Proceedings of the Third International Conference on the Peaceful Uses of Atomic Energy

Held in Geneva
31 August–9 September 1964

Volume 4
Reactor Control

MULTILINGUAL EDITION
ÉDITION MULTILINGUE
МНОГОЯЗЫЧНОЕ ИЗДАНИЕ
EDICIÓN PLURILINGÜE

UNITED NATIONS
New York
1965

EXPLANATORY NOTE

The Proceedings of the Third International Conference on the Peaceful Uses of Atomic Energy comprise a single, multilingual publication of sixteen volumes. This form was prescribed by the General Assembly of the United Nations in approving the Conference budget.

Papers accepted for consideration at the Conference are accordingly printed herein only in the original language of submission, each being followed by its abstract in the other three languages of the Conference.*

The budgetary arrangements for the Conference required also that Governments provide abstracts and papers in two of the Conference languages. One of the three abstracts following each paper is, therefore, in a translation provided by the Government concerned. The abstracts were translated into the other two languages either by the Division of Language Services, International Atomic Energy Agency (IAEA) in Vienna, or, with its assistance, through the intermediary of the national atomic energy authorities in London, Paris, Moscow and Madrid.

The Foreword by the Secretary-General of the United Nations, the Preface by the Director General of IAEA, and this Explanatory Note, together with the records of discussion at each of the six scientific general sessions and thirty-six technical sessions of the Conference, are published in all four languages. All other material, which is largely of a formal nature and is confined to Volumes 1 and 16, is published in the language of submission or delivery, followed in the case of French, Russian and Spanish originals by the English translation.

Governments whose national tongue is not one of the four Conference languages were consulted as to their preference for the language in which their papers should appear in these Proceedings.

The Table of Contents in each volume gives the titles of papers in the original language, or language of choice, followed in the case of French, Russian and Spanish titles by the English translation.

Starting from the 992 abstracts submitted by Governments, specialized agencies and IAEA, the Scientific Secretariat, working under the guidance of the United Nations Scientific Advisory Committee, finally chose 747 papers for inclusion in the Programme of the Conference; of these, 358 were selected for oral presentation at the 42 working sessions.

In arranging the programme, the Scientific Secretariat aimed at achieving a balanced schedule, providing for the oral presentation of as many papers as possible at each session while still leaving adequate time for discussion of the material presented. Two afternoons were left entirely free, to enable informal groups to discuss matters arising out of discussions at the formal sessions of the Conference. No records were taken of such informal meetings.

Wherever possible, the author, or authors, of papers were consulted during the Conference by members of the Scientific Secretariat, who acted as secretaries of session, or by the team of editors made available for the purpose by IAEA,** to ensure maximum accuracy.

The records of discussion at the various sessions, based on notes taken in the meetings by IAEA records officers,** and checked where necessary against the sound recordings made of all sessions, were prepared by the Division of Language Services of IAEA in English, and subsequently translated into French, Russian and Spanish through the intermediary of the atomic energy authorities in the three countries concerned (see third paragraph of the present note).

The editing of the English, French and Spanish papers was carried out at the United Nations Office at Geneva under United Nations supervision by a team of editors, whose services, also, were made available by the atomic energy authorities of their respective countries, with some help from outside consultants. The editing of the Russian papers was done in Moscow in similar circumstances. The following served as editors: Mr. A. de Calmès, Dr. C. E. Granados, Mr. D. H. Hill, Mr. V. F. Kalinin, Cand. Tech. Sc., Dr. R. Lapage, Mr. E. T. Marles, Dr. J. D. C. Mole, Mr. C. Ségot, Mr. J. J. Stobbs, Mr. C. R. Symons and Mr. J. Williamson.

The task of printing this large collection of scientific information has been shared by printers in

* The languages of the Conference were English, French, Russian and Spanish.

** The names of the scientific secretaries, editors and records officers will be found in the list of the Conference Secretariat in Annex 1, Volume 1, of this series.

Belgium, Canada, France, Switzerland, the Union of Soviet Socialist Republics and the United Kingdom.

Full titles of the sixteen volumes of these Proceedings, together with the sessions covered by each volume, are as follows:

Volume No.		*Sessions included*
1	Progress in Atomic Energy	A, B, 1.6, C, H
2	Reactor Physics	3.1
3	Reactor Studies and Performance	3.2, 3.3
4	Reactor Control	3.4, 3.5
5	Nuclear Reactors — I. Gas-cooled and Water-cooled Reactors	1.1, 1.2, 1.3
6	Nuclear Reactors — II. Fast Reactors and Advanced Concepts	1.4, 1.5, 1.7
7	Research and Testing Reactors	D, 1.9, 1.8
8	Reactor Engineering and Equipment	1.10, 1.11, 3.7
9	Reactor Materials	2.8, 2.9, 2.4
10	Nuclear Fuels — I. Fabrication and Reprocessing	2.3, 2.6, 2.7
11	Nuclear Fuels — II. Types and Economics	2.5, 2.1, 2.2
12	Nuclear Fuels — III. Raw Materials	2.11, 2.12, 2.10
13	Nuclear Safety	3.9, 3,8 3.6
14	Environmental Aspects of Atomic Energy and Waste Management	3.10, 3.11
15	Special Aspects of Nuclear Energy and Isotope Applications	E, 4.1, F, G, 4.2
16	List of Papers and Indexes	

NOTE EXPLICATIVE

Les Actes de la troisième Conférence internationale sur l'utilisation de l'énergie atomique à des fins pacifiques sont publiés ici sous la forme d'une édition unique, multilingue, en seize volumes. Cette présentation a été décidée par l'Assemblée générale lorsqu'elle a approuvé le budget de la Conférence.

En conséquence, les mémoires qui ont été acceptés pour la Conférence sont reproduits ici dans la langue originale dans laquelle ils ont été soumis et sont suivis d'un résumé dans les trois autres langues de la Conférence *.

Aux termes des dispositions budgétaires prises en vue de la Conférence, les gouvernements devaient fournir les résumés et les mémoires dans deux des langues de la Conférence. Ainsi, sur les trois résumés qui suivent chaque mémoire, un est une traduction fournie par le gouvernement intéressé. La traduction des résumés dans les deux autres langues a été faite soit par la Division des services linguistiques de l'Agence internationale de l'énergie atomique (AIEA), à Vienne, soit avec son concours, par les soins des organismes nationaux compétents en matière d'énergie atomique à Londres, Paris, Moscou et Madrid.

L'avant-propos du Secrétaire général de l'Organisation des Nations Unies, la préface du Directeur général de l'AIEA et la présente note explicative, ainsi que les comptes rendus de chacune des six séances scientifiques générales et des trente-six séances techniques de la Conférence, sont publiés dans les quatre langues. Tous les autres textes, qui pour la plupart sont d'un caractère non technique et figurent dans les volumes 1 et 16, sont publiés dans la langue dans laquelle ils ont été présentés par écrit ou oralement et sont suivis, lorsque cette langue est l'espagnol, le français ou le russe, d'une traduction en anglais.

Les gouvernements des pays dont la langue officielle n'est pas l'une des quatre langues utilisées à la Conférence ont été consultés pour savoir dans quelle langue ils préféraient voir paraître leurs mémoires.

La table des matières de chaque volume donne les titres des mémoires dans la langue originale ou dans la langue choisie; ces indications sont suivies, pour les titres en espagnol, en français et en russe, de la traduction en anglais.

Sur les 992 résumés présentés par les gouvernements, les institutions spécialisées et l'AIEA, le Secrétariat scientifique, travaillant sous la direction du Comité consultatif scientifique des Nations Unies, en a finalement retenu 747 pour les inscrire au programme de la Conférence; sur ce nombre, 358 ont été présentés oralement aux 42 séances de travail.

En établissant le programme de la Conférence, le Secrétariat scientifique a cherché à réaliser un équilibre: il s'est efforcé de ménager un temps suffisant pour la présentation du plus grand nombre possible de mémoires tout en laissant du temps pour leur discussion. Deux après-midi avaient été laissés entièrement libres afin de permettre aux participants d'organiser des réunions non officielles et de discuter en petits groupes des questions qui se posaient à la suite des séances officielles de la Conférence. Ces réunions n'ont pas fait l'objet de comptes rendus.

Toutes les fois que cela a été possible, l'auteur ou les auteurs des mémoires ont été consultés pendant la Conférence par les membres du Secrétariat scientifique, qui ont assuré le secrétariat des séances, ou par l'équipe d'« éditeurs » que l'AIEA ** avait mis à cet effet à la disposition de la Conférence, afin d'assurer l'exactitude la plus grande.

Les comptes rendus des discussions aux réunions, établis d'après les notes prises en séance par les rédacteurs de comptes rendus de l'AIEA** et comparés toutes les fois qu'il le fallait avec les enregistrements sonores, ont été rédigés en anglais par la Division des services linguistiques de l'AIEA, puis traduits en espagnol, en français et en russe par les soins des organismes compétents en matière d'énergie atomique des trois pays intéressés (voir le troisième alinéa de la présente note).

Les mémoires rédigés en anglais, en espagnol et en français ont été mis au point pour l'impression à l'Office européen des Nations Unies à Genève, sous le contrôle de l'ONU, par une équipe de rédac-

* Les langues de la Conférence étaient l'anglais, l'espagnol, le français et le russe.

** On trouvera les noms des secrétaires scientifiques, des « éditeurs » et des rédacteurs de comptes rendus dans la liste des membres du secrétariat de la Conférence à l'annexe 1 du volume 1.

teurs mis à la disposition de la Conférence par les organismes compétents en matière d'énergie atomiques des pays intéressés, avec l'aide de quelques consultants extérieurs. La mise au point définitive des mémoires rédigés en russe a été faite à Moscou dans les mêmes conditions. Voici les noms des rédacteurs qui ont assuré la mise au point des mémoires: M. A. de Calmès, M. C. E. Granados, M. D. H. Hill, M. V. F. Kalinin, M[lle] R. Lapage, M. E. T. Marles, M[lle] J. D. C. Mole, M. C. Ségot, M. J. J. Stobbs, M. C. R. Symons et M. J. Williamson.

Des entreprises de Belgique, du Canada, de France, du Royaume-Uni, de Suisse et de l'Union des Républiques socialistes soviétiques se sont partagé la tâche que représentait l'impression de cette masse importante de documents scientifiques.

Les titres complets des seize volumes des Actes de la Conférence, ainsi que les numéros des séances sur lesquelles porte chaque volume, figurent ci-après:

Numéro du volume		Séances
1	Progrès accomplis dans le domaine atomique	A, B, 1.6, C, H
2	Physique des réacteurs	3.1
3	Etude des réseaux et performance des réacteurs	3.2, 3.3
4	Contrôle des réacteurs	3.4, 3.5
5	Réacteurs nucléaires — I. Réacteurs refroidis par un gaz et réacteurs refroidis à l'eau	1.1, 1.2, 1.3
6	Réacteurs nucléaires — II. Réacteurs à neutrons rapides et réacteurs d'avant-garde	1.4, 1.5, 1.7
7	Réacteurs de recherche et réacteurs d'essai de matériaux	D, 1.9, 1.8
8	Technologie et équipement des réacteurs	1.10, 1.11, 3.7
9	Matériaux pour réacteurs	2.8, 2.9, 2.4
10	Combustibles nucléaires — I. Fabrication et retraitement	2.3, 2.6, 2.7
11	Combustibles nucléaires — II. Caractéristiques et aspects économiques	2.5, 2.1, 2.2
12	Combustibles nucléaires — III. Matières premières	2.11, 2.12, 2.10
13	Sûreté nucléaire	3.9, 3.8, 3.6
14	Influence sur le milieu de l'emploi de l'énergie nucléaire. Traitement et élimination des déchets	3.10, 3.11
15	Aspects particuliers de l'énergie nucléaire et applications des radioéléments	E, 4.1, F, G, 4.2
16	Liste des mémoires et index	

ПОЯСНИТЕЛЬНАЯ ЗАПИСКА

Труды третьей Международной конференции по использованию атомной энергии в мирных целях представляют собой единое многоязычное издание из шестнадцати томов. Такая форма была предусмотрена Генеральной Ассамблеей Организации Объединенных Наций при одобрении ею бюджета Конференции.

Принятые к рассмотрению Конференцией доклады соответственно опубликованы здесь лишь на языке оригинала; при этом каждый доклад сопровождается аннотацией на других трех языках Конференции*.

Бюджетные постановления в отношении проведения Конференции также предусматривали, что правительства представят аннотации и доклады на двух языках Конференции. Поэтому одна из трех аннотаций, сопровождающих каждый доклад, является переводом, представленным соответствующим правительством. Аннотации были переведены на другие два языка либо Отделом переводов Международного агентства по атомной энергии (МАГАТЭ) в Вене, либо с его помощью при сотрудничестве национальных органов, ведающих вопросами атомной энергии, в Лондоне, Париже, Москве и Мадриде.

Введение и предисловие Генерального Секретаря Организации Объединенных Наций и Генерального директора МАГАТЭ, соответственно, и настоящая пояснительная записка, наряду с протоколами каждого из шести научных пленарных заседаний и тридцати шести секционных заседаний Конференции, публикуются на всех четырех языках. Все другие материалы, которые по своему характеру в основном относятся к числу официальных и содержатся в томах 1 и 16, публикуются на языке оригинала; и когда речь идет о французских, русских и испанских оригиналах, то к ним приложен английский перевод.

С правительствами стран, язык которых не относится к числу четырех языков Конференции, были проведены консультации по поводу того, на каком языке было бы желательно, по их мнению, опубликовать в настоящих трудах представленные ими доклады.

В содержании каждого тома указаны заглавия докладов на языке оригинала либо на другом избранном языке, и в том случае, когда речь идет о французских, русских и испанских заглавиях, их сопровождает английский перевод.

Из 992 аннотаций, представленных правительствами, специализированными учреждениями, а также МАГАТЭ, Ученый секретариат, работая под руководством Научного консультативного комитета Организации Объединенных Наций, в итоге отобрал 747 докладов для включения их в программу Конференции; из них 358 были отобраны для представления в устной форме на 42 рабочих заседаниях.

При составлении программы Ученый секретариат ставил целью добиться сбалансированного расписания, которое дало бы возможность представить в устной форме максимальное количество докладов на каждом заседании при обеспечении достаточного времени для проведения дискуссии по поводу представленного материала. В двух случаях имеющееся во второй половине дня время оставили нераспределенным, с тем чтобы дать возможность неофициальным группам обсудить вопросы, возникшие в ходе дискуссии на официальных заседаниях Конференции. На таких неофициальных заседаниях протоколы не составлялись.

По мере возможности, с автором или авторами докладов консультировались в ходе Конференции члены Ученого секретариата, которые выполняли функции секретарей заседаний, либо такие консультации проводились группой редакторов, которые были выделены МАГАТЭ** для этой цели, с тем чтобы обеспечить максимальную точность.

* Языками Конференции являлись: английский, французский, русский и испанский.

** Фамилии ученых секретарей, редакторов и протоколистов приведены в перечне сотрудников секретариата Конференции в приложении 1-ом к тому 1-му настоящей серии.

Протоколы дискуссии на различных заседаниях, составленные на основе записей, сделанных в ходе заседаний протоколистами МАГАТЭ*, и проверенные, по мере необходимости, путем сравнения со звуковой записью, которая велась на всех заседаниях, были подготовлены Отделом переводов МАГАТЭ на английском языке и впоследствии переведены на французский, русский и испанский языки при сотрудничестве национальных органов, ведающих вопросами атомной энергии, в трех заинтересованных странах (смотри третий абзац пояснительной записки).

Работа по редактированию документов на английском, французском и испанском языках была проведена в Европейском отделении Организации Объединенных Наций, в Женеве, под руководством Организации Объединенных Наций группой редакторов, услуги которых были также предоставлены по линии органов, ведающих вопросами атомной энергии в соответствующих странах, с использованием в некоторой степени помощи приглашенных со стороны консультантов. Русские документы редактировались в Москве в таких же условиях. Нижеследующие лица осуществляли работу в качестве редакторов: д-р К. Э. Гранадос, кандидат технических наук В. Ф. Калинин, г-н А. де Кальмэс, д-р Р. Лепейдж, г-н Э. Т. Марлз, д-р Дж. Д. К. Моул, г-н Ч. Р. Саймонс, г-н Дж. Дж. Стобз, г-н Ш. Сэго, г-н Дж. Уильямсон, г-н Д. Х. Хилл.

В выполнении задачи по печатанию этой обширной научной информации принимали участие типографии в Бельгии, Канаде, Соединенном Королевстве, Союзе Советских Социалистических Республик, Франции и Швейцарии.

Ниже приводятся полные заглавия шестнадцати томов настоящих Трудов, а также указывается, какие сессии охватываются каждым томом:

* Фамилии ученых секретарей, редакторов и протоколистов приведены в перечне сотрудников секретариата Конференции в приложении 1-ом к тому 1-му настоящей серии.

Номер Тома		Заседания, включенные в том
1	Прогресс в работах по атомной энергии	A, B, 1.6, C, H
2	Физика реакторов	3.1
3	Изучение реакторов и их характеристики	3.2, 3.3
4	Регулирование реакторов	3.4, 3.5
5	Ядерные реакторы — I. Реакторы с водяным и газовым охлаждением	1.1, 1.2, 1.3
6	Ядерные реакторы — II. Реакторы на быстрых нейтронах и усовершенствованные реакторы	1.4, 1.5, 1.7
7	Исследовательские и испытательные реакторы	D, 1.9, 1.8
8	Технология и оборудование реакторов	1.10, 1.11, 3.7
9	Реакторные материалы	2.8, 2.9, 2.4
10	Ядерное топливо — I. Изготовление и переработка	2.3, 2.6, 2.7
11	Ядерное топливо — II. Типы и экономика	2.5, 2.1, 2.2
12	Ядерное топливо — III. Сырьевые материалы	2.11, 2.12, 2.10
13	Ядерная безопасность	3.9, 3.8, 3.6
14	Исследование окружающей среды и удаление радиоактивных отходов	3.10, 3.11
15	Специальные аспекты применения ядерной энергии и изотопов	E, 4.1, F, G, 4.2
16	Список докладов и указатели	

NOTA EXPLICATIVA

Las Actas de la tercera Conferencia Internacional sobre la Utilización de la Energía Atómica con Fines Pacíficos están constituidas por una publicación única y plurilingüe compuesta de dieciséis volúmenes, en conformidad con lo dispuesto por la Asamblea General de las Naciones Unidas al aprobar el presupuesto de la Conferencia.

Por consiguiente, las memorias aceptadas para ser examinadas en la Conferencia sólo figuran impresas en el idioma original en que se presentaron, y cada una de ellas va seguida de un resumen de la misma en los otros tres idiomas de la Conferencia *.

En los arreglos presupuestarios para la Conferencia se dispuso también que los gobiernos tenían asimismo que presentar resúmenes y memorias en dos de los idiomas de la Conferencia. En consecuencia, uno de los tres resúmenes que siguen a cada memoria es una traducción facilitada por el gobierno interesado. Los resúmenes fueron traducidos a los otros dos idiomas, ya por la División de Idiomas del Organismo Internacional de Energía Atómica (OIEA) de Viena, o, con su asistencia, por conducto de las autoridades nacionales de energía atómica de Londres, París, Moscú y Madrid.

La introducción del Secretario General de las Naciones Unidas, el prefacio del Director General del OIEA y la presente nota explicativa, junto con las actas de los debates celebrados en cada una de las seis sesiones científicas generales y las treinta y seis sesiones técnicas de la Conferencia, se publican en los cuatro idiomas. El resto del material, que reviste en su mayoría un carácter oficial y está contenido exclusivamente en los volúmenes 1 y 16, se publica en el idioma en que fue presentado o entregado, seguido para los originales en español, francés y ruso, de la traducción en inglés.

Se consultó a los gobiernos cuyo idioma nacional no es uno de los cuatro idiomas de la Conferencia para saber en cuál de ellos preferían que se publicaran sus memorias en estas Actas.

El índice de cada volumen contiene los títulos de las memorias en el idioma original, o en el idioma elegido, seguidos, cuando se trata de títulos en español, francés y ruso, de la traducción en inglés.

De los 992 resúmenes presentados por gobiernos, organismos especializados y el OIEA, la Secretaría Científica, bajo la dirección del Comité Científico Consultivo de las Naciones Unidas, escogió por último 747 memorias que debían ser incluidas en el programa de la Conferencia; de éstas, 358 fueron seleccionadas para ser presentadas oralmente en las 42 sesiones de trabajo.

Al preparar el programa de actividades, la Secretaría Científica trató de conseguir un justo equilibrio, y así se previó la presentación oral del mayor número posible de memorias en cada sesión, pero dejando todavía tiempo suficiente para examinar la información presentada. Se dejaron dos tardes totalmente libres, a fin de que los grupos oficiosos pudieran examinar las cuestiones que surgieran en las sesiones oficiales de la Conferencia. No se levantó acta de tales reuniones.

Siempre que fue posible, el autor, o los autores, de las memorias fueron consultados en el curso de la Conferencia por miembros de la Secretaría Científica, que actuaron de secretarios de sesión, o por un grupo de editores facilitado a dicho efecto por el OIEA**, a fin de asegurar la máxima exactitud.

Las actas de los debates celebrados en las diversas sesiones, basadas en notas tomadas en las reuniones por redactores de actas del OIEA**, y verificadas siempre que fue necesario mediante las grabaciones efectuadas en todas las sesiones, fueron preparadas por la División de Idiomas del Organismo Internacional de Energía Atómica (OIEA) en inglés, y traducidas después al español, el francés y el ruso por conducto de las autoridades de energía atómica de los tres países interesados (véase el tercer párrafo de la presente nota).

La preparación para la publicación del texto de los documentos en español, francés e inglés se efectuó en la Oficina de Ginebra de las Naciones Unidas, bajo la fiscalización de las Naciones Unidas, por un equipo de editores cuyos servicios fueron también proporcionados por las autoridades de energía atómica de sus respectivos países, con alguna ayuda de consultores del exterior. La preparación para la publicación de los documentos en ruso se efectuó en Moscú en circunstancias análogas. Actuaron de editores las personas siguientes: Sr. A. de Calmès, Dr. C. E. Granados, Sr. D. H. Hill,

* Los idiomas de la Conferencia fueron el español, el francés, el inglés y el ruso.

** Los nombres de los secretarios científicos, editores y redactores de actas figuran en la lista de la Secretaría de la Conferencia, en el anexo 1, volumen 1, de esta serie.

Sr. V. F. Kalinin, Dra. R. Lapage, Sr. E. T. Marles, Dra. J. D. C. Mole, Sr. C. Ségot, Sr. J. J. Stobbs, Sr. C. R. Symons y Sr. J. Williamson.

En la impresión de esta gran recopilación de información científica han participado impresores de Bélgica, el Canadá, Francia, el Reino Unido, Suiza y la Unión de Repúblicas Socialistas Soviéticas.

Los títulos completos de los dieciséis volúmenes de estas Actas, junto con las sesiones comprendidas en cada volumen, son los siguientes:

Número del volumen		*Sesiones*
1	Progresos realizados en el dominio atómico	A, B, 1.6, C, H
2	Física de los reactores	3.1
3	Estudios sobre reticulados. Funcionamiento de reactores	3.2, 3.3
4	Control de los reactores	3.4, 3.5
5	Reactores nucleares — I. Reactores refrigerados por gas y por agua	1.1, 1.2, 1.3
6	Reactores nucleares — II. Reactores rápidos y conceptos más avanzados	1.4, 1.5, 1.7
7	Reactores de investigación y de ensayo	D, 1.9, 1.8
8	Tecnología y equipo de los reactores	1.10, 1.11, 3.7
9	Materiales de los reactores	2.8, 2.9, 2.4
10	Combustibles nucleares — I. Fabricación y tratamiento	2.3, 2.6, 2.7
11	Combustibles nucleares — II. Características y estudios económicos	2.5, 2.1, 2.2
12	Combustibles nucleares — III. Primeras materias	2.11, 2.12, 2.10
13	Seguridad nuclear	3.9, 3.8, 3.6
14	Influencia del empleo de la energía nuclear sobre el ambiente. Evacuación de residuos	3.10, 3.11
15	Aspectos especiales de la energía nuclear y empleo de los radioelementos	E, 4.1, F, G, 4.2
16	Lista de documentos e índices	

TABLE OF CONTENTS

Volume 4

Session 3.4 : Reactor kinetics

			Page
	Point-reactor kinetics		
P/270	Gyftopoulos	Point reactor kinetics and stability criteria	3
P/648	Stassis, Mitsonias	Determination of ℓ_{eff} and β_{eff} in a critical reactor by the pulsed neutron technique	12
P/686	Schmid, Zünti	The evolution of fission rate during and after shut-down of a nuclear reactor	16
P/687	Schmid	On the stability of steam-cooled fast reactors with ceramic fuel	25
P/713	Tunkelo	On non-linear reactor kinetics	35
	Spatial kinetics		
P/271	Kaplan *et al.*	Space-time reactor dynamics	41
P/272	Thie	Stochastic processes in nuclear reactors and measurement of dynamic performance characteristics	54
P/685	Norinder	Spatial kinetics of thermal reactors	61
P/842	Koskinen	Generalized potential theory for multi-group diffusion in a general multi-region reactor	67
P/847	Kanai *et al.*	Theoretical kinetic studies of boiling water reactors and multi-region reactors	76
	Kinetic studies of particular reactors		
P/79	Abdon, Chaigne	Etude du comportement dynamique de la pile RAPSODIE *Study of the dynamic behaviour of the reactor RAPSODIE*	89
P/178	Hughes *et al.*	Temperature limits and the optimisation of power output in Calder and Chapelcross reactors	100
P/371	Гаврилов, Подлазов *Gavrilov, Podlazov*	О динамической устойчивости ядерных энергетических установок *On the dynamic stability of nuclear power plants*	109
P/629	Ambrosini *et al.*	Stability analysis and dynamic performance of a chemical system operated for the automatic fine control of a nuclear reactor	118
P/664	Miida *et al.*	Some engineering studies on the analysis of kinetics and control of Tokai Atomic Power Station	128
P/671	Qazi	A reactivity oscillator for swimming pool reactors	139

			Page
P/697	Gilbert *et al.*	An analogical study of the dynamic behaviour of the Lucens Experimental Nuclear Power Station	144
P/848	Miida	Kinetic studies and control of nuclear reactors by statistical methods	151
P/859	Aarset *et al.*	In-core instrument development in the HBWR programme	164
P/860	Ager-Hanssen *et al.*	Dynamics of boiling heavy water reactors based on HBWR research programme	179
Record of session 3.4			192
Compte rendu de la séance 3.4			196
Протокол заседания 3.4			200
Acta de la sesión 3.4			205

Session 3.5 : Reactor control and shielding

Instrumentation

P/80	Furet, Pupponi	Quelques aspects particuliers du contrôle dans les piles atomiques de puissance *Some particular aspects of control in nuclear power reactors*	213
P/500	Podgórski, Szulc	Recent developments in control and safety systems for nuclear reactors at the Institute of Nuclear Research in Poland	220
P/631	Kovanic, Wagner	Outlook for reactor control systems with moving detectors	227
P/633	Kovanic	Optimum digital information treatment and nuclear engineering instrumentation	235
P/647	Sommer	Automatic control of the average core flux by measuring N^{16} coolant activity at the FRM Munich Research Reactor	243
P/815	Bobleter, Vajda	Measurement of high-dose gamma fluxes at reactor pulses and strong gamma sources by the conductivity of cuprous oxide	248

Control systems

P/179	Brown *et al.*	Control, stability and protection of a gas-cooled graphite-moderated reactor	255
P/180	Branson *et al.*	Design of control rod systems for gas-cooled reactors	267
P/274	Radkowsky, Creagan	Poison control of thermal reactors	277
P/354	Орлов и др. *Orlov* et al.	Выбор некоторых оптимальных характеристик компенсирующих элементов ядерных реакторов *Choice of some optimum characteristics of control elements for nuclear reactors*	287

Page

P/375 Кузнецов и др. . . . Экспериментальное изучение способов компенсации избыточной реактивности промежуточных реакторов 297
Kuznetsov et al. *Experimental study of some methods of compensating excess reactivity in intermediate reactors*

P/376 Бать и др. Компенсация больших изменений реактивности деформацией решетки активной зоны 306
Bat et al. . . . . *Compensation of large changes in the reactivity by deformation of the core lattice*

P/795 Conti, Conti . Solid state nuclear safety system . . 314

Automatic control

P/273 Schultz, Legler . . . . Application of digital computer techniques to reactor operation 321

P/677 Iftode *et al.* . . . . . Un nouveau système de contrôle des réacteurs nucléaires 331
A new control system for nuclear reactors

Progress in theoretical and experimental shield-design methods

P/175 Youell *et al.* . . . . . Bradwell Nuclear Power Station: comparison of shielding performance with design calculations . . 339

P/260 Blizard, Mittelman . . . . . Recent advances in reactor shielding in the United States 348

P/364 Абагян и др. . . . . Некоторые новые аспекты применения сопряженных функций и теории возмущений в расчетах реакторов и защиты 359
Abagyan et al. . . . . *Some new aspects of using adjoint functions and perturbation theory in reactor and shielding calculations*

P/377 Лейпунский и др. . Новые результаты физического исследования защиты 372
Leipunsky *et al.* . . . . . *New results of shielding research*

P/657 Kataoka . . . . . Use of response matrix method for multi-layer shield design 386

P/684 Aalto *et al.* . . . . . A new shield design method and some attenuation studies in laminated biological shields 395

P/721 Наумов . . . . . Описание ослабления нейтронного излучения ядерного реактора многослойной биологической защитой с помощью многогрупповой модели в диффузионном приближении 405
Naumov . . . . . *Description of neutron radiation attenuation in-pile by multi-layer biological shielding on a multi-group model in diffusion approximation*

Record of session 3.5 418

Compte rendu de la séance 3.5 422

Протокол заседания 3.5 427

Acta de la sesión 3.5 432

Session 3.4

REACTOR KINETICS

LIST OF PAPERS

			Page
	Point-reactor kinetics		
P/270	Point reactor kinetics and stability criteria	E. P. Gyftopoulos	3
P/648	Determination of ℓ_{eff} and β_{eff} in a critical reactor by the pulsed neutron technique	C. Stassis, C. Mitsonias	12
P/686	The evolution of fission rate during and after shut-down of a nuclear reactor	P. Schmid, W. Zünti	16
P/687	On the stability of steam-cooled fast reactors with ceramic fuel	P. Schmid	25
P/713	On non-linear reactor kinetics	E. Tunkelo	35
	Spatial kinetics		
P/271	Space-time reactor dynamics	S. Kaplan *et al.*	41
P/272	Stochastic processes in nuclear reactors and measurement of dynamic performance characteristics	J. A. Thie	54
P/685	Spatial kinetics of thermal reactors	O. Norinder	61
P/842	Generalized potential theory for multi-group diffusion in a general multi-region reactor	H. Koskinen	67
P/847	Theoretical kinetic studies of boiling water reactors and multi-region reactors	T. Kanai *et al.*	76
	Kinetic studies of particular reactors		
P/79	Etude du comportement dynamique de la pile RAPSODIE *Study of the dynamic behaviour of the reactor RAPSODIE*	R. Abdon, M. Chaigne	89
P/178	Temperature limits and the optimisation of power output in Calder and Chapelcross reactors	H. A. Hughes *et al.*	100
P/371	О динамической устойчивости ядерных энергетических установок *On the dynamic stability of nuclear power plants*	П. А. Гаврилов, Л. Н. Подлазов P. A. Gavrilov, L. N. Podlazov	109
P/629	Stability analysis and dynamic performance of a chemical system operated for the automatic fine control of a nuclear reactor	G. C. Ambrosini *et al.*	118

		Page
P/664	Some engineering studies on the analysis of kinetics and control of Tokai Atomic Power Station ..... J. Miida *et al.*	128
P/671	A reactivity oscillator for swimming pool reactors ..... M. N. Qazi	139
P/697	An analogical study of the dynamic behaviour of the Lucens Experimental Nuclear Power Station ..... J. R. Gilbert *et al.*	144
P/848	Kinetic studies and control of nuclear reactors by statistical methods ..... J. Miida	151
P/859	In-core instrument development in the HBWR programme ..... B. Aarset *et al.*	164
P/860	Dynamics of boiling heavy water reactors based on HBWR research programme ..... H. Ager-Hanssen *et al.*	179

Point reactor kinetics and stability criteria

By E. P. Gyftopoulos*

During the past few years efforts have been devoted to the understanding of the capability and limitations of point reactor kinetics with regard to their relationship to experiments [1-3]. Even though it is generally recognized that point kinetics fail to account for the dynamic behavior of large core reactors, it is not equally well accepted that similar failures may arise in small reactors where relatively small flux shape changes may occur over short periods of time.

One of the purposes of this paper is to re-derive the kinetics equations in an effort to illustrate these failures and to emphasize the need for space-time dependent kinetics for meaningful correlations of experimental measurements. A positive result of this re-derivation is the recognition that point kinetics can always be used to answer questions of overall stability or instability. Thus, the second purpose of the paper is to review existing criteria for nonlinear stability, to indicate how restrictive they are and then suggest some practical considerations which might bridge the discrepancy between analysis and experience.

POINT REACTOR KINETICS

Transport theory and conventional neutron kinetics

The most important variable in reactor dynamics is the fission energy stored in the reactor and its distribution because this energy can be directly related to all other variables and all material and environmental constraints. Even though the stored energy is such a key variable, it has not been possible to measure it and control it directly. Instead, the energy behavior is inferred from measurements of the neutron population, the temperatures of different components, the pressure, etc.

The analysis of the time behavior of the neutron population in a reactor can be treated by a number of alternative models. A basic model is the one implied by transport theory. This theory allows a precise and detailed representation of all conceivable interactions that neutrons undergo in a reactor with a minimum number of assumptions. The equations that result, however, are very difficult to handle analytically. Consequently, they need to be reduced to simpler forms and then be related in an approximate manner to the energy stored in the reactor. To this end, consider a reactor with a stationary fuel. For mathematical simplicity and without any loss of generality, assume that there is only one species of fissionable material and that there is a very large number of neutrons so that statistical fluctuations can be ignored.

The time dependent balance equations for the neutron population and the delayed neutron precursors are:

$$\frac{\delta}{\delta t} N(\bar{r}, E, \bar{\Omega}, t) = \frac{1}{4\pi} f_0(E) \int_{\Omega'} d\bar{\Omega}' \int_0^\infty dE' \nu(E')(1-\beta)\nu'\Sigma_f(\bar{r}, E', t)N(\bar{r}, E'\,\bar{\Omega}', t)$$

$$+ \int_{\Omega'} d\bar{\Omega}' \int_0^\infty dE'\, \nu'\, \Sigma_s(\bar{r}, E' \to E, \bar{\Omega}' \to \bar{\Omega}, t)N(\bar{r}, E', \bar{\Omega}', t) + \frac{1}{4\pi} \sum_{i=1}^{m} \lambda_i f_i(E) C_i(\bar{r}, t) + S(\bar{r}, E, \bar{\Omega}, t)$$

$$+ \bar{\Omega}\, \nu \cdot \mathrm{grad} N(\bar{r}, E, \bar{\Omega}, t) - \nu\Sigma_t(\bar{r}, E, t)N(\bar{r}, E, \bar{\Omega}, t); \qquad (1)$$

$$\frac{\delta}{\delta t} C_i(\bar{r}, t) = \int_{\Omega'} d\bar{\Omega}' \int_0^\infty dE' \nu(E')\beta_j\nu'\Sigma_f(\bar{r}, E', t)N(\bar{r}, E', \bar{\Omega}', t) - \lambda_i C_i(\bar{r}, t)\ ;\ i = 1, 2, \ldots m, \qquad (2)$$

where $N(\bar{r}, E, \bar{\Omega}, t)$ is the neutron density per unit volume, per unit relative neutron energy, E, per unit solid angle, $\bar{\Omega}$, at time t, and $C_i(r, t)$ is the concentration of the ith delayed neutron precursor per unit volume at position $\bar{r}$ and time t. The other symbols have their common usage as described in [1].

The difficulties of Eqs. (1) and (2) stem both from their dependence on seven independent variables $(r, E, \bar{\Omega}, t)$, and from the fact that the macroscopic cross sections are complicated implicit functions of the behavior of the neutron population throughout the entire reactor. Customarily an attempt is made to reduce Eqs. (1) and (2) to a set of ordinary differential equations. The reduction is achieved by a variety of mathematical techniques. Which tech-

* Department of Nuclear Engineering, Massachusetts Institute of Technology, Cambridge, Massachusetts.

nique is more appropriate depends on such considerations as computational expediency, reactor type and/or the particular aspect of dynamic behavior which is under investigation. The following technique has received particular attention. The neutron density is expressed in the form

$$N(\bar{r}, E, \bar{\Omega}, t) = G(t)N_g(\bar{r}, E, \bar{\Omega}, t) \ , \qquad (3)$$

where $G(t)$ is a time dependent function accounting for all growth or decay tendencies of the neutron density, while $N_g(\bar{r}, E, \bar{\Omega}, t)$ is a shape function which is bounded at all times and for all values of $(\bar{r}, E, \bar{\Omega})$ and accounts for the distribution of neutrons in the phase space $(\bar{r}, E, \bar{\Omega})$. With this definition for $N(\bar{r}, E, \bar{\Omega}, t)$ and through consideration of the adjoint density, $N_0^*(\bar{r}, E, \bar{\Omega})$, of an arbitrary source-free critical reference reactor, Eqs. (1) and (2) are reduced to the form:

$$\frac{dG(t)}{dt} = \left(\frac{\rho}{\Lambda} - \frac{\beta_e}{\Lambda}\right) G(t) + \sum_i^m \lambda_i C_i(t) + Q(t)$$

$$- \left[\frac{\delta}{\delta t} \ell n \int_v d\bar{r} \int_0^\infty dE \int_\Omega^i d\bar{\Omega} N_0^*(\bar{r}, E, \bar{\Omega}) N_g(\bar{r}, E, \bar{\Omega}, t)\right] G(t) \ ; \qquad (4)$$

$$\frac{dC_i(t)}{dt} = \frac{\beta_{ie}}{\Lambda} G(t) - \lambda_i C_i(t) + \left[\frac{\delta}{\delta t} \ell n \int_v d\bar{r} \int_0^\infty dE \int_\Omega d\bar{\Omega} N_0^*(\bar{r}, E, \bar{\Omega}) N_g(\bar{r}, E, \bar{\Omega}, t)\right] C_i(t), \qquad (5)$$

where the analytical expressions for $C_i(t)$, $Q(t)$, ρ/Λ and B_{ie}/Λ are given in [1].

The selection of the bounded shape function is arbitrary. One possibility is to normalize $N_g(\bar{r}, E, \bar{\Omega}, t)$ so that

$$\int_v d\bar{r} \int_0^\infty dE \int_\Omega d\bar{\Omega} N_0^*(\bar{r}, E, \bar{\Omega}) N_g(\bar{r}, E, \bar{\Omega}, t) = \text{constant}. \qquad (6)$$

Thus, the logarithmic term disappears from Eqs. (4) and (5), and $G(t)$ describes the time dependent amplitude of the component of $N(\bar{r}, E, \bar{\Omega}, t)$ which has the same shape as the distribution of neutrons in the critical reference reactor. This normalization is practical when the neutron shape distribution does not change appreciably and/or rapidly, because the solutions of Eqs. (4) and (5) can then be correlated unambiguously with the recording of any counter placed around or inside the reactor. Under these conditions, $G(t)$ can be interpreted as the average power of the reactor. The correlation is quite good because the important coefficient ρ/Λ in Eq. (4) is a bilinear average of the differences of cross sections between those of the reactor under consideration and those of the critical reference reactor. As such it can be estimated to a good degree of accuracy. On the other hand, if the neutron shape distribution changes appreciably or very rapidly, assuming that Eq. (6) is valid renders the correlation of $G(t)$ with the reading of a counter ambiguous. The reason is that $G(t)$ is proportional to the amplitude of the fundamental component of the flux while the counter reading depends on the behavior of the flux at the position of the counter. If an attempt is made to include the logarithmic term in Eqs. (4) and (5), then again the correlation becomes difficult both because knowledge of the temporal behavior of the shape function is needed and because association of any counter reading with an average flux requires a time dependent calibration of the counter.

Another technique which may be used to reduce Eqs. (1) and (2) into a set of ordinary differential equations is to write

$$N(\bar{r}, E, \bar{\Omega}, t) = P(t)N_p(\bar{r}, E, \bar{\Omega}, t), \qquad (7)$$

multiply Eqs. (1) and (2) by the fission cross-section and integrate over all $(\bar{r}, E, \bar{\Omega})$. Thus, with appropriate definitions of ρ/Λ, β_{ie}/Λ, $C_i(t)$ and $Q(t)$, a set of equations similar to Eqs. (4) and (5) is found in terms of $P(t)$ instead of $G(t)$. If the shape function is chosen so that

$$\int_v d\bar{r} \int_0^\infty dE \int_\Omega d\bar{\Omega} \Sigma_f(\bar{r}, E, t) N_p(\bar{r}, E, \bar{\Omega}, t) = \text{constant}, \qquad (8)$$

the logarithmic term is missing from the equations, and $P(t)$ is a measure of the average power of the reactor. The difficulty with this formulation is that during appreciable or rapid changes of the neutron density shape function, $N_p(\bar{r}, E, \bar{\Omega}, t)$, the average power $P(t)$ cannot be correlated with the reading of a counter. In addition, the coefficient ρ/Λ for this case is a bilinear average of the absolute cross-sections and consequently subject to large errors.

Finally, a third alternative is to derive a set of ordinary equations by using the counter cross-section as a weighting function instead of $N_0^*(\bar{r}, E, \bar{\Omega})$ or $\Sigma_f(\bar{r}, E, t)$. Thus a set of equations is established which describes directly the counter reading but again, during appreciable or rapid changes of the shape of the neutron density, the counter reading cannot be interpreted as measuring a physically meaningful quantity.

In summary, the essence of all these arguments is that the standard form of point kinetics may not be suitable for rapid transients.

Illustrative example

A. F. Henry, S. Kaplan and J. Yasinsky of Westinghouse performed and contributed the following digital computer experiment for the purposes of this paper. They considered two slab reactors, 60 cm and 240 cm long, respectively, with material properties as shown in Table 1. They computed the space-time dependent fluxes, $\phi_1(x, t)$ and $\phi_2(x, t)$, on the basis of a two-group diffusion theory approximation, using the data also shown in Table 1. Delayed neutrons were neglected since the time of interest was only 10 ms. The computed fluxes were used to find the following quantities:

$$\psi(x, t) = \frac{<\psi^*(x, 0), \frac{1}{\nu_2}\phi_2(x, 0)>}{<\psi^*(x, 0), \frac{1}{\nu_2}\phi_2(x, t)>}\phi_2(x, t), \tag{9}$$

$$G(t) = \frac{<\psi^*(x, 0), \frac{1}{\nu_2}\phi_2(x, t)>}{<\psi^*(x, 0), \frac{1}{\nu_2}\phi_2(x, 0)>}, \tag{10}$$

$$P(t) = \frac{<\nu\Sigma_f, \psi(x, t)>}{<\nu\Sigma_f, \psi(x, 0)>}, \tag{11}$$

$$C(t) = \frac{<\Sigma_c, \psi(x, t)>}{<\Sigma_c, \psi(x, 0)>} = \frac{\psi(z, t)}{\psi(z, 0)}, \tag{12}$$

$$\frac{\rho}{\Lambda} = \frac{<\phi_1^*(x, 0), \delta\nu\Sigma_1^f\phi_1(x, t)> + <\phi_2^*(x, 0), \delta\nu\Sigma_2^f\phi_2(x, t)>}{<\phi_2^*(x, 0), \frac{1}{\nu_2}\phi_2(x, t)>}, \tag{13}$$

where $<, >$ denotes integration over the entire reactor. The results of these computations are summarized in Figs. 1 to 3. Simple inspection of the figures indicates the possible difficulties inherent in point kinetics when they are used for fast transients and/or large reactors as discussed previously.

STABILITY CRITERIA FOR NUCLEAR REACTORS

General remarks

Even though point reactor kinetics may have limitations with regard to meaningful correlations of experimental results, they are quite appropriate to use for investigating questions of stability or instability. Specifically, the neutron density in Eqs. (1) and (2) can always be written as the product of a time dependent function and a bounded shape function. With a convenient normalization of the shape function, the transport theory equations can always be reduced to a set of ordinary differential equations of the form of Eqs. (4) and (5), with or without the logarithmic term. The ordinary differential equations have coefficients ρ/Λ, β_{ie}/Λ, etc. which are bounded functions or functionals of the cross sections and/or other reactor variables. Consequently, the problem of stability of nuclear reactors can be approached by assigning to the coefficients of the point kinetics equations a variety of bounded functional dependences and examining whether the time dependent solutions are stable or unstable. In addition, if by using the above procedure it is possible to establish criteria which: (*a*) guarantee stability; (*b*) can be evaluated experimentally and (*c*) are insensitive to small perturbations of the physical constants of the system, then the question of physical interpretation of the time dependent variables, entering the point kinetics, loses its importance.

In order to present some general techniques which are, or may be used for stability studies, the kinetics equations are taken in the form of Eqs. (4) and (5) without the logarithmic and source terms. For simplicity and without loss of generality, it is assumed that the ratios β_{ie}/Λ are physical invariants of each reactor and that the ratio ρ/Λ can be expressed as a function or a functional of $G(t)$. In other words, the system of equations under consideration is:

$$\frac{dG(t)}{dt} = \left(\frac{\rho}{\Lambda} - \frac{\beta_e}{\Lambda}\right)G(t) + \sum_i^m \lambda_i C_i(t); \tag{14}$$

$$\frac{dC_i(t)}{dt} = \frac{\beta_{ie}}{\Lambda}G(t) - \lambda_i C_i(t); \tag{15}$$

$$\frac{\rho}{\Lambda} = \rho_e + \int_0^t f(t-\tau)[G(\tau) - G_0]d\tau + f_1[G(\tau < t)], \tag{16}$$

where ρ_e is the externally controlled part of ρ/Λ, $f(t)$ is a kernel accounting for the linear dependence of ρ/Λ on $G(t)$, G_0 is a constant representative of the operating power level and $f_1(G(\tau < t))$ is a functional such that ρ/Λ is bounded at all times and all values of $G(t)$.

An immediate property of Eqs. (14) to (16) which results from the boundedness of ρ/Λ is that no reactor admits a finite escape time. There are, however, some reactor models which yield solutions with finite escape times [4].

Review of existing stability criteria

For relatively small variations of ρ_e and $G(t)$, Eqs. (14) to (16) can be linearized and any of a number of linear stability criteria may be used to derive conditions that must be satisfied by $f(t)$ in order for the reactor to be stable. These conditions can be verified experimentally by means of oscillation or correlation tests. It must be recognized, however, that loss of linear stability does not necessarily imply that the solutions of the exact equations are unbounded [5-6].

For larger variations of $G(t)$ and $f_1[G(\tau<t)] \equiv 0$, a stability criterion has been derived by Welton without linearization of Eqs. (14) to (16). Specifically, the sufficient requirement for asymptotic stability is: [7, 8]

$$\int_0^\infty f(t)\cos\omega t dt \leqq 0. \tag{17}$$

The meaning of this condition is that the reactor without delayed neutrons must be globally asymptotically stable or globally bounded, i.e. stable at all operating power levels (0 to ∞) and/or for all inputs ρ_e. The condition is very appealing because it relates nonlinear stability to experimentally detectable linear properties. It is, however, very restrictive and there is hardly any practical reactor that satisfies it.

Liapunov's second method has also been used to investigate the stability of Eqs. (14) to (16) with $f_1[G(\tau < t)] \equiv 0$ [9 to 11]. It has been shown, however, that up to now the results of this approach are either equivalent to or more restrictive than Welton's criterion [12, 13].

Some practical considerations in nonlinear reactor stability

From the preceding discussion, it follows that criteria for nonlinear reactor stability are not satisfactory. The purpose of this section is to discuss a

Table 1. Summary of data for computer experiment

Reactor	60 cm long	240 cm long
Material composition (number of atoms 10^{-24} cm^3)	Homogeneous mixtures of H, O, Zr, U^{235}, U^{238}	
	$N_H = 0.30042 \times 10^{-1}$	$N_O = 0.24106 \times 10^{-1}$
	$N_{Zr} = 0.10706 \times 10^{-1}$	$N_{25} = 0.92358 \times 10^{-3}$
	$N_{28} = 0.69517 \times 10^{-4}$	
Transverse bucklings (cm^{-2})	3 material regions, 12 mesh points	
	Region 1; points 0-3;	$B^2 = 0.01091$
	Region 2; points 3-9;	$B^2 = 0.01200$
	Region 3; points 9-12;	$B^2 = 0.01089$
Two-group constants 1 = fast; 2 = thermal	$D_1 = 1.69531$	$D_2 = 0.409718$
	$\Sigma_1^a = 0.137513 \times 10^{-1}$	$\Sigma_2^a = 0.261361$
	$\Sigma_1^R = 0.164444 \times 10^{-1}$	
	$\nu\Sigma_1^f = 0.213143 \times 10^{-1}$	$\nu\Sigma_1^f = 0.196962 \times 10^{-1}$
	$\nu\Sigma_2^f = 0.544286$	$\nu\Sigma_2^f = 0.497857$
Ramp changes in fission cross-sections in region 1 over 10 ms.	$\nu\Sigma_1^f$ varied from 0.257143×10^{-1} to 0.169143×10^{-1}	$\nu\Sigma_1^f$ varied from 0.213561×10^{-1} to 0.176363×10^{-1}
	$\nu\Sigma_2^f$ varied from 0.656644 to 0.431928	$\nu\Sigma_2^f$ varied from 0.545353 to 0.450361

number of changes which might be introduced in the approach to the problem in order to derive practical results.

The importance of delayed neutrons

In most reactor stability studies delayed neutrons are neglected. Thus the problem becomes easier and the results are always conservative provided that the feedback is not identically equal to zero [14]. If the feedback is equal to zero, then inclusion of delayed neutrons may deteriorate the reactor stability as in the case of sinusoidal oscillations of a critical reactor at zero power [15].

From the practical standpoint, however, the omission of delayed neutrons is an over-simplification because the results may be so conservative that they are impractical [16]. Consequently, delayed neutrons must be included in the analysis.

The admissible operating power levels

Many analyses of nonlinear reactor stability attempt to establish conditions for asymptotic stability at all operating power levels. Designing a reactor, however, to be globally asymptotically stable in most cases is unrealistic and unnecessary because of environmental and material constraints. It is more meaningful to derive stability criteria only for a practical and limited range of operating power levels.

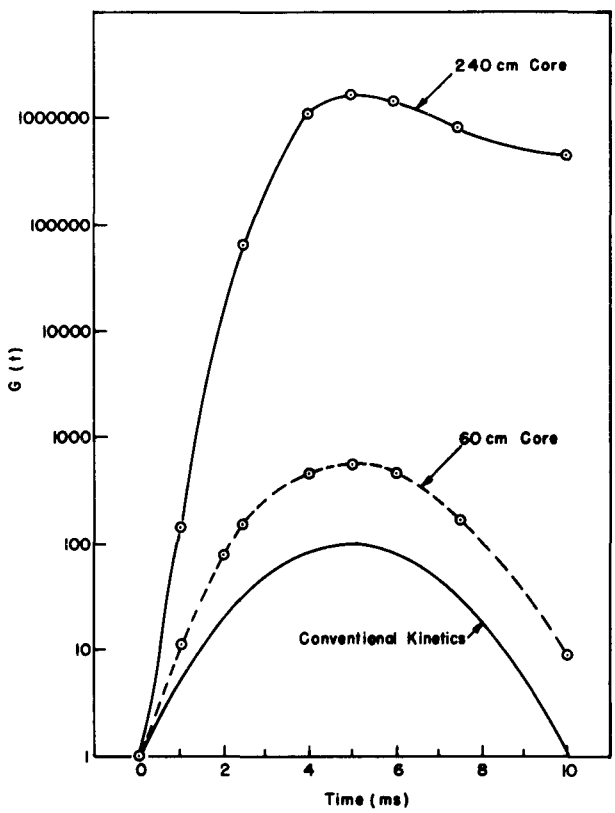


Figure 1. Computed $G(t)$ for 60 cm and 240 cm cores

Asymptotic versus Lagrangian stability

Requirements for asymptotic stability may be often so restrictive that they are impossible for the designer to achieve. In addition, even if a reactor is designed to be asymptotically stable, in practice the inherent noise leads to a mode of operation charac-

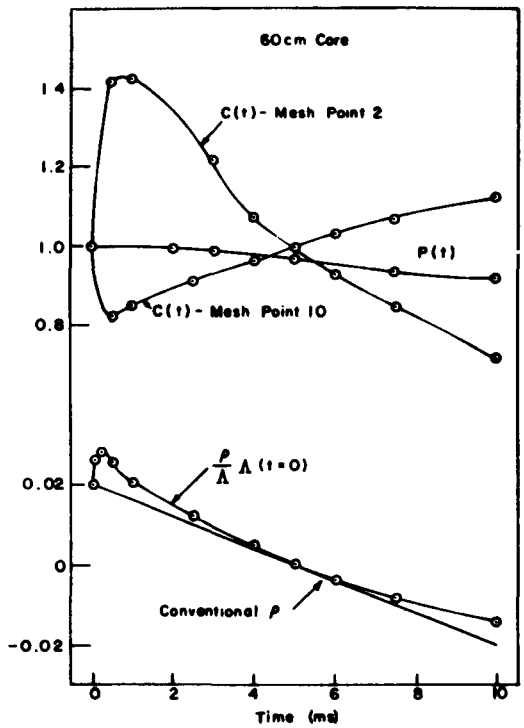


Figure 2. Computed $P(t)$, $C(t)$ and (ρ/Λ) $[\Lambda(t=0)]$ for 60 cm core

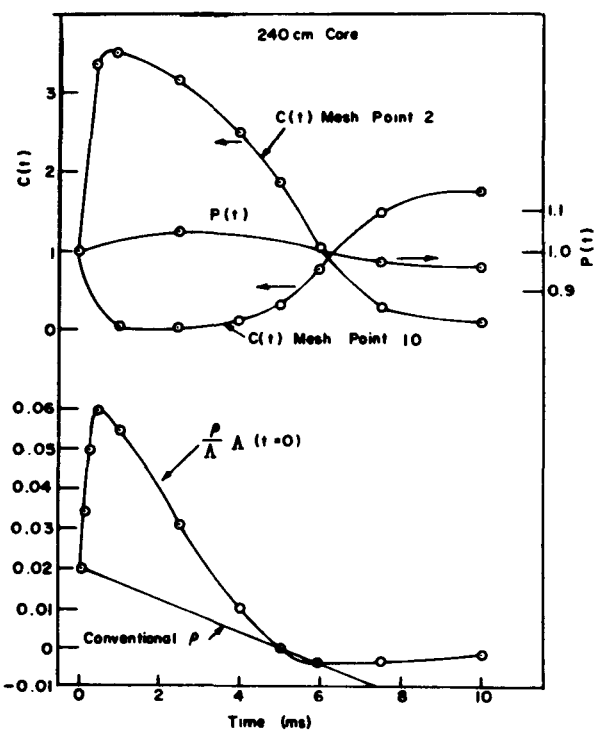


Figure 3. Computed $P(t)$, $C(t)$ and (ρ/Λ) $[\Lambda(t=0)]$ for 240 cm core

terized by bounded variations which are not asymptotically stable. It is, therefore, of interest to examine other types of stability. For example, one possibility is to attempt to establish sufficient requirements for Lagrangian stability [17]. Geometrically speaking, Lagrangian stability implies that the designer is satisfied with the assurance that all the reactor variables are confined within a closed region of the multi-dimensional state variable space instead of requiring that they tend to coalesce at one point. Lagrangian stability may be investigated either by means of Liapunov's second method [18], or by examining the conditions under which the equilibrium states of the kinetics equations at infinity are locally unstable. Satisfaction of the latter conditions implies that the reactor variables are bounded or asymptotically stable depending on the particular topology of the equilibrium states in the finite space [19].

Illustrative examples

A practical criterion for asymptotic stability in the small and Lagrange stability in the large

Consider the stability of the solutions of Eqs. (14) to (16) with regard to step changes of ρ_e. Assume for simplicity that to each ρ_e = constant, there corresponds only one equilibrium state, G_1. If $G(t) = g(t) + G_1$, after some elementary algebra, the kinetics equations can be written as:

$$\frac{\mathrm{d}}{\mathrm{d}t}\left[\int_0^t \int_0^\tau k(\tau-\lambda)g(\tau)g(\lambda)\ \mathrm{d}\tau\mathrm{d}\ \lambda\ \right]$$

$$= g^2(t)\int_0^t f(t-\tau)g(\tau)\mathrm{d}\tau + g(t)(g(t)+G_1)f_2[g(\tau<t)] + g(t)I_0(t), \tag{18}$$

where $k(t)$ is the inverse Laplace transform of $K(s) = s + D(s) - G_1F(s)$, $D(s)$ and $F(s)$ are the Laplace transforms of $d(t)$ and $f(t)$, respectively, $d(t)$ is given by

$$d(t) = \sum_i^m \frac{\beta_{ic}}{\Lambda}(\delta(t) - \lambda_i e^{-\lambda_i t}); \quad t > 0$$

$$= 0 \qquad\qquad\qquad\qquad ; \quad t < 0$$

$\delta(t)$ is the delta function, $f_2[g(\tau<\mathrm{t})] = f_1(g(\tau<t) + G_1) - f_1(G_1)$ and $I_0(t)$ is a well behaved function ($I_0(\infty) = 0$) depending on the initial conditions. If it is further assumed that:

$$f(t) < 0\ ;\ K(s) \text{ is a positive real function} \tag{19}$$

then $g(t)$ is ultimately bounded. Indeed, when $K(s)$ is a positive real function for a finite range of values of G_1, the double integral in the left hand side of Eq. (18) is a positive definite function [20]. Its time derivative becomes negative for large values of $g(t)$. The reason is that if $f(t) < 0$ there is always a level g_1 such that when $g(t) > g_1$ the integral $\int_0^t f(t-\tau)g(\tau)\ \mathrm{d}\tau < 0$ and increasing in absolute value. Above the level g_1 the functional $f_2[g(\tau<t)] > 0$ and varying slower than linearly with $\int_0^t f(t-\tau)g(\tau)\mathrm{d}t$ since ρ/Λ must be a bounded functional. The term $g(t)I_0(t)$ varies only linearly with $g(t)$. Therefore, the sign of the right hand side of Eq. (18) for $g(t) > g_1$ is determined by the first term and it is negative. Since $g(t)$ is physically bounded for $g(t) < -G_1$, it is concluded that $g(t)$ is ultimately bounded or Lagrange stable outside some range $-G_1 < g(t) < g_1$. In other words, conditions (19) guarantee that diverging oscillations do not exist. In addition, the positive real character of $K(s)$ (or of its inverse, which is the reactor transfer function at power) guarantees that $g(t)$ is asymptotically stable for small perturbations $g(t)$.

Conditions (19) can be easily implemented both theoretically and experimentally. They are less restrictive than Welton's criterion which requires that $(-F(s))$ be a positive real function. It must be noted, however, that asymptotic stability in the small and ultimate boundedness in the large do not exclude the possibility of bounded oscillations. Investigation of the existence of bounded oscillations requires more specific information about ρ/Λ.

An illustration of stability derived from investigations of singularities at infinity

Consider the xenon controlled reactor. Its dynamics can be approximated by the normalized set of equations [5, 6 and 19]:

$$\frac{\mathrm{d}\phi}{\mathrm{d}t} = \omega_0(1-X)\phi\ ; \tag{20}$$

$$\frac{\mathrm{d}X}{\mathrm{d}t} = \lambda_x(\alpha\phi + \beta I - X - \gamma\phi X)\ ; \tag{21}$$

$$\frac{\mathrm{d}I}{\mathrm{d}t} = \lambda_i(\phi - I), \tag{22}$$

where all symbols are defined in [6]. The singularities at infinity can be placed in evidence by a transformation into homogeneous coordinates. In other words, if ϕ is replaced by ϕ/Z, X by X/Z and I by I/Z, infinity is mapped on the surface

$Z = 0$. It can be shown that the singularities at infinity are given by:

$$\begin{array}{lll} \text{Singular points:} & \phi = \pm\,\omega_0\,; & X = \pm\,\gamma\lambda_x\,;\ I = 0\,;\ Z = 0 \\ \text{Singular lines:} & \phi = 0 \quad ; & Z = 0 \\ & X = 0 \quad ; & Z = 0 \end{array}$$

The singular points are also equilibrium points. The eigenvalues at these points are found to be $s_1 = s_2 = s_3 = \gamma\lambda_x > 0$ since for the cases of interest both γ and λ_x are positive [6]. Consequently, these two equilibrium points are unstable. The singular line $\phi = 0$; $Z = 0$ is the intersection of the integral surfaces $Z = 0$ and $\phi = 0$. On the integral surface $Z = 0$ the trajectories are lines starting from the singular points $(\pm\,\omega_0\,,\ \pm\,\gamma\lambda_x,\ 0,\ 0)$ and ending on the line $(\phi = 0;\ Z = 0)$. On the integral surface $\phi = 0$ the trajectories are solutions of the linear system;

$$\frac{dX}{dt} = \lambda_x(\beta I - X); \tag{23}$$

$$\frac{dI}{dt} = -\lambda_i I. \tag{24}$$

The eigenvalues at the origin are $s_1 = -\lambda_x$, $s_2 = -\lambda_i$. All trajectories on $\phi = 0$ converge to the origin and therefore the singular line $\phi = 0$, $Z = 0$ has a saddle point character.

Finally, it is readily shown that the singular line $X = 0$; $Z = 0$ does not admit any equilibrium states when the system of equations:

$$X^2 - \left(1 + \frac{\lambda_i}{\omega_0} + \frac{\alpha}{\gamma}\right)X + \frac{\lambda_i(\alpha+\beta)}{\omega_0\gamma} + \frac{\alpha}{\gamma} = 0, \tag{25}$$

$$\frac{I}{\phi} = \frac{\lambda_i}{\omega_0(1-X) + \lambda_i}, \tag{26}$$

does not have real solutions for $c\,\delta_0 < y$. This is true when either

$$c\,\delta_0 < 2\sqrt{(c\,\lambda_i\tau_e y_i)} + y_x - c\,\lambda_i\tau_e\,;\ c\,\lambda_i\tau_e > y_i \tag{27a}$$

$$\text{or} \qquad c\,\delta_0 < y_x + c\,\lambda_i\tau_e\,;\ c\,\lambda_i\tau_e < y_i, \tag{27b}$$

where all symbols are as defined in [5]. If either of inequalities (27) is not satisfied, Eqs. (25) and (26) do admit real solutions; there is a double equilibrium state on $X = 0$; $Z = 0$, and the eigenvalues at this point are $s_1 = -\gamma\lambda_x$, $s_2 = s_3 = 0$.

Summing up, when either of inequalities (27) is satisfied, all equilibrium states at infinity are unstable. Consequently, these inequalities constitute the necessary and sufficient conditions for the reactor model to be Lagrange stable. Whether it is also asymptotically stable or not depends on the eigenvalues at the equilibrium state $\phi = 1$, $X = 1$, $I = 1$, as already discussed in [5, 6].

REFERENCES

1. Henry, A. F., Nuc. Sci. Eng. *3*, 52 (1958).
2. Lewins, J., Nuc. Sci. Eng. *9*, 399 (1961).
3. Gyftopoulos, E. P., and Devooght, J., Nuc. Sci. Eng. *4*, 372 (1961).
4. Shotkin, L. M., Nuc. Sci. Eng. *18*, 271 (1964).
5. Chernick, J., Nuc. Sci. Eng. *8*, 233 (1960).
6. Gyftopoulos, E. P., Nuc. Sci. Eng. *10*, 254 (1961).
7. Welton, T. A., Proceedings of the First International Conference on the Peaceful Uses of Atomic Energy, P/610, Vol. 5, p. 377, United Nations (1956).
8. Gyftopoulos, E. P. and Devooght, J., Nuc. Sci. Eng. *7*, 533 (1960).
9. Ergen, W. K., Lipkin, H. J., and Nohel, J. A., J. Math. and Phys. *36*, 36 (1957).
10. Popov, V. M., Proceedings of the Second International Conference on the Peaceful Uses of Atomic Energy, P/2458, Vol. 11, p. 245, United Nations (1958).
11. Smets, H. B., *Problems in Nuclear Power Reactor Stability*, Presses Universitaires de Bruxelles, Bruxelles (1962).
12. Devooght, J., private communication.
13. Gyftopoulos, E. P., Information and Control *6*, 276 (1963).
14. Gyftopoulos, E. P., and Devooght, J., Nuc. Sci. Eng. *8*, 244 (1960).
15. Ruiz, A. L., HW-SA-2012 (1960).
16. Gyftopoulos, E. P., Proc. of the Conf. on Transfer Function Measurements and Reactor Stability Analysis, USAEC report ANL-6205 (1960).
17. LaSalle, J. and Lefschetz, S., *Stability by Liapunov's Direct Method with Applications*, Academic Press, New York (1961).
18. Gyftopoulos, E. P., Proc. of the Symposium on Reactor Kinetics and Control, Univ. of Arizona, Tucson, Arizona (1963).
19. Barandiaran, M., ScD Thesis, MIT, Nuc. Eng. Dept., Cambridge, Massachusetts (September 1963).
20. KyFan, Mémorial des Sciences mathématiques, Fascicule CXIV (1950).

ABSTRACT - RÉSUMÉ - АННОТАЦИЯ - RESUMEN

A/270 Etats-Unis d'Amérique

Cinétique ponctuelle du réacteur et critères de stabilité

par E. P. Gyftopoulos

Le mémoire a pour objet: *a*) d'examiner la forme des équations de cinétique ponctuelle du réacteur qui peuvent être utilisées pour la corrélation des données expérimentales afférentes à des états transitoires très instables; *b*) de passer en revue les critères de stabilité actuels et d'étudier certains problèmes pratiques d'analyse non linéaire de la stabilité du réacteur.

A cette fin, l'auteur reprend et réinterprète les équations de cinétique ponctuelle obtenues par diffé-

rents auteurs à partir de la théorie fondamentale du transport. Il fait observer que ces équations contiennent des termes qui dépendent de la vitesse de variation de la forme de la distribution du nombre volumique de neutrons dans les diverses parties du cœur. Cette vitesse de variation peut devenir appréciable même si les modifications de forme sont relativement petites mais surviennent dans un laps de temps très court. L'auteur en conclut que l'on devrait tenir compte des modifications de forme lorsqu'on établit une corrélation des données expérimentales afférentes à des états transitoires fortement instables. Pour étayer sa thèse, il présente certains résultats numériques.

On peut tirer d'autres conclusions de la réinterprétation des équations de cinétique:

a) La réactivité est une fonction qui finit par être formée, ce qui est normal étant donné qu'il n'intervient qu'un nombre limité de neutrons par fission;

b) Aucun réacteur ne peut admettre une perte finie de neutrons, car il faudrait pour cela lui injecter du combustible à une vitesse infinie;

c) Les équations de cinétique ponctuelle permettent toujours de répondre à la question de savoir si l'on se trouve, en définitive, en présence d'un état stable ou instable.

L'auteur étudie ensuite les critères de stabilité pour les réacteurs nucléaires. Il fait remarquer que les conditions nécessaires et suffisantes de stabilité en ce qui concerne les petites perturbations sont bien définies, tant en théorie qu'expérimentalement. Il note d'ailleurs que l'instabilité, en ce qui concerne les petites perturbations, ne constitue pas nécessairement un danger pour la sécurité. Il donne des exemples d'oscillations bornées.

En ce qui concerne l'analyse non linéaire de la stabilité, la plupart des critères adoptés pour définir les conditions suffisantes de stabilité d'un réacteur concernent la stabilité asymptotique globale et sont extrêmement prudents. L'auteur suggère que l'on pourrait trouver des conditions de stabilité moins sévères en tenant compte, dans l'analyse, de certaines limitations pratiques, à savoir:

a) Les approximations analytiques pour la réactivité de rétroaction doivent être des fonctions qui finissent par être bornées;

b) L'analyse devrait tenir compte des neutrons retardés, car des critères de stabilité calculés sans tenir compte des neutrons retardés seraient tellement prudents qu'ils n'auraient aucun intérêt pratique;

c) On devrait déterminer les critères de stabilité pour une gamme limitée de niveaux de puissance de fonctionnement et/ou d'entrées de réactivité, étant donné qu'il ne saurait être question de construire un réacteur capable de résister à une puissance infinie ou à un stockage d'énergie infini.

L'auteur admet qu'en tenant compte de ces aspects pratiques dans l'analyse on rend le problème de la stabilité plus complexe, mais il estime qu'on obtient aussi des résultats d'une plus grande utilité pratique. Il donne des exemples pour illustrer cette remarque.

A/270 США

Кинетика точечного реактора и критерии стабильности

Э. П. Гифтопулос

Целью этого доклада является: *а*) проанализировать форму кинетических уравнений для точечных реакторов, которые могут быть использованы для корреляции данных по резким переходным режимам; *b*) обсудить существующие критерии устойчивости, а также рассмотреть некоторые практические стороны нелинейной стабильности реактора.

Дается анализ уравнений точечной кинетики, полученных разными авторами на основе теории переноса, и им дается новая интерпретация. Отмечается, что в эти уравнения входят члены, которые зависят от быстроты изменения кривой распределения плотности нейтронов по всей активной зоне реактора. Эта быстрота изменения может стать значительной, если относительно малые изменения формы происходят в короткий промежуток времени. Делается вывод о том, что изменения формы необходимо принимать во внимание при корреляции экспериментальных данных по резким переходным режимам. Приводятся несколько численных результатов, подтверждающих этот вывод.

На основе новой интерпретации кинетических уравнений можно сделать следующие выводы:

а) реактивность является функцией критически ограниченной, какой она и должна быть, потому что на каждое деление приходится только ограниченное число нейтронов;

b) ни один реактор не может допустить конечного времени до вылета, если не вводить топливо в бесконечном количестве;

c) уравнения точечной кинетики всегда могут быть использованы для решения вопросов предельной устойчивости или неустойчивости.

Затем обсуждаются критерии устойчивости ядерных реакторов. Отмечается, что условия, необходимые и достаточные для устойчивости при небольших возмущениях, хорошо уже доказаны теоретически и экспериментально. Также указывается, что неустойчивость в отношении к небольшим возмущениям не обязательно является опасностью. Приведены примеры ограниченных колебаний.

В отношении нелинейной устойчивости говорится, что большинство из существующих критериев, которые удовлетворяют требованиям устойчивости реактора, относятся к глобаль-

ной асимптотической устойчивости и что все эти критерии приводят к консервативным расчетам. Предлагается установить менее ограничивающие условия для устойчивости путем включения в анализ нескольких практических ограничений, то есть:

a) аналитическое приближенное выражение для обратной связи реактивности должно быть функцией критически ограниченной;

b) в анализ также следует включить запаздывающие нейтроны, так как критерии, установленные для устойчивости без этих нейтронов, могут быть сделаны с таким большим запасом, что они не будут иметь никакого практического значения;

c) критерии устойчивости должны быть получены для ограниченного диапазона рабочих мощностей и/или ввода реактивности, потому что нельзя построить реактор, который бы мог иметь бесконечную мощность или запас энергии.

Конечно, включение практических сторон в анализ осложняет задачу устойчивости, но зато полученные результаты являются более полезными. Приведено несколько практических примеров для пояснения этого очень важного вопроса.

A/270 Estados Unidos de América

Cinética puntual y criterios sobre estabilidad en reactores

por E. P. Gyftopoulos

En el presente informe se trata de: *a*) examinar la forma de las ecuaciones cinéticas puntuales de un reactor, que podrían emplearse en la correlación de resultados experimentales relativos a transitorios importantes; *b*) revisar los criterios existentes sobre estabilidad y discutir algunos aspectos prácticos de la estabilidad no lineal en reactores.

Con este fin, se revisan e interpretan las ecuaciones cinéticas puntuales deducidas por diferentes autores a partir de la teoría fundamental del transporte. Se observa, que estas ecuaciones contienen términos que dependen de la variación de la forma de la distribución de la densidad neutrónica en el núcleo del reactor. Esta variación puede llegar a ser apreciable, incluso cuando los cambios en la distribución son relativamente pequeños pero se producen en un corto intervalo de tiempo. Se llega a la conclusión de que deben considerarse las variaciones en la forma de la distribución al correlacionar resultados experimentales relativos a transitorios importantes. Para corroborar esta conclusión se dan algunos resultados numéricos.

Otras conclusiones que pueden derivarse de la reinterpretación de las ecuaciones cinéticas, son:

a) La reactividad es una función acotada asintóticamente como debe ser, ya que hay solamente un número limitado de neutrones por fisión;

b) Ningún reactor puede admitir un tiempo de escape finito, a menos que el combustible sea inyectado a una velocidad infinita;

c) Las ecuaciones cinéticas puntuales pueden siempre emplearse para resolver problemas sobre estabilidad o inestabilidad asintóticas.

A continuación se discuten los criterios de estabilidad en los reactores nucleares. Se observa que, teórica y experimentalmente, están bien establecidas ciertas condiciones necesarias y suficientes para la estabilidad con respecto a pequeñas perturbaciones. También se observa, sin embargo, que la inestabilidad con respecto a pequeñas perturbaciones no constituye necesariamente un riesgo. Se presentan ejemplos de oscilaciones acotadas.

Con respecto a la estabilidad no lineal, se observa que la mayoría de los criterios de suficiencia obtenidos para la estabilidad en reactores, pertenecen a una estabilidad global asintótica y son muy conservadores. Se sugiere que podrían establecerse condiciones de estabilidad menos restrictivas incluyendo en el análisis algunas limitaciones prácticas. Concretamente:

a) Las aproximaciones analíticas para la realimentación de la reactividad deben ser funciones asintóticamente acotadas;

b) El análisis debe incluir los neutrones retardados, ya que las condiciones de estabilidad deducidas sin tenerlos en cuenta son tan conservadoras que carecen de importancia práctica;

c) Los criterios de estabilidad deben deducirse para un intervalo limitado de niveles de la potencia de funcionamiento o de alimentación de la reactividad, ya que ningún reactor puede construirse para resistir una potencia o un almacenamiento de energía infinitos.

Cierto es que el problema de la estabilidad se complica al tener en cuenta en el análisis estos aspectos prácticos, pero, en cambio, los resultados son más significativos. Este punto importante se ilustra con algunos ejemplos prácticos.

Determination of ℓ_{eff} and β_{eff} in a critical reactor by the pulsed neutron technique

By C. Stassis and C. Mitsonias*

The usual method of measuring the effective lifetime (ℓ_{eff}) of neutrons in a critical reactor by the pulsed neutron technique involves the calculation of ℓ_{eff} from the observed decay constant assuming that β_{eff} is known to be approximately equal to $\beta = \Sigma\beta_i$. This latter assumption may introduce a significant error for measurements on reactors of relatively small dimensions due to the difference in escape probabilities of the prompt and delayed neutrons.

In the present work a method of simultaneous determination of ℓ_{eff} and β_{eff} is described. This method is based on the analysis of the contribution of the fast neutron pulses to the average thermal neutron density of the reactor.

EXPERIMENTAL METHOD

The method used is that of a homogeneous reactor. The response of a reactor to a square fast neutron pulse of intensity S_1 and duration Δ, is given by the solution of the equations:

$$\dot{n} = \frac{k_{ex}-\beta}{\ell_{eff}} n + \sum_i \lambda_i C_i + S \qquad (1)$$

$$\dot{C}_i = \frac{\beta_i}{\ell_{eff}} n - \lambda_i C_i \qquad (2)$$

where n is the thermal neutron density,
C_1 is the delayed neutron precursor concentration.

$$\begin{aligned} S &= S_1 \int_v P(\vec{r})\Phi_0(\vec{r})dr \quad && \text{for } 0 \leqslant t \leqslant \Delta \text{ and} \\ S &= 0 && \text{for } t > \Delta \end{aligned} \qquad (3)$$

$P(\vec{r})$ is the probability for a fast neutron to reach the point $\vec{r}$ as a thermal neutron.

$\Phi_0(\vec{r})$ is the eigenfunction which corresponds to the smallest eigenvalue of the equation:

$$\nabla^2\Phi(\vec{r}) + B_g^2\Phi(\vec{r}) = 0 \qquad (4)$$

and $\Phi(\vec{r}) = 0$ at the extrapolated boundary of the reactor.

If the reactor is critical, $k_{ex} = 0$, and Eqs. (1) and (2) become:

$$\dot{n} = \frac{-\beta}{\ell_{eff}} n + \sum_i \lambda_i C_i + S \qquad (5)$$

$$\dot{C}_i = \frac{\beta_i}{\ell_{eff}} n - \lambda_i C_i \qquad (6)$$

Using Laplace transformation one obtains:

$$n(0 \leqslant t \leqslant \Delta) = n_0 + SBt + S\sum_j A_j(e^{\alpha_j t} - 1) \qquad (7)$$

$$n(t > \Delta) = n_0 + SB\Delta + S\sum_j A_j e^{\alpha_j t}(1 - e^{-\alpha_j \Delta}) \qquad (8)$$

where α_j are the roots of the equation

$$1 + \frac{1}{\ell_{eff}} \sum_{i=1}^{6} \frac{\beta_i}{s+\lambda_i} = 0 \qquad (9)$$

α_6 is the most negative root of Eq. (9) and characterizes the prompt neutron decay.

$$A_j = \prod_{i=1}^{6} (\alpha_j + \lambda_i)/\alpha_j^2 \cdot \prod_{i \neq j} (\alpha_j - \alpha_i) \qquad j = 1,2,\ldots 6 \qquad (10)$$

$$B = 1/(1 + \frac{1}{\ell_{eff}} \sum_{i=1}^{6} \frac{\beta_i}{\lambda_i}) \qquad (11)$$

Assuming $|\alpha_j \Delta| << 1$ Eq. (7) can be written

$$n(0 \leqslant t \leqslant \Delta) = n_0 + SBt + SA_6(e^{\alpha_6 t} - 1) \qquad (12)$$

If $|\alpha_6 t| << 1$, Eq. (12) is reduced to:

$$n(0 \leqslant t \leqslant \Delta) = n_0 + S(B+1)t \qquad (13)$$

since $A_6\alpha_6 \approx 1$.

The change in the power level of the reactor due to the train of fast neutron pulses of period $T >> \frac{1}{|\alpha_6|}$, will be $SB\Delta$ for each pulse of fast neutrons. Consequently, one finds for the rise of the mth pulse,

$$\begin{aligned} &n[(m-1)T \leqslant t \leqslant (m-1)T + \Delta] \\ &= n_0 + (m-1)SB\Delta + S(B+1)t \end{aligned} \qquad (14)$$

where n_0 is the initial power of the reactor and $(m-1)SB\Delta$ the increase of the power due to the previous $(m-1)$ pulses.

In the way the measurements have been done, the results of each pulse are added to the results

* Reactor Department, Nuclear Research Centre Democritus.

of the previous pulses. So the accumulated results of m consecutive pulses of fast neutrons give:

$$n(t) = mn_0 + \frac{m(m-1)}{2} SB\Delta + mS(B+1)t \text{ for } 0 \leqslant t \leqslant \Delta \qquad (15)$$

Equation (15) shows that the rise of the thermal neutron pulse is a straight line the slope of which gives a quantity X proportional to $mS\ (B+1)$.

The measurement of the *initial* background (mn_0) and the *accumulated* background due to the injection of m consecutive pulses, give a quantity Y proportional to $\frac{m(m+1)}{2} SB\Delta$. By combining the measured quantities X and Y, B can be determined. Once B is determined, ℓ_{eff} can be calculated from Eq. (11), supposing λ_i known and given a set of values for B_{ieff}.

The decay constant of prompt neutrons α_6 can be determined as the most negative root of Eq. (9). The constant α_6 so calculated does not necessarily coincide with the one determined experimentally. Then the values of β_{ieff}, that are introduced into the calculation of ℓ_{eff}, are modified in order to find another value of α_6. This process is repeated until the value of α_6 calculated is close to the experimental value, within the order of the experimental errors. In this way one achieves the values of ℓ_{eff} and β_{eff}.

EXPERIMENTAL RESULTS

The method has been used to measure the ℓ_{eff} and β_{eff} of the Democritus Reactor. The experimental equipment consists of a 14 MeV pulse neutron generator, a 512 channel multiscaler and an automatic device to preset the number of pulses. Figure 1 gives a layout of the core with the neutron generator and the counter used.

The measurements have shown that the assumptions of the method are good for $T \geqslant 0.1$ and $\Delta \leqslant 10^{-3}$ seconds. With these conditions the number of the consecutive neutron pulses m should not be over 2 000, otherwise the signal to background ratio is poor. To improve the statistics, the accumulation of 2 000 pulses were repeated under the same experimental conditions many times. The stepping frequency used for the multiscaler was 40 μs. Figures 2 and 3 are plots of the experimental results obtained under these conditions. From the experimental data fitted by the least squares method one finds:

$$X = 60.125 \times 10^5$$
$$Y = 2.8 \times 10^3$$
$$\alpha_6 = 160.256\ s^{-1}$$

A second series of measurements have been made

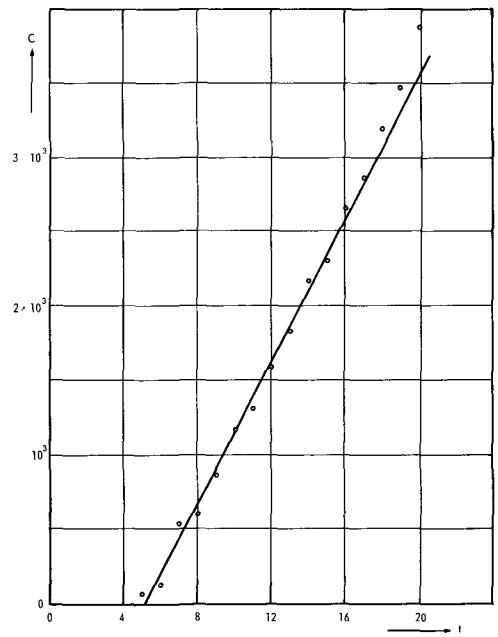


Figure 2. Plot of counts (C) vs. channels (t) for the rise of the thermal neutron pulse

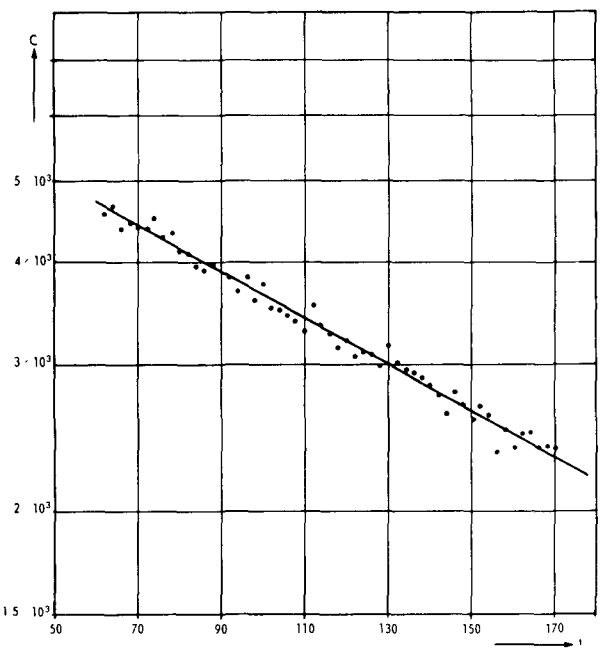


Figure 3. Plot of counts (C) vs. channels (t) for the decay of the thermal neutron pulse

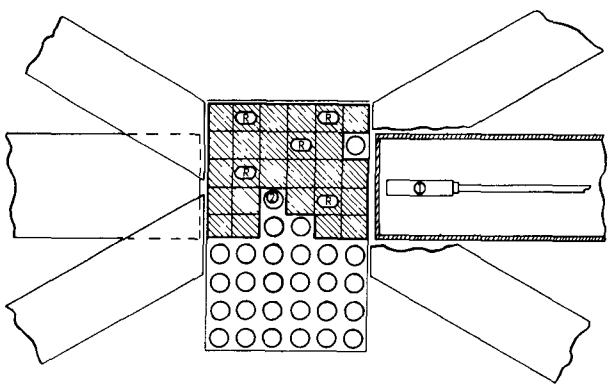


Figure 1. Layout of the core showing the neutron generator (1) and the BF_3 counter (2). R denotes the control rods of the reactor

using a time of flight unit with a channel width of 16 μs. The experimental data are:

$$X = 1.063 \times 10^6$$

$$Y = 494$$

$$\alpha_6 = 96.826 \text{ s}^{-1}$$

Table 1 gives the values of λ_i and β_i found in [1—5] together with the values of β_{ieff} used and the calculated values for β_{eff} and ℓ_{eff}.

The determination of the group of β_{ieff} to be used has been considerably simplified by a calculation using the corrective factors $\gamma_i = \beta_{ieff}/\beta_i$.

CONCLUSIONS

With this method the simultaneous determination of ℓ_{eff} and β_{eff} for a critical reactor is possible. It also permits an estimation of the corrective factors γ_i for the delayed neutrons for the same reactor.

Table 1. Values of λ_i, β_i, β_{ieff} and calculated values of β_{eff} and ℓ_{eff}

λ_i (s^{-1})	β_i	β_{ieff}	β_{eff}	ℓ_{eff} (s)	
				Multiscaler	Time of flight
0.0127	2.46×10^{-4}	2.46×10^{-4}			
0.0317	13.71×10^{-4}	16.505×10^{-4}			
0.1155	12.11×10^{-4}	12.11×10^{-4}	68.94×10^{-4}	4.3×10^{-5}	4.5×10^{-5}
0.3107	26.25×10^{-4}	26.25×10^{-4}			
1.3970	8.24×10^{-4}	9.935×10^{-4}			
3.8710	1.68×10^{-4}	1.68×10^{-4}			

It is remarkable that this method permits the direct determination of S. From Eq. (3), S is proportional to an integrand containing the fundamental eigenfunction of the reactor and the probability $P(\vec{r})$.

ACKNOWLEDGEMENT

The authors want to thank the personnel of the Reactor Department and especially Mr. E. Karageorgos for their assistance during the experiment. Also they are indebted to Mr. F. LaViolette and Mr. A. Nikolitsas for many useful suggestions and to Mr. I. Anoussis for reading the manuscript.

REFERENCES

1. Keepin, G. R., USAEC report LAMS-2215 (1958).
2. Bendt, P. J., Karr, H. J., and Scott, F. R., Nuclear Sci. Eng., *4*, 703-708 (1958).
3. Simmons, B. E., and King, J. S., *ibid.*, *3*, 595-608 (1958).
4. Keepin, G. R., *ibid.*, *5*, 132-136 (1959).
5. Keepin, G. R., Nucleonics, *20* (8), 150-156 (1962).

ABSTRACT - RÉSUMÉ - АННОТАЦИЯ - RESUMEN

A/648 Grèce

Détermination de ℓ_{eff} et β_{eff} d'une pile critique par la méthode des impulsions neutroniques

par C. Stassis et C. Mitsonias

Le mémoire expose une méthode de détermination de ℓ_{eff} et β_{eff} d'une pile critique (Democritos), basée sur l'analyse de la réponse de la pile à une injection de neutrons rapides, c'est-à-dire de la variation de la densité du flux de neutrons thermiques.

L'équipement consiste essentiellement en un générateur d'impulsions neutroniques de 14 MeV, une échelle à 512 canaux et un dispositif automatique pour le préréglage du nombre des impulsions.

A/648 Греция

Определение $l_{эфф}$ и $\beta_{эфф}$ в критическом реакторе с помощью метода пульсирующих нейтронов

С. Стасис, С. Митсониас

Значения $l_{эфф}$ и $\beta_{эфф}$ для критического реактора (DEMOCRITOS) определяются с помощью метода пульсирующих нейтронов. Этот метод основан на анализе нарастания и спада плотности тепловых нейтронов, полученных путем инжекции импульса быстрых нейтронов в реактор.

Измерительная аппаратура состоит из импульсного генератора нейтронов с энергией 14 *Мэв*, универсального пересчетного устройства с 512 каналами и автоматического устройст-

ва для предварительного установления числа импульсов.

A/648 Grecia

Determinación de ℓ_{ef} y β_{ef} en un reactor crítico utilizando una fuente pulsada de neutrones

por C. Stassis y C. Mitsonias

Se han determinado los valores de ℓ_{ef} y β_{ef} para un reactor crítico (Democritos) utilizando la técnica de neutrones pulsados. Este método está basado en el análisis de la disminución y el aumento de la densidad de neutrones térmicos originados por la inyección de un impulso de neutrones rápidos en el reactor.

El equipo de medida es un generador de neutrones de 14 MeV, junto con un analizador de 512 canales y un dispositivo automático para preseleccionar el número de impulsos.

The evolution of fission rate during and after shutdown of a nuclear reactor

By P. Schmid and W. Zünti*

This paper summarizes knowledge about shutdown phenomena acquired at this institute while carrying out computations for reactor safety evaluation and for the development of new techniques to measure the reactivity of subcritical reactors. The following two problems are treated:

Evaluation of the fission rate during and after shutdown of a nuclear reactor from an initially critical equilibrium state

It is assumed that a nuclear reactor has been operated in its delayed critical state at constant fission rate for a time long enough to ensure the equilibrium of all concentrations of delayed neutron precursors. Then, at time $t = 0$, a control device is released, reducing the reactivity, according to a known function of time, to a value $\rho_1 \leqslant -1\,\$$. The latter reactivity value defines the stationary shutdown state which is reached at time t_1 when the control device has arrived in its final position. There are three questions to be answered (problem A). The first concerns close upper and lower bounds for the fission rate during the shutdown, i.e., between $t = 0$ and $t = t_1$. The second requires the determination of an equivalent reactivity step at an intermediate time θ in terms of the known time behaviour of the actual reactivity change. The third question asks for a simple but accurate description of the evolution of the fission rate for $t > t_1$, making use of the formerly determined value of θ. The ways of solving the problem depend essentially on the assumption that the prompt neutron generation time can be neglected. Furthermore, the present treatment disregards all space-dependent effects since their inclusion would lead far beyond the scope of this paper. Depending, however, on the particular problem they must and can, in general, be adequately accounted for.

While all the three parts of problem A are useful as simple but rather accurate estimates for engineering purposes, the description of the fission rate in the stationary shutdown state may well lead to a novel *rod drop* evaluation technique for the determination of shutdown reactivities as part of the operation routines in both research and power reactors.

Evaluation of total fission energy released after the initiation of a fast shutdown

This problem is based on the assumption that a nuclear reactor undergoes a prompt subcritical power excursion characterized by a constant, non-negative period, T_0, for a sufficiently long time to ensure the dynamic equilibrium of all concentrations of delayed neutron precursors. Reactivity changes due to thermal effects are supposed to be negligible. During the time interval $0 < t < t_1$ the reactivity is reduced from $\rho_0 \geqslant 0$ to $\rho_1 < 0$ by means of a fast shutdown device. The question to be answered is complementary to those already mentioned and refers to a more general case: what is the total fission energy released after the initiation of the trip? The answer is to be found in such an analytical form that the importance of both the reactivity worth and the travel time of the shutdown device is recognized independently and as clearly as possible.

The solution of the latter problem (provided that non-fission heat sources, approximate rates of heat production and removal, and heat capacities are all properly taken into account) proves useful for certain safety evaluation problems—in particular for the critical examination of specifications for shut-down devices.

Derivation and interpretation of a simplified integral equation

If the ratio of the fission rate at time t to the constant fission rate at time $t = 0$ is designated as $r(t)$ the *basic integral equation of reactor kinetics* [1-4] may be expressed by

$$r(t) = 1 + \int_0^t G_\sigma(t-t')\,[r(t')\,(\rho(t')-\sigma) + \sigma]\mathrm{d}t' \qquad (t \geqslant 0), \tag{1}$$

where

$$\rho = \frac{k_{\mathrm{eff}} - 1}{\bar{\beta}\, k_{\mathrm{eff}}} = \text{reactivity in dollar units,} \tag{2}$$

σ is an arbitrary non positive constant and $G_\sigma(t)$ is Green's function for a reactor at reactivity σ, defined by its Laplace transform [5]

* Swiss Federal Institute for Reactor Research, Würenlingen.

$$\mathcal{L}\{G_\sigma(t)\} \equiv \bar{G}_\sigma(s) = \frac{1}{s[\tau + \bar{W}(s)] - \sigma} \quad (\sigma \leqslant 0). \tag{3}$$

Here τ is the reduced generation time which is put equal to zero henceforth. $\bar{W}(s)$ and its inverse transform are defined by

$$\bar{W}(s) = \sum_{\mu=1}^{M} b_\mu/(s + \lambda_\mu), \tag{4}$$

$$W(t) = \sum_{\mu=1}^{M} b_\mu \, e^{-\lambda_\mu t}. \tag{5}$$

λ_μ designates the decay constant of the μth group of delayed neutron precursors. If $\bar{\beta}_\mu$ is the effective fraction of delayed neutrons from this group, then b_μ is defined by

$$b_\mu = \bar{\beta}_\mu/\bar{\beta}\,; \quad \bar{\beta} \equiv \sum_{\mu=1}^{M} \bar{\beta}_\mu. \tag{6}$$

Taking the Laplace transform of (1) and using (3) with $\tau = 0$ and $\sigma = 0$ yields, after rearrangement

$$\mathcal{L}\{r(t)\rho(t)\} - \bar{r}(s) = -\bar{W}(s) + \bar{r}(s)(s\bar{W}(s) - 1). \tag{7}$$

It is easily seen that the following identical relation holds between $\bar{W}(s)$ and the Laplace transform, $\bar{D}(s)$, of the delay distribution function, $D(t)$:

$$s\bar{W}(s) \equiv 1 - \bar{D}(s), \tag{8}$$

with

$$\bar{D}(s) = \sum_{\mu=1}^{M} b_\mu\lambda_\mu/(s + \lambda_\mu), \tag{9}$$

$$D(t) = \sum_{\mu=1}^{M} b_\mu\lambda_\mu e^{-\lambda_\mu t}. \tag{10}$$

Back transformation of (7) thus results in the following simplified integral equation,* whereby the reactivity has been removed from the convolution integral:

$$r(t) = \frac{\int_0^t D(t-t')r(t')\mathrm{d}t' + W(t)}{1 - \rho(t)}. \tag{11}$$

This expression has an immediate interpretation [3]. The numerator is proportional to the strength of delayed neutron sources, whereas the denominator is proportional to the *prompt multiplication* of these sources. The first part of the numerator represents the neutron source strength due to those precursors which are produced at positive times, but $W(t)$ accounts for delayed neutrons from the *old precursors*, i.e., precursors produced before $t = 0$. This interpretation enables one to find lower and upper bounds to $r(t)$ by putting $r(t')$ in the convolution integral equal to zero and one, respectively. This leads to

$$\frac{(W(t)}{1 - \rho(t)} \leqslant r(t) \leqslant \frac{1}{1 - \rho(t)} \tag{12}$$

if

$$\rho(t) \begin{cases} = 0 \text{ for } t \leqslant 0 \\ < 0 \text{ for } t > 0. \end{cases} \tag{13}$$

These limits diverge more and more as time proceeds. They are, therefore, only appropriate immediately after the initiation of a shutdown. A more precise evaluation of lower and upper bounds, based on the same integral equation, is presented below.

Narrow bounds for the fission rate during and after shutdown of a nuclear reactor from an initially critical equilibrium state

Consider the problem defined in the first section and let the reactivity be given by

$$\rho(t) = \rho_1\phi(t), \quad (\rho_1 < 0), \tag{14}$$

where $\phi(t)$, which will be called the *normalized shutdown function* has the following properties:

$$\phi(t) \begin{cases} = 0 \text{ for } t < 0, \\ \text{is non-decreasing for } 0 < t < t_1, \\ = 1 \text{ for } t > t_1. \end{cases} \tag{15}$$

Then the *prompt multiplication* term in (11) can be written as

$$\frac{1}{1 - \rho(t)} = \frac{1}{1 - \rho_1}(1 + \Phi(\rho_1; t)), \tag{16}$$

where

$$\Phi(\rho_1; t) \equiv \frac{1 - \phi(t)}{\phi(t) - 1/\rho_1} \tag{17}$$

will be called the *transient prompt multiplication*. Obviously $\Phi(\rho_1; t)$ has an initial value of $-\rho_1 > 0$ at $t < 0$ and decays to zero during the travel time of the shutdown device.

Now the actual fission rate $r(t)$, as given by (11), is formally split into two parts, the first, $r_1(t)$, corresponding to the transient part of the *prompt multiplication* according to (16):

$$r(t) = r_1(t) + r_\Phi(t). \tag{18}$$

Inserting this into the convolution integral in (11) and taking the Laplace transform permits one to solve for $\bar{r}_1(s)$. $\bar{r}_\Phi(s)$ still appearing as an unknown function:

$$\bar{r}_1(s) = \frac{\bar{D}(s)\bar{r}_\Phi(s) + \bar{W}(s)}{1 - \bar{D}(s) - \rho_1}. \tag{19}$$

* As was shown in [1] and [3] this expression, which neglects the reduced generation time, is a good approximation to the exact equation (1) if $\mathrm{d}\rho(t)/\mathrm{d}t \ll (1-\rho)^2/\tau$ and $\rho < 1$.

Now lower and upper bounds for $\bar{r}_\Phi(s)$ are obtained by applying the principle shown by (12) and (13) to $r_\Phi(t)$:

$$\frac{1}{1-\rho_1}\,\Phi(\rho_1;t)W(t) \leqslant r_\Phi(t) \leqslant \frac{1}{1-\rho_1}\,\Phi(\rho_1;t). \tag{20}$$

Taking Laplace transforms of (20), inserting them into (19), solving for $r(t)$ and inverting leads to:

$$\int_0^t G_{\rho_1}(t-t')W(t')\Big[1+\Phi(\rho_1;t')\Big]\,dt' \leqslant r(t) \leqslant \int_0^t G_{\rho_1}\ (t-t')\Big[W(t')+\Phi(\rho_1;t')\Big]\,dt'. \tag{21}$$

It is advisable to subtract the fission rate $r_s(t)$ defined as $r_1(t)$ in the limit $t_1 \to 0$, i.e., the response to an ideal step at time $t = 0$. $r_s(t)$ is given by [1]:

$$r_s(t) = 1 + \rho_1 \int_0^t G_{\rho_1}(t')\,dt' = \int_0^t G_{\rho_1}(t-t')W(t')\,dt'. \tag{22}$$

Then the following bounds are found (considering that $\Phi(t') = 0$ for $t' > t_1$):

$$\int_0^{\mathrm{Min}(t,\,t_1)} G_{\rho_1}(t-t')W(t')\Phi(\rho_1;t')\,dt' \leqslant r(t) - r_s(t) \leqslant \int_0^{\mathrm{Min}(t,\,t_1)} G_{\rho_1}(t-t')\Phi(\rho_1;t')\,dt'. \tag{23}$$

If one is interested in these bounds only for $t < t_1$, t_1 being of the order of one second, Green's function (with $\tau \to 0$) can be approximated fairly well by (Ref. [1], Fig. 7)

$$G_{\rho_1}(t') \approx \frac{\delta(t')}{1-\rho_1} + \frac{\Lambda_1^1(0)}{(1-\rho_1)^2}\,e^{-\omega t'}\ ;\quad \omega = \frac{\Lambda_2^2(0)}{\Lambda_1^1(0)} - \frac{\Lambda_1^1(0)}{1-\rho_1}\quad (0 < t' < t_1), \tag{24}$$

where $\Lambda_\nu^\nu(0)$ is defined by Eq. (37) and numerical values are given in a later footnote.

$$\frac{1}{1-\rho_1}\left[W(t)\Phi(\rho_1;t) + \frac{\Lambda_1^1(0)e^{-\omega t}}{1-\rho_1}\int_0^t W(t')\Phi(\rho_1;t')\,dt'\right] \leqslant r(t) - r_s(t) \leqslant \frac{1}{1-\rho_1}\left[\Phi(\rho_1;t) + \frac{\Lambda_1^1(0)}{1-\rho_1}\int_0^t \Phi(\rho_1;t')\,dt'\right] \quad (0 < t < t_1 \lesssim 1\ \mathrm{s}) \tag{25}$$

Together with the definitions (14) to (17) this answers the first question of problem A, provided that $r_s(t)$ is known. The determination of the latter function is the subject of the following section.

Close approximation of the fission rate after a negative reactivity step

Using again the definitions and assumptions of earlier sections, $\bar{r}_s(s)$ is obtained by taking the Laplace transform of (22), second form:

$$\bar{r}_s(s) = \frac{\bar{W}(s)}{1-\bar{D}(s)-\rho_1}. \tag{26}$$

If $\rho_1 < -1$ \$ (this is an additional restriction to the foregoing assumptions) then (26) may be expanded into the following series of functions (*cf.* Ref. [5], p. 201 *et seq.*):

$$\bar{r}_s(s) = \frac{1}{-\rho_1}\,\frac{\bar{W}(s)}{1-\dfrac{1-\bar{D}(s)}{\rho_1}} = \frac{\bar{W}(s)}{-\rho_1}\sum_{k=0}^{\infty}\left(\frac{1}{\rho_1}\right)^k\Big[1-D(s)\Big]^k. \tag{27}$$

In the present case $\bar{r}_s(s)$ can be inverted term by term, leading to

$$r_s(t) = \frac{1}{-\rho_1}\sum_{k=0}^{\infty}\left(\frac{1}{\rho_1}\right)^k F_k(t). \tag{28}$$

The functions $F_k(t)$ are defined by the following recurrence relation:

$$F_k(t) = F_{k-1}(t) - \int_0^t D(t-t')F_{k-1}(t')\,dt';$$

$$F_0(t) \equiv W(t) = \sum_{\mu=1}^{M} b_\mu e^{-\lambda_\mu t} \tag{29}$$

Figure 1 shows $F_k(t)$ for $k = 0, 1, 2, 3, 4$ based on delayed neutron data by Keepin *et al.* [6] for fast neutron induced fission of U^{235}. Figure 2 demonstrates how well the partial sums

$$r_{sK}(t) \equiv \frac{1}{-\rho_1}\sum_{k=0}^{K}\left(\frac{1}{\rho_1}\right)^k F_k(t) \tag{30}$$

approach the accurate function $r_s(t)$ (full curve) which was obtained by numerical solution of (22). The comparison shown in Fig. 2 refers to reactivities of $\rho_1 = -1$ \$ * and $\rho_1 = -2$ \$, with $K = 2$; 3; 3.5 and 4, where $K = 3.5$ means that the member with $k = 4$ of the alternating series (30) is included only with a weighting factor of 0.5. Figure 3 represents the time integrals $E_k(t)$ of the functions $F_k(t)$, which are useful for the approximate evaluation of the fission energy released during finite time intervals.

* This reactivity is just on the boundary of the region of convergence.

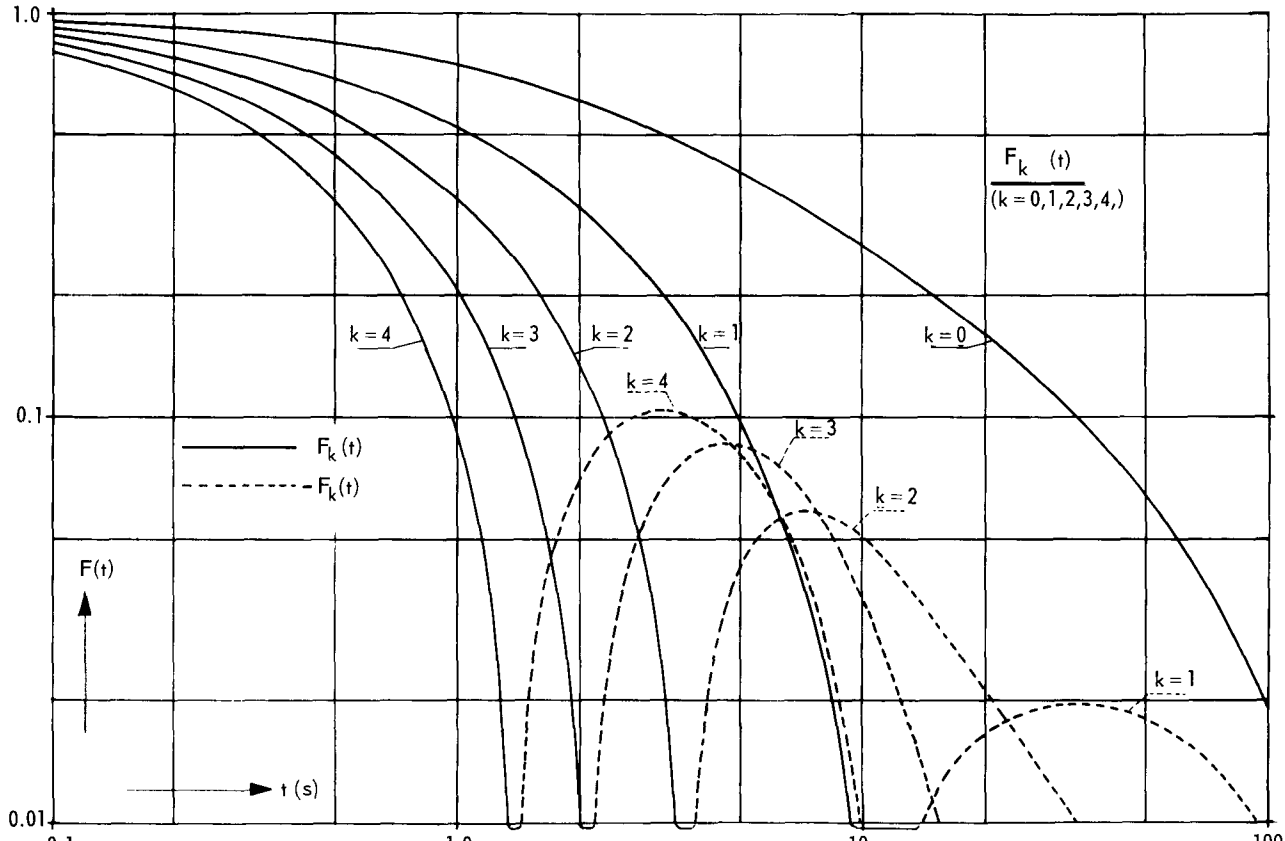


Figure 1

Definition and determination of an equivalent reactivity step

The second question to problem A requires the determination of a reactivity step from zero to $-\rho_1$ at such a time $\theta > 0$ that the corresponding response of the fission rate

$$r_\theta(t) \begin{cases} = 1 \text{ for } 0 < t < \theta \\ = r_s(t-\theta) \text{ for } t > \theta \end{cases} \tag{31}$$

coincides as well as possible with the actual fission rate $r(t)$ for times later than t_1. It can be shown (Ref. [5], p. 209 *et seq.*) that matching of the respective moments amounts to the first order* to an asymptotic fit of $\bar{r}_\theta(s)$ to $\bar{r}(s)$ for $s \to 0$.

From (31) and (22) follows [5]:

$$\bar{r}_\theta(s) = \frac{1 - e^{-\theta s}}{s} + e^{-\theta s}\,\bar{G}_{\rho 1}(s)\bar{W}(s) \to \theta - \frac{\bar{W}(0)}{\rho_1}\ (s \to 0). \tag{32}$$

The lower bound, say $r_I(t)$, of $r(t)$ is given by (21), left hand side, which leads, according to well known rules of Laplace transformation [5], to

$$\bar{r}_I(s) = \bar{G}_{\rho 1}(s)\,\mathcal{L}\left\{W(t)\left(1 + \Phi(\rho_1; t)\right)\right\}$$

$$= \bar{G}_{\rho 1}(s)\left[\bar{W}(s) + \sum_{\mu=1}^{M} b_\mu \bar{\Phi}(\rho_1; s + \lambda_\mu)\right]. \tag{33}$$

The Laplace transform of $\Phi(\rho_1; t)$ can be expanded as follows [5]:

$$\bar{\Phi}(\rho_1; s) = \sum_{\nu=0}^{\infty} \frac{(-1)^\nu}{\nu!}\,\Psi_\nu(\rho_1)\,s^\nu, \tag{34}$$

where $\Psi_\nu(\rho_1)$ denotes the νth moment of $\Phi(\rho_1; t)$, i.e.

$$\Psi_\nu(\rho_1) = \int_0^\infty \Phi(\rho_1; t)\,t^\nu\,dt\,. \tag{35}$$

Inserting (34) into (33) leads to

$$\lim_{s \to 0} \bar{r}_I(s)$$

$$= \frac{1}{-\rho_1}\left[\sum_{\nu=0}^{\infty} \frac{(-1)^\nu}{\nu!}\,\Lambda_\nu^\nu(0)\Psi_\nu(\rho_1) + \bar{W}(0)\right], \tag{36}$$

where **

$$\Lambda_\nu^\nu(p_0) \equiv \sum_{\mu=1}^{M} \frac{b_\mu \lambda_\mu}{\lambda_\mu + p_0}\,\lambda_\mu^\nu\,. \tag{37}$$

* From Fig. 4 it is recognized that matching of the zeroth moment results in practically perfect coincidences of $r(t)$ and $r_s(t-\theta)$ for times later than 1,5 t_1.

** For fast neutron fission of U^{235} the following values are obtained [1]: $\Lambda_0^0(0) = 1$; $\Lambda_1^1(0) \approx 0.435\ s^{-1}$; $\Lambda_2^2(0) \approx 0.682\ s^{-2}$; $\Lambda_3^3(0) \approx 1.871\ s^{-3}$; $\Lambda_4^4(0) \approx 6.328\ s^{-4}$.

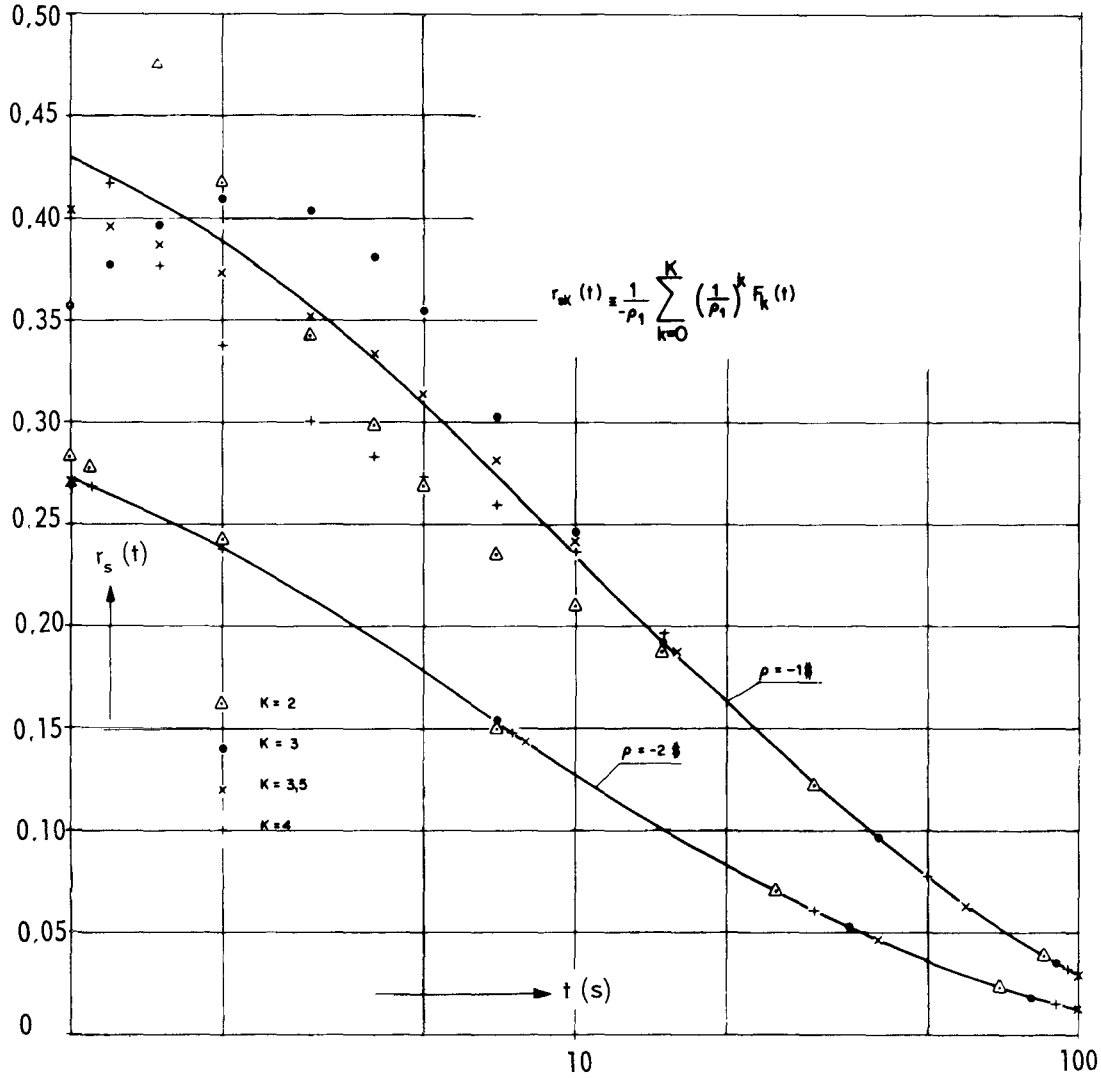


Figure 2. Successive approximation of actual fission rate after step reactivity change to $\rho_1 = -1$ \$ and $\rho_1 = -2$ \$ by finite series:

$$r_{sK}(t) \equiv \frac{1}{-\rho_1} \sum_{k=0}^{K} \left(\frac{1}{\rho_1}\right)^k F_k(t)$$

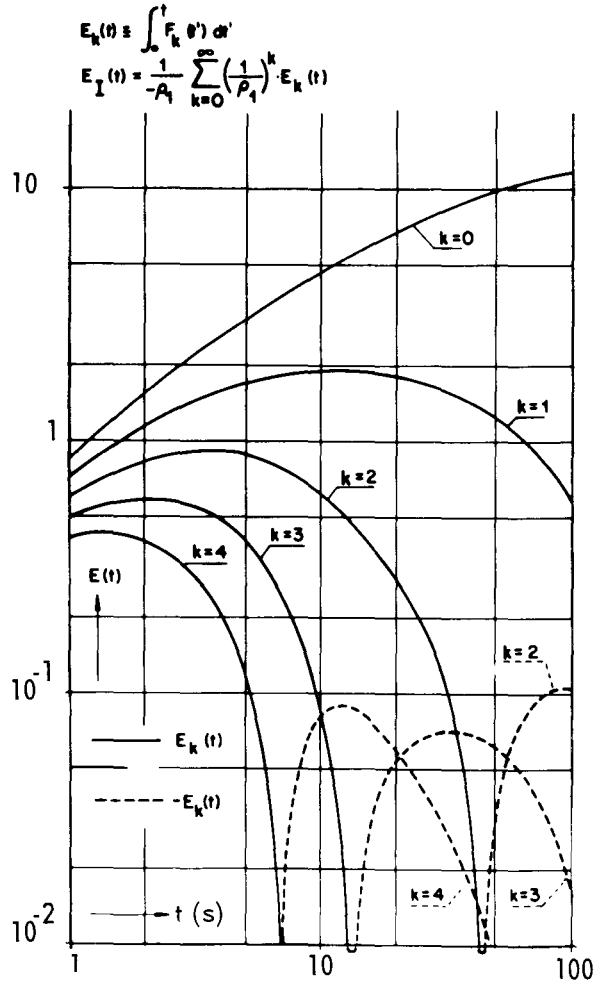


Figure 3. Functions $E_k(t)$ for synthesis of the energy released after an idealized shutdown at $t = 0$:

$$E_k(t) \equiv \int_0^t F_k(t')dt'$$

$$E_I(t) = \frac{1}{-\rho_1} \sum_{k=0}^{\infty} \left(\frac{1}{\rho_1}\right)^k E_k(t)$$

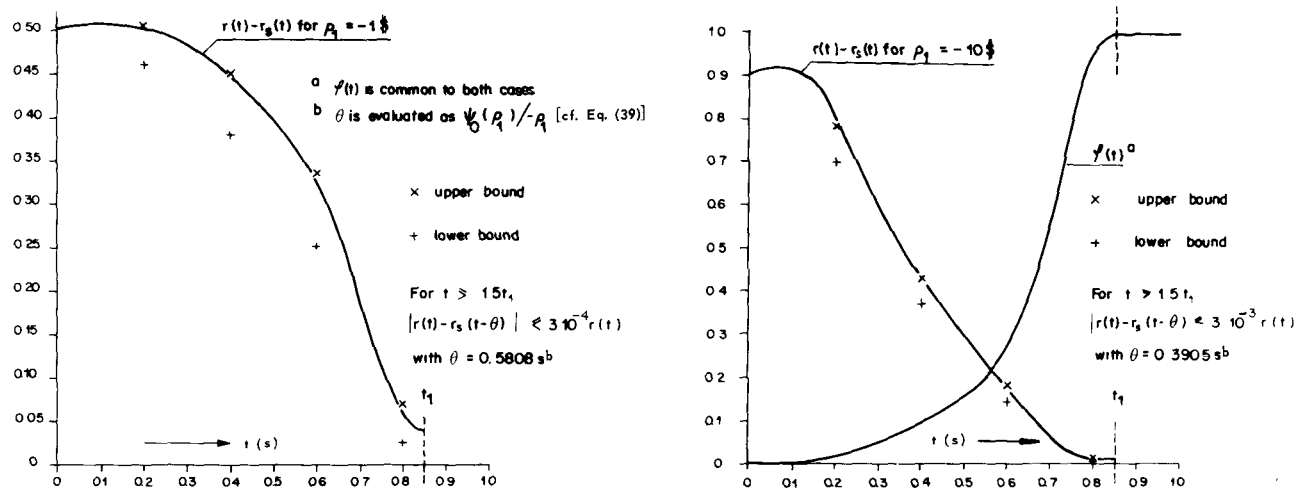


Figure 4. Comparison of the present approximations to the evolution of the fission rate with precise numerical results

Similarly the upper bound, $r_u(t)$, as given by (21), right hand side, leads to

$$\lim_{s \to 0} \bar{r}_u(s) = \frac{1}{-\rho_1} \left[\Psi_0(\rho_1) + \bar{W}(0) \right]. \tag{38}$$

From (32), (36) and (38) follow the lower and upper bounds to θ:

$$\frac{1}{-\rho_1} \sum_{\nu=0}^{\infty} \frac{(-1)^\nu}{\nu!} \Lambda_\nu^\nu(0) \Psi_\nu(\rho_1) \leqslant \theta \leqslant \frac{1}{-\rho_1} \Psi_0(\rho_1) . \tag{39}$$

For most practical purposes the upper bound can be used as a very good approximation of θ (Fig. 4). For a step at $t = t_1$, for instance, it gives the exact answer. For certain applications it is worthwhile to notice that, to the first order, a displacement of θ is exactly compensated by a fictitious change of the initial amplitude. If both the amplitude and θ can be selected at will it is even possible to fit simultaneously the zeroth and the first moments of $r_\theta(t)$ and $r(t)$.

Adaptation of the model to a reactor initially undergoing a subpromptcritical power excursion

In previous work [2] one of the authors has shown that the *basic integral equation* is applicable in a slightly generalized form if the initial fission rate is not constant, but given by an exponential with period $T_0 = 1/p_0$:

$$r(t) = e^{t/T_0} = e^{p_0 t} \text{ for } t < 0. \tag{40}$$

The generalization requires the following substitutions to be made:

$$r(t) \text{ is replaced by } r^*(t) \equiv r(t)\, e^{-p_0 t}, \tag{41}$$

$$\lambda_\mu \text{ is replaced by } \lambda_\mu^* \equiv \lambda_\mu + p_0, \tag{42}$$

$$b_\mu \text{ is replaced by } b_\mu^* \equiv b_\mu \lambda_\mu (\lambda_\mu + p_0), \tag{43}$$

$$\rho(t) \text{ is replaced by } {}^*\rho^*(t) \equiv \rho(t) - \rho_0, \tag{44}$$

* This substitution must not be applied to the simplified form (11) of the *basic integral equation of reactor kinetics*. This follows easily from a derivation analogous to that in an earlier section.

where ρ_0 is related to p_0 by the well-known inhour equation.

In case of Green's function, $G_\rho(t)$, the substitutions (42) to (44) are equivalent to the following displacement of its Laplace transform:

$$\bar{G}_{\rho 1}(s) \text{ is replaced by } \bar{G}_{\rho 1}(s + p_0) \tag{45}$$

A final adaptation of the model to a system being shut down from a noncritical state concerns the *prompt multiplication* (16). If $\phi(t)$ still represents the *normalized shutdown function* Eq. (14) must be generalized as follows:

$$\rho(t) = \rho_0 + \Delta\rho\ \phi(t); \quad \Delta\rho \equiv \rho_1 - \rho_0 < 0. \tag{46}$$

It is then found that the forms of (16) and (17) remain the same if ρ_1 is replaced by $\hat{\Delta}\rho$:

$$\hat{\Delta}\rho \equiv \frac{\Delta\rho}{1 - \rho_0} = \frac{\rho_1 - \rho_0}{1 - \rho_0} < 0. \tag{47}$$

In order to take full advantage of the generalization explained in this chapter it is necessary to note that, according to well-known rules from the theory of Laplace transforms [5]:

$$E \equiv \int_0^\infty r(t)\,dt = \int_0^\infty r^*(t) e^{p_0 t}\,dt = \lim_{s \to -p_0} \bar{r}^*(s). \tag{48}$$

Total fission energy released after initiation of a fast shutdown

According to the rules quoted above, Eq. (33) transforms to

$$\bar{r}_l^*(s) = \bar{G}_{\rho 1}(s+p_0)\sum_{\mu=1}^{M}\frac{b_\mu\lambda_\mu}{\lambda_\mu+p_0}\left[\frac{1}{s+\lambda_\mu+p_0}+\bar{\Phi}(\hat{\Delta\rho};s+\lambda_\mu+\rho_0)\right]. \quad (49)$$

Similarly one obtains from the right hand sideof (21):

$$\bar{r}_u^*(s) = \bar{G}_{\rho 1}(s+p_0)\left[\sum_{\mu=1}^{M}\frac{b_\mu\lambda_\mu}{\lambda_\mu+p_0}\frac{1}{s+\lambda_\mu+p_0}+\bar{\Phi}(\hat{\Delta\rho};s)\right]. \quad (50)$$

Remembering (48) leads to

$$\bar{r}_l^*(-p_0) \leqslant E \leqslant \bar{r}_u^*(-p_0). \quad (51)$$

If that contribution to both $\bar{r}_l^*(-p_0)$ and $\bar{r}_u^*(-p_0)$ which is independent of $\bar{\Phi}$, i.e. the expression corresponding to an ideal reactivity step from ρ_0 to ρ_1 at $t=0$, is designated as E_I, one obtains:*

$$E_I = \frac{1}{-\rho_1}\bar{W}(p_0) = \frac{\rho_0 T_0}{-\rho_1}. \quad (52)$$

For the contribution E_Φ to the total fission energy which is due to the finite travel time of the shutoff device the following bounds are found from (49), (50) and (51):

$$\frac{1}{-\rho_1}\sum_{\nu=0}^{\infty}\frac{(-1)^\nu}{\nu!}\Lambda_\nu^\nu(p_0)\Psi_\nu(\hat{\Delta\rho}) \leqslant E_\Phi \leqslant \frac{1}{-\rho_1}\sum_{\nu=0}^{\infty}\frac{p_0^\nu}{\nu!}\Psi_\nu(\hat{\Delta\rho}). \quad (53)$$

Finally one obtains the total fission energy release, E, as the following sum:

$$E \equiv \int_0^\infty r(t)\,dt = E_I + E_\Phi. \quad (54)$$

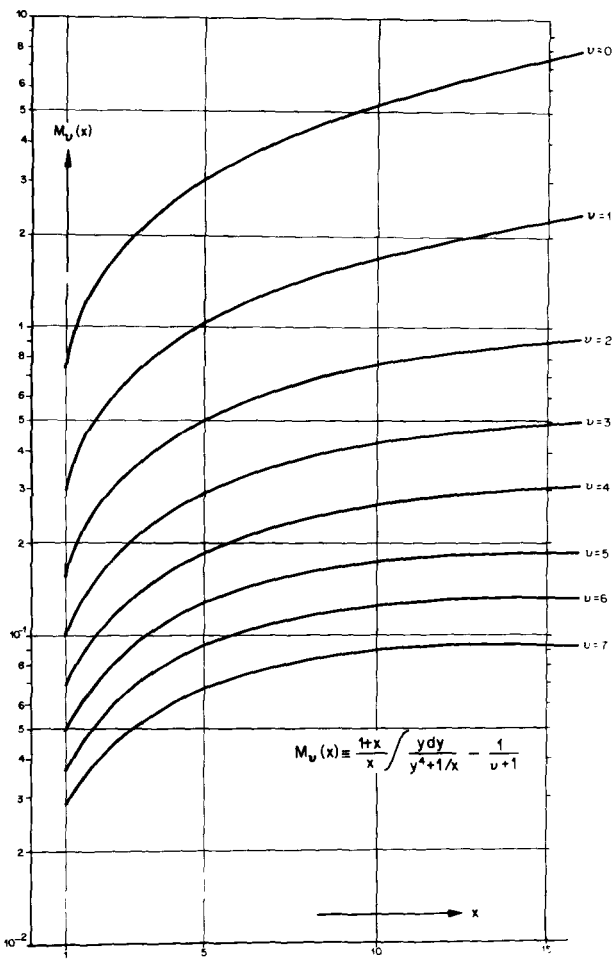


Figure 5

The effectiveness of a shutdown device in terms of its reactivity worth and its equivalent travel time

Consider a shutoff device moving with constant acceleration, g, from an initial position $z(0)$ to a final position $z(t_1) = H$. Suppose that the reactivity change as a function of position can be fitted well to $(z/\tilde{H})^2$ near $z=0$, where $\tilde{H}$ can be regarded as an equivalent total travel distance. The *normalized shutdown function*, $\phi(t)$, is then approximated by

$$\phi(t) \approx (gt^2/2\tilde{H})^2 \qquad (0 \leqslant t \leqslant \Theta), \quad (55)$$

where Θ replaces t_1 and will be called the *equivalent travel time*:

$$\Theta = (2\tilde{H}/g)^{1/2}. \quad (56)$$

The moments of $\Phi(\hat{\Delta\rho};t)$ are then given by [7]

$$\Psi_\nu(\hat{\Delta\rho}) \approx \Theta^{\nu+1}M_\nu(|\hat{\Delta\rho}|), \quad (57)$$

where

$$M_\nu(x) \equiv \frac{1+x}{x}\int_0^1\frac{ydy}{y^4+1/x}-\frac{1}{\nu+1}, (x>0). \quad (58)$$

The functions (58) ($\nu = 0, 1, 2, \ldots. 7$) are plotted in Fig. 5 in the range of $1 \leqslant x \leqslant 16$.

If $\Theta/T_0 \leqslant 1$ and $\Theta^{\nu+1}\Lambda_\nu^\nu(p_0) \leqslant 1$ ($\nu = 1, 2, \ldots.$) then E_Φ is closely approximated by E_Φ as given by (59):

$$\frac{\Theta}{-\rho_1}\left(1-\rho_0+\frac{\tau}{T_0}-0.4\,\frac{\Theta T_0\Lambda_1^1(0)\Lambda_2^2(0)}{\Lambda_1^1(0)+T_0\Lambda_2^2(0)}\right)$$

$$M_0\left\{\frac{\rho_0-\rho_1}{1-\rho_0}\right\} \leqslant E_\theta \leqslant \frac{\Theta}{-\rho_1}e^{\theta/2T}M_0\left\{\frac{\rho_0-\rho_1}{1-\rho_0}\right\}, \quad (59)$$

* It can be shown that the final expression $\rho_0 T_0/(-\rho_1)$ is strictly correct even if the prompt neutron generation time is different from zero. The fractional fission energy released during finite time intervals may be obtained by synthesis, using the functions plotted in Fig. 3.

where τ is the reduced generation time (i.e., prompt neutron generation time divided by $\bar{\beta}k_{\text{eff}}$) and $M_0(x)$ is closely approximated by

$$M_0(x) \approx 0.7688\, x - 0.03805\, x^2 + 0.00131\, x^3 \quad (1 \leqslant x \leqslant 16)$$

$$M_0(x) \approx \frac{\pi}{2\sqrt{2}}\,(1+x)\, x^{-0.25} - 1 \quad (16 < x \to \infty) \qquad (60)$$

Final remarks

Figure 4 compares the approximation elaborated in this paper with the results of two numerical computations [8] concerning actual shutdown functions of the Swiss research reactor SAPHIR.

The authors express their gratitude for stimulating discussions and assistance with numerical computation to the following members of this Institute: Mr. R. Alpiar, Dr. T. Hürlimann, Dr. J. Patry, Mr. F. Riccard, Dr. H. Soodak and Mr. K. Zumbrunn.

REFERENCES

1. Schmid, P., Nukleonik, *4*, 331-347 (1962).
2. Schmid, P., Nukleonik, *4*, 251-255 (1962).
3. Schmid, P., *Derivation of a Basic Integral Equation of Reactor Kinetics*, Proceedings of the Second International Conference on the Peaceful Uses of Atomic Energy, P/232, Vol. 11, p. 277, United Nations (1958).
4. Ash, M. C., J., Appl. Phys., *27*, 1030-1031 (1956).
5. Doetsch, G., *Anleitung zum praktischen Gebrauch der Laplace-transformation*, 2nd ed. Oldenbourg, München (1961).
6. Keepin, G. R., Wimett, T. F., and Zeigler, R. K., J. Nuclear Energy, *6*, 1-21 (1957).
7. Schmid, P., Interne Technische Mitteilung TM-PH 128 des Eidg. Institutes für Reaktorforschung (1963).
8. Patry, J., Neue Technik, *4*, 383-394 (1962).

ABSTRACT - RÉSUMÉ - АННОТАЦИЯ - RESUMEN

A/686 Suisse

Evolution du taux de fission pendant et après l'arrêt d'une pile atomique

par P. Schmid et W. Zünti

L'évolution du taux de fission pendant et peu de temps après l'arrêt brusque d'un réacteur peut contribuer de façon essentielle au dégagement total de chaleur dans le combustible; l'estimation de cette évolution est donc nécessaire, aussi bien aux constructeurs qu'aux responsables de la sécurité. De plus, l'allure de la fonction représentant le flux de neutrons en un endroit quelconque en fonction du temps écoulé depuis l'insertion soudaine des absorbeurs de contrôle contient des informations essentielles et sûres sur la réactivité à l'état d'arrêt. Ce dernier fait a été exploré au moyen de certaines techniques de mesure de la réactivité développées récemment et nommées « méthode modifiée de la chute des barres ».

Le mémoire résume certaines connaissances utiles acquises dans l'Institut de Würenlingen au cours de calculs et d'expériences du type mentionné plus haut. Des limites supérieures et inférieures sont déduites pour le taux de fission pendant la durée finie du mouvement du système d'arrêt. On définit alors un saut équivalent de réactivité tel que l'évolution asymptotique du taux de fission soit reproduite. On exprime le taux de fission, à partir du moment où le dispositif d'arrêt a atteint sa position finale, au moyen d'un développement en série de fonctions caractéristiques du temps. Les coefficients de ce développement sont donnés par les puissances de l'inverse de la réactivité exprimée en dollars. Ce développement converge bien pour des valeurs de réactivité finales inférieures à — 1 $ et se montre d'une grande utilité, non seulement pour des estimations rapides du taux de fission, mais aussi pour une analyse optimale d'expériences du type « méthode modifiée de la chute des barres ». Une approximation pour l'énergie totale de fission dégagée depuis le début de l'insertion rapide des barres est présentée pour des excursions sous-critiques promptes dont les périodes initiales sont plus grandes ou égales au temps de chute (convenablement défini) du dispositif d'arrêt, celui-ci étant introduit avec une accélération constante.

A/686 Швейцария

Изменение плотности делений во время и после остановки ядерного реактора

П. Шмид, В. Цюнти

Изменение плотности делений во время и после внезапной остановки реактора может существенным образом способствовать выделению тепла в топливе; как для конструкторов, так и для тех, кто отвечает за безопасность, необходима оценка этого изменения. Кроме того, вид функции, представляющей поток нейтронов в каком-либо месте в зависимости от прошедшего времени с момента внезапного введения регулирующих поглотителей, дает существенные надежные данные о реактивности в состоянии

остановки. Это явление было исследовано с помощью некоторых методов измерения реактивности, разработанных недавно и названных модифицированным методом падения стержня.

В настоящем докладе обобщаются некоторые полезные данные, накопленные этим институтом в ходе расчетов и экспериментов вышеупомянутого типа. Верхние и нижние пределы выводятся для изменения плотности делений во время конечной длительности движения регулирующей системы. Затем определяют эквивалентный скачок реактивности таким образом, что воспроизводится асимптотическое изменение плотности делений. Плотность делений выражают, исходя из момента, когда приспособление для остановки достигает конечного положения, с целью развертывания ряда характерных функций времени. Коэффициенты этого развертывания выражаются мощностями в противоположность реактивности, выражаемой в долларах. Развертывание хорошо сходится для конечных значений реактивности меньше —1 долл. и является весьма полезным не только для быстрых оценок плотности делений, но также и для оптимального анализа опытов типа модифицированного метода падения стержня. Приближение для общей энергии деления E, освобождаемой с начала остановки, представлено для мгновенных подкритических разгонов, у которых начальный период T_0 больше или равен времени падения Θ (определенным соответствующим образом) устройства для остановки, причем последнее вводится с постоянным ускорением.

A/686 Suiza

Evolución del índice de fisiones durante la parada de un reactor y después de la misma

por P. Schmid y W. Zünti

La evolución del índice de fisiones durante la parada brusca de un reactor, y poco después de la misma, puede contribuir de manera muy importante al desprendimiento total de calor en el combustible. En consecuencia, la estimación de esa evolución es necesaria, tanto en lo que respecta a los constructores como a los responsables de la seguridad. Además, la forma de la ecuación que representa el flujo neutrónico en un punto cualquiera en función del tiempo transcurrido desde la inserción repentina de los absorbentes de control, contiene información sumamente importante y fiel sobre la reactividad en estado de parada. Este factor se ha investigado por medio de ciertas técnicas de medición de la reactividad, ideadas recientemente y denominadas "método modificado de la caída de barra" (*modified rod drop method*).

En la memoria se resumen ciertos conocimientos útiles adquiridos en el Instituto en el curso de cálculos y experimentos del tipo antes mencionado. Se deducen límites superiores e inferiores para la evolución del índice de fisiones durante la duración finita del movimiento del sistema de control. Seguidamente, se define un salto equivalente de reactividad tal que la evolución asintótica del índice de fisión sea reproducida. Se expresa ese índice a partir del momento en que el dispositivo de parada ha alcanzado su posición final, por medio de un desarrollo en serie de funciones de tiempo características. Los coeficientes de este desarrollo vienen dados por las potencias de la inversa de la reactividad expresada en dólares. Este desarrollo es convergente para valores finales de reactividad inferiores a — 1 dólar y resulta sumamente útil, no sólo para el cálculo rápido del índice de fisiones, sino también para el análisis óptimo de experimentos del tipo "método modificado de la caída de barra". Se presenta una aproximación para la energía total de fisión E desprendida desde el comienzo de la parada, para saltos subcríticos inmediatos cuyos períodos iniciales T_0 son superiores o iguales al tiempo de caída θ (oportunamente definido) del dispositivo de parada, que se introduce con una aceleración constante.

On the stability of steam-cooled fast reactors with ceramic fuel

By P. Schmid*

By virtue of their short generation times fast reactors may be considered as particularly safe, provided their reactivity feedback is governed by a prompt negative contribution from effects inherent to the system. In large ceramic-fuelled reactors this is ensured by the Doppler coefficient of reactivity. It is generally known that stability may be jeopardized by sufficiently large delayed contributions of either sign to the total reactivity feedback. Nevertheless one has to cope with the fact that uranium-plutonium oxide fuelled fast breeder reactors with core volumes larger than a few hundred liters exhibit sizable positive void coefficients if they are cooled by steam. The present paper derives stability criteria which allow determination of the maximum permissible ratio of magnitudes of the positive steam void coefficient and the negative Doppler coefficient of reactivity. Two models are considered, according to the types of instability to be prevented.

Space-independent model assuming Newton's law of cooling with coupled heat transfer

This "point model" neglects the finite dimensions of the reactor core, as well as the influence of those parts of the closed steam loop which are outside the reactor core. Using a theorem by Popov [1] necessary and sufficient conditions for asymptotic stability in the large are obtained. These conditions state that:

(*a*) The equilibrium net power coefficient must be negative,

(*b*) A power pulse must result in an initial drop in reactivity,

(*c*) Redistribution of heat following the power pulse must not cause any further decrease of reactivity.

According to the inherent limitations of the first model the satisfaction of these conditions is considered to ensure against selfsustained oscillations with periods comparable to or shorter than the coolant transit time through the core.

* Swiss Federal Institute for Reactor Research, Würenlingen.

Space-dependent model including linear reactivity feedback from out-of-pile components

The second model of reactivity feedback is more realistic if possible instabilities at intermediate and lower frequencies are to be considered. Heat transfer from the fuel element to dry steam as well as the performance of out-of-pile parts of the coolant loop are described in a rather general and flexible manner by a series of characteristic parameters, valid at least in the neighbourhood of the considered equilibrium state. Applying the "First stability theorem" by Smets [2], a necessary condition for the asymptotic stability in the large is derived for such a system with linear reactivity feedback. Using some approximations well justified in the light of published design characteristics of a 300 MW(e) steam-cooled fast breeder reactor power plant, a simplified version of the former criterion is found. The ratio of the Doppler coefficient to the steam void coefficient must be greater or equal to an elementary expression containing only two essential characteristics, which are an average relaxation time for heat removal from the fuel and a suitable parameter which characterizes the efficiency of heat removal from the primary steam loop.

Uses and limitations of the proposed models

It is expected that an analytical understanding of the stability of an actual fast breeder reactor power plant, expressed in terms of a few representative over-all characteristics, will be helpful while deciding on main design aspects and finding the optimum lay-out of a certain concept. The two models proposed in this paper are believed to contribute to such an understanding. There might, however, exist a substantial gap between the two, a gap which may well need to be filled by generalization of the second model to include coupled heat transfer. There is no doubt that the actual lay-out of a power reactor should be based on much more advanced digital or analogue computations. Nevertheless it is hoped that the present approach, which lies halfway between simple analytical criteria concerning over-simplified models and extended parametric studies with sophisticated models, will become useful tools, once their limitations have been clearly recognized.

SPACE-INDEPENDENT MODEL OF REACTIVITY FEEDBACK AND NONLINEAR STABILITY CRITERIA

The adopted reactivity feedback mechanism

Let n be the reactor power, the fractions η_j of which are generated in the fuel ($j = 1$) and the coolant ($j = 2$). The respective heat capacities shall be designated by ϵ_1 and ϵ_2. θ_1 and θ_2 shall designate respectively the average temperatures of fuel and coolant, measured above ambient temperature, i.e., above the inlet temperature of the coolant in an open cooling circuit. According to Newton's law of cooling, the following differential equations govern the time behaviour of the temperatures θ_1 and θ_2:

$$\epsilon_1\dot{\theta}_1 = \eta_1\ n(t) - \lambda_1(\theta_1 - \theta_2), \tag{1}$$

$$\epsilon_2\dot{\theta}_2 = \eta_2\ n(t) + \lambda_1(\theta_1 - \theta_2) - \lambda_2\theta_2 \tag{2}$$

where $\dot{\theta}_j$ means the time derivative $\mathrm{d}\theta_j(t)/\mathrm{d}t$ and λ_j are the heat transfer coefficients for heat transfer from the fuel to the coolant ($j = 1$) and heat removal from the coolant ($j = 2$).

There exist two equilibrium points, namely the shut-down equilibrium $n = \theta_1 = \theta_2 = 0$ and a non-trivial solution called the "operating equilibrium point" with the following coordinates:

$$\theta_{10} = \frac{n_0}{\lambda_2} + \eta_1\frac{n_0}{\lambda_1},\quad \theta_{20} = \frac{n_0}{\lambda_2};\ (\eta_1 + \eta_2 \equiv 1). \tag{3}$$

Choosing this point as the origin of the new coordinates

$$N \equiv \frac{n - n_0}{n_0},\quad T_1 \equiv \frac{\theta_1 - \theta_{10}}{n_0},\quad T_2 \equiv \frac{\theta_2 - \theta_{20}}{n_0} \tag{4}$$

leads to

$$\epsilon_1\dot{T}_1 = \eta_1 N - \lambda_1(T_1 - T_2), \tag{5}$$

$$\epsilon_2\dot{T}_2 = \eta_2 N + \lambda_1(T_1 - T_2) - \lambda_2 T_2. \tag{6}$$

Let the "prompt reactivity" be defined by:

$$\rho_\mathrm{p} \equiv \frac{k_{\mathrm{p\,eff}} - 1}{k_{\mathrm{p\,eff}}} = \rho_{\mathrm{p\,E}} + \rho_{\mathrm{p\,I}}, \tag{7}$$

where $k_{\mathrm{p\,eff}}$ is the effective prompt multiplication constant or prompt criticality factor, $\rho_{\mathrm{p\,E}}$ and $\rho_{\mathrm{p\,I}}$ are designating those parts of ρ_p which are externally controlled and caused by internal temperature changes, respectively. Furthermore let the "internal reactivity" be linearly dependent on the temperatures of both fuel and coolant

$$\rho_{\mathrm{p\,I}} = -\alpha_1'\theta_1 - \alpha_2'\theta_2. \tag{8}$$

Since in the operating equilibrium point ρ_p must vanish, the following relation is obtained from (7) and (8):

$$\rho_{\mathrm{p\,E}_0} = \alpha_1'\theta_{10} + \alpha_2'\theta_{20}. \tag{9}$$

The basic differential equation of reactor kinetics, neglecting both delayed neutrons and extraneous neutrons, is given by:

$$\Lambda_\mathrm{p} n(t) = \rho_\mathrm{p} n(t), \tag{10}$$

where Λ_p is the prompt neutron generation time.

Using the transformations (3) and

$$\frac{\alpha_j'}{\Lambda\mathrm{p}} \equiv \alpha_j \qquad (j = 1,2) \tag{11}$$

leads to

$$N(t) = (-\alpha_1 n_0 T_1 - \alpha_2 n_0 T_2)(1 + N). \tag{12}$$

In order to apply Popov's theorem [1] it is convenient to introduce

$$N = f(\sigma) = \mathrm{e}^\sigma - 1,\ \sigma \equiv \ell n(N + 1). \tag{13}$$

$f(\sigma)$ is then said to belong to class A, i.e., $f(\sigma)$ is continuous and satisfies

$$f(0) = 0 \text{ and } \sigma f(\sigma) > 0 \text{ for } \sigma \neq 0. \tag{14}$$

The dynamic behaviour of the system is then governed by the following set of differential equations:

$$\sigma = -\alpha_1 n_0 T_1 - \alpha_2 n_0 T_2, \tag{15}$$

$$\dot{T} = -\frac{\lambda_1}{\epsilon_1}(T_1 - T_2) + \frac{\eta_1}{\epsilon_1} f(\sigma), \tag{16}$$

$$\dot{T}_2 = \frac{\lambda_1}{\epsilon_2} T_1 - \frac{\lambda_1 + \lambda_2}{\epsilon_2} T_2 + \frac{\eta_2}{\epsilon_2} f(\sigma). \tag{17}$$

The application of Popov's Theorem [1] to this model

Popov's Theorem [1] may be applied to an even more general set of differential equations which is obtained from (15) to (17) by subtracting $rf(\sigma)$ from (15), where r is a constant. According to Popov the term $f(\sigma)$ is to be linearized by substituting $z\sigma(0 < z < \infty)$ instead. If the characteristic equation of the linearized system is given by:

$$s^3 + a_1 s^2 + a_2 s + z(rs^2 + b_1 s + b_2) = 0, \tag{18}$$

where, by proper definitions, a_1 and a_2 are positive, and b_1 is assumed to be different from zero *, then the following conditions are *necessary and sufficient for asymptotic stability in the large*

$$r \geqslant 0,\ b_1 > 0,\ b_2 > 0,$$
$$\sqrt{b_2} < \sqrt{(ra_2)} + \sqrt{(a_1 b_1)}. \tag{19}$$

The application of these conditions to the characteristic equation of the system of differential equations (15) to (17) leads to:

$$\lambda_1(\alpha_1 + \alpha_2) + \lambda_2\eta_1\alpha_1 > 0 \tag{20}$$

* For $b_1 = 0$ special investigations would be necessary (*cf.* [6]).

$$\frac{\eta_1\alpha_1}{\epsilon_1} + \frac{\eta_2\alpha_2}{\epsilon_2} > 0 \; * \tag{21}$$

$$\frac{\alpha_1}{\epsilon_1}(\eta_2\epsilon_1 - \eta_1\epsilon_2) + \frac{\alpha_2}{\epsilon_2}\left[\eta_1\epsilon_2 - \eta_2\epsilon_1\left(1 + \frac{\lambda_2}{\lambda_1}\right)\right] < 0. \tag{22}$$

Discussion of the obtained stability criterion, disregarding delayed neutrons

It is easily recognized that (20) and (21) are equivalent to the requirements (*a*) and (*b*) stated in an earlier section. In previous work [3] the author has demonstrated that (22) expresses explicitly condition (*c*) in that section immediately after an idealized power pulse (Dirac δ-function). There it was also proved that the three conditions (20) to (22) are, for the present model, identical to Welton's stability criterion [4] which requires the phase lag of the feedback transfer function to remain smaller than 90 degrees for all real frequencies between zero and infinity (it should be remembered, however, that Welton's criterion was only shown to be sufficient but not necessary, if applied to the most general type of reactivity feedback mechanism). From this and from Smets' discussion (*cf.* Ref. [2], p. 20) follows the interpretation expressed by condition (*c*), valid not only immediately after the supposed power pulse, but for all later times. As in all practical cases $\eta_2 << \eta_1$ this means that a certain amount of heat must reduce the reactivity more if it is produced in the fuel than if it were deposited in the coolant. It is thus clearly recognized that a strongly negative temperature coefficient of the coolant is not even desirable from the point of view of stability. This was found by Kinchin [5] in 1956. It is not so obvious, but may be understood if one realizes the potential phase lag of the reactivity feedback due to coolant temperature changes, which may approach 180 degrees at high frequencies.

Recently Shotkin [6] has shown that the conditions expressed by (20) to (22) are not only necessary and sufficient for asymptotic stability in the large, but also necessary to guarantee simple stability. If (20) is violated, essentially there no longer exists any stable operating equilibrium point. If only condition (22) is violated there do not even exist centres i.e., non-isolated periodic motions whose amplitude and frequency depend on initial conditions. There remain only the possibilities of stable limit cycles and of solutions with finite escape time. The latter are only possible if condition (21) is violated, too, and the initial conditions are in favour of them.

Stability criteria including delayed neutrons

According to another theorem by Popov [7], which is applicable to the present model, the system including delayed neutrons is asymptotically stable in the large even if it were only simply stable without delayed neutrons. This means that the conditions (20) and (22) are sufficient all the more. On the other hand, it is evident that stable limit cycles and solutions with a finite escape time persist in the neighbourhood of sufficiently high operating equilibrium powers, even if delayed neutrons tend to stabilize them.** This means that the conditions (20) and (22) are not only sufficient, but also necessary to ensure asymptotic stability in the large for the considered reactivity feedback model, including delayed neutrons. Nevertheless delayed neutrons may ensure asymptotic stability in the small for a considerable range of initial conditions, even if the system without delayed neutrons would oscillate, particularly if these oscillations would be of the type of stable limit cycles or narrow spiral trajectories.

STABILITY CRITERIA CONSIDERING THE REACTIVITY FEEDBACK FROM DRY STEAM CIRCULATION IN A CLOSED COOLANT LOOP

Formulation of the problem

Consider the model of a representative section of a reactor core and out-of-pile equipment as shown schematically in Fig. 1. The given design data are in rough agreement with those published for a 300 MW(e) steam-cooled fast breeder reactor power plant fuelled with U-Pu oxide [8]. They correspond to operating equilibrium values the perturbations of which are only considered in the following treatment. It is supposed that all material properties, such as heat capacities, thermal conductivities, heat transfer coefficients etc. remain constant during the considered perturbations. Likewise the mass flow rates and velocities averaged along the whole coolant loop shall remain constant in time. Local velocities may change, however, in so far as density changes are involved. These propagate with the velocity of sound which is assumed to be very much higher than the average flow velocity. This means that the equilibria defined by the equations of state are reached instantaneously. These assumptions justify the application of a linear reactivity feedback model.

* This condition corresponds to $b_1 > 0$. As in the present model r vanishes, it is easily recognized that condition (21) is a consequence of conditions (20) and (22), a_1 being positive.

** At present the author has not yet proved this statement rigorously. His opinion is supported by Shotkin's paper [6] in the sense that the generation time is defined in [6] as an average one, including delayed neutrons. The author of the present paper agrees, however, with Shotkin's treatment of delayed neutrons only if the considered periods are long compared with the average generation time.

Consider an operating equilibrium point characterized by an equilibrium power n_0, and an equilibrium reactivity ρ_0. Any linear reactivity feedback mechanism may be characterized by a reactivity feedback kernel $K(t)$, such that the reactivity change $\delta\rho(t)$ is related to any change of the power $\delta n(t) = n(t) - n_0$ by the following linear functional:

$$\delta\rho(t) = -\int_0^t K(t-t')\,[n(t') - n_0]\,dt'. \quad (23)$$

According to Smets' first stability theorem (*cf.* Ref. [2], p. 17) a nuclear reactor is asymptotically stable in the large at the power equilibrium state when this state exists and when the cosine Fourier transform of $K(t)$ is positive or equal to zero for all non negative real frequencies;

$$\int_0^\infty K(t)\cos\omega t\,dt \geqslant 0 \qquad (0 \leqslant \omega < \infty) \quad (24)$$

or $\quad \mathrm{Re}\,\bar{K}(i\omega) \geqslant 0, \qquad (0 \leqslant \omega < \infty) \quad (25)$

where $\bar{K}(s)$ is the Laplace transform [9] of $K(t)$. It is the aim to find an approximation to $\bar{K}(i\omega)$ which comes close enough to the truth to be significant under typical conditions and is yet simple enough for its real part to be expressed in terms of a few main characteristics of the plant.

The Doppler contribution to the reactivity feedback kernel

It is assumed that the power density is constant over the cross section of each fuel element. Furthermore the reactivity change due to the Doppler effect shall be proportional to the total energy deposited per unit height at a specified height z of the kth fuel element. If an ideal power pulse

$$\delta n(t) = E_0\delta(t) \qquad [\delta(t) = \text{Dirac } \delta\text{-function}] \quad (26)$$

is superimposed on the equilibrium power, the extra energy produced at height z per unit height in the kth fuel element shall be designated by $\delta q_k(z;0)$. Due to the heat transfer through the oxide fuel and the canning to the coolant, $\delta q_k(z;t)$ will eventually decay to zero according to a law of the following type:

$$\delta q_k(z;t) = E_0\alpha_k(z)\sum_{l=1}^{L}\beta_{kl}(z)\,e^{-\nu_l t}, \quad (27)$$

where

$$\sum_{l=1}^{L}\beta_{kl}(z) = 1 \text{ for all } k \text{ and } -\frac{H}{2} \leqslant z \leqslant \frac{H}{2}. \quad (28)$$

Obviously it has been assumed that the heat transfer properties neither change radically along the axis of each fuel element nor from one fuel element to the other. Appreciable changes due to the different equilibrium temperatures may, however, be considered by different spectral amplitudes $\beta_{kl}(z)$. If $\alpha_k^+(z)$ denotes the reactivity change due to the Doppler effect if unit energy is deposited at height z of the kth fuel element then the reactivity response to the power pulse (26) is given by:

$$\delta\rho(t) \equiv -E_0K_D(t) = E_0\sum_{l=1}^{L} e^{-\nu_l t}\sum_k\int_{-H/2}^{+H/2}\alpha_k^+(z)\alpha_k(z)\beta_{kl}(z)dz \quad (29)$$

or, in abbreviated form

$$K_D(t) = -\sum_{l=1}^{L} D_lQ_l e^{-\nu_l t}, \quad \bar{K}_D(s) = -\sum_{l=1}^{L}\frac{D_lQ_l}{s+\nu_l} \quad (30)$$

where

$$Q_l \equiv \sum_{k=1}^{M}\int_{-H/2}^{+H/2}\alpha_k(z)\beta_{kl}(z)dz\,; \quad \sum_{l=1}^{L} Q_l \equiv 1 \quad (31)$$

and

$$D_l \equiv \frac{\sum_{k=1}^{M}\int_{-H/2}^{+H/2}\alpha_k^+(z)\alpha_k(z)\beta_{kl}(z)dz}{Q_l} \quad (32)$$

It is thus recognized that the Doppler coefficient has a spectral representation such that the equilibrium reactivity change due to unit power change, i.e., the *Doppler power coefficient*, is given by:

$$\langle D\rangle = \frac{1}{\Delta n}\int_0^\infty\sum_{l=1}^{L} D_lQ_l e^{-\nu_l t}\cdot\Delta n\,dt = \sum_{l=1}^{L}\frac{Q_l}{\nu_l}D_l \quad (33)$$

whereas the instantaneous reactivity change due to a power pulse, i.e., the *Doppler energy coefficient*, is given by:

$$\hat{D} = \sum_{l=1}^{L} D_lQ_l. \quad (34)$$

The fuel-to-coolant heat transfer function

Newton's law of cooling would require considering the rate of heat flowing from fuel to coolant as proportional to the difference between a significantly averaged fuel temperature and an average coolant temperature. Although such "coupled heat transfer" may be expressed implicitly by (27) it is recognized that the temperature changes of the cooling steam are so low compared with the corresponding changes of the fuel temperature that they may well be neglected in the explicit heat transfer equations. From the preceding section it immediately follows that the rate of heat transfer from fuel to coolant after a power pulse $\delta n(t) = E_0\delta(t)$ is given by:

$$E_0 G(t) \equiv -E_0 \frac{\mathrm{d}}{\mathrm{d}t} \sum_{l=1}^{L} Q_l \mathrm{e}^{-\nu_l t}, \qquad (35)$$

so that the Laplace transform of Green's function for heat transfer is given by:

$$\bar{G}(s) = \mathscr{L}\{G(t)\} = \sum_{l=1}^{L} \frac{\nu_l Q_l}{s+\nu_l}. \qquad (36)$$

This treatment disregards the spatial distribution of the heat released to the coolant. This is justified because the fundamental time constant responsible for heat transfer to the coolant, ν_1^{-1}, is of the order of 0.5 seconds whereas the time for any volume element of the coolant to pass through the core is only about 0.005 seconds.

Reactivity feedback from changes of the steam density

A uniform change of the steam density in large U-Pa oxide reactor cores leads to two competing effects. On the one hand the leakage is changed at lower neutron energies, while on the other k_∞ *is* changed as a consequence of the spectral shift. In typical power reactor projects the spectral effect predominates, so that a density reduction leads to a reactivity increase.

Consider a fictitious injection of heat into the coolant contained in the considered core section:

$$E_0\delta(t). \qquad (37)$$

This increases the local steam temperature, acting in two competing ways on the local density. On the one hand—assuming that the dry steam behaves like an ideal gas—there is an instantaneous increase of the pressure in the whole loop, $\delta p(0)$. If p_0 designates the equilibrium pressure,* then

$$\frac{\delta p(0)}{p_0} = \frac{E_0}{U_0} \qquad (38)$$

where U_0 is the total energy of all the steam contained in the loop. On the other hand there is a local decrease of the steam density due to the increase of the local temperature. If $h_{0k}(z)$ is the enthalpy of the steam contained per unit height at height z in the channel surrounding the kth fuel element, then an "averaged" total enthalpy of the steam in the kth channel shall be defined by:

$$< h_{0k} > = \int_{-H/2}^{+H/2} \alpha_k(z)\mathrm{d}z \Big/ \int_{-H/2}^{+H/2} \frac{\alpha_k(z)}{h_{0k}(z)}\, dz. \qquad (39)$$

If $< d_{0k} >$ and $< \delta d_k(0) >_T$ designate respectively the average operating equilibrium steam density and the average, temperature-induced, instantaneous change of the steam density in the whole channel surrounding the kth fuel element, then the following relations hold:

$$\frac{< \delta d_k(0) >_T}{< d_{0k} >} = -\frac{\alpha_k E_0}{< h_{0k} >} \quad (k = 1, \ldots . M), \qquad (40)$$

where α_k determines the fraction of the total energy E_0 which is injected into the kth fuel element

$$\alpha_k \equiv \int_{-H/2}^{+H/2} \alpha_k(z)\mathrm{d}z, \qquad \left(\sum_{k=1}^{M} \alpha_k \equiv 1\right). \qquad (41)$$

Now the fractional change of overall pressure (38), which causes a fractional density perturbation of equal sign and magnitude, may be superimposed on (40) to give the initial net change of the fractional average steam density in the kth channel

$$\frac{< \delta d_k(0) >}{< d_{0k} >} = \frac{E_0}{U_0} - \frac{\alpha_k E_0}{< h_{0k} >}. \qquad (42)$$

If the individual steam velocities in the different fuel channels are properly matched to the distribution of heat sources, α_k, all the $< h_{0k} >$ $(k = 1, \ldots M)$ are identical and equal to $< h_0 >$. Let the averaged local change of reactivity in the kth channel be given by σ_k times the fractional density change. Then the instantaneous change of reactivity due to the injection of heat defined by (37) is expressed by:

$$-\delta p(0) = E_0 \sum_{k=1}^{M} \alpha_k \left(\frac{\alpha_k}{< h_0 >} - \frac{1}{U_0}\right). \qquad (43)$$

Now the following abbreviations are introduced:

$$S_T \equiv \frac{-1}{< h_0 >} \sum_{k=1}^{M} \alpha_k \sigma_k > 0 \qquad (44)$$

$$S_P \equiv +\frac{1}{U_0} \sum_{k=1}^{M} \sigma_k < 0. \qquad (45)$$

From (43) and (38) the following contributions to the Green function involved

$$H(t) \equiv -\frac{\delta\rho(t)}{E_0} = H_T(t) + H_P(t) \qquad (46)$$

are obtained;

$$H_T(0) = -S_T, \quad H_P(0) = -S_P. \qquad (47)$$

As time proceeds the contributions $H_T(t)$ and $H_P(t)$ behave differently. This is illustrated in Fig. 2. The

* Stationary pressure drops along the loop are disregarded here. Their inclusion would not introduce appreciable modifications to the results obtained.

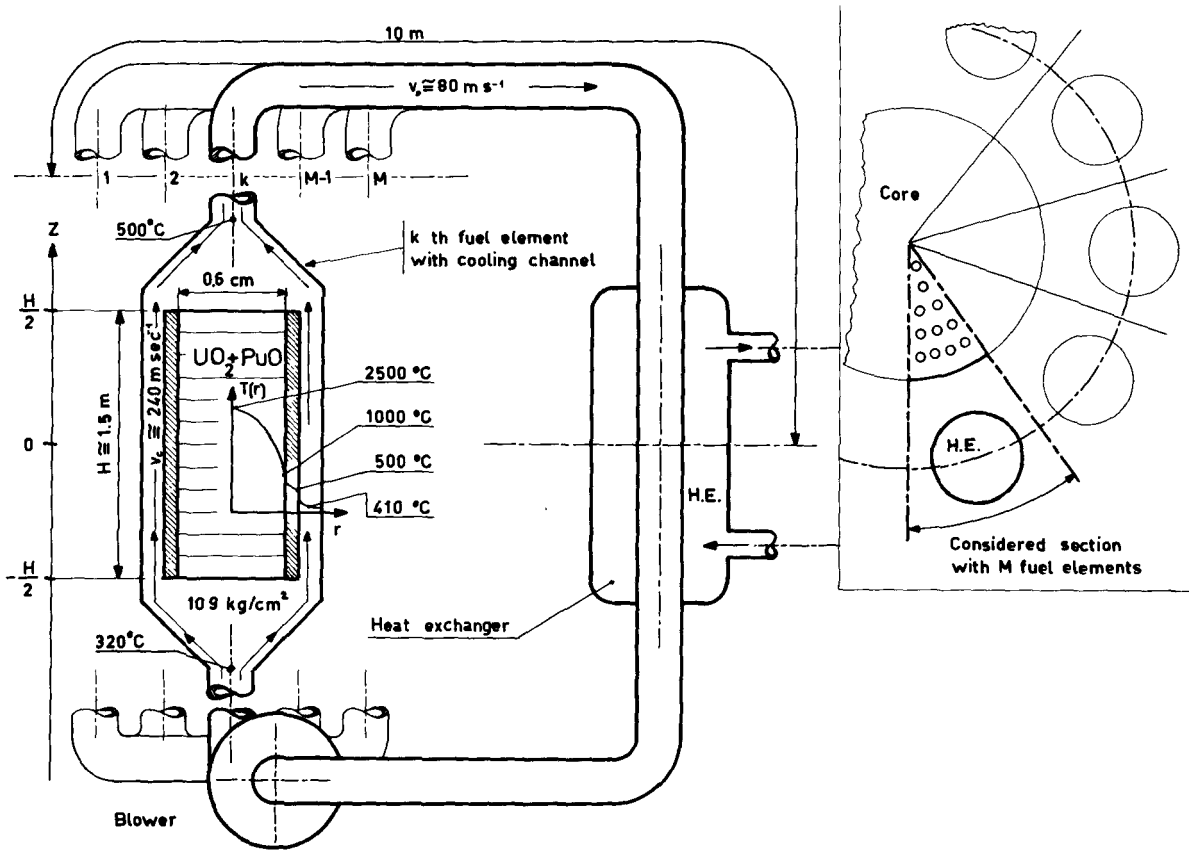


Figure 1. Representative section of reactor core and steam loop. Characteristic data are in rough agreement with published project of a 300 MW(e) steam-cooled fast breeder power plant [8]

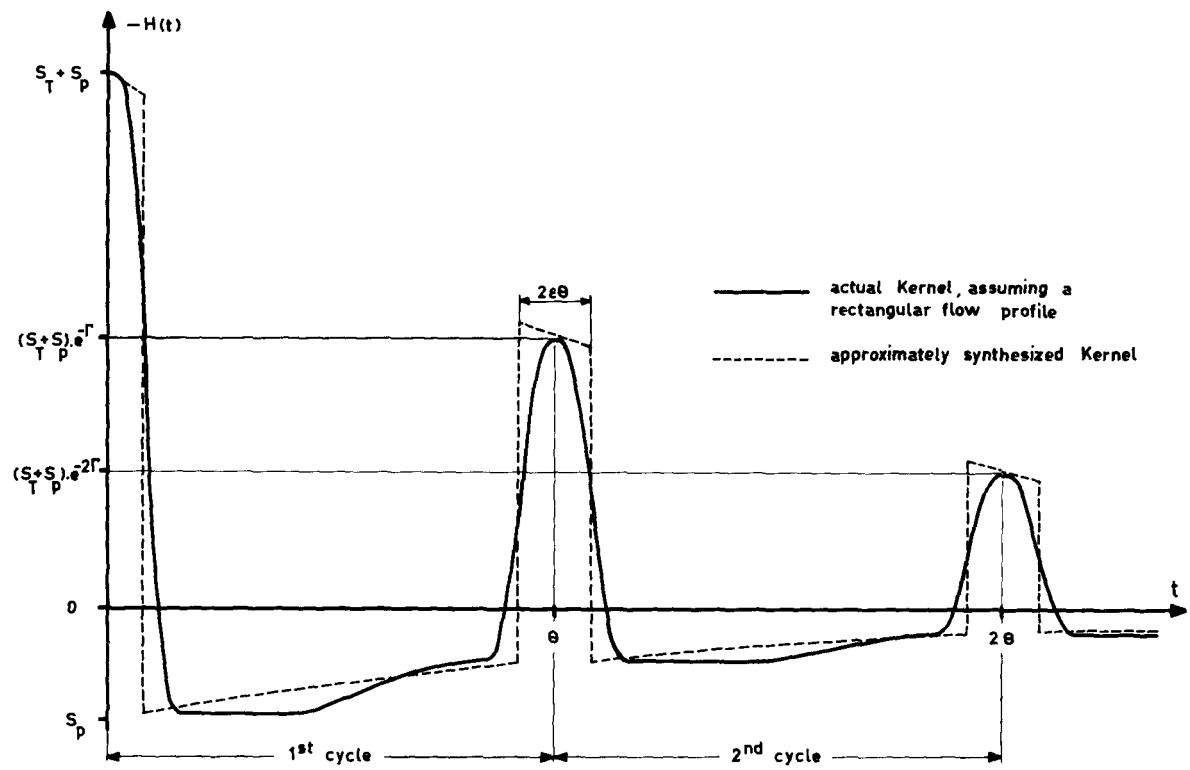


Figure 2. Partial negative feedback kernel $-H(t)$ which demonstrates the reactivity perturbation by changes of the steam density if at $t = 0$ unit thermal energy is injected into the steam surrounding the fuel elements

"hot steam plug" causing the initial effect $H_T(0)$ will soon be pushed out of the core, so that $H_T(t) = 0$ until this "plug" re-enters the core. Meanwhile the "plug" has passed the heat exchanger where the fraction $(1 - e^{-\Gamma})$ of its heat content has been removed, $H_P(t)$ decreasing then to $H_P(0)e^{-\Gamma}$. This is repeated during all the following cycles of the "hot steam plug" around the loop as illustrated in Fig. 2.* θ is the loop period, Γ designates a factor characteristic of the differential effectiveness of the heat exchanger, which is usually of the order of 1. The Laplace transforms of the approximations to $H_T(t)$ and $H_P(t)$, as indicated in Fig. 2 by dotted lines, are obtained as follows:

$$\mathcal{L}\{H_T(t)\} = \bar{H}_T(s) \approx \frac{-S_T}{s + \Gamma/\theta}\left[\frac{e^{\epsilon\theta(s+\Gamma/\theta)} - e^{-\epsilon\theta(s+\Gamma/\theta)}}{1 - e^{-\theta(s+\Gamma/\theta)}} - e^{-\epsilon\theta(s+\Gamma/\theta)} + 1\right] \tag{48}$$

$$\mathcal{L}\{H_P(t)\} = \bar{H}_P(s) \approx -\frac{S_P}{s + \Gamma/\theta}. \tag{49}$$

ϵ, as defined by the graphic approximation in Fig. 2, is roughly given by the equilibrium fraction of the mass of steam in the loop which is inside the core.

The total reactivity feedback transfer function

The Laplace transform of the reactivity feedback kernel $\bar{K}(i\omega)$ is obtained from (30), (36), (48) and (49)

$$\bar{K}(i\omega) = \bar{K}_D(i\omega) + \bar{G}(i\omega)[\bar{H}_T(i\omega) + \bar{H}_P(i\omega)]. \tag{50}$$

Its real part is given by:

$$-\mathrm{Re}\{\bar{K}(i\omega)\} = \sum_{l=1}^{L} \frac{Q_l\mu_l\theta}{\mu_l^2 + \Omega^2}\left\{D_l + \frac{S_T}{\Gamma^2 + \Omega^2}\left[(\mu_l\Gamma - \Omega^2)(C + F_2) + \Omega(\mu_l + \Gamma)F_1\right]\right\} \tag{51}$$

where

$$\Omega \equiv \theta\omega\,, \quad \mu_l \equiv \theta\nu_l\,, \tag{52}$$

$$F_1 \equiv F_1(\Omega, \Gamma, \epsilon) \equiv \left(\frac{(e^{\Gamma} - \cos\Omega)\cos h\epsilon\Gamma}{\cos h\,\Gamma - \cos\Omega} - 1\right)\sin\epsilon\,\Omega\,, \tag{53}$$

$$F_2 \equiv F_2(\Omega, \Gamma, \epsilon) \equiv \left(\frac{(e^{\Gamma} - \cos\Omega)\cos h\epsilon\Gamma}{\cos h\,\Gamma - \cos\Omega} + 1\right)\cos\epsilon\,\Omega\,, \tag{54}$$

$$C \equiv 1 + \frac{S_P}{S_T} - e^{-\epsilon\Gamma} \approx \epsilon(\Gamma - \kappa)^{**} \qquad (\kappa = Cp/C_v \approx 1.33) \tag{55}$$

The stability criterion quoted earlier could, of course, be applied immediately to (51), using the definitions (52) to (55). It is desirable, however, to sacrifice some precision in order to gain more insight into the nature of the stability conditions. In this sense the following functions are defined:

$$T(\Omega) \equiv \sum_{l=1}^{L} \frac{Q_l\,\mu_l}{\Omega^2 + \mu_l^2}\,, \tag{56}$$

$$U(\Omega) \equiv \sum_{l=1}^{L} \frac{Q_l\,\mu_l^2}{\Omega^2 + \mu_l^2}\,, \qquad X(\Omega) \equiv U(\Omega)/T(\Omega) \tag{57}$$

$$V(\Omega) \equiv \sum_{l=1}^{L} \frac{Q_l\mu_l D_l}{\Omega^2 + \mu_l^2}\,, \qquad Y(\Omega) \equiv V(\Omega)/T(\Omega)\,. \tag{58}$$

Inserting these functions into Eq. (50) and applying Smets' first stability criterion leads to:

$$\Omega^2[(C + F_2)S_T - Y] - \Omega S_T F_1[\Gamma + X] - \Gamma[\Gamma Y + S_T(C + F_2)X] \gtrless 0. \tag{59}$$

It should be noticed that F_1, F_2, X and Y are all functions of Ω, so that (59) does not seem to be a second order equation in Ω. As ϵ is of the order of 0.02 it is recognized, however, that F_2, X and Y change very slowly with varying Ω. Obviously (59) must be satisfied in the limits $\Omega \to 0$ and $\Omega \to \infty$.

This means that:

(a) *For* $\Omega \to 0$

$$Y(0) = \langle D\rangle/\bar{\tau}, \text{ where } \bar{\tau} \equiv \sum_{l=1}^{L} Q_l/\nu_l, \tag{60}$$

$$X(0) = \theta/\bar{\tau}, \tag{61}$$

* The assumption of a rectangular flow profile in the tubes of the coolant loop is, of course, a large simplification. This is surely in the sense of a conservative estimate of stability conditions.

** This approximation is rough but sufficient to demonstrate that $|C| << 1$.

$$F_2(0) \approx \frac{2}{\Gamma}\left[1+\Gamma+\frac{\Gamma^2}{12}+0(\Gamma^4)\right], \qquad (\Gamma^2<<30;\ (\epsilon\Gamma)^2<<2). \tag{62}$$

Thus, neglecting C (*cf.* Eq. (55)) against F_2;

$$S_T \lesssim \frac{-<D>\Gamma^2/2\theta}{1+\Gamma+\Gamma^2/12} \qquad (\text{for } <D> \textit{ cf.} \text{ Eq. (33)}) \tag{63}$$

(b) *For* $\Omega \to \infty$

$$Y(\infty) = \sum_{l=1}^{L} Q_l D_l \nu_l \Big/ \sum_{l=1}^{L} Q_l \nu_l \equiv \tilde{D} \tag{64}$$

$$\operatorname*{Min}_{\Omega\to\infty} F_2(\Omega) = -F_2(0) \tag{65}$$

Thus, again neglecting C against F_2;

$$S_T \lesssim \frac{-\tilde{D}\Gamma/2}{1+\Gamma+\Gamma^2/12} \tag{66}$$

(c) *For intermediate frequencies*

Obviously the "linear part" in Ω gives a negative contribution to (59) at such frequencies where $\sin \epsilon\,\Omega$ is positive. Since both Γ and X are of the order of unity and since $|F_2| > |F_1|$ the "linear term" in Ω can compete with the quadratic term in Ω only at frequencies below $\Omega = 1$. As in a typical case, ϵ is of the order of 0.02 this means that $\sin \epsilon\,\Omega$ is equivalent to $\epsilon\,\Omega$ in this "critical" domain. If F_1 is approximated, using this equivalence, then it turns out that the second term is also quadratic in Ω, but has a coefficient the magnitude of which is much smaller than the positive coefficient of the first term in (59). Therefore (59) cannot become negative if the practically inevitable condition

$$\epsilon << 1 \tag{67}$$

is satisfied.

ACKNOWLEDGEMENTS

The author is much indebted to Dr. W. Häfele, head of the Karlsruhe Fast Breeder Reactor Project, for his suggestions and his encouragement to undertake this problem. Many valuable discussions with Dr. L. Caldarola, Dr. K. Ott, E. G. Schlechtendahl, Dr. H. Soodak and Dr. D. Smidt are gratefully acknowledged. Finally the author would like to express his appreciation to the directors of this Institute, Dr. W. Zünti and Dr. A. F. Fritzsche, as well as to Professor U. Hochstrasser, delegate for Atomic Energy Affairs to the Swiss Federal Government, for their encouragement to start work connected with the development of the oxide fuelled fast breeder reactor concept.

REFERENCES

1. Popov, V. M., Automation and Remote Control, *19*, 1-7 (1958).
2. Smets, H. B., *Problems in Nuclear Power Reactor Stability*, Presses universitaires de Bruxelles (1956).
3. Schmid, P., *Desirable Properties of Linear Reactivity Feedback in Fast Nuclear Reactors*, Swiss Federal Institute for Reactor Research internal report TM-PH 125 (1963).
4. Welton, T. A., *Kinetics of Stationary Reactor Systems*, Proceedings of the First International Conference on the Peaceful Uses of Atomic Energy, P/610, Vol. 5, p. 377, United Nations (1956).
5. Kinchin, D., *The Stability of Fast Reactors*, UKAEA report AERE-RP/M 83 (1956).
6. Shotkin, M., Nuclear Sci. Eng., *18*, 271-279 (1964).
7. Popov, V. M., *Notes on the Inherent Stability of Nuclear Reactors*, Proceedings of the Second International Conference on the Peaceful Uses of Atomic Energy, P/2458, Vol. 11, p. 245, United Nations (1958).
8. Sofer, G., Hankel, R., Goldstein, L., and Birman, G., *Steam Cooled Power Reactor Evaluation. Steam Cooled Fast Breeder Reactor*, USAEC report NDA-2148-4 (1961).
9. Doetsch, G., *Anleitung zum praktischen Gebrauch der Laplace Transformation*, 2nd ed. Oldenbourg, München (1961).

ABSTRACT - RÉSUMÉ - АННОТАЦИЯ - RESUMEN

A/687 Suisse

Stabilité des piles à neutrons rapides, refroidies par vapeur et utilisant un combustible céramique

par P. Schmid

En raison de leur court temps de génération les piles à neutrons rapides peuvent être considérées comme particulièrement sûres, pourvu que la contre-réaction de réactivité soit dominée par une contribution négative prompte provenant d'effets inhérents au système. Dans les grandes piles à combustible céramique, ceci doit être assuré par le coefficient Doppler de réactivité. On sait que la stabilité peut être compromise par des contributions retardées suffisamment grandes, de l'un ou l'autre signe, à la contre-réaction totale. Il est d'autant plus nécessaire

de se rendre maître du phénomène que les piles rapides utilisant un mélange d'oxydes d'uranium et de plutonium et ayant un cœur de volume supérieur à quelques centaines de litres présentent, lorsqu'elles sont refroidies par vapeur, des coefficients cavitaires positifs appréciables. Le mémoire établit des critères de stabilité qui permettent de déterminer le rapport maximal admissible entre les valeurs absolues du coefficient cavitaire positif de la vapeur et du coefficient Doppler négatif. Deux modèles sont considérés.

Le premier modèle suppose un refroidissement suivant la loi de Fourier, avec transmission de chaleur couplée, mais néglige l'influence des parties du circuit de vapeur qui se trouvent hors du cœur. On établit des conditions nécessaires et suffisantes pour la stabilité asymptotique contre des perturbations quelconques en partant d'un théorème de Popov. Ces conditions sont:

a) Le coefficient net de puissance doit être négatif pour l'état d'équilibre;

b) Une très courte impulsion de puissance doit causer initialement une chute de réactivité;

c) La nouvelle répartition de la chaleur à la suite de l'impulsion de puissance ne doit pas provoquer de baisse subséquente de la réactivité.

En tenant compte des limitations inhérentes au premier modèle, on peut admettre que si les conditions sont satisfaites, on sera assuré contre des oscillations auto-entretenues à périodes voisines ou inférieures au temps de passage du réfrigérant à travers le cœur du réacteur.

Le deuxième modèle est plus approprié à la discussion des instabilités propres, aux fréquences intermédiaires et basses. La transmission de chaleur de l'élément de combustible à la vapeur sèche et l'influence de la partie extérieure du circuit sont traitées d'une façon générale et flexible, en choisissant un nombre de paramètres caractéristiques supposés constants, au moins à proximité de l'état d'équilibre considéré. A partir du premier théorème de stabilité donné par Smets, on établit une condition nécessaire assurant la stabilité asymptotique contre des perturbations quelconques pour un système à contre-réaction de réactivité linéaire. On obtient une simplification de cette condition lorsqu'on fait quelques approximations justifiées au vu des caractéristiques nominales publiées pour une centrale de 300 MW(e) utilisant une pile rapide surrégénératrice refroidie par vapeur; on trouve ainsi que le rapport des valeurs absolues du coefficient Doppler et du coefficient cavitaire du réfrigérant doit être supérieur ou égal à une expression simple qui ne contient que deux caractéristiques essentielles du système, à savoir un temps de relaxation moyen pour l'évacuation de la chaleur dégagée dans le combustible, et un paramètre qui indique l'efficacité d'évacuation de la chaleur hors du circuit primaire de vapeur.

A/687 Швейцария

Стабильность реакторов на быстрых нейтронах, охлаждаемых паром и использующих керамическое топливо

П. Шмид

Вследствие короткого времени жизни поколения реакторы на быстрых нейтронах могут считаться особенно надежными при условии, что вклад отрицательной мгновенной реактивности, возникающей в результате эффектов, свойственных системе, определяет обратную связь по реактивности. В крупных реакторах с керамическим топливом это обеспечивается допплеровским коэффициентом реактивности. Известно, что на стабильность может повлиять достаточно большой вклад запаздывающих нейтронов того или другого знака с общей обратной связью. Тем более необходимо использовать тот факт, что реакторы на быстрых нейтронах, использующие смесь окиси урана и плутония и имеющие активную зону объемом больше нескольких сотен литров, при охлаждении паром обладают заметными положительными пустотными коэффициентами. В настоящем сообщении устанавливаются критерии стабильности, которые позволяют определить максимально допустимое отношение абсолютных значений положительного пустотного коэффициента пара и отрицательного допплеровского коэффициента. Рассматриваются две модели.

Первая модель предполагает охлаждение в соответствии с законом Фурье со спаренной передачей тепла, но не учитывает влияния частей парового контура, находящихся вне активной зоны. Исходя из теоремы Попова, устанавливают необходимые и достаточные условия асимптотической стабильности против некоторых пертурбаций. Эти условия следующие:

а) чистый коэффициент мощности должен быть отрицательным для состояния равновесия;

б) очень короткий импульс мощности должен первоначально вызвать снижение реактивности;

в) новое распределение тепла после импульса мощности не должно вызывать последующего снижения реактивности.

Учитывая ограничения, свойственные первой модели, можно признать, что, если условия удовлетворяются, обеспечивается уверенность против регенеративных колебаний с периодами, сравнимыми или меньше времени прохождения теплоносителя через активную зону реактора.

Вторая модель больше подходит для обсуждения собственных нестабильностей с промежуточными и низкими частотами. Передача тепла от тепловыделяющего элемента сухому пару и влияние внешней части контура рассматрива-

ются в общем виде с достаточной гибкостью путем выбора ряда характерных параметров, предполагаемых постоянными по крайней мере в приближении к рассматриваемому равновесному состоянию. Исходя из первой теоремы стабильности Сметса, устанавливают необходимое условие, обеспечивающее асимптотическую стабильность против каких-либо пертурбаций для системы с линейной обратной связью реактивности. Получают упрощение этого условия, когда делают несколько оправданных приближений, принимая во внимание опубликованные упомянутые характеристики для атомной электростанции электрической мощностью 300 *Мвт* с реактором-размножителем на быстрых нейтронах, охлаждаемым паром. Таким образом находят, что отношение абсолютных значений коэффициента Допплера и пустотного коэффициента охлаждения должно быть выше или равно простому выражению, которое содержит только две основные характеристики системы, а именно: среднее время релаксации для отвода выделяющегося в топливе тепла и параметр, который показывает эффективность отвода тепла из первичного парового контура.

A/687 Suiza

Acerca de la estabilidad de los reactores de neutrones rápidos refrigerados por vapor y alimentados con combustible cerámico

por P. Schmid

En razón de su breve tiempo de generación, los reactores de neutrones rápidos pueden considerarse particularmente seguros, siempre que la contrarreacción de reactividad esté dominada por una contribución negativa inmediata proveniente de efectos inherentes al sistema. En los grandes reactores de combustible cerámico, esto debe ser garantizado por el coeficiente Doppler de reactividad. Como se sabe, la estabilidad puede ser afectada por contribuciones retardadas suficientemente grandes, de uno u otro signo, a la contrarreacción total. Por ello, es preciso tener en cuenta que los reactores rápidos alimentados con una mezcla de óxidos de uranio y de plutonio, y cuyo núcleo tiene un volumen superior a varios contenares de litros, presentan, cuando se refrigeran por vapor, apreciables coeficientes cavitarios de signo positivo. En la memoria se establecen criterios de estabilidad que permiten determinar la razón máxima admisible de los valores absolutos del coeficiente cavitario positivo del vapor y del coeficiente Doppler negativo. Se consideran dos modelos.

El primer modelo supone una refrigeración según la ley de Newton, con transmisión de calor acoplado, pero prescinde de la influencia de las partes del circuito de vapor situadas fuera del núcleo. Se definen las condiciones necesarias y suficientes para la estabilidad asintótica contra cualesquiera perturbaciones partiendo de un teorema de Popov. Estas condiciones son:

a) El coeficiente neto de potencia debe ser negativo para el estado de equilibrio;

b) Un impulso de potencia debe causar inicialmente una merma de reactividad;

c) La redistribución de calor consecutiva al impulso de potencia no debe provocar una disminución subsiguiente de reactividad.

Teniendo en cuenta las limitaciones inherentes al primer modelo, se puede admitir que siempre que las condiciones sean satisfechas, se estará a salvo de oscilaciones regeneradoras de períodos comparables o inferiores al tiempo de paso del refrigerante a través del núcleo del reactor.

El segundo modelo es más apto para el examen de las inestabilidades propias, de frecuencias intermedias y bajas. La transmisión de calor del elemento combustible al vapor seco y la influencia de la parte exterior del circuito se trata de manera general y flexible, eligiendo un número de parámetros característicos que se suponen constantes, al menos en las proximidades del estado de equilibrio considerado. Basándose en el primer teorema de estabilidad enunciado por Smets, se establece una condición necesaria que garantiza la estabilidad asintótica contra cualesquiera perturbaciones para un sistema de contrarreacción de reactividad lineal. Se obtiene una simplificación de esta condición si se procede a ciertas aproximaciones, justificadas en vista de las características publicadas para una central de 300 MW(e), alimentada por un reactor reproductor rápido refrigerado por vapor: se observa que la razón de los valores absolutos del coeficiente de Doppler y del coeficiente cavitario del refrigerante debe ser superior o igual a una expresión simple que sólo contiene dos características esenciales del sistema, a saber: un tiempo de relajación medio para la disipación del calor generado en el combustible, y un parámetro que indica la eficacia con que el calor se extrae del circuito primario de vapor.

On non-linear reactor kinetics

By E. Tunkelo*

The kinetics of nuclear reactors contain many features which do not lend themselves to description in terms of linear equations. The most important of these is related to the multiplicative nature of the chain reaction process. This leads to an exponential time behaviour which itself can be handled by linear means although any effect changing the multiplication of the reactor, e.g., the temperature dependance of reactivity, causes non-linear effects. Another source of apparent non-linearity is connected with the common practice of using lumped constant or space independent descriptions of reactor kinetics. Actually, all phenomena in the reactor are three dimensional and consequently any spatial separation between the cause of a change and its effect is manifested as non-linear behaviour in the space independent model.

There are a large number of studies of the non-linear properties of reactor kinetics [1-3]. Most of them consider a model reactor where the cooling is constant, independent of reactor power and temperature. In this paper we discuss a case in which cooling is proportional to fuel temperature. This is a fairly realistic model and gives good results when applied to reactors where the fuel elements are surrounded by light water which acts as both a moderator and a coolant. We assume additionally that the change in reactivity as the result of a change in temperature is immediate as is the case in the TRIGA reactor which was used in the experimental studies.

There are two basically different methods which can be used for studies of non-linear phenomena [4, 5]. One is the direct study of the non-linear equations governing the system and the interpretation of the properties of their solutions in terms of appropriately selected independent variables. Normally two independent variables are selected and the solutions are represented as trajectories in the so called phase space formed by them. The second approach is a direct extension of the conventional frequency response analysis or transfer function analysis of linear systems. In the non-linear case the response, however, depends on the amplitude of the input and the harmonics as well as subharmonics of the fundamental frequency which is generated in the system. Both of these approaches can be used in both theoretical and experimental studies. They will both be utilized in the present paper and some of the interrelations between them will be studied.

We limit our discussion to the non-linearities in the lumped constant description of the reactor dynamics, restricting ourselves to few remarks about possible spatial effects. The experimental studies were performed with the TRIGA Mark II reactor of the Institute of Technology, Helsinki, and the theoretical results were derived taking into consideration the particular features of this reactor, nevertheless the results will certainly have a wider applicability.

POWER EXCURSIONS FOLLOWING A FINITE INJECTION OF REACTIVITY

The space independent reactor kinetic equations when a linear negative temperature coefficient of reactivity is taken into consideration and the heat transfer from fuel to coolant is approximated with only one heat conduction term, are

$$\begin{aligned} \frac{dP}{dt} &= \frac{\Delta k_p - \alpha T}{\ell} P + \Sigma \lambda_i C_i \\ \frac{dC_i}{dt} &= \frac{\beta_i}{\ell} P - \lambda_i C_i \qquad (1) \\ C_0 \frac{dT}{dt} &= P - kT. \end{aligned}$$

In these equations P is the reactor power, C_i the delayed neutron precursor populations expressed in power units and T the average fuel temperature increase above the initial temperature. The following symbols have been used for the various parameters describing the reactor:

ℓ = prompt neutron lifetime
Δk = $\Delta k_p + \beta$ = reactivity inserted by control rods
α = negative temperature coefficient of reactivity
λ_i = delayed neutron group decay constants
λ_0 = $\Sigma \beta_i \lambda_i / \beta$ = weighted average of the delayed neutron decay constants
β_i = effective delayed neutron group yield fractions
β = $\Sigma \beta_i$ = effective delayed neutron fraction
C_0 = total fuel heat capacity
k = heat transfer coefficient from fuel to water

* Institute of Technical Physics, Institute of Technology, Helsinki.

We will study the solutions of these equations after a certain reactivity Δk is inserted in the reactor, the reactor being in the initial condition $P = P_0$, $T = 0$. The initial value of temperature can always be selected to be equal to zero compensating for a part of the inserted reactivity Δk. We plot the solution in the P-T plane as a trajectory describing the sequence of instantaneous values of P and T during the excursion.

During the initial power surge immediately after the insertion of reactivity we can neglect the delayed neutrons and the cooling term in Eqs. (1). In this case the equations can be easily integrated giving

$$P - P_0 = \frac{C_0}{\ell} \left(\Delta k_p T - \frac{\alpha}{2} T^2\right). \tag{2}$$

The maximum power reached is

$$P_p = C_0(\Delta k_p)^2/2\alpha\ell$$

and the temperature at the moment of maximum power is

$$T_p = \Delta k_p/\alpha .$$

Corrections to these values to account for the delayed neutrons have been considered elsewhere [6] and in the first approximation lead to the result that the maximum power

$$P_{max} = C_0(\Delta k_p)^2/2\alpha\ell + \frac{C_0\beta\lambda_0}{\alpha} \left(0.1932 + 2\,\frac{\beta}{\Delta k_p}\right) \tag{3}$$

is reached when the temperature is

$$T_{peak} = \Delta k_p/\alpha + 2\ell\beta\lambda_0/\alpha\Delta k_p . \tag{4}$$

After the maximum, the power decreases but does not decay to the initial value P_0 but, because of the delayed neutrons, the precursors of which were born during the pulse, attains instead an almost constant value which we obtain by setting $dP/dt = 0$ in Eqs. (1).

$$P_{tail} = \frac{\ell \sum \lambda_i C_i}{\alpha T - \Delta k_p} . \tag{5}$$

This power, evaluated elsewhere [6], is a constant, independent of the reactivity inserted:

$$P_{tail} = \frac{2C_0\beta\lambda_0}{\alpha} . \tag{5}$$

During this phase the temperature is also approximately constant:

$$T_{tail} = \frac{2\Delta k_p}{\alpha} \left[1 + 1.6449\left(\frac{k\ell}{C_0\Delta k_p}\right)^2\right]. \tag{6}$$

Subsequently, the power starts to decrease while the temperature increases until it reaches a maximum:

$$T_{max} \approx kP_{tail} = \frac{2kC_0\beta\lambda_0}{\alpha} . \tag{7}$$

Finally the power and the temperature approach values given by the asymptotic solutions of Eqs. (1).

$$T_\infty = \frac{\Delta k}{\alpha}$$

$$P_\infty = kT_\infty = \frac{k\Delta k}{\alpha} . \tag{8}$$

To study the approach to this point in more detail we start with Eqs. (1). During this phase the change of power and temperature is so slow that we can neglect the time delay of the delayed neutrons, although we must pay special attention to those delayed neutrons which are emitted by the precursors born during the maximum of the pulse. Although the precursors have decayed for several half lives the number produced is so high that the number of neutrons being emitted by them is still appreciable. We may describe these delayed neutrons by a source term which we suppose to be a constant or slowly decreasing function of time.

$$\frac{dP}{dt} = \frac{\Delta k_p + \beta - \alpha T}{\ell} P + S$$

$$C_0 \frac{dT}{dt} = P - kT . \tag{9}$$

Changing to new, dimensionless variables

$$p = (P - P_\infty)/P_\infty$$

$$u = (T - T_\infty)/T_\infty$$

and using the relationships (8) between the asymptotic quantities we obtain

$$\frac{dp}{dt} = -\alpha' u(p+1) + s$$

$$\frac{du}{dt} = k'(p-u) \tag{10}$$

where we have used the notation

$$\alpha' = \alpha T_\infty/\ell$$

$$k' = k/C_0$$

$$s = S/P_\infty .$$

Dividing the first of Eqs. (10) by the second we obtain the differential equation of the trajectories in the neighbourhood of the point $p = 0$, $u = 0$, or $P = P_\infty$, $T = T_\infty$ which is the only singular point in the P-T plane.

$$\frac{dp}{du} = \frac{-\alpha' u(p+1) + s}{k'(p-u)} . \tag{11}$$

To study the behaviour of the trajectories in the immediate vicinity of the origin we linearize Eqs. (10).

$$\frac{dp}{dt} = -(\beta' + \alpha')p - 2\alpha' u$$

$$\frac{du}{dt} = k'p - k'u \tag{12}$$

where $\beta' = \beta/\ell$. The solutions of these equations form a group of curves which converge at the origin.

To study their behaviour in more detail we evaluate the roots of the characteristic equation of (12). They are

$$-\tfrac{1}{2}(\alpha'+\beta'+k') \pm (\tfrac{1}{4}(\alpha'+\beta'+k')^2 - (\alpha'+\beta')k' - 2\alpha'k')^{\frac{1}{2}}$$

From this we see that solution is aperiodic and that the point $P = P_\infty$, $T = T_\infty$ is a node if

$$(\alpha'+\beta'+k') > 2\,(k'(\beta'+3\alpha'))^{\frac{1}{2}}, \qquad (13)$$

otherwise the solution is periodic and the point is a focus. In either case this point is, however, a stable point. For both cases the form of the trajectories is shown in Fig. 1. In most practical cases the condition given by (13) exists and there is a stable node in the *P-T* plane corresponding to the asymptotic solution of Eqs. (1). An over-all representation of the trajectories describing power excursions following different reactivity injections is shown in Fig. 2. From this we see that there is at all times only one pulse being produced by a certain reactivity injection and that the maximum power and temperature during the excursion is given by Eqs. (3) and (7). After the excursion the reactor assumes the power and temperature corresponding to the asymptotic solution (8) which is a stable situation.

EXPERIMENTAL DETERMINATION OF THE PROPERTIES OF POWER EXCURSIONS

The experimental work was done using the TRIGA Mark II reactor of the Institute of Technology in Otaniemi. For each measurement, the reactor was brought to criticality and held at a constant power level of about 1 W. After equilibrium was reached, a pneumatically operated control rod was driven out of the core to a predetermined position, giving the reactivity injection needed. The motion of the rod took less than 200 ms. The power of the reactor was subsequently measured and continuously recorded with one or more of the methods to be described later. The temperature of the fuel elements was measured with thermocouples inbedded in the fuel and recorded on a recording oscillograph.

The power produced in the reactor, which is proportional to the neutron flux, was measured during and after the reactivity injection using three different methods:

(*a*) Using an uncompensated boron coated ionization chamber, which was located at the outer surface of the graphite reflector. The current of the chamber was recorded directly without any additional amplification using an appropriate galvanometer in a recording oscillograph.

(*b*) Detecting the bluish Cerenkov radiation produced in the light water moderator surrounding the fuel elements. It is mainly due to fission product beta and gamma rays and is accordingly proportional to the rate of fission and thus to the power generated. With an optical arrangement light from the water was directed onto the photo-cathode of a photomultiplier the current of which was recorded directly and simultaneously with the same recording oscillograph that was measuring the current of ionization chamber.

(*c*) Detecting the time variation of a beam of fast (cadmium filtered) neutrons emerging from the core. Only a monochromatic group of 8 eV neutrons corresponding to the strong resonance in the samarium cross section at this energy was detected. The capture gamma rays produced in a thin samarium sample were detected using a liquid scintillator and recorded using a 512 channel time analyser having a channel width between 2 to 10 ms depending on the measurements.

From these measurements which are described in detail elsewhere [6] a trajectory of the excursion was constructed in the *P-T* plane. The family of these trajectories is shown in Fig. 3. Unfortunately one could not go further along these trajectories because the reactor automatically shuts down a few seconds after the injection of the reactivity. In any case these results are in good agreement with the theoretical results developed previously. Inability to study the later stages of the trajectory is compensated partly by the fact that the kinetic behaviour of the reactor in that part of the *P-T* plane can be studied independently using sinusoidal variations of reactivity and measuring the amplitude dependence of the frequency response of the reactor.

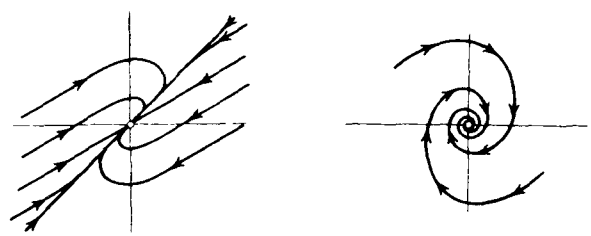


Figure 1. Trajectories in the neighbourhood of the point of asymptotic solution $P=P_\infty$, $T=T_\infty$ when there is (*a*) a node and (*b*) a focus

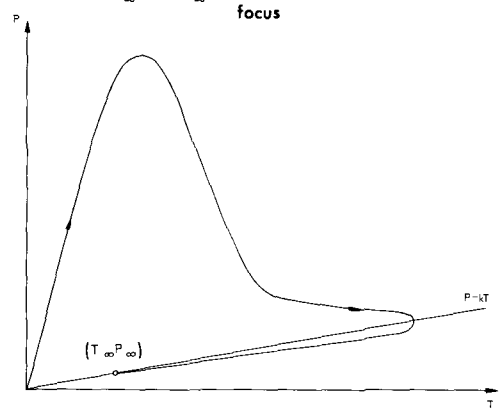


Figure 2. Trajectory of a power excursion in *P-T* plane

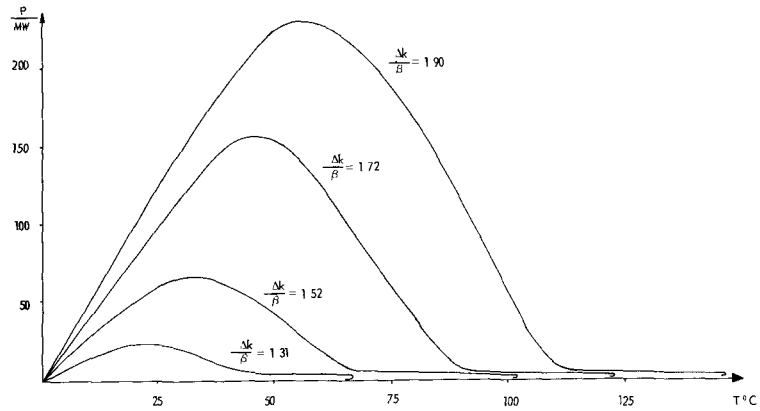


Figure 3. Experimental trajectories of power excursions produced by reactivity injections of different sizes in a TRIGA Mark II reactor

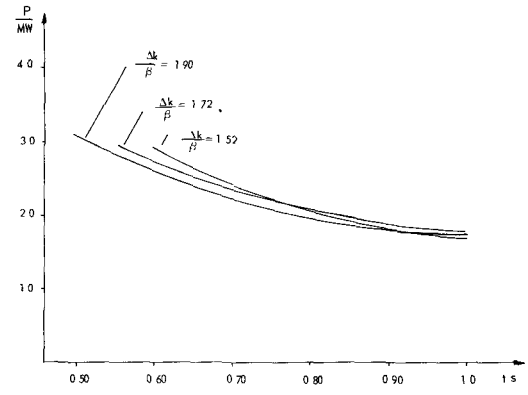


Figure 4. The power during the *tail* of a power excursion as a function of time. It is, to a first approximation, independent of the reactivity injected

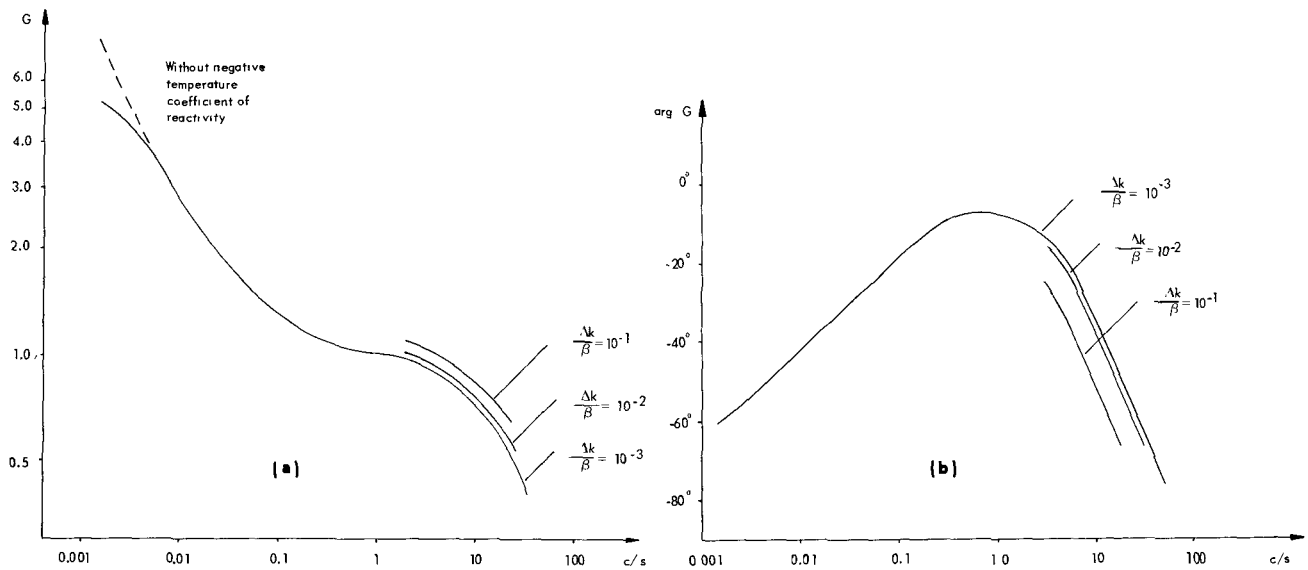


Figure 5. (a) Amplitude and (b) phase of transfer function of TRIGA Mark II reactor for different reactivity amplitudes

The tail of the pulse is very interesting. The fact that its intensity is almost independent of the reactivity injected is surprising. This fact is experimentally confirmed by the experimental results shown in Fig. 4.

RESPONSE TO SINUSOIDAL VARIATION OF REACTIVITY

The zero power transfer function i.e., the linearized transfer function of the reactor has been the subject of numerous studies [7] and is well known. In order to study the effects of the non-linearities and the effect of the negative temperature coefficient of reactivity Eqs. (1) were programmed on an analogue computer and the properties of the solutions studied.

First the transfer functions were measured using a very small reactivity amplitude in order to reproduce a linearized transfer function for reference. The effect of negative temperature coefficient was found to reduce the transfer function to a constant value for frequencies smaller than 0.002 c/s as expected. Then a series of measurements with increasing reactivity amplitudes $\Delta k/\beta$ between 10^{-2} and 10^{-1} were made. Markedly non-sinusoidal outputs were recorded and analyzed in terms of the fundamental and two lowest harmonic components. The fundamental frequency transfer function with the reactivity amplitude as a parameter is shown in Fig. 5 in terms of the amplitude and phase angle. The amplitude of the two lowest harmonics are shown in Fig. 6.

This part of the study was partly initiated by the results of Park [8] who, using a TRIGA Mark II reactor, found an anomaly in their transfer function measurements with a pile oscillator. In spite of very careful analysis of the present measurements no indication corresponding to their anomaly has been found and accordingly the conclusion is that if any such resonance exists in the experimental transfer function of the reactor concerned it is not due to the non-linearities of the reactor kinetics but must

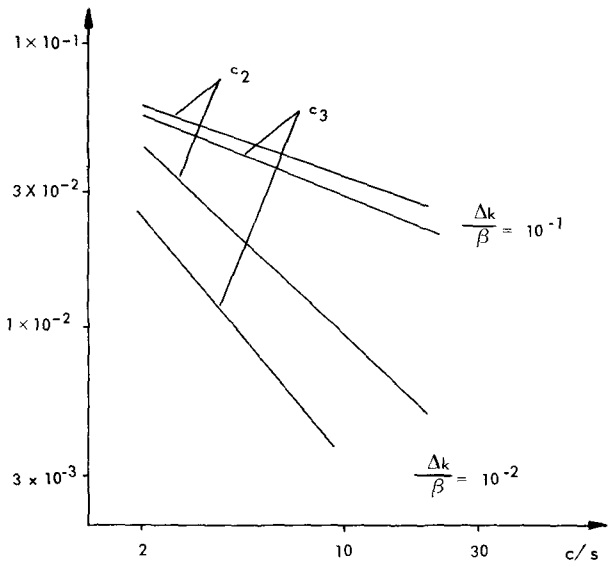


Figure 6. Amplitude of the second and third harmonic in the response of the TRIGA Mark II reactor as a function of frequency

be related to some spatial effects in the reactor core. The following mode which might produce a resonance-like peak in the transfer function at the frequency considered is suggested. The velocity of a disturbance produced in the reactor core by e.g., a pile oscillator, propagates with an average velocity

$$c = 2v(\Sigma_a D)^{\frac{1}{2}}$$

where v is the average neutron velocity, Σ_a is the macroscopic absorption cross section and D the diffusion constant of the moderator. From this we obtain an estimate of the velocity of propagation in the core of the TRIGA reactor equal to 35 m/s. If the pile oscillator and the detector are in different places in the core there is a delay between the production and detection of the disturbance. A small distance between the oscillator and detector is not enough, however, to produce the effect but the disturbance might be reflected from the graphite reflector where the velocity of propagation of the disturbance is about an order of magnitude higher. Interference of the directly arriving and reflected disturbances at the detector might be able to produce an anomaly in the transfer function at or about the frequency 20 c/s.

REFERENCES

1. Anselini, A. M., *Reactor Kinetics and Behaviour of Nuclear Power Plants under Variable Operating Conditions,* Comitato Nazionale Energia Nucleare (Italy), report RT/ING *13* (1962).
2. Nyer, W. E., and Forbes, S. G., *Dynamic Properties of Heterogeneous Water Reactors,* USAEC report IDO-16701 (1961).
3. Weinberg, A. M., and Wigner, E. P., *The Physical Theory of Neutron Chain Reactors,* University of Chicago Press, Chicago (1958).
4. Graham, D., and McRuer, D., *Analysis of Nonlinear Control Systems,* John Wiley and Sons Inc., New York (1961).
5. Mirorsky, N., *Nonlinear Oscillations,* Van Nostrand Company Inc., Princeton, N.J. (1962).
6. Tunkelo, E., *The Effect of the Delayed Neutrons on the Shape of the Power Pulse of the Triga Reactor,* Department of Technical Physics, Institute of Technology, report No. 3 (1963).
7. Proceedings of the Conference on Transfer Function Measurements and Reactor Stability Analysis, USAEC report ANL-6205 (1960).
8. Park, I. Y., *TRIGA Mark II Transfer Function Measurement and the Dynamic Analysis,* Atomic Energy Research Institute, Republic of Korea report AERI E/R-1C (1963).

ABSTRACT - RÉSUMÉ - АННОТАЦИЯ - RESUMEN

A/713 Finlande

Sur la cinétique non linéaire des réacteurs

par E. Tunkelo

Les caractéristiques non linéaires de la cinétique du réacteur, y compris l'effet du coefficient négatif rapide de température de la réactivité sont étudiés expérimentalement et théoriquement. Deux cas extrêmes sont considérés: régime transitoire après une augmentation soudaine de la réactivité et réponse en régime stationnaire lors d'une variation sinusoïdale de la réactivité. Les expériences ont été faites sur un réacteur TRIGA Mark II.

Dans les expériences sur le régime transitoire, l'asymétrie de la pulsation produite et la « queue » subséquente sont étudiées. La détermination expérimentale de la forme de l'impulsion a été effectuée par trois méthodes différentes: *a*) une chambre d'ionisation à revêtement de bore reliée à un oscillographe enregistreur; *b*) enregistrement de l'intensité de la radiation de Cerenkov dans le cœur par un photomultiplicateur muni d'un système optique approprié; et *c*) enregistrement, par un analyseur de temps multiple, de l'intensité du rayonnement gamma de capture de la résonance 8,2 eV du samarium. La théorie développée montre que les effets mesurés peuvent être décrits d'une manière satisfaisante par les propriétés des groupes de neutrons retardés et par le transfert de chaleur du combustible au modérateur à eau légère.

La réponse d'un réacteur à une variation sinusoïdale de la réactivité est étudiée en considérant des composantes fondamentales, harmoniques ainsi que sous-harmoniques; une analyse de la réponse est également présentée du point de vue de la physique. Les fonctions de transfert non linéaires du réacteur pour les grandes variations de la réactivité

sont développées et discutées du point de vue de leurs relations avec les propriétés des régimes transitoires.

A/713 Финляндия

Нелинейные переходные процессы в реакторе

Э. Тинкело

Нелинейные характеристики кинетики реактора, включающие мгновенный отрицательный температурный коэффициент реактивности, изучаются как экспериментально, так и теоретически. Рассматриваются два предельных случая: переходные процессы, вызванные мгновенным ростом реактивности, и чувствительность реактора в стационарном состоянии к синусоидальным изменениям реактивности. Эксперименты проводились на реакторе TRIGA-II.

В экспериментах по кинетике изучаются несимметрия получаемых импульсов и сопровождающие их «хвосты». Экспериментальное измерение импульсов выполняется тремя различными методами: *a*) с помощью ионизационной камеры, покрытой бором, в сочетании с записывающим осциллографом; *b*) путем регистрации интенсивности черенковского излучения в активной зоне с помощью фотоумножителя, соединенного с соответствующей оптической системой; *c*) с использованием многоканального временного анализатора для регистрации интенсивности γ-излучения, образующегося при захвате самарием нейтронов, с энергией 8,2 *эв* (резонанс самария). Развитая впоследствии теория показывает, что измеренные результаты могут удовлетворительно описываться свойствами групп запаздывающих нейтронов и передачей тепла от топлива к водяному замедлителю.

Чувствительность реактора к синусоидальным изменениям реактивности изучается для основных гармоник и некоторых компонент более низких гармоник и субгармоник. Анализ чувствительности выполнен также на основе физических концепций. Выводятся нелинейные передаточные функции в реакторе для больших амплитуд отклонения реактивности, обсуждается их отношение к свойствам переходных процессов.

A/713 Finlandia

Acerca de la cinética no lineal del reactor

por E. Tunkelo

El autor ha estudiado teórica y experimentalmente las características no lineales de la cinética del reactor, concretamente el efecto del coeficiente de temperatura negativo instantáneo de la reactividad. Ha considerado dos casos extremos: el estado transitorio producido por una adición instantánea de reactividad y la respuesta del reactor en régimen estacionario a una variación sinusoidal de la reactividad. La parte experimental del estudio se realizó con un reactor TRIGA Mark II.

En el trabajo experimental de los estados transitorios se estudió la asimetría del impulso producido y la «cola» que le sigue. La determinación experimental del impulso se efectuó por tres métodos distintos: *a*) con una cámara de ionización revestida de boro, conectada a un oscilógrafo registrador; *b*) por registro de la intensidad de la radiación de Cerenkov en el núcleo con un fotomultiplicador adaptado a un sistema óptico apropiado y *c*) empleando un analizador de tiempos multicanal para registrar la intensidad de los rayos gamma de captura neutrónica originados por la resonancia del samario a los 8,2 eV. El desarrollo teórico demuestra que las propiedades medidas pueden explicarse satisfactoriamente en función de las propiedades de los grupos de neutrones retardados y de la transmisión de calor del combustible al agua moderadora.

El autor estudia la respuesta del reactor a una variación sinusoidal de la reactividad en función del componente fundamental y de algún armónico de orden inferior, así como de componentes subarmónicos; también analiza la respuesta basándose en conceptos físicos. Deduce las funciones de transferencia no lineales del reactor para variaciones de reactividad de mayor amplitud y discute su relación con las propiedades transitorias.

Space-time reactor dynamics

By S. Kaplan, A. F. Henry, S. G. Margolis and J. J. Taylor *

During the past several years it has become both necessary and possible to describe in some detail the space-time dynamics of neutrons in assemblies of reactor materials. The necessity has arisen for two reasons. First, the current trend in power reactors is towards very large sizes for which space-time effects can become limiting design considerations. Second, certain useful experimental techniques for measuring basic reactor parameters and for verifying the adequacy of theoretical models require that space-time phenomena be accounted for, either as an essential part of the analysis or to insure that they are not perturbing the experimental conditions. The possibility of providing a detailed description of space-time effects has arisen from an improved understanding of the basic theory and from an increased capacity to determine numerical solutions to the governing equations through the use of digital computers.

The purpose of this paper is to survey and correlate the work in space-time dynamics emphasizing developments in the USA since the 1958 Geneva Conference. The next section reviews work relating to the basic mathematical theory of the reactor space-time equations; the section following that describes approximation methods for obtaining numerical solutions to these equations, and the last section discusses the applications of space-time analysis that have been made to various experiments and to the problem of xenon spatial stability.

PROPERTIES OF THE REACTOR KINETICS EQUATIONS

The space dependent and point kinetics equations

Most reactor calculations are based on group diffusion theory. According to this model, and with the assumption of stationary fuel and one type of fissionable isotope, the governing equations are:

$$[\nabla . D \nabla - A + (1-\beta)\chi_p F^T]\phi(r,t) + \sum_{i=1}^{6} \lambda_i \chi_i C_i(r,t) + q(r,t) = V^{-1}\frac{\partial}{\partial t}\phi(r,t) \tag{1a}$$

$$\beta_i F^T \phi(r,t) - \lambda_i C_i(r,t) = \frac{\partial}{\partial t} C_i(r,t)\,, \tag{1b}$$

where $\phi(\vec{r},t)$ is a column of group fluxes and the rest of the notation is explained in the appendix.

If there is no feedback, the matrix operators $\nabla . D \nabla, A, F^T$ are linear, and using their transposes the set of adjoint equations may be written

$$[\nabla . D \nabla - A^T + (1-\beta)F\chi_p^T]\phi^*(r,t) + \sum_{i=1}^{6} \beta_i F C_i^*(r,t) + q^*(r,t) = -V^{-1}\frac{\partial}{\partial t}\phi^*(r,t)$$

$$\lambda_i \chi_i^T \phi^*(r,t) - \lambda_i C_i^*(r,t) = -\frac{\partial}{\partial t} C_i^*(r,t) \tag{2}$$

To derive the point reactor kinetics equations replace the flux in (1) by the neutron density $N(r,t) = V^{-1}\phi(r,t)$. Then, introduce a weighting matrix, $W^T(r) = \text{row}\,[W^1(r) \ldots W^G(r)]$, which is for the moment considered arbitrary, and define $T(t)$ as the integral of this matrix with the density, N,

$$T(t) \equiv \int_{\text{reactor, R}} W^T(r) N(r,t)\,dr\,. \tag{3}$$

Let $\eta(r,t)$ be the ratio of N to T so that:

$$N(r,t) = \eta(r,t)T(t)\,. \tag{4}$$

Thus the neutron density is expressed as an amplitude $T(t)$ times a shape function, $\eta(r,t)$, which is itself time dependent [1]. If Eq. (1a) is now multiplied by W^T and Eq. (1b) by $W^T\chi_i$ and both integrated over the reactor the result is the point kinetics equations:

* Bettis Atomic Power Laboratory, Pittsburgh, Pennsylvania.

$$\frac{\rho-\bar{\beta}}{\Lambda}\,T(t)+\sum_{i=1}^{6}\lambda_i\int_R W^T\chi_i C_i\mathrm{d}r+\int_R W^T q\mathrm{d}r=\frac{\mathrm{d}}{\mathrm{d}t}\,T(t) \tag{5a}$$

$$\frac{\bar{\beta}_i}{\Lambda}\,T(t)-\lambda_i\int_R W^T\chi_i C_i\mathrm{d}r=\frac{\mathrm{d}}{\mathrm{d}t}\int_R W^T\chi_i C_i\mathrm{d}r \tag{5b}$$

where the parameters ρ, β, Λ are defined by:

$$\Lambda\equiv\frac{1}{F}\int_R W^T\eta\mathrm{d}r=\frac{1}{F}\qquad\bar{\beta}_i\equiv\frac{1}{F}\int_R W^T\chi_i F^T V\eta\mathrm{d}r$$

$$\rho\equiv\frac{1}{F}\int_R W^T[\nabla\cdot D\nabla-A+(1-\beta)\chi_p F^T+\sum_{i=1}^{6}\beta_i\chi_i F^T]V\eta\mathrm{d}r$$

with
$$F\equiv\int_R W^T[(1-\beta)\chi_p F^T+\sum_{i=1}^{6}\beta_i\chi_i F^T]V\eta\mathrm{d}r\qquad\bar{\beta}=\sum_{i=1}^{6}\bar{\beta}_i. \tag{6}$$

This reformulation of the space-time Eqs. (1) into the form of ordinary differential Eqs. (5) is only a formality since the unknown space shape, $\eta(\vec{r},t)$ is involved in the evaluation of the parameters (6). In those cases where the shape is constant and known during the transient the reformulation reduces the entire kinetics problem to the solution of Eqs. (5). Most often, however, it is necessary to approximate $\eta(r,t)$. Since most kinetics problems are concerned with perturbations about some steady state the usual approximation is to use the shape, $\eta_0(r)$, corresponding to the steady state. In this case it is advantageous to choose the weighting-matrix $W(r)$ as the steady state adjoint $\phi_0^*(r)$. This choice causes the first order part of the error in the computation of ρ to vanish [1, 2]. Other choices of weighting function have been made, however. These choices are discussed and compared by Gozani [3].

Meaning of the adjoint

The physical interpretation of the adjoint function is now well understood as a result of the work of Hurwitz [4] and Ussachoff [5] in the critical case, Selengut [6] and Kadomtsev [7] in the subcritical case, and Lewins [8] and Marchuk and Orlov [9] in the time dependent case. It turns out that if any inhomogeneous terms appearing either in the adjoint equation (2), or in the boundary or initial conditions, are interpreted as efficiency functions of neutron detectors, then the adjoint function evaluated at any point and time has an interpretation as the total response of these detectors to a source of neutrons introduced at that point and time.

Eigenvalue problems associated with the kinetics equations

In connection with the reactor kinetics Eqs. (1), (2), (5), it is customary to distinguish three types of eigenfunctions. The first, which we designate lambda modes, are the solutions of:

$$[-\nabla\cdot D\nabla+A]\psi(r)=\frac{1}{\lambda}\,[(1-\beta)\chi_p+\sum_{i=1}^{6}\beta_i\chi_i]F^T\psi(r)\,. \tag{7}$$

This eigenvalue problem is the type solved readily by common computer programs. The second, called "omega-p modes", corresponds to the modes of a reactor with no delayed neutron source:

$$[\nabla\cdot D\nabla-A+(1-\beta)\chi_p F^T]\psi(r)=\omega_p V^{-1}\psi(r)\,. \tag{8}$$

The third type, omega-d modes, are the natural modes of the reactor with delayed neutrons. These modes have a flux component, ψ, and delayed components, ξ_i.

$$[\nabla\cdot D\nabla-A+(1-\beta)\chi_p F^T]\psi(r)+\sum_{i=1}^{6}\lambda_i\chi_i\xi_i(r)=\omega_d V^{-1}\psi(r) \tag{9a}$$

$$\beta_i F^T\psi(r)-\lambda_i\xi_i(r)=\omega_d\xi_i(r)\,. \tag{9b}$$

Identification of these modes gives rise to questions concerning their existence, completeness, positivity and other properties. In the last few years considerable progress has been made towards answering these questions.

The situation is simplest in the case of the finite difference approximations to these defining equations. Here Birkhoff and Varga [10] have shown, for all three types of mode (and for the corresponding adjoint modes as well), that there exists a unique, positive eigenvector which corresponds to a real, simple eigenvalue. This eigenvalue, in the case of the λ modes, is larger than the absolute value of any other eigenvalue and, in the case of omega modes, is larger than the real part of any other eigenvalue. Completeness of the eigenvectors and

Table 1. Nomenclature used

ϕ^g	:	flux in energy group g
ϕ	:	col $[\phi^1 \ldots \phi^G]$: column matrix of group fluxes
D^g	:	diffusion coefficient in group g
D	=	diag $[D^1 \ldots D^G]$
Σ^g	:	total macroscopic cross section in group g
Σ^{gj}	:	scattering cross section from group j to group g $\Sigma^{gg}=0$
A	=	diag $[\Sigma^1 \ldots \Sigma^G] - [\Sigma^{gj}]$: absorption and scattering matrix
$\nu\Sigma_f^g$	:	neutrons per fission $\times$ fission cross section in group g
F^T (F transpose)	=	row $[\nu\Sigma_f^1 \ldots \nu\Sigma_T^G]$
χ_p	=	col $[\chi_p^1 \cdots \chi_p^G]$: emission spectrum for prompt neutrons
χ_i	=	col $[\chi_i^1 \cdots \chi_i^G]$: emission spectrum of delayed neutrons of type i
β_i	:	fraction of fission neutrons appearing as delayed type i
C_i	:	concentration of delayed neutron precursors of type i
λ_i	:	decay constant of precursors of type i
v^g	:	velocity of neutrons in energy group g
V^{-1}	=	diag $\left[\frac{1}{v^1}, \ldots \frac{1}{v^G}\right]$
q	=	col $[q^1, \ldots q^G]$: external source
G	:	number of energy groups
Φ	=	col $[\phi, C_1, C_2, \ldots C_6]$ combined column unknown
Φ^*	=	col $[\phi^*, C_1^*, C_2^*, \ldots C_6^*]$
q	=	diag $[V^{-1},1,1,1,1,1,1]$
Q^*	=	col $[q^*,0,0 \ldots 0]$
$\mathscr{L}$	=	$[\nabla \cdot D\nabla - A + (1-\beta)\chi_p F^T + \sum_{i=1}^{6} \beta_i \chi_i F^T]$
$\eta_k(r)$	=	col $[\eta_{k1}(r), \ldots \eta_{kG}(r)]$ basis functions for a modal analysis
σ_x	=	row $[\sigma_x^1 \ldots \sigma_x^G]$ xenon microscopic cross sections
$T(x,y,z)$	=	temperature at a point x,y,z in the reactor Steady state is denoted by subscript zero

generalized eigenvectors [11] is immediate in the finite difference case since one deals here only with matrices.

For the differential form of the group diffusion equations existence and uniqueness of the positive dominant eigenfunction and its adjoint have been proven, for the λ and ω_p cases, by Habetler and Martino [12]. In the ω_p case these authors also show, for homogeneous bare reactors and for heterogeneous but one-dimensional reactors, that the eigenfunctions and generalized eigenfunctions form a complete set.

For more exact reactor models (e.g., the transport equation), Birkhoff [13-15], using an abstract setting and hypotheses which are physically reasonable, has sketched extensions of the proofs of existence and uniqueness of the positive dominant eigenfunction and its adjoint. Important work on the nature of the spectrum of the transport operator has been done by Jorgens [16], Van Norton [17], and Lehner and Wing [18].

Very little appears to be known of the properties of the higher eigenfunctions. Such questions as: are there complex eigenfunctions? how many nodes are there in each energy group? are the nodal lines for each energy group coincident?—are virtually unexplored. However, computer codes [3, 19] have recently been developed which are capable of finding higher modes. It is to be hoped that experimentation with these codes will yield empirical and perhaps stimulate theoretical answers to these questions.

Certain properties of the higher modes are known at least qualitatively [20, 21]. For example, the omega-d modes appear to come in clusters of $6+G$ each, all members of a given cluster having roughly the same spatial shape. Of these, the ones having the G most negative eigenvalues are very closely approximated by a corresponding cluster of G omega-p modes [22]. The remaining 6 have flux components almost identical to each other and very similar to that of a corresponding lambda mode [13, 23].

Some further properties of the omega-d modes become evident if one integrates Eqs. (9) with the weighting matrix $W^T(r)$. The result of these operations is

$$
0 = \begin{array}{|cccccc|c|}
\hline
\frac{\rho-\bar{\beta}}{\Lambda} - \omega & \lambda_1 & \lambda_2 & \ldots & \lambda_6 & \langle W^T V^{-1}\psi \rangle \\
\frac{\bar{\beta}_i}{\Lambda} & -\lambda_1-\omega & 0 \ldots & & 0 & \frac{1}{\Lambda}\langle W^T, \chi_i \xi_i \rangle \\
\vdots & \vdots & \vdots & & \vdots & \vdots \\
\frac{\bar{\beta}_6}{\Lambda} & 0 & \ldots & & -\lambda_6-\omega_6 & \frac{1}{\Lambda}\langle W^T, \chi_6 \xi_6 \rangle \\
\hline
\end{array} \qquad (10)
$$

where $\rho, \Lambda, \bar{\beta}$ are defined as in (6) with ψ replacing η. Setting the determinant of this matrix to zero yields the inhour equation:

$$\frac{\rho - \bar{\beta}}{\Lambda} - \omega + \frac{1}{\Lambda} \sum_{i=1}^{6} \frac{\bar{\beta}_i \lambda_i}{\lambda_i + \omega} = 0 . \qquad (11)$$

Thus every omega-*d* eigenvalue is a root of the inhour equation. The converse however, is not precisely true. Every root of the inhour equation is not an omega-*d* eigenvalue since ψ, and thus ρ, $\bar{\beta}$, Λ, are different for each eigenvalue. However, in a one-group, uniform bare reactor model, the ψ are in fact the same for a given cluster. In reactors which are "almost" uniform bare, ψ is approximately the same for those modes corresponding to the seven most positive $\omega - d$ eigenvalues in any given cluster. If one assumes that ψ is the same for these seven modes then the seven eigenvalues satisfy not only Eq. (11) but several other interesting identities which follow from considering the eigenvectors of Eq. (10). For example, one such identity is

$$\sum_{j=1}^{7} \frac{\dfrac{\bar{\beta}_k \lambda_\ell}{(\lambda_k + \omega_j)(\lambda_\ell + \omega_j)}}{\Lambda + \displaystyle\sum_{i=1}^{6} \frac{\bar{\beta}_i \lambda_i}{(\lambda_i + \omega_j)^2}} = 0 . \qquad k \neq \ell \quad (12)$$

These identities have been found useful in interpreting pulsed source experiments [23, 24].

METHODS FOR APPROXIMATE SOLUTION OF THE KINETICS EQUATIONS

Analysis of a practical reactor transient problem requires the solution of the "physics" equation (1), along with a set of "engineering" equations describing heat transfer, coolant flow and pressure behavior. Together these constitute a cumbersome set of coupled partial differential equations which typically are to be solved for a complicated geometrical configuration. In practice it is necessary to develop approximate versions of these equations which can be solved numerically. For the engineering equations, this simplification usually takes the form of a "lumped parameter" treatment of the spatial dependence. For the physics equations the natural approach is to try to break the space-time equations into separate space equations and time equations, the space equations to be solved on digital computers (which are well suited to the geometrical complexity) and the time equations to be combined with those from the engineering model and solved either digitally, by discretizing the time variable, or by analog computer with time varying continuously.

The remainder of this section outlines the methods which have been used or proposed for accomplishing this breakdown of the physics equations.

Adiabatic method

Most reactor dynamics studies and computer programs use the point kinetics equations assuming the space shape is constant [Eq. (5) with $\eta(r, t) = \eta(r)$]. The adiabatic method [25, 26] attempts to improve on this assumption while still retaining the point kinetics formulation. The basic idea is to replace the true shape function, $\eta(r, t)$ at any instant by the fundamental lambda mode, ψ, corresponding to the reactor condition at that instant. The space part now consists of finding the ψ from static calculations and the time part consists of solving (5).

The replacement of η by ψ implies that the flux shape responds instantaneously to changes of the reactor properties. This is probably a reasonable approximation for small reactors. However, changes in shape are retarded by the delayed neutrons in the same way as are changes in the over-all power level [22, 27]; hence the application of the adiabatic approximation to large reactors is questionable.

Nodal analysis

The basic idea of this method is to view the reactor as divided into regions or "nodes" and to derive a set of time dependent equations involving the average fluxes or power at each node. The space part of the problem consists of the determination of parameters governing neutron leakage from node to node.

Finite difference techniques [28] may be considered as a limiting form of nodal analysis in which the nodes are small and closely spaced. This approach has been used for analog studies [29, 30] and digital computer programs [31, 35] that solve the space-time problems including, in some cases, temperature and flow feedback, boiling and Doppler coefficient effects [32-34, 36]. However, this approach leads to programs with long running times and therefore it has been used primarily with simplified reactor models having only one spatial variable and often only one energy group. For somewhat larger nodes a "higher order" difference approximation such as that used by Riese [37] is appropriate. Here the flux within each region is approximated by a simple function such as a polynomial.

When the nodes are few and represent gross regions of the core different concepts are needed and leakage parameters must be inferred from experiment, or from fine mesh, time independent spatial calculations. Two examples of the latter are the determination of the parameters, k_{ij}, in Avery's theory of coupled reactors [38], and the determination of the channel transfer coefficients in Wachspress' multichannel flux synthesis [39, 40].

When a nodal analysis is used it is often convenient to introduce quantities representing a reactivity for each node. Since these reactivities differ in definition from Eq. (6) the inhour equation relating them to the reactor period is in general different from Eq. (11). Modified inhour relations of this type have been used in the analyses of the Argonaut reactor by Baldwin [41], Danofsky and Uhrig [42], and in the analyses of reflected reactor

kinetics by Cohn [43] and Gamble [44]. In the latter case the modification takes the form of an additional group of delayed neutrons which the authors associate with neutrons slowed down in the reflector and returned to the core.

Modal analysis

The central idea of the modal analysis approach is to approximate the unknown function of space and time by a linear combination of known space functions (modes) with unknown time dependent coefficients. The space part of the problem is the selection or construction of the modes; the time part is the determination of the coefficients.

Of the many versions of modal analysis perhaps the most basic and common is to expand each flux and precursor group separately in a series of ordinary orthogonal functions (e.g., solutions of the Helmholtz equation). This approach is primarily suitable for one-dimensional uniform reactor models [22, 45] although it has also been applied to non-uniform and two-dimensional models [46, 47]. For more complicated models it is advisable to use modes which are more specific to the problem at hand, e.g., the lambda or omega modes [48]. Generally speaking the more effort put into finding the modes the less is required in finding the time dependent coefficients. Thus if the natural modes of the system are used, ordinarily only a few are needed and the coefficient of each may be found independently of all the others. On the other hand if Helmholtz modes are used for a typical complicated reactor configuration many modes are needed and all the expansion coefficients must be solved for simultaneously.

As mentioned earlier, the question of completeness of the lambda and omega modes is not fully settled. To the designer, however, this question is academic since for practical computations he is able to use only a small number of modes in any event. Therefore the idea has grown recently that one need not necessarily use eigenfunctions as the basis functions. Instead, one has the freedom to use any functions which intuition or experience suggest may yield an adequate approximation. Thus Dougherty and Shen [49] propose the use of Greens Function Modes obtained by solving the diffusion equations with sources fixed in various subregions of the reactor. Another suggestion [50, 51] is the use of synthesis modes which are shapes that in some sense bracket the actual shape at all times during the transient.

When the space functions such as the synthesis modes are used the usual orthogonality properties which determine the expansion coefficients are absent. Instead, one may have recourse to methods of the Galerkin [52] or weighted residual type [53]. Suppose in Eq. (1) an approximation of the form

$$N(\vec{r}, t) = V^{-1}\phi(\vec{r}, t) \approx \sum_{k=1}^{K} \eta_k(\vec{r}) T_k(t) \qquad (13)$$

is desired. This form is inserted into Eq. (1) and the resulting residual required to be orthogonal to a succession of weighting matrices, $W_j^T(r)$ for Eq. (1a) and $W_j^T(r)\chi_i$ for Eq. (1b). If we define $[F]$ as the matrix whose j, k^{th} entry is

$$\int_R W_j^T[(1-\beta)\chi_p F^T + \sum_{i=1}^{6} \beta_i \chi_i F^T] V \eta_k dr\,, \qquad (14)$$

$[\rho]$ as $[F]^{-1}$ times the matrix with entries

$$\int_R W_j^T[\nabla \cdot D\nabla - A + (1-\beta)\chi_p F^T + \sum_{i=1}^{6} \beta_i \chi_i F^T] V \eta_k dr \qquad (15)$$

and similarly for the other quantities in (6), then the result of the weighted residual process is a set of "multimode kinetics" equations

$$\Lambda^{-1}\{[\rho] - [\bar{\beta}]\} \begin{bmatrix} T_1(t) \\ \vdots \\ T_k(t) \end{bmatrix} + \sum_{i=1}^{6} \lambda_i \begin{bmatrix} \int_R W_1^T \chi_i C_i dr \\ \vdots \\ \int_R W_k^T \chi_i C_i dr \end{bmatrix} + \begin{bmatrix} \int_R W_1^T q dr \\ \vdots \\ \int_R W_k^T q dr \end{bmatrix} = \frac{d}{dt} \begin{bmatrix} T_1(t) \\ \vdots \\ T_k(t) \end{bmatrix} \qquad (16a)$$

$$\Lambda^{-1}[\bar{\beta}_i] \begin{bmatrix} T_1(t) \\ \vdots \\ T_k(t) \end{bmatrix} - \lambda_i \begin{bmatrix} \int_R W_1^T \chi_i C_i dr \\ \vdots \\ \int_R W_k^T \chi_i C_i dr \end{bmatrix} = \frac{d}{dt} \begin{bmatrix} \int_R W_1^T \chi_i C_i dr \\ \vdots \\ \int_R W_k^T \chi_i C_i dr \end{bmatrix} \qquad (16b)$$

which stand in direct analogy to Eq. (5).

These equations and the bracketing idea have been successfully tested for simple one-dimensional examples [51]. The bracketing idea has also been applied to a space variable to construct three-dimensional flux shapes using only two-dimensional calculations [51]. By this means it has been found practical to determine few-group flux shapes for a geometrical model involving several million mesh points. These facts suggest that if the idea is applied simultaneously to the space and time variables, the result will be a practical procedure for computing space-time transients in realistic, three-dimensional reactor models.

APPLICATIONS OF SPACE-TIME ANALYSIS

The need for accurate description of space-time effects can arise: (*a*) in carrying out experiments to measure some isolated reactor parameter such as the diffusion cooling coefficient, the slowing down time, etc.; (*b*) in verifying simplified models of space-time phenomena; (*c*) in designing a reactor and its control system, in predicting its transient operating behavior, and in assessing the consequences of accidents. Since the analytical approach is dictated by the feedback effects involved, the applications will be discussed accordingly.

No feedback effects

Non-multiplying media

Time dependent experiments in non-multiplying media are generally performed to measure some isolated integral parameter. Frequently the experiment is designed to pick out an effect associated with some particular spatial or energy mode. Space-time analysis is required to insure that that mode exists and that the interference of other modes is negligible.

Several analytical approaches have been investigated. For example Daitch and Ebeoglu [54] discuss the behavior of a neutron pulse in a slab moderator using a multigroup, P_L expansion. They relate the asymptotic time decay constants to the buckling, B, associated with an assumed spatial shape e^{iBx}.

The problem of the relationship between B and the physical thickness of the slab is complicated. Ferziger and Leonard [55] have attacked this by studying, for the case of isotropic scattering, the transport solution for the angular and energy dependent flux associated with the smallest decay constant. The extension of this method to the case of anisotropic scattering and to more than one dimension is difficult. Thus, although the spatial boundary conditions are accounted for naturally by attacking the transport equation directly, the expansion in Legendre components is probably a more suitable procedure for the analysis of actual experiments.

Perez and Uhrig [56] are concerned with a neutron wave experiment involving a point source of neutrons oscillating at the center of the end face of a long rectangular column of moderating material. They point out that the pulsed source and the neutron wave technique can be made to yield equivalent information. Thus the wave experiment can be used to avoid the difficulty in interpretation which occurs in the pulse experiment when the extrapolation length is an appreciable fraction of the shortest physical dimension.

In most applications of the pulsed source technique only the final asymptotic die-away constant is measured. There have, however, been exceptions. For example, Lopez and Beyster [57], for a 44.5 cm $\times$ 44.5 cm $\times$ 48.9 cm volume of light water, measure the die-away as a function of distance from the surface at which the pulse is created. Energy modes and transverse spatial modes have died out but spatial modes in the axial dimension are still present. The decay constants of four of these are inferred from the data.

Bernard *et al.* [58] have measured the time dependent spectrum of neutrons emanating from the center of a 60 cm $\times$ 62.2 cm $\times$ 71.1 cm graphite block pulsed by a 1 μs burst of neutrons. In this case the high leakage rate from the graphite causes higher spatial harmonics to die out very quickly so that the spectrum measured is composed of energy modes belonging to the fundamental spatial mode.

Multiplying media

In applying the pulse neutron technique to subcritical multiplying assemblies, considerable effort is made to measure the prompt decay constant of the fundamental ω_P mode of the system without any interference from other, faster-decaying modes. As a result there has not been strong motivation for examining space-time effects in this connection. One exception is the paper of Krieger and Zweifel [59], which extends asymptotic reactor theory to the time-dependent case and thereby provides an accurate method for computing slowing-down time for the case of bare homogeneous systems.

Krieger and Zweifel do not account explicitly for delayed neutron effects. In experiments which measure only the asymptotic die-away of the neutron flux due to prompt neutrons, delayed neutrons contribute only to the background. Garelis and Russell [24] have shown for a one-group uniform bare slab reactor that this background, despite the fact that it is composed of many modes, can be made to yield significant information which permits the determination of both ρ/Λ and β/Λ for the fundamental mode. Their method assumes that, for the mathematical model used and the physical situation examined, β/Λ is the same for all modes. For reflected or inhomogeneous assemblies, this approximation can be poor. The method will still yield the correct value $\rho - \beta/\Lambda$ for the fundamental mode; however, the precise interpretation of the individual quantities ρ/Λ, β/Λ is open to doubt [23].

A similar doubt attaches to measurement of the reactivity to power transfer function at high frequencies [60, 61]. It is not clear that either reactivity (Eqs. 6) or power can be measured at high frequencies. Moreover, even if spatially dependent transfer functions between measured observables are determined, many modes will be involved and careful planning will be necessary if interpretable data about reactor parameters or the validity of a mathematical model are to be obtained.

Fast feedback effects

Space-time transients occurring in the time range microseconds-to-minutes give rise to fast feedback

effects. Transients having time durations in the first part of this range (μs-to-ms) are usually referred to as runaways. Those in the latter part of the range generally fall into the categories of maneuvering transients (for example, change of power level) or operational accidents (for example, failure of a coolant pump).

For runaways, the primary interest is on the magnitude of the neutron concentration. As a result it is usually sufficient to describe the neutron behavior during such a runaway by the conventional kinetics equations, *provided* ρ/Λ and the β_i/Λ are computed using a flux shape approximating that during the initial phase of the runaway. The proviso is quite important if the flux shape during the runaway differs significantly from the unperturbed shape. Under these circumstances $\rho - \bar{\beta}/\Lambda$ can change by a factor of two or three depending on which shape is used to compute it. For very large reactors, a question of importance to the safety analyses is whether catastrophic local disturbances will propagate to affect all the reactor or whether the excursion (and consequent fission fragment release) will be confined to a small part of the reactor.

When maneuvering transients or operational accidents are analysed, a proper description of neutron space-time behavior can become extremely important. It is generally a requirement of a power reactor that it be capable of experiencing such transients without suffering damage. Since such requirements frequently dictate design limitations, failure to predict the effects of transients to within 20 or 30 per cent can be quite serious.

Slow feedback–xenon stability

The xenon feedback effect is the most important in the time range minutes-to-days. Instabilities and transient distortions of the spatial flux shape resulting from this effect can present a practical problem in the design and operation of large power reactors. Xenon spatial oscillations have been observed in the Shippingport reactor [62], the Savannah River reactor [63], and large graphite reactors [64]. Analyses have given qualitative agreement with the measured periods and amplitudes of the oscillations [65]. A thorough summary of operational experience with xenon instabilities and analytical studies of them may be found in a recent paper by Wilson [63].

In the analysis of xenon effects, there are two basic approaches: stability in the large and stability in the small. In the former, one considers the full governing equations with non-linear terms present and asks how the system will behave given various initial conditions. In the latter, one adopts the viewpoint of classical small vibrations theory and considers the reactor system in the vicinity of some steady operating condition. The governing equations are linearized and the natural vibration modes of the resulting linear system examined.

Two trends have been discernible in recent years. These are the replacement of highly idealized one-group, uniform bare representations [66-68] with more elaborate few-group treatments [30, 69, 70], and the appreciation of the importance of operator and plant interaction with the xenon transient. The first trend parallels the development of improved methods in reactor statics. The second follows the recognition by Beckjord [71], Lellouche [72], Margolis [73] and others [74-76] that the operator, in attempting to control a xenon oscillation, may actually make it worse.

Formulation of the xenon problem

On the time-scale of xenon oscillations, the neutron flux may be treated quasi-statically. Thus Eq. (1) is used in the form $\mathscr{L}\phi = 0$ where the delayed neutrons, the source q and the $V^{-1}\,\mathrm{d}\phi/\mathrm{d}t$ term have been omitted. To this must be added the iodine and xenon equations and equations governing the density and temperature, for example:

$$T(x,y,z) = T_{\mathrm{in}} + \int_0^z KF^{\mathrm{T}}(x,y,z')\phi(x,y,z')\,\mathrm{d}z'. \quad (17)$$

Equations describing the behavior of the inlet temperature, T_{in}, need not be explicitly considered. For any xenon concentration, T_{in} will adjust itself so that the reactor is just critical at a power level which equals the power demand, and this adjustment will take place in a short length of time compared to the time required for the xenon change.

Finally, it is necessary to describe the effects of temperature and control rods on the operator $\mathscr{L}$, and to specify the control policy. In some reactors, the policy is to observe averages, $\bar{T}_j$, of the core inlet and outlet temperatures in local regions of the reactor. If the $\bar{T}_j$ are within specified dead bands, no action is taken. If a T_j moves outside its band, the rods in that region are moved to bring $\bar{T}_j$ back to the center of the band. Stabilizing monitor and control systems have been demonstrated in practice with light water [62] and graphite moderated [64] reactors and have been designed for gas-cooled [77] and heavy moderated [78] reactors now under development.

Stability in the small

For an analysis in the small, one expresses $\phi, X, I, T_{\mathrm{in}}$ as the sum of values at the steady state and deviations from those values; e.g., $\delta\phi = \phi_0 + \delta\phi$ etc. Similarly, the operator $\mathscr{L}$ is $\mathscr{L}_0$ plus changes which are taken to be linear functions of the changes $\delta\phi$, δX etc. Thus

$$\mathscr{L} = \mathscr{L}_0 + \left(\frac{\partial \mathscr{L}}{\partial X}\right)\delta X + \left(\frac{\partial \mathscr{L}}{\partial \delta\phi}\right)\delta\phi + \left(\frac{\partial \mathscr{L}}{\partial T_{\mathrm{in}}}\right)\delta T_{\mathrm{in}} + \frac{\partial \mathscr{L}}{\partial C}\,\delta C \quad (18)$$

where for example

$$\left(\frac{\partial \mathscr{L}}{\partial \delta\phi}\right)\delta\phi = \left(\frac{\partial \mathscr{L}(x,y,z)}{\partial T}\right)\int_0^z KF_0^{\mathrm{T}}(x,y,z')\delta\phi(x,y,z')\mathrm{d}z' \tag{19}$$

δC represents the change in the control rods from their equilibrium position, and for simplicity we consider here only the case of a single control variable.

If one uses these expressions and eliminates products of deviations there results

$$\begin{bmatrix} \mathscr{L}_0 + \frac{\partial \mathscr{L}}{\partial \delta\phi}\phi_0 & 0 & \frac{\partial \mathscr{L}}{\partial X}\phi_0 \\ \frac{\gamma_I}{\nu}F_0^{\mathrm{T}} & -\lambda_I & 0 \\ \frac{\gamma_X F_0^{\mathrm{T}}}{\nu} - \sigma_x \mathbf{X}_0 & \lambda_I - \lambda_X - \sigma_X\phi_0 & \end{bmatrix} \begin{bmatrix} \delta\phi \\ \delta I \\ \delta X \end{bmatrix} = \begin{bmatrix} 0 & 0 & 0 \\ 0 & 1 & 0 \\ 0 & 0 & 1 \end{bmatrix} \frac{\partial}{\partial t} \begin{bmatrix} \delta\phi \\ \delta I \\ \delta X \end{bmatrix} - \begin{bmatrix} \left(\frac{\partial \mathscr{L}}{\partial \delta T_{\mathrm{in}}}\phi_0\right)\delta T_{\mathrm{in}} + \left(\frac{\partial \mathscr{L}}{\partial C}\phi_0\right)\delta C \\ 0 \\ 0 \end{bmatrix} \tag{20}$$

To this, in lieu of the plant description, one adds the power level constraint

$$\int_{\mathrm{R}} F_0^{\mathrm{T}}\delta\phi\,\mathrm{d}\vec{r} = 0 \tag{21}$$

and a linearized control policy relating δT_{in} to ∂C, for example $\delta C \equiv 0$ (which corresponds to a wide dead band) or $\delta T_{\mathrm{in}} \equiv 0$ (zero width dead band).

Equations (20) and (21) are the governing equations in the vicinity of the steady point. If we require the time dependence e^{pt} for all variables, then Eq. (20) (although it appears to be inhomogeneous) when taken together with constraint (21), constitutes an eigenvalue problem having solutions for only discrete values p_j. This problem defines the natural modes for the system in the small. If all the p_j have negative real parts, the reactor is stable in the small. If any have positive real parts, it is unstable.

Although no computer programs are available at present for the direct solution of this eigenvalue problem, a program does exist [69] which solves the corresponding problem for the more limited case of no temperature and control feedback. This program finds the natural modes and complex eigenvalues for a one-dimensional core by a Wieland t-type iterative process [79]. It has also been pointed out [80] that assuming the xenon and flux perturbation to be 180 ° out of phase leads to a simplified set of equations [19] which often gives quite accurate results [69].

An alternate to the direct approach is to attack the eigenvalue problem corresponding to (20, 21) by modal expansion. Many variations of this procedure are possible depending on the type of mode used [69, 81-83, 91], on whether ϕ, I and X are all expanded (or just ϕ) [84], on whether modal interaction terms are retained [85], and on whether the eigenvalues are found explicitly or whether a Nyquist type criterion is employed to determine if any lie in the right half plane [84].

Whenever an analysis in the small is used questions arise concerning its validity [86, 87]. If the linearized analysis indicates stability it does so for sufficiently small initial disturbances from the equilibrium state, but does not find the maximum permissible size of such disturbances. Conversely if the linear analysis indicates instability the initial disturbance will grow but the linear theory does not predict how much it will grow. Thus the role of analysis in the small is only to predict the onset of xenon instability. In this role, there is no practical or theoretical reason to employ anything but linear theory.

Stability in the large

Although attempts [87] have been made to apply methods of the Lyapounov type to the spatial xenon problem, most analyses in the large employ the brute force approach of programming all the equations for a computer and following the transients for various initial conditions. Both analog [68, 88] and digital [89] computers have been used for both modal and nodal treatments. When digital techniques are used, results are found to depend on the time-step length. Typically, lengthy computations involving 15 minute to one hour time-steps are required. Thus the methods given recently by Barss and Davison [70, 90] for extrapolating to zero time-step length may prove to be a valuable contribution.

In real reactors, spatial oscillations which are divergent in the linear range will eventually be limited at amplitudes which may be large or small depending upon what nonlinearities are present. Two studies [66, 88] using highly simplified models have indicated that the flux-xenon product nonlinearity by itself does not limit the amplitude of xenon oscillations until they have become fairly sizable.

CONCLUSIONS

The problems of reactor space-time dynamics may be considered to be of two types—namely, linear problems in which the neutron behavior is sought in an assembly of known nuclear properties, and nonlinear problems in which it is necessary to account for the feedback from the neutron behavior to the nuclear properties of the reactor. At the present time studies of the former category may be

said to be in a reasonably satisfactory state. The properties of the basic equations are fairly well understood, the adequacy of various approximations has been explored and the equations are supported by sufficiently accurate microscopic nuclear data to make meaningful both detailed computations and sophisticated experimentation.

This relatively clear picture becomes obscure when feedback is included. Feedback mechanisms involve a wide variety of phenomena ranging from plate expansion and void formation to the actions of the reactor operator, and the formulation and solution of analytical models for these effects is often difficult. Nevertheless simplified studies have been useful for example in describing the character of xenon oscillations, in providing stability criteria and semi-quantitative descriptions of the kinetic behavior of particular reactor systems.

With the trend to large power reactors, it is likely that space-time problems will receive greatly increased attention in coming years. Often the performance objectives of these large reactors cannot be met by designing them to be inherently stable, but rather they must be stabilized through external, spatially-dependent control. This situation adds to the need for computational tools with which the nuclear designer can follow transients on realistic three-dimensional models of his reactor. Preliminary versions and segments of such tools are already available. For example, there are now computer programs which treat the transient temperature and flow equations for reactor and external plant in considerable detail. (These usually involve empirical thermal hydraulic correlations and are presently linked to simplified treatments of the neutron equations.) In addition, there are programs for treating the neutron equations in three-dimensional detail (but without time-dependence or temperature feedback). A major obstacle to the merger of these two types of programs has been the cost of solving the three-dimensional neutron equations repeatedly as must be done for a transient calculation. However some of the approximation methods described above (in section "Methods for approximate solution of the kinetics equations") give promise of reducing this cost drastically. Also, there is continuing development of more efficient iterative processes and rapid strides in the development of faster computers. In view of these developments it is reasonable to expect that the goal of a detailed yet practical design tool for space-time kinetic studies will be attained in the near future.

REFERENCES

1. Henry, A. F., Nuclear Sci. Eng., *3*, 52 (1958).
2. Lewins, J., Nuclear Sci. Eng., *8*, 95 (1960).
3. Gozani, T., Nukleonik, *5* (2), 55-62 (1963).
4. Hurwitz, Jr., H., *Note on the Theory of Danger Coefficients*, USAEC report KAPL-98 (1948).
5. Ussachoff, L. N., *Equation for the Importance of Neutrons, Reactor Kinetics and the Theory of Perturbation*, Proceedings of the First International Conference on the Peaceful Uses of Atomic Energy, P/656, Vol. 5, p. 503, United Nations (1956).
6. Selengut, D. S., *Variational Analysis of Multi-Dimensional Systems*, USAEC report HW-59126 (1958).
7. Kadomtsev, B. B., Doklady Akad. Nauk S.S.S.R., *113*, 3 (1957).
8. Lewins, J., Nuclear Sci. Eng., *1*, 268 (1960).
9. Marchuk, G. I., and Orlov, V. V., *The Theory of Adjoint Functions*, P24, *Soviet Progress in Neutron Physics* (Krupchitskii, P. A., ed.) Consultants Bureau, New York (1963).
10. Birkhoff, G., and Varga, R. S., J. Soc. Ind. Appl. Math., *6*, 354-377 (1958); see also USAEC report WAPD-166.
11. Friedman, B., *Principles and Techniques of Applied Mathematics*, John Wiley, New York (1956).
12. Habetler, B. J., and Martino, M. A., Proc. Symp. in Appl. Math., Amer. Math. Soc., 127-139 (1961); see also USAEC report KAPL-1886 (July 1958).
13. Birkhoff, G., Proc. Symp. in Appl. Math., Vol. XI, pp. 116-126 (1961).
14. Birkhoff, G., Rendiconti di Mathematica, 1-2, Vol. 22, pp. 102-126 (1963).
15. Birkhoff, G., Trans. Amer. Math. Soc., *85*, 219-227 (1957).
16. Jorgens, K., Pure and Appl. Math., XI, 218-242 (1958).
17. Van Norton, R. N., *The Spectrum of the Neutron Transport Operator*, New York University Report, NYO-9085 (1960).
18. Wing, G. M., *An Introduction to Transport Theory*, John Wiley and Sons, New York (1962).
19. Ewen, R. L., *MULE — A FORTRAN Program for the Calculation of Three Types of Overtone Modes*, USAEC report WAPD-TM-369 (1963).
20. Weinberg and Wigner, *The Physical Theory of Neutron Chain Reactors*, U. of Chicago Press (1958).
21. Soodak, H., Proc. Symp. in Appl. Math., Vol. II, p. 238 (1959).
22. Garabedian, H. L., Proc. Symp. Appl. Math., Vol. XI, pp. 256-288 (1961).
23. Henry, A. F., *The Application of Inhour Modes to the Description of Nonseparable Reactor Transients*, USAEC report WAPD-T-1671 (1964).
24. Garelis, E., and Russell, Jr., J. L., Nuclear Sci. Eng., *16*, 263 (1963).
25. Henry, A. F., and Curlee, N. J., Nuclear Sci. Eng., *4*, 727 (1958).
26. Curlee, N. J., Nuclear Sci. Eng., *6*, 1 (1959).
27. Kaplan, S., and Margolis, S. G., Nuclear Sci. Eng., *7* (3), 277 (1960).
28. Varga, R. S., *Numerical Solution of the Two-Group Diffusion Equation in x-y Geometry*, USAEC report WAPD-159 (1956).
29. Klefer, C. N., Just, L. C., and Morehouse, Jr., N. F., Nuclear Sci. Eng., *11*, 285-289 (1961).
30. Pearce, R. M., Nuclear Sci. Eng., *11*, 328 (1961).
31. Cadwell, W. R., Henry, A. F., and Vigilotti, A. J., *WIGLE — A Program for the Solution of the Two-Group Space-Time Diffusion Equations in Slab Geometry*, USAEC report WAPD-TM-416 (1964).
32. Crowther, R. L., and Wolf, W. H., Trans. ANS, *6* (2), 210 (1963).

33. Cook, M. J., Okrent, D., Statkus, D., and Lazarus-Wells, M. B., *AX-1 — A Computing Program for Coupled Neutronics Hydrodynamics Calculations on the IBM-704*, USAEC report ANL 5977 (see also Trans. ANS, *2*, 1 (1959)).
34. Tiller, R. E., and Oster, C. A., *CLUMSY-1 — A Time and Space Dependent Reactor Kinetics Code for the IBM-7090 Computer*, USAEC report HW-77221.
35. Agresta, J., Nuclear Sci. Eng., *7*, 64-68 (1960).
36. Curtis, A. R., Tyror, J. G., and Wrigley, H. E., *STAB — A Kinetic Three-Dimensional One-Group Digital Computer Program*, UKAEA AEEW report 77 (1961).
37. Riese, J. W., *VARIQUIR — A Two-Dimensional Time Dependent Multigroup Diffusion Code*, USAEC report WANL-TNR-133 (1963).
38. Avery, R., *Theory of Coupled Reactors*, Proceedings of the Second International Conference on the Peaceful Uses of Atomic Energy, P/1858, Vol. 12, p. 182, United Nations (1958).
39. Wachspress, E. L., Burgess, R. D., and Baron, S., Nuclear Sci. Eng., *12*, 381-389 (1962).
40. Wachspress, E. L., *Digital Computation of Space-Time Variation of Neutron Fluxes*, USAEC report KAPL-2090 (1960).
41. Baldwin, G. C., Nuclear Sci. Eng., *6*, 320 (1959).
42. Danofsky, R. A., and Uhrig, R. E., Trans. ANS, *3* (1), 119 (1960), Nuclear Sci. Eng., *16*, 131 (1963).
43. Cohn, C. E., Nuclear Sci. Eng., *13*, 12-17 (1962).
44. Gamble, D. P., Trans. ANS, *3* (1), 122 (1960).
45. Kaplan, S., Margolis, S. G., and Harris, D. R., *Transient Response of the Spatial Flux Distribution in an Initially Uniform Bare Reactor to Arbitrary Nonuniform Changes in Materials Properties*, USAEC report WAPD-BT-17, 69-83 (1960).
46. Garabedian, H. L., and Thomas, D. H., Nuclear Sci. Eng., *14*, 266 (1962).
47. Garabedian, H. L., and Lynch, R. E., *Non Linear Reactor Kinetics Analysis*, General Motors Corporation Report, GMR-416.
48. Cohn, R., *Some Topics in Reactor Kinetics*, Proceedings of the Second International Conference on the Peaceful Uses of Atomic Energy, P/629, Vol. 11, p. 302 (1958).
49. Dougherty, D. E., and Shen, C. N., Nuclear Sci. Eng., *13*, 141-148 (1962).
50. Bewick, J., Henry, A. F., and Kaplan, S., Trans. ANS, *5* (1), 177-178 (1962).
51. Kaplan, S., Marlowe, O. J., and Bewick, J., Nuclear Sci. Eng., *18*, 2 (1964).
52. Kantorovich, L. V., and Kryloff, V. I., *Approximate Methods of Higher Analysis*, Interscience, New York (1959).
53. Crandall, S. H., *Engineering Analysis*, McGraw-Hill (1956).
54. Daitch, P. B., and Ebeoglu, D. B., Nuclear Sci. Eng., *17*, 212 (1963).
55. Ferziger, J. H., and Leonard, A., Trans. ANS, *6*, 290 (1963).
56. Perez, R. B., and Uhrig, R. E., Nuclear Sci. Eng., *17*, 90 (1963).
57. Lopez, W. M., and Beyster, J. R., Nuclear Sci. Eng., *12*, 190 (1962).
58. Barnard, E., Khan, N. A., McLatchie, R. C. F., Poole, M. J., and Tait, J. H., Nuclear Sci. Eng., *17*, 513 (1963).
59. Krieger, T. S., and Zweifel, P. F., Nuclear Sci. Eng., *5*, 21 (1959).
60. Loewe, W. E., Trans. ANS, *6*, 215 (1963).
61. Hansson, P. T., and Foulke, L. R., Nuclear Sci. Eng., *17*, 528 (1963).
62. Leonard, J. H., *Nuclear Behaviour of the Shippingport Reactor Through Three Seeds*, Trans. ANS, 5 (1), 136 (1962).
63. Wilson, J. V., Nuc. Safety, Vol. 5 (3), 124.
64. Fullmer, G. C., *Xenon Instability in Graphite Reactors*, USAEC report HW-69084 (1961).
65. *PWR Technical Progress Reports*, USAEC reports WAPD-MRP-97, WAPD-MRP-104, WAPD-MRP-106 (February 1962-October 1963).
66. Randall, D., and St. John, D. S., Nucleonics, *16*, 3 (1958).
67. Ward, A. G., *The Problem of Flux Instability in Large Power Reactors*, Atomic Energy of Canada Ltd. report CRRP-657 (AECL-345) (1956).
68. Henry, A. F., and Germann, J. D., Nuclear Sci. Eng., *2*, 4 (1957).
69. Ewen, R. L., Trans. ANS, *5*, 179 (1962).
70. Barss, W. M., *Digital Simulation of Xenon Instability in Reactors*, AECL report (AECL-1226) (1961).
71. Beckjord, E. S., and Harker, W. H., USAEC report ANL-6205 (1960).
72. Lellouche, G. S., *Control of Xenon Spatial Oscillations*, USAEC report BNL-6330 (1962).
73. Margolis, S. G., *Operator Induced Xenon Oscillations*, USAEC report WAPD-BT-29 (1963).
74. Harris, D. R., Internal Communication, June 1962.
75. Hitchcock, A., *Nuclear Reactor Stability*, London, Temple Press, 35-46 (1960).
76. Fonda, A., Nuclear Power, *5* (49), 93-96 (1960).
77. Carstairs, R. L., and Taylor, R. W., *The Occurrence and Control of Spatial Instabilities in Large Reactors*, GEC Atomic Energy Review, *2* (2), 89-97 (1959).
78. Sidall, E., *Reactivity Control in the CANDU Reactor*, AECL report AECL-1692 (1963).
79. Wachspress, E. L., Nuc. Sci. Eng., *8*, 164-170 (1960).
80. Harris, D. R., and Lacy, P. S., Trans. Am. Nuc. Soc., *3* (2), 437-438 (1960).
81. Lellouche, G. S., Nuclear Sci. Eng., *12*, 482-489 (1962).
82. Shotkin, L. M., and Abernathy, F. H., Nuclear Sci. Eng., *15*, 2 (1963).
83. St. John, D. S., *Reactor Stability Report*, USAEC report DP-517, E. I. du Pont de Nemours and Co., 82 (1960).
84. Margolis, S. G., Trans. ANS, *3* (2), 437 (1960).
85. Gyorey, G. L., Nuclear Sci. Eng., *13*, 338-344 (1962).
86. Chernick, J., Lellouche, G., and Wollman, W., Nuclear Sci. Eng., *10* (2), 120 (1961).
87. Lundquist, S., and Weissglass, P., Nuclear Sci. Eng., *15* (4), 474 (1963).
88. Margolis, S. G., and Kaplan, S., Trans. ANS, *3* (1), 183 (1960).
89. Barss, W. M., *Digital Simulation of Xenon Instability in Reactors*, AECL report CRRP-1002 (1961).
90. Davison, B., *Correction for Non-Zero Time Step in the Numerical Simulation of Spatial Xenon in a Nuclear Reactor*, AECL report (AECL-1292) (1961).
91. Mochizuki, K., and Takeda, A., Nuclear Sci. Eng., *7* (4), 336 (1960).

ABSTRACT - RÉSUMÉ - АННОТАЦИЯ - RESUMEN

A/271 Etats-Unis d'Amérique

Dynamique d'un réacteur dans l'espace et dans le temps

par S. Kaplan *et al.*

Pour pouvoir extraire de la chaleur d'un réacteur avec un bon rendement et en toute sécurité, il faut que les bureaux d'études puissent calculer de façon détaillée la distribution spatiale de la puissance. En principe, ils devraient pouvoir calculer cette distribution pour tous les moments de la vie du réacteur, pour toutes les conditions de fonctionnement statiques et transitoires, et pour divers états transitoires accidentels possibles. Dans la pratique, il n'existe pas de moyens de calcul permettant de le faire; au contraire, dans les études de réacteur, on représente généralement ce dernier par un modèle à une ou deux dimensions et, pour les calculs d'états transitoires, on le représente souvent par un seul point dans l'espace.

On s'était contenté jusqu'à présent de cette approximation, mais le besoin se fait de plus en plus sentir d'un traitement plus précis des effets spatiaux, tant dans les calculs statiques que dans les calculs dynamiques. Cela découle en partie de la tendance vers les réacteurs de très grandes dimensions dans lesquels les effets spatiaux deviennent significatifs. Dans les grands réacteurs, les courbes de puissance tendent à accuser de grandes distorsions sous l'effet de petites perturbations. Ces courbes dépendent fortement des conditions d'exploitation et de la gestion du combustible; elles peuvent osciller spontanément à la suite d'une rétroaction due au xénon.

Le mémoire évalue l'importance des problèmes espace-temps dans les études de réacteur, énumère les méthodes analytiques et les instruments de calcul utilisables, présente les données expérimentales pertinentes, décrit les nouveaux instruments de calcul étudiés ou mis au point et indique comment on pourrait les vérifier à l'aide d'une série d'expériences sur réacteur. Il classe et compare les différentes méthodes analytiques.

Il y a trois manières de traiter le problème de la stabilité sous l'effet xénon. La première consiste à étudier les équations linéarisées qui décrivent le système au voisinage immédiat d'un point d'équilibre et à déterminer des critères de stabilité pour ce point. La deuxième méthode consiste à étudier de grandes régions de l'espace des états, par exemple par des méthodes du type Lyapunov, pour chercher des cycles limites, des régions de stabilité asymptotique, etc. Enfin, on peut faire un calcul détaillé d'un état transitoire dû au xénon en observant sa formation et sa désintégration. On a alors le choix entre la méthode brutale qui utilise un code de diffusion-appauvrissement avec de petits échelons de temps et la méthode de la représentation approximative de la dépendance par rapport à l'espace (décrite plus loin) complétée par un traitement analogique ou numérique de la dépendance par rapport au temps.

On peut considérer le calcul des états transitoires généraux espace-temps comme comprenant trois opérations simultanées. La première consiste à résoudre les équations des neutrons pour déterminer la distribution de la puissance instantanée. La deuxième est la résolution des équations du flux thermique et du fluide de refroidissement pour déterminer la distribution des températures et des densités à partir de la distribution de la puissance. La troisième consiste à calculer la section efficace nucléaire, c'est-à-dire les coefficients des équations nucléaires, à partir de la température et de la densité instantanées.

Il ne saurait être question actuellement de faire des calculs avec une description spatiale détaillée à trois dimensions; aussi s'intéresse-t-on surtout aux méthodes d'approximation de la dépendance par rapport à l'espace. Les auteurs distinguent quatre méthodes: *a*) la méthode adiabatique; *b*) la méthode des différences d'ordre supérieur ou méthode de la cellule; *c*) l'analyse nodale; *d*) l'analyse modale. Ils les décrivent et donnent des exemples de calculs.

A/271 США

Динамика реактора во времени и пространстве

Дж. И. Тайлор *et al.*

Чтобы безопасно и с наименьшими потерями отвести тепло из ядерного реактора, конструктор должен детально рассчитать пространственное распределение энерговыделения. Теоретически он должен рассчитать это распределение на все время существования реактора при всех статических и переходных режимах и при всяких случайных переходных процессах. Практически нет таких расчетных средств, которыми он мог бы эти распределения получить. Вместо этого конструктор делает свои расчеты при помощи одно- или двухразмерной модели, а переходные процессы он часто рассчитывает при помощи точечной модели.

В связи с все возрастающим интересом к более точному изучению пространственного эффекта в статических и в переходных случаях эти методы не дают необходимой точности. Частично это объясняется стремлением к строительству более крупных энергетических реакторов, в которых пространственные эффекты приобретают важную роль. В больших реакторах кривые энерговыделения склонны к боль-

шим искажениям при маленьких возмущениях. Кривые энерговыделения зависят в большой мере от рабочего режима и топливного цикла и могут спонтанно колебаться в результате обратной связи, возникающей при отравлении ксеноном.

Дается оценка значения задач пространства и времени при проектировании реактора. Рассматриваются аналитические методы и методы расчетов для решения указанных задач и соответствующие экспериментальные данные. Описываются новые планируемые или разрабатываемые методы расчетов и указываются возможные способы проверки этих методов путем тщательных экспериментов в реакторе. Определяются и классифицируются разные аналитические подходы и указываются связи этих подходов.

Имеются три подхода к решению задачи устойчивости ксенона. Первый подход — это так называемый подход в малом размере. При этом методе конструктор рассматривает линейные уравнения, которые описывают систему в близи от точки равновесия, а потом пытается получить критерии устойчивости для этой точки. Пользуясь вторым подходом, конструктор проверяет большие объемы пространственного состояния и, наверное, применяет при этом методы, похожие на методы Ляпунова, чтобы найти предельные частоты, области асимптотической устойчивости и т. д. В третьем можно точно рассчитать нестационарное отравление ксеноном, наблюдая его накопление и распад. При этом можно использовать метод грубой силы, то есть применить код диффузии — истощения с короткими промежутками времени или применить приблизительное представление пространственной зависимости, как описывается ниже, с последующей цифровой или аналоговой обработкой временной зависимости.

Можно рассматривать расчеты простых переходных случаев в пространстве и времени как состоящие из трех отрезков с одновременно происходящими действиями. Во-первых, надо решить уравнения нейтронов, чтобы установить мгновенное распределение энергии. Во-вторых, зная распределение энергии, разрешить уравнения теплового потока и теплоносителя, чтобы установить температуры и плотности распределения. Третий отрезок — это расчет ядерного сечения, то есть коэффициентов ядерных уравнений, на основе значений мгновенной температуры и плотности.

Выполнение этих расчетов с подробным описанием пространства в трех размерах сейчас не возможно, и поэтому главный интерес направлен на методы аппроксимации пространственной зависимости. Различаем четыре метода: a — адиабатический; b — разностный метод высшего порядка, или ячеечный; c — узловой анализ и, d — анализ рабочего режима. Описываются эти методы и приводятся примеры расчетов.

A/271 Estados Unidos de América

Dinámica espacial y temporal de reactores

por S. Kaplan *et al.*

Para extraer de un modo eficaz y seguro el calor de un reactor nuclear, el proyectista debería poder calcular la distribución espacial detallada de la generación de potencia. En principio, debería poder hacerlo para cualquier instante de la vida del reactor, para todas las condiciones estáticas y transitorias de funcionamiento y para los diversos transitorios accidentales que se postulen. En la práctica no se ha podido disponer de métodos que permitan realizar este programa por lo que, en los cálculos de estática, se representa el reactor por un modelo uni o bidimensional y en los cálculos de transitorios se representa frecuentemente por un solo punto espacial.

Hasta ahora, tales métodos han sido suficientes. Sin embargo, hay un interés creciente en tratar con más precisión los efectos espaciales en los cálculos dinámicos y estáticos. Esto se debe en parte a la tendencia a construir grandes reactores de potencia, en los que los efectos espaciales llegan a ser importantes. En los reactores grandes, pequeñas perturbaciones originan grandes distorsiones en la distribución de potencia. Esta tiende a depender considerablemente de las condiciones de funcionamiento y de los ciclos de combustible y puede oscilar espontáneamente debido a la realimentación del xenon.

El documento evalúa la importancia de los problemas espacio-temporales en el diseño del reactor, se examinan los métodos analíticos y de cálculo disponibles para su investigación, se revisan los datos experimentales pertinentes, se describen nuevos medios de cálculo que se están desarrollando o se encuentran en estudio, y se indican las posibilidades futuras para comprobar estos métodos mediante experimentos detallados de reactor. En la discusión se clasifican y relacionan entre sí los diferentes métodos analíticos.

Hay tres maneras de abordar el problema de la estabilidad del xenon. La primera es la de la "estabilidad en pequeñas regiones", que parte de las ecuaciones linealizadas que describen el sistema en la proximidad de un punto de equilibrio y pretende así obtener criterios para la estabilidad de este punto. En la segunda, se examinan grandes regiones del espacio de estados, posiblemente con métodos del tipo de Lyapunov, para buscar ciclos límites, regiones de estabilidad asintótica, etc. En la tercera, se intenta calcular detalladamente un transitorio del xenon, observando su crecimiento o decaimiento. Esto puede hacerse por el método de la "fuerza bruta", empleando un código de difusión y de quemado con pequeños intervalos de tiempo, o bien empleando una representación aproximada de la dependencia espacial (como se describe más adelante), y un tratamiento analógico o digital de la

dependencia temporal. El cálculo de los transitorios espacio-temporales se puede considerar como resultado de tres procesos simultáneos. El primero, es la resolución de las ecuaciones neutrónicas para determinar la distribución instantánea de potencia. El segundo, es la resolución de las ecuaciones de transmisión de calor y del movimiento del refrigerante para determinar las distribuciones de temperatura y densidad, conociendo la distribución de potencia. El tercero, es el cálculo de las secciones eficaces, es decir, los coeficientes de las ecuaciones nucleares, partiendo de la temperatura y de la densidad instantáneas.

Actualmente, no cabe pensar en efectuar estos cálculos con una detallada representación tridimensional, por lo que se ha dado más importancia a los métodos que aproximan la dependencia espacial. Distinguimos aquí cuatro métodos: *a*) método adiabático; *b*) método de las diferencias de orden superior o método de la celda; *c*) análisis nodal y *d*) análisis modal. Estos métodos se describen e ilustran con el cálculo de algunos ejemplos.

Stochastic processes in nuclear reactors and measurement of dynamic performance characteristics

By J. A. Thie*

An area of reactor technology which has grown rapidly within the last few years is that of the utilization of intrinsic stochastic processes or "noise" in reactors to give information about their dynamic properties. A wealth of experience has accumulated in this field [1-2].

METHODS

In reactor applications it is often desired to obtain information such as system time constants, resonant frequencies, and stability indicators. Stochastic signals from ion chambers, thermo-couples, etc., are a source of this information. A large number of different experimental methods for extracting this information have been introduced and proven out in practice. These are listed in Table 1.

As with other experimental methods of reactor dynamics, one may work either in the time or in the frequency domain. If $n(t)$ is a randomly varying function of time to be investigated, one may work directly with it. Alternatively, one may consider it to be a superposition of various frequencies

$$n(t) = \int n(f) \exp(i\omega t)\, \mathrm{d}f \qquad (1)$$

and work with the Fourier amplitude $n(f)$. The latter approach is used more often. Table 2 shows the specific functions of time or frequency which have been utilized in reactor noise analysis. The end results of the methods in Table 1 as manifested by quantities in Table 2 in general must be compared with theory in order to obtain an understanding of the dynamics of the reactor being studied.

To select from these methods the one most suitable in a given situation involves compromises among results desired, accuracy, cost, and experimental convenience. The following is a list of some of the more significant considerations:

(*a*) The source of the stochastic process may be intrinsic to the reactor itself. An ion chamber or some other transducer may indeed provide a time function containing adequate signal information in the time or frequency range of interest. In zero power reactors, an in-core or nearby detector giving one event per 10 000 or less fissions is required to exceed inherent detector noise; the requirements are much less stringent in power reactors. Otherwise external excitation by random (or, more customarily, periodic or step) functions is needed—such as the pseudorandom binary reactivity signal excitation of KIWI A3 [3];

(*b*) The information desired, together with theoretical considerations, determines whether one or more than one signal is needed for analysis. For information about the source of the stochastic fluctuations in reactor power, analysis of coolant temperature, flow, etc., may be needed;

(*c*) Digital techniques generally offer greater flexibility than analog methods. However, when a fixed type of analysis is performed repeatedly it is more economical and efficient to use a continuous or analog data processing method;

(*d*) The precision of the results generally varies as $T^{-\frac{1}{2}}$, where T is the duration of $n(t)$ available for analysis. Its Fourier spectrum $n(f)$ can be determined at frequencies Δf, $2\Delta f$, $3\Delta f$, . . . , etc., with reasonable precision if the resolution of $\Delta f \gg 1/T$;

(*e*) It is advantageous to search for information over a restricted frequency range, such as near f_0 (or, correspondingly, to seek time constants near $\tau = 1/2\pi f_0$). The resolution is chosen adequately below f_0, but not too far below. Frequencies below Δf are advantageously omitted, and similarly frequencies above some f_1 (which is a few times f_0) are also omitted or filtered out.

ZERO POWER REACTORS

From a Laplace transform solution of the neutron kinetics equations in which the source function is taken to be a noise spectrum $S(f)$ one obtains

$$\left|\frac{n(f)}{S(f)}\right|^2 = \left[1 + \frac{1}{\omega^2 \bar{\lambda}^2}\right] \frac{\left[\frac{(1-\beta)k_{\mathrm{eff}}-1}{\ell}\right]^2}{\omega^2 + \left[\frac{(1-\beta)k_{\mathrm{eff}}-1}{\ell}\right]^2} \qquad (2)$$

where $\bar{\lambda}$ is the average decay constant of the six delayed neutron groups, $\omega = 2\pi f$, β is the effective delayed neutron fraction, ℓ the neutron lifetime and k_{eff}, though equal to unity in critical systems, may

* Consultant, Minneapolis, Minnesota.

Table 1. Experimental methods used in the investigation of stochastic processes in reactors [2]

Detectors	Method	Reactors investigated
Two counters	Rossi alpha delayed coincidence	Cornell University Reactor, Godiva 1, ZPR3, ZPR5
Counter	Variance from gate-scaler	Ford Nuclear Reactor, SPERT2 ZPR4', ZPR5
Ion chamber	Variance from integrated currents	ZPR4'
Regulating rod	Variance from integrated positions	ATSR
Ion chamber	Spectrum from digitized charts	BORAX 4, EBWR, Elk River, Iowa State UTR10, VBWR
Ion chamber	Spectrum from an electronic analyzer	BSR1, BSR2, Dresden, EBWR, Indian Point, KEWB, ML1, N.S. *Savannah* Critical, N.S. *Savannah* Reactor, ORNL Pool Critical Assembly, Saxton, SRE, TTR, University of Florida Training Reactor, Westinghouse Critical Experiment Station, Yankee, ZPR3, ZPR4', ZPR5, ZPR7, Argonaut
Ion chamber	Probability counts of chart events	BORAX 1, BORAX 2, BORAX 4, HRE2, TRX
Ion chamber	Cross correlation of power and control rod's random position	Brookhaven Neutron Source Reactor, Godiva 2, KIWI A3, University of Florida Subcritical Assembly
Gamma chamber	Spectrum from an electronic analyzer	Dresden
Thermocouples, Ion chamber, Flowmeter	Spectra and cross correlations from an electronic analyzer	Saxton, SNAP
Thermocouples, Ion chamber, Flowmeter	Spectra and cross correlations from digitized charts	Elk River, VBWR

Table 2. Time and frequency functions commonly used in stochastic analyses

Function	Definition [a]
Autocorrelation function	$\phi(\tau) = \frac{1}{T}\int_{-T/2}^{T/2} n(t)n(t-\tau)\mathrm{d}t$
Standard deviation	$\sigma = \phi(0)^{\frac{1}{2}}$
Cross correlation function	$\phi_{n\theta}(\tau) = \frac{1}{T}\int_{-T/2}^{T/2} n(t)\theta(t-\tau)\mathrm{d}t$
Variance	$\overline{c^2} - (\bar{c})^2 = \frac{1}{N}\sum_{1}^{N} c_i^2 - \left[\frac{1}{N}\sum_{1}^{N} c_i\right]^2$
Spectrum [b]	$\lvert n(f)\rvert^2 = \left\lvert \int_{-T/2}^{T/2} n(t)\exp(-i\omega t)\mathrm{d}t \right\rvert^2$
Cross-spectrum	$\mathrm{n}(f)^*\theta(f) = \int_{-T/2}^{T/2} n(t)\exp(i\omega t)\mathrm{d}t \int_{-T/2}^{T/2} \theta(t)\exp(-i\omega t)\mathrm{d}t$

[a] Random functions $n(t)$ and $\theta(t)$ are taken to have a zero mean value; c_i is a random sequence.
[b] Alternatively $\lvert n(f)\rvert^2$ may be defined in terms of the cosine transform of $\phi(\tau)$.

be significantly less than unity in the case of subcritical reactors. Thus, by measuring the spectrum of a zero power assembly at frequencies near $f_0 = [(1-\beta)k_{\mathrm{eff}} - 1]/2\pi\ell$ one may evaluate β/ℓ, k_{eff}, or both.

One of the most practical applications of noise analysis to zero power reactors is that of monitoring the value of k_{eff} in a subcritical reactor [4]. If two widely spaced frequencies f_1 and f_2 on either side of f_0 are chosen with $f_1 < f_2$, then

$$\left|\frac{n(f_2)}{n(f_1)}\right|^2 = \frac{\omega_1^2 + \left[\frac{(1-\beta)k_{\mathrm{eff}} - 1}{\ell}\right]^2}{\omega_2^2 + \left[\frac{(1-\beta)k_{\mathrm{eff}} - 1}{\ell}\right]^2} \quad (3)$$

provided f_1 is somewhat greater than $1/2\pi\bar{\lambda}$. Experimental data obtained on the Westinghouse Critical

Experiment Station reactor by a Milletron shutdown reactivity meter [5] is shown in Fig. 1. The amplified in-core ion chamber current is Fourier-analyzed electronically at 10 and 300 c/s by sine wave multiplication. Previously calibrated control rods inserted below their critical positions provided various values of k_{eff} at which $n(300)/n(10)$ was measured. The agreement with Eq. (3), with ℓ selected for normalization at $k_{eff} = 1$, is sufficiently good to show that this method can be used to determine k_{eff} when it is not otherwise known.

Successful analysis of stochastic processes has also been possible in the time domain. If many counts c_i are taken in a fixed time interval τ, their variance (see Table 2) will exceed their mean in the case of in-core detectors; the ratio of variance to mean may be derived from zero power neutron kinetics [6]:

$$\frac{\overline{c^2} - (\bar{c})^2}{\bar{c}} = 1 + 0.795\,\epsilon\left[\frac{(1-\beta)^2}{(\beta-\rho)^2}\left(1 - \frac{1 - e^{-(\beta-\rho)\tau/\ell}}{\frac{\beta-\rho}{\ell}\tau}\right) + 41\,000\left(1 - \frac{1 - e^{-0.277\tau}}{0.277\tau}\right)\right] \quad (4)$$

Here ρ is $1 - k_{eff}^{-1}$ and ϵ is the number of counts per fission. If ϵ is somewhat greater than $1/\beta^2 = 0.0001$, the initial 1 in Eq. (4) may be neglected. Under these circumstances this equation is the time domain analog of Eq. (2), since an additive background term is neglected in the latter.

Figure 2 shows measurements of the variance-to-mean ratio obtained for the Ford Nuclear Reactor [6] by using a counter feeding a gate-scaler with various gate times τ. Fitting Eq. (4) to these data allows a determination of $(\beta-\rho)/\ell = 122\ s^{-1}$, corresponding to: $\beta = 0.0065$, $\rho = -0.0022$ and $\ell = 0.0000715$ s. Thus, subcritical reactivities may also be determined in this manner, as was also experimentally verified on SPERT2 [7]. An additional useful quantity determined from the fit to the data in Fig. 2 is $\epsilon = 0.0014$ counts per reactor fission—an absolute power calibration of the in-core counter.

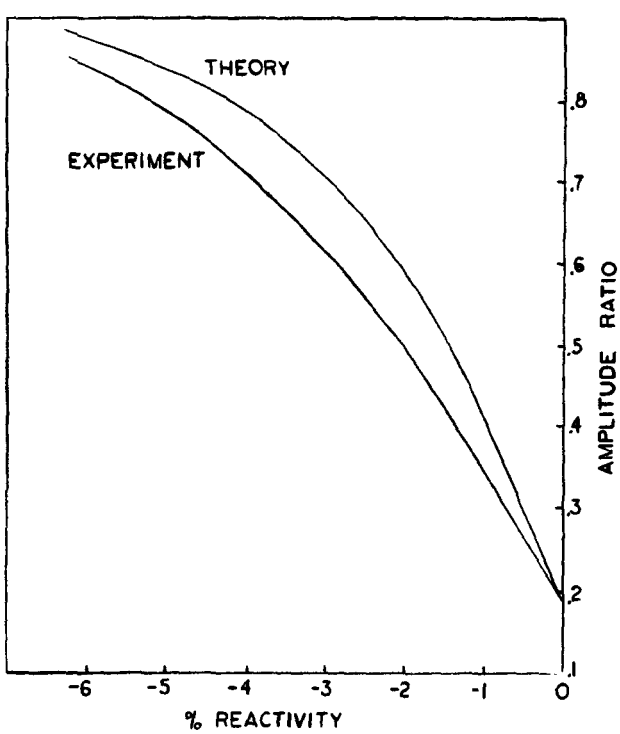


Figure 1. Subcritical reactivity measurements on the Westinghouse Critical Experiment Station reactor. The ratio of the spectral amplitude values at 300 cycles per second and 10 cycles per second is measured for various control rod insertions below criticality and also computed from Eq. (3)

POWER REACTORS

In power reactors, a stochastic reactivity function $\rho_{in}(t)$ generally exists with a magnitude sufficient to produce power fluctuations $n(t)$ well in excess of those due to the random fission process phenomena of zero power reactors. Measurements of the spectra $|n(f)|^2$ of current fluctuations in externally located ion chambers will give information about both the reactor transfer function $G(f)$ and $\rho_{in}(f)$:

$$|n(f)|^2 = \bar{N}^2 |G(f)|^2 |\rho_{in}(f)|^2 \quad (5)$$

where $\bar{N}$ is the mean reactor power. A common application of this equation is to measure the details of a resonance at $f = f_r$ in $G(f)$, owing to a reactor's unstable tendencies. This is done by measuring $n(f)$, and in this application it is not necessary to know the details of $\rho_{in}(f)$.

Table 3 lists specific applications of noise analysis to many power reactors. It is seen that the motivations are the detection of possible instabilities and an added understanding of the reactor's dynamic behavior. For some reactors listed it was possible to obtain $G(f)$ from a rod oscillator experiment. In such cases it was found that spectrum determinations and rod oscillator experiments complement each other; the two together providing more

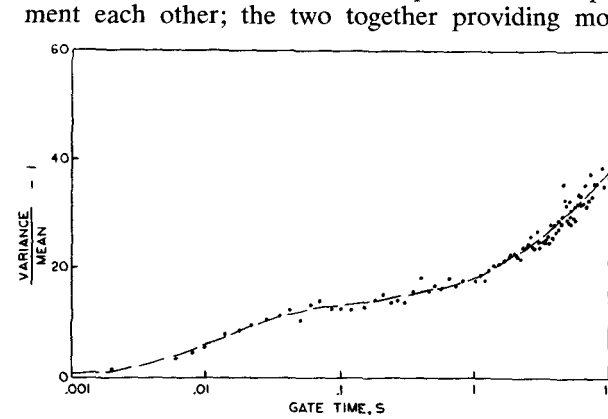


Figure 2. The variance-to-mean ratio of the Ford Nuclear Reactor measured at various gate times. The curve through the data corresponds to Eq. (4)

information than either separately—such as uniquely determining $\rho_{in}(f)$.

To facilitate the interpretation of reactor spectra it is advantageous to have a theoretical understanding of $\rho_{in}(f)$ as well as the more commonly measured and calculated $G(f)$. The stochastic function which is responsible for the reactivity excitation of a power reactor is usually the small temperature or density fluctuations in its coolant and/or moderator. When coolant flow is the fundamental stochastic function, it is converted to temperature and/or density fluctuations in the core before manifestation as $\rho_{in}(f)$. Table 4 indicates the experimental method, the results, and the interpretation used to deduce the noise source for several reactors.

One of the more conclusive methods used in studying noise sources is to obtain the cross-correlation function (see Table 2) between reactor power fluctuations $n(t)$ and fluid temperature fluctuations $\theta(t)$. If it is large in the region of some time lag τ, then a causal relationship is established between these variables, phased by approximately τ. Table 4 also shows that the amount of reactor power noise as measured by the standard deviation in a given frequency band $f_2 - f_1$:

$$\sigma_n]_{f2\,-\,f1} = [\int_{f1}^{f2} | n(f) |^2 df]^{\frac{1}{2}} \qquad (6)$$

can be related to quantitative measures of its cause, such as $\sigma_\theta]_{f2\,-\,f1}$.

Since spectrum measurements have been used often in stablility studies, Fig. 3 shows several of these. The least stable reactor here is the EBWR at 100 MW, since the resonance due to void reactivity feedback has a Q value (defined as f_r divided by the width of peak three decibels down) of five. An indication of nucleate boiling in the Saxton pressurized water reactor is shown by its resonant peak [1]. The area below this peak in various spectra correlated well with the thermodynamically computed core surface area undergoing nucleate boiling at various pressures and temperatures, as mentioned in Table 4.

SPATIAL EFFECTS

Since loose dynamic coupling in large power reactors has already been observed in conjunction with xenon instabilities, a possible application of reactor noise analysis is to monitor for other possible spatial instabilities. Because of experimental simplicity, zero power assemblies have offered a means of developing techniques for studying stochastic processes in space and time. In addition, a better insight into zero power reactor dynamics is also obtained while setting the groundwork for related investigations in power reactors.

The zero power transfer functions between pairs of detectors shown in Fig. 4 were obtained on a natural uranium, light water, subcritical ($k_{eff} = 0.9$)

Table 3. Results obtained in applying stochastic analysis techniques to power reactors [1, 2]

Results	Reactors
Details of spectral resonance due to boiling	BORAX 4, EBWR, Elk River, VBWR, Saxton, TTR
Details of spectral resonance due to fuel effects	HRE2, SRE
Stability of control system	KIWI A3
Stability monitoring	Dresden, Indian Point, ML1, N.S. *Savannah*, Saxton, SNAP, Yankee
Attributing noise source to temperature or flow fluctuations	Dresden, Elk River, HRE2, Saxton, SNAP
Shutdown margin	Saxton

Table 4. Identification of the noise source responsible for reactor power fluctuations

Reactor	Noise source determination
Dresden [8]	Spectra of gamma radiation in primary flow piping indicate a hydraulic oscillation at the same frequency as the resonance in the reactor power spectrum
Elk River [1]	$\sigma_n]f_2$—f_1 is linearly related to $\sigma_n]f_2$—f_1 of a thermocouple below the core under a variety of operating conditions. Also a gravitational oscillatory resonance in the natural circulation feedwater return was identified with a similar resonance in reactor power spectra
HRE2 [9]	A hydraulic mock-up of the reactor flow fluctuations in combination with an analog computer gave the same statistical distribution of power peaks as the reactor under a variety of flow conditions
Saxton [1]	A cross-spectrum of the reactor power and flow indicated a causal relationship. Also the area under a high frequency resonance varied linearly with the core area undergoing nucleate boiling under a variety of operating conditions
SNAP [1]	A cross-spectrum of the reactor power and flow indicated a causal relationship

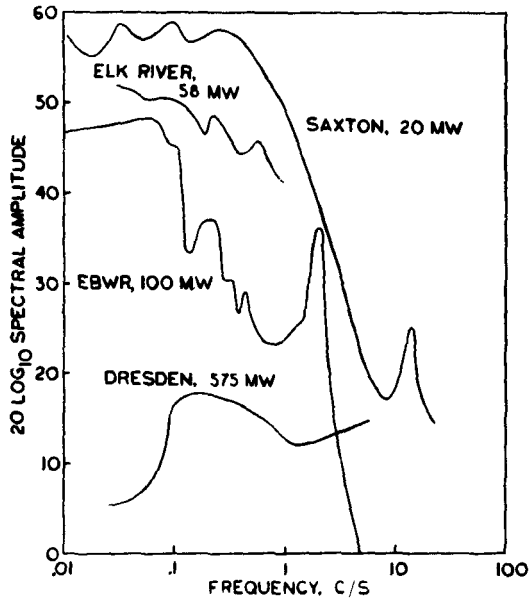


Figure 3. Spectra from ion chamber fluctuations for various power reactors

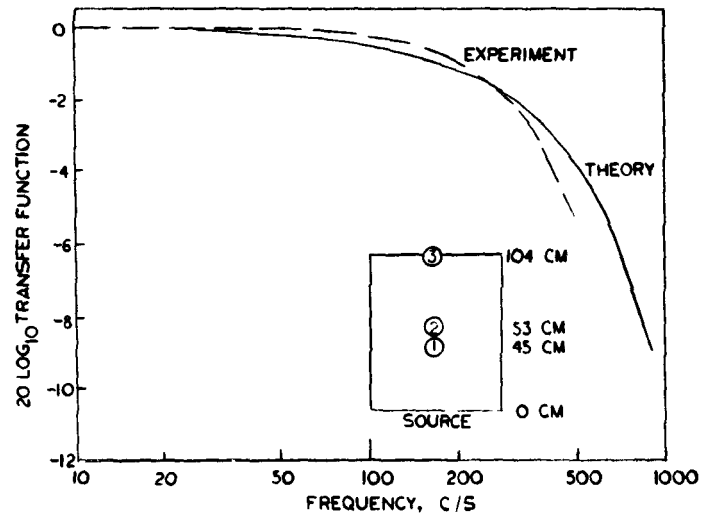


Figure 4. Transfer function between ion chambers located at the center and edge of the University of Florida subcritical assembly. Measurements of the cross correlation functions between chambers located at 2 and 1 and between chambers located at 3 and 1 were used in Eq. (7) to obtain this transfer function

assembly at the University of Florida [1]. The neutron source was pulsed according to a pseudo-random signal in order to achieve ample signal strength with which to obtain cross-correlation functions $\phi_{13}(\tau)$ and $\phi_{12}(\tau)$ and hence a transfer function;

$$\text{transfer function between chambers 3 and 2} = \frac{\int \phi_{13}(\tau)\exp(-i\omega\tau)\,d\tau}{\int \phi_{12}(\tau)\exp(-i\omega\tau)\,d\tau}. \qquad (7)$$

The reduced transmission of frequencies above 400 c/s over this 51 cm distance corresponds to an effective time lag of 0.0004 s between these two locations: $\phi_{12}(\tau)$ is maximum at $\tau = 0$ while $\phi_{13}(\tau)$ is maximum at $\tau = 0.0004$ s. Time dependent Fermi age and diffusion theory is the basis for the theoretical curve adequately describing the experiment.

In power reactors there are spatially distributed stochastic functions $\theta(\vec{r},t)$ which must be taken into account in addition to these spatial effects in zero power theory. The spatial correlation function to be considered is

$$\overline{\phi(\vec{s},t)} = \overline{\frac{1}{V}\int \theta(\vec{r},t)\theta(\vec{r}+\vec{s},t)\,dV} \qquad (8)$$

where the bar denotes a time average over the reactor volume V. Should this function have a simple $\exp(-2|\vec{s}|/d)$ dependence, it can be shown that the reactor behaves as if there were V/d^3 independent noise sources, d being the mean correlation distance [1].

In the VBWR, spectra of in-core ion chamber currents at various locations in a fuel element indicated that the high frequency components of the noise differ as shown in Fig. 5 [10]. This is attributed to local void fluctuations influencing thermal neutron diffusion, since the function $\phi(\vec{s},t)$ for water density has a correlation distance much less than the core height of three feet. The externally located ion chamber responds to the average fast neutron flux of the core rather than to local in-core thermal fluxes.

OUTLOOK

From the variety of reactor dynamics phenomena already studied by means of stochastic signals, it is safe to assume that this analytical tool will continue to be used at least as extensively as at present. With

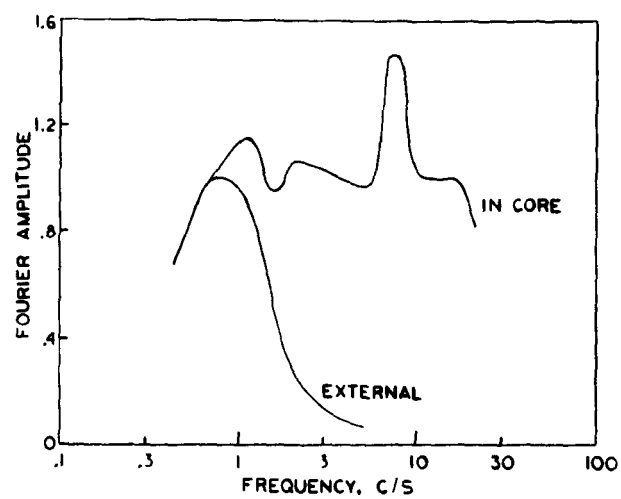


Figure 5. Comparison of in-core and external ion chamber spectra for the VBWR. Though both have a boiling resonance at 1 cycle per second, the in-core chamber also shows local high frequency effects

techniques and equipment rather highly developed, the application of stochastic signal analysis to reactors is relatively easy, although interpretation is often difficult. It is not unreasonable to expect the future to exhibit additional fruitful applications beyond those presented here.

REFERENCES

1. Proceedings of the Symposium on Noise Analysis in Nuclear Systems, University of Florida, Gainesville, Florida, to be published (1964).
2. Thie, J. A., *Reactor Noise,* Rowman and Littlefield, New York (1963).
3. Balcomb, J. D., Demuth, H. B., and Gyftopoulos, E. P., Nuclear Sci. Eng., *11*, 206 (1961).
4. Uhrig, R. E., Trans. Amer. Nuclear Soc., *4* (1), 85 (1961).
5. Garrett, S. J., Schultz, M. A., and Yang, C. M., *Shutdown Reactivity Meter Development*, USAEC report NYO-10492 (1963).
6. Albrecht, R. W., Nuclear Sci. Eng., *14*, 153 (1962).
7. Schroeder, F., ed., Quarterly Technical Report, SPERT Project, USAEC report IDO-16687 (1960).
8. Beckjord, E. S., Trans. Amer. Nuclear Soc., *3* (2), 433 (1960).
9. Lawson, C. G., *et al.*, *ibid.*, *4* (2), 315 (1961).
10. VBWR Stability Test Report, USAEC report GEAP-3971 (1963).

ABSTRACT - RÉSUMÉ - АННОТАЦИЯ - RESUMEN

A/272 Etats-Unis d'Amérique

Phénomènes stochastiques dans les réacteurs nucléaires et mesure des caractéristiques dynamiques

par J. A. Thie

L'auteur présente les nombreuses méthodes spécialement mises au point pour obtenir des données expérimentales sur les phénomènes stochastiques, ainsi que des procédés d'analyse de ces données. Cet inventaire va des méthodes approchées et peu coûteuses aux méthodes très compliquées et extrêmement précises. Il s'efforce d'en déduire un certain nombre de principes directeurs pour le choix de la méthode qui convient le mieux dans chaque cas.

Etant donné que la dynamique théorique des réacteurs et les mathématiques des phénomènes stochastiques ont été étudiées très à fond, il n'est pas surprenant qu'on puisse, en les combinant, construire une théorie valable du bruit dans les réacteurs. Ainsi, pour les réacteurs de puissance zéro, on a mesuré avec succès la durée de vie des neutrons, le niveau de puissance absolue et la marge de réactivité à l'arrêt. Les données fournies pour le réacteur du Centre d'expériences critiques montrent que l'on peut déterminer la valeur absolue de k-efficace en comparant les amplitudes de Fourier aux fréquences f_1 et f_2 du flux d'un réacteur sous-critique, dont les variations sont aléatoires. Ce principe a servi de base à l'étude d'un appareil de mesure simple, qui contrôle constamment la réactivité d'un réacteur à l'arrêt et permet d'étalonner les barres de contrôle.

Dans plusieurs réacteurs de puissance, on a constaté que l'origine des fluctuations aléatoires en $n(t)$ peut être trouvée dans les fluctuations de la température dans le fluide de refroidissement et de ralentissement. Mais, dans les réacteurs à eau bouillante, ces fluctuations de la température se répercutent sur les cavités produites par la vapeur, et il en résulte une fonction stochastique de la réactivité dont dépend l'excitation du réacteur. L'auteur fournit des données pour étayer ces conclusions.

Dans le cas des réacteurs à eau bouillante, l'auteur a obtenu beaucoup de spectres de bruit à partir d'analyses fourieristes des fluctuations aléatoires de $n(t)$. Il récapitule ces résultats sous forme de tableaux afin de fournir une base pour déterminer la stabilité relative des futurs réacteurs à eau bouillante. Il étudie ensuite les problèmes de sécurité du réacteur en cherchant une fréquence de résonance dans le spectre des amplitudes de Fourier de $n(t)$. On montre qu'il existe des méthodes d'analyse optimales et préférables en raison de cette bande de fréquences limitée qui présente de l'intérêt.

A/272 США

Стохастические процессы в ядерных реакторах и измерение рабочих характеристик при динамическом режиме

А. Тай

Приводятся таблицы отдельных методов получения экспериментальных данных о стохастических процессах и методы анализа этих данных. Среди этих методов имеются дешевые, приближенные подходы и точные. Благодаря этому обзору можно установить известные критерии, которые помогут выбрать подходящий метод к разрешению поставленной задачи.

Не удивительно, что при хорошо развитых теоретической динамике реактора и математике стохастического процесса существует надежная теория о шуме реактора. Так, для реактора нулевой мощности большие успехи были достигнуты при измерении времени жизни нейтронов, абсолютной мощности и избытка отрицательной реактивности при остановке. Из данных, приведенных для реактора опытной установки критичности, видно, что эффективный коэффициент размножения можно определять из отношения амплитуд Фурье на часто-

тах f_1 и f_2 беспорядочного изменяющегося подкритического потока реактора. На этом принципе построен простой измерительный прибор, который постоянно контролирует реактивность остановочного реактора, а также калибрирует регулирующие стержни.

В нескольких энергетических реакторах было найдено, что причиной беспорядочных флуктуаций нейтронного потока являются температурные колебания теплоносителя. Однако в кипящих реакторах эти колебания превращаются во флуктуации паровых полостей, обусловливающих возникновение стохастической функции реактивности, возбуждающей реактор. Приводятся данные и методы анализа, подтверждающие эти выводы.

Многие шумовые спектры кипящих реакторов были получены путем анализа Фурье беспорядочных флуктуаций нейтронного потока. Все эти данные обобщены и их характеристики сведены в таблицу, чтобы установить фон, по которому можно приблизительно определить относительную устойчивость новых кипящих реакторов. Безопасность реактора изучается исследованием резонансной частоты в спектре амплитуд Фурье нейтронного потока. Показано наличие оптимальных и предпочтительных приемов анализа, в основе которых лежит представляющая интерес узкая полоса частот.

A/272 Estados Unidos de América

Procesos estocásticos en reactores nucleares y medida de las características de rendimiento dinámico

por J. A. Thie

Se dan tablas de los muchos métodos específicos para obtener información experimental acerca de los procesos estocásticos y de las técnicas de análisis de datos. Estas abarcan desde procedimientos aproximados y poco costosos hasta métodos muy refinados y precisos. Con este estudio es posible obtener ciertos principios de orientación que ayuden a cada uno a elegir el método adecuado a sus necesidades.

Existiendo una dinámica teórica de reactores y una teoría matemática de fenómenos estocásticos sumamente desarrollada, no es de extrañar que con la combinación de ambas se obtenga una teoría aceptable del ruido de reactores. De este modo, en reactores de potencia cero, se ha obtenido gran éxito en la medida de la vida de los neutrones, del nivel absoluto de potencia y del exceso de reactividad tras la parada del reactor. Los datos dados para el reactor de la Estación de Experiencias Críticas muestran que la k efectiva puede determinarse absolutamente a partir de la relación de amplitudes de Fourier a las frecuencias f_1 y f_2 de las variaciones azarosas de flujo en el reactor subcrítico. Este es el fundamento de un aparato de medida que examina continuamente la reactividad de un reactor parado y calibra las barras de control.

Se ha encontrado en varios reactores de potencia que las fluctuaciones azarosas de $n(t)$ son atribuíbles a fluctuaciones de temperatura en el refrigerante del moderador. Sin embargo, en los reactores de ebullición éstas se transforman en fluctuaciones del coeficiente de vacío por el vapor, las cuales generan la función de reactividad estocástica que excita al reactor. Se dan datos y métodos de análisis que prueban estos descubrimientos.

Para reactores de ebullición se han obtenido numerosos espectros de ruido a partir del análisis de Fourier de las fluctuaciones azarosas de $n(t)$. Se resumen estos datos y se tabulan sus características para proporcionar una base a partir de la cual pueda determinarse la estabilidad relativa de futuros reactores en ebullición. La seguridad del reactor se estudia investigando una frecuencia de resonancia en el espectro de amplitudes de Fourier de $n(t)$. Se demuestra que existen procedimientos óptimos y preferibles de análisis a causa de esta limitada e interesante banda de frecuencias.

Spatial kinetics of thermal reactors

By O. Norinder*

The large power reactors being built or planned in Sweden use fuel transpositioning to attain flux flattening and high burn-up. The lattice parameters of the reactor core consequently are macroscopically heterogeneous. The knowledge of thermal reactor spatial kinetics that is assembled in Sweden therefore should be valid for macroscopically heterogeneous reactors. A general understanding of the kinetics of such reactors is promoted by considering expansions in the flux shape eigenfunction system. The eigenvalue difference of the eigenfunctions show that the significant part of a spatial transient in a three-dimensional power reactor is contained in the fundamental mode and in three higher modes. The latter modes correspond to oscillations with three nodal planes, that are orthogonal to each other.

GROUPING OF TRANSIENTS

Different time characteristics of the neutron flux transients in thermal reactors make it convenient to sub-divide the transients into different groups. The fastest phenomena is the prompt jump transient. This arises when the prompt neutrons adjust themselves to changes in the distribution of neutron multiplication properties and neutron sources. The prompt jump transient might be approximately described as an approach with a simple time constant. In the Marviken reactor this time constant is about 0.1 second for transients far from prompt critical.

The heat transport in the fuel, the steam transport in the boiling channels and the delayed neutrons give rise to transients, the time scale of which is some seconds. In the transients where the external heat circuits are significant a minute time scale is appropriate.

The important xenon transients might have a duration of several days. The depletion transients have the slowest time scale. Weeks, months and years are significant time intervals here.

THE SPACE- AND TIME-DEPENDENT ONE-GROUP NEUTRON FLUX EQUATIONS

The space- and time-dependent equations governing the neutron flux will be stated in a clear form. Let D, Σ_f and Σ_a be space- and time-dependent parameters, the significance of which is clear from Eq. (1). Let as usual β be the space-dependent fraction of delayed neutrons. Let γ_i be the space-dependent relative fraction of delayed neutrons of the ith precursor. Some average value of the diffusion constant is $\bar{D}$. The average neutron velocity is $\bar{v}$. The mean life of the ith precursor is τ_i. The following equations describe the neutron flux:

$$\nabla\left(\frac{D}{\bar{D}}\nabla\phi\right) + \frac{1}{\bar{D}}(\Sigma_f - \Sigma_a)\,\phi + \frac{1}{\bar{D}}\Sigma_f\beta\left(-\phi + \sum_{i=1}^{n}\gamma_i C_i\right) = \frac{1}{\bar{D}\,\bar{v}}\frac{\partial\phi}{\partial t} \tag{1}$$

$$\tau_i\frac{\partial C_i}{\partial t} = -C_i + \phi \quad ; \; i = 1(1)n \tag{2}$$

THE CONCEPT OF SPATIAL STABILITY

It is well known that most power reactors are inherently unstable in the fundamental flux mode due to xenon poisoning. However, due to the slow time scale of the xenon transient, stable operation is easily attained by moving control rods. Xenon might also cause spatial instability, by which is meant spatial transients that are not suppressed by a specified control system and the action of which is for instance to keep the reactor power constant. A possibility of spatial instability is also present with void distribution. Finally, one might visualize a mechanism giving spatial instability with a temperature distribution and the ensuing fluid streaming in a fluid moderator. However, truly nuclear flux spatial instability of the two last species has, to the author's knowledge, never been observed in reactors.

XENON SPATIAL STABILITY

Xenon spatial stability is well understood in the linearized description, that is as small oscillations about the equilibrium distribution. The theory is for instance noted in an article by Randall and St. John [1]. Some Swedish work is noted in [2], [3] and [4]. The two latter references give eigenfunction tables for two-zone slabs and for two-zone cylinders. All data necessary for xenon spatial stability calculations are tabulated and [3] contains

* AB Atomenergi, Stockholm.

the pertinent formulae. The tables make possible stability analysis for a considerable variety of different fluxes, that might be approximated in symmetrical slab geometry or in R-dependent cylinder geometry. The neutron flux should be described by one energy group when the tables are used. A sufficient one-group description exists and might be formulated in the engineering design of thermal reactors. However, it is not possible to separate the flux in one slab geometry and one cylinder geometry description in all practical cases.

Results of numerical analysis with two-group description of the neutron flux is given in [2]. The results have made possible some general conclusions, which are noted in the reference.

In engineering practice it should be sufficient to investigate xenon spatial stability by analysis of the situation regarding the non-fundamental flux eigenfunctions. If the stability margin is found insufficient, one must introduce a control system that measures and controls the spatial flux distribution.

General results valid for xenon perturbations that are not small in comparison to the equilibrium distribution are few. Some attempts to develop general theory have been made in Sweden by Lundquist and Weissglas [5].

THERMAL REACTOR NEUTRON FLUX SPATIAL STABILITY WITH FLUX-VOID INTERACTION

The treatment to be presented of the denominated problem is new. Therefore it will be given in some detail. A more complete account is to be found in [6].

Perturbed one-group equations

The time-dependent neutron flux is represented by the one-group diffusion equation with a flux variation time constant. By a suitable choice of the constant one might take account of the effect of the delayed neutrons. The relative diffusion constant $E = D/\bar{D}$, the buckling Q and the flux time constant τ_ϕ are introduced. The system of Eqs. (1) and (2) will then be approximately represented by the following single equation:

$$\nabla (E \nabla \phi) + Q \phi = \tau_\phi \frac{\partial \phi}{\partial t} \tag{3}$$

The mean difference between the local fuel temperature and the coolant is denoted by U. The local power transfer from fuel to coolant is also proportional to U, which by a time constant follows the neutron flux. This gives

$$U + \tau_U \frac{\partial U}{\partial t} = \phi \tag{4}$$

To investigate the conditions at small deviations from the equilibrium values the variables are redefined. The majuscules are used to signify the equilibrium values and the minuscules to signify the deviations. Thus $\phi \leftarrow \phi + \phi$, $E \leftarrow E + e$, $U \leftarrow U + u$ and $Q \leftarrow Q + q$. The new variables are introduced in Eqs. (3) and (4), first-order increments only retained and the relation $\nabla(E\nabla\phi) + Q\phi = 0$ for the equilibrium flux observed. One gets the abridged equation

$$\nabla (E \nabla \phi) + Q\phi + \nabla (e \nabla \phi) + \phi q = \tau_\phi \frac{\phi \varrho}{\partial t} \tag{5}$$

For the temperature increment, one gets

$$u + \tau_U \frac{\partial u}{\partial t} = \phi \tag{6}$$

The increments e and q are, with possibly space-dependent factors γ, α and β dependent on the void increment v and the increment u according to the equations

$$e = \gamma v(\bar{x}, t) \tag{7}$$

$$q = \alpha u(\bar{x}, t) + \beta v(\bar{x}, t) \tag{8}$$

Variables describing the coolant behaviour of a boiling reactor are governed by fundamentally non linear equations when one has net boiling, particularly if all or a significant part of the momentum sources come from the buoyancy of the steam. However, the limit equations for deviations from equilibrium values are linear.

If there is a small power increment in some small part of the reactor space there will result a space- and time-dependent void increment, in general over the whole reactor space. If the reactor is hydrodynamically stable the void increment will tend to a final space-dependent value.

In the linearized approximation the final void increment distribution is dependent on the power increment distribution by a kernel integral. This follows from the fact that the void increment depends linearly on the power increment in every part of the reactor space. In the equations used the channel power is proportional to the temperature increase in the fuel.

In the following, the equations are simplified by treating the void increment as if it instantaneously assumes the final shape due to a power increment. The following integral is then valid:

$$v(\bar{x}, t) = \int K(\bar{x}, \bar{x}') u(\bar{x}', t) \mathrm{d}V' \tag{9}$$

Expansion in flux modes

A numerical treatment of the equations might use approximation by finite differences or expansion in some system of space-dependent functions with time-dependent coefficients. In the following the flux-mode system is used as this often gives small cross-coupling terms between different modes.

As stated earlier the equilibrium flux satisfies $\nabla (E \nabla \phi) + Q\phi = 0$ with space-dependent relative diffusion coefficient $E(\bar{x})$ and material buckling $Q(\bar{x})$. The flux modes are defined as the eigenfunctions $g_\nu(\bar{x})$ to the equation

$$\nabla (E(x) \nabla g_\nu(x)) + Q(x) g_\nu(x) + \mu_\nu^2 g_\nu(x) = 0 \quad (10)$$

$g_\nu = 0$ on the (extrapolated) boundary of the reactor flux space.

With every eigenfunction is connected an eigenvalue μ_ν^2, zero is the smallest eigenvalue and its eigenfunction is proportional to the equilibrium flux. As Eq. (10) is self-adjoint the solutions are orthogonal. The solutions are normalized by adjusting their magnitude.

Modal expansion of the flux and fuel temperature increments yields the following expressions:

$$\phi(\bar{x}, t) = \sum_{\nu=0}^{\infty} y_\nu(t)\ g_\nu(\bar{x}) \quad (11)$$

$$u(\bar{x}, t) = \sum_{\nu=0}^{\infty} w_\nu(t)\ g_\nu(\bar{x}) \quad (12)$$

Let $v_\nu(\bar{x})$ be the void increment resulting from the fuel temperature increment $g_\nu(\bar{x})$. The linearity of Eq. (9) then makes valid the following expansion of the void

$$v(\bar{x}, t) = \sum_{\nu=0}^{\infty} w_\nu(t)\ v_\nu(\bar{x}) \quad (13)$$

The expansions (11)-(13) are used in Eqs. (5)-(8). The expressions resulting are multiplied by $g_\kappa(\bar{x})$ and integrated over the reactor space. One observes the relation

$$\nabla (g_\kappa e(\nabla \phi)) = e(\nabla g_\kappa) \cdot (\nabla \phi) + g_\kappa (\nabla (e(\nabla \phi))) \quad (14)$$

Every value of κ gives two linear equations for the coefficients $y_\nu(t)$ and $w_\nu(t)$. The equations are expediently written in matrix form. After Laplace transformation (and redefinition) one finds:

$$(A + sB)(y_0, w_0, y_1, w_1, y_2, w_2, y_3, w_3, y_4, w_4, \ldots\ldots)^T = 0 \quad (15)$$

T indicates transpose. The structures of the square matrices A and B will be given:

$$A = \begin{Vmatrix} 0 & c_{00} & 0 & c_{01} & 0 & c_{02} & 0 & c_{03} & \\ 1 & -1 & 0 & 0 & 0 & 0 & 0 & 0 & \\ 0 & c_{10} & -\mu_1^2 & c_{11} & 0 & c_{12} & 0 & c_{13} & \\ 0 & 0 & 1 & -1 & 0 & 0 & 0 & 0 & \\ 0 & c_{20} & 0 & c_{21} & -\mu_2^2 & c_{22} & 0 & c_{23} & \\ 0 & 0 & 0 & 0 & 1 & -1 & 0 & 0 & \\ & & & & & & & & \\ & & & & & & & & \end{Vmatrix} \quad (16)$$

$$B = \begin{Vmatrix} -\tau_\phi & 0 & 0 & 0 & 0 & 0 & 0 & 0 & \\ 0 & -\tau_U & 0 & 0 & 0 & 0 & 0 & 0 & \\ 0 & 0 & -\tau_\phi & 0 & 0 & 0 & 0 & 0 & \\ 0 & 0 & 0 & -\tau_U & 0 & 0 & 0 & 0 & \\ 0 & 0 & 0 & 0 & -\tau_\phi & 0 & 0 & 0 & \\ 0 & 0 & 0 & 0 & 0 & -\tau_U & 0 & 0 & \\ & & & & & & & & \\ & & & & & & & & \end{Vmatrix} \quad (17)$$

For the coupling terms $c_{\kappa\nu}$ is valid:

$$c_{\kappa\nu} = -\int \gamma\, \nu_\nu(\bar{x})(\nabla)(\nabla g_\kappa(\bar{x}))(\nabla \phi(\bar{x}))\, dV + \int \alpha\, g_\kappa(\bar{x})\ g_\nu(\bar{x})\ \phi(\bar{x})\, dV + \int \beta\, \nu_\nu(\bar{x})\ g_\kappa(\bar{x})\ \phi(\bar{x})\, dV \quad (18)$$

Possibilities of spatial oscillations

The dynamic properties of the equations representing the reactor are evident from the eigenvalues and eigenvectors of Eq. (15). In some cases the cross coupling terms might be neglected. If they are neglected one finds that the κth mode is stable if

$$c_{\kappa\kappa} < \mu_\kappa^2 \quad (19)$$

Principles of numerical treatment

The spatial functions $\phi(\bar{x})$, $g_0(\bar{x})$, $g_1(\bar{x})$, ..., $\nu_0(\bar{x})$, $\nu_1(\bar{x})$, ... must be known or approximated to make possible a numerical treatment. One might also introduce γ, α β as spatial functions.

Only a finite number of eigenfunctions might be used in a numerical treatment. The flux tables [3] and [4] show that the fundamental eigenfunction and the eigenfunction next in line should give a good indication of the spatial stability properties when the analysis is made in one spatial dimension.

Numerical calculations for the Marviken reactor

To investigate the conditions at the Marviken reactor numerical calculations have been made for two different equilibrium power distributions. Only the vertical (Z) co-ordinate was represented in the calculations. The first flux (a) corresponds to case 72 of the slab flux table [3]. This is a "ditch" flux with min/max = 0.73. The second flux (b) corresponds to case 13 of [3] and is flat for 65% of a slab geometry. The void distributions corresponding to the $g_0(Z)$ and $g_1(Z)$ perturbations were calculated by a computer code created for general analysis of boiling channel equilibrium and transient void distributions. The code is described in another paper to this Conference [7]. A Mercury Autocode computing the space integrals (eighteen) has been written. The eigenproblem was solved by the Atomenergi standard program GEROL [8]. A more complete documentation of the calculations is found in [6].

Conclusions regarding void spatial stability

Although only eighteen cases have been calculated as described above it was possible to draw important conclusions regarding void oscillations. The conclusions are valid for many reactors but particularly evident for Marviken.

(a) Void-induced space harmonics in the neutron flux are stabilized by the neutron leakage. This is evident from the form of the matrix A of Eq. (16). The property has solidly manifested itself in the numerical calculations;

(b) In many investigations involving void transients the neutron flux can be treated as a function of space multiplied by a function of time. This is particularly the case when void stability and hydraulic transients are examined;

(c) It is very unlikely that a boiling reactor, that has been found to be stable for fundamental mode oscillations, will exhibit flux-void induced spatial instability.

THE COMPUTER PROGRAMME RZT-1F

In Sweden the computer programme RZT-IF has been created for calculating in finite cylinder (RZ) geometry time dependent neutron flux and fuel temperature transients. The neutron flux is represented by one energy group. Two groups of delayed neutrons are used. The influence of control rods is represented by parameter increments, which are added to the initial parameters. Control rod movement is represented by a variable boundary parallel to the R co-ordinate axis in the RZ plane considered.

The main presentation of results is graphically made as isoflux and isothermal curves in the RZ plane. The programme also has options for calculating the stationary flux distributions for different prescribed control rod configurations. The control rod influence must be represented by homogeneous parameters. Such parameters are calculated by the CRCC programme [9].

Some calculations have been made by the programme RZT-1F. Future calculations will be designed among other things to demonstrate the difference between the space transient from the programme and a sequence of instantaneous static flux distributions corresponding to the space-time variation of the nuclear parameters.

Some observations regarding the need for exact calculation of space-time transients will be noted. Violent flux and thermal transients are avoided in power reactors and are in practice only obtained when the reactor is shut down by scram. It is hard to define other accidental transients in advance and in most cases a proposed reactor with a finite probability of such transients will not be built. The scram transient is more advantageously treated as a sequence of static flux distributions corresponding to different positions of the bank of scram rods as will be explained in the next paragraph.

An exact calculation of the scram transient will be valid for and only for the situation aimed at in the calculations. With the "static-sequence" description it is possible to state general expressions valid for different kinetic parameters and different time functions for the position of the scram control rod bank.

CALCULATION OF SPACE-TIME TRANSIENTS FROM A SEQUENCE OF STATIC FLUX DISTRIBUTIONS

The neutron flux of a thermal reactor adapts itself to the neutron sources, which at power operation always come from the delayed neutron emitters. The adaption in the practical cases occurs with a time constant of about a tenth of a second and thus is fast in comparison with the velocity of control rods, coolant, heat from the fuel and other entities that influences the reactivity.

The old flux history will manifest itself as a "drag" on the instantaneous static flux picture. This "drag" comes from the part of the old sources that has not decayed and that has a spatial shape different from the shape of the sources belonging to the instantaneous flux picture. In most cases the "drag" is small and might be neglected. The facts noted have been clearly stated in [10].

Rather general expressions for the space-time transient of the Marviken reactor have been developed from a sequence of calculated static flux distributions. The expressions are particularly used to calculate the temperature transients of the superheater fuel elements after a turbine trip.

THE SPACEPOWER PROGRAMMES

A system of programmes denoted SPACEPOWER for three-dimensional calculation of the heat power and other variables of thermal reactors is planned in Sweden. The neutron flux is described in two energy groups. The difference equations for the fast and thermal flux are formulated to describe the reaction rates and neutron interchanges between fuel elements, water holes and control rods. Therefore a checkerboard lattice corresponding to the real reactor lattice is used in the horizontal plane. In the vertical dimension the "checkerboard pillars" are divided into a number of cells of equal height and it is thought that approximately cubic cells should be used in most calculations. The first versions of SPACEPOWER that are currently being coded in FORTRAN 4 will contain special provisions for supplying the sequences of static flux distributions required for calculation of spatial transients. In the distant future there might ensue from the SPACEPOWER programme sequence codes that will directly calculate spatial reactor transients.

REFERENCES

1. Randall, D., and St. John, D. S., *Xenon Spatial Oscillations*, Nucleonics, *16* (3), 82-86, 129 (March 1958).
2. Norinder, O., *Two-Group Analysis of Xenon Stability in Slab Geometry by Modal Expansion*, AB Atomenergi report AE-108 (May 1963).
3. Norinder, O., *Flux-Shape Eigenfunction Tables for Two-Zone Slabs*, AB Atomenergi internal report (1963).
4. Norinder, O., *Flux-Shape Eigenfunction Tables for Two-Zone Cylinders*, AB Atomenergi internal report (1963).
5. Lundquist, S., and Weissglas, P., *A Method for Determination of Spatial Stability*, Nuclear Sci. Eng., *15*, 474-475 (April 1963).
6. Norinder, O., *Thermal Reactor Neutron Flux Spatial Stability with Flux-Void Interaction*, AB Atomenergi internal report (1964).
7. Becker, K. M., Jahnberg, S., Haga, I., Hansson, P. T., and Mathisen, R. P., *Hydrodynamic Instability and Dynamic Burnout in Natural Circulation Two-Phase Flow. An Experimental and Theoretical Study*, P/607, Vol. 8, these Proceedings.
8. Norinder, O., *GEROL — A General Root-Locus Program in Mercury Autocode*, AB Atomenergi internal report (1962).
9. Norinder, O., and Nyman, K., *Two-Group Current-Equivalent Parameters for Control Rod Cells. Autocode Programme CRCC, Nukleonik, 5 (1)*, 19-23 (1963).
10. Ross, P. N., ed., *Technical Progress Report. Reactor Physics and Mathematics, for the Period September 1, 1959 to December 1, 1959*, USAEC report WAPD-MRJ-8 (December 1959).

ABSTRACT - RÉSUMÉ - АННОТАЦИЯ - RESUMEN

A/685 Suède

Cinétique spatiale des réacteurs thermiques

par O. Norinder

On étudie, en Suède, la théorie de la cinétique spatiale des réacteurs et on s'efforce de rendre cette théorie plus claire et d'en simplifier l'interprétation. On accorde une attention particulière aux études visant à élucider les propriétés cinétiques du réacteur de Marviken. Pour être applicable à ce réacteur, la théorie doit être valable pour les noyaux macroscopiquement hétérogènes. La description du flux du réacteur et d'autres variables est généralement basée sur l'équation de la diffusion des neutrons à groupe unique en fonction du temps. Par développement dans le système des fonctions propres du flux, on obtient une description graphique du comportement dans le temps. La partie significative du phénomène transitoire est représentée par la fonction propre fondamentale et les trois fonctions propres supérieures. A partir des caractéristiques de vitesse des phénomènes transitoires, il est possible de grouper ces phénomènes selon les catégories suivantes: neutrons instantanés, transport de chaleur de combustible et neutrons retardés, circuits de chaleur extérieurs, xénon et appauvrissement.

Dans les recherches cinétiques sur les réacteurs, on applique généralement plusieurs conceptions de stabilité. Celles-ci doivent être définies. Dans le cas d'un réacteur, la totalité du système doit toujours être stable. La stabilité spatiale peut être commodément définie comme étant la stabilité sans système de réglage ou avec un système de réglage commandé par une variable réelle. La stabilité spatiale du xénon peut être étudiée à l'aide des fonctions propres du flux. On décrit les tables qui ont été calculées pour ces fonctions.

Une théorie nouvelle de la stabilité spatiale de distribution du vide est présentée, cette théorie permettant des estimations numériques aux conditions de la stabilité.

Pour le calcul des phénomènes transitoires, il est nécessaire le plus souvent d'étudier séparément les phénomènes dans l'espace d'une part et dans le temps d'autre part. Dans la plupart des cas, il est possible de retenir les caractéristiques significatives pour le projet du réacteur lorsque des descriptions séparées dans l'espace et dans le temps sont utilisées. On donne une description succinte d'un code de calcul des phénomènes transitoires spatiaux. Les possibilités d'estimer le comportement transitoire spatial à partir de calculs de flux statique sont étudiées.

A/685 Швеция

Пространственная зависимость кинетики реакторов на тепловых нейтронах

О. Нориндер

В Швеции изучаются теоретические вопросы кинетики реакторов и делаются попытки внести в эту теорию определенную ясность и упростить ее интерпретацию. Исследования кинетики реактора имеют практическое значение. Чтобы использовать результаты этой теории для определенного реактора, она должна быть применима к макроскопическим гетерогенным активным зонам. Обычно поток нейтронов в реакторе и другие переменные описываются одногрупповым диффузионным уравнением нейтронов с временно́й зависимостью. Путем анализа системы с моделируемым потоком можно получить графическое изображение временно́й зависимости. Главная часть переходного процесса представлена основным типом и тремя более высокими типами. По скоростным характеристикам переходные процессы можно группировать следующим образом: мгновенный скачок, теплоотдача топлива и запаздывающие нейтроны, внешний тепловой контур, ксенон и медленные переходные процессы.

В исследованиях кинетики реакторов в основном используют несколько концепций стабильности. Следует определить эти концепции. Реактор как система в целом всегда должен быть стабильным. Пространственную стабильность удобно определять как стабильность без системы регулирования или с системой регулирования, возбуждаемой реальными отклонениями. Пространственная стабильность, обусловленная наполнением ксенона, может быть исследована с помощью собственных функций потока. Приводятся таблицы численных значений этих функций.

Описана новая теория стабильности, обусловленная пространственным распределением пустот. Теория позволяет сделать возможные численные оценки условий стабильности.

При расчете переходных процессов по большей части необходимо отделить пространственную зависимости от временно́й зависимости. Разделение пространственной и временно́й зависимости обычно позволяет сохранить наиболее важные характеристики переходных процессов при проектировании реакторов. Приводится краткое описание программы расчета пространственной зависимости переходных процессов. Исследуются возможности оценить пространственную зависимость переходных процессов от результатов расчета статического потока.

A/685 Suecia

Cinética espacial de reactores térmicos

por O. Norinder

En Suecia se estudia la teoría de la cinética espacial de reactores y se ensayan perfeccionamientos que la hagan más clara y simplifiquen su interpretación. Se ha concedido particular atención a los estudios que expliquen las propiedades cinéticas del reactor de Marviken. Para que sea aplicable a este reactor, la teoría debe ser válida para núcleos macroscópicamente heterogéneos. La descripción efectiva del flujo del reactor y de otras variables se basa principalmente en la ecuación de difusión neutrónica para un grupo de neutrones, dependiente del tiempo. Mediante el desarrollo en serie de flujos propios se obtiene una descripción gráfica del comportamiento temporal. La parte dominante del transitorio está representada por el modo fundamental y por los tres siguientes. Según sea su dependencia temporal pueden agruparse los transitorios en transitorios instantáneos, de transmisión de calor del combustible y de neutrones retardados, de circuito térmico exterior, de xenón y de empobrecimiento. En las investigaciones relativas a la cinética de reactores se usan, en general, varios conceptos de estabilidad que deben definirse. Para un reactor, todo el sistema debe ser estable. Conviene definir la estabilidad espacial como estabilidad sin sistemas de control o con un sistema de control accionado por una variable real. Puede estudiarse la estabilidad espacial del xenón utilizando los flujos propios. Se describen tablas calculadas de tales funciones.

Se da una nueva teoría de la estabilidad espacial de la distribución de huecos. La teoría permite estimar numéricamente las condiciones de estabilidad.

Para el cálculo de transitorios es necesario, en la mayoría de los casos, separar las dependencias espacial y temporal. Es muy probable que se conserven las características dominantes de los transitorios que influyen en el diseño de reactores cuando se emplea una descripción por separado en espacio y tiempo. Se describe brevemente un programa para el cálculo de transitorios espaciales. Se estudian las posibilidades de estimar el comportamiento espacial de los transitorios partiendo de los cálculos de flujos estáticos.

Generalized potential theory for multi-group diffusion in a general multi-region reactor

By H. Koskinen *

We shall consider the formulation of the multi-group diffusion equations for a general multi-region reactor in terms of generalized potential theory. Under potential theory for boundary value problems, one includes the transformation of the partial differential equations of the problem into a set of integral equations for certain functions defined on one or more surfaces present in the system. The expression *generalized potential theory* is used because we do not use Green's functions for the Laplace-operator as in classical potential theory. Instead, in order to avoid volume terms, the transformation mentioned above is performed substituting the fluxes and Green's functions corresponding to a more general elliptic or even parabolic operator into Green's formulae. Furthermore, we extend our considerations to cases where the normal derivative is not a point function but rather a distribution or an absolutely additive function of point sets in the sense of Radon [1-3]. In such cases the function is described by means of functions of bounded variation.

There are several slightly different formulations of potential theory for boundary value problems. They are distinguished by the different boundary conditions prescribed for Green's functions. Consequently the unknown functions are often not the boundary values of the problem, but other layer strengths closely related to these. The author has chosen the most straightforward version, which, although not used as often as the others, seems to be the most natural and to uncover the most essential mathematical features of the problem. In this investigation only Green's functions for infinite regions are used. The functions sought are just the surface fluxes and currents or normal derivatives.

The elements of potential theory are not completely new in reactor diffusion theory, although systematic use of potential theory has, as far as is known to the present author, never been made here. The matrix method [4] for one-dimensional reactors or reactors reflected in only one direction may be considered as a part of potential theory. Here integral operators are reduced to real numbers due to the presence of a high degree of symmetry. In the small source representations of heterogeneous reactor theory, the layer sources are distributed on infinitely thin cylindrical surfaces permitting the replacement of the variable source point in the integration by a point on the axis of the cylinder. Several attempts to generalize these methods for large source reactors have been made [5, 6], but the connection with potential theory has not been accomplished. In the hitherto most complete analysis of multi-group diffusion [7-9], Habetler and Martino have made some use of the terminology of potential theory, but not for the same purpose as in the present work. Finally, the treatment based on potential theory has interesting connections with the invariant imbedding formulation of the problem recently advanced by Shimizu [10].

The author has been greatly influenced by the above-mentioned classical works of Radon; see also [11]. More recent applications of classical or generalized potential theory are to be found in [12-14]. The problem of uniqueness and related questions in multi-region diffusion theory not considered in detail below may be treated by the methods of Sobolev presented in [15].

DERIVATION OF POTENTIAL THEORY FOR TIME INDEPENDENT CASES

The most general multi-region reactor geometry is shown in Fig. 1. A reactor is a connected region in an at most three-dimensional Euclidean space, in which region diffusion theory is applied. The portions of the space in which diffusion theory is *not* applied are shaded in Fig. 1. The outer boundary of R is denoted by S_0 and may be at infinity. S_0 is also a boundary of the multiply connected region V_0. The other boundaries of V_0 consist of a collection of disjoint surfaces S_k $(k = 1, 2, \ldots, m)$. Some of these S_k form *outer boundaries* of the regions in which diffusion theory will be applied. The remaining S_k surfaces we shall call *interfaces*. They form the outer limits of the sub-regions V_k, each of which may have the same general internal topology as R itself. In this manner one may theoretically continue to infinity. However, the most important special cases of the general geometry are the multi-zone reactor and the (large source) heterogeneous

* Institute of Technical Physics, Institute of Technology, Helsinki.

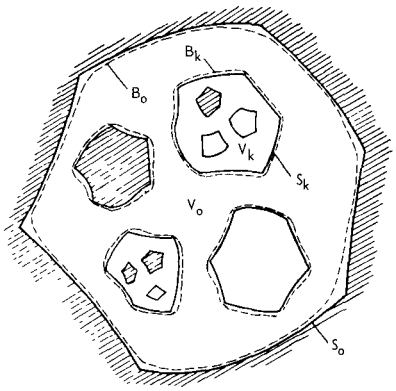


Figure 1. A general multi-region reactor geometry in two dimensions and the approach to the boundaries in it

reactor. We allow all the surfaces to possess a finite number of *corners*, but not cusps.

It is assumed that the diffusion coefficients, removal and slowing-down cross sections $D_i(\bar{r})$, $\Sigma_i(\bar{r})$ and $\Sigma_i'(\bar{r})$ respectively, of each energy group i, have constant values within every region, but are discontinuous across the interfaces. For formal simplicity, we allow only spontaneous sources of volume measure zero in the system because these can be replaced by boundary conditions. The simplest possible multi-group model is used below.

There are two equivalent ways of writing the multi-group diffusion equations in the present case of discontinuous coefficients, both of which can be used to establish the potential theory. The first one, which is the starting point for several overall expansion methods, could be called an operational form because it contains generalized functions or distributions [15]. In terms of classical analysis, this form has meaning only as a limiting form for a sequence of equations with continuous coefficients, or, alternatively, when multiplied by a well-behaved function and integrated over the reactor volume. If the concentrated sources located either within the regions or on the interfaces are denoted by $Q_i(\bar{r})$, one has:

$$\left.\begin{aligned} -\nabla D_i(\bar{r})\cdot\nabla\phi_i(\bar{r}) + \Sigma_i(\bar{r})\phi_i(\bar{r}) &= \Sigma'_{i+1}(\bar{r})\phi_{i+1}(\bar{r}) + Q_i(\bar{r}) \quad (i = 1, 2, \ldots, n-1) \\ -\nabla D_n(\bar{r})\cdot\nabla\phi_n(\bar{r}) + \Sigma_n(\bar{r})\phi_n(\bar{r}) &= k\Sigma_1(\bar{r})\phi_1(\bar{r}) + Q_n(\bar{r}). \end{aligned}\right\} \tag{1}$$

These equations are accompanied by boundary conditions for the fluxes $\phi_i(\bar{r})$ on the outer boundaries $(S_0, S_k, \ldots)$ of R, which can be interpreted as special of the general form

$$\phi_i(\bar{s}_k) + \lambda_i(\bar{s}_k)\frac{\partial\phi_i(\bar{s}_k)}{\partial n_{s_k}} = h_i(\bar{s}_k) \quad (i = 1, 2, \ldots, n). \tag{2}$$

Here the set of surface co-ordinates needed to specify the position of the point on S_k is denoted by s_k, while $\partial/\partial n_s$ signifies differentation in the direction of the surface normal at $\bar{s}_k$. We do not discuss the allowed classes of the given functions λ_i and h_i. We note that in many practical cases a condition of the form (2) is required *almost everywhere* (if for instance $\partial/\partial n$ is not everywhere defined). If the behaviour of the fluxes at these exceptional points is not separately specified, the result is identification of certain classes of functions with their representative elements [8, 11].

The second formulation is

$$\begin{aligned} -D_i(\bar{r})\nabla^2\phi_i(\bar{r}) + \Sigma_i(\bar{r})\phi_i(\bar{r}) &= \Sigma'_{i+1}(\bar{r})\phi_{i+1}(\bar{r}) \quad (i = 1, 2, \ldots, n-1), \\ -D_n(\bar{r})\nabla^2\phi_n(\bar{r}) + \Sigma_n(\bar{r})\phi_n(\bar{r}) &= k\Sigma_1(\bar{r})\phi_1(\bar{r}). \end{aligned} \tag{3}$$

It is equivalent to (1) and is valid almost everywhere in R, combined with the conditions (2) and a set of new boundary conditions due to the omission of the terms $Q_i(\bar{r})$ of (1). Furthermore, (3) must be supplied with appropriate interface conditions, which are rigorously derived using the sequence of equations defining the limiting form (1). We point out that these conditions generally state the continuity (or more general relations) of the currents in a *weak* form [15].

We shall now indicate how the potential theory is established using (1) as a basis. For brevity, we consider a two-region reactor in two-dimensional space with smooth surfaces. Let us consider a one-group equation describing this reactor:

$$-\nabla D(\bar{r})\cdot\nabla\phi(\bar{r}) + \Sigma(\bar{r})\phi(\bar{r}) = Q(\bar{r}); \quad \phi(\bar{s}_0) \equiv 0. \tag{4}$$

$Q(\bar{r})$ may represent a quite general source distribution for the energy group under question. The values of the diffusion coefficient and the cross section in the core (V_1) are denoted by D_1 and Σ_1, and those in the reflector (V_0) by D_0 and Σ_0 respectively. Equation (4) can be modified as follows,

continuously in the symbolic sense:

$$\left.\begin{aligned} D\nabla^2\phi - \Sigma\phi &= -\nabla D\cdot\nabla\phi - Q \\ \nabla^2\phi - \kappa^2\phi &= \nabla(1/D)\cdot D\nabla\phi - (1/D)Q \;;\; \kappa^2 = \Sigma/D \\ \nabla^2\phi - \kappa_0^2\phi &= (\kappa_1^2 - \kappa_0^2)\phi c_1 + \nabla(1/D)\cdot D\nabla\phi - (1/D)Q \;;\quad \phi(\bar{s}_0) \equiv 0, \end{aligned}\right\} \tag{5}$$

where $c_1 = c_1(\bar{r})$ is the characteristic function for the region V_1 and has the value 1 in V_1 and 0 in V_0. If we perform all differentiations in the direction of the outward normal, it follows that

$$\nabla(1/D) = (1/D_0 - 1/D_1)\delta(\bar{r} - \bar{s}_1)\,, \tag{6}$$

where $\delta(\bar{r} - \bar{s}_1)$ is a delta-function at the point $\bar{s}_1$ on the interface S_1. Using Green's function for an infinite region $G_0(\bar{r}, \bar{r}') = (1/2\pi)K_0\,(\kappa_0|\,\bar{r} - \bar{r}'\,|)$ for the operator on the left side of the last of Eqs. (5) and accounting for the leakage through S_0, we obtain, if $V_1 + V_0 = V$

$$\phi(\bar{r}) = (\kappa_1^2 - \kappa_0^2)\int_{V_1} G_0(\bar{r}, \bar{r}_1)\phi(\bar{r}_1)\mathrm{d}V_1 - \int_V G_0(\bar{r}, \bar{r}_1)(1/D)Q(\bar{r}')\mathrm{d}V'$$
$$+ \left(\frac{D_1}{D_0} - 1\right)\oint_{S_1} G_0(\bar{r}, \bar{s}_1)\,\frac{\partial\phi}{\partial n_{s_1}}\,\mathrm{d}s_1 + \oint_{S_0} G_0(\bar{r}, \bar{s}_0)\,\frac{\partial\phi}{\partial n_{s_0}}\,\mathrm{d}s_0\,. \tag{7}$$

There are still volume terms on the right side of (7). These can be eliminated by expressing the core flux $\phi(\bar{r}_1)$ by means of its boundary values $\phi(\bar{s}_1)$ and $\partial\phi(\bar{s}_1)/\partial n_{s_1}$. For example, by writing Eq. (4) specifically for the core and applying Green's theorems one obtains

$$\phi(\bar{r}) = K_1\phi_1(\bar{s}_1) + K_2\,\frac{\partial\phi_1(\bar{s}_1)}{\partial n_{s_1}} + K_3\,\frac{\partial\phi_0(\bar{s}_0)}{\partial n_{s_0}} + f(\bar{r})\,. \tag{8}$$

The notation K_ν has been used for certain integral operators some of which may imply double integration; $f(\bar{r})$ is a given function. The desired representation is achieved by letting $\bar{r} \to \bar{s}_1$, and by letting $\bar{r} \to \bar{s}_1$ accompanied by simultaneous differentiation in the normal direction, and finally by letting $\bar{r} \to \bar{s}_0$ accompanied by normal differentiation. During these operations, careful attention must be paid to the correct application of the limit theorems of potential theory [12, 13].

Since the theory of generalized functions has been applied only to distributions on smooth surfaces, a more reliable method of obtaining the potential theory is that of (3). One considers a multiply connected reactor region such as V_0 in Fig. 1, but the boundary conditions are not yet fixed on S_0 nor S_k $(k = 1, 2, \ldots, m)$. Some of these may be outer boundaries, others interfaces. Corners or edges are specifically allowed. We enclose S_0 internally and the S_k externally (Fig. 1) by sufficiently smooth surfaces B_0 and B_k $(k = 1, 2, \ldots, n)$, which in a later phase are considered to converge towards the actual surfaces S. The multi-group Eqs. (3) can be transformed for each of the fluxes $\phi_1 = \phi_i\,(\bar{r})$ in V_0 into the following forms

$$(\nabla^2 + B_1^2)(\nabla^2 + B_2^2)\cdots(V^2 + B_n^2)\phi_i(\bar{r}) \equiv [\prod_{j=1}^{n}(\nabla^2 + B_j^2)]\phi_i(\bar{r}) = 0 \;\; (i = 1, 2, \ldots, n). \tag{9}$$

The bucklings B_j^2 will in general be both positive and negative. We neglect the consideration of possible multiple roots. It is assumed that the fluxes ϕ_i can be expressed as linear combinations

$$\phi_i = \sum_{j=1}^{n} c_{ij}\,\phi_j \quad (i = 1, 2, \ldots, n), \tag{10}$$

where the functions $\phi_j = \phi_j(\bar{r})$ satisfy the individual equations

$$(\nabla^2 + B_j^2)\phi_j(\bar{r}) = 0 \tag{11}$$

If we set $c_{1j} = 1$ $(j = 1, 2, \ldots, n)$, the other coefficients c_{ij} are determined by the *coupling* relations. The given matrix $[c_{ij}]$ is denoted by C and its inverse by C^{-1}. We note that the above special property of the multi-group equations enables one to specify the potential theory by means of simple and double layers only, without the use of multiple layers.

Within the multiply connected regions bounded by the surfaces B_0 and B_k $(k = 1, 2, \ldots, m)$, each function $\phi_j(\bar{r})$ can, by Green's second theorem, be expressed in terms of its boundary values as follows:

$$\phi_j(\bar{r}) = \oint_{B_0}\left[G_j(\bar{r}, \bar{b}_0)\,\frac{\partial\phi_i(\bar{b}_0)}{\partial n_{b_0}} - \frac{\partial G_j(\bar{r}, \bar{b}_0)}{\partial n_{b_0}}\,\phi_j(\bar{b}_0)\right]\mathrm{d}b_0$$
$$- \sum_{k=1}^{m}\oint_{B}\left[G_j(\bar{r}, \bar{b}_k)\,\frac{\partial\phi_i(\bar{b}_k)}{\partial n_{b_k}} - \frac{\partial G_j(\bar{r}, \bar{b}_k)}{\partial n_{b_k}}\,\phi_j(\bar{b}_k)\right]\mathrm{d}b_k\,. \tag{12}$$

All normal derivatives in (12) are taken in the outward direction from the point of view of the individual regions. For the first integral the surface is approached from the inside, while for the others from the outside. We use the notations $\bar{b}_k$ and $\mathrm{d}b_k$ instead of $\bar{s}_k$ and $\mathrm{d}s_k$ to denote the set of surface coordinates and a surface element of B_k. As the infinite region Green's functions we use with the notations of [12]

Geometry	$B_j^2 > 0$	$B_j^2 < 0$ (temporarily we denote B_j^2 by $-\kappa_j^2$)
2-dim.	$\frac{1}{2\pi i} H_0^{(1,2)}(B_j \lvert \bar{r} - \bar{r}' \rvert)$	$\frac{1}{2\pi} K_0(\kappa_j \lvert \bar{r} - \bar{r}' \rvert)$
3-dim.	$\frac{1}{4\pi} \frac{e^{\pm iB_j \lvert \bar{r} - \bar{r}' \rvert}}{\lvert \bar{r} - \bar{r}' \rvert}$	$\frac{1}{4\pi} \frac{e^{-\kappa j \lvert \bar{r} - \bar{r}' \rvert}}{\lvert \bar{r} - \bar{r}' \rvert}$

(13)

If we let $\bar{r} \to \bar{b}_0$ and $\bar{r} \to \bar{b}_k$ in turn, we obtain the limit relations [12, 13]:

$$\begin{aligned}
\tfrac{1}{2}\phi_j(\bar{b}_0) &= \oint_{B_0} \left[G_j(\bar{b}_0, \bar{b}'_0) \frac{\partial \phi_j(\bar{b}'_0)}{\partial n_{b'_0}} - \frac{\partial G_i(\bar{b}_0, \bar{b}'_0)}{\partial n_{b'_0}} \phi_j(b'_0) \right] \mathrm{d}b'_0 \\
&\quad - \sum_{k=1}^{m} \oint_{B_k} \left[G_j(\bar{b}_0, \bar{b}_k) \frac{\partial \phi_j(\bar{b}_k)}{\partial n_{b_k}} - \frac{\partial G_j(\bar{b}_0, \bar{b}_k)}{\partial n_{b_k}} \phi_j(\bar{b}_k) \right] \mathrm{d}b_k \\
\tfrac{1}{2}\phi_j(\bar{b}_k) &= \oint_{B_0} \left[G_j(\bar{b}_k, \bar{b}_0) \frac{\partial \phi_j(\bar{b}_0)}{\partial n_{b_0}} - \frac{\partial G_j(\bar{b}_k, \bar{b}_0}{\partial n_{b_0}} \phi_j(\bar{b}_0) \right] \mathrm{d}b_0 \\
&\qquad\qquad\qquad\qquad\qquad\qquad\qquad\qquad (k = 1, 2, \ldots, m) \\
&\quad - \sum_{k'=1}^{m} \oint_{B_{k'}} \left[G_j(\bar{b}_k, \bar{b}_{k'}) \frac{\partial \phi_j(\bar{b}_{k'})}{\partial n_{b_{k'}}} - \frac{\partial G_j(\bar{b}_k, \bar{b}_{k'})}{\partial n_{b_{k'}}} \phi_j(\bar{b}_{k'}) \right] \mathrm{d}b_{k'}
\end{aligned} \tag{14}$$

All integrals above are to be understood as Cauchy principal values when the points denoted by $\bar{b}_k$ or $\bar{b}_0$ and $\bar{b}'_k$ or $\bar{b}'_0$ lie on the same surface. The $m+1$ Eqs. (14) constitute a linear operator equation of Fredholm type for the vectors $(\phi_{j0}, \phi_{j1}, \phi_{j2}, \ldots, \phi_{jm})$ and $(\partial\phi_{j0}/\partial n_0, \partial\phi_{j1}/\partial n_1, \partial\phi_{j2}/\partial n_2, \ldots, \partial\phi_{jm}/\partial_{nm})$ where the argument notations have been dropped. When Eqs. (14) are written for all values of $j (j = 1, 2, \ldots, n)$, the result is a similar relation between two vectors with $n(m+1)$ components. The components of one vector are the functions ϕ_{jk}, while these of the other vector are the functions $\partial_{\phi jk}/\partial_{nk}$ $(j = 1, 2, \ldots, n;\ k = 0, 1, 2, \ldots, m)$. The relation (10) holds as well for the boundary values of the functions ϕ_{jk} and ϕ_{jk} and their derivatives, for each boundary B_k $(k = 0, 1, 2, \ldots, m)$ separately. Therefore, we can transform the last operator equation into an equation for new vectors x and y whose components are the fluxes $x_{ki} = \phi_{ki}$ and $y_{ki} = \partial\phi_{ki}/\partial n_k$, which are functions of the surface co-ordinates. This is achieved by means of the inverse transformation C^{-1}. The equation takes the form

$$x - Ax = Ty, \tag{15}$$

or, in the component representation

$$x_\nu - \sum_\mu A_{\nu\mu} x_\mu = \sum_\mu T_{\nu\mu} y_\mu \tag{16}$$

where we have introduced the abbreviations ν or μ for the ordered pairs (k, i) or (k', i'). We recall that the components of x and y are defined and so the whole Eq. (15) is valid for the artificial *smooth* surfaces $(k = 0, 1, 2, \ldots, m)$. If in addition the actual surfaces S_k $(k = 0, 1, 2, \ldots, m)$ are smooth, the present part of the treatment naturally can be applied directly to them. Equation (15) is a compatibility condition for the vectors x and y. The following linear vector space E is introduced: $x \in E$, if $x = (x_0, x_1, \ldots, x_k, \ldots, x_m)$, where $x_k = (x_{k1}, x_{k2}, \ldots, x_{ki}, \ldots, x_{kn})$, $x_{ki} \in \bar{C}(B_k)$, or x_{ki} belongs to the space of *complex-valued* continous functions on B_k. By introduction of a norm $\|x\|$ in E:

$$\|x\|^2 = \sum_k \|x_k\|^2, \quad \|x_k\|^2 = \sum_i \|x_{ki}\|^2, \quad \|x_{ki}\|^2, = \sup_{b_k \in B_k} |x_{ki}|^2, \tag{17}$$

it is made a Banach-space, as is easily seen. The transformations A and T, whose matrix elements are integral operators with bounded or weakly singular kernels, map E into itself. Eq. (15) has, in addition, two very important properties. Firstly, if we assume that x and y are a pair of compatible solutions, then if x is real, y is also real, and vice versa. This is seen by decomposing A and T into their real and imaginary parts:

$$x - (A_1 + iA_2)x = (T_1 + iT_2)y \tag{18}$$

Because of the regularity of the imaginary parts of

the kernels (13) application of Green's second formula yields for the imaginary parts of the operators $A_2x = T_2y$, from which the statement follows. Secondly, the existence of a non-trivial solution of the equation $x - Ax = 0$ is identified with the possibility of criticality under homogeneous Neumann conditions of the *considered region alone*. This is seen directly from Eq. (15). Thus in practical cases, when there are still other regions in the multi-region system, the inverse operator $(I - A)^{-1}$ is known to exist, and can be obtained in a discrete version by the method of successive approximations. As is seen in the more general case below, the boundary and interface conditions would for smooth surfaces yield a second equation, possibly homogeneous, of the same type as (15). Both equations.

$$x - Ax = Ty \qquad x - Bx = S(y + f) \quad (19)$$

would then provide the solution of the problem. We remark that in cases of very symmetric smooth surfaces even scalar products may be introduced and E becomes a Hilbert-space.

We continue with the consideration of the more general case, where the interfaces are not smooth, and let the B_k surfaces converge towards the S_k surfaces of Fig. 1 ($k = 0, 1, 2, \ldots, m$). It is assumed at first that no concentrated sources are present on the interfaces, so that the fluxes are everywhere finite. Later it will be indicated how such sources can be accounted for.

$$A_{\nu\mu}\, x_\mu = \oint_{B_{k'}} \frac{\partial Gi(\bar b_k, \bar b_{k'})}{\partial n_{b_{k'}}}\, x_{i'}(\bar b_{k'})\, db_{k'}\,,$$

In the case $k = k'$ the line or surface integrals are interpreted as Cauchy principal values. From now on our considerations will be limited to two-dimensional cases because the formal representation of functions of point sets becomes very simple. The line integrals (20) can be written using Stieltjes-integrals as follows:

$$\left.\begin{aligned} A_{\nu\mu}\, x_\mu &= \oint_{B_{k'}} x_{i'}(b_{k'})\; \mathrm{d}\int_0^{b_{k'}} \frac{\partial Gi(b_k,\, b'_{k'})}{\partial n_{b'_{k'}}} db'_{k'}\,, \\ T_{\nu\mu}\, y_\mu &= \oint_{B_{k'}} G_i(b_k, b_{k'})\; \mathrm{d}\int_0^{b_{k'}} y_{i'}(b'_{k'})\; db'_{k'} \end{aligned}\right\} (21)$$

The question is, what limits do the inner integrals in the expressions (21) approach when $B_k \to S_k$. For the latter integral of (21) these limits are determined by the choice of the space of the x-functions i.e. the boundary *fluxes*. As a result of the limit

$$T_{\nu\mu}\, y_\mu = \oint_{B_{k'}} Gi(\bar b_k, \bar b_{k'})\; y_{i'}\,(\bar b_{k'})\, db_{k'}\,. \qquad (20)$$

process it can be shown [2, 3, 11] that the compatible function spaces for the flux and its normal derivative are no longer the same space E, but we now have:

$$k \in E \;\therefore \lim_{B_{k'} \to S_{k'}} \int_0^{b_{k'}} y_{i'}(b'_{k'})\, db'_k$$

$$= Y_{i'}\,(S_{k'}) \in \bar V(S_{k'}) \quad \begin{pmatrix} i' = 1, 2, \ldots, n \\ k' = 0, 1, \ldots, m \end{pmatrix}, \quad (22)$$

where $\bar V(S_{k'})$ is the space conjugate to $\bar C(S_{k'})$, i.e. the space of complex-valued functions of bounded variation on $S_{k'}$. This means that, if the boundary fluxes are *continuous* functions of the arc coordinates, the Y-solutions will be found in the spaces of *functions of bounded variation*. Furthermore, the elements of the spaces $\bar C(S_k)$ are to be identified with elements in their second conjugate spaces.

Let $Y \in E^*$, if Y

$$= (Y_0, Y_1, \ldots, Y_k, \ldots, Y_m),\; Y_k = (Y_{k1}, Y_{k2}, \ldots, Y_{kj}, \ldots, Y_{kn}),\; Y_{kj} = Y_{kj}(s_k) \in \bar V(s_k)\,. \quad (23)$$

By using the norm

$$\| Y \|^2 = \sum_k \| Y_k \|^2,\; \| Y_k \|^2 = \sum_j \| Y_{kj} \|^2,\; \| Y_{kj} \|^2 = \operatorname*{Var}_0^{b_k} | Y_{kj} |^2 \qquad (24)$$

E^* becomes a Banach-space.

As a result of the limit process, Eq. (15) assumes the form

$$x - A'x = T'Y\,, \qquad (25)$$

or, in the component form,

$$x_\nu - \sum_\mu A'_{\nu\mu}\, x_\mu = \sum_\mu T'_{\nu\mu}\, Y_\mu\,. \qquad (26)$$

Typical terms in the sums have the forms

$$A'_{\nu\mu}\, x_\mu = \oint_{S_{k'}} x_{i'}(s_{k'})\; \mathrm{d}G_i^{s_k}\,(s_{k'}), \qquad T'_{\nu\mu}\, Y_\mu = \oint_{S_{k'}} G_i(s_k, s_{k'})\; \mathrm{d}Y_{i'}\,(s_{k'})\,, \qquad (27)$$

where $A'_{\nu\mu}$ is a mapping $[\bar C(S_{k'}) \to \bar C(S_k)]$ and $T'_{\nu\mu}$ a mapping $[\bar V(S_{k'}) \to \bar C(S_k)]$ (strictly $\bar C_{s_k}$ should read $\bar C^{**}_{s_k}$ in the latter). In Eqs. (27) $G_i^{s_k}(s_{k'})$ is in general a function of bounded variation obtained from the limit process (21).

The same statements concerning the generally complex solutions and the existence of non-trivial

solutions of $x - A'x = 0$ which were given in connection with Eq. (15) apply to Eq. (25) as well. We note that a simple matrix multiplication transforming the variables ϕ, $\partial\phi/\partial n$ into the new variables J_+ and J_- reveals interesting similarities between the present treatment and invariant imbedding.

Assume that forms corresponding to (25) are given for the sub-regions V_k, irrespective of whether they are simply connected or have sub-structures. That is,

$$x_k - B'_k\ x_k = S'_k\ Y_k\ ,(k = 1,\ 2,\ \ldots,\ r \leq m) \quad (28)$$

where a factor D_0/D_k arising from the continuity of the current (not normal derivative) is still included in the matrix elements. It appears that, even if homogeneous boundary conditions are given on the rest of the S_k surfaces including S_0, they can be written in the same form as (28). The result is a pair of equations:

$$x - A'x = T'Y \qquad x - B'x = S'Y. \quad (29)$$

If there are sources, concentrated fuel or absorber layers or lines or points distributed on the surfaces one has to distinguish between the inner boundary values, x_i and Y_i, and outer boundary values, x_0 and Y_0, of the vectors x and Y. Thus one has

$$x_0 - A'x_0 = T'Y_0 \qquad x_i - B'x_i = S'Y_i \quad (30)$$

rather than (29). To these equations, however, must be added two linear, possibly inhomogeneous, relations between the four vectors, stating the behaviour of the fluxes in crossing the surfaces. Thus in some cases the norm of the relevant spaces must be changed; perhaps the spaces must be extended. Unfortunately it is not possible to give a detailed presentation of the general numerical methods to be used in solving (29) or the corresponding inhomogeneous system at this time; for these see [13]. Elsewhere the author will apply this method in treating overall reflected rectangular and cylindrical cores.

POTENTIAL THEORY FOR REACTOR KINETICS

We must limit ourselves to one example of the possibilities for extending the potential theory for reactor kinetics. Let us consider a two-dimensional reactor region whose boundary curve is generally time-dependent, i.e. $F(x, y, t) = 0$. It is assumed that the surface of this reactor region is smooth with respect to all variables in x, y, t-space (Fig. 2) and that all parameters such as cross sections and so on remain constant. The one-group equation without delayed neutrons

$$L\phi \equiv \nabla^2\phi - \kappa^2\phi - \frac{1}{c^2}\frac{\partial\phi}{\partial t} = 0\ ;\quad c^2 = Dv \quad (31)$$

is considered, and the initial condition $\phi(\bar{r}, 0) = \phi_0(\bar{r})$ is taken. We wish to transform the boundary value problem for $\phi(\bar{r}, t)$ into an integral relation connecting the time dependent boundary values $\phi(\bar{s}, t)$, $(\partial\phi/\partial n)$ $(\bar{s}, t)$ and $\phi_0(\bar{r})$ together. The time dependent Green's function $G(\bar{r}, t; \bar{r}', t')$ for the operator L in a two-dimensional geometry which satisfies

$$LG(\bar{r}, t; \bar{r}; t') = \delta(\bar{r} - \bar{r}')\ \delta(t - t'),\quad t > t'$$

and vanishes for $t < t'$ and for $|\bar{r} - \bar{r}'| \to \infty$ is

$$G(\bar{r}, t; \bar{r}', t') = \begin{cases} \dfrac{1}{4\pi(t - t')} \exp\left[-\kappa^2 c^2(t - t') - \dfrac{|\bar{r} - \bar{r}'|^2}{4c^2(t - t')}\right], & t \geqq t' \\ 0, & t < t' \end{cases} \quad (32)$$

We will also use Green's function $G^*(\bar{r}, t; \bar{r}', t')$ for the adjoint operator:

$$L^*\phi = \nabla^2\phi - \kappa^2\phi + \frac{1}{c^2}\frac{\partial\phi}{\partial t}. \quad (33)$$

$G^*(\bar{r}, t; \bar{r}', t')$ is obtained from G by inversion of the time direction,

$$G^*(\bar{r}, t; \bar{r}', t') = G(\bar{r}, -t; \bar{r}', -t'). \quad (34)$$

When Green's second theorem is applied to the functions $\phi(\bar{r}', t')$ and $G^*(\bar{r}', t'; \bar{r}, t)$ as well as to the operator L, one obtains the following expression

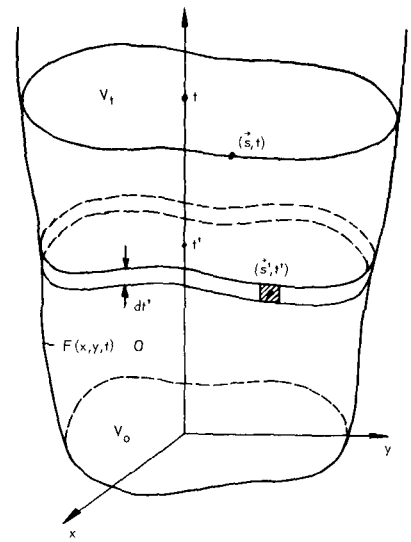


Figure 2. A reactor region with time-dependent boundaries as a region of x, y, t-space

by integrating over the reactor region from $t = 0$ to $t_1 > t$ in x, y, t-space

$$\phi(\bar{r},t) = \int_0^t \mathrm{d}t' \oint_{s_{t'}} \left[G(\bar{r},t;\bar{s}',t') \frac{\partial\phi(\bar{s}',t')}{\partial n_{s'}} - \frac{\partial G(\bar{r},t;\bar{s}',t')}{\partial n_{s'}} \phi(\bar{s}',t') \right] \mathrm{d}S_{t'}$$

$$- \frac{1}{c^2} \int_{V_0} G(\bar{r},t,\bar{r}',t')\phi(\bar{r}',0)\mathrm{d}V'_0 \qquad (35)$$

In the above equation, $\mathrm{d}S_t$ denotes the surface element at time t in the neighbourhood of the surface point $\bar{s}$. Normal differentiation $\partial/\partial n_{s'}$, is performed in the direction of the outward normal of the reactor surface. The desired representation is finally obtained from (35) by letting $\bar{r} \to \bar{s}$. The result, analogous to Eq. (14), is

$$\tfrac{1}{2}\phi(\bar{s},t) + \int_0^t \mathrm{d}t' \oint_{s_{t'}} \frac{\partial G(\bar{s},t;\bar{s}',t')}{\partial n_{s'}} \phi\bar{s}',t')\mathrm{d}S_{t'}$$

$$= \int_0^t \mathrm{d}t' \oint_{s_{t'}} G(\bar{s},t;\bar{s}',t') \frac{\partial\phi(\bar{s}',t')}{\partial n_{s'}} \mathrm{d}S_{t'} - \frac{1}{c^2}\int_{V_0} G(\bar{s},t,\bar{r}',0)\phi(\bar{r}',0)\mathrm{d}V'_0 \,. \qquad (36)$$

The functions $\phi(\bar{s},t)$ and $\partial\phi(\bar{s},t)/\partial n_s$ can be interpreted as the strengths of double and simple layers distributed on the surface $F(x,y,t) = 0$. The integral transformations appearing in (36) can also be interpreted as transformations of a suitable Banach-space into itself, and the method of successive approximations can be used in practical calculations. The extension of the treatment to multigroup kinetics provides certain difficulties because a decomposition comparable to (9) could not be found in the general case.

CONCLUSIONS

In this paper the author has emphasized the qualitative presentation based on generalized potential theory of a possible treatment of the multi-region diffusion equations. Despite the fact that even the theory of the integral equations of potential theory still contains some open questions, this approach seems to constitute a connecting link between some, often not very well founded, calculational methods of reactor diffusion theory. The relationship between the boundary values of any boundary value problem is a central question, which in eigenfunction expansion methods is obscured. It is probable that this method has significance also as a tool for numerical calculations, but as yet its main interest seems to lie on more theoretical questions. There are still possibilities for the extension of the approach under questions. One of them is the consideration of more general fuel distributions, with generally piece continuous space-dependent parameters. In such cases one would use the functions of Levi instead of Green's functions.

REFERENCES

1. Radon, J., Sitzungsber. Akad. Wiss. Wien, *122*, Abt. IIa, 1295-1438 (1913).
2. Radon, J., *ibid.*, *128*, 1083-1121 (1919).
3. Radon, J., *ibid.*, *128*, 1123-1167 (1919).
4. Schulze, O., in *Nuclear Engineering Handbook* (Etherington, H., ed.), pp. 6-70—6-74, McGraw-Hill Book Company, Inc., New York (1958).
5. Stippel, H., Proceedings of the Second International Conference on the Peaceful Uses of Atomic Energy, P/1440, Vol. 16, p. 639, United Nations (1958).
6. Galanin, A. D., Kernenergie, *2*, 141-146 (1961).
7. Martino, M. A., USAEC report KAPL-1867 (1957).
8. Habetler, G. J., and Martino, M. A., USAEC report KAPL-1886 (1958).
9. Habetler, G. J., and Martino, M. A., in Proc. of Symposia in Applied Mathematics (Birkhoff, G. and Wigner, E. P., eds.), Vol. 6, pp. 127-139, Amer. Math. Soc., Providence, Rhode Island (1961).
10. Shimizu, A., J. Atomic Energy Soc. Japan, *5* (5), 359-368 (1963).
11. Riesz, F., and Sz.-Nagy, B., *Vorlesungen über Funktionalanalysis*, pp. 195-200 and 209-211, VEB Deutscher Verlag der Wissenschaften, Berlin (1956).
12. Kupradse, W. D., *Randwertaufgaben der Schwingungstheorie und Integralgleichungen*, VEB Deutscher Verlag der Wissenschaften, Berlin (1956).
13. Kupradse, V. D., *Dynamical Problems of Elasticity*, North-Holland Publ. Co., Amsterdam (1964).
14. Jaswon, M. A., Proc. Roy. Soc. A, *275*, 23-32 (1963).
15. Sobolev, S. L., *Applications of Functional Analysis in Mathematical Physics*, Amer. Math. Soc., Providence, Rhode Island (1963).

ABSTRACT - RÉSUMÉ - АННОТАЦИЯ - RESUMEN

A/842 Finlande

Théorie du potentiel généralisé pour la diffusion multigroupe dans un réacteur à plusieurs régions

par H. Koskinen

Ce mémoire présente la base mathématique pour un nouveau traitement des équations de diffusion à plusieurs groupes dans des géométries générales, à bien des égards analogue à la théorie classique du potentiel. L'auteur s'est déjà référé à ce traitement dans une publication antérieure.

Les équations aux dérivées partielles conformes à la théorie de diffusion décrivant le comportement statique ou cinétique d'un réacteur à plusieurs régions peuvent être transformées en un système d'équations intégrales linéaires pour les flux aux *surfaces* et pour les dérivées normales des flux. Si les surfaces de séparation contiennent des arêtes ou des singularités dues aux sources concentrées ou d'autres singularités, la dérivée normale est remplacée par des fonctions d'ensemble additives qui définissent une mesure de Radon dans les équations intégrales correspondantes. Les fonctions de Green utilisées sont celles du milieu infini des opérateurs

$$A_i = \nabla^2 - \kappa_i^2$$

pour le cas statique, et

$$A_i = \nabla^2 - \kappa_i^2 - \frac{1}{c_i^2}\frac{\partial}{\partial t}$$

pour le cas cinétique. Les fonctions de Green singulières et leurs dérivées normales sur les surfaces apparaissent comme noyaux dans les équations.

Selon la théorie du potentiel, chaque comportement cinétique du réacteur peut être interprété comme le résultat, soit d'un changement de forme survenu dans une certaine région du réacteur (limites mobiles), soit d'un changement en fonction du temps des conditions limites aux surfaces stationnaires (longueur d'extrapolation dépendant du temps, etc.). Même dans le cas cinétique, les flux $\Phi_i(x,y,z,t)$ peuvent donc être représentés par des potentiels généralisés des couches simples ou doubles distribuées sur les surfaces de l'espace (x,y,z,t).

Dans chaque cas, le système des équations intégrales obtenu peut être présenté comme une équation linéaire

$$x - Kx = f \qquad x, f \in \mathrm{E}$$

pour un élément x d'un certain espace de Banach E. Des composantes du vecteur x sont des fonctions définies sur les surfaces du réacteur. K est une transformation linéaire de l'espace E en lui-même. Même dans le cas des géométries les plus générales, il existe des méthodes bien connues pour effectuer la solution numérique des équations; dans les cas particulièrement simples, des solutions approchées peuvent être obtenues. Cette formulation est particulièrement utile pour l'explication de quelques aspects théoriques des solutions.

A/842 Финляндия

Обобщенная потенциальная теория для многогрупповой диффузии в реакторе с многими областями

Х. Коскинен

В статье содержится математическая основа для нового подхода к многогрупповым диффузионным уравнениям в общей геометрии, во многих отношениях аналогичного классической потенциальной теории. Этот подход упоминался автором в предыдущей работе.

Парциальные дифференциальные уравнения, описывающие статическое или кинетическое поведение реактора со многими областями в диффузионном приближении, можно преобразовать в систему линейных интегральных уравнений для поверхностных потоков и для нормальных производных потоков на поверхностях. Если поверхности раздела имеют углы, или концентрированные источники, или другие особенности, роль нормальной производной будет играть аддитивная серийная функция, из которой получается радонный делитель в соответствующих интегральных уравнениях. Используемые функции Грина являются функциями бесконечной среды операторов

$$A_i = \nabla^2 - \varkappa_i^2$$

для статического случая или

$$A_i = \nabla^2 - \varkappa^2 - \frac{1}{i^2}\frac{\partial}{\partial t}$$

для кинетического случая. Сингулярные функции Грина и их производные, перпендикулярные к поверхности, являются ядрами в уравнениях.

В свете потенциальной теории всякое кинетическое поведение реактора может рассматриваться как результат либо изменения формы областей реактора (передвижные границы), либо изменения во времени граничных условий на стационарных поверхностях (экстраполированная длина, зависящая от времени, и т. п.). Следовательно, даже в кинетическом случае потоки Фi (x, y, z, t) можно представить при помощи обобщенных потенциалов одинарного или двойного слоев, распределенных по поверхности в (x, y, z, t)-пространстве.

В обоих главных случаях полученный ряд интегральных уравнений можно записать в виде линейного уравнения

$$x - Kx = f, \quad f \in E$$

для элемента x определенного пространства Банаха E. Вектор x содержит компоненты, которые являются несколькими функциями по поверхностям, присутствующим в реакторе. K — это линейное связанное преобразование пространства в самом себе. Даже для большинства общих геометрий имеются стандартные методы численного решения этого уравнения, но в некоторых особенно простых случаях можно найти приближенные решения. Эта формулировка имеет особое значение для объяснения некоторых теоретических аспектов решений.

A/842 Finlandia

Teoría del potencial generalizado para la difusión con varios grupos en un reactor general de varias regiones

por H. Koskinen

Este artículo contiene el fundamento matemático de un nuevo tratamiento de las ecuaciones de difusión con varios grupos, en geometrías generales, tratamiento que es, en muchos aspectos, análogo a la teoría clásica del potencial. Este método ha sido citado por el autor en una memoria anterior.

Las ecuaciones en derivadas parciales que describen el comportamiento estático o cinético de un reactor con varias regiones, dentro de la aproximación de la teoría de la difusión, pueden transformarse en un sistema de ecuaciones integrales lineales en los flujos de *superficie* y en las derivadas normales de los flujos en las superficies. Si las superficies de separación presentan esquinas, fuentes concentradas u otras singularidades, el papel de la derivada normal lo representa una función aditiva de conjunto de la que se deduce una medida de Radon en las ecuaciones integrales correspondientes. Las funciones de Green empleadas son las correspondientes a un medio infinito para los operadores

$$A_i = \nabla^2 - \kappa_i^2$$

en el caso estático, o para

$$A_i = \nabla^2 - \kappa_i^2 - \frac{1}{c_i^2}\frac{\partial}{\partial t}$$

en el caso cinético. Las funciones singulares de Green y sus derivadas normales a las superficies aparecen como núcleos integrales en las ecuaciones.

Desde el punto de vista de la teoría del potencial, el comportamiento cinético de un reactor puede interpretarse como el resultado bien sea de una variación en la forma de las regiones del reactor (contornos móviles) o como una variación temporal de las condiciones de contorno en superficies estacionarias (longitud extrapolada dependiente del tiempo, etc.). Por consiguiente, aun en el caso cinético, los flujos $\Phi_i\ (x, y, z, t)$ pueden representarse por medio de potenciales generalizados de una y de dos capas, definidos sobre superficies del espacio (x, y, z, t).

En ambos casos principales, el sistema de ecuaciones integrales que resulta puede expresarse como ecuación lineal

$$x - Kx = f \qquad x, f \in E$$

en un elemento x de un determinado espacio E de Banach. Las componentes del vector x son funciones definidas sobre las superficies del reactor, K es una transformación lineal acotada del espacio en sí mismo. Incluso para las geometrías más generales, hay métodos conocidos para la resolución numérica de dicha ecuación, pero en algunos casos particularmente simples pueden obtenerse soluciones aproximadas. Este método es especialmente potente para explicar algunos aspectos teóricos de las soluciones.

Theoretical kinetic studies of boiling water reactors and multi-region reactors

By T. Kanai,* T. Kawai,* J. Miida,** N. Suda,** S. An*** and A. Oyama***

THEORETICAL DYNAMIC ANALYSIS OF BOILING WATER REACTORS

T. Kanai, T. Kawai, J. Miida and N. Suda

The dynamic behaviour of two-phase flow is an important consideration in the dynamic analysis of boiling water reactors. The authors have derived a void equation which describes the time-space dependent behaviour of void fraction in a one-dimensional channel based on the fundamental laws of conservation of mass, energy and momentum. Then these equations are simplified and combined with other equations to form a complete mathematical model of the boiling water reactor. Finally, using the model, simplified transfer functions are obtained, which can be considered a compromise between completeness and moderate complexity, and which make it possible to investigate readily dynamic characteristics from the design parameters. The transient characteristics and the stability of the whole system dynamics are also investigated.

Void equation [1]

Derivation of void equation

Assuming no correlation between the pressure and velocity components in the turbulence, and also some space independence of correlation between velocity components, macroscopic conservation laws for two-phase flow are derived:

$$\frac{\partial}{\partial t}\{\rho_w(1-f)+\rho_s f\}+\frac{\partial}{\partial z}\{\rho_w(1-f)V_w+\rho_s f V_s\}=0 \tag{1}$$

$$\frac{\partial}{\partial t}\{\rho_w i_w(1-f)+\rho_s i_s f\}+\frac{\partial}{\partial z}\{\rho_w i_w(1-f)V_w+\rho_s i_s f V_s\}=Q' \tag{2}$$

$$\frac{\partial}{\partial t}\{\rho_w V_w(1-f)+\rho_s V_s f\}+\frac{\partial}{\partial z}\{\rho_w V_w^2(1-f)+\rho_s V_s^2 f\}=-\frac{\partial}{\partial z}p-F_r \tag{3}$$

where all variables ρ, i, f, p, and V are quantities averaged over the channel section. The viscous dissipation of energy is neglected in Eq. (2).

In addition to these fundamental equations, the usual experimental slip relation is further assumed:

$$V_s=rV_w \tag{4}$$

where the slip ratio r is assumed to be a function of void volume fraction f. In principle, the relation between V_s and V_w should be derived from the microscopic fundamental equation, but the present knowledge of two phase turbulence seems insufficient to obtain it theoretically.

When equations (1) through (4) are solved, they yield a solution which includes the pressure wave accompanying void compression. If the sound velocity is high compared with water and vapour velocities, as is usually the case, pressure is considered to be a function of time only, which is determined by external conditions. In this case void volume fraction can be determined without the momentum equation (3). The inlet velocity $V_0(t)$ is considered as a boundary condition.

From Eqs. (1), (2) and (4), the following equations for f are obtained:

$$\frac{\partial f}{\partial t}+U\frac{\partial f}{\partial z}=q \tag{5}$$

$$q=\frac{1}{\rho_w\rho_s\Delta i}\frac{\rho_w V_w(1-f)+\rho_s V_s f}{V_w(1-f)+V_s f}\left[Q'-\frac{dp}{dt}\left\{\rho_w\frac{\partial i_w}{\partial p}(1-f)+\rho_s\frac{\partial i_s}{\partial p}f\right\}\right]+\frac{dp}{dt}\frac{f(1-f)}{1-f+rf}\left(r\frac{1}{\rho_w}\frac{d\rho_w}{dp}-\frac{1}{\rho_s}\frac{d\rho_s}{dp}\right) \tag{6}$$

$$U=\{r+f(1-f)(\partial r/\partial f)\}V_w/(1-f+rf) \tag{7}$$

where U is the velocity with which the void fraction f is transmitted, and it may be called *the void transmission velocity*.

* Hitachi Central Research Laboratory.
** Japan Atomic Energy Research Institute.
*** Tokyo University.

Table 1. Components of the effective void source q

	Evaporation by heat	Flashing or condensation	Compression or expansion of steam	Compression or expansion of water
Direct effect	$\frac{Q}{\rho_s \Delta i}$	$I = \frac{-1}{\rho_s \Delta i} \{(1-f)\rho_w i'_w + f\rho_s i'_s\} \times \frac{dp}{dt}$	$J = \frac{-f\rho'_s}{\rho_s} \frac{dp}{dt}$	0
Indirect effect	$\frac{Q}{\rho_s \Delta i} \frac{-rf(1-\rho)}{1-f+rf}$	$I \times \frac{-rf(1-\rho)}{1-f+rf}$	$J \times \frac{-rf}{1-f+rf}$	$\frac{(1-f)fr}{1-f+rf} \frac{\rho'_w}{\rho_w} \times \frac{dp}{dt}$
Net effect	$\frac{Q}{\rho_s \Delta i} \frac{1-f+rf\rho}{1-f+rf}$	$I \times \frac{1-f+\rho rf}{1-f+rf}$	$J \times \frac{1-f}{1-f+rf}$	As above

$' = d/dp \qquad \rho = \rho_s/\rho_w$

Physical interpretation of void transmission velocity and void source

In order to clarify the physical interpretation of each term in the void equation (5), consider the formula

$$\frac{\partial f}{\partial t} + \frac{\partial}{\partial z}(V_s f) = \frac{1}{\rho_s \Delta i} - \left[Q' - \frac{dp}{dt} \left\{ \rho_w \frac{di_w}{dp}(1-f) + \rho_s \frac{di_s}{dp} f \right\} \right] - \frac{dp}{dt} f \frac{1}{\rho_s} \frac{d\rho_s}{dp} \tag{8}$$

which is obtained by eliminating $\frac{\partial(1-f)V_w}{\partial z}$ from Eqs. (1) and (2). The right-hand side of Eq. (8) represents the direct effects of void formation by vaporization, flashing or condensation, as well as compression or expansion. The term $\frac{\partial}{\partial z}(V_s f)$ is split into two terms:

$$\frac{\partial}{\partial z}(V_s f) = \left(V_s + f \frac{\partial V_w}{\partial f} \right) \frac{\partial V_w}{\partial z} + fr \frac{\partial V_w}{\partial z} \tag{9}$$

where

$$fr \frac{\partial V_w}{\partial z} = \frac{fr(\rho_w - \rho_s)}{\rho_w \rho_s \Delta i (1-f+rf)} \left[Q' - \frac{dp}{dt} \left\{ \rho_w \frac{di_w}{dp}(1-f) + \rho_s \frac{di_s}{dp} f \right\} \right] - \frac{rf}{1-f+rf} f \frac{1}{\rho_s} \frac{d\rho_s}{dp} \frac{dp}{dt} - \frac{rf(1-f)}{1-f+rf} \frac{1}{\rho_s} \frac{d\rho_s}{dp} \frac{dp}{dt} \tag{10}$$

This is a part of the void source term in the void equation that arises from velocity change. Therefore, this should be interpreted as an *indirect void source* compared with the direct one in Eq. (8). In Table 1 the effective void source is classified according to four physical origins and resolved into direct and indirect effects. The indirect effect is always smaller in magnitude than the direct one and is opposite in sign (Fig. 1).

From Eq. (9) the void transmission velocity U is obtained:

$$U = V_s + f(\partial V_s / \partial f) ,$$

which differs from the vapour velocity V_s. In general, the magnitude of U is not always between V_s and V_w.

Figures 2 and 3 show examples of the response of void distribution to a step change in each disturbance.

Among the four disturbances, the effect of inlet velocity change turns out to be indistinguishable from that of the heat source. Void reactivity is also computed from the perturbation theory, and is shown in Fig. 4.

Boiling water reactor transfer functions

Formulation of transfer function [2]

Transfer functions are derived from the void Eq. (5) by dividing the variables into steady state values and small deviations from the steady state, and then ignoring all the products of two or more deviation terms:

$$\frac{\partial \delta f}{\partial t} + U^* \frac{\partial \delta f}{\partial z} = L_1 \delta f + L_2 \delta z_1 + L_3 \frac{\delta Q}{Q^*} + L_4 \frac{\delta V_o}{V_o^*} + L_5 \frac{d\delta p}{dt} + L_6 \delta p \tag{11}$$

where L_1 through L_6 are functions of the stationary void distribution. Three disturbances, δQ, δV_0 and δp, are considered as sources external to the void. The boiling boundary shift δz_1, which is not present in the original void equation, may be considered another independent disturbance, although it is dependent on the conditions in the subcooled region.

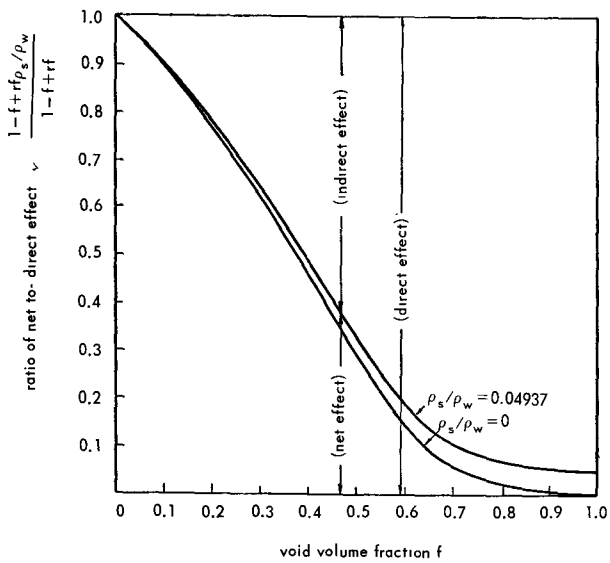


Figure 1. Ratio of net to direct effect in the effective void source q

Eq. (11) is further simplified when it is assumed that the slip ratio is unity and the distribution of heat flux along the channel is uniform. Upon Laplace transformation of the equation thus obtained and solving it with respect to z, one obtains $\delta f(z, s)$ in explicit form. The space-dependent void transfer functions, which relate the local void fraction to the four variables δQ, δV_0, δz_1 and δp are obtained from this equation. Integration of the local void fraction over the whole boiling region of the core gives the total void volume in the core. Void transfer functions relating the total void volume to the four variables $G_1(s)$ through $G_4(s)$ are thus obtained and given in [2].

Core boiling boundary transfer functions are obtained by linearizing in the same way the fundamental equation of the water temperature in the subcooled region. They are given by $G_5(s)$ through $G_8(s)$ in [2].

The reactor vessel is divided into two zones: the upper part occupied by saturated steam and water and the lower part occupied by the subcooled water.

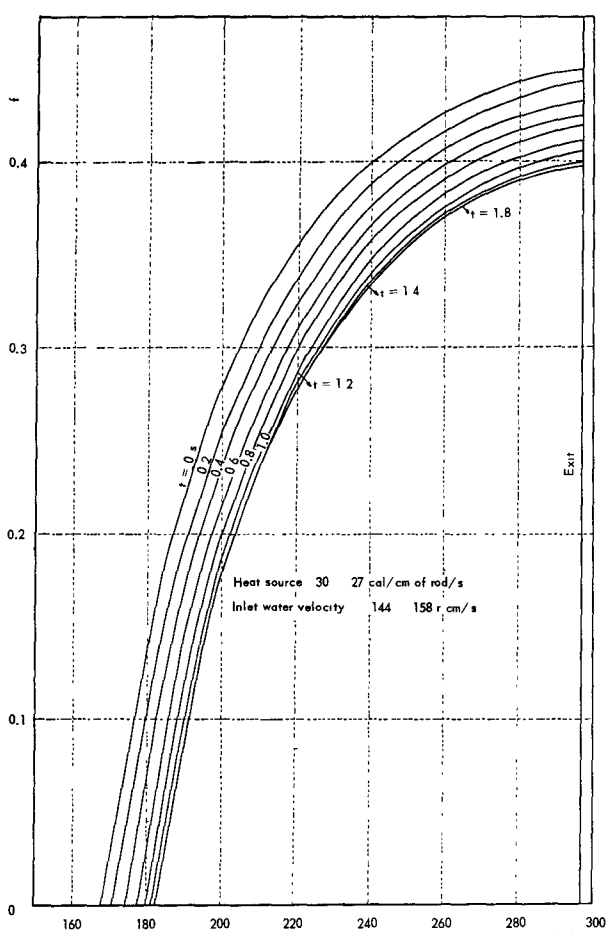


Figure 2. Void distribution response for step change of heat source or inlet water velocity

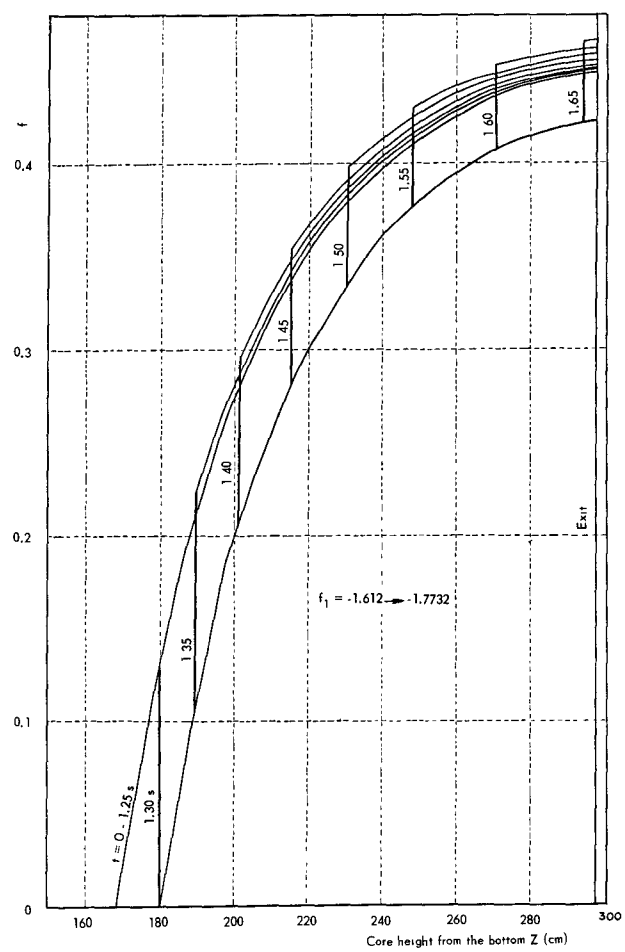


Figure 3. Void distribution response for step change of subcooling

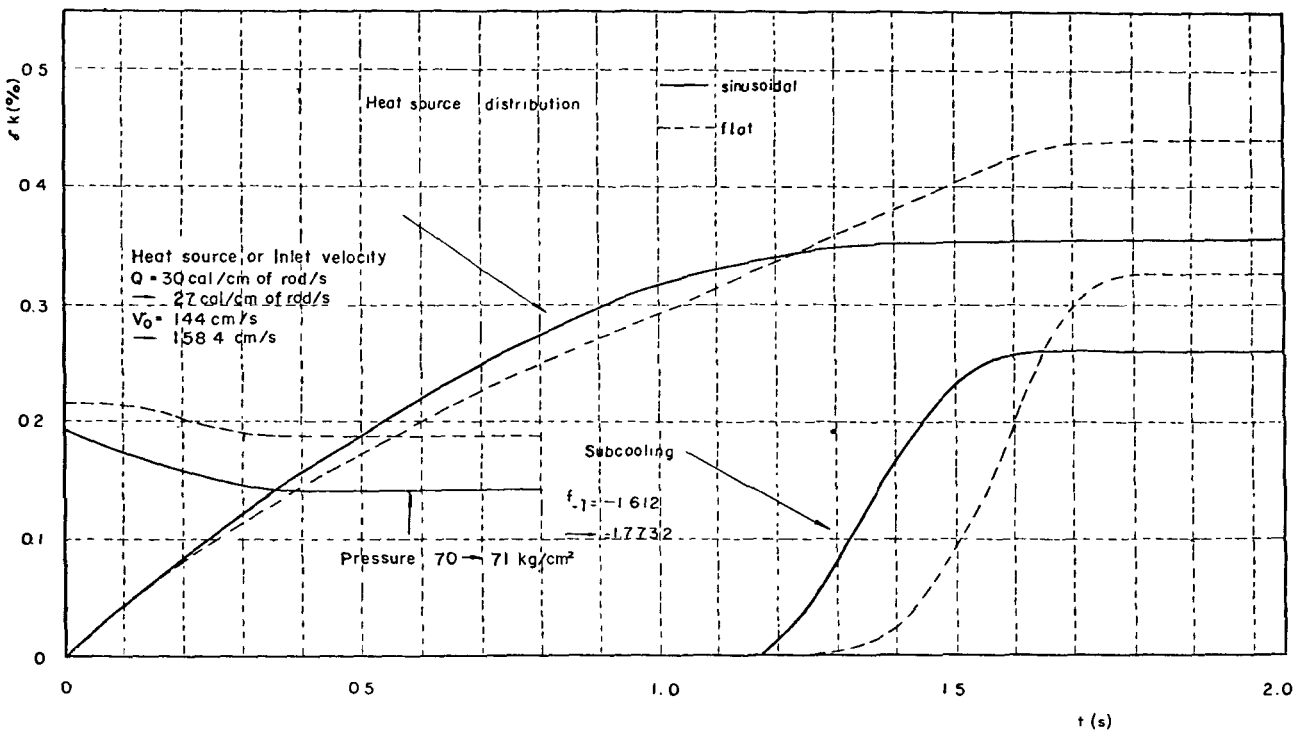


Figure 4. Void reactivity response for step change of heat source, subcooling and pressure

From the fundamental equations based on mass balance, energy balance, and conditions of constant volume, the vessel pressure transfer functions are obtained as $G_{16}(s)$ through $G_{19}(s)$ in [2].

The inlet water enthalpy transfer functions are obtained by regarding the downcomer as a single tube and by assuming complete mixing between feedwater flow and recirculation flow at the top of the subcooled region. The transfer functions obtained from these assumptions are $G_{22}(s)$ through $G_{24}(s)$ in [2].

The inlet velocity transfer functions have been obtained from the fundamental equations of hydrodynamics of the natural circulation loop, but computer studies have indicated that their effect on the whole system dynamics may be ignored.

The recirculation flow transfer functions also have been obtained from the fundamental equations of vessel pressure dynamics, of which also the effect has been shown to be negligible.

The relations between these transfer functions are shown in Fig. 5.

Simplified transfer functions [3]

The transfer functions derived above are simplified, and approximate forms are obtained. Most of them are in the form of combinations of single time constant delays whose time constants and static gains are readily evaluated from design parameters. The results are summarized in Table 2 and the interrelations between these transfer functions are shown in Fig. 6. The parameters appearing in Table 2 are summarized in Table 3 in terms of design parameters. For obtaining an approximate formula for the single time constant, the 45°-phase-lag method [3] is adopted throughout the simplification process, since it has been found to give the best result of several methods.

Most of the numerical calculations of the transfer functions for the full power condition of JPDR have been obtained in order to demonstrate the validity of the simplification. The frequency characteristics of $G_1(s)/Q^*$ and its approximation from the simplified transfer function given in Table 2 are shown in Fig. 7. The frequency characteristics of $G_4(s)$ and its approximation are shown in Fig. 8. The results are quite satisfactory. The frequency characteristics of the void feedback transfer function obtained from Fig. 6 are shown in Fig. 9.

It should be noted that several important conclusions are obtained from the void transfer functions:

(*a*) Time constant T_1 of the whole void volume in the boiling region for power change is seen from Table 3 to be roughly 40% of the void transit time τ_{12}. Other time constants T_3 and T_4 are seen to be roughly 70% and 60% respectively of τ_{12}. The result is quite general under the assumptions adopted here;

(*b*) Time constants are almost independent of the power level;

(*c*) Gain constants and time constants of void transfer functions have proved [3] to be almost constant when power level and operating pressure are changed proportionally; the dynamic behaviour of the core void does not change under such a

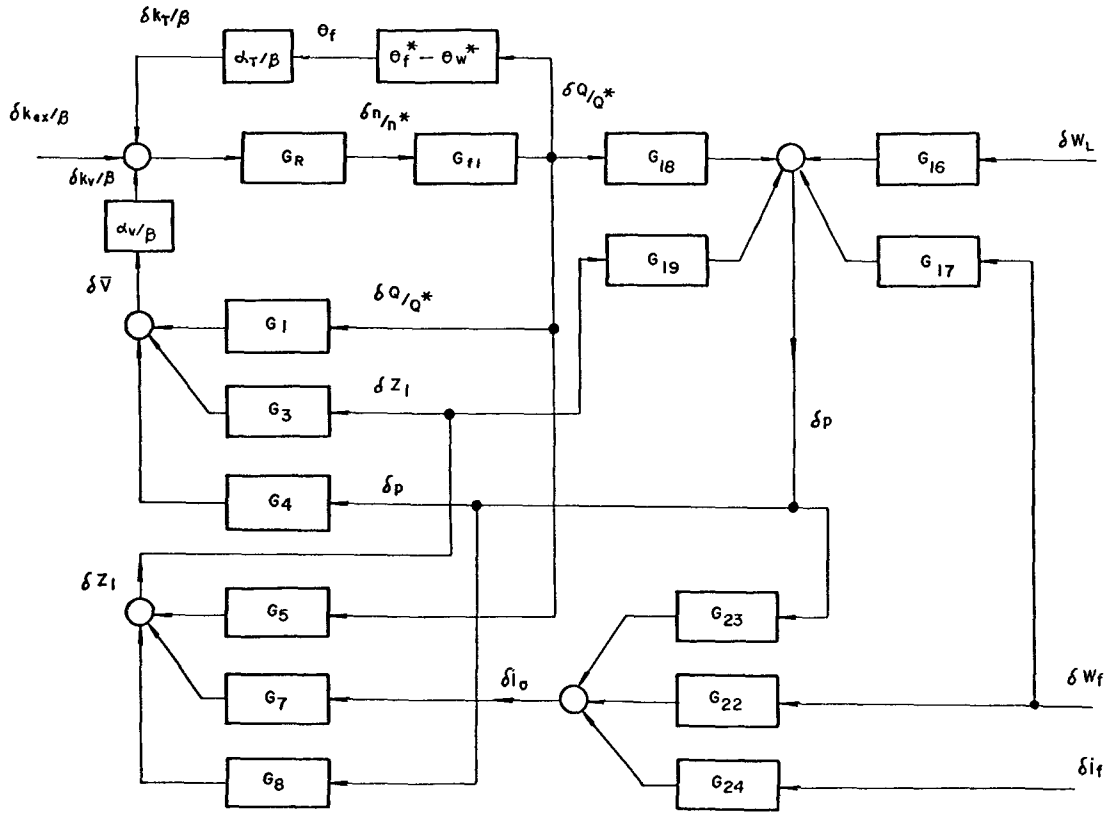


Figure 5. Transfer functions of a natural circulation boiling water reactor

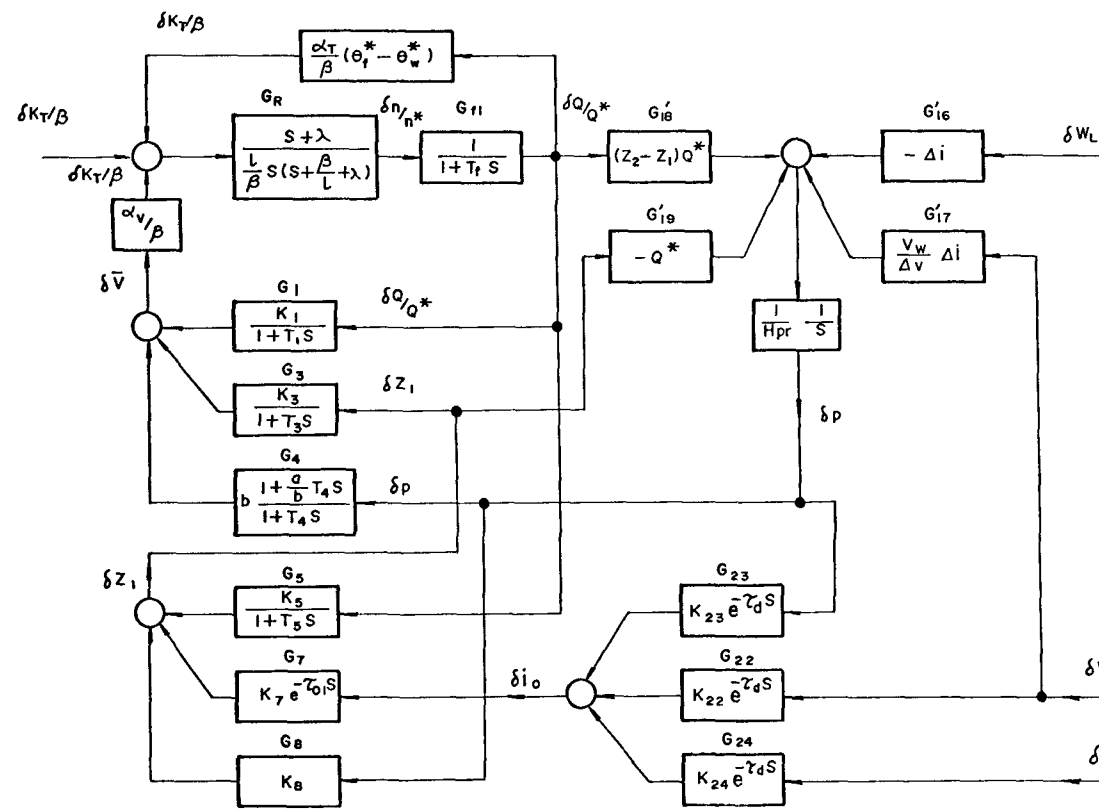


Figure 6. Simplified block diagram

condition. This conclusion is quite important and useful, and is also consistent with the measured transfer functions of EBWR [4].

Simplified model with small time constants neglected

In order to further simplify the model shown in Fig. 6 the feedback transfer function is reduced to two feedback paths; one from power to void and the other from power through pressure to void, by eliminating δz_1 and δi_0. For studies on the control of boiling water reactors it is possible to ignore smaller time constants, for example those less than one second.

Thus, a further simplified model is obtained and shown in Fig. 10. The frequency characteristics of the void feedback transfer function based on Fig. 10 are shown by the dotted line in Fig. 9. The discrepancy in the high frequency region is due to having neglected small time constants.

Some characteristics of the whole system dynamics

Transient analyses based on the simplified transfer functions derived in Fig. 6 are made on an analog computer. Some of them are shown in Fig. 11. The diagrams indicate that the initial transients of all variables die out in 20 to 30 seconds and thereafter

Table 2. Simplified transfer functions

Symbol	Output / Input	Transfer function	Symbol	Output / Input	Transfer function
G_R	$\frac{\delta n/n^*}{\delta k/\beta}$	$\frac{s+\lambda}{\frac{\ell}{\beta}s\,(s+\frac{\beta}{\ell}+\lambda)}$	G_8	$\frac{\delta z_1}{\delta p}$	K_8
G_{f1}	$\frac{\delta Q/Q^*}{\delta n/n^*}$	$\frac{1}{1+T_f\cdot s}$	G_{16}	$\frac{\delta p}{\delta W_L}$	$-\Delta i\,\frac{1}{H_{pr}}\cdot\frac{1}{s}$
G_{f2}	$\frac{\delta\theta_f}{\delta n/n^*}$	$\frac{\theta_f{}^*-\theta_w{}^*}{1+T_f\cdot s}$	G_{17}	$\frac{\delta p}{\delta W_f}$	$\frac{v_w}{\Delta v}\,\Delta i\,\frac{1}{H_{pr}}\cdot\frac{1}{s}$
G_1	$\frac{\delta\bar{V}}{\delta Q/Q^*}$	$\frac{K_1}{1+T_1\cdot s}$	G_{18}	$\frac{\delta p}{\delta Q/Q^*}$	$(z_2-z_1)Q^*\,\frac{1}{H_{pr}}\cdot\frac{1}{s}$
G_3	$\frac{\delta\bar{V}}{\delta z_1}$	$\frac{K_3}{1+T_3\cdot s}$	G_{19}	$\frac{\delta p}{\delta z_1}$	$-Q^*\,\frac{1}{H_{pr}}\cdot\frac{1}{s}$
G_4	$\frac{\delta\bar{V}}{\delta p}$	$b\,\frac{1+\frac{a}{b}T_4\cdot s}{1+T_4\cdot s}$	G_{22}	$\frac{\delta i_0}{\delta W_f}$	$K_{22}\,e^{-\tau_d\cdot s}$
G_5	$\frac{\delta z_1}{\delta Q/Q^*}$	$\frac{K_5}{1+T_5\cdot s}$	G_{23}	$\frac{\delta i_0}{\delta p}$	$K_{23}\,e^{-\tau_d\cdot s}$
G_7	$\frac{\delta z_1}{\delta i_0}$	$K_7\,e^{-\tau_{01}\cdot s}$	G_{24}	$\frac{\delta i_0}{\delta i_f}$	$K_{24}\,e^{-\tau_d\cdot s}$

Table 3. Parameters appearing in simplified transfer functions (Table 2)

$$K_1 = (\frac{v_s}{\Delta v}V_0{}^*A_{co})\tau_{12}\,(1-\frac{y_2-1}{y_2\,\ell n\,y_2}),\quad T_1 = \tau_{12}(0.3816+0.0109\,y_2)$$

$$K_3 = -(\frac{v_s}{\Delta v}A_{co})\,\frac{y_2-1}{y_2},\qquad T_3 = \tau_{12}(0.6080+0.050\,y_2)$$

$$a = -(\frac{v_s}{\Delta v}V_0{}^*A_{co})\,\tau_{12}\,\{D'+(A'-C')\,\frac{y_2-1}{y_2\,\ell n\,y_2}-\frac{E}{y_2}\}$$

$$b = -(\frac{v_s}{\Delta v}V_0{}^*A_{co})\,\tau_{12}\,(A'-C')\,(1-\frac{y_2-1}{y_2\,\ell n\,y_2})$$

$$T_4 = 0.636\,\tau_{12}$$

$$K_5 = -(z_1-z_0),\qquad T_5 = 0.637\,\tau_{01}$$

$$K_7 = -(z_1-z_0)\,\frac{\rho_w}{\tau_{01}Q^*},\qquad K_8 = (z_1-z_0)\,\frac{\tau_e}{\tau_{01}}\cdot B'$$

$$H_{pr} = (H_{pr})_{ves} = \{M_s{}^*(A+B)+M_w{}^*B\}-\frac{\Delta i}{\Delta v}\{M_s{}^*(C+D)+M_w{}^*D\}-\frac{\bar{V}_{sat}}{J}$$

$$K_{22} = -\frac{W_R{}^*}{W_0{}^*}\cdot\frac{i_w-i_f}{W_R{}^*+W_f{}^*},\quad K_{23} = \frac{W_R{}^*}{W_0{}^*}\cdot B,\quad K_{24} = \frac{W_f{}^*}{W_0{}^*}$$

the deviations of all variables continue to increase with an almost constant period. This divergent tendency results from the fact that the steam flow to load is kept constant so that mismatch results between the power generated and that removed. It can be shown that the closed loop transfer functions have several smaller time constants, as well as a single large time constant associated with a small positive real root of the characteristic equation. Since the divergent tendency associated with this small positive root is very slow, it is not a serious concern from the viewpoint of control and safety.

The stability of the whole system will be investigated by means of the Nyquist stability criterion and with the roots of the characteristic equation. The open loop transfer function is schematically shown in Fig. 12. It is concluded from this figure that the system has a single positive real root based on Nyquist stability criterion.

It is evident on the basis of the Nyquist diagram of Fig. 12 that, if the phase lag exceeds 180 ° at a higher frequency, an instability appears as the loop gain increases, which will have an oscillatory tendency. It is tentatively assumed that the fuel heat transfer dynamics are of a single time constant model; thus, the phase lag of the open loop transfer function is equal to 180 ° at $\omega \to \infty$. However, when a more accurate model is adopted, the phase lags more than 180 ° at $\omega \to \infty$.

Nomenclature

Symbols

A_{co} : flow area of core
$A = \partial \Delta i / \partial p$
$A' = A / \Delta i$
$B = \partial i_w / \partial p$
$B' = \Delta v / \Delta i \cdot B / v_w$
$C = \partial \Delta v / \partial p$
$C' = C / \Delta v$
$D = \partial v_w / \partial p$
$D' = D / v_w$
$E = A' - B' - C' + D'$
$F = -A' - B' + C' + D'$
f : void fraction
f_2 : void fraction at core exit
$G_{f1}(s)$: fuel heat transfer function
$Gf_2(s)$: fuel heat transfer function
$G_R(s)$: zero power transfer function
H_{pr} : defined in Table 3
i_s : specific enthalpy of saturated steam
i_w : specific enthalpy of saturated water
$\Delta i = i_s - i_w$
i_{sub} : average enthalpy of water in subcooled region
i_f : specific enthalpy of feedwater
$i_w - i_{sub}$: subcooling
J : mechanical equivalent of heat
δk_{ex} : reactivity change
δk_{void} : void reactivity change
δk_T : reactivity change caused by temperature
ℓ : average neutron life time
M_s : saturated steam mass in vessel (excluding core and riser)
M_w : saturated water mass in vessel (excluding core and riser)
n : neutron density
p : pressure
Q : heat source per unit length
Q' : heat source per unit volume
q : effective void source
r : slip ratio
T_f : fuel time constant
U : void transmission velocity
V : flow velocity
V : void volume in the core
$\bar{V}_{sat}$: saturated steam and water volume in vessel (excluding core and riser)
$\bar{V}_{sub}$: subcooled water volume in vessel (excluding core and riser)
V_o^* : inlet water velocity
$v_s = 1/\rho_s$
$v_w = 1/\rho_w$
$\Delta v = v_s - v_w$
W_L : steam flow to load
W_o : water flow at core inlet
W_R : recirculation flow
W_f : feedwater flow
$y(z)$: defined as $\left(V_o^* + \frac{z - z_1}{\tau_e}\right) / V^*$
$y_2 = y(z_2)$
z : position in axial direction (the origin at the inlet of core)

Subscripts

w : water
s : steam
d : downcomer
o : core inlet

Superscripts

* : steady state value
α_T : temperature coefficient of reactivity
α_v : void coefficient of reactivity
β : delayed neutron fraction
θ : temperature
θ_f : fuel average temperature
θ_w : water temperature
θ_{sat} : saturation temperature
ρ_s : density per unit length of saturated steam
ρ_w : density per unit length of saturated water
$\tau_e = \frac{\Delta i}{Q^* \Delta v}$: steam raising time, i.e., time during which the unit volume of steam is raised per unit volume of water
$\tau_{o1} = (z_1 - z_o) / V_o^*$
$\tau_{12} = \tau_e \ell n y_2$: void transit time in boiling region
τ_d : time taken by flow from feedwater inlet to core inlet

1 : boiling boundary
2 : top of core
sub : subcooled
sat : saturated

ANALYSIS OF MULTI-REGION REACTOR KINETICS

S. An and A. Oyama

An analysis of multi-region reactor kinetics has been undertaken, with the use of the perturbation method and regional kinetics. In the perturbation method equations are introduced relating reactor period to perturbation conditions for a multi-region reactor. In regional kinetics one set of regional kinetic equations is derived by integrating the time dependent diffusion equation over each region of the reactor.

Perturbation method [5]

Perturbation method taking account of the effect of delayed neutrons

The following equations are obtained for eigenvalues and eigenfunctions:

$$\vec{M}\vec{v}_\alpha = \omega_\alpha \vec{v}_\alpha \qquad \tilde{\vec{M}}\vec{v}_\beta^{+} = \omega_\beta \vec{v}_\beta^{+}$$

where M denotes matrix operator of diffusion equation, $\vec{v}$ is a vector whose elements are neutron fluxes and concentrations of delayed neutron precursors, and ω is the reciprocal of the reactor period. Superscripts $^+$ and $\tilde{}$ mean adjoint and transpose, respectively. The dependence of neutron flux on reactor period is discussed elsewhere [6-7]. The computer code (IBM 7090) has been written to calculate neutron flux and reactor period. One of the calculations is shown in Fig. 13. $\tilde{M}$ being an adjoint operator, the following equation is obtained by the perturbation method:

$$<\vec{v}_\beta^{+} P \vec{v}_\alpha'> = (\omega_\alpha' - \omega_\beta) <\vec{v}_\beta^{+} \vec{v}_\alpha'> \tag{12}$$

$$\Delta\omega_\alpha \approx <v_\alpha^{+} P v_\alpha'> / [\sum_{i=1}^{N} \int \phi_{i\alpha}^{+} \phi_{i\alpha} dV + \sum_{j=1}^{N}\sum_{k=1}^{M} \int \frac{\phi_{d\alpha}^{+} \nu_d \lambda_{jk} \beta_{jk} \nu_j \phi_{j\alpha} \Sigma_{fj}}{(\omega_\alpha^{+} + \lambda_{jk})^2} dV] \tag{13}$$

where P denotes the perturbation term, ϕ_i and ϕ_d the neutron flux of the ith group and that corresponding to the energy of delayed neutrons, respectively and superscript $'$ means a perturbed variable. This equation would appear to be useful for multi-region reactors with a different β in each region. Making a non critical reactor critical by changing the number of fission neutrons, the equation relating reactor period to static reactivity can be derived from the above equations. We can discuss the in-hour equation of a multi-region reactor, using this equation.

Neutron life time and β_{eff} of reflected reactors

Values of statically and dynamically defined parameters are compared with each other. Some of the results obtained are listed in Table 4.

Surface perturbation method [8]

The surface perturbation method is used for calculating the reactor period resulting from variation of the external boundary of a reactor. Denoting the perturbed surface by S', which is included in the initial volume:

$$\Delta\omega = \int_{S'} (\phi^{+} \nu D \nabla\phi')_\nu dS / \int \vec{v}^{+} \vec{v}' dv \tag{14}$$

The denominator is integrated over the perturbed volume. Usually, we approximate $\vec{v}'$ by $\vec{v}$, but if ϕ' is replaced by ϕ:

$$\omega \approx \int_{S'} (\phi^{m} D \nabla\phi)_\nu dS / [\int \frac{\phi^{m}}{v} \phi dv + \int \frac{\beta \phi^{m} \eta \Sigma_f \phi}{\lambda + \omega} dv] \tag{15}$$

where superscript m means importance. In order to compare the above mentioned procedure with the rigorous treatment, periods of a reflected spherical reactor are calculated for different thicknesses of the reflector. The results are shown in Fig. 14.

Regional kinetics

Derivation of basic equations

Integrating the time dependent diffusion equations over each region of a multi-region reactor, we obtain one set of regional kinetic equations. The equations are given below as an example:

$$\frac{\alpha_{11}}{\ell_1}(1-\beta_1)N_1 + \frac{\alpha_{12}}{\ell_2} N_2 + \lambda C_1 - \frac{N_1}{\ell_1} + S_1 = \frac{dN_1}{dt} \tag{16}$$

$$\frac{\alpha_{22}}{\ell_2}(1-\beta_2)N_2 + \frac{\alpha_{21}}{\ell_1} N_1 + \lambda C_2 - \frac{N_2}{\ell_2} = \frac{dN_2}{dt} \tag{17}$$

$$\frac{\alpha_{11}}{\ell_1}\beta_1 N_1 - \lambda C_1 = \frac{dC_1}{dt} \tag{18}$$

$$\frac{\alpha_{22}}{\ell_2}\beta_2 N_2 - \lambda C_2 = \frac{dC_2}{dt} \tag{19}$$

where α_{ii} denotes the number of neutrons produced divided by that disappearing from the ith region, defined as $\alpha_{ii}/\ell_i = \nu_i k_i \Sigma_i$, α_{ij} denotes the number of incident neutrons flowing to the ith from the adjacent jth region divided by that disappearing in the jth region and ℓ_i denotes neutron life time of the ith

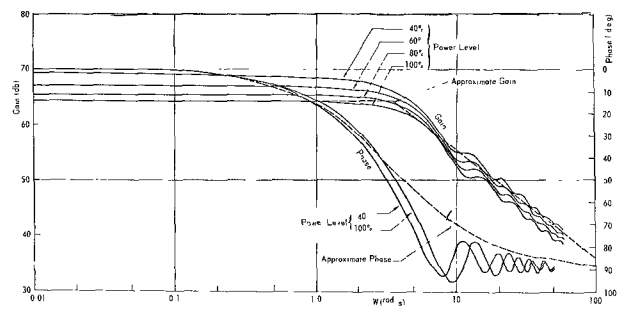


Figure 7. Frequency characteristics of $G_1(s)/Q^*$

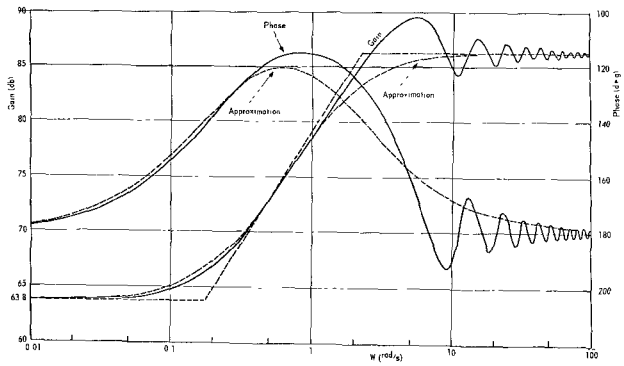


Figure 8. Frequency characteristics of $G_4(s)$

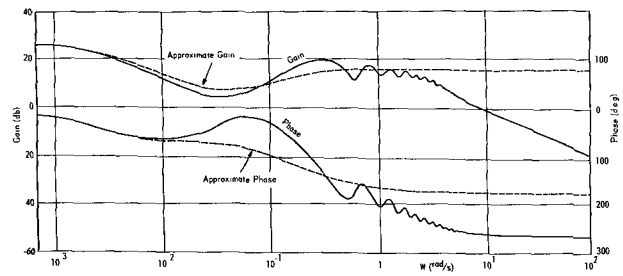


Figure 9. Frequency characteristics of feedback transfer function which relates $\delta k_v/\beta$ to $\delta Q/Q^*$

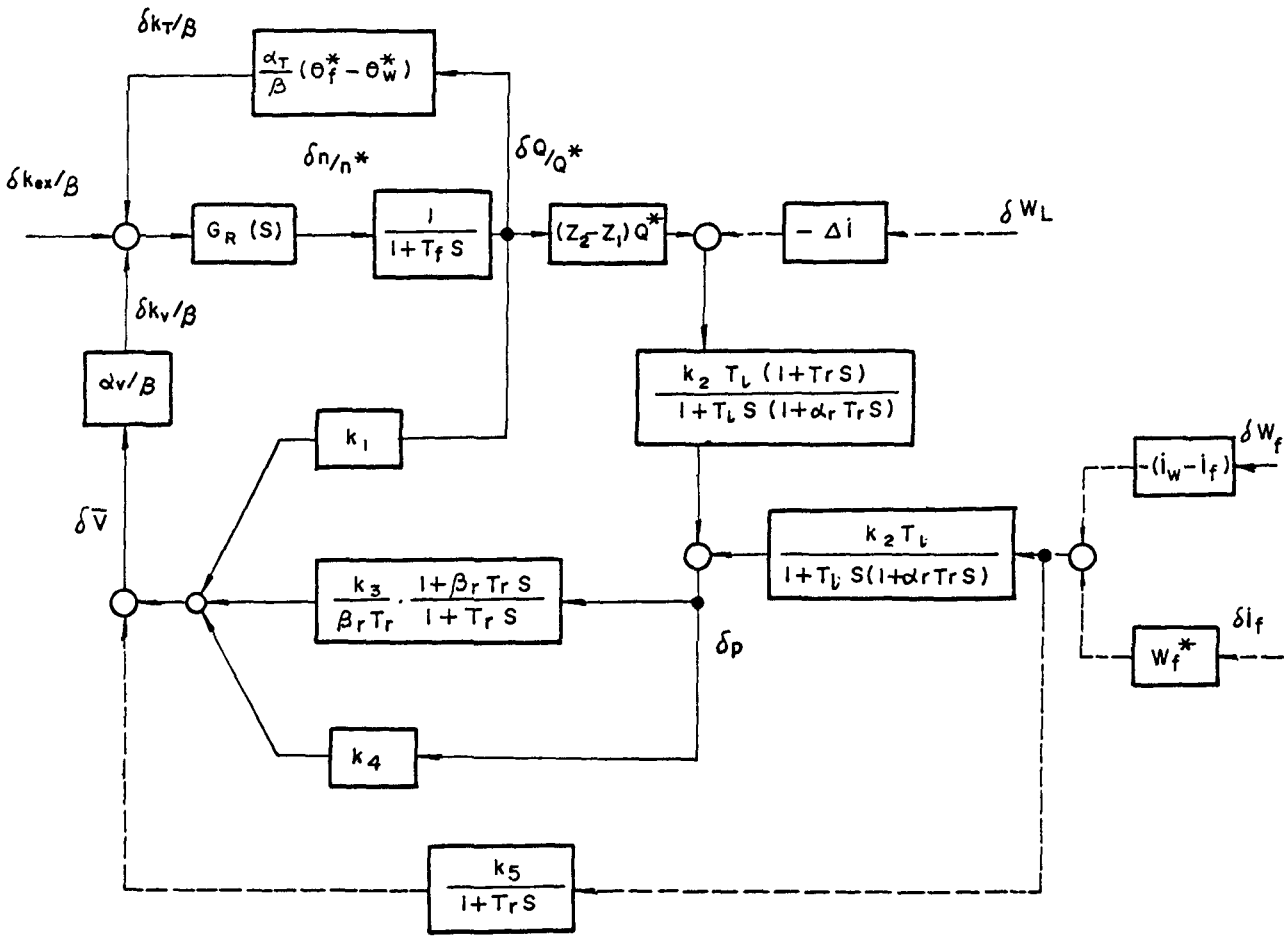


Figure 10. Further simplified block diagram

$$K_1 = V_o^* A_{co}\,\tau_{12}\,(1 - \frac{y_2-1}{y_2\,\ell n\,y_2}) + (z_1-z_0)A_{co}\frac{y_2-1}{y_2}$$

$$K_3 = A_{co}\,\frac{y_2-1}{y_2}\,\frac{W_o^* T_r B}{Q^*}$$

$$K_2 = \frac{1}{H_{pr}+W_o^* T_r B}$$

$$B_r = (1 - \frac{W_R^*}{W_o^*})^{-1}$$

$$\alpha_r = H_{pr} \times k_2$$

$$K_4 = -V_o^* A_{co}\,\tau_{12}\,(A'-C') \times (1 - \frac{y_2-1}{y_2\,\ell n\,y_2})$$

$$T_r = \tau_{01} + \tau_d$$

$$K_5 = \frac{A_{co}}{Q^*}\,\frac{y_2-1}{y_2}$$

$$T_L = \frac{H_{pr}}{\alpha_r W_o^* B}\,(1 - \frac{W_R^*}{W_o^*})^{-1}$$

Table 4. Kinetic parameters of a uranium-fuelled, H_2O-moderated reactor with a H_2O reflector

Thickness of reflector	20 cm	15 cm	10 cm	5 cm
$\beta_{\text{eff.s}}/\beta$	1.179	1.180	1.185	1.191
ℓ_s (seconds)	7.23×10^{-5}	7.22×10^{-5}	7.21×10^{-5}	7.10×10^{-5}
ℓ_d (seconds)	1.01×10^{-4}	9.47×10^{-5}	8.26×10^{-5}	6.27×10^{-5}

region. The relation between variation of source δS_1 and variation of leakage terms δL_1, δL_2 and δL_0 is obtained by the invariant imbedding method [9-10], L_1 denoting the number of leakage neutrons or current as shown in Fig. 15. The incident neutron current L to one region, the reflected current L_R and the transparent current L_T are related by $\bar{L}_R = R\bar{L}$ and $\bar{L}_T = T\bar{L}$, where superscript $^-$ denotes Laplace-transformed variables. The neutron current L_S is related to S by $\bar{L}_S = Q\bar{S}$. R, T and Q are derived by solving diffusion equations under certain boundary conditions. Combining Laplace-transformed equations with the above mentioned relations, one obtains:

$$\delta\bar{N}_1/\delta\bar{S}_1 = \{ Q_1 - R_2Q_1 + (1-R_1R_2) \}/[\frac{\alpha_{11}}{\ell_1}\{ 1-\beta_1+\frac{\lambda\beta_1}{s+\lambda} \} - \nu_1\Sigma_1 - s](1-R_1R_2) \tag{20}$$

$$\delta\bar{N}_2/\delta\bar{S}_1 = \{ R_2Q_1 - Q_1 + T_2Q_1 \} / [\frac{\alpha_{22}}{\ell_2}\{1-\beta_2+\frac{\lambda\beta_2}{s+\lambda}\} - \nu_2\Sigma_2 - s](1-R_1R_2) \tag{21}$$

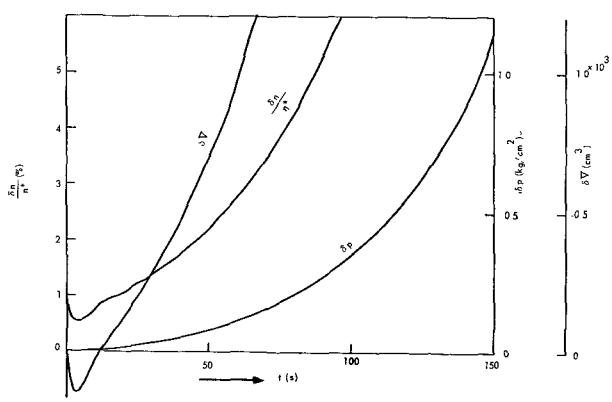


Figure 11. Response of $\delta n/n^*$, δp and δV to step change in $\delta k = 1$ cent

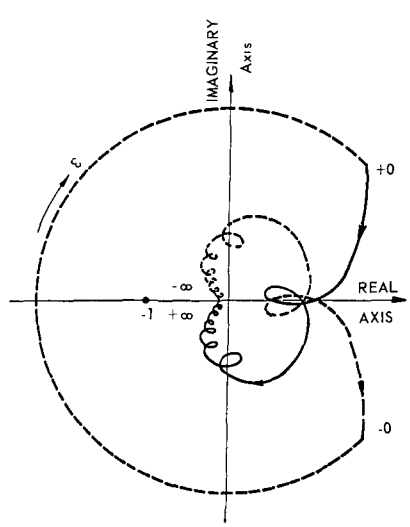


Figure 12. Schematic Nyquist plot of open loop transfer function which relates $-\frac{1}{\beta}(k_V + k_T)$ to net reactivity

Approximation in the range of low frequency

Equations (20) and (21) are very complicated, and so it is assumed that the frequency ω is less than β/ℓ and that the two regions are each sufficiently subcritical, while their combined system is critical. Then, four transfer functions, $\delta\bar{N}_1/\delta\bar{S}_1$, $\delta\bar{N}_1/\delta\bar{S}_2$, $\delta\bar{N}_2/\delta\bar{S}_1$ and $\delta\bar{N}_2/\delta\bar{S}_2$ are expressed explicitly in terms of α parameters and neutron life time of critical state.

Criticality condition and reactivity

The critical condition for one energy group and two regions is $(1-\alpha_{11})(1-\alpha_{22}) = \alpha_{12}\alpha_{21}$. Re-

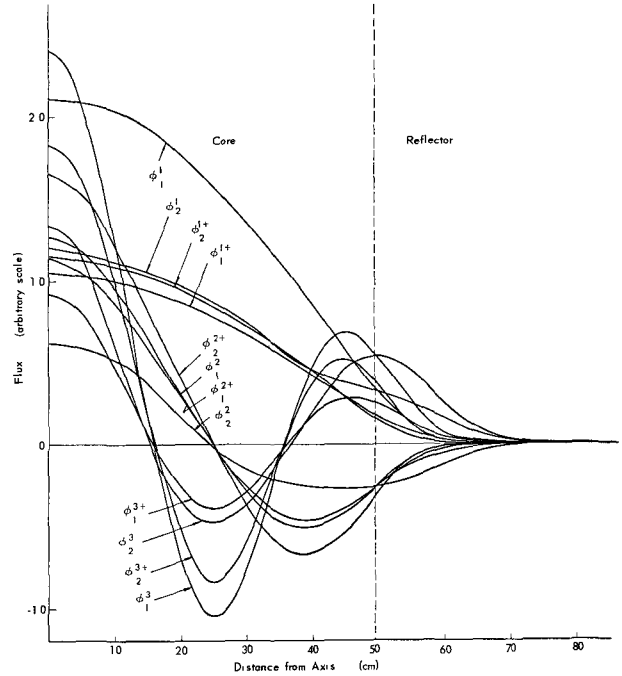


Figure 13. Neutron flux and adjoint flux corresponding to delayed neutrons (uranium-fuelled, H_2O-moderated reactor with a H_2O reflector)

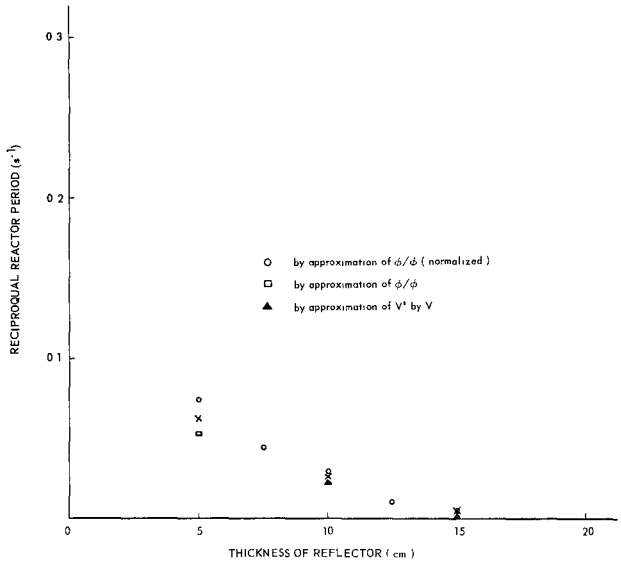


Figure 14. Reciprocal reactor period of a uranium-fuelled reactor with a H_2O reflector

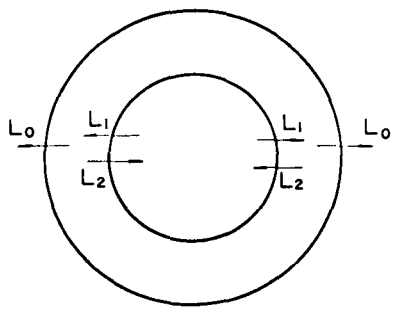


Figure 15. Leakage current from each region

activity ρ can be expressed in terms of α parameters. Source transfer functions are transformed to reactivity transfer functions by the use of the above relations. The frequency characteristics—except the gain, dependent on the position of source—are roughly similar throughout the whole core under the above mentioned conditions. However, error from the approximation becomes larger for larger ω, and the frequency response becomes different from region to region. The effective neutron life time of the whole core is given by: $[(1-\alpha_{11})\ell_2+(1-\alpha_{22})\ell_1]/[(1-\alpha_{11})\alpha_{22}+(1-\alpha_{22})\alpha_{11}]$ and β_{eff} is $[\alpha_{11}\beta_1(1-\alpha_{22})+\alpha_{22}\beta_1(1-\alpha_{11})]/[(1-\alpha_{11})\alpha_{22}+(1-\alpha_{22})\alpha_{11}]$. Some results of the calculations are represented in Fig. 16.

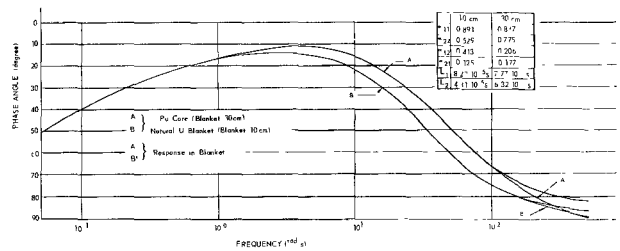


Figure 16. Frequency response of a spherical two-region reactor (source at core centre)

REFERENCES

1. Kanai, T., *et al.*, J. Atomic Energy Soc. Japan, *3* (3), 168-178 (1961).
2. Miida, J., *et al.*, Japan Atomic Energy Research Institute report JAERI-1044 (1962).
3. Miida, J., *et al.*, *ibid.*, JAERI-1061 (1964).
4. Deshong, J.A., Jr., *et al.*, USAEC report ANL-5850 (1958).
5. An, S., J. Atomic Energy Soc. Japan, *3*, 841-848 (1961).
6. Harasawa, S., private communication.
7. Gozani, T., Nucleonik, *5*, 55-61 (1963).
8. Lewins, J., Nucleas Sci. Eng., *7*, 481-486 (1960).
9. Kawai, T., private communication.
10. Shimizu, A., J. Atomic Energy Soc. Japan, *5*, 359-368 (1963).

ABSTRACT - RÉSUMÉ - АННОТАЦИЯ - RESUMEN

A/847 Japon

Etudes théoriques de cinétique des réacteurs à eau bouillante et des réacteurs à plusieurs régions

par T. Kanai *et al.*

Le mémoire comprend deux parties. La première est constituée par une analyse dynamique théorique des réacteurs à eau bouillante; la seconde est une analyse de la cinétique des réacteurs à plusieurs régions. La première partie commence par l'établissement des équations décrivant la formation de vide transitoire dans le cœur; ces équations sont ensuite simplifiées et combinées avec d'autres équations pour former un modèle mathématique complet des réacteurs à eau bouillante. Enfin, grâce à ce modèle, on étudie la stabilité du réacteur.

Une « équation simplifiée du vide », décrivant le comportement en fonction du temps et de l'espace de la fraction de volume du vide due aux changements de puissance du réacteur, du sous-refroidissement, de la vitesse d'entrée du réfrigérant et de la pression du système, a été déduite des lois de conservation de la masse et de l'énergie; des calculs numériques ont été effectués pour la réactivité en relation avec le vide transitoire, utilisant cette équation du vide et la théorie habituelle des perturbations.

Les fonctions de transfert du vide sont obtenues en mettant sous forme linéaire l'équation du vide.

Dans ce cas, on suppose une distribution uniforme de puissance et on ne tient pas compte du glissement. En dehors de ces deux simplifications, les fonctions de transfert résultantes sont les modèles paramétriques de distribution les plus complets que l'on ait jamais établis.

En plus des fonctions de transfert du vide, on obtient un autre ensemble complet de fonctions de transfert, à savoir, la fonction de transfert de vitesse d'entrée, la fonction de transfert de la pression du caisson, celle du sous-refroidissement et celle du débit de recirculation.

Les fonctions de transfert ainsi obtenues sont alors simplifiées et on obtient des formes approximatives par des combinaisons de simples retards de constante de temps, dont les constantes de temps et les gains statiques sont immédiatement évalués à partir des paramètres déterminés par la conception du réacteur.

Les caractéristiques dynamiques des fonctions de transfert de réaction et la stabilité du système sont aussi étudiées.

Dans la seconde partie, on a entrepris une analyse de la cinétique des réacteurs à plusieurs régions, en utilisant la méthode des perturbations et la cinétique des régions. Dans la méthode des perturbations on introduit des équations mettant en relation la période du réacteur et les conditions de perturbation pour un réacteur à plusieurs régions. Ces équations sont appliquées au calcul des périodes du réacteur associées à la variation d'épaisseur du réflecteur et pour l'examen de l'équation donnant la mesure de la réactivité. En cinétique de région, on établit un système d'équations de cinétique de région en intégrant l'équation de diffusion en fonction du temps sur chaque région du réacteur. Ces équations sont exprimées explicitement en fonction des paramètres physiques de chaque région. Partant de ces équations, on examine les fonctions de transfert et les caractéristiques de fréquence de chaque région.

A/847 Япония

Теоретические исследования кинетики реакторов с кипящей водой и многозонных реакторов

Ц. Канаи *et al.*

Доклад состоит из двух частей. Первая часть посвящена теоретическому анализу динамики реакторов с кипящей водой, а вторая — анализу кинетики многозонных реакторов. Первая часть начинается с вывода уравнений, описывающих переходное образование пустот в активной зоне, затем эти уравнения упрощаются и комбинируются с другими уравнениями для получения полной математической модели реакторов с кипящей водой. Наконец, исследуется стабильность реакторов с использованием модели.

Упрощенное уравнение пустотности, описывающее в зависимости от времени и пространства поведение пустотной фракции, обусловливаемое изменениями мощности реактора, недогрева, скорости теплоносителя на входе и давления в системе, было получено из законов сохранения массы и энергии; были проведены численные расчеты переходной пустотной реактивности с использованием этого уравнения пустотности и обычной теории возмущений.

Пустотные передаточные функции получены путем линеаризации уравнения пустотности. Здесь распределение мощности принимается однородным, а скольжением пренебрегают. За исключением этих двух упрощений полученные передаточные функции являются наиболее полной моделью распределения из когда-либо рассмотренных.

Кроме пустотных передаточных функций был получен целый ряд других передаточных функций, а именно передаточная функция скорости на входе, передаточная функция давления в сосуде, передаточная функция недогрева и передаточная функция рециркулирующего потока.

Полученные выше передаточные функции еще упрощены и аппроксимированы путем комбинирования постоянных запаздывания, чьи временные константы и статический прирост легко оценить из параметров конструкции.

Исследованы также динамические характеристики передаточных функций обратной связи и стабильность системы.

Во второй части проводится анализ кинетики многозонного реактора с использованием метода возмущений и региональной кинетики. В методе возмущений вводятся уравнения, связывающие период реактора с условиями возмущений для многозонного реактора. Эти уравнения применяются для расчета периодов реактора, связанных с изменением толщины отражателя, и для проверки уравнения обратных часов. В региональной кинетике один ряд уравнений региональной кинетики получен путем интегрирования зависящего от времени диффузионного уравнения для каждой зоны в реакторе. Эти уравнения выражены в явных членах физических параметров для каждой зоны. Основываясь на этих уравнениях, удалось проверить передаточные функции и частотные характеристики каждой зоны.

A/847 Japón

Estudios de cinética teórica de reactores de agua hirviente y reactores de varias regiones

por T. Kanai *et al.*

Este trabajo consta de dos partes. La primera se refiere a un análisis dinámico teórico de reactores

de agua hirviente, la segunda parte es un análisis de la cinética de reactores de varias regiones. La primera parte comienza con la deducción de las ecuaciones que describen el transitorio de formación de huecos en el núcleo, luego estas ecuaciones se simplifican y combinan con otras ecuaciones para formar un modelo matemático completo de los reactores de agua hirviente. Por fin, se investiga la estabilidad del reactor empleando el modelo.

Se ha deducido una ecuación de huecos simplificada, que describe el comportamiento dependiente del tiempo y del espacio de la proporción de huecos debida a variaciones de potencia del reactor, refrigeración insuficiente, velocidad de entrada del refrigerante y presión del sistema. Se ha deducido partiendo de las leyes de conservación de masa y energía y se han realizado cálculos numéricos referentes a la reactividad transitoria de huecos empleando esta ecuación de huecos y la teoría de perturbaciones.

Las funciones de transferencia de huecos se obtienen linearizando la ecuación de huecos. Aquí se supone que la potencia está distribuida uniformemente y no se tiene en cuenta el deslizamiento. Aparte de estas dos simplificaciones, las funciones de transferencia que resultan forman el modelo de parámetros distribuidos más completo que se haya desarrollado nunca.

Además de las funciones de transferencia de huecos se deduce un sistema completo de otras funciones de transferencia, a saber: la función de transferencia de velocidad de entrada, de la presión de la vasija, la subrefrigeración y la del flujo de recirculación.

Las funciones de transferencia deducidas más arriba se simplifican más aún y se aproximan mediante combinaciones de retardos de una constante de tiempo única, cuyas constantes de tiempo y ganancias estáticas se calculan fácilmente a partir de los parámetros de diseño.

También se investigan las características dinámicas de las funciones de transferencia de realimentación y la estabilidad del sistema.

En la segunda parte se emprende un análisis de la cinética de reactores de varias regiones, empleando el método de perturbaciones y la cinética de regiones. En el método de perturbaciones se introducen ecuaciones que relacionan el período del reactor con las condiciones de la perturbación para reactores de varias regiones. Dichas ecuaciones se aplican al cálculo de los períodos del reactor asociados a la variación de espesor del reflector y para examinar la ecuación de la hora inversa. En la cinética de regiones se deduce un sistema de ecuaciones de cinética regional integrando la ecuación de difusión dependiente del tiempo, sobre cada región del reactor. Dichas ecuaciones se expresan como función explícita de parámetros físicos de cada región. Basándose en estas ecuaciones se examinan funciones de transferencia y características de frecuencias de cada región.

Etude du comportement dynamique de la pile RAPSODIE*

par R. Abdon** et M. Chaigne**

Le développement des réacteurs surrégénérateurs à neutrons rapides pose des problèmes nouveaux, en particulier en ce qui concerne leur comportement dynamique et leur sécurité.

La pile RAPSODIE — qui fait par ailleurs l'objet d'un mémoire à la présente Conférence, auquel on voudra bien se reporter pour la description générale de l'installation [11, 1] — a été l'objet de nombreuses études dynamiques effectuées sur machines analogiques et digitales pour deux versions du combustible (métal et oxyde).

Après élaboration des modèles mathématiques représentatifs de l'ensemble de l'installation (bloc pile et ses deux circuits de refroidissement) et mise au point des schémas analogiques et codes digitaux [2-3], nous avons effectué:

a) L'étude des incidents envisageables avec et sans fonctionnement du système de sécurité. Ces dernières études ont principalement été effectuées pour le rapport préliminaire de sûreté de la pile (par voie analogique pour les études d'ensemble, et sur machines digitales pour les études détaillées);

b) L'étude de la conduite du réacteur (sur machines analogiques);

c) L'étude de sa stabilité (par voie digitale).

Enfin, l'ensemble de ces études a été concrétisé par la mise au point d'un simulateur d'entraînement à la conduite de la pile.

Le combustible oxyde ayant été choisi pour première charge de la pile, nous illustrerons en général ce texte en choisissant — en raison de la place limitée dont nous disposons — les cas les plus typiques concernant cette version.

Hypothèses

Le schéma général — du point de vue dynamique — de l'installation est indiqué par la figure 1. Dans le cadre des études dynamiques, nous avons été amenés à faire les hypothèses suivantes [5]:

a) Les plaquettes placées entre les assemblages de combustible au voisinage du plan médian du cœur assurent la rigidité mécanique de celui-ci dès lors que le gradient thermique nominal (90 °C) est atteint (la validité de cette hypothèse a été vérifiée sur la maquette RAPSODIE [12]);

b) Le débit de convection naturelle est pris égal à 6% du débit initial, ce qui permet l'évacuation de la puissance résiduelle due aux produits de fission, dont la valeur calculée est de 6% de la puissance initiale (nous avons vérifié cette hypothèse pour des gradients de température cœur de l'ordre de 150 à 200 °C);

c) On ne tient pas compte de la conduction thermique dans le sens axial pour le combustible et le réfrigérant, ni dans le sens radial pour ce dernier; la capacité calorifique de la gaine est négligée; enfin la conductibilité du combustible est supposée indépendante de la température.

Coefficients de réactivité

Nous nous limiterons ici au cas du combustible oxyde.

Coefficient Doppler

Dans le cas de RAPSODIE, l'effet Doppler est négligeable: ce coefficient est de l'ordre de 10^{-8} $(\delta k/k)/°C$. Ceci est dû au fait que, dans les petits réacteurs, le spectre est très dur.

Coefficient de dilatation du combustible

La dilatation radiale des barreaux de combustible n'a pas d'influence sur la réactivité, les déplacements de matière se compensant en moyenne. La dilatation axiale des barreaux a pour conséquence d'augmenter la hauteur du cœur et de diminuer la densité moyenne du combustible. Nous avons supposé (guidés par des résultats d'irradiation d'aiguilles de combustible) que le barreau était fretté à sa gaine sur sa périphérie: le coefficient combustible (tenant compte de l'association à la gaine) doit donc être associé à la température de la gaine, peu différente de celle du réfrigérant. Ce coefficient a pour valeur: $-0{,}6 \cdot 10^{-5}$ $(\delta k/k)/°C$.

Coefficient de dilatation du sodium

Il est dû, d'une part, à la variation de densité du sodium et, d'autre part, à la dilatation radiale de la gaine. Dans le cas des petits réacteurs cet effet est négatif. Pour RAPSODIE, ce coefficient est de: $-1{,}3 \cdot 10^{-5}$ $(\delta k/k)/°C$.

* Ce mémoire a été préparé dans le cadre de l'Association EURATOM-CEA sur les réacteurs à neutrons rapides.
** Commissariat à l'Energie atomique.

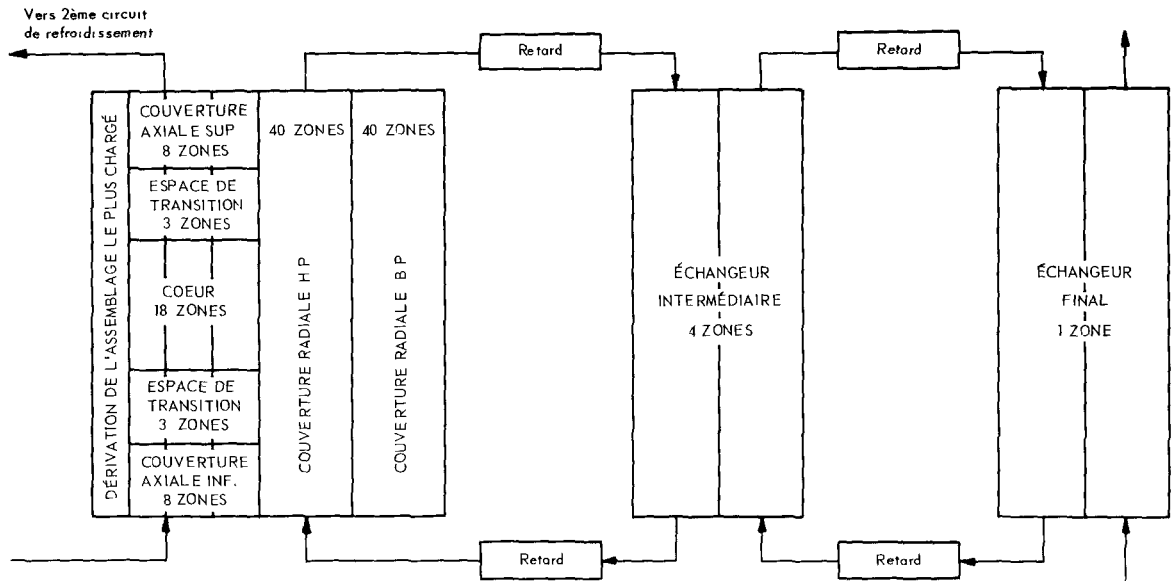


Figure 1. Schéma général de l'installation

Coefficients dus aux structures

Comme nous l'avons indiqué dans les hypothèses, nous avons supposé que le cœur était compact dès lors que le gradient thermique normal entre l'entrée et la sortie du sodium était établi. Il en résulte qu'une augmentation de température au niveau des plaquettes dont il a été question ci-dessus conduit à une expansion radiale du cœur et provoque ainsi une diminution de la réactivité. Le coefficient dû aux plaquettes est de: $-1{,}3 \cdot 10^{-5}\ (\delta k/k)/°C$.

Le positionnement des plaquettes a par ailleurs été étudié pour obtenir un effet d'arcage négatif qui donne un coefficient de réactivité pratiquement négligeable.

Formulation et constantes

Les hypothèses énoncées ci-dessus conduisent à la formulation générale que nous indiquons brièvement ci-après:

Cinétique

Les équations sont classiques: on néglige dn/dt devant les termes du second membre de (1). On a avec les notations habituelles:

$$\begin{cases} 0 = [(\delta k - \beta)/l]n + \Sigma \lambda_i C_i & (1) \\ dC_i/dt = (\beta_i/l)n - \lambda_i C_i & (2) \end{cases}$$

avec $l \approx 10^{-7}$s et $\beta \approx 550 \cdot 10^{-5}\ \delta k/k$

Contre-réaction de température

$$\delta k = \delta k_{\text{ex.}} + \delta k_{\text{th.}}$$

$$\delta k_{\text{th}_i^j} = 1/\ (z_2 - z_1)\left[\xi \int_{z_1}^{z_2} \Delta T(z)\,dz + \eta \int_{z_1}^{z_2} \Delta U(z)\,dz\right]$$

avec:

ΔT et ΔU: écarts de température du combustible et du sodium

z_1 et z_2: cotes limites de la zone i de la dérivation j de débit

ξ et η: coefficient de température du combustible et du sodium

Échanges thermiques

a) Dans le bloc-pile:

$$\begin{cases} C_T(\partial T/\partial t) + H(T - U) = \lambda(z)q(t) \\ H(T - U) = C_U(\partial U/\partial t) + vC_U(\partial U/\partial z) \end{cases}$$

Le cœur a été découpé en 18 zones axiales pour les études détaillées effectuées en digitale, 3 zones ayant été utilisées pour les études effectuées en analogique. Les couvertures axiales et radiales ont été représentées par un nombre plus limité de zones (1 à 5).

b) Dans les échangeurs intermédiaires:

$$\begin{cases} C_U(\partial U/\partial t) + m_U(\partial U/\partial z) = H_U(V - U) \\ H_v(U - V) = C_v(\partial V/\partial t) + m_v(\partial V/\partial z) \end{cases}$$

Les échangeurs ont été découpés en 4 zones, tant pour les études menées par voie digitale, que pour celles menées par voie analogique.

Les notations relatives aux deux alinéas précédents sont les suivantes:

- T : température moyenne du combustible
- G : température moyenne de la gaine
- U : température moyenne du sodium primaire
- V : température moyenne du sodium secondaire
- C_i : capacité calorifique par unité de longueur de l'élément i
- H_i : coefficient d'échange par unité de longueur de l'élément i
- v : vitesse du sodium primaire
- m_i : débit calorifique du fluide

ÉTUDES D'INCIDENTS [5, 10]

On peut classer les incidents en incidents de réactivité (chutes intempestives ou remontées accidentelles de barres, par exemple) et en incidents de réfrigération (arrêt de pompes, par exemple).

Suivant l'état de l'installation du moment de l'incident (démarrage, fonctionnement à pleine puissance, un seul ou deux circuits de refroidissement en service) et selon que l'on considère que le système de sécurité fonctionne (action du contrôle) ou non (sécurité intrinsèque), les incidents envisageables peuvent avoir des répercussions très différentes.

Certaines associations très pessimistes d'hypothèses peuvent conduire en effet à des incidents dont les conséquences seraient un changement d'état des constituants: ébullition du sodium à 880 °C ou fusion du combustible oxyde à 2 500 °C (par exemple, grippage simultané des pompes primaires avec non-fonctionnement du système de sécurité), mais la probabilité de tels événements est si faible qu'il est normal (pour des raisons de simplification et d'économie) de ne pas en tenir compte pour l'organisation du système de sécurité ou pour le dessin de l'installation. En tout état de cause, leurs conséquences seraient très loin d'être aussi dommageables que dans le cas de l'accident hypothétique maximal que nous ne pouvons présenter ici mais dont on trouvera la description dans les rapports [2] et [3].

Nous allons présenter ci-après les principaux incidents que nous avons étudiés pour la version oxyde; ils concernent tous le bloc pile et les circuits de refrigération primaires, la place nous manquant pour présenter les incidents sur les circuits secondaires ou tertiaires, dont les conséquences ne sont d'ailleurs pas du tout sévères pour l'installation.

Incidents de réfrigération

Grippage de la pompe primaire à 10 MW à débit nominal 340 m³/h avec un seul circuit en fonctionnement

La figure 2 montre que l'ébullition du sodium se produit quatre secondes après le début de cet incident en cas de défaillance du système de sécurité, ce qui nous a conduits à n'autoriser le fonctionnement avec un seul circuit en service qu'à une puissance limitée au tiers de la puissance nominale théorique correspondant au débit de fonctionnement (3 MW, par exemple, au débit 340 m³/h, qui correspond à la puissance nominale 10 MW) pour éviter le changement d'état du refroidisseur.

Notons que le modèle mathématique que nous avons utilisé n'est pas représentatif des phénomènes qui se passent après l'ébullition (courbe en pointillés sur la figure). Nous reprendrons plus loin l'étude de ce cas.

Sur la même figure on voit que, si les barres de sécurité chutent dès la détection du grippage, la température maximale atteinte par le sodium

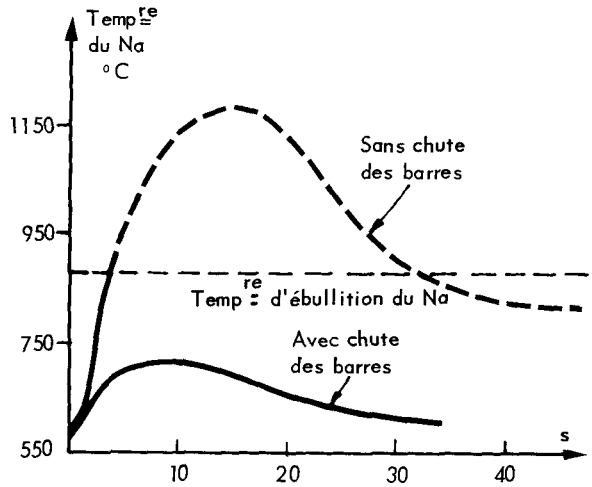


Figure 2. Grippage de la pompe primaire à 10 MW

(715 °C) reste inférieure à sa température d'ébullition (880 °C).

Arrêt des pompes primaires sur l'inertie de leur groupe d'alimentation à 20 MW à débit nominal 680 m³/h avec deux circuits de refroidissement

La figure 3 montre que, même si le système de sécurité ne fonctionne pas, le sodium n'atteint pas l'ébullition, du fait que l'arrêt des pompes s'effectue sur l'inertie des groupes d'alimentation Ward-Leonard équipés de volants tels que l'inertie ramenée sur l'arbre de la pompe soit d'environ 30 kgm²; cette inertie minimale a été déterminée après une étude paramétrique pour éviter que l'arrêt des pompes (incident qui peut être relativement fréquent: panne de secteur) n'entraîne l'ébullition du sodium qui se produirait en cas de défaillance du système de sécurité. Si ce dernier fonctionne, la marge de sécurité, comme le montre également la figure 3, est beaucoup plus grande.

Enfin, signalons que toutes les précautions sont

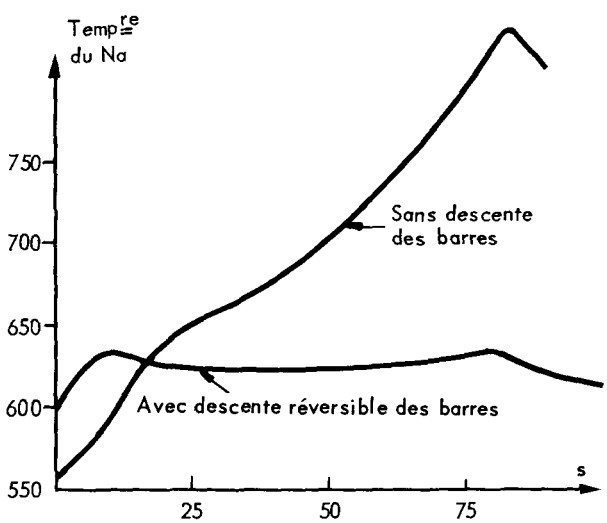


Figure 3. Arrêt des pompes primaires sur l'inertie du groupe à 20 MW

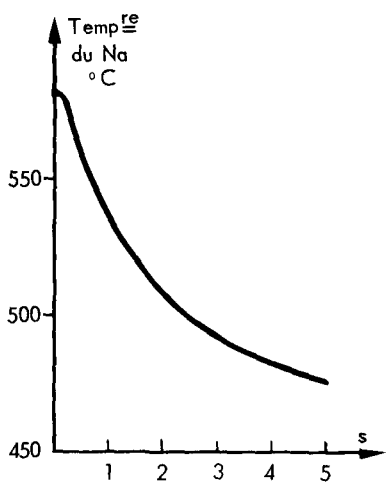


Figure 4. Arrêt d'urgence (chute des barres) à 20 MW

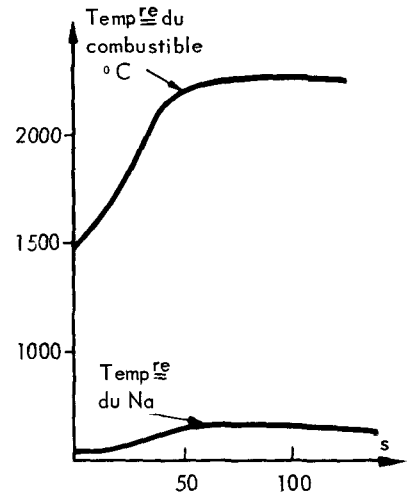


Figure 5. Accident de pilotage (sans chute des barres) à 20 MW

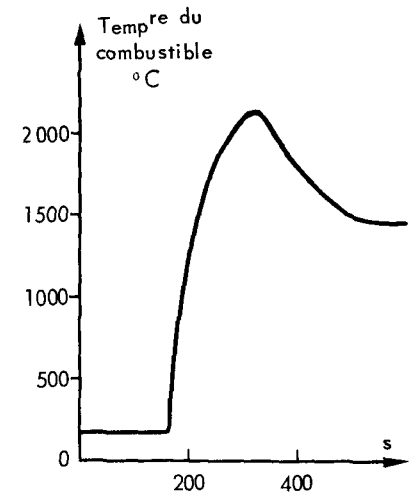


Figure 6. Accident de démarrage (sans chute des barres)

prises pour éviter une coupure d'alimentation entre les groupes et les pompes (principalement du côté du dispositif de régulation); un tel incident survenant sur un circuit aurait d'ailleurs des conséquences beaucoup moins graves que le grippage étudié plus haut.

Incidents de réactivité

Chute accélérée des barres à 20MW (arrêt d'urgence) (figure 4)

Le choc thermique froid sur les gaines des aiguilles combustibles est de 90 °C avec un gradient de 60 °C/s, que la chute accélérée des barres soit accompagnée de l'arrêt des pompes primaires sur l'inertie des groupes d'alimentation (cas normal: arrêt d'urgence du réacteur en cas d'incident) ou non (chute intempestive des barres).

En fait la loi théorique de décélération des pompes qui permettrait de réduire le choc thermique étant proche du grippage, nous avons préféré, mises à part les difficultés technologiques du freinage, calculer les structures pour les contraintes citées, plutôt que de courir le risque grave d'un fonctionnement intempestif du dispositif de freinage des pompes.

Remontée accidentelle d'une barre de pilotage à 20 MW (accident de pilotage)

On suppose ici qu'une barre de pilotage remonte sans contrôle, produisant un accroissement de réactivité de 5 ¢ à raison de 1 ¢/s, et que le dispositif de sécurité ne fonctionne pas. Les températures maximales du combustible et du sodium, données par la figure 5 montrent que ni la fusion de l'oxyde ni l'ébullition du sodium ne sont atteintes.

Nous ne donnons pas l'évolution de la température du sodium pour cet incident dans le cas de la chute accélérée des barres qui intervient du fait de l'action du système de sécurité, la courbe représentative de l'évolution de ce paramètre ayant été donnée dans la figure 4.

Remontée accidentelle d'une barre de compensation au démarrage (1 watt) (accident de démarrage)*

On suppose qu'une barre de sécurité/compensation remonte sans contrôle à la vitesse de 0,3 ¢/s et que le dispositif de sécurité ne fonctionne pas. Précisons que la température initiale est de 150 °C, et que le débit d'air est nul. La figure 6 montre que la température de fusion de l'oxyde n'est pas atteinte dans la zone centrale de l'aiguille de combustible.

Ébullition accidentelle du refroidisseur

Le modèle que nous avons en général utilisé pour les études d'incidents n'est pas représentatif du comportement de la pile, en cas de changement d'état du réfrigérant ou du combustible. Ces changements d'état ne se produisent que pour des incidents extrêmement improbables et/ou en cas de défaillance totale du système de sécurité. Néanmoins, leur étude étant utile pour déterminer le degré de sécurité intrinsèque de l'installation, nous avons mis au point un code complémentaire spécial qui permet une approche de l'évolution du réacteur en cas de commencement d'ébullition du sodium.

Nous avons été amenés dans ce but à faire les hypothèses simplificatrices suivantes:

a) L'ébullition s'effectue à pression constante, donc à température constante;

b) On ne tient pas compte de la convection naturelle;

c) On considère un mélange homogène du sodium à l'état liquide et du sodium à l'état vapeur.

Les équations d'échange thermique dans le cœur que nous avons explicitées plus haut sont remplacées, dès que $U \geqslant U_b$ [température d'ébullition

* Précisons que cet incident a été étudié en tenant compte du coefficient de réactivité dû aux structures dès que le gradient de température du cœur cesse d'être négligeable, ce qui n'est pas tout à fait exact mais influe peu sur les résultats.

du sodium (880 °C)], respectivement par les équations suivantes:

$$\begin{cases} C_T(\partial T/\partial t) + H(T-U_b) = \lambda(z)q(t) \\ H(T-U_b) = K\,B\,m_U\,(\partial v_s/\partial z) + KC_V\,(\partial v_s/\partial t) \end{cases}$$

v_s étant le volume spécifique de la phase liquide-vapeur et K une constante; avec, en outre (équation de continuité), ρ étant la densité et V la vitesse du sodium: $(\partial\rho/\partial t) + [\partial(\rho V)/\partial z] = 0$.

On peut ainsi déterminer la cote à laquelle apparaît l'ébullition, la vitesse et le sens de propagation de celle-ci pendant les instants qui suivent, et les conséquences du changement d'état pour la température du combustible et la puissance [9].

Les figures 7 et 8 sont relatives au cas que nous avons déjà examiné du grippage de la pompe primaire en fonctionnement avec un seul circuit à 10 MW.

On voit sur la figure 8, qui représente les variations de la puissance et de la réactivité, que la vaporisation du sodium correspond à une forte insertion d'antiréactivité. La figure 7 montre la variation de la densité du sodium en fonction de la cote à différents instants. On voit ainsi que l'ébullition apparaît approximativement aux trois quarts de la hauteur du cœur et se propage préférentiellement ensuite vers le haut.

Détermination des caractéristiques du système de contrôle

Un des premiers buts des études entreprises a été d'une part la détermination de la vitesse et de l'antiréactivité des barres de pilotage et des barres de sécurité, ainsi que la détermination des lois de variation de débit des pompes; d'autre part, le choix des paramètres utilisables pour le système de sécurité automatique du réacteur.

Les études paramétriques effectuées dans le cas des incidents les plus probables nous ont amenés à choisir:

a) Pour chacune des deux barres de pilotage, une vitesse de 1¢/s et une valeur de 35¢;

b) Pour chacune des quatre barres de sécurité, une vitesse de montée de 0,3¢/s, une vitesse de descente de 3¢/s et une valeur d'environ 4 dollars;

c) Pour les pompes primaires, une inertie de 30 kgm² pour les volants placés sur les groupes d'alimentation.

Toutefois, pour le premier démarrage de la pile et la phase pendant laquelle les premières mesures expérimentales seront effectuées pour vérifier les calculs, il a été décidé d'adopter temporairement des valeurs plus faibles pour les vitesses ou valeurs des barres, cette procédure allant dans le sens de la sécurité et nous assurant contre les conséquences d'éventuelles erreurs.

Les paramètres principaux retenus pour le déclenchement successif d'actions correctrices de plus en plus efficaces sont les suivants:

a) La puissance neutronique;

b) La période;

c) La comparaison du débit à la puissance neutronique;

d) Les débits ou vitesses des pompes primaires;

e) Les températures de sortie du sodium des assemblages du cœur et leur moyenne.

Étude des chocs thermiques sur les structures

Le tableau 1 résume les caractéristiques des chocs maximaux (pour le combustible qui donne dans chaque cas les valeurs les plus défavorables) susceptibles d'affecter les structures à la suite d'incidents.

Comparaison des comportements des cœurs oxyde et métal

Les coefficients d'échange étant beaucoup plus faibles pour l'oxyde que pour l'alliage, la chaleur

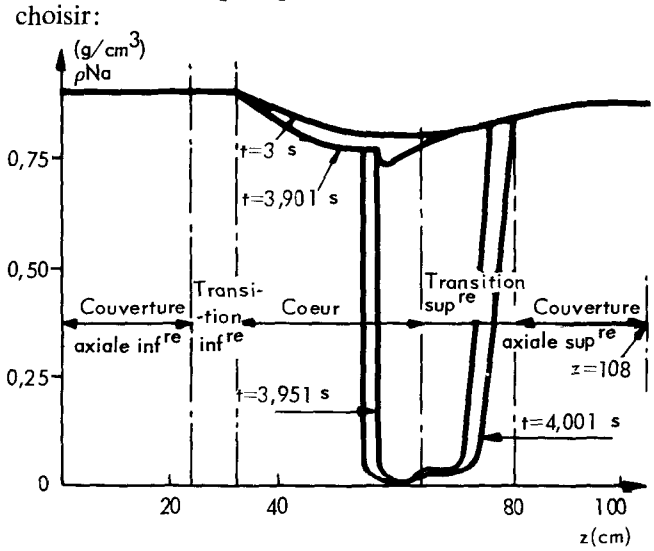


Figure 7. Grippage de la pompe primaire. Variations de ρNa en fonction de la cote z (paramètre: temps)

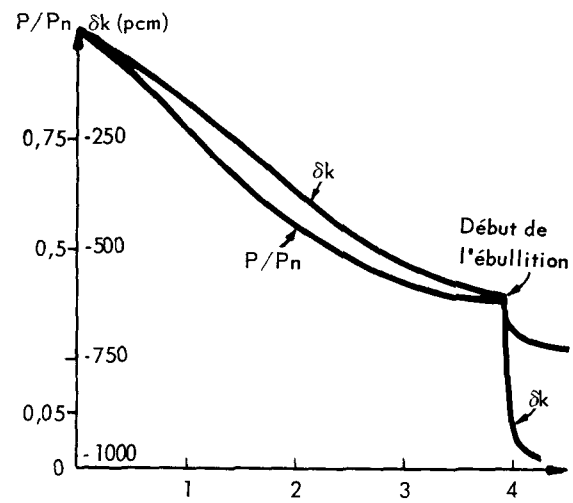


Figure 8. Grippage de la pompe primaire. Variation de la puissance relative P/Pn et de la réactivité totale δ k en fonction du temps

Tableau 1. Chocs thermiques

Nature du choc	Cause	Etat initial de l'installation	Gradient et amplitude
Choc froid à la sortie du cœur	Arrêt d'urgence (chute accélérée des barres avec arrêt des pompes primaires sur l'inertie de leur groupe)	20 MW 2 circuits	—100 °C/s —80 °C
Choc chaud à la sortie du cœur	Arrêt des pompes primaires sur l'inertie de leur groupe et descente réversible des barres	20 MW 2 circuits	+6 °C/s +40 °C
Choc froid sur le sommier HP	Augmentation linéaire du débit air sans action du système de sécurité	1 MW 1 circuit	—1 °C/s —45 °C
Choc chaud sur le sommier HP	Grippage de la pompe secondaire sans action du système de sécurité	10 MW [a] 1 circuit	+5 °C/s +80 °C

[a] Cas théorique, puisque le fonctionnement à cette puissance avec un seul circuit sera prohibé.

se propage moins bien dans l'aiguille d'oxyde que dans l'aiguille d'alliage. En schématisant, on peut dire que les températures de l'alliage suivent les températures du sodium, alors que les températures de l'oxyde sont davantage liées aux variations de puissance. Il en résulte que, du point de vue du combustible, les accidents de refroidissement sont en général plus sévères pour l'alliage que pour l'oxyde, alors que la situation inverse se présente pour les accidents de réactivité.

ÉTUDES DE CONDUITE

Ces études ont été menées sur machines analogiques, avec simulation indépendante des deux circuits thermiques. Trois procédures principales ont été examinées:

a) Démarrage avec débits accordés à la valeur finale de la puissance à atteindre;

b) Démarrage avec débits minimaux des pompes;

c) Démarrage avec débits maximaux des pompes.

La première procédure a l'avantage de simplifier la conduite, seules les commandes neutroniques et les commandes de débit d'air étant à manœuvrer pendant toute la montée en puissance; par contre, son inconvénient principal réside dans le fait que le gradient de température dans le cœur n'est établi qu'à la fin de la dernière phase et qu'on ne bénéficie ainsi que tardivement de l'action du coefficient de contre-réaction de puissance.

Dans la deuxième procédure, les avantages et inconvénients sont inverses, la conduite est plus compliquée du fait qu'il faut actionner simultanément les commandes de barres, de débits primaires, secondaires, et air, mais le gradient de température dans le cœur est établi dès le début de la montée en puissance.

La troisième procédure (qui est celle utilisée en général sur les réacteurs de puissance) semble peu intéressante pour le cas de RAPSODIE, du fait qu'elle cumule les inconvénients des deux premières sans en avoir les avantages.

Actuellement, notre préférence va à la première procédure, du fait de sa simplicité et parce que la stabilité de la pile aux faibles débits est très satisfaisante, comme nous allons le montrer ci-après.

ÉTUDES DE STABILITÉ

On sait l'importance qu'on attache, depuis l'incident survenu à EBR1, à la stabilité des piles rapides.

Nous avons effectué ces études dans le domaine linéaire pour les cœurs alliage et oxyde de RAPSODIE en nous limitant à l'étude du bloc pile. On montre, en effet, que les circuits de refroidissement ne peuvent pas, par eux-mêmes, apporter d'instabilité à un bloc pile stable [8].

Préalablement à l'étude proprement dite de RAPSODIE, nous avons mené à bien une étude complète des différents modèles mathématiques envisageables pour représenter le comportement thermodynamique du barreau combustible. Alors que les modèles employés pour les études d'incidents sont tous du type discontinu en r et z, ceux qui sont envisageables pour les études de stabilité sont mixtes, continus et discontinus, ou même entièrement continus. Nous avons essayé d'apporter une amélioration aux modèles les plus simples (comportant une ou deux zones radiales où la température du combustible est moyennée) en raison de l'intérêt que présente, pour les combustibles les plus réfractaires comme les oxydes UO_2, PuO_2, l'accès à la température au centre du barreau. Des solutions analytiques exactes sont représentatives des fonctions de transfert du système en analyse harmonique comme nous l'indiquons ci-après.

Formulation

A partir des équations fondamentales d'échange thermique dans le cœur, les notations étant celles indiquées plus haut

$$\begin{cases} \rho C \int_0^R 2\pi r [\partial T(r)/\partial t] dr = \lambda(z) q(t) - H_G(T_R - G) & (1) \\ C_G(\partial G/\partial t) = H_G(T_R - G) - H_U(G - U) & (2) \\ C_U(\partial U/\partial t) = H_U(G - U) - V C_U(\partial U/\partial z) & (3) \end{cases}$$

Si l'on considère des oscillations autour du régime d'équilibre $X = X_0 + \delta X$, il vient, après application de la transformation de Laplace, en remarquant que le terme $H_G (T_R - G)$ peut se mettre

sous la forme $-2\pi K R [(d/dr)\ \delta T(r)]r = R$ et en différenciant par rapport à r l'équation (1)

$$\frac{d^2\delta T}{dr^2} + \frac{1}{r}\frac{d\delta T}{dr} - \rho\frac{\rho C}{K}\delta T = -\frac{\lambda(z)\delta q}{\pi R^2 K}$$

une solution particulière de l'équation sans second membre est:

$$\delta T/\delta q = C_1 J_o(\theta) + C_2 \gamma_o(\theta)$$

J_o et γ_o étant les fonctions de Bessel de première et deuxième espèces d'ordre 0, avec

$$\theta = j\, r \sqrt{(\rho C p/K)}$$

Finalement, après élimination de δG entre les équations (2) et (3), et détermination de C_1 et C_2 par les conditions aux limites pour $r = 0$ et $r = R$, il apparaît que la solution générale de (1) est de la forme:

$$\delta U/\delta q = e^{-B/V(z-z_0)}\ [\delta U_o + (1/AV)\int_{z_0}^{z} e^{B/V(z-z_0)}\lambda(z)dz]$$

On remonte alors facilement aux valeurs de:

$$\delta G/\delta q,\quad \delta T_R/\delta q,\quad \delta \bar{T}/\delta q,\quad \delta T_A/\delta q$$

($\delta \bar{T}$ étant la température moyennée sur la section du barreau et δT_A la température au centre du barreau de combustible).

Nous avons utilisé ce modèle pour les études, sur machine digitale, de la stabilité des versions alliage et oxyde de RAPSODIE.

Le code mis au point permettrait, outre le relevé des fonctions de transfert température/réactivité, le relevé des fonctions de transfert température/température d'entrée et température/débit.

Résultats

Du point de vue de la stabilité, le comportement des cœurs oxyde et alliage est différent, du fait que le coefficient d'échange thermique est beaucoup plus faible pour l'oxyde que pour l'alliage (respectivement 0,035 W/cm °C et 0,3 W/cm °C).

Dans les deux cas, la pile est très stable. Les puissances critiques d'instabilité aux différents débits sont très grandes; par exemple, dans le cas le plus défavorable (cœur oxyde avec hypothèse combustible lié à la gaine), les valeurs suivantes ont été relevées:

Débit (m³/h)	700	175	43,75
Puissance nominale (MW)	20	5	1,5
Puissance critique (MW)	2 000	500	60

Dans tous les cas, les lieux de Nyquist ne coupent pas l'axe réel ou le coupent en des points très voisins de l'origine. Nous donnons dans les figures 9 et 10 les courbes (normalisées à 1 MW) relatives au cas cité ci-dessus pour l'oxyde et au cas de l'alliage.

ÉTUDE ET MISE AU POINT DU SIMULATEUR

Toutes les études effectuées sur la dynamique de RAPSODIE ont été concrétisées par la mise au point d'un simulateur destiné, d'une part, à permettre la sélection, l'entraînement et le perfectionnement du personnel chargé de la conduite du réacteur; d'autre part, à effectuer des études complémentaires sur son comportement dynamique et à mener à bien des essais technologiques lors de la mise en service du contrôle commande de la pile [6]. Il se compose:

a) D'un pupitre de contrôle analogue à celui du réacteur;

b) D'un pupitre « moniteur » permettant de simuler pannes et incidents et de contrôler le comportement de l'élève;

c) D'une calculatrice analogique, qui reçoit les commandes de réactivité et débits des pupitres, résout en temps réels les équations dynamiques de la pile (bloc pile et circuits thermiques) et restitue aux pupitres tous les paramètres représentatifs de l'état de l'installation (puissance, période, température, etc.) aussi bien en fonctionnement normal que dans le cas des divers incidents possibles.

Calculatrice

La calculatrice analogique se compose de deux machines PACE type 231 R*, dont on utilise environ 220 amplificateurs, 14 servomultiplieurs et 13 générateurs de fonction à diodes.

* Installées dans les locaux de la section d'électronique et d'instrumentation au CEN de Cadarache, France.

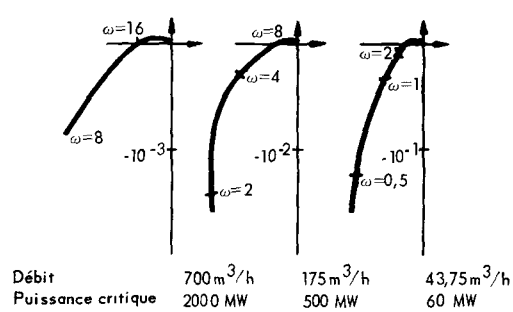


Figure 9. Critère de Nyquist (version oxyde)

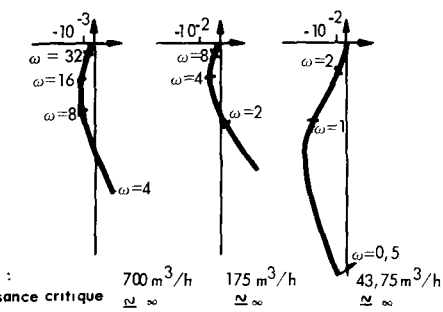


Figure 10. Critère de Nyquist (version alliage)

La formulation utilisée, qui concerne le bloc pile et les deux circuits de réfrigération, a été décrite plus haut; le découpage optimisé, qui résulte d'une pré-étude effectuée sur machine digitale (le critère adopté étant de conserver une précision meilleure que 10% par rapport au modèle de référence pour les transitoires les plus violents) consiste à diviser le cœur en quatre zones, la couverture radiale étant représentée par une seule zone. Les échangeurs intermédiaires comportent quatre zones, alors que les échangeurs terminaux sont représentés par une seule zone. Grâce à l'utilisation d'un système de commutation automatique, la cinétique est simulée sur neuf décades. Ce dispositif se compose essentiellement d'intégrateurs utilisés comme mémoires et diviseurs, et d'un relayage de commutation utilisé également pour fournir au pupitre la puissance sous forme logarithmique.

Les retards dans les tuyauteries sont simulés au moyen de dispositifs à capacité tournante.

Pupitres

Le pupitre de contrôle est similaire à celui de la pile. Il comporte:

a) Les commandes des quatre barres de sécurité/compensation, des deux barres de pilotage;

b) Les commandes des quatre pompes primaires et secondaire et des deux ventilateurs;

c) Les indications de puissance, période, température entrée et sortie cœur et des échangeurs intermédiaires et finals.

Le pupitre moniteur, outre la répétition des principales informations sur l'état de la pile, comporte une centaine de clefs permettant la simulation de toutes les pannes et incidents principaux envisageables sur l'installation.

Couplage avec une machine digitale

Enfin nous avons réalisé, à titre expérimental et en vue d'applications futures, le couplage en temps réel du pupitre de contrôle du simulateur avec une calculatrice arithmétique rapide (type CAE 530) conformément au schéma de la figure 11.

La simulation était limitée au bloc pile seul, découpé en trois zones pour le cœur et une zone pour la couverture radiale. Le pas de calcul choisi était 300 ms, ce qui permettait une représentation valable de l'évolution des paramètres pour les incidents déjà cités. La cinétique était traitée en virgule flottante, du fait de la variation sur huit décades de la puissance; par contre, les équations d'échange thermique étaient traitées en virgule fixe, les températures n'évoluant que sur une décade au plus.

Nous comptons poursuivre ces essais par la simulation d'ensemble de la pile et de ses circuits.

CONCLUSIONS

Nous avons vu que, même dans les configurations les plus défavorables, la stabilité de la pile était très grande. De l'étude d'ensemble des incidents possibles, il ressort que, moyennant certaines précautions, aucun dommage (chocs thermiques inacceptables, changements d'état du combustible ou du réfrigérant) — même en cas de défaillance du système de sécurité — ne peut affecter l'installation. Quelques incidents extrêmement improbables pourraient conduire à des dommages qui resteraient cependant très inférieurs à ceux pouvant résulter de l'accident hypothétique maximal.

Enfin, l'utilisation du simulateur permettra de compléter les études de conduite et d'assurer la formation du personnel chargé de l'exploitation de la pile.

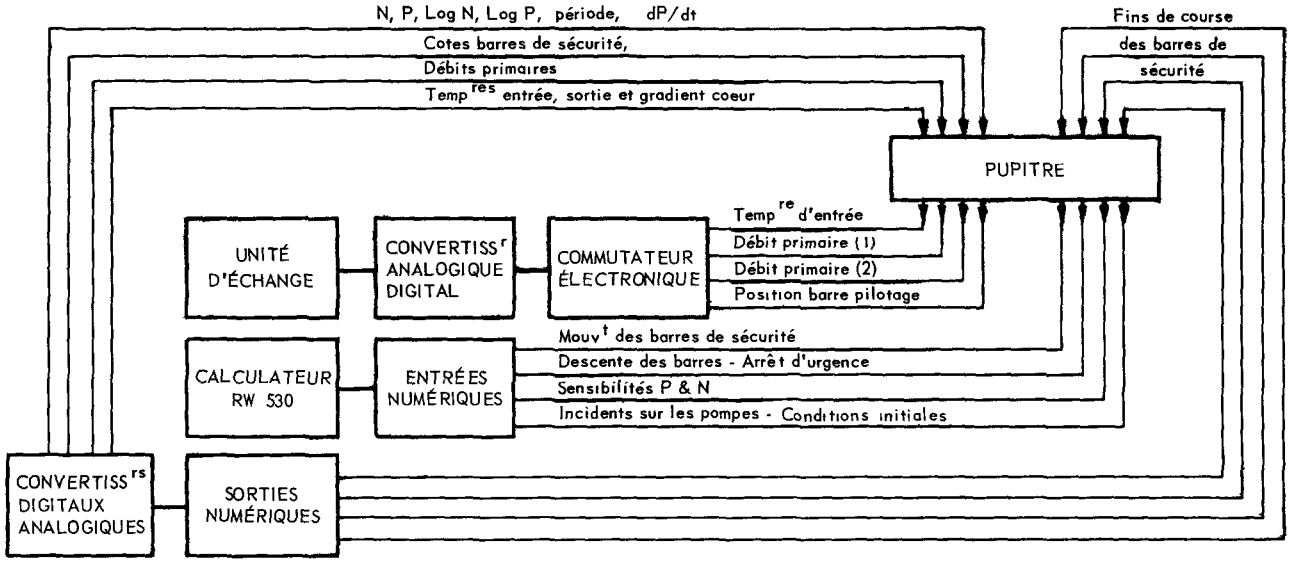


Figure 11

REMERCIEMENTS

Nous remercions toutes les personnes qui ont dirigé le travail dont la synthèse fait l'objet du présent mémoire ou qui y ont participé. Les études ont été effectuées, d'une part, dans le cadre de l'Association EURATOM-CEA pour les neutrons rapides, dont le chef du projet est M. G. Vendryès, au Service d'études des piles rapides, dirigé par M. C. P. Zaleski, les ingénieurs y ayant collaboré étant: MM. J. Ladet, I. Puig et M. Jallade; d'autre part, pour les études traitées par voie analogique à la Section autonome d'électronique des réacteurs du Département d'électronique du CEA, dont le chef est M. Weill, par M. Caillet, avec la collaboration de M^me^ List et MM. Bory et Vallat. Enfin les calculs digitaux ont été menés au Service de calcul électronique dirigé par M. Amouyal.

RÉFÉRENCES

1. Zaleski, C. P., et Vautrey, L., *Le réacteur surgénérateur RAPSODIE,* Symposium sur les réacteurs de puissance expérimentaux, Conférence de Vienne, 1961, Rapport CEA 2193.
2. Campan, J. L., Chaumont, J. M., Clauzon, P. P., Chesquière, G., Leduc, J., et Zaleski, C. P., *Généralités sur le comportement dynamique des piles rapides. Etudes préliminaires de RAPSODIE,* Rapport CEA 2293.
3. Abdon, R., Chaumont, J. M., Clauzon, P. P., et Chesquière, G., *Etudes des régimes transitoires et de la stabilité des piles rapides,* Symposium sur les réacteurs de puissance expérimentaux, Conférence de Vienne, 1961.
4. Abdon, R., Ladet, J., Puig, I., et Chesquière, G., *Etudes comparatives effectuées sur le comportement dynamique des piles rapides du type RAPSODIE,* Symposium "Advances in Reactor Theory", Karlsruhe, avril 1963.
5. Abdon, R., *et al., RAPSODIE: Etudes neutroniques, hydrauliques, thermiques et dynamiques et études de stabilité,* Rapport CEA 2450.
6. Abdon, R., et Chaigne, M., *Le simulateur RAPSODIE,* Rapport CEA en préparation.
7. Abdon, R., Ladet, J., et Mitaine, J., *Utilisation d'une calculatrice arithmétique pour la simulation en temps réel d'un réacteur nucléaire, Application à RAPSODIE,* Rapport CEA en préparation.
8. Puig, I., *Etude de la stabilité des piles rapides. Application à RAPSODIE,* Rapport CEA en préparation.
9. Ladet, J., et Jallade, M., *Contribution à l'étude de l'ébullition accidentelle du réfrigérant dans les piles rapides refroidies au sodium. Application à RAPSODIE,* Rapport CEA en préparation.
10. Caillet, C., et Chaigne, M., et les ingénieurs des Groupes de calcul analogique de Saclay et Cadarache, *Comportement dynamique de RAPSODIE,* Rapport CEA à paraître.
11. Vendryès, G., *et al., RAPSODIE,* Voir les présents Actes, P/42, Vol. 6.
12. Chalot, A., Sauvage, M., et Venturino, G., *Montage de la maquette RAPSODIE. Point des études et essais à la date d'avril,* Rapport CEA en préparation.

ABSTRACT - RÉSUMÉ - АННОТАЦИЯ - RESUMEN

A/79 France

Study of the dynamic behaviour of the reactor RAPSODIE

By R. Abdon and M. Chaigne

It is known that fast neutron breeder reactors pose new problems in the fields of mechanics and heat technology, as well as in respect to their dynamic behaviour and safety.

The reactor RAPSODIE has been the object of numerous dynamic studies on analogue and digital computors for two types of fuel (metal and oxide).

After elaborating the mathematical models representing the whole of the installation (reactor block and cooling circuit) from the point of view of neutrons as well as thermodynamics, the analogue diagrams and digital codes required for simulating incidents, control and stability of the reactor have been established.

Considerable effort was made to obtain a greater precision than in the usual methods, either by using smaller intervals, or by the use of formulations closer to the real system, or even analytically soluble.

The study of incidents was carried out on an analogue computer for the whole system, and a digital computer for the reactor block alone or the installation functioning with a single thermal circuit.

A special complementary programme—which, so far as we know, was used for the first time here for sodium reactors—that takes into account the behaviour of the reactor beyond the boiling point of sodium, was refined on the basis of some simplifying assumptions.

The investigation of incidents has served to determine:

(*a*) The intrinsic safety of the reactor, i.e. its behaviour under accident conditions without the intervention of the safety systems;

(*b*) The behaviour of the installation under normal accident conditions, i.e. with the safety systems functioning, and the definition and organisation of the latter;

(*c*) The comparison of the two versions investigated (metal or oxide fuel) for the choice of the first loading of the reactor;

(*d*) The determination of thermal shocks (amplitudes and gradients suffered by the structures during probable incidents) to be used in the test on the full-scale model of the reactor.

The stability tests were carried out digitally. The investigation of the control, carried out on an

analogue computer, served to determine the different possible means of starting and changing the conditions of the reactor as well as its automatic control.

The calculations were examined as a whole by the construction of a training simulator composed of a board similar to the control board of the reactor, all of whose commands (reactivity and flows) work on an analogue computer which resolves in the real time the dynamic equations of the reactor and which reproduces simultaneously all the parameters representing the state of the installation (power, period, temperatures, etc.) in the case of various incidents as well as under normal conditions of functioning.

A/79 Франция

Изучение динамического поведения реактора „RAPSODIE"

Р. Абдон, М. Шенье

Известно, что разработка реакторов-размножителей на быстрых нейтронах ставит новые проблемы как в области механики и термодинамики, так и в отношении динамического поведения таких реакторов и безопасности работы.

Реактор RAPSODIE явился объектом многочисленных динамических исследований, проводившихся на счетно-решающих и цифровых машинах для двух видов топлива (в виде металла и в виде окиси).

После разработки математических моделей, представляющих совокупность реактора (реакторный блок и контур охлаждения) как в отношении нейтронов, так и в отношении термодинамики, были созданы аналоговые схемы и цифровые коды, которые использовались для имитации аварий, поведения и стабильности реактора.

Старались получить более высокую точность по сравнению с обычными методами путем деления на более тонкие зоны, путем использования более типичных формулировок действительной системы, решаемых даже аналитическим путем.

Аварии изучались с помощью счетно-решающей машины для всей установки и с помощью цифровой машины для изучения только реакторного блока или установки, работающей с одним тепловым контуром.

Путем усреднения упрощенных гипотез была составлена специальная дополнительная программа, дающая представление о поведении реактора при температуре выше температуры кипения натрия. По мнению автора, она впервые была применена для реакторов с натриевым теплоносителем.

Изучение аварий позволило уточнить:

— безопасность, свойственную реактору, т. е. его поведение в аварийном режиме без включения системы безопасности;

— поведение установки в нормальном аварийном режиме, т. е. при включении системы безопасности, и определение и организацию последней;

— сравнение двух изучаемых моделей (с топливом в виде металла и в виде окиси) для выбора первой топливной загрузки реактора;

— определение тепловых ударов (амплитуда и тепловые градиенты, испытываемые конструкцией во время возможных аварий) для испытания на макете реактора в натуральную величину.

Изучение стабильности осуществлялось с помощью цифровой машины. Изучение поведения, проводившееся на счетно-решающих машинах, позволило уточнить различные процедуры, предусматриваемые для пускового режима и изменений режима работы реактора, а также для автоматического управления.

Совокупность всех этих исследований была конкретизирована путем создания пускового моделирующего устройства, состоящего из пульта, подобного пульту управления реактора, но на котором все команды (реактивность и выходы) приводят в действие счетно-решающую машину, решающую в реальное время динамические уравнения реактора, которая одновременно выдает все параметры, характеризующие состояние установки (мощность, период, температуры и т. д.), как при нормальной работе, так и в случае различных возможных аварий.

A/79 Francia

Estudio del comportamiento dinámico de la pila RAPSODIE

por R. Abdon y M. Chaigne

Se sabe que el desarrollo de reactores reproductores de neutrones rápidos presenta problemas nuevos en los campos mecánico y térmico por una parte y en lo que respecta a su comportamiento dinámico y a su seguridad por otra.

La pila RAPSODIE ha sido objeto de numerosos estudios dinámicos efectuados con máquinas analógicas y digitales para dos versiones del combustible (metal y óxido).

Después de la elaboración de los modelos matemáticos representativos del conjunto de la instalación (bloque del reactor y circuito de refrigeración), tanto desde el punto de vista neutrónico como desde el punto de vista termodinámico, se han puesto a punto los esquemas analógicos y los códigos utilizables para efectuar la simulación de incidentes anormales, de operación normal y de estabilidad del reactor.

Por lo que respecta a los métodos habituales, se ha puesto interés en obtener una precisión mayor por descomposición en zonas más estrechas y por el empleo de formulismos que representen mejor el sistema real y que sean incluso solubles analíticamente.

Los estudios de incidentes han sido efectuados por medios analógicos para el conjunto de la instalación y por medios digitales para el estudio del bloque del reactor aislado o de la instalación funcionando con un solo circuito térmico.

Mediante ciertas hipótesis simplificadoras, se ha puesto a punto un programa complementario especial que informa del comportamiento del reactor más allá de la ebullición del sodio y que, a nuestro juicio, ha sido empleado aquí por primera vez para las pilas de sodio.

Los estudios de incidentes han permitido precisar:

a) La seguridad intrínseca del reactor, es decir, su comportamiento en régimen accidental sin intervención del sistema de seguridad;

b) El comportamiento de la instalación en régimen accidental normal, es decir, con funcionamiento del sistema de seguridad según sus características nominales;

c) La comparación entre las dos versiones estudiadas (combustible metálico y combustible óxido) con objeto de elegir la primera carga de la pila;

d) La determinación de choques térmicos (amplitud y gradientes sufridos por las estructuras en el momento de los incidentes probables) con vistas a pruebas en la maqueta a escala 1 de la pila.

Los estudios de estabilidad han sido efectuados por medios digitales. Los estudios de operación, efectuados con máquinas analógicas, han permitido precisar los diferentes procedimientos aceptables para el arranque y cambios de régimen de la pila, así como su control automático.

Todos estos estudios han sido materializados por la puesta a punto de un simulador de entrenamiento provisto de un pupitre similar al pupitre de control de la pila pero cuyos mandos (reactividad y caudal de circulación de fluidos) accionan una calculadora analógica que resuelve en tiempo real las ecuaciones dinámicas del reactor y entrega simultáneamente todos los parámetros que representan el estado de la instalación (potencia, período, temperaturas, etc.) tanto en funcionamiento normal como en el caso de distintos incidentes posibles.

Temperature limits and the optimisation of power output in Calder and Chapelcross reactors

By H. A. Hughes, D. S. Briggs, R. Dodds and R. M. Horsley*

The maximum output of a power reactor is determined by the operating limits specified for various items of the plant. These limits serve two purposes: first, they ensure continued safe operation under normal conditions, and secondly, they minimise the risk of hazardous conditions arising in the event of a fault. At the design stage, and during the early period of operation, it is necessary to allow appreciable margins in setting some of the limits because of uncertainties in fundamental parameters and in actual operating conditions. As operational experience grows, some of these uncertainties are reduced, and also predictive models can be tested using experimental measurements. Irradiation experiments at accelerated dose-rates enable extrapolations to be made of changes in irradiation-dependent parameters, and the validity of such extrapolations can be checked against actual reactor measurements. Consequently, operating limits and reactor performance can be gradually refined.

For various reasons temperature is one of the most important factors determining the performance of the major reactor components — fuel elements, moderator, pressure vessel. The operating temperatures of fuel elements must be such that their mechanical strength and oxidation characteristics give satisfactory behaviour during irradiation under normal conditions. In addition, a limitation is imposed by the criterion that there must be a reasonable probability that the Magnox will not ignite in a depressurisation incident. Following such an incident, graphite temperatures will be affected by the release of stored energy and the exothermic reaction between air and graphite. This leads directly to the imposition of limits on the conditions under which the graphite moderator can be irradiated. The limits on fuel element temperatures and on the moderator, although important under normal operating conditions, are also intended to minimise the consequences of a fracture of the pressure circuit. Thus the limitations placed on the pressure vessel are of crucial importance, not only in deciding the ultimate safety and life of the reactor, but also in determining the attainable power output. It is the way in which criteria are defined for these interrelated limits that forms the theme of this paper.

* U.K.A.E.A., Production Group, Windscale.

FUEL ELEMENT TEMPERATURE LIMITS

The temperature criterion

Initially, the power of the Calder and Chapelcross reactors was controlled by a limit of 408 °C on the maximum can surface temperature [1]. This limit was based on a combination of available information on the canning material (Magnox) and calculations of the temperature conditions required to achieve the design output. Assessments to ensure that the limit was not exceeded could be made properly only for the channels in which can thermocouples were installed and these were severely restricted in number and position by the existing operational limitations.

Several complementary developments eventually made practicable a more rationally-based temperature criterion, in which account is taken of the temperature in every channel. The objective laid down was that no widespread can melting should occur in the temperature transient following the worst credible reactor fault. Analysis showed this fault to be fracture of an inlet duct and consequent failure of the blowers.

The temperature criterion which has been applied since early in 1962 is that the operating temperature distribution shall be such that in the initial transient following an inlet duct failure, the sum of the probabilities of can temperatures reaching the ignition point of Magnox (taken for the present as 630 °C) shall not exceed 0.1 with 90% confidence. The ignition temperature of Magnox depends on the air and moisture content of the CO_2 coolant and on the rate of rise of temperature. For the Calder and Chapelcross reactors, a conservative value of 630 °C is currently used pending further assessments. In choosing the probability and confidence level a compromise must be made between overall risk (bearing in mind the low probability of the fault occurring), and economic penalty. It may be noted that changing the probability from 0.1 to 0.01 would reduce the permitted can temperatures by 6-7 °C. Furthermore, the assessed probability cannot take into account channels in which, for example, flow is restricted by partial blockage; the risk of such conditions must be kept low by suitable inspection and operational procedures. Can-failure

rates and post-irradiation examination have confirmed that the temperatures attained under the criterion are not too high for the metallurgical and physical properties of the cans, provided that the measured temperatures are kept below 495 °C to avoid incompatibility between Magnox and the stainless-steel thermocouple sheath. It has been shown that the alpha-beta transition temperature of uranium is never closely approached. The requirements for the operation of such a criterion are an adequate model for the prediction of steady-state temperatures, a method of calculating the transient rise in temperature, and a method of application which ensures that the stipulated conditions are always satisfied. These three features are discussed in the following section.

The steady-state temperature distribution

The first essential in developing a predictive model is a method of calculating the flux in every fuel channel which will take into account, in sufficient detail, the reactor core and reflector regions and the fuel and absorber loadings, including variations in irradiation. Of several computer programmes written for this purpose, the one which has been used at Calder and Chapelcross is FTD2 [2]. This is a two-group, two-dimensional programme which uses finite difference methods to solve the diffusion equations. The flux predictions were first shown to be satisfactory by comparison with measurements made during reactor commissioning and operation [3]. The programme then calculates the maximum can temperature (T_{sm}) in each channel from a formula which requires a knowledge of a combined mass flow and heat transfer parameter for each channel. Such a parameter can be obtained by direct correlation of predicted and measured values of T_{sm}, or by measurements of the individual mass flow and heat transfer parameters from commissioning or rig tests. Since many reliable can temperature measurements were available, the direct correlation method was used. Whatever method is adopted it is important to determine the systematic effects which occur.

The existence of some effects may be readily predicted though their magnitude is difficult to determine. Such effects arise, for example, from the fact that the problem is three-dimensional while the programme treats only two dimensions. Thus FTD2 assumes a cosine axial flux distribution corresponding to the control rods being fully withdrawn. Partial insertion of the control rods affects both the radial and the axial distribution of flux and hence of temperature. These effects have been determined by means of: flux measurements; can and channel gas outlet temperature measurements; programmes which treat the axial distribution only, and the three-dimensional programme FTD3. The result is a series of corrections to apply to the FTD2 predictions for any insertion of the control rods.

Other systematic effects may not be anticipated in design and may escape detection in operation for some time. Three such effects, taken into account by assessment of experimental data, are gas and heat leakage, quadrantal flow asymmetry, and the perturbation of flow caused by the diagrid girders [1].

Comparison of individual measured and predicted temperatures for 30 reactor charges covering the range of operating conditions has shown that T_{sm} in any channel is now predicted with a standard deviation of 8.3 °C.

The transient rise in temperature

Fracture of an inlet duct would cause rapid depressurisation of the reactor with drastic reduction in core coolant flow. The control rods would trip after a delay time which is characteristic of the reactor safety circuit. With the reduction in coolant flow, fuel element temperatures would rise and reach a maximum in about a minute when the falling heat input rate from delayed neutron and fission product sources first equalled the rate of heat loss by radiation and convection. The transient rise in temperature for any channel is taken to be the difference between the maximum can temperature in the steady-state and the maximum can temperature reached in the transient, although these will in general occur at different axial positions.

The transient rise can be obtained only from a computer calculation. This must take into account, with the appropriate time-dependence where necessary: coolant flow; trip delay time (taken to be that corresponding to the second fastest independent tripping mechanism); reactivity held by the control rods and their insertion time, fission product heating, can emissivity; thermal capacity of uranium and can [4]. The variation of the transient rise with channel power and mass flow, with control rod insertion, and with irradiation, must be found in order to determine the transient rise for every channel under any operating conditions.

Since it is difficult to obtain a realistically-based error for the estimate of transient rise, no error is assumed but, instead, the calculation is made deliberately pessimistic, particularly in respect of the variation most difficult to determine—namely, the variation of coolant flow with time. Transient experiments, in which the blowers have been tripped and the control rods held out, have been performed on a reactor in order to check the model used in the nuclear part of the calculation [5].

Application of the criterion

The proper application of the criterion requires, first, that operating limits are specified for all possible reactor conditions with a given fuel and absorber loading and, secondly, that the method of checking that these limits are not exceeded is simple and quick. If any significant change is made in the fuel or absorber loading (including irradiation

changes), the operating limits must be recalculated. In addition, the thermocouples installed must give an adequate, unbiased sample of the temperatures in the reactor.

The first requirement in determining the operating limits is the distribution of peak transient temperatures for the expected reactor power and any given rod insertion. This is calculated by FTD2 from the T_{sm} distribution and the transient rise for a given channel rating. Next, a temperature T^* must be found which will be exceeded with only 0.1 probability at the 90% confidence level. The temperature which is exceeded with a probability α and with confidence $(1 - \beta)$ is given by a relation involving the normal deviates corresponding to α and β and the number of temperature readings used in normalising the model and in estimating the standard deviation.

The quantity $(630 - T^*)$ °C is added to the predicted T_{sm} for each instrumented channel to give "permitted T_{sm}'s". From the axial temperature distribution the permitted temperature for each installed thermocouple can be derived. The criterion is satisfied, for the reactor power and rod insertion assumed in the above calculation, if the average of the thermocouple readings does not exceed the average permitted temperature $(\bar{P})$.

The above calculation should strictly be repeated for several different rod insertions and reactor powers in order to obtain $\bar{P}$ for any power and rod insertion. Calculation time can be saved by making simplifying, pessimistic assumptions. If reactor power is limited by can temperatures, this will, of course, mean an economic penalty. If small changes are made in the reactor core, for example by additional insertion of a few control rods, the resulting changes in the flux and temperature distribution can be obtained from the changes in the installed thermocouples. The operating limits can then be revised without the use of FTD2. Even if no such changes are made, however, the operating limits must be recalculated at suitable intervals using FTD2, to take account of the change in irradiation.

GRAPHITE TEMPERATURE LIMITS

Limits on the operating temperature of the graphite moderator are determined by the permissible accumulation of irradiation damage, and the influence of temperature on the course of certain fault conditions. Three main criteria can be recognised. The first is that normal operation of the reactor should not be adversely affected during its design lifetime by changes in graphite properties. The second is that property changes should not affect the consequences, as distinct from the time scale of a credible fault, e.g. a single channel fire in an intact reactor should not spread. The third criterion is that property changes should not dangerously shorten the time-scale of credible reactor faults. The magnitude of acceptable changes are interlinked to the operating conditions of the plant.

Consideration of the first two criteria lead to limitations on growth and stored energy respectively, during the reactor lifetime. The damage restriction may lead to a requirement for an increase in inlet gas temperature to decrease the rate of damage, or the application of an annealing procedure to reduce the damage accumulated at a given time, depending on the effectiveness of these procedures. It should be noted that present-day knowledge allows a more exact specification of a minimum graphite temperature to avoid excessive irradiation damage than was possible when the first Calder reactors were designed. On three Chapelcross reactors, for example, the introduction of sleeves increased the graphite temperatures in the plane of maximum damage by 40 °C above that in the unsleeved reactors, and thus effectively eliminated the damage problem. The third criterion involves stored energy, graphite oxidation and graphite operating temperature. Assuming that stored energy is limited by the second criterion and that sufficient information exists on the reactivity of the graphite throughout the moderator, an upper limitation on the operating temperature can be derived.

Dimensional change

Under irradiation Calder reactor grade-A graphite shrinks parallel to the direction of extrusion and grows perpendicular to this direction; this is illustrated in Table 1 by results obtained from specimens irradiated in DIDO. In designing the core, Wigner gaps were included to allow the anticipated dimensional changes to be accommodated without distortion of the structure [6].

Table 1. Dimensional changes in grade A graphite

Temperature [6] (°C)		Perpendicular to extrusion		Parallel to extrusion	
Rig	Calder equivalent	Equivalent dose MWd/ate[a]	% change	Equivalent dose MWd/ate	% change
150	129	5 000	+ 3	6 000	— 1
200	173	5 000	+ 1	6 000	— 0.8
350	300	25 000	— 1	20 000	— 1

[a] ate = adjacent tonne.

Specimens, pre-cut to high precision, are irradiated throughout the reactor life to monitor the dimensional changes. However, the laboratory programme has recently been supplemented, indeed almost replaced, by a direct in-pile measurement. A clear picture of the Wigner gaps, and a permanent photographic record, may be obtained using a television camera carrying a calibrated scale. Measurements are made in a number of X-holes and a sufficiently large number of axial locations to allow the growth profile to be determined. The design tolerances on

gap sizes and the accuracy of measurement are such that the design values of gap sizes can be accepted as the zero irradiation datum. The agreement between these direct measurements and predictions from accelerated dose measurements is shown in Fig. 1. In-pile monitoring will be continued to confirm this agreement between the behaviour of large bricks and small samples at higher irradiations.

The first significant milestone indicating the effects of growth is the closing of the first Wigner gap. In the unsleeved reactor this will occur for the 3 mm gap in zones A and B after about 14 years operation. Subsequent closing of gaps at the common level will cause overall lateral growth such that at 20 years core lifetime a 2.5 mm displacement between core bricks Nos. 1 and 2 could have developed in the outer channels of zone B; this is unlikely to embarrass charge-discharge operations. Dimensional change of bricks and tiles (which separate bricks in the vertical plane) is such that the tiles may start to protrude into the channels after 17 years operation, but even after 20 years the protrusion should not exceed 1.5 mm, which is unlikely to be of any consequence in refuelling operations. For the sleeved reactor, the first Wigner gap should not close until 26 years of operation have elapsed, and several more years of operation could be expected before the dimensional changes became troublesome. Changes are progressive over many years, and are irreversible, but the rate of dimensional change is sensitive to temperature and could be reduced by increasing the reactor inlet temperature.

Stored energy

The variation of stored energy with neutron dose in the temperature range of importance in these reactors has been discussed by Bell and others [7]. They showed that the rate of increase of total stored energy with dose decreases markedly as the irradiation temperature increases and that it also decreases with increasing dose at any given temperature. The rate of release of stored energy (dE/dT), important in safety calculations, is simply related to the total stored energy, and is similarly sensitive to the irradiation temperature.

Measurements of the total stored energy of a specimen of graphite are made in a bomb calorimeter and rate of release determinations in a linear rise calorimeter [8]. Samples for measurements are taken either from monitoring specimens loaded into the reactors during commissioning, or from specimens cut directly from the bulk graphite moderator or from the channel sleeves. The variation of rate of release of stored energy with effective dose [9] under Calder conditions is shown in Fig. 2.

Early calculations on the spread of a single channel fire in a CO_2 atmosphere were very pessimistic; for example, it was assumed that there was no cooling of the channels surrounding the burning channel, and that the closest approach between dE/dT and specific heat was maintained up to 1 100 °C. Such a calculation led to a requirement that for non-spread, the minimum effective specific heat should be 0.07 cal/g deg C. Calculations are in hand to redefine the acceptable value of dE/dT using more realistic assumptions, and are expected to allow a much closer approach to the value of specific heat.

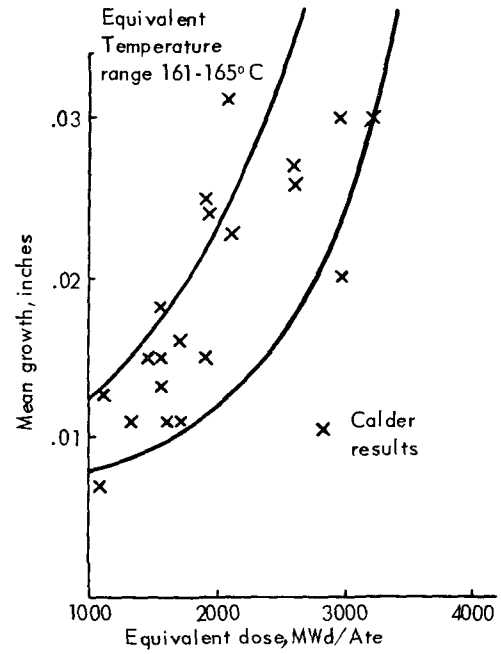


Figure 1. Change in Wigner gap size with equivalent dose

95% of the accelerated dose rig data lie within the two curves

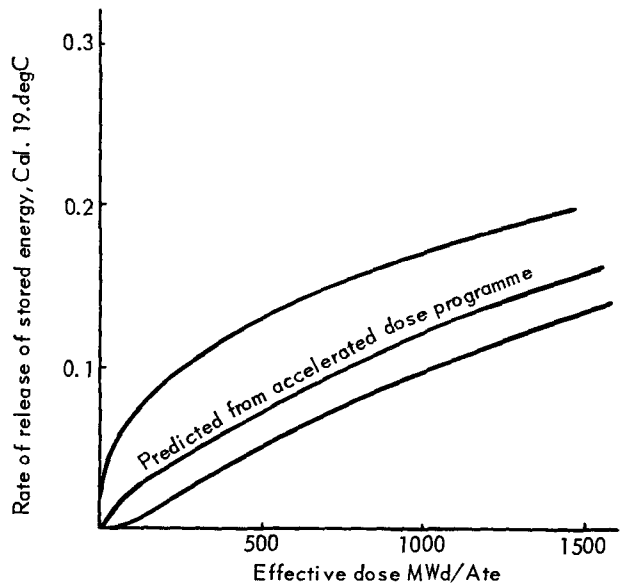


Figure 2. Variation of stored energy with effective dose

90% of experimental points from Calder samples lie within the two outer curves

Maximum operating temperature

If substantial quantities of air are drawn into the coolant circuit after a depressurisation incident, the rate of rise of reactor temperatures will be governed by fission product decay heat, the stored energy liberated from the graphite when the temperature exceeds its operating temperature by about 50 °C, and the heat of oxidation which is strongly related to temperature by an Arrhenius equation. This rate of rise should be such that sufficient time is available for the operator to take reasonable emergency actions which will effectively control the incident, such as isolation or repair of the fracture, CO_2 purging and restoration of main circulators.

The oxidation rate of virgin A-grade graphite in air at 400 °C has an average value of 3×10^{-6} g/g h. Reactivity measurements have been made on both monitoring and trepanned graphite samples from the Calder reactors, and the results confirm that this value tends to increase as a result of reactor exposure. The possible reasons for this increase and also a prediction of its extent over the course of a lifetime of a Magnox reactor are given by Beattie, Lewis and Lind [10], who suggest that a reactivity of the order of 100×10^{-6} g/g h might ultimately be reached. Results to date from the Calder reactors show a considerable degree of scatter, but are in broad agreement with this prediction. A reduction in overall reaction rate can be expected from the effect of in-pore diffusion control provided that bulk flow of gas through the graphite is negligible [10]. Such would be the case if the standby pony motor flow only were available.

The general effect on the graphite temperature vs. time curves of various assumptions such as the addition of a large feed-rate of CO_2 and the restoration of main circulators has been illustrated by Beattie *et al.* [10]. Application of this type of analysis to Calder and Chapelcross reactors show that it is unnecessary to impose a restrictive limit on the maximum permitted graphite operating temperature, as even with the pessimistic assumptions temperatures would remain under control for at least several hours after duct fracture. The present limit of 420 °C, comfortably above normal operating temperatures of about 380-400 °C., is reviewed annually using up-to-date values of the appropriate parameters with a statistical approach to take account of local variations.

PRESSURE VESSEL TEMPERATURE LIMITS

The design and construction of the Calder pressure vessels has been described by Brown *et al.* [11]. The specification adopted was B.S.1500, which permits a maximum membrane stress of 25% of the ultimate tensile stress of the steel plate. Whilst this provides a safeguard against tensile failure it does not specifically cover other modes of failure or deformation, such as brittle fracture, excessive creep deformation, stress rupture, fatigue and fast ductile fracture. Consideration of the first three of these types of failure leads to the definition of temperature limitations in the pressure vessel and associated duct work.

Brittle fracture

From general considerations a special high-notch-ductility, fully-killed steel, Lowtem, was specified, which would allow a convenient minimum temperature of operation, taking into account the effect on the ductile/brittle transition temperature, T_t, of irradiation damage and strain-aging. To define the value of T_t for the original unirradiated steel used at Calder and Chapelcross, the UKAEA have used an isothermal crack arrest temperature test developed from that of Robertson [12], which yields a temperature of about 0 °C. The large size of specimens required for the Robertson test precluded their use in-pile for monitoring purposes, and hence a correlation was obtained out-of-pile for the change in transition temperature (induced by strain-aging) measured by both the Robertson test and by the analysis of conventional Charpy V-notch impact tests so that the smaller Charpy test pieces could be used as in-pile monitoring specimens in positions where the damage flux and temperature were representative of important regions of the pressure vessel. Normal properties were also monitored using tensile specimens. As the change in T_t in the steel of the vessel, and hence also in the above specimens, was likely to be small, specimens were loaded in Calder fuel channels and in high flux reactors to give accelerated effects, the results being corrected to the appropriate temperature and flux as for graphite damage. From a correlation between these results and a neutron damage model, it can be estimated that an increase of only 13 °C in T_t will occur after 20 years at a representative point on the vessel [13]. Even when allowance is made for uncertainties in this estimate, and for the effect of strain-aging, predicted to be about 20 °C in 20 years, the minimum vessel temperature limit is much lower than the presently accepted operational value of 80 °C.

It should be noted that maintenance of a pressure vessel above the appropriate value of T_t does not guarantee freedom from risk of fast fracture. Irvine, Quirk and Bevitt [14] have shown that above a critical crack length, fast fracture is possible over a temperature interval which embraces the full range of Charpy values.

Low deformation creep

The permissible creep strain in the top dome of the vessel is limited to 0.2% by the requirements of charge tube alignment. The most pessimistic interpretation of data from uni-axial creep tests shows that this value would be reached in 200 000 hours (the design life of the vessel) if the temperature of

the steel was 365 °C with the top-dome membrane stress of 5 tons/in² (8 kg/mm²). In an equi-bi-axial system, as exists in the top dome, a further margin of 10 °C may well be in hand, but this margin could be required for possible enhancement of creep rates resulting from irradiation damage. Actual measurements on the top-dome indicate that the maximum temperature does not exceed 310 °C, and at the centre 280 °C, accounted for by the presence of a stagnant layer of gas below the cooled, unlagged dome. Additionally, capacitance-type strain gauges mounted on the dome of one reactor at Chapelcross show extremely low creep values.

Stress rupture

Although low deformation creep is not restrictive on the Calder and Chapelcross vessels, the creep-rupture characteristics require assessment for the highly stressed regions, where the steel temperature is more nearly equal to that of the outlet gas. The assessment must distinguish between the relative risks of stress rupture in the vessel plate, and the weld material. Under the same conditions weld material will generally rupture at a higher stress but at a lower strain than the plate. It appears likely that the strain criterion will not be infringed, and thus the following discussion refers to the properties of the plate.

Data from uni-axially stressed specimens has been analysed in an attempt to determine the relationship between stress, temperature and time-to-rupture. In order to produce rupture of the specimens in a reasonably short time, the process was accelerated by using much higher temperatures and/or stresses than exist in the reactor. Consequently a considerable extrapolation was required between the experimental and plant operating conditions, and the data is periodically re-analysed as it becomes available from the longer term tests. The form of the analysis is illustrated in a paper by Haskey and Wood [15], where it is shown that the long term stress behaviour can be described by a parameter of the form $(\log t - \log t_0)/(1/T - 1/T_0)$, where t is the time to rupture at a temperature T for constant stress, the subscript referring to a datum condition. From the relationship derived for Lowtem steel it may be shown that at 350 °C an increase of 6 °C in temperature or an increase of 1 ton/in² (1.6 kg/mm²) halves the time to rupture.

In order to use the relation to determine a limiting temperature in the operating reactor, further information is necessary on the detailed temperature distribution at a given power level and the detailed stress distribution as a function of operating time, bearing in mind the extreme sensitivity of the time to rupture on both temperature and stress, and the fact that the rupture stress calculated by this semi-empirical relation at a particular time and temperature may have a spread of up to 4 tons/in² (6 kg/mm²) between different casts of steel. An examination of bi-axial creep rupture data indicates that the assumption that failure is governed by the maximum principal stress should lead to a pessimistic assessment. Furthermore, experimental evidence suggests that the periodic cycling experienced during operation should not invalidate the use of the relation.

Additional thermocouples attached to the surface of the outlet ducts of Calder reactors in a plane about 4 metres from the junction with the vessel indicated that temperatures at some points in this plane exceeded the bulk gas temperature measured by the originally installed thermocouples by about 10 °C, and that considerable azimuthal asymmetry in temperature existed, indicating that incomplete mixing of the gas was taking place. Experiments with individually-inserted control rods showed that the temperature distribution around a duct could be made more uniform and that the general level of duct metal temperatures could be reduced below the measured bulk gas outlet temperature. Although thermocouples adjacent to strain gauges near the outlet ducts on a Chapelcross reactor indicate a temperature some 8 °C lower than the bulk gas outlet temperature, similar measurements on the duct have not been made, and thus considerable uncertainty still exists about the temperature distribution in the high-stress region around the outlet duct. Until more direct measurements can be made, the duct metal thermocouples are used for control purposes, and absorber patterning is arranged to minimise temperature variations around each duct and between the four ducts on each reactor.

Some uncertainty also exists about the appropriate value of the time-dependent stress which should be used for calculation of a limiting temperature. An assessment can be made from a study of the original design calculations, strain-gauge data obtained during the pressurising of the vessel at the commissioning stage, strain gauge data obtained during operation on one of the Chapelcross reactors, and data from uni-axial creep relaxation tests. This leads to pessimistic figures of 14 tons/in² (22 kg/mm²) and 7 tons/in² (11 kg/mm²) for the circumferential and longitudinal stresses respectively, at the points of highest stress. The Haskey-Wood relation shows that a stress of 14 tons/in² (22 kg/mm²) should produce rupture in 200 000 hours at a temperature of 365 °C. Thus by operating at the present limit of 345 °C as measured on the outlet ducts an ample margin appears to be in hand for uncertainties in all the data. As the reactor power is controlled by this limit, efforts are being made to derive a more realistic value. A suggested form of criterion which can be applied is that the worst operating conditions should be such that the probability of stress rupture occurring before 200 000 hours does not exceed some specified low value. Application of this criterion demands a better knowledge of the appropriate stress, the uncertainties in the use of the

Haskey-Wood relation, and actual measurements of temperature at the critical points for control purposes.

CONCLUSION

The operating limits discussed earlier in this paper fall into three categories:

(*a*) Limits which are essential for immediate safety or economy (e.g., maximum fuel element temperatures based on compatibility considerations, minimum pressure vessel temperature);

(*b*) Limits based on reactor lifetime requirements (e.g., reactor inlet temperatures and graphite growth or stored energy, reactor outlet temperatures and pressure vessel stress rupture);

(*c*) Limits based on fault studies which minimise the consequences of a primary fault in some other component (e.g., fuel element temperature criterion, maximum graphite temperature).

Given adequate experimental and theoretical data it is usually not difficult to set limits to avoid failure of a primary component, since the problem can be defined unequivocally, and the margin between operating level and failure condition can be specified with reasonable precision. It is less easy to agree on a limit based on assessments of the safe working life of a component, usually with inadequate experimental data on which to predict future behaviour. The extent to which it is permissible to operate a reactor to gain increased power at the expense of a marginal decrease in working life over a 20- or 30-year period is a balance between short-term economic advantage and long-term power and policy requirements. The third category of operating limit is even harder to specify since the power is restricted on the results of a safety calculation based on a hypothetical fault, under conditions that are necessarily not amenable to experimental verification. The refinement of operating limits and the optimisation of power output is therefore a continuing commitment throughout the working life of the reactor.

REFERENCES

1. Hughes, H. A., and Horsley, R. M., J. British Nuclear Energy Soc., to be published.
2. Enderby, J. A., UKAEA TRG report 46 (R) (1961).
3. Horsley, R. M., Briggs, D. S., and Enderby, J. A., Nucl. Power, *7*, 55-60 (1962).
4. Wilson, B., and Dodds, R., J. British Nuclear Energy Soc., to be published.
5. Jenkinson, P., and Smith, D., Symposium on the Physics of Graphite-Moderated Reactors, The Institute of Physics and the Physical Society, Bournemouth (April 1962).
6. Dent, K. H., Long, E., and Prince, K., *In the design of gas-cooled, graphite-moderated reactors* (Poulter, D. R., ed.) Oxford University Press, London, pp. 319-348 (1963).
7. Bell, J. C., Bridge, H., Cottrell, A. H., Greenough, G. B., Reynolds, W. N., and Simmons, J. H. W., Phil. Trans. Roy. Soc. Series A., *254*, 361-395 (1963).
8. Cottrell, A. H., *et al.*, Proceedings of the Second International Conference on the Peaceful Uses of Atomic Energy, P/2485, Vol. 7, pp. 315-327, United Nations (1958).
9. Bridge, H., and Nairn, J. S., *In the design of gas-cooled graphite-moderated reactors* (Poulter, D. R., ed.), Oxford University Press, London, pp. 171-220 (1963).
10. Beattie, J. R., Lewis, J. B., and Lind, R., *Graphite oxidation and reactor safety*, P/185, Vol. 13, these Proceedings.
11. Brown, G., Noone, M. J., and Bishop, R. F., J. British Nuclear Energy Conf., *2*, 132-145 (1957).
12. Robertson, T. S., Iron Steel Inst. J., *175*, 361-374 (1953).
13. Hanstock, R. F., unpublished work.
14. Irvine, W. H., Quirk, A., and Bevitt, E., J. British Nuclear Energy Soc., *3*, 31-48 (1964).
15. Haskey, H. W., and Wood, D. S., UKAEA TRG report 555 (C) (1963).

ABSTRACT - RÉSUMÉ - АННОТАЦИЯ - RESUMEN

A/178 Royaume-Uni

Limites de température et rendement optimal en puissance dans les réacteurs de Calder et de Chapelcross

par H. A. Hughes *et al.*

Les conditions limites de fonctionnement qui sont spécifiées pour les différents organes de l'installation déterminent les performances d'un réacteur de puissance. Ces limites sont conçues pour assurer un fonctionnement sûr et satisfaisant dans les conditions normales et pour réduire au minimum les risques possibles dans le cas d'une défaillance. Les données accumulées durant l'exploitation du réacteur réduisent les incertitudes initiales touchant les paramètres fondamentaux et les conditions réelles de fonctionnement, et dont il faut tenir compte lorsqu'on fixe les limites initiales. On peut ainsi améliorer les performances du réacteur.

La température constitue l'un des plus importants paramètres limitatifs pour déterminer le comportement des éléments de combustible, du modérateur et de la cuve sous pression. Outre que rien ne devrait empêcher le comportement satisfaisant du combustible durant l'irradiation dans des conditions normales de fonctionnement, une limitation se trouve imposée par le critère qu'il devrait être raisonnablement possible d'éviter: l'incendie de canaux indépendants dans le cas de l'accident le plus grave possible, un incident de dépressurisation. On décrit les calculs et interprétations des données expérimentales qui permettent de lever l'incertitude de la prévision de la distribution complète de température à

l'état stationnaire, le calcul des élévations transitoires subies par chaque canal et l'application de ces calculs et autres données à la détermination des limites de fonctionnement.

Les limitations concernant l'étendue des dégâts d'irradiation dans le graphite, phénomène qui dépend également de la température, peuvent être définies à la fois du point de vue fonctionnement et du point de vue sécurité. Les principales propriétés discutées dans le mémoire sont les variations dimensionnelles, l'énergie emmagasinée et l'oxydation à l'air, les deux premières étant limitées par une température minimale du graphite et la troisième par une température maximale. Les dimensions sont contrôlées par les variations des espacements relatifs à l'effet Wigner, les mesures étant comparées avec les changements dimensionnels produits par irradiation de spécimens dans des réacteurs à flux élevé après correction de ces derniers résultats pour des différences de température et débit de dose. Une température limite est imposée par le critère qu'aucune difficulté d'exploitation ne devrait se produire au cours de la durée utile du réacteur. Les limites touchant l'énergie emmagasinée sont dictées par le critère que l'inflammation d'un seul canal ne devrait pas s'étendre aux autres canaux. L'oxydation du graphite introduit une source supplémentaire de chaleur lors d'une rupture du circuit primaire lorsque de l'air est aspiré dans le réacteur, et on détermine une température maximale qui tient compte des mesures correctives que l'on pourrait raisonnablement prendre si un tel accident se produit.

Les limites de température concernant la cuve sous pression sont fixées par la nécessité d'éviter deux phénomènes principaux. Le premier, qui gouverne la température minimale, est la rupture par fragilité, et on l'étudie par mesures sur spécimens hors pile et en pile. Le second phénomène est la rupture sous contrainte, qui fixe la limite de température supérieure de telle façon que le temps de résistance à la rupture aux contraintes existant dans les cuves, en tenant compte de la détente due au fluage, dépasse la vie utile requise. On décrit les résultats des analyses de données de rupture sous contrainte dans des spécimens et l'application de ces résultats aux conditions particulières.

A/178 Соединенное Королевство

Температурные ограничения и оптимизация выходной мощности реакторов в Колдер-Холле и Чэпел-Кроссе

Х. А. Хьюз *et al.*

Эксплуатационные ограничения, специфичные для каждой установки, определяют характеристики энергетического реактора. Эти ограничения устанавливаются в процессе проектирования с целью обеспечения безопасности и удовлетворительной работы при нормальных условиях эксплуатации, а также снижения возможных опасных последствий в случае аварии. Накопление данных в процессе эксплуатации реактора позволяет уточнить первоначально принятые значения основных параметров и определить реальные условия эксплуатации, которые требуют введения определенных допусков при установлении первоначальных ограничений. Таким образом можно усовершенствовать характеристики реактора.

Температура является одним из наиболее важных лимитирующих параметров в определении характеристики тепловыделяющих элементов, замедлителя и корпуса давления. В дополнение к требованию удовлетворительного поведения тепловыделяющих элементов в процессе облучения при нормальных условиях эксплуатации налагается ограничение, обеспечивающее разумную вероятность избежания расплавления отдельных каналов в случае самой тяжелой из возможных аварий — потери давления. Описываются расчеты и оценки экспериментальных данных, позволяющих определить неточность в предсказании полного распределения температуры при установившемся режиме, расчеты скоростей переходных процессов для каждого канала и применимость этих расчетов и других данных для определения эксплуатационных ограничений.

Ограничения, обусловленные радиационным повреждением графита, которые также зависят от температуры, могут быть определены как из рассмотрения опыта эксплуатации, так и из условий безопасности. Основными результатами радиационного повреждения графита, обсуждаемыми в докладе, являются рост размеров, накопление энергии и окисление в атмосфере воздуха. Первые два фактора ограничиваются минимальной температурой графита, а третий — максимальной температурой. Рост размеров контролируется изменением вигнеровского зазора. Результаты измерений сопоставляются с изменениями геометрических размеров образцов, облученных в реакторах с высоким потоком нейтронов. При этом для результатов, полученных при измерении образцов, вводится поправка, учитывающая разницу в температурах и мощности дозы облучения. Температурные ограничения определяют ряд критериев, обеспечивающих нормальную эксплуатацию реактора в течение всего срока службы. Ограничения, обусловленные накоплением энергии, требуют обеспечения условий, при которых сгорание одного канала не влечет за собой разрушение других каналов. Окисление графита создает дополнительный источник тепла, усугубляющий аварию со снижением давления при попадании воздуха в реактор, и устанавливается максимальная температура, которую нужно учитывать при разработке правил

эксплуатации, которые, как предполагают, могут быть выполнены в случае такой аварии.

Температурные ограничения, характерные для корпуса давления, обусловливаются необходимостью избежать двух основных явлений. Первым фактором, определяющим минимальную температуру корпуса, является образование трещин из-за охрупчивания, которое изучается в ходе внереакторных и внутриреакторных измерений образцов. Вторым фактором является разрушающее напряжение, которое устанавливает верхний температурный предел, так что время разрушения при уровнях напряжений, существующих в корпусе (с учетом необходимого допуска на релаксацию из-за ползучести) будет превышать требуемый срок службы. Описываются результаты анализа данных по разрушающему напряжению образцов и использованию их применительно к определенным эксплуатационным условиям.

A/178 Reino Unido

Los límites de temperatura y la optimización de la potencia producida en los reactores de Calder y de Chapelcross

por H. A. Hughes *et al.*

Los límites de funcionamiento que se especifican para los diversos componentes de la instalación determinan el comportamiento de un reactor de potencia. Se fijan estos límites para garantizar el funcionamiento seguro y satisfactorio durante las condiciones normales de explotación y para que los riesgos posibles que resulten de una avería sean mínimos. La acumulación de los datos que se obtienen durante el funcionamiento del reactor reduce las incertidumbres iniciales de los parámetros fundamentales y de las condiciones reales de funcionamiento, incertidumbres que deben tenerse en cuenta al establecer los límites originales. De esta manera puede mejorarse el comportamiento del reactor.

La temperatura es uno de los parámetros limitativos más importantes en la determinación del comportamiento de los elementos combustibles, del moderador y de la vasija de presión. Además del requisito de que no debe sufrir cambio la conducta satisfactoria del combustible durante la irradiación en condiciones normales de funcionamiento, se impone una limitación más con el criterio de que debe existir una probabilidad razonable de evitar la combustión de canales aislados en el caso de la avería máxima verosímil, un accidente de pérdida de presión. Se describen los cálculos y la estimación de los datos experimentales que permiten determinar la incertidumbre en la predicción de la distribución estacionaria de la temperatura, el cálculo de los estados transitorios de cada canal y la aplicación de estos cálculos y de otros datos a la determinación de los límites de funcionamiento.

Se pueden definir, a partir de consideraciones de seguridad y de funcionamiento, limitaciones en la magnitud del deterioro producido por la irradiación al grafito, fenómeno dependiente también de la temperatura. Las propiedades más importantes que se discuten en la memoria son la hinchazón, la energía almacenada y la oxidación por el aire, las primeras limitadas por una temperatura mínima del grafito y la tercera por una temperatura máxima. La hinchazón se vigila midiendo las variaciones en la magnitud de los intersticios de Wigner, y relacionando las medidas con los cambios dimensionales producidos en muestras irradiadas en reactores de flujo elevado, después de corregir los resultados para tener en cuenta las diferencias de temperatura y de la dosis de irradiación. Se fija entonces la temperatura límite utilizando el criterio de que no se presentarán dificultades de funcionamiento durante la vida del reactor. Los límites en la energía almacenada se fijan mediante el criterio de que un incendio en un canal no debe propagarse a los otros. La oxidación del grafito introduce una fuente adicional de calor en el accidente de pérdida de presión al entrar aire en el reactor; se fija una temperatura máxima que tiene en cuenta las medidas que razonablemente se supone se tomarían en el caso de que ocurriese el accidente.

Los límites de temperatura de la vasija de presión se fijan al tener que impedir la presencia de dos fenómenos principales. El primero, que gobierna la temperatura mínima, es la fractura frágil y se estudia midiendo los efectos en probetas irradiadas o no irradiadas. El segundo fenómeno es la ruptura por tensiones, que fija el límite superior de la temperatura de modo que el tiempo hasta la ruptura a las tensiones de trabajo de la vasija, teniendo en cuenta la relajación por fluencia, sea superior a la vida deseada. Se describen los resultados del análisis de los datos de la tensión de ruptura obtenidos de las muestras, y de la aplicación de aquéllos a casos concretos.

О динамической устойчивости ядерных энергетических установок

П. А. Гаврилов, Л. Н. Подлазов

Ядерные энергетические установки, предназначенные для работы в труднодоступных районах страны, должны обладать не только высокой надежностью, но и определенными динамическими характеристиками.

Энергетическая установка небольшой мощности, работающая вне энергетической системы на небольшое число потребителей, может испытывать значительные колебания внешней нагрузки. Практически она должна быть стабильной и выдерживать сброс и введение полной внешней нагрузки. При этом из соображений экономичности питание приводов насосов, системы управления и прочего электрооборудования установки целесообразно осуществлять от того же турбогенератора, что и внешних потребителей. Кроме того, система управления установкой должна быть очень простой, не требующей для обслуживания специалистов высокой квалификации.

Поэтому представляется необходимым для регулирования мощности в максимальной степени использовать свойства саморегулируемости самих энергетических систем.

Целью настоящей работы было изучение особенностей и характера протекания нестационарных процессов в ядерных энергетических установках, в которых парогенератор имеет свободный уровень кипящей воды. Как показали исследования, установки этого класса по своим динамическим свойствам неплохо отвечают требованиям «малой энергетики».

Обычно парогенераторы со свободным уровнем кипящей воды имеют относительно большие водяные емкости по вторичному контуру. Переходные процессы в энергетических установках с таким парогенератором, связанные с изменениями параметров вторичного контура (отбор пара, расход питательной воды и ее температура), протекают с большой инерционностью, медленно по сравнению с переходными процессами в реакторе. Поэтому последние можно рассматривать как квазистатические, и при исследовании динамической устойчивости системы в целом реактор можно учитывать лишь в квазистационарном асимптотическом приближении. Это означает, что в передаточной функции реактора не учитывается влияние членов высоких порядков. При этом может оказаться, что вся система в целом апериодически устойчива даже при колебательной устойчивости реактора. Поскольку высокие частоты колебаний, которые могут по разным причинам возникать в реакторе, фильтруются в парогенераторе и прочих достаточно больших емкостях первичного контура и не проходят на вход реактора, система оказывается как бы «разомкнутой» по высоким частотам. Вопрос об устойчивости замкнутой системы можно свести к исследованию динамической устойчивости реактора на этих частотах и замкнутой системы, в которой реактор представлен в квазистационарном приближении.

При написании системы уравнений динамики нами был принят ряд упрощающих предположений, законность которых достаточно очевидна. Основными из них являются следующие:

а) принималось, что расход теплоносителя по первичному контуру остается постоянным;

б) принималось, что отбор пара на турбину прямо пропорционален нагрузке;

в) считалось, что подача питательной воды зависит от изменения расхода пара на турбину и осуществляется через инерционное звено первого порядка;

г) в уравнениях кинетики рассматривалась одна группа запаздывающих нейтронов;

д) недогрев питательной воды до температуры насыщения учитывался в общем энергетическом балансе тепла в парогенераторе;

е) конечной скоростью подъема пара в испарительной зоне пренебрегалось, то есть изменение уровня кипящей воды из-за изменения объемного паросодержания не учитывалось;

ж) зависимость температуры насыщения от давления принималась линейной;

з) коэффициенты теплопередачи принимались постоянными; для реактора это является следствием предположения о постоянстве расхода теплоносителя; для парогенератора это справедливо, если коэффициент теплопередачи слабо зависит от теплового потока;

и) предполагалось, что изменения реактивности будут малыми и допустима линеаризация уравнений кинетики;

к) транспортные запаздывания в трубопроводах аппроксимировались апериодическим звеном первого порядка.

Решение системы уравнений динамики реактора в этих достаточно общих предположениях можно выразить в виде передаточной функции $\alpha(S)$, которая характеризует изменения температуры теплоносителя на выходе из реактора при возмущениях температуры на входе в него. Условно назовем эту функцию «передаточной функцией реактора», хотя под последней обычно понимают функцию, характеризующую зависимость изменения мощности от изменения реактивности:

$$\alpha(S) = -\frac{\widetilde{\vartheta}_{\text{вых}}}{\vartheta_{\text{вх}}} = -\frac{F_1(S)}{F_0(S)}, \qquad (1)$$

где

$$F_0(S) = S(S+T_м^p)(S+T_{\parallel}^p+0{,}5T_{\perp}^p) - \\ -0{,}5ST_м^pT_{\perp}^p - \alpha_e^* A_0 T_{\perp}(S+T_0); \qquad (2)$$

$$F_1(S) = S(S+T_м^p)(T_{\parallel}^p-0{,}5T_{\perp}^p) + \\ +0{,}5ST_м^pT_{\perp}^p + \alpha_i^* A_0 T_{\perp}(S+T_0).$$

Функции $\alpha_e^*(S)$ и $\alpha_i^*(S)$ соответственно равны

$$\alpha_e^*(S) = \alpha_e + \beta_0 S;$$

$$\alpha_e = 0{,}5\alpha_т\bar{\theta}_0\left\{1+\left(2\frac{T_{\parallel}^p}{T_{\perp}^p}+1\right)\frac{\beta_т}{\alpha_т}\right\}; \qquad (3)$$

$$\beta_0 = \beta_т\frac{\bar{\theta}_0}{T_{\perp}^p};$$

$$\alpha_i^*(S) = \alpha_i = 0{,}5\alpha_т\bar{\theta}_0\left\{1+\left(1-2\frac{T_{\parallel}^p}{T_{\perp}^p}\right)\frac{\beta_т}{\alpha_т}\right\}.$$

Изменение реактивности $\widetilde{\varrho}_т$ можно представить в виде функции температуры теплоносителя на входе и выходе из реактора

$$\widetilde{\varrho}_т = \alpha_i^*(S)\widetilde{\vartheta}_{\text{вх}} + \alpha_e^*(S)\widetilde{\vartheta}_{\text{вых}}. \qquad (4)$$

Из соотношений (1) и (2) видно, что реактор как динамическая система имеет характеристическое уравнение третьего порядка. Однако в большинстве случаев функция $\alpha(S)$ может быть упрощена за счет пренебрежения членами порядка S^3 и S^2, так как коэффициент теплоотдачи и теплопроводность тепловыделяющих элементов, а следовательно, и динамические постоянные реактора обычно оказываются достаточно большими. Кроме того, в замкнутой реакторной системе высокочастотные составляющие в функции изменения температуры теплоносителя на входе пренебрежимо малы.

Если принять, что уровень кипящей воды в парогенераторе при всех переходных процессах поддерживается примерно постоянным за счет регулируемой подачи питательной воды и остается выше уровня змеевиков, то из решения уравнений теплопередачи в парогенераторе легко получить соотношение между $\vartheta_{\text{вх}}$ и $\widetilde{\vartheta}_{\text{вых}}$

$$\widetilde{\vartheta}_{\text{вх}} = f(S)\left\{A_1\widetilde{\vartheta}_{\text{вых}} + (S+T_1)\frac{\psi A_2}{T_1}\widetilde{P}, \qquad (5)\right.$$

где

$$f(S) = \frac{T^{\text{пг}}T_1T_2}{(S+T^{\text{пг}})(S+T_1)(S+T_2)}. \qquad (6)$$

Функция $f(S)$ может рассматриваться как передаточная функция последовательно соединенных апериодических звеньев. По физическому смыслу динамические коэффициенты $T^{\text{пг}}$, T_1, T_2 всегда положительны. Поэтому сам парогенератор как динамическая система является абсолютно устойчивой системой по возмущениям выходной температуры и давлению во вторичном контуре.

Введя эффективное время запаздывания $\tau^{\text{эфф}} = \tau_1 + \tau_2 + \tau^{\text{пг}}$, функцию $f(S)$ можно представить звеном первого порядка

$$f(S) = \frac{T^{\text{эфф}}}{(S+T^{\text{эфф}})}, \qquad (7)$$

где

$$T^{\text{эфф}} = \frac{\tau_0}{\tau^{\text{эфф}}}.$$

При наличии системы регулирования систему уравнений динамики необходимо дополнить уравнениями автоматического регулятора мощности, которые с учетом возможной коррекции по технологическим параметрам (давлению, температуре и т. д.) можно записать в виде

$$S\widetilde{\varrho}_{\text{ст}} = \varkappa_1(\widetilde{n}-\widetilde{n}_з); \qquad (9)$$

$$S\widetilde{n}_з = \varkappa_2\widetilde{n}_з + \varkappa_3\widetilde{P} + 2(\varkappa_4+\varkappa_5 S)\widetilde{\vartheta}_4.$$

В этом случае изменение реактивности системы при возмущениях по давлению (внешней нагрузке) при введении коррозии на задатчик мощности по давлению пара может быть «разложено» на две составляющие: «температурную» $\widetilde{\varrho}_т$, обусловленную изменениями температуры теплоносителя, и «составляющую по давлению» $\widetilde{\varrho}_P$. Кроме того, можно ввести третью составляющую $\widetilde{\varrho}_{\text{ск}}$, характеризующую нерегулируемое случайное возмущение по реактивности.

Таким образом,

$$\widetilde{\varrho}(S) = \widetilde{\varrho}_m^{\text{эфф}}(S) + \widetilde{\varrho}_P(S) + \widetilde{\varrho}_{\text{ск}}(S), \qquad (10)$$

где

$$\widetilde{\varrho}_m^{\text{эфф}}(S) = \alpha_i^{\text{эфф}}(S)\widetilde{\vartheta}_{\text{вх}} + \alpha_e^{\text{эфф}}(S)\widetilde{\vartheta}_{\text{вых}}; \qquad (11)$$

$$\widetilde{\varrho}_P(S) = \varkappa_P^{\text{эфф}}(S)\widetilde{P}.$$

При этом эффективные «температурные» коэффициенты реактивности ($\alpha_i^{\text{эфф}}(S)$, $\alpha_e^{\text{эфф}}(S)$) и эффективный коэффициент реактивности «по давлению» могут быть выражены через технологические параметры реактора и параметры регулятора мощности следующим образом:

$$\alpha_i^{эфф}(S)=\frac{\alpha_i^*(S-\varkappa_2)S-\varkappa_1(\varkappa_4+\varkappa_5 S)}{(S-\varkappa_2)(S^2-\varkappa_1 S-\varkappa_1 T_0)}S;$$

$$\alpha_e^{эфф}(S)=\frac{\alpha_e^*(S)(S-\varkappa_2)S-\varkappa_1(\varkappa_4+\varkappa_5 S)}{(S-\varkappa_2)(S^2-\varkappa_1 S-\varkappa_1 T_0)}S; \quad (12)$$

$$\varkappa_P^{эфф}(S)=\frac{\varkappa_1\varkappa_3}{(S-\varkappa_2)(S^2-\varkappa_1 S-\varkappa_1 T_0)}S.$$

Соответственно в силу линейности системы уравнений динамики изменение других технологических параметров (например, $\widetilde{\vartheta}_{вых}$, $\widetilde{n}$) также можно формально «разложить» на составляющие по «температуре», «давлению» и «скачку реактивности». Например,

$$\widetilde{\vartheta}_{вых}=\frac{F_1(S)}{F_0(S)}\widetilde{\vartheta}_{вх}+\frac{F_P(S)}{F_0(S)}\widetilde{P}+\frac{F_{ск}(S)}{F_0(S)}\widetilde{\varrho}_{ск}, \quad (13)$$

где $F_0(S)$ и $F_1(S)$ по форме совпадают с функциями (2), в которые вместо α_e^* и α_i^* входят соотношения (12), а $F_P(S)$ и $F_{ск}(S)$ соответственно равны

$$F_P(S)=\frac{\varkappa_P^{эфф}(S)}{S}(S+T_0)A_0T_\perp^p=$$

$$=-\frac{\varkappa_1\varkappa_3 A_0T_\perp^p(S+T_0)}{(S-\varkappa_2)(S^2-\varkappa_1 S-\varkappa_1 T_0)}; \quad (14)$$

$$F_{ск}(S)=\frac{\varkappa_{ск}^{эфф}(S)}{S}(S+T_0)A_0T_\perp^p=$$

$$=\frac{A_0T_\perp^p S(S+T_0)}{(S-\varkappa_2)(S^2-\varkappa_1 S-\varkappa_1 T_0)}.$$

Заметим, что для обеспечения наилучшего качества переходных процессов системы автоматического регулирования мощности проектируются таким образом, что постоянные времени изменения уставки мощности реактора и коррекций оказываются много большими постоянной времени регулятора нейтронной мощности, то есть

$$|\varkappa_1|\gg|\varkappa_2,\ \varkappa_3,\ \varkappa_4,\ \varkappa_5|.$$

Это означает, что скорость изменения нейтронной мощности значительно больше скорости изменения уставки мощности, мощность успевает отслеживать изменения уставки задатчика мощности, то есть в каждый момент времени. Кроме того, скорость перемещения стержней АР при автономной настройке регулятора обычно выбирается такой, чтобы АР мог преодолеть «сопротивление» отрицательного температурного эффекта реактивности и обеспечить хорошее качество переходного процесса по мощности реактора. Это означает, что первое слагаемое в числителе выражений для $\alpha_i^{эфф}(S)$ и $\alpha_e^{эфф}(S)$ в формуле (12) должно быть много меньшим при всех характерных для реактора частотах. Поэтому, пренебрегая влиянием температурного эффекта при работающем автоматическом регуляторе мощности и считая, что АР отстроен настолько хорошо, что не вносит в замкнутую реакторную динамическую систему систематических возмущений низких частот, можно вместо соотношений (12) написать соотношения

$$\alpha_i^{эфф}(S)=\alpha_e^{эфф}(S)\simeq S\frac{\varkappa_4+\varkappa_5 S}{(S-\varkappa_2)(S+T_0)};$$

$$\varkappa_P^{эфф}(S)\simeq S\frac{\varkappa_3}{(S-\varkappa_2)(S+T_0)}; \quad (15)$$

$$\varkappa_{ск}^{эфф}(S)\simeq S\frac{S}{\varkappa_1(S+T_0)}.$$

При наличии системы автоматического регулирования мощности с учетом соотношений (15) функции $F_0(S)$ и $F_1(S)$ принимают вид

$$F_0(S)=(S-\varkappa_2)[(S+T_м^p)(S+T_\parallel^p+$$

$$+0{,}5T_\perp^p)-0{,}5T_м^pT_\perp^p]-A_0T_\perp^p(\varkappa_4+\varkappa_5 S); \quad (16)$$

$$F_1(S)=(S-\varkappa_2)[(S+T_м^p)(T_\parallel^p-0{,}5T_\perp^p)+$$

$$+0{,}5T_м^pT_\perp^p]+A_0T_\perp^p(\varkappa_4+\varkappa_5 S). \quad (17)$$

Здесь множитель $(S-\varkappa_2)$ в знаменателе опущен как несущественный.

В качестве примера приведем некоторые результаты исследования динамических свойств установки АРБУС. Так как характерные времени протекания процессов в установке АРБУС составляют несколько десятков секунд, а характерные времени теплопередачи и переноса тепла $\tau_\parallel^p$, $\tau_\perp^p$, $\tau_м^p$ составляют секунды, то тепловые процессы в реакторе можно рассматривать в квазистационарном приближении. Это позволяет записать функции $F_0(S)$ и $F_1(S)$ из соотношений (2) в виде

$$F_0(S)\simeq K_e(S+T_e);$$

$$F_1(S)\simeq K_i(S+T_i). \quad (18)$$

Выражения для K_e, K_i, T_i, T_e приведены в таблице.

Характеристическое уравнение системы в этом случае запишется следующим образом:

$$S^3+\chi S^2+\zeta S+B_0=0, \quad (19)$$

где

$$\chi=\frac{1}{1-f}\left\{\left[D\left(2-\frac{T^{эфф}(T_1+T_2)}{T_1T_2}(1-A_1)\right)+\right.\right.$$

$$+T_e\left(1-\frac{DT^{эфф}}{T_1T_2}(1-A_1)\right)+$$

$$\left.\left.+T^{эфф}\left(1-A_1\frac{K_i}{K_e}\right)\right]+\left[\varkappa_3'\frac{D}{T_1}\frac{A_0T_\perp^p}{K_e}\right]\right\}; \quad (20)$$

$$\zeta=\frac{1}{1-f}\left\{\left[T_eT^{эфф}\left(1-A_1\frac{K_iT_i}{K_eT_e}\right)+\right.\right.$$

$$+DT^{эфф}(1+A_1)\left(1-\frac{K_i}{K_e}\right)+$$

$$\left.\left.+DT_e\left(2-\frac{T^{эфф}(T_1+T_2)}{T_1T_2}(1+A_1)\right)\right]+\right.$$

$$\left.+\left[-\varkappa_3'D\frac{A_0T_\perp^p}{K_e}\left(1+\frac{T^{эфф}}{T_2}-\frac{T^{эфф}}{T_1}\right)\right]\right\}; \quad (21)$$

$$B_0=DT^{эфф}T_e(1+A_1)\left(1-\frac{K_iT_i}{K_eT_e}\right)-$$

$$-\varkappa_3'DT^{эфф}\frac{A_0T_\perp^p}{K_e}. \quad (22)$$

Эффективные динамические параметры реактора

При наличии системы автоматического регулирования	Саморегулирование
$K_i = T^p_{\text{м}} T^p_{\parallel} \left\{ 1 - \varkappa_2 \frac{T^p_{\parallel} - 0{,}5 T^p_{\perp}}{T^p_{\text{м}} T^p_{\parallel}} - \varkappa_5 \alpha_p \right\}$	$K_i = T^p_{\text{м}} T^p_{\parallel} \{1 + \alpha_i \alpha_p\}$
$K_e = T^p_{\text{м}} T^p_{\parallel} \left\{ 1 - \varkappa_2 \frac{T^p_{\text{м}} + 0{,}5 T^p_{\perp} + T^p_{\parallel}}{T^p_{\text{м}} T^p_{\parallel}} - \varkappa_5 \alpha_p \right\}$	$K_e = T^p_{\text{м}} T^p_{\parallel} \{1 - (\alpha_e + \beta_0 T_0) \alpha_p\}$
$T_i = - \frac{\varkappa_2 + \varkappa_4 \alpha_p}{1 - \varkappa_2 \frac{T^p_{\parallel} - 0{,}5 T^p_{\perp}}{T^p_{\text{м}} T^p_{\parallel}} - \varkappa_5 \alpha_p}$	$T_i = \frac{\alpha_i \alpha_p T_0}{1 + \alpha_i \alpha_p}$
$T_e = \frac{\varkappa_2 + \varkappa_4 \alpha_p}{1 - \varkappa_2 \frac{T^p_{\text{м}} + T^p_{\parallel} + 0{,}5 T^p_{\perp}}{T^p_{\text{м}} T^p_{\parallel}} - \varkappa_5 \alpha_p}$	$T_e = - \frac{\alpha_e \alpha_p T_0}{1 - \alpha_e \alpha_p}$

Коэффициент подобия τ_0 определяется из условия обращения в единицу B_0 в уравнении (22).

Применительно к установке АРБУС коэффициенты уравнения (19) и τ_0 равны

$$\tau_0 \simeq 81;$$
$$\zeta \simeq 3{,}2;$$
$$\chi \simeq 2{,}6.$$

Для исследования корней характеристического уравнения (19) можно воспользоваться диаграммами Вышнеградского (рис. 1), представленными в работе [2]. На рис. 1 приведены следующие обозначения:

τ_S, τ_{S_i} — период удвоения экспоненциальной составляющей переходного процесса; β — безразмерная частота колебаний периодической составляющей переходного процесса; ϱ — характеристика затухания амплитуды колебаний периодической составляющей переходного процесса.

Положение определяющей точки с координатами (χ, ζ), соответствующими динамическим параметрам системы на диаграмме Вышнеградского, позволяет судить о характере переходных процессов в ней. Из рис. 1 видно, что установка АРБУС как динамическая система является устойчивой, слабо колебательной системой. Период удвоения апериодической составляющей переходного процесса

$$t_0 = \frac{\tau_0 \tau_S}{0{,}693} \simeq 140 \text{ сек},$$

период колебаний

$$T = \frac{2\pi\tau_0}{\beta} \simeq 500 \text{ сек},$$

степень затухания периодической составляющей

$$d = \frac{\beta \ln \varrho}{2\pi} \simeq |-3|.$$

Кривые изменения во времени мощности и давления пара при скачкообразном возмущении по внешней нагрузке на 45% от номинальной, полученные независимо на моделирующей машине для полной исходной нелинейной системы и без упрощающих предложений относительно реактора, приведены на рис. 2. Из приведенных оценок и кривых видно, что протекание переходных процессов в установке АРБУС носит почти апериодический характер, так что колебательной составляющей практически можно пренебречь. Это означает, что переходный процесс можно практически аппроксимировать передаточной функцией, эквивалентной апериодическому звену типа $S = \frac{0{,}693^{-1}}{\tau_S}$, где τ_S зависит от параметров установки через коэффициенты χ и ζ.

Было проведено сравнение результатов исследования характера переходных процессов на аналоговой машине с использованием полной нелинейной системы уравнений и уравнений, полученных по диаграммам Вышнеградского [1,2] при использовании характеристического уравнения третьего порядка (19). Сравнение показало, что это характеристическое уравнение дает достаточно хорошие по точности результаты и может быть использовано для исследования влияния различных динамических факторов на устойчивость.

Заметим, что динамические коэффициенты D, $T^{\text{эфф}}$, A и K_i/K_e, T_i, T_e, входящие в коэффициенты характеристического уравнения (26), зависят соответственно: D — от конструктивных и теплофизических параметров вторичного контура; A_1, $T^{\text{эфф}}$ характеризуют теплопередачу в парогенераторе и транспортный перенос тепла по трубопроводам и парогенераторам в первичном контуре; K_i/K_e, T_i, T_e выражаются через конструктивные физические и теплофизические параметры реактора.

Это обстоятельство дает возможность исследовать отдельно влияние параметров реактора, парогенератора и емкостей теплоносителя в первичном и во вторичном контурах на положение определяющей точки на диаграмме Вышнеградского и соответственно на изменение динамических характеристик установки варьированием всего нескольких обобщенных параметров.

На рис. 3 показано влияние $T^{эфф}$ $\alpha_т$ и D на положение определяющей точки в пространстве параметров χ и ζ. Заметим, что увеличение $T^{эфф}$ физически эквивалентно уменьшению времени транспортного запаздывания в трубопроводах и парогенераторе по первичному контуру и улучшению условий теплопередачи в нем. Из приведенных на рис. 3 кривых видно, что при увеличении примерно до 0,15 (то есть в 10 раз) при прочих равных условиях определяющая точка переходит в область апериодической устойчивости.

Влияние динамических параметров реактора на устойчивость замкнутой энергетической системы, работающей в режиме саморегулируемости, можно оценить, выразив коэффициенты K_i/K_e, T_i, T_e через величину температурного коэффициента реактивности ($\alpha_т$).

На рис. 3 приведена кривая изменения положения определяющей точки в фазовом пространстве в зависимости от величины $\alpha_т$ при постоянном $\beta_т$ и постоянном комплексе $\alpha_p T_0$, определяемом характеристиками реактора. Из кривой видно, что при увеличении отрицательного коэффициента реактивности определяющая точка перемещается в область апериодической устойчивости.

При уменьшении $|\alpha_т|$ кривая огибает область апериодической устойчивости, оставаясь в области колебательной устойчивости. При положительном коэффициенте реактивности $\alpha_т > 0$, по величине близкой к значению отрицательного коэффициента реактивности по горючему $|\beta_т|$, динамическая замкнутая система скачком переходит в область абсолютной неустойчивости. На рис. 3 приведена зависимость положения определяющей точки от параметров вторичного контура, выраженных в обобщенном динамическом коэффициенте. Из рассмо-

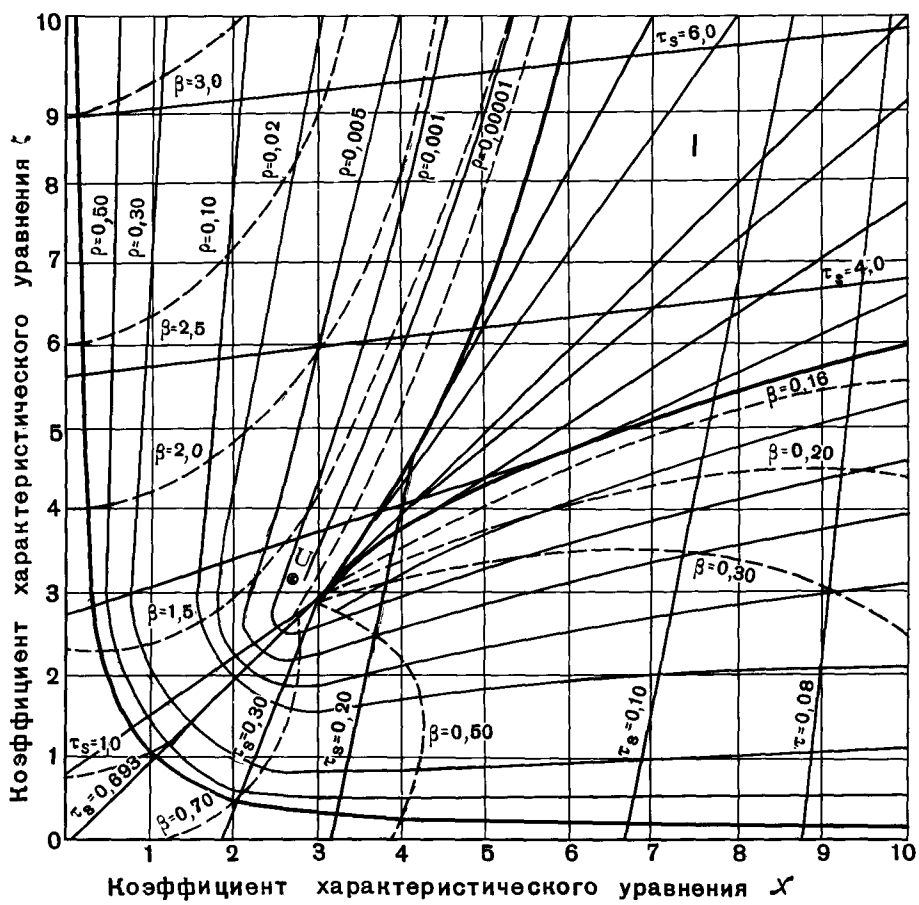


Рис. 1. Диаграмма параметров переходного процесса в динамических системах третьего порядка. (Точка U соответствует параметрам установки АРБУС):

I — область апериодической устойчивости; *II* — область колебательной устойчивости

трения кривых рис. 3 можно заключить, что изменение параметров ядерной энергетической установки типа АРБУС в весьма широких пределах не переводит ее в область динамической неустойчивости, если температурные коэффициенты реактивности остаются отрицательными.



Рис. 2. Изменение мощности реактора и давления пара при сбросе и последующем увеличении нагрузки:

1—относительная мощность реактора; *2*—давление пара

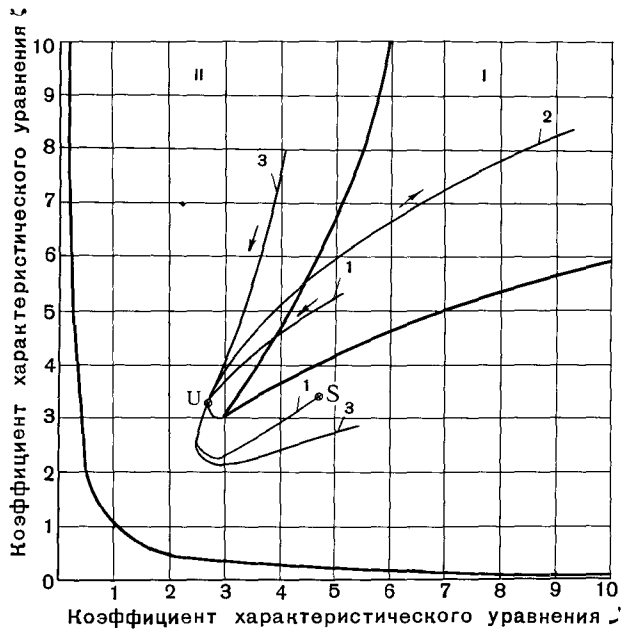


Рис. 3. Траектории определяющей точки в зависимости от изменения параметров установки АРБУС, работающей в режиме саморегулирования (направление стрелок на кривых соответствует возрастанию параметров):

1—α_T от $-\infty$ до $+0{,}001$; *2*—$T^{эфф}$ от $0{,}5\cdot10^{-2}$ до 0,5; *3*—D от $0{,}5\cdot10^{-3}$ до 0,10

Поскольку определяющая точка при этих изменениях перемещается вблизи области апериодической устойчивости, огибая ее, характер переходных процессов в безразмерном времени мало меняется (то есть переходные процессы носят почти апериодический характер с большим декрементом затухания).

При большом отрицательном температурном коэффициенте и при малых транспортных запаздываниях по первичному контуру реакторная система типа АРБУС имеет тенденцию к переходу в область апериодической устойчивости.

Из соотношений (20—22) и таблицы, а также кривых рис. 3 можно оценить влияние некоторых параметров системы регулирования. Так, коэффициенты $\varkappa_4$, $\varkappa_5$ по своему смыслу весьма похожи на «температурные» коэффициенты реактивности α_i и α_e. Поэтому при их возрастании определяющая точка будет стремиться к границе апериодической устойчивости так же, как и при росте $|\alpha_T|$. Коэффициент $\varkappa_2$ похож по смыслу на β_0.

При выборе оптимальных динамических параметров существенным является не только характер переходного процесса, но и величина асимптотического отклонения технологических параметров установки (в частности, наименьшее отклонение давления пара от номинального при любых возмущениях по нагрузке).

Расчеты показали, что асимптотическая величина давления ($S \to 0$) при работе установки в режиме саморегулирования тем меньше, чем лучше условия теплопередачи в парогенераторе.

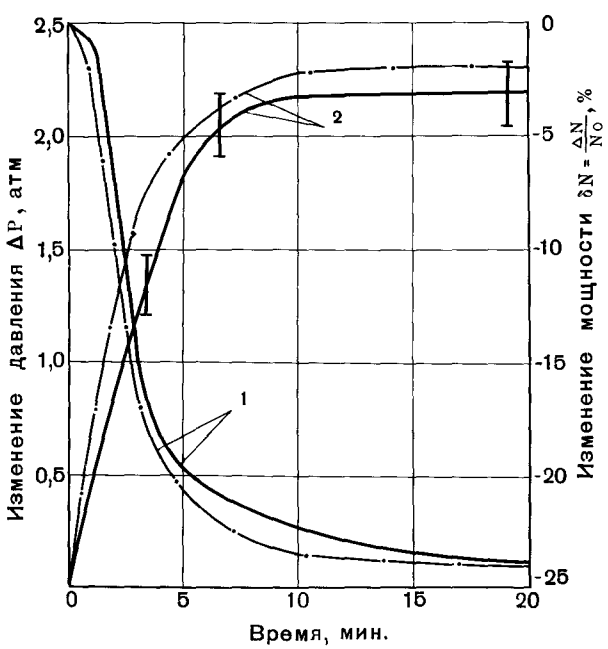


Рис. 4. Изменение мощности и давления при сбросе нагрузки:

—·—·—расчетная кривая; ——— —экспериментальная кривая; *1*—мощность, %; *2*—давление, *атм*

(KF), и зависит от исходного уровня давления

$$\Delta P_\infty = -\frac{(A_3+A_5)\left(1+\frac{\alpha_i}{\alpha_e}A_1\right)}{D(1+A_1)\left(1+\frac{\alpha_i}{\alpha_e}\right)}\Delta W_т \simeq$$

$$\simeq -\frac{\Gamma+\Delta_i'}{\left(\frac{\vartheta T_3}{\vartheta Q}\right)_{\rho_0}\cdot KF}\Delta W_т. \qquad (23)$$

Для установки АРБУС при работе в режиме саморегулирования относительное отклонение давления при сбросе всей внешней нагрузки, составляющей около 60% от полной мощности, равно примерно 25% от P_0 (то есть около 6 *атм*).

Учитывая близкий к апериодическому характер переходных процессов и величину отклонения давления от номинального, можно утверждать, что установка АРБУС может устойчиво работать в режиме саморегулирования (без АР), по крайней мере в условиях, когда изменения внешней нагрузки не превышают 30% от полной мощности.

Отклонение давления от номинального (ΔP_∞) при данном типе парогенератора можно снизить путем введения коррекции по давлению в автоматический регулятор мощности ($\varkappa_3 \neq 0$) и подбором соответствующих параметров $\varkappa_2$ и $\varkappa_3$, $\varkappa_4$. Тогда

$$\Delta P_\infty = -\frac{(A_3+A_5)\left[(1-A_1)-(1+A_1)\alpha_p\frac{\varkappa_4}{\varkappa_2}\right]}{D(1+A_1)\alpha_p\left(\frac{\varkappa_4}{\varkappa_2}+\frac{1}{\psi}\frac{\varkappa_3}{\varkappa_2}\right)}\Delta W_т.$$

В установке АРБУС введение коррекции по давлению позволяет снизить величину относительного изменения давления при сбросе 60% от полной мощности примерно до 12% P_0 (то есть до $\Delta P_\infty \simeq 3$ *атм*).

Однако при больших отношениях $\varkappa_3/\varkappa_2$ несколько ухудшается качество переходных процессов, увеличивается их колебательность. В самом деле, при увеличении $|\varkappa_3|$ уменьшается χ и увеличивается ζ, что эквивалентно увеличению частоты колебаний и уменьшению степени затухания колебаний.

Результаты теоретических исследований динамических свойств по изложенной здесь методике были подтверждены в ходе предварительных экспериментальных исследований при пусконаладочных работах на установке АРБУС [3]. На рис. 4 сравниваются экспериментальные и расчетные кривые изменения мощности давления при сбросе 24% внешней электрической нагрузки.

За счет введения коррекции по изменению давления на задатчик автоматического регулятора мощности можно обеспечить устойчивую работу установки АРБУС при сбросах и увеличении всей внешней нагрузки. При этом отклонение давления пара от номинального не будет превышать 2,5 *атм*.

ОСНОВНЫЕ ОБОЗНАЧЕНИЯ

τ_0 — масштаб времени
λ — постоянная распада эмиттеров запаздывающих нейтронов
ϱ — реактивность
$\varrho_{ст}$ — реактивность стержней регулирования
$\alpha_т$ — температурный коэффициент реактивности по теплоносителю
$\beta_т$ — температурный коэффициент реактивности по горючему
C — удельная теплоемкость
M — масса
KF — полный поток тепла на единицу температурного перепада
φ — расход теплоносителя по первичному контуру
$W_т$ — расход пара на турбину
N_0 — номинальная мощность реактора
$\bar{\theta}_0$ — номинальная средняя температура теплоносителя в реакторе
γ', γ'' — плотности соответственно воды и пара на линии насыщения
r — удельная теплота парообразования
i' — энтальпия воды на линии насыщения
$i_{пв}$ — энтальпия воды на входе в реактор
$V_{пар}$ — паровой объем вторичного контура
$V_{вод}$ — объем кипящей воды во вторичном контуре
T_S — температура воды на линии насыщения
$\varkappa_i$ — коэффициенты системы автоматического регулирования
τ_1, τ_2 — времена транспортного запаздывания в трубопроводах соответственно от реактора до парогенератора и обратно
n — изменение относительной мощности реактора
c — изменение относительной концентрации эмиттеров запаздывающих нейтронов
$\vartheta_{вх}$, $\vartheta_{вых}$ — изменение относительной температуры теплоносителя первичного контура соответственно на входе и выходе из реактора
ϑ_1, ϑ_2 — изменение относительной температуры теплоносителя первичного контура на входе и выходе из парогенератора
u — изменение относительной средней температуры тепловыделяющих элементов
P — изменение относительного давления пара во вторичном контуре

Индексы

p — коэффициент относится к реактору
ПГ — коэффициент относится к парогенератору
о — означает, что данная величина соответствует исходным значениям параметров установки

ДИНАМИЧЕСКИЕ ПАРАМЕТРЫ УСТАНОВКИ

$$T_i = \frac{\tau_0}{\tau_i} \qquad \tau_M,\ \tau_\perp = \left[\frac{C_p M}{KF}\right]$$

$$\tau_1,\ \tau_2,\ \tau_{||} = \left[\frac{M}{G}\right]$$

$$\tau_0^p = \lambda^{-1}$$

$$A_0 = \frac{N_0\tau_0}{(CM)_M^p\bar{\theta}} \qquad T^{пг} = T_{||}^{пг} + 0{,}5T_\perp^{пг}$$

$$A_1 = \frac{T_{\parallel}^{\text{пг}} - 0{,}5T_{\perp}^{\text{пг}}}{T_{\parallel}^{\text{пг}} + 0{,}5T_{\perp}^{\text{пг}}} \qquad T_{\text{в}} = \frac{W_{\text{то}}\tau_0}{P_0\left(\frac{\partial\gamma''}{\partial P}\right)_0 V_{\text{пар}}}$$

$$A_2 = 1 - A_1 \qquad T_{\text{по}} = \frac{\overline{K}F\cdot\theta_0\tau_0}{P_0\left(\frac{\partial\gamma''}{\partial P}\right)_0 V_{\text{пар}}}$$

$$A_3 = \frac{i' - i_{\text{пв}}}{\Gamma}\cdot\frac{T_{\text{в}}}{1+\varkappa\frac{V_{\text{пар}}}{V_{\text{вод}}}} \qquad D = \psi A_4$$

$$A_4 = \frac{0{,}5T_{\text{по}}}{1+\varkappa\frac{V_{\text{пар}}}{V_{\text{вод}}}} \qquad \psi = \left(\frac{\partial T_S}{\partial P}\right)_0 \frac{P_0}{\bar{\theta}_0}$$

$$A_5 = \frac{T_{\text{в}}}{1+\varkappa\frac{V_{\text{пар}}}{V_{\text{вод}}}} \qquad \varkappa = \left(\frac{\partial i'\gamma'}{\partial P}\right)_0 \Big/ \Gamma\left(\frac{\partial\gamma''}{\partial P}\right)_0$$

$$\alpha_p = \frac{A_0 T_{\perp}^{p}}{T_M^{p} T_{\parallel}^{p}} \qquad f = \frac{DA_2 T^{\text{эфф}}}{T_1 T_2}$$

ЛИТЕРАТУРА

1. И. А. Вышнеградский и др. Теория автоматического регулирования. М., Изд-во АН СССР, 1949.
2. В. И. Крутов. Анализ работы систем автоматического регулирования. М., Машгиз, 1961.
3. Атомная энергетическая установка с органическим теплоносителем, наст. издание.

ABSTRACT - RÉSUMÉ - АННОТАЦИЯ - RESUMEN

A/371 USSR

On the dynamic stability of nuclear power plants

By P. A. Gavrilov and L. N. Podlazov

The stability of nuclear power plants with a steam generator operating at a free level is considered when turbogenerator load and reactivity are changing.

A dynamic equation system is given and confirmed. Transfer functions for several parameters (in particular, power and pressure) are obtained in the form suitable for different modes of regulation including self-regulation.

In practice, it is shown that in most interesting cases transfer functions may be used as fractional rational functions with a characteristic equation of not higher than the fifth power.

A method of defining plant general parameters is presented ensuring a plant aperiodic stability with load and reactivity perturbations.

Nomograms are given to determine the plant dynamic characteristics (characteristic equation roots, decrements of attenuation, oscillation frequencies, etc.). The nomograms may be directly used to select optimal characteristics and analyse dynamics of designed reactor and control systems.

As an example, the model developed is applied to the analysis of the ARBUS dynamics.

It is shown that the ARBUS dynamic parameters are in the vicinity of the aperiodic stability boundary when the turbogenerator load is changing. Some recommendations are given aimed at improving dynamic characteristics of the plant.

The results of the ARBUS dynamics on an analogue computer are compared with those on nomograms.

A choice of regulation model of the ARBUS is provided.

It is shown that there is no need for an automatic power regulator and that it is possible to use self-regulation for the operation of nuclear power plants.

A/371 URSS

Stabilité dynamique des centrales nucléaires

par P. A. Gavrilov et L. N. Podlazov

Le mémoire étudie la stabilité des centrales nucléaires avec générateur de vapeur à niveau libre lorsque varient la charge de consommation extérieure et la réactivité.

On établit un système d'équations de dynamique. On obtient les fonctions de transfert pour une série de paramètres (fréquence, puissance et pression) sous une forme qui ne dépend pas des divers moyens de contrôle, y compris l'autorégulation.

On montre que dans la majorité des cas intéressants pour la pratique, les fonctions de transfert peuvent être réduites en fonctions rationnelles fractionnaires à équation caractéristique ne dépassant pas la puissance 5.

On propose une méthode de détermination des paramètres généralisés de l'installation qui garantit la stabilité apériodique de l'installation au cours des perturbations de la charge et de la réactivité.

Le rapport donne les nomogrammes qui permettent de déterminer les caractéristiques dynamiques de l'installation (racines de l'équation caractéristique, décréments d'amortissement, fréquences des oscillations, etc.). Les nomogrammes peuvent être directement utilisés pour le choix de caractéristiques optimales et pour l'analyse des propriétés dynamiques dans les études de réacteurs et de systèmes de contrôle.

L'analyse des propriétés dynamiques de l'installation ARBUS sert d'exemple à cette méthode.

Les paramètres dynamiques de l'installation ARBUS sont proches des limites de stabilité apériodique au cours des variations de la charge extérieure. On donne des indications pour l'amélioration de ses propriétés dynamiques.

Les résultats de l'étude de la dynamique d'ARBUS sur simulateur sont comparés aux résultats d'une étude sur nomogrammes.

On donne les raisons du choix du système de contrôle de l'installation ARBUS.

On démontre qu'il est possible en principe de renoncer au régulateur automatique de puissance et d'adopter l'autorégulation pour les installations énergétiques.

A/371 USSR

Estabilidad dinámica de las centrales nucleares

por P. A. Gavrilov y L. N. Podlazov

En la memoria se estudia la estabilidad de las centrales nucleares con generador de vapor de nivel libre para variaciones de la carga de consumo exterior y de la reactividad.

Se establece el sistema de ecuaciones dinámicas. Las funciones de transferencia se obtienen para una serie de parámetros (la frecuencia, la potencia y la presión) de manera tal que su forma no dependa de los diferentes procedimientos de regulación, incluido el control automático.

Se demuestra que en la mayoría de los casos interesantes en la práctica, las funciones de transferencia se pueden reducir a fracciones racionales de ecuación característica de grado no superior al quinto.

Se propone un método para determinar los parámetros generalizados de la instalación que asegura la estabilidad aperiódica de la misma fuente a perturbaciones de la carga y de la reactividad.

Los nomogramas que se presentan permiten determinar las características dinámicas de la instalación (raíces de la ecuación característica, coeficientes de amortiguamiento, frecuencias de las oscilaciones, etc.) y pueden utilizarse directamente para elegir las características óptimas y para el análisis de las propiedades dinámicas de los reactores en proyecto y de los sistemas de control.

Como ejemplo se aplica este método al análisis de las propiedades dinámicas de la instalación ARBUS.

Se demuestra que los parámetros dinámicos de la instalación ARBUS se encuentran cerca del límite de estabilidad aperiódica respecto de los cambios de la carga exterior. Se hacen algunas recomendaciones para mejorar sus propiedades dinámicas.

Los resultados del estudio dinámico del reactor ARBUS llevado a cabo en su modelo se comparan con los resultados obtenidos con los nomogramas.

Se justifica también la elección del sistema de control de la instalación ARBUS.

Se señala que es posible en principio renunciar al control automático de potencia y adoptar el control automático de las instalaciones nucleares.

Stability analysis and dynamic performance of a chemical system operated for the automatic fine control of a nuclear reactor

By G. C. Ambrosini,* T. Bozzoni,* G. Cipollina,* E. Colussi** and R. Garroni*

The chemical control of a nuclear reactor is realized by varying the reactivity through the injection and the extraction, from the reactor coolant or moderator, of a neutron absorber in the form of a soluble compound [1]. This kind of control presents many advantages in comparison with conventional systems using rods; the main features are:

(*a*) A low capital investment: the control rods and their expensive drive mechanisms are partially or completely eliminated; the vessel structure is simplified and the sealing problems concerning the rod-drive coupling are avoided; the design of the refuelling machine is made easier by the absence of the rods;

(*b*) The maintenance is simplified: there are no mechanical moving parts inside the reactor vessel; the only parts of the circuit which need maintenance are valves and pumps, which may be located in accessible zones;

(*c*) Possibility of controlling large reactivity values: by injecting poisoning liquids into the moderator it is possible to reach very high reactivity values, not attainable with control rods. There is thus the possibility of having high initial reactivity values and therefore a long neutron life of the reactor core;

(*d*) Elimination of axial flux peaks due to partially withdrawn control rods and therefore more favourable axial hot channel factors. This allows higher specific power and more uniform fuel element burn-up.

Chemical control is generally considered for shim purposes since reactivity changes due to a variation of the soluble poison concentration are generally slow and, consequently, such a system does not appear to be convenient for fine control purposes. This is true when the poison is injected directly into the moderator but other solutions of the problem are possible which allow the design of a chemical fine control system with performances comparable with those of conventional systems. The purpose of this paper is to describe the design of a neutron flux automatic control system, utilizing a soluble poison solution circulating in a tube located in the reactor core, showing good stability characteristics and dynamic response. A prototype of this system has been successfully tested in the swimming pool reactor AVOGADRO-RS-1 of the Saluggia Nuclear Centre. The paper deals particularly with the dynamic characteristics of such a type of control and does not emphasise other kinds of problems, like those concerning the corrosion, the radiation damage, the boric acid recovery from the exhausted solution and the poison deposition on the piping.

* Divisione Tecnologica, CNEN, Rome.
** Società Ricerche e Impianti Nucleari, Centro Nucleare Saluggia.

ANALYTICAL STUDY

The relationships describing the physical phenomena are elaborated in order to obtain the *transfer functions* which correlate the so-called input variables to the output variables. This procedure, usually adopted in the feedback theory, permits solution of the stability problem of the system in the small, i.e., for the case of small deviations around a steady state position. Consideration shall be given also to the stability in the large, involving the non-linearity of the system, leaving the analogue study to confirm the validity of the analytical linear approach.

System description

Figure 1 shows the flow diagram of the circuit. The hydraulic circuit consists of a stainless steel loop in which an aqueous solution of boric acid is circulated by means of a centrifugal pump. The in-pile section of the loop is in the form of a U-tube. Two pressurized tanks, filled respectively with water and saturated boric acid solution, are connected to the loop through two automatically controlled valves. These valves may be driven by an electrical signal to inject water or saturated boric acid solution (chosen as poison for its good neutron absorbing characteristics) into the circuit. An expansion tank completes the hydraulic circuit. Under normal conditions the concentration of the circulating solution is kept constant by closing both these injection valves. A variation in the concentration value and

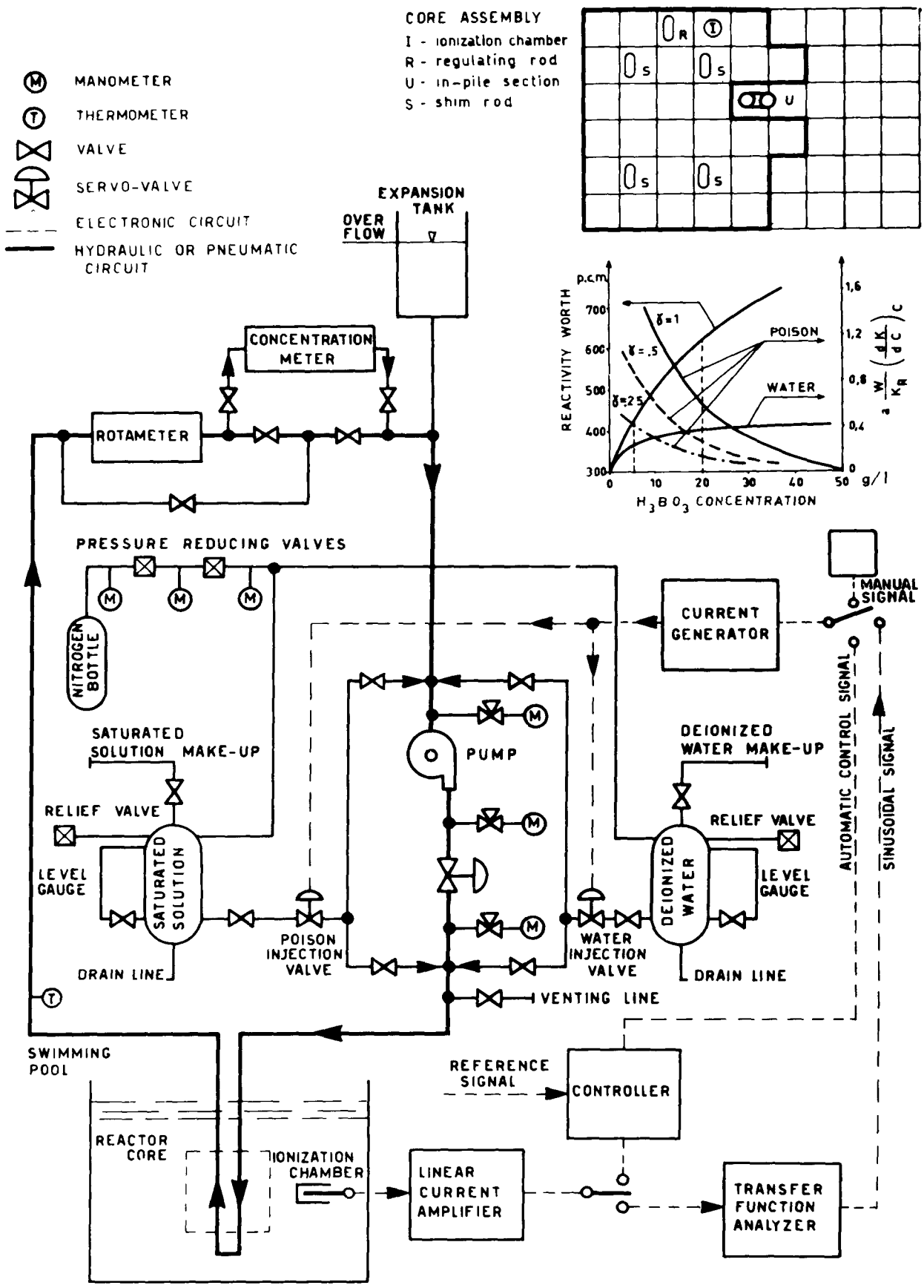


Figure 1. Simplified flow diagram

therefore in the reactivity worth of the in-pile section is obtained by injecting water or concentrated poison solution.

System transfer functions

The transfer functions of the several blocks into which the system may be subdivided are deduced in the following sections.

Injection valves

The transfer function relating the current signal actuating the valve positioners to the fractional opening of both valves is assumed to be:

$$G_v = \frac{x(s)}{i_c(s)} = \frac{G_v(0)}{(s/\omega_0)^2 + 2\zeta(s/\omega_0) + 1} \quad (1)$$

and can be determined from the experimental dynamic characteristics. Actually the valve and the electro-pneumatic actuator are a complex feedback system, with several non-linearities, as for instance the finite stroke.

Flow rate versus injection valve opening

The injection and the in-pile section flow rates determine completely the hydraulics of the system because of the relationship: $W_e = W - W_i$. Applying the dynamic Bernouilli equation to the several parts of the hydraulic circuit, one obtains a set of equations, which may be linearized to give the following transfer functions:

$$G_{i1} = \frac{W_i(s)}{x(s)} = \frac{1}{C_v}\left(\frac{P_0 - P_B}{g\rho}\right)^{1/2} = \text{constant} \quad (2)$$

$$G_{i2} = \frac{W(s)}{x(s)} = \frac{1}{C_v}\left(\frac{P_0 - P_B}{g\rho}\right)^{1/2} \frac{\alpha_e s + 2\chi_e W - dH/dW}{\alpha s + 2\chi W - dH/dW} \quad (3)$$

where C_v is a constant, characteristic of the injection valve, relating the pressure drop to the flow rate. Considering the numerical values relative to the hydraulic circuit, it can be seen that the time constants may be neglected in comparison with others affecting the system dynamics.

Poison concentration versus injection flow rate

The poison concentration $C(z, t)$ in the circuit is time and space dependent. The solution concentration at the mixing point after the injection is given in a linearized and Laplace transformed scheme by the relationship:

$$C_m(s) = \frac{C_p - C}{W} W_p(s) - \frac{C}{W} W_w(s) + C_e(s) \quad (4)$$

where $C_e(s)$ is related to $C_m(s)$ by

$$C_e(s) = C_m(s) \exp(-sT)/(1+s\tau_1)(1+s\tau_2) \quad (5)$$

T being the total loop transit time and τ_1, τ_2 two mixing time constants. The solution concentration at the reactor inlet is:

$$C_i(s) = C_m(s) \exp(-sT_1)/(1+s\tau) \quad (6)$$

The desired transfer function results in

$$G_c(s) = \frac{C_i(s)}{W_i(s)} = a\bar{G}_c(s) = a \frac{\exp(-sT)/(1+s\tau_1)}{1-\exp(-sT)/(1+s\tau_1)(1+s\tau_2)} \quad (7)$$

where $a = \frac{C_p - C}{W}$ or $-\frac{C}{W}$ for poison or water injection respectively. Therefore, Eq. (7) presents different gain values for poison or water injection. The concentration response to a step in the injection flow rate, if one neglects the mixing time constants, is a sequence of steps with a period equal to the total main transit time. In the actual system the gain is changing as a function of the concentration and the steps are decreasing with time. For low frequencies the transfer function $G_c(s)$ behaves like an integrator:

$$\bar{G}_c(s) \approx \frac{1}{s(T+\tau_1+\tau_2)} \quad (8)$$

Reactivity versus concentration

The reactivity versus concentration transfer function is defined as the reactivity-worth variation of the in-pile section versus the poison concentration at the reactor inlet. The reactivity-worth variation of a unit length of the in-pile section, located at a distance z from the reactor core inlet, versus the solution concentration entering the reactor is given by

$$K(s) = (dk/dC)_c C_i(s) \exp[-(z/v)s]\phi(z) \quad (9)$$

where $(dK/dC)_c$ is the slope of the characteristic giving the reactivity versus poison concentration at steady state; $\phi(z)$ is a weighing factor correlated to the neutron flux axial distribution which—assuming a sinusoidally shaped flux, and approximating the in-core loop length with twice the extrapolated core length L'—results in:

$$\phi(z) = \frac{1}{2L'}\left(1 - \cos\frac{2\pi}{L'} z\right) \quad (10)$$

Integrating (8) along the whole in-pile section one has:

$$G_k(s) = \frac{K(s)}{C_i(s)} = \left(\frac{dK}{dC}\right)_c \frac{1-\exp(-sT_r)}{T_r \cdot s\ [1+(sT_r/4\pi)^2]} \quad (11)$$

The time constants of $G_K(s)$ are, for the case of the Avogadro control loop, about ten times smaller than the corresponding main loop transit time. It may be shown that the transfer function $G_K(s)$ does not look in this case very important from the stability point of view.

Nuclear power versus reactivity

The following well-known kinetic transfer function with no feedback effect is taken:

$$G_r(s) = \frac{N(s)}{N_0 K(s)} = 1/s(l^* + \Sigma_i \beta_i/s+\lambda_i) \quad (12)$$

The ion chamber transfer function is assumed to be a constant gain G_0.

Control system design

Figure 2 shows the complete block diagram of the system. The given scheme is of the non-linear type and the open loop gain of the system is varying according to the steady state poison concentration value because of the two terms: C/W or $(C_p-C)/W$ and $(dK/dC)_c$. This second factor is due to the non-linear reactivity-concentration characteristic. The dynamic behaviour of the system under study is also characterized by the pure delays due to the fluid circulation. From this point of view the conventional system may be considered as a particular case, where all the delays are zero: in fact, with this assumption, the given transfer function is reduced to that of a velocity servo system, and the mixing time constants may be interpreted as those relative to the mechanical system inertia.

System specifications

The performances desired from the chemical system are those typical of a conventional system:

(*a*) Useful reactivity control range of about 200 pcm;

(*b*) Zero steady state power error. This is obtained by means of an integrating function relating the power error signal to the reactivity. This is usually accomplished by a velocity-servo and in our case by the step-by-step integration following the fluid circulation;

(*c*) Satisfying transient behaviour. In the linear approximation used, the system is assumed to be sufficiently fast if its cut-off frequency is at least of 0.2 radians/s. The cut-off frequency is defined as the one for which the system gain is one, and therefore it is the frequency value for which the phase margin is calculated. An analogical study is in every way necessary to analyse the transient behaviour, because of the many non-linearities of the system;

(*d*) The system, in case of a fully open injection valve, has to produce a reactivity rate of at least 5 pcm/s in the whole control range.

To meet these specifications, the in-pile section was located in a fuel element position in the outer ring of the core, and two additional fuel elements were set in the positions shown in Fig. 1, where the experimental diagram of the in-pile section reactivity worth versus boric acid concentration is also given. The reactivity worth of the in-pile section pipe filled with clean water is 300 pcm. The system cannot utilize the whole concentration interval from 0 to C_p because of the strong gain variation. The rate of reactivity insertion is given by the following expression:

$$\dot{K} = a\frac{W_i}{T^*}\left(\frac{dK}{dC}\right)_c = \frac{W_i K_r}{W T^*}\left(aW\frac{(dK/dC)_c}{K_r}\right) \quad (13)$$

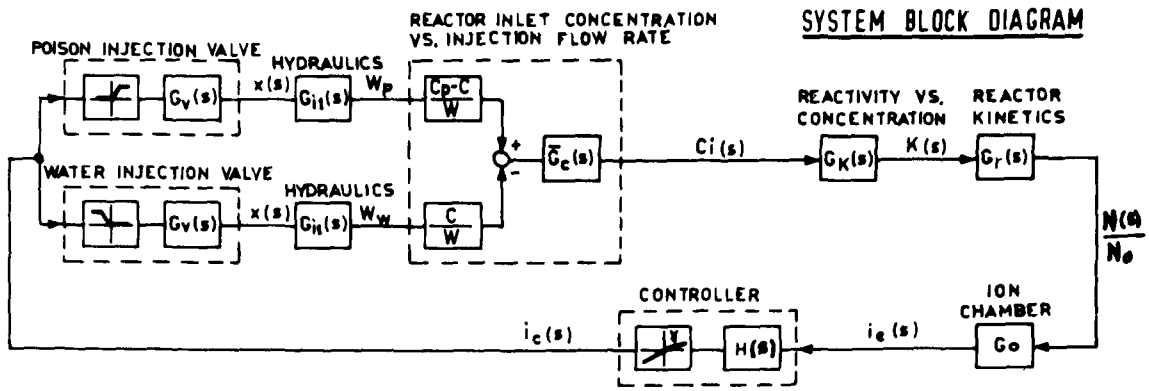
In Fig. 1 the factor $aW\frac{dK/dC}{K_r}$ is plotted against the solution concentration for the case of water and of poison injection. It may be seen that the higher gain variation is obtained in the case of poison injection at low concentration values where there is no self-shielding effect. In the useful concentration range the gain variation should be smaller than a factor of three. With this limitation in mind and selecting the operating range symmetrically around the concentration value corresponding to the same water and poison injection gain, i.e. 25 g/l, the resulting useful reactivity range is then 115 pcm. However, it is possible to vary by a factor of γ the poison injection gain by means of a convenient non-linear controller, in order to get a wider reactivity range. If one assumes for γ a value of 0.5, the reactivity range is of 160 pcm, and for a value of 0.25, of about 200 pcm, the corresponding operating concentration range varying from 5 to 20 g/l. The minimum rate of the reactivity variation, with the above assumptions, results for water injection. In order to have a reactivity insertion rate of at least 5 pcm/s in the case of a fully open water valve without perturbing the system hydraulics and having a convenient injection to main flow ratio, one must have a total loop circulation time not longer than 10 seconds. Design considerations aimed at reducing the pressure loss have suggested the selection of the same pipe cross section for the loop as in the in-pile section.

System dynamics

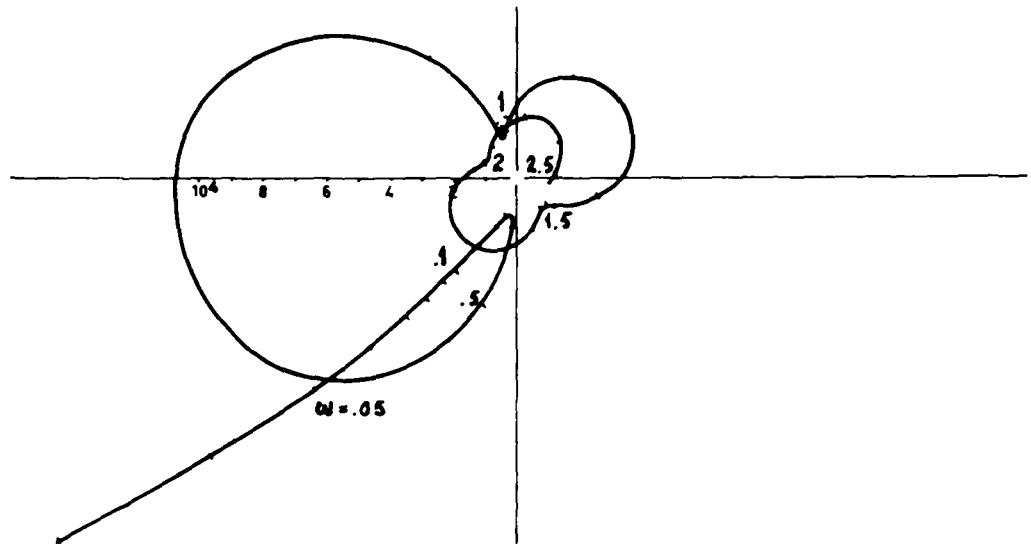
The open loop system transfer function is $F(s) = F_0 \bar{F}(s)$, where:

$$\bar{F}(s) = \frac{T^*\exp(-sT_1)/(1+s\tau_1)}{1-\exp(-sT)/(1+s\tau_1)(1+s\tau_2)} \times \frac{1-\exp(-sT_R)}{sT_r[1+(sT_r/4\pi)^2]} \times \frac{1}{(s/\omega_0)^2+2\zeta(s/\omega_0)+1} G_r(s) \quad (14)$$

To study the system stability, the Nyquist diagram of the $\bar{F}(s)$ function has been plotted in Fig. 2, assuming the following numerical values derived for a flow rate of 1.8 l/s and corresponding to the AVOGADRO experimental loop: $T = 10$ seconds; $T_1 = 4$ seconds; $T_r = 0.6$ seconds; $\tau_1 = 0.25$ seconds; $\tau_2 = 1.3$ seconds; $\omega_0 = 5$ seconds; $\zeta = 0.8$. The values of β_i and λ_i are stated by Keepin [2] and the mean neutron lifetime is assumed to be 7×10^{-5} s. The fluid circulation affects the transfer



NYQUIST DIAGRAM OF THE OPEN LOOP TRANSFER FUNCTION $\bar{F}(s)$ FOR A CIRCULATION TIME OF 10 s



BODE DIAGRAM OF THE OPEN LOOP TRANSFER FUNCTION $\bar{F}(s)$ FOR A CIRCULATION TIME OF 9,3 s

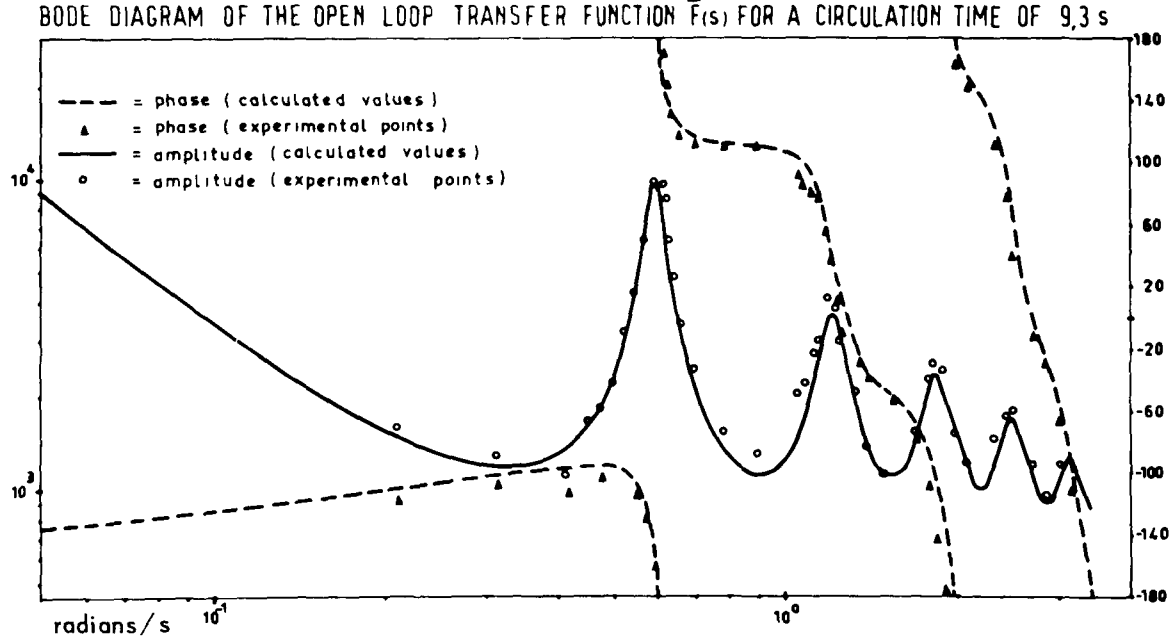


Figure 2

function $F(s)$ in the frequency range interesting the control system and interferes with the stabilizing neutronic kinetic lead effect. This influence of the fluid circulation may be split into two factors: (*a*) the first term of (14), which relates to the loop circulation time. The open loop gain should be infinite for frequency value multiples of $2\pi/T$, if the mixing were neglected. Actually there are resonance peaks for such frequency values. Furthermore, there is the opposite interference effect for frequencies: $\omega = (2n + 1)(\pi/T)$; (*b*) the delay term $\exp(-sT_1)$ which makes the Nyquist diagram rotate around the origin in a clockwise sense.

The phase shift between two resonance peaks is mainly a function of the ratio T_1/T.

Owing to the non-monotone behaviour of the amplitude of the overall open-loop system transfer function, it may be seen from the Nyquist diagram of Fig. 2 that, when a proportional controller is used such that the total open loop gain is unity for the cut-off frequency of 0.2 radians/s, the system reveals a satisfactory behaviour in the range of frequency interesting the reactor control. The system, however, is unstable for higher frequencies, belonging to the first resonance peak. Therefore it is necessary to use a compensating network to modify the overall open loop transfer function at the resonance frequencies.

The system dynamic characteristics have been studied as a function of several parameters, amongst which the most important were:

(*a*) The main loop flow rate, in the range from 1.8 to 4 l/s. The dynamic behaviour is improved by an increase in the mass flow because the resonance peaks are shifted to higher frequencies, over the range interesting from the stability point of view, and because the delay T_1 decreases. For instance, with a flow rate of 4 l/s and a total transit time of 4.5 seconds, a conventional controller having only proportional action might be used;

(*b*) The mixing time constants of the circuit. They strongly affect the resonance peaks. A parametric study is necessary due to the present lack of knowledge of the hydraulic behaviour.

Controller synthesis

The design has been developed firstly following the classic feedback theory suitable for linear systems. Following this, the whole system has been simulated on an analogue computer and more accurate values of the controller parameters have been obtained. The non-linearity corresponding to the different poison and water injection gains (see Fig. 2) has been compensated for by means of a convenient non-linear element in the controller. This compensation is actually a function of the frequency of the input signal, because of the position of the injection valve transfer function $G_v(s)$ between the two non-linearities. The accuracy of the approximation is obviously increasing as more input signal harmonics belong to the range where $G_v(s)$ is constant in amplitude and phase. In order to have a control system with satisfactorily fast and stable performances, the $F(s)$ Nyquist diagram shows the necessity of modifying also the overall open loop transfer function. In designing the controller transfer function, the inverse function criterion has been followed. In fact, to avoid the instability phenomena inherent in the first term given in (14) concerning the closed loop circulation time, an ideal controller should have a transfer function of the type $[1\text{-}\exp(-sT)]/sT$ when the mixing time constants are neglected; furthermore, to compensate for the delay relative to the injection point-core inlet transit time, a lead term can be introduced. Actually a controller has been designed whose transfer function $H(s)$ approximates to that of the ideal controller in a convenient frequency range, expressing the $\exp(-sT)$ term in a Padé series of the fourth order, which corresponds to the compensation of the first resonance peak only.

EXPERIMENTAL RESULTS

The control system described has been tested and operated extensively on the AVOGADRO swimming pool reactor of the Saluggia Nuclear Centre. The analytical and analogical studies were confirmed by the experimental results. Neutron flux transients typical of a research reactor routine operation were performed, for instance reactivity insertions and variations in power demand. A precision better than 1% was obtained in the neutron flux level regulation; a limiting factor in this respect was found to be the injection valves dead zone. The saturation effect due to full opening of an injection valve was important only for step reactivity insertions of about 100 pcm. Figure 3 shows the response of the system to a ramp of 7 pcm/s up to $\pm$ 50 pcm in the case of a circulation time of about 10 seconds, which means a mass flow of 1.8 l/s. Figure 3 illustrates also the transient following a step of $\pm$ 15% in the power demand. Some reactor transients have been performed for a circulation time of 15 seconds with the purpose of checking if satisfactory control performance with a lower installed pumping power was possible; however, for such a low flow the resulting power error and the transient duration were intolerably high. The transfer function of the reactor power versus the electrical input signal to the injection valves was determined experimentally. The Bode diagram plotted in Fig. 2 shows the experimental points and the calculated values for the case of a 9.3 seconds circulation time. From this operational experience one may conclude that the control system examined here seems to have satisfactory dynamic characteristics as regards the fine control of the neutron flux level. There are no particular operation and maintenance problems. The whole system appears to be quite reliable, rugged and easy to handle.

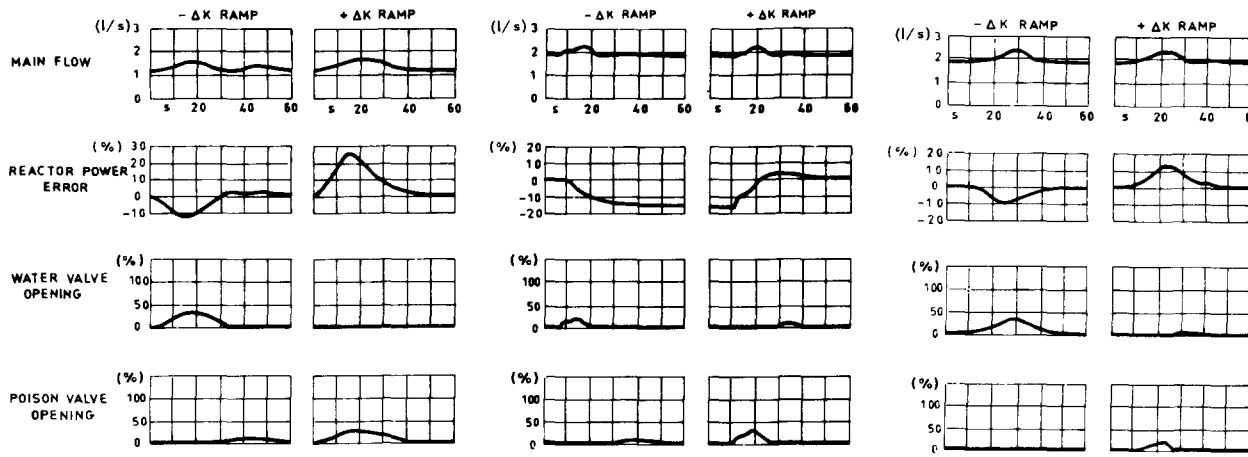


Figure 3. AVOGADRO experimental loop dynamic behaviour

Response of the system to a ramp of 7 pcm/s up to ± 50 pcm. Circulation time: 15 seconds. Steady state concentration: 13 g/l

Transient of the system following a step of ± 15% in the power demand. Circulation time: 10 seconds. Steady state concentration: 13 g/l

Response of the system to a ramp of 7 pcm/s up to ± 50 pcm. Circulation time: 10 seconds. Steady state concentration: 13 g/l

FURTHER CONSIDERATIONS

Chemical control appears to be advantageous for any kind of nuclear reactor; particularly for the elimination of the axial neutron flux peaks, due to partially withdrawn control rods, and is thus interesting for power reactors as it allows an increase in the power of a core in comparison with the case of reactivity control effected by means of rods. It should be noted that in research reactors or in prototypes of power reactors, where one has to test different core assemblies, the absence of rods eliminates any problem concerning the control rod positioning and the following fuel element pitch limitations. Chemical control also looks attractive for materials testing reactors, where it is desired to keep the neutron flux distribution constant and uniform in the experimental channels. Another possibility arising from the use of soluble poisons could be local neutron flux control in an attempt to have a flux value which is independent of the reactor power behaviour, in zones containing samples of materials under test, e.g., one may place the samples in a tube where a boric acid solution circulates and whose concentration is conveniently related to the local flux value, this flux being directly measured or indirectly determined by means of more easily detectable variables.

NOMENCLATURE

A : pipe cross section
a : $(C\rho - C)/W$ or $-C/W$
C : solution concentration
C_e : concentration entering injection point
C_i : reactor inlet solution concentration
C_m : concentration leaving injection point
Cp : saturated solution concentration
$F(s)$: open loop transfer function
F_0 : open loop gain
$\bar{F}(s)$: open loop normalized transfer function
$G_c(s)$: hydraulic transfer function
$G_c(s)$: normalized $G_c(s)$ transfer function
$G_1(s)$: hydraulic transfer function
$G_k(s)$: K versus C_i transfer function
$G_0(s)$: ion chamber transfer function
$G_r(s)$: reactor transfer function
$G_v(s)$: injection valves transfer function
g : gravity constant
$\frac{dH}{dW}$: pump characteristics
$H(s)$: controller transfer function
i_c : injection valves imput signal
i_e : ion chamber current
K : reactivity excess
K_r : in-pile section maximum reactivity-worth
$(dK/dC)_c$: slope of the K versus C diagram
L : total loop length
L' : extrapolated core length
L_e : loop length from expansion tank to injection point
l^* : neutron mean life time
N : nuclear power
N_0 : steady state power
P_b : injection point pressure
P_0 : injection tank pressure
s : Laplace operator
T : total circulation time
T^* : $T + \tau_1 + \tau_2$
T_1 : injection point — reactor inlet time delay
T_2 : reactor outlet — injection point time delay
T_r : in-pile section transit time
v : solution velocity
x : injection valve fractional opening
W : in-pile flow rate
W_i : injection flow rate
$W\rho$: poison injection flow rate

W_w : water injection flow rate
α_e : L_e/Ag
α : L/Ag
β_i : delayed neutrons i^{th} group yield
γ : poison to water gain ratio
λ_i : delayed neutrons i^{th} group decay constants
ρ : solution density
τ_1 : injection point — reactor inlet mixing time constant
τ_2 : reactor outlet — injection point mixing time constant
ζ : injection valve damping factor
$\phi(z)$: weighing factor
χ_e : expansion tank — injection point pressure drop factor
χ : total pressure drop factor
ω_0 : injection valve natural frequency

REFERENCES

1. Breden, C. R., Brown, W. S., and Sivetz, M., *Soluble Poisons in Reactor Control,* USAEC report ANL-5244 (November 1955).
2. Keepin, G. R., Wimett, T. F., and Zeigler, R. K., Phys. Rev., *107,* 1044 (1957).

ABSTRACT - RÉSUMÉ - АННОТАЦИЯ - RESUMEN

A/629 Italie

Analyse de stabilité et de comportement dynamique d'un système chimique utilisé pour le réglage automatique d'un réacteur nucléaire

par G. C. Ambrosini *et al.*

On a projeté et expérimenté avec satisfaction un système automatique de réglage fin, où barre de réglage et servo-moteur de vitesse sont remplacés par une solution d'acide borique circulant dans un tube près du cœur du réacteur.

Toute variation de réactivité jusqu'à 200 pcm est obtenue en injectant de l'eau pure ou une solution concentrée d'acide borique dans le circuit hydraulique principal. Il s'agit là d'un circuit du type fermé muni d'un récipient d'expansion avec trop-plein pour évacuer l'excès du débit au cours des phénomènes transitoires de réactivité.

Le contrôle de la réactivité, effectué au moyen de poison soluble au lieu des absorbeurs traditionnels à état solide, présente de nombreux avantages, qu'il s'agisse de réacteurs de puissance ou de réacteurs de recherche. Il reste néanmoins à résoudre quelques problèmes additionnels concernant la chimie des solutions acides, le comportement des matériaux et le comportement dynamique du système.

L'analyse de stabilité et de comportement dynamique est un des facteurs essentiels qui décide si un système chimique convient ou non au réglage d'un réacteur nucléaire.

On trouvera dans le mémoire une étude détaillée sur un modèle linéaire du système réel, utilisant les méthodes graphique et analytique traditionnelles de la théorie des systèmes à rétroaction.

Les calculs ont été réalisés à l'aide d'un calculateur digital IBM-704 et du diagramme de Nyquist obtenu pour la fonction de transfert du circuit ouvert de l'ensemble du système.

Voici ci-après quelques caractéristiques d'un système de contrôle à circulation de poison soluble en circuit fermé:

a) Un gain fortement variable du système en fonction de la valeur de la concentration stationnaire. Ceci est dû principalement aux différents effets résultant de l'injection d'une égale quantité d'eau ou d'une solution concentrée d'acide borique; évidemment on obtient un effet d'injection d'eau pure supérieur si l'on augmente la concentration de la solution; c'est l'inverse qui se passe dans le cas d'une injection d'acide borique. Un autre effet résulte de la caractéristique non linéraire du diagramme de réactivité en fonction de la concentration pour un tube en forme de U, utilisé dans la section à l'intérieur du réacteur, compte tenu du phénomène d'auto-absorption aux valeurs élevées de concentration d'acide borique.

b) Les délais normaux dus à l'écoulement de la solution ont deux effets principaux qui influencent fortement le comportement dynamique du système. Tout d'abord, la phase de délai entre le point d'injection et le réacteur compromet la stabilité du système, vu qu'il s'agit d'une longue constante de temps; en deuxième lieu, on observe une tendance à des oscillations auto-entretenues à des fréquences multiples de $1/T$, T étant le délai de transit total.

Pour obtenir un comportement dynamique du circuit de réglage comparable à celui d'un système classique à vitesse asservie automatiquement, les régulateurs proportionnels, intégraux et dérivés se révèlent inadéquats, et un circuit plus élaboré a été élaboré.

La validité du modèle linéaire a été ensuite contrôlée par simulation de l'ensemble du système sur une machine à calculer analogique; on trouve que certains effets non linéaires, tels que la saturation de la soupape d'ouverture, ont de l'importance dans les transitoires du réacteur qui impliquent de grosses insertions de réactivité. On obtient des valeurs de paramètres de régulateur plus précises.

Le système de réglage a été expérimenté et utilisé avec succès sur le réacteur AVOGADRO. On a effectué des transitoires de puissance typiques du fonctionnement ordinaire d'un réacteur de recherche, ainsi que des insertions de réactivité et des variations de puissance de préréglage, et on a obtenu une précision supérieure à 1% dans le réglage du niveau du flux de neutrons.

On a également mesuré la fonction de transfert du système et les points expérimentaux ont coïncidé parfaitement avec les calculs du diagramme de Nyquist.

A/629 Италия

Анализ устойчивости и динамические характеристики химической системы, применяемой для автоматического плавного регулирования ядерного реактора

Дж. Амброзини *et al.*

Разработана и удовлетворительно эксплуатируется автоматическая система плавного регулирования реактора, в которой регулирующие стержни и скоростные сервоприводы заменены раствором борной кислоты, циркулирующим в трубе около активной зоны реактора.

Любое изменение реактивности достигается путем впрыскивания чистой воды или концентрированного раствора борной кислоты в основной гидравлический контур. Этот контур имеет вид замкнутой петли; для отвода излишнего потока во время переходных изменений реактивности предусмотрен расширительный бак со сливной трубой.

Регулирование реактивности с помощью растворимого поглотителя нейтронов вместо обычных твердых поглотителей имеет большие преимущества для энергетических и исследовательских реакторов. Однако необходимо решить некоторые дополнительные проблемы, связанные с химией кислотных растворов, поведением материалов и динамикой системы.

Динамическая устойчивость и анализ характеристик представляют собой два из основных факторов проектирования химической системы, предназначенной для плавного регулирования ядерных реакторов.

В докладе подробно описывается исследование, проведенное на линеаризованной модели реальной системы с применением обычного графического и аналитического методов теории системы с обратной связью.

Расчеты производились с помощью электронной цифровой вычислительной машины IBM-704. Была получена диаграмма Найквиста для передаточной функции незамкнутой петли всей системы.

Система регулирования с циркуляцией растворенного поглотителя нейтронов в замкнутой петле имеет следующие особенности:

a) Большое переменное усиление системы в зависимости от величины рабочей равновесной концентрации. Это объясняется главным образом различными эффектами, получаемыми в результате впрыскивания одинакового количества воды или концентрированного раствора борной кислоты. Более сильный эффект воды достигается при повышении концентрации раствора, а при впрыскивании борной кислоты наблюдается обратное явление. Другой эффект вытекает из нелинейной характеристики диаграммы зависимости реактивности от концентрации для U-образных труб, применяемых внутри реактора, так как при повышенных концентрациях борной кислоты наблюдается явление самопоглощения.

b) Задержки, связанные с протеканием раствора, приводят к двум основным эффектам, сильно влияющим на динамическое поведение системы. Во-первых, задержка между точкой инжекции и реактором отрицательно влияет на устойчивость системы, будучи эквивалентной долговременной постоянной; во-вторых, тенденция к самоподдерживающимся колебаниям наблюдается при частотах $1/T$, где T — полное время пролета.

Было установлено, что для получения петли регулирования с динамическими характеристиками, аналогичными характеристикам обычной системы с механическим приводом стержней и скоростными сервоприводами, интегральные и производные регуляторы использовать нельзя, и была разработана более точная схема.

Затем была проверена пригодность линейной модели путем имитации всей системы на моделирующем устройстве. Было установлено, что некоторые нелинейные эффекты, как, например, насыщение, при котором клапан открывается, играют важную роль при переходных режимах реактора и вызывают сильное увеличение реактивности. Были получены более точные значения параметров регуляторов.

Система регулирования была успешно испытана и использована на реакторе AVOGADRO. Производились переходные изменения мощности, типичные для обычной эксплуатации исследовательских реакторов, как, например, увеличение реактивности и изменение заданной мощности. Была достигнута точность выше 1% при регулировании уровня потока нейтронов.

Измерялась также передаточная функция системы, и экспериментальные точки хорошо согласовались с диаграммой Найквиста.

A/629 Italia

Análisis de estabilidad y comportamiento dinámico de un sistema químico empleado para el control automático fino de un reactor nuclear

por G. C. Ambrosini *et al.*

Se ha diseñado y hecho funcionar satisfactoriamente un sistema automático de control de precisión, en el que la barra de regulación y el servo de velocidad han sido sustituidos por una solución de ácido

bórico que circula por un tubo cerca del núcleo del reactor.

Se puede obtener cualquier variación de reactividad hasta 200 pcm inyectando agua pura o disolución concentrada de ácido bórico en el circuito hidráulico principal. Este es del tipo de circuito cerrado provisto de un depósito de expansión con un rebosadero para evacuar el exceso de caudal durante los regímenes transitorios de reactividad.

El control de la reactividad por medio de veneno soluble en vez de los absorbentes sólidos clásicos ofrece muchas ventajas tanto en reactores de investigación como de potencia. Sin embargo, deben resolverse algunos problemas adicionales relacionados con la química de disoluciones ácidas, el comportamiento de los materiales y la dinámica del sistema.

El análisis de la estabilidad dinámica y comportamiento del sistema son los factores principales en el diseño de un sistema químico adecuado para el control fino de reactores nucleares.

Esta memoria describe con detalle el estudio realizado según un modelo linealizado del sistema real, utilizando los métodos gráfico y analítico normales en la teoría de servomecanismos.

Se realizaron los cálculos con la ayuda de una calculadora digital IBM-704 y se obtuvo el diagrama de Nyquist para la función de transferencia en circuito abierto del sistema completo.

A continuación se incluyen algunas de las características típicas de un sistema de control de circuito cerrado con circulación de veneno soluble:

a) Una ganancia del sistema muy variable, dependiente del valor de la concentración estacionaria de funcionamiento. Esto se debe principalmente a los efectos diferentes obtenidos por la inyección de cantidades iguales de agua o disolución concentrada de ácido bórico; evidentemente se obtiene un mayor efecto del agua pura aumentando la concentración de la disolución, ocurriendo lo inverso en el caso de una inyección de ácido bórico.

Otro efecto resulta de las características no lineales del diagrama de la reactividad en función de la concentración para el tubo en forma de U empleado dentro del reactor, a causa del fenómeno de autoabsorción que tiene lugar para valores elevados de concentración de ácido bórico.

b) Los retardos causados por la circulación de la disolución tienen dos efectos principales que afectan grandemente al comportamiento dinámico del sistema. En primer lugar el retardo entre el punto de inyección y el reactor pone en peligro la estabilidad del sistema, siendo equivalente a un constante de tiempo grande; en segundo lugar se observa una tendencia hacia oscilaciones automantenidas a frecuencias del orden de $1/T$, donde T es el tiempo total de tránsito.

Se encontró que los reguladores de control proporcional, integral y derivado no eran adecuados para obtener un circuito de control con un comportamiento semejante al de una barra de control clásica con un servosistema de velocidad, y se proyectó un sistema más perfeccionado.

Se comprobó a continuación la validez del modelo lineal por simulación del sistema completo en una calculadora analógica; se encontró que algunos efectos no lineales tales como la saturación de apertura de la válvula son importantes en transitorios del reactor que implican inserciones de reactividad grandes y se obtuvieron valores más precisos para los parámetros de los reguladores.

El sistema de control se probó con éxito en el reactor AVOGADRO. Se experimentaron transitorios de potencia típicos del funcionamiento normal de un reactor de investigación, tales como inserciones de reactividad y variaciones de la demanda de potencia, obteniéndose una precisión mayor del 1% en la regulación del nivel de flujo neutrónico.

Se midió también la función de transferencia del sistema, estando los puntos experimentales en excelente acuerdo con el diagrama de Nyquist.

Some engineering studies on the analysis of kinetics and control of Tokai Atomic Power Station

By J. Miida,* N. Suda,* M. Toyoda,** T. Kagayama,** A. Takeda** and M. Yoshic***

In natural uranium gas-cooled reactors, the moderator temperature coefficient of reactivity becomes positive at a certain fuel burn-up level. With this positive temperature coefficient of reactivity the possibility of instability of the reactor as a whole, as well as of xenon-induced, spatial flux oscillations arises.

A series of analyses has been made on the kinetics, control and operational characteristics of the British type of gas-cooled reactor. The present numerical calculations have been made mainly for the Tokai Atomic Power Station, but the analytical results obtained are quite general for this type of reactor.

Preliminary analyses

Since the British type of gas-cooled reactors has a positive temperature coefficient of reactivity, the stability of this type of reactor is of concern. General criteria for the stability of reactors with two feedback paths have been derived [1]. Application of these criteria has revealed that the British type of reactor is unstable at high fuel burn-up [2]. Transient analyses by means of an analogue computer were made of three reactors, namely, Calder Hall, Hunterston and Tokai [2, 3]. Some of the transient responses obtained are shown in Figs. 1 and 2. The Hunterston and Tokai reactors have a graphite sleeve around each fuel element. The effect of the sleeve on the transient responses was also investigated. The reactor with the sleeve shows a more favourable behaviour as shown in Fig. 3, primarily because the change in the moderator temperature is reduced [2].

Due to the large size of the core, spatial oscillations of the flux may occur in these reactors. The threshold values of the moderator temperature coefficient for stability in each mode of spatial oscillation are shown in Fig. 4 [4-6]. Again the reactors with and without the sleeves are compared. In this case, however, the sleeve has an unfavourable effect, that is, higher mode oscillations are more easily excited in the reactor with sleeve. Analogue computer studies of spatial oscillations in axial as well as radial and azimuthal directions have been extensively performed [7, 8].

A view of modal transfer function of reactor spatial kinetics

Since the main aim in developing the kinetic theory of a reactor is reactor control, the transfer function is taken as the form of representation. On the other hand, numerous studies have been performed in the spatial kinetic problem in which, however, the treatment is not as simple, and is therefore not easily adaptable to ordinary control theory. From this point of view, some attempts have been made to extend the reactor transfer function to the spatial kinetic problem to permit its utilization by control engineers. A summary of this work is given in this paper.

In the spatial kinetic problem, spatial eigenfunctions are known to be one of the most promising approaches to the problem. One of the present authors tried to combine this with the transfer function, by designating a modal transfer function to each eigenfunction for a zero power reactor. Thus in this series of transfer functions the ordinary zero power reactor transfer function in lumped treatment is included as that related to the lowest eigenfunction. A distinctive feature of the modal transfer function is to incorporate the eigenvalue of the mode instead of spatial parameters.

Space dependent reactor kinetics can therefore be treated as the sum of an infinite series of independent fictitious reactors which have no spatial dependency [9].

The power reactor has a number of inherent feedback effects such as xenon poisoning, temperature coefficients and so forth. These effects introduce non-linear effects into the kinetic equation. But as far as small perturbations are concerned, we can make a linear approximation, as is well known. In this process the modal transfer function of these feedback effects can be derived for each mode as an approximation. The sector control rod system such as adopted in the Tokai reactor gives a space dependent feedback effect to the reactor. Even for such a system the modal transfer function can be derived for each eigenfunction [9].

Though an advantage of using the modal transfer

* Japan Atomic Energy Research Institute.
** Japan Atomic Power Co. Ltd.
*** Fuji Electric Manufacturing Co. Ltd.

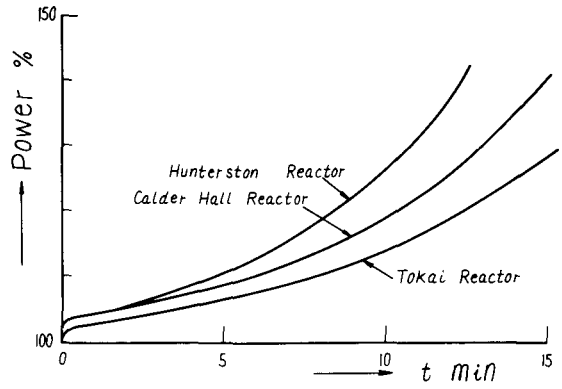


Figure 1. Comparison of transient power in different reactors (reactivity disturbance 1.2 × 10^{-4})

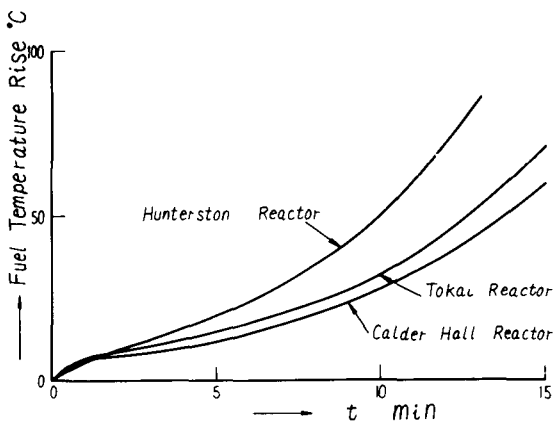


Figure 2. Comparison of fuel temperature rise in different reactors (reactivity disturbance 1.2 × 10^{-4})

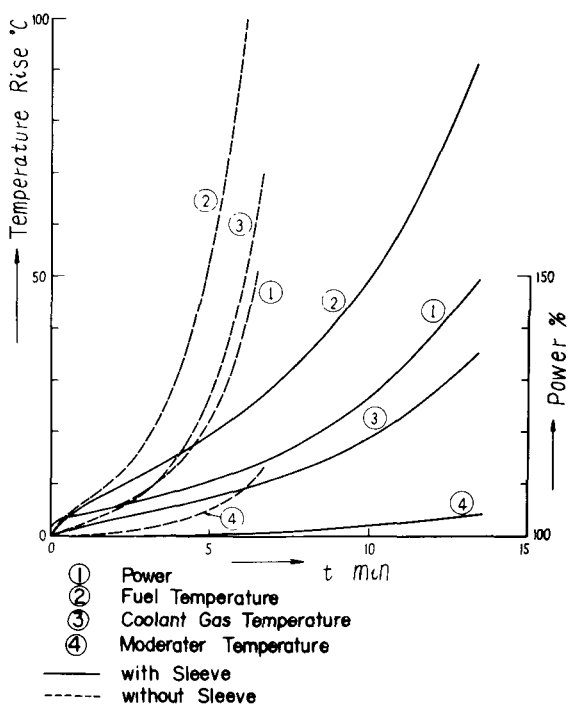


Figure 3. Comparison of responses of reactors with and without sleeve (reactivity disturbance 1.2 × 10^{-4})

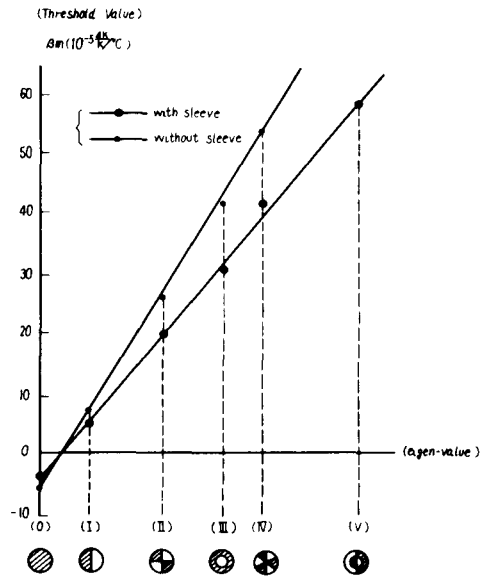


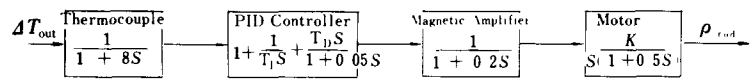
Figure 4. Threshold values of moderator temperature coefficient for instability

function is to treat each fictitious space independent reactor as an isolated system independent of the others, mutual inteference between them can only be neglected as an approximation. One such mutual interference arises from the linear approximation made of the feedback effect, but this is usually small and can be neglected. The only important case of this type of mutual interference is for axial spatial kinetics in which the forced coolant flow from bottom to top in the core gives rise to strong thermal connection between modes [10]. Another type arises from the sector control rod system, and finally there is the multi-region effect. The sector control rod system is an artificial device so that any system of infinite complication could be introduced. But fortunately in the present case we can apply the mode independent approximation to the actual control system excluding the axial kinetic problem [9]. The multi-region effect provides us with many interesting problems. Usually we can also neglect the mutual connection between modes arising from this effect. But once strong non-homogeneity of the core is explicitly taken into account, such as a large reflector part, mutual connection between modes introduced by the delayed neutron effect can be neglected no longer. In general a matrix representation should be adopted for such a mutual connecting system [11]. The elements of the matrix are the space independent transfer functions. The diagonal elements of the matrix are the modal transfer functions, already defined, and the off-diagonal elements represent the mutual connecting effect between modes. Since the mutual connection is a kind of feedback effect from one mode to another, the matrix representation can be formally dissolved to a feedback transfer function matrix and a forward transfer function matrix [11]. The feedback to the original mode is also included in this feedback matrix. Such generalization is help-

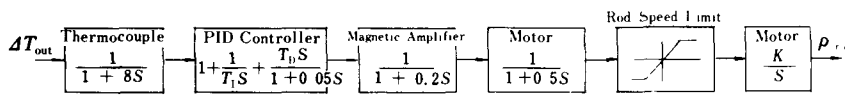
ful for our understanding of the space dependent kinetics, but at the same time we lose the advantage of simplicity, which was one of our original aims.

In order to relieve this situation, each mode is dissolved into groups of submodes, each of which corresponds to one of the characteristic roots of the transfer function of the main mode. We can eliminate the mutual connection by introducing these groups of submodes to replace the main modes [11]. But this time we sacrifice our other aim, which was to maintain the original form of the transfer function, which expresses a clear physical meaning. The transfer function to the submode is the first order delayed system.

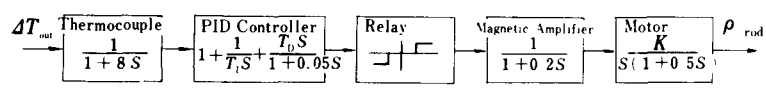
Thus both of the alternative ways of representing the reactor spatial kinetics involving mutual interference between modes have their respective merits and shortcomings. In our analysis of the Tokai reactor, mutual connection between modes is not as significant in the radial-azimuthal direction including the sector control rod system, and so the mode independent analysis was adopted. For the Tokai



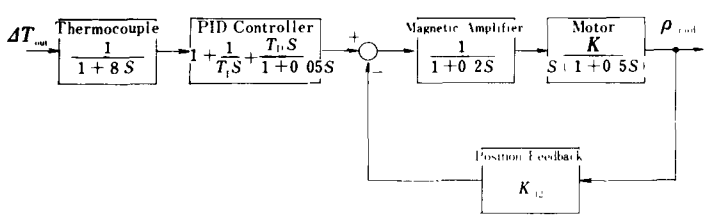
(a) Controller for Basic System



(b) Controller for Continuous Control with Rod Speed Saturation



(c) Controller for Discontinuous Control System



(d) Controller for Continuous Control with Position Feedback

Figure 5. Block diagrams of controller

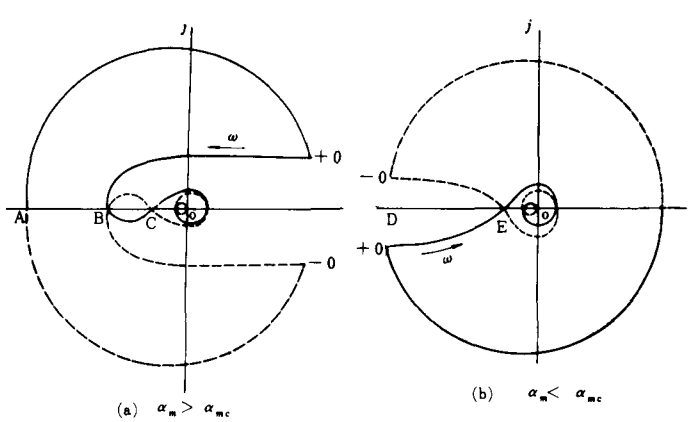


Figure 6. Vector locus of open loop transfer function $G_0(jw)$

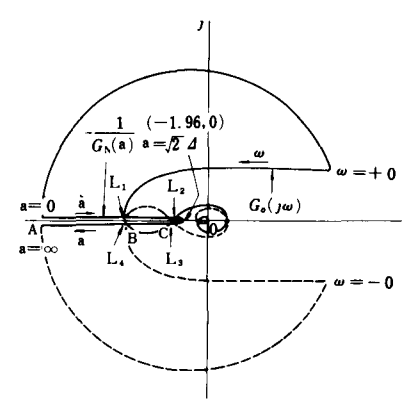


Figure 7. Vector locus of $G_0(jw)$ and $-1/G_N(a)$

Table 1. Comparison of optimum responses

System	T_I (s)	T_D (s)	K (10^{-5}/s °C)	K_{f2} (°C)	Transient peak in ΔT_{out} (°C)	Transient peak in Δq (%)	Settling time (s)	Effects of saturation in rod speed
Without (w/o) position feedback	∞	30	0.05	—	2.7	1.4	260	No effect if $R_{max} > 10^{-5}$/s
With (w/w) position feedback	80	20	3	10^4	0.85	0.9	200	No effect if $R_{max} > 2 \times 10^{-5}$/s. Very little effect for $R_{max} = 10^{-5}$/s

NOTES: Reactivity disturbance $\rho_{ex} = 2 \times 10^{-4}$. Settling time is defined to be the time after which ΔT_{out} remains within ±0.1°C.

reactor, the axial kinetic analysis is the only case in which we have to take into account the mutual connection between modes. And in this case, the matrix representation is useful for describing the effect of coolant flow and partially inserted control rod movement on mutual connection between axial modes [10].

Stability analysis of control systems

The Tokai reactor is controlled by measuring the gas temperature at the core outlet and moving the control rods according to its deviation from the reference temperature. The systematic stability analysis of such control systems by means of the generalized Nyquist criteria was initiated in 1959 [12]. The analysis was extended to various types of controllers as shown in Fig. 5 [13-16]. If the reactor is unstable and has one pole in the right half of the s-plane [1, 2], the continuous system (Fig. 5a) is unstable when the controller gain is either too high or too low, that is, in the Nyquist diagram of Fig. 6a the point (−1, 0) must be on segment BC of the real axis. For a stable reactor, however, the system is stable if the gain is low enough (Fig. 6b). In the actual system the control rod speed is always limited (Fig. 5b) but this saturation in speed does not significantly affect the system response. The stability of a discontinuous control system (Fig. 5c) was investigated by means of Kochenburger's describing function. The vector locus of the linear transfer function $G_0(j\omega)$ and of the inverse describing function $-1/G_N(a)$ are shown in Fig. 7. It is noted that four limit cycles L_1 to L_4 exist, of which L_1 and L_3 are stable and L_2 and L_4 are unstable. The control system either undergoes sustained oscillation corresponding to L_1 or L_3, or it diverges, depending upon the magnitude of the external disturbance introduced. An example of oscillations corresponding to L_3 is shown in Fig. 8. The effect of control rod position feedback (Fig. 5d) was also examined. The Nyquist diagrams have two different forms (Fig. 9) depending upon the magnitude of the feedback coefficient K_{f2}. If K_{f2} is too large (Fig. 9b) the system is always unstable, otherwise (Fig. 9a) the system is stable if the point (−1, 0) is on segment BC. Numerical computation shows that the stable region BC in Fig. 9a is larger than that of the conventional system in Fig. 6a. The optimum responses with rod position feedback are compared with those without the feedback in Fig. 10. The details of the responses were shown in Table 1. Thus as far as

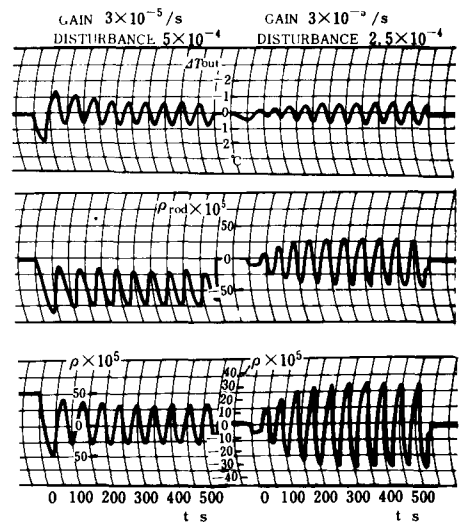


Figure 8. Examples of transient responses

this analysis is concerned, it is concluded that rod position feedback increases the stability and improves system performance.

Non-interacting controls for spatial instabilities [17] [18]

In order to control the spatial instabilities induced by xenon and the positive temperature effect, it is generally proposed to provide an independent control system in each of the several sectors. In this division plan, however, too much attention seems to be focussed on the individual controls in the divided sectors while the effects being exerted on the reactor as a whole are overlooked. Viewing therefore

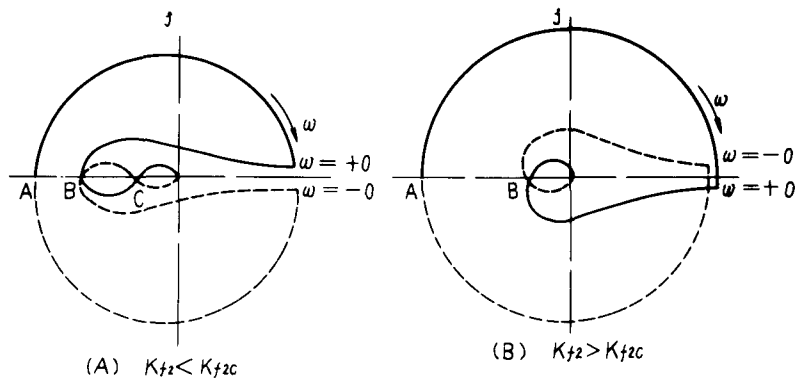


Figure 9. Vector locus of open loop transfer function

the reactor as a whole, consideration is given to developing an overall procedure of control system in which all the sector controllers work in combination.

Xenon oscillation being a phenomenon observed in large scale reactors, we can apply the Laplace transform directly to a one-group diffusion equation.

The resultant equation is a partial differential equation in respect of the space dependent variables with a parameter s (variable in frequency domains) instead of the time variable t. This method is quite different from the treatment of xenon oscillation used hitherto, and takes the axial heat transportation by coolant flow as a perturbation term. Hence by solving an eigenvalue problem in the frequency domains, we can get the frequency response of the reactor represented by an absolutely and uniformly convergent series in the complex plane of s, where eigenvalues are a function of frequency having a close relationship with the so-called modal transfer function.

Now making a hypothetical division of the reactor with the centre as 0-domain and Q radial domains designated 1 to Q-domains, we take the reactivity variations due to control rod motion and coolant flow variations as reactor system input, i.e., the manipulated variables. As reactor system output, i.e., the controlled variables, we consider the average outlet temperature in each domain and the neutron flux, from which we obtain the block diagram of the whole system illustrated in Fig. 11, where the

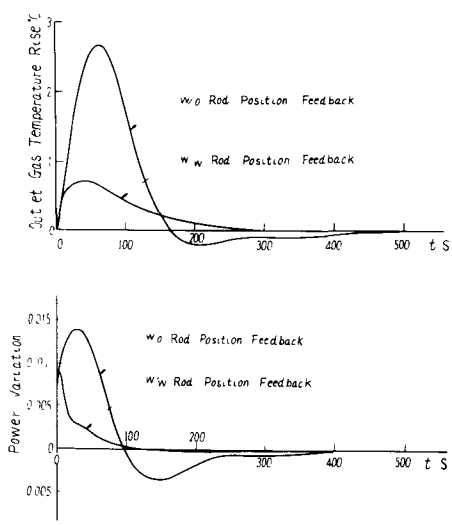


Figure 10. Comparison of optimum responses

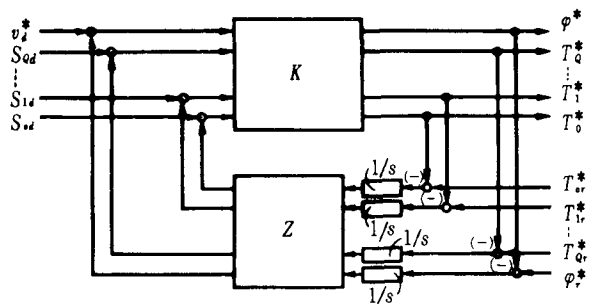
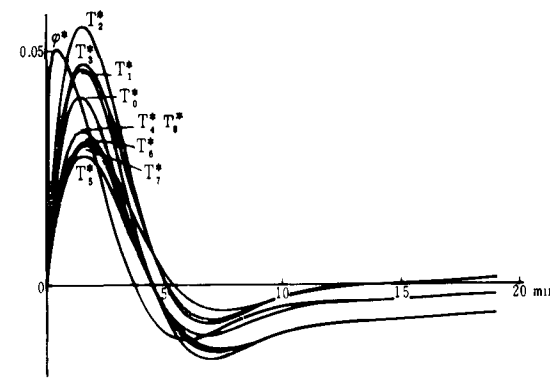
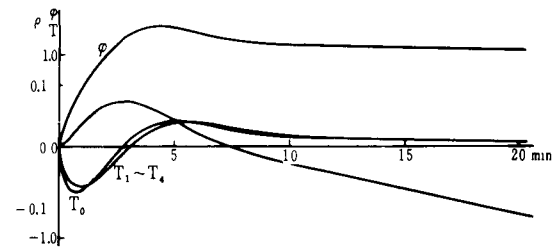


Figure 11. Block diagram of whole system



(a) Response to Reactivity Step Disturbance



(b) Response to Step Change in Coolant Flow

Figure 12. Response to step change

reference and the disturbance are respectively denoted by the suffixes r and d. In addition, we show the integral action separately in order to eliminate offset in the controlled variables.

In view of the symmetric arrangement of control rods and temperature measuring instruments, the transfer function of the reactor K is expressed by the symmetrical and recurrent matrix, the elements of which can be obtained by calculating the expansion coefficients of the reactor frequency response obtained previously. Since it is natural to assume that the controller matrix Z is symmetrical and recurring in a similar manner, symmetry and recurrence are maintained in the KZ matrix, which might well be called the loop transfer matrix.

Consequently, as is well known, the KZ matrix undergoes principal axis transformation by the characteristic unitary matrix, where the characteristic equation of the whole system is invariant. Further, if the diagonal elements of the transformed matrix are taken to be equal to each other, the KZ matrix proves to be diagonal which satisfies the noninteraction condition; at the same time calculation of the roots of the characteristic equation is greatly simplified, and enables us to synthesize easily the control system by drawing the root loci.

Applying this procedure to the Calder Hall type of reactor, we have the analogue computer solutions shown in Figs. 12a and b, in which we can discern co-operative control action.

Dynamics and control of power stations

Outline of power plant

Figure 13 shows a partial diagram of the power plant which comprises a reactor having four steam raising units (heat exchangers) and two turbo-generators. The gas is circulated by gas circulators driven by back pressure steam turbines.

The steam pressure at the inlet of the low pressure steam turbine is held constant by a gas flow controller and thus heat exchanger output is adjusted to demanded power. Steam pressure control by high pressure range and drum level control are also shown in this figure.

Dynamics of each bank of heat exchangers

As an illustration, several dynamic equations are selected for a superheater and an evaporator [19].

(*a*) For mean temperature of gas, steel wall and steam in a high pressure superheater

$$C_{p1}\frac{dT_{p1}}{dt} = -U_1(T_{p1}-T_{m1}) + \frac{c_{p1}G_1}{4}(T_o - T_i),\ C_{p1} = c_{p1}H_{p1},\ T_{p1} = \frac{T_o+T_i}{2}$$

$$C_{m1}\frac{dT_{m1}}{dt} = U_1(T_{p1}-T_{m1}) - U_1'(T_{m1}-T_{v1}),\ C_{m1} = c_{m1}I_{m1},\ T_{v1} = \frac{T_{vH}+T_{sH}}{2}$$

$$C_{v1}\frac{dT_{v1}}{dt} = U_1'(T_{m1}-T_{v1}) - \frac{c_{v1}g_H}{4}(T_{sH}-T_{vH}),\ C_{v1} = c_{v1}S_{v1}$$

(*b*) For heat transmission to boiling water in a high pressure evaporator

$$U_3'(T_{m3}-T_{vH}) - (h_{fH}-h_{5H})\frac{G_{5H}}{4} - (h_{vH}-h_{fH})\frac{g_H}{4}$$

$$= \left[\left(W_H\frac{dh_{fH}}{dp_H} + w_H\frac{dh_{vH}}{dp_H}\right) - (h_{vH}-h_{fH})\frac{w_H dv_{vH}}{v_{vH}dp_H}\right]\frac{dp_H}{dt}$$

Symbols in the above equations are as follows, each suffix expressing a position indicated in Fig. 13:

T,T': Temperature

U,U': Heat transfer coefficient

G, g_H, G_{5H}: Mass flow rate of gas, high pressure steam and feed water

C_{p1}, C_{m1}, C_{v1}: Specific heat of gas, steel wall and steam

H_{p1}, I_{m1}, S_{v1}: Weight of gas, steel wall and steam

h: Enthalpy

v: Specific volume

W, w: Water and steam content in evaporator

p: Pressure

t: Time.

These equations are linearized, so that the approximate transfer function for each bank is determined from the form of indicial response given by applying a step input.

Dynamics of power plants

Dynamic equations of turbo-generator, individual controllers etc. are combined with the above heat exchanger dynamics, and an overall control system for the whole installation excepting the reactor can be established [19]. One example of transient response of the power plant is shown in Fig. 14. Ten per cent change corresponds to 0.2 c/s change in this case. In this study, the gas temperature T_0 at reactor outlet is assumed constant. Preliminary control plans can be drawn up in this manner.

Analysis of large load changes

The dynamic behaviour of the reactor during large load changes, both positive and negative, were

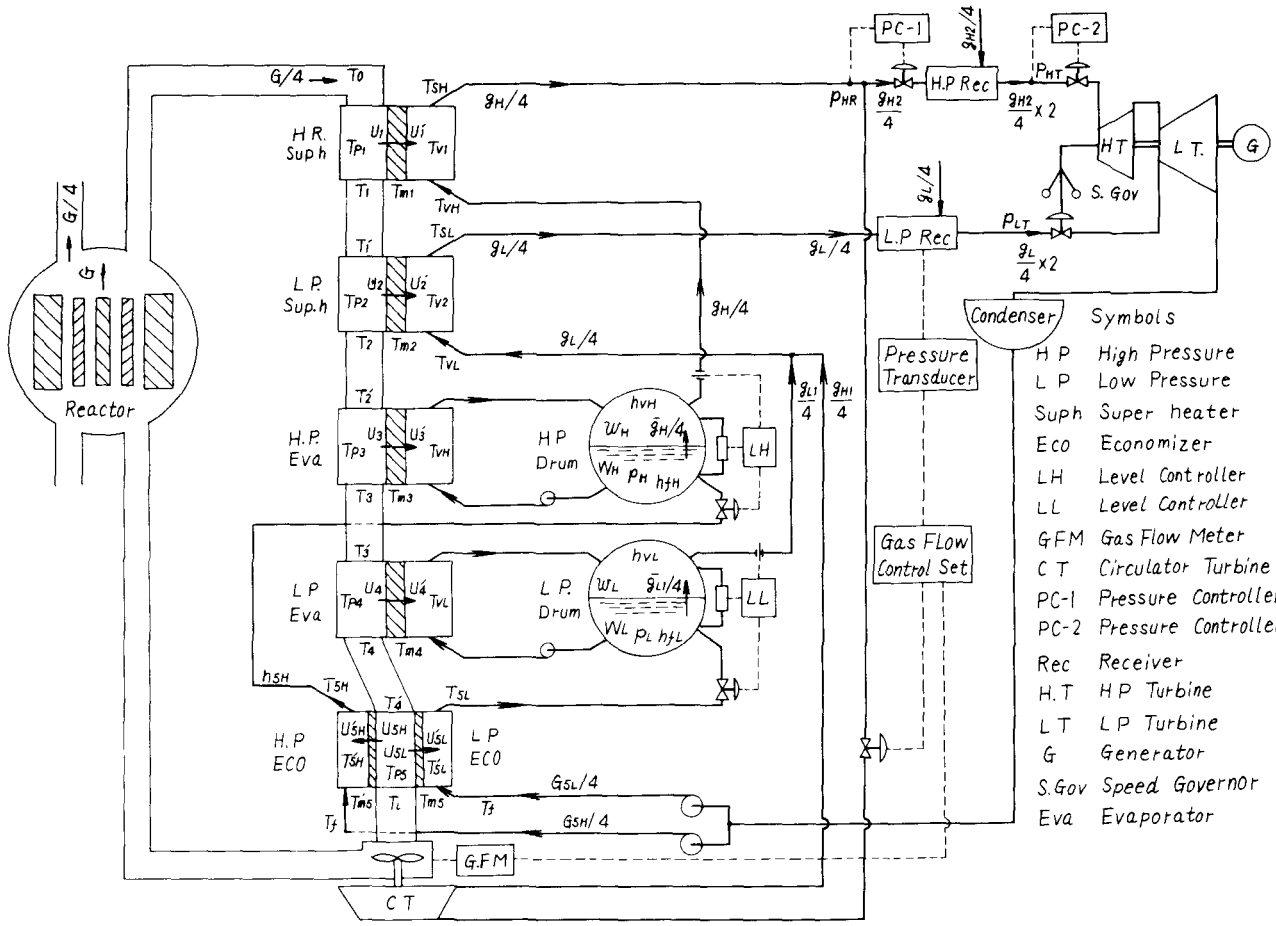


Figure 13. Skeleton diagram of power plant

studied by means of an analogue computer [20-23]. Both continuous and discontinuous systems were investigated (Figs. 5a and c). Some of the conclusions obtained are as follows.

(*a*) The stable region of the control system is determined. Optimum values of controller parameters are obtained as shown in Table 2;

(*b*) The rate of normal load change is expected to be 5%/min. Load changes at a rate twice as rapid are easily controlled;

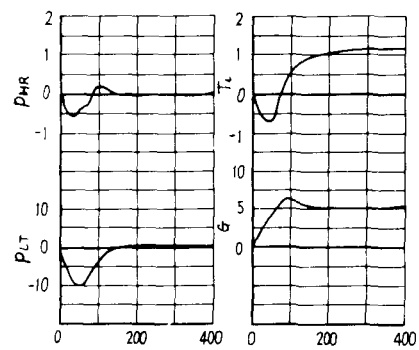


Figure 14. Transient response for 10% increase of low pressure steam (g_L). Ordinate (% change), abscissa (s); p_{HR}, p_{LT}: pressure indicated in Fig. 13; T_i: temperature at inlet of reactor

Table 2. Optimum controller parameters for large load changes

Controller	Gain	T_I	T_D
Continuous	$K_c=0.2\times10^{-5}$/s °C	∞	50 s
Discontinuous	$K_d=1\times10^{-5}$/s °C	∞	50 s

(*c*) Generally speaking the system is found more stable at higher power levels;

(*d*) The reactivity worth required for the control rods is −1.7% to increase power from 25% to 100% (full power) and +2.4% to decrease power from 100% to 25%;

(*e*) The maximum rod speed required is found to be $\pm4-5\times10^{-6}$/s to decrease and to increase power;

(*f*) Comparisons are made between a reactor with positive temperature coefficient and that with a negative one. There are no significant differences in the transient behaviour of power and temperature, except that the control rods move in opposite directions;

(*g*) Continuous control is favourable from the viewpoint of stability, compatibility with excessive

Table 3. Upper limit of scram levels from safety considerations

	Continuous rod withdrawal				Failure of gas circulators		
	During start-up		At full power		2	3	4
Disturbance	0.3 $\delta k/k/s$	1.0 $\delta k/k/s$	1.0 $\delta k/k/s$	1.3 $\delta k/k/s$	100→50%	100→25%	100→0%
Period	20	10	—	—	—	—	—
Excess power (%)	32	58	169	171	—	—	—
Excess fuel cladding temperature (°C)	495	488	573	572	577	555	497
Excess outlet temperature (°C)	439	407	480	479	518	490	—

Table 4. Peak values of transients due to disturbances during normal operation

	Refueling	Control rod withdrawal	Drop of fuel rod	Failure of a gas circulator
Disturbance	0.5 $\delta k/k/s \times 2$ min	0.05 $\delta k/k/s \times 30$ min	20 $\delta k/k$ step	−30% step in flow
Period (s)	~ 1 000	∞	~ 100	—
Power (%)	105	101	105	—
Fuel cladding temperature (°C)	460	450	455	483
Outlet gas temperature (°C)	401	394	398	429

Table 5. Upper and lower limits of scram levels obtained from Tables 3 and 4

Scram signals	Upper limit	Lower limit
Short period (s)	20	100
Excess power (during start-up) (%)	32	—
Excess power (at full power) (%)	169	105
Excess fuel cladding temperature (°C)	488	483
Excess outlet gas temperature (°C)	479	429

rate of load change and so on. The transient responses with optimum setting of controller parameters do not differ significantly;

(*h*) The maximum rate of change in fuel temperature is approximately 0.3 °C/s;

(*i*) If the load is decreased exponentially rather than linearly with time, the transient change in fuel temperature is reduced.

Analysis of abnormal conditions

Analogue computer studies of transients under abnormal conditions were made in order to determine the appropriate settings for the scram levels [24]. The scram levels should be low enough to prevent the fuel cladding temperature from exceeding the melting point even if with the occurrence of any of the following accidents: (i) start-up accidents, (ii) continuous rod withdrawal at power or (iii) failure of more than two gas circulators. On the other hand they should be high enough so that the reactor is not scrammed following any disturbances which may take place during the normal operation of plant, such as: (i) refuelling, (ii) control rod withdrawal during refuelling, (iii) drop of a single fuel rod by mishandling or (iv) failure of a gas circulator. In the analysis, four kinds of scram signal are postulated: (i) short reactor period, (ii) excess reactor power, (iii) excess fuel cladding temperature and (iv) excess outlet gas temperature. The appropriate settings thus determined are summarized in Tables 3-5.

REFERENCES

1. Miida, J., *et al.*, Nuclear Sci. Eng., *11*(1), 55 (1961).
2. Miida, J., *et al.*, JAERI report 1006-B (1959).
3. Miida, J., *et al.*, Proceedings of the Third Symposium on Nuclear Energy, Paper II-11, pp. 143-153, National Science Council of Japan (1959).
4. Mochizuki, K., JAERI report 1006-C (1959).
5. Mochizuki, K., *et al.*, Ref. [3], Paper II-16, pp. 175-180.
6. Mochizuki, K., *et al.*, Nuclear Sci. Eng., *7*, 336 (1960).
7. Mochizuki, K., *et al.*, National Nuclear Congress Paper (1960) B 24, not published.
8. Mochizuki, K., *et al.*, Annual Meeting of the Japan Institute of Electrical Engineers (JIEE), July 1960, Paper 550, not published.
9. Takeda, A., J. Atomic Energy Soc., Japan, *2*(4), 175 and UKAEA report AERE-TRANS 881 (1) (1960).
10. Takeda, A., *ibid.*, *4*(6), 377-385 (1962).
11. Takeda, A., *ibid.*, *2*, 523 and UKAEA report AERE-TRANS 888 (2) (1960).

12. Suda, N., JAERI, Inst. & Controls Lab. Internal Memo 24 (1959).
13. Miida, J., *et al.*, National Nuclear Congress Paper, 1960, B27, not published.
14. Miida, J., *et al.*, Automatic Control, *7*(3), 14 (1960).
15. Suda, N., *et al.*, Annual Meeting of Atomic Energy Soc. of Japan C48 (1963).
16. Suda, N., *et al.*, JAERI report 1042 (1963).
17. Kagayama, T., Annual Meeting of JIEE, 1959, Paper 345, not published.
18. Kagayama, T., J. Atomic Energy Soc., Japan, *2*(2), 78-88 and UKAEA report AERE-TRANS 879 (1960).
19. Miida, J., *et al.*, Internal report on the Undertaken Works for JAPC by JAERI (1961).
20. Miida, J., *et al.*, National Nuclear Congress, 1960, Paper B31, not published.
21. Suda, N., *et al.*, Annual Meeting of JIEE, July 1960, Paper 552, not published.
22. Miida, J., *et al.*, J. Atomic Energy Soc. Japan, *2*(12), 742-749 (1960).
23. Miida, J., *et al.*, *ibid.*, *3*(1), 33-39 (1961).
24. Japan Atomic Power Co. Technical Report No. 7 (1963).

ABSTRACT - RÉSUMÉ - АННОТАЦИЯ - RESUMEN

A/664 Japon

Quelques études techniques sur les analyses de cinétique et de contrôle à la Centrale nucléaire de Tokai

par J. Miida *et al.*

Une série d'analyses a été effectuée sur la cinétique, le contrôle et les caractéristiques d'opération des réacteurs de type britannique refroidis par un gaz et ayant un coefficient de température positif de réactivité. Ces analyses préliminaires ont fourni des données quantitatives sur les réponses transitoires des réacteurs de ce type, en même temps que des conclusions générales sur la stabilité des réacteurs avec des rétroactions relatives à la température et au xénon, ainsi que sur l'effet des manchons de graphite sur la stabilité. Des recherches poussées ont été effectuées sur les oscillations du flux spatial, provoquées par le xénon dans les directions radiale, azimutale et axiale. On a ainsi trouvé que la méthode classique employée pour simuler le comportement dynamique du réacteur était quelquefois inadéquate. C'est pourquoi des recherches ont été effectuées sur les fonctions de transfert dépendant de l'espace à la fois de la cinétique nucléaire et des transitoires de température. La représentation par fonctions de transfert de la cinétique nucléaire dépendant de l'espace, s'est révélé un bon moyen pour la synthèse de système de contrôle exposée ci-dessous.

Les analyses de stabilité et de performance du système de contrôle de la température ont été effectuées à l'aide du critère généralisé de Nyquist et de la méthode de la fonction de description de Kochenburger. En premier lieu, les conditions de stabilité aussi bien que la disposition optimale du dispositif de contrôle ont été obtenues pour les dispositifs classiques. On en a conclu que: *a*) le système continu est instable lorsque le gain du dispositif de contrôle est soit trop élevé, soit trop bas; *b*) la limitation de la vitesse de la barre de contrôle n'affecte pas d'une façon significative la réponse du système, et *c*), lorsque le contrôle discontinu est adopté, le système diverge ou bien subit des oscillations entretenues, correspondant aux cycles limites stables. Ensuite, on a examiné l'effet produit lorsqu'on a une réaction de position de la barre de contrôle sur le dispositif de contrôle. On a noté que ce système à réaction de position de la barre avait une stabilité plus grande et des performances meilleures que celles du système classique de contrôle.

Afin de contrôler l'oscillation spatiale provoquée par le xénon, des dispositifs de contrôle avaient été affectés à chacun des secteurs du cœur. Une méthode a été développée pour la synthèse du contrôle sans interaction entre ces dispositifs au moyen de la transformation unitaire de la matrice de la fonction de transfert. En plus des résultats analytiques généraux, on a présenté des solutions obtenues au moyen d'un calculateur analogique afin de démontrer que le contrôle est fait sans interactions.

On a fait aussi des recherches sur la dynamique du système de production de vapeur et du turbo-alternateur. Les variations transitoires de température et de pression du système, lors des changements de charge, ont été examinées.

On a étudié le comportement dynamique du réacteur pour de grands changements de puissance. On a obtenu le taux maximal admissible de changement de la puissance et la valeur de réactivité demandée aux barres de contrôle.

Des analyses ont été effectuées sur les accidents de démarrage, le retrait continu de barres pendant le fonctionnement en puissance et les accidents de perte de réfrigérant. Elles ont fourni des informations nécessaires sur la disposition appropriée des niveaux d'arrêt brusque.

A/664 Япония

Некоторые исследования технологии и анализ кинетики и регулирования атомной электростанции в Токаи-Мура

Ю. Миида *et al.*

Проведен ряд анализов кинетики, регулирования и эксплуатационных характеристик реак-

торов типа английских с газовым охлаждением, имеющих положительный температурный коэффициент реактивности. Предварительный анализ позволяет получить количественные данные по переходным реакциям реакторов этого типа, а также сделать общие выводы о стабильности реакторов с температурной обратной связью и обратной связью, обусловленной отравлением ксеноном. Рассмотрено влияние графитовых втулок на стабильность. Проведены обширные исследования по пространственным колебаниям потока, вызванным отравлением ксеноном, в радиальном, азимутальном и аксиальном направлениях. Выявилось, что обычный подход-имитация динамического поведения реактора иногда неприемлем. Следовательно, были проведены исследования по зависящим от пространства передаточным функциям как ядерной кинетики, так и температурных переходов. Представление передаточной функции для ядерной кинетики, зависящей от пространства, оказалось удобным средством для синтеза системы регулирования, что описано ниже.

Анализ стабильности и характеристик системы регулирования по температуре был проведен с использованием обобщенного критерия Найквиста и метода описательных функций Кохенбургера. Прежде всего для обычных регулирующих устройств были получены условия стабильности, а также оптимальные установки приборов управления. Установлено: *a*) что постоянная система нестабильна, если усиление прибора управления слишком высокое или слишком низкое; *b*) что насыщение скорости регулирующих стержней не очень сильно влияет на срабатывание системы и *c*) если принять непрерывное регулирование, система либо расходится, либо испытывает сдерживаемые колебания, соответствующие пределам стабильного цикла. Изучено также влияние наличия обратной связи в регулировании положений стержней на приборах управления. Отмечается, что система с обратной связью положения регулирующих стержней обладает повышенной стабильностью и более совершенными характеристиками по сравнению с обычными системами регулирования.

Чтобы регулировать пространственные колебания потока, обусловленные отравлением ксеноном, были установлены регулирующие устройства, каждое на одном из секторов активной зоны. Был разработан метод объединения независимого регулирования между этими регулирующими устройствами путем унитарного преобразования матрицы передаточных функций. Кроме общих аналитических результатов представлены решения на электронной вычислительной машине, показывающие независимое регулирование.

Исследованы также динамика системы генерации пара и турбогенератора. Изучены переходные колебания температуры и давления в системе, связанные с изменениями электрической нагрузки.

Изучено динамическое поведение реактора во время больших изменений мощности. Определены максимально допустимая скорость изменения мощности и цена реактивности, необходимая для регулирующих стержней.

Проведен анализ неисправностей при запуске непрерывного выведения стержней на мощности и аварий, связанных с потерей теплоносителя. Это позволило собрать необходимые данные для определения соответствующего уровня для аварийной системы.

A/664 Japón

Algunos estudios de ingeniería sobre el análisis de la cinética y el control de la Central Nuclear de Tokai

por J. Miida *et al.*

Se han realizado una serie de análisis sobre la cinética, el control y las características de funcionamiento de los reactores refrigerados por gas de tipo británico con coeficiente positivo de reactividad con respecto a la temperatura. Los análisis preliminares proporcionan información cuantitativa sobre la respuesta transitoria de los reactores de este tipo así como conclusiones generales sobre la estabilidad de reactores con realimentación de temperatura y xenón y el efecto de la envuelta de grafito sobre la estabilidad. Se realizaron amplias investigaciones sobre las oscilaciones espaciales del flujo, inducidas por xenón, en las direcciones radial, azimutal y axil. Se encontró que a veces no es adecuado el método clásico empleado para simular el comportamiento dinámico del reactor. Por esto, se realizaron investigaciones sobre las funciones de transferencia con dependencia espacial de la cinética nuclear y de los transitorios de temperatura. La representación por funciones de transferencia de la cinética nuclear con dependencia espacial ha demostrado ser un medio adecuado para la síntesis del sistema de control descrito a continuación.

Los análisis de la estabilidad y comportamiento del sistema de control de temperatura se realizaron empleando el criterio generalizado de Nyquist y el de las funciones descriptivas de Kochenburger. En primer lugar se obtuvieron las condiciones de estabilidad así como las condiciones óptimas de los aparatos de control corrientes. Se llegó a la conclusión de que: *a*) el sistema continuo es inestable cuando la ganancia del aparato de control es muy alta o muy baja, *b*) la saturación de la velocidad de la barra de control no afecta significativamente a la respuesta del sistema y *c*) cuando se adopta control continuo, el sistema es divergente o sufre oscilaciones sostenidas que corresponden a los ciclos límites estables. Se estudió también el efecto de realimentación de la posición de la barra al circuito de control. Se

notó que el sistema con realimentación de la posición de la barra de control proporciona un aumento en estabilidad y un comportamiento mejor del sistema en comparación con el sistema clásico de control.

Para controlar las oscilaciones espaciales provocadas por el xenón se emplearon grupos de control asignados a cada una de las zonas del núcleo. Se desarrolló un método para síntesis del control sin interacción entre estos conjuntos de control por medio de una transformación unitaria de la matriz de la función de transferencia. Además de los resultados analíticos generales, se presentan soluciones de calculadora analógica para demostrar la posibilidad de control sin interacción.

Se investigó también la dinámica del sistema de producción de vapor y del turbogenerador. Se examinaron variaciones transitorias de la temperatura y presión del sistema cuando éste queda sometido a las variaciones de carga.

Se estudió el comportamiento dinámico del reactor durante cambios grandes de potencia. Se obtuvieron la velocidad máxima permisible de cambio de potencia y el valor en reactividad necesario para las barras de control.

Se realizaron análisis de accidentes de arranque, extracción continua de barra en carga y pérdida de refrigerante. Estos análisis proporcionaron la información necesaria para la selección de los niveles adecuados de parada rápida.

A reactivity oscillator for swimming pool reactors

By M. N. Qazi*

Although there are various methods for the experimental determination of the frequency response of a nuclear reactor [1], the reactivity oscillation and the random noise techniques are by far the most popular. The choice of the technique largely depends on the type of the reactor of which the frequency response is to be measured. For swimming pool reactors, which are becoming increasingly popular as valuable tools of research and education with the research institutes and universities around the world, the method of reactivity oscillation seems to be better suited. Some of the important considerations which favour the oscillation method are listed below.

(*a*) In the random noise technique, the basic assumption that the reactor spectrum driving function is *white* throughout the frequency range is not valid as shown by Griffin and Randall [2]. They have recently obtained data on the Sodium Reactor Experiment (SRE) which shows that this function is not white at frequencies lower than 0.1 c/s for reactors running at low powers;

(*b*) The accuracy of the noise technique is limited due to the uncertainties resulting from the disturbances which enter the system [3];

(*c*) The noise technique can only be used to obtain the amplitude portion of the frequency response whereas the oscillation method is capable of furnishing both the amplitude and phase information;

(*d*) In a swimming pool reactor, the core is easily accessible for the location of the reactivity oscillator.

There are, however, certain problems associated with the oscillation technique which require careful consideration. The design of the oscillating device must be such that the resulting reactivity oscillations will be between certain well-defined limits, set by the needs of the experiment, and at the same time meet the stringent requirements imposed by reactor safety considerations. Then there is the problem of activation of the device, which has to be kept at a minimum.

THEORY

Basic reactor kinetic equations are [4]

$$\frac{dn}{dt} = \frac{n}{\ell^*}\delta k - \sum_{i=1}^{6} \frac{dc_i}{dt} \qquad (1)$$

and

$$\frac{dc_i}{dt} = \frac{\gamma_i \beta_i}{\ell^*} n - \lambda_i C_i \qquad (2)$$

where

n = neutron flux ($cm^{-2}s^{-1}$) or power level (watts)
δk = excess reactivity ($\Delta k/k$)
ℓ^* = prompt neutron lifetime (s)
β_i = true fraction of delayed neutrons in the ith group
c_i = concentration of the ith group delayed neutron precursors (cm^{-3})
γ_i = relative effectiveness (in producing fission) of the ith group delayed neutrons compared with prompt neutrons
λ_i = decay constant for the ith group delayed neutron precursors (s^{-1}).

These equations are first linearized by substituting

$$n = n_0 + \delta n$$

and

$$c_i = c_{i0} + \delta c_i$$

and then after simplification they are Laplace transformed. Assuming zero initial conditions, these transformed equations are

$$s\delta n(s) = \frac{n_0}{\ell^*}\delta k(s) - s\sum_{i=1}^{6} \delta c_i(s) \qquad (3)$$

and

$$s\delta c_i(s) = \frac{\gamma_i \beta_i}{\ell^*}\delta n(s) - \lambda_i\, \delta c_i(s) \qquad (4)$$

The frequency response or the transfer function in the usual form is given by

$$\frac{\delta n(j\omega)}{\delta k(j\omega)} = \frac{n_0/\ell^*}{j\omega\left[1 + \sum_{i=1}^{6} \frac{\gamma_i \beta_i}{\ell^*(j\omega + \lambda_i)}\right]} \qquad (5)$$

where

$$j = \sqrt{-1}$$

and

ω = angular frequency (radians/s)

The only restriction on expression (5) is that due to the process of linearization. This expression is valid only if the power level fluctuations are limited to a few per cent of the steady state value.

The approximate reactor transfer function equation using a single group of delayed neutrons is

* Atomic Energy Centre, Lahore.

easily derived if the following replacements are made in Eq. (5).

$$\lambda_i = \bar{\lambda}$$

and

$$\sum_{i=1}^{6} \gamma_i \beta_i = \bar{\beta}$$

where $\bar{\beta}$ is the total effective fraction of all the delayed neutrons and $\bar{\lambda}$, the properly averaged value of the decay constant, is given by

$$\bar{\lambda} = \bar{\beta} \Big/ \sum_{i=1}^{6} \frac{\gamma_i \beta_i}{\lambda_i}$$

This substitution gives

$$\frac{\delta n(j\omega)}{\delta k(j\omega)} = \frac{n_0}{\ell^*} \cdot \frac{(j\omega + \bar{\lambda})}{j\omega(j\omega + \bar{\lambda} + \bar{\beta}/\ell^*)} \qquad (6)$$

Since $\bar{\lambda}$ is of the order of 0.1 and $\bar{\beta}/\ell^*$ of 100, for all practical purposes $\bar{\lambda} << \bar{\beta}/\ell^*$. Therefore Eq. (6) reduces to

$$\frac{\delta n(j\omega)}{\delta k(j\omega)} = \frac{n_0}{\ell^*} \cdot \frac{(j\omega + \bar{\lambda})}{j\omega(j\omega + \bar{\beta}/\ell^*)} \qquad (7)$$

Using the data of Keepin and Wimett [5] on the delayed neutron parameters, $\bar{\lambda}$ was calculated to be 0.077 and the value of $\bar{\beta}$ was taken to be 0.008 which was determined experimentally for a compact loading of the Bulk Shielding Reactor 1, at the Oak Ridge National Laboratory [6].

Equations (7) and (9) were both coded in FORTRAN for the Pennsylvania State University's digital computer IBM-7074 to calculate the theoretical results of the transfer function for different ℓ^* values.

APPARATUS

The entire set-up for the measurement of ℓ^* is shown schematically in Fig. 1. It can be divided into three major systems:

(i) Oscillator drive system;
(ii) Oscillatory mechanism;
(iii) Output measuring system.

Oscillator drive system

This system consisted of a variable speed DC drive unit of the Servo-Tek Products Company, a speed reducer unit, a pair of Selsyn servo motors of the Bendix Aviation Corporation and a variable voltage supply.

The ¼ hp shuntwound DC control motor of the drive unit was rated for a maximum output speed of 3 600 rpm. It was controlled by an infinitely adjustable, ten-turn precision potentiometer. Since the direct coupling of the motor could effectively be used down to 60 rpm only, a specially designed and machined pulley system was employed to suit the requirements of the experiment. Use of this pulley system (speed reducer unit) made it possible to achieve speeds less than 1 rpm. This speed reducer unit was mechanically coupled to the master Selsyn servo motor and mounted on a single aluminium base plate. Belts of the speed reducer unit were required to be changed only once during the entire operation.

The slave Selsyn servo motor was placed at one end in the aluminium tube which carried the oscillatory mechanism. The two servo motors were connected by five, thirty-foot long leads, placed in a ¾ inch diameter Tygon tube to make them water-tight.

Oscillatory mechanism

Reactivity oscillations were obtained by rotating a 3⅜ inch diameter aluminium disc which was partially covered by 20 mil thick cadmium sheets. These cadmium sheets covering two opposite quadrants of the disc were mechanically secured to stop them falling apart during high speed rotation of the disc—a situation undesirable for obvious reasons of reactor safety. The aluminium disc was mounted at one end of a ¼ inch diameter and 18 inch long steel shaft with the help of a set screw. The other end of the shaft was coupled to the slave motor. This entire unit consisting of the cadmium carrying disc, the steel shaft and the slave motor were housed in a water-tight aluminium tube specially designed for this purpose and referred to throughout this report as the oscillator. This oscillator is shown schematically in Fig. 2. It can be seen that the aluminium housing tube could be opened at either end by

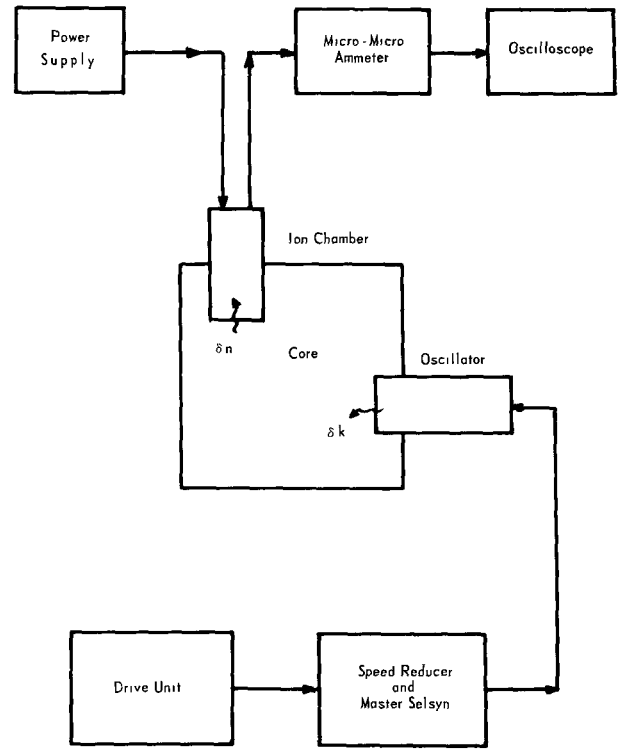


Figure 1. Block diagram of the apparatus

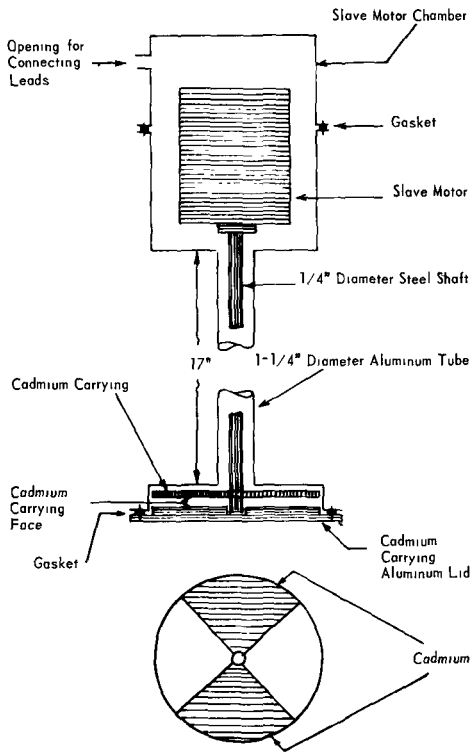


Figure 2. Schematic diagram of the oscillator

removing the lid which is held in position by screws. This provided access to the slave motor and the aluminium disc, for carrying out inspection, adjustment and replacement of components as necessary. The inside of the lid facing the aluminium disc also carried two symmetrically placed cadmium quadrants identical to those on the disc. When this lid was held in position and the disc rotated, the two sets of cadmium quadrants alternately covered and exposed each other resulting in the variation of net exposed cadmium surface area from a minimum of two quadrants to a maximum of four. These oscillations in the effective amount of the cadmium resulted in the oscillatory change in the core reactivity.

The frequency of the reactivity oscillations being twice that of the disc, it was possible with this system to achieve reactivity oscillation frequencies higher than 100 c/s.

Since the disc was removable the oscillator had great flexibility. It was possible to try a number of discs having various amounts of cadmium along with their respective lids to determine their suitability experimentally.

In the actual experiment, the oscillator was mounted horizontally on the instrument bridge in the reactor pool with its cadmium carrying end facing the reactor core. The oscillator was then lowered into the pool and brought against the core face.

The peculiar shape of the oscillator and its horizontal position against the core restricted the intense neutron exposure to only one end of the device and the major portion was shielded by water.

Output measuring system

A compensated ion-chamber was used to detect the power level fluctuations. The signal from the ion-chamber was fed into a model 410C Keithley micro-microammeter using RG62 A/U coaxial cable. The micro-microammeter is a sensitive current measuring device able to measure extremely small currents. The output of this instrument was displayed on a type 53IA Tektronix oscilloscope using a type Z plug-in differential comparator which made it possible to see only the differential component of the signal. The oscillations on the screen of the oscilloscope were recorded on a Polaroid camera.

RESULTS AND DISCUSSIONS

The apparatus was bench tested and calibrated for the entire frequency range with the help of a strobotac. The net change in the reactivity worth of the oscillator was experimentally determined using the safety rod No. 3 of the Pennsylvania State Reactor control system. This turned out to be 0.01% $(\Delta k/k)$, well below the value 0.1% $(\Delta k/k)$ stipulated by the Safeguards Committee for this reactor. This value of reactivity would result in approximately 5% of the power level fluctuations at a frequency of 0.01 c/s [7] and hence was considered satisfactory for the requirements of the linearization process.

To measure the amplitude transfer function, the reactor was operated at 20 watts with core loading No. 38 [8]. Measurements were made on Monday mornings when the residual power level due to fission product gammas was less than 3 watts. On other mornings this level was usually more than 10 watts.

Four runs were conducted on different dates scattered over a period of one month. These results are shown in Fig. 3 along with those obtained theoretically for l^* values of 55, 65 and 75 micro seconds. For comparison, the experimental and theoretical results were both arbitrarily normalized to zero decibels at 1 c/s. It is clear from these

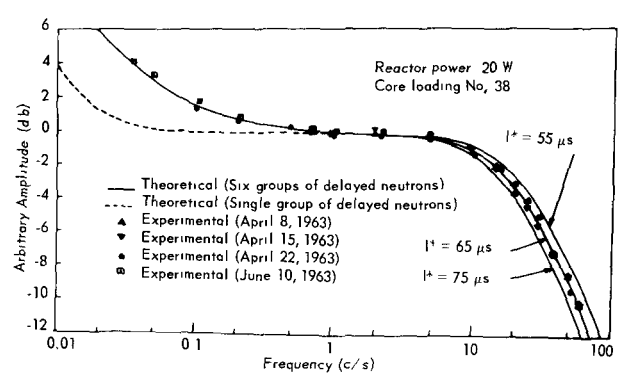


Figure 3. Amplitude transfer function plots

results that the experimental data agrees well with the theoretical results corresponsing to ℓ^* equal to 65 micro-seconds. The error in the value of ℓ^* was considered to be of the order of ± 3 micro seconds and was mainly due to the error in reading the amplitude from the pictures of the power level fluctuations taken by the Polaroid camera. It was, therefore, concluded that the value of ℓ^* for the reactor was 65 $\pm$ 3 micro seconds which was about 18% higher than the one quoted by Breazeale *et al.* [9].

It can also be seen from Fig. 3 that the single-group approximation can be used for the determination of ℓ^* if the break frequency, given by $\bar{\beta}/\ell^*$, lies above 2 c/s.

CONCLUSION

This reactivity oscillator is very simple and reliable. It can be easily set up in any pool type reactor. The entire experiment of measuring the amplitude transfer function can be accomplished in about 4½ hours which makes it particularly attractive as a teaching device.

REFERENCES

1. Qazi, M. N., *An Oscillator Measurement of the Prompt Neutron Lifetime in the Pennsylvania State University Reactor*, Master's thesis (1963).
2. Griffin, C. W., and Randall, R. L., *At-Power, Low-Frequency, Reactor-Power-Spectrum Measurements and Comparison with Oscillation Measurements*, Nuclear Sci. Eng., *15* (2) (February 1963).
3. Rajgopal, V., *Determination of Reactor Transfer Functions by Statistical Correlation Methods*, Nuclear Sci. Eng., *12* (2) (February 1962).
4. Soodak, H., *Reactor Handbook*, Vol. 3, Part A, Interscience Publishers (1962).
5. Keepin, G. R., and Wimett, T. F., *Reactor Kinetic Functions: A New Evaluation*, Nucleonics, *16* (10) (October 1958).
6. Perez-Belles, R. *et al.*, *A Measurement of the Effective Delayed Neutron Fraction for the Bulk Shielding Reactor I*, Nuclear Sci. Eng., *12* (4) (April 1962).
7. Lundholm, Jr., J. G. *et al.*, *Measurement of Zero Power Frequency Response of the SRE*, USAEC report NAA-SR-3762 (November 1959).
8. *Core Loading Log Book*, Pennsylvania State University, University Park, Pa., USA unpublished.
9. Breazeale, W. M. *et al.*, *Low Power Experiments with the Pennsylvania State University Reactor*, NYO 7895 (September 1956).

ABSTRACT - RÉSUMÉ - АННОТАЦИЯ - RESUMEN

A/671 Pakistan

Oscillateur pour réacteur piscine

par M. N. Qazi

L'auteur décrit en détail la mise au point et les essais d'un oscillateur très simple et sûr.

L'appareil est spécialement adapté pour un réacteur piscine, mais il est utilisable soit tel quel, soit avec de légères modifications dans des réacteurs de type similaire.

Ses principaux avantages sont la facilité et la commodité avec lesquelles on peut l'installer et faire les expériences qui permettent de mesurer la fonction de transfert d'amplitude. L'appareil permet de faire l'opération complète de mesure de la fonction de transfert d'amplitude, y compris sa mise en place, en quatre heures et demie environ, ce qui le rend particulièrement intéressant pour l'enseignement. Il peut disposer d'un intervalle de fréquences ajustable entre 0,01 Hz et plus de 100 Hz; l'ajustement se fait au moyen d'un moteur à courant continu et à vitesses variables associé à un système de poulies spécialement conçu. On évite l'emploi d'un rotor en utilisant deux servo-moteurs Selsyn, ce qui est un grand perfectionnement. On obtient les oscillations de la radioactivité en faisant osciller la quantité de cadmium entre un minimum et un maximum, et cela par rotation d'un disque d'aluminium, portant des feuilles de cadmium symétriquement disposées, sur un autre disque d'aluminum fixe exactement semblable au premier. Les variations de la densité des neutrons dans le cœur, qui en résultent, sont décelées par une chambre d'ionisation et sont présentées sur un oscilloscope.

Une chambre à lames Polaroïd est utilisée pour enregistrer ces variations à partir de l'image sur l'écran de l'oscilloscope.

L'appareil a été utilisé pour mesurer la fonction de transfert de l'amplitude dans le réacteur de l'Université de l'Etat de Pennsylvanie.

On compare les courbes de la fonction de transfert de l'amplitude obtenues par voie expérimentale avec celles qui sont construites d'après les résultats théoriques de calculs sur IBM 7074, pour différentes valeurs de ℓ^* (durée de vie des neutrons instantanés). Pour obtenir les résultats théoriques, on a utilisé une valeur de 0,008 pour le paramètre $\bar{\beta}$ (fraction effective totale des neutrons différés); cette valeur est fondée sur une détermination expérimentale faite dans BSR1 au Laboratoire d'Oak Ridge. La durée de vie des neutrons instantanés dans le réacteur nucléaire de l'Université de l'Etat de Pennsylvanie a été ainsi fixée à 65 μs.

A/671 Пакистан

Осциллятор реактивности для реакторов погружного типа

М. Н. Кази

В этом докладе детально описаны разработка и испытание очень простого и надежного ос-

циллятора реактивности. Хотя этот осциллятор специально разработан для погружных реакторов, он может быть использован и для других аналогичных типов реакторов либо в его настоящем виде, либо с небольшими модификациями. Главным преимуществом являются легкость и удобство установки и проведения эксперимента по измерению амплитуды передаточной функции. Весь эксперимент измерения амплитуды передаточной функции, включая установку аппарата, может быть выполнен примерно за 4,5 *ч*, что делает этот прибор очень удобным для учебных целей. Устройство может обеспечить бесконечно регулируемый диапазон частоты от 0,01 до более 100 *гц*, что достигается за счет использования мотора постоянного тока с переменной скоростью в сочетании со специально разработанной системой блоков. Необходимость в длинном вале ротора устраняется благодаря использованию двух сельсинных сервомоторов, что является значительным усовершенствованием. Колебания реактивности получаются путем изменений количества кадмия от минимума до максимума. Это осуществляется путем вращения алюминиевого диска с симметрично расположенными кадмиевыми слоями над другим стационарным алюминиевым диском, точно подобным первому. Возникающие колебания плотности нейтронов активной зоны детектируются ионизационной камерой и передаются на осциллоскоп. Для записи этих колебаний с экрана осциллоскопа используется поляроидная камера. Этот аппарат был использован для измерения амплитуды передаточной функции на реакторе Пенсильванского университета. Экспериментально полученные графики амплитуд передаточной функции сравнивались с графиками, теоретически рассчитанными на машине IBM-7074 для различных значений l^* времени жизни мгновенных нейтронов. При вычислении теоретических значений для параметра β -полной эффективной доли запаздывающих нейтронов была использована величина 0,008, основанная на экспериментальном определении в реакторе BSR-1 в Окриджской национальной лаборатории. Таким путем для времени жизни мгновенных нейтронов в реакторе Пенсильванского университета было найдено значение 65 *мксек*.

A/671 Pakistán

Oscilador de reactividad para reactores tipo piscina

por M. N. Qazi

La memoria describe detalladamente los trabajos y pruebas de un oscilador de reactividad de funcionamiento sencillo y seguro, concebido especialmente para reactores de tipo piscina, pero que puede emplearse en otros tipos similares, ya sea en su forma actual o con ligeras modificaciones. El aparato lleva a cabo medidas de amplitud de la función de transferencia y su principal ventaja reside en la facilidad y rapidez con que puede ponerse a punto y ejecutar el propio experimento, que no dura en total sino unas 4 horas y media, lo cual le hace particularmente atractivo como instrumento de enseñanza. Puede proporcionar una gama de frecuencias de ajuste continuo entre 0,01 Hz y más de 100 Hz utilizando un motor de corriente continua de velocidad variable, acoplado a un sistema de poleas de construcción especial. El empleo de dos servomotores Selsyn ha eliminado ventajosamente la necesidad de utilizar un eje de rotor excesivamente largo. Las oscilaciones de reactividad se han conseguido haciendo fluctuar la cantidad de cadmio de un mínimo a un máximo mediante un disco de aluminio con láminas de cadmio colocadas de manera simétrica que gira sobre otro disco estacionario idéntico. Las fluctuaciones resultantes en la densidad neutrónica se detectan con una cámara de ionización y aparecen en la pantalla de un osciloscopio, fotografiándose mediante una cámara Polaroid. Con este aparato se midió la amplitud de la función de transferencia en el reactor de la Universidad del Estado de Pensilvania, los datos experimentales se compararon con los calculados teóricamente mediante una IBM-7074 para varios valores de la vida de los neutrones instantáneos l^* y un valor de 0,008 para la fracción efectiva total de neutrones diferidos $\bar{\beta}$ (según determinación experimental en el BSR1 del Laboratorio Nacional de Oak Ridge). La vida de los neutrones rápidos medida en el reactor de la Universidad del Estado de Pensilvania resultó ser de 65 μs.

An analogical study of the dynamic behaviour of the Lucens Experimental Nuclear Power Station

By J. R. Gilbert, Y. Fishman, P. Doroszlai and E. Bühler *

The Lucens experimental station has been described in detail elsewhere [1].

Broadly outlined, it is a 30 MW(th) reactor burning slightly enriched metallic uranium, moderated by heavy water and gas-cooled (CO_2); it has two mono-tube steam generators and one turbo-alternator set.

The control devices have been conceived with the object of enabling energy to be delivered over a wide output range, while ensuring thermal operating conditions as constant as possible for the plant.

Preliminary studies led to the adoption for the output control of a method consisting of influencing the reactor first, and modifying the coolant flow in order to minimize the temperature variations inside the reactor. Two modes of operation are envisaged; as an interconnected and as an isolated station.

When operating as an interconnected station, the output is maintained at a set value and energy is delivered in accordance with a predetermined programme. The speed of the turbo-alternator set is dictated by the frequency of the mains grid to which it is connected.

When operating as an isolated station, the plant is the sole supplier of an independent grid. Regulation of the frequency is assured by the turbine speed governor. Steam pressure variations resulting from fluctuations in the load act via a control sequence on the reactor control rods, which thus automatically adapt the output to the demands of the grid.

DESCRIPTION OF THE CONTROL EQUIPMENT

The main control circuits are represented in Fig. 1. For controlling the reactor there are 10 absorber rods available, acting one after the other to provide automatic regulation according to a sequential system. The drive signal to the servomotor of the control rod is given by the flux regulator, which is characterized as follows:

(*a*) The controlled condition is the logarithm of the flux, giving the system a dynamic behaviour unaffected by the output level;

(*b*) The inverse of the period, $\frac{1}{\phi}\frac{d\phi}{dt}$, is inserted naturally in the regulator; this signal ensures damping of the system and limitation of the rate of flux variation;

(*c*) Flux regulation is subordinated to the thermal output regulator.

In the *interconnected station* the thermal output is regulated to a set value. The flow of gas in the primary loop is taken as a representative value for the output delivered by the reactor. This choice, favourable from the dynamic aspect, is justified by the fact that the gas temperature varies very little at the reactor inlet, and that it is automatically maintained constant at the outlet.

The opening of the butterfly valves in the primary loop is dictated by the gas temperature regulator, which also introduces the reactor output as an anticipatory signal. This regulation system provides continuous adaptation of the coolant flow to the reactor output.

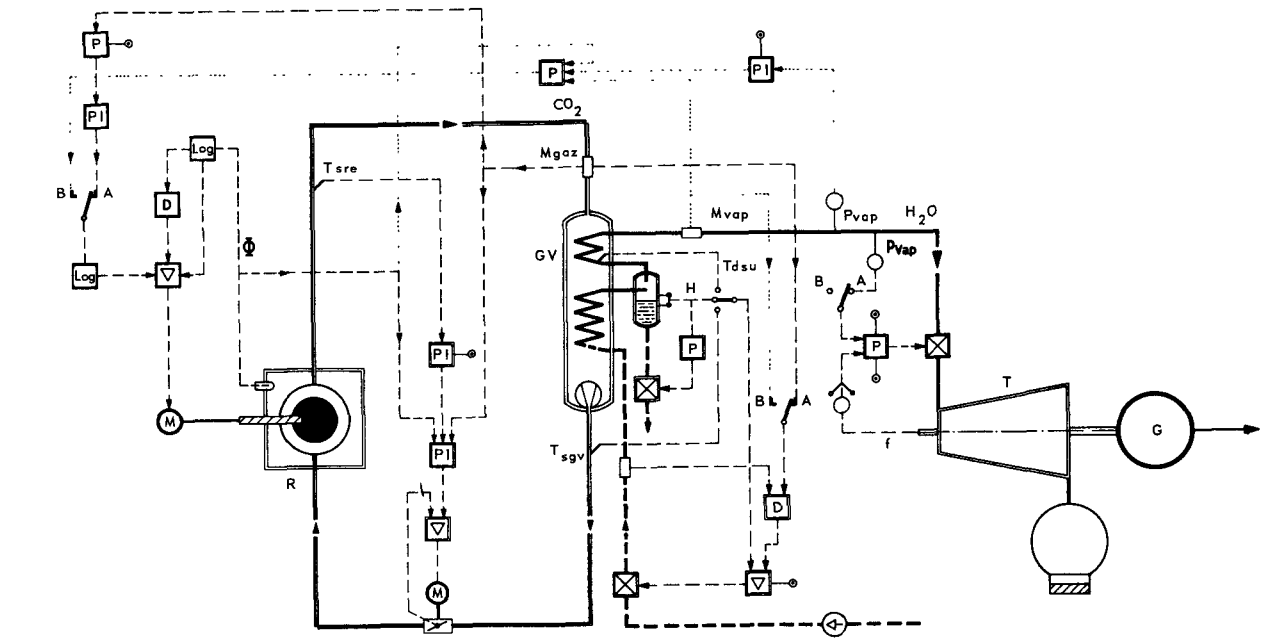
For the *mono-tube steam generators* three methods of regulation are available, depending on whether the controlled variable selected is the water level—in the separator, the steam temperature at the superheater inlet T_{dsu}, or the gas temperature at the outlet from the steam generator T_{sgv}. In all three cases, the regulating condition is the feedwater flow rate. Moreover, the gas flow is generally utilized as an anticipatory signal.

In the case of the regulation of the water level in the separator, a second control circuit enables the blow-down flow rate to be adjusted to the desired value.

As for the live steam pressure, the turbine governor keeps it constant by acting on the admission valves.

In the *isolated station*, the speed of the set is regulated by the turbine governor, assuming that there is no other station supplying the grid envisaged. Thus the variations in the pressure and flow of live steam are transmitted to a regulator which acts on the reactor through the intermediary of the flux control circuit. The thermal output regulator is cut out of action. The other regulation devices function as in the interconnected station, except that the anticipatory signal for the feedwater regulation is preferably proportional to the live steam flow.

* Therm-Atom Ltd.



R Reactor
GV Steam generator
T Turbine
G Alternator

P Proportional control unit
PI Proportional plus integral control unit
D Derivative control unit

Control amplifier
Servo-motor
Valve with Servo-motor

A Interconnected station
B Isolated station
Control circuits in general
Control circuits, case B

Figure 1. Control system of the Lucens nuclear power station

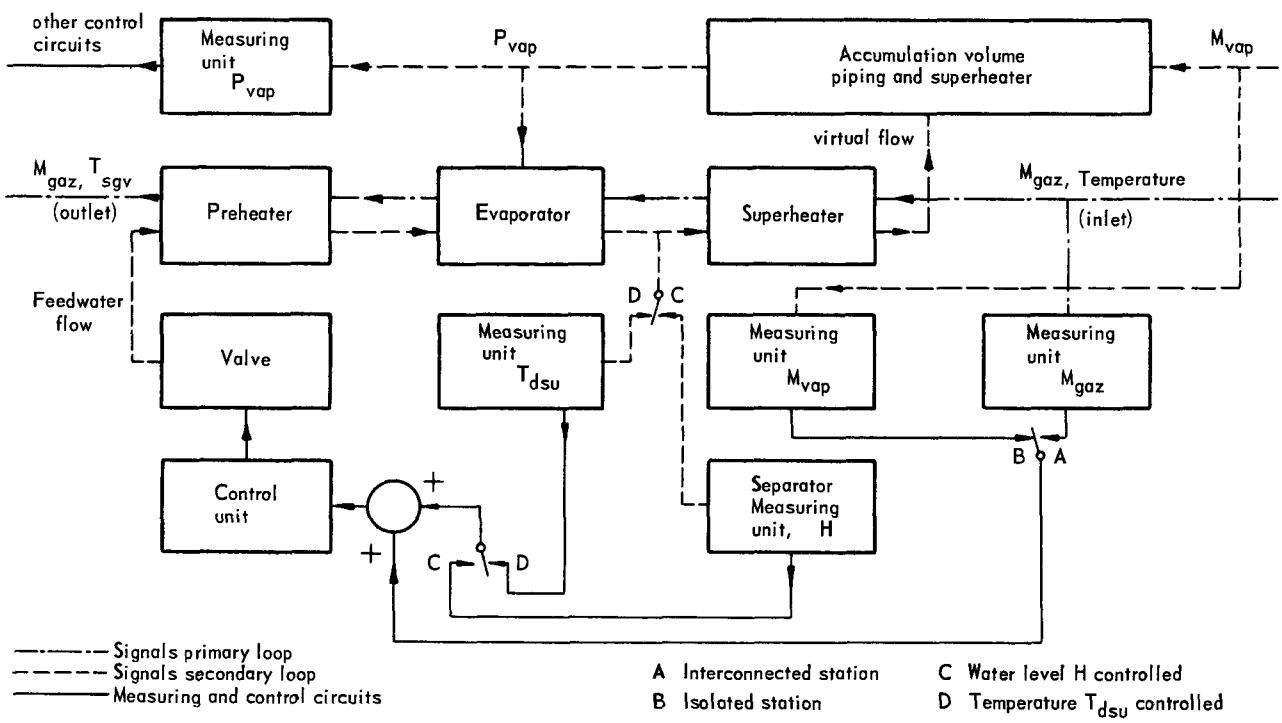


Figure 2. Operational diagram of the steam generator

BASES FOR ANALOGICAL CALCULATION

Reactor

From the nuclear viewpoint it is assumed that the distribution of the neutron flux in space does not vary and the classical equations of neutron kinetics are employed [2]. Because the frequency range corresponding to the dynamic problems under consideration is limited, it is sufficient to introduce two suitably chosen imaginary groups of delayed neutrons. On the other hand, no allowance is made for the effect of temperature on reactivity; the temperature of the moderator (D_2O) practically does not vary, the influence of the temperature variations on the uranium remains slight (the controlled behaviour of the plant is being studied), and the coolant (CO_2) does not make any contribution.

After an exhaustive study of the thermal behaviour of the reactor, it was ascertained that it was sufficient to establish the equations governing the exchanges of energy for a single fuel element, considering only four vertical zones: the rod of uranium, its canning, the cooling duct and the corresponding gas inlet duct. It did not prove necessary to subdivide the element along the reactor axis. The dead times simulate the transport of gas in the primary loop.

Steam generator

Although the installations comprise two steam generators, a single unit has been assumed for calculation. The steam generator consists of a preheater, an evaporator and a superheater. The calculations are based in part on existing theories [3]. Since it is necessary to consider not only the heat transfer from the primary to the secondary sides, but likewise the retroaction of the latter on the primary side, moreover making due allowance for the influence of the pressure variations, theoretical study has had to be pursued further. Fig. 2 shows the functional components affecting the calculations. As for the reactor, the equations with partial derivatives are replaced by equations with finite differences, and the steam generator is sub-divided into several zones. In view of the fact that the capacity of the analogue computer is not unlimited, it was necessary to restrict the number of basic subdivisions. The choice was made on the basis of the transfer behaviour of the different elements. Thus the preheater, which has the slowest behaviour, is sub-divided into two zones; dead times are introduced in their simulation. The evaporator and the superheater are not sub-divided spatially.

Turbo-alternator set

The equation was written for the movement of the whole set, under the assumption that the torque is proportional to the flow of live steam, the latter being determined on the one hand by the opening of the admission valves and on the other by the steam pressure. With regard to the electrical part, an exact description of the behaviour of the grid was not attempted, on account of the excessive complexity of the problem. Only the active power brought into play is considered, and the load is broken down into several terms: the first equivalent to a pure resistance, the others corresponding to different types of machines encountered in the grid with their particular characteristic in function of the frequency.

Control devices

In general, the calculations are straightforward, though special attention must be given to the measuring devices and the regulators. Analysis leads either to neglecting the time constant of certain elements, or to investigating the approximations compatible with the dynamic behaviour of the whole plant. On the other hand it is important to make allowance for various non-linearities, such as the dead zones of control elements, limiting speed (synchronous) of servomotors, valve characteristics, etc.

RESULTS AND COMMENTS

By way of examples a few aspects of the dynamic behaviour of the station are shown in Figs. 3 to 8. The working method consists of applying a disturbance to the plant starting from a stationary condition, and recording the corresponding responses of the principal variables.

With the interconnected station the disturbance consists of a ramp function in the set value for the thermal output (0.33% per second over 15 seconds), and with the isolated station of an instantaneous load increase of 5%.*

The curves for reactor output and gas flow being practically identical on the time scale chosen, only the gas flow is plotted on the various diagrams.

The results for the *interconnected station* (Figs. 3 and 4) already reveal the good temperature maintenance of the primary loop, regardless of the output level and the method employed for controlling the steam generator. The introduction of an anticipatory signal derived from the gas flow notably improves the dynamic behaviour of the latter. On the other hand it gives rise to a certain delay in the establishment of the new steady state, especially under high load (Fig. 3). Finally the presence of the anticipatory signal has virtually no influence on the behaviour of the primary loop: apart from calculating errors the curves obtained for M_{gaz} and T_{sre} are the same, and here also only one curve has been reproduced in the diagrams.

The results for the *isolated station* (Figs. 5 to 8) all refer to 50% load. Consequently they permit a

* The relative values given as percentages refer to the nominal output.

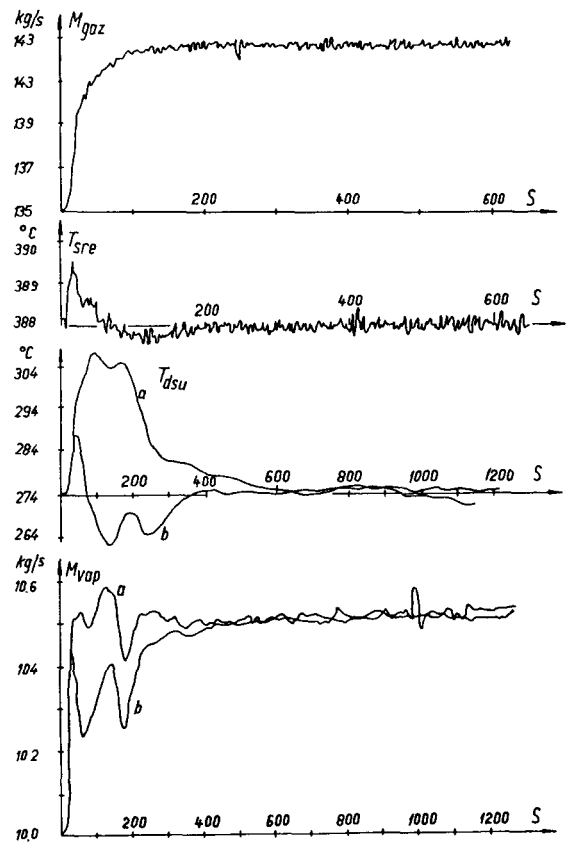


Figure 3. Interconnected station 90% load, steam temperature at superheater inlet (T_{dsu}) regulated
a: Without anticipatory signal; *b*: anticipatory signal from gas flow

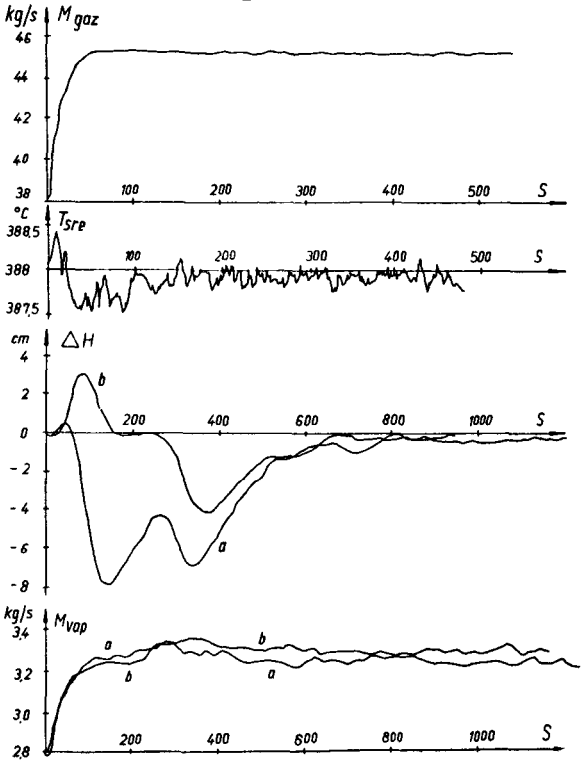


Figure 4. Interconnected station, 25% load, water level *H* regulated
a: Without anticipatory signal; *b*: anticipatory signal from gas flow

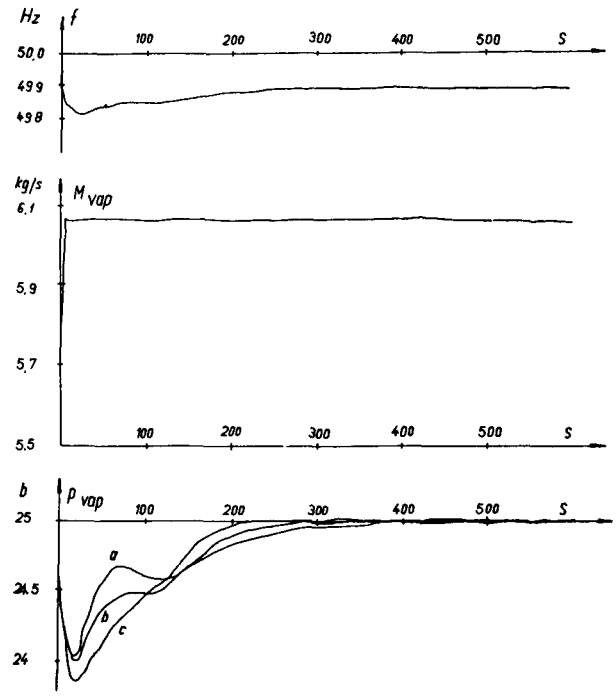


Figure 5. Isolated station, 50% load, water level *H* regulated
a: Without anticipatory signal; *b*: anticipatory signal from gas flow; *c*: anticipatory signal from steam flow

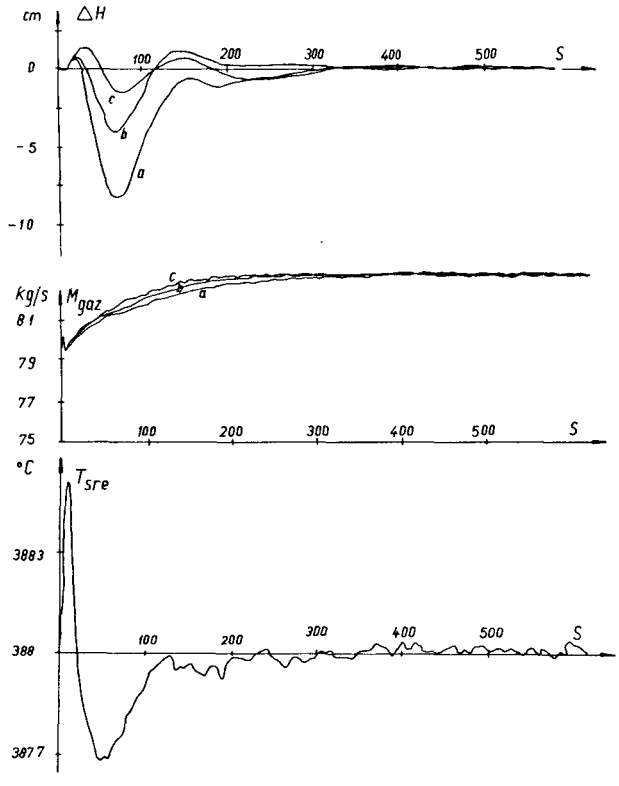


Figure 6. Isolated station, 50% load, water level *H* regulated
a: Without anticipatory signal; *b*: anticipatory signal from gas flow; *c*: anticipatory signal from steam flow

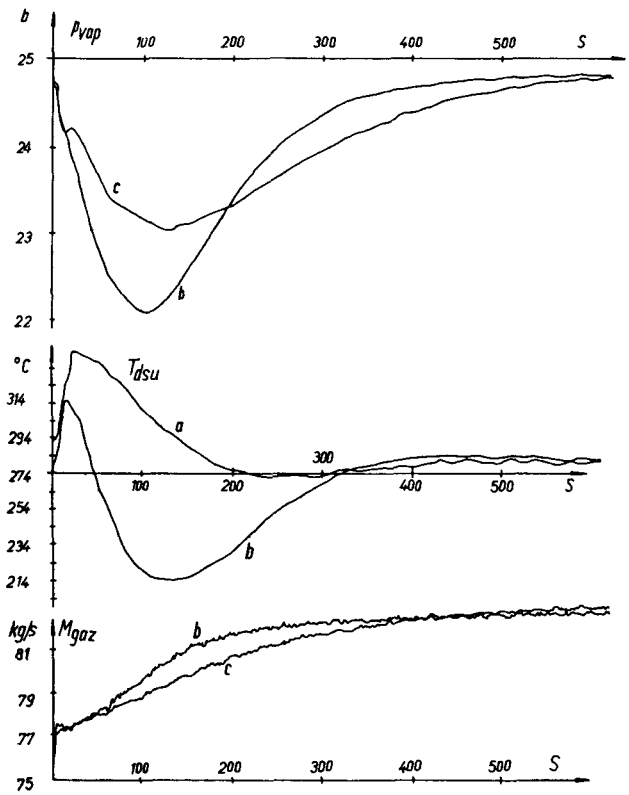


Figure 7. Isolated station, 50% load, steam temperature at superheater inlet (T_{dsu}) regulated

a: Without anticipatory signal; *b*: anticipatory signal from gas flow; *c*: anticipatory signal from steam flow

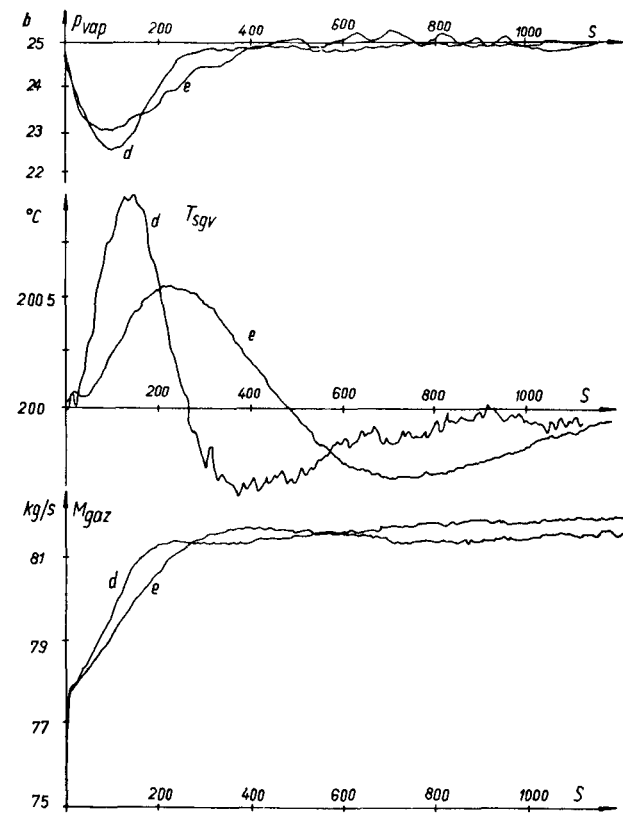


Figure 8. Isolated station, 50% load, gas temperature at steam generator outlet (T_{sgv}) regulated

d: Without differential temperature signal; *e*: with differential temperature signal

valid comparison between the various methods of regulating the steam generator. The frequency and steam flow curves are only reproduced in one case (Fig. 5), since they differ little from one case to another. With the level regulation H it will be noted that the transient phenomena last 300 seconds at the most (Figs. 5 and 6). This interval is hardly any longer in the case of the temperature regulation T_{sgv} (Fig. 8). On the other hand, regulation takes somewhat longer where the temperature T_{dsu} is regulated (Fig. 7). Using an anticipatory signal always assists the thermal behaviour of the steam generator, and the signal originating from the steam flow gives the best results. In the case of regulation of the gas temperature at the outlet from the steam generator (T_{sgv}), improvement is obtained by introducing a signal proportional to the time derivative of the gas temperature in a suitably chosen zone of the steam generator (this device is not shown in Fig. 1); the anticipatory signal is derived from the gas flow in this case. Finally the variations in the gas temperature at the reactor outlet (T_{sre}) are very slight (Fig. 6: the variations are of the same order of magnitude in the other cases).

CONCLUSIONS

The results of the calculations demonstrate that the control equipment selected will ensure satisfactory dynamic behaviour of the station and that the latter will meet the requirements imposed upon it from the thermal aspect. Experience with the Lucens station itself will reveal the extent to which these predictions are realized.

NOMENCLATURE

T_{sre} : gas temperature at reactor outlet (°C)

T_{sgv} : gas temperature at steam generator outlet (°C)

T_{dsu} : steam temperature at superheater inlet (°C)

M_{gaz} : total gas flow in primary loop (kg/s)

M_{vap} : total live steam flow (kg/s)

$\triangle H$: variation of water level in separator (cm)

p_{vap} : live steam pressure (bar)

f : frequency of turbo-alternator set (c/s)

REFERENCES

1. Krafft, P., *The Lucens Experimental Nuclear Power Station*, P/692, Vol. 5, these Proceedings.

2. Schmid, P., Nukleonik, *4*, 331-347 (1962).

3 Profos, P., *Die Regelung von Dampfanlagen*, pp. 124-182, Springer-Verlag, Berlin (1962).

ABSTRACT - RÉSUMÉ - АННОТАЦИЯ - RESUMEN

A/697 Suisse

Etude analogique du comportement dynamique de la centrale nucléaire expérimentale de Lucens

par J. R. Gilbert *et al.*

Le comportement en régime variable de l'ensemble de la centrale de Lucens a été étudié sur une calculatrice analogique de grande capacité. Le but de cette étude était d'analyser le fonctionnement de l'usine, d'en contrôler la stabilité, de comparer divers modes d'exploitation ainsi que diverses méthodes de réglage, et enfin de procéder au choix des coefficients donnant les meilleures performances.

Dans la première partie, les auteurs décrivent les dispositifs de réglage envisagés pour le réacteur, le circuit primaire, le générateur de vapeur, et le groupe turbo-alternateur. Ces dispositifs sont conçus de telle façon que la centrale puisse fonctionner soit à partir du réacteur, selon un programme de fourniture d'énergie déterminé (centrale « interconnectée »), soit à partir du réseau (centrale « isolée »). Dans le premier cas, la puissance nucléaire est imposée; dans le second cas, le réacteur fournit l'énergie que lui demandent les consommateurs. Le débit du réfrigérant (CO_2) dans le circuit primaire est toujours adapté automatiquement à la puissance nucléaire, de manière à maintenir constante la température du gaz à la sortie du réacteur.

Dans une deuxième partie, les bases du calcul sont présentées. La capacité de la machine analogique, quoique appréciable, étant limitée, il a fallu procéder à un certain nombre de simplifications.

On ne considère qu'un seul générateur de vapeur (au lieu de deux, prévus dans les installations). Les modèles thermiques du réacteur et du générateur de vapeur sont subdivisés en zones pour lesquelles on définit des valeurs moyennes. Les constantes de temps petites par rapport au comportement de l'ensemble sont négligées.

On introduit les équations classiques de la cinétique neutronique sous leur forme non linéaire, en ne considérant toutefois que deux groupes fictifs de neutrons retardés. D'autres non-linéarités sont également conservées dans la simulation du réacteur et du circuit primaire. Les modèles du générateur de vapeur, du groupe turbo-alternateur et du réseau sont décrits par des équations linéarisées. Les coefficients de celles-ci dépendent donc du niveau de puissance. Dans la troisième partie, les auteurs montrent et commentent quelques exemples de résultats obtenus par la simulation de l'ensemble de la centrale. On enregistre la réponse de diverses grandeurs caractéristiques à de petites perturbations à partir d'un état d'équilibre, à différents niveaux de puissance. En centrale interconnectée, par exemple, la perturbation consiste en une variation de la consigne de puissance, tandis qu'en centrale isolée on simule un saut de la puissance absorbée par le réseau. On étudie également divers modes de réglage du générateur de vapeur, ainsi que l'influence particulière de certains signaux d'anticipation.

On constate que la centrale est en mesure de réagir rapidement aux variations de régime demandées et que les fluctuations des grandeurs réglées restent dans des limites acceptables. En particulier, la température du gaz à la sortie du réacteur varie peu et les écarts de fréquence observés en centrale isolée sont faibles.

A/697 Швейцария

Исследование с помощью моделирующего вычислительного устройства динамического поведения экспериментальной атомной электростанции в Люценсе

Ж. Р. Жильбер

С помощью моделирующего устройства с большой разрешающей способностью изучалось поведение в переходном режиме системы атомной электростанции в Люценсе. Целью настоящего исследования являлось проанализировать функционирование установки, проконтролировать ее стабильность, сравнить различные способы эксплуатации, а также различные методы управления и приступить к выбору коэффициентов, дающих наилучшие характеристики.

В первой части доклада авторы описывают системы управления, предусматриваемые для реактора, первичного контура, парогенератора и турбогенераторной группы. Эти системы задуманы таким образом, чтобы электростанция могла работать при заданной мощности реактора в соответствии с определяемой программой подачи энергии («объединенная» электростанция) или с учетом условий сети («изолированная» электростанция). В первом случае ядерная мощность предписывается, во втором — реактор дает такое количество энергии, которое требуют потребители. Расход теплоносителя (CO_2) в первичном контуре автоматически приспособляется к мощности реактора таким образом, чтобы температура газа на выходе из реактора поддерживалась постоянной.

Во второй части доклада представлены основы расчета. Поскольку счетно-решающая машина имеет значительную, но ограниченную разрешающую способность, потребовалось произвести некоторые упрощения. Рассматривается только один парогенератор (вместо двух, предусматриваемых для установки). Тепловые

модели реактора и парогенератора подразделяются на зоны, для которых определяются средние значения. Не учитываются постоянные времени, которые невелики по отношению к поведению всей установки.

Вводятся классические уравнения кинетики нейтронов в нелинейной форме, причем рассматриваются только две фиктивные группы запаздывающих нейтронов. В моделировании реактора и первичного контура сохраняются также и другие нелинейности. Модели парогенератора, турбогенераторной группы и сети описываются линеаризованными уравнениями. Коэффициенты последних зависят от уровня мощности. В третьей части доклада авторы приводят некоторые результаты, полученные методом моделирования системы электростанции, и комментируют их. Отмечается реакция различных величин, характерных для небольших возмущений, исходя из состояния равновесия, на различные уровни мощности. Например, на объединенной электростанции нарушение заключается в изменении мощности, а на изолированной электростанции моделируют скачок мощности, потребляемой сетью. Исследуются также различные методы управления парогенератора, а также особое влияние некоторых предварительных сигналов.

Отмечается, что электростанция может быстро реагировать на требуемые изменения режима и что колебания регулируемых величин остаются в допустимых пределах. В частности, температура газа на выходе из реактора изменяется мало и отклонения частоты, наблюдаемые на изолированной электростанции, невелики.

A/697 Suiza

Estudio analógico del funcionamiento de la central nuclear experimental de Lucens

por J. R. Gilbert *et al.*

Se ha estudiado con una calculadora analógica de gran capacidad el comportamiento en régimen variable de la central de Lucens para analizar su funcionamiento, verificar su estabilidad, comparar diversos modos de explotación y métodos de control y, por último, seleccionar coeficientes que proporcionen resultados óptimos.

En la primera parte los autores describen los dispositivos de control previstos para el reactor, el circuito primario, el generador de vapor y el grupo turbo-alternador. Estos dispositivos se han concebido de manera tal que la central pueda funcionar ya sea según un programa determinado de suministro de energía (central "interconectada"), o bien en dependencia con la red (central "aislada"). En el primer caso la potencia nuclear viene impuesta, mientras que en el segundo el reactor suministra la energía que demanda el consumidor. El caudal de refrigerante (CO_2) del circuito primario se adapta siempre automáticamente a la potencia nuclear para que la temperatura del gas a la salida del reactor se mantenga constante.

En la segunda parte se exponen las bases del cálculo. Como la capacidad de la calculadora analógica, aunque apreciable, es limitada, ha sido preciso efectuar un cierto número de simplificaciones, y así se considera solamente un generador de vapor (en lugar de dos, previstos en la instalación), los modelos térmicos del reactor y del generador de vapor se dividen en zonas para las que se definen valores medios y se prescinde de las constantes de tiempo, pequeñas en relación con la importancia del conjunto.

Se introducen las ecuaciones clásicas de la cinética neutrónica en su forma no lineal, si bien solamente se consideran dos grupos ficticios de neutrones retardados, e igualmente se mantienen otras expresiones no lineales en la simulación del reactor y del circuito primario. Los modelos del generador de vapor, del grupo turbo–alternador y de la red se representan por ecuaciones lineales cuyos coeficientes dependen, pues, del nivel de potencia. En la tercera parte los autores exponen y comentan algunos ejemplos de resultados obtenidos por la simulación del conjuno de la central. Se señala la reacción de diversas magnitudes características ante pequeñas perturbaciones de un estado de equilibrio, para diferentes niveles de potencia. Por ejemplo, en una central interconectada, la perturbación consiste en una variación de la potencia asignada mientras que, en una central aislada, se simula un salto de la potencia absorbida por la red. Se estudian diversos procedimientos de control del generador de vapor, así como la influencia particular de ciertas señales de aviso.

Se comprueba que la central está en condiciones de reaccionar rápidamente a las variaciones de régimen exigidas y que las fluctuaciones de las magnitudes controladas no exceden de límites aceptables. En particular, la temperatura del gas a la salida del reactor varía poco y las oscilaciones de frecuencia en la central aislada son pequeñas.

Kinetic studies and control of nuclear reactors by statistical methods *

By J. Miida**

Statistical analyses of nuclear reactors have been made both by the direct power spectrum measurement method and the cross-correlation method using binary noise. The experimental and analytical studies of reactor kinetics by these methods are given in the present paper, with special emphasis on the noise spectrum of various reactors at critical and subcritical states obtained by direct measurement, and on the development of binary noise techniques. Finally, the automatic start-up of a research reactor by a digital method is described.

DYNAMIC BEHAVIOUR AT POWER, LOW FREQUENCY, OF A WATER BOILER REACTOR IN NORMAL OPERATION

Y. Kuroda and K. Sumita

Use was made of both band pass filter and digital auto-correlation methods to analyse the low frequency characteristics of JRR1 (water boiler reactor) at power in normal operation.

Band pass filter analysis was performed at power levels of 20, 30, 35 and 40 kW, over 0.008-10 c/s using fm recording and speed-up techniques (Fig. 1) [1-3]. However, discussion is limited here to the frequency region below 2 c/s. From these experiments we have established that: (*a*) reactor noise is most violent at 37-38 kW, is independent of noise from coolant flow and increases with decreasing in-core pressure, and vice versa; (*b*) there exists a resonance peak at about 0.06 c/s for a given power level, whose slope on the higher frequency side is 60-80 db/dec, which can be explained using simple models (Fig. 2). The peak shifts to the higher frequency side with increasing power level; (*c*) another resonance peak seems to be located at a frequency lower than 0.01 c/s.

Digital auto-correlation analysis was performed at 40 kW, in the frequency region below 1 c/s using Blackman-Tukey's method [4]. The main feature of the data processing is presented in Table 1, where Hamming was used as a smoothing window. It turned out that: (*a*) there exists an approximate local stationarity in the wider sense, as proved by investigating the variability of power spectral densities; (*b*) there exists a pair of resonance peaks: one located at about 0.06 c/s, the other at about 0.008-0.01 c/s, as shown in Fig. 3; the former agreed well with that obtained from band pass filter techniques.

Results by pile oscillator [5] indicated only one resonance peak at 0.008 c/s as shown in Fig. 1, which agreed with that computed from the Skinner-Hetrick model [6], as well as the Moore noise model [7].

It is concluded from these results that the resonance peak at 0.008 c/s is due to the power gain of the reactor.

Concerning the other resonance peak at the higher frequency side, we may consider it a radiolytic void reactivity effect, as inferred from Fig. 4(a). Since local stationarity is valid in the process observed, there would exist a stable void noise reactivity power gain $|H_R(f)|$ (Fig. 4(a)). Comparing the power spectrum of reactor noise $\Phi_{nn}(f)$ with the power gain $|G(f)|$ measured by pile oscillator [8], we have $|H_R(f)|^2 = k[(k'\Phi_{nn}(f)/|G(f)|^2)-1]$, where Φ_{nn} = power spectrum of reactor noise, $k = C/C'$ and $k' = 1/C$, assuming that the external noise $b(t)$ with power spectrum C and an equivalent void noise $v(t)$ with power spectrum C' are uncorrelated and white Gaussian in the narrow frequency band concerned. From experimental data, it is seen that $|H_R(f)|^2$ behaves somewhat like a second order system in the neighbourhood of the resonance peak as shown in Fig. 5, where k and k' are normalized.

Meanwhile, in the Skinner-Hetrick model we have, in form, as power gain of noise reactivity feedback corresponding to $|H_R(f)|$,

$$|H'_R(f)|^2 = k'\Big[\sum_{i=1}^{4}\Phi_{ii}(f) + \sum_{i,\,j=1}^{4}\mathrm{Re}\,\Phi_{ij}(f)\Big]\,|H_T(f) + H_v(f)|^2$$

where $\Phi_{ij}(f)$'s are cross-power spectra between $g_i(t)$ and $g_j(t)$, $g_i(t)$'s, $H_T(f)$ and $H_v(f)$ are defined in Fig. 4.

* With contributions by Y. Kuroda, Tokai University; S. Yamada, Hitachi Central Research Laboratory; T. Nomura and S. Goto, Nippon Atomic Industry Group Co., Ltd.; K. Sumita, M. Hara and N. Suda, Japan Atomic Energy Research Institute; Y. Takahashi and S. Takamatsu, Tokyo Shibaura Electric Co., Ltd.

** Japan Atomic Energy Research Institute.

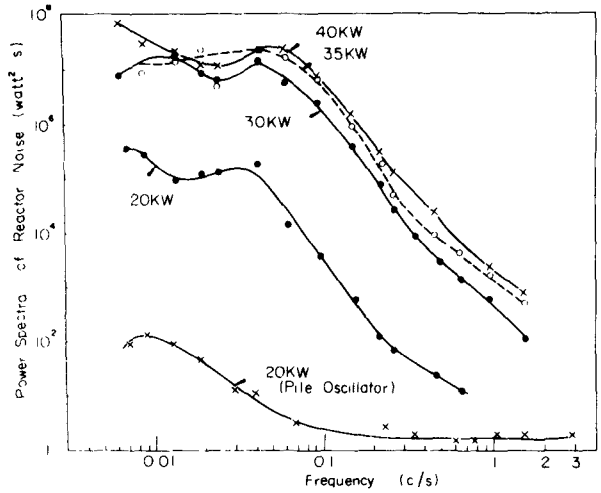


Figure 1. Power spectra of reactor noise in JRR1 by band pass filter and pile oscillator methods

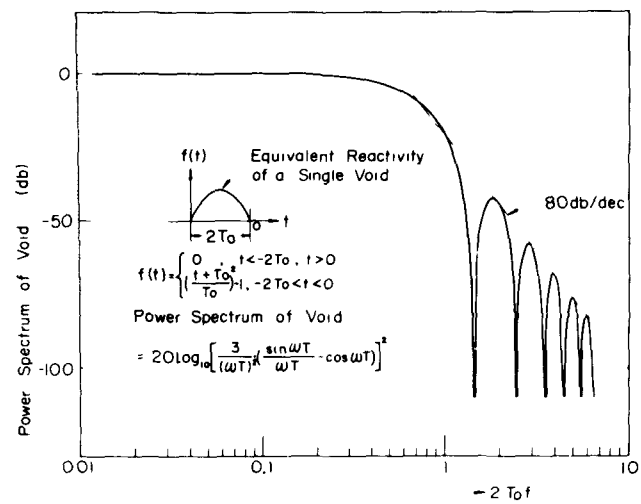


Figure 2. A power spectrum of void noise

Supposing $|H_R(f)|^2$ would agree with $|H'_R(f)|^2$, $\Phi_{24}(f)$ among $\Phi_{ij}(f)$ should most likely contribute to the resonance peak concerned, when the power level exceeds a certain threshold. This cross-power spectrum would somehow relate to thermal convection, circulating liquid flow and low frequency oscillation of the liquid surface in the core.

Consequently the second resonance peak as a result of noise seems most likely to be due to a transfer mechanism of radiolytic void through the temperature field, and not a simple effect of random void formation. Concerning the effect of boiling in the core at 80 °C, we have not yet arrived at an acceptable conclusion.

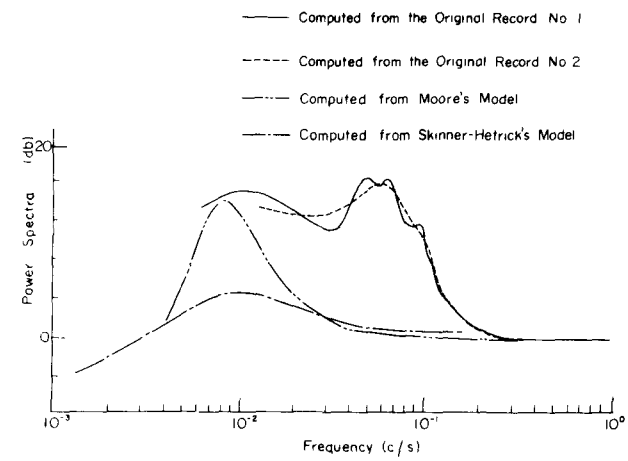


Figure 3. Power spectra of reactor noise in JRR1 at 40 kW, low frequency, by digital auto-correlation method

DEVELOPMENTS IN BAND PASS FILTER TECHNIQUES AND ITS APPLICATION TO FREQUENCY MEASUREMENTS AND POWER CALIBRATION OF HTR [9]

S. Yamada

Noise analysis of HTR (swimming pool type) has been done with the system shown in Fig. 6. The noise current derived from an ionization chamber was fed into an ultra low frequency ac amplifier. The output of the amplifier was recorded on tape with an fm magnetic tape recorder, and re-recorded to permit playback at 2, 8, 16 and 32 times the original recording speed. Speed-up of the tape permitted playback of thirty minutes of data in one minute. The output of the tape recorder demodulator was fed into a selective amplifier with twin-T band pass filters in the feedback circuit. Various combinations of resistances and capacitances could be switched in to obtain a wide range of resonant frequencies from 0.1 to 500 c/s while maintaining a constant Q-value (selected to be about 10).

Table 1. Main feature of data processing

	Sampling interval Δt (s)	Resolution Δf(c/s)	Max. shift number m	Sample number N	$\{1/[(N/m)-\frac{1}{3}]\}^{\frac{1}{2}}$ r.m.s error of power spectral estimate (%)
Original record No. 1	0.5	0.00625	160	1860	30
Original record No. 2	0.5	0.0125	80	1860	21
1st half of original record No. 2	0.5	0.025	40	930	21
2nd half of original record No. 2	0.5	0.025	40	930	21

The spectral density was determined by measuring the mean square value of the output of the selective amplifier and dividing it by the band-width of the filter at each particular frequency. A voltage proportional to the square of the output of the selective amplifier was obtained by feeding this output into an electronic multiplier, and the mean value of this voltage was obtained using an integrator. With tape speed-up and speed-down of thirty-two times, the band pass filters from 0.1 to 30 c/s gave band pass resolution from 0.003 to 1 K c/s. It is important, especially at low frequencies below 10 c/s, to integrate the whole information recorded on the tape, since if it is integrated partially, different values may be obtained depending on the parts of tape taken up.

The frequency response of the amplifier and electrometer were measured with a low frequency signal oscillator, and also from statistical white noise from the detector when exposed to a 4 000 curie Co^{60} source. The absolute value of the mean square noise amplitude may be calculated from the output value of the integrator. Background noises were measured by short-circuiting the input terminal of the ac amplifier, recording the output, and analysing the recorded data for the power spectrum.

The spectra of reactor noise were measured at power levels of 0.2W, 1W, 5W, 100W, 500W, 5kW and 100kW, and the resulting spectra are shown in Fig. 7. The effect of detector white noise appeared in the data at frequencies above 100 c/s. If the reactivity noise is assumed to be nearly true white noise at low power, the power spectral density in Fig. 7 would be proportional to the square modulus of the reactor transfer function. Calculations by the least squares method were made with a HIPAC-103 computer, and the prompt neutron mean life time was $(7.58 \pm 1.58) \times 10^{-5}$ s, based on an effective delayed neutron fraction of 0.0082. The noise spectra at low power are in agreement with the zero power transfer function, but at higher power the spectra reveal resonances and have much higher amplitude within a certain frequency range.

The absolute values of the mean square noise amplitude were obtained from the output value of the integrator. Charge q produced per neutron absorbed was observed to be $(3.9 \pm 2.7) \times 10^{-15}$ As. Schröder found $q = 2.62 \times 10^{-15}$ As [10]. Figure 8 shows the relation between the power indicated on the power meter and that obtained by noise analysis based on Cohn's noise model [11]. The power meter was calibrated by absolute measurements with gold foil activation. The two agreed to within 3%.

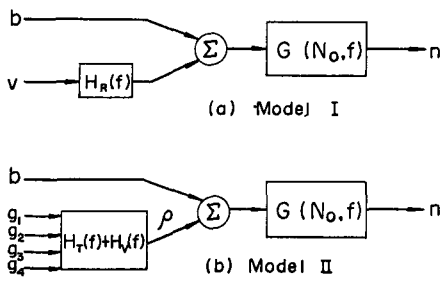


Figure 4. A void-temperature noise feedback

$G(N_0,f)$ = over-all transfer function of a water boiler reactor

$H_R(f)$ = void noise reactivity feedback transfer function

$H_T(f)$ = average temperature reactivity feedback transfer function

$$= \frac{K}{s + \langle r \rangle}, \quad r(t) = \langle r \rangle + r(t)$$

$H_v(f)$ = average void feedback reactivity transfer function

$$= \frac{G}{s + \langle \sigma \rangle}, \quad \sigma(t) = \langle \sigma \rangle + \sigma'(t)$$

$n(t)$ = power noise

$\rho(t)$ = feedback reactivity due to noise

$b(t)$ = external noise

$v(t)$ = equivalent void noise through temperature field

$g_1(t)$ = $[-n(t) + G\rho(t)]r'(t)$ equivalent temperature noise due to $r(t)$

$g_2(t)$ = power dependent term

$g_3(t)$ = $[-\rho(t) + Kn(t)]\sigma'(t)$ equivalent void noise due to $\sigma(t)$

$g_4(t)$ = power dependent term

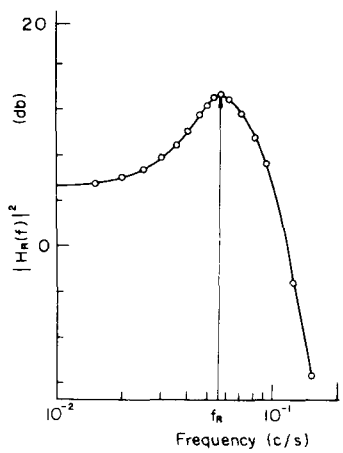


Figure 5. Behaviour of $|H_R(f)|^2$ at 40 kW around the resonance frequency $f_R \approx 0.06$ c/s

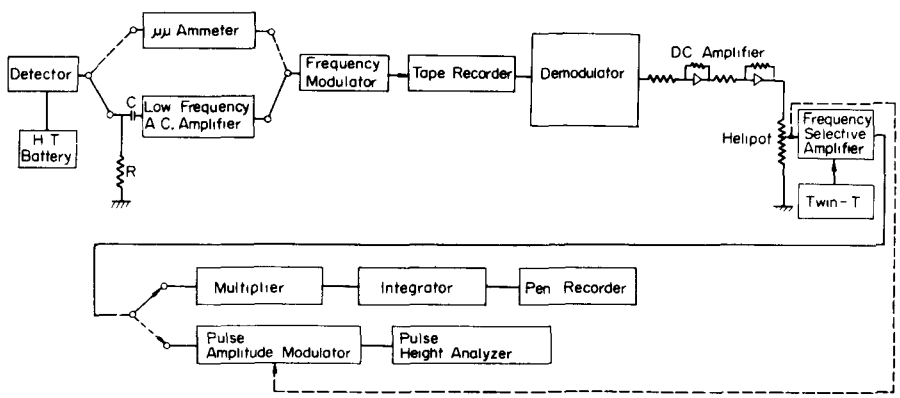


Figure 6. Experimental arrangement

SUBCRITICAL REACTIVITY MEASUREMENTS IN TTR1 DURING POWER DECAY

T. Nomura and S. Goto

This chapter describes a theory and an experiment related to the subcritical reactor transfer function of a two-energy group model. From this theory, it became evident that subcritical reactivity, as well as thermal and fast neutron life time may be determined by means of reactor power spectral density measurements. The measurements of subcritical reactivity were made under several shutdown conditions of TTR1 (swimming pool type).

Theory of two-energy group subcritical reactor transfer function [12-14]

Subcritical reactor transfer functions can be obtained by using a two-energy group model as follows:

$$N^f(s) = \frac{1}{f(s)}\ \delta\Sigma_a\ \frac{\kappa}{p\ell^s}\ \{(1-\beta)s+\lambda\} \qquad \text{thermal source, fast group}$$

$$N^s(s) = \frac{1}{f(s)}\ \delta\Sigma_a\ (s+\frac{1}{\ell^f})\ (s+\lambda) \qquad \text{thermal source, thermal group}$$

$$N^f(s) = \frac{1}{f(s)}\ \delta S_0\ (s+\frac{1}{\ell^s})\ (s+\lambda) \qquad \text{fast source, fast group}$$

$$N^s(s) = \frac{1}{f(s)}\ \delta S_0\ \frac{p}{\ell^f}\ (s+\lambda) \qquad \text{fast source, thermal group}$$

$$f(s) = (s-\lambda\frac{\rho/\beta}{1-\rho/\beta})\ \{s+\frac{\beta}{\ell^f+\ell^s}\ (1-\frac{\rho}{\beta})\}\ \{s+(\frac{1}{\ell^s}+\frac{1}{\ell^f})-\frac{\beta}{\ell^f+\ell^s}\ (1-\frac{\rho}{\beta})\ \}$$

These frequency characteristics are shown in Fig. 9. In theory, since each break frequency is related to reactor parameters, it is possible to determine these parameters by means of reactor power spectral density measurements. In practice, direct measurements of both thermal and fast neutron life times have not been successful because of chamber noise and chamber frequency characteristics. Particular interest was concentrated on the determination of subcritical reactivity related to the break frequency. This frequency is the same as that derived from the usual mono energy group reactor kinetic equations. From these equations, assuming random fluctuation parameters ρ/ℓ, β/ℓ and S_0 (source term), one obtains the reactor power spectrum in a high frequency region as follows:

$$|N(j\omega)|^2 = \frac{F_{11}}{\omega^2+[\beta/\ell(1-\rho/\beta)]^2}\ ;\quad \ell=\ell^f+\ell^s$$

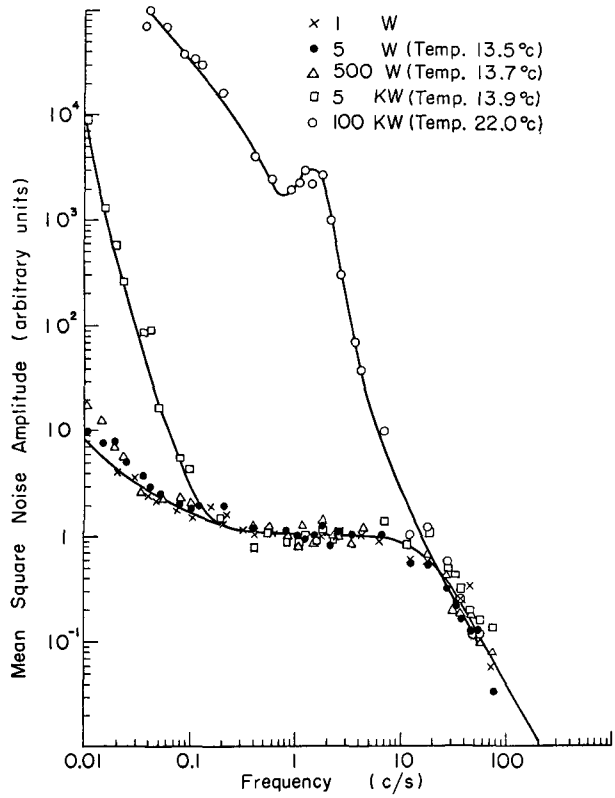


Figure 7. Noise spectra measurements of various powers

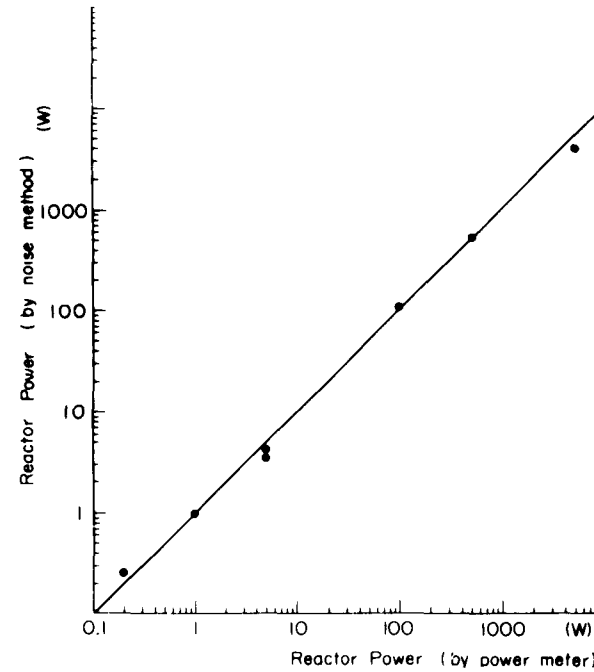


Figure 8. Reactor power calibration

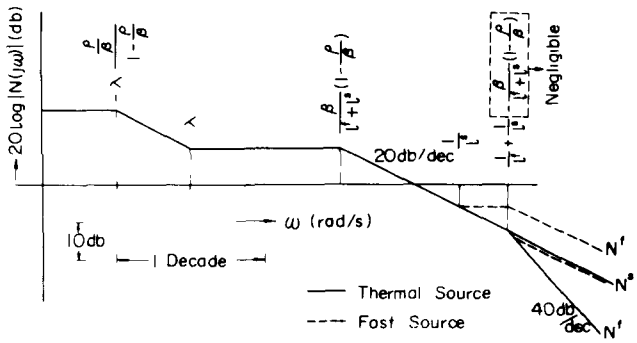


Figure 9. Two-energy group subcritical reactor transfer function

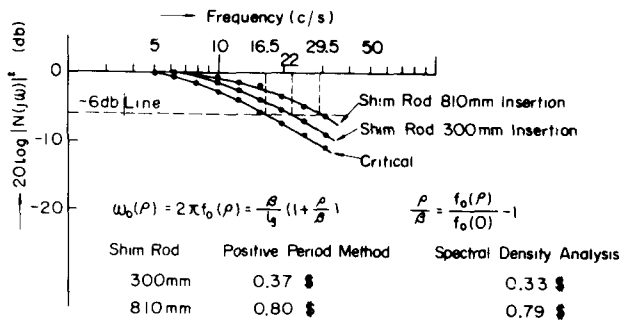


Figure 10. Reactor power spectra

Break frequency $\beta/\ell(1-\rho/\beta)$ corresponds to the decay constant of the neutron flux obtained by pulsed neutron technique.

The observed break frequency is equated to the theoretical formula $\beta/\ell\ (1-\rho/\beta)$, and then the negative reactivity is estimated from this equation with other parameters determined from a critical experiment.

These theories were developed in 1961 by the author [12-14] independently of Uhrig's theory [15]. The aims of both are very similar as far as the determination of subcritical reactivity is concerned; however, Uhrig ignored β in comparison with 1 and therefore obtained $(1-\kappa)/\ell$ for large subcriticality instead of $\beta/\ell\ (1-\rho/\beta)$.

Method and experimental equipment

Subcritical reactivity measurements were made on a cold clean reactor by Ricker [16-17] and Schultz [18]. At about the same time, subcritical reactivity measurements were made on TTR1 using a new method developed by the authors [19, 20] with ordinary simple instrumentation.

In order to obtain a high neutron flux level at a subcritical state and to be free from the spatial effect of ordinary neutron sources, an attempt was made to obtain a frequency spectrum while the power was slowly decreasing by rod drop with a constant period associated with the long delayed neutron decay constant.

Results of experiment

The reactivities determined by spectral density measurements in each of the two subcritical conditions were compared with the values obtained with the positive period method (Fig. 10).

It is clear that the subcritical break frequency shifts to the higher frequency, and that the reactivity obtained by this method is quite favourable particularly to measurements of large negative reactivity. The possible range of measurement, however, is limited by chamber efficiency.

This limitation may be eased by putting the chamber closer to the reactor core or by using several chambers.

Certain sources of error should be taken into account for this method. Firstly there are sources of error in the instrumentation. These errors, however, are not grave for this particular method. The second is due to finite sampling time and the non-stationary process.

Since the subcritical system itself, however, is linear, this particular non-stationarity problem is not very important. Qualitatively, because of the long decay constant of the neutron flux, the change of the neutron flux level is negligible over a short time. When data are taken over a longer time (about 30 seconds in this case), it is equivalent to an ensemble of short samples, each of which has an instantaneous power spectrum of the same shape for a frequency region as high as the break frequency of the subcritical reactivity determination.

The results from this experiment are sufficiently encouraging to warrant further investigation.

DEVELOPMENT OF BINARY NOISE TECHNIQUE FOR REACTOR TRANSFER FUNCTION MEASUREMENTS

M. Hara, N. Suda and J. Miida

The cross-correlation method has the advantage of providing us with information on both the gain and the phase of the reactor transfer function. A particular type of input signal, the binary noise, is often used, because its auto-correlation function is very close to the δ-function and therefore the cross-correlation function obtained is approximately equal to the system weighting function $g(t)$.

$$\phi_{io}(\tau) = \int_{-\infty}^{\infty} g(t-\tau)\ \phi_{ii}(t)dt \approx g(\tau)$$

Since the transfer function $G(j\omega)$ is the Fourier transform of $g(t)$, it is approximately equal to the cross-power spectrum $\Phi_{io}(j\omega)$. Using binary noise also simplifies the delay element and the multiplier needed for computing the cross-correlation function.

The two types of binary noise most frequently used are the random interval binary noise (RIBN) and the discrete interval binary noise (DIBN). In the case of RIBN the transitions from one state to the other occur independently and the number of

such transitions in any fixed interval is Poisson distributed. In the case of DIBN the times at which transitions can occur are explicitly specified and the state for any interval is chosen independently of the state in any other interval. More detailed comparisons of RIBN and DIBN have been discussed elsewhere [21]. It is concluded that, because of the limitation imposed by the response of the reactivity generator, the average rate of transitions κ for RIBN should be less than 5 s^{-1}, and the minimum interval between transitions, Δ for DIBN should be 0.02 s. The power density spectra of such binary noises are shown in Fig. 11. Since we are interested in the reactor transfer function for $\omega = 0.03$ to 30 rad/s, RIBN does not have a sufficiently wide bandwidth. Thus DIBN is considered to be more favourable.

The auto-correlation function of DIBN of infinite length is given by

$$\phi_{ii}(\tau) = 1 - \frac{|\tau|}{\Delta} \qquad \text{for } |\tau| \leq \Delta$$

and is zero for $|\tau| > \Delta$. However, DIBN actually used in experiments is always of finite duration and its auto-correlation function has *side-lobes* as shown in Fig. 12. The magnitude of the side-lobes follows the binominal distribution with a standard deviation of $1/\sqrt{N}$, if the total length of the noise is $N\Delta$. To estimate the error in the measured transfer function due to this side lobe, the reactor system was simulated on a digital computer and its transfer function measured using DIBN of $N = 10\,000$ [22]. The magnitude $1/\sqrt{N}$ of the side lobe is approximately 1%. The error in $\Phi_{io}(j\omega)$, however, amounted from 0.5 to 1 db in gain and from 5 to 10 degrees in phase as shown in Fig. 13. Thus error due to the side lobe is not always negligible.

It is known that a particular type of pseudo-random binary noise can be synthesized, whose auto-correlation function is shown by the broken line in Fig. 12. By using this type of binary noise, which may be called the binary noise of maximum period sequence of MSBN, the error due to the side lobe is eliminated. MSBN is synthesized by means of a sequency filter, if N is an integer having the form $2^n - 1$, and by quadratic residue method if N is a prime number of the form $4\kappa - 1$ [23]. If some external noise exists in the system, one period of MSBN is not sufficient to reject the effect of external noise. Hence identical MSBN are repeated 10 to 20 times in actual experiment.

A series of experiments were performed on a zero power critical assembly, SHE [24-26] and a heavy water reactor JRR3 [27], at zero power. Details of the experiments are shown in Table 2. The experimental set-up was almost the same for all measurements, and the block diagram of the data acquisition system for a recent measurement on JRR3 is shown in Fig. 14. Several types of reactivity generators were tried and one using a pulse motor was found to be the most reliable.

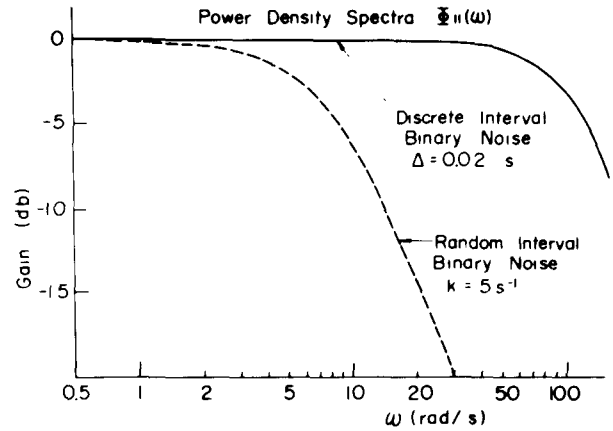


Figure 11. Comparison of bandwidth for discrete interval binary noise and random interval binary noise

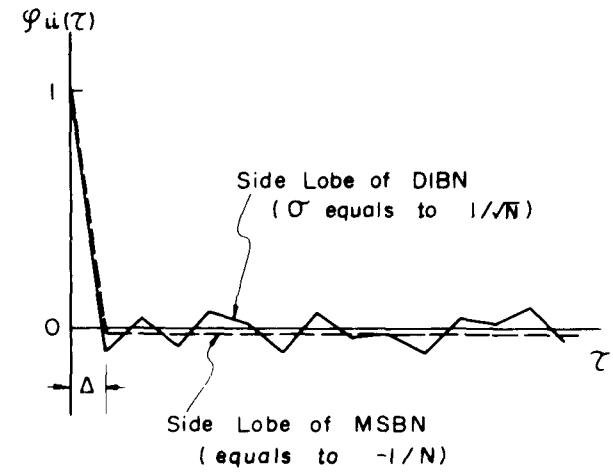


Figure 12. Side lobes in auto-correlation functions of DIBN and MSBN

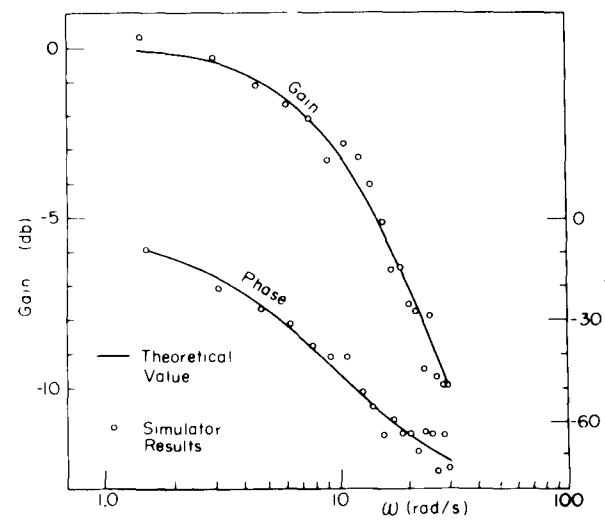


Figure 13. Transfer function of simulator obtained using a finite length DIBN

Table 2. Details of binary noise experiments

Reactor:	SHE [24-25]	SHE [21, 26]	JRR3 [27]	JRR3 [27]
Date:	Feb. 1962	Sept. 1962	Aug. 1963	Sept. 1963
Input binary noise				
Type	RIBN ($\kappa = 2\ s^{-1}$)	DIBN ($\Delta = 26$ s)	MSBN ($\Delta = 26$ to 104 ms)	MSBN ($\Delta = 26/65$ ms)
Length	180 s	$N = 10\,000$ or 300 s	$N = 511$ 10/20 chains	$N = 3\,463$ 10 chains
Reactivity generator				
Type	servo motor	servo motor	pulse motor	pulse motor
Worth	3.2 cents	1.45 cents	1.4 cents	1.4 cents
Neutron detector	WL-6377	RSN-77A	WL-6377	WL-6377
Amplifier	Keithley model 410	Keithley model 415	Keithley model 415	Keithley model 415
Prewhitening filter	$\frac{s}{s+0.08}$	$\frac{s}{(s+0.08)\ (s+16)}$	$\frac{s}{(s+0.008)\ (s+33)}$	$\frac{s}{(s+0.08)\ (s+33)}$
Magnetic recorder	Sony correlator	Sony data recorder	Sony data recorder	Sony data recorder
Date reduction	Sony analogue correlator	Sony analogue correlator	Sony analogue correlator	Sony analogue correlator and digital computer

The data thus recorded on a magnetic tape are reproduced and the cross-correlation function is computed on an analogue correlator. The cross-correlation function for large values of τ is obtained by replaying the magnetic tape at a speed higher than the recording speed. The Fourier transform of the cross-correlation function is computed with an IBM-650. One of the JRR3 transfer functions thus obtained is shown in Fig. 15, along with the theoretical value and the results obtained with the conventional rod oscillation technique.

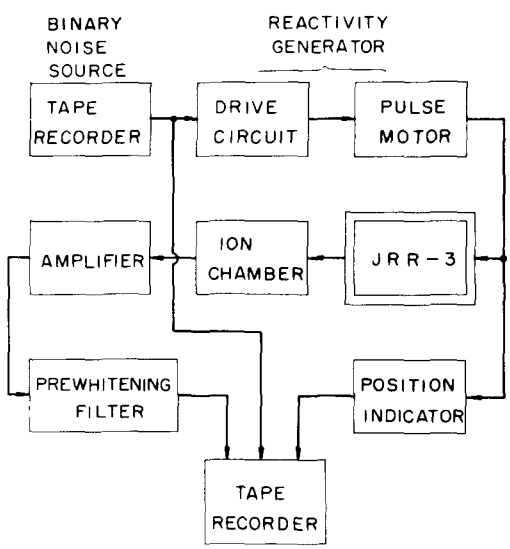


Figure 14. Block diagram of data acquisition system

The studies summarized above show that reactor transfer function is measured with fair accuracy by means of the binary noise method and that MSBN is most suitable for this purpose.

DIGITAL START-UP CONTROL OF A RESEARCH REACTOR

Y. Takahashi and S. Takamatsu

It is advantageous in light water moderated reactors to have the period signal in a digital rather than an analogue form, since pulse type detectors are used for measuring low power level in reactor start-up. Studies on digital start-up control are reported elsewhere [28-30]. A digital system has been successfully developed for starting up the TTR1 from source to power level.

A specially designed digital computer counts pulse signals from BF_3 counters every Δt seconds, and at the same time calculates reactor period for indication and inverse period for control using approximate formulas derived with particular attention to reduce random fluctuation of the calculated results. The calculated inverse period together with power signal is compared with the start-up programme preset on the push-buttons of the control panel to send digital control signals to the control rod drive-mechanism. The parameters set on the push-buttons in binary numbers are two inverse periods, a count rate at which the programmed inverse period is changed, a count rate at which the power control takes over the period control, a count

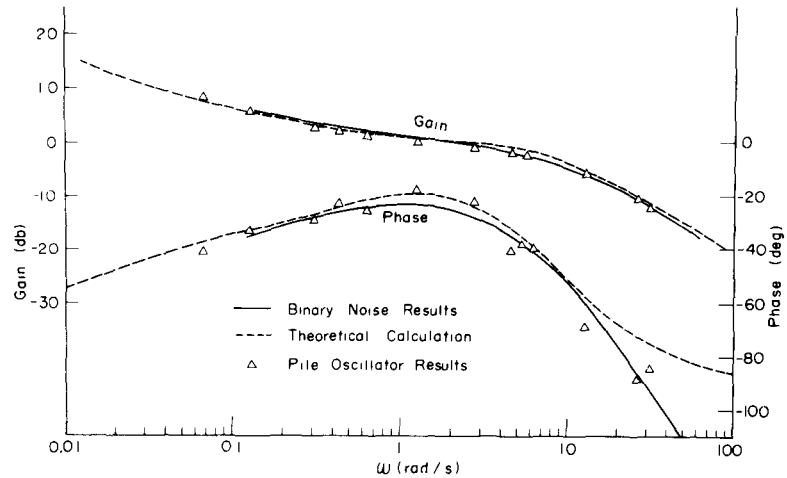


Figure 15. JRR3 transfer function obtained using MSBN

rate designating the final power level, reciprocal gain of the period control and a dead-band width. The control signal determines the speed of the control rod movement in proportion to the deviation of the inverse period or the power level from the program. Two BF_3 counters are used: one placed at a fixed position, and the other movable between two different positions. These three positions make possible measurements of power level over six decades. Reactor power and inverse period during the start-up programme are schematically shown in Fig. 16.

Reactor power is obtained by counting the number of pulses n during a predetermined sampling interval Δt. Reactor period and inverse period are calculated by the formula $T' = [n(t) + n(t - m\Delta t)]\, m\Delta t/2\, [n(t) - n(t - m\Delta t)]$, where m is an integer. Error of approximation in the above formula is of the order of $(m\Delta t/T)^2$. n is a random number of Poisson distribution. It is shown that an approximate inverse period S', defined as $1/T'$, roughly obeys the Gaussian distribution law. The ratio of standard deviation to mean value is plotted in Fig. 17 as a function of $T/m\Delta t$, which shows that fluctuations of S' increase for larger period and smaller number of counts. Results of the experiment are shown in Fig. 18, where reactor power is increased with a constant period without control. $m\Delta t$ should be large in order to reduce the fluctuation. On the other hand

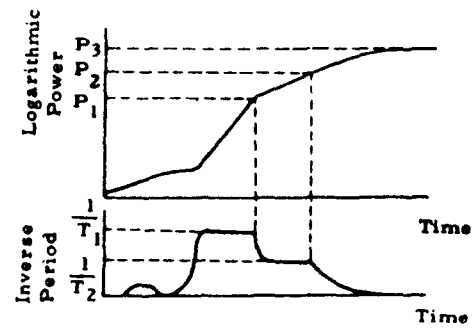


Figure 16. Increase of reactor power during start-up programme

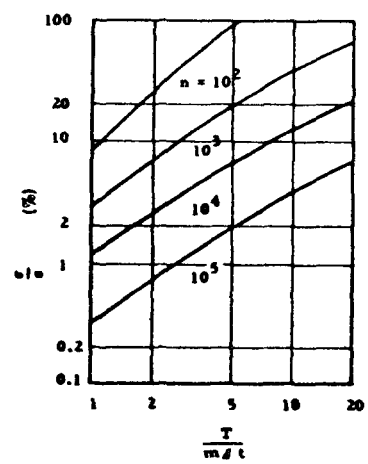


Figure 17. Fluctuation of inverse period

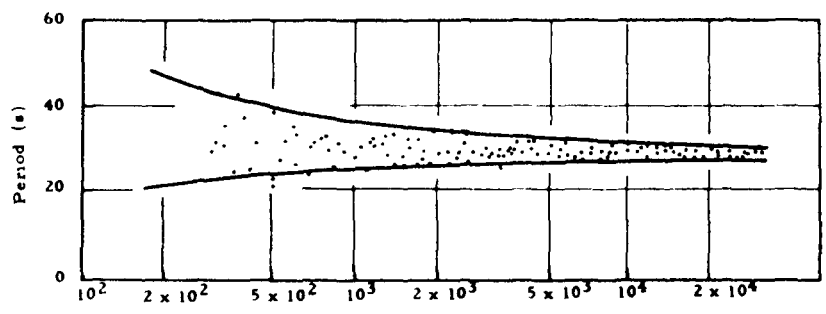


Figure 18. Period vs. count rate

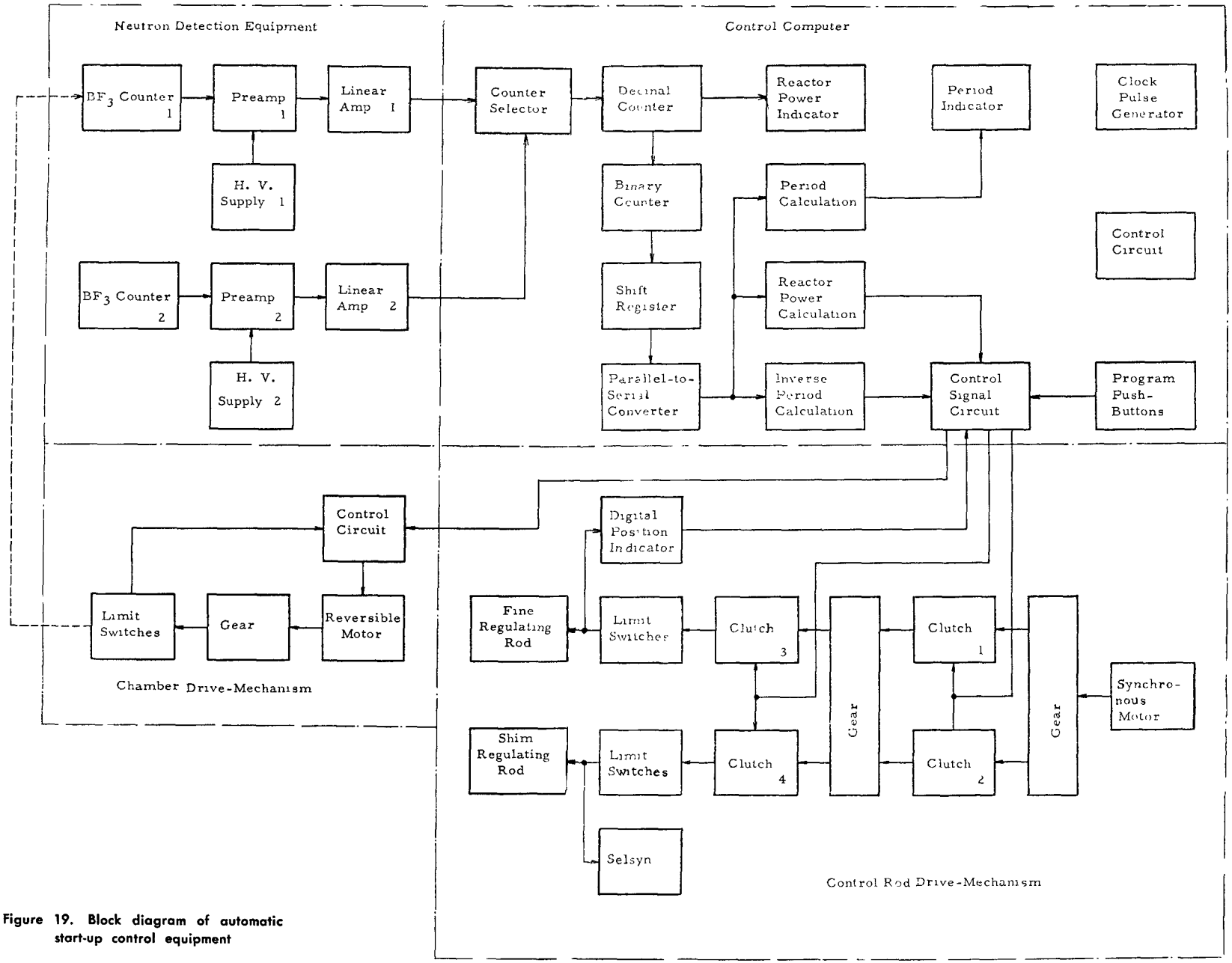


Figure 19. Block diagram of automatic start-up control equipment

large $m\Delta t$ means a large time lag in the period computation, resulting in an unfavourable effect on the control system. Thus the stability of the computed period and the response of the control system are incompatible. The optimum values of $m\Delta t$ and the count rate must be determined by compromise, and m was finally decided to be 4, and Δt to be 8, 4 and 2 seconds for $T > 100$, $100 > T > 50$ and $T < 50$, respectively.

The digital start-up control system consists of a neutron detection system, chamber drive-mechanism, control rod drive-mechanism, control computer and control circuit as shown in Fig. 19. The control computer is a special purpose digital computer where numbers are represented by 24-bit serial binary numbers, including a sign bit. The pulses from neutron detectors are also counted with binary counters. The counted number is sent into a set of shift registers. The numbers stored in the first and the last shift registers $n(t)$ and $n(t - 4\Delta t)$ respectively are led into an adder and to a subtracter to obtain $n(t) + n(t - 4\Delta t)$ and $n(t) - n(t - 4\Delta t)$ respectively. $n(t) + n(t - 4\Delta t)$ is now multiplied by $2\Delta t$ and is led into an accumulator from which the absolute value of $n(t) - n(t - 4\Delta t)$ is repeatedly subtracted until the minuend becomes negative. The number of subtractions is the approximate reactor period. Once the period is obtained, the content of the accumulator is replaced by the absolute value of $n(t) - n(t - 4\Delta t)$ multiplied by 2^{10}. $n(t) + n(t - 4\Delta t)$ is now repeatedly subtracted from the accumulator until the minuend is again negative. The number of subtractions is counted by an eight-bit binary counter. The number of counts in the counter is the approximate inverse period in units of 2^{-10} s^{-1}.

The automatic start-up of TTR1 was successfully carried out after testing the equipment with a reactor kinetic simulator. One of the results obtained is shown in Fig. 20. The control parameters used in this experiment are as follow: $T_1 = 30$ s, $T_2 = 170$ s, $P_1 = 8\,192$ cps, $P_2 = 16\,384$ cps. Final power $= 16\,384$ cps. Gain of period control $= 27.3$ cm, gain of power control $= 10.24$ cm, dead-band $= \pm 1/512$ s^{-1}.

REFERENCES

1. Sumita, K., *et al.*, Second National Nuclear Congress, Japan (1961), B65, not published.
2. Sumita, K., *et al.*, First Reactor Physics Fall Meeting of Atomic Energy Soc. of Japan (1961), Paper No. 40, 41.
3. Sumita, K., *et al.*, JAERI, Inst. & Controls Lab. Internal Memo 159 (1962).
4. Kuroda, Y., School of Eng. report, Tokai Univ., No. 1 (1963).
5. Sumita, K., *et al.*, First Reactor Engineering Fall Meeting of Atomic Energy Soc. of Japan (1963), Paper No. 5.
6. Skinner, R. E., *et al.*, Nuclear Sci. Eng., *3*, 573-594 (1958).

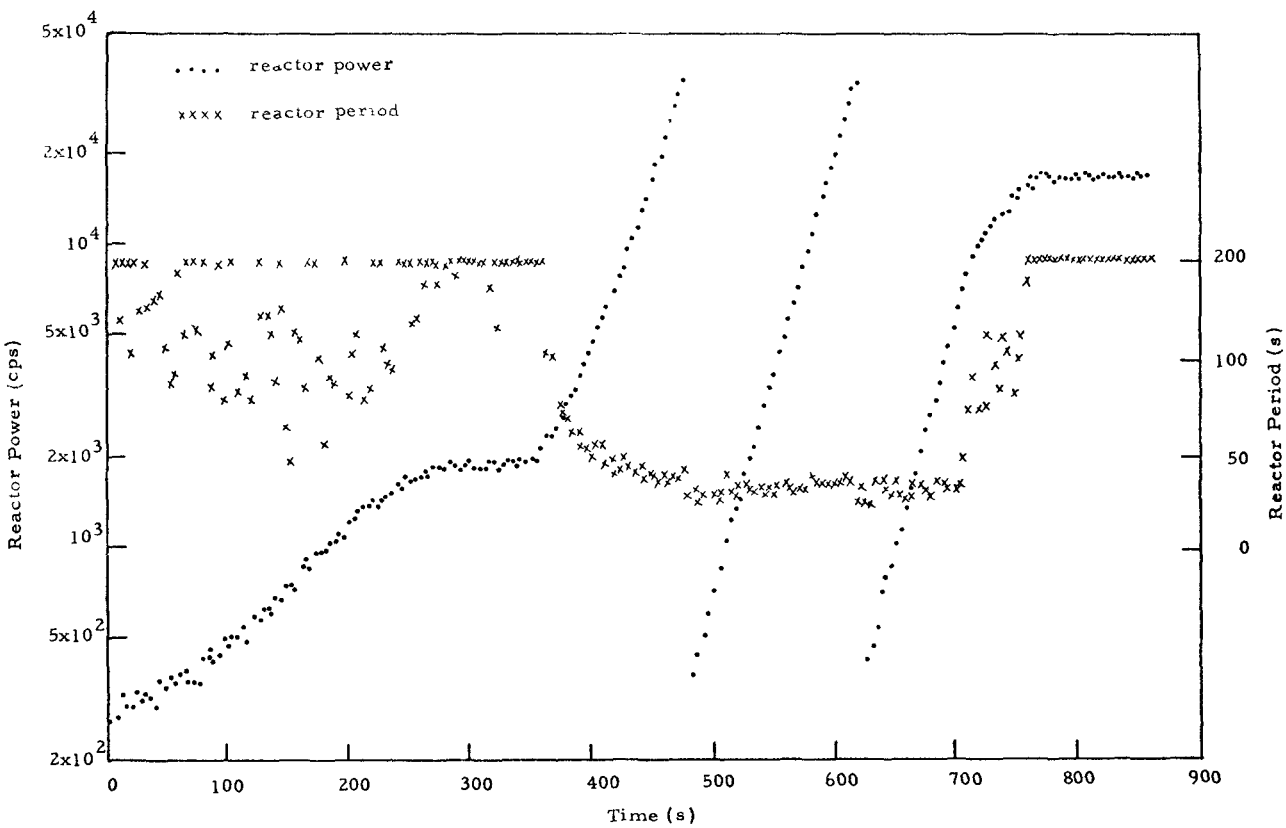


Figure 20. Reactor power and reactor period during automatic start-up

7. Moore, M. N., *ibid.*, *6*, 448-452 (1959).
8. Griffin, C. W., *ibid.*, *15*, 131-138 (1963).
9. Yamada, S., J. Nuclear Sci. and Tech., in press.
10. Schröder, V. R., Nucleonik, *4* (5), 277 (1962).
11. Cohn, C. E., Nuclear Sci. Eng., *5*, 331 (1959).
12. Nomura, T., First Reactor Physics Fall Meeting of Atomic Energy Soc. of Japan (1961), Paper No. 34.
13. Nomura, T., JIEE Professional Technical Committee on Control of Nuclear Plant (1961), Preprint No. 58.
14. Nomura, T., J. Nuclear Sci. and Tech., in press.
15. Uhrig, R. E., Trans. Amer. Nuclear Soc., *4*, 85-86 (1961).
16. Ricker, C. W., *et al.*, *ibid.*, *6* (1963).
17. Ricker, C. W., *et al.*, Trans. of the Symposium on Noise Analysis in Nuclear Systems (1963), No. 2-4.
18. Schultz, M. A., *ibid.*, No. 2-3.
19. Nomura, T., *et al.*, First Reactor Engineering Fall Meeting of Atomic Energy Soc. of Japan (1963), Paper No. 35.
20. Miida, J., *et al.*, Proc. of the Symposium on Noise Analysis in Nuclear Systems, to be published.
21. Hara, M., *et al.*, JAERI-Memo 1243 (1963).
22. SUDA, N., *et al.*, First Reactor Engineering Fall Meeting of Atomic Energy Soc. of Japan (1963), Paper No. 34.
23. Suda, N., JAERI Inst. & Controls Lab., Internal Memo 244 (1963).
24. Miida, J., *et al.*, Third National Nuclear Congress, Japan (1962), D75, not published.
25. Miida, J., *et al.*, JAERI Inst. & Controls Lab., Internal Memo 141 (1962).
26. Miida, J., *et al.*, Annual Meeting of Atomic Energy Soc. of Japan (1963), C58.
27. Okumura, Y., *et al.*, Annual Meeting of Atomic Energy Soc. of Japan (1964), F7.
28. Lehr. S. H., *et al.*, AIEE Trans., Pt. I, *79*, 369 (1960).
29. Schmidt, J. D., *et al.*, IRE Trans., NS-8, *3*, 1 (1961).
30. Takahashi, Y., *et al.*, Second National Nuclear Congress, Japan (1961), C27, not published.

ABSTRACT - RÉSUMÉ - АННОТАЦИЯ - RESUMEN

A/848 Japon

Etudes de cinétique et de contrôle des réacteurs nucléaires par des méthodes statistiques

par J. Miida

Les analyses statistiques des réacteurs nucléaires sont données par la méthode directe de mesure du spectre de puissance et par la méthode de corrélation mutuelle utilisant le bruit binaire. Le mémoire donne un résumé des études expérimentales et analytiques de cinétique de réacteur par ces méthodes, en faisant ressortir le spectre de bruit de différents réacteurs à l'état critique et sous-critique, par mesures directes, et aussi en mettant l'accent sur le développement des techniques de bruit binaire.

Finalement, on décrit la mise en marche automatique d'un réacteur de recherches par méthode digitale.

L'analyse de bruit de JRR 1 (type eau bouillante) a été effectuée par la méthode du filtre à bandes passantes, à différents niveaux de puissance (20 à 40 kW) et, également, par la méthode d'autocorrélation digitale à 40 kW. A des niveaux de puissance élevés, deux sommets sont apparus dans la région de basse fréquence: l'un était en accord avec le sommet obtenu sur le modèle de Moore ainsi que sur le modèle de Skinner-Hetrick; l'autre, non expliqué sur le modèle de Moore, semble être causé par une fluctuation de vide due à la radiolyse de l'eau.

Les mesures du spectre de puissance sur HTR (pile piscine), à différents niveaux de puissance (0,2 W à 100 kW) ont été effectuées par la méthode du filtre à bandes passantes avec des filtres jumeaux-T et des techniques d'accélération d'enregistreur sur bande. A puissance élevée, quelques-uns des sommets de résonance ont été trouvés dans la région de basse fréquence. La valeur absolue de la puissance du réacteur, obtenue par l'analyse du bruit basée sur le bruit de Cohn était, en dessous de 5kW, la même que sur l'indicateur de puissance.

Une analyse de bruit de réacteur, pendant le transitoire d'arrêt, a été proposée pour déterminer la réactivité négative de TTR 1 (pile piscine). En vue d'obtenir un niveau élevé de flux de neutrons en état sous-critique et d'être libéré de l'effet spatial des sources ordinaires de neutrons, on a essayé d'obtenir le spectre de fréquence de bruit du réacteur par la méthode du filtre à bandes passantes avec enregistrement sur bande pendant la baisse de puissance obtenue par chute des barres avec une période constante associée à la constante de neutrons retardés la plus grande possible. Des essais ont été effectués dans diverses conditions d'arrêt. Les fréquences limites observées ont été mises en équation dans la formule théorique $\beta/\ell(1-\rho/\beta)$ puis la réactivité négative a été estimée à partir de cette équation, à l'aide d'autres paramètres déterminés grâce à une expérience critique.

Les mesures de fonction de transfert de réacteur par la fonction de corrélation mutuelle entre la puissance du réacteur et l'apport de réactivité ont été effectuées en utilisant la variation de réactivité sous la forme de plusieurs types de bruits binaires. D'abord, une comparaison est faite entre les bruits binaires à intervalle aléatoire et à intervalle discret. Du point de vue de la largeur de bande, le dernier est favorable. Mais une analyse d'erreurs révéla que le bruit binaire pseudo-aléatoire de séquence de période maximale est préférable aux bruits binaires vraiment aléatoires. Le générateur de réactivité construit pour ces essais est actionné par le bruit binaire enregistré sur bande. La réactivité et la puissance du réacteur sont enregistrées simultanément sur bande

magnétique. Les deux techniques — analogique et digitale — sont utilisées pour évaluer la fonction de corrélation mutuelle.

Le démarrage automatique de TTR 1, depuis son niveau de source jusqu'à son niveau de puissance, est réalisable avec un calculateur digital. Un calculateur digital spécialement conçu compte les signaux d'impulsions venant de compteurs BF_3, toutes les Δt secondes et, en même temps, calcule la période du réacteur pour l'indication et pour le contrôle. Une formule approximative permet de calculer la période du réacteur. La valeur approximative ainsi obtenue donne, particulièrement à des bas taux de comptage, une estimation plus stable de la période qu'un périodemètre analogique ordinaire. Le signal de contrôle est déterminé de telle sorte que la vitesse de la barre de contrôle soit proportionnelle à un signal d'erreur de période inverse.

Le système de démarrage digital décrit est une partie du programme destiné à établir un système à réacteur de recherche entièrement contrôlé par des calculateurs. Il assurera également la sécurité dans l'exploitation des réacteurs.

A/848 Япония

Исследование кинетики и регулирования ядерных реакторов статистическими методами

Ю. Миида

Описан статистический анализ ядерных реакторов методом прямых измерений спектра мощности и методом взаимной корреляции с использованием двойных шумов. Суммированы данные по экспериментальному и аналитическому изучению кинетики реакторов этими методами, причем особое внимание уделено спектру шумов различных реакторов в критическом и подкритическом состояниях путем непосредственных измерений и развитию методики двойных шумов.

Наконец, описан автоматический запуск исследовательского реактора с применением цифровой вычислительной машины.

Анализ шумов реактора JRR-1 (с кипящей водой) был проведен по методу полосового фильтра при различных уровнях мощности (0,5 *вт* — 40 *квт*), а также по методу цифровой автокорреляции при мощности 40 *квт*. При более высоких уровнях мощности в области низких частот появляется пара пиков, один из которых согласуется с пиком, полученным из модели Мура, а также модели Скиннера — Хетрика. Однако другой пик, который не удается объяснить моделью Мура, по-видимому, обусловлен флуктуациями пустот из-за радиолитического разложения воды.

Измерения частотного спектра мощности реактора на реакторе HTR (погружного типа) при различных уровнях мощности (0,2 *вт* — 100 *квт*) были проведены по методу полосового фильтра со сдвоенными Т-образными фильтрами и высокоскоростной записью на магнитную ленту. При большой мощности в области низких частот было найдено несколько резонансных пиков. Абсолютное значение мощности реактора, полученное методом анализа шумов, основанным на шумах Кона, для мощности ниже 5 *квт* согласуется с показаниями измерителя мощности.

Было предложено провести анализ шумов реактора в процессе выключения, чтобы определить отрицательную реактивность реактора TTR-1 (погружного типа). Чтобы получить высокий уровень нейтронного потока при подкритическом состоянии и освободиться от пространственного эффекта обычных нейтронных источников, попытались определить частотный спектр шумов реактора по методу полосового фильтра с записью на магнитную ленту, когда мощность уменьшается вследствие падения стержня с постоянным периодом, связанным с самой большой постоянной распада запаздывающих нейтронов. Эксперименты проводились в различных условиях выключения. Наблюдаемые точки излома частотной характеристики приравнивали к теоретической формуле $\frac{\beta}{l}\left(1-\frac{\rho}{\zeta}\right)$, после чего отрицательную реактивность можно было оценить из этого уравнения, но с другими параметрами, определенными в критическом эксперименте.

Измерения передаточной функции реактора при помощи функции взаимной корреляции между мощностью реактора и величиной реактивности проводились с использованием изменений реактивности в виде различных типов двойных шумов. Прежде всего сравнивали двойные шумы с беспорядочными интервалами и дискретными интервалами. С точки зрения ширины полосы последние были предпочтительнее. Однако анализ ошибок показал, что по сравнению с обычными шумами предпочтительнее псевдобеспорядочные двойные шумы с максимальным периодом следования. Серийный генератор реактивности запускается двойными шумами, записанными на магнитную ленту. Реактивность и мощность реактора записываются на магнитную ленту одновременно. Для расчета функции взаимной корреляции были использованы оба метода как электронно-аналоговый, так и цифровой.

Автоматический запуск реактора TTR-1 от уровня с источником до уровня на мощности стал возможен с использованием цифровой вычислительной машины. Специально сконструированная цифровая вычислительная машина считает сигналы импульсов от счетчика с трехфтористым бором каждые Δt секунд и в то же время вычисляет период реактора для указания

и для регулирования. Период реактора вычисляется по приближенной формуле. Полученная таким образом приближенная величина дает более стабильную оценку периода, в особенности при меньшей скорости счета, чем обычный аналоговый измеритель периода. Регулирующий сигнал определен таким образом, что скорость регулирующего стержня пропорциональна сигналу ошибки обратного периода. Описанная система регулирования запуска при помощи цифровой машины является частью программы разработки полностью автоматизированной системы регулирования исследовательского реактора при помощи вычислительной техники. Эта система также обеспечивает безопасную эксплуатацию реактора.

A/848 Japón

Estudios cinéticos y control de reactores nucleares por métodos estadísticos

por J. Miida

Se describe el análisis estadístico de reactores nucleares por el método directo de medida del espectro de potencia y también por el de intercorrelación usando ruido binario. Se resumen los estudios analíticos y experimentales de cinética de reactores mediante estos métodos, poniendo un énfasis especial en el espectro de ruido de varios reactores en estados críticos y subcríticos obtenido por medida directa, así como en el desarrollo de técnicas de ruido binario.

Finalmente se describe la puesta en marcha automática de un reactor de investigación con un método digital.

El análisis de ruido de JRR 1 (tipo hervidor de agua) se llevó a cabo mediante el método de filtros pasabanda a varios niveles de potencia (20 a 40 kW) y también por el método de autocorrelación digital a 40 kW. A niveles de potencia más elevados aparecen dos picos en la región de baja frecuencia, uno de los cuales se corresponde con el obtenido con los modelos de Moore así como con el de Skinner-Hetrick. Sin embargo, el otro pico, que no es explicado por el modelo de Moore, parece ser debido a fluctuaciones de burbujas por descomposición radiolítica del agua.

Se hicieron medidas del espectro de frecuencia de potencias en HTR (tipo piscina) a varios niveles de potencia (0,2 W a 100 kW) por el método de filtros pasabanda con filtros doble T y técnicas rápidas de registro en cinta. A potencias elevadas algunos de los picos de resonancia aparecieron en la región de bajas frecuencias. El valor absoluto de la potencia del reactor deducido del análisis de ruido basado en el modelo de Cohn concordaba con la indicación del medidor de potencia en menos de 5 kW.

Se ha propuesto el análisis de ruido del reactor durante el transitorio que sigue a una parada como método para determinar la reactividad negativa del TTR 1 (tipo piscina). A fin de obtener un alto nivel de flujo neutrónico en estado subcrítico y estar libre del efecto espacial de las fuentes ordinarias de neutrones, se intentó obtener el espectro de frecuencia del ruido del reactor mediante el método de los filtros pasabanda con un registrador de cinta magnética mientras la potencia descendía, por caída de la barra, con un período constante asociado con la constante de desintegración más larga de los neutrones retardados. Se llevaron a cabo experimentos en diferentes condiciones de parada. Las máximas de frecuencia observadas se igualaron a la expresión teórica, $\beta/\ell\ (1 - \rho/\beta)$ y entonces se dedujo de la ecuación la reactividad negativa, una vez que se habían determinado los valores de los otros parámetros a partir de una experiencia crítica.

Las medidas de la función de transferencia del reactor a través de la función de intercorrelación entre potencia del reactor y reactividad, se han llevado a cabo usando variaciones de reactividad en forma de varios tipos de ruido binario. En primer lugar se comparan los ruidos binarios para intervalo aleatorio e intervalo discreto. Desde el punto de vista de la anchura de banda, el último es favorable. Sin embargo, un análisis de errores demostró que es preferible el ruido binario pseudoaleatorio de máximo período a los aleatorios reales. El ruido binario registrado en cinta magnética acciona un generador de reactividad diseñado para este objeto. La reactividad y la potencia del reactor se registran simultáneamente sobre las cintas magnéticas. Se utilizan técnicas analógicas y digitales para calcular la función de intercorrelación.

Mediante una calculadora digital se ha hecho posible la puesta en marcha automática del TTR1 desde el nivel de fuente hasta nivel de potencia. Una calculadora digital especialmente diseñada cuenta los impulsos de los contadores de BF_3 cada Δt segundos, y al mismo tiempo calcula el período del reactor para indicación y para control. El período se calcula mediante una fórmula aproximada. El valor aproximado así obtenido proporciona una estimación más estable del período que con un medidor analógico convencional, en especial a ritmos de recuento bajos. La señal de control se determina de modo que la velocidad de la barra de control es proporcional a una señal de error de período inverso. El sistema descrito de control digital para la puesta en marcha automática forma parte de un programa con el fin de establecer un reactor de investigación completamente controlado con calculadora digital. Ello permitirá también una operación de los reactores libre de riesgos.

In-core instrument development in the HBWR programme *

By B. Aarset, H. P. Olson, R. D. Smith and O. Vapaavuori **

HBWR is the only boiling heavy water reactor [1]. It has been internationally operated as an OECD project for the last five years to demonstrate the feasibility of the boiling D_2O concept and to explore the limitations of the system.

The key to a new HBWR programme is an extensive system of in-core instrumentation and read-out developed in the last 2½ years in connection with the experimental reactor dynamics programme. In the effort to reduce present conservatism in design, about twenty-five test fuel assemblies will be equipped with instruments to measure channel power, monitor flow, measure void fraction, monitor fuel central and surface temperatures, and protect test fuel in various other ways.

The continuous measurement of critical parameters will permit in-pile experiments to be conducted under conditions that might otherwise involve considerable risk to programme continuity. It is evident that similar approaches to fuel design and heat load improvements are being followed in other test reactors. The pressurized water reactor at Saxton [2] and the boiling light water reactor at Vallecitos [3] both employ in-core instrumentation on elements unique in design or heat rating. There are, however, differences in approach and reactor system designs, apart from the differences in moderator and coolant, that tend to make the HBWR facility unique for the fuel test programme. Some of these are:

(*a*) The reactor (Fig. 1) employs individual fuel element penetrations. A completely instrumented test assembly can be inserted very rapidly in any of the *200 vacant core positions*. The natural circulation mode of cooling eliminates the need for costly instrumented external loops and heat exchange equipment. The flexible leads from the fuel instruments run directly to the junction boxes leading the signals out of the reactor hall and into the data processing system;

(*b*) The open lattice and fuel stringer pitches of D_2O reactors lead to a degree of instrumentability not obtainable in tighly-packed H_2O cores (this feature may ultimately have a strong implication on power reactors where the ability to install instrumentation may permit power densities not possible in light water cores). An example of this might be found in either the stability monitoring or burn-out protection techniques now being applied at HBWR to high specific power test channels;

(*c*) The ability that exists in HBWR to operate any given test channel in the forced circulation non-boiling condition, forced circulation boiling condition, or natural circulation boiling condition (while the rest of the core operates in a normal natural circulation boiling mode) provides the possibility of direct (flow $\times$ ΔT) power calibration of gamma or neutron sensing instruments located within the test fuel. The calibrated flux instruments can then be used for direct channel power measurement when the channel is converted to natural or forced circulation boiling;

(*d*) The extent and variety of instrumentation that has been proved and is available for any new HBWR test fuel element, is believed to exceed that available in any other boiling test facility. Figure 2 shows the locations in which instrumented assemblies have been placed. Figure 3 shows a pictorial drawing of the most recently installed instrumented fuel assembly, IFA-4. This assembly has been in-pile since November 1963 and all of the instruments are performing satisfactorily. Table 1 gives the history and future of in-core instrument development at HBWR. Figures 4 through 10 show some of the instruments and give highlights of their development.

STATUS OF DEVELOPMENT

In the recent dynamics programme, the use of in-core instruments to permit direct measurement of the microscopic parameters such as channel steam void, fuel and channel coolant temperatures and local coolant velocities was recognized as the most promising approach to the verification of models that could justify extrapolation. This need for direct measurement of microscopic parameters, together with an absence of proven instruments for those purposes, led to the development of in-core instrumentation for dynamic measurement in HBWR.

It was decided in 1961 to install moderator temperature measuring thermocouples, in-core fission chambers and four instrumented fuel assemblies containing thermocouples, inlet and outlet turbine flow meters and dynamic void gauges. The ways in which the instruments have been used in various

* One of the joint undertakings of the OECD European Nuclear Energy Agency.

** Institutt for Atomenergi, OECD Halden Reactor Project, Halden.

combinations to measure critical in-core parameters are indicated in Table 2.

A boiling loop for testing electrically heated replicas of HBWR fuel elements, was constructed in late 1962 to study fuel element burn-out and hydraulic performance, evaluate instruments, and to study the validity of hydraulic extrapolation from a single element in a closed loop to the reactor situation.

By early 1964 about 100 in-core and loop signals were available.

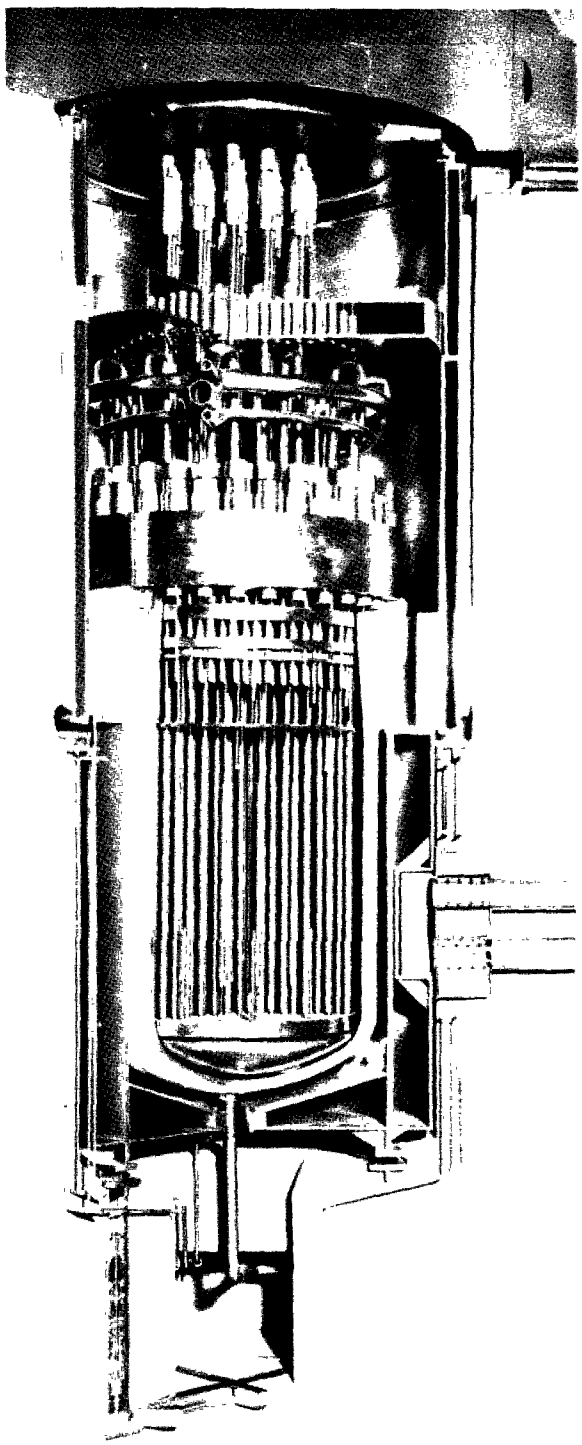


Figure 1. The reactor is located in a 30 feet deep pit inside a small mountain. The minimum rock overburden is about 90 feet. The section shows the original metallic fuel charge of 296 elements

DATA REDUCTION

Any signals can be selected for comparison with theoretical predictions in dynamic experiments. To permit simultaneous analysis of the time behaviour of a large number of in-core signals, an extensive system for automatic data reduction was installed in the spring of 1963. The system employs a two-channel transfer function analyser, a special analogue computer for noise correlation studies, high speed visual recording equipment, a 60 amplifier analogue computer for reducing instrument signals to meaningful dynamic parameters before analysis, an analogue-to-digital converter and a small, but fast, digital computer.

NEW DEVELOPMENT AIMS

Fuel test programme

The new HBWR programme incorporates the long term and high specific power irradiation of oxide and metal fuel elements embodying metallurgical and structural features that lead to reduced cost, or ease fabrication. The irradiation behaviour of these fuel assemblies will be assessed by the combination of special in-core instrumentation, by periodic removal and visual examination, and by post-irradiation destructive examination. The first 10 of a total of about 25 test assemblies are specified and are in various phases of design and construction (Table 1, Future).

The instrument development effort to complement the fuel test programme includes systems for measuring direct channel power, axial form factor, central oxide temperature and fission gas pressure, and instrumentation for protecting against heat transfer burn-out, and hydraulic instability. A fuel failure location system is being developed.

Dynamic experiments

Dynamic experiments will be carried out with instrumented tubular fuel elements to be installed late in 1964 and early 1965. The elements will be subjected to periodic flux and flow perturbations and, from the responses in the various in-core parameters, it will be possible to compare in-pile and out-of-pile hydrodynamic behaviour and assess the effect of hydraulic coupling between adjacent channels in a D_2O boiling reactor.

For this programme, instrument development is being extended to include electromagnetic in-core flow oscillators, channel void gauges and high speed gamma thermometers.

Table 1. Instrumented

	PAST	PRESENT				
	TR-1, 2, 3	TTR-1	FR-1	IFA-1	IFA-2	IFA-3
Description	Moderator temperature rods for moderator temperature mapping during 0 power high temperature physics experiments	Moderator temperature and cable corrosion test rods	Dynamic axial flux measurement	Instrumented second charge fuel assembly 1½ wt % UO_2	Instrumented second charge fuel assembly 1½ wt % UO_2	Instrumented second charge fuel assembly 1½ wt % UO_2
Date in	March-May 1962	July 1962	Dec. 1962	Oct. 1962	Feb. 1963	June 1963
Instruments contained	5 Chromel Alumel t/c's 304 SS clad Alumina insulated 1 mm diameter	8 Chromel Alumel t/c's with cladding of 304 SS 321 SS 347 SS Inconel	3 GE miniature fission chambers at ¼, ½ and ¾ points in fuel charge	2 turbine flow meters 1 void gauge 3 surface t/c's 5 coolant t/c's 1 calibration valve All cables 1 mm SS clad	2 turbine flow meters 1 void gauge 3 surface t/c's 5 coolant t/c's 1 calibration valve All cables Inconel clad	2 turbine flow meters 1 void gauge 3 surface t/c's 5 coolant t/c's 1 calibration valve 3 gamma thermometers 1 central oxide t/c
In-core instrument problems identified (later resolved)	Rapid corrosion of SS clad t/c's observed leakage of sheaths resulted in loss of accuracy	Similar corrosion of type 304 and 321 cables	None	(1) SS cable corrosion reduced turbine signals Failed void gauge, reduced accuracy of thermocouples (2) Calibration valve sluggish in operation	(1) Turbine pocket leakage reduced signals (2) Central oxide fabrication failures penetration and mechanical design (3) Awkward assembly main seal (4) Channel power measurement natural circulation imprecise (5) Flow pattern effect on turbine calibration (6) Nicrobraze and silver-solder penetrations not desirable or reliable	(1) Central oxide t/c failed mechanically during irradiation (2) Coolant t/c location critical to forced circulation power measurement (3) Errors in moderator heat transfer determination (4) Gamma thermometer signal smaller than design value
Date out	1963	Indefinite	Indefinite	January 1963	Indefinite	Indefinite

assemblies in HBWR

		FUTURE			
IFA-4	MVR-1	IFA-5	IFA-6	IFA-7-10	IFA-11-28
Instrumented second charge fuel assembly 6 wt % UO_2	Moderator void rod — 5 impedance void gauges on rod for testing new seal and flashing void tests	(Swedish) Instrumented Marviken fuel assembly 2½ wt % UO_2 6 rods Long segments, spacer clips	(British) Instrumented prototype SGHWC fuel assembly 6 or 7 rods Long segments, thin canning	Instrumented tubular metallic fuel assemblies natural uranium tubes External cooling for hydrodynamic tests	Instrumented test fuel assemblies Britain, Sweden, Norway Testing: spacers oxides rods and tubes heat ratings instruments claddings
Nov. 1963	Oct. 1963	Apr. 1964	July 1964	Sept. 1964	1964-1966
2 turbine flow meters 2 void gauges 2 surface t/c's 5 coolant t/c's 1 calibration valve 3 gamma thermometers 1 central oxide t/c 1 burn-out protector 1 sampling tube 1 injection tube 1 fission gas transducer Removable instruments and shroud	5 impedance void gauges using high compression mechanical ceramic-to-metal seal	1 turbine flow meter 4 coolant t/c's 1 calibration valve 3 gamma thermometers 1 central oxide t/c 1 sampling tube	2 turbine flow meters 4 coolant t/c's 1 calibration valve 3 gamma thermometers 1 sampling tube Removable shroud	2 turbine flow meters 2 void gauges 5 coolant t/c's 1 calibration valve 3 gamma thermometers 1 burn-out protector 1 sampling tube 1 flow oscillator Removable shroud Replaceable instruments Alternate cooling	Instrumented to fit test objectives 1 sampling tube
None identified	(1) High compression seals within three days in reactor				
Indefinite	Indefinite	August 1964	July 1966	Indefinite	

IN-CORE INSTRUMENTS

Background

The in-core instrument development concurrent with the first and second charge research programmes has made it possible to move directly to in-pile fuel testing and hydrodynamic programmes at high specific channel powers. The programme for development of instruments supporting the experimental dynamics investigations was formulated early in 1961 and has been revised as the shift in emphasis toward high specific power and long term fuel testing materialized. Basic development problems had been recognized earlier and work had already begun in 1960 on the specification for flux meters (Fig. 4), principle testing of impedance void gauges (Fig. 5) and in-core cabling (Fig. 8) at the Kjeller Research Centre and at HBWR. The In-Core Instrument Meeting at HBWR in May 1961 [4] and the Advanced Course on In-Core Instrumentation for Water Cooled Reactors [5], held in August of the same year, brought together specialists from Europe and the US and enabled the HBWR development programme to utilize and depart from technology developed at other sites. A symposium was held in Oslo in June 1964 to re-establish these bases for future work.

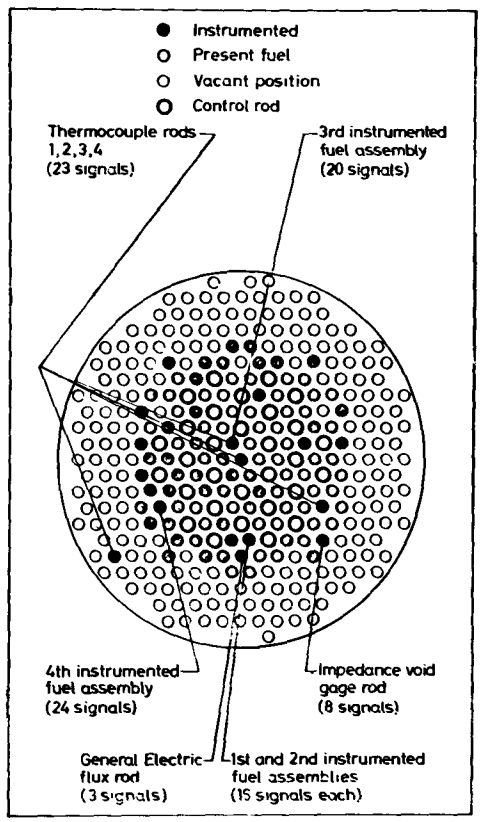


Figure 2. The top lid of HBWR contains 336 holes. 100 holes are presently occupied by second charge fuel in an open hexagonal arrangement with 30 control rods occupying central positions. Test fuel elements are located in the lattice as desired, displacing standard elements to outer positions. The black spots show positions in which instrumented assemblies have been located during the present programme

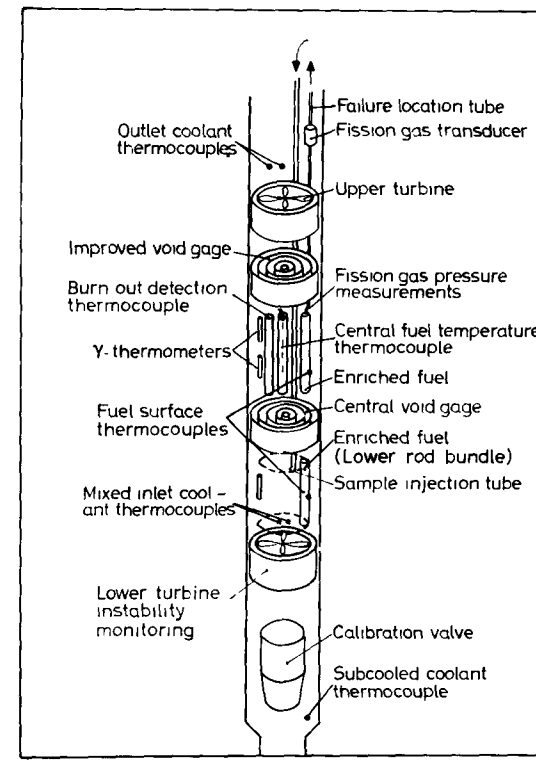


Figure 3. The fourth instrumented fuel assembly, IFA-4, contains all instruments developed earlier for the dynamic experiments plus prototypes of new instruments, including burn-out detector, steam-sampler, central void gauge, improved central oxide thermocouple. The element is designed for post irradiation replacement of instruments and uses 6 wt% UO_2 fuel to operate up to double normal fuel powers. First irradiation started in November in low flux position. All instruments are working properly

The record of assemblies containing in-core instruments that have been installed in HBWR is indicated on the lattice diagram of Fig. 2, and Figs. 4 to 10 briefly describe the instruments employed, their precision, and in-pile application.

Table 1 summarizes the design, history and experience with various instrumented assemblies installed in HBWR since 1961. The fourth instrumented fuel assembly (IFA-4) installed on 4 November 1963, embodies improved versions of all fuel instrumentation previously tested [6] and in addition contains instruments undergoing their first in-pile evaluations.

Instrument development problems

A discussion of the detailed mechanical and electronic development problem encountered in the construction, calibration and application of the system of in-core instrumentation now in use at HBWR

Table 2. Functions of in-core instruments

	Power and Flow							Physics and Hydraulics Studies													High Specific Power Studies	
	Forced circulation	Total power of fuel channel: Boiling: Static	Total power of fuel channel: Boiling: Dynamic	% Subcooled power in fuel channel	Channel coolant flow (dynamic and static)	Temperature reactivity coefficients	Void reactivity coefficients	Channel exit void: Static	Channel exit void: Dynamic	Channel average void (dynamic and static)	Channel exit void: Static	Channel exit quality: Dynamic	Channel exit quality: Static	Channel exit slip: Dynamic	Channel exit slip: Static	Axial flux shape: Dynamic	Fuel time constant	Coolant transit time and void formation in moderator	UO_2 conductivity and central temperature	Gas pressure release in fuel stringer	Fuel failure location	Heat transfer burnout protection
Bottom turbine	•			•	•		•	•		•		•	•	•							•	
Top turbine	•						•	•		•		•	•	•								
Top void gages							•		•	•		•		•								
Central void gages										•												
In-core flux chambers			•												•	•						
γ-thermometers		•				•	•				•		•		•							•
Fuel surface t/c's																•						
Inlet coolant t/c's		•		•							•											
Outlet coolant t/c's	•	•																				
Subcooled inlet t/c's	•			•							•											
Calibration valve	•																					
Central oxide t/c's						•													•	•		
Fission gas transducer																				•		
Burnout detector t/c's																						•
Active sample injector																					•	
Steam samplers																					•	
Moderator void gages																	•					
Moderator t/c's						•											•					
Subcooled plenum pressure				•							•											

is outside the scope of this paper. Table 1 does, however, indicate the past growth of the programme and identifies some of the more significant problems. For further information on these problems the series of Halden Project Quarterly Progress reports [7] is comprehensive. The results of in-pile measurements made with the first three instrumented fuel assemblies are also documented and discussed in the progress reports and in [6]. The experiments with the fourth instrumented fuel assembly, IFA-4, have been the most extensive.

Figures 4 to 10 attempt to highlight the instruments individually and present a sample of the problems, calibration data and actual in-pile results. It is hoped that this series of figures with their captions will stand alone to present a summary picture of the scope of the programme.

IFA-4

The fourth instrumented fuel assembly (IFA-4), installed on 4 November 1963, embodies improved versions of all fuel instrumentation previously tested [6] and in addition contains instruments undergoing their first in-pile evaluations.

The recognition, in early 1963, that high specific power fuel testing would play an important part in future HBWR activities led to the design of the fourth instrumented fuel assembly (Fig. 3) to contain instruments especially applicable to that kind of programme, and enabled early experience to be gained. The list of instruments in IFA-4 is shown in the figure and will not be repeated here.

The calibration runs with IFA-4 have included:

(*a*) Forced circulation non-boiling experiments, up to 250 kW channel power, to: (i) determine base points for fission gas pressure build-up (Figs. 10c and 10d); (ii) determine calibrations for the three gamma thermometers (Fig. 7) in terms of specific channel power (Fig. 6); (iii) measure (in perturbation experiments) the transfer functions of the gamma thermometers, burn-out protector, and the fuel itself (Fig. 9e) and intercalibrate all thermocouples (Fig. 9c);

(*b*) Forced circulation boiling experiments in which the theoretical boiling boundary was changed by varying sub-cooling in the range from 0-100%

Table 3. Void fractions in typical boiling reactors

Reactor	Type	Pressure (atm)	Maximum channel exit void fraction: Existing	Maximum channel exit void fraction: Planned
Kahl	Light water	71	62	—
VBWR	Light water	70	46	72
Dresden	Light water	70	45	—
HBWR	Heavy water	30	82	94
Marviken	Heavy water	50	—	72

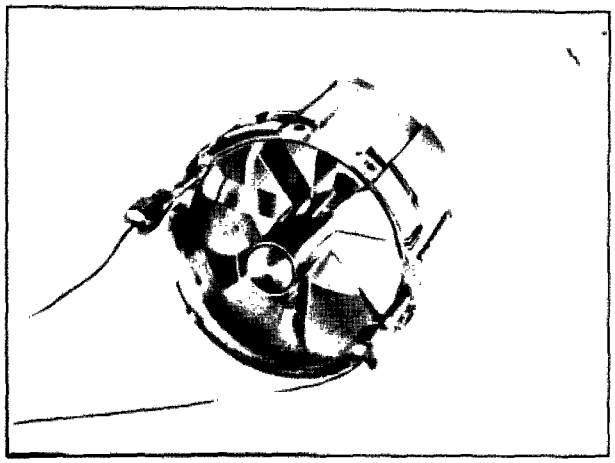


FIG. a Two flow meters of this type have operated since February 1963 and retain calibrations. Turbine responses are flat to 10 c/s. Eight have been employed so far.

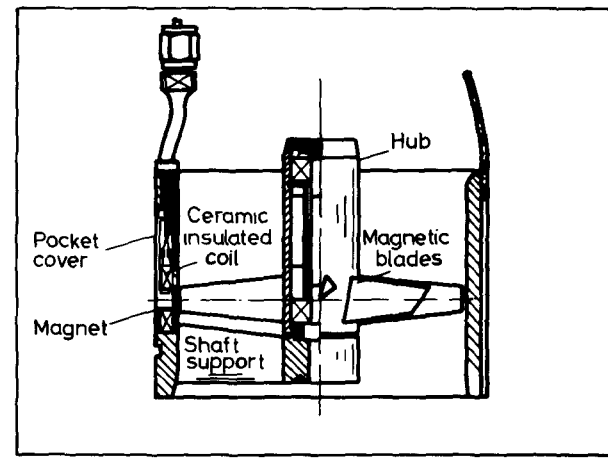


FIG. b The turbines employ 2 flat, coil-wrapped permanent magnets inside sealed housing pockets and use 8 magnetic blades of 19 cm pitch. Graphite bearings are in hub.

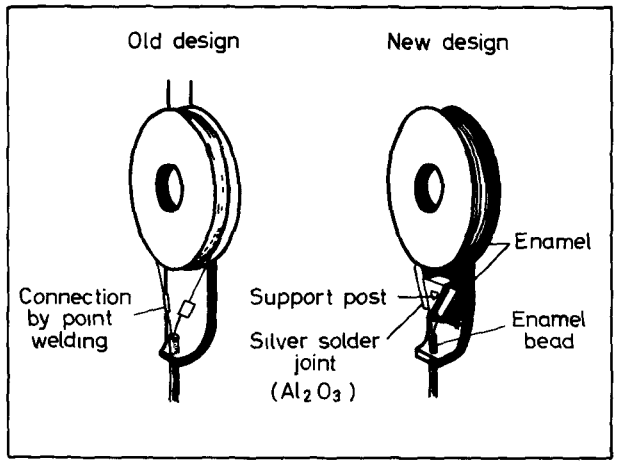


FIG. c Leakage into the turbine pick-up pockets was reliably prevented by all-stainless-steel mechanical seals, and internal pocket improvements prevented shorting.

$$\alpha = 1 - \frac{V_{LT}}{V_{UT}}(1-x)(1-x+Sx)$$

$$x = \frac{Q_F + Q_M - Q_{SC}}{V_{LT} \cdot A \cdot \rho_W \cdot r}$$

$$S = \frac{1-\alpha}{\alpha}\,\frac{x}{1-x}\,\frac{\rho_W}{\rho_S}$$

Q_M - Heat transferred from moderator into channel

ρ_W, ρ_S - Water and steam densities

A - Turbine area

x - For other nomenclature see other Figs.

FIG. d Readings of turbines below and above the fuel bundle combine to give : flow, exit void fraction, and exit steam-to-coolant velocity ratio (slip).

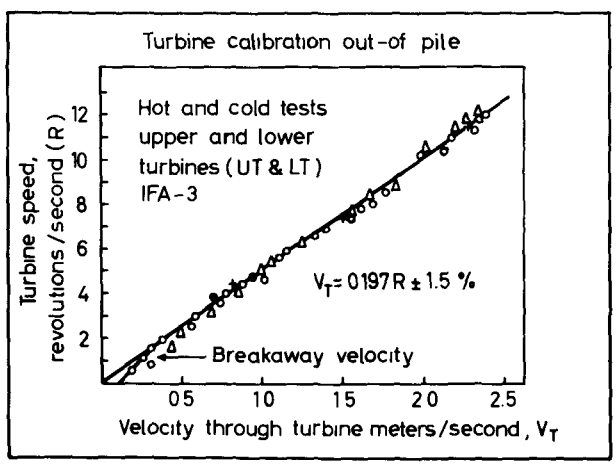


FIG. e Out-of-pile calibrations with full liquid flow give individual calibration curves for each turbine meter. Forced circulation runs in-pile check calibrations.

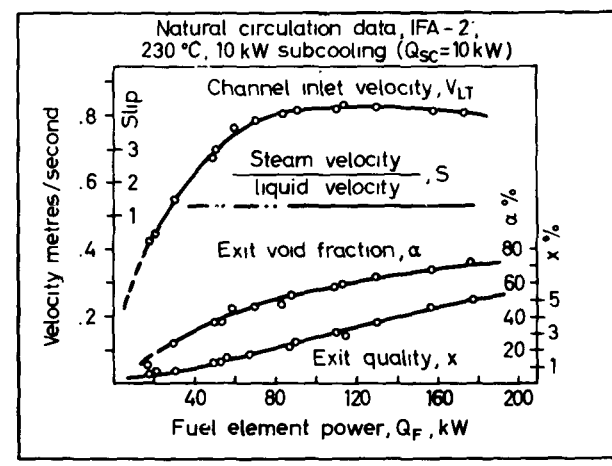


FIG. f Natural circulation hydraulic data from instrumented fuel assemblies are now being extended to explore power limits with the specially enriched fuel element, IFA-4.

Figure 4. Turbine flow meters give flow, void and slip

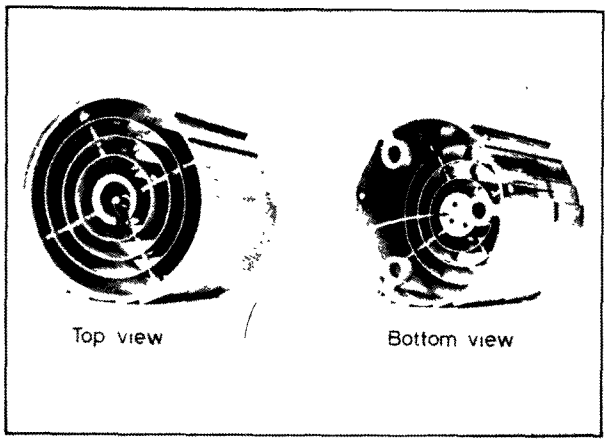


FIG. a Ten impedance void gauges of this type have been tested in HBWR ; 4 at fuel channel exits, 1 mid channel, 5 in moderator.

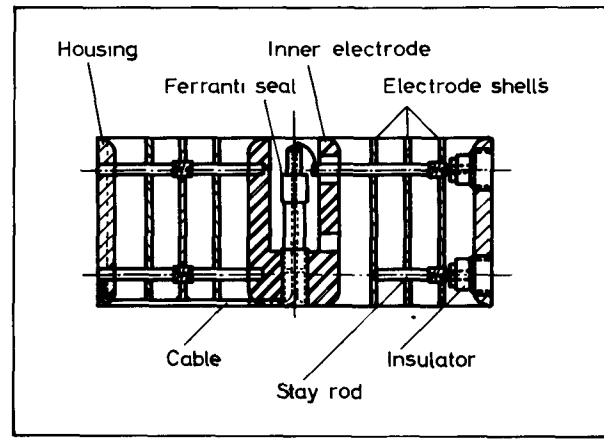


FIG. b Alternate concentric plates make impedance ratio insensitive to radial void distribution. Plates are held by radial steel bars and Al_2O_3 bushings.

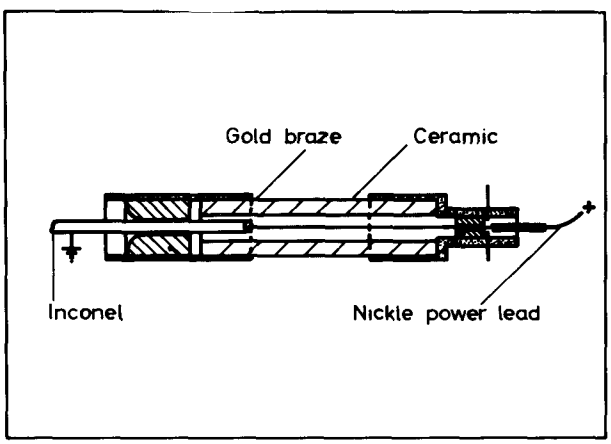


FIG. c A gold brazed Ferranti seal prevents leakage into the inconel clad power cable. The units operate on 1000 cycle per second AC.

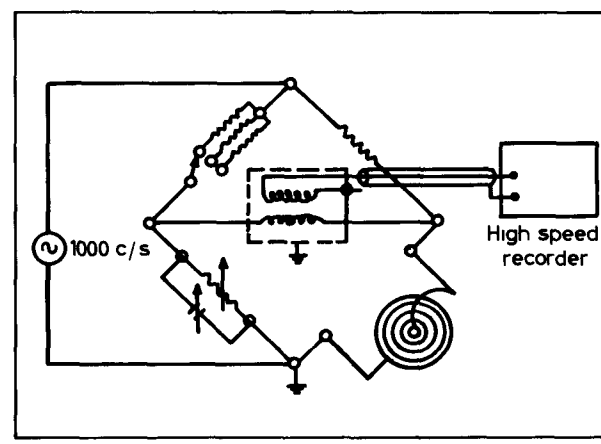


FIG. d The impedance of the circuit is recorded dynamically. The circuit is balanced to give full scale meter deflection with only liquid in gauge.

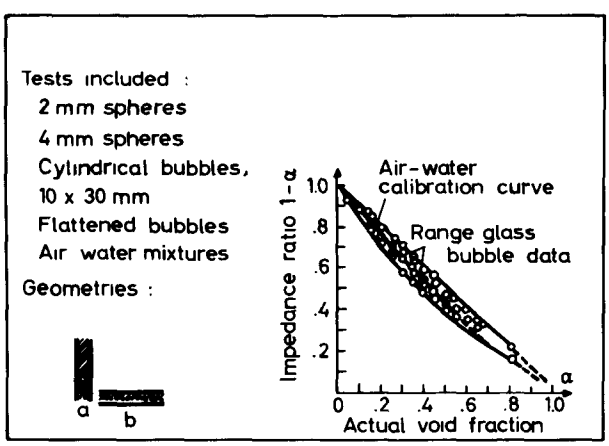


FIG. e The curves show deviations from linearity for various glass "bubble" simulations and air-water mixtures in out-of-pile experiments.

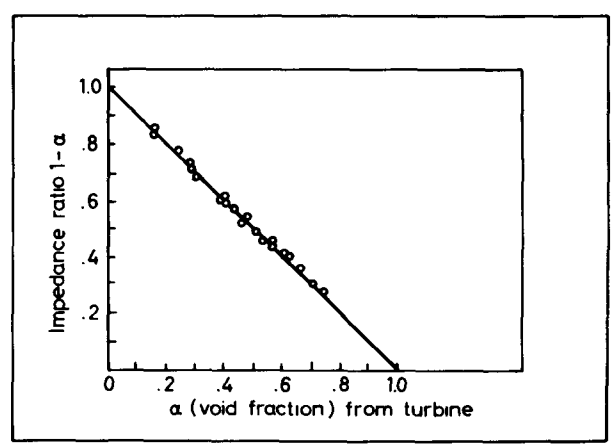


FIG. f In-pile steady state comparisons of void from turbine flow meters and void gauges agree. Gauges augment turbines when quality is oscillating.

Figure 5. Impedance gauges give dynamic void fraction

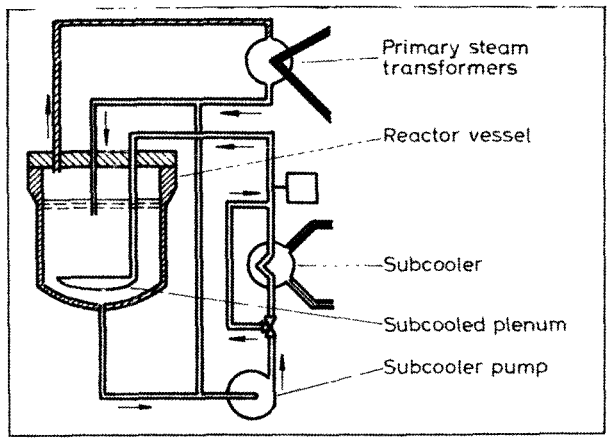


FIG. a The presence of 15-20°C subcooled D_2O in a plenum chamber below the fuel charge permits the non-boiling operation of test fuel.

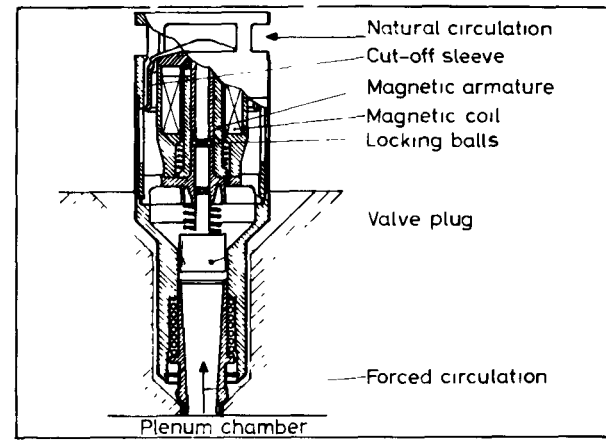


FIG. b Remote unlatching of calibration valve in bottom of test fuel shuts off natural circulation and admits 13 tons/h of subcooled water.

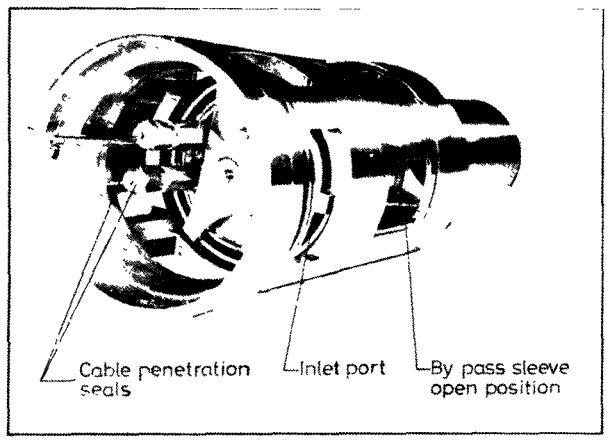


FIG. c Calibration valves have been in all four instrumented fuel assemblies. With no boiling flow and ΔT are measured to give power.

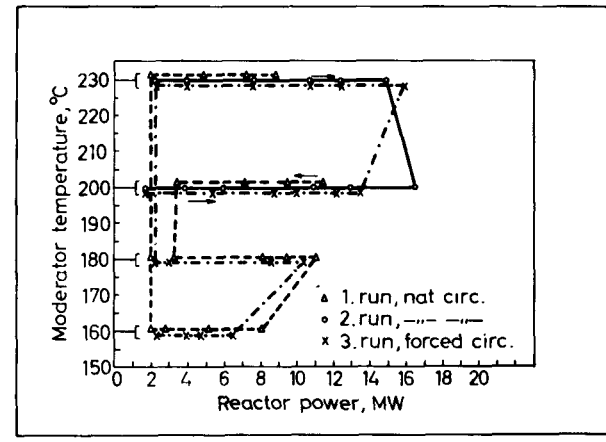


FIG. d Forced circulation runs permit calibration of flux chambers, γ-thermometers, turbines, and t/c's, and measurement of time constants.

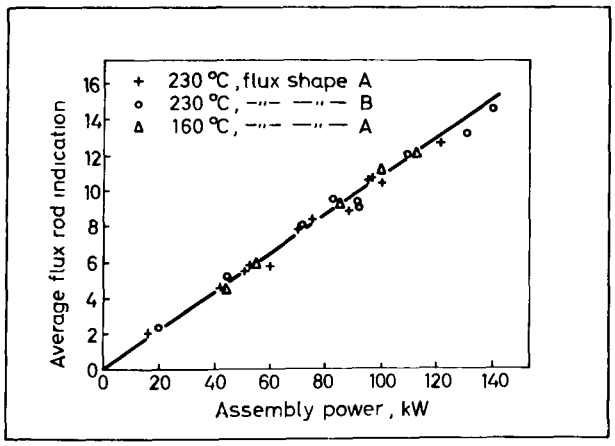


FIG. e With IFA-2 the adjacent flux rod containing three fission chambers was calibrated against flow x ΔT at various axial flux shapes. Curve was later used in boiling runs.

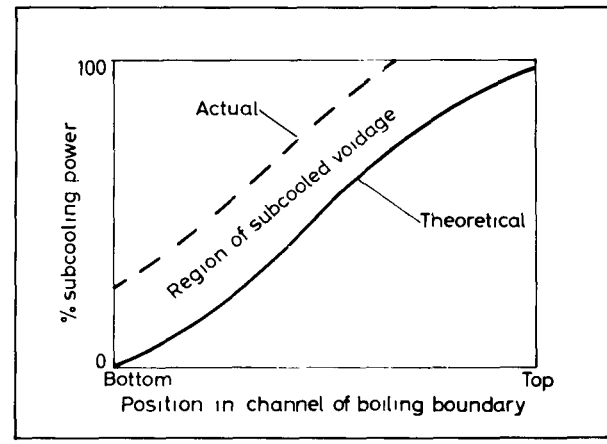


FIG. f Subcooled water temperature is increased to produce forced circulation boiling with calibration valve open. Boiling boundary is being studied in-pile with IFA-4.

Figure 6. Direct power measurements of boiling channels

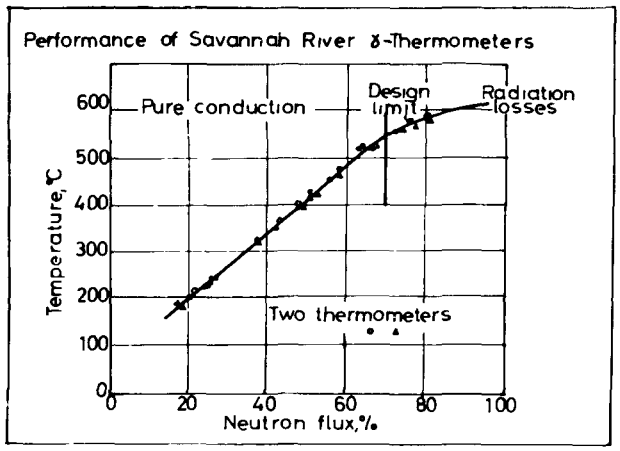


FIG. a *α-Thermometer development started at du Pont, SRP.* Development continues at HBWR. Rugged, reproducible, proportional to power, not flux.

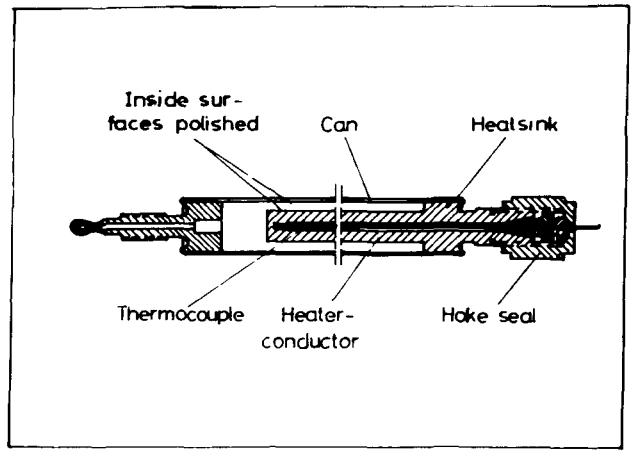


FIG. b *The heat generation in a SS cylinder is proportional to* α-energy absorbed. Temperature rise is controlled by path to the heat sink.

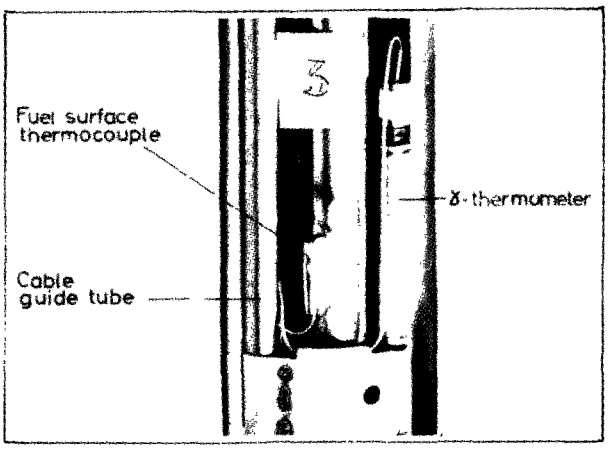


FIG. c Three α-thermometers are in each of the latest IFA's. They have been calibrated against flux wires and channel powers.

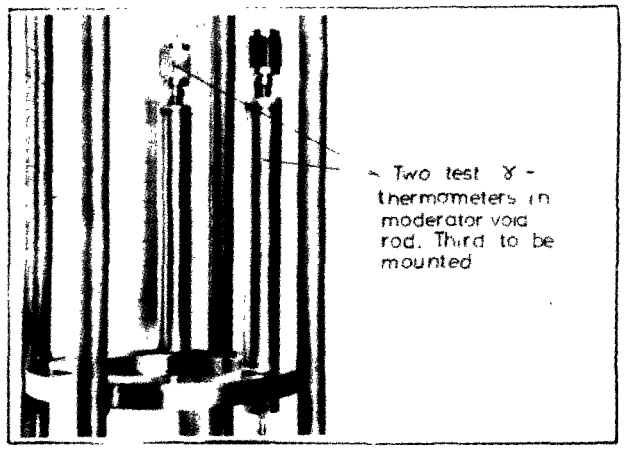


FIG. d Three α-thermometers were identically located in an inactive assembly to prove reproducibility as made. Temperature rises were small but agreed well.

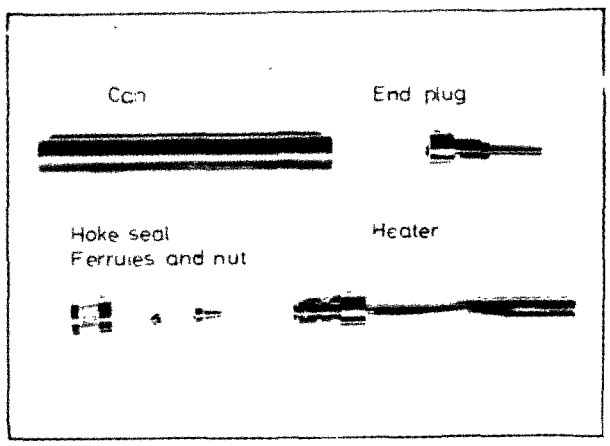


FIG. e The α-thermometers now used are about 7 cm long 7 mm diameter. The space between heater and can is gas-filled at low pressure.

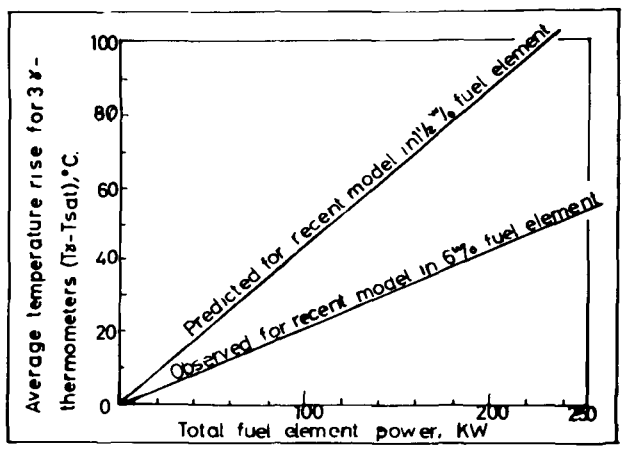


FIG. f The curves compare power calibration when α-thermometers are used in 6 $^{w}/_{o}$ and 1½ $^{w}/_{o}$ enriched fuel in the 1½ $^{w}/_{o}$ enriched HBWR core.

Figure 7. γ-thermometers measure power of test fuel

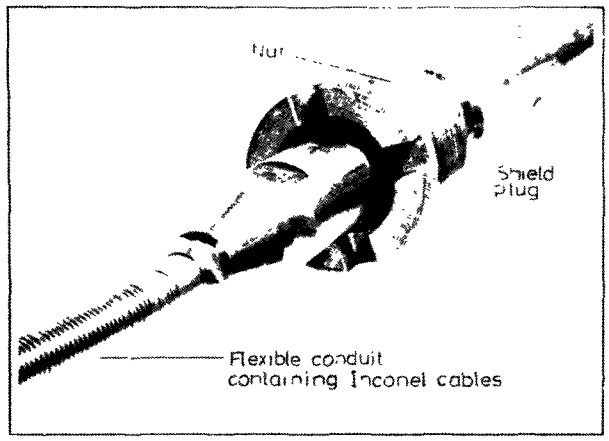


FIG. a Up to 24 leads and tubes penetrate a single top gland, pass through flexible conduit to terminal strips.

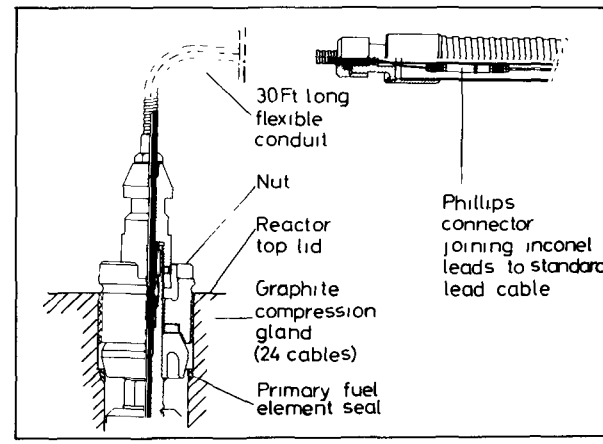


FIG. b Fuel elements are individually sealed in HBWR top lid; 200 holes are available for new test fuel.

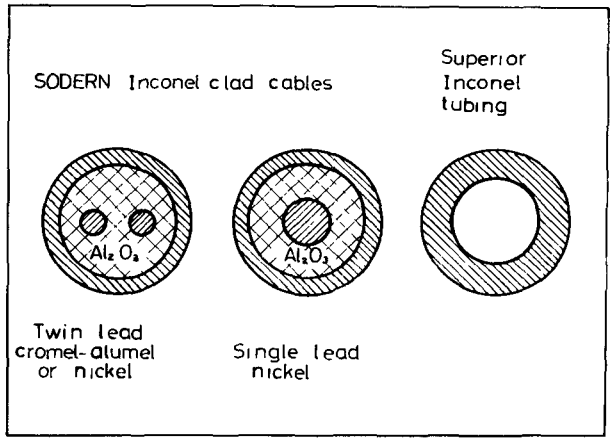


FIG. c Cables have 1 mm od Inconel sheath; no sheath failures have occurred in 18 months service. Tubes are 1 mm od Inconel.

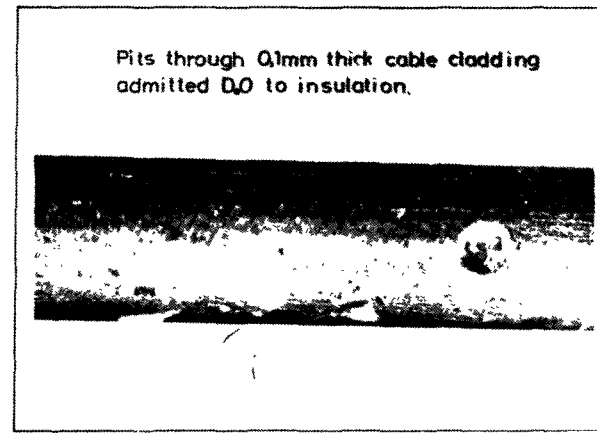


FIG. d Rapid pitting of 304 L SS sheathed t/c's at the D_2O level in early tests led to removal of first instrumented fuel assembly, and selection of Inconel.

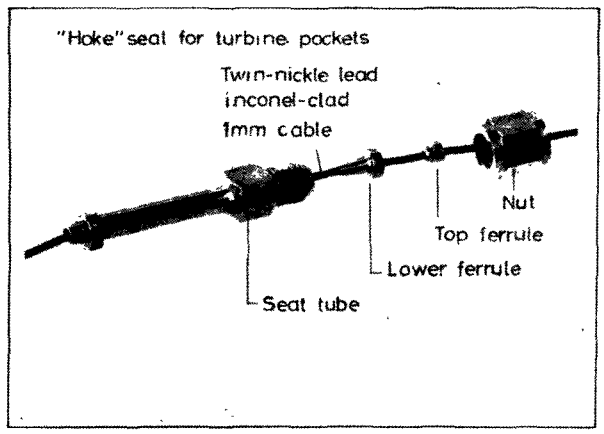


FIG. e Miniature tube fittings of stainless steel are used for single penetrations with 100% performance. Results with metallurgical seals and compression glands were poor.

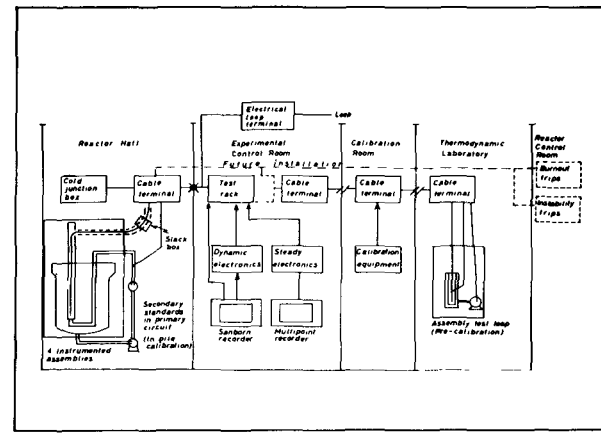


FIG. f Flexible cables from test elements lead to terminals connected by a cable network to the calibration and data-reduction systems.

Figure 8. Inconel cables and mechanical seals are used

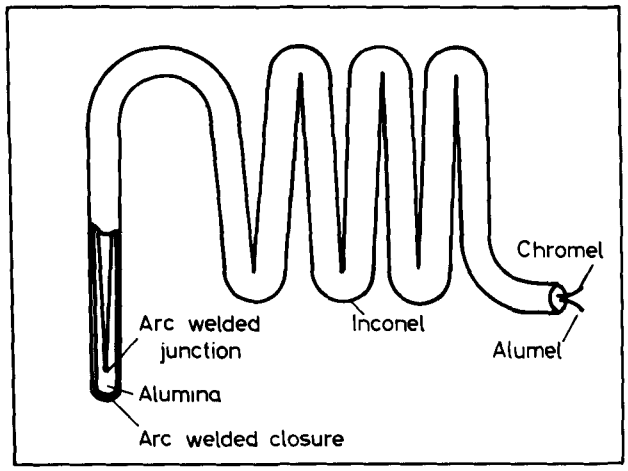


FIG. a *The 1 mm od thermocouples used in most instruments are made by* SODERN, Paris and have proved flexible and rugged.

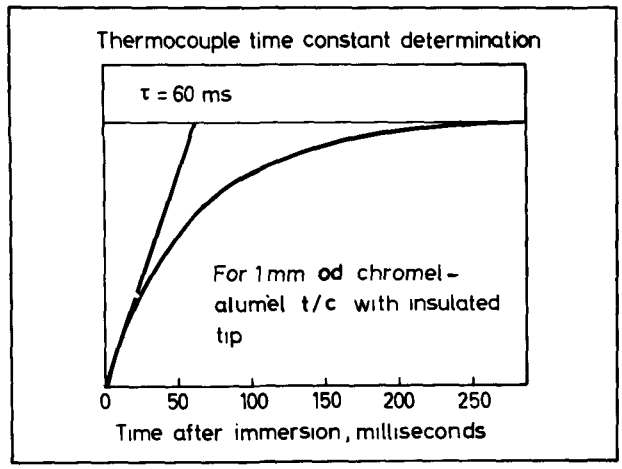


FIG. b Time constants were approximated by controlled immersion of tips into warm water.

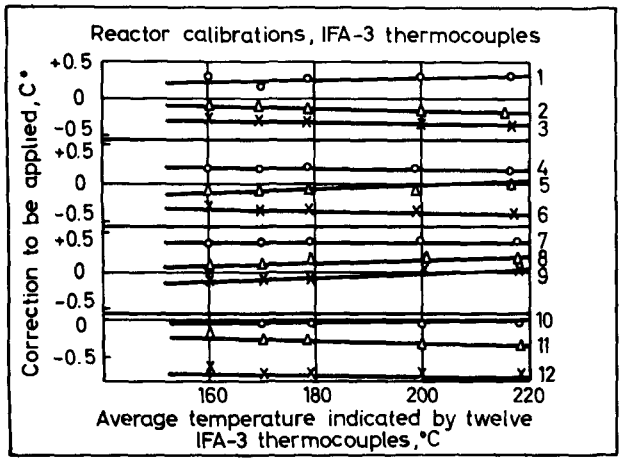


FIG. c *The reactor produces an isothermal bath for thermocouple intercalibration with an unirradiated instrumented fuel assembly.*

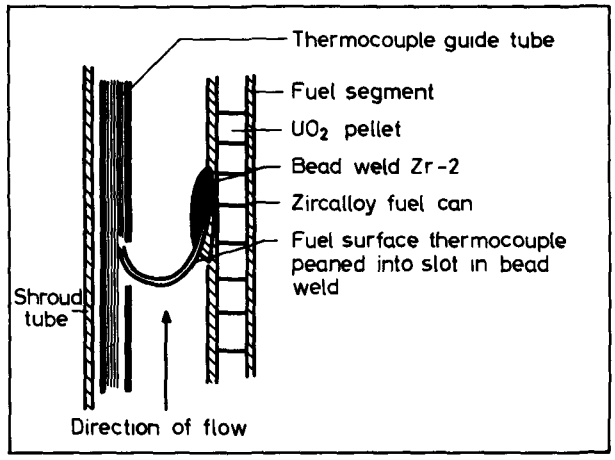


FIG. d The thermocouple application pictured does not measure true surface temperature but does respond quickly to changes in surface heat flux.

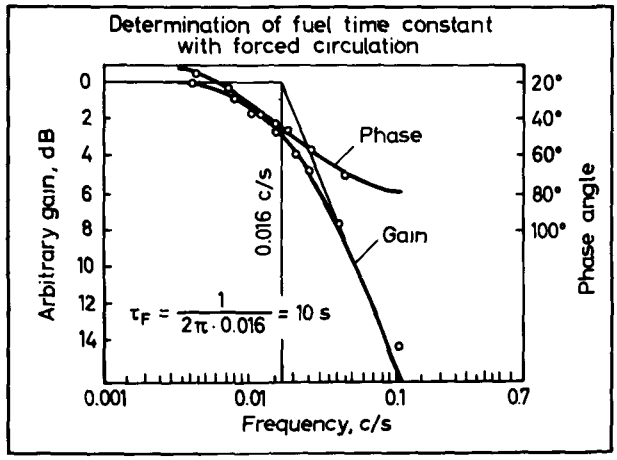


FIG. e Fuel thermal time constants were measured by determining transfer functions between flux chambers and fuel surface t/c's *during reactivity perturbations.*

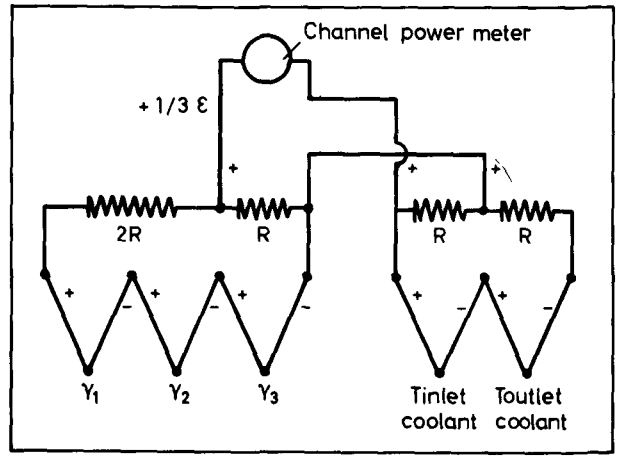


FIG. f Connecting γ thermometer and fuel coolant thermocouples produces a signal giving fuel power to ± 6%, independent of axial flux shape.

Figure 9. Δ T's to 0.1 deg C accuracy after in-pile calibration

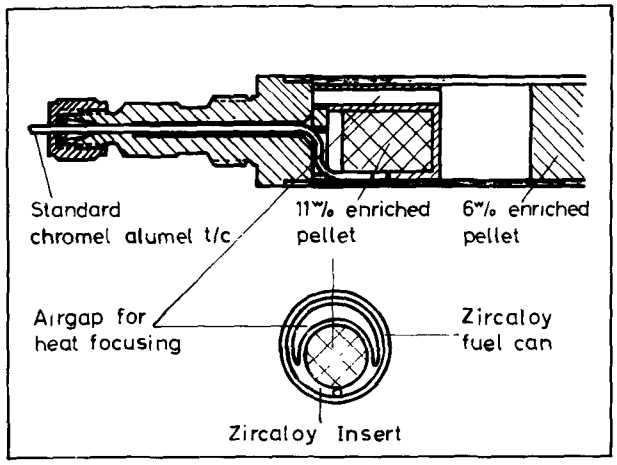


FIG. a Temperature rise of the burnout thermocouple, resulting from steam blanketing, will scram the reactor. Trip instrument also monitors inlet flow oscillation.

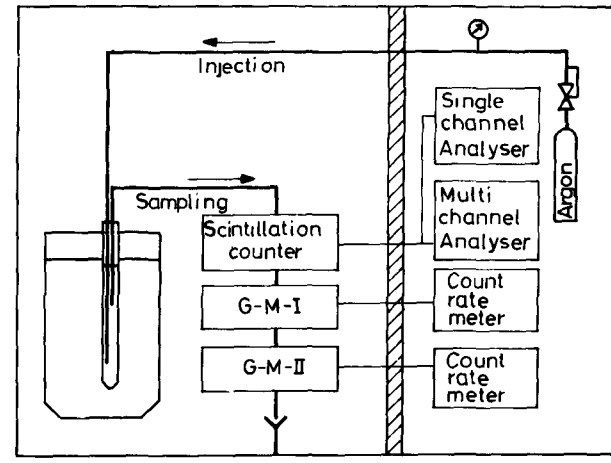


FIG. b Continuous steam sample from IFA-4 passes monitoring equipment. Later test fuel will also be sampled to quickly locate offending element if failure occurs.

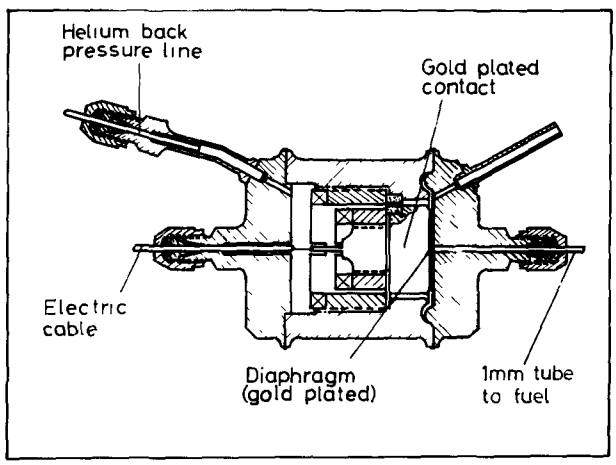


FIG. c IFA-4 contains a device to measure build up of fission gases inside fuel can with exposure and check for sudden release when oxide temp. nears melting point.

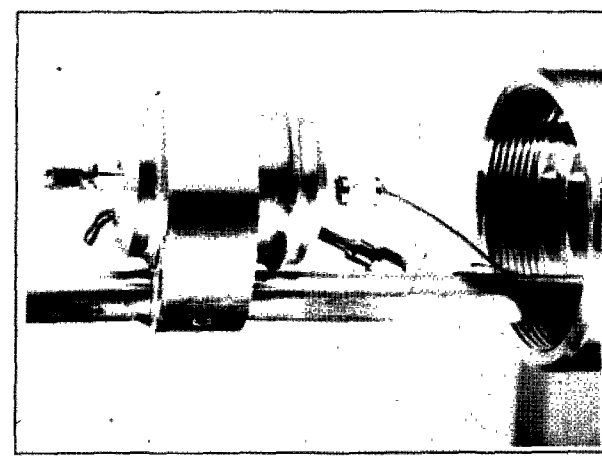


FIG. d The transducer is connected to a fuel stringer gas space by a 1 mm Inconel tube. Helium back pressure is applied to break electrical contact.

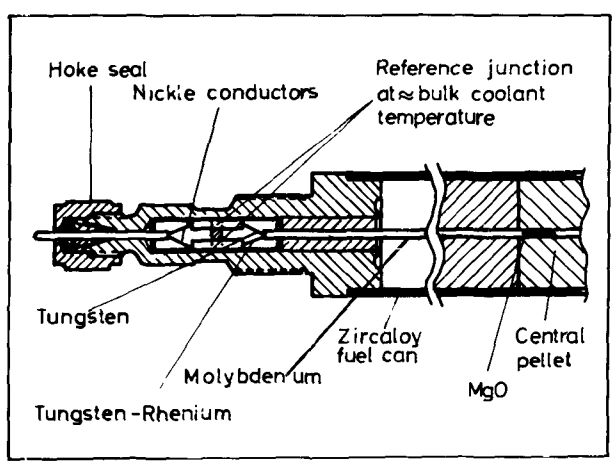


FIG. e Tungsten-Rhenium thermocouples clad in Molybdenum tubing and insulated with MgO have been applied in both IFA-3 and IFA-4.

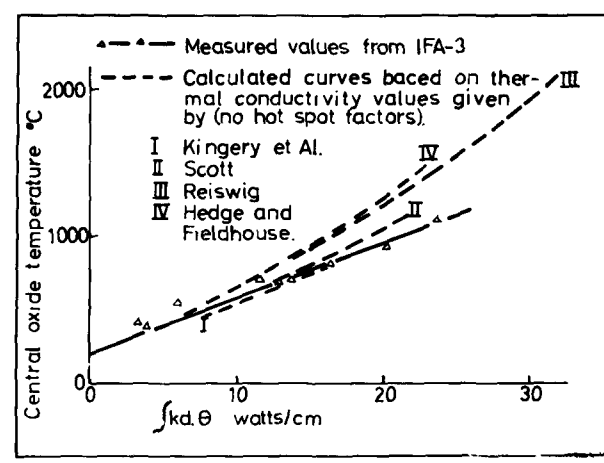


FIG. f Data from IFA-3 and IFA-4 agree and could confirm the conductivities of UO_2 presented by either Scott or Kingery.

Figure 10. IFA-4 instruments protect test channels

of channel power (Fig. 6f). The void gauges have been used in these experiments to compare real and theoretical channel void contents;

(*c*) Natural circulation boiling experiments. In February 1964 IFA-4 was operated in natural circulation at a power of 500 kW which produced a void fraction of 94%. Hydraulic instability occurred at a channel power of 385 kW. The power of the channel was increased to 500 kW without burn-out indication. Further increases were prevented by the limits on total reactor power. The conditions piloted with IFA-4 are believed to have produced higher void fractions than in any previous in-pile natural or forced circulation boiling reactor (Table 3). The range of test powers may be increased for IFA-4 in the spring of 1964 by raising reactor power above its present 20 MW limit.

Electrical loop experiments with an identically instrumented mock-up of IFA-4 (with actual reactor axial heat flux profile and using the automatic data processing system of HBWR) are now being conducted in an effort to establish conclusively (in cooperation with the in-pile experiments) that the in-pile channel is reliably protected from damage by the burn-out protector thermocouple trip circuits.

CONCLUSIONS

If and when the IFA-4 in-pile and electrical mock-up tests confirm that it is possible to protect reliably a boiling channel in-pile against damage due to the sudden disruption of steady state heat transfer conditions, a significant gain in specific powers of boiling reactor cores may be achieved through reduction of operating burn-out margins.

The problem of exact control and knowledge of operating conditions in a unique boiling test element, placed in a foreign lattice, has been solved through instrumentation in HBWR (Fig. 6). This will permit numbers of experimental fuel assemblies to be operated at frontier conditions without imposing unnecessary test fuel power limits that often reduce the value of such tests but are necessary to avoid risk to the continuity of reactor operation. Direct power measurements with trip circuits will replace conservatisms for uncertainty in flux calculation, possible power overshoot, or flux distortion; continuous axial flux shape monitoring will replace large conservative allowances for distorted form factors; in-pile burn-out protection may replace conservative extrapolation of non-reproducible laboratory boiling burn-out data; continuous radiation monitoring of steam from test fuel pieces will minimize failure location problems and further justify operation with narrow heat transfer margins and minimum design conservatism.

The aquisition of experience necessary to reduce conservatism in mechanical design, heat transfer rating, and material selection for boiling reactor fuel elements is the main objective of the new HBWR programme. The application of in-core instrumentation can speed-up the acquisition of the needed experience, and insure the validity of the test results.

REFERENCES

1. Editorial, *The World's Reactors, No. 21 Halden,* Nuclear Engineering (March 1959).
2. Rees, D. R., and Powell, E. U., *Saxton Tests Lead toward Better Power Reactors,* Nucleonics, 21 (11), 72 (1963).
3. USAEC report GEAP 3781 (1961).
4. Proceedings of the Boiling Water Reactor In-Core Instrumentation Meeting, report HPR-16, OECD Halden Reactor Project, Halden, Norway.
5. *Advanced Course on In-Core Instrumentation for Water-Cooled Reactors,* Institutt for Atomenergi, Kjeller, Norway.
6. Vapaavuori, O. *et al., Natural Circulation Hydrodynamics of HBWR Fuel,* OECD Halden Reactor Project, Halden, Norway (September 1963).
7. Quarterly Progress Reports, OECD Halden Reactor Project, Halden, Norway. Development sections in the following reports give instrument experience: HPR-18, HPR-24, HPR-28, HPR-29, HPR-30, HPR-31 and HPR-32.

ABSTRACT - RÉSUMÉ - АННОТАЦИЯ - RESUMEN

A/859 Norvège

Mise au point d'instruments pour mesures diverses dans le cœur du réacteur à eau lourde bouillante de Halden

par B. Aarset *et al.*

Afin de permettre des mesures dynamiques continues et de comparer durant les expériences de perturbation les paramètres spécifiques au cœur du réacteur, il s'est avéré nécessaire d'entreprendre, dans le cadre du programme de recherche du réacteur à eau lourde bouillante de Halden (HBWR), la mise au point de débitmètres à turbines pour la mesure du débit et du coefficient de vide dans les canaux de combustible, de jauges dynamiques de vide et d'instruments de mesure du flux de chaleur et de la puissance dans les canaux à l'ébullition. Ce type d'instruments ayant fonctionné avec succès durant de longues périodes dans le réacteur, le programme de mise au point a été alors orienté vers des instruments de protection et de mesure dans le cœur pour des éléments de combustible expérimentaux à haute puissance fonctionnant aux limites réelles du transfert de chaleur. Des appareils de ce genre ont été ou sont étudiés dans les canaux

d'essai d'éléments de combustible et comprennent des détecteurs de caléfaction, des thermomètres pour rayonnement gamma, des thermocouples centraux pour oxyde et des détecteurs d'instabilité.

Dans de nouveaux essais à HBWR, les instruments de mesure de perturbations du débit dans les canaux seront essayés avec des assemblages de combustible métallique tubulaire contenant des instruments à faible constante de temps.

Dans les essais effectués avec les anciens assemblages de combustible contenant des instruments, les mesures hydrauliques de la circulation naturelle en régime constant comportaient comme paramètres: la pression, la puissance par canal, le sous-refroidissement et la distribution du flux axial; des différences entre ces mesures, les valeurs calculées et les prévisions basées sur les données d'une boucle électrique ont été observées.

A/859 Норвегия

Разработка приборов для проведения внутриреакторных измерений по программе Халленского тяжеловодного кипящего реактора

В. Аарсет *et al.*

Была начата разработка приборов для измерения потока и пустот в топливных каналах, динамических вакуумметров, приборов для измерения теплового потока и мощности кипящих каналов. Разработка велась для осуществления программы экспериментальных исследований в области динамики на Халленском тяжеловодном кипящем реакторе путем непрерывных динамических измерений и сравнения внутриреакторных параметров с переходными режимами.

Затем программа была направлена на разработку приборов системы защиты реактора, установленных внутри реактора, и измерительных приборов для испытательных образцов тепловыделяющих элементов с высоким энерговыделением, работающих на предельных режимах теплопередачи. Приборами этого типа являются детектор пережога, гамма-термометр, центральные окисные термопары и измеритель неустойчивости.

Во время новых исследований в области динамики на Халленском реакторе с кипящей водой будут испытываться внутриреакторные приборы для измерения расхода теплоносителя через канал вместе с трубчатыми металлическими топливными сборками, оснащенными приборами с малой временной постоянной.

В процессе таких испытаний топливных сборок были проведены статические гидравлические измерения естественной циркуляции. При этом измерялись давление, мощность канала, недогрев и осевое распределение потока. Наблюдались расхождения в данных, полученных путем расчета на основе экспериментов с электрической петлей.

A/859 Noruega

Desarrollo de instrumentación del interior del núcleo en el programa HBWR

por B. Aarset *et al.*

Se inició el desarrollo de turbinas de medidas de flujo en los canales de combustible y de proporciones de vacío, de indicadores de vacío dinámico y de dispositivos de medida del flujo de calor y de potencia del canal de ebullición para respaldar el programa experimental de investigaciones de la dinámica del HBWR al permitir medidas dinámicas continuas y la comparación entre parámetros del interior del núcleo durante una perturbación. Con el comportamiento satisfactorio a largo plazo de estos dispositivos, el programa de desarrollo de instrumentos se desvió hacia dispositivos de protección y de medida en el interior del núcleo para pruebas de elementos combustibles a altas potencias funcionando en los límites reales de transferencia de calor. Los dispositivos de este tipo que han sido o están siendo verificados en los canales de combustible de prueba, son el detector del grado de quemado, el termómetro gamma, termopares de óxido central y un dispositivo de observación de inestabilidades.

Respecto a nuevas investigaciones de la dinámica del HBWR se probarán dispositivos de perturbación del flujo de los canales en el interior del reactor, en unión de conjuntos de elementos combustibles metálicos tubulares e instrumentación de constante de tiempo corta.

En el proceso de comprobación de conjuntos de instrumentos y elementos combustibles se han hecho medidas hidráulicas de la circulación natural en estado estacionario, tomando como parámetros la presión, la potencia del canal, el subenfriamiento y la forma del flujo axial. Se han observado diferencias entre los cálculos y la predicción a partir de los datos de redes eléctricas.

Dynamics of boiling heavy water reactors based on HBWR research programme*

By H. Ager-Hanssen, T. Eurola, Y. Fishman and J. E. Lunde**

At HBWR, which is the only heavy water boiling reactor in operation, extensive experimental and theoretical work investigating the dynamic behaviour of such reactors has been conducted in the period from 1959 to 1963 [1-7].

Two fuel charges have been used in the investigations, a natural metallic uranium charge operating at low coolant power densities, and a 1.5% enriched uranium oxide fuel charge permitting operation at high coolant power densities.

The present paper summarizes the experience obtained at HBWR on the dynamics of natural circulation boiling heavy water reactors and it gives indications of the effect upon stability of the different design parameters. Other papers to this Conference [8-10] describe the experience obtained on in-core instrument development, water chemistry and reactor operation at HBWR.

Incentives for HBWR dynamic studies

Power reactors in which the coolant is boiling water offer attractive economic advantages and a large number of such reactors are either in operation or under construction [11]. Although most of these reactors are moderated by light water, there has recently been an increasing interest in boiling heavy water-moderated systems. Thus in Sweden, construction has started on a 200 MW(e) boiling D_2O-moderated reactor with natural circulation (Marviken) and in the UK a 100 MW(e) D_2O-moderated reactor cooled by boiling light water (SGHWR) is under construction.

Since the experiments with light water boiling reactors (e.g. the BORAX reactors and EBWR) showed that this reactor type presents stability problems at high core power densities [12, 13], it was considered important to investigate in HBWR whether D_2O boiling reactors also present such problems.

It has been shown [14] that void coupled instabilities in light water boiling reactors can be produced (*a*) by purely hydrodynamic effects, and (*b*) by void reactivity feedback effects. Although the effects are distinct they will usually interact, and their separation in an integral reactor experiment is complicated.

Although it was realized that the dynamic experiments with the metallic fuel charge would not permit sensitive testing of core dynamics models, it was considered important to get information on plant dynamics since few systematic experiments of this type have been reported.

In early measurements with the oxide fuel charge, low frequency ($\sim$ 0.005 c/s) oscillations were observed at certain reactor conditions [5]. These oscillations are believed to be due to steam flashing in the moderator. Since this phenomenon had not been expected, emphasis was placed on the study of the dynamic behaviour at low frequency, in contrast to the studies performed for light water boiling reactors where instabilities have been observed to occur at high frequency ($\sim$ 1 c/s). The large fuel thermal time constant ($\sim$ 10 s) for the HBWR oxide fuel charge actually prevents void reactivity feedback instability at high frequency.

Brief description of HBWR

To obtain a defined flow pattern in the reactor, the fuel elements have shrouds separating upstreaming steam-water mixture from the downstreaming water between the elements. Water from the moderator enters the shrouds through ports in the lower section, steam-water mixture leaving them through perforations at the top. Steam is collected in the space above the water level. The total body of water in the reactor is approximately at saturation temperature.

Figure 1 presents a simplified flow diagram for HBWR. The heavy water steam circulates through steam transformers where it is condensed to produce light water steam in the secondary circuit. Heavy water can be withdrawn from the tank, subcooled in a separate circuit and reintroduced.

The two fuel charges that have been used in the experiments are described in Table 1. A more detailed description of HBWR can be found in [1].

Techniques used in the dynamics measurements

Suitable experimental techniques and instruments have been developed both for perturbing the reactor

* One of the joint undertakings of the OECD European Nuclear Energy Agency.

** Institutt for Atomenergi, OECD Halden Reactor Project, Halden.

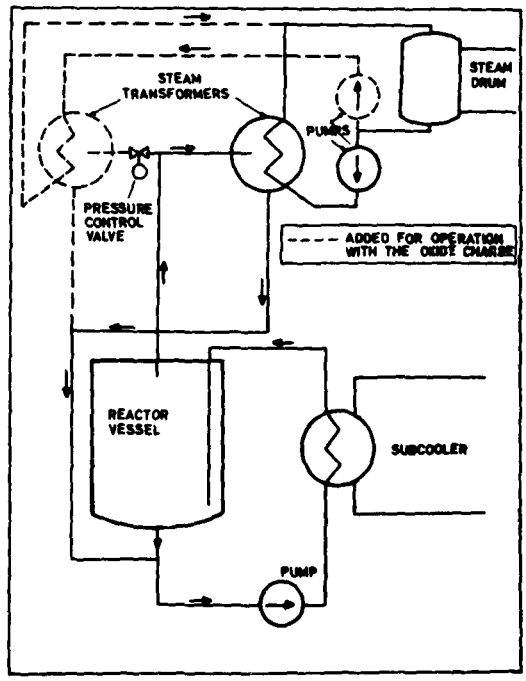


Figure 1. HBWR simplified flow diagram

and for measuring the responses of dynamically important variables.

The most common way of expressing results of dynamic measurements is by transfer functions. Such functions have been obtained at HBWR both by using sinusoidal and multi-frequency perturbations of reactivity and steam flow. Sinusoidal reactivity perturbations were obtained by means of a reactivity oscillator [3, 5, 6] installed in the central core position. The multi-frequency perturbation for the metallic charge was a binary signal whose Fourier spectrum had several characteristic peaks [3], while for the oxide charge it was a white noise type binary signal [7].

Noise analysis of the various signals was also performed [15, 16] and responses to steps in both reactivity and steam flow have been measured [3, 5, 7].

It was soon realized that measuring responses of macroscopic parameters such as nuclear power, pressures and flows alone was not sufficient for a complete dynamic analysis. Therefore considerable effort has been placed on the development of in-core instruments for the measurements of important microscopic parameters [8, 17, 18]. Thus exit void fractions, coolant inlet and outlet velocities, fuel thermal time constants, temperatures in the downcomer, axial power and flux shapes have been measured by means of impedance void gauges, turbine flow meters, thermocouples, flux chambers and gamma thermometers.

To permit simultaneous analysis of the time behaviour of a large number of in-core signals, an extensive system [18, 19] for automatic data reduction has been installed at HBWR. The system employs a two channel transfer function analyser, a special analogue computer for noise correlation studies, high speed visual recording equipment, a 60 amplifier analogue computer for reducing instrument signals to meaningful dynamic parameters before analysis, an analogue-to-digital converter and a small, but fast, digital computer.

DESCRIPTION OF THE HBWR DYNAMIC BEHAVIOUR

The experiments with the two fuel charges have been performed at markedly different pressures, powers, and power densities (Table 1), resulting in considerably different dynamic behaviours. The main difference observed was that for the metallic charge stability increased with increasing power level, whereas the opposite was true of the oxide charge. This is illustrated by the reactivity to power transfer functions, Figs. 2c and 2d. The peak in the gain curve decreased with increasing power in the first case, and increased in the second. Responses of power to reactivity steps gave similar results. For a given step, the peak in the response decreased with increasing power level in the case of the metallic charge, but increased with increasing power level in the case of the oxide charge.

Another difference is shown in Figs. 2a and 2b. While the power responses to positive and negative reactivity steps were not symmetric in either case, the responses to positive steps were larger than to negative steps for the metallic charge, whereas the opposite occurred with the oxide charge.

Measurement of the power spectrum of the nuclear power noise, performed with both charges, yielded results illustrated in Figs. 2e and 2f. For the metallic charge no peak was observed while for the oxide charge a marked peak, which increased with in-

Table 1. HBWR fuel charges

	Metal charge	Oxide charge
Uranium-235 content, %	0.71	1.5
Fuel rod diameter, cm	2.54	1.26
Canning material	Aluminium	Zircaloy
Canning thickness, cm	0.18	0.076
Number of fuel rods per element	1	7
Total weight of fuel, kg	7000	1466
Inner diameter of coolant shroud, cm	7.14	7.08
Fuel length, cm	237	171
Number of fuel elements	296	100
Lattice pitch, cm	13	13
Lattice configuration	Triangular	Hexagonal
Maximum moderator temperature, °C	150	230
Maximum pressure, atm (a)	4.8	28.5
Maximum nuclear power, MW	6	20
Maximum channel power, kW	35	270
Maximum channel exit void fraction, %	43	82
Maximum heat flux, W/cm^2	20	66
Average coolant channel power density, kW/l	2.4	42

creasing power level, occurred at the resonance frequency.

Figure 3 illustrates the effect on the HBWR dynamics of changing operating conditions in the case of the oxide charge, the reactor being less sensitive to such changes in the case of the metallic charge.

The effect of changing the power level has already been described (Fig. 2). Increasing the subcooling ratio is seen to increase stability, Fig. 3a, decreasing moderator temperature has a stabilizing effect, Fig. 3b, as has a decrease in moderator level, Fig. 3c.

The heat transfer characteristics of the steam transformers seem to have a negligible influence on stability since no change in the reactivity to power transfer function occurred when one of the two steam transformers was closed off on the secondary

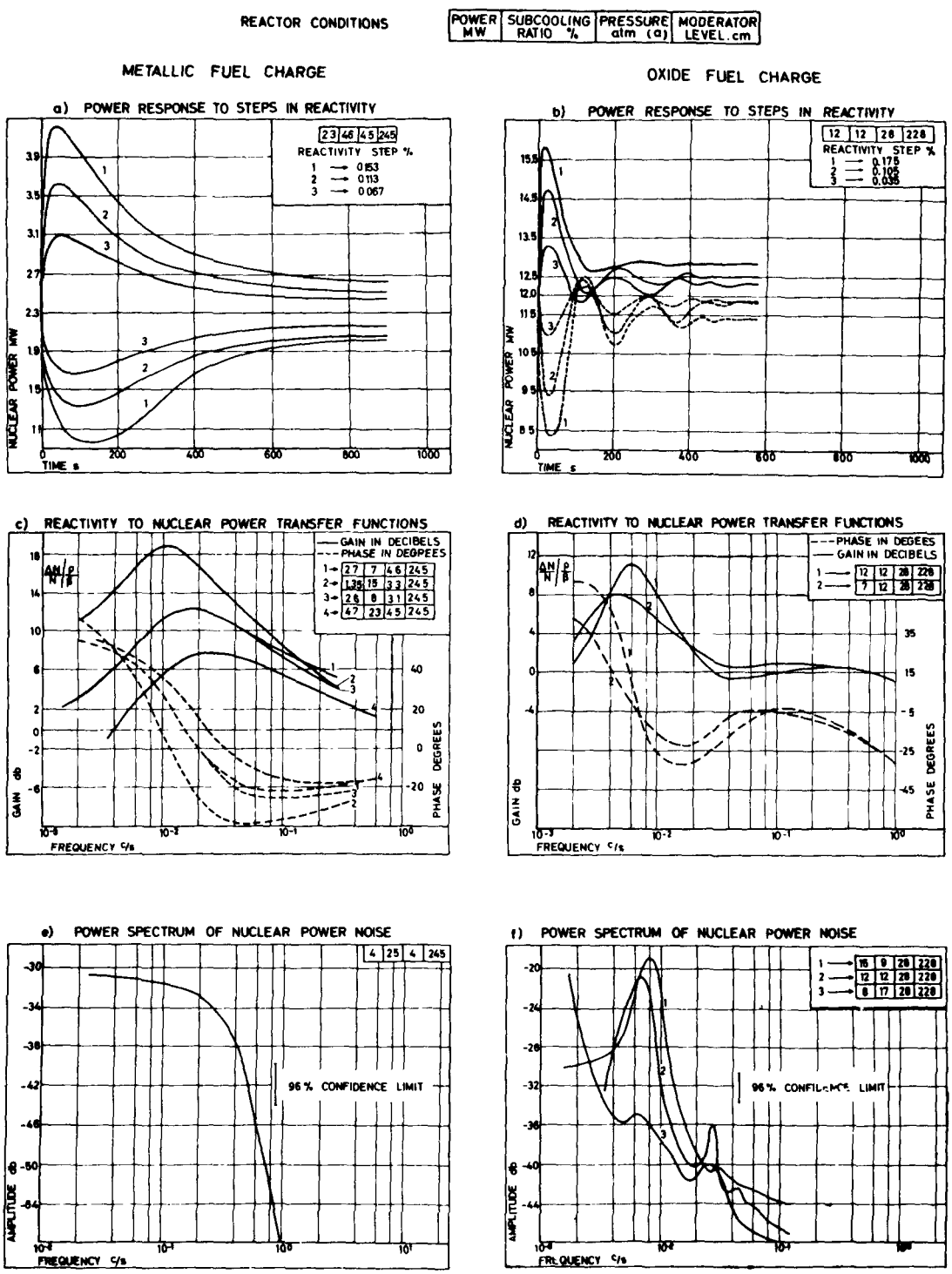


Figure 2. Measured dynamic characteristics of the two fuel charges

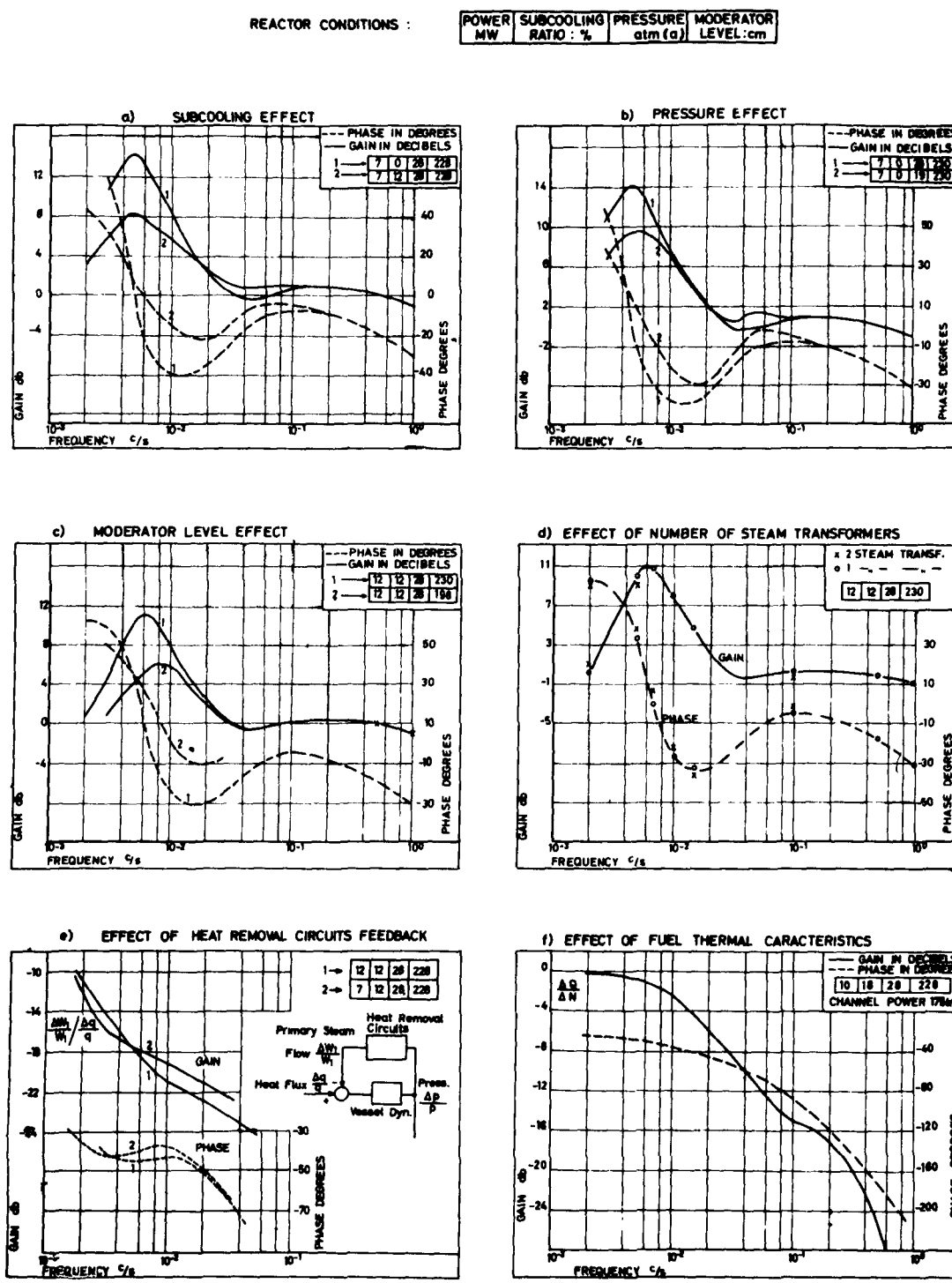


Figure 3. Effect of design parameters on the dynamic behaviour of the reactor

side, Fig. 3d and 3e show the transfer function from heat flux into the coolant to steam flow in the primary circuit. The gain at the resonance frequency in this transfer function is as small as 0.1 (—20 db), indicating that the pressure at above this frequency is mainly dependent on the heat flux.

The transfer function from nuclear power to heat flux is shown in Fig. 3f. It is observed that at low frequencies it is acceptable to use a fuel thermal time constant of approximately 10 seconds.

In contrast to its behaviour with the metallic charge, the reactor exhibited self-sustained power oscillations with the oxide charge. At 28 atm(a), and 228 cm moderator level, the onset of the oscillations was in the vicinity of 7 MW total power, without subcooling, and 10 MW with 1.5 MW subcooling.

The oscillations, whose frequency lies between 0.005 and 0.009 c/s, increase in amplitude with increasing power, pressure, moderator level, and decreasing subcooling. The frequency of the oscillations increases with increasing power level. Figure 4a shows the self-sustained oscillations observed at 12 MW and a subcooling ratio of 12%. The peak to peak amplitude was about 1.5 MW. Above 15 MW with maximum subcooling (12%), the oscillations diverged.

Keeping the pressure constant by means of automatic control stopped the oscillations. Figure 5 shows the reactivity to power transfer function, measured with the multi-frequency technique, with and without pressure control. (The measured points are joined by a broken line through which a smooth curve is interpolated). Figure 6 is the feedback from power to reactivity, with and without pressure control, calculated from the curves of Fig. 5, and from the zero power transfer function.

Standard HBWR oxide fuel elements operating at powers up to a maximum of 270 kW did not exhibit high frequency ($\sim$ 1c/s) hydraulic oscillations. Such oscillations were obtained in an instrumented, 6% enriched, pilot fuel element, which is close in design to the standard oxide elements and equipped with burn-out protection [7, 19, 20] when its power reached 390 kW. At 490 kW, these oscillations became so large that there were indications of periodic flow reversal. Even at this condition, where the exit void fraction was more than 90%, there was no indication that the element was close to a burn-out condition. Fig. 4b is an example of the inlet flow oscillations obtained at 412 kW.

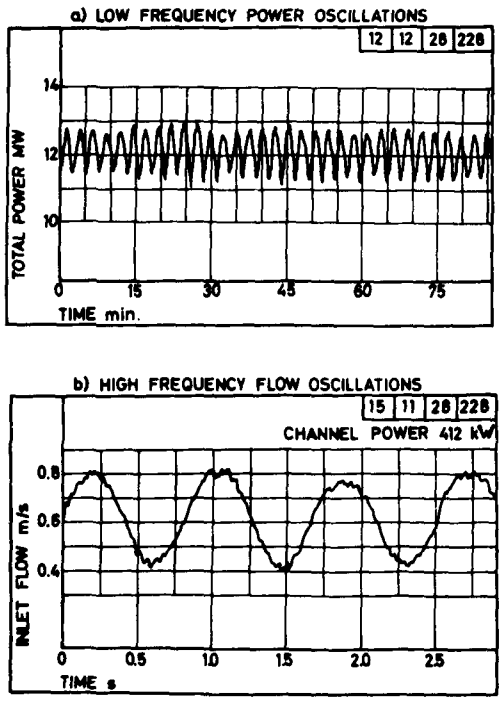


Figure 4. *Self-sustained oscillations*

REACTOR CONDITIONS :

POWER MW	SUBCOOLING RATIO : %	PRESSURE atm (a)	MODERATOR LEVEL : cm

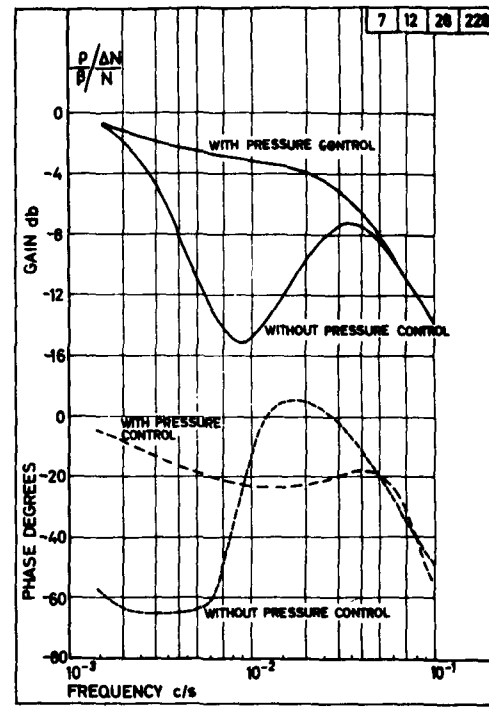


Figure 5. Reactivity to power transfer function with and without pressure control

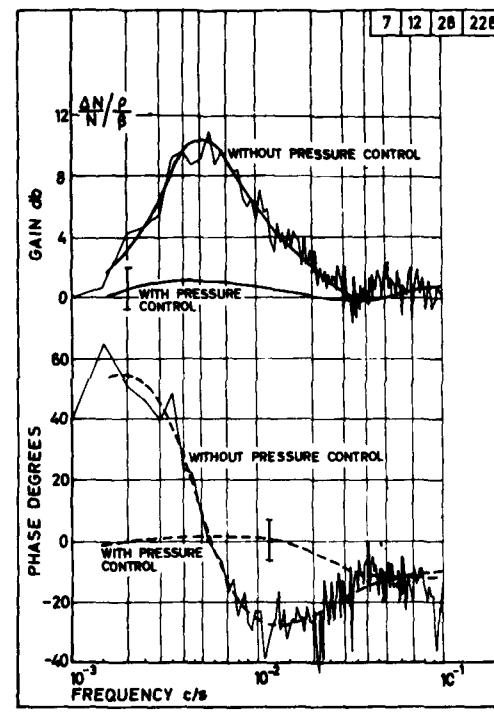


Figure 6. Power to reactivity feedback with and without pressure control

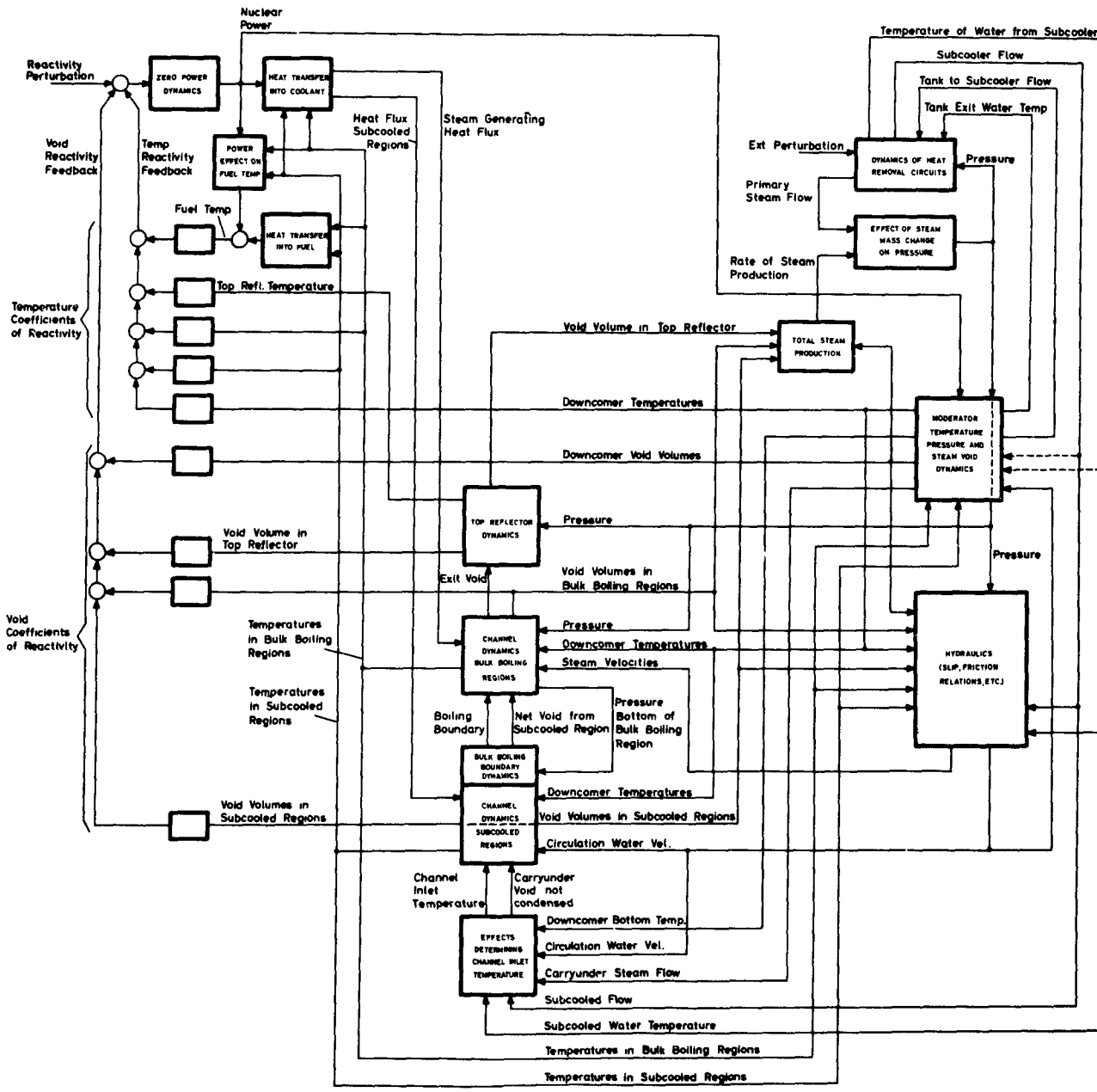


Figure 7. Principle diagram of HBWR dynamics

THEORETICAL DESCRIPTION OF THE DYNAMICS OF HBWR

The dynamics model development for HBWR has proceeded on the basis outlined in the principle diagram of Fig. 7, which shows how the main phenomena are interconnected. As it was realized that the low frequency instability originated from flashing of the moderator, emphasis was placed on a detailed description of the pressure effects.

Because of the relatively weak hydraulic coupling between individual fuel channels and the possibility of having the downcomer in the core region of natural circulation heavy water boiling reactors (cf. HBWR), a provision for dividing the fuel channels and the downcomer in radial regions is included in the principle diagram. Each of these regions, if necessary, can be subdivided into a number of axial regions to allow for a better spatial description.

The zero power dynamics and the heat transfer phenomena are reasonably well understood and can be treated linearly or non-linearly and in as much detail as the desired accuracy requires. The heat transfer is primarily dependent on the nuclear power and the channel temperatures.

The channel dynamics (void and temperature distributions in the coolant channels) are determined by the heat flux from the fuel and the moderator into the coolant, and by the steam pressure, the

steam and water velocities, the channel inlet temperature and eventually the carry-under of the steam.

The moderator (downcomer) dynamics (void and temperature distributions in the moderator) are determined by the steam pressure, the water velocities and the power input. The power input to the moderator comes from gamma heating, from heat transfer to the moderator and from changes in subcooling power. The existence of steam void in the downcomer introduces a non-linear effect in the sense that the steam bubbles can disappear with increasing pressure, whereas there is no such limitation with decreasing pressure. The inclusion of this saturation effect has been found to be important in HBWR dynamics.

The top reflector dynamics (void and temperature distribution in the top reflector) are essentially determined by the steam pressure and the void fraction and steam velocity at the exit of the coolant channels.

The hydraulics block in Fig. 7a contains the description of steam and water velocities both in the channels and downcomer regions. It includes the effects of slip, buoyancy and friction. These are influenced by the coolant and moderator densities, which are in turn determined by the pressures and temperatures. The effect of subcooling is also included in the model.

The steam pressure depends on the rate of steam production and the rate of steam removal (primary steam flow).

The void and temperature distributions in various parts of the system and the steam pressure, finally determine the reactivity feedbacks.

Basic assumptions

The general system described above takes the effect of most parameters into account. In order to solve the mathematical problem, various simplifying assumptions have been formulated [21-25].

Two different models were used for the description of the dynamics of the metallic fuel charge. The first model was a direct application of the scheme developed by Beckjord for the EBWR [21], while the second was a further development of the work by Fleck [23]. The way these two models were applied to HBWR is described in detail in [4] and [26] and more concisely in [1].

The model for the oxide fuel charge has had as its basis the mathematical formalism used by Kirchenmayer [14]. This model, which is somewhat more detailed than the above two, has been extended to include space dependence of coolant velocities in the channels [27], as well as the void and temperature distributions in the downcomer [28]. Moreover, the description of the steam pressure has been improved [7]. The previously mentioned non-linearity in the moderator dynamics as well as the non-linearity due to the bottom of the channel constituting a limit to the boiling boundary, have been taken into account [6].

The main assumptions and simplifications used in the present version of the model for the oxide charge are:

(i) The channels are radially identical and axially divided into two regions, non-boiling and boiling;

(ii) The downcomer (including the outer reflector) is radially treated as one region and axially divided into several regions;

(iii) The channel velocities are separable in space and time;

(iv) The slip ratio is constant in space and time;

(v) The heat exchange between the coolant channels and the downcomer is negligible;

(vi) The subcooled boiling is negligible;

(vii) There is no steam carry-under;

(viii) The effect of temperatures on densities is neglected (in subcooled regions);

(ix) Reactivity coefficients are constant in time (not in space).

The above assumptions eliminate many of the interconnections shown in Fig. 7. The large thermal time constant of the oxide charge makes it possible to describe the hydraulics and channel dynamics in a simple way as apparent in the above assumptions.

Comparison of theoretical and experimental results

As a limited number of variables (nuclear power, steam flows and pressures) could be measured in the case of the metallic fuel charge, it was only possible to compare certain overall theoretical transfer functions with the experimental ones. Since a detailed account of this work is given in [1] and [4], it will not be treated in this paper.

In the case of the oxide fuel charge, the extensive in-core instrumentation has made possible a more refined check of the theory than for the metallic fuel charge. This work is still underway, for which reason only a few overall theoretical transfer functions are, in this report, compared with the measurements at two different operating conditions. References [5-7] present the progress in the model development work in detail.

Figures 8a and 8b show the calculated and measured reactivity to power transfer functions at two conditions. For both, the resonance peak at a frequency of about 0.006 c/s as observed in the measurements is predicted by the theory. For the 12 MW condition (Fig. 8a), the agreement in the resonance region is very good in both phase and peak frequency, while the theoretical gain is smaller than the experimental one by about 4 db. At 7 MW (Fig. 8b) it is observed that the resonance frequency is also predicted reasonably well. The phase is predicted to within 15 degrees in the resonance region and the gain which decreases rapidly below the resonance frequency is predicted to within 1 db at the peak.

Figures 8c and 8d present the nuclear power to pressure transfer functions. For the 12 MW condition (Fig. 8c) discrepancy in gain is seen to be less than 2 db, whereas the discrepancy in phase increases toward high frequencies. These comments are applicable also for the 7 MW case.

Figures 8e and 8f show the pressure to moderator temperature transfer functions with the temperature measured close to the bottom of the downcomer. The agreement between theory and experiments for the phase of the transfer function is quite good, but the gains differ at high frequencies.

It is apparent from the above comparisons that the model is not satisfactory yet. Various improvements are being studied at present.

FUTURE PROGRAMME

The metallic and the oxide fuel charges were originally designed to demonstrate the feasibility of

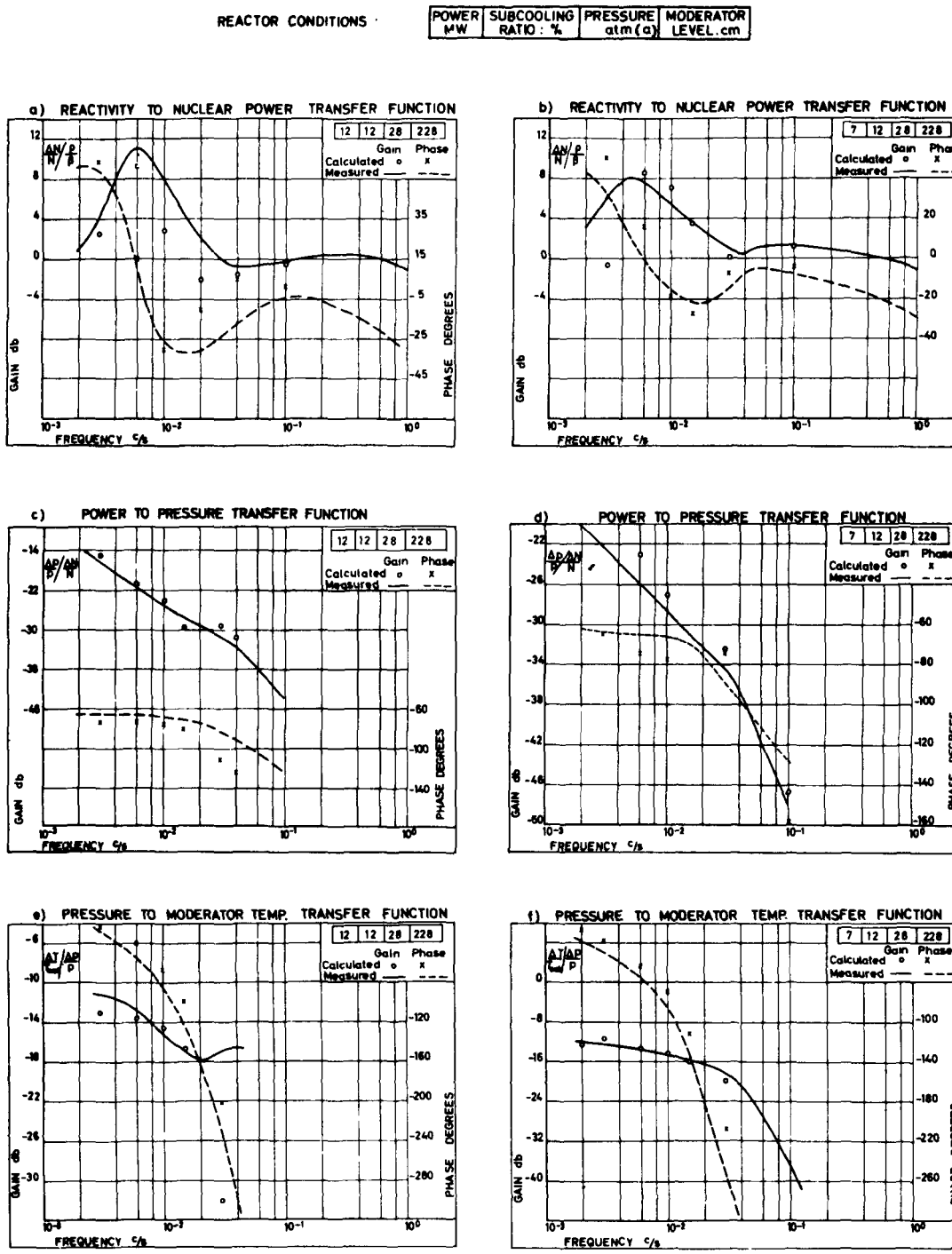


Figure 8. Comparison of experimental and theoretical results

a heavy water boiling reactor with natural circulation, and no emphasis was placed on incorporating in the core designs the necessary flexibility for systematic core dynamic studies. In effect, the sluggish response of the oxide charge to reactivity changes and the low power density of the metallic fuel charge, have limited the extent to which verifications of core dynamic models could be made, to the low frequency range. For this reason it has been decided to extend the dynamics programme by performing measurements with four instrumented tubular metallic fuel assemblies, which will operate at high coolant power densities and which will respond rapidly to reactivity changes. Flow oscillators installed in the tubular fuel assemblies will permit perturbation in the natural circulation flows.

Perturbations of reactivity and flow will make possible determination of transfer functions between fuel assembly power, circulation velocity and exit and local void fractions. Loop experiments with mock-up test assemblies containing identical instrumentation will be conducted concurrently, and the comparison with the reactor experiments will serve to determine whether the effects of steam carry-under, radiation, thermal capacity and moderator circulation patterns will significantly alter the in-pile behaviour predicted from the loop experiments.

The degree of hydraulic coupling between tubular fuel assemblies installed adjacent to each other, will also be determined by measuring transfer functions between flow perturbations in one fuel assembly, to flow and void variations in the others. If it can be shown that the coupling effects between channels are weak in a reactor of the HBWR type, then the potential exists for operating such reactors at higher coolant power densities than would be permissible in natural circulation light water boiling reactors where the whole core acts as an up-comer.

In the high specific power testing of tubular fuel it will be possible to compare power thresholds at which the self-excited flow oscillations occur with those determined in loops, where poor simulation of downcomer momentum, flux shape, and heat capacity may give erroneous indications. Experiments performed with a high specific power, 6% enriched, fuel assembly of the same design as the standard oxide fuel assemblies, have indicated that the instability threshold may differ substantially from that predicted in loop experiments under simulated reactor conditions.

CONCLUSIONS

The dynamic experiments conducted with both HBWR fuel charges, lead to the following general conclusions concerning the characteristics of D_2O natural circulation boiling water reactors:

(*a*) Reactors of this type can become unstable as a result of flash boiling of moderator between coolant channels. This instability must either be controlled or avoided by appropriate design.

Reactors using a subcooled moderator avoid the problem (e.g., in the Swedish Marviken reactor the subcooled water from the condenser is introduced at the bottom of the reactor vessel between coolant channels resulting in a subcooled moderator).

A large steam space is observed to have a stabilizing influence.

An increase in operating pressure is observed to have an adverse effect on the flashing instability in contrast with the influence of pressure on the high frequency instabilities observed in light water boiling reactors.

(*b*) The models previously developed for natural circulation light water boiling reactors are not directly applicable to natural circulation heavy water boiling reactors. In a light water reactor dynamic model, the entire core is usually considered as a single upcoming boiling channel, while the downcomer is in the reflector. In heavy water reactors of the HBWR type, the coolant channels are separate with a large downcomer space between the coolant channels, resulting in weak hydraulic coupling. This feature must be incorporated in the dynamic model for the heavy water reactor.

(*c*) A large fuel thermal time constant will have a stabilizing effect on the high frequency reactivity feedback instability. Thus only hydraulic instability is considered to impose a possible power density limitation in oxide fuelled reactors.

(*d*) A heavy water boiling reactor will generally have less reactivity in voids [1] than its light water counterpart. This is because in the heavy water reactor, boiling takes place only in the small part of the moderator inside the coolant housings, while in the light water reactor, boiling extends throughout the complete moderator. The small void reactivity coefficients in D_2O moderated reactors may eliminate the problem of high frequency reactivity feedback instability in such reactors. This is indicated by the reactivity to power transfer functions observed in the experiments with both HBWR fuel charges. These experiments show negligible reactivity feedback effects for frequencies above 0.1 c/s. This may make it possible to achieve higher coolant power densities stably in D_2O reactors, than in H_2O reactors, with any type of fuel. This assumes, however, that the net power reactivity coefficient is not positive.

(*e*) Since D_2O boiling reactors may be designed to have a weak hydraulic coupling between coolant channels, large channel void fluctuations may be tolerable. The reactivity fluctuations resulting from random hydraulic oscillations tend to combine to maintain constant net void reactivity worth, and thus constant nuclear power. This makes it possible to achieve higher coolant power densities than in H_2O reactors, assuming hydraulic instability to be the power limiting factor.

(*f*) The 91% maximum exit void fraction obtained in HBWR, which is believed to be the highest

Table 2. Void fractions in typical boiling reactors

Reactor	Type	Pressure (atm)	Maximum channel exit void fraction	
			Already	Planned
Kahl	Light water	71	62	—
VBWR	Light water	70	46	72
Dresden	Light water	70	45	—
HBWR	Heavy water	30	91	94
Marviken	Heavy water	50	—	72

in any natural or forced circulation boiling reactor (Table 2), was measured with an instrumented pilot element in the reactor. Although the channel flow was oscillating strongly under these conditions, this may be close to an acceptable condition even in the complete core of a natural circulation heavy water boiling reactor.

The operating limit imposed on channel exit void fraction is the best measure of the heat transfer performance of natural boiling reactor fuel elements. Both heat transfer burn-out and hydrodynamic instability are more closely related to the steam void fraction in the channel than to other parameters. Raising system pressure will reduce void fraction at a given specific power and thus permit an increase in power.

ACKNOWLEDGEMENT

The developments in boiling water reactor dynamics at Halden are the result of the work of several persons, of which the following should be mentioned: G. Ambrosini, A. Andersson, R. W. Bowring, A. Brouwers, P. la Cour Christensen, J. Freycenon, R. Grumbach, A. Hellsten, A. Höld, K. Jahren, A. Olsen, N. Rydell, H. Schmidl, E. Sokolowski, L. Stevens, V. Tosi, O. Vapaavuori, H. Vollmer and F. Åkerhielm.

REFERENCES

1. Ager-Hanssen, H., Enger, F. H., Kåsa, O. R., and Rose, R., *Experience from the Operation of the Halden Heavy Water Boiling Reactor on its First Fuel Charge, June 1959 to April 1961*, report HPR-26 (1962).
2. Ager-Hanssen, H., *Halden Operating and Research Experience*, Nuclear Power, *17*(79), 57 (1962).
3. La Cour Christensen, P., Hellsten, A., and Akerhielm, F., *Dynamic Experiments with HBWR First Fuel Charge*, report HPR-21 (1962).
4. Schmidl, H., and Stevens, L., *Interpretation of the Dynamic Experiments with HBWR First Fuel Charge*, report HPR-25 (1962).
5. HBWR Quarterly Progress Report, October to December 1962, report HPR-29 (1963).
6. HBWR Quarterly Progress Report, January to March 1963, report HPR-30 (1963).
7. HBWR Quarterly Progress Report, October to December 1963, report HPR-33 (1964).
8. Aarset, B., Olson, H. P., Smith, R. D., and Vapaavuori, O., *In-Core Instrument Development in the HBWR Programme*, P/859, this volume.
9. Hammar, L., Rose, R., and Allison, G. M., *Water Chemistry Research at HBWR*, P/595, Vol. 9, these Proceedings.
10. Jamne, E., Firing, J. A., Øvreeide, M., and Wullum, T., *Operation Experience on the Second Charge for the Halden Boiling Heavy Water Reactor*, P/594, Vol. 5, these Proceedings.
11. Appleby, E. R., *Review of Power and Heat Reactor Designs*, USAEC report HW-66666 REV 2 (1963).
12. Dietrich, J. R., Lichtenburger, H. V., and Zinn, W. H., *Design and Operating Experience of a Prototype Boiling Reactor*, Proceedings of the First International Conference on the Peaceful Uses of Atomic Energy, P/581, Vol. 13, p. 56, United Nations (1956).
13. Harrer, J. M., *et al.*, *Performance Evaluation of Direct Cycle Boiling Water Nuclear Power Plants Based on Recent EBWR and BORAX Data*, Proceedings of the Second International Conference on the Peaceful Uses of Atomic Energy, P/2379, Vol. 9. p. 264, United Nations (1958).
14. Kirchenmayer, A. L., *Dynamics of Boiling Water Reactors*, Advanced Course on the Dynamic Behaviour of Boiling Water Reactors, Institutt for Atomenergi, Kjeller, Norway, report KR-35, Vol. 2 (1962).
15. Freycenon, J., *Reactor Noise Experiments with HBWR First Fuel Charge*, report HPR-23 (1962).
16. Eurola, A. T., *Reactor Noise Experiments on the Halden Boiling Water Reactor*, Proceedings of the Symposium on Noise Analysis in Nuclear Systems, University of Florida (1963), to be published.
17. Bowring, R. W., Proceedings of the Boiling Water Reactor In-Core Instrumentation Meeting at Halden May 15-18, 1961, report HPR-16 (1961).
18. Ager-Hanssen, H., and Smith, R. D., Nucleonics, *22*(4), 49-56 (1964).
19. HBWR Quarterly Progress Report, April to June 1963, report HPR-31 (1963).
20. HBWR Quarterly Progress Report, July to September 1963, report HPR-32 (1963).
21. Beckjord, E. S., *Dynamic Analysis of Natural Circulation Boiling Water Reactors*, USAEC report ANL-5799 (1958).
22. Thie, J. A., *Theoretical Reactor Statics and Kinetics of Boiling Reactors*, Proceedings of the Second International Conference on the Peaceful Uses of Atomic Energy, P/638, Vol. 11, p. 440, United Nations (1958).
23. Fleck, J. A., Jr., *The Dynamic Behaviour of Boiling Water Reactors*, J. Nuclear Energy, *11*, 114 (1960).
24. Kirchenmayer, A. L., *On the Kinetics of Boiling Water Reactors*, J. Nuclear Energy, Part A, Reactor Science, *12*(4), 155 (1960).
25. Akcasu, A. Z., *Theoretical Feedback Analysis in Boiling Water Reactors*, USAEC report ANL-6221 (1960).
26. Schmidl, H., Ambrosini, G., Rydell, N., and Vapaavuori, O., *A Transfer Function Model of the HBWR Plant*, report HPR-5 (1960).
27. HBWR Quarterly Progress Report, April to June 1962, report HPR-27 (1962).
28. HBWR Quarterly Progress Report, July to September 1962, report HPR-28 (1962).

ABSTRACT - RÉSUMÉ - АННОТАЦИЯ - RESUMEN

A/860 Norvège

Dynamique des réacteurs à eau lourde bouillante sur la base du programme de recherche du réacteur à eau lourde bouillante de Halden

par H. Ager-Hanssen *et al.*

De 1959 à 1963 des recherches étendues portant sur la statique et la dynamique des réacteurs ont été entreprises avec le réacteur à eau lourde bouillante de Halden (HBWR), en vue de mettre au point des modèles décrivant le comportement de réacteurs à eau lourde bouillante et à circulation naturelle. Deux charges de combustible ont été utilisées pour ces recherches: d'une part, une charge d'uranium naturel métallique gainé d'aluminium à densité de puissance peu élevée et d'autre part, une charge d'oxyde d'uranium enrichi à 1,5% gainé de zircaloy et à haute densité de puissance.

Les techniques et l'équipement nécessaires pour obtenir les fonctions de transfert du réacteur ont été mis au point et utilisés avec succès dans le programme d'essais dynamiques effectués avec la charge de combustible métallique. Au cours de ce programme, les valeurs de paramètres intégraux tels que la puissance, le débit de vapeur, la pression et les températures de la vapeur et de l'eau ont été mesurées au cours d'expériences de perturbations. Cependant, le nombre des paramètres intervenant dans le modèle dynamique est si grand et le nombre de ces paramètres mesurés si petit, qu'il a fallu procéder à des ajustements empiriques des modèles afin de les faire correspondre aux résultats expérimentaux pour les différentes conditions d'essais. Il s'est avéré difficile dans ces conditions d'ajustements macroscopiques de mettre au point des modèles qui puissent être extrapolés avec confiance à d'autres projets de réacteurs.

Il a été reconnu dès le début qu'en plus des paramètres intégraux, la mesure directe des paramètres microscopiques tels que le coefficient de vide de la la vapeur dans les canaux, les températures du combustible et du fluide de refroidissement dans les canaux et les vitesses locales du fluide de refroidissement, était la méthode la plus prometteuse pour la mise au point de modèles permettant l'extrapolation. En conséquence, et compte tenu du fait que des instruments éprouvés pour de telles mesures n'existaient pas, on a entrepris la mise au point d'instruments destinés à être insérés dans le cœur du réacteur pour les mesures du programme d'études dynamiques avec une charge de combustible en oxyde. Le programme de mise au point d'instruments à insérer dans le cœur est décrit dans une autre communication soumise à cette conférence.

Afin de permettre l'analyse simultanée du comportement dans le temps d'un grand nombre de signaux provenant du cœur, conformément au programme d'essais dynamiques avec la charge de combustible en oxyde, un système complexe de traitement des informations a été mis au point. Le système comprend un analyseur à deux canaux pour fonctions de transfert, une calculatrice analogique spéciale pour des études de corrélation des bruits, un équipement visuel d'enregistrement rapide, une calculatrice analogique à 60 amplificateurs pour la réduction des signaux provenant des instruments en paramètres dynamiques significatifs préalable à leur analyse, un convertisseur analogique-digital et une petite calculatrice digitale rapide.

Sur la base des expériences des perturbations de la charge, entreprises avec le combustible métallique à basse densité de puissance, on a observé que la puissance nucléaire suivait de façon uniforme les variations de la charge, sans transitoires fâcheux comme dans le cas des réacteurs à eau légère bouillante et à grand coefficient de vide de la réactivité (négatif). Par contre, un comportement différent a été observé avec le combustible en oxyde. Dans ce cas, le réacteur (fonctionnant à plus de 10 MW) présente une variation transitoire très violente de la puissance nucléaire lorsque la demande en vapeur est augmentée. Cet effet s'est avéré être dû à une ébullition brusque du modérateur résultant d'une baisse de pression dans la cuve produite par l'augmentation de la demande de vapeur. Une longue période d'instabilité a même été observée à des puissances supérieures à 15 MW. On peut conclure de l'analyse de cette instabilité que: *a*) les instabilités d'ébullition ont une fréquence assez faible pour pouvoir être réduites par le système de contrôle rétroactif nucléaire; *b*) que les réacteurs à eau légère comportant une réactivité cavitaire du fluide de refroidissement élevée et avec un retour de ce fluide vers le bas dans le réflecteur où le coefficient cavitaire est petit, ne seront normalement pas sujets à une telle instabilité; et que *c*) l'instabilité peut être évitée en sous-refroidissant le modérateur (comme par exemple dans le réacteur suédois de Marviken).

Sur la base de ces recherches sur la dynamique, on peut conclure que les modèles qui ont été mis au point précédemment en vue de prédire la stabilité des réacteurs à eau légère bouillante ne sont pas applicables dans le cas d'un réacteur à eau lourde bouillante et à circulation naturelle. Si dans le modèle dynamique des réacteurs à eau légère bouillante, le cœur entier peut être considéré généralement comme un canal d'ébullition unique avec courant ascendant, le retour vers le bas se faisant dans le réflecteur, dans le cas d'un réacteur à eau lourde bouillante, le couplage hydraulique entre les différents canaux est très faible. Cette différence entre les réacteurs bouillants à eau lourde et à eau légère permet d'obtenir de façon stable des densités de

puissance dans le réfrigérant plus élevées dans les réacteurs à D_2O que dans les réacteurs à H_2O.

A/860 Соединенное Королевство

Данные о динамике кипящих тяжеловодных реакторов, полученные по программе исследований на HBWR

Н. Агер-Ханссен

Рассматриваются исследования статики и динамики реактора с 1959 по 1963 год на установке HBWR. Целью исследований была разработка моделей, характеризующих поведение кипящих тяжеловодных реакторов с естественной циркуляцией. В ходе исследований использовались две топливные загрузки: загрузка из природного металлического урана в алюминиевом покрытии с низкой плотностью энерговыделения и загрузка из окиси урана 1,5%-ного обогащения в циркалоевом покрытии с высокой плотностью энерговыделения.

Необходимое оборудование и экспериментальные методы для получения передаточных функций реактора были разработаны и успешно применены в ходе программы исследований динамики, проводившихся на топливной загрузке из металлического урана. По этой программе во время экспериментов по возмущениям была измерена реакция на такие интегральные параметры, как мощность, расход и давление пара, температуры пара и воды. Однако количество параметров, вводимых в динамические модели, было настолько большим, а количество измеренных параметров настолько незначительным, что путем эмпирического регулирования можно было добиться того, что эти модели воспроизводили экспериментальные результаты за пределами условий испытания. При таких микроскопических параметрах оказалось трудным разработать модели, которые с уверенностью можно было бы экстраполировать на другие конструкции реакторов. Были сделаны выводы о том, что самым перспективным направлением разработки моделей, позволяющих производить экстраполяцию, является прямое измерение таких микроскопических параметров, как объем, занимаемый паром в каналах, температуры топлива и теплоносителя в каналах и местные скорости теплоносителя в дополнение к интегральным параметрам. Были разработаны приборы для измерений параметров в активной зоне при изучении динамики, когда в качестве топлива служит окись урана. Программа разработки приборов для проведения таких измерений дана в другом докладе, представленном на Третью Женевскую конференцию.

Была разработана обширная система автоматической обработки экспериментальных данных для анализа одновременного поведения во времени большого числа сигналов, поступающих из активной зоны по программе изучения динамики с окисью урана в качестве топлива. Система состоит из двухканального анализатора передаточных функций; специального счетного устройства непрерывного действия для изучения корреляции шума; скоростного оборудования для визуальной регистрации; счетного устройства непрерывного действия с 60 усилителями для преобразования сигналов приборов в смысловые динамические параметры перед их анализом; аналого-цифрового преобразователя и небольшой, но быстродействующей цифровой вычислительной машины.

В результате экспериментов с возмущениями нагрузки, которые проводились при использовании в качестве топлива металлического урана с низкой плотностью энерговыделения, было установлено, что мощность плавно изменяется с изменением нагрузок без резких переходных колебаний, характерных для кипящих реакторов на обычной воде, имеющих большие (отрицательные) пустотные коэффициенты реактивности. Однако при использовании загрузки из окиси урана наблюдалась совершенно иная картина. При такой загрузке происходило увеличение потребления пара (работа на мощности около 10 *Мвт*) и наблюдались сильные переходные колебания мощности. Оказалось, что этот эффект объясняется испарением замедлителя в результате снижения давления в баке. Длительный период неустойчивости отмечался при работе на мощностях свыше 15 *Мвт*. На основании анализа этой неустойчивости можно сделать следующие выводы:

1) частота неустойчивости испарения довольно небольшая, чтобы ее можно было контролировать с помощью регулирования с обратной связью;

2) реакторы на обычной воде, имеющие большой пустотный коэффициент реактивности теплоносителя и циркуляционную трубу в отражателе, где пустотный коэффициент реактивности невелик, не будут, как правило, иметь такой неустойчивости;

3) этой неустойчивости можно избежать с помощью переохлаждения замедлителя (как это делается, например, на шведском реакторе в Марвикене).

На основании проведенных исследований динамики можно сделать вывод о том, что модели, разработанные до этого для определения устойчивости кипящих реакторов на обычной воде с естественной циркуляцией, не применимы для тяжеловодных реакторов с естественной циркуляцией. Если в динамической модели кипящего реактора на обычной воде вся активная зона рассматривается как один кипящий канал с восходящим потоком, имеющий циркуляционную трубу в отражателе, то в тяжеловодном кипящем реакторе существует лишь очень слабая гидравлическая связь между различными каналами. Эта разница между кипя-

щими реакторами на обычной и тяжелой воде позволяет устойчиво получать в реакторах на тяжелой воде более высокую плотность энерговыделения теплоносителя, чем в реакторах на обычной воде.

A/860 Noruega

Dinámica de los reactores de agua hirviendo basada en el programa de investigación HBWR

por H. Ager-Hanssen *et al.*

Desde 1959 a 1963 se han realizado en el HBWR diversas investigaciones sobre estática y dinámica de reactores para desarrollar modelos que describan el comportamiento de los reactores con circulación natural de D_2O hirviendo. Se han utilizado dos cargas de combustible: una de uranio natural, revestido de aluminio, de baja densidad de potencia, y otra de óxido de uranio enriquecido al 1,5% revestido de Zircaloy, de densidad de potencia elevada.

Se ha desarrollado y empleado con éxito el equipo necesario y las técnicas experimentales para obtener la función de transferencia del reactor, dentro del programa de dinámica realizado con cargas de elementos combustibles metálicos. En este programa se ha medido la respuesta de parámetros integrales tales como potencia, flujo de vapor, presión de vapor y temperatura de vapor y agua durante los experimentos de perturbación. Sin embargo, el número de parámetros que entran en los modelos dinámicos es tan grande y las medidas de esos parámetros son tan escasas que los modelos deben limitarse a reproducir resultados experimentales mediante ajustes empíricos en los intervalos indicados en las condiciones de prueba. Se ha encontrado dificultad en esta aproximación macroscópica para desarrollar modelos que puedan ser extrapolados con confianza a otros diseños de reactores.

Se aceptó desde un principio que las medidas directas de los parámetros macroscópicos tales como vacío de vapor en los canales, temperaturas en el combustible y en los canales de refrigeración, velocidades locales del refrigerante, etc., junto con los parámetros integrales eran las más prometedoras para el desarrollo de modelos que permitiesen extrapolaciones. Este hecho, unido a la ausencia de instrumentos normalizados para tales medidas, condujo al desarrollo de una instrumentación destinada al interior del núcleo del reactor durante el programa dinámico con combustible en forma de óxido. El desarrollo de esta instrumentación se describe en otra memoria de esta Conferencia.

Para realizar un análisis simultáneo del comportamiento temporal de un gran número de señales en el núcleo en el programa dinámico con combustible en forma de óxido, se ha desarrollado un amplio programa para la reducción automática de datos. El sistema emplea un analizador de dos canales para la función de transferencia, un calculador analógico especial para los estudios de correlación de ruido, un equipo de registro visual de velocidad elevada, un calculador analógico amplificador 60 para reducir las señales de los instrumentos a parámetros dinámicos antes del análisis, un convertidor de analógico a digital, y un pequeño calculador digital rápido.

En los experimentos de perturbación de la carga realizados con el combustible metálico de baja densidad de potencia, se ha observado que la potencia sigue suavemente las variaciones de la carga sin que aparezcan los transitorios anormales característicos de los reactores de agua hirviendo, con elevados coeficientes de vacío (negativos). Con el combustible en forma de óxido se observó un comportamiento diferente. Cuando se sometía el reactor a un aumento en la demanda de vapor (operando el reactor a potencias superiores a 10 MW), se observó un transitorio violento en la potencia. Este efecto se explicó como consecuencia de la disminución de presión de la vasija, unido al aumento de la demanda de vapor. Se observó una inestabilidad de largo período a potencias superiores a 15 MW. Del análisis de esta inestabilidad se concluyó: *a*) que la inestabilidad es de una frecuencia suficientemente baja para ser controlada por métodos de control por realimentación; *b*) en los reactores de agua ligera con valor elevado de coeficiente de vacío en el refrigerante y circulación descendente en el reflector donde el valor de este coeficiente es menor, no aparece esta inestabilidad; *c*) la inestabilidad puede ser evitada subenfriando en moderador (por ej., como se ha hecho en el reactor sueco de Marviken).

A partir de las investigaciones dinámicas realizadas, se puede concluir que los modelos previamente desarrollados para las predicciones de estabilidad de los reactores con circulación natural de agua hirviendo no son aplicables a los reactores con circulación natural de agua pesada hirviendo. Mientras que en los reactores de agua natural hirviendo el modelo dinámico del núcleo entero es normalmente un canal con circulación ascendente y circulación descendente en el reflector, hay un acoplamiento pequeño entre los distintos canales de un reactor de agua pesada hirviendo. Esta diferencia entre los reactores de agua pesada hirviendo y agua natural permite alcanzar unas densidades de potencia en el refrigerante superiores en los reactores de D_2O que las que se pueden obtener en los reactores de H_2O.

Record of Session 3.4

Reactor kinetics

Chairman: S. Yiftah (Israel)

Point and spatial kinetics

GENERAL DISCUSSION

H. SMETS (Belgium): In paper P/687, Dr. Schmid derives the stability properties of a reactor from considerations in which delayed neutrons are neglected, and he obtains exact results in the particular case he studied. However, I think it should be pointed out that delayed neutrons do not always improve the stability of reactors. Reactors with delayed neutrons may be unstable even though stable when delayed neutrons are neglected. The power at which the reactor reaches its stability limit may be lower when delayed neutrons are taken into account, and damping of oscillations can be decreased by the delayed neutrons.

These facts are not generally known, and many doubtful statements have been made in the past, as well as in some of the papers presented at this Conference, on the effect of delayed neutrons.

P. SCHMID (Switzerland): I quite agree with Dr. Smets. In his 1958 Geneva paper (Ref. [7] of my paper), V. M. Popov proved that delayed neutrons always lead to asymptotic stability in the large provided that simple stability of the system without delayed neutrons can be proved *by establishing a second-order Lyapunov function.* For systems with two independent temperature coefficients, which are mathematically equivalent to my first model, Popov derived such a Lyapunov function, so that its existence can be taken for granted. This should suffice to justify the remarks in my paper.

For my second model I applied Smets' *first stability theorem*, which was obtained from a suitable Lyapunov function, including delayed neutrons. I think it can be said, therefore, that the criteria needed for my second model to be asymptotically stable in the large have been rigorously derived and that the effect of delayed neutrons has been adequately taken into account.

J. CHERNICK (United States of America): I should like to add a few words to the comments of Dr. Smets and Dr. Schmid. The question of whether delayed neutrons add stability or not frequently depends on the mathematical model, which may or may not represent the physical situation. It also depends on whether the dynamic system is free or forced. I believe that the physical conditions demanded by Dr. Schmid would in fact lead to damping in all cases. However, where there is a forced oscillation, as I pointed out a few years ago at a meeting of the American Nuclear Society in Boston, the simple case of a sinusoidal reactivity oscillation leads to antidamping on the part of the delayed neutrons.

E. P. GYFTOPOULOS (United States of America): I generally agree with what Smets and Chernick have said. However, the proof that delayed neutrons improve stability is based on the assumption that the system of equations describing the reactor without delayed neutrons has feedback and admits solutions which are asymptotically stable at all power levels. In these conditions there is no doubt that delayed neutrons improve stability.

T. GOZANI (Israel): I have a general comment which concerns all these papers on point and spatial kinetics, but in particular, possibly, the paper of Kaplan and Taylor (P/271) and that of Stassis and Mitsonias (P/648).

In recent years there have been great improvements in the use of pulsed neutron sources, both in the techniques themselves and in the evaluation of the results. Powerful and relatively cheap neutron generators have become available. The new evaluation procedures* make it possible to determine reactivity directly in dollar units, practically without harmonic systematic errors and without recourse to the assumption that prompt-neutron generation time is independent of the subcritical state. This is done by not rejecting the delayed neutron background following the pulses.

Any functional relationship between the prompt and delayed neutron populations, complemented by the prompt decay constant of the persisting mode,

* Gozani, T., Nukleonik, *4*, 348 (1962), and Garelis, E., and Russel, J. L. Jr., Nucl. Sci. and Eng., *16*, 263 (1963).

yields both reactivity and prompt generation in dollar units. With this evaluation procedure it is not necessary to have very short pulses or to wait until the delayed neutron population has reached equilibrium. It is proposed that this should be used as a standard method for precise reactivity measurements wherever possible.

E. P. GYFTOPOULOS (United States of America): I think it should be said that reactivity is not a basic quantity without which we cannot analyse a reactor. Whenever we use the concept of reactivity we should not fail to ask ourselves why we are doing so. In large reactors, or in reactors undergoing very fast transients, it may be purposeless or actually misleading.

V. A. KUZNETSOV (USSR): I should like to comment on paper P/648. The authors suggest a method which in their opinion should make it possible to obtain independently, from a single experiment, two important physics characteristics (β_{eff} and l_{eff}) which enter into all kinetic equations in the form of a ratio. However, the two equations from which the authors derive these characteristics are clearly not independent. They too contain, essentially, only one characteristic, namely $\alpha = \beta_{\text{eff}}/l_{\text{eff}}$, and this is, unfortunately, the only relation which can be determined experimentally by the method they propose.

T. GOZANI (Israel): It is in fact impossible to determine β_{eff} by kinetic methods. The only way of determining it is to compare reactivity, ρ, measured in dollar units, by any kinetic method one likes to use for the purpose, with a calculated value for precisely the same system. Several years ago, Kaplan and Henry in the United States used boron poisoning to carry out such a measurement on a light water system. However, by applying the new pulsed-source evaluation procedures (as mentioned above) to calculable systems, one can determine β_{eff} with relative ease. Preliminary measurements have been carried out at Würenlingen (EIR) in Switzerland.

A. B. WHITELEY (United Kingdom): I might mention, in connection with paper P/271, that the Central Electricity Generating Board has made extensive use of the United Kingdom Atomic Energy Authority's three-dimensional kinetic programmes STAB and STABLE. These involve a solution in one-group diffusion theory with about 1 500 mesh points and solution of the associated thermodynamic equations corresponding to a gas-cooled, graphite-moderated reactor. However, in cases where local disturbances arise—e.g., through withdrawal of a single rod—we have found that these programmes are not sufficiently detailed. Our efforts are now concentrated, therefore, on an extension of the three-dimensional SKIP programme (a joint enterprise of the CEGB and the UKAEA), which is to become a time-dependent programme with about 8 000 mesh points, giving very flexible representation of local absorbers and associated control systems. This programme is being written mainly in FORTRAN for the IBM 7094.

J. J. TAYLOR (United States of America): In our work on space-time analysis, reported in the paper you refer to, we have been placing emphasis on methods of modal analysis, using synthesis techniques, rather than on the nodal analyses employed in the United Kingdom programmes. Nevertheless, we have been following the British work with great interest and are gratified to see how well programmes using a relatively small number of mesh points have succeeded in predicting the space-time kinetic characteristics of gas-cooled, graphite-moderated reactors.

Kinetic studies of particular reactors

Papers P/859 and P/860 (presented jointly by H. Ager-Hanssen)

DISCUSSION

M. A. SCHULTZ (United States of America): I see that you are planning to use in-core instrumentation as safety equipment. How long do you expect these devices to last, and on the basis of what experience can you predict their lifetime?

H. AGER-HANSSEN (Norway): We plan to install the safety instrumentation with the core rather than with the pressure vessel. We believe that the instruments will have a lifetime similar to that of the fuel charge, that is between one and two years. There should be no difficulty in meeting this requirement; turbines and thermocouples have been in operation at Halden for more than two years without giving rise to any problems.

B. G. DUBOVSKY (USSR): During start-up of the Beloyarsk reactor (a high-specific-power reactor) we tested certain equipment designed to improve the control system. The instrumentation includes an automatic power-level recorder, a reactivity gauge showing changes in the reactivity curve and a gauge indicating the position of control rods belonging to the automatic control mechanism; there is also a co-ordinating oscillator which makes a time indication (every 100 s) on the recording potentiometer charts for all three of the above instruments.

This equipment has made possible a speedy analysis of the reactor's state during changes in the operating régime, including emergencies. It has enabled us to improve our control over the precise operation of the automatic control mechanism and over the actions of operating staff. In short, it has proven its value.

J. A. THIE (United States of America): My question concerns the use of noise spectra in the HBWR

as a means of detecting the instability. Power plant operators often prefer this technique to other dynamic tests because it does not disturb the reactor or upset its operating schedule. For a proper interpretation of noise test results, it is advantageous to know the source of the random reactivity fluctuations in the core. My paper (P/272) discusses this problem in connection with several reactors and I conclude that randomness in coolant flow is the cause most frequently found. However, fluctuations of coolant inlet temperature have also been shown to be the cause of noise in some reactors. Have either of these effects, or possibly others, been established as the source of reactivity noise in the HBWR?

T. EUROLA (Finland): May I answer that question? A study of noise sources has been part of our work on noise at Halden. So far, because of the complexity of the system, we have been unable to pinpoint the source or sources of noise. I can only say that the reactivity-to-power transfer function, as measured in non-oscillating reactor conditions, does not seem to be identical with the power spectrum of nuclear power. This seems to indicate that the source of noise is not the bubble formation, but that it might be temperature and flow fluctuations at the channel inlet or turbulence in the moderator region. For instance, the power spectrum of the coolant flow seems to be close to white. However, as I said before, we dare not be too firm in our conclusions as yet.

J. A. THIE (United States of America): The use of a burn-out protector in the Halden reactor is very interesting, especially if the experience makes it possible to use similar instruments in other reactors. Could Mr. Ager-Hanssen tell us what in-pile or out-of-pile experience exists? In particular, have deliberate attempts been made to induce burn-out, and did the protection in all cases prevent burn-out by a trip? If burn-out protectors are to have practical application elsewhere, can one be absolutely sure that they are installed in the right place to monitor the channel which is to undergo burn-out?

H. AGER-HANSSEN (Norway): So far we have not been able to take the fuel assembly to a power level approaching burn-out conditions. However, we have now requested a licence to operate the reactor at 25 MW, that is 5 MW above the present nominal rating, and we hope then to be able to bring our high-specific-power assembly (IFA4) to a point where burn-out may occur but fuel melting will be prevented by the burn-out detector. The design of this instrument is based on the observation that burn-out is likely to occur at the exit of a channel where the void fraction is highest. We also make use of an observed radial effect which indicates that burn-out will occur at the point furthest removed from an opposing surface; the heat-focusing technique used in our burn-out detector takes advantage of this effect.

O. VAPAAVUORI (Finland): I should like to add a few remarks to the papers presented by Mr. Ager-Hanssen. The results of certain measurements made with the IFA4 fuel assembly were obtained after the paper on in-core instrument development had been written, and they might be of general interest:

(*a*) The maximum peak-to-peak oscillations in inlet flow, during the measurements, were of the order of $\pm$ 200% (relative to the steady-state value). The measured inlet velocities were 1.5 m/s upwards and 0.5 m/s downwards;

(*b*) The total number of hydraulic oscillations was of the order of 10^5, without any fuel element failure; the outlet void fraction (α_{ex}) was always very near 90% at the onset of hydraulic oscillations;

(*c*) The maximum power level attained beyond the instability threshold was about 60% higher than this threshold. No burn-out phenomena were in evidence and

(*d*) A noise technique has been used successfully in the reactor to determine the instability threshold of fuel assemblies.

Paper P/79 (presented by R. Abdon)

DISCUSSION

J. J. TAYLOR (United States of America): I have two questions. First, could you describe the specific compensating effects which keep reactivity steady when radial expansion of an individual fuel element occurs? Secondly, have you done any analyses using the digital computer *tied in* with the analogue computer and, if so, could you elaborate on how the *tie-in* is accomplished?

R. ABDON (France): Radial expansion of the fuel elements has a negligible effect on reactivity as the movements of material are, on the average, self-compensating. A positive effect due to fuel moving closer to the centre of the core is compensated by a negative effect due to the material expanding towards the outside.

In reply to your second question, we have not yet coupled the analogue and digital computers used with the RAPSODIE simulator, mainly because of the practical inconvenience of getting them together; at the moment they are five kilometres apart. We are nevertheless planning to couple them later on.

J. CHERNICK (United States of America): Would you explain the use of plaquettes to obtain a negative structural coefficient in RAPSODIE?

R. ABDON (France): The plaquettes make the

core more compact as soon as the sodium temperature reaches its design value for reactor operation and the temperature gradient of 90 degC between the inlet and outlet is established (in fact, probably even before the gradient is established). On the full-scale thermal mock-up of the reactor constructed at Cadarache we found that the play between the assemblies was very slight and we were therefore able to predict that the core would become compact as a result of expansion.

J. CHERNICK (United States of America): What information applicable to the technology of fast power reactors do you expect to obtain from RAPSODIE?

R. ABDON (France): The purpose of RAPSODIE is threefold. We hope in the first place to verify the methods of calculation used for the project. Secondly, we want to perfect certain technologies which can then be extended to other reactors of this type, particularly those having to do with the sodium coolant loops, the reactor block and the remote handling equipment. Lastly, RAPSODIE will be used to irradiate fast-reactor fuel elements.

Paper P/664 (presented by J. Miida)

DISCUSSION

K. WOOD (United Kingdom): The matrix methods for a reflected reactor, discussed in your paper, involve lengthy computer programmes and the use of much computer time. In design studies for large gas-cooled reactors, adequate information can generally be obtained from an unreflected homogeneous reactor model with a single neutron energy group; either harmonic or finite-difference methods of solution can be used for both stability and transient analysis.

Simulation of controllers with dead bands or saturation may be preferred to describing function analysis. It is then possible to investigate directly the effects of signal or controller noise on transient behaviour.

Although the position feedback proposed in the paper gives some improvement in control system response, it is usually avoided in United Kingdom designs because it introduces an additional controller input which could fail in service. Satisfactory control can be achieved in all conditions with a simple bad-lag phase advance.

J. MIIDA (Japan): I cannot say offhand whether the matrix method for a reflected reactor requires more time than other methods or not. Of course, simulation by computer is useful in this type of study. However, parameter studies by simulation can be quite time-consuming, and simulation cannot give us the effect of particular parameters on the system studied. In such cases approximation by describing function analysis is very useful.

Theoretically, rod position feedback improves response and lessens the effect of the limit cycles. I cannot agree that it introduces an additional input which could fail in service; in fact, in this case I don't quite see what failure in service could mean.

Paper P/272 (read by title only)

DISCUSSION

B. G. DUBOVSKY (USSR): Dr. Thie tells us, in paper P/272, that it is possible to measure subcriticality by investigating the statistical fluctuations (noise) of a reactor. I should like to know what magnitude of subcriticality can be measured in this way. If it is a question of only $\sim 2\%$ the prospect is not particularly attractive because there are other, simpler methods of doing the job; but if subcriticalities of $\sim 6\%$ or greater can be measured, the method will become extremely valuable. Perhaps Dr. Thie, or others, could tell us what are the specific advantages of noise methods.

J. A. THIE (United States of America): Measurements of shutdown reactivities greater than 5% are interesting though difficult. The Milletron company in the United States is engaged in research on measurements of these large negative reactivities, even in the presence of large gamma fields. For subcritical reactivities nearer criticality than 5%, increasing precision is possible, and this is fortunately in the region where higher accuracy is desirable (for reasons of safety, for example).

In measurements of shutdown reactivities, noise methods do have certain definite advantages over methods such as rod drop, subcritical count, and so on. One of these is that noise methods are not sensitive to source and detector geometry.

M. A. SCHULTZ (United States of America): As Dr. Thie says, subcritical noise measurements provide a simple means of obtaining high accuracy near critical and are therefore interesting even though the answers obtained at, say, 10% negative reactivity are a good deal less precise. Experiments such as rod worth or fuel addition can be carried out when the reactor is subcritical without any necessity of resorting to period measurements or rod bumping. However, the basic apparatus commercially available today is intended primarily for use as a safety device.

E. P. GYFTOPOULOS (United States of America): In my view, noise measurements in subcritical reactors have the same advantage as noise measurements in other conditions—specifically, that the reactor is "excited" by the inherent noise and not by the experimenter. Of course, this advantage is gained at a price. As Dr. Thie says at the end of paper P/272, the experimental results may often be difficult to interpret.

Compte rendu de la séance 3.4

Cinétique des réacteurs

Président: S. Yiftah (Israël)

Cinétique ponctuelle et spatiale

DISCUSSION GÉNÉRALE

H. SMETS (Belgique): Dans le mémoire P/687, M. Schmid déduit les propriétés de stabilité d'un réacteur de considérations dans lesquelles on néglige les neutrons retardés, et il obtient des résultats exacts dans le cas particulier de son étude. Cependant, je crois qu'il faudrait bien faire ressortir que les neutrons retardés n'améliorent pas toujours la stabilité des réacteurs. Des réacteurs à neutrons retardés peuvent être instables, même s'ils sont stables lorsqu'on néglige les neutrons retardés. La puissance à laquelle le réacteur atteint sa limite de stabilité peut être plus faible lorsqu'on tient compte des neutrons retardés, et l'amortissement des oscillations peut être réduit par les neutrons retardés.

Ces faits ne sont pas connus en général, et bien des affirmations douteuses sur l'effet des neutrons retardés ont été faites dans le passé, ainsi que dans quelques-uns des mémoires présentés à cette conférence.

P. SCHMID (Suisse): Je partage entièrement l'avis de M. Smets. Dans son mémoire présenté à la conférence de Genève de 1958 (référence [7] de mon mémoire), V. M. Popov a démontré que les neutrons retardés conduisent toujours asymptotiquement à la stabilité en général, pourvu que la stabilité simple du système sans neutrons retardés puisse être démontrée *par l'établissement d'une fonction de Lyapunov du second ordre*. Pour des systèmes avec deux coefficients de température indépendants, qui du point de vue mathématique sont équivalents à mon premier modèle, Popov arrive à une telle fonction de Lyapunov, aussi l'existence de celle-ci peut-elle être tenue pour acquise. Ceci devrait suffire à justifier les remarques faites au début de mon mémoire.

Pour mon second modèle, j'ai appliqué le « premier théorème de stabilité » de Smets, obtenu à partir d'une fonction convenable de Lyapunov, tenant compte des neutrons retardés. Je crois que l'on peut donc dire que les conditions nécessaires pour que mon second modèle tende vers la stabilité en général ont été déduites en toute rigueur et que l'on a convenablement tenu compte des neutrons retardés.

J. CHERNICK (Etats-Unis d'Amérique): Je voudrais ajouter quelques mots aux remarques faites par M. Smets et par M. Schmid. Que les neutrons retardés améliorent ou non la stabilité dépend souvent du modèle mathématique, qui peut être représentatif ou non de la situation physique. Cela dépend aussi du caractère libre ou contraint du système dynamique. Je pense que les conditions physiques imposées par M. Schmid conduiraient en fait à l'amortissement dans tous les cas. Cependant, quand il existe une oscillation forcée, comme je l'ai montré voici quelques années à un congrès de l'American Nuclear Society à Boston, le cas simple d'une oscillation sinusoïdale de réactivité conduit à un anti-amortissement du fait des neutrons retardés.

E. P. GYFTOPOULOS (Etats-Unis d'Amérique): Dans l'ensemble, je suis d'accord avec ce qu'ont dit Smets et Chernick. Cependant, la preuve de l'amélioration de la stabilité par les neutrons retardés se fonde sur l'hypothèse que le système d'équations représentant le réacteur sans neutrons retardés fonctionne en rétroaction et admet des solutions qui tendent vers la stabilité à tous les niveaux de puissance. Dans ces conditions, il est hors de doute que les neutrons retardés améliorent bien la stabilité.

T. GOZANI (Israël): Je voudrais faire une remarque d'ensemble qui concerne tous ces mémoires sur la cinétique ponctuelle et spatiale, mais surtout, peut-être, le mémoire de Kaplan et Taylor (P/271) et celui de Stassis et Mitsonias (P/648).

Ces dernières années, on a beaucoup perfectionné l'emploi de sources de neutrons pulsés, à la fois dans les techniques elles-mêmes et dans l'interprétation des résultats. Des générateurs de neutrons puissants et d'un prix relativement bas sont apparus sur le marché. Les nouvelles méthodes d'évaluation* rendent possible la détermination de la réactivité directement en dollars, pratiquement sans erreur systématique d'harmonique et sans qu'il soit besoin de supposer que le temps de génération des neutrons

* Gozani, T., Nukleonik, *4*, 348 (1962), et Garelis, E., et Russel, J. L., Jr., Nuclear Sci. and Eng., *16*, 263 (1963).

instantanés est indépendant de l'état sous-critique. On y parvient en n'éliminant pas le bruit de fond dû aux neutrons retardés qui suivent les impulsions.

Toute relation entre les populations de neutrons instantanés et de neutrons retardés, complétée par la constante de décroissance des instantanés selon le schéma permanent, donne à la fois la réactivité et la génération instantanée en dollars. Avec cette méthode d'évaluation, il n'est pas nécessaire d'avoir des impulsions très brèves, ni d'attendre que la population de neutrons retardés ait atteint son équilibre. On propose de suivre cette méthode type de mesures précises de réactivité chaque fois que c'est possible.

E. P. GYFTOPOULOS (Etats-Unis d'Amérique): Je crois qu'il faudrait dire que la réactivité n'est pas une grandeur fondamentale sans laquelle on ne peut analyser un réacteur. Chaque fois que nous nous servons de la notion de réactivité, nous ne devrions pas manquer de nous demander pourquoi nous le faisons. Dans les gros réacteurs, ou dans ceux qui subissent des régimes transitoires très rapides, cela peut être sans objet ou même trompeur.

V. A. KUZNETSOV (URSS): Je voudrais faire quelques observations sur le mémoire P/648. Les auteurs suggèrent une méthode qui, à leur avis, permet d'obtenir indépendamment, en une seule expérience, deux importantes caractéristiques physiques (β_{eff} et l_{eff}) qui figurent dans toutes les équations cinétiques sous la forme d'un rapport. Cependant, les deux équations dont les auteurs tirent ces caractéristiques ne sont manifestement pas indépendantes. Elles aussi ne contiennent au fond qu'une seule caractéristique, qui est $\alpha = \beta_{eff}/l_{eff}$, et c'est là, malheureusement, la seule relation que l'on puisse déterminer expérimentalement par la méthode qu'ils proposent.

T. GOZANI (Israël): En fait, il est impossible de déterminer β_{eff} par des méthodes cinétiques. La seule méthode pour le déterminer est de comparer la réactivité ρ, mesurée en dollars, par une méthode cinétique quelconque choisie à cette fin, avec une valeur calculée pour le même système exactement. Il y a plusieurs années, Kaplan et Henry, aux Etats-Unis, ont utilisé l'empoisonnement au bore pour effectuer une mesure sur un système à eau ordinaire. Cependant, l'application que j'ai mentionnée des nouvelles méthodes d'évaluation avec neutrons pulsés à des systèmes accessibles au calcul permet de déterminer β_{eff} assez facilement. Des mesures préliminaires ont été effectuées à Würenlingen (EIR) en Suisse.

A. B. WHITELEY (Royaume-Uni): Je peux signaler, à propos du mémoire P/271, que le Central Electricity Generating Board s'est abondamment servi des programmes cinétiques à trois dimensions STAB et STABLE de l'United Kingdom Atomic Energy Authority. Ces programmes comportent une solution en théorie de la diffusion à un groupe avec environ 1 500 points de réseau et la solution des équations thermodynamiques associées correspondant à un réacteur refroidi par un gaz et modéré au graphite. Cependant, dans les cas où apparaissent des perturbations locales — par exemple le retrait d'une seule barre — nous avons trouvé que ces programmes n'étaient pas assez détaillés. Nos efforts sont donc maintenant concentrés sur une extension du programme à trois dimensions SKIP (entrepris en commun par le CEGB et l'UKAEA), qui doit devenir un programme fonction du temps avec environ 8 000 points de réseau, donnant une représentation très souple des absorbants locaux et des systèmes de contrôle associés. Ce programme est en cours de rédaction, principalement en FORTRAN, pour un ensemble IBM 7094.

J. J. TAYLOR (Etats-Unis d'Amérique): Dans nos travaux sur l'analyse espace-temps, rapportés dans le mémoire auquel vous vous référez, nous avons mis au premier plan les méthodes d'analyse modale qui utilisaient des techniques de synthèse, plutôt que l'analyse modale utilisée dans les programmes du Royaume-Uni. Néanmoins, nous avons suivi les travaux britanniques avec beaucoup d'intérêt, et nous sommes satisfaits de voir avec quel bonheur des programmes utilisant un nombre relativement faible de points de réseau ont réussi à prédire les caractéristiques cinétiques d'espace-temps des réacteurs refroidis par gaz et modérés au graphite.

Études cinétiques de réacteurs particuliers

Mémoires P/859 et P/860 (présentés ensemble par H. Ager-Hanssen)

DISCUSSION

M. A. SCHULTZ (Etats-Unis d'Amérique): Je vois que vous envisagez d'employer des instruments placés dans le cœur comme système de sécurité. Combien de temps comptez-vous que ces appareils pourront durer, et sur quelle expérience vous fondez-vous pour prédire leur durée de vie?

H. AGER-HANSSEN (Norvège): Nous avons l'intention de lier l'installation de l'appareillage de sécurité à celle du cœur plutôt qu'à celle du caisson. Nous croyons que les appareils auront une durée semblable à celle du chargement de combustible, soit entre un et deux ans. Il ne devrait pas y avoir de difficulté à obtenir ces performances; des turbines et des thermocouples ont fonctionné à Halden pendant plus de deux ans sans causer aucun problème.

B. G. DUBOVSKY (URSS): Au cours du démarrage du réacteur de Beloyarsk (à forte puissance spécifique), nous avons soumis à des essais certains appareils conçus pour améliorer le système de contrôle. L'appareillage comprend un enregistreur automatique du niveau de puissance, un indicateur de réactivité montrant les changements de la courbe de réactivité, et un indicateur donnant la position des

barres de contrôle qui appartiennent au dispositif automatique de contrôle; il y a aussi un oscillateur de synchronisation qui marque un repère de temps (toutes les 100 s) sur les bandes des enregistreurs potentiométriques des trois appareils précédents.

Cet appareillage a rendu possible une analyse rapide de l'état du réacteur au cours de modifications du régime de fonctionnement, y compris des alarmes. Il nous a permis de mieux diriger le fonctionnement exact du dispositif automatique de contrôle et la conduite du personnel d'exploitation. Bref, il a fait la preuve de son efficacité.

J. A. THIE (Etats-Unis d'Amérique): Ma question vise l'emploi des spectres de bruit dans le HBWR comme moyen de déceler l'instabilité. Les exploitants des centrales préfèrent souvent cette technique à d'autres tests dynamiques, parce qu'elle ne perturbe pas le réacteur et ne change rien à son programme d'exploitation. Pour interpréter convenablement les résultats d'essais de bruit, on a intérêt à connaître la source des fluctuations aléatoires de réactivité dans le cœur. Mon mémoire (P/272) discute ce problème à propos de plusieurs réacteurs, et je déduis que les phénomènes aléatoires dans l'écoulement du caloporteur sont la cause la plus fréquente. Cependant, des fluctuations de la température d'entrée du caloporteur se sont aussi révélées être la cause de bruit dans quelques réacteurs. L'un ou l'autre de ces effets, ou d'autres peut-être, a-t-il été reconnu comme la source de bruit de réactivité dans le HBWR?

T. EUROLA (Finlande): Puis-je répondre à cette question? Une étude des sources de bruit a été faite parmi nos travaux sur le bruit à Halden. Jusqu'ici, à cause de la complexité du système, nous ne sommes pas arrivés à déterminer exactement la source ou les sources de bruit. Je puis seulement dire que la fonction de transfert réactivité-puissance mesurée dans les conditions d'un réacteur non oscillant ne semble pas identique au spectre d'énergie de la puissance nucléaire. Cela semble indiquer que la source de bruit n'est pas la formation de bulles, mais qu'elle se trouve peut-être dans les fluctuations de température et de débit à l'entrée du canal ou dans la turbulence dans la zone du modérateur. Par exemple, le spectre d'énergie de l'écoulement du caloporteur semble proche du blanc. Cependant, je l'ai déjà dit, nous n'avons pas encore le droit d'affirmer nos conclusions.

J. A. THIE (Etats-Unis d'Amérique): L'emploi d'un dispositif anti-caléfaction dans le réacteur de Halden est très intéressant, surtout si l'expérience établit la possibilité d'employer des appareils semblables dans d'autres réacteurs. M. Ager-Hanssen pourrait-il nous dire quelle est l'expérience acquise en pile et hors pile? En particulier, a-t-on fait des essais délibérés pour provoquer la caléfaction, et la protection a-t-elle par son déclenchement empêché la caléfaction dans tous les cas? Si des dispositifs anti-caléfaction doivent avoir des applications pratiques ailleurs, peut-on avoir la certitude absolue qu'ils sont placés à l'endroit convenable pour contrôler le canal qui va subir la caléfaction?

H. AGER-HANSSEN (Norvège): Jusqu'ici nous n'avons pas pu porter les éléments de combustible à un niveau de puissance approchant les conditions de caléfaction. Cependant nous avons à présent demandé l'autorisation de porter le réacteur à 25 MW, soit 5 MW de plus que la valeur nominale actuelle, et nous avons bon espoir de pouvoir amener notre élément à forte puissance spécifique (IFA4) à un point où la caléfaction peut se produire, mais où la fusion du combustible sera empêchée par le détecteur de caléfaction. La conception de cet appareil s'appuie sur la remarque que la caléfaction risque de se produire à la sortie d'un canal où la fraction de vide est le plus élevée. Nous utilisons aussi nos observations d'un effet radial, qui indiquent que la caléfaction se produira au point le plus éloigné d'une surface en opposition. La technique de focalisation de la chaleur utilisée dans notre détecteur de caléfaction met à profit cet effet.

O. VAPAAVUORI (Finlande): Je voudrais ajouter quelques remarques aux mémoires présentés par M. Ager-Hanssen. Les résultats de certaines mesures faites avec l'assemblage de combustible IFA4 ont été obtenus après la rédaction du mémoire sur la mise au point des instruments insérés dans le cœur et peuvent présenter un intérêt général:

a) Le maximum des oscillations crête à crête dans le débit d'entrée pendant les mesures était de l'ordre de $\pm 200\%$ (valeur relative à valeur de régime). Les vitesses d'entrée mesurées étaient 1.5 m/s de bas en haut et 0.5 m/s de haut en bas;

b) Le nombre total d'oscillations hydrauliques était de l'ordre de 10^5, sans aucune rupture d'élément combustible; la fraction de vide à la sortie (α_{ex}) était toujours très proche de 90% à l'établissement des oscillations hydrauliques;

c) Le niveau maximal de puissance atteint au-delà du seuil d'instabilité était d'environ 60% au-dessus de ce seuil. Il n'apparaissait aucun phénomène de caléfaction;

d) Une technique de bruit a été utilisée avec succès dans le réacteur pour déterminer le seuil d'instabilité des éléments combustibles.

Mémoire P/79 (présenté par R. Abdon)

DISCUSSION

J. TAYLOR (Etats-Unis d'Amérique): J'ai deux questions à poser. D'abord, pourriez-vous décrire les effets spécifiques compensateurs qui maintiennent la réactivité constante quand se produit l'expansion radiale d'un élément combustible?

Deuxièmement, avez-vous fait des analyses en couplant le calculateur numérique au calculateur analogique, et dans ce cas pourriez-vous expliquer ce couplage dans le détail?

R. ABDON (France): L'expansion radiale des éléments combustibles a sur la réactivité un effet négligeable car les mouvements de matière sont, en moyenne, auto-compensés. Un effet positif dû au mouvement du combustible se rapprochant du centre du cœur est compensé par un effet négatif dû à l'expansion de matière vers l'extérieur.

Pour répondre à votre deuxième question, nous n'avons pas encore réalisé de couplage entre calculateur analogique et calculateur numérique principalement à cause de difficultés pratiques pour les réunir; ils sont en ce moment à 5 km l'un de l'autre. Néanmoins nous avons l'intention de réaliser ce couplage plus tard.

J. CHERNICK (Etats-Unis d'Amérique): Voudriez-vous expliquer l'emploi de plaquettes pour obtenir un coefficient négatif des structures dans RAPSODIE?

R. ABDON (France): Les plaquettes rendent le cœur plus compact dès que la température du sodium atteint sa valeur normale pour le réacteur en exploitation et que le gradient de température de 90 °C est établi entre l'entrée et la sortie (en fait, même probablement avant l'établissement du gradient). Sur la maquette en vraie grandeur construite à Cadarache, nous avons trouvé que le jeu entre les assemblages était très faible, et nous avons donc pu prédire que le compactage du cœur se produirait comme conséquence de l'expansion.

J. CHERNICK (Etats-Unis d'Amérique): Quels renseignements applicables à la technologie des réacteurs rapides de puissance comptez-vous tirer de RAPSODIE?

R. ABDON (France): Le but de RAPSODIE est triple. Nous espérons d'abord vérifier les méthodes de calcul utilisées pour le projet. En deuxième lieu, nous voulons perfectionner certaines technologies qui peuvent s'étendre à d'autres réacteurs de ce type, principalement celles qui ont trait aux boucles de refroidissement au sodium, au bloc pile et à l'appareillage de manutention à distance. Enfin, RAPSODIE servira aux irradiations d'éléments combustibles de réacteurs rapides.

Mémoire P/664 (présenté par J. Miida)

K. WOOD (Royaume-Uni): Les méthodes matricielles pour un réacteur avec réflecteur, discutées dans votre mémoire, demandent de longues programmations et beaucoup de temps de calculateurs. Dans les études de projets de grands réacteurs refroidis par un gaz, des informations convenables peuvent être obtenues en général à partir d'un modèle de réacteur homogène sans réflecteur avec un seul groupe d'énergie de neutrons; on peut employer l'une ou l'autre des deux méthodes de résolution, soit celle des harmoniques soit celle des différences fines, pour analyser à la fois la stabilité et les transitoires.

On peut préférer la simulation de contrôleurs avec des bandes perdues ou la saturation à la description de l'analyse de fonction. Il est alors possible de rechercher directement les effets du signal ou du bruit du contrôleur sur le régime transitoire.

Bien que la rétroaction de positionnement proposée dans le mémoire améliore quelque peu la réponse du système de contrôle, on l'évite en général au Royaume-Uni, car elle demande la mise en action d'un contrôleur supplémentaire susceptible de panne en exploitation. Un contrôle satisfaisant est réalisable dans toutes les conditions avec un simple rattrapage de déphasage.

J. MIIDA (Japon): Je ne peux pas dire immédiatement si la méthode matricielle pour un réacteur avec réflecteur demande ou non plus de temps que d'autres méthodes. Assurément, la simulation par calculateur est utile dans ce genre d'étude. Toutefois, les études paramétriques par simulation peuvent prendre beaucoup de temps, et la simulation ne peut nous donner l'effet de paramètres particuliers pour le système étudié. Dans de tels cas, l'approximation par la description de l'analyse de fonction est très utile.

En théorie, la rétroaction de positionnement des barres améliore la réponse et réduit l'effet des cycles limites. Je ne peux partager l'avis selon lequel elle introduit une mise en action supplémentaire susceptible de panne en exploitation; en fait, dans ce cas, je ne vois pas très bien ce que pourrait être le sens de « panne en exploitation ».

Mémoire P/272 (présenté par son titre seulement)

B. G. DUBOVSKY (URSS): M. Thie nous dit, dans le mémoire P/272, qu'il est possible de mesurer la sous-criticité en étudiant les fluctuations statistiques (bruit) d'un réacteur. Je voudrais savoir quel ordre de grandeur de sous-criticité peut être ainsi mesurée. S'il ne s'agit que de 2%, la recherche ne présente pas un intérêt particulier, car il existe d'autres méthodes plus simples pour faire ce travail; mais si l'on peut mesurer des sous-criticités de 6% ou davantage, la méthode deviendra extrêmement précieuse. Peut-être M. Thie ou d'autres participants pourraient-ils nous dire quels sont les avantages spécifiques des méthodes de bruit.

J. A. THIE (Etats-Unis d'Amérique): Des mesures de réactivité d'arrêt supérieure à 5% sont intéressantes malgré leur difficulté. La Compagnie Milletron aux Etats-Unis fait des recherches sur ces mesures de grandes anti-réactivités, même en présence d'importants champs gamma. Pour des anti-réactivités s'approchant de la criticité de moins de 5%, une augmentation de la précision est possible, et c'est heureusement dans ce domaine qu'une plus grande précision est souhaitable (pour des raisons de sécurité, par exemple).

Dans des mesures de réactivité d'arrêt, les méthodes de bruit présentent bien en fait certains

avantages précis sur des méthodes telles que chute de barre, comptage sous-critique, etc. L'un de ces avantages est que les méthodes de bruit ne sont pas sensibles à la géométrie des sources et des détecteurs.

M. A. SCHULTZ (Etats-Unis d'Amérique): Comme le dit M. Thie, des mesures sous-critiques de bruit fournissent un moyen simple d'obtenir une grande précision au voisinage de l'état critique et sont donc intéressantes même si les réponses obtenues à, par exemple, 10% d'anti-réactivité sont beaucoup moins précises. Des expériences telles que mesures de la valeur d'une barre ou addition de combustible peuvent se faire quand le réacteur est sous-critique sans qu'il soit besoin d'avoir recours à des mesures de période ou à des chutes de barres. Cependant, l'appareillage de base aujourd'hui sur le marché est prévu en premier lieu pour l'emploi comme dispositif de sécurité.

E. P. GYFTOPOULOS (Etats-Unis d'Amérique): A mon avis, les mesures de bruit dans des réacteurs sous-critiques présentent les mêmes avantages que les mesures de bruit dans d'autres conditions — à savoir, essentiellement, que le réacteur est « excité » par le bruit inhérent et non pas par l'expérimentateur. Assurément, cet avantage se paie un certain prix. Comme le dit M. Thie à la fin du mémoire P/272, les résultats expérimentaux peuvent être souvent difficiles à interpréter.

Протокол заседания 3.4

Кинетика реакторов

Председатель: С. Х. Ифта (Израиль)

Точечная и пространственная кинетика

ОБЩАЯ ДИСКУССИЯ

Х. СМЕТС (Бельгия): В докладе P/687* д-р Шмид выводит характеристики стабильности реактора из рассмотрения, в котором запаздывающие нейтроны не учитываются, и получает довольно точные результаты для исследованного им частного случая. Однако, по моему мнению, полученные результаты показывают, что запаздывающие нейтроны не всегда играют существенную роль в устойчивости работы реакторов. Реакторы с учетом запаздывающих нейтронов могут быть неустойчивыми, хотя устойчивость имеет место без учета запаздывающих нейтронов. Мощность, при которой реактор достигает границы устойчивости, может быть ниже в случае учета запаздывающих нейтронов. Запаздывающие нейтроны могут уменьшать затухание колебаний.

Эти факты, вообще говоря, не являются общеизвестными. За последнее время сделано много неопределенных заявлений (в том числе в некоторых докладах, представленных на эту конференцию) по поводу влияния запаздывающих нейтронов.

П. ШМИД (Швейцария): Я совершенно согласен с д-ром Сметсом. В своем докладе, представленном на Женевскую конференцию 1958 г. (см. ссылку [7] моего доклада) В. М. По-

Для своей второй модели я применил *первую теорему устойчивости* Сметса, которая была получена из соответствующей функции Ляпунова, включая запаздывающие нейтроны. В связи с этим можно сказать, что критерии, необходимые для моей второй модели асимптотической устойчивости крупных установок, определены с достаточной точностью и что влияние запаздывающих нейтронов было соответствующим образом учтено.

Дж. ЧЕРНИК (США): Я хочу добавить несколько слов к выступлениям д-ра Сметса и д-ра Шмида. Вопрос о влиянии запазды-

* Настоящее издание, этот том, стр. P /687

пов доказал, что запаздывающие нейтроны всегда ведут к асимптотической стабильности крупных установок при условии, что простая стабильность системы без учета запаздывающих нейтронов может описываться *функцией Ляпунова второго порядка*. Для систем с двумя независимыми температурными коэффициентами, которые математически эквивалентны моей первой модели, Петров получил функцию Ляпунова, существование которой может считаться доказанным. Это в достаточной степени подтверждено в моем докладе.
вающих нейтронов на устойчивость часто зависит от математической модели, которая может или не может отражать физическую картину. Это также зависит от того обстоятельства, свободная или связанная динамическая система. Я полагаю, что физические условия, определенные Шмидом, в действительности должны привести к уменьшению амплитуды колебаний во всех случаях. Однако для связанных колебаний, как я указывал несколько лет назад на конференции Американского ядерного общества в Бостоне, в простейшем случае синусоидальные колебания реактивности не ведут к уменьшению амплитуды колебаний, обусловленному запаздывающими нейтронами.

Э. П. ГИФТОПУЛОС (США): Я, вообще говоря, согласен с выступлениями Сметса и Черника. Однако доказательство того, что запаздывающие нейтроны улучшают стабильность, основано на предположении, что система уравнений, описывающих реактор без запаздывающих нейтронов, имеет обратную связь и допускает решения, которые асимптотически устойчивы для всех уровней мощности реактора. При этих условиях запаздывающие нейтроны без сомнения повышают стабильность.

Т. ГОЗАНИ (Израиль): Я хочу высказать несколько общих замечаний, которые касаются всех докладов и в особенности доклада Каплана и Тэйлора (P/271) и доклада Стассиса и Митсониаса (P/648).

За последние годы значительные усовершенствования были сделаны в использовании импульсных источников нейтронов. Это относится как к самой методике, так и к оценке получаемых результатов. Мощные и относительно дешевые нейтронные генераторы становятся более доступными. Новые оценочные методики * позволяют определять реактивность прямо в долларовых единицах без систематических гармонических ошибок и использования предположения, что время генерации мгновенных нейтронов зависит от подкритического состояния. При этом учитывается фон запаздывающих нейтронов после импульса.

Любое функциональное отношение между плотностью мгновенных и запаздывающих нейтронов, дополненное постоянной мгновенного распада существующего вида, дает реактивность и генерацию мгновенных нейтронов в долларовых единицах. При использовании этой оценочной методики отпадает необходимость иметь очень короткие импульсы или ждать, когда плотность запаздывающих нейтронов достигнет равновесия. Полагают, что эта методика может быть использована в качестве стандартного метода для прецизионных измерений реактивности там, где это возможно.

Э. П. ГИФТОПУЛОС (США): Я должен сказать, что реактивность не является основной количественной характеристикой, без которой мы не можем анализировать реактор. Когда же мы используем концепцию реактивности, мы должны спрашивать себя, для чего мы это делаем. В крупных реакторах или в реакторах с кратковременными переходными процессами это может быть бесполезным или в действительности обманчивым.

В. А. КУЗНЕЦОВ (СССР): Я хотел бы сделать замечание по докладу P/648. Авторы предлагают метод, который, по их мнению, даст возможность получить из одного эксперимента две важные независимые физические характеристики $\beta_{эфф}$ и $l_{эфф}$, которые входят в кинетическое уравнение реактора в виде их отношения. Однако два уравнения, из которых авторы определяют эти характеристики, не являются независимыми. По существу они содержат только одну характеристику, а именно отношение $\alpha = \beta_{эфф}\, l_{эфф}$, и, к сожалению, только это отношение может быть получено экспериментально с использованием предложенного авторами метода.

Т. РОЗАНИ (Израиль): Действительно невозможно определить $\beta_{эфф}$ с помощью кинетических методов. Единственным методом определения этой характеристики является сравнение реактивности ρ, измеренной в долларовых единицах каким-либо подходящим для этой цели кинетическим методом с расчетным значением, полученным для той же самой системы. Несколько лет назад Каплан и Генри в США использовали борный поглотитель для проведения таких опытов на водяной системе. Однако при использовании новой оценочной методики импульсного источника для расчета системы можно определить $\beta_{эфф}$ сравнительно просто. Предварительные экспериментальные измерения были проведены в Швейцарии на установке EDR.

А. Б. УАЙТЛИ (Соединенное Королевство): Я могу отметить в связи с докладом P/271, что Центральное энергетическое управление широко использует трехмерные кинетические программы STAB и STABLE Управления по атомной энергии Соединенного Королевства. Эти программы включают решения на основе одногрупповой диффузионной теории с 1500

* T. Gosani. Nukleonik, *4*, 348 (1962); E. Garelis and J. L. Russel, Jr. Nucl. Sci. and Eng., *16*, 263 (1963).

узлами сетки и решение связанных термодинамических уравнений применительно к реактору с графитовым замедлителем и газовым охлаждением. Однако в тех случаях, когда имеют место локальные возбуждения (например, удаление одного стержня), мы обнаружили, что эти программы не дают удовлетворительных решений. В настоящее время наши усилия направлены на разработку трехмерной программы SKIP (разрабатывается совместно Управлением по атомной энергии и Центральным энергетическим управлением), которая будет программой с временной зависимостью и с 8000 узлами сетки. Эта программа позволит определять влияние локальных поглотителей и связанных систем регулирования. Она разрабатывается главным образом на основе кода FORTRAN применительно к машине IBM-7094.

Дж. Дж. ТЭЙЛОР (США): В нашей работе по пространственно-временному анализу, на которую Вы ссылаетесь в своем докладе, основное внимание уделяется методам модального анализа, использующим методику синтеза, а не узловой анализ, на котором основаны программы Соединенного Королевства. Тем не менее мы с большим интересом следим за работами в Соединенном Королевстве и с удовлетворением отмечаем, что программы, использующие небольшое число узлов сетки, успешно предсказывают пространственно-временные кинетические характеристики реакторов с графитовым замедлителем и газовым охлаждением.

Изучение кинетики отдельных реакторов

Доклады P/859 и P/860 (представил X. Агер-Ханссен)

ДИСКУССИЯ

М. А. ШУЛЬЦ (США): Вы планируете использование приборов внутри активной зоны для контроля за безопасностью работы реакторов. Сколько времени эти приборы могут проработать в активной зоне и на основании какого опыта Вы можете предсказывать срок их службы?

X. АГЕР-ХАНССЕН (Норвегия): Мы планируем смонтировать приборы по контролю за безопасностью непосредственно к активной зоне, а не на корпусе давления. Мы полагаем также, что срок службы этой аппаратуры будет такой же, как длительность кампании топливной загрузки, то есть 1—2 года. Мы не ожидаем каких-либо трудностей при выполнении этого требования. Турбины и термопары работали в Халлене в течение более двух лет, при этом не возникало каких-либо проблем.

Б. Г. ДУБОВСКИЙ (СССР): Во время пуска реактора Белоярской атомной электростанции (реактор с высокой удельной мощностью) нами была испытана аппаратура, предназначенная для усовершенствования системы управления. Эта аппаратура включала автоматический самописец мощности, измеритель реактивности, показывающий изменение хода реактивности, и прибор, указывающий положение автоматических регулирующих стержней. Имелся также координатор времени, который через каждые 100 *сек* делал временные отметки на ленте записывающих потенциометров всех трех вышеуказанных приборов.

Использование этого оборудования позволяло быстро анализировать состояние реактора при изменении режима его работы, в том числе и аварийного режима. Это усовершенствование позволило усилить контроль за работой автоматического регулятора и действиями эксплуатационного персонала. Комплект удовлетворительно зарекомендовал себя в работе.

Дж. А. ТАЙ (США): Мой вопрос касается использования спектра шумов в реакторе HBWR в качестве средства для определения стабильности реактора. Операторы атомных энергетических установок часто предлагают эту методику для других динамических испытаний, поскольку при этом не возникают различные возмущения в реакторе и не нарушается его рабочий режим. Для правильной интерпретации результатов исследования реакторных шумов необходимо знать источник случайных флуктуаций реактивности в активной зоне. В моем докладе P/272 эта проблема обсуждается в связи с некоторыми реакторами и я пришел к выводу, что случайности наиболее часто обнаруживаются в потоке теплоносителя. Однако было показано, что флуктуация входной температуры теплоносителя является источником шумов в некоторых реакторах. Установлено ли, что эти или другие эффекты являются источниками флуктуаций реактивности в реакторе HBWR?

Т. ЮРОЛА (Финляндия): Может быть, я отвечу на этот вопрос? Исследование источников шумов составляло часть нашей работы по шумам, проведенной в Халлене. Из-за сложности системы мы не могли точно определить источник или источники шумов. Я могу только сказать, что передаточная функция реактивность — мощность, измеренная в условиях неосциллирующего реактора, оказалась не тождественной энергетическому спектру. Это показывает, что образование пузырьков не является источником шумов. Такими источниками могут быть флуктуации температуры и потока на входе в канал или турбулентность в области замедлителя. Например, оказалось, что энергетический спектр в потоке теплоносителя почти не меняется. Однако, как я уже упоминал, мы еще не уверены в правильности наших выводов.

Дж. А. ТАЙ (США): Использование устройства, предотвращающего пережог топлива в Халленском реакторе, является очень интересным, особенно если опыт покажет пригодность подобного оборудования для других реакторов. Может ли Агер-Ханссен сказать, какие проводятся внереакторные или внутриреакторные эксперименты? В частности, предпринимались ли попытки достичь условий кризиса кипения и ликвидировать их во всех случаях с помощью предохраняющего устройства? Если устройство, предотвращающее кризис кипения, может иметь практическое применение где-нибудь в другом месте, то можно ли иметь абсолютную уверенность, что это устройство установлено действительно в том месте контролируемого канала, в котором может наблюдаться кризис кипения?

Х. АГЕР-ХАНССЕН (Норвегия): Пока мы не в состоянии поднять мощность топливной сборки, приближающуюся к условиям кризиса кипения. Однако в настоящее время мы просим разрешения на повышение мощности реактора до 25 *Мвт*, то есть на 5 *Мвт* выше существующего номинального уровня. Мы надеемся, что в наших сборках типа IFA-4, рассчитанных на высокую удельную мощность, будут области, в которых могут возникнуть условия кризиса кипения, но расплавление топлива будет предотвращено указанным детектором пережога. Конструкция этого устройства основана на том, что кризис кипения, вероятно, может возникать на выходе канала, где содержание пустот самое высокое. Мы также использовали наблюдаемый радиальный эффект, который показывает, что кризис кипения будет возникать в местах, наиболее удаленных от противоположной поверхности. Использованная в нашем детекторе пережога методика тепловой фокусировки успешно обнаруживает этот эффект.

О. ВИПААВОУРИ (Финляндия): Я хотел бы добавить несколько замечаний к докладу, представленному Агер-Ханссеном. Результаты некоторых измерений, выполненных с топливной сборкой IFA-4, были получены после написания доклада о разработке внутриреакторного устройства и поэтому они могут представлять определенный интерес:

а) максимальное колебание входного потока во время измерений составляло $\pm$ 200% (по отношению к стабильному потоку). Измеренные входные скорости были равны 1,5 *м/сек* (верхнее значение) и 0,5 *м/сек* (нижнее значение);

б) общее число гидравлических колебаний достигало порядка 10^5 без повреждения тепловыделяющих элементов; доля пустот на выходе в начале гидравлических колебаний была почти всегда близка к 90%;

в) уровень мощности, достигнутый после порога нестабильности, был на 60% выше этого порога. Явление кризиса кипения не было очевидным;

г) в реакторе успешно использовалась методика шумов для определения порога нестабильности топливных сборок.

Доклад P/79 (представил Р. Абдан)

ДИСКУССИЯ

Дж. ТЭЙЛОР (США): Я хочу задать два вопроса. Во-первых, могли бы Вы объяснить, какие компенсирующие эффекты поддерживают постоянную реактивность в случае радиального расширения отдельных тепловыделяющих элементов? Во-вторых, проводили ли Вы какой-либо анализ с использованием цифровой вычислительной машины, связанной с аналоговой машиной и, если проводили, то можете ли Вы поподробнее объяснить, как эта связь осуществлялась?

Р. АБДОН (Франция): Радиальное расширение тепловыделяющих элементов очень слабо влияет на реактивность, поскольку перемещения материала в среднем взаимно компенсируются. Положительный эффект, обусловленный уплотнением топлива к центру активной зоны, компенсируется отрицательным эффектом, обусловленным расширением зазоров между элементами по направлению к периферии активной зоны.

Относительно Вашего второго вопроса я хотел бы сказать, что мы еще не соединили аналоговую и цифровую вычислительную машины, используемые на моделирующем устройстве реактора RAPSODIE. Причиной этого является в основном то обстоятельство, что эти машины находятся друг от друга на расстоянии 5 *км*. Несмотря на это, мы планируем соединить их вместе несколько позже.

Дж. ЧЕРНИК (США): Можете ли Вы объяснить использование приспособлений, обеспечивающих отрицательный конструкционный коэффициент реактивности в реакторе RAPSODIE?

Р. АБДОН (Франция): Эти устройства делают активную зону более компактной после достижения проектной температуры натрия в работающем реакторе и установления градиента в 90° С между входной и выходной температурой (в действительности, вероятно, даже до установления этого градиента). На полномасштабной тепловой модели реактора, сооруженной в Кадараше, мы нашли, что взаимодействие между сборками очень слабое, на основании чего можно предположить, что активная зона становится более компактной в результате расширения топлива.

Дж. ЧЕРНИК (США): Какие данные Вы предполагаете получить на реакторе RAPSODIE, которые можно было бы использовать для энергетических реакторов на быстрых нейтронах?

Р. АБДОН (Франция): Реактор RAPSODIE предназначен для решения трех задач. Во-первых, мы надеемся подтвердить методы расчета, использованные при разработке проекта. Во-вторых, мы хотим усовершенствовать определенные методики, которые затем могут быть распространены на другие реакторы подобного типа, в особенности это относится к петлям с натриевым охлаждением, реакторному блоку и дистанционному оборудованию для перегрузки. И наконец, реактор RAPSODIE будет использоваться для облучения тепловыделяющих элементов реакторов на быстрых нейтронах.

Доклад P/664 (представил И. Миида)

ДИСКУССИЯ

К. ВУД (Соединенное Королевство): Матричные методы расчета реактора с отражателем, обсуждаемые во втором разделе Вашего доклада, включают очень длинные машинные программы и требуют значительного машинного времени. При изучении конструкций крупных реакторов с газовым охлаждением необходимая информация может быть получена на модели гомогенного реактора без отражателя с одной энергетической группой нейтронов. Для анализа устойчивого состояния или переходного процесса может быть использован метод гармоник или метод конечных разностей. Моделирование регулирующих устройств с диапазонами нечувствительности или насыщения может быть представлено функциональным анализом. Затем можно исследовать влияние сигнала или шумов регулирующего устройства на переходные процессы.

Хотя положительная обратная связь, указанная в моем докладе, дает некоторое улучшение характеристик системы управления, обычно в конструкциях Соединенного Королевства она не используется, поскольку это вводит дополнительный сигнал на вход регулирующего устройства, который затруднит и усложнит обслуживание. Надежное регулирование может быть достигнуто во всех условиях с использованием простого запаздывающего опережения по фазе.

И. МИИДА (Япония): Я не могу в данный момент сказать, требует ли матричный метод расчета реактора с отражателем большего или меньшего машинного времени по сравнению с другими методами. Конечно, моделирование с использованием вычислительной машины является полезным для такого рода исследований. Однако исследование параметров с помощью моделирования может занять много времени и моделирование может не обнаружить влияния основных параметров на исследуемую систему. В таких случаях аппроксимация с помощью функционального анализа является очень полезной.

Теоретически обратная положительная связь регулирующего стержня улучшает характеристики и снижает влияние предельных циклов. Я не могу согласиться с утверждением, что при этом вводится дополнительный сигнал на вход регулирующего устройства, который может усложнить обслуживание. В этом случае я совершенно не понимаю, что может означать «недостаток или усложнение обслуживания».

Доклад P/272 (зачитано только название доклада)

ДИСКУССИЯ

Б. Г. ДУБОВСКИЙ (СССР): В докладе P/272 д-р Тай указал на возможность использования статистических флуктуаций (шумов) реактора для измерения степени подкритичности. Я хотел бы узнать, какая степень подкритичности может быть измерена таким методом. Если этим методом можно измерить подкритичность порядка 2%, то он не представляет практического интереса, поскольку существуют другие более простые методы. Если можно измерить подкритичность порядка 6% и более, то этот метод становится очень ценным. По-видимому, д-р Тай или кто-либо другой может рассказать о существенных преимуществах метода реакторных шумов.

Дж. А. ТАЙ (США): Измерение реактивности остановленного реактора выше 5% является интересной, хотя и трудной задачей. Фирма «Миллетрон» в США занимается измерениями таких больших отрицательных значений реактивности даже в присутствии γ-полей значительной интенсивности. Для степени подкритичности с менее чем 5% до критического состояния можно повысить точность измерений, что особенно необходимо в диапазоне, где желательна более высокая точность измерений (например, определение аварийных причин). При измерении реактивности остановленного реактора метод шумов должен иметь определенные преимущества перед такими методами, как сброс стержня, отсчет в подкритическом состоянии и другие. Преимуществом метода шумов является то, что он не чувствителен к источнику и геометрии детектора.

М. А. ШУЛЬЦ (США): Д-р Тай сказал, что измерение шумов в подкритическом состоянии является простым средством для получения высокой точности определения реактивности вблизи критичности. Поэтому этот метод интересен, даже если менее точные результаты, полученные, скажем, для 10% отрицательной реактивности, хорошо согласуются между собой. Такие эксперименты, как определение компенсирующей способности стержня или добавление топлива, могут проводиться в подкри-

тическом состоянии реактора без необходимости измерения периода или резкого перемещения стержня. Однако имеющаяся в настоящее время в продаже основная аппаратура используется главным образом в качестве аварийных приборов.

Э. П. ГИФТОПУЛОС (США): По моему мнению, измерение шумов в подкритических реакторах имеет те же преимущества, что и измерение шумов в других условиях, в особенности когда реактор «возбуждается» присущим ему шумом, а не экспериментатором. Конечно, это преимущество является ценным. Как указывает д-р Тай в конце доклада P/272, часто экспериментальные результаты очень трудно интерпретировать.

Acta de la sesión 3.4

Cinética de reactores

Presidente: S. Yiftah (Israel)

Cinética puntual y espacial

DISCUSIÓN GENERAL

H. SMETS (Bélgica): En el documento P/687, el Dr. Schmid deriva las propiedades de estabilidad de un reactor partiendo de consideraciones en las que se desprecian los neutrones retardados y obtiene resultados exactos en el caso particular que estudia. Sin embargo, yo creo que debería hacerse notar que los neutrones retardados no siempre mejoran la estabilidad de los reactores. Los reactores pueden ser inestables con neutrones retardados, aun cuando sean estables si se desprecian los neutrones retardados. La potencia a la que el reactor alcanza su límite de estabilidad puede ser menor cuando se tienen en cuenta los neutrones retardados, y dichos neutrones pueden hacer disminuir el amortiguamiento de las oscilaciones.

Estos hechos no son conocidos generalmente, y se han dado, tanto anteriormente como en algunos de los trabajos presentados en esta Conferencia, muchas informaciones dudosas sobre el efecto de los neutrones retardados.

P. SCHMID (Suiza): Estoy completamente de acuerdo con el Dr. Smets. V. M. Popov demuestra en su documento de la Conferencia de 1958 (Ref. [7] de mi documento) que los neutrones retardados conducen siempre a la estabilidad asintótica si se hace la hipótesis de que se puede demostrar la simple estabilidad del sistema sin neutrones retardados, *estableciendo una función de Lyapunov de segundo orden.* Popov derivaba tal función de Lyapunov para sistemas con dos coeficientes de temperatura independientes, que son matemáticamente equivalentes a mi primer modelo, de modo que pueda darse por supuesta la existencia de dicha función. Esto bastaría para justificar las notas de mi artículo.

Para mi segundo modelo, he aplicado el « teorema de primera estabilidad » de Smets, que fue obtenido a partir de una función de Lyapunov adecuada, incluyendo neutrones retardados. Así pues, creo que se puede decir que se han derivado rigurosamente los criterios que necesita mi segundo modelo para ser asintóticamente estable y que se ha considerado de forma adecuada el efecto de los neutrones retardados.

J. CHERNICK (Estados Unidos de América): Quisiera añadir unas palabras a los comentarios de los doctores Smets y Schmid. La cuestión de si los neutrones retardados añaden o no estabilidad depende del modelo matemático que puede representar o no la situación física. También depende de si el sistema dinámico es libre o forzado. Yo creo que las condiciones físicas exigidas por el Dr. Schmid conducirían en efecto a la amortiguación en todos los casos. Sin embargo, allí donde hay una oscilación forzada, como ya apunté hace unos años en una reunión de la American Nuclear Society en Boston, el simple caso de una oscilación sinusoidal de reactividad conduce a la antiamortiguación sobre la parte de los neutrones retardados.

E. P. GYFTOPOULOS (Estados Unidos de América): En general, estoy de acuerdo con lo dicho por Smets y Chernick. Sin embargo, la demostración de que los neutrones retardados mejoran la estabilidad se basa en la suposición de que el sistema de ecuaciones que describe el reactor sin neutrones retardados es realimentado y admite soluciones que son asintóticamente estables a cualquier nivel de energía. En estas condiciones no hay duda de que los neutrones retardados mejoran la estabilidad.

T. GOZANI (Israel): Quiero hacer un comentario que concierne a todos los artículos sobre cinética puntual y espacial, pero posiblemente en particular, al documento de Kaplan y Taylor (P/271) y al de Stassis y Mitsonias (P/648).

En los últimos años, se han hecho grandes progresos en el uso de fuentes pulsadas de neutrones, tanto en las técnicas mismas como en la evaluación de resultados. Se dispone ahora de generadores de neutrones potentes y relativamente baratos. Los nuevos procedimientos de cálculo* permiten determinar la reactividad directamente en unidades de dólares, prácticamente sin errores sistemáticos de armónicos y sin recurrir a la suposición de que el tiempo de generación de los neutrones instantáneos es independiente del estado subcrítico. Esto se hace no despreciando el fondo de neutrones retardados que siguen a los impulsos.

Cualquier relación funcional entre las poblaciones de neutrones instantáneos y retardados, junto con la constante de desintegración de los instantáneos del modo persistente, proporciona la reactividad y la generación instantánea en unidades de dólares. Con este procedimiento de cálculo, no es necesario tener impulsos muy cortos o esperar hasta que la población de neutrones retardados haya alcanzado el equilibrio. Se propone que este método debería usarse como método típico para medidas precisas de reactividad, siempre que fuera posible.

E. P. GYFTOPOULOS (Estados Unidos de América): Creo que debería decirse que la reactividad no es una magnitud básica sin la cual no se puede analizar un reactor. Cada vez que usamos el concepto de reactividad, no deberíamos dejar de preguntarnos por qué lo estamos haciendo. En los reactores grandes, o en los reactores que sufren transitorios muy rápidos, estos puede ser inútil y hasta erróneo.

V. A. KUZNETSOV (URSS): Me gustaría comentar el documento P/648. Los autores sugieren un método que, en su opinión, permitiría obtener independientemente, con un solo experimento, dos características físicas importantes (β_{ef} y ℓ_{ef}) que intervienen en forma de cociente en todas las ecuaciones cinéticas. Sin embargo, las dos ecuaciones, de las cuales derivan los autores estas características, son evidentemente no independientes. Estas ecuaciones contienen, esencialmente, sólo una característica que es $\alpha = \beta_{ef}/\ell_{ef}$ y ésta es, desgraciadamente, la única relación que se puede determinar por el método propuesto.

T. GOZANI (Israel): Es, en efecto, imposible determinar β_{ef} por métodos cinéticos. La única manera de determinarla es comparar la reactividad ρ medida en unidades de dólares, usando para ello el método cinético que se quiera, con un valor calculado para el mismo sistema. Hace varios años, Kaplan y Henry en los Estados Unidos usaron envenenamiento por boro para realizar tal medida en un sistema de agua ligera. Sin embargo, aplicando los nuevos procedimientos de cálculo para fuentes pulsadas a sistemas calculables, se puede determinar β_{ef} con relativa facilidad. Se han realizado medidas preliminares Würenlingen (EIR) en Suiza.

A. B. WHITELEY (Reino Unido): Quiero mencionar, en relación con el documento P/271, que el Central Electricity Generating Board ha utilizado ampliamente los programas cinéticos de tres dimensiones STAB y STABLE de la Atomic Energy Authority del Reino Unido. Estos proporcionan una solución en la teoría de difusión de un grupo, con unos 1 500 puntos reticulares, y también la solución de las ecuaciones termodinámicas asociadas, correspondientes a un reactor con moderador de grafito y refrigerado por gas. Sin embargo, en los casos en que surgen perturbaciones locales, por ejemplo, extrayendo una sola barra, hemos encontrado que estos programas no son suficientemente finos. Debido a esto, nuestros esfuerzos se concentran ahora en hacer una extensión del programa tridimensional SKIP (empresa conjunta del CEGE y la UKAEA) que será un programa dependiente del tiempo con unos 8 000 puntos reticulares, dando una representación muy flexible de los absorbentes locales y sistemas de control asociados. Este programa se está escribiendo principalmente en FORTRAN para la IBM 7094.

J. J. TAYLOR (Estados Unidos de América): En nuestro trabajo acerca del análisis espacio–tiempo, descrito en el documento a que Vd. se refiere, hemos insistido principalmente en los métodos de análisis nodal usando técnicas de síntesis, más que en el análisis nodal empleado en los programas del Reino Unido. Con todo, seguimos con gran interés el trabajo británico, y estamos satisfechos de ver con qué éxito estos programas, usando un número relativamente pequeño de puntos reticulares, predicen las características cinéticas espacio–tiempo de los reactores moderados con grafito y refrigerados por gas.

Estudios sobre la cinética de algunos reactores

Documentos P/859 y P/860 (presentados a la vez por H. Ager-Hanssen)

DISCUSIÓN

M. A. SCHULTZ (Estados Unidos de América): Veo que tienen Vds. el proyecto de usar instrumentación en el núcleo como equipo de seguridad. ¿Cuánto tiempo esperan que duren estos dispositivos y en qué experiencia pueden basarse para predecir su tiempo de vida?

H. AGER-HANSSEN (Noruega): Tenemos la intención de instalar la instrumentación de seguridad con

* Gozani, T., Nukleonik, *4*, 348 (1962); y Garelis, E., y Russel, J. L., Jr., Nucl. Sci. and Eng., *16*, 263 (1963).

el núcleo, más bien que con la vasija de presión. Creemos que los instrumentos tendrán un tiempo de vida similar al de la carga de combustible, que es entre uno y dos años. No debería haber ninguna dificultad en conseguir esto; en Halden se ha operado con turbinas y pares termoeléctricos que han funcionado durante más de dos años sin dar lugar a ningún problema.

B. O. DUBOVSKY (URSS): Durante la puesta a punto del reactor de Beloyarsk (un reactor de alta potencia específica) hemos probado cierto equipo diseñado para mejorar el sistema de control. La instrumentación comprende un registrador automático de nivel de potencia, un medidor de reactividad que indica los cambios en la curva de reactividad y un medidor que indica la posición de las barras de control pertenecientes a los mecanismos de control automático; hay también un oscilador de coordenación que hace una indicación periódica (cada 100 s) sobre los mapas del potenciómetro registrador para los tres instrumentos citados.

Este equipo ha hecho posible un análisis rápido del estado del reactor durante los cambios en el régimen de operación, incluidas las emergencias. Nos ha permitido mejorar nuestro control sobre la operación precisa del mecanismo de control automático y sobre las acciones del personal operador. En resumen, el equipo ha demostrado su eficacia.

J. A. THIE (Estados Unidos de América): Mi pregunta se refiere al uso de los espectros de ruido en el HBWR como medio de detectar la inestabilidad. Los operadores de plantas de potencia prefieren a menudo esta técnica a otras pruebas dinámicas, porque no perturba el reactor ni altera su programa de operación. Para una interpretación correcta de los resultados de la prueba de ruido, es conveniente conocer el origen de las fluctuaciones de reactividad al azar en el núcleo. Mi documento P/272 discute este problema en conexión con varios reactores y llego a la conclusión de que el carácter aleatorio en el flujo del refrigerante es la causa encontrada con más frecuencia. Sin embargo, se ha demostrado que las fluctuaciones en la temperatura de entrada del refrigerante son también la causa del ruido en algunos reactores. ¿Se ha establecido si uno de estos dos efectos u otros es la causa del ruido de reactividad en el HBWR?

T. EUROLA (Finlandia): ¿Puedo contestar a esta cuestión? Parte de nuestro trabajo sobre el ruido en Halden, ha sido precisamente un estudio de sus causas. Hasta ahora y debido a la complejidad del sistema, hemos sido incapaces de localizar la fuente o fuentes de ruido. Sólo puedo decir que la función de transferencia de reactividad a potencia, medida en condiciones de reactor no oscilante, no parece coincidir con el espectro de potencia del reactor nuclear. Esto parece indicar que el origen del ruido no es la formación de burbujas, pero sí podría ser las fluctuaciones de temperaturas y flujo en el canal de entrada o turbulencias en la región del moderador. Por ejemplo, el espectro de potencia del flujo del refrigerante parece ser próximo al blanco. Sin embargo, como dije antes, no nos atrevemos aún a ser categóricos en nuestras conclusiones.

J. A. THIE (Estados Unidos de América): El uso de un protector de combustión en el reactor de Halden es muy interesante, especialmente si la experiencia permite el uso de instrumentos semejantes en otros reactores. ¿Podría el Sr. Ager-Hanssen decirnos qué experiencias existen dentro o fuera de la pila? En particular, ¿se han hecho intentos deliberados para inducir la combustión? y la protección ¿defiende en todos los casos contra la combustión producida por una escapada? Si los protectores de combustión van a tener aplicación práctica en otra parte ¿puede uno estar completamente seguro de que están instalados en el lugar correcto para mandar el canal que se va a quemar?

H. AGER-HANSSEN (Noruega): Hasta ahora no hemos podido llevar el conjunto combustible a un nivel de potencia próximo a las condiciones de combustión. Sin embargo, hemos pedido permiso para operar el reactor a 25 MW, esto es 5 MW más que el nivel nominal presente, y esperamos entonces poder llevar nuestro conjunto de alta potencia específica (IFA4) a un punto en que pueda ocurrir la combustión pero tal que el detector de quemado evitará la fusión del elemento combustible. El diseño de este instrumento se basa en la observación de que es más probable que la combustión ocurra a la salida de un canal donde la fraccion de huecos es más alta. También hacemos uso de un efecto radial observado que indica que la combustión ocurrirá en el punto más alejado de una superficie opuesta; la técnica de focalización del calor usada en nuestro detector de combustión es favorecida por este efecto.

O. VAPAAVUORI (Finlandia): Querría añadir algunas observaciones a los documentos presentados por el Sr. Ager-Hanssen. Los resultados de ciertas medidas hechas con el conjunto combustible IFA4 se han obtenido después de escrito el artículo sobre el desarrollo de instrumentos en el núcleo y pueden ser de interés general:

a) Las máximas oscilaciones pico a pico en el flujo de entrada durante las medidas fueron del orden de $\pm 200\%$ (relativas al valor de estado estacionario). Las velocidades de entrada medidas fueron de 1,5 m/s hacia arriba y 0,5 m/s hacia abajo;

b) El número total de oscilaciones hidráulicas fue del orden de 10^5, sin fallo de ningún elemento combustible. La fracción de huecos de salida (α_{ex}) fue siempre muy próxima a 90% en el arranque de las oscilaciones hidráulicas;

c) El máximo nivel de potencia alcanzado por encima del umbral de inestabilidad fue aproximada-

mente 60% más alto que este umbral. No se tuvo prueba de fenómenos de quemado, y

d) Se ha utilizado con éxito en el reactor una técnica de ruido para determinar el umbral de inestabilidad de los conjuntos combustibles.

Documento P/79 (presentado por R. Abdon)

DISCUSIÓN

J. J. TAYLOR (Estados Unidos de América): Tengo que hacer dos preguntas. Primero: ¿podría Vd. describir los efectos de compensación específica que mantienen estacionaria la reactividad cuando ocurre la dilatación radial de un elemento combustible individual?

Segundo: ¿ha hecho Vd. algún análisis usando el calculador digital «enlazado» con el calculador analógico y, si es así, podría Vd. detallar cómo se efectúa el «enlace»?

R. ABDON (Francia): La dilatación radial de los elementos combustibles tiene un efecto despreciable en la reactividad puesto que los movimientos de material son en valor medio autocompensados. Un efecto positivo debido al acercamiento del combustible al centro del núcleo, se compensa con un efecto negativo debido a la expansión del material hacia el exterior.

Como respuesta a su segunda pregunta, no hemos acoplado todavía las calculadoras analógicas y digital usadas con el simulador de RAPSODIE, debido sobre todo a la dificultad práctica de tenerlos juntos; por el momento están a 5 km. de distancia. Sin embargo, estamos planeando acoplarlos en lo sucesivo.

J. CHERNICK (Estados Unidos de América): ¿Querría Vd. explicar el uso de plaquetas para obtener un coeficiente de estructura negativo en RAPSODIE?

R. ABDON (Francia): Las plaquetas hacen más compacto el núcleo tan pronto como la temperatura del sodio alcanza su valor requerido para la operación del reactor y se establece el gradiente de temperatura de 90 °C entre la entrada y la salida (en realidad, probablemente aún antes de establecerse el gradiente). Sobre el modelo térmico a escala natural del reactor, construido en Cadarache, encontramos que el juego entre los conjuntos era muy ligero y pudimos por lo tanto predecir que el núcleo se haría compacto como resultado de la dilatación.

J. CHERNICK (Estados Unidos de América): ¿Qué información aplicable a la tecnología de reactores rápidos de potencia espera Vd. obtener de RAPSODIE?

R. ABDON (Francia): RAPSODIE tiene un triple objeto. En primer lugar, esperamos comprobar los métodos de cálculo usados para el proyecto. En segundo lugar, queremos perfeccionar ciertas tecnologías para que sean aplicables a otros reactores de este tipo, particularmente a las que tengan relación con circuitos refrigeradores de sodio, el bloque del reactor y el equipo de manejo a distancia. Y por fin se utilizará RAPSODIE para irradiar elementos combustibles de reactores rápidos.

Documento P/664 (presentado por J. Miida)

DISCUSIÓN

K. WOOD (Reino Unido): Los métodos de matrices para un reactor reflejado, discutidos en su documento, implican muchos programas de cálculo, y el uso de mucho tiempo de calculadora. En general, en estudios de diseño de reactores grandes refrigerados por gas, se puede obtener información adecuada a partir de un modelo de reactor homogéneo no reflejado, con un solo grupo de energía de los neutrones; se pueden usar los métodos de solución por armónicos o de diferencias finitas para el análisis de la estabilidad y de los transitorios.

Se puede preferir la simulación de controladores con bandas muertas o saturación, a describir el análisis de la función. Es posible así investigar directamente los efectos de señal o de ruido del controlador sobre el comportamiento de los transitorios.

Aunque la posición de realimentación propuesta en el documento mejora algo la respuesta del sistema de control, se suele evitar en los diseños del Reino Unido, porque introduce una entrada de control adicional que podría fallar en servicio. Se puede conseguir un control satisfactorio en todas las condiciones con un simple avance de fase mal retrasada.

J. MIIDA (Japón): No puedo decir sin pensarlo si el método de matrices para un reactor reflejado requiere o no más tiempo que otros métodos. Desde luego la simulación por un calculador es útil en este tipo de estudio. Sin embargo los estudios de parámetros por simulación pueden llevar mucho tiempo y la simulación no puede darnos el efecto de parámetros particulares sobre el sistema estudiado. En tales casos es muy útil la aproximación que describa el análisis de la función.

Teóricamente la realimentación de posiciones de barras mejora la respuesta y disminuye el efecto de los ciclos límites. No puedo estar de acuerdo en que se introduce una entrada adicional que podría fallar en servicio; en realidad, en este caso no veo bien lo que puede querer decir fallo en servicio.

Documento P/272 (se enunció solamente el título)

DISCUSIÓN

B. G. DUBOVSKY (URSS): El Dr. Thie nos dice, en el documento P/272, que se puede medir la subcriticidad investigando las fluctuaciones estadísticas (ruido) de un reactor. Me gustaría saber qué cantidad de subcriticidad se puede medir de este

modo. Si sólo es una cuestión del 2%, el método no es muy atractivo porque hay otros métodos más simples de realizar este trabajo; pero si se pueden medir subcriticidades del 6% o mayores, el método sería extremadamente útil. Quizá el Dr. Thie o algún otro, puedan decirnos cuáles son las ventajas específicas de los métodos de ruido.

J. A. THIE (Estados Unidos de América): Las medidas de reactividades de detención mayores del 5% son interesantes aunque difíciles. La Compañía Milletron en los Estados Unidos se ha comprometido a investigar sobre medidas de estas grandes reactividades negativas, aún en presencia de grandes intensidades gamma. Para reactividades subcríticas más próximas al 5% de la criticidad, es posible aumentar la precisión y afortunadamente es la región donde se requiere mayor precisión (por razones de seguridad por ejemplo). En las medidas de reactividades de parada, los métodos de ruido presentan ciertas ventajas definidas sobre métodos tales como el sacar barras, recuento subcrítico, etc. Una de estas ventajas es que los métodos de ruido no son sensibles a la geometría de la fuente y del detector.

M. A. SCHULTZ (Estados Unidos de América): Como dice el Dr. Thie, las medidas de ruido subcrítico proporcionan una manera simple de obtener alta precisión cerca de la criticidad y son, por lo tanto, interesantes aun cuando las respuestas obtenidas, digamos 10% de reactividad negativa, sean considerablemente menos precisas. Se pueden realizar experimentos tales como importancia de barras o adición de combustible, cuando el reactor es subcrítico, sin necesidad de recurrir a medidas del período o caída de barras. Sin embargo, los aparatos básicos existentes hoy en el comercio están destinados principalmente a dispositivos de seguridad.

E. P. GYFTOPOULOS (Estados Unidos de América): En mi opinión, las medidas de ruido en reactores subcríticos tienen las mismas ventajas que las medidas de ruido en otras condiciones, concretamente, cuando el reactor es « excitado » por el ruido inherente y no por el experimentador. Naturalmente esta ventaja está sometida a un precio. Como el Dr. Thie dice al final de su documento P/272, los resultados experimentales son, a menudo, difíciles de interpretar.

Session 3.5

REACTOR CONTROL AND SHIELDING

LIST OF PAPERS

			Page
	Instrumentation		
P/80	Quelques aspects particuliers du contrôle dans les piles atomiques de puissance *Some particular aspects of control in nuclear power reactors*	J. Furet, J. Pupponi	213
P/500	Recent developments in control and safety systems for nuclear reactors at the Institute of Nuclear Research in Poland	J. Podgórski, P. Szulc	220
P/631	Outlook for reactor control systems with moving detectors	P. Kovanic, K. Wagner	227
P/633	Optimum digital information treatment and nuclear engineering instrumentation	P. Kovanic	235
P/647	Automatic control of the average core flux by measuring N^{16} coolant activity at the FRM Munich Research Reactor	M. Sommer	243
P/815	Measurement of high-dose gamma fluxes at reactor pulses and strong gamma sources by the conductivity of cuprous oxide	O. Bobleter, P. Vajda	248
	Control systems		
P/179	Control, stability and protection of a gas-cooled graphite-moderated reactor	J. Brown *et al.*	255
P/180	Design of control rod systems for gas-cooled reactors	P. B. Branson *et al.*	267
P/274	Poison control of thermal reactors	A. Radkowsky, R. J. Creagan	277
P/354	Выбор некоторых оптимальных характеристик компенсирующих элементов ядерных реакторов *Choice of some optimum characteristics of control elements for nuclear reactors*	В. В. Орлов и др. *V. V. Orlov* et al.	287
P/375	Экспериментальное изучение способов компенсации избыточной реактивности промежуточных реакторов *Experimental study of some methods of compensating excess reactivity in intermediate reactors*	В. А. Кузнецов и др. *V. A. Kuznetsov* et al.	297

			Page
P/376	Компенсация больших изменений реактивности деформацией решетки активной зоны	Г. А. Бать и др.	306
	Compensation of large changes in the reactivity by deformation of the core lattice	*G. A. Bat* et al.	
P/795	Solid state nuclear safety system	L. Conti, M. Conti	314
	Automatic control		
P/273	Application of digital computer techniques to reactor operation	M. A. Schultz, F. C. Legler	321
P/677	Un nouveau système de contrôle des réacteurs nucléaires	I. Iftode *et al.*	331
	A new control system for nuclear reactors		
	Progress in theoretical and experimental shield-design methods		
P/175	Bradwell Nuclear Power Station: comparison of shielding performance with design calculations	F. P. Youell *et al.*	339
P/260	Recent advances in reactor shielding in the United States	E. P. Blizard, P. S. Mittelman	348
P/364	Некоторые новые аспекты применения сопряженных функций и теории возмущений в расчетах реакторов и защиты	А. А. Абагян и др.	359
	Some new aspects of using adjoint functions and perturbation theory in reactor and shielding calculations	*A. A. Abagyan* et al.	
P/377	Новые результаты физического исследования защиты	О. И. Лейпунский и др.	372
	New results of shielding research	*O. I. Leipunsky* et al.	
P/657	Use of response matrix method for multi-layer shield design	I. Kataoka	386
P/684	A new shield design method and some attenuation studies in laminated biological shields	E. Aalto *et al.*	395
P/721	Описание ослабления нейтронного излучения ядерного реактора многослойной биологической защитой с помощью многогрупповой модели в диффузионном приближении	В. А. Наумов	405
	Description of neutron radiation attenuation in-pile by multi-layer biological shielding on a multi-group model in diffusion approximation	*V. A. Naumov*	

Quelques aspects particuliers du contrôle dans les piles atomiques de puissance

par J. Furet* et J. Pupponi**

La mesure et le contrôle du flux neutronique dans les piles de puissance posent encore de nombreux problèmes. Ces problèmes semblent plus difficiles à résoudre dans le cas des piles à haut flux.

Les études actuellement entreprises dans le domaine des piles atomiques à haut flux doivent apporter une contribution importante à la solution de ces problèmes, qui intéressent bien entendu les spécialistes du contrôle des piles de puissance.

L'état de ces études entreprises en France est analysé et les résultats relatifs aux différents travaux effectués dans les laboratoires du Commissariat à l'énergie atomique sont donnés.

LES DÉTECTEURS DE NEUTRONS ET L'INSTRUMENTATION NUCLÉAIRE

Les exigences nouvelles imposées par le développement des piles atomiques de puissance sont essentiellement: une température de fonctionnement élevée et des flux neutroniques et gamma importants, une plus grande précision dans la mesure des flux de neutrons dans les champs de rayonnement mixte (neutron et gamma).

Développement de détecteurs et câbles susceptibles de fonctionner à haute température et sous rayonnement γ élevé [1, 2, 3]

Il est exigé dans certains cas que les détecteurs de neutrons fonctionnent à des températures de l'ordre de 400 à 500 °C. Cela présente des difficultés qui sont essentiellement d'ordre technologique et qui concernent surtout les matériaux isolants. Il faut en effet disposer d'isolant qui conserve à des températures d'environ 600 °C: une bonne résistivité électrique, une parfaite étanchéité, une bonne résistance mécanique, la possibilité de scellement étanche au vide avec les métaux. L'alumine frittée répond actuellement le mieux à ces exigences. Il faut utiliser une alumine de grande pureté à texture fine.

Si l'on ne peut pas recourir à une discrimination extérieure du type électronique, il est nécessaire d'utiliser dans la construction des détecteurs des matériaux ayant une faible section efficace d'activation. Mais le bruit le plus important est dû aux gammas de pile. La tendance actuelle est de développer des chambres à fissions à réponse rapide pour pouvoir atteindre une discrimination gamma possible même avec des rayonnements de 10^6 R/h.

Plusieurs types de chambres à fission en acier inoxydable, à isolement d'alumine frittée, permettent un fonctionnement à 400 °C; les caractéristiques de ces appareils sont regroupées dans le tableau 1.

Tableau 1. Caractéristiques des chambres à fission haute température

Chambres à fission	Type CFU 3	Type CFU 6	Type CFU 7
Caractéristiques technologiques			
Matériaux de structure	acier inox-alumine frittée	acier inox-alumine frittée	acier inox-alumine frittée
Température maximum d'utilisation °C	400	400	400
Charge développée (10^{-13} cb)	1	1	0,5
Temps de collection (10^{-9} s)	200	200	40
Sensibilité aux neutrons (c/s par n/cm² s)	0,15	0,15	0,02
Tenue aux rayonnements neutrons (n/cm²)	10^{19}	10^{19}	10^{19}
Rayonnement γ (Roentgens)	10^{10}	10^{10}	10^{10}

Applications des techniques d'électronique rapide à la mesure des flux neutroniques sous rayonnement γ élevé [4, 5]

La mesure des flux de neutrons faibles en présence de rayonnement γ intense est possible si on élimine les impulsions « γ » en séparant dans l'électronique associée à la chambre les impulsions d'amplitude faible et les impulsions « neutrons » d'amplitude importante et cela grâce au discriminateur d'amplitude. Cette discrimination ne peut se faire bien entendu que si les deux types d'impulsions apparaissent individuellement et séparément avant l'étage discriminateur. On admet actuellement que la probabilité d'empilement des impulsions élémentaires γ croit non seulement avec l'intensité de rayonnement mais avec le temps de collection du détecteur et le temps de résolution de l'électronique. Aussi la

* Commissariat à l'énergie atomique.
** Electricité de France.

mesure de flux neutronique faible sous rayonnement γ est d'autant plus aisée que le temps de collection du détecteur et le temps de résolution de l'électronique sont faibles. L'expérimentation a montré pour un détecteur du type chambre à fissions de temps de collection 100 ns, que si la mesure de flux de neutrons faibles en présence de rayonnement γ de 10^5 R/h est possible avec une électronique de temps de résolution de 1 μs, elle est encore possible avec une électronique de temps de résolution de 40 ns. Par ailleurs, la diminution du temps de résolution de l'électronique permet d'augmenter le taux de comptage maximal, donc la dynamique de mesure. Elle permet de ne pas élargir les impulsions brèves fournies par le détecteur. Les charges électriques de ces impulsions ne sont alors intéressées pendant leur propagation que par une faible partie de la capacité du câble entre détecteur et électronique, ce qui permet de lever une restriction parfois désagréable sur la longueur de câble entre détecteur et électronique. Il est nécessaire bien entendu d'adapter l'impédance d'entrée de l'amplificateur à l'impédance caractéristique du câble pour éviter les réflexions. Des ensembles d'électroniques rapides pour détecteurs de neutrons fonctionnant en impulsions, de temps de résolution de 40 ns, ont été développés par le département d'électronique générale. Certains sont installés sur la pile CABRI pour permettre l'enregistrement de la puissance en régime dynamique.

L'ORGANISATION DES CHAÎNES DE MESURES NEUTRONIQUES DANS L'ENSEMBLE DU CONTRÔLE DES PILES ATOMIQUES

Les perturbations apportées aux mesures neutroniques et les moyens de les corriger [6, 7]

Dans les piles à haut flux fonctionnant en régime de puissance, les mesures de flux neutronique en certains points du réacteur ne sont pas proportionnelles à la puissance neutronique ou thermique. En effet, des variations lentes apparaissent en cours de fonctionnement dans la valeur du rapport entre le flux neutronique sur le détecteur et le flux moyen dans le cœur (effet de position des barres de contrôle par exemple). Ces variations lentes peuvent être corrigées au moyen d'un paramètre variable lié à des grandeurs susceptibles d'être facilement mesurables, à savoir par exemple: la dose de rayonnement γ en un point judicieusement choisi, la puissance thermique dégagée dans le cœur du réacteur, l'activité en ^{16}N du fluide de réfrigération.

Méthode du déplacement automatique des détecteurs pendant les opérations de démarrage [8-13]

L'utilisation d'un détecteur en mouvement pour commander l'évolution de la pile depuis le niveau sous-critique jusqu'au niveau de puissance nominale a déjà été l'objet de travaux et de publications, en particulier celles de Kovanits et Kulka, Anderson et Winterberg. L'avantage essentiel de cette utilisation est de pouvoir contrôler l'évolution de puissance des piles atomiques sur un grand nombre de décades avec le nombre minimal de détecteurs.

Les différents systèmes proposés sont tous fondés sur la remarque suivante: l'indication (N) donnée par un détecteur est une fonction de la puissance (P) de la pile et de sa position (x) par rapport au cœur de la forme:

$$N = P \cdot f(x)$$

Si l'on connaît à chaque instant l'indication N, la position x et la loi d'atténuation $f(x)$ du flux neutronique en fonction de l'éloignement, on en déduit le niveau de puissance de la pile.

Les principes de base de fonctionnement des différents systèmes peuvent se classer en deux groupes:

Premier groupe. Le détecteur est asservi de façon à rester dans un flux neutronique constant. Le démarrage de la pile est fait en commandant l'extraction des barres de contrôle, le détecteur s'éloignant dès que le flux neutronique augmente.

Deuxième groupe. Le détecteur est éloigné suivant un certain programme, choisi de telle sorte que si l'on maintient un flux neutronique constant sur le détecteur par une action automatique sur les barres de contrôle, la pile évolue alors suivant une loi déterminée (par exemple: période constante). Ce système permet de faire un démarrage automatique.

Il est toujours nécessaire, bien entendu, de trouver au voisinage du cœur de la pile une zone dans laquelle on puisse déplacer facilement le détecteur, de façon à l'approcher au moment du démarrage et à l'éloigner pendant la montée en puissance. Les piles dont le cœur est entouré d'eau, piles-piscines par exemple, présentent ces caractéristiques; de plus, le programme de retrait nécessaire pour une automatisation du démarrage est extrêmement simple, puisque l'atténuation du flux neutronique en fonction de la distance est exponentielle, soit $f(x) = e^{-kx}$, dans ces conditions il suffit d'éloigner le détecteur à vitesse constante $V = 1/KT$ et de maintenir le flux neutronique constant sur le détecteur pour obtenir une divergence à période constante égale à T.

Un système de démarrage de ce type est installé sur la pile TRITON depuis 1962, un système analogue est en projet sur la pile MÉLUSINE.

Pour la pile OSIRIS, pile à eau légère du type piscine dont la construction est commencée à Saclay, le contrôle de l'évolution du flux neutronique depuis l'état sous-critique jusqu'à un niveau légèrement inférieur au niveau d'opération normale, est fait par trois ensembles électroniques associés chacun à une chambre à fission mobile. Les différents automatismes de commande de déplacement de la chambre à fission et de commande des barres sont mis en service, lorsque le taux de comptage N prend un

certain nombre de valeurs particulières indiquées dans le tableau 2.

Tableau 2. Actions automatiques sur les barres de contrôle et la chambre à fission à partir des taux de comptage

Taux de comptage	Action sur les barres de contrôle	Action sur la chambre à fission
$< N_1 \approx 10$ c/s	Chute des barres (2/3)	
$< N_2 \approx 10^3$ c/s		Rapprochement
$> N_0 \approx 5.10^3$ c/s	(Voir note [a] ci-dessous)	Eloignement
$> N_3$ arrêt des barres	Arrêt des barres (1/3)	
$> N_4 \approx 2.10^4$ c/s	Chute des barres (2/3)	

[a] Lorsque le taux de comptage est supérieur à N_0, puisque la chambre à fission s'éloigne à vitesse constante, le démarrage peut alors être commandé automatiquement en asservissant la barre de contrôle au maintien du niveau constant sur le détecteur.

Les équipements à détecteurs mobiles coexistent encore avec des ensembles de mesure et de sécurité associés à des détecteurs en position fixe. Il est possible néanmoins d'envisager dans un avenir proche, lorsqu'on aura acquis une plus grande expérience dans le fonctionnement de ces systèmes et une plus grande confiance dans la sûreté des ensembles électroniques à impulsions, une utilisation plus systématique de ces équipements.

LE DÉMARRAGE RAPIDE DES PILES ATOMIQUES

L'intérêt du démarrage rapide des piles atomiques est presque essentiellement économique. Il permet sur les piles expérimentales à haut flux un gain de temps très appréciable.

Les difficultés de redémarrage liées à la dynamique des empoisonnements xénon et samarium [14, 15]

Les évolutions des empoisonnements xénon et samarium ont une influence très importante sur le bilan de réactivité après arrêt dans le cas des piles à neutrons thermiques à haut flux. Les résultats de calculs faits en supposant dans le cœur une répartition uniforme du flux neutronique sont indiqués sur la figure 1.

Etant donné les réactivités disponibles, il semble que les redémarrages après arrêt rapide ne soient possibles qu'avec des vitesses de libération de réactivité élevées. On peut même constater que pour des flux supérieurs à 6.10^{14} n/cm^2 s, le redémarrage après arrêt semble impossible.

Les difficultés de corrélation entre vitesse de démarrage et bilan de réactivité [16, 17, 18]

La logique du point de vue sécurité impose dans le cas du démarrage rapide les deux critères suivants: *a*) vitesse de libération de réactivité grande si réactivité < 0; *b*) vitesse de libération de réactivité faible si réactivité > 0.

Plusieurs méthodes ont été étudiées pour la mesure de la réactivité, la pile se trouvant généralement à l'état sous-critique. Mais il apparaît que pour l'instant aucune de ces méthodes ne semble conduire à un appareillage susceptible d'assurer une sécurité automatique pendant la période de démarrage rapide. Aussi, des méthodes nouvelles de démarrage sont envisagées [19, 20].

Les méthodes de démarrage rapide liées à la mesure du taux de fission en fonction du temps

Lorsque l'efficacité différentielle et l'efficacité totale en réactivité des barres de contrôle sont mal connues, on peut envisager le démarrage en libérant à grande vitesse la réactivité par paliers. Du point de vue sécurité, la libération de réactivité entre chaque palier doit être inférieure à β (fraction des neutrons retardés). Cette programmation de libération de réactivité est interrompue lorsque le rapport de deux taux de comptage pendant le palier dépasse une certaine valeur (voir figure 2). Cette méthode de démarrage analysée au moyen d'un simulateur de pile a donné les résultats suivants: pour des réactivités $\leqslant -2\,500$ pcm, la relation puissance réactivité peut se mettre sous la forme $N_1 \rho_1 = N_2 \rho_2$, $N_1 \rho_1$: puissance et réactivité initiales, $N_2 \rho_2$ puissance et réactivité après la libération de $\rho_2 - \rho_1$ à grande vitesse. La durée des paliers pour effectuer la mesure du rapport des puissances neutroniques n'est fonction que de la durée nécessaire aux comptages pour obtenir une certaine précision. Pour des réactivités $> -2\,500$ pcm, le rapport puissance finale du palier/puissance initiale du palier varie assez peu pour des durées de palier comprises entre 10 s et 100 s et des variations de réactivité inférieures à β. La procédure de démarrage rapide automatique peut être alors la suivante: variation de réactivité pour chaque saut de l'ordre de $\beta/2$, palier à réactivité constante d'une durée de 10 s; arrêt de la procédure lorsque le rapport puissance finale du palier/puissance initiale du palier est $\geqslant 1{,}2$. La fréquence des arrêts de barre conduit à des vitesses

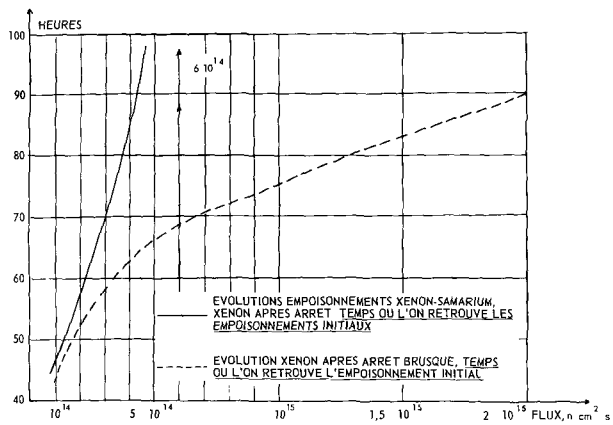


Figure 1. Evolution des empoisonnements xénon et samarium, résultats des calculs en supposant dans le cœur une répartition uniforme du flux neutronique

moyennes de libération de réactivité comprises entre 20 et 40 pcm/s.

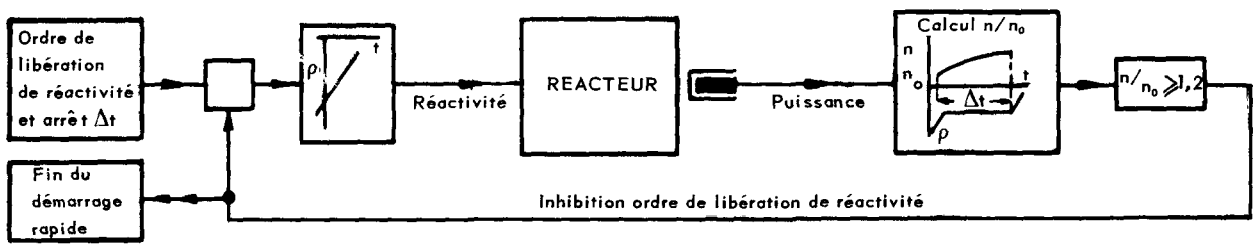
Une procédure un peu différente semble permettre d'aller encore plus vite dans la phase libération de réactivité, la pile étant sous-critique. Cette procédure est la suivante: à partir de l'état initial sous-critique réactivité ρ_0, puissance N_0, on retire du cœur de la pile les barres de contrôle à vitesse a élevée et ceci jusqu'à ce que le niveau de puissance passe de N_0 à $2\ N_0 = N_{10}$. La réactivité n'évoluant plus alors, on attend un temps Δ au bout duquel le niveau N_{10} est devenu $N_{1\Delta}$. Si $N_{1\Delta}$ est plus petit que pN_0 (p facteur de proportionnalité à fixer), on recommence alors à libérer de la réactivité à vitesse a et on arrête cette libération de réactivité lorsque la puissance N est devenue $N_{20} = 2N_{1\Delta}$; il y a attente pendant Δ et comparaison de $N_{2\Delta}$ par rapport à $N_{1\Delta}$. D'une manière générale, on continue à libérer de la réactivité tant que $N_{i\Delta}/N_{(i-1)\Delta}$ est $< p$. La libération de réactivité est stoppée lorsque $N_{i\Delta}/N_{(i-1)\Delta} = p$, c'est-à-dire qu'à ce moment, la pile atomique se trouve dans un état voisin de la criticité. L'analyse de cette procédure automatique de démarrage sur simulateur de pile pour des vitesses de libération de réactivité comprises entre 50 pcm/s et 200 pcm/s et pour des temps de vie moyens des neutrons de 10^{-5} s et 10^{-3} s a montré que la valeur optimale à donner à p est 2, 3.

Dans le cas d'une vitesse $a = 100$ pcm/s les résultats de cette analyse sont indiqués dans le tableau 3.

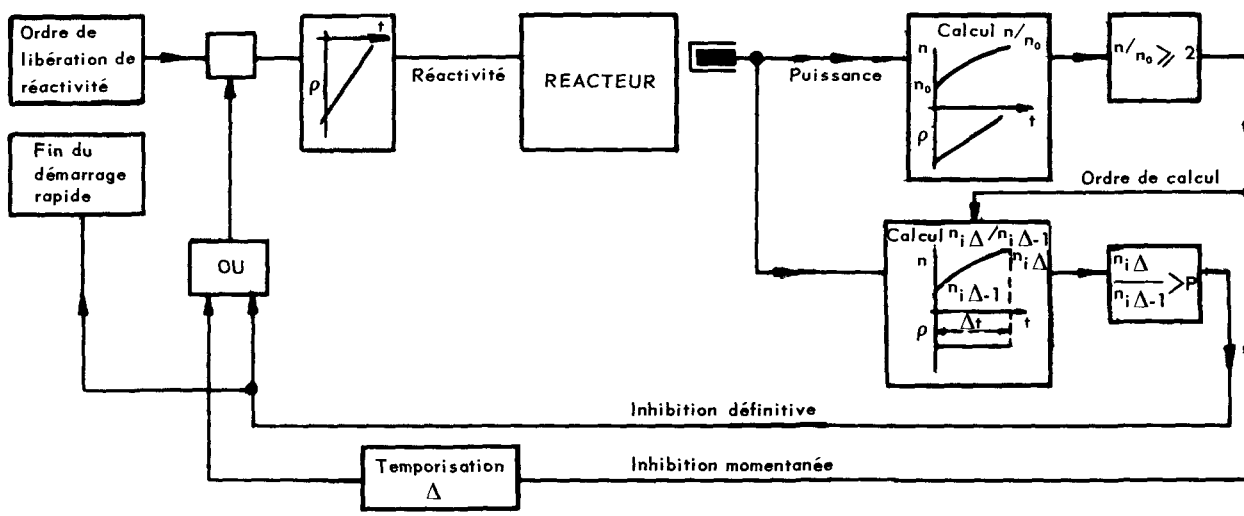
Tableau 3. Résultats de l'analyse de la procédure de démarrage rapide dans le cas d'une libération de réactivité de 100 pcm/s

Réactivité initiale (pcm)	Finale (pcm)	Durée (s)
500	21	4,79
800	185	6,19
1 000	295	7,05
2 000	216	27,8
3 000	495	35
4 000	180	58
5 000	330	67
6 000	470	80
7 000	100	99
8 000	177	108
10 000	320	125
12 000	466	145
13 000	530	154
14 000	91	180
16 000	116	198

Ces procédures de démarrage rapide nécessitent des mesures proportionnelles au niveau de puissance précises. Il est indispensable de disposer de niveaux de source importants. L'automatisation de ces dispositifs ne pose pas de problèmes particuliers. Leur expérimentation a commencé sur la pile CABRI à



DEMARRAGE RAPIDE 1e PROCEDURE



DEMARRAGE RAPIDE 2e PROCEDURE

Figure 2. Procédures de démarrage rapide

Cadarache au début du mois d'août. Le choix de ce réacteur pour l'expérimentation est lié à la possibilité de disposer en toute sécurité des vitesses de libération de réactivité élevées.

MESURE DE LA PUISSANCE NEUTRONIQUE À EDF3

Dans cette centrale il est nécessaire de suivre l'évolution de la puissance sur plus de huit décades. Cet impératif a été réalisé à l'aide de quatre types de chaînes de mesures distinctes composées chacune de trois voies.

Description et caractéristiques des chaînes de mesure de la puissance neutronique

Nous décrivons plus particulièrement, dans ce qui suit, les chaînes bas flux qui sont placées dans le cœur du réacteur et pour lesquelles des solutions originales et délicates ont été adoptées.

Chaînes bas flux. Ces chaînes sont réparties dans trois puits de barres de contrôle sur la périphérie du réacteur de manière à fournir un signal de pilotage à partir de 10 W et jusqu'à 10^5 W.

Les caractéristiques de fonctionnement, à la puissance nominale et à l'emplacement des chambres, sont les suivantes: *a*) atmosphère CO_2, pression 27 bars, température 400 °C; *b*) flux en neutrons thermiques 10^{12} n/cm²s, flux gamma 10^6 R/h.

Ces caractéristiques ont entraîné l'étude et la réalisation: *a*) d'une chambre de faible sensibilité nécessitée par le flux important; *b*) d'un câble de liaison entre la chambre et le préamplificateur d'une âme en nickel, d'un isolant en perles d'alumine et d'une tresse d'inconel:

Diamètre de courbure	19 cm
Résistance d'isolement à la température ambiante	$10^{13}\ \Omega$/m
Résistance d'isolement à 400 °C	$10^{10}\ \Omega$/m
Capacité au mètre	40 pF
Gaine isolante externe en laine de verre d'un préamplificateur spécial capable de résister à une pression de 27 bars de CO_2	

Un logement pour le recevoir a été prévu à l'intérieur du treuil automatique, dont le rôle est de remonter la chambre à partir d'un certain niveau de puissance. La liaison au préamplificateur est réalisée par prise tournante. Le moteur de commande du treuil doit être lubrifié à sec. L'ensemble bouchon, treuil, préamplificateur, câble et chambre peut être absorbé par l'appareil de chargement-déchargement situé sur la dalle supérieure du réacteur.

Démarrage automatique

Le démarrage est entièrement automatique et réalisé grâce aux dispositifs suivants:

a) Les chaînes de puissance neutronique; outre leur rôle de contrôle et de sécurité, elles élaborent les signaux de puissance et réactivité;

b) Un programmeur numérique de montée en puissance; il permet de suivre une loi tenant compte des conditions initiales qui suivent un arrêt plus ou moins long;

c) Un calculateur numérique servant par ailleurs au traitement des informations; il assure la mise en marche des différents auxiliaires de la centrale depuis l'arrêt jusqu'à la marche nominale.

RÉFÉRENCES

1. Duchêne, J., *Détecteurs de neutrons,* Bulletin d'informations scientifiques et techniques, *61,* 6-15 (1962).
2. Duchêne, J., *High temperature fission chambers,* International symposium on aerospace nuclear propulsion, Las-Vegas, Nevada, USA, 9, 23. 27 (1961).
3. Duchêne, J., *Développements récents des détecteurs pour le contrôle des réacteurs,* Conférence INSTN 4 (1964).
4. Bourdel, J., et Buisson, J., *Nouvel ensemble d'impulsions pour chambres à fission,* Etude CEN, Saclay, DE, 1714/SAER/1058.
5. Recyclage INSTN 64, *Evolution de l'instrumentation de contrôle des piles atomiques,* INSTN, 4 (1964).
6. Cabellos, E., Felix, M., et Jover, P., *Etude analogique d'un problème de régulation de réacteur par la puissance thermique,* Etude CEN, Saclay, DE, 1731/SAER/1069 (1963).
7. Bory, M., Pansart, F., et Weil, P., *Démarrages et changements de régime du réacteur RAPSODIE,* Etude CEN, Saclay, DE, 1678/SAER/1029 (1961).
8. Kovanits, P., et Kulka, M., *Automatic reactor control systems,* Journal of Nuclear Energy, part B, reactor technology, vol. 1 (1959).
9. Anderson, J. L., et Winterberg, R. E., *Servo fission chamber,* ORNL 2787 (Instruments).
10. Jover, P., et Roselli, G., *Contrôle automatique d'un réacteur nucléaire au moyen d'un détecteur mobile,* Etude CEN, Saclay, DE, 1598/SAER/992 (1962).
11. Ailloud, J., Chandanson, P., Berthoin, J., et Letour, C., *Appareillage de démarrage sous programme de TRITON à partir de l'état sous-critique,* note 227/62, DEP/SEPP (1962).
12. Kovanits *et al., Nouveau système automatique de contrôle et de sécurité du réacteur VVR-S,* Atomnaya energia, tome 13, n° 4 (1962).
13. Jover, P., *Avant-projet contrôle OSIRIS,* Etude CEN, Saclay, DE, 1711/SAER/1055 (1963).
14. Furet, J., *Influence de l'empoisonnement xénon dans les piles à haut flux sur la vitesse des barres de contrôle,* Rapport CEA 2080 (1962).
15. Furet, J., *Cinétique de l'empoisonnement samarium dans les piles à très haut flux,* Rapport CEA 2389 (1963).
16. Valat, J., et Stern, T., *Analyse de la précision de certaines méthodes de mesures des très basses réactivités,* Etude CEN, Saclay, DE, 1540/SAER/983 (1961).
17. Stern, T., Valat, J., Blaquière, A., et Cazemajou, J., *Mesures de très basses réactivités à partir de la réponse impulsionnelle d'un réacteur déterminée par intercorrélation,* Rapport CEA à paraître.
18. Beliard, L., Cazemajou, J., et Froelicher, B., *Compte rendu de manipulations par la méthode d'intercorrélation ULYSSE,* Etude CEN, Saclay, DE, 1757/SAER/1089 (1963).
19. Weill, J., et Furet, J., *Procédé nouveau de démarrage rapide des réacteurs nucléaires,* c.r. Académie des Sciences de Paris, t. 258, p. 887-889 (1964).
20. Furet, J., *La sécurité période pendant le démarrage des piles atomiques,* Rapport CEA 2411.

ABSTRACT - RÉSUMÉ - АННОТАЦИЯ - RESUMEN

A/80 France

Some particular aspects of control in nuclear power reactors

By J. Furet and J. Pupponi

There are still many problems in the field of measurement and control of neutron flux. The present studies in connexion with high flux reactors contribute to the solution of these problems which concern specialists in reactor control.

The present state of this investigation and the results of different studies carried out in France by the CEA and the EDF are as follows:

(*a*) In the nuclear instrumentation field, work is at present devoted to the technologies used to develop detectors and cables that have to work at high temperatures and in a high γ background; fast electronic techniques are applied to fission counters to measure low neutron fluxes in a high γ background (10^6 r/h).

(*b*) In the control and safety field, there is a real need for studies on the behaviour of reactors in the subcritical state. This increases the margin of security during restarts when poison effects must be overcome.

The perturbations due to control rod movements necessitate a new organisation of power level safety and control assemblies, in connection with thermal or activation measurements.

Two methods of fast start-up are described. They are related to the fission rate measurement as a function of time. This is done either continuously by a constant and high reactivity change, or step by step.

The application of automatic techniques to detector motion seems to give the answer to control and safety in normal start-up.

(*c*) The scope of these studies covers the methods used for the control of EDF3, which are described.

A/80 Франция

Некоторые специфические проблемы контроля энергетических реакторов

Ж. Фюре, Ж. Пуппони

Проблемы измерения и контроля нейтронного потока в энергетических реакторах еще полностью не решены. Исследования, проводимые в настоящее время в области реакторов с высокой плотностью нейтронного потока, должны внести значительную ясность в решение этих проблем, представляющих интерес для специалистов по управлению энергетическими реакторами. Дан анализ современного состояния этих исследований и приведены результаты различных работ, выполненных во Франции в различных лабораториях Комиссариата по атомной энергии и фирмы «Электрисите де Франс».

a) В области контрольно-измерительных приборов эти исследования направлены в настоящее время на методы разработки детекторов и измерительных кабелей, пригодных для работы в условиях высоких температур и интенсивного γ-облучения, и на технику быстродействующей электроники, применяемую в счетчиках деления, с помощью которых измеряют нейтронный поток под сильным γ-излучением (10^6 *р/ч*).

b) В области контроля и безопасности трудности повторного пуска реактора, связанные с отравлением продуктами деления, требуют глубокого изучения поведения реактора в подкритическом режиме.

Нарушения нейтронных измерений, вызываемые движением регулирующих стержней, потребовали нового устройства цепей измерения и нейтронной безопасности, вынудив изменить уровень мощности регулирующих параметров, таких как тепловая мощность, температура, активация N^{16}.

Описаны два новых метода, относящиеся к быстрым пускам реакторов и связанные в основном с измерениями плотностей делений в функции времени в случае непрерывного освобождения при постоянной скорости и повышенной реактивности или в случае освобождения реактивности по горизонтальной кривой. Кроме того, применение метода автоматического перемещения детекторов при обычных пусках, по-видимому, дает разумное решение проблемы контроля и безопасности.

c) В рамках изложенных методов описаны устройства, предназначенные для измерения и контроля мощности реактора электростанции EDF-3.

A/80 Francia

Algunos aspectos particulares del control de los reactores nucleares de potencia

por J. Furet y J. Pupponi

La medida y el control del flujo neutrónico en los reactores de potencia plantea todavía muchos problemas. Los estudios emprendidos actualmente en el campo de los reactores de flujo alto, aportarán, sin duda, una contribución importante a la solución de estos problemas que interesan a los especialistas del control de los reactores de potencia.

Se analiza el estado actual de estos estudios y se dan los resultados de los diferentes trabajos efectuados en Francia por los diversos laboratorios del

Commissariat à l'énergie atomique y de Electricité de France.

a) En el campo de la instrumentación, estos estudios versan actualmente sobre las tecnologías utilizadas para el desarrollo de detectores y de cables capaces de funcionar a altas temperaturas y bajo una radiación γ elevada — y sobre las técnicas de electrónica rápida aplicadas a las cámaras de fisión que permiten hacer medidas del flujo de neutrones bajo radiación γ elevada (10^6 r/h).

b) En el campo general del control y de la seguridad, las dificultades de la puesta en marcha después de una parada del reactor, debidas al envenenamiento por los productos de fisión, obligan a efectuar un profundo estudio sobre el comportamiento del reactor en régimen subcrítico.

Las perturbaciones provocadas, en las medidas neutrónicas, por el movimiento de las barras de control hacen precisa una nueva organización de los sistemas de medida y de seguridad neutrónica, en la que se haga intervenir, a cada nivel de potencia, unos parámetros correctores como: potencia térmica, temperatura, actividad del nitrógeno-16.

Por lo que respecta a los arranques rápidos, se describen dos nuevos métodos relacionados esencialmente con la medida del número de fisiones en función del tiempo, bien sea en el caso de un aumento continuo de reactividad de forma constante y rápida o cuando se trate de un aumento por escalones. Por otra parte, la aplicación de las técnicas de desplazamiento automático de los detectores, en el caso de arranques normales, parece aportar una solución racional para el control y la seguridad.

c) Dentro de las técnicas mencionadas anteriormente, se describen también los dispositivos adoptados para la medida y el control de la potencia del reactor EDF3.

Recent developments in control and safety systems for nuclear reactors at the Institute of Nuclear Research in Poland

By J. Podgórski and P. Szulc *

The Polish reactor construction program has necessitated the creation at the Institute for Nuclear Research of specialized groups for elaborating and developing basic reactor-control instrumentation and for designing and examining reactor control systems by means of analogue computers.

The first task of these groups was the design and construction of a complete control system for the zero power reactor, ANNA, and the low power reactor, MARYLA. Development work on the instrumentation began in 1960; both reactors came into operation in 1963. A short account of the control units for both the above mentioned reactors is given below in the next two sections of this paper. There follows a section devoted to detectors used for reactor control and another on some newly developed control systems for research reactors.

In connection with the plan to construct a high flux reactor and, in the future, power reactors requiring several tens or hundreds of control points of parameters (such as temperature, flow-rate, pressure etc.), a fast point-by-point scanning and measurement system using standardised equipment has been developed. The main features of this system are described.

CONTROL SYSTEM OF THE ZERO POWER REACTOR ANNA [1, 2]

A block diagram of the ANNA Reactor control system is shown in Fig. 1. It has been constructed as a highly reliable system with the basic control channel composed of 3 lines, and other channels each of 2 independent lines. The instrumentation is therefore considerably in excess of that justified by the operational requirements of a zero-power reactor. This concept, however, is providing some useful experience for designing control systems for large research reactors.

The principal tasks of individual control lines are as follows.

Channel A (pulse start-up control) [3] covers the power range of 5 decades and assures the signalisation of the presence of the neutron source and the "warning" and "scram" period values. (Rate-meter range 10^1 to 10^5 pulse/s; period-meter range -30 to $+3$; trips: one for minimum pulse-rate, (control for the presence of the source) and two for warning and shut-down period controls adjusted in the 15 to 7 s and 7 to 3 s range). The detectors used are either BF_3 counters or 1RW-502 fission chambers. Each line output can in addition be switched over to the linear rate-meter and parallel scaler with a loudspeaker for start-up auditory control.

Channel C is used for logarithmic dc period measurement and signalisation [4]. Neutron ionisation chambers of the RAKJ-5 type ** are used as detectors. The current range of each line is 10^{-12} to 10^{-7} A, period meter and trip blocks are the same as in Channel A except for the neutron source presence trip. The normal functioning of each block is controlled and signalled, and the control system can function with only one C line in working order.

Channel E assures an additional signal of the maximum power level. Special gamma-sensitive G-M counters in the current region (range 10^{-12} to 10^{-7}) are used as detectors, having relatively high output currents ($\sim 10^{-5}$ A). A very simple trip amplifier is used as an alarm device adjusted to 115-150 per cent of the required power level.

Channel B (linear, dc) [5] is the basic channel for measurement, regulation and safety purposes. It works on the "2 out of 3" principle. RAKJ-5 type ionisation chambers are used as in Channel C. Each line consists of:

(*a*) A linear dc amplifier (input current range of over two decades, 5×10^{-11} to 8×10^{-9} A, output voltage respectively 1 125 to 180 V with 1 per cent accuracy, zero 8 h stability less than 10 mV);

(*b*) Power-level-exceeding triggers in two blocks: ZMN (warning 110 per cent and scram 120 per cent of the required power) and ZMM (scram step-II, 150 per cent of maximum permissible power level); and

(*c*) Specially developed comparison circuits, SRP, which control output voltages between each

* Institute of Nuclear Research, Świerk.

** The various types of equipment listed in this paper are produced in Poland. Tables 1 and 2 give their characteristics.

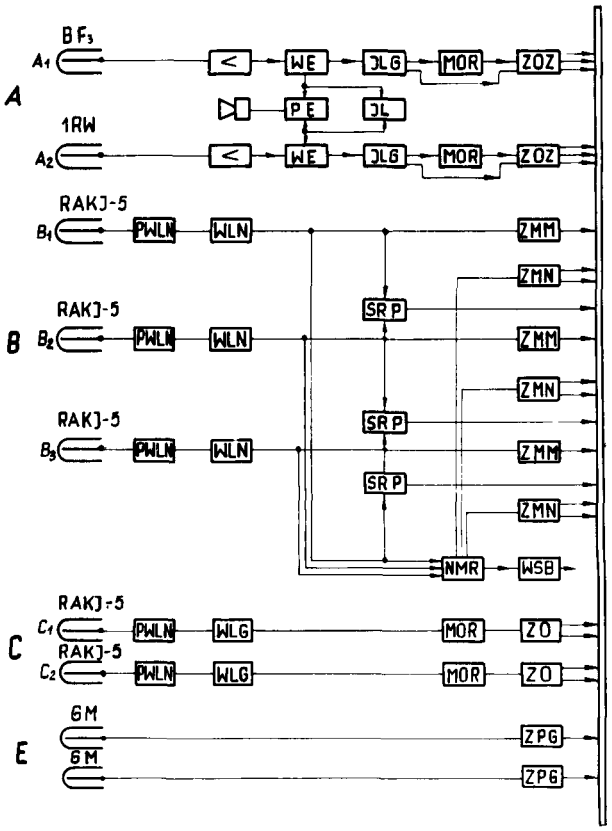


Figure 1. Control system of the zero power reactor ANNA (block diagram)

"<": pulse amplifier; WE: discriminator; JLG: logarithmic counting-rate/meter; MOR: period meter; ZOZ: trip block; PWLN, WLN: linear pre-amplifier and amplifier; SRP: comparison circuit; NMR: required power set; ZMM: max. power trip; ZMN: required-power exceeding trips; PWL, WLG: log dc pre-amplifier and amplifier; ZO: period trips; ZPG: gamma level trip; WSB: error signal amplifier

of the two-lines and signal the line with an output differing from others by more than the preselected percentage, 4, 10, 20 or 40%, of the respective output voltage. Since it was assumed that the reactor power might often be changed within the two-decade range, the comparison circuits were developed as having constant relative sensitivity in comparison with the output voltage level (varying from 1 to 180 V).

Figure 2 illustrates the operating principle of the SRP circuit: both voltages U_1 and U_2 are suitably divided in proportion to the required percentage sensitivity in block N_c and are compared by means of the vibrator P_t. If U_1 and U_2 are not equal, the input of the amplifier W receives a square waveform voltage of an amplitude proportional to the difference between U_1 and U_2; the amplifier voltage passes to a diode discriminator Ogr, polarised with U_{sr} (proportional to the mean value of both U_1 and U_2). When the preset percentage difference between U_1 and U_2 is exceeded, the discriminator passes an impulse, and owing to the complete positive feed-

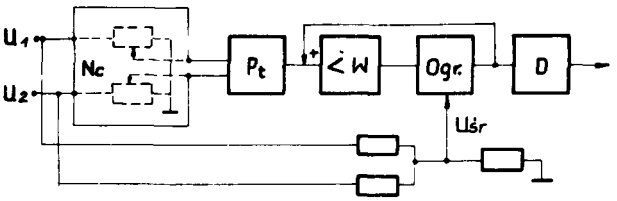


Figure 2. Comparison circuit SRP (block diagram)

U_1, U_2: compared output voltages of two lines; N_c: sensitivity set; P_t: chopper; W: amplifier; Ogr: diode discriminator; D: pulse integrator and trigger

back, a series of impulses of the vibrator frequency is generated. These pulses are fed to the input of a simple diode-pump integrator and trigger (trip) D giving an output signal. The simple integrating circuit causes an insignificant 0.2 s delay in the response time, but ensures insensitivity to random disturbances.

The SRP circuits check the efficient functioning of the B Channel lines. Both SRP, ZMN and ZMM trip circuits operate on the "fail-safe" principle, and the whole channel can be considered as ensuring the high reliability of the reactor. On the other hand, as the neutron flux distribution in the reactor core may often be changed, as a function of fuel and absorber loading, Channel B detectors are equipped with a simple servo-drive so that the position of the chambers can easily be chosen and the currents of the different lines equalized.

The automatic regulator channel [6] may be switched over to each of the 3 B lines. It consists of a block NMR (required power set) and a magnetic error signal amplifier supplying a two-phase reversive ac servo-motor of the automatic control rod drive.

The ANNA Reactor is equipped with 4 safety rods, 2 or 3 shim-rods, and 1 automatic control rod. The step-I scram signal (e.g., 120 per cent of required power) causes the safety rods to drop: the step-II scram signal (e.g., 150 per cent of maximum power) in addition causes a deduction from the critical mass of two special fuel elements which drop from electro-magnets, by which they are normally suspended.

The ANNA Reactor operates at present at power levels up to about 100 W. Since the source level of the shut-down reactor is only about 1 mW, the above-described control system is capable of ensuring complete control of period and power level changes over the full power range.

CONTROL SYSTEM OF THE LOW POWER SWIMMING-POOL REACTOR MARYLA [7]

Instrumentation for the MARYLA Reactor control system has been developed with a large margin of safety. The measuring ranges of individual channels overlap to a considerable extent. The instrumentation is ample, and it was made so in view of the fact that: (*a*) the reactor safety commission

postulated rigorous precautions because of the location of MARYLA within the hall of the 2 mW EWA Reactor; (*b*) all the instrumentation consisted of prototypes designed in the Institute.

The block diagram of the MARYLA Reactor control system is shown in Fig. 3. It consists of:

A logarithmic current channel similar to Channel C in ANNA, with an extended current range up to 7 decades, 10^{-12} to 10^{-5} A. It covers the whole power range from about 1 mW source level to above 1 kW maximum power.

The linear current channel [8] is basic for control and regulation, and consists of 3 lines. KHK-53 (USSR-made) compensated neutron ionization chambers are used as detectors. The detector current passes on to the electrometer linear amplifier with five, decade-per-decade switched ranges, 10^{-10} to 10^{-5} A; the output voltage corresponding to each decade varies from 3 to 30 V, with a 20 mV daily zero drift. The amplifier is followed by a trigger block with 3 trips: (*a*) required power, (*b*) warning, 110 per cent of required power, and (*c*) alarm (scram), 120 per cent of required power. Triggers were designed on the "fail-safe" principle. The efficient working of the measuring lines is checked by means of trigger-based comparison circuits of pre-selected voltage sensitivity, in the range of 1 to 20 V of deviation between outputs of the two compared lines. The detectors are fed from a $\pm$ 500 V supply with a stability factor better than 10^{-3}. The presence of high voltage is also checked automatically.

Alarm signals (by 3 efficient lines) are given only as the result coincidence of at least 2 lines. In order to obtain better operational reliability, the comparison blocks are doubled and operate on the "4 out of 6" principle.

Step-II Safety channel [9]. G-M counters in the current region (DOB-60 type) are used as gamma detectors. The current output (4 to 60 μA) is proportional to the logarithm of the gamma dose in the range of 0.4 40 r/h. The channel consists of 3 measuring lines. Each line consists of a trip amplifier with the trips corresponding to 30, 40 and 50 μA input current and comparing circuits signalling the deviation of output currents between each two lines with adjustable sensitivities corresponding to 10 15 μA input current deviation.

The instrumentation of the step-II safety channel is based completely on solid-state electronics (transducers and semiconductor devices), and is supplied from a dc 48 V power source. By changing the location of detectors, the sensitivity of trips may be changed over to the order of 20 W, but essentially the task of the step-II channel is to ensure the signalisation of power exceeding the highest permissible level, i.e., 1.5 kW 15 kW. The power level trips operate on the "2 out of 3" system, and the doubled comparison circuits operate on the "4 out of 6" system. An excess of the step-II safety level

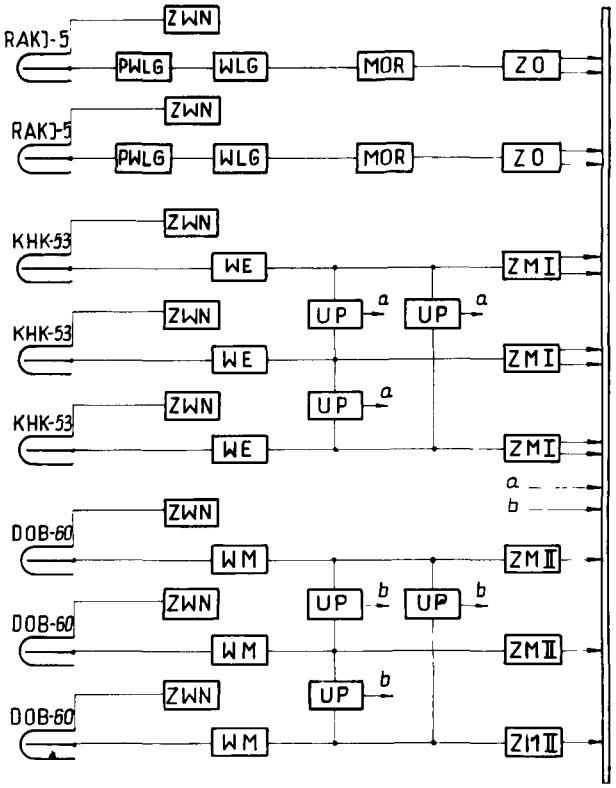


Figure 3. Control system of the low-power reactor MARYLA (block diagram)

RAKJ-5 KHK-53: compensated ionization chamber; DOB-60: G-M counter in current region; ZWN: high voltage power supply; PWLG: log dc pre-amplifier; WLG: log dc amplifier; MOR: period meter; ZO: period trips; WE: electrometer linear amplifier; ZMI: trip amplifier; UP: trigger-based electronic and magnetic comparison circuits; WM: magnetic amplifier; ZMII: magnetic trip amplifier

brings about shut-down which results not only from dropping the safety rods but also from deducting one fuel element from the critical mass.

The control rods have a specially constructed tube-type drive mechanism [10] of a maximum outer diameter of 82 mm. It consists of a dc motor, a selsyn position transmitter, two planetary gear boxes, an electro-magnet, and an air-brake (dashpot), etc. The outer 82 mm diameter permits easy positioning of control rods in many places. In this manner high flexibility of the configuration of the MARYLA Reactor core is achieved.

DETECTORS FOR REACTOR CONTROL

As the result of a few years work on the design of various reactor detectors, preceding that described above, Polish-made detectors were used for checking reactor control channels of the EWA Reactor and were used in MARYLA and ANNA.

At present, many types of detectors are used and after several years of work they have proved very reliable. Some of them are described below.

BF_3 proportional counters of various types for start-up pulse channels are produced on an industrial

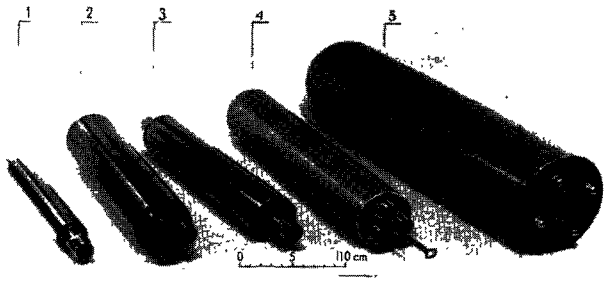


Figure 4. Polish reactor detectors

1: 9 RW-100; 2: RAKJ-5; 3: 1 RW-502; 4: RAKJ-5; 5: KPDG-1/10

scale. The design and production technique was developed at the Institute of Nuclear Research [11].

Fission chambers (Fig. 4) for start-up pulse channels are now made in two types: RW-502 type chamber of 500 cm^2 coated surface and RW-100 type chamber of 100 cm^2 coated surface. To obtain a greater range of chamber sensitivity, the electrodes are coated with uranium of various enrichments. The technical parameters of the chambers are shown in Table 1 [12].

Stainless steel electrodes supported on ceramic insulators are situated in a stainless steel housing. Connections to the internal electrodes are made via ceramic-to-metal seals.

Compensated ionization chambers of three different types (Fig. 4) are made: RAKJ-5 argon-filled made of aluminum with ceramic insulators, and RAKJ-6 and RWKJ-6 types consisting of aluminum electrodes which are placed in a stainless steel housing with ceramic insulators and ceramic-to-metal seals. RAKJ-6 is filled with argon, and RWKJ-6 with hydrogen. The parameters of these chambers are presented in Table 2 [12, 13].

Precise adjustment of gamma current compensation in these chambers is achieved by appropriately changing the operating voltage of the compensatory electrode.

Apart from the detectors described above, various special detectors for reactor measurements and reactor physics experiments have been developed.

Table 1. Fission chambers

Type	Fissile coating	Sensitivity per unit flux (cps)	Overall diameter (mm)	Length (mm)	Capacity (pF)
9RW-502	90% U^{235}	0.35	47	350	100
1RW-502	10% U^{235}	4×10^{-2}	47	350	100
RW-502	Natural uranium	3×10^{-3}	47	350	100
9RW-100	90% U^{235}	7×10^{-2}	31	270	45
1RW-100	10% U^{235}	8×10^{-3}	31	270	45
RW-100	Natural uranium	6×10^{-4}	31	270	45

Table 2. Compensated ionization chambers

Type		RAKJ-5	RAKJ-6	RWKJ-6
Max. length ...	mm	365	345	345
Overall diameter	mm	59	58	58
Neutron sensitivity	A/nv	2.10^{-14}	2.10^{-14}	8.10^{-15}
Gamma sensitivity (non-compensated)	A/r h	1.10^{-11}	1.10^{-11}	2.10^{-12}
Max. current . .	μA	100	100	200
Operating voltage max.	V	1000	1000	1000
Coating material .		Natural boron	Natural boron	Natural boron

NEWLY DEVELOPED CONTROL SYSTEMS FOR RESEARCH REACTORS

Experience gained during the design, construction and commissioning of the ANNA and MARYLA control systems have proved very useful in the design of new large reactors. In the high-flux research reactor (20-30 MW) which is now in the design stage it was decided to have a modified control and safety system based partly on the "Maxtrel" [14] principle.

Such a control system consists of three dc linear, and three dc logarithmic lines. The output signals of both linear and logarithmic lines are added electrically and compared with the pre-set required value. The error signal passes to the input of the signalling triggers and to the automatic control rod drive amplifier (which maintains either the required constant rate of change of the power level during the start-up, or the required constant power level in the steady-state condition).

Instruments now being developed or tested for that control system are completely transistorized. In the above-mentioned system, there are no comparison circuits between the outputs of 3 independent measuring lines. In each line, not the absolute value of the measured parameter, but the deviation from the required level is signalled. Each line consists of 3 triggers: two (warning and scram) signalling the increase and one the decrease below the required level. Signals coming only from a single line are considered as evidence of inefficient working of that line. Signals coming in coincidence from 2 or 3 lines either give warning or initiate the scram. The authors consider that this principle simplifies considerably the control of the efficient functioning of the lines, and fulfils the requirements for maximum structural reliability of the reactor safety control system.

MULTIPLE-POINT SCANNING, MEASUREMENT AND SIGNALIZATION SYSTEM FOR REACTOR OPERATIONAL PARAMETERS

Many types of power and research reactors need several hundreds or thousands of measurement points

of temperature, pressure, flow-rate etc. Reliability and simplicity of the measuring and signalling systems is required both as regards safety and economics. The most simple system may for example be composed of:

(*a*) A number of detectors (or other sensing instruments giving electrical output signals proportional to the measured parameter value);

(*b*) A scanning (or commutation) system, able to perform fast point-by-point switching of many detectors to one input of the measuring and signalling system;

(*c*) A measuring and signalling system, including an analogue or digital display of measured values and positions of points as well as programming devices for adjusting the signalled levels, and suitable outputs for external signalization and for recording devices.

In order to obtain such a simple system that will work with thermocouples (or other detectors giving the dc signals between tens of microvolts and hundreds of millivolts) a transistor scanning device was developed. A basic module of that device has 16 inputs and 1 output, and works with a switching time of 1 ms. Many individual modules may be connected; in this way a system for scanning several hundreds of detectors per second can be formed. A model that has been tested has an analogue output and shows the temperature-distribution image on the screen of a kinescope tube. Further development of the system, i.e., digital output for recording and for joint operation with a digital computer, is envisaged. Other fast scanning systems for other types of flow, temperature, pressure etc. and detectors (e.g., giving an ac output of a frequency proportional to the measured value) are also at the development stage.

ACKNOWLEDGEMENTS

The authors would like to express their gratitude to all collaborators at the Institute of Nuclear Research, who have contributed to the work described in this paper and particularly to those enumerated in the enclosed bibliography, whose papers were very instrumental in the preparation of this survey.

REFERENCES

1. Dabek, W., Domosławski, Z., Janikowski, A., and Szczechla, B., *Control and safety system for critical experiment on the water-graphite critical assembly of the 2nd Polish Reactor,* Institute of Nuclear Research, Swierk, Report 104/IX (March 1963) (in English).
2. Filipczak, N., *Control and safety system of the zero power reactor ANNA,* Institute of Nuclear Research, Swierk, Report 413/XII (March 1963) (in Russian).
3. Krzycki, A., *Pulse start-up channel "A" of the zero power reactor ANNA,* Institute of Nuclear Research, Swierk, Report 416/XII (March 1963) (in Russian).
4. Kuliszkiewicz, W., *The log.-current channel "C" of the ANNA zero power reactor control system,* Institute of Nuclear Research, Swierk, Report 415/XII (March 1963) (in Russian).
5. Zieliński, T., *A linear dc channel "B" of the control and safety system for zero power reactor ANNA,* Institute of Nuclear Research, Swierk, Report 417/XII (March 1963) (in Russian).
6. Filipczak, W., Grzejszczak, J., and Krzycki, A., *The automatic control system of the zero power reactor ANNA,* Institute of Nuclear Research, Swierk, Report 406/XII (March 1963) (in Russian).
7. Bajbor, Z., and Podgórski, J., *Critical assembly MARYLA,* Report on the Reactor Physics and Technology Conference in Bucharest (1961) (in Russian).
8. Podgórski, J., *D.C. Measurement channel for the control and safety system of the critical assembly MARYLA,* Institute of Nuclear Research, Swierk, Report 419/XI (March 1963) (in German).
9. Korytkowski, J., and Malanowski, K., *Transduktorowy układ zabezpieczeń reaktora MARYLA-I,* Internal report of Institute of Electronics Warsaw, Międzylesie, 1963 (in Polish).
10. Kurkiewicz, A., and Długołęcki, J., *Control and Safety Rod Drives for the Critical Assembly MARYLA,* Institute on Nuclear Research, Swierk, Report 109/XI (March 1963) (in Russian).
11. Kazimierski, A., *Konstrukcja, technologia oraz właściwości liczników proporcjonalnych z trójfluorkiem boru,* Nukleonika, *4,* No. 2, 199-220 (1959).
12. Dąbek, W., Jabłońska, J., Janikowski, J., and Topa, J., *A Survey of the Detectors Developed in the Reactor Engineering Department of the Institute of Nuclear Research in Swierk,* Institute of Nuclear Research, Swierk, Report 411/IX (March 1963) (in English).
13. Dąbek, W., Jabłońska, J., Janikowski, A., Szczechla, B., and Topa, J., *Referaty z II Krajowej Narady Elektroniki,* Przegląd Elektroniki, *4,* No. 7, 372-413 (July 1963) (in Polish).
14. Filipczak, N., and Filipczak, W., *The "MAXTREL" Control and safety system for Nuclear Reactors,* Institute of Nuclear Research, Swierk, Report 418/XII (March 1963) (in Russian).

ABSTRACT - RÉSUMÉ - АННОТАЦИЯ - RESUMEN

A/500 Pologne

Perfectionnements des organes de contrôle et de sécurité pour réacteurs nucléaires à l'Institut polonais de recherches nucléaires

par J. Podgórski et P. Szulc

Les auteurs décrivent des organes de contrôle de l'assemblage critique ANNA et du réacteur piscine de petite puissance MARYLA, qui ont été mis en service au Centre atomique de Swierk en 1963, ainsi que les perfectionnements apportés aux organes de contrôle pour les réacteurs nucléaires actuellement à l'étude en Pologne.

L'assemblage critique ANNA étant la maquette nucléaire d'un réacteur de recherche à haut flux de 20 à 30 MW, on l'a équipé d'organes de contrôle plus perfectionnés que ceux qu'exigent normalement

les assemblages critiques, en vue d'acquérir l'expérience du fonctionnement de ces organes.

L'ensemble comprend les principales chaînes de mesure ci-après:

a) Chaîne de démarrage avec détecteurs à impulsions (deux lignes) pour la mesure du temps de doublement dans un domaine de puissance couvrant cinq décades;

b) Chaîne logarithmique (deux lignes identiques) pour la mesure du temps de doublement dans un domaine de puissance couvrant cinq décades;

c) Chaîne linéaire (trois lignes identiques fonctionnant selon le principe « 2 sur 3 ») pour la mesure de la puissance dans un domaine couvrant deux décades;

d) Chaîne de stabilisation automatique de la puissance.

L'électronique du système comporte des circuits spéciaux de contrôle de la fiabilité. La chaîne linéaire est équipée d'un comparateur dont la sensibilité relative est indépendante du niveau de puissance dans un domaine couvrant deux décades.

Les organes de contrôle du réacteur MARYLA comprennent les chaînes suivantes:

a) Chaîne logarithmique (deux lignes identiques) pour la mesure du temps de doublement dans un domaine de puissance couvrant sept décades (de 1 mW à plusieurs kW);

b) Chaîne linéaire fonctionnant selon le principe « 2 sur 3 » dans un domaine de puissance allant de 50 mW à 1 kW;

c) Chaîne de sécurité du deuxième degré, fonctionnant selon le principe « 2 sur 3 », à seuil de déclenchement réglable dans une gamme allant de quelques centaines de W à plusieurs kW; cette chaîne est équipée de compteurs Geiger-Müller utilisés comme détecteurs de « puissance gamma ».

Les chaînes logarithmiques et linéaires sont utilisées pour la mesure du temps de doublement et de la puissance et leur stabilisation. Le système de sécurité du deuxième degré joue le rôle d'un « coupe-circuit » supplémentaire. Son déclenchement entraîne l'arrêt du réacteur par éjection d'une section d'éléments de combustible. La chaîne de démarrage transistorisée avec détecteurs à impulsions et la chaîne de stabilisation automatique de la puissance en sont au stade des études.

Les auteurs décrivent les deux systèmes de contrôle ainsi que l'électronique associée, les détecteurs et les mécanismes des barres de commande.

A l'heure actuelle, on met au point de nouveaux systèmes de contrôle et de sécurité pour des réacteurs de recherche de 5 et 30 MW (système « 2 sur 3 » modifié). Ils font l'objet d'essais pour vérifier la fiabilité. Le matériel pour la mesure de la température et du débit en de nombreux points, muni de commutateurs à action rapide, est à l'étude.

A/500 Польша

Опыт работ в области управления и защиты ядерных реакторов в Институте ядерных исследований в Польше

П. Шульц, Я. Подгурски

В докладе рассматриваются системы управления и защиты критической сборки ANNA и реактора малой мощности погружного типа — MARYLA (обе установки введены в эксплуатацию в атомном центре в Сверке в 1963 году), а также дальнейшее развитие систем управления ядерных реакторов, проектируемых в настоящее время в Польше.

Критическая сборка ANNA, являющаяся ядерной моделью исследовательского реактора мощностью в 20—30 *Мвт* с высоким потоком нейтронов, снабжена более совершенной системой управления по сравнению с требованиями, которые обычно предъявляются к таким системам для критических сборок. Это вытекает из необходимости накопления опыта эксплуатации такой системы, состоящей из следующих основных измерительных каналов:

1) импульсного пускового канала (две линии), контролирующего период реактора в диапазоне мощности пяти декад;

2) логарифмического канала (две одинаковые линии), контролирующего период реактора в диапазоне мощности пяти декад;

3) линейного канала (три одинаковые линии, действующие по принципу «два из трех»), контролирующего уровень мощности в диапазоне двух декад;

4) канала автоматического регулятора мощности.

Электронная аппаратура в этой системе снабжена специальными схемами контроля неисправности. В линейном канале применена специальная сравнивающая схема, относительная чувствительность которой не зависит в пределе двух декад от измеряемого уровня мощности.

Система управления и защиты реактора MARYLA состоит из следующих каналов:

1) логарифмического канала с двумя одинаковыми линиями, контролирующего период реактора в диапазоне семи декад (1 *мвт* — несколько киловатт);

2) линейного канала с переключателем диапазонов от 50 *мвт* до 1 *квт*, действующего по принципу «два из трех»;

3) канала аварийной защиты второй степени, действующего по принципу «два из трех», с порогом срабатывания, устанавливаемым в пределах от 100 *вт* до 1,5 *квт;* в этом канале применены токовые счетчики Гейгера — Мюллера в качестве детекторов «гамма-мощности».

Логарифмический и линейный каналы служат для измерений и защиты реактора по периоду и по уровню мощности.

Вторая ступень аварийной защиты играет роль добавочного «предохранителя». Ее срабатывание вызывает сброс одной технологической секции из активной зоны вниз. Разрабатывается транзисторизованный импульсный пусковой канал, а также канал автоматического регулирования мощности.

В докладе описываются обе системы вместе с электронной аппаратурой, детекторами и приводами регулирующих стержней.

Сейчас разрабатываются новые системы управления и защиты для исследовательских реакторов мощностью 5 и 30 *Мвт*. В стадии испытаний находится новая система (модифицированная система «два из трех») с высокой структурной надежностью. Разрабатываются многоточечные быстродействующие приборы для измерения температур и расходов.

A/500 Polonia

Trabajos sobre los sistemas de control y seguridad de los reactores nucleares, realizados en el Instituto de Investigaciones Nucleares de Polonia

por J. Podgórski y P. Szulc

En esta memoria se describen los sistemas de control y seguridad del conjunto crítico ANNA y del reactor de poca potencia, del tipo piscina, MARILA; las dos instalaciones fueron inauguradas en el Centro de Svierk, el año 1963. También se incluye una descripción de los adelantos conseguidos en los sistemas de control de los reactores nucleares que se están proyectando actualmente en Polonia.

El conjunto crítico ANNA, por ser un modelo nuclear del reactor de investigación, de alto flujo neutrónico (de 20–30 MW) está provisto de un sistema de control más complejo que el corrientemente instalado en los conjuntos críticos, por la necesidad de adquirir experiencia del funcionamiento de dicho sistema.

Este sistema consta de los siguientes canales principales de medida:

a) Canal de puesta en marcha (dos líneas); controla el período del reactor en un intervalo de potencia de 5 décadas.

b) Canal logarítmico (dos líneas iguales); controla el período del reactor en un intervalo de potencia de 5 décadas.

c) Canal lineal (tres líneas iguales que actúan según el principio « dos de tres »); controla el nivel de potencia en un intervalo de 2 décadas.

d) Canal de regulación automática de la potencia.

El equipo electrónico de este sistema está provisto de circuitos especiales de control de la seguridad de funcionamiento. En el canal lineal se ha adoptado un circuito comparador especial cuya sensibilidad relativa no depende, dentro de un límite de dos décadas, del nivel de potencia que se está midiendo.

El sistema de control y seguridad del reactor MARILA consta de los siguientes canales:

a) Canal logarítmico con dos líneas iguales; controla el período del reactor en un intervalo de 7 décadas (1 mW hasta varios kW).

b) Canal lineal con conmutador del intervalo de medida, desde 50 mW hasta 1 kW; actúa según el principio « dos de tres ».

c) Canal de seguridad de segundo grado; actúa según el principio « dos de tres » con nivel de disparo ajustable entre 100 W y 1,5 kW; en este canal se utilizan contadores Geiger-Müller como detectores de « potencia-gamma ».

Los canales logarítmico y lineal sirven para la medición del período y de la potencia, y además para la seguridad del reactor por estos mismos conceptos. El canal de seguridad de segundo grado desempeña un papel de seguridad adicional. Su disparo produce la caída, fuera del núcleo, de una sección de elemento combustible. Actualmente se está tratando de transistorizar el canal de puesta en marcha y el canal de regulación automática de la potencia.

En la memoria se describen ambos sistemas y el equipo electrónico, los detectores y los mecanismos de transmisión de las barras de control.

Actualmente se están desarrollando nuevos sistemas de control y seguridad para dos reactores de investigación proyectados, de 5 MW y 30 MW. Un nuevo sistema (una modificación del sistema « dos de tres »), de gran solidez estructural, está en fase de ensayo. Se están desarrollando también instrumentos de respuesta rápida para la medición, en varios puntos, de temperaturas y caudales.

Outlook for reactor control systems with moving detectors

By P. Kovanic* and K. Wagner**

The essential characteristics of control systems using fixed and moving ion chambers or fission counters are given in this paper and the advantages of the system with such moving detectors are explained by comparing them. Furthermore, the transfer function of these systems as well as the results obtained is mentioned. The automatic control of the Czechoslovakian VVR-S reactor, which has operated on this principle since 1961, is described in more detail. Finally, other applications of the systems with moving detectors are discussed. The paper deals with Czechoslovakian research in this field.

THE REACTOR CONTROL AND SAFETY SYSTEM USING FIXED DETECTORS

Generally a reactor control and safety system comprises three types of loop having different functions. The first loop controls the reactor start-up, the second controls the reactor at high power and the third loop is used as a safety system. The basic scheme for all three loops is the same: the detector signal is processed, is compared to a pre-set value (programme) and in the case of a disagreement acts on the reactor (reactivity). The loops are closed across the reactor and detectors. The processing of a signal from the detector in the case of a safety system is accomplished by amplification (power control), or by logarithmic counting and differentiating (period control). The programme to be compared with the signal is represented by a number of levels, which if surpassed act on the reactor causing an alarm or even scramming. The processing of the start-up circuit detector signal is done by determining the power and period, the programme determining the power and period as a function of time. The deviations from the programme cause relatively high reactivity changes by means of the control rods. The power level control differs from the start-up control essentially only by the detector sensitivity and sometimes also with the transfer function which determines the action on the reactivity, which is varied to some extent by control rods. An essential feature of the control systems with fixed detectors is that at a change of power demand the detector output also changes.

These are only the basic functions of the three loops. The loops, however, must fulfil other subsidiary functions, the principal ones being:

(*a*) Maintaining operation at various reactor power levels;

(*b*) Checking the system before start-up;

(*c*) Continuous checking of correct operation.

At power variations over a broad range the sensitivity of the measuring instrumentation must be switched over and the power dependence of the reactor gain must be compensated. It is necessary to switch the input circuits or displace the detectors to another position or to replace them with other detectors.

Additional, sometimes complex measures must be taken, especially if the system includes non-linear circuits e.g., logarithmic amplifiers. The safety system also includes switching at pre-set values of power variation, as an auxiliary operation.

REACTOR CONTROL AND SAFETY SYSTEM WITH MOVING DETECTORS

The idea of consequently using servo systems with moving detectors for designing a unified reactor control and safety system originated at the beginning of 1958 after an analysis of the complications which arose when attempting to automate control of a reactor using fixed detectors.

The possibility of using a servo system with a moving detector for measuring reactor power was described earlier by Schulz [1], the main advantage of the arrangement being that it avoids the need to switch measuring ranges. According to Schultz the principal disadvantage of such a system is the non-linear dependence of the detector position on reactor power. The essential feature in considering this problem is simply that this non-linearity turns out to be an essential advantage in the case of a natural exponential distribution of the neutron flux along the detector path, which passes through the moderator. This allows the possibility of using the moving detector directly for measuring the logarithmic power and reactor period. A further important step was the design of a control system on the same principle. Still another logical step was the design of the measuring and control loops combined in one system which may be adequate for accomplishing full automation by simple means [2].

* Nuclear Research Institut, Řež, Prague.
** Lenin Works, Pilsen.

In the case of a moving detector, neutron space distribution is used in such a way that its co-ordinate is varied as a function of the reactor power at a constant detector signal (the power measurement and safety system loop), or reactor power is varied as a function of the detector co-ordinate (power and period control loop). The signal processing is done for example by amplification, the constant signal of an auxiliary source representing the programme to be compared with the signal, and the difference between them causing detector displacement (power and period measurement) or acting on the control rod (power and period control). An unambiguous link exists between the detector position and reactor power and between the velocity of the detector movement and the reactor period. In the case of an exponential distribution of neutron flux along the detector path the exponential power increase corresponds to the linear displacement of the detector so that the moving detector scale is logarithmic, although the system does not consist of logarithmic amplifiers. The logarithmic power is given by the detector co-ordinate.

COMPARISON OF SYSTEMS WITH FIXED AND MOVING DETECTORS

The structure of the reactor control and safety system with a moving detector is simpler, as it does not include new components as compared with the system using fixed detectors; it is assumed that the detector had to be displaced in any case to attain coarse sensitivity variations as well as to be protected against overloading. It may for example include only amplifiers operating in the range of the zero input signal. In this case the accuracy of the system operation is not affected by amplification variations. The circuits with fixed detectors cannot function in the whole range of reactor power and it is necessary, therefore, to use several circuits functioning at various levels and to switch them over when necessary. The number of circuits (channels) of the system with moving detectors may be smaller, as in measuring both at start-up and at a high power as well as for period and power control system a single measuring channel may be used. It must be considered furthermore that both types of loop, measuring and control loops, may be interchanged after a simple switching so that a common stand-by system may be used for both loops, and that the single circuit with a moving detector may measure both power and period, which is not always possible with fixed detectors. It means that an important reduction in the number of independent channels may be attained with the use of moving detectors in comparison with fixed detectors.

With the use of moving detectors auxiliary functions are also simplified. Detector movement is the principle of the system and it is carried out automatically without any other intervention. The input circuits need not be switched over when the reactor power varies. The system sensitivity is increased automatically by detector movement away from the active zone. It may be checked simply that the system is ready for operation by the use of the servo system principle. The compensating input circuit facilitates a continuous check as most failures in any loop result in the occurrence of a high signal at some loop point or in the detector movement. Both these two effects may be identified as signalling a loop failure or unwanted behaviour in the reactor operation. The instrumentation failure may be distinguished from the emergency reactor state by comparing the indications from different channels. Setting the alarm power levels is performed automatically e.g., by duly disconnecting or connecting the servo system loop. As the detectors remain at the same position at a stationary reactor power corresponding to the preset power, the detector signal is equal to the preset value even after the disconnection of the loop and the difference signal, therefore, is equal to zero. A deviation of the power from the preset value, corresponding to the detector position, is accompanied by the appearance of a signal in the loop. This method of setting emergency signals by deviation from the preset value is simpler in comparison with fixed detectors and its applicability is not limited to a certain part of the full range of the power variations.

The operation of the system with moving detectors is associated, unlike that with fixed detectors, with mass displacement. It is possible that this fact will lead to higher delays in this system and to an insufficiently fast function. We shall discuss this problem in more detail. With normal operation of the instrumentation the rate of the reactivity variations is limited for safety reasons in such a way that the velocity of the detector movement and its acceleration are within the limits in which mechanical delay is not significant. The detector of the measuring loop may follow the power, and other variations (by its displacement) because these variations are given by the movement of a control detector of the same design. In emergency cases however, the power variations may be so quick that the detector of the measuring (alarm) loop cannot follow the power variations owing to its mechanical inertia. But in this case the larger the inertia of the moving parts the larger is the signal that appears in the loop. If we imagine that the detector did not move at all during the emergency state, then the alarm loop with the moving detector turns out to be a loop with a fixed detector and, as it does not comprise any other elements with respect to the latter, a similarly quick function of both loop types may be expected.

THE DEVELOPMENTAL STAGE OF THE SYSTEM WITH MOVING DETECTORS

The studies which were carried out in Czechoslovakia with the co-operation of the Nuclear Research Institute and the Lenin Works in Pilsen

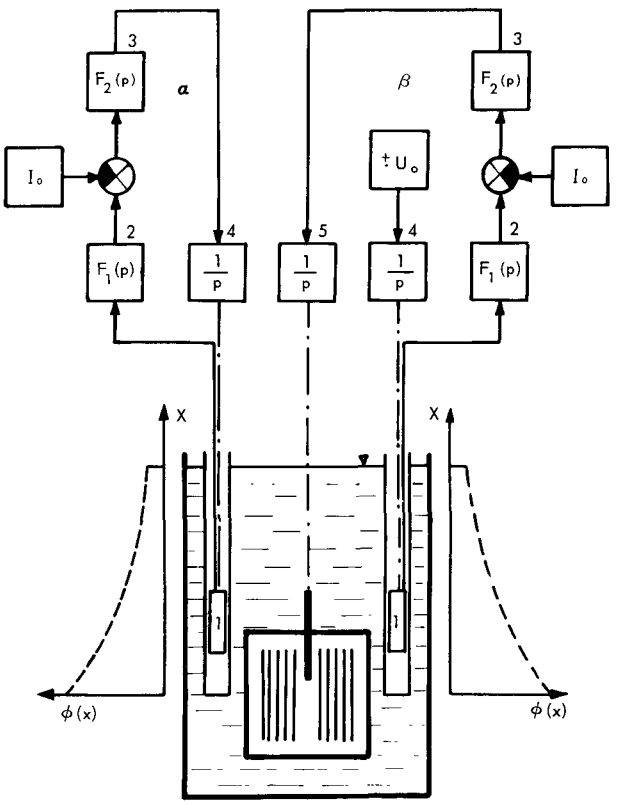


Figure 1. Block diagram of the control and measuring systems

during the last six years have accumulated experience with the design and operation of the system with moving detectors. A theory for the measuring and control loop was elaborated for devices of the analogue type. The block scheme of such systems is given in Fig. 1. The detector (1) signal is processed by the element (2) (an amplifier or count ratemeter), the output of which is compared to a constant value I_0. The difference signal is amplified by the element (3) and fed to the motor (4) of the detector (at the measuring loop) or to the motor (5) of the control rod (at the control loop). The source (6) sets the controlled period. The transfer functions of individual elements are also shown on the figure. For a steady state ($p \longrightarrow 0$) it may be assumed that:

$$\lim_{p \to 0} F_1(p) = K_1 \; ; \; \lim_{p \to 0} F_2(p) = K_2 \; ;$$
$$\text{where } K_1 > 0; \; K_2 > 0.$$

The distribution of the neutron flux along the detector channel may be characterized by the function:

$$\phi = \phi_0 [t] \exp\left(-\frac{x}{L}\right)$$

where L is a constant on the part of the detector path considered, and $\phi(t) = K\phi N(t)$ is a quantity proportional to the reactor power.

The transients in these systems are described with non-linear differential equations with variable coefficients. In simple cases the main characteristics of the systems described with these equations may be found by analyzing singular points in the phase plane [3]. The most efficient calculation method is the application of transfer functions, which may be obtained by transforming the equations with certain acceptable assumptions.

The transfer function of the measuring system is

$$\frac{\delta x(p)/L}{\delta n(p)} = \frac{[(1 + \alpha L/K_2 I_0) I_0/L]\,[F_1(p)/K_1]\,F_2(p)}{p + [(1+\alpha L/K_2 I_0) I_0/L]\,[F_1(p)/K_1]\,F_2(p)}$$

where:

$\delta x(p) = \mathcal{L}\{\delta x(t)\}$; $\delta x(t) = x - \alpha L t + \epsilon$;

$\epsilon/L + \alpha L/K_2 I_0$ is the stationary relative dynamic error at the period $1/\alpha$;

$$\delta n(p) = \mathcal{L}\{\delta n(t)\} \; ;$$

and $\delta n(t) = N(t) - N_0 \exp(\alpha t)$, the relative power deviation from the exponential value.

This transfer function holds under the following conditions:

$|\delta n(t)| \ll 1$; $\quad |\delta x(t)/L| \ll 1$

$I_0 = K_1 K_2 N_0$; $\quad |\alpha L/K_2 \phi_0| \ll 1$

The transfer function does not depend on power but depends slightly on the period $1/\alpha$

The transfer function of the control system is:

$$\frac{\delta p(p)/\delta n(p)}{} = -(1/p) I_0 \{F_1(p)/K_1\} F_2(p) \left[1 - \frac{\delta x(p)/L}{\delta n(p)}\right]$$

where:

$\delta p(p) = \mathcal{L}\{p(t) - p_0\}$

$p(t)$ is the reactivity of the reactor which varies with time

p_0 is the constant component of the reactivity which corresponds to the period $1/\alpha$, and

$\delta x^*(p)$ is the transform of the variation of the detector co-ordinate.

The transfer function of the control loop holds again at small deviations from the quasi-stationary state with an exponential power variation and depends neither on reactor power nor period. The transfer function of the closed loop control system for the reactor depends, however, on the period on which the reactor transfer function also depends.

The transfer functions mentioned above may be used for the analysis and synthesis of the systems with moving detectors, and this has been checked experimentally.

Experience has shown that a pulsed fission chamber is a convenient type of moving detector because

of its high sensitivity to neutron flux, a minimum effect of gamma radiation and the possibility of easy and reliable checking.

It appears that the neutron flux distribution in the water shield of the most common type of research reactor, with light water as reflector and shielding, is quite suitable for the function of this system with the moving detector, if the detector channels are filled with water. The calibration of the power scale does not change during operation and, in practice, does not depend on the operational programme of the reactor.

THE FACILITY FOR FULLY AUTOMATIC CONTROL OF THE VVR-S REACTOR

On the basis of the results of these studies the facility for the fully automatic control of the Czechoslovak VVR-S reactor was designed and put into operation in the summer of 1961.

The facility comprises three servosystems with a moving detector as basic parts. Each channel contains:

A moving pulsed fission chamber;
A pulse amplifier with a pulse-height discriminator;
A pulse ratemeter ($T_i = 0.1$ s);
A voltage source;
An electronic amplifier of the difference signal;
An output magnetic amplifier (reversible);
A servomotor for the ionization chamber and control rods.

Each system may be operated in the following modes:

CRM: count rate (power) meter with a fixed detector (the first stage of the automatic start-up);
PPM: reactor power and period meter with a moving detector;
PPC: automatic power and period control instrumentation;
PDM: power deviation from the preset meter value;
B: system is blocked (automatically at its own failure or hand operated by the operator).

The detector of the blocked system passes automatically into its top position. Blocking of each individual loop is equivalent to the onset of all alarm signals of this loop. Each signal originating from a single loop is considered as an alarm. A high signal of power or period given by two out of three functioning loops, by one out of two functioning loops, or by the blocking of two loops, is considered as the scram signal for the rods to drop. In any reactor situation at least two independent systems are in operation. In the case of blocking the control loop one of the functioning loops takes over its task.

An automatic reactor start-up is only possible after a successful checking: when a chosen power level and the executive command for start-up is given, the automatic check that the system is ready begins. All other operations are accomplished automatically till the chosen level is stabilized. The check uses the pulses produced by α-particles of the fission chambers. A discriminator with two discriminating levels is provided before the ratemeter. Neutron counts only are registered at the operational discrimination level. During the check all background level discrimination of input circuits is suppressed and neutron and α-counts are registered. During the check the α-count signal causes the displacement of all loops in the PPM-function into the extreme upper position producing all alarm signals. When the operational discrimination level is re-established the detecting chambers re-occupy their original position. The check of the arrangement is successful, if all checking operations are ended within due time (approximately 80 s). After a successful check, the start-up begins immediately. If the check conditions are not fulfilled, the arrangement signals an alarm and the sequence is interrupted. The loop which is hand blocked before the check is not controlled and its behaviour does not affect the result of the check.

At the beginning of the start-up the loops are in the CRM-function. On completion of the check the safety rods are gradually pulled up, the control rod occupies its operational position and the reactivity is increased, in steps, with compensating rods. When an output of 10 W is attained, the measuring chambers, which are in the lowest position, indicate 40 000 cps. At this moment the second phase of the start-up begins by switching one loop to the PPC-function and two loops to the PPM-function. The linear reactivity increase is stopped. The detector of the PPC loop moves at a given velocity to the position which is determined by the power preselection. The detectors of the remaining loops measure the power really attained. When the detector of the PPC loop attains the determined position, the reactor power is established at the preset value. After the end of the transient process two measuring loops are disconnected to measure the deviation from the given position (PDM function).

The continuous check of the correct functioning and finding of a faulty loop is done by mutual comparison of the voltages at the output of magnetic amplifiers or at the auxiliary source of the control detector. With normal operation of the loops and with small deviations of the reactor state from that required, the voltages to be compared may differ by little and only for a short period. The loop whose voltage differs from others by an impermissible value is blocked automatically. If two measuring chambers only remain functioning, then the disagreement of their indications results in at least one of them blocking and thereby in reactor scramming.

The comparison system reveals some incorrect functions immediately, but the failures which originate during the PDM-function are registered by

the system only at the following power variation. The incorrect functioning of two loops could lead to the blocking of the single correct loop. The check means are, therefore, still effective. The minimum counting rate is checked in all detectors both in the CRM (approximately 20 cps) and in other functions (40 000 cps). At a decrease of the count rate the loop is blocked.

At a failure (e.g. in the discriminator) leading to an increase of the integrator output, an alarm signal is given.

A dangerous reactor state is signalled very simply owing to the use of the servo-system principle for all loops. At a deviation of the reactor state from that required, the reactor is scrammed by one combination of the alarm and blocking signals. The operator obtains the information of the reactor state at a power above 10 W from the detector position (power) and mean voltage on the loop output (inverse period).

At a power below 10 W the state is indicated by the logarithmic count integrator. This device is used only for the information of the operator and it does not interfere with the automatic control.

The dependence of the reactor power on the detector co-ordinate is shown in Fig. 2. At a normal counting rate of 40 000 cps the measuring and control loops function from 10 W to the emergency level of 3.6 MW. It may be seen from Fig. 2 that the loop could be used without any other dispositions up to approximately 100 MW, if the reactor, of course, could be operated at such a level.

The minimum period value at which the detector follows the power is 2.1 s. At shorter periods the detector velocity does not increase further, the unambiguous coupling of the period and detector velocity is perturbed, the neutron flux at the detector position rises and the system gives an emergency signal independently from the period value. The period-meter time constant used ($\tau = 0.5$ s) provides a reliable period measurement up to 50 s. Negative periods may be measured by the system in the same manner as the positive ones. The dependence of the dynamic error on the measured period $1/\alpha$ is determined by an approximative expression $\epsilon = 0.5\ \alpha$ where ϵ is expressed in relative units, i.e. $\epsilon = 0.1$ corresponds to the power error of 10%.

The experimentally determined mean square error of the measurement of the constant power with a moving pulsed chamber is 0.6-0.7% in the given case. Besides errors due to the statistical nature of the input signal, short term electronic errors, errors of measuring the detector coordinate and others are included. The maximum instantaneous deviation from the mean value as observed once in 15 min is 2%.

In the linear region of the automatic control the amplification is $3.5 \times 10^{-5}\ \delta k/s$ with respect to 1% of the power deviation. The mean square error of the power level control is 0.6% owing to the use of

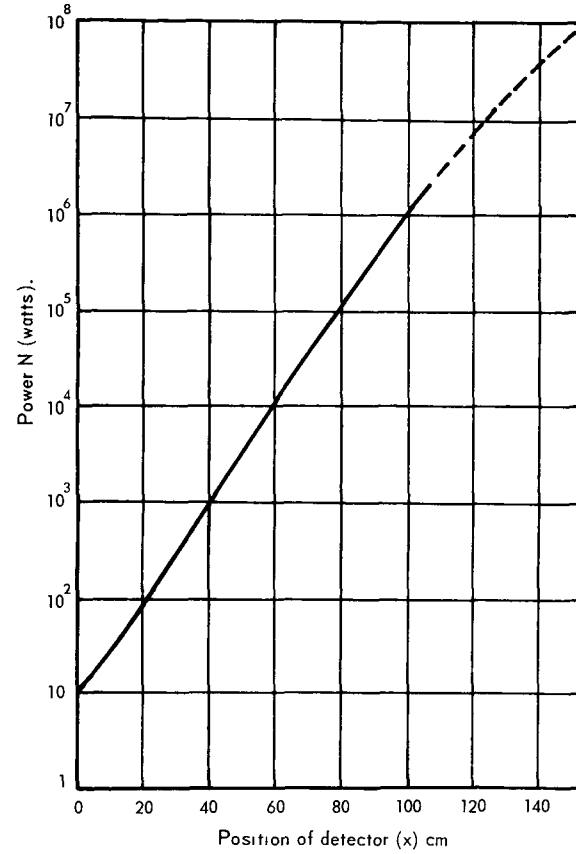


Figure 2. Calibration curve of the moving detector system

the pulse detector. The transient at reactivity perturbations lasts approximately 7 s. At this setting the control loop can control the periods up to $1/\alpha = 3.5$ s. The established error of the power and period control is equal to zero. The requirement for an automatic control of short periods is inconsistent with the effort to decrease total efficiency of the control rod. This efficiency at the given geometry is $\delta k = 3.4 \times 10^{-3}$ which is insufficient for an automatic facility. Some measures were taken for maintaining the control rod in the middle, linear, region of the path both by using compensating rods and by adjusting the programme of power variations to the instantaneous possibilities of the means of control. All this is accomplished automatically.

Negative periods up to −80 s may also be controlled by the facility. Difficulties arise in the control of shorter periods within a wide power range, which is due to the nature of the reactor.

The characteristics of the system described enabled the rates of the reactivity variations in the first phase of the start-up to be increased to the value of $2.8 \times 10^{-4}\ \delta k/s$. In such a case the reactor start-up from the subcritical state to full power including the check lasts 5-7min (depending upon the initial state of the reactor). In daily operation approximately half this rate is usual.

During reactor operation the system correctly fulfils all functions mentioned. The deficiencies which

have appeared up to the present are technological and may be avoided. Any changes of the relative neutron distribution which could affect essentially the calibration curves of the power dependence on the detector co-ordinate have not been observed so far.

A more detailed description of the facility is given in [4].

SOME IDEAS ON OTHER POSSIBLE DEVELOPMENTS IN THE USE OF A SYSTEM WITH MOVING DETECTORS

There is no need to solve the principal problems for using systems with moving detectors in experimental reactors of most present types, but it is necessary to make some technical improvements in instrumentation, to use contactless systems and to improve the lifetime of the devices. The problems connected with the use of these systems in power reactors have another aspect. There is insufficient experience in this field. Difficulties are assumed especially for an essentially lower neutron flux which would be available for the detectors, and the necessity to provide an exponential neutron distribution by some additional means. Similar difficulties appear in low power experimental reactors. With a poor input signal and also for simplifying the scheme, nonlinear circuits of the relay type and digital processing of input and output signals seem to be indicated.

Present studies lie in this direction. The aim is to design a means of automatic control for a heavy-water reactors of low power and to equip the first Czechoslovak nuclear power plant with an experimental facility of this type.

REFERENCES

1. Schultz, M. A., *Control of Nuclear Reactors and Power Plants*, McGraw-Hill Book Company, Inc.
2. Kovanic, P., and Kulka, M., *A complex automation of nuclear reactor control*, Atomnaya Energia, N 10 (1958).
3. Kovanic, P., *Basic Equations of the Servosystems with Moving Detectors for Nuclear Reactor Control*, International Conference on the Physics and Technology of Nuclear Reactors, Prague (April 1963).
4. Kovanic, P., Rygl, J., Wagner, K. and Teska, J., *A New System of the Automatic Control of the WR-S Reactor*, Atomnaya Energia, *13*, N 14 (October 1962).

ABSTRACT - RÉSUMÉ - АННОТАЦИЯ - RESUMEN

A/631 Tchécoslovaquie

Systèmes de contrôle des réacteurs utilisant des détecteurs mobiles et leurs perspectives d'avenir

par P. Kovanic et K. Wagner

En Tchécoslovaquie, on s'efforce depuis le début de 1958 de mettre au point un système de contrôle des réacteurs utilisant des servomécanismes avec des détecteurs mobiles. Ce système présente les avantages suivants: *a*) grand champ d'utilisation; *b*) applicabilité universelle; *c*) possibilité d'automatiser le contrôle avec des moyens simples. Les auteurs décrivent, pour information, le principe de fonctionnement de systèmes utilisant des détecteurs mobiles.

Les principes de ces systèmes ayant été entièrement confirmés et leur théorie établie, on a étudié les propriétés de systèmes utilisant des chambres d'ionisation mobiles, à l'aide d'une installation expérimentale qui était le prototype d'un système de contrôle de réacteur entièrement automatique. On a étudié aussi les caractéristiques de servosystèmes utilisant des détecteurs mobiles du type à impulsions. Sur la base des résultats satisfaisants donnés par toutes ces recherches, on a montré un système de contrôle entièrement automatique utilisant des chambres mobiles à fission, qui a été mis en service en 1961 sur le réacteur de recherche tchèque VVR-S. Depuis lors, le système fonctionne durant l'exploitation normale du réacteur. Il assure le contrôle entièrement automatique de son propre état de fonctionnement, du démarrage du réacteur jusqu'à un niveau préréglé, de la puissance en régime stationnaire et en régime transitoire, ainsi que la vérification constante de sa propre exactitude et du régime du réacteur. L'efficacité du fonctionnement de ce type de dispositif a confirmé les avantages que l'on attendait de systèmes utilisant des détecteurs mobiles.

Tous les problèmes fondamentaux que pose l'utilisation de systèmes munis de détecteurs mobiles dans la plupart des réacteurs de recherche actuels sont maintenant résolus. Il reste à apporter des perfectionnements techniques à leurs éléments. L'utilisation de ces systèmes dans les réacteurs de puissance pose d'autres problèmes, car il faut prendre des mesures particulières pour assurer une distribution longitudinale adéquate du flux de neutrons dans les canaux des détecteurs. L'analyse a montré que les avantages présentés par des systèmes utilisant des détecteurs mobiles justifiaient les mesures supplémentaires visant à établir les conditions physiques qui permettent à ces systèmes de fonctionner, là où ces conditions ne sont pas une propriété naturelle du milieu entourant le cœur du réacteur.

En Tchécoslovaquie, on étudie actuellement un système de contrôle automatique destiné à un réacteur à eau lourde de puissance zéro et fondé sur ce principe. Le réacteur de la première centrale nucléaire tchèque sera également pourvu d'un dispositif expérimental de ce genre en vue de faire l'expérience de son fonctionnement dans un grand réacteur de puissance. Dans les deux cas ceci implique l'emploi de méthodes numériques.

A/631 Чехословакия

Перспективы развития системы с подвижными детекторами для управления реакторами

П. Кованиц, К. Вагнер

С начала 1958 года в Чехословакии производится разработка аппаратуры для полной автоматизации управления ядерными реакторами с помощью сервосистем с подвижными детекторами. Преимуществом этих систем является широкий рабочий диапазон, универсальность и пригодность к полной автоматизации управления при простой структуре. Для информации приведено описание принципа действия систем с подвижными детекторами.

После принципиальной проверки работы этих систем и после разработки их теории исследовались свойства систем с подвижными ионизационными камерами на экспериментальной установке, являющейся упрощенным прототипом системы для автоматического управления реактором. В дальнейшем исследовались особенности работы сервосистем с подвижными детекторами импульсного типа. На основе удовлетворительных результатов исследований была создана и в 1961 году введена в эксплуатацию на реакторе ВВР-С полностью автоматизированная система управления реактором с подвижными камерами деления. С этого времени система работает при нормальной эксплуатации реактора. Установка автоматически выполняет проверку своей готовности к работе, разгон реактора на заданную мощность и регулирование мощности в установившемся и в переходных состояниях, непрерывный контроль за собственной исправностью и за состоянием реактора. Результаты ее работы подтверждают ожидаемые преимущества систем с подвижными детекторами.

Для применения систем с подвижными детекторами на экспериментальных реакторах большинства из существующих типов нет уже необходимости в решении каких-либо вопросов принципиального характера. Предстоит проведение технического усовершенствования элементов этих систем. Несколько другой характер имеют пока работы, связанные с введением этих систем на энергетических реакторах, где вопрос заключается в возможности создания подходящего пространственного распределения нейтронного потока вдоль каналов детекторов. Анализ показывает, что выгодные свойства систем с подвижными детекторами могут служить достаточным доводом для дополнительных мер по обеспечению физических условий работы этих систем и у тех типов реакторов, где они не являются естественным свойством среды, окружающей реактор.

В Чехословакии в настоящее время проводятся работы по созданию автоматической системы управления тяжеловодным реактором нулевой мощности на том же принципе. Реактор первой чехословацкой ядерной станции будет также снабжен экспериментальной аппаратурой этого типа с целью получения опыта работы в условиях большого энергетического реактора. В обоих этих случаях предполагается использовать элементы цифровой техники.

A/631 Checoslovaquia

Perspectivas de los sistemas de control con detectores móviles

por P. Kovanic y K. Wagner

Desde principios de 1958 se está efectuando en Checoslovaquia el desarrollo de un sistema de control de reactores nucleares a base de servomecanismos con detectores móviles. Las ventajas de estos sistemas son las siguientes: *a*) amplio campo de operación, *b*) aplicabilidad universal, *c*) posibilidad de automatización del control con medios sencillos. Se describe a título de información el principio de funcionamiento de estos sistemas.

Una vez realizada la investigación y desarrollada la teoría, se examinaron las propiedades de sistemas con cámaras de ionización móviles en una instalación experimental, prototipo de un sistema de control totalmente automático para un reactor. Además, se investigaron las características de servosistemas con detectores de impulsos, móviles. En vista del resultado satisfactorio de la investigación se diseñó un sistema de control con cámaras de fisión móviles totalmente automático, que se puso en funcionamiento en 1961 en el reactor checoslovaco de investigación VVR-S. Desde entonces el sistema está en régimen de funcionamiento normal de forma totalmente automática. El aparato es capaz de realizar su propia puesta a punto, puesta en marcha del reactor hasta un nivel prefijado, el control de potencia en condiciones estacionarias y en transitorias y la comprobación continua de su propio comportamiento y del estado del reactor. El buen funcionamiento del sistema confirmó las ventajas que se le suponían.

Las principales cuestiones planteadas por el uso de sistemas con detectores móviles en la mayor parte de los reactores actuales de investigación han sido resueltas. Quedan por introducir mejoras técnicas en sus elementos. Hay otro tipo de problemas que surgen en los reactores de potencia, en los que hay que hacer un montaje especial para tener la seguridad de que existe la distribución apropiada de flujo en los canales de detección. El análisis muestra que las ventajas de los sistemas con detectores móviles justifican que se adopte medidas adicionales que aseguren las condiciones físicas de operación de dichos sistemas aun en aquellos reactores en los que

estas condiciones no son una propiedad natural del medio que rodea al núcleo del reactor.

Actualmente se ha diseñado en Checoslovaquia un sistema de control automático, apoyado en este principio, para un reactor de agua pesada de potencia nula. Además, el reactor de la primera central nuclear de potencia checoslovaca irá dotado de un dispositivo experimental de este tipo para obtener experiencia de operación en un gran reactor de potencia. En ambos casos se usa una técnica digital.

Optimum digital information treatment and nuclear engineering instrumentation

By P. Kovanic*

The measurements carried out with nuclear instrumentation are subjected to statistical variations which are partly inherent in the processes investigated and partly due to measuring channels. The optimum treatment of continuous signals with instruments of the analogue type, i.e. optimum filters designed by Wiener theory, is practically possible only in simple cases and at limited accuracy requirements. For this reason and for others also [1], digital methods are rather preferred. Digital methods exist for solving automatic control problems [2] which may also be used for the more special problem of treating signals in the presence of random variations [3]. By using these methods each calculation step is based on the results obtained in the previous step.

Some problems of the type mentioned may be solved in a simpler way. In this paper the optimum operation is carried out as a scalar product of two vectors: that of input values and that of the operator resulting from the problem conditions. The aim of this paper is to give the information necessary for the practical application of this method. The formulae used are not derived, their derivation is given in [4].

THE FORMULATION OF THE PROBLEM

Consider a function $f(t)$ which is characterized as follows:

(*a*) The function $f(t)$ has all derivatives in a certain sufficiently broad interval of the argument t;

(*b*) The approximate values of this function are given in the points $t_0, t_1, \ldots, t_n$ of the definition interval.

The values $Y_0, Y_1, \ldots, Y_n$ may be assumed as a sum of accurate values of the function $f(t_i)$ and errors y_i, i.e.

$$Y_i = f(t_i) + y_i, \qquad (i = 0, 1, \ldots, n) \tag{1}$$

The errors are assumed to have a random nature. The following relations are supposed for mean values:

$$\overline{y_i} = 0 \quad \text{(for all values of } i\text{)} \tag{2}$$

$$\overline{y_i y_j} = 0 \quad (i \neq j) \tag{3}$$

$$\overline{y_i^2} = \text{const} \quad \text{(for all values of } i\text{)} \quad (i = 0, 1, \ldots, n) \tag{4}$$

Averaging is done over the realisation set. The quantities Y_i are assumed to be mutually not-correlated stationary random quantities with zero mean value.

For abbreviation we define a one row matrix

$$\boldsymbol{Y} = (Y_0\ Y_1 \ldots\ldots\ldots\ldots\ldots\ Y_n). \tag{5}$$

The desired quantity is the product of a linear transformation of the function $f(t)$; it is the numerical value of the transformed function obtained from $f(t)$ in the point $t = t_r$. We denote the desired quantity as x. The simplest case is the determination of the function $f(t)$ in the point $t = t_r$, i.e. the determination of $[f(t)]_{t=t_r}$.

At $t_r = t_n$ or $t_r = t_0$ we can speak of the "filtration" of the $f(t)$-value, at $t_0 < t_r < t_n$ of interpolation, and at $t_r < t_0$ or $t_n < t_r$ of extrapolation of $f(t)$ values. Not only the $f(t)$-values but also the kth derivatives of this function, integral values or linear combinations of the function, derivatives and integrals may be filtered, interpolated or extrapolated. The function $\mathscr{L}$, the linear transformation of the function $f(t)$, is approximated by the calculation, i.e. the number $x = [\mathscr{L}\{f(t)\}]_{t=t_r}$. (6)

Expression (6) may in a special case be of the form

$$x_0 = [f(t)]_{t=t_r} \qquad x_I = \left[\int_{t_s}^{t} \ldots \int_{t_s}^{t} f(\tau)\mathrm{d}\tau \ldots \mathrm{d}\tau\right]_{t=t_r}$$

$$x_D = [f^{(k)}(t)]_{t=t_r} \qquad x_K = \left[\int_{t_s}^{t} k(t,\tau) f(\tau)\mathrm{d}\tau\right]_{t=t_r}$$

or their linear combination.

We must content ourselves with an approximation owing to the presence of statistical variations in the

* Institute of Nuclear Research, Řež, Prague.

rigorous solution, but also because of the fact that the given $n + 1$ parameters may be insufficient for a rigorous solution of the given problem in the general case. The problem may be considered as solved if we find such a one-column matrix Ω,

$$\Omega = \begin{bmatrix} \Omega_0 \\ \Omega_1 \\ \vdots \\ \Omega_n \end{bmatrix}, \tag{7}$$

that yields the required approximate solution by multiplying the matrix. This solution is optimum in a certain meaning

$$(x) = \boldsymbol{Y}\Omega \tag{8}$$

The parentheses denote here the one row and one-column matrix, the number x being its element.

Such a solution x will be considered as the optimum approximate solution which yields the minimum mean square error $\overline{(x - \bar{x})^2}$, i.e. minimum variance, in the presence of statistical fluctuations and which satisfies the condition of analytical accuracy at the same time. This condition may be formulated as follows: the approximate and accurate solutions must be equal if input values are given accurately (i.e. without any statistical error) and if the function $f(t)$ is a polynomial of the order m (where $m \leq n$).

The formulation of the problem may, therefore, be resumed as follows: such Ω must be found that the conditioned minimum

$$\overline{(x - \bar{x})^2} = \text{Min}, \tag{9}$$

would be attained under the conditions of analytical accuracy:

$$\boldsymbol{t}'\Omega = \omega$$

$$\text{where } (x) = \boldsymbol{Y}\Omega. \tag{10}$$

$$\boldsymbol{t} = \begin{bmatrix} t_0^0 & t_0^1 & \vdots & t_0^m \\ t_1^0 & t_1^1 & \vdots & t_1^m \\ \vdots & \vdots & \vdots & \vdots \\ t_n^0 & t_n^1 & \vdots & t_n^m \end{bmatrix}, \tag{11}$$

and $\boldsymbol{t}'$ is the transposed matrix $\boldsymbol{t}$; also

$$\omega = \begin{bmatrix} \omega_0 \\ \omega_1 \\ \vdots \\ \omega_m \end{bmatrix} \tag{12}$$

$$\text{and} \qquad \omega_i = [\mathscr{L}\{t^i\}]_{t=t_i} \tag{13}$$

SOLUTION OF THE PROBLEM

It may be proved that a solution of the problem exists if all values of t_i are mutually different. The necessary and sufficient condition for solving is that Ω_i is the value of the polynomial of the degree m of the variable t in the point $t = t_i$, i.e.

$$\Omega_i = \sum_{s=0}^{s=m} F_s t_i^s. \tag{14}$$

Denoting

$$\boldsymbol{F} = \begin{bmatrix} F_0 \\ F_1 \\ \vdots \\ F_m \end{bmatrix} \tag{15}$$

then

$$\boldsymbol{F} = (\boldsymbol{t}'\boldsymbol{t})^{-1}\omega, \tag{16}$$

where $(\boldsymbol{t}'\boldsymbol{t})^{-1}$ is the inverse matrix to the matrix $(\boldsymbol{t}'\boldsymbol{t})$.

Therefore

$$\Omega = \boldsymbol{t}(\boldsymbol{t}'\boldsymbol{t})^{-1}\omega = \boldsymbol{t}\boldsymbol{F} \tag{17}$$

and the desired numerical value is found as

$$(x) = \boldsymbol{Y}\boldsymbol{t}(\boldsymbol{t}'\boldsymbol{t})^{-1}\omega. \tag{18}$$

The variance of the result is minimum at given conditions and equals:

$$\overline{[(x - \bar{x})^2]}_{\text{Min}} = \overline{y^2}(\omega'(\boldsymbol{t}'\boldsymbol{t})^{-1}\omega). \tag{19}$$

If any other polynomials of the mth degree different from Eq. (14) are used for the calculation, the variance of the result will be higher than that of Eq. (19).

In the special case of the filtration, interpolation and extrapolation of the $f(t)$ values

$$\omega = \boldsymbol{t}_r$$

where

$$\boldsymbol{t}_r = \begin{bmatrix} t_r^0 \\ t_r^1 \\ \vdots \\ t_r^m \end{bmatrix} \tag{20}$$

In this case, smoothing of $(n + 1)$ inaccurate values of the function $f(t)$ is carried out with the polynomial of the degree m. The value of the smoothing polynomial in the point $t = t_r$ is given by expressions (18) and (20)

$$(\tilde{Y}_r) = \boldsymbol{Y}\boldsymbol{t}(\boldsymbol{t}'\boldsymbol{t})^{-1}\boldsymbol{t}_r \tag{21}$$

Substituting $t_r = t_i$ we can get the values of the smoothing polynomial in the nodal points and the deviations $\tilde{Y}_i - Y_i$ of the smoothing polynomial from the input values may be determined.

It may be shown that by solving the problem formulated in agreement with the expression (18) not only the variance minimum of the result of Eq. (19) is attained, but also the sum of the deviations squared of the smoothing polynomial in the nodes is a minimum, i.e. the expression

$\sum_{i=0}^{n} (\tilde{Y}_i - Y_i)^2$. This minimum value of the sum of the square of the deviations is equal to

$$\left(\left[\sum_{i=0}^{n} (\tilde{Y}_i - Y_i)^2 \right]_{\text{Min}} \right) = \boldsymbol{Y}(\boldsymbol{I} - \boldsymbol{t}(\boldsymbol{t}'\boldsymbol{t})^{-1}\boldsymbol{t}')\boldsymbol{Y}' . \tag{22}$$

The inverse is also valid: by smoothing the input values $Y_0, Y_1, \ldots, Y_n$ with a polynomial of the degree m by the least squares method, i.e. to minimize the quantity $\sum (\tilde{Y}_i - Y_i)^2$, and by linear transformation $\mathscr{L}$ of the smoothing polynomial, the minimum variance is obtained. For solving given problems it is convenient, therefore, to use the well-known method of orthogonal polynomials or other numerical methods. It may be advantageous, however, to use the inverse matrix $(\boldsymbol{t}'\boldsymbol{t})^{-1}$ for considerations of a more general nature.

We shall give the inverse matrices up to $m = 2$ for the case of a constant step τ

$$t_r = r\tau \tag{23}$$

$m = 0$:

$$(\boldsymbol{t}'\boldsymbol{t})^{-1} = \left(\frac{1}{n+1} \right) \tag{24}$$

$m = 1$:

$$(\boldsymbol{t}'\boldsymbol{t})^{-1} = \frac{1}{n(n+1)(n+2)} \cdot \begin{bmatrix} \frac{n(4n+2)}{\tau^0} & -\frac{6n}{\tau^1} \\ -\frac{6n}{\tau^1} & \frac{12}{\tau^2} \end{bmatrix} \tag{25}$$

$m = 2$:

$$(\boldsymbol{t}'\boldsymbol{t})^{-1} = \frac{1}{(n-1)n(n+1)(n+2)(n+3)} \cdot \begin{bmatrix} \frac{(n-1)n(9n^2+9n+6)}{\tau^0} & -\frac{18(n-1)n(2n+1)}{\tau^1} & \frac{30n(n-1)}{\tau^2} \\ -\frac{18(n-1)n(2n+1)}{\tau^1} & \frac{192n^2+24n-36}{\tau^2} & -\frac{180n}{\tau^3} \\ \frac{30n(n-1)}{\tau^2} & -\frac{180n}{\tau^3} & \frac{180}{\tau^4} \end{bmatrix} \tag{26}$$

Both the inverse matrix calculation and application is complicated in the general case with larger values of m. An important case is to increase the node number within the observation interval $(t_0 ; t_n)$. It may be proved that just at a sufficiently large n the matrix inversion may be carried out in a general form. Denoting by S_{jk} the element of the inverse matrix for a sufficiently large n and a constant step τ, the expression (23) being valid, we have

$$S_{jk} = \frac{1}{n} \cdot \left(\frac{-1}{n\tau} \right)^{j+k} \cdot \frac{1}{j+k+1} \cdot \frac{1}{(j!\,k!)^2} \cdot \frac{(m+j+1)!}{(m-j)!} \cdot \frac{(m+k+1)!}{(m-k)!} . \tag{27}$$

FILTRATION, INTERPOLATION AND EXTRAPOLATION OF THE INPUT FUNCTION

In this case

$$\mathscr{L}\{t^i\}_{t=t_r} \equiv t_r^i \tag{28}$$

Again, constant intervals between the nodes of the observation interval are considered; therefore we have, in agreement with (23) and (13),

$$\omega_i = (r\tau)^i . \tag{29}$$

This case is best illustrated by an example.

From (26) and from general equations we have the ith component of the vector operator Ω for $m = 2$:

$$\Omega_i = [(n-1)n(n+1)(n+2)(n+3)]^{-1} . \{3n(n-1)[(3n^2+3n+2)r^0 - 6(2n+1)r^1 + 10r^2]i^0$$
$$+ [-18(n-1)n(2n+1)r^0 + (192n^2+24n-36)r^1 - 180nr^2]i^1 + 30[n(n-1)r^0 - 6nr^1 + 6r^2]i^2\} . \tag{30}$$

The variance of the required value is, with regard to (19),

$$\overline{(x_0 - \bar{x}_0)^2} = \overline{y^2} \, \frac{3n(n-1)(3n^2+3n+2)r^0 - 36(n-1)n(2n+1)r^1 + (252n^2-36n-36)r^2 - 360nr^3 + 180r^4}{(n-1)n(n+1)(n+2)(n+3)} \tag{31}$$

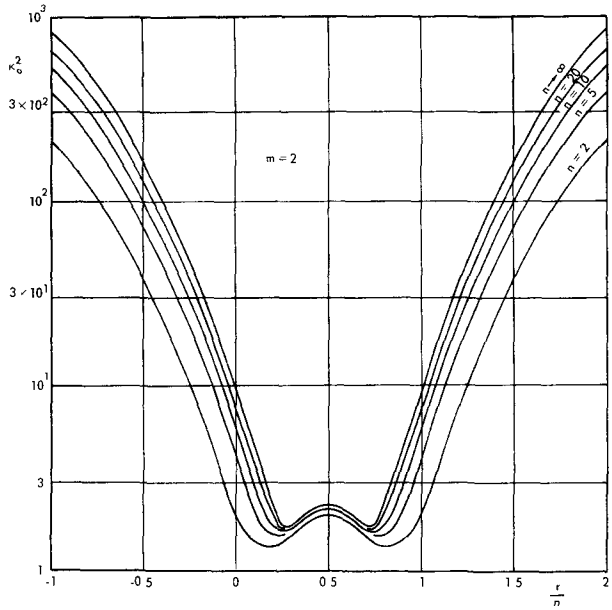


Figure 1. Relative variance $\kappa_0^2 = \frac{\overline{(x_0 - \bar{x}_0)^2}}{\overline{y^2}}$ n of the value of the smoothing polynomial of the 2nd degree in the point $\frac{r}{n}$ in smoothing the measured values $Y_0, \ldots, Y_n$

We may write:

$$\frac{\overline{(x_0 - \bar{x}_0)^2}}{\overline{y^2}} = \frac{\kappa_0^2}{n}. \tag{32}$$

In Fig. 1 the dependence of κ_0^2 on $\frac{r}{n}$ for various $n(m = 2)$ is shown to give an idea of the effect of the choice of n as well as of $\frac{r}{n}$. The interval from $\frac{r}{n} = 0$ to $\frac{r}{n} = 1$ is the observation interval where the nodes, i.e. the points with given input values, are situated at regular intervals of a length $\tau = \frac{T}{n}$. The values of $\frac{r}{n} = 0$ and $\frac{r}{n} = 1$ characterize the operation which is carried out as a mere filtration of input values eliminating random errors, whereas $0 < \frac{r}{n} < 1$ characterizes the interpolation, and $\frac{r}{n} < 0$ or $\frac{r}{n} > 1$ the extrapolation of the input values. All curves are symmetrical with regard to the observation interval, the symmetry axis being $\frac{r}{n} = 0.5$. The increase of n and simultaneous decrease of the step τ at a constant length of the observation interval $T = n\tau$ leads to a decrease of the result variance if the $\overline{y^2}$ is independent of the size of τ i.e. if Eqs. (2) to (4) hold. In [5] an important case is analyzed which refers to treatment of a pulse sequence having Poisson distribution where the situation is substantially different.

Figure 1 suggests that the variance of the value interpolated need not have the minimum in the centre of the observation interval.

It is interesting to compare the values κ_0^2 calculated for various m (Fig. 2) and for high n. The increase of m and the increase of the analytical accuracy of the result at the same time leads essentially to the increase of the variance of this result, except in the case of points for which the curves in Fig. 2 approach one another.

FILTRATION, INTERPOLATION OR EXTRAPOLATION OF THE KTH DERIVATIVE OF THE INPUT FUNCTION

We have

$$\left[\mathcal{L}\{t^i\}\right]_{t=t_r} \equiv \left[\frac{\mathrm{d}^k(t^i)}{\mathrm{d}t^k}\right]_{t=t_r} = \frac{i!}{(i-k)!}\, t_r^{i-k} \tag{33}$$

At a constant step between nodes we have

$$\omega_i = \frac{i!}{(i-k)!}\,(r\tau)^{i-k} \tag{34}$$

As an example, if we have for $m = 4$ and third derivative for a sufficiently large n and a regular step τ:

$$(\Omega_D)_i = \frac{1}{n(n\tau)^3}\left\{\left[-8400 + 15120\left(\frac{r}{n}\right)\right]\left(\frac{i}{n}\right)^0 + \left[161280 - 302400\left(\frac{r}{n}\right)\right]\left(\frac{i}{n}\right)^1 + \left[-705600 + 1360800\left(\frac{r}{n}\right)\right]\left(\frac{i}{n}\right)^2 + \left[1075200 - 2116800\left(\frac{r}{n}\right)\right]\left(\frac{i}{n}\right)^3 + \left[-529200 + 1058400\left(\frac{r}{n}\right)\right]\left(\frac{i}{n}\right)^4\right\} \tag{35}$$

Other examples are given in Ref. [5]

A SIMPLE OPTIMUM ESTIMATOR

The operation mentioned above permits one to simplify calculations which are carried out in treating experimental results as it enables one to calculate once and for all the components of the vector operator for a given type of a frequently occurring problem; the numerical calculation itself may then be limited to carrying out the scalar product $\sum_{i=0}^{n} Y_i\Omega_i$. If the conditions for this operation are fulfilled, the calculations which are associated with

smoothing by the least squares method and which are usually carried out with computers may be done with a desk calculator: or else the computer programme can be substantially simplified. But, it is also possible to treat the measurement results either directly during the measurements or later using a convenient recording method and with the aid of a simple, special digital computer. Such a device is called an *estimator*. Let us suppose that this estimator is capable of performing calculations according to the formula

$$x = \frac{\boldsymbol{Y}\Omega_a}{\boldsymbol{Y}\Omega_b}$$

where Ω_a and Ω_b are any vector-operators and $\boldsymbol{Y}$ is an input-vector.

AN ACCURATE MEASUREMENT OF THE REACTOR PERIOD BY MEANS OF THE ESTIMATOR

The measurement of the reactor period for the purposes of control and safety requires quick treating of the input signal with limited accuracy; usually this is done by computers of the analogue type. But reactor period measurement is also an essential operation in some physical experiments. Physical measurements of the reactor period, however, require high accuracy as compared with operational measurements and often they are performed at a limited reactor power, i.e. with low neutron flux at the position of the detector and in the presence of statistical fluctuations of the input signal. But the required speed is not so high, the periods measured being tenths to hundredths of a second. Both the accuracy requirements and the need to measure long reactor periods oppose the use of operational instrumentation. The method of directly measuring the power-doubling-time with a stop watch, which is often used, is tedious and means performing experiments repeatedly. Therefore, the reactor start-up curve is sometimes recorded numerically and later the reactor period is determined with the computer by handling the record by the least squares method. This method is handicapped by the fact that the measured quantity is not available to the experimenter immediately during the experiment. An economic solution of this problem may appear by the use of the estimator. The input vector $\boldsymbol{N}$ is represented by $(n+1)$ the "newest" data from the detector, which are fed to the estimator in the moments $k_0\tau_1(k_0+1)\tau_1 \ldots (k_0+n)\tau_1$. The vector Ω_a is calculated introducing Eq. (29) into Eq. (17); the vector Ω_b is obtained by introducing Eq. (34) into Eq. (17) for $k = 1$.

We have thus

$$T\text{est} = \frac{\boldsymbol{N}\Omega_a}{\boldsymbol{N}\Omega_b} \cong \frac{[N]_{t=r\tau}}{\left[\frac{dN}{dt}\right]_{t=r\tau}} = T_x$$

where N is the reactor power, T_x is the reactor period.

The period may be also measured indirectly by the power ratio

$$\frac{N_{k+r}}{N_k} = \left[N_0 \exp\left(\frac{t_k + t_r}{T_x}\right)\right] \cdot \left[N_0 \exp\left(\frac{t_k}{T_x}\right)\right]^{-1} = \exp\left(\frac{t_r}{T_x}\right)$$

where t_r is a conveniently chosen interval. This method does not yield directly the value of the reactor period but may be advantageous as it does not use the derivative which results in a higher variance of the result. This measurement may also be carried out with the estimator of the type mentioned.

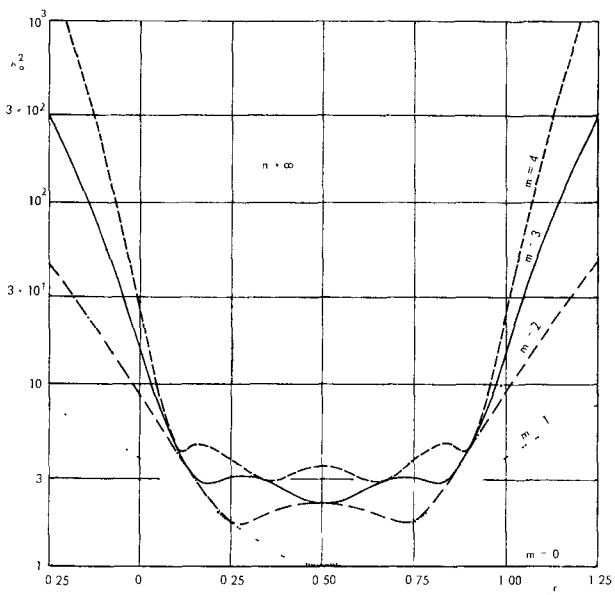


Figure 2. Relative variance $\kappa_0^2 = \frac{\overline{(x_0 - \bar{x}_0)^2}}{\overline{y^2}}$ n of the value of the smoothing polynomial of the degree m of the point $\frac{r}{n}$ in smoothing the measured values $Y_0, \ldots, Y_n$ at a high value of n

MEASUREMENT OF THE REACTOR REACTIVITY BY THE ESTIMATOR

From the kinetics equation we obtain the reactivity

$$\delta k = \frac{T_0 \frac{dN}{dt} + \mu N - T_0 \sum_j C_j \lambda_j}{N},$$

where

- N is the quantity proportional to the reactor power,
- T_0 is the neutron life in the reactor,
- $\mu = \sum_j \mu_j$ is the contribution of delayed neutrons to the multiplication factor,
- μ_j and λ_j are the constants of delayed neutrons, and

C_j is the solution of the equation for the jth group of delayed neutrons.

As has been already shown above, each of the quantities in this ratio may be written as a scalar product of the vector of input values N and a conveniently chosen vector-operator; the reactivity, therefore, may be determined as the ratio of scalar products with the estimator of the type mentioned.

OTHER POSSIBILITIES FOR USING THE SIMPLE OPTIMUM ESTIMATOR

In the applications so far mentioned the estimator gets new input values and so treats the input function in steps. In other cases, however, a whole range of input function may be stored and the required operation carried out, eventually repeatedly, with different operators. In this way the values measured may be smoothed, i.e. we can find the values $\tilde{Y}_0, \ldots, \tilde{Y}_n$ of the smoothing polynomial. For example, by introducing the logarithms of the measured values into the estimator, parameters a_i of the function $\exp(\sum_j a_j z^j)$ optimally fitted in the vicinity of the measured values may be easily found. The estimator with a conveniently chosen vector-operator determines the optimum approximation of the required parameter as a linear combination of the derivatives of the polynomial $\sum_j dj\, z^j$ at a conveniently chosen point z_r. This group of applications, in addition to others, comprises treating the results of measurement of the spatial distribution of the neutron flux and determination of diffusion and relaxation lengths, etc. In measuring the reactor period, the estimator determines the logarithmic derivative with respect to time. If the abscissa of the neutron flux distribution curve near the diffusion boundary is the argument, the estimator can determine the extrapolation length as the ratio of the "filtered" value of the flux on the boundary to its derivative. Another possible application is suggested in measuring the buckling using the flux distribution: the wave equation for neutron flux is decomposed after separating variables into one-dimensional differential equations of the second order. Corresponding Laplacians may be determined from each of such wave equations for a chosen value of the argument as a linear combination of the first and second flux derivatives divided by the value of the flux at a chosen point; this is again of the form convenient for treating the measurement results of the flux distribution with the estimator.

A concluding example for the application of the optimum estimator of the type described from a different field is given. For an optimum control it is often necessary to introduce a feed-back signal derived from a controlled quantity; this signal is obtained by different analytical operations including the use of higher order derivatives. The analogue technique has only limited possibilities in this field. The required operations may easily be carried out with the estimator. The calculations of the vector-operator may be carried out as given, for example in Ref. [6].

Though the optimum estimator, which determines the ratio of the scalar products of vectors is relatively simple, its possible field of application is very wide.

SUMMARY

The numerical operation of the filtration, interpolation and extrapolation of a function, the values of which are obtained with statistical errors, or similar operations with derivatives or integrals of this function or linear combinations thereof, may be carried out by determining the scalar product of the vectors of input values and the vector-operator. The method for calculating the vector-operator which minimizes the variance of the results of the operation is given, and a close coupling with the method of smoothing the input data with a polynomial method minimizing the sum of the squares of the errors in nodes is shown. The method is used to solve a number of problems. A simple optimum estimator calculating the ratio of the scalar products may be used for the realisation of the operations mentioned. Possible applications comprise the accurate measurement of the reactor period, dynamic reactivity measurement, treatment of the results of physical measurements, application in optimum control systems, etc. The method may also be used for simplifying the calculations when using the least squares method and especially for determining the errors originating in such calculations.

REFERENCES

1. Furet, J., *La digitalisation dans le contrôle des piles atomiques*, French Atomic Energy Commission report CEA No. 2175.
2. Tou, J. F. and Joseph, P. D., *Modern Syntheses of Computer Control Systems*, IREE Trans. Appl. Ind., No. 66, pp. 61-65 (May 1963).
3. Joseph, P. D., *Optimum Design of Linear Multivariable Digital Control Systems*, Thesis, Purdue University (1961).
4. Kovanic, P., *On the digital solution of some problems in statistical dynamics*, Nuclear Research Institute, Řež, report no. 1028.
5. Kovanic, P., *Optimum digital information treatment and nuclear engineering instrumentation*, Nuclear Research Institute, Řež, report no. 1030.
6. Volgin, L. N., *The elements of the control machines theory*, Soviet Radio, Moscow (1962).

ABSTRACT - RÉSUMÉ - АННОТАЦИЯ - RESUMEN

A/633 Tchécoslovaquie

Traitement optimal des données numériques et appareils de mesures nucléaires pour réacteurs

par P. Kovanic

Les signaux traités par des appareils de mesures nucléaires sont fréquemment sujets à des perturbations statistiques propres à ces mesures. Ces perturbations sont dues à la nature statistique des processus physiques; sur ces processus, des données ne peuvent être recueillies qu'au moyen d'un traitement des signaux d'entrée. Du point de vue théorique, le problème du traitement optimal des données en présence de perturbations statistiques se résoud par la théorie de Wiener.

Une structure relativement simple de la calculatrice, la possibilité de déterminer d'une manière simple la limite de précision théorique et la possibilité d'exploiter « presque complètement » les données d'entrée sont les résultats intéressants que l'on a pu obtenir en utilisant l'algorithme suivant: le signal d'entrée est un vecteur de dimension finie. Les composantes de ce vecteur sont données par la série finie de sommes de valeurs de fonctions stochastiques et non stochastiques, les paramètres statistiques fondamentaux de ces valeurs étant donnés. Le signal de sortie est le produit scalaire du vecteur d'entrée et du vecteur opérateur. Les composantes du vecteur opérateur sont déterminées par la précision analytique donnée, la dispersion minimale du résultat et le type de la transformation linéaire appliquée à la fonction non stochastique d'entrée. Parmi les cas spéciaux de ce problème, on peut citer les suivants: interpolation numérique, extrapolation et filtration des valeurs d'entrée de la fonction non stochastique, de ses dérivés, de ses intégrales et de ses transformations linéaires.

Ces opérations s'effectuent à partir de valeurs imprécises de la fonction d'entrée, qui sont données en différents points de l'intervalle fini d'observation. La tâche de la calculatrice est la même que celle des filtres optimaux à mémoire finie qui reçoivent des signaux continus.

L'avantage de l'algorithme choisi est que l'on peut calculer une fois pour toutes le vecteur opérateur et simplifier ainsi la calculatrice. Pour passer d'un problème à un autre, il suffit de modifier les composantes du vecteur opérateur sans modifier pour autant la structure ou les parties constitutives des appareils.

Le mémoire fait état des résultats théoriques fondamentaux qui sont indispensables pour des calculs pratiques. L'auteur donne des exemples de l'emploi de cette méthode d'approximation pour la solution de certains problèmes de physique et de génie nucléaires. Parmi ces possibilités d'utilisation, il cite notamment la mesure exacte de la puissance et de la période du réacteur, la mesure de la réactivité instantanée à l'aide des équations de la cinétique des réacteurs, etc. Il est d'autant plus utile d'avoir recours aux calculatrices que le degré de précision voulu est plus grand et que la transformation que la machine doit effectuer est plus complexe; cette complexité dépend surtout des composantes statistiques du signal d'entrée.

A/633 Чехословакия

Оптимальная цифровая обработка информации и приборы для ядерной техники

П. Кованиц

Характерным для сигналов, обрабатываемых приборами ядерной физики и техники, является во многих случаях наличие статистических помех. Эти помехи являются следствием статистического характера физических процессов, о которых приборы должны давать информацию на основе обработки входных сигналов. Проблема оптимальной обработки информации при наличии статистических помех решена теоретически теорией Винера, однако применение приборов и фильтров этого типа ограничивается простыми случаями или случаями с невысокими требованиями к точности работы.

Интересные результаты, то есть относительно простую структуру цифрового устройства и возможность простого определения теоретического предела точности задачи, так же как и возможность «почти полного» исчерпания входной информации, дает следующий алгорифм: входным сигналом является вектор; составляющие этого вектора конечного размера даны конечной последовательностью сумм цифровых значений неслучайной функции и случайной функции с заданными основными статистическими параметрами. Выходной сигнал получается как скалярное произведение входного вектора на вектор-оператор. Составляющие вектора-оператора определены на основе требования заданной аналитической точности, минимума дисперсии результата и типом линейного преобразования, выполняемого на входной неслучайной функции. Частными случаями этой задачи являются: цифровое интерполирование, экстраполирование или фильтрация значений входной неслучайной функции, ее производных, интегралов или их линейных преобразований.

Эти операции проводятся на основе неточно известных значений входной функции, данных в разных точках конечного промежутка «наблюдения». Цифровое устройство здесь играет роль, аналогичную роли оптимальных филь-

тров с конечной памятью, работающих с непрерывными сигналами.

Преимуществом выбранного алгорифма является возможность рассчитать для данной задачи раз навсегда вектор-оператор и упростить таким образом цифровое устройство. Переход на другую задачу осуществляется путем замены цифр составляющих вектора-оператора без изменения структуры и компонент устройства.

В докладе приводятся основные результаты теории, необходимые для практических расчетов. Далее указываются примеры применения указанного подхода к некоторым задачам ядерной физики и техники. Из возможных областей применения следует указать точное измерение мощности и периода реактора с использованием уравнений кинетики реактора и др.

Необходимость перехода к устройствам цифрового типа возрастает с повышением требований к точности и с повышением требований к сложности преобразований, выполняемых аппаратурой, и особенно зависит от того, насколько может быть входной сигнал «чист» от статических составляющих.

A/633 Checoslovaquia

Tratamiento óptimo de la información digital e instrumentación de ingeniería nuclear

por P. Kovanic

Las señales que se manejan en física y en instrumentación nucleares están sujetas en muchos casos a perturbaciones estadísticas cuya presencia constituye su propiedad característica. Estas perturbaciones se deben a la naturaleza estadística de los procesos físicos acerca de los cuales se obtiene información mediante el tratamiento adecuado de las señales de entrada. El problema del tratamiento óptimo de la información en presencia de perturbaciones estadísticas se resuelve teóricamente con la teoría de Wiener, pero el correspondiente tipo de aparatos y filtros sólo puede aplicarse en casos sencillos y cuando no se exige una gran precisión.

Usando el algoritmo que se indica a continuación se obtuvieron resultados interesantes, tales como una estructura de la calculadora digital relativamente simple, posibilidad de determinar de modo sencillo el límite teórico de precisión y, al mismo tiempo, posibilidad de una explotación "casi completa" de la información de entrada. Dicho algoritmo consiste en asimilar la señal de entrada a un vector de dimensión finita. Las componentes de este vector están dadas por las series finitas de sumas de valores de funciones no aleatorias y de funciones aleatorias, dándose los parámetros estadísticos básicos de las últimas. La señal de salida se obtiene como producto escalar del vector de entrada y del operador vector. Las componentes del operador vector están determinadas por los requerimientos de precisión analítica, por la dispersión mínima de los resultados y por el tipo de la transformación lineal aplicada a la función no aleatoria de entrada. Casos especiales de estos problemas son los siguientes: interpolación digital, extrapolación y filtrado de los valores de entrada de la función no aleatoria, sus derivadas, sus integrales y sus transformaciones lineales.

Estas operaciones se efectúan partiendo de los valores imprecisos de la función de entrada que se obtienen en diferentes puntos del intervalo finito de observación. La calculadora digital tiene la misma misión que los filtros óptimos con memoria finita que se alimentan con señales continuas.

El algoritmo seleccionado tiene la cualidad de permitir calcular, de una vez para siempre, el operador vector para una aplicación dada y de este modo simplificar la calculadora digital. Es posible el paso a otro problema mediante el intercambio de dígitos (componentes del operador vector) sin cambio en la estructura y en los componentes de la instrumentación.

En la memoria se mencionan los resultados teóricos fundamentales necesarios para cálculos prácticos. Se dan ejemplos de empleo de esta aproximación en algunos problemas de física e ingeniería nucleares. Como posibles campos de empleo se dan medidas precisas de potencia y de período de reactores, medidas de reactividad debida a neutrones inmediatos empleando las ecuaciones cinéticas del reactor, etcétera. La necesidad de empleo de calculadoras digitales crece al aumentar la precisión exigida y al aumentar la complejidad de las transformaciones a efectuar, influyendo especialmente en ello las componentes estadísticas de la señal de entrada.

Automatic control of the average core flux by measuring N^{16} coolant activity at the FRM Munich Research Reactor

By M. Sommer *

Neutron beam experiments at several beam-tubes and sample irradiations at various locations in research reactors bring up the problem of maintaining a constant flux at all locations and for any given period of time. Usually the flux at the reflector of the core is measured in order to control the total flux. As a result the flux at the neutron detector is kept constant, but this leaves the possibility open for the average core flux to vary by as much as 20% because of a variation in flux distribution in and around the core. In most cases this variation is due either to a rearrangement of the experimental set-up or to positional changes of the control rods during operation. Often research reactors are operated at constant power in equilibrium xenon concentration over an extended period of time. This state is reached after about 40 hours of operation and requires only small changes in the rod positions to result in a constant core flux.

In the case of short or intermittent operations, flux constancy is poor, especially since the flux is detected at one position only. To improve this, another control system was developed for the FRM which is based on the N^{16} coolant activity. The use of N^{16} coolant activity as a power indication has been reported by several authors [1-6]. This paper describes an automatic control system keeping the N^{16} coolant activity constant and thereby the average core flux.

MEASUREMENT OF N^{16} ACTIVITY

As is known, the unstable nitrogen N^{16} isotope is produced by a (n,p) reaction from the oxygen isotope O^{16} of the water during its flow through the core. This reaction involves fission neutrons only, and therefore the number of N^{16} nuclei produced per unit volume of water is proportional to the average fission flux. The N^{16} nuclei decay under β-emission accompanied by high energy γ-radiation (6.14,7.11, ... MeV) in 74% of all decays. The half-life is 7.3 seconds.

An ionization chamber detects the γ-radiation of the N^{16} activity. This chamber consists of a sealed nitrogen-filled tube with guard rings and coaxially arranged copper electrodes. It is mounted parallel and close to the coolant pipe. The effective volume is 3 000 cm^3. For 1 MW reactor power the chamber current is of the order of 10^{-9} amperes. An accurate measurement of this current necessitates careful protection of the signal line against humidity. The current is measured by a vibrating reed electrometer, the input resistance of which is stabilized by a thermostat. The output is recorded, and measured by a digital voltmeter, which in turn gives the signal for the control system described below. The stability of the set-up was tested over a period of one week using a Co^{60} γ-source. The variations did not exceed 0.2%.

It is a particular advantage, that the N^{16} activity does not vary with limited fluctuations of the flow rate provided the activity is measured some distance from the core. The influence of fluctuations may be derived from Eq. (1), which gives the N^{16} activity per unit volume of water at any location in the pipe system:

$$a = n\sigma\emptyset_s \left(1 - e^{\frac{-\lambda V_1}{D}}\right) e^{\frac{-\lambda V_2}{D}} \qquad (1)$$

a = N^{16} activity per unit volume of water
n = number of O^{16} nuclei per unit volume of water
σ = effective cross section of N^{16} for a fission spectrum
$\emptyset_s$ = average fission flux in the core
λ = decay constant of N^{16}
D = coolant flow rate
V_1 = volume of the core
V_2 = volume of the section of the pipe between core exit and chamber location

Equating the differential quotient da/dD to 0 leads to Equation (2)

$$\left(1 + \frac{V_1}{V_2}\right) e^{\frac{-\lambda V_1}{D}} = 1 \qquad (2)$$

$$\text{or } \frac{\lambda V_2}{D} = 1 - \tfrac{1}{2}\frac{V_1}{V_2} + \tfrac{1}{3}\left(\frac{V_1}{V_2}\right)^2 - + \cdots$$

Disregarding powers higher than one, gives the result

$$\tfrac{1}{2}\frac{V_1}{D} + \frac{V_2}{D} = \frac{1}{\lambda} \qquad (3)$$

Obviously the sum $V_1/2D + V_2/D$ is the average transport time T_1, which elapses between generation of the N^{16} nuclei in the core and their detection in the measuring chamber. This time, T_1, is equivalent

* Technische Hochschule München.

to $1/\lambda$ (10.5 s). For a given coolant flow rate, the transport time T_1 can be used to determine the distance between the core and the optimum position of the chamber on the tube. Small flow rate fluctuations do not influence the activity at the chamber position, since an increased decay due to an increased transport time is compensated by an increase of the activation time in the core and vice versa. Figure 1 shows the dependence of the activity on the flow rate, Fig. 2 the variation of the N^{16} activity at the optimum position of the chamber for small changes of the coolant flow rate. The observed fluctuations stay within $\pm$ 4% and the resulting error always remains below 0.1%.

Other possible sources of error are activities other than that of N^{16}. The activities of N^{17} and O^{19} are small compared with that of N^{16}, and of fixed ratio to it. The activity due to impurities in the water depends on the past and present operating conditions of the reactor. It has been shown that the only impurities of importance are Al^{28}, Mg^{27} and Na^{24}, originating from aluminium corrosion, and Ar^{41}. These all have a long decay time compared with N^{16} and their activities may accumulate over several coolant cycles. For example, the Na^{24} equilibrium concentration in the coolant is approximately reached after 60 hours of constant power operation. The influence of impurities on the measurement of N^{16} activity has been determined experimentally. After 170 hours of operation at a constant power of 1 MW, the reactor was shut down and the N^{16} chamber current continued to be recorded for another hour. This current was caused by the activity of impurities produced before shut-down. The analysis of the decreasing current led to the conclusion that in our case the error caused by the maximum possible activity of impurities always stays below 0.06%.

A change in coolant density may also be a source of error. Such a change originates from an increase of pool water temperature during operation. At the FRM, these temperatures ranged from 18° to 24°C. The decrease of activity due to such a decrease of density cannot exceed 0.2%.

All these errors add up to a maximum possible error of 0.5%. The output of the N^{16} circuit is related to the average flux within this limit.

The instantaneous activity at the chamber position varies due to fluctuations in coolant mixing, which originate from the turbulence in the coolant mixing chamber following the core. These variations may however be averaged, resulting in a time independent detection of the mean activity. The N^{16} circuit is therefore damped with a time constant of $T_2 = 5$ s.

AUTOMATIC CONTROL SYSTEM

The time delay T_2 together with the transport time T_1 must be taken into account when setting up a system for the automatic control of the average core flux. It is obvious that this time delay prohibits a secure and stable control of the flux by means of the N^{16} circuit only. A fast auxiliary circuit based on the current on a neutron chamber supplements the former system.

Figure 3 shows the complete control system. The compensated chamber of the fast auxiliary circuit measures the neutron flux at the reflector near the core. The current of this chamber is measured by means of operational amplifiers and compared with a nominal value which in turn is influenced by the N^{16} circuit. The deviation of the ionisation current from this nominal demand is amplified and converted into alternating current and drives the control rod motor. Thus the usual requirements of a reactor control system for fast equalisation of changes in reactivity and neutron flux can be satisfied, and furthermore the average core flux is kept constant. The digital output of the N^{16} circuit is compared with a preset value. In case the difference between these two values exceeds an allowable magnitude, a reversible motor slowly takes the place of the nominal demand of the auxiliary circuit until the average neutron flux has again reached the desired value. The possible variation rate of the nominal demand of the last auxiliary circuit is limited to 0.2% per minute. This rate is sufficient to control all variations of the average flux with respect to the flux at the auxiliary chamber. It is, however, small enough to leave the control system insensitive to short-time variations of the N^{16} activity due to mixture fluctuations as discussed above. The system is stable in spite of the time delay of 15 s. It has been proved very safe under operation and is now a part of the reactor instrumentation.

FLUX DISTRIBUTION FOR A CONSTANT AVERAGE CORE FLUX

Flux measurements were made to test for variations in the flux distribution which remain after introducing the N^{16} control system in-core. A U^{235}-thermophile was constructed to determine the vertical flux distribution in some special fuel elements of the core. As an example Fig. 4 shows the flux curves determined for two different settings of the control rods TS2 and TS3. The two settings correspond to different poisoning states of the reactor, the state one hour after start-up (dotted lines) and the state of equilibrium xenon concentration after 46 hours of operation at a constant power of 1 MW (solid lines). An analysis of the flux measurements verifies the assumption that the average core flux is kept constant by the N^{16} control system for various states of operation. The remaining local flux variations, which develop even for a constant average flux, are caused by the changes of the control rod positions. These variations are unavoidable, but may however be reduced to a minimum by choosing a special core arrangement. The control rods, which are driven to compensate for poisoning and burn-up, are placed

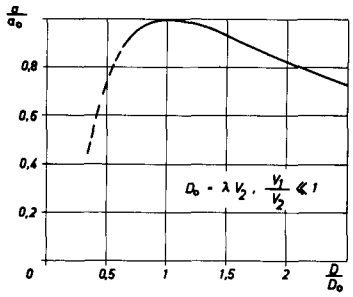


Figure 1. N^{16} activity a as a function of the water flow rate D (normalized with respect to a_0 at $D_0 = \lambda V_2$)

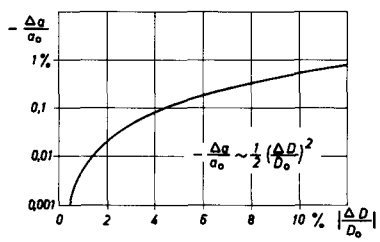


Figure 2. Variation $\Delta a/a_0$ of the N^{16} activity for small changes $\Delta D/D_0$ of the coolant flow rate at the optimum chamber position

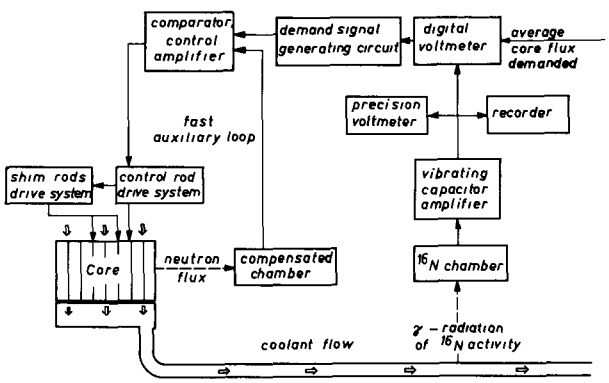


Figure 3. N^{16} control system

symmetrically with respect to the vertical axis of the core. Their control range centres around the position half way down the core. Figure 5 shows the flux distribution for an improved arrangement of the core. The stability of local fluxes due to the constant average flux and the chosen core arrangement is obvious.

The N^{16} control system proved to be very useful. For instance, the variations of intensity of a neutron beam, which was monitored over a period of several weeks under intermittent reactor operation, stayed below 1.8%. For continuous operation at a constant power of 1 MW the variations were smaller than 0.7% as compared with former variations of 12% at the same beam tube.

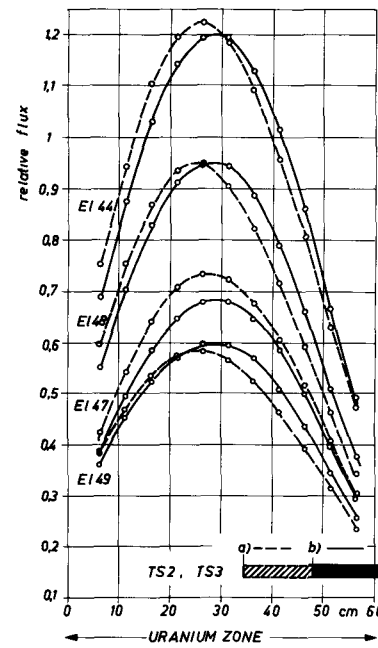


Figure 4. Vertical flux distribution for various fuel elements (*a*) one hour after start-up, (*b*) after 46 hours of operation at constant N^{16} coolant activity

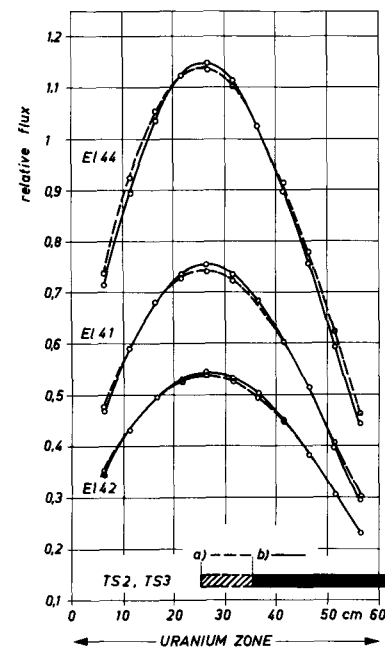


Figure 5. Flux distribution in a symmetric core (*a*) one hour after start-up, (*b*) after 48 hours of operation at constant N^{16} coolant activity

ACKNOWLEDGEMENT

The author would like to express his gratitude to Dr. L. Koester for helpful advice and many stimulating discussions.

REFERENCES

1. Drucker, E. E., and Wallace, W. D., *Determination of Reactor Power by Coolant Activity Monitoring,* Nuclear Sci. Eng., *3,* 215-231 (1958).
2. Lalere, J., *Contrôle de la puissance d'une pile par la mesure de l'activité du fluide de refroidissement — cas particulier de EL 3,* French Atomic Energy Commission report CEA No. 1196 (1959).
3. Krock, R. E., and Kresny, H. S., *Nitrogen N^{16} monitoring systems,* WCAP 6043, 12-34, USA (1960).
4. Krock, R. E., *Evaluation of N^{16} monitoring in WTR primary coolant for measuring flow and reactor power,* WCAP 6045, USA (1961).
5. Kongso, A. E., Skanborg, P. Z., Nielsen, K. O., *Power measurement at the Danish reactor DR 2 based on N^{16} activity of the primary coolant,* Riso report No. 29 (1961).
6. Tiberghien, R., *Chaîne de puissance "Azote 16" sur le circuit de réfrigération de MELUSINE,* thèse; Faculté de Sciences de l'Université de Grenoble (1962).

ABSTRACT - RÉSUMÉ - АННОТАЦИЯ - RESUMEN

A/647 République fédérale d'Allemagne

Contrôle automatique du flux neutronique moyen dans le cœur du réacteur de recherche FRM de Munich, par la mesure de l'activité de l'azote 16 dans le refroidisseur

par M. Sommer

La précision des expériences faites avec un réacteur de recherche est souvent limitée par les variations du flux en valeur moyenne et en distribution spatiale. En règle générale, le flux est contrôlé en un point arbitraire au bord du cœur et les mouvements inévitables des barres de commande causent de grandes variations du flux local. Nous nous sommes efforcés d'apporter à cette méthode deux améliorations: nous contrôlons le flux moyen et, par suite, la puissance du réacteur en utilisant l'activité de l'azote 16 dans l'eau de refroidissement. Les barres de commande peuvent ainsi être placées dans des positions favorables où leurs mouvements causent le minimum de perturbations dans la distribution du flux. L'activité de l'azote 16 par unité de volume d'eau est proportionnelle au flux moyen et par conséquent à la puissance du réacteur. Le rayonnement gamma est mesuré dans un certain volume du courant d'eau de refroidissement à quelque distance du cœur. On montre que pour un temps de transport de 10,5 s l'activité au détecteur ne varie pas lorsque les fluctuations du débit restent entre certaines limites. Le retard résultant empêche un contrôle sûr et stable du réacteur au moyen du circuit à azote 16 utilisé seul. Une boucle auxiliaire rapide fonctionnant d'après le courant d'un détecteur de neutrons complète le circuit à azote 16. Les changements rapides du flux de neutrons sont compensés par le circuit auxiliaire. Le flux moyen est maintenu constant en utilisant le circuit à azote 16.

Pour observer les variations de la distribution de flux qui persistent après l'introduction du système de contrôle qui vient d'être décrit, on a fait des mesures de flux dans le cœur. Les variations restantes de flux local résultent des changements de position des barres de commande. Ces variations sont inévitables. Toutefois, elles peuvent être réduites au minimum en choisissant une disposition spéciale du cœur. Les barres de commande qui sont insérées pour compenser l'empoisonnement et la combustion sont placées symétriquement par rapport à l'axe vertical du cœur. Les positions courantes sont au voisinage de la position de demi-insertion dans le cœur. Les mesures de flux montrent la stabilité des flux locaux qui résulte de la stabilité du flux moyen et de l'amélioration de la disposition du cœur.

A/647 ФРГ

Автоматический контроль среднего потока в Мюнхенском исследовательском реакторе FRM путем измерения активности N^{16} в теплоносителе

М. Зоммер

Точность экспериментов, проводимых в исследовательском реакторе, часто ограничивается как флуктуациями среднего значения, так и пространственного распределения потока. Обычно поток нейтронов контролируется в произвольно выбранной точке вблизи активной зоны. Перемещение регулирующих стержней неизбежно вносит значительные изменения локальных потоков. Мы регулируем средний поток нейтронов и, таким образом, мощность реактора путем использования активности N^{16} в охлаждающей воде. При этом способе контроля регулирующие стержни могут находиться в подходящих положениях, соответствующих минимальному возмущению распределения потока. Активность N^{16} в единичном объеме воды пропорциональна среднему потоку и, следовательно, мощности реактора. γ-активность измеряется в потоке охлаждающей воды на некотором расстоянии от активной зоны. Было показано, что за время прохождения воды 10,5 *сек* активность детектора слабо меняется при ограниченной флуктуации скорости потока воды. Результирующее запаздывание не обеспечивает надежного и устойчивого регулирования реактора с использованием только схемы с N^{16}. Помимо схемы с N^{16} имеется быстродей-

ствующая вспомогательная схема, основанная на использовании сигнала от нейтронного детектора. Кратковременные применения нейтронного потока регулируются дополнительной схемой.

Средний поток поддерживается постоянным с помощью схемы с N^{16}. С целью применения изменений в распределении потока, которые возникают после введения описанной системы регулирования в активную зону были проведены соответствующие изменения потока. Остаточные применения локального потока обусловливаются перемещением регулирующих стержней. Эти изменения неизбежны. Однако они могут быть сведены до минимума в результате выбора соответствующей конструкции активной зоны. Регулирующие стержни, которые используются для компенсации поглощения и выгорания, размещаются симметрично относительно вертикальной оси активной зоны. Регулирующий участок этих стержней вводится в активную зону на половину своей длины. Измерения потока показали стабильность локальных потоков благодаря постоянному значению среднего потока, а также в результате усовершенствования конструкции активной зоны.

A/647 República Federal de Alemania

Control automático del flujo medio en el núcleo por medio de la medida de la actividad de ^{16}N en el refrigerante en el reactor de investigación FRM de Munich

por M. Sommer

A menudo la precisión de los experimentos que se hacen con un reactor de investigación está limitada por las fluctuaciones tanto del flujo medio como de su distribución espacial. De ordinario el flujo se gobierna en un lugar cualquiera cercano al núcleo y los movimientos inevitables de las barras de control producen grandes variaciones del flujo local. Se ha intentado introducir dos mejoras: por medio de la actividad del nitrógeno-16 en el agua de refrigeración se controla el flujo medio y, por tanto, la potencia del reactor. Si se hace así, las barras de control pueden situarse en posiciones favorables, donde sus movimientos causan una perturbación mínima en la distribución de flujo. La actividad del ^{16}N producido por unidad de volumen de agua es proporcional al flujo medio y por ello a la potencia del reactor. Se fija un cierto volumen de la corriente de agua a cierta distancia del núcleo y se mide su actividad gamma. Se demuestra que, con un tiempo de transporte de 10,5 s, el recuento del detector no varía con variaciones limitadas del caudal. El retraso que así se introduce hace que no pueda controlarse el reactor sólo con el circuito de ^{16}N de forma segura y estable y se le suplementa con un circuito rápido auxiliar mandado por la corriente de un detector neutrónico. El circuito auxiliar nivela los cambios rápidos del flujo neutrónico. El circuito de ^{16}N mantiene constante el flujo medio.

Se han realizado medidas de flujo en el interior del núcleo a fin de comprobar las variaciones de la distribución de flujo que subsisten tras la introducción de este sistema de control. Las variaciones locales del flujo que persisten se deben a los cambios de posición de las barras de control y son inevitables. Pero si se elige una disposición especial del núcleo se pueden reducir a un mínimo. Las barras de control que se mueven para compensar el envenenamiento y el quemado se colocan simétricamente respecto del eje vertical del núcleo. Su zona de control se centra hacia la mitad de la altura del núcleo. Las medidas de flujo muestran la estabilidad de los flujos locales debida a la constancia del flujo medio y a la mejora en la disposición del núcleo.

Measurement of high-dose gamma fluxes at reactor pulses and strong gamma sources by the conductivity of cuprous oxide

By O. Bobleter and P. Vajda*

In radiation dosimetry today frequent use is made of the fact that semiconductors greatly change their physical properties under high energy radiation. Among others, silicon (for α particles) [1], germanium (for β particles) [2], cadmium sulphide (for γ radiation) [3], indium phosphide (for fast neutrons) [4] are successfully employed. A characteristic feature is that semiconductors, which are also known as photoconductors, are efficient as radiation detectors. On account of this we decided to examine more closely cuprous oxide (Cu_2O), which has been somewhat neglected in this field.

Most pertinent work on cuprous oxide deals with its properties as a photoconductor. In this connection basic results were more recently obtained by Pastrnyak and Kužel [5], A. F. Joffe and co-workers [6] and the group Gorbanj *et al.* [7].

Up to date, cuprous oxide has not been examined especially as a detector for γ radiation; only relative measurements with and without neutrons were made [8], and the usefulness of cuprous oxide rectifiers under reactor radiation conditions was examined by the Lark-Horovitz group in Oak Ridge [9]. We therefore made a systematic examination of the changes of electric conductivity of cuprous oxide under γ irradiation. Cuprous oxide was tested to see how far it can be employed as a high dose sensitive material.

The main object of this investigation was to examine the extent to which the changes in the conductivity of cuprous oxide constitute a measure for high doses of strong gamma sources; and how far very short gamma pulses can be recorded, as can be produced by the TRIGA-Mark II Pulsing Reactor or may occur accidentally in excursions in nuclear reprocessing and fission plants.

PREPARATION OF SAMPLES

Cuprous oxide is a typical vacancy type semiconductor, whose electric conductivity is due mainly to deviation from the stoichiometric composition. Its crystal lattice shows a deficiency in copper ions, while the oxygen ions are in excess. The copper vacancies act as acceptor levels for the electrons in the valence band, so that at room temperature there is constantly a considerable vacancy type conductivity. This behaviour is particularly strongly marked at the grain boundaries of the polycrystalline material, as here the vacancy concentration is especially high. It was obvious, therefore, that the dependency of the electric conductivity on the number of crystal grains per unit area should be examined in order to determine the most favourable conditions for the production of the desired form of cuprous oxide.

The cuprous oxide was produced according to the method developed by Blankenburg and co-workers [10]. Copper plates ($1 \times 20 \times 80$ mm in size) were freed of the oxide layer by emery paper, degreased with acetone, and etched in $1N$ nitric acid. The copper was rinsed in distilled water and put in a cold crucible furnace. To support the copper samples 0.1 mm thick platinum was used, which was clamped into small chamotte stones. A 1 mm thick copper plate was oxidized to cuprous oxide in the following way: the copper sample was glowed to copper oxide (CuO) for 48 hours at 950 ± 4 °C under access of air (150 torr oxygen pressure (p_{O_2})). Immediately afterwards it was reduced to cuprous oxide (Cu_2O) at 1 020 °C under 1.5 torr p_{O_2} for twenty hours. For this purpose technical grade nitrogen was used, which contained 1.5 torr oxygen. The use of this gas considerably simplified the procedure. For further twenty hours the material was annealed at 1 080 °C and 1.5 torr p_{O_2} in order to obtain a relatively strong growth of the crystal grains. Then the furnace was turned off and the cuprous oxide left in the closed furnace (still under 1.5 torr p_{O_2}) until it had cooled to approximately 650 °C, then removed and chilled in air.

The oxide layer which had formed during the cooling process was removed with emery cloth of different coarseness. The cleaned cuprous oxide was polished and etched in $1N$ nitric acid, to make the grain boundaries of the crystals visible. In general it was established that, when the same thickness of copper was used, the grain-size of the crystals was greater at higher annealing temperatures.

* Atominstitut der Österreichischen Hochschulen, Vienna (present address: Research Establishment RISÖ, Roskilde-Denmark).

The maximum temperature for annealing was 1 090 °C, and in this instance it was possible to obtain crystal grains with a surface area of 10-12 mm^2. At still higher temperatures plastic deformation of the material occurred.

The electrical contacts were obtained by covering the samples partly with a thin layer (about 500 Å) of gold by high vacuum evaporation, and fixing copper wires (0.3 mm diameter) with a silver plastic mass. It was proved with a curve-tracer that these contacts gave no rectifier effects. The samples were then dipped in a solution of polyvinylacetic acid and acetone, dried and sealed in light-proof plastic envelopes.

DEPENDENCY OF ELECTRICAL CONDUCTIVITY ON THE GRAIN SIZE

As has already been mentioned, the concentration of defects on the grain boundaries is especially high, so that material of a finely grained nature will behave differently in respect of its electrical properties from that of a coarse crystalline structure. To investigate this behaviour in the case of cuprous oxide, several samples of varying grain size were examined under the microscope (constant field of vision approximately 35-fold magnification), and tested, together with some single crystals, for their electrical resistance. The samples were tested in a room under a constant temperature of ± 0.1 °C, and the resistance determined with a precision Wheatstone bridge. The results of the measurements are given in Fig. 1.

The dependency of the conductivity (σ) on the number of grains per unit area (n) shows two regions: for the one, in the case of larger numbers of grains per unit area, the conductivity is proportional to n (A in Fig. 1); for the other, in the case of smaller numbers of grains per unit area, the conductivity levels off at a constant value (B in Fig. 1). If one assumes that at the grain boundaries the crystal defects are accumulated and that this contributes considerably to the conductivity, the result is in fact that, with increasing fineness of grain-size, the current is conducted only over the grain boundaries, and the conductivity increases proportionally to the number of grains per unit area. In the case of large crystals, the conduction of current through the interior of the grains plays an increasing role, so that in the extreme case of single crystals a constant electrical conductivity is obtained (at constant temperature), more or less independently of their origin. Andrijewskij *et al.* [11] also obtained similar results, but have proved only the linear part of the conductivity curve.

IRRADIATION WITH HIGH DOSE RATES FROM GAMMA SOURCES

1 c caesium-317, 1 c, 1 000 c and 2 000 c cobalt-60 activities were used as sources. The constant

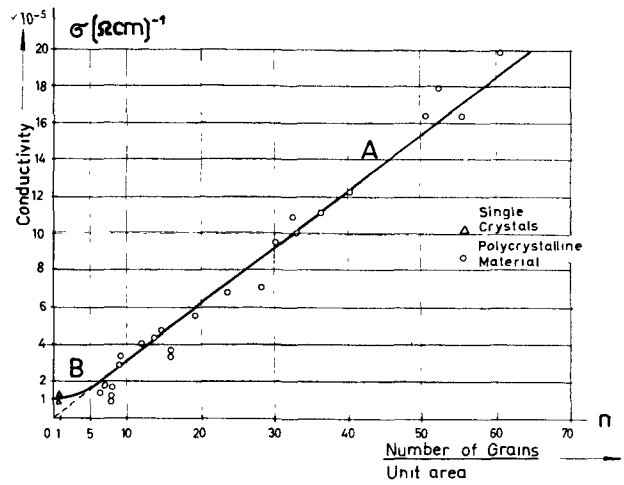


Figure 1. Conductance of cuprous oxide as function of number of grains per unit area

temperature (± 0.01 °C) necessary for the experiment was maintained by covering the plates with foam-type heat-insulating polystyrene. The constancy of temperature was controlled with the Wheatstone bridge, which was in use in resistance measurements (measurement accuracy 0.03%). The dose-rates of the radiation sources were measured either with a pocket ionisation dosimeter or with a chemical dosimeter (according to Fricke).

The values of the electrical resistance of three cuprous oxide samples under irradiation at the caesium and cobalt sources are given graphically in Fig. 2. The curve Fig. 2(a) represents the measurements of a polycrystalline material (number of grains per unit area = 11), while for the curves Fig. 2(b) and 2(c) single crystals were used. In all irradiation experiments the samples show the same behaviour qualitatively: the resistance, which is practically constant without irradiation, decreases rapidly within a few seconds of the commencement of radiation, after 1 to 2 minutes the curve becomes less steep, and then falls linearly. When the irradiation ceases, the resistance suddenly increases (but not as strongly as the decrease at the commencement of irradiation) and after a few minutes remains at a constant value. When irradiation is renewed, the resistance again decreases steeply, as in the first irradiation, but quantitatively somewhat more weakly. The linear part is a little flatter than at first; in the case of especially fine-grained samples the resistance in fact increases in spite of continued irradiation.

The results of the measurements at the caesium source were used as the basis for examining the relation between grain size per unit area (n) and the relative decrease in resistance ($\Delta R/R$) (Fig. 3). ΔR is the resistance decrease which occurred in a ten-minute irradiation period, from the fifth to the fifteenth minute after commencement of irradiation, that is, in the linear region of the curve. It can clearly be seen from the behaviour of the curve that the coarse crystalline samples are considerably more sensitive to radiation than the fine-grained. One

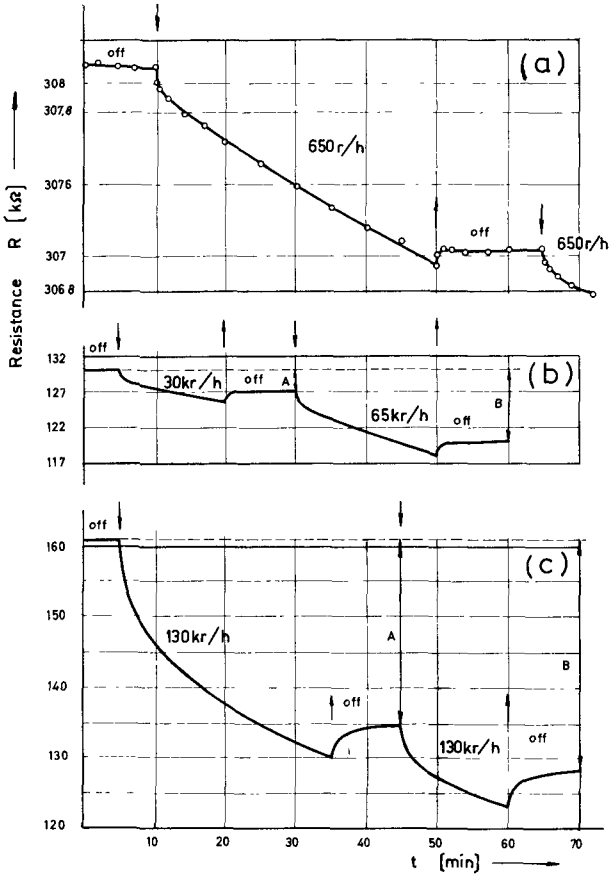


Figure 2. Resistance as function of time of irradiation with different dose-rates

(*a*) Polycrystalline material; 650 r/h; 1 c caesium-137
(*b*) Single crystal; 30 and 65 kr/h; 2 000 c cobalt-60
(*c*) Single crystal; 130 kr/h; 2 000 c cobalt-60

can therefore assume that the latter, even without irradiation, already have so many charge carriers, that those supplementarily generated by radiation cause only little additional effect. Therefore only coarse crystalline material was used for further experiments.

An analysis was made to establish any existing relationship between the resistance decrease or change in conductivity and the gamma dose-rate. It can be seen from Fig. 2(b) that, at relative moderate dose-rates, there is in fact an approximate proportionality between the resistance decrease and the dose: the difference A in resistance is in the ratio 1:3.33 to difference B, while the ratio of the first dose to the sum of both doses is 1:3.87. Therefore dose-rates can be determined approximately by the decrease in resistance of cuprous oxide.

With higher doses, however, the error in the resistance ratios (Fig. 2(c)) is too great to give useful values for the dose-rates. Further experiments, of which Fig. 4 is an example, showed that a quantitative relation between the dose-rate and the conductivity of the cuprous oxide sample does exist.

On the assumption that the concentration of defects (N), which are caused by the effect of the

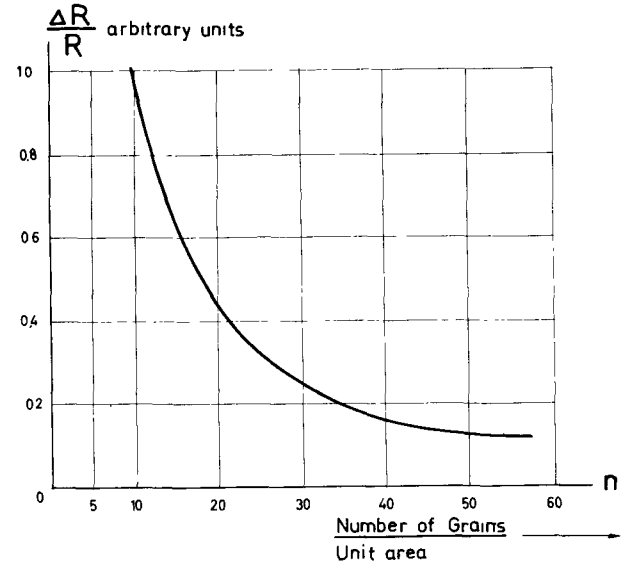


Figure 3. Relative decrease in resistance as function of the number of grains per unit area: radiation source 1 c caesium-137

dose (r) on cuprous oxide, is responsible for the change in conductance, there would have to be a direct proportionality between N and r. Since this proportionality is lost at higher doses, it must be assumed that the defects recombine. And since the recombination of defects formed by radiation often takes place with already existing defects (N_0), and since the latter occur in excess in cuprous oxide (N_0 = constant), the recombination can be written in the form of a zero order-reaction:

$$\frac{dN}{dr} = k_1 - k_2 N_0 N \qquad (1)$$

Equation (1) becomes upon integration

$$N = k_1/k_2 N_0 - C \exp(-k_2 N_0 r) \qquad (2)$$

and in logarithmical form and by the introduction of the change in conductance ($\Delta\sigma$) instead of the concentration of defects N we get

$$\log(K_1 - \Delta\sigma) = K_2 r - K_3 \qquad (3)$$

Table 1 gives the conductance values and doses obtained from Fig. 4. If log $\Delta\sigma$ is plotted versus dose r (Fig. 5), a curve (A) is obtained. For several samples the K_1 value could be uniformly taken as 2.50×10^{-6} [Ω^{-1}] with relatively great accuracy. The plotting of log $(2.50 \times 10^{-6} - \Delta\sigma)$ versus the dose (r) therefore is a linear function (B in Fig. 5).

Using cuprous oxide samples, the gamma flux of gamma sources of different strengths was determined, according to the method described. Moreover, with the aid of small samples sealed in watertight envelopes the dose-rate of the TRIGA-Mark II reactor (when shut down) was measured in certain places only accessible with great difficulty for other detectors, and calculated according to Eq. (3). The samples were first measured in a thermostatic bath, immersed for a certain period (e.g. 5-10 minutes)

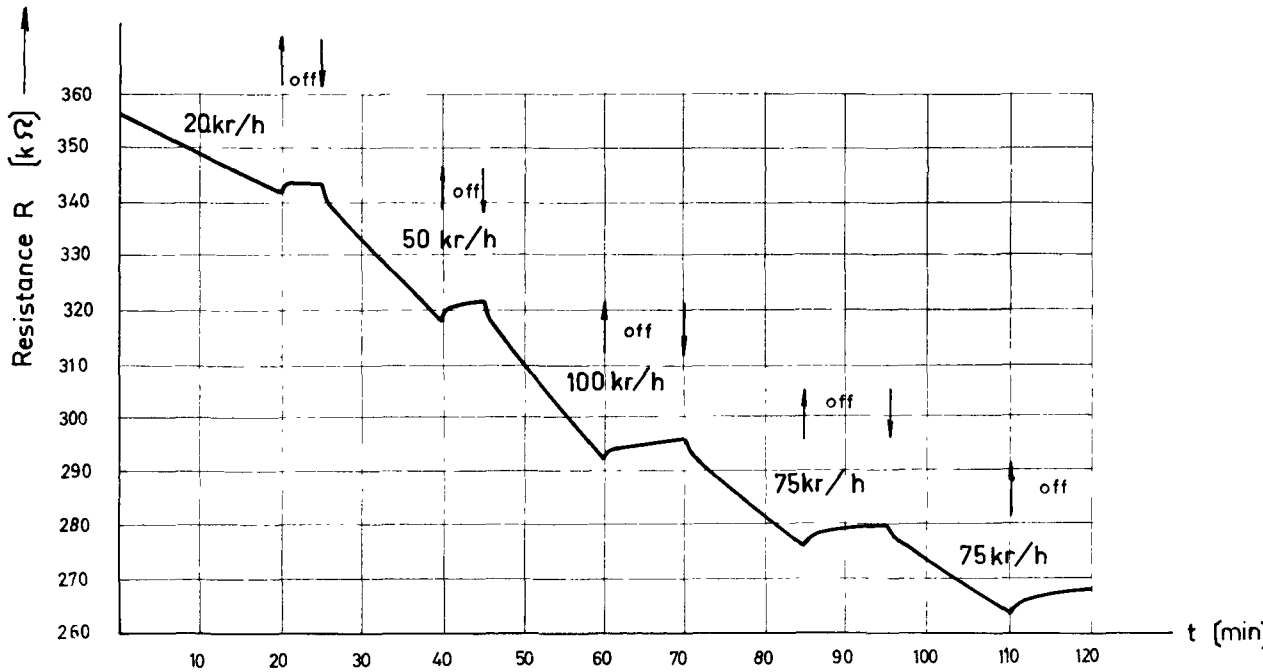


Figure 4. Changes in resistance under different dose rates
Polycrystalline material; radiation source 2 000 c cobalt-60

in the reactor, and then the resistance was again determined at the same temperature.

HIGH DOSE GAMMA FLUXES AT REACTOR PULSES

Because of the inherent safety of the TRIGA-Mark II reactor it is possible to produce short, extraordinarily high power pulses. The half-width of such a reactor pulse is only approximately 30 ms and the power peak can be as high as 250 MW, while the maximum continuous power level is only 100 kW. With the aid of such pulses it is possible to simulate the excursion of a fuel reprocessing or a nuclear fission reactor. It was therefore of interest to examine how far the change in the conductivity of cuprous oxide represents a simple method for measuring these pulses.

In order to avoid activation of the material, the cuprous oxide detector was put into a corner of the reactor (thermal column) in which only thermal neutrons were present. The cuprous oxide samples were shielded with cadmium. Therefore only gamma rays reached the samples.

The electronic circuit used for these experiments was very simple. The circuit elements are shown in Fig. 6(a). A cuprous oxide sample and a resistor (approximately 500 kΩ) were connected in series to a 9-volt battery. The decrease of the resistance of the cuprous oxide during the reactor pulse causes a change of the voltage drop. This signal is coupled over a 10 μF capacitor to a recording instrument, for example an oscilloscope. This registration can be transmitted over quite a distance.

The doses were measured with pocket ionisation dosimeters, which were also packed in cadmium. Fig. 6(b) shows a pulse recorded by a Tectronix oscilloscope. Our measurements showed that proportionality exists between the voltage pulse height and the dose, and therefore also between the pulse height and the reactor power peak. The sample responds immediately to the irradiation and returns to the original value almost simultaneously with the end of the radiation period. The half-width of the curve (40 ms) is somewhat greater than that of the reactor pulse (35 ms). Although the doses applied to the samples were relatively small (35-

Table 1. Resistance and conductance values with corresponding doses taken from Fig. 4

	Resistance R kΩ	$1/R$ $\Omega^{-1} \times 10^6$	$1/R - 1/R_0 = \Delta\sigma \times 10^6$	$(K_1 - \Delta\sigma) = (2\,50 \times 10^{-6} - \Delta\sigma) \times 10^6$	Total dose kr
R_0	356	2.81	—	—	—
R_1	343	2.92	0.11	2.39	6.67
R_2	322	3.10	0.29	2.21	19.17
R_3	296	3.38	0.57	1.93	44.17
R_4	280	3.57	0.76	1.74	62.92
R_5	268	3.73	0.92	1.58	81.67

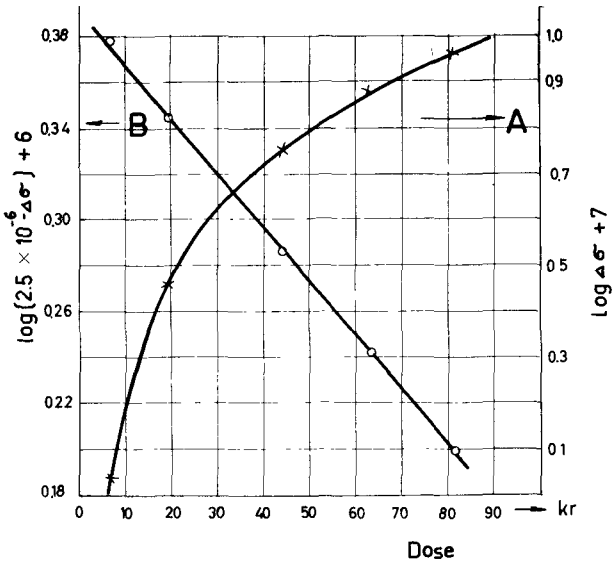


Figure 5. Conductance as function of the applied dose, corresponding to Fig. 4 and Table 1

Curve A: $\log \Delta\sigma$ versus dose (r)
Curve B: $\log (2.50 \times 10^{-6} - \Delta\sigma)$ versus dose (r)

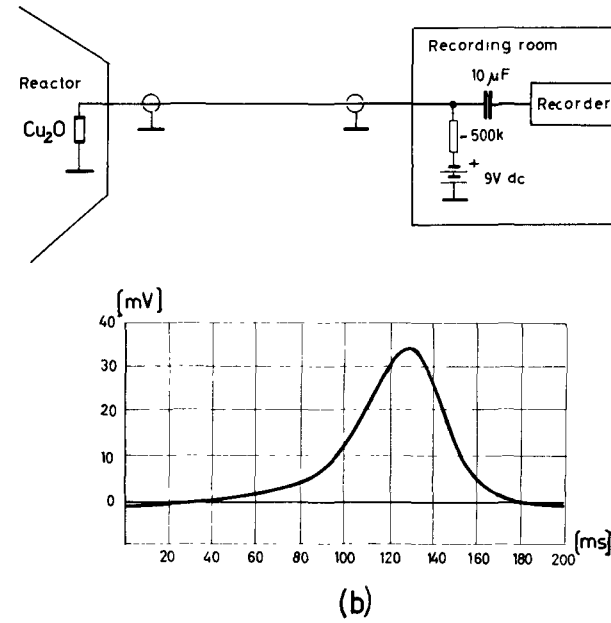


Figure 6

(*a*) Electric circuit for the cuprous oxide detector. The cuprous oxide sample is placed in the reactor and the recording device in a separate room; (*b*) the signal obtained by a 250 MW reactor pulse: total dose of 70 r at the detector position

70 r), the dose-rate was very high (several Mr/h) because of the short pulse duration. However, the samples underwent no noticeable change and could therefore be used repeatedly.

DISCUSSION

The results of all experiments indicate that property changes in cuprous oxide which take place under high dose irradiation of gamma rays are based on two different mechanisms: the one, quick and reversible; the other slow and with a long lifetime. The first case is verified by the steep fall and rise of the resistance-dose curve (Fig. 2) and by the pulse measurements. This behaviour can be explained by a direct ionisation of the material, in which electrons are moved from the valence band to the conduction band, and return to the valence band after radiation has ended. The second case can be attributed to the formation of Frenkel defects when irradiation takes place over a longer period. In Fig. 2 this behaviour can be seen in the change in resistance remaining after the shut-down of radiation.

The temperature behaviour of the samples which were not irradiated shows that acceptor levels at energies of 0.60 eV are present. Of these a considerable number recombine at a temperature of 100 to 120 °C. The defects recombining at this temperature are therefore due to the production procedure. After intense irradiation new levels could be found, which differ by approximately 0.05 eV from those found in samples which were not irradiated.

Small cuprous oxide detectors, either as single crystals (approximately 10 mm^2 surface area) or as polycrystalline samples (several cm^2 surface area), can be exposed to intense gamma radiation in places where access is difficult. The proportionality of the conductance values $\log (2.50 \times 10^{-6} - \Delta\sigma)$ and the doses (r) allows a simple calculation of the doses obtained by measuring the resistance difference before and after irradiation.

Power pulses in nuclear plants, whether carried out in inherently safe systems or occurring accidentally, can be measured with cuprous oxide detectors by a very simple electronic circuit. The signals thereby obtained can be recorded at a safe distance from the nuclear plant. This device can therefore be used as a monitoring system.

REFERENCES

1. Engler, H. D., Nukleonik, *2*, 6, 215 (1960).
2. Engler, H. D., Z. f. Naturf., *15a*, 82 (1960).
3. Crawford, J. H., Nuclear Power, 84, Aug. 1959.
4. Gremmelmaier, R., and Welker, H., Z. Naturf., *11a*, 420 (1956).
5. Pastrnyak, J., and Kužel, R., Czech. J. Phys., *6*, 217 (1956).
6. Joffe, A. F., Physik der Halbleiter, Akademieverlag, Berlin (1960).
7. Gorbanj, J. S., Gritsenko, Yu. I., and Rudjko, S. N., Soviet Phys. Solid State, *3*, 1559 (1962).
8. Nikitine, S., Grosmann, M., and Brun, J. B., Compt. Rend., *255*, 6, 1087 (1962).
9. Cleland, J. W., *et al.*, ORNL-865, Phys. Div., 87 (period ending Sept. 1950); ORNL-782, Phys. Div., 71 (period ending June 1950).
10. Blankenburg, G., and Kassel, K., Ann. Phys., *10*, 201 (1952).
11. Andrijewskij, A. J., *et al.*, Dokl. Ak. Nauk. SSSR, *90*, 521 (1953).

ABSTRACT - RÉSUMÉ - АННОТАЦИЯ - RESUMEN

P/815 Autriche

Utilisation de la conductibilité de l'oxyde cuivreux pour la mesure de flux gamma intenses dus à des réacteurs pulsés ou à des puissantes sources gamma

par O. Bobleter et P. Vajda

Un procédé spécial d'oxydation a permis d'obtenir à partir de plaques de cuivre (1 × 20 × 80 mm) de l'oxyde cuivreux possédant une structure cristalline grossière. La conductibilité électrique spécifique de ce produit est la même que celle d'un monocristal. Pour un spécimen à cristaux fins, la conductibilité augmente proportionnellement au nombre de cristaux par unité de surface. Ce phénomène provient d'une concentration plus élevée de défauts à la surface des cristaux.

La conductibilité augmente sous l'influence des rayons X et gamma. Plus la conductibilité initiale du produit est basse, plus grand est l'effet relatif. Les résultats obtenus font apparaître une relation linéaire et démontrent que Cu_2O cristallin à structure grossière convient très bien pour la détermination de hautes doses de flux gamma.

Immédiatement après le début de l'irradiation par une source intense de rayons gamma, on peut mesurer une très nette diminution de la résistance de Cu_2O; quelques minutes après, la courbe s'étale et se transforme en une ligne droite. Quand on interrompt l'irradiation, la première diminution de résistance est presque complètement compensée en un temps très court, tandis que les défauts causés par l'irradiation, qui se traduisent par la portion linéaire de la courbe, sont compensés très lentement, d'où un effet à long terme.

Des changements réversibles de la conductibilité des spécimens de Cu_2O ont été obtenus dans le réacteur (TRIGA Mark II) sous l'action de courtes impulsions gamma. Grâce au système de sécurité inhérent au réacteur, des excursions de puissance atteignant 250 MW sont possibles. La largeur à mi-hauteur des impulsions est environ de 30 ms. Les échantillons de Cu_2O étaient recouverts de cadmium et placés là où le débit de dose gamma pouvait atteindre plusieurs MR/h (30 — 70 R par excursion). La courbe de conductibilité mesurée pendant l'impulsion est presque identique à celle de la puissance du réacteur. Ce système de mesure relativement simple, basé sur la conductibilité de Cu_2O, permet de déterminer la puissance maximale de l'excursion du réacteur et de transmettre électroniquement les résultats obtenus. Si on admet qu'une excursion provoquée du réacteur peut simuler l'état d'un réacteur de centrale nucléaire sur le point de s'emballer, la méthode décrite basée sur la conductibilité de Cu_2O peut servir la prévention des accidents par excursion de puissance.

En outre, cette forme de Cu_2O peut servir à mesurer de puissants flux gamma provenant de sources continues, si on l'expose aux radiations pendant un certain temps et si on mesure ensuite sa conductibilité. Le mécanisme de la conductibilité et l'influence de l'irradiation sur les défauts cristallins sont brièvement examinés.

A/815 Австрия

Измерение мощных потоков γ-излучения в импульсах реактора и больших источников γ-излучения по проводимости закиси меди

О. Боблетер, П. Вайда

Закись меди с крупной кристаллической структурой получали из медных пластинок размером 1×20×80 *мм* путем специального процесса окисления. Удельная электропроводность этого материала не отличается от электропроводности монокристаллов. Для мелкокристаллических образцов проводимость увеличивается пропорционально числу кристаллов на единицу площади. Такое поведение является результатом более высокой концентрации дефектов кристаллов на поверхности зерен.

Под влиянием γ- и рентгеновского излучения проводимость увеличивается. Чем ниже начальная проводимость материала, тем больше относительный эффект. Полученные таким образом результаты показывают линейную зависимость и свидетельствуют о том, что крупнокристаллическая закись меди является наиболее подходящим материалом для определения мощных потоков γ-излучения.

Немедленно после начала облучения мощным источником γ-излучения измеряется резкое уменьшение сопротивления закиси меди; через несколько минут кривая становится менее крутой и переходит в линейную часть. Когда облучение прерывают, первое уменьшение восстанавливается почти полностью за очень короткое время, тогда как отжиг дефектов, характеризуемый линейной частью кривой, происходит очень медленно и поэтому является длительным эффектом.

Обратимые изменения проводимости в образцах закиси меди в действительности были получены в результате коротких импульсов γ-излучения в реакторе TRIGA, модель 2. Благодаря особым характеристикам безопасности, присущим этому реактору, можно было полу-

чить импульсы мощностью до 250 *Мвт*. Полуширина импульса составляла приблизительно 30 *мсек*. Образцы закиси меди покрывали слоем кадмия и помещали в позиции, где мощность дозы γ-излучения составляла несколько миллионов рентген в час (30—70 *р* за время импульса). Кривая проводимости, измеренная за время импульса, почти идентична кривой мощности реактора. При помощи этого сравнительно простого устройства для измерения проводимости закиси меди можно измерить пиковую мощность реактора в импульсе и передать полученные данные при помощи электронной схемы. Поскольку импульс реактора может быть использован для имитации выбросов мощности на установках с ядерным топливом, этот метод измерения проводимости закиси меди может быть использован в системах контроля ядерных аварий.

Более того, образцы закиси меди могут быть использованы для измерения мощных потоков γ-излучения от непрерывно излучающих источников путем установки образца на некоторое время в определенное место и последующего измерения проводимости. Кратко обсуждаются механизм проводимости и влияние излучения на дефекты кристаллов.

A/815 Austria

Empleo de la conductividad del óxido cuproso para medir intensos flujos gamma emitidos por fuentes y reactores pulsados

por O. Bobleter y P. Vajda

Un procedimiento especial de oxidación permitió obtener óxido cuproso de estructura cristalina gruesa a partir de placas de cobre de 1 × 20 × 80 mm. La conductividad eléctrica específica de este material no difiere de la de los monocristales. En el caso de muestras de estructura cristalina fina, la conductividad aumenta proporcionalmente al número de cristales por unidad de superficie. Ello se debe a la mayor concentración de defectos en la superficie de los cristales.

La conductividad aumenta bajo el efecto de los rayos gamma y de los rayos X. Cuanto menor es la conductividad inicial del material, mayor es el efecto relativo. Los resultados obtenidos pueden representarse por una relación lineal y demuestran que el Cu_2O de estructura cristalina gruesa es el que mejor se presta para la determinación de intensos flujos gamma.

Inmediatamente después del comienzo de la irradiación mediante una fuente gamma de alta actividad, se observa una neta disminución de la resistencia del Cu_2O; al cabo de unos minutos, la pendiente de la curva disminuye y ésta se transforma en una recta. Cuando la irradiación se interrumpe, la primera disminución queda casi completamente compensada en un tiempo muy breve, mientras que el recocido de los defectos que se reflejan en el tramo recto del gráfico se produce muy lentamente, por lo que constituye un efecto a largo plazo.

En la práctica, se han provocado cambios reversibles de la conductividad de muestras de Cu_2O mediante breves impulsos gamma en el reactor TRIGA Mark II. Debido a la seguridad intrínseca de este reactor, pueden obtenerse impulsos de potencia de hasta 250 MW. La semianchura del impulso es del orden de los 30 ms. Las muestras de Cu_2O se recubrieron de cadmio y se colocaron en posiciones en que se podían obtener dosis de varios Mroentgens/h (30 a 70 roentgens por duración del impulso). La curva de conductividad medida durante el impulso es casi idéntica a la de potencia del reactor. Este método de medición relativamente sencillo, basado en la conductividad del Cu_2O, permite determinar la potencia máxima del impulso del reactor y trasmitir electrónicamente los resultados obtenidos. En la medida en que un impulso de reactor puede considerarse representativo del estado de un reactor a punto de escapar al control, el método de medición de la conductividad del Cu_2O descrito en la memoria puede utilizarse para prevenir accidentes en los centros nucleares.

Asimismo, las muestras de Cu_2O pueden utilizarse para medir intensos flujos gamma emitidos por fuentes continuas de radiación colocando la muestra durante cierto tiempo en el lugar apropiado y midiendo consecutivamente la conductividad. Se examina brevemente el mecanismo de la conductividad y la influencia de las radiaciones sobre los defectos de la red cristalina.

Control, stability and protection of a gas-cooled graphite-moderated reactor

By J. Brown, A. B. Whiteley and M. J. Whitmarsh-Everiss*

The first nine twin-reactor nuclear stations now in operation or under construction in the United Kingdom are CO_2-cooled and graphite-moderated, using natural uranium fuel. All but the two latest, at Oldbury and Wylfa, have a steel pressure vessel containing the core from which ducts convey the coolant to and from the boilers; at Oldbury and Wylfa, core and boilers have been placed inside a pre-stressed concrete pressure vessel. The limitations on the steady state operating temperatures, imposed either by physical properties of the fuel element canning material and the uranium metal fuel rods, or by transient temperature rises during the worst possible fault conditions, are discussed elsewhere [1].

Reactivity faults have not been given detailed consideration until recently, and the main effort in this paper is devoted to this class of fault. Philosophically, all faults should be detected by two means, preferably using different physical parameters, e.g. reactivity faults by flux and temperature, both parameters being effective in preventing the fuel cladding from igniting. Sequencing interlocks between rod groups did not form any part of the protective system, and similarly, no excess margin trips were fitted to either shut-down or temperature trip amplifiers; excess margin alarms were provided, purely to assist the operator. The use of alarms instead of trips, however, meant that reactors had to be proved safe against all reactivity faults with the protection assumed at its full-power operating value. Modifications to this philosophy are described in the text of the paper, together with the design changes which have been required.

Five years ago the standard kinetics simulation used a point model to represent the reactor, which assumed that axial and radial flux shapes were known, and remained constant during the transient. However, one-dimensional models were being developed, in which a single channel represents a reactor, so that axial flux shapes are correctly given although the radial shape is constant; this model has been extensively used on analogue and digital computers but under-estimates peak transient temperatures as a result of incorrect reactivity feed back. This difficulty has been overcome by the use of 2 and 3 channel models such as KINAX (see appendix). The next advance was to 2-dimensional models, wherewith a steady-state picture of temperatures in every channel could be obtained (FTD2) [2], or transient effects could be obtained in which radial and axial flux shapes varied but azimuthal symmetry was assumed (STAB R, Z) [3]. Finally, very fast digital computers have enabled 3-dimensional models to be set up, and it is, at this moment, possible to examine steady states along every channel (SKIP) [4], and to calculate transient conditions in axial and radial directions when azimuthal conditions are asymmetric (STABLE) [5].

REACTOR STEADY STATE CONDITIONS

Three methods of flattening are illustrated in historical order as normalised flux plots across a diameter, nominally within the flattened region, Fig. 1. In case X, flattening is by steel fittings on the fuel elements within the flattened zone augmented by control rods (C). The centre flux is depressed by the source (S), the trim rod (T) and the off-centre stability rod (R). Control rods including (C) and flux scanning positions lie on interstitials. In case Y, there are no interstitials, and channels allocated to control rods, graphite samples and flux scanning appear as vacancies (V) giving flux rises. Flattening is by absorber rods (A) having similar weight to the fuel and positioned in fuel channels. In case Z, flattening is by absorber rods (A) in interstitial positions. The improvement in radial form factor by adopting the latter method is obvious. The difficulties of producing an optimised radial form factor are aggravated considerably if asymmetric stability or xenon override rod distributions are employed. Care is also necessary in the distribution of graphite samples and thermocouple runs. Flattening distributions are studied using FTD2 [2].

Three-dimensional steady states may be studied using SKIP [4] but are more frequently studied assuming the axial and (r, θ) distributions are separable. Axial steady state distributions are shown on Fig. 2 for a single and 4-group bulk rod lift. The normalised axial flux shapes for the 4-group lift at all xenon concentrations and the full power, equilibrium xenon concentration single group lift, assuming criticality is maintained on bulk rod penetration, lie within

* Central Electricity Generating Board, London.

the envelope *B*. In the case of the single group lift, at zero xenon concentration, 50% bulk rod group penetration is required to take up 2% in reactivity. The resultant flux distortion is shown on curve *A*. The axial steady state temperature distributions corresponding to *A* and the envelope of *B* are given by curves *C* and *D* respectively. If curve *E* defines the trip level setting at any axial position, it is clear that a full power zero xenon concentration steady state cannot be obtained in the case of a single group lift if trip thermocouples are positioned below 50% core height. The latter is normally the case as shown in a later section, and for this reason the obtainable power at start-up is related to the xenon time constant. An indication of the operational single group lift temperature differentials as a function of fractional mass flow is given on Fig. 3. Curve *Y* shows the temperature differential between a steady state tripping plane at 90% core height and the full power trip level (E of Fig. 2). The curves *Z* show the differential between the steady state at 90% core height and the maximum axial temperature. The full and broken lines are zero and equilibrium xenon concentration. *A* and *B* indicate 0 and 3 000 MWd/t. The normalisation criteria assumed that trip levels at neither 40% nor 90% core height, nor the maximum can temperature, could be exceeded.

(r, θ) rod patterns are studied using FTD2 to reduce maximum to average gas temperature differentials, to bias the can temperatures to the (r, θ) position of trip thermocouples and to study the effect of rods missing from optimised distributions since the latter may invalidate fault protection. Isothermal can temperature plots for the 4th group of a 4-group lift and for a single group lift are shown on Figs. 4 and 5 respectively. Mal-distribution limits the initial obtainable power at start-up and may invalidate fault protection.

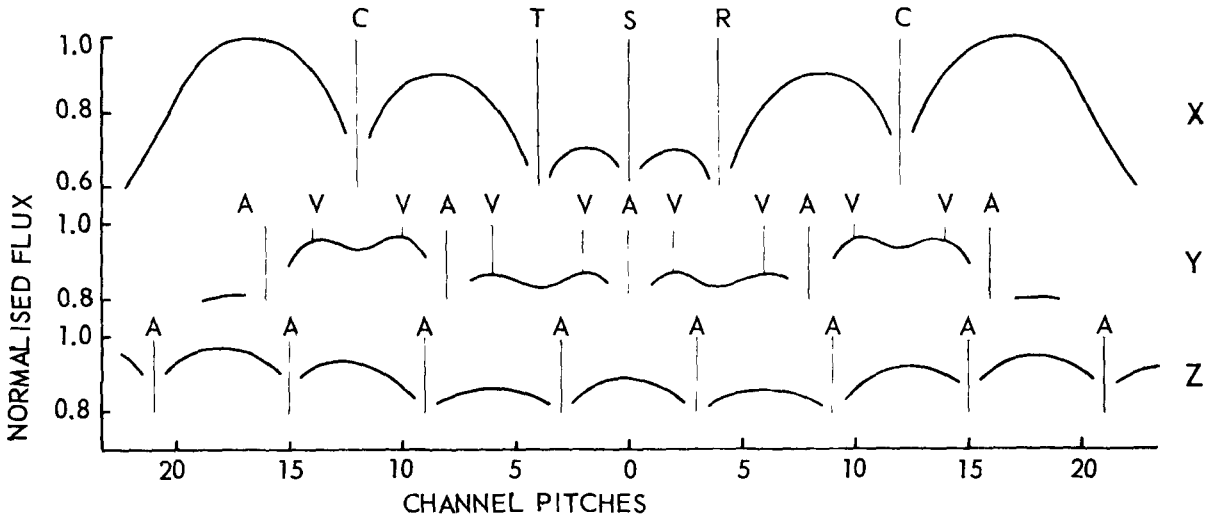


Figure 1. Methods of flux flattening

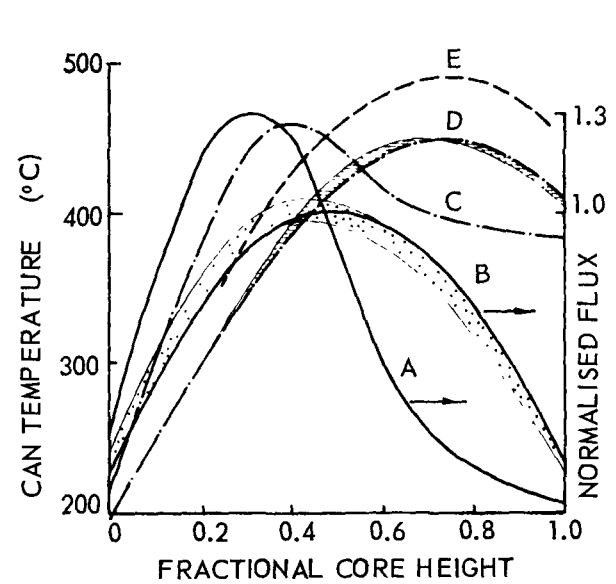


Figure 2. Axial flux and temperature distributions

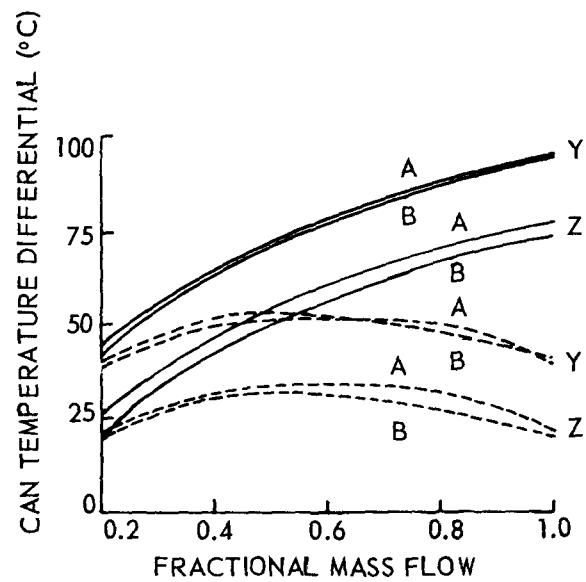


Figure 3. Single group lift temperature differentials

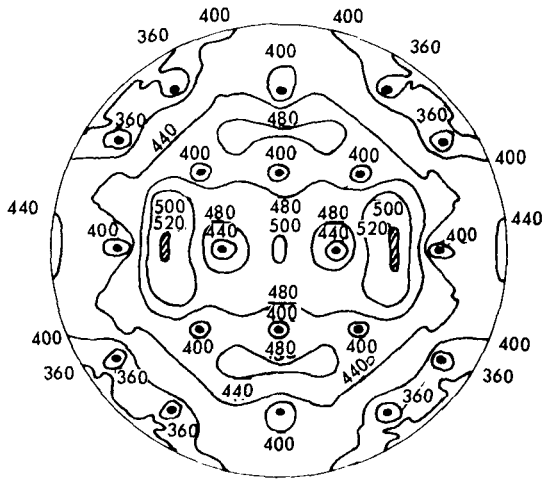


Figure 4. *Can surface temperature distribution: 4-group lift*

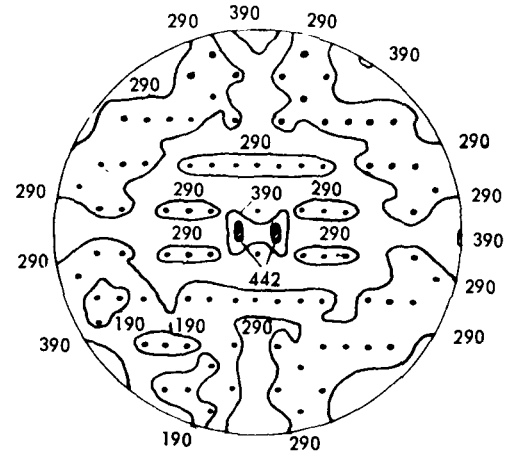


Figure 5. Can surface temperature distribution: 1-group lift

CONTROL ROD INVESTMENT

The rod investment criterion requires that:

Maximum k_{eff} (rods at maximum penetration) $\leqslant 1 - \Delta k(\text{s—d}) - \Delta k(\ell) - \Delta k(\text{c}) - \Delta k(\text{s})$

where

Δk (s—d) : shutdown investment = 0.005
Δk (s) : investment in safety rod group = 0.005
Δk (ℓ) : allowance for errors in lattice calculations = 0.005
Δk (c) : allowance for errors in control rod calculations = 0.005

In practice errors in lattice calculations are taken up by absorber and $\Delta k(\ell) = 0$. The reactor is assumed cold and at zero xenon concentration with three months delay in absorber loading. At commissioning, Δk(c) is replaced by the error in rod calibration (<0.005). A graph of the variation of $(1 - k_{eff})$ with time, assuming (*a*) the design flattening distribution, (*b*) no flattening absorber, (*c*) three months absorber loading delay, for the cold core, is given on Fig. 6. The Δk due to absorber loading delay is 0.004. After 140 weeks the minimum k_{eff} is 0.955. This effect may be used to increase start-up rates by the deletion of control rods and increased rod speeds, giving shorter start-up times and releasing rod sites for improved rod distribution. Since $\Delta k(\text{s} - \text{d})$ and $\Delta k(\text{s})$ are dependent on rod distribution which is a function of the (r, θ) temperature distributions at power with low xenon concentration a 2-dimensional calculation (FTD2) [2] is the minimum requirement. It has been demonstrated theoretically (FTD2) and experimentally, that removal of a small number of control rods from the area of peak shut-down flux can cause criticality and the shut-down criterion should now be related to this condition. The reactivity change due to the removal of a small number of control rods from a poor rod distribution (Fig. 7) is illustrated on Fig. 8, with the corresponding bulk rod radial flux shape. On Fig. 7, *B* denotes bulk rods, *S* safety rods and *R* stability rods. The fault may be avoided by designing the on-load rod handling facility such that the number of rods that can be removed at any one time is less than that for criticality.

REACTOR INSTABILITIES

Xenon and temperature instabilities have been treated elsewhere [6]. Radial/azimuthal instabilities are controlled by servos which in their simplest form comprise 1 central stability rod and 8 peripheral stability rods positioned in the radial peak of the first azimuthal mode at 45° to one another. Each rod is driven at a velocity proportional to a

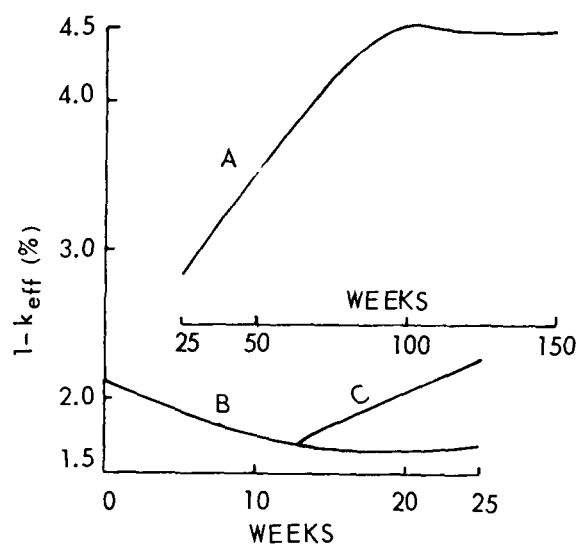


Figure 6. Variation of $(1 - k_{eff})$ with time

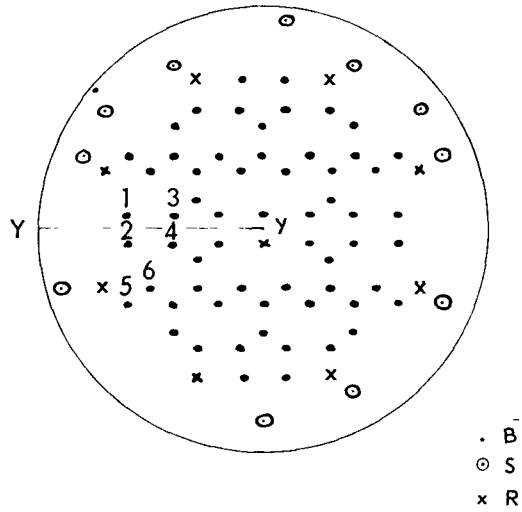


Figure 7. Example of control rod distribution

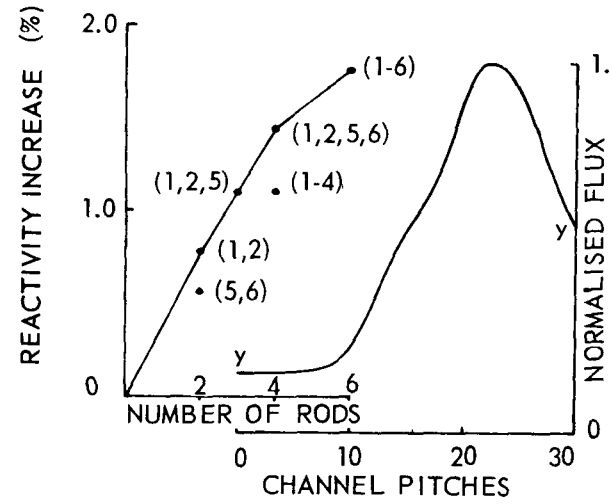


Figure 8. Reactivity and flux changes due to rod removal

temperature error signal, this signal being formed from demanded and measured sector coolant outlet temperature [7]. In order to accommodate temperature excursions due to on-load refuelling, absorber loading and control rod maintenance, power may have to be reduced when operating to a maximum can temperature criterion. This loss of output is kept to a minimum by optimising the stability rod distribution and control parameters to these disturbances. The stability rod system is also an inherent part of the station control system [7] and controls power changes at rates up to 10%/minute. Low power engagement of the stability rod system is of great assistance in controlling the positive reactivity feed back from an irradiated core at start-up since a bulk rod sub-group on fast in-speed will have a low rate of negative reactivity injection if the sub-group penetration is low.

STABILITY ROD FAULTS

Given a stability rod system of the generic type discussed above it can be postulated that any rod in the system may withdraw from the core at the saturation speed due to an electrical fault. The resultant transient has been studied, starting from the 100% power, equilibrium xenon concentration steady state at 3 000 MWd/t. A parametric survey has been made of initial rod penetration (assuming all stability rods in line and on automatic control), control rod reactivity investment and rod withdrawal speed. Studies of this nature require a 3-dimensional solution, and the STABLE [5] programme was employed using Bradwell design parameters having an average moderator temperature coefficient of 11.5 mN/°C and a uranium temperature coefficient, $a_u = -1.4$ mN/°C. The predicted change in maximum can temperature (δT_s) with time is shown on Fig. 9 for a 40 mN stability rod with initial penetration from which the fault occurs, and withdrawal speed as parameters, whilst Fig. 10 shows the δT_s/time curve for a constant rod withdrawal speed of 1.27 cm/s with initial penetration and control rod reactivity investment as parameters. Figure 11 is the maximum coolant outlet temperature (δT_c) equivalent of Fig. 10. The stability rod movements corresponding to the withdrawal of the 40 mN rod (Fig. 10), from 50, 70 and 100% penetration, are given on Fig. 12. The geometric position of the peripheral rods is shown on Figs. 14 and 15 by the azimuthal coordinate J. R_0 denotes the central rod. The relationship between rod reactivity investment, initial penetration and time from the start of the fault is given on Fig. 13 for $\delta T_s = 70$ °C. Isothermal can temperature diagrams at 70% core height for a 45.3 mN rod (X) withdrawn from $J = 9$ at 1.27 cm/s are drawn for a peak δT_s of 106 °C on Fig. 14 and 15, from initial penetrations of 70 and 100%, at times of 17 min and 8 min respectively from the start of the fault. The effect of a_u on the δT_s/time curve is illustrated on Fig. 16 for 50, 70 and 100% initial

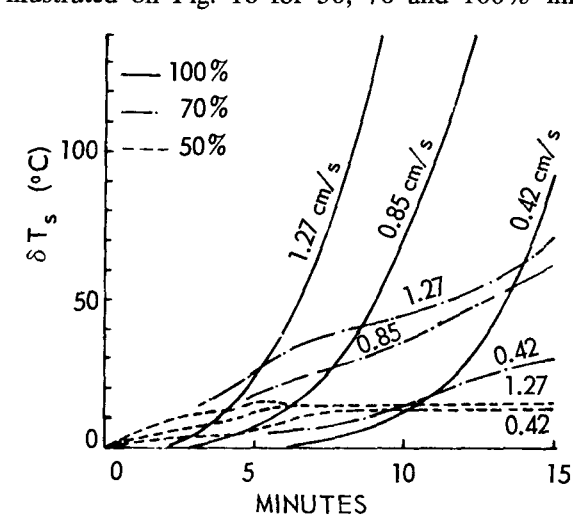


Figure 9. Peripheral stability rod fault: effect of withdrawal speed and insertion

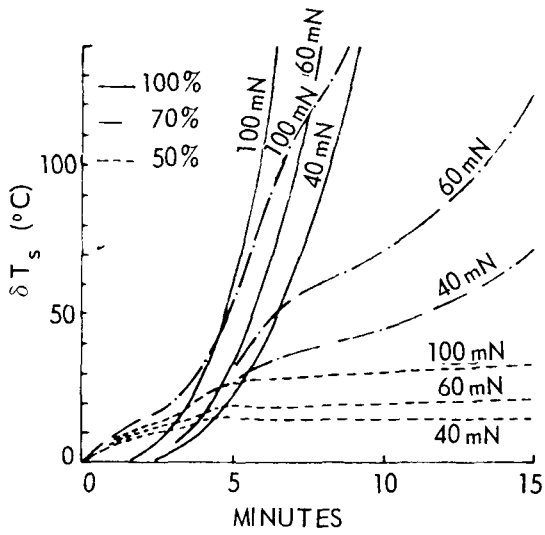


Figure 10. Peripheral stability rod fault: effect of reactivity investment and insertion

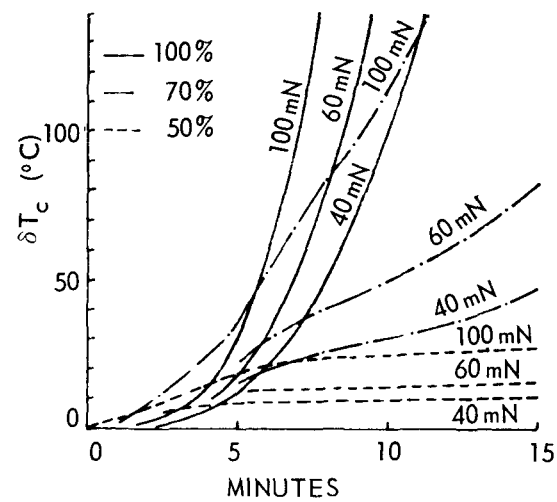


Figure 11. Peripheral stability rod fault: coolant outlet temperatures

rod penetrations for a 45.3 mN rod withdrawn at 1.27 cm/s. From the above transient data and the axial steady state single group lift temperature differentials shown in Fig. 3 it was considered that protection could be achieved by a constant margin to trip and to alarm. This can be achieved by using a servo driven trip margin having a saturation rate of 10 °C/min below the setting of the auto-speed inhibition interlock and 2 °C/min above. A high margin trip, approach to trip alarms, and an absolute level trip are provided. A detailed examination shows that 27 servo reset devices, 3 per sector, are required. Diversity on automatic tripping can be claimed for a fault from 100% penetration. For faults from 70% penetration one automatic trip from the sector containing the rod withdrawn under fault and a minimum of 7 minutes operator correction time from the approach to trip alarm, and a greater time from rod penetration alarms, may be claimed. Faults from

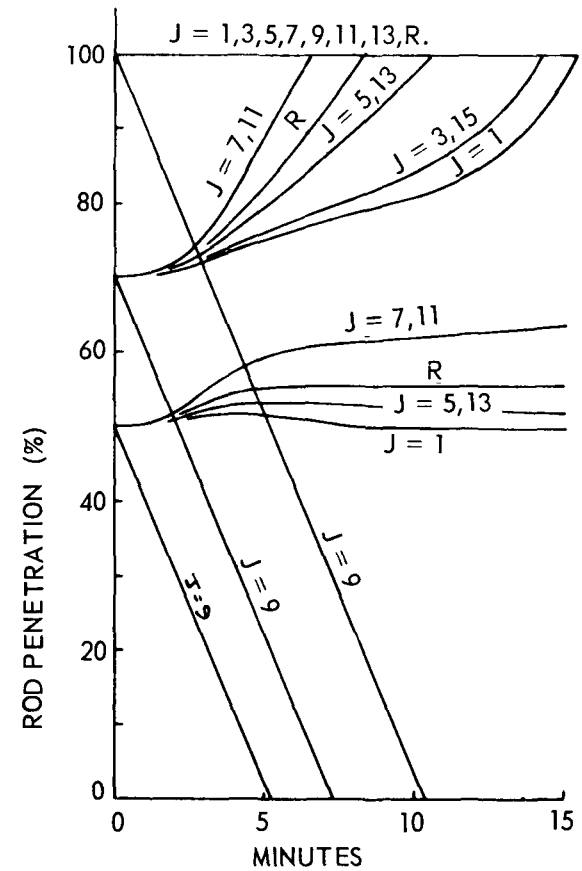


Figure 12. Peripheral stability rod fault: movement of stability rods

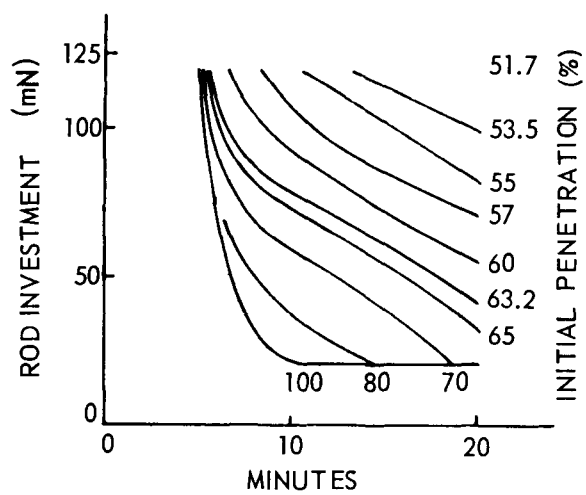


Figure 13. Peripheral stability rod fault: investment and insertion versus time

50% penetration have longer than 600 minutes operator correction time, two stimuli being claimed as before. Operator correction times of as low as 2 minutes can be supported by detailed time studies. An exhaustive treatment of the 4-group lift peripheral stability rod fault has not been made but it appears that fixed level protection may prove adequate.

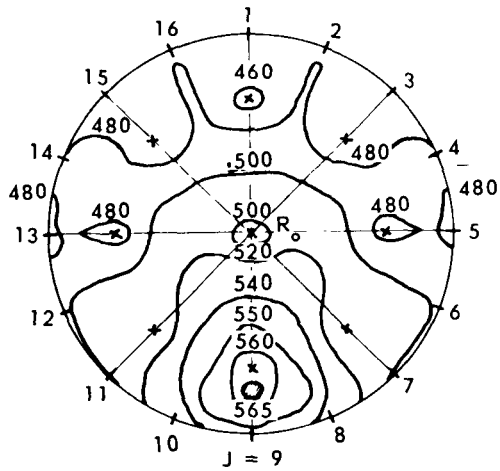


Figure 14. Peripheral stability rod fault: isothermals from 70% at 17 min

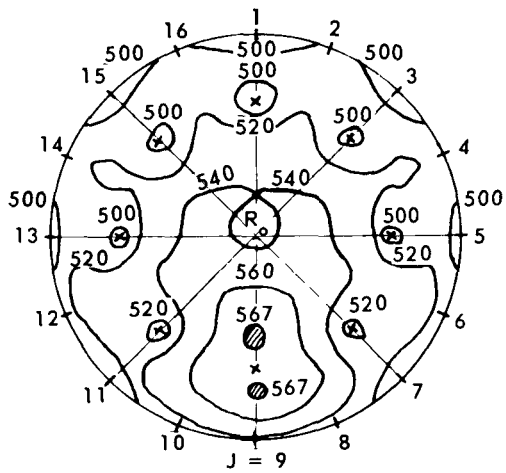


Figure 15. Peripheral stability rod fault: isothermals from 100% at 8 min

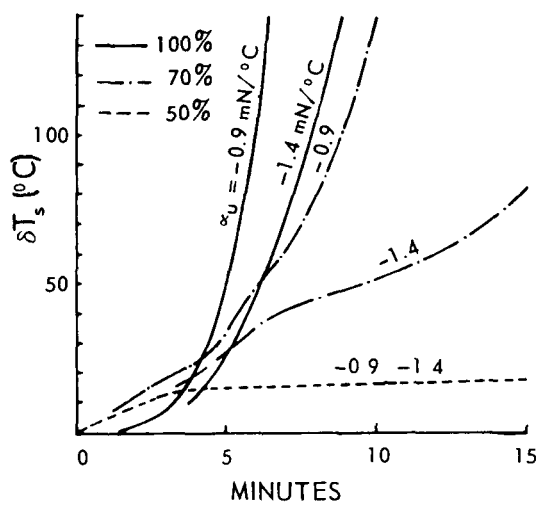


Figure 16. Peripheral stability rod fault: effect of fuel temperature coefficient

A Berkeley STABLE model transient solution has been compared with a Berkeley peripheral stability rod experiment at 420 MW in which a 50.6 mN peripheral stability rod was withdrawn from 57% penetration with the remaining central rod and 7 peripheral stability rods on automatic control at nominally the same penetration. A comparison of the change in can temperature (δT_s) with time as predicted by STABLE (continuous line) and as measured by 3 thermocouples (X) local to the rod at 70% core height is given on Fig. 17 together with a graph of the corresponding rod withdrawal speed (S). The good agreement obtained gives confidence in the method of solution.

The number of azimuthal planes in the STAB/STABLE models, 8 and 16 respectively, required to give adequate (r, θ) temperature representation has been the subject of doubt. The peripheral stability rod transient for a 45.3 mN rod withdrawn from 70% penetration at 1.27 cm/s for $a_u = -0.9$ mN/°C had a particular (r, θ, z) temperature distribution at 9 minutes and this has been compared with an FTD3 (a 3-dimensional version of FTD2) steady state solution, using STABLE to derive rod penetrations and reactivity feed backs with suitable scaling for the discrepancy in flux and thermal power. The agreement at 75% core height is illustrated by Fig. 18, which shows a radial can temperature plot through the rod withdrawn under fault. The azimuthal agreement is illustrated by Fig. 19 for 7/9 core radius. The STABLE solution is shown as a continuous line, the point (×) being the FTD3 solution and the broken line the scaled STABLE distribution. Comparison suggests that 16 azimuthal planes are adequate to predict the transient (r, θ) temperature distributions.

SYMMETRIC REACTIVITY FAULTS

Reactivity faults are the boundary condition to reactor start-up. In early designs bulk rod investment was related to the shutdown criteria and speed to the bulk rod reactivity fault. Stability rods had not been introduced. Their introduction increased reactivity release rates from 0.5 to 2.3 mN/s. A reactivity fault was then postulated in which the bulk rod group was withdrawn from source power with the stability rod group withdrawn at criticality. Such a symmetric fault is very difficult to protect by temperature in the case of a single-group lift due to the axial flux distortion, heat transfer effects, and rate of change of temperature up to 30 °C/s. The axial flux distortion may be reduced by the use of group lift systems. Single, 4 and 8-group lifts were investigated with a view to reducing axial distortion. It was found that the improvement in axial flux (ϕ) shape between 4 and 8 groups was marginal (Fig. 20), as were the axial can temperature (T_s) distributions at trip, but that (r, θ) temperature distortions for an 8-group lift were untenable. 4-group lift systems were introduced from Trawsfynydd

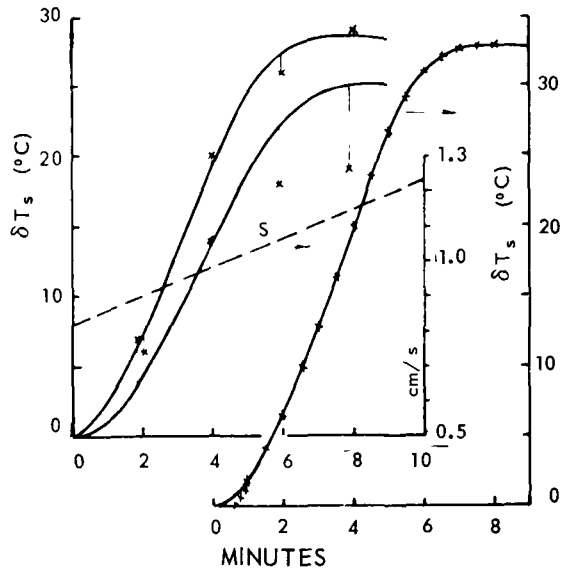


Figure 17. Peripheral stability rod fault: comparison with Berkeley experiment

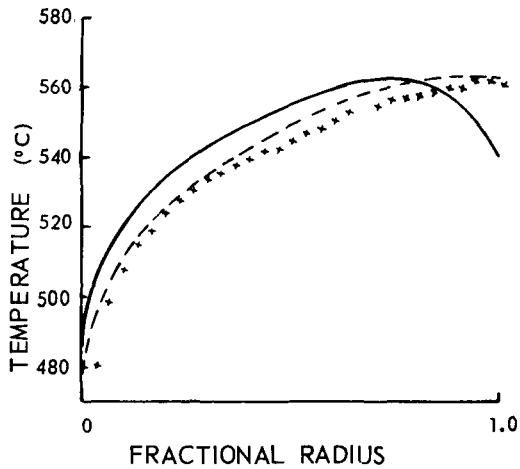


Figure 18. Peripheral stability rod fault: comparison between STABLE and FTD3

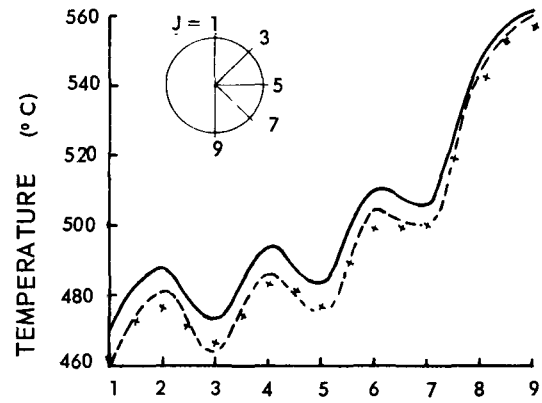


Figure 19. Peripheral stability rod fault: azimuthal comparison, STABLE and FTD3

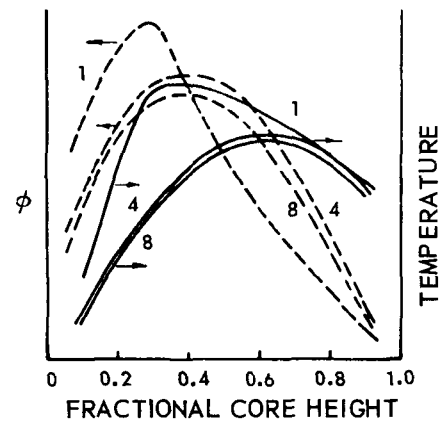


Figure 20. Axial flux and temperature distortions: single and multi-group lifts

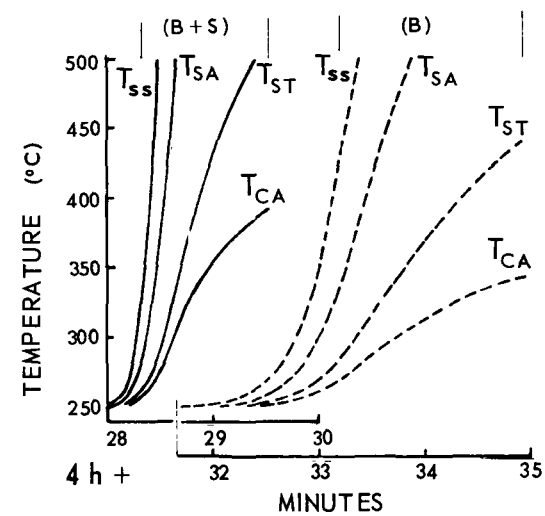


Figure 21. Symmetrical bulk + stability rod withdrawal fault

onwards. Using the KINAX programme, a (bulk + stability) rod withdrawal fault, denoted by (B + S), and bulk rod withdrawal fault, denoted by (B), are illustrated on Fig. 21, where T_{ss} is the temperature in a peak systematic channel, T_{SA} that in the average channel as defined by the (r, θ) flux plot of Fig. 22 for the 3rd ($\times$) and 4th ($\cdot$) sub-groups at 100% penetration, and T_{ST} is the temperature in the trip sensor channel, chosen on a redundancy argument relative to the (r, θ) can temperature isothermals of Fig. 23. T_{CA} is the average coolant outlet temperature. The corresponding flux (ϕ) and rod movements are shown on Fig. 24. Considerations of release rate and (r, θ) temperature distortion require interlocks which preclude withdrawal of more than one sub-group at a time and allow of the withdrawal order 1, 2, 3, 4 only. Because (B) and (B + S) faults require temperature protection from a sharply defined core height (40%), because of (r, θ) temperature distortions, and because of difficulty in protecting against the (bulk + asymmetric stability rod) fault, stability rod movement is inhibited until 15% power

by two parameters, T_{CA} and ϕ, and the fast symmetric and asymmetric faults are designed out. Protection is now claimed as follows: below the auto-speed inhibition interlock setting where only bulk rods can move, flux level trip (low log) and temperature (40% core height); above the interlock setting, two lines of temperature protection at say, 40 and 90% core height, there being no high margin trip on flux shutdown amplifiers.

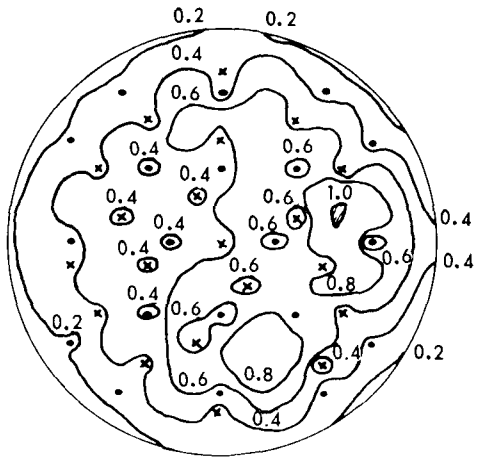


Figure 22. Flux plot: third and fourth groups inserted

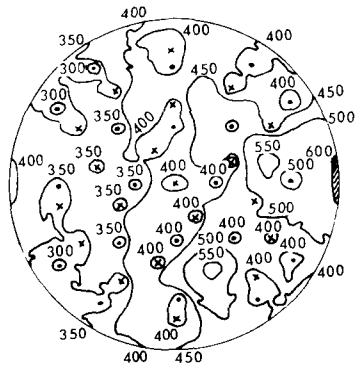


Figure 23. Isothermals: third and fourth groups inserted

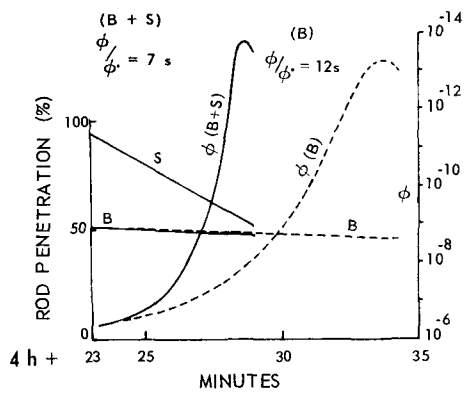


Figure 24. Flux changes with time: rod withdrawal faults

REACTOR START-UP AND FAST START-UP

A single-group lift start-up is drawn on Fig. 25, divided into logical terminations, the bands (*A-H*) between terminations having particular limitations in respect of start-up rate. Safety group withdrawal is shown at *Q*, where the limitation (*A*) is safety philosophy. Start-up times following a spurious trip may be reduced by connecting this group into the shutdown counter channel only. Stability rod group withdrawal is shown at *R*; the limitation (*B*) is by operational sequencing interlocks. This group may be disconnected from the safety circuits without invalidating fault philosophy, providing the auto-speed inhibition interlock is maintained. Bulk rod withdrawal is shown at *S*. The limitation (*C*) is on rod withdrawal speed as required by reactivity fault protection. The speed was related to protection of the (bulk + stability) rod fault; this is designed out by auto-speed inhibition interlocks so that the bulk rod group speed could be increased by a factor of 4. After 140 weeks the number of control rods may be decreased and the rod speed increased.

The notation used in the remainder of Fig. 25 is: T = coolant inlet temperature, U = coolant outlet temperature, V = indicated can temperature, W = assessed maximum can temperature, X = mass flow, Y = thermal power, Z = stability rod group movement. The approach to criticality D is required to confirm the plant reactivity state. Limitations at E and G are metallurgical, the rate of change of can temperature limit being 10 °C/min. Rates of change of mass flow may be increased from 4–10%/min but this requires low power engagement of the stability control system. Limitation F is due to 40% core height trip levels, and may increase time to 75% power by 100 hours. The remedy is to use the 4-group lift (Fig. 2); some alleviation may be obtained by servo-reset devices. Limitation H is due to can temperature limitations, and to point rating burst duct limitations [1] (Fig. 26), where δU is the difference between coolant outlet temperature and the design maximum. These two limitations are overcome by using a 4-group lift. A further limitation is imposed by poor (r, θ) rod distribution (compare Figs. 5 and 23 with Fig. 4).

PART LOAD OPERATION AND XENON OVERRIDE

Xenon and temperature override is provided for reactor power reductions equivalent to the loss of one turbo-alternator set on a ranged station. For two sets per station this is equivalent to 50% load reduction per reactor. The override is invested either in the stability rod system, in control rods used as absorber (Fig. 1, X), in a xenon override group or by raising the coolant inlet temperature if the moderator temperature coefficient is positive. The

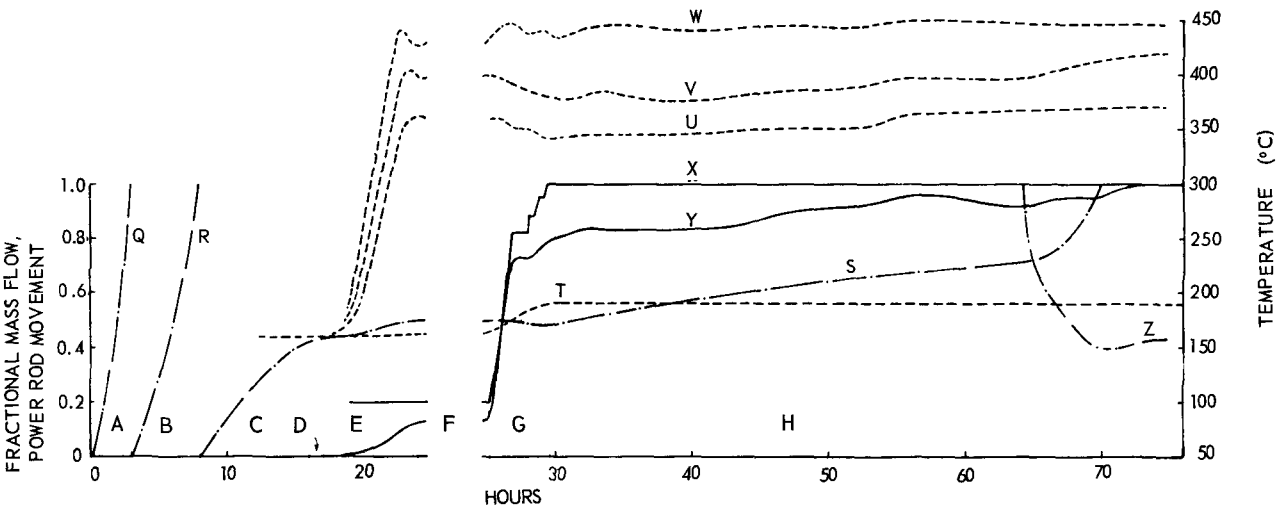


Figure 25. Limitations during reactor start-up

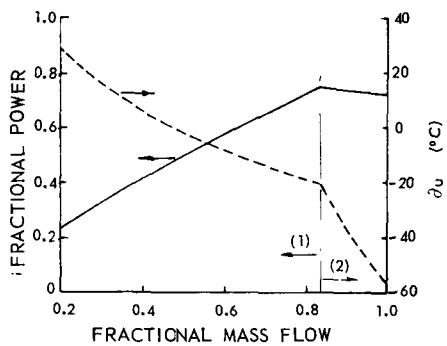


Figure 26. Point rating limitations during reactor start-up

latter method is associated with use of stability rods at low irradiations.

CONCLUSIONS

The severity of reactivity faults caused by control rod withdrawal has been increased by the necessity to use stability rods capable of high reactivity release rates. The worst symmetrical faults have been designed out, and an adequate protection scheme has been developed for asymmetrical faults.

ACKNOWLEDGEMENT

The authors wish to acknowledge the assistance of their colleagues both within the CEGB organisation and in the UK nuclear power industry.

APPENDIX

Computational methods employed

The KINAX one-dimensional reactor kinetic programme

The KINAX programme has been written in FORTRAN for the IBM 7090 and solves the one-dimensional, one-group neutron diffusion equation in its kinetic form with up to six delayed neutron groups for an "average" reactor channel. The heat transfer and xenon equations are solved and their reactivity effects are fed back explicitly into the diffusion equation. Certain nuclear and thermal properties in addition to k_∞ are allowed temperature dependence. Two additional non-averaged channels are represented in which the heat source is derived from that computed in the "average" channel via arbitrary scaling factors. Certain thermal characteristics in these extra channels may be different from those in the average channel and from each other. The "average" channel has its properties appropriately averaged in the radial and azimuthal directions, the second channel then represents one in which the trip sensors are located, whilst the third is the peak systematic channel. Hence temperature and xenon reactivity effects are correctly represented for the reactor as a whole and give the correct time behaviour of the neutron flux. The steady state may be set up as either a source (subcritical), fixed (i.e., specified) critical flux shape or computed critical flux shape (eigenvalue problem). In the latter case alternative criticality options are available. In both critical options the power level may be normalised to satisfy several alternative criteria, i.e., channel power, maximum can temperature, etc. Other features of the programme include four independent control rod groups and single control rod with associated automatic control loop and fission product heating. Practicable time steps lie in the range 0.01 s for rapid changes, e.g., high rates of negative reactivity injection, to 30 s to 1 min for slow transients. Running times on the computer depend on the number of axial points and on whether the extra channels are included. Typical cases with 20 axial points take 2-5 s per time step, depending on the options used. Except for rapid transients, the overall computation is faster than real time. Typical running times for 3-dimensional programmes [3, 5] are 2-5 min per time step, an a complete transient would take between 1 h and 5 h on the IBM 7090. The

KINAX programme is used regularly by the CEGB and has almost completely superseded analogue calculations of a similar type.

Current trend of CEGB reactor calculations

The main fields of reactor calculation are safety and operation. Hence computational methods have been developed in which increasing physical and thermal detail may be represented, although the neutronic section of the calculations is normally confined to one-group diffusion theory using "smeared" macroscopic data. The potential output from any one run is enormous, running into millions of numbers in some cases. Hence elaborate editing routines and carefully designed output formats are essential. A number of the deficiencies of STAB and STABLE [3, 5] are being overcome in a new 3-dimensional kinetic programme based on the SKIP steady state programme [4]. This programme together with an associated 2-dimensional programme is being developed by the CEGB and will be written in (x, y, z) and (x, y) geometry respectively. There will be 10 times as many mesh points available than in STAB (1368), and greater flexibility in the representation of absorbers and automatic control systems.

REFERENCES

1. Bainbridge, G. R., Bowles, L. F., Cave, L., Harrison, J. R., and Yellowlees, J. M., *The Safety of UK Gas Cooled Reactors — A Review*, P/183, Vol. 13, these Proceedings.
2. Enderby, J. A., *FTD2; A 2-Dimensional Flux and Temperature Distribution Programme for Thermal Reactors*, UKAEA report TRG 46(R), H.M.S.O., London (1961).
3. Curtis, A. R., *et al.*, *STAB: A Kinetic Three-Dimensional, One-Group Digital Computer Programme*, UKAEA report AEEW — R.77, H.M.S.O., London (1961).
4. Whiteley, A. B., Prescott, R., Syrett, J. J., Walsh, J., Buckler, A. N., Tyror, J. C., and Wrigley, H. E., *Calculation of Reactor Power and Temperature Distribution in Three Spatial Dimensions*, P/169, Vol. 2, these Proceedings.
5. Wrigley, H. E., *STABLE: A Digital Computer Programme for Solving the Time, Three-Dimensional, One Group Neutron Diffusion Equation*, UKAEA report AEEW — R.223 (1963).
6. Hitchcock, A., *Nuclear Reactor Stability*, Temple Press, London (1960).
7. Coxon, T., *Reactor Control*, Fifth International Instruments and Measurements Conference, Stockholm (1960).

ABSTRACT - RÉSUMÉ - АННОТАЦИЯ - RESUMEN

A/179 Royaume-Uni

Contrôle, stabilité et sûreté des réacteurs refroidis par un gaz et ralentis au graphite

par J. Brown *et al.*

Cet exposé se limite au contrôle, à la stabilité du flux et à la protection contre les défauts de réactivité dans les grands réacteurs modérés au graphite et refroidis au CO_2 actuellement en exploitation ou en construction en Grande-Bretagne. On décrit les limitations nominales pour l'état stationnaire, limitations imposées par les critères concernant les propriétés de l'élément de combustible lors d'incidents. On discute, avec exemples à l'appui, les difficultés rencontrées pour aplatir correctement le flux radial d'un tel réacteur.

On examine les suppositions faites pour déterminer l'équipement en barres de contrôle nécessaire pour arrêter un réacteur dans toutes les conditions de température et d'irradiation et on montre que, pour obtenir l'économie la plus grande, la disposition des barres doit être soigneusement choisie. On traite l'effet du retrait local de barres de contrôle d'un réacteur complètement arrêté.

La stabilité du flux du réacteur est examinée à la fois dans les directions radiale/azimutale et axiale et on conclut qu'une certaine forme de contrôle est nécessaire pour empêcher les instabilités possibles dans la direction radiale/azimutale mais non dans la direction axiale. On décrit l'utilisation dans ce but de barres de contrôle légèrement absorbantes en prenant comme exemple un grand réacteur type. Bien que ces barres soient prévues pour empêcher les instabilités, on a trouvé commode de les incorporer dans l'ensemble du système de commande du réacteur. Cependant des défauts dans le système de commande de ces barres peuvent conduire à des élévations locales de température, et on effectue un examen complet et détaillé de ce qui se produit à l'intérieur du réacteur en cas d'accident de ce genre.

On discute les problèmes relatifs à la mise en marche du réacteur et on fait l'historique du développement des systèmes de manœuvre des barres de contrôle par groupes, depuis le système de relevage en un seul groupe tel qu'il est utilisé à Calder Hall. On montre que la distorsion du flux axial est ainsi réduite mais que si la disposition des barres de contrôle n'est pas soigneusement choisie, les distorsions du flux radial/azimutal peuvent provoquer des élévations locales de température dans les éléments de combustible. On insiste sur le fait que la symétrie de la disposition du cœur du réacteur doit être considérée comme un concept essentiel de construction.

On montre que les incidents de réactivité généralisés, provoqués lorsque toutes les barres se déplacent simultanément, sont très graves, bien que la gravité dépende de la disposition relative des groupes de barres lorsque le réacteur devient critique. On démontre la nécessité de prévoir des interverrouillages ayant des degrés de sécurité élevés pour empêcher que de tels incidents se produisent. On

montre néanmoins que l'on peut arriver à des démarrages rapides sur ce type de réacteur pourvu que certaines exigences techniques fondamentales puissent être satisfaites économiquement.

On discute le fonctionnement du réacteur à charge partielle et on décrit les méthodes pour remédier à l'empoisonnement dû au xénon à la suite d'une réduction de charge.

Le progrès des méthodes de calcul utilisant de grandes calculatrices numériques et analogiques a permis de se rendre compte de l'existence de bien des problèmes discutés. En utilisant le calcul numérique on décrit une méthode qui permet d'étudier les états transitoires du réacteur dans les trois dimensions et on présente également une autre méthode unidimensionnelle pour les calculs de transitoires; ces méthodes ont été utilisées pour les graphiques joints au mémoire.

A/179 Соединенное Королевство

Управление, устойчивость и защита реактора с газовым охлаждением и графитовым замедлителем

Дж. Браун *et al.*

Работа ограничивается рассмотрением регулирования, стабильности потока и способов предотвращения падения реактивности в крупных реакторах с графитовым замедлителем, охлаждаемых углекислым газом, аналогичных реакторам, работающим или сооружаемым в настоящее время в Великобритании. Формулируются ограничения, связанные с конструкцией, которые определяются характеристиками тепловыделяющих элементов. Обсуждаются, например, трудности выравнивания формы радиального потока такого реактора и приводятся примеры.

Проверяются предположения, сделанные относительно необходимости введения регулирующих стержней для остановки реактора при всех возможных значениях температуры и облучения, и показано, что для более эффективного использования регулирующих стержней расположение должно быть выбрано тщательно. Поясняется влияние локального удаления регулирующих стержней из полностью остановленного реактора.

Рассматривается устойчивость потока реактора как в радиально-азимутальном, так и в аксиальном направлениях, делается заключение, что необходим некоторый вид регулирования, чтобы предотвратить возможные радиально-азимутальные нестабильности. Описывается использование для этой цели регулирующих стержней со слабым поглощением; в качестве примера приводится обычный крупный реактор. Хотя такие стержни применяются для предотвращения нестабильностей, найдено удобным включать их во все схемы регулирования реактора. Нарушение в системе управления этих стержней может однако привести к локальным высоким температурам, и в связи с этим дается детальный анализ этого типа неисправностей в реакторе.

Обсуждаются вопросы, связанные с запуском реактора, и рассматривается усовершенствование одновременного вывода нескольких групп регулирующих стержней, начиная с вывода одной группы, как это делается в реакторе в Колдер-Холле. Показано, что при этом уменьшается искажение аксиального потока, но, если расположение регулирующих стержней выбрано не тщательно, искажение радиально-азимутального потока может привести к локальному повышению температуры в тепловыделяющих элементах. Придается особое значение симметрии компоновки активной зоны.

Показано, что падение реактивности, вызванное одновременным перемещением всех регулирующих стержней, очень критично, хотя эта критичность зависит от относительного расположения групп стержней, когда реактор проходит через критическое состояние; демонстрируется необходимость обеспечения блокировок для повышения степени безопасности, чтобы предотвратить распространение таких падений реактивности. Показано, тем не менее, что быстрый запуск может быть достигнут на такого типа реакторе при условии возможности экономического выполнения основных проектных требований.

Обсуждается операция по частичной загрузке реактора, описываются способы снижения отравления ксеноном после уменьшения нагрузки.

Обсуждаются проблемы, связанные с разработкой усовершенствованных методов расчета с применением больших цифровых и аналоговых счетных машин. Описывается трехмерный метод расчета, допускающий проверку переходных процессов в реакторе; представлен также другой одномерный метод расчета переходных процессов; результаты расчета представлены в виде графиков.

A/179 Reino Unido

Control, estabilidad y protección de un reactor moderado por grafito y refrigerado por gas

por J. Brown *et al.*

Esta memoria se limita al control, estabilidad del flujo y protección contra accidentes de reactividad en reactores de gran tamaño refrigerados por CO_2, y moderados por grafito, del tipo actualmente en funcionamiento o en construcción en Gran Bretaña. Se plantean las limitaciones del proyecto en estado estacionario, derivadas de los límites impuestos por

los criterios de seguridad en relación con las propiedades de los elementos combustibles. Se discuten, con ejemplos, las dificultades de aplanar correctamente la distribución radial del flujo en un reactor de este tipo.

Se examinan las suposiciones hechas para calcular la inversión en barras de control que se necesita para apagar el reactor en cualesquiera condiciones de temperatura e irradiación y se demuestra que, para una máxima economía en la inversión, la distribución de las barras de control debe escogerse cuidadosamente. Se explica el efecto de la extracción local de barras de control en un reactor completamente apagado.

Se estudia la estabilidad del flujo en las direcciones radial/azimutal y axil y se concluye que se necesita alguna forma de control para impedir la primera, pero no la última, de estas posibles formas de inestabilidad. Se describe el empleo con este propósito de barras de control poco absorbentes y se utiliza como ejemplo un reactor grande típico. Aunque se han dispuesto barras de este tipo para impedir la inestabilidad, se ha encontrado que es conveniente integrarlas en una configuración global de control. Sin embargo, los fallos en un sistema de control con esas barras pueden originar altas temperaturas locales. Se hace un estudio completo y detallado de este tipo de fallos en el reactor.

Se discuten los problemas relacionados con el arranque del reactor y se sigue el desarrollo de los mecanismos de extracción de grupos múltiples de barras de control a partir de los de extracción de grupos sencillos tal como se usan en Calder Hall. Se demuestra que con ellos se disminuye la distorsión axil del flujo, pero que, a menos que se elija cuidadosamente la distribución de las barras de control, las distorsiones del flujo radial/azimutal pueden ocasionar altas temperaturas locales en los elementos combustibles. Se subraya la importancia de la simetría de la distribución del núcleo como criterio de proyecto.

Se demuestra que los accidentes de reactividad, causados al mover simultáneamente todas las barras, son muy graves, aunque la gravedad depende de la posición de los grupos de barras cuando el reactor pasa por la criticidad. Se indica la necesidad de emplear enclavamientos con altas características de seguridad para evitar que ocurran tales fallos. Se demuestra, sin embargo, que se pueden conseguir arranques rápidos con este tipo de reactor siempre que se puedan satisfacer económicamente ciertos requisitos básicos de proyecto.

Se discute el funcionamiento del reactor a cargas parciales y se describen métodos para contrarrestar el envenenamiento por xenón que sigue a una reducción de carga.

El conocimiento de la existencia de muchos de los problemas discutidos se debe al desarrollo de métodos de cálculo perfeccionados empleando grandes máquinas calculadoras digitales y analógicas. Se describe un método de cálculo que emplea las primeras y que permite examinar los regímenes transitorios del reactor en 3 dimensiones. Se presenta también otro método unidimensional para cálculo de transitorios. Ambos métodos han sido empleados para obtener las curvas presentadas en esta memoria.

Design of control rod systems for gas-cooled reactors

By P. B. Branson, * R. L. Carstairs * and A. J. Spurgin *

The control requirements recognized a few years ago for gas-cooled, graphite-moderated thermal reactors were comparatively simple, the reactors being expected to operate usually at full load and to be stable in all conditions. Subsequently, however, it has been shown that these reactors can become divergently unstable, both in the fundamental mode and in various spatial modes, and greater operational flexibility is now required. Local flux and temperature distortions produced by partially inserted control rods have been found to be larger than was anticipated, and trimming operations to maintain a good power distribution require more care than was previously thought necessary. Also, fault conditions are now examined in greater detail, with particular reference to the effects of possible gas circuit rupture.

This paper summarises, from the design point of view, the current control requirements for large gas-cooled reactors of the type developed in the United Kingdom, and describes in general terms the calculational methods suitable at the design stage. The principles for selecting control rod arrangements are discussed, and illustrated by consideration of the systems developed for two contrasting reactor designs.

REACTOR CONTROL REQUIREMENTS

The neutron absorbers which are used to control a large gas-cooled reactor are arranged in various groups. The power distribution is flattened by inserting fixed absorbers or a group of movable flattening rods into a central region of the core. One or more coarse control rod groups provide manual control of large reactivity changes and a separate small safety rod group is held out of the core in reserve for unforeseen circumstances. Automatic control of conditions in several independent regions is necessary to control core instabilities, and partially inserted spatial control rods are used for this purpose.

Two other control functions may also be required. Firstly, an override group of partially inserted rods can be provided to compensate for xenon and temperature reactivity changes following a reduction in power level. Depending on the part-load performance requirements, however, the reactivity override may be contributed by the spatial control group or by the variable flattening group, if present. Secondly, in some designs a secondary shut-down group is included to supply a fast and guaranteed rate of reactivity reduction in the event of gas circuit rupture faults, and may also be required to deal with special hazards such as earthquakes; this group can either consist of a sub-group of the coarse control rods, with special release mechanisms, or can be a physically different system.

Reactor control requirements may be considered under two headings. "Static" control requirements are concerned with achieving an adequate shut-down reactivity margin in all conditions and with the effects of inserted control rods on power distribution; steady-state analysis is sufficient to satisfy these requirements. "Kinetic" control requirements relate to the achievement of satisfactory behaviour in all transient conditions, including fault conditions which may involve mal-operation of the control system itself. Consideration of kinetic requirements involves the choice of permissible rates of control rod movement as well as some aspects of the grouping, spatial allocation and reactivity investment of the rods, and in general requires space-and-time variant analysis.

The primary static requirement is that sufficient coarse control rods must be provided to give an adequate margin of shut-down reactivity (usually 0.5% k in the United Kingdom) in all feasible normal and fault conditions of the reactor. In current United Kingdom practice the safety rod group must control at least 0.5% k. An additional static requirement, essentially an economic one, is that any rod groups which are normally inserted in the operating reactor should be arranged to produce the best possible power distribution (usually a flattened one) and should form an integrated pattern both with each other and with any fixed flattening absorbers that are used.

An aspect of the spatial distribution of the rod groups which has recently gained prominence concerns the phenomenon sometimes described as "local criticality". This can occur in a supposedly shut-down reactor if a sufficiently large region is devoid of rods, and gives rise to a potentially unsafe critical condition with a severe local flux peak in the driving region, against which it may be difficult

* United Power Company, London.

to achieve automatic protection. Care is necessary in the rod allocation to avoid local criticality, particular attention being needed where the removal of rods for maintenance is involved.

With regard to the kinetic requirements, it is important that normal operational transients are of an acceptable magnitude; alarms or trips should not occur and fuel thermal cycling must not be excessive in these conditions. The core reactivity during a transient may vary widely from the steady-state value, due to changes in fuel and moderator temperatures and xenon level; this influences the choice of the ratio of fixed to movable absorber investment, since override of the core reactivity changes must be provided by movable absorber.

In large reactors, independent automatic control over a number of regions is required to enable the intrinsic core instability to be controlled. The spatial control rods used for this purpose act independently to control the transients following local operational disturbances and in unison to control the total power level; control of the transient behaviour following a failure of one or more coolant circulators may also be required. Rod reactivity rates and controller parameters must be suitable for these purposes, with allowance for the variation of control reactivity rate with rod insertion in various core conditions.

The rates of change of control reactivity for either local or overall core control are limited by safety requirements: the maximum possible reactivity rates during local or group control rod runaway must be such as to permit the various tripping devices to operate without unacceptable temperatures being reached anywhere in the core. It is desirable that the time available before a trip occurs should be such that manual intervention is possible to prevent the trip; this may be particularly important if no alternative tripping system is provided, as may apply for runaway of a single automatic control group.

Current safety philosophy requires that the probability of fuel can melting following any fault condition shall be acceptably low, and assumes that the reactor automatic tripping system functions correctly. The rates of absorber addition to the core following a trip must be satisfactory. Gas circuit rupture calculations suggest that in certain special conditions temporary core flow stagnation and consequent very rapid fuel temperature rises could occur. A more rapid addition of absorber to the core following a trip in these circumstances is needed than that required for other trips. The special secondary shut-down mechanisms used for this purpose must operate sufficiently quickly and may have to function in particularly severe conditions; for example, during an earthquake.

DESIGN ANALYSIS METHODS

The understanding of large reactor behaviour has increased considerably in the last few years to the extent that extremely complex representations of conditions in reactors are now studied. Three-dimensional kinetic and steady-state computer codes have been developed, usually employing finite-difference methods, but because of their size and complexity these codes require long computation times and are expensive to run; they are therefore used mostly for detailed operational studies of completed designs.

Where a large number of calculations is needed for parameter surveys or other design work, simplified methods have been developed which enable computation to be carried out speedily and economically, whilst still being sufficiently accurate for design purposes; these methods assume separability of one or more space variables, or use averaged quantities for the complete core, and consider a simplified model of the core geometry.

In static design calculations the reactor is represented as a number of homogeneous regions, and two neutron-diffusion energy groups are commonly used; a discrete source-sink simulation of individual fuel channels is rarely necessary. The main problem concerns the determination of reactivity investment and sometimes the flux distributions for various patterns of control rods. For reactivity calculations, particularly when the rod pattern is fairly uniform, a one-dimensional radial model provides a rapid means of finding how the investment varies with temperature and irradiation conditions, but it is usually necessary to normalise the results by comparison with a two-dimensional x,y or r,θ calculation which takes specific account of the discrete absorber positions. A one-dimensional axial model is usually sufficient at the design stage to determine the axial characteristics of partly inserted rod groups. For the one-dimensional studies both analytic and finite-difference methods are used; for two-dimensional problems finite-difference methods are most common but harmonic expansion methods are occasionally employed.

In cases where an accurate flux or power distribution is required a two-dimensional x,y or r,θ method (again with discrete absorber representation) is necessary, since flux shapes are very sensitive to individual absorber strengths and positions. A full three-dimensional approach is, however, rarely needed for design purposes; and even for systems using partially inserted flattening rods a combination of two-dimensional x,y and r,z calculations is sufficient.

Kinetic models for design calculations usually consider the neutron diffusion equation with one thermal energy group in a homogeneous core; two delayed neutron groups are sufficient if used with suitably averaged data. Neutron kinetic and heat transfer representations of core averaged conditions, of axially (z,t) variant, or of radial-azimuthally (r,θ,t) variant conditions are used; these are often called point, axial and radial-azimuthal models respectively. Harmonic expansion methods are com-

monly used for radial-azimuthal analysis, since a finite-difference two-dimensional representation would require a large number of mesh points. A finite-difference approach is preferred, however, for axial studies, since an adequate representation of the effects of partially inserted control rods would require too many harmonics.

Kinetic studies are usually associated either with the investigation of the uncontrolled or controlled core stability in various conditions or with the determination of the system transient behaviour following particular disturbances. Point equation frequency-response studies of the controlled reactor fundamental mode behaviour give approximate ranges of automatic control system parameters and corresponding gain and phase margins; these can be interpreted in terms of the unison reactor transient response quality, the phase margins being the more sensitive to parameter variation. The results of these studies are confirmed using point transient analysis. Spatial stability studies are undertaken to determine the shape and time behaviour of the various controlled and uncontrolled radial-azimuthal core flux modes, and to determine the stability margin for the uncontrolled first axial harmonic flux mode as a function of automatic control rod insertion.

Radial-azimuthal transient studies determine the response of the controlled reactor to local disturbances, such as refuelling operations or the removal of in-pile control rods for maintenance purposes; fault conditions with one or more automatic control rod groups inoperative or running away are also considered. Axial transient studies, representing the average or hottest channels in a core, or both, are used to study normal operations such as start-up, shut-down, or load change, and for studies of fault conditions such as control rod group runaway or gas circuit de-pressurization. Control parameters suggested by the point frequency-response analysis are generally adequate for spatial studies.

DESIGN APPLICATIONS

General remarks

The coarse control rods will normally be withdrawn when the reactor is at full power, but, following a start-up, approximately one-quarter of the absorption of these rods will be needed to compensate for the absence of xenon whilst the core is initially at a high power level. Coarse rods may be present in the core for longer periods if they are used as additional reactivity absorbers during, for example, the approach to a fuel cycle equilibrium state. It is therefore desirable that at least some of the coarse rods be distributed uniformly over the core in a way which causes minimum perturbation to the operating power distribution.

Various methods of grouping the coarse rods for withdrawal during start-up are available, the simplest being to use a single group. This method leads, however, to large axial flux distortions which can cause difficulty in the achievement of adequate automatic temperature protection, and it is often not possible to select the total coarse rod pattern so that a good radial power distribution is obtained when the rods are inserted. Another disadvantage is a reduction in axial stability margins, though this does not normally cause an operational limitation. A solution to these problems is to divide the coarse rods into a number of roughly equal groups which are withdrawn sequentially. As the number of these groups is increased the axial distortion is reduced but for more than about four groups no significant further reduction occurs; also, above this number it becomes difficult to maintain adequate radial flux distribution within each group. Thus the use of about four groups presents the best compromise solution. With this scheme the distribution within the last group to be withdrawn is the most important as regards the effect on power distribution, but a good arrangement is relatively easy to obtain from any reasonable coarse rod pattern. Other start-up schemes, such as sequential withdrawal in annular groups, may have special advantages in some circumstances but the uniformly distributed group scheme is generally preferable.

The automatic spatial control rods operate in each region to maintain the local average gas outlet temperature as nearly constant as possible. The distribution of these rods is particularly important; they must be placed so that adequate local control is ensured and it is desirable to allow for the possibility of one of the controllers being inoperative for maintenance or other reasons. In most of the gas-cooled reactors so far designed in the United Kingdom a sector layout of spatial control rods has been used; this arrangement has an outer ring of rod groups or single rods, usually eight in number, placed at roughly equal azimuthal separation, together with one rod group controlling the central region. The sector layout was originally chosen since it suited the cylindrical geometry and the sizes and ratings of early Magnox reactors. It is now thought desirable, particularly for very large reactors, to associate the spatial control rods with regions of similar shape and area: this leads to an (x,y) pattern with reasonably uniform distribution.

Since the spatial control rods are normally inserted in the reactor at power, they must be considered as an integral part of the flux flattening. Some compromise may be necessary between the best positions for control and those for flattening; in particular it is advantageous to avoid locating the spatial rods in the unflattened region of the core because of consequent reduced output, due both to loss of reactivity and to local flux disturbances. Because these rods operate to keep the average coolant gas outlet temperature constant in the different core regions, they act also to provide automatic flatten-

ing; and although because of other control requirements only small variations in insertion are permissible for this purpose, a useful degree of automatic flattening can still be achieved.

Control reactivity rates must be large enough for adequate control and at the same time small enough to result in satisfactory behaviour in control rod runaway fault conditions; these requirements are in opposition, but it is possible to achieve a satisfactory compromise in practice. Maximum reactivity rates of about 10^{-5} k/s for the automatic control system operating in unison are typical, with approximately half this value for individual coarse or override control groups. Faster rates can be justified in some circumstances, for example during the early stages of start-up.

A basic design choice in a reactor using absorber flattening is between fixed or variable absorbers. In a fixed system the flattening can only be changed by the fuelling machine and, even with on-load refuelling, it is relatively inflexible. A further disadvantage arises since these absorbers usually lie on a different lattice from that of the spatial control rods, thus making the achievement of an integrated pattern more difficult.

In the variable flattening scheme, some of the control rod positions in the flattened region are used for partially inserted flattening rods. This allows easy and rapid adjustment both of total reactivity by bulk movement and of power distribution shape by differential movement of individual rods or groups of rods. Furthermore, reactivity override is easily provided and, in some cases, the axial flux shaping produced by the partly inserted absorbers can result in a worthwhile reduction of a few degrees in maximum can temperature. The disadvantages to be set against the operational convenience of variable flattening are that extra penetrations of the pressure vessel may be required, which may be particularly undesirable in a concrete pressure vessel, and that additional expenditure on control rod motors, supplies, etc. is involved, compared with the fixed system. It is thus not possible to make a unique choice between the two arrangements without consideration of other design features, but some measure of movable flattening control is very desirable even in a predominantly fixed flattening scheme.

It has been mentioned that some of the coarse rods need to be more or less uniformly distributed; a high degree of symmetry is also advantageous. This is particularly so with the combined flattening and spatial control rod pattern, where an imbalance in the distribution can lead to a significant reduction in the ratio of mean to maximum power, and applies to a lesser extent to any group of the coarse control rods which can be present in the core at power for significant periods. An incidental advantage of symmetrical patterns is the significant simplification of complex two- and three-dimensional calculations. Rotational symmetry is sometimes employed in absorber patterns, but there is a greater advantage by utilising planes of reflection. Two such planes (quadrantal symmetry) occur with rectangular and hexagonal geometry and four planes (octantal symmetry) can be used with a square array of positions.

The Tokai reactor

This relatively small (150 Mw(e)) natural uranium, Magnox reactor, which is in an advanced state of construction, provides an example of current control requirements applied to an existing design. The core was constructed to resist earthquake hazards, and so did not permit the use of interstitial holes in the graphite. The standpipes, which contain the various control devices, are located above fuel channel positions on an equilateral-triangular basis, with one position to each twelve fuel channels. A variable flattening system is incorporated, rather than fixed absorber in fuel channels, and in addition to the normal boron steel control rods a secondary shut-down system, of different design, is also employed which uses boron steel balls; these provide both a guaranteed degree of reactivity control in the event of core displacement during an earthquake and a rapid shut-down rate against core de-pressurisation faults. Positions for all control devices and for flux plotting and other functions have to be accommodated within the single standpipe array.

The use of movable flattening clearly makes a heavy demand on the standpipes within the flattened region; however, positions must be left for other functions and local criticality during rod removal for maintenance must be avoided. About one-third of the positions within the flattened region can be used for flattening and spatial control rods, one-third are required for coarse control rods and the remainder accommodate secondary shut down units and other equipment. For reactor designs such as Tokai it is necessary to study the important features of any chosen patterns with the use of at least a two-dimensional representation which takes account of specific absorber positions.

The main features of the design standpipe allocation are shown in Fig. 1. The flattening and spatial control rods are of identical steel construction and form an integrated pattern, which at the fuel cycle equilibrium condition gives a power averaging factor of 0.77, only 5% less than the ideal value with fully homogenised absorber. The flattening pattern is such that variations in anticipated reactivity can be easily accommodated by differential insertion of rings of rods. It is of interest that no simple rules for the selection of this type of flattening pattern are known; a considerable amount of trial and error with many two-dimensional calculations was involved in the present case, and in particular several patterns which appeared to be far more uniform that that of Fig. 1 gave worse results.

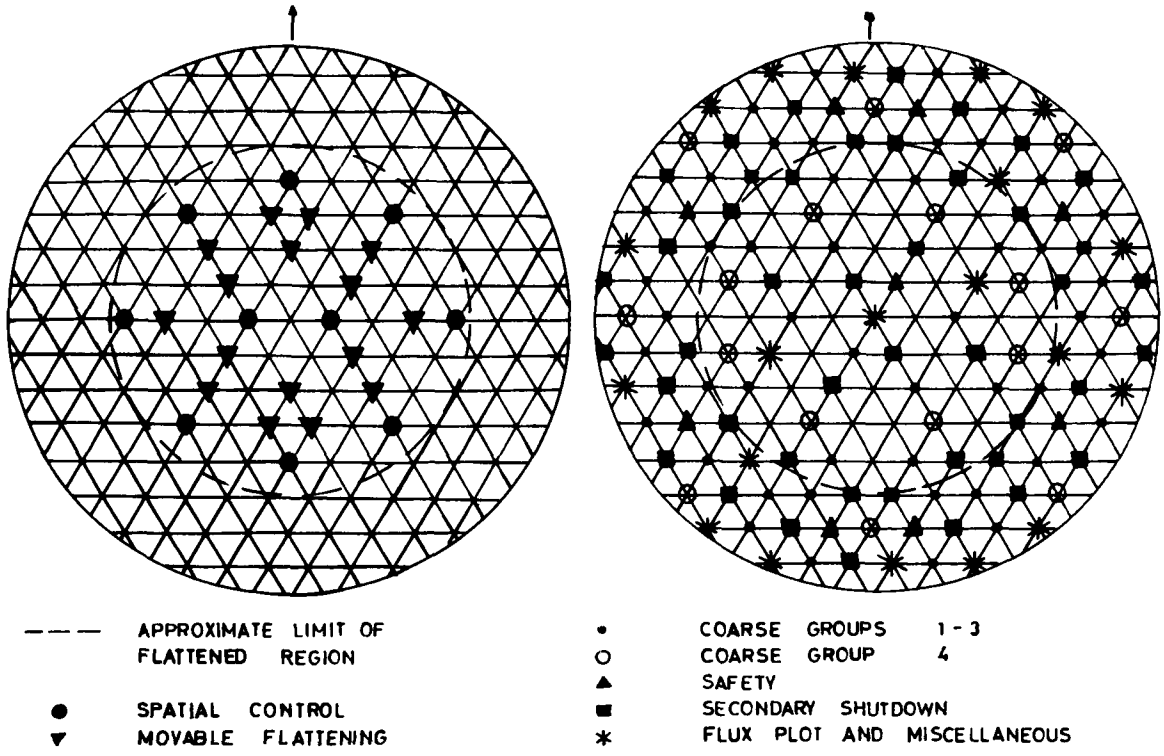


Figure 1. Allocation of Tokai reactor control groups

The Tokai spatial control rods are arranged in a sector configuration; two rods are used in the centre to maintain quadrantal symmetry (the centre hole not being available) and the eight outer rods, one per sector, lie just inside the flattened region. Fig. 2 shows typical spatial transient behaviour of the reactor following a step movement of absorber in the core. The transient spatial changes of outlet gas temperature are shown for one disturbance position, and the dotted curve shows the maximum values of the changes for similar absorber movements at all radial positions.

Transient studies of sector control systems for the Tokai reactor and others have enabled rules to

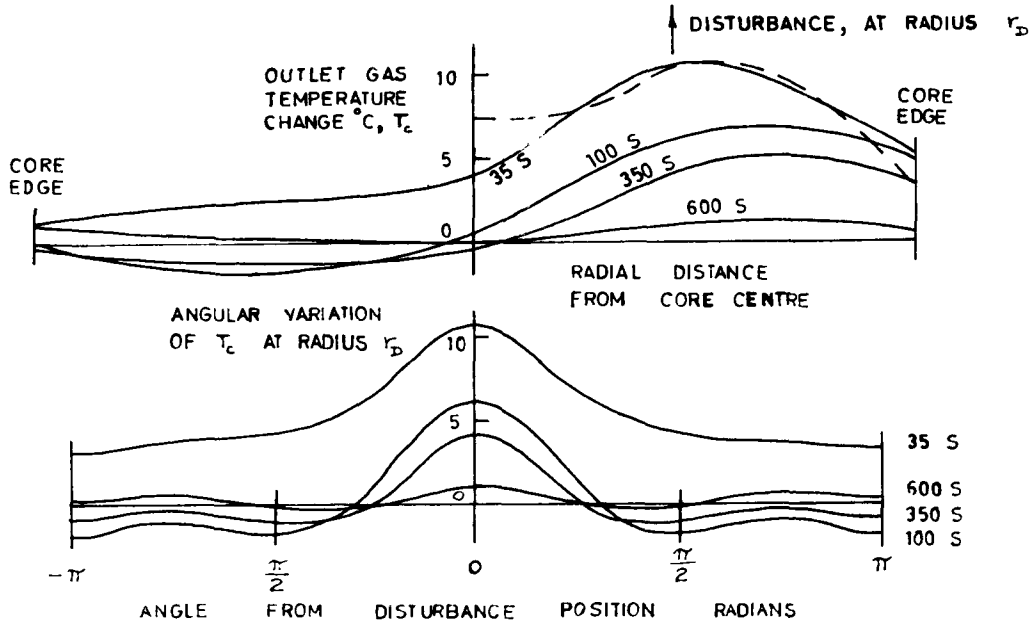


Figure 2. Tokai reactor. Spatial response to 20 $\times$ 10^{-5} k single absorber step movement. All controllers operating

be formulated for positioning those channel outlet gas thermocouples which are used for automatic control. The thermocouple positions should be distributed as evenly as possible within each control region, except that positions are not needed near the core edge, where conditions are effectively determined if satisfactory control is obtained elsewhere. It is desirable to avoid positions adjacent to sector rods or other movable in-pile rods; the local flux and temperature depression surrounding a rod varies in phase with the rod movement, and can adversely affect the response of the associated controller to the average temperature change of this region.

Apart from the limitations imposed in the flattened region, the control rods and secondary shut-down devices are distributed fairly uniformly over the core to maximise reactivity investment and minimise local criticality. The coarse control rods are required to have about 8% reactivity investment to cover all reactor conditions and the secondary shut-down system is chosen to give about half this investment. With regard to the possibility of local criticality in the coarse rod pattern, the centre is the most sensitive region; however, with the worst combination of reactor conditions and uncertainties in prediction, more than five rods would have to be deliberately removed from adjacent positions before criticality could occur, and even in this extreme condition the safety rods hold over 0.5% of reactivity. Since the reactor operating rules permit the removal of only one rod at a time for maintenance the possibility of local criticality is eliminated.

A large reactor design

A recent design study for a large uranium Magnox reactor (500 Mw(e)) in a concrete pressure vessel shows some features of interest which contrast with the Tokai design. In this case, because of limitations in the number of pressure vessel penetrations, completely variable flattening cannot be used and a predominately fixed scheme is incorporated. No secondary shut-down system is needed because of the impossibility of rapid gas circuit de-pressurisation, so that most standpipe positions are available for coarse control rods, and local criticality presents no special problems. However, the very large size of core means that particular care is necessary in the design of the spatial control rod layout. For a large reactor an (x,y) spatial control arrangement can be more easily integrated with both the fixed flattening scheme and any override rods (if present) than can a scheme based on the sector arrangement. For the design discussed here an (x,y) lattice of steel spatial control rods, one to each controlled region, is used, as shown in Fig. 3. Because of the very large flattened radius it is possible to locate all these rods within the flattened region. A similar set of steel override rods is provided which are intermeshed as regularly as possible with the spatial control rods; these are operated in unison to control the temperature and xenon reactivity changes associated with power variations, and individually for regional reactivity trimming. This scheme gives better trimming and automatic flattening than is possible with other arrangements; the improved core efficiency in a large reactor more than offsets the cost of the larger number of control mechanisms. Figure 4 illustrates typical transient behaviour of the reactor following a local step movement of absorber, corresponding to a refuelling operation. Figure 5 gives the time constants and periods of

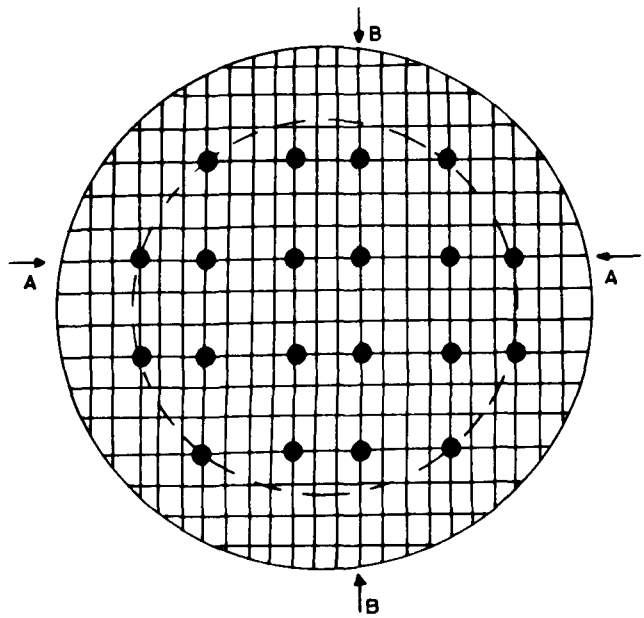


Figure 3. Spatial control rod allocation for large reactor design

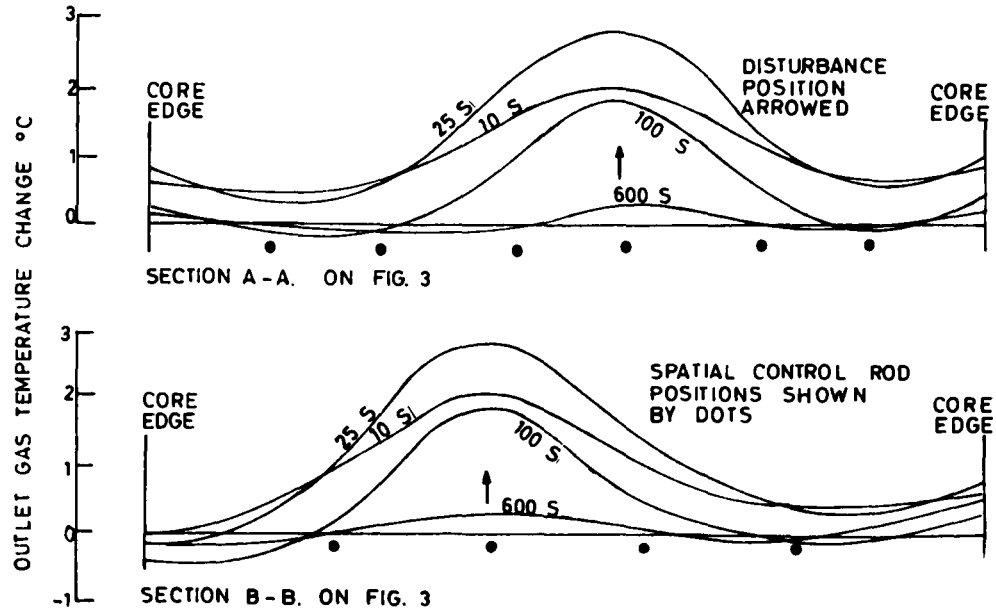


Figure 4. Large reactor design. Spatial response to 4 × 10^{-5} k single absorber step movement, all controllers operating

typical radial-azimuthal flux modes. The controlled system is spatially stable with any one controller out of operation; stability with one control region inoperative, whilst desirable, is not essential, because the response rate in an uncontrolled region sometime after a disturbance is comparatively slow. However, stability in these conditions is a good indication of satisfactory local transient spatial behaviour in general.

Future reactors

The next stage in the commercial development of gas-cooled reactors is typified by the Advanced Gas-Cooled Reactor (AGR) for which the control principles discussed in this paper remain broadly applicable, although with some shift of emphasis. AGR designs are likely to employ re-entrant coolant flow arrangements, so that off-lattice holes will not normally be available for control absorbers. Thus, for economic reasons, the use of large numbers of either fixed or variable flattening absorbers is precluded, because of the consequent reduction of channels available for fuel. A lower limit on numbers of control rods will however be set by the severity of local criticality effects with enriched fuel.

The greater durability of steel-canned uranium oxide fuel and the choice of enrichment value allows either fuel interchange, or graded enrichment, or both, to be adapted for flattening purposes, leading to greater neutron economy. With these methods alone, however, it is likely that only a relatively poor control of the radial power shape will be possible, so that a moderate amount of movable absorber trimming will still be needed.

For a given power output, spatial control can be more easily achieved for an AGR than for a Magnox reactor, mainly because of its smaller size, but also because moderator temperatures will be less affected by reactivity disturbances if a re-entrant coolant flow system is used.

Greater flexibility in station operation is likely to be required in the future, and the reactors will need to be more closely integrated with the conventional plant. Core inlet and outlet gas temperatures may be arranged to have particular variations with load,

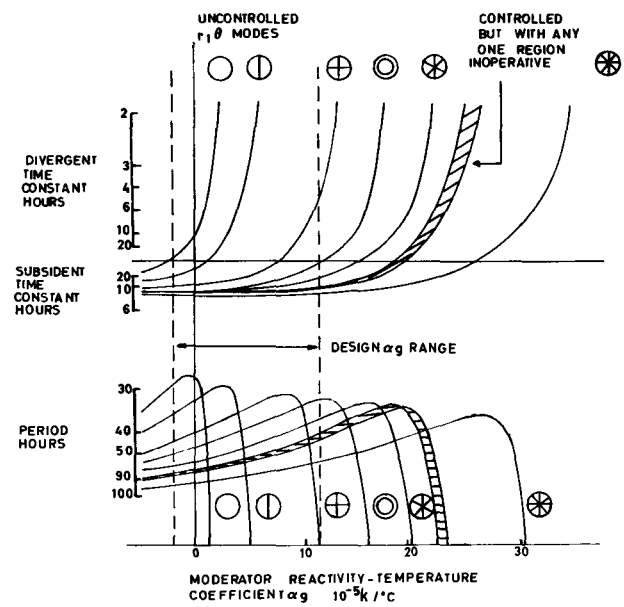


Figure 5. Large reactor design. Radial-azimuthal stability at full power

to assist in control of steam conditions or to reduce the override reactivity requirements. Considerations of this type will not, however, affect control rod system design principles.

CONCLUSIONS

The uranium Magnox reactor is now well developed, and the design methods of analysis are fairly well established. Although current control requirements are more complex than was originally envisaged, existing designs have been or can be adapted to satisfy them. The various control requirements are often conflicting, but satisfactory compromise solutions can be found.

The design principles outlined in this paper are likely to be applicable to future designs of gas-cooled reactors, in which it will be possible to improve the integration of the spatial control and override rods with the flattening absorbers, so leading to better flux shape control and enhanced core efficiency.

ABSTRACT - RÉSUMÉ - АННОТАЦИЯ - RESUMEN

A/180 Royaume-Uni

Étude des systèmes de pilotage pour réacteurs refroidis par un gaz

par P. B. Branson *et al.*

On discute l'application pratique des principes de pilotage aux réacteurs refroidis par un gaz et modérés au graphite, surtout en ce qui concerne le groupage, la distribution spatiale et les vitesses de déplacement des absorbeurs de réglage. On considère à la fois les aspects statiques et cinétiques du pilotage; certaines exigences ne peuvent s'exprimer que qualitativement, d'autres sont incompatibles et nécessitent des compromis; une surveillance appropriée des conditions dans le réacteur est essentielle.

Des méthodes rapides et économiques d'analyse des projets à l'étude sont nécessaires pour compléter les méthodes d'analyse détaillée, qui conviennent mieux pour les études du comportement des réacteurs en fonctionnement. On décrit des méthodes d'étude types qui conviennent pour l'analyse du contrôle statique et cinétique.

On considère les différents groupages des barres de réglage grossier pour le démarrage et on montre qu'une disposition par quatre groupes fournit probablement la meilleure configuration. On décrit l'utilisation de barres automatiques de régulation spatiale à la fois pour le réglage global et pour le réglage localisé; on discute des exigences opposées affectant les vitesses de déplacement et on présente une autre disposition (x, y) de l'arrangement classique en secteurs. On compare les avantages des absorbeurs fixes et mobiles pour l'aplatissement de la courbe de puissance; on souligne la nécessité de considérer les groupes de barres de régulation spatiale et de compensation comme faisant partie intégrante de l'aplatissement de la puissance, et l'importance de la symétrie dans les groupes de barres.

Les principes de régulation discutés ci-dessus sont illustrés par le cas de deux systèmes différents. Tout d'abord on considère l'étude du réacteur de Tokai; il s'agit d'un réacteur relativement petit, dont la construction est assez avancée, avec de nombreuses caractéristiques communes à d'autres réacteurs Magnox du stade 1. L'équipement comporte des dispositifs d'arrêt rapide secondaires, utilisant des billes d'acier au bore, en tant que protection supplémentaire contre les risques de tremblement de terre. On décrit la manière dont ces dispositifs, ainsi que les groupes de barres de commande et le système d'aplatissement variable de la puissance, sont logés dans une simple grille de tubes fixes, une attention particulière étant accordée à l'élimination du risque de «criticité locale». On expose le comportement type transitoire spatial pour la disposition en secteurs des barres et on indique les effets de l'emplacement des thermocouples de contrôle par rapport aux barres.

Ensuite, on considère un nouveau type de cœur et on décrit le système de régulation; ce cœur est beaucoup plus grand que celui du réacteur de Tokai et on utilise l'aplatissement fixe de la puissance. A cause des grandes dimensions, il est possible d'étendre l'intégration des barres de régulation spatiale et de compensation avec l'aplatissement de la puissance; ceci améliore à la fois l'efficacité du cœur et l'effet d'aplatissement automatique du flux des barres de régulation spatiale. On discute des avantages d'une disposition (x, y) des barres de régulation spatiale pour un cœur de grandes dimensions. On donne les résultats des études de stabilité radiale-azimutale et les effets transitoires à la suite d'un déplacement local d'absorbeurs.

On discute les tendances probables des systèmes de pilotage pour les réacteurs futurs, tels que le réacteur amélioré à réfrigérant gazeux, y compris une intégration plus étroite avec une installation classique, un meilleur asservissement du réacteur en fonction de la demande de puissance, et un fonctionnement de plus en plus souple.

A/180 Соединенное Королевство

Конструкция систем регулирования реакторов с газовым охлаждением

П. Б. Брансон *et al.*

Обсуждается практическое применение принципов регулирования к реакторам с газовым охлаждением и графитовым замедлителем, особый упор делается на группирование, пространственное распределение и скорости движения регулирующих поглотителей. Рассматриваются как статические, так и кинетические аспекты регулирования; некоторые требования выражены только качественно, а часть их является спорной, в отношении которых необходимо идти на компромисс; существенным является соответствующий контроль режима реактора.

Быстрые и экономичные расчетные методы анализа необходимы в дополнение к детальным методам анализа, которые более удобны для тщательного рабочего исследования режима работы реактора. Описываются методы расчета, удобные для статического и кинетического анализа регулирования.

Рассматриваются различные способы группирования стержней грубой регулировки при запуске; показано, что четырехгрупповая схема является, вероятно, наилучшей. Описывается применение группы автоматических регулирующих стержней как при одновременном действии, так и регулирование отдельными стержнями; обсуждаются противоположные требования, влияющие на скорости движения стержней, и в обычную секторную схему вводится переменный слой (x, y). Сравниваются достоинства неподвижных и подвижных поглотителей для выравнивания мощности; подчеркивается необходимость рассмотрения группового регулирования и регулирования одиночными стержнями как составная часть выравнивания мощности и важность симметрии в группах стержней.

Обсужденные выше принципы регулирования иллюстрируются ссылкой на две различные системы. Во-первых, рассматривается проект реактора в Токаи-Мура. Это сравнительно небольшой реактор, находящийся в стадии сооружения; многие конструктивные особенности его подобны другим магноксовым реакторам первой очереди. Конструкция включает дополнительное устройство для остановки реактора с шарами из бористой стали, которое является дополнительной мерой предосторожности против сейсмической опасности. Описывается способ, которым эти устройства вместе с группой регулирующих стержней и системой выравнивания компонуются на решетке технологических каналов; особое внимание уделяется исключению возможности появления локальной критичности. Приводятся типичные переходные характеристики для случая размещения групп регулирующих стержней по секторам и указывается на влияние размещения термопар на стержнях.

Во-вторых, рассматривается новая конструкция активной зоны и описывается система регулирования; эта активная зона значительно больше активной зоны реактора в Токаи и в ней используется фиксированное выравнивание. Благодаря большому размеру активной зоны возможно объединение регулирования групной стержней и одиночными стержнями с системой выравнивания мощности; это улучшает как коэффициент полезного действия, так и эффект автоматического выравнивания группы регулирующих стержней. Обсуждаются преимущества регулирования группой стержней и отдельными стержнями для активной зоны больших размеров. Приводятся результаты изучения радиально-азимутальной устойчивости и влияния локального перемещения поглотителя на переходные процессы.

Обсуждаются возможные направления развития систем регулирования будущих реакторов, таких как усовершенствованный реактор с газовым охлаждением, с учетом опыта эксплуатации современных атомных станций, последующего увеличения нагрузки и повышения гибкости в процессе эксплуатации.

A/180 Reino Unido

El diseño de los sistemas de control de los reactores refrigerados por gas

por P. B. Branson *et al.*

Se discute la aplicación práctica de los principios de control a los reactores moderados por grafito y refrigerados por gas, haciendo particular referencia al agrupamiento, distribuciones espaciales y velocidades de desplazamiento de los absorbentes de control. Se consideran los dos aspectos del control, estático y cinético. Algunos requerimientos sólo pueden formularse cualitativamente, otros son antagónicos y exigen un compromiso. Una vigilancia adecuada de las condiciones del reactor es fundamental.

Se necesitan métodos analíticos de diseño, rápidos y económicos, como complemento de los muy detallados que son más apropiados para estudios minuciosos del comportamiento del reactor en operación. Se describen métodos típicos de diseño, adecuados al estudio analítico del control en su doble aspecto, estático y cinético.

Se consideran varias formas de agrupar las barras de control grueso para la fase de arranque, y se demuestra que la disposición de cuatro grupos es probablemente la mejor. Se describe el empleo de barras de control espacial automático de acción tanto conjunta como local, se discuten los requisitos

antagónicos que afectan a las velocidades de desplazamiento, y se introduce una configuración (x, y) distinta al esquema convencional de sectores. Se comparan las ventajas de los absorbentes fijos con las de los desplazables en el aplanamiento de la potencia. Se resalta la necesidad de considerar el control espacial y excluir los grupos de barras como partes integrantes del aplanamiento. Se destaca también la importancia de la simetría en los grupos de barras.

Se ilustran los principios de control anteriormente discutidos en referencia a dos sistemas en contraste. En primer lugar se considera el diseño del proyecto Tokai, un reactor relativamente pequeño y en avanzado estado de construcción, que contiene muchas características comunes a otros reactores de magnox de la serie 1. El diseño incluye dispositivos secundarios de parada, utilizando esferas de acero al boro, para aumentar la protección frente a posibles seísmos. Se describe la forma en que estos dispositivos, así como los grupos de control y el sistema de aplanamiento variable, se sitúan dentro de un enrejado único de tubos de soporte, prestando especial atención a eliminar el riesgo de criticidad local. Se detalla el comportamiento de la disposición de elementos de control por sectores ante transitorios espaciales típicos, y se mencionan los efectos producidos en las barras en relación con la situación de los termopares de control.

En segundo lugar se considera un nuevo diseño de núcleo y se describe el sistema de control. Este núcleo es mucho mayor que el del reactor de Tokai y se emplea un sistema de aplanamiento fijo. Debido a sus grandes dimensiones es posible incluir el aplanamiento en el control espacial y excluir las barras; esto supone un mejoramiento, tanto en la eficiencia del núcleo como en el efecto de aplanamiento automático de las barras de control espacial. Se discuten las ventajas de una configuración (x, y) de control espacial y de la exclusión de barras, para un núcleo de gran tamaño. Se exponen los resultados de estudios sobre estabilidad radial-azimutal y los transitorios que siguen a desplazamientos locales de absorbente.

Se discuten las directrices más probables para los sistemas de control de futuros reactores, tales como los avanzados de refrigeración por gas, incluyendo una integración más ligada a la planta convencional, con una mejor acomodación a la potencia de carga, y una mayor flexibilidad de funcionamiento.

Poison control of thermal reactors

By A. Radkowsky * and R. J. Creagan **

The control of nuclear reactors has been accomplished in large measure through the motion of neutron absorbing materials known as control rods. The use of such moving control rods, while straightforward conceptually, has limitations from the standpoints of mechanical complexity and the amount of reactivity which can be controlled. Thus several means of supplementing or partly eliminating control rods have been explored. In the soluble poison method, which is applicable to liquid cooled reactors, the neutron absorbing material is dissolved in the coolant. This requires means for injecting and removing the neutron absorber from the coolant. On the other hand, in the burnable poison method the neutron absorbing material is fixed in the reactor at the start of life and automatically removed by neutron absorption as the reactor operates; burnable poison can be utilized in either liquid-cooled or gas-cooled reactors [1].

Both of these control methods, soluble poison and burnable poison, have their advocates, and relative advantages and disadvantages. In this paper each method is described in a separate section without attempting to evaluate their relative merits. Comparisons cited in each section are with cores controlled entirely by mechanical rods. We shall not discuss use of soluble and burnable poisons in combination [2] in view of limited applications in this area.

SOLUBLE POISON CONTROL

R. J. Creagan

Boric acid dissolved in the coolant moderator has been used to compensate for cold-to-hot reactivity change in a number of power reactors, Yankee, Indian Point, BR3, and Saxton. The extension to power operation for control of reactivity loss due to depletion and fission product accumulation, called chemical shim, has been practiced to a limited extent in EBWR, BORAX, Yankee, and BR3. More recently, Saxton has completed nine months of full chemical shim operation with up to 1 200 ppm of boron as boric acid. This approaches the concentration range (1 100 to 1 600 ppm) which would be typical of large, high burn-up reactors.

A brief review is presented of the physics and chemistry aspects of the use of boric acid for chemical shim in closed-cycle water reactors.

Physics

The primary advantages of chemical shim control stem from core design considerations. It permits a reduction in the number of control rods, drive mechanism, and associated equipment by more than 50%. It also yields improved core performance through a reduction in the maximum-to-average power density. Finally, it permits significantly higher fuel burn-ups.

Changing the concentration of a chemical neutron absorber dissolved in the primary coolant is inherently a slow process. As a consequence, the dissolved neutron absorber is used only to compensate for such slowly varying reactivity effects as cold-to-operating moderator temperature change, fission product poisoning effects, and fuel depletion. A typical large water-moderated reactor, however, requires roughly 20% excess reactivity (at ambient temperature) for a fuel burn-up of 8 000 megawatt days/metric ton of uranium between fuel loadings [3]. Over two-thirds of this may be controlled by chemical shim. The control rod reactivity requirements in a typical core which utilizes chemical shim are roughly 6%. Although control rod worth is reduced slightly in the presence of boron, this effect is very small ($\sim$ 12%).

Since fuel depletion effects are controlled by the dissolved neutron absorber, the reactivity worth of control rods does not place a fuel burn-up limitation on the core. Fuel burn-ups in the range of 24 000 megawatt days per ton or higher can be controlled easily by chemical shim.

Chemical shim control permits a reactor to be operated at full power in the steady-state condition, with all control rods in the "out" position except for a small rod insertion for transient control. Since the distribution of neutron poison is uniform and independent of the amount of reactivity being controlled, the fuel loading distribution is much more easily "designed" to yield a uniform power distribution. For example, the density of fissionable material may be distributed in concentric zones about the axis of the reactor to maintain a very favorable power distribution, and local power peaking effects caused by control rods are minimized.

* United States Atomic Energy Commission.
** Westinghouse Electric Corporation, Atomic Power Division.

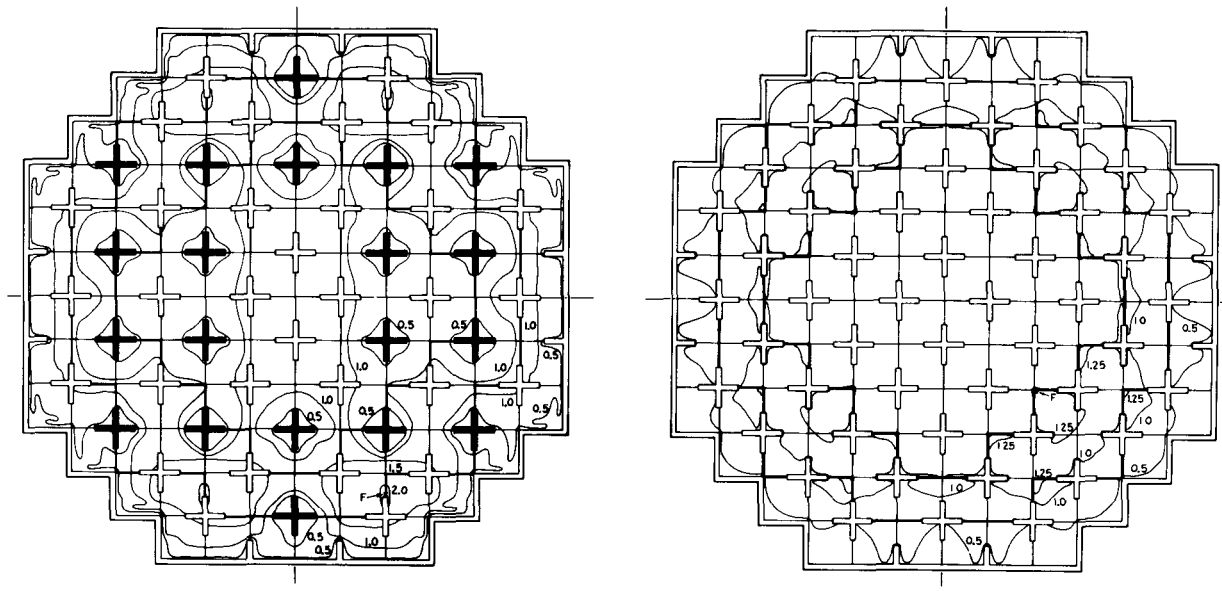


Figure 1. (left) Power distribution in 3-region core using rod control; (right) power distribution in 3-region core using chemical shim control

Figure 1 illustrates these effects with a 120 fuel assembly core, loaded in three concentric regions in a large pressurized water reactor. Each region contains 40 fuel assemblies. The region boundaries are represented by darker lines than those outlining fuel assemblies, and control rods are represented by black cruciforms. The core cross section on the right shows the power contour map through a transverse section of a core controlled by a uniform chemical poison. The cross section on the left shows an identical mechanical design in which neutron absorbing control rods are used to compensate for roughly 6% excess reactivity.

The major disadvantage of controlling solely by rods is that the optimum fuel loading distribution with one control rod pattern may be far off power density optimum for other patterns. A control rod program specification, however, requires many costly calculations to show that an acceptable power distribution is achievable with multiple control rod patterns to suit the varying excess reactivity requirements of the core throughout its life. The control rod pattern at the left of Figure 1 is representative of the worst transverse power distribution which might be obtained during a core lifetime with an optimum control rod program, and is equivalent to a maximum-to-average power density of 2.5. This is a 50% increase over the maximum-to-average shown on the right side of the figure.

The temperature coefficient of reactivity with chemical shim [4] is less negative than in a rodded core. Neutron leakage to control rods contributes a negative increment to the coefficient and, in chemical shim, the rods are nearly removed. Also, chemical poison density decreases with water density at temperature, giving rise to a positive component of moderator coefficient directly proportional to poison concentration (Fig. 2). Since chemical poison is used to control excess reactivity for burn-up, the initial temperature coefficient becomes less negative as design burn-up increases. With sufficient boron, the coefficient can become positive, especially at lower temperatures with the core less undermoderated than at operating temperatures. With respect to accident the uncontrolled transient response is determined by the prompt Doppler coefficient which is unaffected by boron additions.

It is found that with a zero or even positive moderator temperature coefficient, core stability is

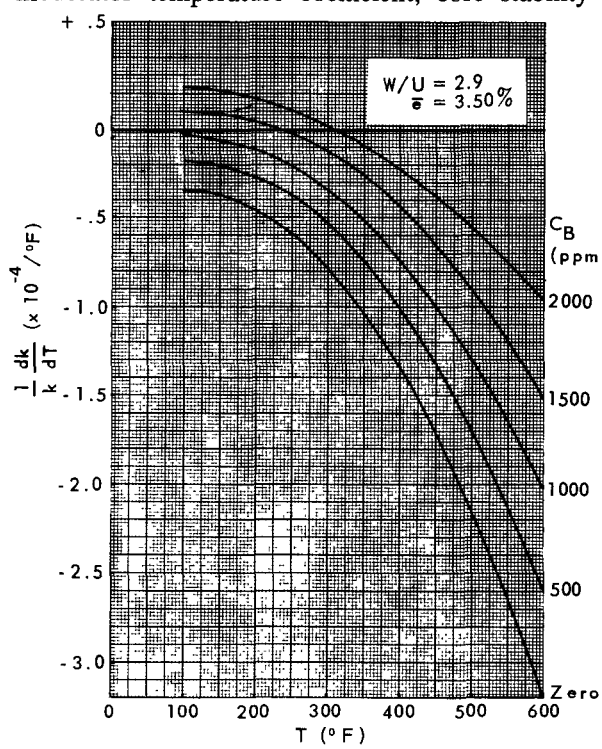


Figure 2. Moderator temperature coefficient vs. moderator temperature at different boron concentrations

not adversely affected if the net coefficient (Doppler plus moderator) remains only slightly positive. A case studied (typical of 400 to 500 MW(e) plants) with a net coefficient of $+ 1 \times 10^{-4}$/ °F indicated no difficulties. The selective accumulation of boron in the core during operation is the only significant potential safety problem associated with chemical shim. Sudden release of accumulated boron to the coolant would cause a ramp increase in reactivity as the coolant containing the released boron left the core. The maximum allowable release of such accumulations (or hideout) is calculable for a given core and stated operating conditions.

Because the maximum release corresponds to a rather small concentration change, it has been found more practical to monitor hideout by a continuous follow of core reactivity changes rather than depending on inventory control.

Chemistry

Following the preliminary evaluation at Argonne National Laboratory [5] and Westinghouse, leading to the conclusion that boron as boric acid was the best candidate material for chemical shim, many questions still remained to be answered, particularly with respect to safety and plant application problems. Accordingly, as part of the Large Reactor Research and Development Program carried out by Westinghouse Atomic Power Division for the U.S. Atomic Energy Commission, these problems were investigated in detail in the laboratory and in the operation of the Saxton Reactor (Saxton Nuclear Experiment Corporation) with chemical shim. Other chemical shim operations at the Yankee Reactor were followed closely and the results correlated with the overall program. The laboratory program is essentially complete [6, 7, 8, 9, 10]. A substantial body of laboratory data and plant operating experience has been accumulated from which significant conclusions on the utilization of chemical shim in power reactors can be drawn.

Laboratory results

Limitations of space preclude any treatment other than a summary of the findings of the laboratory program and brief résumé and interpretation of the plant operating experience, as follows:

(*a*) The major potential safety problem in chemical shim is the possible sudden release from the core of deposits of transport corrosion products (crud) containing boron adsorbed or precipitated from the coolant;

(*b*) Based on tracer tests with artificial crud it is inferred that significant boron accumulation in crud deposits (hideout) can occur only with thick deposits, and only when boiling occurs at the deposit site (sub-cooled or bulk boiling);

(*c*) Operation with 10^{-4} molar alkali additive tends to decrease quantity and concentrating ability of deposits;

(*d*) Materials suitable for core and plant construction in neutral or alkaline water are, in general, also suitable for use in chemical shim plants. There are possible exceptions, such as nickel plate;

(*e*) Corrosion product release rates and consequent plant contamination, although somewhat increased compared with those from pure water, are at acceptable levels, based on nine-month corrosion test data;

(*f*) Boric acid solutions can be purified by borate form ion exchange in the same manner, and essentially to the same practical degree, as pure water with alkali additive;

(*g*) Some problems exist in waste disposal because of the volatility of boric acid. The problem can be overcome by neutralization of the waste and ion exchange of evaporator overheads. Waste disposal in a chemical shim plant is more expensive than in a plant with rod control, but less than in plants with only hot-to-cold reactivity control with chemical poison, with the other control by rods. This results from the higher average ratio of operating to shutdown poison concentration in a chemical shim plant compared with a plant with hot-to-cold reactivity control only.

Plant operating experience

Yankee, Consolidated Edison Indian Point, Saxton, and BR3 all use boric acid for hot-to-cold reactivity control, and have experienced no significant problems in this application. BR3 operated for about one month, and Saxton has operated for nine consecutive months [11, 12] with chemical shim, without short-period reactivity effects or operational problems, except waste disposal as previously noted. Based on successful short chemical shim tests on Yankee Cores 1 and 2 [13], Yankee Core 3 has been designed with higher reactivity and has operated on chemical shim for its first 2 months. Slow reactivity changes have been observed in BR3 and Saxton [12], but none of these are attributable to boron hideout. The most important observation has been that of the increase of reactivity with increase of coolant pH. The effect has been observed at Saxton at power, with or without nucleate boiling over a significant area of the core, but not at zero power. It has been observed at Saxton and Yankee [13] with and without significant boron levels in the coolant. The addition of lithium and potassium (equivalent to pH 10 to 10.5 in pure water) produces an increase in reactivity of 0.25% $\Delta k/k$ at Saxton. A similar addition of ammonia results in a 0.5 to 0.6% $\Delta k/k$ increase at Yankee. Removal of the alkali results in a corresponding loss of reactivity. The rate of change of reactivity is slow, the full effect requiring from 10 to 20 hours after step additions of alkali. No satisfactory explanation for this effect has been developed. The "pH" effect cannot be correlated with

the poison content of the coolant or corrosion products, including trace quantities of control rod materials. A careful reactivity balance at Saxton [11] showed a maximum difference of 0.15% $\Delta k/k$ between observed and calculated reactivity. In subsequent operation for a total of nine months, this figure was not exceeded. Hot laboratory examination of core deposits following this period of operation showed trivial quantities of residual poison on the core (boron and control rod materials). Yankee fuel removed from Cores 1 and 2 was as clean or cleaner than Saxton fuel.

The experience cited demonstrates that chemical shim is a safe and practical method of operation for closed-cycle water reactors, providing important advantages in design and operating economics.

BURNABLE POISON CONTROL

A. Radkowsky

General survey

Burnable poisons either are used uniformly mixed with the fuel (distributed poisons) or are placed discretely as separate fixed elements in the reactor (lumped or self-shielded poison). The arrangement and quantities of the burnable poisons are designed to maintain reactivity nearly constant over core life.

The use of burnable poisons has several significant advantages:

(*a*) Core endurance can be greatly increased because the reactivity effect of the fuel is balanced by the absorption of the burnable poison so that core lifetime achievable now becomes essentially limited only by metallurgy and irradiation;

(*b*) By use of burnable poison the maximum reactivity of the core can be adjusted to be close to the value at end of core life so that the required number of mechanical control rods is much reduced;

(*c*) Power distributions can be significantly improved for two reasons:

(i) Control rods, except those required for transient xenon and samarium and for mismatch are removed from the core during operation, which reduces flux distortions; and

(ii) A further improvement can be obtained by locating burnable poison at points where the flux tends to peak, which reduces the peaks and leads to a uniform power distribution through the core;

(*d*) Burnable poison tends to make the reactivity temperature coefficient of the core more negative, which results in increased safety, stability, and self-regulation. Flexibility in location of burnable poisons provides the nuclear designer an additional degree of freedom which can be utilized in zoning arrangements to enhance core performance in many important respects. Since the burnable poison is confined to the core, the beneficial effects of the reflector on power distributions and neutron moderation are retained.

Figure 3 [14] shows some of the salient features of the use of burnable poison versus control rods for the control of reactivity effects due to depletion. Note the much greater control swing and therefore larger number of control rods required when burnable poison is not used. In fact the endurance obtainable with the burnable poison is far beyond that which could be controlled by mechanical rods.

The material which has received most consideration for burnable poison application is boron, although, as discussed later, other materials are advantageous in special situations. Nuclearly, boron has the advantage that its absorbing isotope, B^{10}, has a cross section sufficient to compensate for the depletion of U^{235} fuel and build-up of fission products and that its reaction products, Li^7 and helium, have negligible absorption. Furthermore, physics predictions of the performance of cores utilizing boron are facilitated by the $1/v$ energy dependence of the boron absorption cross section, which means that the depletion of boron relative to U^{235} fuel will be nearly independent of the thermal spectrum shape. While epithermal fissioning becomes important in highly loaded cores, the ratio of boron to U^{235} microscopic absorption cross section, averaged over all neutron energies, is nearly constant (varying between 5.5 and 5.6) for a wide range of average neutron thermal energy [15]. For high fuel loadings the use of boron homogeneous with the fuel results in too great a reactivity excursion and it is necessary to reduce the average flux "seen" by boron relative to fuel by using the boron in self-shielded form. By combinations of distributed and self-shielded boron it appears possible in most practical cases to provide good regulation of reactivity and still leave only a small poison residue, avoiding undue increases in fuel inventory.

In contrast to its desirable nuclear properties, boron has relative undesirable physical character-

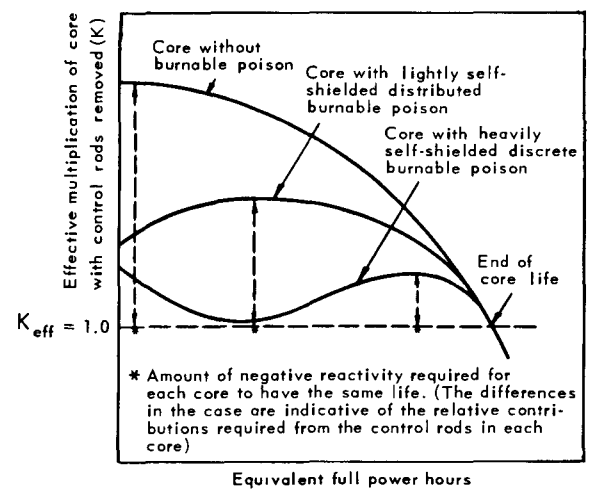


Figure 3. Reactivity with control rods removed from cores containing (a) no burnable poison, (b) lightly self-shielded distributed burnable poison, and (c) heavily self-shielded discrete poison

istics, particularly when distributed in the fuel. There is an increased tendency towards swelling of fuel elements and decreased corrosion resistance and ductility.

Since a review paper on burnable poisons was given at the 1958 Geneva Conference [16], the remainder of this section will emphasize development over the last 6 years.

Application to reactors containing fertile materials

Two types of reactor concepts containing fertile material have been extensively studied: the seed-blanket type in which fertile material is in natural form and highly enriched material is placed in seed regions [17], and the uniformly enriched type in which fertile and fissionable fuels are mixed homogeneously in one or more zones of enrichment.

In application of burnable poison to seed-blanket reactors it is evident that the poison need be placed only in the seed, which controls the core reactivity. The amount of burnable poison required for control is relatively small, since the seeds are usually designed as highly buckled regions in order to increase the blanket power output. Thus in Shippingport Core 1, in which only a moderate increase in seed endurance was sought, 0.04 wt % of natural boron was added uniformly to the fuel alloy.

In Shippingport Core 2 the seed average energy density has been increased by a factor of more than $2\frac{1}{2}$ and power density nearly doubled. The blanket irradiation is sufficiently great to change the blanket multiplication factor by amounts appreciably affecting core reactivity. It is desirable to employ burnable poison elements designed to result in a slight rise (about $1.5\% \Delta k$) in core reactivity, thereby minimizing the residue of burnable poison at end of seed life. Further, the burnable poison must be carefully located so as to promote a uniform power distribution. Figure 4 shows schematically the arrangement of the burnable poison in the Shippingport Core 2 design. Poison elements are fabricated from stainless steel containing 0.8 wt % boron-10. The elements are located at corners of each seed cluster to supress flux peaks as much as possible. Power distribution can be still further improved by local zoning of fuel. Such zoning has a relatively large effect on the power, which is proportional to the product of thermal flux and fuel density, but has little effect on flux shapes or control rod worths. The relatively narrow burnable poison elements provide flexibility during the course of the design for varying either self-shielding, by adjusting poison density, or the poison quantity, by varying the plate widths.

Because of $1/v$ dependence of the boron cross section, discrete poison elements will be more self-shielded and therefore less effective when the core is cold than hot. This does not necessarily mean that the cold core is more difficult to shut down

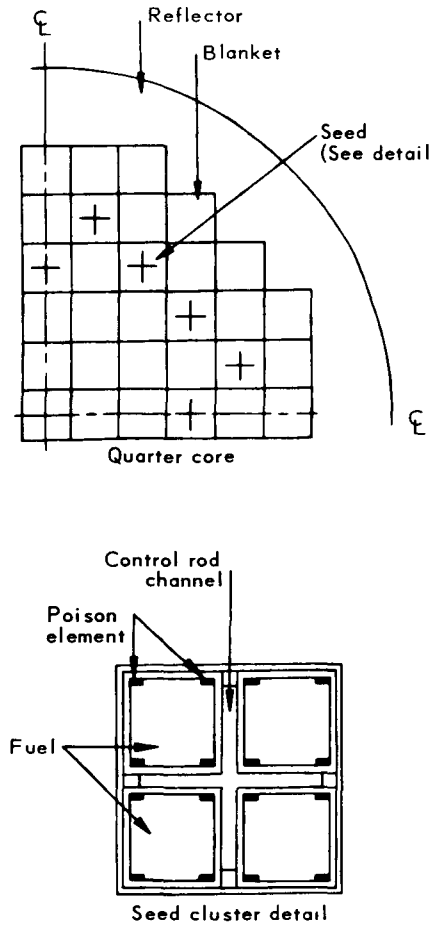


Figure 4. Schematic arrangement of burnable poison in Shippingport Core 2 geometry

when a control rod is completely withdrawn (the criterion usually adopted for shutdown adequacy). As is evident from Fig. 4, with one control rod withdrawn, the flux would tend to peak at the poison elements near the control rod channel and enhance their worth, thus partly offsetting the effect of increase in self-shielding.

For poison elements of plate form, diffusion theory is usually used to calculate the boron absorptions with plate diffusion parameters selected to fit blackness theory [15]. In many cases, however, the poison elements are in the form of short plates (Fig. 4) or other geometry for which a one-dimensional treatment is inadequate. A Monte Carlo calculation is then needed, but even with modern high speed computers it is still not feasible to apply Monte Carlo methods to a complex core configuration. A useful procedure is to select a model geometry and fit parameters for the poison elements in diffusion theory such that the ratio of captures in poison to fuel agree with Monte Carlo. It is then found that this equivalence holds almost regardless of the external medium, provided that the characteristics and mesh spacing of the poison region are unchanged.

In uniformly enriched cores both homogeneous and discrete boron can be employed. Thus the Indian Point Reactor (U^{235} plus thorium fuel) utilized boron in the fuel element cladding. For uniformly enriched uranium cores it is possible to select self-shielded boron elements which will result in a close reactivity match and small poison residue. The following values are typical [17]:

Enrichment (wt % U^{235})	Initial value of self-shielding for boron element
2	1.25
3	1.9
4	2.1

These calculations were for batch loading. The use of fuel management presents a more difficult problem, since first-cycle fuel is moved in the reactor to a location of different neutron importance; thus, in the usual case, partially depleted fuel is shifted from the periphery of the core to the center. The ideal burnable poison would then be such as to maintain the multiplication factor of the fuel at a relatively high value during the first cycle, and at a lower value during the second cycle. This behavior could be approximated in a practical case by use of heavily self-shielded poison elements (Fig. 3). Still better performance can be obtained by combinations of lightly and heavily self-shielded elements, and neutron economy is improved over that with a uniform macroscopic poison cross section throughout the reactor.

Burnable poisons other than boron

Materials other than boron most frequently considered as burnable poisons [15] are discussed below.

Samarium is especially convenient as a supplementary burnable poison to boron to increase core shutdown at the beginning of life by the amount of negative reactivity which will be introduced by build-up of permanent samarium. It is then feasible to reduce the amount of boron required initially, and, consequently, the amount of self-shielding, which leads to a somewhat smaller boron residue and increased endurance for a given fuel loading. Use of samarium would not be expected to introduce additional metallurgical problems since it builds into fuel elements as a fission product.

The SNAP 10 reactor, which contains uranium-zirconium-hydride elements and is liquid metal cooled, is controlled by samarium burnable poison and temperature variation. In this design the high cross section of samarium results in a rise of reactivity which offsets the rapid loss of reactivity due to hydrogen redistribution.

A combination of samarium and europium [15] has been considered for shimming EBWR, loaded for the Plutonium Recycle study [19].

Dysprosium depletes much less rapidly than boron and may avoid the need for poison self-shielding in a long-lived core. Unfortunately, residual absorption (from dysprosium daughter isotopes) always exceeds 20% of the initial value and increases with higher fuel loads and resultant hardening of the thermal spectrum. In the Dresden boiling water reactor pellets of dysprosium oxide are used in the ends of the fuel elements.

Erbium has a unique property, resulting from the low lying resonances and $1/v$ behavior in the thermal range in that the addition of the element to a well moderated core results in enhancement of the negative temperature coefficient. This is important in some cases from a self-protection standpoint. Erbium is employed for this reason in TRIGA reactors and its use has been considered in superheat reactors to ensure safety in case of flooding. Erbium depletes at a rate which maintains a close reactivity match in well moderated thermal reactors. The residue is appreciable but helps to ensure a negative temperature coefficient at the end of core life.

Gadolinium has a cross section (46 000 barns at 2 200 m/s) which is so large relative to fuel that the element must be self-shielded as a burnable poison. All incident neutrons in the thermal energy range will be absorbed on the surface of a gadolinium lump. Thus the lump reactivity worth is proportional to its surface area [20]. For a gadolinium cylinder depletion reduces the effective lump area linearly with flux time since absorption cross sections of daughter isotopes are small. By proper shaping and selection of cylinder dimensions reactivity can be regulated very closely for a wide range of reactor compositions. This has been studied in the Allis Chalmers Shaped Burnable Poison Program. Figure 5 shows results for a large boiling reactor with zirconium clad uranium fuel elements, enriched to 3.3 wt % U^{235}, and 2.6 water/fuel volume ratio; the computed lifetime is 18 500 MWd/t. An even better reactivity match could be obtained with fewer cylinders of larger diameter.

The high cross section of gadolinium permits use of small Gd_2O_3 lumps which may be mixed with uranium oxide fuel. From a safety standpoint, in case of a nuclear excursion, gadolinium oxide would probably diffuse into the fuel, giving a strong negative reactivity effect.

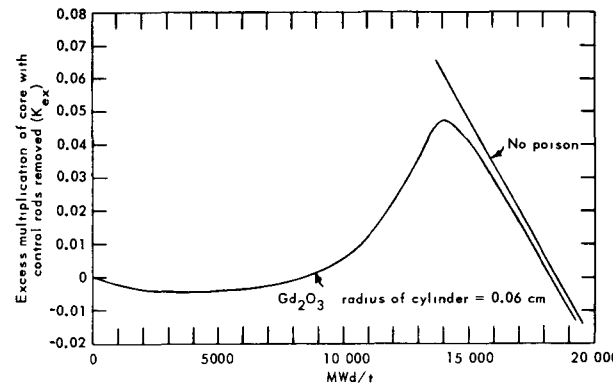


Figure 5. Reactivity of a large boiling water reactor

By combination of gadolinium and erbium [2] homogeneously distributed in the fuel it appears possible to reduce the reactivity temperature defect without affecting the negative temperature coefficient at power, but depletion effects have not been studied.

Experimental techniques

In analyzing lifetime behavior of cores utilizing boron burnable poison it is important to determine the ratio of boron absorptions to fuel fissions. Since boron does not activate, determination of boron absorptions presents a problem experimentally.

The usual recourse has been to mix an activating or "spiking" material in low concentration uniformly with several of the boron elements in a critical assembly. The activating material then yields a measure of boron absorptions, provided that corrections are made for the amount by which the cross section of the activating material as a function of energy differs from that of boron. The activating material most commonly used is manganese, for which basic techniques were worked out by W. Baer of Bettis Atomic Power Laboratory. Unfortunately manganese has a high resonance absorption which necessitates large corrections, making accurate determination of the boron absorption difficult.

Use of vanadium as an activating material in connection with boron absorption measurements has been suggested by D. A. Gavin of Knolls Atomic Power Laboratory. W. Skolnik, also of Knolls, has suggested nickel. Ni^{64} and V^{51} have very little resonance absorption.

Skolnik has recently completed a comparative study of all three materials as activators in boron, using gamma counting, and has obtained good agreement. Corrections for resonance absorption in the activating materials are made by measurements with and without cadmium sleeves, to obtain in effect the thermal component of the activation. By intercalibration of thin foils of the activating material and of fuel in a known flux and assuming that the activating material has $1/v$ absorption in the thermal range, the ratio of boron absorptions to fuel fissions can be found.

It is important to correct for gamma-ray self-absorption in the activating material. To do this an activation sample, of nickel-boron, for example, was made up of thin foils. One of the foils was activated and placed in different positions in the sample, and count rates were determined, which gave the effective gamma self-absorption for each foil.

In the case of manganese the samples consisted of boron steel in which manganese was used as a hardening alloy. There is a threshold reaction of iron, Fe^{56} (n,p)Mn^{56}, which complicates the Mn^{55} (n,γ)Mn^{56} reaction used as an indicator. This was corrected for by first using a sample containing almost no manganese.

With suitable corrections all three activating materials yielded equal values for boron absorption within experimental error and agreed with a Monte Carlo calculation.

Each activator material has advantages and disadvantages. Nickel requires the smallest epithermal correction, but, because of low natural content of Ni^{64}, a high activation level must be used. Manganese occurs as an element in boron-stainless material often used in critical assemblies, but requires large epithermal corrections. Vanadium has a small epithermal correction and the natural element is 100% active, but the short half-life of the gamma radiation requires special techniques. The choice of activator thus depends on the experimental situation.

Conclusion

The use of burnable poison permits the attainment of very significant advantages in reactor performance, including greatly increased endurance, reduction in mechanical control, improvement in power distribution, and improved stability and safety. Flexibility in location of burnable poison elements provides an additional degree of design freedom which further enhances these advantages. While burnable poisons have been employed primarily in aqueous reactors, they are applicable to other fixed fuel types. In most cases the burnable poison is boron, but other materials are valuable in special circumstances. Analytical and experimental techniques have been worked out to predict burnable poison effects.

Acknowledgement

The author wishes to acknowledge assistance and advice received from members of the Bettis and Knolls Atomic Power Laboratories, and is grateful to P. Lacy of Allis Chalmers and L. S. Nims of Atomics International for information on the Shaped Burnable Poison and SNAP programs, respectively.

REFERENCES

1. Nuclear Engineering, 630A G.E. Marine Reactor, p. 51 (February 1964).
2. Bick, J. H., *Poison Mixtures Which Improve Thermal Reactor Operating Characteristics*, NAA-SR-8225 (1963).
3. Poncelet, C. G., *Analysis of the Reactivity Characteristics of Yankee Core I*, USAEC report WCAP-6050.
4. Miller, D. L., *Control Rod Requirements in a Chemical Shim Core*, WCAP-3727; French, R. J., and Miller, D. L., *Nuclear Performance of Large Pressurized Water Reactors Controlled by Soluble Poison*, TID-7672.
5. Breden, G. R., and Abers, A., *Corrosion and Stability Tests on Chemical Poisons in High Temperature Water*, USAEC report ANL-5147 (Rev.), (September 1953).
6. Fletcher, W. D., *Ion Exchange in Boric Acid Solutions with Radioactive Decay*, Westinghouse Atomic Power Division, USAEC report WCAP-3716 (November 1962).

7. Byrnes, D. E., *Some Physicochemical Studies of Boric Acid Solutions at High Temperatures*, Westinghouse Atomic Power Division USAEC report WCAP-3713, (September 1962).
8. Picone, L. F., *The In-Pile Test of Chemical Shim*, Westinghouse Atomic Power Division USAEC report WCAP-3729 (June 1963).
9. Picone, L. F., Whyte, D. D., and Taylor, G. R., *Radiotracer Studies of Hideout at High Temperature and Pressure*, Westinghouse Atomic Power Division USAEC report WCAP-3731 (June 1963).
10. Fletcher, W. D., Krieg, A., and Cohen, P., *The Behavior of Austenitic Stainless Steel Corrosion Products in High Temperature Boric Acid Solutions*, Westinghouse Atomic Power Division USAEC report WCAP-1689, revision (May 1961).
11. Bartnoff, S., Weisman, J., Impink, A. J., Layman, W. A., and Hetrick, D. E., *The Saxton Experiment on Chemical Shim*, Trans. Amer. Nucl. Soc., *6*, 305 (1963).
12. Fletcher, W. D., and Swift, R. F., *Water Technology of the Saxton Nuclear Experiment*, presented before the Division of Water and Waste Chemistry, American Chemical Society, Philadelphia, Pennsylvania (April 5-10, 1964).
13. Reed, G. A., *Operating and Refueling Experience at the Yankee Atomic Electric Power Plant*, presented at the Canadian Nuclear Association International Conference on Operating Experience and Future Development of Power Reactors, Montreal, Canada (May 27-29, 1963).
14. Anderson, W. K., and Theilacker, J. S., *Neutron Absorber Materials for Reactor Control* (1962).
15. Radkowsky, A., *Burnable Poisons*, Naval Reactors Physics Handbook, *1*, Chapter 4.7 (1964).
16. Radkowsky, A., *Theory and Application of Burnable Poisons*, Proceedings of the Second International Conference on the Peaceful Uses of Atomic Energy, P/1900, Vol. 13, pp. 426-445, United Nations (1958).
17. Schwoerer, F., *Economic Potential of the Seed-Blanket Reactor*, WAPD-237 (1960).
18. *Gas Cooled Reactor Program*, USAEC report ORNL-3523, 277 (1963).
19. *Reactor Development Program Progress Report*, USAEC report ANL-6698, 53 (1963).
20. Holl, R. J., *Highly Self-Shielded Burnable Poisons*, thesis, Ann Arbor, Michigan, University of Michigan (1963).

ABSTRACT - RÉSUMÉ - АННОТАЦИЯ - RESUMEN

A/274 Etats-Unis d'Amérique

Utilisation de poisons pour le contrôle des réacteurs à neutrons thermiques

par A. Radkowsky et R. J. Creagan

Les auteurs étudient l'utilisation de poisons combustibles et de poisons solubles pour le contrôle des réacteurs.

Un absorbeur de neutrons en solution dans le fluide de refroidissement et de ralentissement d'un réacteur à eau a été utilisé pour l'arrêt à froid et en cours de fonctionnement. Les auteurs étudient les conséquences de son utilisation du point de vue des études de cœurs de réacteur, par exemple la possibilité d'élever la puissance spécifique, de réduire les besoins en barres de contrôle, ainsi que les incidences du coefficient de température sur le réglage et la stabilité du réacteur. Ils traitent des moyens permettant d'introduire dans le réacteur ou d'en retirer des agents chimiques de régulation. Les auteurs mentionnent l'expérience acquise dans l'exploitation de Yankee, d'Indian Point, de Saxton et du réacteur BR3, qui utilisent tous l'acide borique pour compenser l'accroissement de réactivité lors du refroidissement.

Le poison combustible qui s'est révélé le plus utile à ce jour est le bore. Même dans le cas de la fission épithermique, le rapport entre les sections efficaces du bore et de l'uranium 235, lorsqu'on a fait la moyenne pour toutes les énergies importantes du point de vue du fonctionnement d'un réacteur, est presque indépendant du spectre des neutrons thermiques. L'hélium produit par la désintégration du bore 10 soulève des problèmes de métallurgie, mais des chargements de bore dilué semblent acceptables.

Après étude, l'utilisation comme poisons combustibles d'un grand nombre d'éléments autres que le bore semble se justifier dans certains cas. Ainsi, l'erbium permet parfois d'obtenir un coefficient de température négatif de valeur absolue plus élevée, ce qui augmente l'autoprotection; il est utilisé dans les réacteurs TRIGA.

Des éléments ayant une très grande section efficace, comme le samarium, sont parfois utilisés comme poisons combustibles d'appoint, afin de faciliter l'arrêt d'un nouveau cœur non empoisonné.

Le mélange homogène de poisons combustibles et de combustible nucléaire ne convient souvent pas si l'on veut obtenir un taux de combustion élevé et une longue durée. En pareil cas, il devient nécessaire d'introduire le poison en masses ou autoprotégé ou de combiner les poisons homogènes et les poisons en masses.

Les auteurs soulignent les incidences de l'utilisation de poisons combustibles sur l'ensemble des caractéristiques d'un réacteur, en citant à titre d'exemple les cœurs de Shippingport dans lesquels les poisons combustibles permettent de prolonger la durée de vie et d'améliorer la distribution de puissance. Ils exposent des méthodes pratiques pour évaluer les effets des poisons combustibles homogènes et en masses.

Les auteurs étudient l'utilisation combinée de poisons combustibles et de poisons multi-isotopiques. Leurs analyses portent notamment sur la répartition localisée et générale des poisons combustibles et du

combustible nucléaire, ainsi que sur les récents travaux concernant les profilés de poisons combustibles.

Dans le cas de réacteurs utilisant du combustible à taux d'enrichissement uniforme, des recherches récentes montrent que si l'on combine de façon appropriée des poisons autoprotégés, on peut utiliser un chargement unique de poison combustible pendant la durée de vie utile du combustible et éviter ainsi d'avoir à remplacer le poison combustible lorsque l'on modifie la répartition du combustible nucléaire.

Pour ce qui est de l'application de poisons combustibles à l'étude pratique des réacteurs, il importe de déterminer le rapport entre les absorptions de poisons combustibles et les fissions de combustible nucléaire, car cette quantité détermine essentiellement l'appauvrissement du poison par rapport au combustible. Dans le cas du bore, un problème particulier se pose sur le plan expérimental, en ce sens que le bore n'a pas d'effet d'activation. Les auteurs ont étudié la possibilité d'utiliser différents produits de « renforcement » comme le manganèse, le vanadium et le nickel. Les résultats obtenus au moyen de chacun de ces matériaux ont concordé. En outre, les données obtenues expérimentalement sont maintenant en bon accord avec les résultats de nombreux calculs par la méthode de Monte-Carlo.

A/274 США

Регулирование реакторов на тепловых нейтронах с использованием выгорающих поглотителей

А. Радковский и Р. Криган

В настоящем докладе рассматриваются вопросы использования для управления реактором растворимых и выгорающих поглотителей.

Вещества, поглащающие нейтроны, растворенные в теплоносителе-замедлителе водяного реактора, использовались для холодной остановки и во время раооты на мощности. Приводятся соображения по конструкции активных зон, как, например, возможности повышения удельной мощности, снижения требований, предъявленных к регулирующим стержням, и вопросы по связи температурного коэффициента замедлителя с управлением и стабильностью реактора. В докладе рассматриваются вопросы, связанные с добавлением химического компенсирующего вещества, с управлением и извлечением из реактора. Опыт использования этой установки можно применить для реакторов фирмы «Янки», реакторов в Индиан-Пойнте и в Сакстоне и реактора BR-3, в которых используется для контроля реактивности борная кислота.

В настоящее время наилучшим выгорающим поглотителем считается бор. Даже если принять во внимание деление на надтепловых нейтронах, отношение сечения бора к сечению U^{235}, усредненное по всем энергиям, которые существенны для реакторов, почти не зависит от спектра тепловых нейтронов. Хотя гелий, получаемый при распаде B^{10}, нежелателен с металлургической точки зрения, добавки разбавленного бора, по-видимому, допустимы.

Кроме бора было изучено большое количество элементов с целью их использования в качестве выгорающих поглотителей, и, по-видимому, их можно применять в отдельных случаях. Например, использование эрбия иногда дает возможность получить большие отрицательные температурные коэффициенты реактивности и, следовательно, повысить, самозащиту, что нашло применение в реакторах типа TRIGA.

Элементы с очень большими сечениями, как, например, самарий, иногда используются в качестве дополнительных выгорающих поглотителей для ускорения остановки реактора со сгораемых отрав, чтобы увеличить степень подкритичности новой чистой активной зоной.

Для получения высокого выгорания и длительного срока службы топлива часто бывает недостаточно просто смешать выгорающий поглотитель с топливом до получения однородной смеси. В этом случае необходимо использовать выгорающий поглотитель в виде блоков или в виде самоэкранирующегося поглотителя или применять сочетание однородного поглотителя с поглотителем в виде блоков.

Подчеркивается важность использования выгорающих поглотителей в конструкциях реактора, и в качестве примера приводятся активные зоны Шиппингпортского реактора, в котором выгорающие поглотители позволяют удлинить срок службы активной зоны и улучшить распределение энергии. Представлены практические методы расчета эффективности при использовании блочных и гомогенных сгораемых отрав, выгорающих поглотителей, и даются соображения относительно их конструкции.

Обсуждаются вопросы использования сочетаний выгорающих поглотителей и применение многоизотопных поглотителей. Включены как местное, так и общее распределения выгорающих поглотителей и топлива, а также последние работы по формированию выгорающих поглотителей.

В случае реакторов с однородным обогащением с контролируемой эксплуатацией топлива, как показывают последние работы, использование подходящих сочетаний самоэкранирующихся поглотителей позволяет использовать одну загрузку выгорающего поглотителя в течение всего срока службы топлива, что дает возможность отказаться от необходимости замены выгорающего поглотителя при перераспределении топлива.

В связи с применением выгорающих поглотителей в практических конструкциях реакторов очень важно определить отношение поглощения в выгорающем поглотителе к делению топлива, поскольку от него в основном зависит истощение поглотителя. В отношении бора возникает особая проблема, так как бор не активируется. Изучалось применение таких материалов, как марганец, ванадий и никель. Результаты, полученные для каждого из этих материалов, были согласованы. Кроме того, экспериментальные результаты хорошо согласуются с вычислениями методом Монте-Карло.

A/274 Estados Unidos de América

Control de reactores térmicos con "venenos"

por A. Radkowsky y R. J. Creagan

Este informe se refiere al empleo de venenos solubles y venenos consumibles para el control de reactores.

Se han empleado productos químicos absorbentes de neutrones disueltos en el refrigerante–moderador de un reactor de agua para la parada en frío y durante el funcionamiento a potencia. Se hacen notar consideraciones acerca del diseño del núcleo de un reactor tales como la posibilidad de aumentar la densidad de potencia, la de disminuir el número de barras de control necesarias y las implicaciones del coeficiente de temperatura del moderador en relación con el control y la estabilidad del reactor. El informe trata de los medios por los que se adiciona, controla y extrae del reactor el absorbente químico para control a largo plazo. Se menciona la experiencia operacional de las centrales Yankee, Indian Point, Saxton y BR3 cuyos reactores todos emplean el ácido bórico para el control de reactividad en todos los márgenes.

Hasta los momentos actuales el boro es el veneno consumible que ha demostrado ser más útil. Incluso teniendo en cuenta las fisiones epitérmicas, la relación de las secciones eficaces de boro a U^{235}, promediada a todas las energías de interés en reactores, es casi independiente del espectro térmico. Aunque el helio producido en la desintegración del boro-10 no es conveniente desde el punto de vista metalúrgico, las cargas de boro diluido parecen ser aceptables.

Además del boro se ha estudiado un gran número de elementos para empleo como venenos consumibles y se ha encontrado que pueden tener ventajas en aplicaciones especializadas. El erbio, por ejemplo, da lugar, en algunos casos, a un coeficiente de temperatura para la reactividad más negativo, aumentando así la autoprotección; por esta razón se emplea en los reactores TRIGA.

Algunas veces se emplean como venenos consumibles suplementarios, elementos con secciones eficaces muy elevadas, tales como el samario, con objeto de aumentar el margen de apagado de un núcleo nuevo.

Frecuentemente la mezcla homogénea del combustible con un veneno consumible no es adecuada para alcanzar un grado elevado de quemado y una larga resistencia del combustible. En este caso es necesario colocar el veneno consumible en forma agrupada o autoblindada o emplear combinaciones de veneno en forma homogénea y agrupada.

Se da gran importancia a la aplicación de venenos consumibles en el diseño global de un reactor, y se toman los núcleos de Shippingport como ejemplos en los que se emplean venenos consumibles para lograr una vida más larga y una mejor distribución de potencia. Se presentan métodos prácticos para el cálculo de los efectos de venenos agrupados u homogéneos y se hacen consideraciones acerca de su diseño.

Se discute el uso de combinaciones de venenos consumibles y el de venenos "multi–isotópicos". Se incluye el estudio de distribuciones locales y por zonas de los venenos consumibles y del combustible así como trabajos recientes sobre venenos consumibles distribuidos según una determinada forma.

Trabajos recientes indican que, en el caso de reactores uniformemente enriquecidos que emplean cambios de posición del combustible, mediante el empleo de combinaciones adecuadas de venenos autoblindados se puede utilizar una sola carga de veneno consumible durante la vida útil del combustible, evitando así la necesidad de sustituir el veneno cuando se redistribuye el combustible.

Por lo que se refiere a la aplicación de venenos consumibles al diseño práctico de reactores, es de gran importancia determinar la relación de absorciones en el veneno consumible a fisiones en el combustible, puesto que esta magnitud determina esencialmente el agotamiento relativo del veneno y en relación con el del combustible. En el caso del boro se presenta un problema experimental especial ya que éste no se activa. Se ha explorado el empleo de inclusiones de distintos materiales tales como manganeso, vanadio y níquel mezclados con el boro. Se han obtenido resultados concordantes con cada uno de estos materiales. Además, los resultados experimentales están de acuerdo con cálculos realizados por el método de Monte Carlo.

Выбор некоторых оптимальных характеристик компенсирующих элементов ядерных реакторов

В. В. Орлов, В. С. Андреянов, Е. И. Гришанин, Л. Я. Исакова, А. Г. Калашников, Ю. Г. Пашкин, Г. И. Тошинский, В. В. Чекунов

Система компенсации избыточной реактивности реакторов может оказывать существенное влияние на физические и эксплуатационные показатели реакторов. Это влияние возрастает при компенсации больших запасов реактивности. Поэтому наряду с задачами оптимизации основных характеристик реактора значительный интерес представляют задачи, связанные с выбором оптимальных характеристик систем компенсации реактора. В первой части доклада рассмотрены некоторые вопросы, связанные с выбором оптимальных характеристик выгорающих поглотителей. Во второй части рассмотрена задача выбора оптимального состава смеси резонансных поглотителей в регулирующих стержнях.

I. ВЫГОРАЮЩИЕ ПОГЛОТИТЕЛИ

Наряду с подвижными органами компенсации избыточной реактивности в реакторах широко применяются выгорающие поглотители [1]. Ряд вопросов теории расчета и применения выгорающих поглотителей изложен в работах [2-5]. В работах [2,3] эти вопросы рассмотрены применительно к реакторам на тепловых нейтронах, в работе [4] изложены некоторые частные случаи для реактора на промежуточных нейтронах. В более общем случае методика расчета выгорающих поглотителей в реакторах изложена в работе [5].

Основной целью применения выгорающих поглотителей является уменьшение реактивности, компенсируемой подвижными органами. Таким образом, выбор оптимального выгорающего поглотителя прежде всего заключается в выборе поглощающих материалов и способе их размещения, обеспечивающих наилучшее согласование между их выгоранием и выгоранием горючего. При этом остаточное отравление реактора невыгоревшим поглотителем, а также другими изотопами, имеющимися в исходном материале и образовавшимися при выгорании, должно быть минимальным. Для того чтобы остаточное отравление реактора за счет не выгоревшего к концу кампании поглотителя было минимальным, скорость выгорания поглотителя должна быть значительно больше скорости выгорания горючего.

Если для рассматриваемого реактора можно подобрать такой поглотитель, то гомогенное размещение поглотителя в реакторе приведет к его быстрому выгоранию и преждевременному освобождению реактивности. В этом случае более эффективным оказывается гетерогенное размещение поглотителя, при котором из-за депрессии потока нейтронов в области его расположения (эффект самоэкранирования) скорость выгорания поглотителя уменьшается, что позволяет уменьшить разбаланс реактивности от несоответствия законов выгорания горючего и поглотителя.

Если же для рассматриваемого реактора такой поглотитель подобрать не удается, то гетерогенное размещение приводит к большой потере реактивности вследствие не выгоревшего к концу кампании поглотителя и гомогенное размещение может оказаться более целесообразным.

А. Гомогенное размещение поглотителя

Случай гомогенного размещения поглотителя подробно рассмотрен в работе [5], в которой приводятся графики, позволяющие определить значение максимального разбаланса реактивности и остаточное отравление в конце кампании от невыгоревшего поглотителя, если известны времена жизни горючего и поглотителя в реакторе.

Б. Гетерогенное размещение поглотителя

а) **Поглотитель в виде пластин.** В работе [5] рассмотрен случай гетерогенного размещения поглотителя в плоской геометрии. Найдены критерии, позволяющие определить характеристики поглотителя, обеспечивающие максимальное сокращение количества (или эффективности) подвижных органов регулирования.

В соответствии с методикой, изложенной в работе [5], были произведены расчеты для определения области эффективного применения поглотителя в виде пластин. Для расчета изме-

нения реактивности от выгорания поглотителя и выгорания горючего и зашлаковывания использовался метод теории возмущений[6]. Приближенные формулы для расчета изменения реактивности во времени от этих процессов, полученные в работе [5], имеют вид

$$\varrho_{\text{п}}(Y)/\varrho_{\text{п}}(0) = \\ = Z(Y)\,[1+\gamma\beta_0]/[1+\gamma\beta_0 Z(Y)]\cdot\left[1-\frac{Y}{X_{\text{г}}}\right] \quad (1)$$

и

$$\varrho_{\text{г шл}}(Y)/\varrho^0_{\text{г шл}} = Y\left(1-\frac{1}{X_{\text{г}}}\right)\Big/\left(1-\frac{Y}{X_{\text{г}}}\right). \quad (2)$$

Здесь приняты следующие обозначения: $\varrho_{\text{п}}(Y)$— реактивность, вносимая поглотителем в реактор в момент времени Y;

Y — безразмерное время в долях кампании, $Y=\frac{t}{T}$;

t — время работы реактора в пересчете на номинальную мощность;

T — длительность кампании;

β_0 — оптическая толщина пластины поглотителя в начале кампании $\beta_0 = N_{\text{п}}(0)\,\sigma^{\text{п}}_c\Delta$;

$N_{\text{п}}(0)$ — концентрация ядер поглотителя в пластине в начале кампании;

$\sigma^{\text{п}}_c$ — микросечение поглотителя, усредненное по спектру нейтронов;

Δ — геометрическая толщина пластины поглотителя;

γ — параметр, дающий наилучшее приближенное представление зависимости фактора самоэкранирования пластины $f(\beta)$ от ее оптической толщины функцией вида $f(\beta) = 1/(1+\gamma\beta)$;

$X_{\text{г}}$ — безразмерное время жизни горючего, $X_{\text{г}} = 1/T\int \sigma^{\text{г}}_c(u)\,\Phi_0(u)\,du$;

$\sigma^{\text{г}}_c$ — микросечение поглощения горючего;

$\Phi_0(u)$ — поток нейтронов в реакторе в начале кампании, нормированный на номинальную мощность;

$\varrho_{\text{г шл}}(Y)$ — реактивность, требующаяся для компенсации процесса выгорания горючего и зашлаковывания в момент времени Y;

$\varrho^0_{\text{г шл}}$ — начальный запас реактивности на выгорание горючего и зашлаковывание;

$Z(Y)$ — относительная концентрация ядер поглотителя $Z = N_{\text{п}}(Y)/N_{\text{п}}(0)$;

$N_{\text{п}}(Y)$ — средняя по толщине пластины концентрация ядер поглотителя в момент времени Y;

$Z(Y)$ определялась из уравнения работы [5] (см. также [4]):

$$Z\cdot e^{-\gamma\beta_0(1-Z)} = \left(1-\frac{Y}{X_{\text{г}}}\right)\frac{X_{\text{г}}}{X_{\text{п}}}, \quad (3)$$

$X_{\text{п}}$— безразмерное время жизни поглотителя, $X_{\text{п}} = 1/T\int \sigma^{\text{п}}_c(u)\,\Phi_0(u)\,du$.

Формулы (1), (2), (3) получены при использовании ряда следующих предположений, существенно упрощающих расчеты:

1) поток и ценность нейтронов не зависят от координат и равны средним значениям по объему реактора;

2) спектр нейтронов со временем не меняется, т. е. $\Phi(uY) = S(Y)\cdot\Phi_0(u)$, где $S(Y) = 1/\left(1-\frac{Y}{X_{\text{г}}}\right)$;

3) начальное распределение горючего и поглотителя в активной зоне не зависит от координат;

4) горючее размещено гомогенно (или в случае гетерогенного размещения фактор экранирования горючего считается не зависящим от времени);

5) образование новых делящихся изотопов в реакторе отсутствует;

6) размер образцов поглотителя мал по сравнению с транспортной длиной в окружающей их среде, так что эффектом внешнего самоэкранирования можно пренебречь;

7) точное выражение фактора экранирования аппроксимировалось функцией $f(\beta) = 1/(1+\gamma\beta)$;

8) сечение поглотителя в зависимости от летаргии представлялось в виде $\sigma^{\text{п}}_c(u) = \text{const}$ при $u \geqslant u_0$ и $\sigma^{\text{п}}_c(u) = 0$ при $u < u_0$.

Из уравнений (1) и (2) можно получить выражения для определения величины разбаланса реактивности и остаточного отравления от не выгоревшего к концу кампании поглотителя.

$$\varrho_{\text{р}}(Y)/\varrho^0_{\text{г шл}} = \frac{1-\varrho_{\text{п}}(Y)/\varrho_{\text{п}}(0)}{1-\varrho_{\text{п}}(1)/\varrho_{\text{п}}(0)}\,m - \varrho_{\text{г шл}}(Y)/\varrho^0_{\text{г шл}}, \quad (4)$$

$$\varrho_{\text{п}}(1)/\varrho^0_{\text{г шл}} = \frac{\varrho_{\text{п}}(1)/\varrho_{\text{п}}(0)}{1-\varrho_{\text{п}}(1)/\varrho_{\text{п}}(0)}\,m, \quad (5)$$

где $m = [\varrho_{\text{п}}(0) - \varrho_{\text{п}}(1)/\varrho^0_{\text{г шл}}]$ отношение реактивности, освобождающейся к концу кампании выгорающим поглотителем, к начальному запасу реактивности на выгорание горючего и зашлаковывание;

$\varrho_{\text{р}}(Y)$ — разбаланс реактивности в момент времени Y;

$\varrho_{\text{п}}(1)$— остаточное отравление в конце кампании.

Как было показано в работе [5], максимальное сокращение подвижных органов регулирования осуществляется при таких значениях начальной оптической толщины пластины β_0, когда максимальное значение разбаланса $[\varrho_{\text{р}}(Y)/\varrho^0_{\text{г шл}}]_{max}$ равно доле начального запаса реактивности на выгорание горючего и зашлаковывание $(1-m)$, компенсируемой подвижными органами регулирования; при этом разбаланс реактивности один раз на протяжении кампании должен обращаться в нуль.

Расчеты были произведены для значений $X_{\text{г}} = 2{,}76$ и ∞ (глубина выгорания горючего $1/X_{\text{г}}$ 0,36 и 0) в диапазоне изменения $X_{\text{п}}\varepsilon$ (0 ÷ ÷ 0,3), что охватывает большинство практи-

чески интересных случаев, когда применение поглотителя в виде пластин может оказаться приемлемым. На рис. 1 приведена зависимость начальной оптической толщины пластины поглотителя β_0, обеспечивающей максимальное сокращение подвижных органов регулирования, от времени жизни поглотителя $X_п$. На рис. 2 приведены зависимости максимального разбаланса реактивности и остаточного отравления от времени жизни поглотителя $X_п$, рассчитанные для значений β_0, определенных выше.

Как видно из рис. 2, область наиболее эффективного применения выгорающего поглотителя в виде пластин одинаковой толщины лежит в диапазоне $X_п$ 0,1 ÷ 0,25. При $X_п >$ $> 0{,}25 \div 0{,}30$ остаточное отравление становится слишком большим, а при $X_п < 0{,}05 \div$ $\div 0{,}1$ сильно растет величина максимального разбаланса реактивности, достигающая при $X_п = 0$ значения $1/(1 + \sqrt{1-1/X_г})$.

Применение поглотителей с очень большими сечениями ($X_п \ll 1$) обеспечивает их полное выгорание, однако при размещении поглотителя в виде пластин создается большой разбаланс реактивности. Разбаланс может быть уменьшен при использовании комбинации пластин с различными оптическими толщинами.

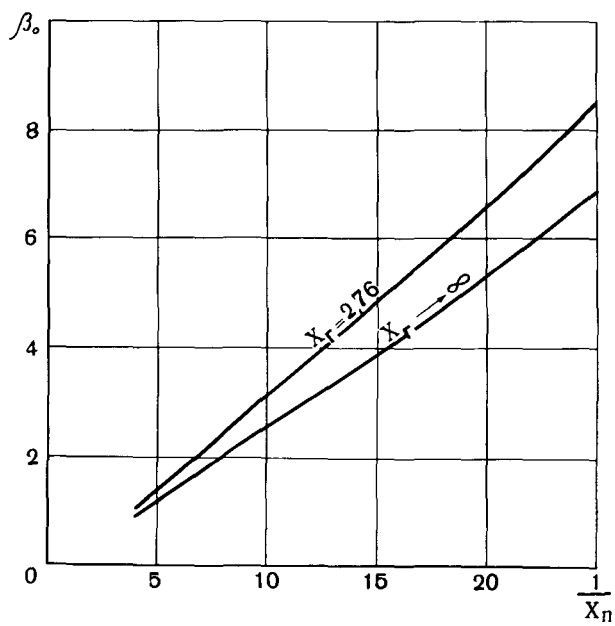


Рис. 1. Зависимость начальной оптической толщины пластины поглотителя, обеспечивающей максимальное сокращение подвижных органов регулирования, от времени жизни поглотителя $X_п$

б) **Поглотители в виде стержней.** Более простым решением является размещение поглотителя с большим сечением в виде цилиндрических стержней * с оптической толщиной $\beta_0 \gg 1$, что позволяет одновременно получить и малое остаточное отравление, и малый разбаланс реактивности.

В этом случае стержень будет выгорать только в узком поверхностном слое. Диаметр «черноты» стержня и, следовательно, освобождающаяся реактивность будут изменяться по закону, близкому к требующемуся для компенсации потери реактивности от выгорания горючего и зашлаковывания. Противоречие между величиной разбаланса реактивности и остаточным отравлением снимается, поскольку при очень больших сечениях выгорание оказывается практически полным. Поглотители с поверхностным выгоранием в отличие от поглотителей с умеренным самоэкранированием образно можно назвать обгорающими поглотителями.

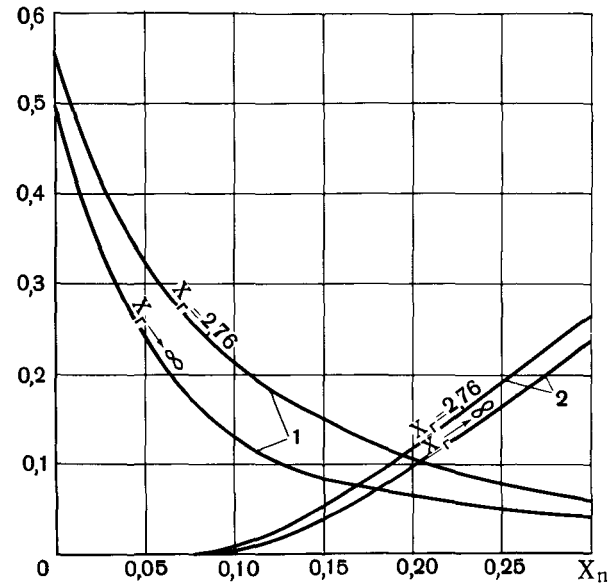


Рис. 2. Максимальный разбаланс реактивности $(\varrho_р/\varrho^0_{г\,шл})_{max}$ (*1*) и остаточное отравление $\varrho_п(1)/\varrho^0_п$ (*2*) реактора при оптимальном значении оптической толщины пластины в зависимости от времени жизни поглотителя $X_п$

Для выяснения физических особенностей обгорающих поглотителей полезно рассмотреть предельный случай для поглотителя с очень большим сечением захвата, представив последнее в виде $\sigma_c^п = \infty$ при $u \geqslant u_0$ и $\sigma_c^п = 0$ при $u < u_0$. Тогда нейтроны будут поглощаться в бесконечно тонком слое. Закон изменения радиуса «черноты» стержня со временем можно

* Можно показать, что поперечное сечение стержня может иметь не только форму круга, но и форму выпуклого многоугольника, в который вписывается окружность.

установить из следующих соображений *. За время dt число поглощенных нейтронов будет равно $\frac{\Phi(t)}{4} 2\pi r dt$, где $\Phi(t)$ — интегральный поток нейтронов в области энергий, где сечение поглотителя отлично от нуля; r — радиус «черноты» стержня. С другой стороны, соответствующее изменение объема стержня за счет выгорания ядер с его поверхности равно $2\pi r dr$. Следовательно, можно написать следующее соотношение

$$\frac{\Phi(t)}{4} 2\pi r\, dt = 2\pi r N_{\text{п}}^0\, dr. \qquad (6)$$

При интегрировании соотношения (6) в соответствующих пределах получим

$$\int_0^t \Phi(t')\, dt' = 4RN_{\text{п}}^0 \left(1 - \frac{r}{R}\right).$$

Отсюда видно, что радиус «черноты» стержня, а вместе с ним и его поглощающая способность уменьшаются примерно линейно со временем, что обеспечивает малую величину разбаланса реактивности. Оценим баланс реактивности, возникающий вследствие неполного соответствия законов выгорания поглотителя и горючего. При

$$\Phi(t) = S(t) \int_{u_0}^{\infty} \Phi(u)\, du, \text{ где } S(t) = 1/\left(1 - \frac{Y}{X_{\text{г}}}\right)$$

и при требовании полного выгорания поглотителя к моменту кампании $Y = Y_0$ выражение для изменения радиуса стержня можно записать в следующем виде

$$1 - r(Y)/R = \ln\left(1 - \frac{Y}{X_{\text{г}}}\right) \Big/ \ln\left(1 - \frac{Y}{X_{\text{г}}}\right), \qquad (7)$$

при этом начальная оптическая толщина стержня $\beta_0 = -\frac{1}{2}\frac{X_{\text{г}}}{X_{\text{п}}} \ln\left(1 - \frac{Y_0}{X_{\text{г}}}\right)$; здесь для удобства введено конечное сечение поглотителя.

При использовании выражения (7), можно получить выражение для реактивности, освобождающейся при обгорании стержня

$$1 - \varrho_{\text{п}}(Y)/\varrho_{\text{п}}(0) = 1 - r(Y)\, S(Y)/R =$$

$$= 1 - \left[1 - \ln\left(1 - \frac{Y}{X_{\text{г}}}\right) \Big/ \ln \times \left(1 - \frac{Y_0}{X_{\text{г}}}\right)\right] \Big/ \ln\left(1 - \frac{Y}{X_{\text{г}}}\right) \text{ при } Y \leqslant Y_0 \qquad (8)$$

и $1 - \varrho_{\text{п}}(Y)/\varrho_{\text{п}}(0) = 1$ при $Y < Y \leqslant 1$.

Из соотношений (8) и (2) получим выражение для относительного разбаланса реактивности при условии, что обгорающим поглотителем в начале кампании компенсируется доля m от полного запаса реактивности на выгорание и зашлаковывание:

$$\varrho_{\text{р}}(Y)/\varrho_{\text{г шл}}^0 = m\left\{1 - \left[1 - \ln\left(1 - \frac{Y}{X_{\text{г}}}\right) \Big/ \ln \times \left(1 - \frac{Y}{X_{\text{г}}}\right)\right] \Big/ \ln\left(1 - \frac{Y}{X_{\text{г}}}\right)\right\} -$$

$$- Y\left(1 - \frac{1}{X_{\text{г}}}\right) \Big/ \left(1 - \frac{Y}{X_{\text{г}}}\right) \text{ при } Y \leqslant Y_0 \qquad (9)$$

и $\varrho_{\text{р}}(Y)/\varrho_{\text{г шл}}^0 = m - Y\left(1 - \frac{1}{X_{\text{г}}}\right) \Big/ \left(1 - \frac{Y}{X_{\text{г}}}\right)$ при $Y < Y \leqslant 1$.

Приравнивая нулю производную по Y от выражения (9) при $Y \leqslant Y$, можно получить соотношение для определения максимального разбаланса реактивности в области $Y \leqslant Y_0$:

$$\varrho_{\text{р}}(Y_{\max})/\varrho_{\text{г шл}}^0 = (X_{\text{г}} - 1 + m)\left\{1 + \left[e^{\frac{X_{\text{г}}-1+m}{m}} \left(1 - \frac{Y_0}{X_{\text{г}}}\right)^{\frac{X_{\text{г}}-1+m}{m}} \ln\left(1 - \frac{Y}{X_{\text{г}}}\right)\right]^{-1}\right\}, \qquad (10\text{а})$$

$$Y_{\max} = X_{\text{г}}\left[1 - e\left(1 - \frac{Y_0}{X_{\text{г}}}\right)^{\frac{X_{\text{г}}-1+m}{m}}\right].$$

При $Y = Y_0$ разбаланс реактивности равен

$$\varrho_{\text{р}}(Y_0)/\varrho_{\text{г шл}}^0 = m - Y_0\left(1 - \frac{1}{X_{\text{г}}}\right) \Big/ \left(1 - \frac{Y_0}{X_{\text{г}}}\right), \qquad (10\text{б})$$

а в конце кампании ($Y = 1$)

$$\varrho_{\text{р}}(1)/\varrho_{\text{г шл}}^0 = -(1 - m). \qquad (10\text{в})$$

Из выражения (10а) легко показать, что максимальный разбаланс реактивности всегда отрицателен. Это означает, что в начале кампании обгорающим поглотителем можно скомпенсировать не весь запас реактивности на выгорание и зашлаковывание, а лишь его долю m. Очевидно, что оставшаяся часть запаса реактивности $(1 - m)$ должна компенсироваться подвижными органами, причем $(1 - m)$ должна быть не меньше величины максимального разбаланса реактивности. Так как нашей целью является максимальное сокращение подвижных органов регулирования, то следует положить $1 - m = -\varrho_{\text{р}}(Y_{\max})\, \varrho_{\text{г шл}}^0$, откуда получается уравнение, связывающее Y и m.

$$1 = -e^{\frac{X_{\text{г}}}{m}} \left(1 - \frac{Y_0}{X_{\text{г}}}\right)^{\frac{X_{\text{г}}-1+m}{m}} \ln\left(1 - \frac{Y_0}{X_{\text{г}}}\right). \qquad (11)$$

В зависимости от значения параметра Y_0 разбаланс реактивности при $Y = Y_0$ (формула 10б) может быть положительным, отрицательным или равным нулю. Можно показать, что оптимальным является случай равенства нулю разбаланса при $Y = Y_0$. Отсюда получается второе уравнение, связывающее величины Y_0 и m,

$$m = Y_0\left(1 - \frac{1}{X_{\text{г}}}\right) \Big/ \left(1 - \frac{Y_0}{X_{\text{г}}}\right). \qquad (12)$$

Из уравнений (11) и (12) получается уравнение для определения оптимальной величины m

* Здесь и далее используются допущения, сделанные ранее в подпункте *а*.

$$\varkappa \ln \frac{\varkappa}{\varkappa-1} = 1 + \ln(\varkappa + M) + \ln \ln \frac{\varkappa}{\varkappa-1}, \quad (13)$$

где

$$\varkappa = \frac{X_\text{г} - 1 + m}{m}, \quad M = \frac{1-m}{m}.$$

Результаты расчета, представленные на рис. 3, показывают, что минимальный разбаланс реактивности $(1 - m)$ в случае размещения выгорающих поглотителей с очень большим сечением захвата в виде стержней существенно меньше, чем в случае пластин. Таким образом, применение обгорающих поглотителей с бесконечным сечением захвата нейтронов сводит к минимуму необходимое количество подвижных органов компенсации, не приводя к потере реактивности за счет невыгоревшего поглотителя. Переход от идеальной модели к реальным поглотителям вызывает ряд дополнительных вопросов, из которых можно остановиться на следующих:

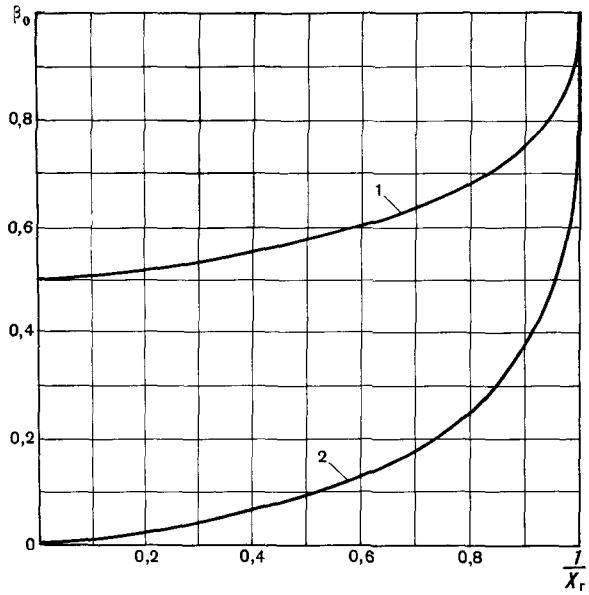


Рис. 3. Максимальный разбаланс реактивности поглотителей с бесконечно большим сечением для плоской *1* и цилиндрической *2* геометрии в зависимости от глубины выгорания горючего за кампанию $(1/X_\text{г})$

1. Для выяснения кинетики выгорания поглотителя с конечным сечением $\sigma_c^\text{п}$ рассмотрим задачу о распределении поглотителя в полубесконечной среде, на которую падает нормально к поверхности поток нейтронов J *нейтр/см²·сек*. Если начальное распределение поглотителя было равномерным N_0 *атомов/см³*, то к моменту времени t это распределение будет иметь вид

$$N_\text{п}(X, t) = N_\text{п}^0 [1 + (1 - e^{-J\sigma t}) \cdot e^{(J\sigma t - \sigma N_\text{п}^0 X)}]^{-1}. \quad (14)$$

Используя эту формулу, можно показать, что поглощающая способность стержня сначала в течение времени $t \lesssim \tau = \frac{1}{J\sigma}$ падает медленно. Ко времени $t \sim \tau$ образуется фронт распределения $N(X)$ с шириной $\Delta x \sim \frac{1}{N_\text{п}^0 \sigma}$, который движется с постоянной скоростью $\frac{dx}{dt} = \frac{J}{N_\text{п}^0}$ внутрь поглотителя (рис. 4). Таким образом, при конечной величине σ следует ожидать отклонения от линейной зависимости $r(t)$ в течение времени $\tau \sim \frac{1}{2J\sigma}$ в первый период работы (в случае изотропного падения ширина фронта уменьшается в 2 раза по сравнению со случаем нормального падения нейтронов, при этом $J = \frac{\Phi}{4}$). Отклонение от формулы (7) будет наблюдаться и на конечном этапе выгорания, когда оптическая толщина стержня уменьшится до величины $\beta \sim 1$, вследствие чего скорость выгорания увеличится. Суммарная длительность участков нелинейности оказывается равной приблизительно $\tau = \frac{1}{J\sigma}$ и, для того чтобы она не превышала, например, 10% кампании, необходимо, чтобы $\tau \leqslant 0{,}1\ T$ или $\frac{1}{J\sigma} \simeq 0{,}1/\Phi\sigma_\text{г}$. Эта оценка показывает, что в качестве обгорающих поглотителей могут быть использованы изотопы с $\sigma_c^\text{п} \geqslant 40\ \sigma_c^\text{г}$.

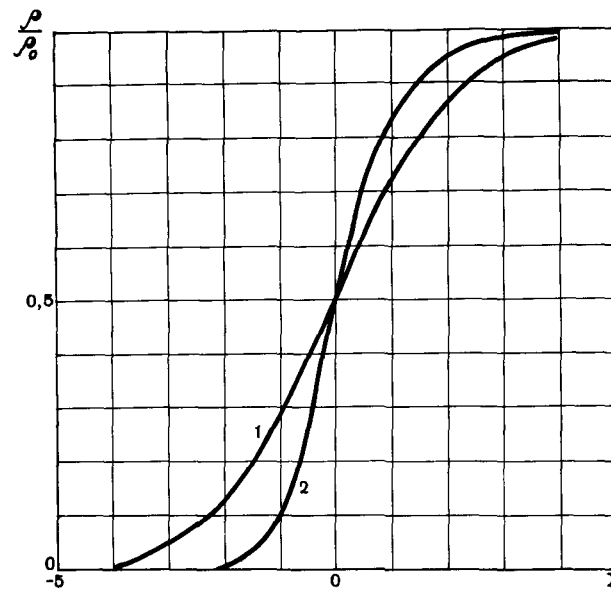


Рис. 4. Установившееся распределение ядер поглотителя в переходной области:

1 — нормально направленный поток; *2* — изотропно распределенный поток

Сечения, столь сильно превышающие сечения делящихся изотопов, встречаются лишь в тепловой области, когда энергия одного из резонансов оказывается близкой к нулю. Поэтому обгорающие поглотители практически могут быть использованы только в реакторах на тепловых нейтронах, причем из стабильных изотопов лишь Cd^{113}, Sm^{149}, Gd^{155} и Gd^{157} удовлетворяют указанному условию.

2. Объемное выгорание поглотителя за счет захвата нейтронов в области энергий, где сечения невелики, также приводит к изменению закона выгорания. Очень большие сечения захвата нейтронов в тепловой области, обусловленные низколежащим резонансом, спадают с ростом энергии согласно формуле Брейта — Вигнера по закону $\sigma_c \sim \frac{1}{E^{5/2}}$. Если спектр падающих на стержень нейтронов есть $\Phi(E)$, то число нейтронов, поглощенных стержнем при энергиях $E > E_{гр}$, когда их пробег $\lambda(E) > \lambda_{гр} = 2R$ равно

$$A_v \simeq \int_{E_{гр}}^{\infty} \Phi(E) V N_п^0 \sigma_c(E)\, dE \simeq$$

$$\simeq V N_п^0 \sigma(E_{гр}) \int_{E_{гр}}^{\infty} \left(\frac{E_{гр}}{E}\right)^{7/2} dE =$$

$$= \frac{2}{5} V N_п^0 \sigma_c(E_{гр}) E_{гр} \Phi(E_{гр}),$$

причем $N_п^0 \sigma_c(E_{гр}) = \frac{1}{2R}$, так что окончательно

$$A_v \simeq \frac{S}{10} E_{гр} \Phi(E_{гр}) = \frac{S}{10} \Phi_т \cdot \frac{\Sigma_c}{\xi \Sigma_s}.$$

Здесь предполагается, что в области $E \sim E_{гр}$ спектр Ферми. Количество нейтронов, поглощенных на поверхности, равно $A_s \simeq \frac{S}{4} \times \int_0^{E_{гр}} \Phi(E)\, dE$, следовательно, доля объемного поглощения есть $A_v/A_s \simeq \frac{2}{5} \cdot \frac{\Sigma_c}{\xi \Sigma_s}$, что в тепловых реакторах составляет обычно величину $\leqslant 0{,}1$.

К величине A_v надо добавить также поглощение в резонансной области, которое для перечисленных выше изотопов мало. Эффект объемного поглощения приводит к некоторому увеличению скорости освобождения реактивности по мере выгорания.

3. Депрессия потока нейтронов в окрестности стержня (внешняя экранировка) приводит к уменьшению скорости выгорания в начале кампании. При использовании стержней малого диаметра ($d < \lambda_{тг}$) этот эффект становится небольшим.

Распределение поглотителя в активной зоне

Соображения, приведенные выше, позволяют выбрать поглощающие стержни (количество, диаметр и плотность поглотителя в них), обеспечивающие малое изменение коэффициента размножения в некотором элементе объема реактора, если заранее известна глубина выгорания горючего в этом объеме, достигаемая к концу кампании. Так как поле энерговыделения в реакторе само зависит от расположения стержней, то возникает нелинейная задача, которая может быть решена методом последовательных приближений.

В идеализированном виде эта задача может быть сведена к следующему нелинейному уравнению. Предположим, что: а) поглотитель обеспечивает постоянство со временем коэффициента размножения K_∞ в каждой точке реактора, б) вероятность поглощения в точке $\vec{r}$ нейтрона, рожденного в точке $\vec{r}'$, $P(\vec{r}, \vec{r}')$ также не изменяется в процессе выгорания (подобная ситуация имеет место, например, в реакторах с водяным замедлителем, где $L^2 \ll \tau$). Тогда плотность генерации нейтронов $Q(\vec{r})$ (или пропорциональная ей плотность энерговыделения) опишется следующим уравнением

$$Q(\vec{r}) = K_\infty(\vec{r}) \int Q(\vec{r}') P(\vec{r}, \vec{r}')\, d\vec{r}'. \qquad (15)$$

Величина K_∞ может быть выражена через глубину выгорания горючего, достигаемую к концу кампании в точке $\vec{r}$ $1/X_г(\vec{r}) \sim Q(\vec{r})$. Таким образом, для $Q(\vec{r})$ получается нелинейное уравнение

$$Q(\vec{r}) = K_\infty[Q(\vec{r}), \vec{r}] \int Q(\vec{r}') P(\vec{r}, \vec{r}')\, d\vec{r}. \qquad (16)$$

Разлагая $Q(\vec{r}')$ в ряд около $\vec{r}$ и ограничиваясь тремя членами разложения, получим при $P = P(|\vec{r} - \vec{r}'|)$

$$\nabla^2 Q - \frac{K_\infty(Q, \vec{r}) - 1}{K_\infty(Q, \vec{r})\, M^2} = 0, \qquad (17)$$

где $M^2 = \int P(r) r^4\, dr \Big/ \int P(r) r^2\, dr$ — площадь миграции.

Граничные условия для Q могут быть записаны с использованием альбедо отражателя. Зная распределение мощности и пропорциональное ему распределение глубин выгорания, нетрудно найти закон распределения поглотителя по активной зоне реактора, обеспечивающий постоянство K_∞ в каждой точке $\vec{r}$. Это распределение не только обеспечивает постоянство реактивности реактора в течение кампании, но и неизменность распределения мощности по реактору *, одновременно выравнивая его (по сравнению с непрофилированным расположением органов компенсации).

---

* Задача о системе компенсации реактивности, обеспечивающей постоянство распределения мощности в реакторе, была поставлена и решена В. Н. Шараповым.

II. РЕЗОНАНСНЫЕ ПОГЛОТИТЕЛИ ДЛЯ РЕГУЛИРУЮЩИХ СТЕРЖНЕЙ

Для регулирующих стержней существенное значение имеет энергетическая зависимость сечения поглощения применяемых материалов. Применение резонансных поглотителей позволяет в известных пределах создать наиболее выгодную для данного реактора энергетическую зависимость сечения поглощения как с точки зрения увеличения эффективности, так и с точки зрения уменьшения величины искажения нейтронного поля вблизи стержня. Последнее обстоятельство наиболее важно для реакторов с тепловым спектром.

Для увеличения эффективности стержней или уменьшения искажений нейтронного потока вблизи стержней представляет интерес использование смесей различных резонансных поглотителей. В этом случае за счет уменьшения эффекта самоэкранирования резонансов каждого компонента общее резонансное поглощение может быть больше, чем поглощение компонента с наибольшим резонансным интегралом. Например, если имеется n поглотителей с узкими и сильными резонансами, отличающихся друг от друга только положением резонансов, то максимальное значение резонансного интеграла смеси будет в $\sqrt{n}$ раз больше резонансного интеграла одного поглотителя. Реальные поглотители отличаются друг от друга ядерной плотностью, расположением и параметрами резонансов и т. п. Кроме того, значительную долю в полном поглощении составляет поглощение слабыми резонансами и «гладкой» частью сечения поглощения. Поэтому оптимальный состав смеси зависит от свойств выбранных поглотителей, а также от формы спектра нейтронов в реакторе, температуры и т. п.

А. Определение оптимального состава смеси резонансных поглотителей для получения максимальной эффективности стержня

Согласно теории возмущений[6], эффективность стержня равна

$$\varrho = \frac{1}{\text{ЦНД}} \int_{V_{\text{ст}}} dv \int du\, W(u) \times \times \sum_{i=1}^{n} N_i \sigma_c^i(u)\, f_i(d, N_k, \sigma_c^k(u)), \quad (18)$$

где $W(u)$ — произведение потока нейтронов энергии E на их ценность;

f_i — фактор самоэкранирования сечения поглощения i-элемента, зависящий в общем случае от всех σ_c^k и N_k, $k = 1, 2, \ldots, n$;

ЦНД — ценность нейтронов деления;

d — диаметр стержня;

n — число компонентов смеси.

Для определения максимального значения эффективности стержня заданного размера из смеси резонансных поглотителей необходимо найти максимум выражения (18) при условии $\sum_i v_i = 1$ (v_i — объемная доля компонента i). Эта задача является задачей на условный экстремум и решается методом неопределенных множителей Лагранжа. В соответствии с этим методом необходимо найти безусловный экстремум функции $F = \varrho + \lambda L$, где $L = \sum_i v_i - 1$, а Λ — неопределенный множитель. Необходимые условия максимума функции F

$$\frac{\partial F}{\partial N_i} = 0, \quad \frac{\partial F}{\partial \lambda} = L = 0 \quad (19)$$

приводят к системе $(n + 1)$ уравнений с неизвестными N_i и λ, которая определяет оптимальную объемную долю каждого компонента смеси v_i. Система (19) в общем случае решается методом итераций. При вычислении факторов самоэкранирования необходимо учитывать взаимную экранировку резонансов ядер различных сортов, самоэкранирование резонансов «гладкой» частью сечения, эффект Допплера для разрешенных и для неразрешенных уровней.

На рис. 5 приведены зависимости эффективности образцов диаметром 10 *мм* в реакторе ПФ-4 [7] (отношение ядер Be и U^{235} составляет 106) от состава смеси Be + Eu_2O_3. Результаты расчета, приведенные на рис. 5, указывают на существование максимального значения эффективности, заметно превышающего эффективность образца из отдельного компонента. Дальнейшее увеличение эффективности стержней можно получить при использовании смеси оптимального состава из трех и более компонентов.

Б. Оптимальный состав смеси резонансных поглотителей для получения минимальных искажений поля энерговыделения в тепловом реакторе

Для реакторов на тепловых нейтронах энергетическая зависимость сечения поглощения имеет значение не только с точки зрения эффективности стержня, но и с точки зрения величины искажений нейтронного поля вблизи стержня. Искажение нейтронного поля можно снизить уменьшением поглощения в каждом стержне за счет увеличения их числа и применением в качестве поглощающих материалов резонансных поглотителей, позволяющих изменять соотношение между поглощением в тепловой и надтепловой областях. Действительно, чем больше нейтронов будет поглощаться стержнем в надтепловой области энергий, тем меньше будет поглощение в тепловой области при фиксированной эффективности стержня, и, следовательно, будет меньше искажение потока нейтронов в тепловой области, где происходит большая часть делений. Наименьшее искаже-

ние поля энерговыделения будет в предельном случае, когда все поглощение перенесено в надтепловую область. В качестве примера рассмотрим поглощение в пластинчатых стержнях. Используя для эффективного резонансного интеграла выражение $J = a + b/\sqrt{Nd}$ (a и b — постоянные, N — плотность ядер, d — толщина пластины) и предполагая, что постоянная a определяется в основном поглощением за счет $1/v$-сечения, полное резонансное поглощение I-i в пластине можно представить в виде

$$I = l\,[\beta_0 2\sqrt{E_0/E_{гр}} + \varepsilon\sqrt{\beta_0}], \qquad (20)$$

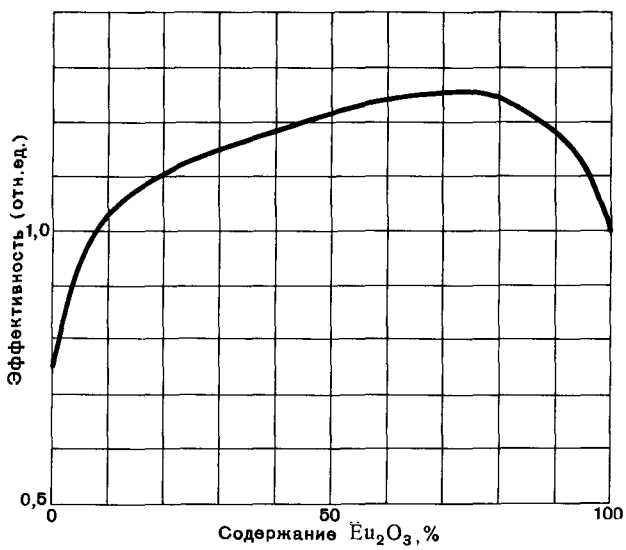


Рис. 5. Эффективность стержня диаметром 10 *мм* в реакторе ПФ-4 в зависимости от содержания окиси европия в смеси Re—Eu_2O_3

где l — поверхность пластин на единицу объема активной зоны;

$\beta_0 = \sigma_c^0 Nd$ — оптическая толщина пластин для нейтронов с энергией $E_0 = 0{,}0253$ *эв*;

$E_{гр}$ — граничная энергия между максвелловским спектром и спектром замедления. Из уравнения (20) видно, что величиной $\varepsilon = b/\sqrt{\sigma}$ удобно характеризовать вклад поглощения, обусловленный сильными резонансами. Эта величина не зависит от концентрации ядер и спектра реактора и является лишь функцией резонансных параметров. Среди резонансных поглотителей наилучшим соотношением между поглощением в резонансной и тепловой областях обладают Hf ($\varepsilon = 1{,}56$), Ta ($\varepsilon = 1{,}14$), In ($\varepsilon = 1{,}04$), Sb ($\varepsilon = 1{,}07$), Eu ($\varepsilon = 1{,}02$) и Re ($\varepsilon = 0{,}92$). Для $1/v$-сечения эта характеристика равна нулю. Наихудшей энергетической зависимостью сечения поглощения обладают Cd и Gd, у которых плавная часть сечения поглощения спадает значительно быстрее по сравнению с $1/v$-поглотителем. Вклад их резонансов, расположенных выше кадмиевой границы, ничтожен, и поэтому этим элементам следует приписывать отрицательные значения ε.

На рис. 6 приведена оптическая толщина пластин β_0 для нейтронов с энергией $E_0 = 0{,}025$ *эв* в зависимости от величины ε, необходимая для компенсации водо-водяного реактора с соотношением ядер H и U^{235}, равным ~ 200 при шаге квадратной решетки пластин 10 *см*. Там же приведена зависимость от ε коэффициента неравномерности потока тепловых нейтронов K в элементарной ячейке.

При использовании смеси оптимального состава можно увеличить величину ε до значений, значительно больших, чем у отдельных элементов. В этом случае оптимальный состав

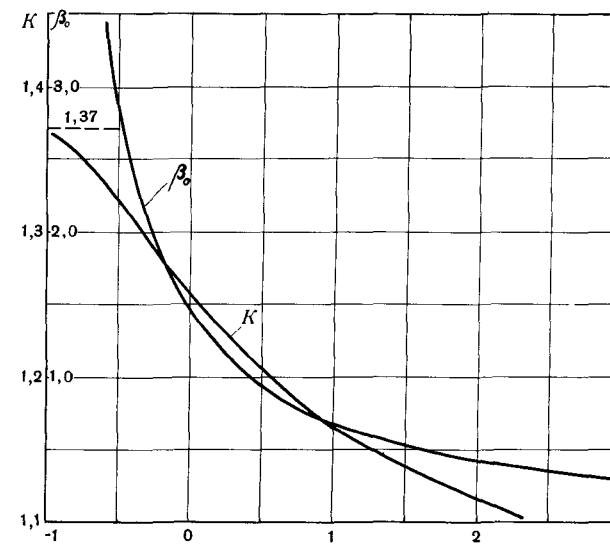


Рис. 6. Оптическая толщина пластин, необходимая для компенсации запаса реактивности водо-водяного реактора, и коэффициент неравномерности потока тепловых нейтронов в его элементарной ячейке в зависимости от ε

находится из требования максимального значения полного резонансного поглощения пластины $I = \sum_i I_i$ при дополнительном условии

$$\sum_i \beta_i = \beta_0.$$

Эта задача с помощью метода неопределенных множителей Лагранжа может быть решена аналитически, если предположить, что резонансные уровни элементов не перекрываются и неблокируемое поглощение обусловлено только $1/v$-сечением (т. е. $\frac{a_i}{\sigma_i} = \text{const}$, $i = 1,2$). Тогда оптимальное весовое содержание P_i-компонента с атомным весом A_i и сечением для тепловых нейтронов σ_i будет определяться выражением

$$P_i = \frac{\varepsilon_i^2 A_i/\sigma_i}{\sum_k \varepsilon_k^2 A_k/\sigma_k}, \qquad (21)$$

а максимальное значение полного резонансного поглощения будет равно

$$I_{\max} = l\left[\beta_0 \cdot 2\sqrt{\frac{E_0}{E_{\text{гр}}}} + \varepsilon_{\max}\sqrt{\beta_0}\right], \quad (22)$$

$$\varepsilon_{\max} = \sqrt{\sum_k \varepsilon_k^2}.$$

Ниже в таблице приведены оптимальные составы и значения $\varepsilon_{\max}$ для смесей некоторых резонансных поглотителей

Материал	In – Ag		Hf – Ta		Hf – Ta – W			Hf – Ta – Eu		
P_i, %	37	63	26,3	73,7	21,1	59,1	19,8	27	73	0,2
ε_i	1,04	0,78	1,57	1,14	1,57	1,14	0,64	1,57	1,14	1,02
$\varepsilon_{\max}$	1,30		1,94		2,04			2,18		

ЛИТЕРАТУРА

1. А. П. Александров и др. Атомный ледокол «Ленин». Труды Второй международной конференции по мирному использованию атомной энергии, Женева, 1958, Доклады советских ученых, P/2140, т. *2*, М., Атомиздат, 1959, стр. 60.
2. А. Радковский. Теория и применение выгорающих поглотителей нейтронов. Труды Второй международной конференции по мирному использованию атомной энергии, Женева, 1958, Доклады советских ученых, P/1900, т. *3*, М., Атомиздат, 1959, стр. 717.
3. В. С. Волков и др. Применение выгорающих поглотителей в ядерных реакторах. Атомная энергия, *11*, вып. 2 (1961).
4. The Physics of Intermediate Spectrum Reactors. USAEC. 1958.
5. Г. И. Тошинский и А. Г. Калашников. Методы расчета выгорания поглотителя в реакторах. Теория и методы расчета ядерных реакторов, М., Госатомиздат, 1962.
6. Л. Н. Усачев. Уравнение для ценности нейтронов, кинетика реактора и теория возмущений. Материалы международной конференции по мирному использованию атомной энергии, Женева, 1955, P/656, т. V, Москва.
7. И. В. Гордеев, Д. А. Кардашев и А. В. Малышев. Ядерно-физические константы. М., Атомиздат, 1963.
8. А. И. Лейпунский и др. Экспериментальные исследования некоторых физических особенностей промежуточных реакторов с бериллиевым замедлителем. Доклад № SM18180 на Международном симпозиуме по физике быстрых и промежуточных реакторов, Вена, 1962.

ABSTRACT - RÉSUMÉ - АННОТАЦИЯ - RESUMEN

A/354 USSR

Choice of some optimum characteristics of control elements for nuclear reactors

By V. V. Orlov *et al.*

The first part of this paper describes a method of determination of optimum burnable absorber characteristics and the technique of distributing them over the core to flatten the shape of heat release during the reactor life-time. Requirements for the absorption cross section of burnable isotopes and some techniques of using burnable absorbers are formulated. A possibility of reaching zero unbalance of reactivity is discussed, based on an ideal case of infinite absorption cross section. The practical recommendations for choosing the geometry of rods are given on the basis of this analysis. As specific examples the following practically important types of burnable absorbers are investigated:

(*a*) Homogeneous;

(*b*) Medium self-shielding factor;

(*c*) Large macroscopic absorption cross section.

The second part of this paper deals with the method of determining optimum composition of an arbitrary mixture of resonant absorbers for control rods from the standpoint of increasing rod efficiency, decreasing distortions of neutron fields due to the rods, etc.

The method is illustrated by an example of optimum mixture corresponding to the maximum efficiency of rods of given dimensions in the intermediate reactor PF-4 ($\rho_{\text{Be}}/\rho_{\text{U}} = 90$). Efficiency increases by 30% (compared with those of the same sized iridium rod) were observed for the optimum mixture of Ir, Re, Eu, Dy and Hf.

This method has also been used to calculate the optimum plate control rod composition for a water-moderated water-cooled reactor ($\rho_{\text{H}}/\rho_{\text{U}} = 280$), corresponding to minimum neutron field distortions near these rods.

Calculated results are compared with experimental data.

A/354 URSS

Choix de certaines caractéristiques optimales des éléments de compensation des réacteurs nucléaires.

par V. V. Orlov *et al.*

La première partie du mémoire expose une méthode permettant de déterminer les caractéristiques optimales des absorbeurs consommables et leur disposition dans le cœur aux fins d'aplatissement du dégagement de chaleur dans le cas de variations très faibles, au cours de toute la durée de vie du réacteur. On détermine les conditions à imposer à la section d'absorption des isotopes consommables selon le mode d'utilisation de ces isotopes. On examine la possibilité d'obtenir une variation nulle de la réactivité au cours de la durée de vie du réacteur dans le cas idéal d'une section d'absorption infiniment grande. Cette analyse donne lieu à des recommandations pratiques sur le choix de la géométrie des barres contenant du poison consommable. Les formes suivantes, importantes en pratique, de poisons consommables sont étudiées en tant qu'exemples concrets:

a) Homogène;

b) Modérément protégé;

c) A grande section d'absorption microscopique.

La deuxième partie du mémoire expose la méthode de détermination de la composition optimale d'un mélange quelconque d'absorbeurs résonants dans les barres de contrôle du point de vue de l'efficacité des barres, de la diminution des distortions du champ neutronique, provoquées par les barres, etc.

La méthode est illustrée par le calcul de la composition optimale correspondant à l'efficacité maximum des barres d'une dimension donnée dans un réacteur intermédiaire PF-4 ($\rho_{Be}/\rho_U = 90$). Pour le mélange optimal Ir, Re, Eu, Dy, Hf, on a observé une augmentation d'efficacité de 30% (par rapport à une barre à Ir de mêmes dimensions).

Cette même méthode a été employée pour calculer la composition optimale de barres de contrôle à lames d'un réacteur refroidi et ralenti par l'eau ($\rho_H/\rho_U = 280$) correspondant à des distorsions minimales du champ de neutrons à proximité de ces barres.

Les résultats des calculs sont comparés aux données expérimentales.

A/354 URSS

Elección de algunas características óptimas de los elementos compensadores en los reactores nucleares

por V. V. Orlov *et al.*

En la primera parte de la memoria se expone un método de determinación de las características óptimas de los absorbentes quemables y la manera de distribuirlos en el núcleo con el fin de uniformar espacialmente la producción de calor, reduciendo a la vez al mínimo los cambios de posición durante la vida del reactor. Se formulan las condiciones a que debe ajustarse el valor de las secciones de absorción de los isótopos quemables para los diferentes procedimientos de utilización de esos isótopos. En el caso ideal de una sección de absorción infinita, se analiza la posibilidad de conseguir una variación de reactividad nula durante toda la vida del reactor. Se recomiendan algunos criterios prácticos, basados en aquel análisis, con vistas a la elección de la forma geométrica de las barras con absorbentes quemables. Como ejemplos concretos se consideran los siguientes casos, importantes en la práctica, de absorbentes quemables:

a) Absorbente homogéneo;

b) Absorbente parcialmente blindado;

c) Absorbente con sección microscópica de absorción elevada.

En la segunda parte de la memoria se presenta un método para determinar la composición óptima de una mezcla cualquiera de absorbentes, con resonancias, en las barras de control desde el punto de vista de aumentar la eficacia de las mismas, de disminuir la alteración del campo neutrónico provocada por ellas, etc.

Se ilustra el método con un ejemplo de cálculo de composición óptima correspondiente a la máxima eficacia de una barra de dimensiones dadas en el reactor intermedio PF-4 ($\rho_{Be}/\rho_U = 90$). Para la mezcla óptima de Ir, Re, Eu, Dy y Hf se observó un aumento de la eficacia del 30% (con relación a una barra de Ir de iguales dimensiones).

El mismo método se aplicó al cálculo de la composición óptima de placas de control en reactores agua-agua ($\rho_H/\rho_U = 280$) con miras a minimizar la deformación del campo neutrónico cerca de las mismas.

Los resultados de los cálculos se comparan con los datos experimentales.

Экспериментальное изучение способов компенсации избыточной реактивности промежуточных реакторов

В. А. Кузнецов, А. И. Могильнер, Л. А. Чернов, В. В. Чекунов, В. И. Шарадин

В работе, отдельные результаты которой приводятся в данном докладе, проводилось сравнительное изучение трех возможных способов компенсации избыточной реактивности в промежуточном реакторе для определения их возможностей, достоинств и недостатков:

а) с помощью системы поглощающих стержней;

б) с помощью компенсирующих цилиндров (КЦ), расположенных в боковом отражателе, часть боковой поверхности которого облицована поглотителем (по типу [1,2]);

в) путем раздвижения двух половин активной зоны на высоте.

Абсолютные значения изменений реактивности и перекосов полей, приведенные в докладе, не претендуют на общность ввиду их очевидной зависимости от размеров и состава активной зоны и отражателей, а также от спектра нейтронов в реакторе.

Подробное описание конструкции стенда ПФ-4, предназначенного для исследования физических особенностей промежуточных реакторов, на котором проводились описанные ниже эксперименты, приведено в работе[1].

Измерения изменений реактивности в экспериментах проводились методом обратного счета и методом наращивания высоты активной зоны.

Первый метод применялся в подкритических опытах. При этом использовалось известное соотношение, связывающее изменение скорости счета внешнего детектора $(N_1 - N_2)$ с изменением реактивности (ΔK) подкритической системы с источником:

$$\Delta K = C \frac{N_1 - N_2}{N_1 N_2}. \qquad (1)$$

Коэффициент C определяется с помощью эталона реактивности, в качестве которого использовался один из регулирующих стержней реактора. В ходе опытов величина C менялась весьма существенно, что было обусловлено перекосами нейтронных полей в реакторе. С целью исключения связанной с этим ошибки величина C измерялась для каждого состояния системы.

Во втором методе подкритичность, сообщаемая критическому реактору, компенсировалась в основном добавлением к активной зоне предварительно проградуированных в единицах реактивности слоев горючего и замедлителя (в том же соотношении, что и в активной зоне) и небольшими перемещениями регулятора.

Распределения нейтронного потока в активной зоне измеряли с помощью малогабаритной камеры деления наружным диаметром 7 *мм*. Измерения проводили на уровне мощности 25 *квт*, поддерживаемом с помощью автомата АППМ[1]. Ионизационная камера автомата в данном случае являлась манитором. Малый диаметр камеры деления позволял размещать ее в полостях между рабочими каналами. Этим достигалось минимальное искажение полей при измерениях.

ЭКСПЕРИМЕНТАЛЬНОЕ ИЗУЧЕНИЕ ВЗАИМНОГО ВЛИЯНИЯ (ИНТЕРФЕРЕНЦИИ) ПОГЛОТИТЕЛЕЙ*

Часто приходится компенсировать значительную величину начальной избыточной реактивности большим числом компенсирующих стержней-поглотителей (КС). В процессе физических исследований такого рода реакторов возникают трудности в определении запаса реактивности вследствие взаимного влияния КС, которое приводит к отличию полного запаса реактивности от суммы эффективностей КС, измеренных порознь в первоначально критическом реакторе.

На стенде ПФ-4 было предпринято специальное экспериментальное исследование взаимного влияния (интерференции) пары поглощающих КС на одной из уран-бериллиевых сборок (ПФ-4-16) без отражателя ($\varrho_{Be}/\varrho_{U^5} = 75$).

Цилиндрические компенсирующие стержни имели диаметр 20 *мм* и содержали карбид

* В работе принимал участие Ю. Г. Пашкин.

бора с плотностью по бору 1,7 *г/см*^{3}. Один из КС (первый) помещался вблизи центра активной зоны, другой (второй) мог перемещаться в радиальном направлении. Измерения проводились в подкритических опытах.

Методика измерения интерференционного члена состояла в следующем. Измерялась эффективность ϱ_{10} одного из стержней (например, первого) в отсутствии второго, затем измерялась эффективность ϱ_{12} того же (первого) стержня в присутствии второго. Интерференционный член Δ_{12}, учитывающий влияние второго стержня на эффективность первого, находился из соотношения

$$\varrho_{12} = \varrho_{10} + \Delta_{12}. \qquad (2)$$

Эффективность второго КС в присутствии первого равна

$$\varrho_{21} = \varrho_{20} + \Delta_{21}. \qquad (3)$$

Эффективность пары КС ϱ_{1+2} составляет

$$\varrho_{1+2} = \begin{cases} \varrho_{21} + \varrho_{10} = \varrho_{10} + \varrho_{20} + \Delta_{21}, \\ \varrho_{12} + \varrho_{20} = \varrho_{10} + \varrho_{20} + \Delta_{12}, \end{cases} \qquad (4)$$

откуда следует, что $\Delta_{21} = \Delta_{12}$.

В опытах по изучению интерференции использовалась относительная единица реактивности, в качестве которой принималась эффективность 1 *см* линейной части характеристики регулятора стенда. Результаты измерений приведены в табл. 1.

Таблица 1

Расстояние между КС, *мм* . .	20	36	73	109	146	182
Эффективность одиночного КС, *см*	216	213	191	148	110	77
Интерференционный член Δ_{12}, *см*	—95	—67	—34	—21	—8	+3

Полученные результаты анализировались в простом предположении, что при относительной малости $\Delta_{12}(\Delta_{12} \ll \varrho_{10}$ и $\Delta_{12} \ll \varrho_{20})$ величина последней пропорциональна как значению ϱ_{10}, так и значению ϱ_{20} с коэффициентом пропорциональности, зависящим от расстояния x_{12} между осями КС:

$$\Delta_{12} = \varrho_{10}\varrho_{20} f(x_{12}). \qquad (5)$$

На рис. 1 нанесены экспериментальные точки, вычисленные по данным табл. 1 с помощью соотношения (5). Рассматривая эти данные, можно сделать следующие выводы.

1. Возмущение, вносимое центральным КС, охватывает весь реактор.

2. При близких расстояниях между КС их совместная эффективность ниже суммы невозмущенных эффективностей этих КС.

3. Начиная с некоторого расстояния (в данном случае 164 *мм*) интерференционный член меняет знак.

4. Зависимость фактора $f(x) = \Delta_{12}/\varrho_{10}\varrho_{20}$ от расстояния близка к линейной. Заметное отклонение коэффициента пропорциональности $f(x)$ при близких расстояниях от линейной зависимости в сторону более высоких значений $\Delta(x)$ можно объяснить тем, что неравенство $\Delta \ll \varrho$ выполняется в этом случае наиболее слабо, и дополнительным снижением эффективности второго КС за счет «теневого эффекта» от первого КС.

Приведенные выше выводы относятся к паре КС, один из которых смещается в радиальном направлении. Однако область справедливости этих выводов гораздо шире. На рис. 2 приводятся данные, полученные на стенде ПФ-4 (при том же отношении $\varrho_{Be}/\varrho_{U5}$, сборка ПФ-4-17), когда избыток загрузки компенсировался группой КС. При анализе результатов предполагалось, что влияние группы КС на один из них можно рассматривать как суперпозицию влияний каждого из членов группы. Иными словами, предполагается, что при $\Delta \ll \varrho$ основной вклад в интерференцию дают парные взаимодействия, то есть взаимодействие пары КС не зависит от присутствия других КС.

Кривая *1* на рис. 2 построена как зависимость $f(x_{ik}) = \Delta_{ik}/\varrho_i\varrho_k$, где эффективности ϱ_i и ϱ_k измерены в присутствии других членов группы КС. Линейная форма $f(x_{ik})$ является некоторым основанием для применения принципа суперпозиции и может быть использована для уточнения статистического выравнивания величин Δ_{ik}, а иногда и для их предсказания.

В предположении, что расстояние между осями КС достаточно велико, чтобы не чувствовался «теневой эффект», и зависимость $f(x)$ линейна, из значений Δ_{ik}, относящихся к паре КС (i, k), можно построить квадратную симметричную матрицу с диагональными членами $\Delta_{ii} = \varrho_{i0}$, где ϱ_{i0} есть эффективность i-го КС в отсутствии всех других КС. Число строк и столбцов матрицы равно числу КС. Вклад в реактивность какого-либо (i-го) КС равен сумме матричных элементов соответствующего (i-го) столбца или строки

$$\varrho_i = \sum_k \Delta_{ik} = \sum_k \Delta_{ki}. \qquad (6)$$

При удалении того или иного КС следует вычеркнуть соответствующий столбец и строку. Для получения эффективности всей группы КС следует сложить диагональные члены и все Δ_{ik} выше (или ниже) диагонали.

Легко видеть, что измерение $\Delta_{ik}(i \neq k)$ и ϱ_i позволяет в соответствии с соотношением (6)

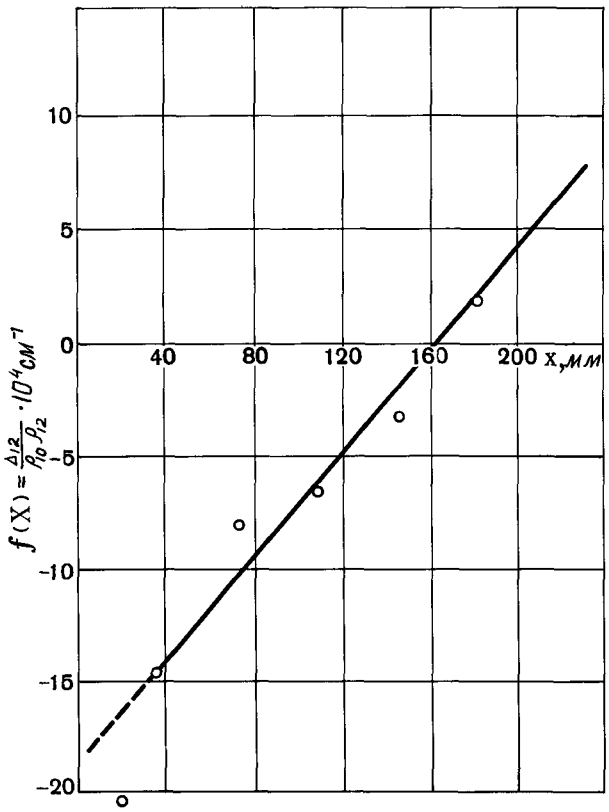


Рис. 1. Зависимость $f(x) = \frac{\Delta_{12}}{\varrho_{10}\varrho_{20}}$ от расстояния между осями КС

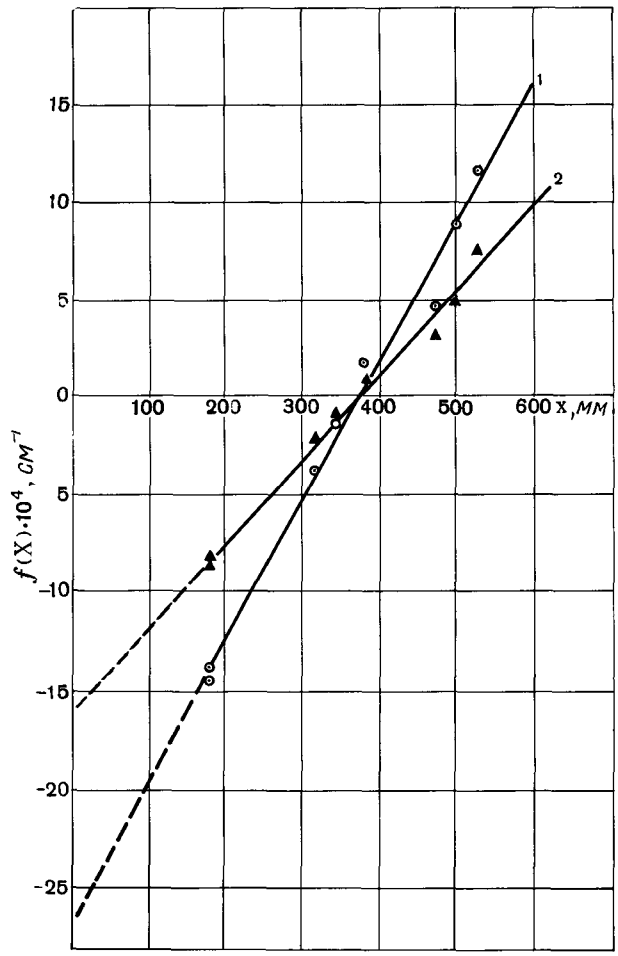


Рис. 2. Зависимость $f(x_i)_k = \frac{\Delta_{ik}}{\varrho_i \varrho_k}$ (кривая *1*) и $f(x) = \frac{\Delta_{ik}}{\varrho_{i0}\varrho_{k0}}$ (кривая *2*) от расстояния между осями КС

получить значение ϱ_{i0}. Кривая *2* на рис. 2 построена как зависимость $f_0(x) = \Delta_{ik}/\varrho_{i0}\varrho_{k0}$. Обе кривые хорошо аппроксимируются прямыми, пересекающими ось абсцисс в одном и том же месте.

ИЗУЧЕНИЕ СПОСОБА КОМПЕНСАЦИИ С ПОМОЩЬЮ КОМПЕНСИРУЮЩИХ ЦИЛИНДРОВ (КЦ)

Изучение проводилось на реакторе ПФ-4-10 диаметром активной зоны, равном 417 *мм*, и отношением $\varrho_{Be}/\varrho_{U^5} = 106$. Эквивалентная толщина бокового бериллиевого экрана составляла 140 *мм*. Макет КЦ представлял собой гексогональную призму, набранную из 19 стандартных алюминиевых каналов (труб) диаметром 50 × 1 *мм* (рис. 3). Шесть каналов, расположенных во внешнем ряду призмы, содержали пеналы с насыпным карбидом бора ($\gamma_{B_4C} = 1{,}06\ г/см^3$), которые имитировали поглощающую облицовку КЦ. Высота облицовки была равна высоте активной зоны. Остальные 13 каналов представляли собой обычные каналы бериллиевого отражателя. Конструкция макета КЦ позволяет менять толщину слоя поглотителя (5 и 10 *мм*), величину дуги облицовки поглотителем, образовывать воздушный зазор между активной зоной и КЦ, а также осуществлять дискретные повороты КЦ через 30°. Поворот КЦ имитировался последовательной перестановкой каналов с поглотителем.

На рис. 4 схематично показан КЦ в различных положениях. Для определения эффективности КЦ с так называемыми нейтронными ловушками за слоем поглотителя в КЦ устанавливались три обычных канала, заполненных на высоту активной зоны парафином. Все эксперименты проводились с одиночным КЦ.

А. Зависимость компенсационной способности (КЦ) от угла поворота

В табл. 2 и на рис. 5 приведены результаты измерений компенсационной способности КЦ в функции угла поворота φ, полученные на стенде ПФ-4-10 для одиночного КЦ с другой

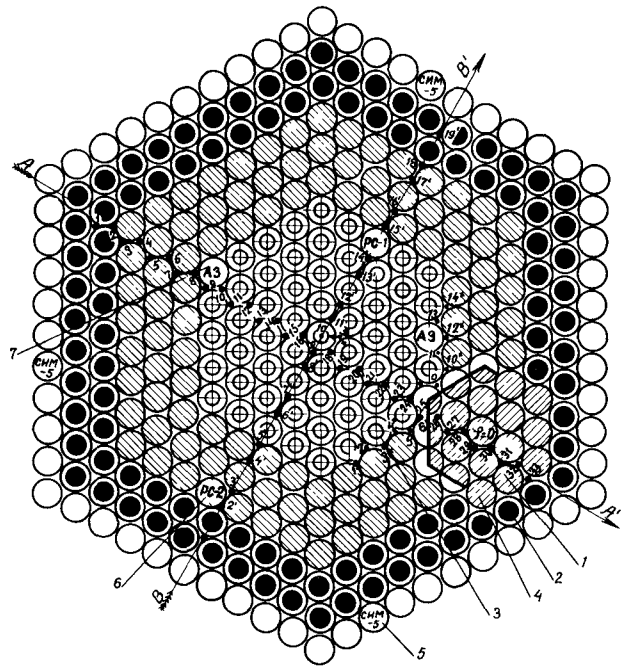


Рис. 3. Картограмма критической сборки ПФ-4-10 с компенсирующим цилиндром в положении $\varphi=0°$:

1 — источник; *2* — пакет стального отражателя; *3* — рабочий пакет; *4* — пакет бериллиевого отражателя; *5* — датчик импульсной аппаратуры; *6* — регулирующий стержень; *7* — стержень аварийной защиты; *1, 2, 3 ...*, *n* — номера точек, в которых производились измерения нейтронного поля

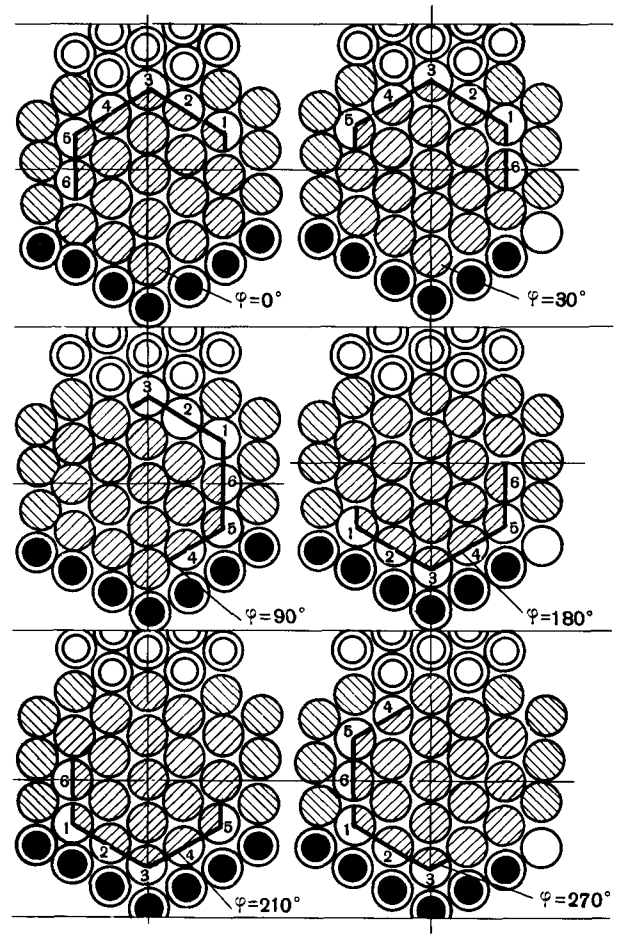


Рис. 4. Схема различных положений одиночного КЦ в критической сборке ПФ-4-10

облицовки $\theta = 180°$ и толщиной облицовки $\delta_{B_4C} = 5$ *мм*. Компенсационная способность КЦ $\left.\frac{\Delta k}{k}\right|_{15°}^{\varphi}$ определялась как изменение реактивности системы при повороте КЦ из положения минимальной реактивности системы при $\varphi = 15°$ (когда поглощающая облицовка КЦ наиболее приближена к активной зоне) в положение φ.

Таблица 2

Угол поворота КЦ φ, удар	Компенсационная способность КЦ $\left.\frac{\Delta k}{k}\right\|_{15°}^{\varphi}$, %		То же за вычетом реактивности от воздушного зазора
	Метод обратного счета	Метод догрузки активного материала	
15 (375)	0,00	0,00	0,00
30 (0, 360) *	0,06	0,06	0,06
60 (330)	0,785	0,79	0,575
90 (300)	1,685	1,85	1,255
120 (270)	2,51	2,74	1,764
150 (240)	3,17	3,28	2,31
180 (210) *	3,84	3,77	2,91
195	3,90	3,85	2,97

* Изменение реактивности при повороте КЦ от 30 до 15° и от 180 до 195° получены интерполяцией кривой $\frac{\Delta k}{k} = f(\varphi)$.

В этих же экспериментах определялось влияние воздушного зазора между активной зоной и КЦ на компенсационную способность последнего. Для этого из макета КЦ извлекались пеналы с карбидом бора и определялось изменение реактивности системы при повороте КЦ из положения $\varphi = 30°$ в положение $\varphi = 180°$ дискретно через каждые 30°. Эти измерения позволили получить характеристики КЦ $\frac{\Delta k}{k} = f(\varphi)$ без учета и с учетом воздушного зазора. «Паразитная» реактивность от КЦ, определяемая по изменению критического положения регулятора при введении в отражатель невозмущенного реактора пакета КЦ в положении наибольшей критичности системы ($\varphi = 210°$), составила $\frac{\Delta k}{k} = 0{,}32\%$.

Данные табл. 2 и рис. 5 свидетельствуют о хорошем согласии результатов измерений эффективности КЦ в различных его положениях принятыми методами. Наблюдаемое расхождение находится в пределах точности экспериментов.

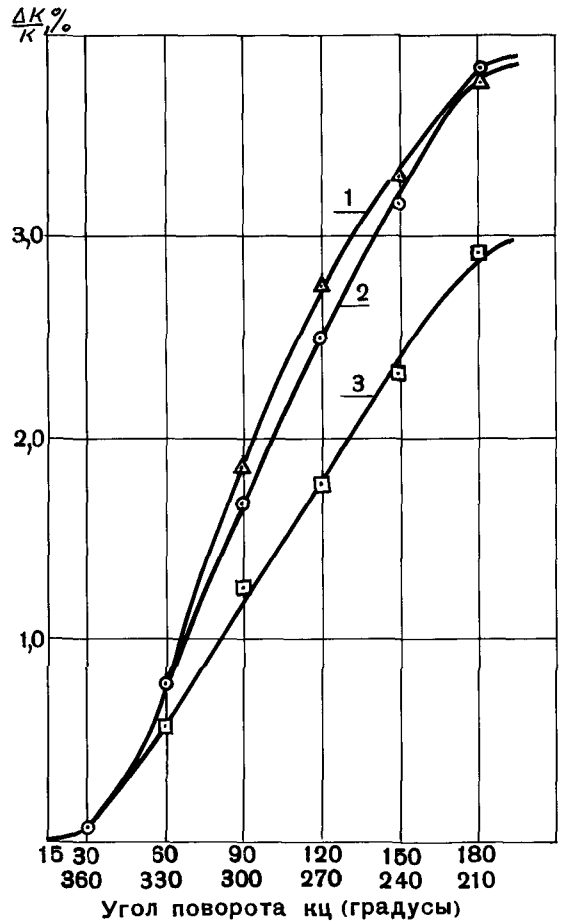


Рис. 5. Характеристики компенсирующего цилиндра:
1 — метод догрузки активного материала; *2* — метод обратного счета; *3* — характеристика КЦ за вычетом эффекта воздушного зазора

Б. Зависимость компенсационной способности КЦ от величины дуги облицовки

Качественный анализ изменения компенсационной способности КЦ от величины дуги облицовки указывает на наличие оптимального значения этой величины, обеспечивающей максимальную компенсационную способность КЦ при минимально возможной «паразитной» реактивности. Для определения оптимальной величины дуги облицовки на сборке ПФ-4-10 были проведены опыты по определению изменений реактивности, вносимой КЦ, в положениях максимальной и минимальной реактивности системы для макетов КЦ с дугами облицовки $\theta = 180$, 150 и 120° при $\delta_{B_4C} = 5$ *мм*. Изменение дуги облицовки осуществлялось заменой каналов с поглотителем на обычные каналы бериллиевого отражателя.

Результаты измерений на сборке ПФ-4-10 приведены в табл. 2. Из таблицы видно, что из трех величин оптимальной дугой облицовки компенсирующего цилиндра для реактора ПФ-4-10 является дуга $\theta = 120°$, так как в этом случае компенсационная способность КЦ является наибольшей, а «паразитная» реактивность минимальна. По характеру изменения реактивности, вносимой КЦ в положении $\varphi = 0$, следует ожидать, что дальнейшее уменьшение дуги облицовки приведет к уменьшению компенсационной способности КЦ.

В. Зависимость компенсационной способности КЦ от толщины слоя поглотителя

Наименование компенсационной способности КЦ с изменением толщины слоя поглотителя изучалось на сборке ПФ-4-10. Результаты измерений показывают, что увеличение толщины слоя карбида бора с 5 до 10 *мм* приводит к увеличению компенсационной способности КЦ с дугой облицовки $\theta = 150°$ в 1,27 раза.

Г. Компенсационная способность КЦ с нейтронными ловушками

Опыт проводился на сборке ПФ-4-10 с малетом КЦ $\theta = 180°$ и $\delta_{B_4C} = 5$ *мм*. Установлено, что три канала с парафином, помещенные в КЦ за слоем карбида бора, увеличили его компенсационную способность на $\frac{\Delta k}{k} \simeq 1\%$. При этом наблюдалось также и увеличение отрицательной паразитной реактивности

$$\frac{\Delta k}{k} \sim -0{,}12\ \%.$$

Д. Поля энерговыделения по радиусу активной зоны при различных положениях КЦ

Можно предполагать, что КЦ не создает существенного искажения поля по высоте активной зоны. Поэтому в данной работе были исследованы искажения нейтронного поля только по радиусу активной зоны и по ее границе в районе расположения КЦ. Поля были сняты для невозмущенной системы, а также при возмущениях, вносимых одиночным КЦ в положениях $\varphi = 270°$ и $\varphi = 30°$. Положение камеры по высоте соответствовало центру активной зоны.

Результаты измерений поля по направлению центр активной зоны — центр КЦ (см. *AA'* на рис. 3) представлены на рис. 6. Поскольку измерение полей при различных положениях КЦ проводилось на различных уровнях мощ-

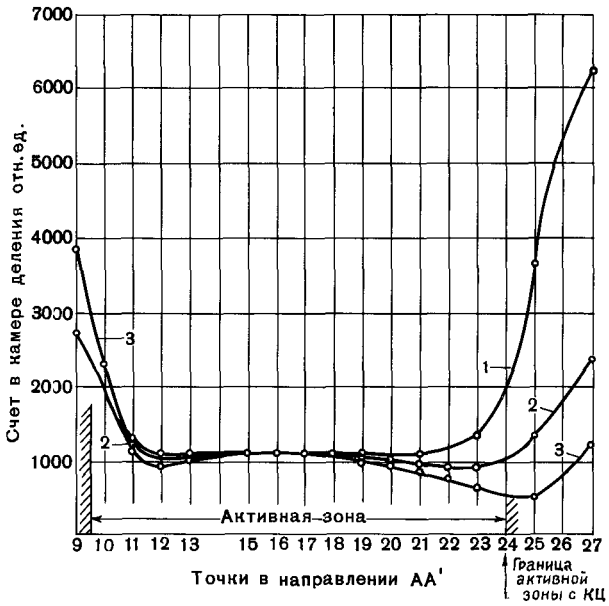


Рис. 6. Распределение плотности делений, измеренное утановой камерой деления по радиусу реактора ПФ-4-10 в направлении AA':

1 — невозмущенное поле; *2* — поле для КЦ в положении $\varphi=270°$; *3* — поле для КЦ в положении $\varphi=30°$

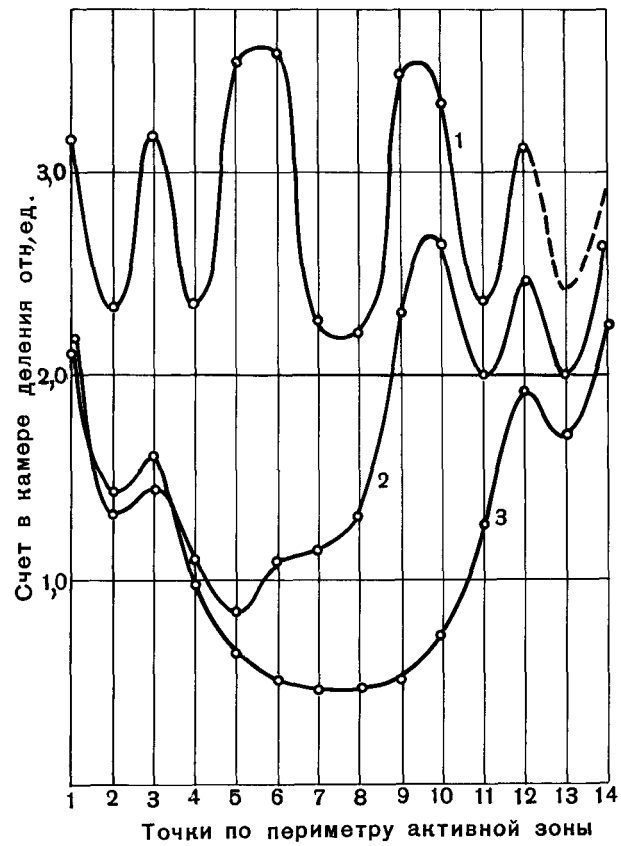


Рис. 7. Распределение плотности делений, измеренное урановой камерой деления по периметру активной зоны реактора ПФ-4-10 в районе расположения КЦ. Все кривые нормированы к значению плотности делений в центре активной зоны, невозмущенному действием КЦ:

1 — невозмущенное поле; *2* — поля для КЦ в положении $\varphi=270°$; *3* — поля для КЦ в положении $\varphi=30°$

ности, нормировка полей сделана на значение в центре активной зоны.

На рис. 7 приведены поля энерговыделения по периметру активной зоны в районе расположения КЦ, отнормированные на значение поля в центре активной зоны, не возмущенное действием КЦ.

ИЗУЧЕНИЕ СПОСОБА КОМПЕНСАЦИИ ПУТЕМ РАЗДВИЖЕНИЯ АКТИВНОЙ ЗОНЫ

Способ компенсации раздвижением активной зоны на две половины был исследован на сборках ПФ-4-09, ПФ-4-13, ПФ-4-10 и ПФ-4-12 (в диапазоне изменения ядерных концентраций $\varrho_{Be}/\varrho_{U^5}$ от 0 до 106).

Измерения изменений реактивности, обусловленных раздвижением зоны и увеличением утечки нейтронов из нее, производились в подкритическом режиме методом обратного счета. В качестве эталона реактивности при этом использовался один из стержней-регуляторов. Предполагалось, что эффективность стержня при раздвижении зоны существенно не меняется, что было подтверждено экспериментально до раздвижения 40 *мм*.

На рис. 8 представлена схема раздвижения активной зоны. Раздвижение активной зоны осуществлялось с помощью дистанционирующих тонкостенных алюминиевых трубок, вводимых между половинами активной зоны. Во всех экспериментах изучалось раздвижение только активной зоны. В других сборках изменение реактивности от раздвижения сравнивалось с изменением реактивности, происходящим при равномерном «разбавлении» активных зон по урану и бериллию при неизменном диаметре и соответствующем увеличении высот активных зон.

В табл. 3 представлены значения изменений реактивности при раздвижении активных зон различных сборок. Те же данные для сборок ПФ-4-09 и ПФ-4-10 представлены на рис. 9. Из данных табл. 3 и рис. 9 следует, что эффективность раздвижения активной зоны на 1 *см*

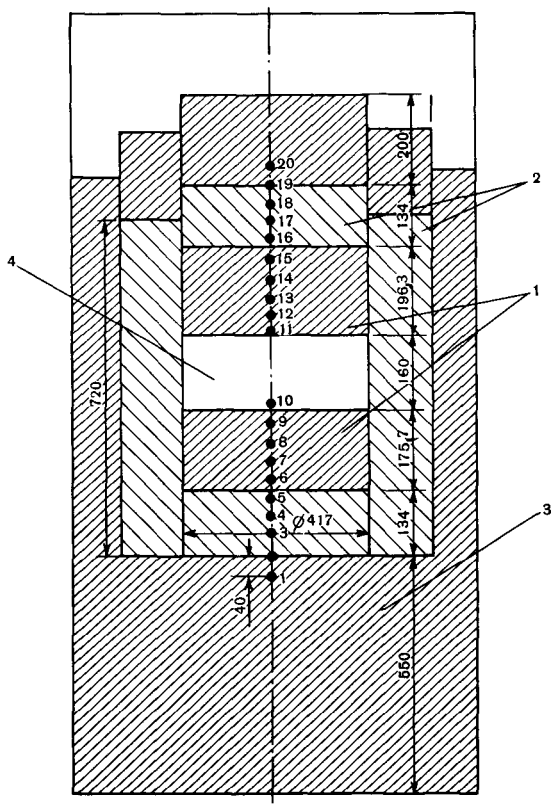


Рис. 8. Схема раздвижения активной зоны реактора ПФ-4-10:

1 — активная зона; *2* — бериллиевый отражатель; *3* — стальной отражатель; *4* — промежуточный воздушный слой

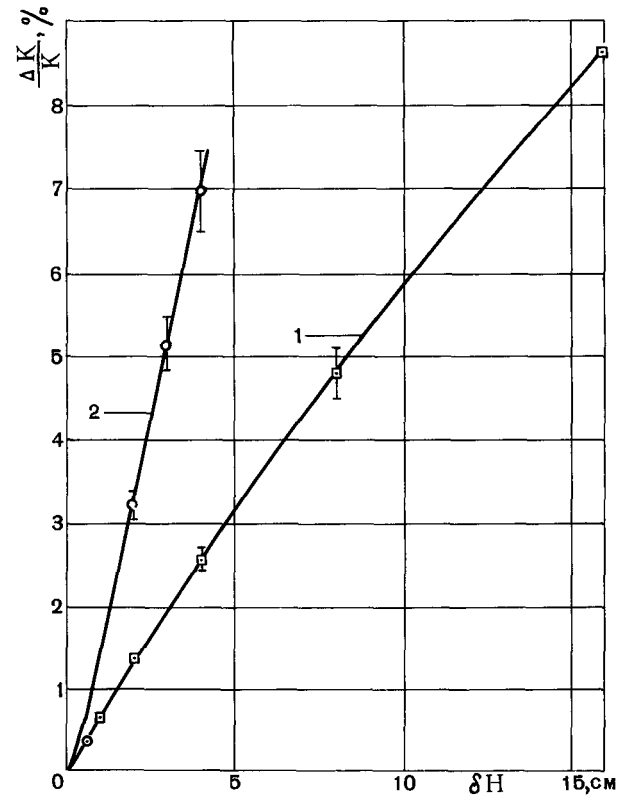


Рис. 9. Характеристики изменения реактивности системы при раздвижении реакторов стенда ПФ-4:

1 — сборка ПФ-4-13; *2* — сборка ПФ-4-10

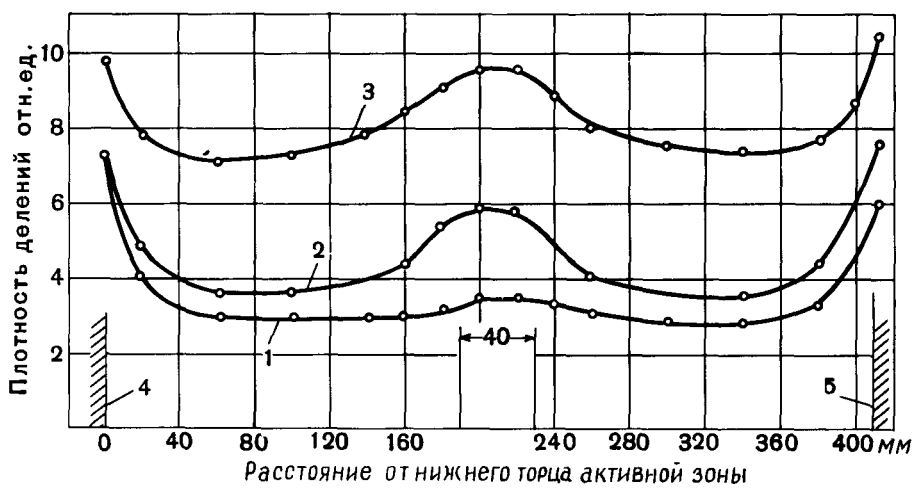


Рис. 10. Распределение плотности делений по высоте активной зоны критической сборки ПФ-5-10 с отношением $\varrho_{Be}/\varrho_{U^5} = 106$ в различных точках по радиусу, измеренное урановой камерой деления. Поля отнормированы к значению в центре активной зоны при нулевом раздвижении:

1 — $r = 29{,}5$ *мм* (точка 16 картограммы рис. 3); *2* — $r = 147{,}0$ *мм* (точка 6 картограммы рис. 3); *3* — $r = 206{,}0$ *мм* (точка 5 картограммы рис. 3)

Таблица 3

Сборка	Величина раздвижения ΔH, *мм*	Эффективность раздвижения на две равные половины $\frac{\Delta k}{k}$, %	Эффективность равномерного «разбавления», эквивалентного раздвижению на величину ΔH $\frac{\Delta k}{k}$, %
ПФ-4-09	10	1,76±0,07	—
	20	3,20±0,16	3,17±0,14
	30	5,14±0,35	—
	40	6,96±0,53	—
ПФ-4-13	10	0,85±0,05	—
	20	1,90±0,05	—
	40	3,20±0,05	—
	80	4,0±0,06	—
ПФ-4-10	10	0,78±0,004	—
	20	1,365±0,017	—
	40	2,56±0,18	—
	80	4,77±0,18	—
	160	8,50±0,75	—
ПФ-4-12	40	3,71±0,21	2,68±0,20

увеличивается с уменьшением $\varrho_{Be}/\varrho_{U_5}$, что связано в основном с уменьшением размеров сборок при уменьшении $\varrho_{Be}/\varrho_{U_5}$.

Сравнение эффективности раздвижения активной зоны на две половины с эффективностью ее равномерного раздвижения (разбавления воздухом) показало, что значения этих эффективностей относятся между собой как значения квадратов потока быстрых нейтронов в центре активной зоны и его среднего значения по высоте. Это можно объяснить, если иметь в виду, что вклад в реактивность вылетающих через щель быстрых нейтронов, которые главным образом и определяют эффективность раздвижения, пропорционален произведению их потока на ценность.

Наряду с величиной изменения реактивности представляет интерес вопрос о распределении плотности делений по высоте активной зоны с центральной горизонтальной щелью.

Распределение плотности делений по высоте активной зоны измерялось с помощью камеры деления. Результаты измерений для сборки ПФ-4-10 при раздвижении на 40 *мм* представлены на рис. 10. Из приводимых графиков следует, что в областях активной зоны, граничащих с зазором и боковым отражателем, наблюдается подъем плотности давлений, обусловленный притоком замедляющихся нейтронов из бокового отражателя.

ЛИТЕРАТУРА

1. А. И. Лейпунский, В. А. Кузнецов, Г. Я. Артюхов, А. И. Могильнер, Ю. А. Прохоров, В. М. Стекловский, Л. А. Чернов. Экспериментальные исследования некоторых физических особенностей промежуточных реакторов с бериллиевым замедлителем. Доклад SM-18/80 на семинаре по физике быстрых и промежуточных реакторов, Вена, 1961.
2. I. R. Stehn. The Physics of Intermediate Spectrum Reactors Editor US AEC, 1958.
3. И. И. Бондаренко и др. Нейтронно-физические характеристики U + Be и U + BeO систем, Р/362, наст. издание.

ABSTRACT - RÉSUMÉ - АННОТАЦИЯ - RESUMEN

A/375 USSR

Experimental study of some methods of compensating excess reactivity in intermediate reactors

By V. A. Kuznetsov *et al.*

The paper contains results of experimental investigations of methods of compensation of high excess reactivity by separating two halves of the core or by inserting compensating cylinders enclosed in boron-containing material into a side beryllium reflector.

The efficiency of these methods of compensation is compared with that of a single boron carbide rod placed in the centre of the core. The distortion of the neutron density distribution is presented as a function of the angular position of the recompensation cylinder and of the separation between two halves of the core.

An attempt was made to evaluate the efficiency of separating halves of the core for intermediate reactors by numerical computations based on one-group theory.

The results of the investigation of the absorbing rods interference prove that the main contribution to the interference comes from pair interactions. The experimental data permit evaluation of the efficiency of the absorbing rod system.

The experiments were carried out with the beryllium-moderated intermediate zero power reactors on the PF-4 physical assembly described elsewhere.

A/375 URSS

Etude expérimentale des méthodes de compensation d'un excédent de réactivité dans les réacteurs à neutrons intermédiaires

par V. A. Kuznetsov *et al.*

Ce mémoire présente les résultats d'une étude expérimentale des méthodes de compensation d'un excédent important de réactivité grâce à des cylindres de compensation à revêtement au bore, insérés dans le réflecteur latéral au béryllium, et à la division de la zone active en deux moitiés.

L'efficacité de chacun de ces moyens de compensation est comparée à celle d'une barre unique en carbure de bore placée au centre de la zone active. Les auteurs donnent les résultats de mesures de déformations des champs de neutrons en fonction de l'angle de rotation du cylindre de compensation et de l'écartement entre les deux moitiés de la zone active.

On fait un essai d'estimation de l'efficacité de cet écartement dans les réacteurs à neutrons intermédiaires par le calcul par approximation à un groupe.

Les auteurs donnent les résultats de l'étude de l'interférence des barres absorbantes; on peut en conclure que la principale contribution à l'interférence est donnée par les interactions paires. Les résultats obtenus permettent d'estimer l'efficacité du système de compensation.

Les expériences ont été faites avec l'installation PF-4, décrite antérieurement, sur des réacteurs à modérateur de béryllium et à spectre intermédiaire de neutrons dans la zone active.

A/375 URSS

Estudio experimental de los métodos de compensación de grandes excesos de reactividad en reactores de neutrones intermedios

por V. A. Kuznetsov *et al.*

La memoria expone los resultados del estudio experimental de los métodos de compensación de grandes excesos de reactividad mediante el montaje, dentro del reflector lateral de berilio, de cilindros de compensación con revestimiento de boro, y la separación del núcleo en dos mitades.

La eficacia de estos métodos se compara con la de una sola barra de carburo de boro situada en el centro del núcleo. En el trabajo se presentan los resultados de las medidas de las deformaciones de los campos neutrónicos en función del ángulo de giro del cilindro de compensación y de la separación entre las dos partes del núcleo.

Se describe un intento de estimar la eficacia de la separación del núcleo en los reactores de neutrones intermedios mediante el cálculo en la aproximación de un solo grupo.

Se presentan los resultados del estudio de la interferencia de las barras absorbentes, resultados que ponen de manifiesto que la mayor parte de la interferencia se debe a las interacciones pares. Los resultados obtenidos permiten estimar la eficacia de un sistema de compensación.

Los experimentos se llevaron a cabo en la instalación de ensayos PF-4, anteriormente descrita, en reactores con moderador de berilio y espectro intermedio de neutrones en el núcleo.

Компенсация больших изменений реактивности деформацией решетки активной зоны

Г. А. Бать, Г. В. Мухина, Д. М. Парфанович, Д. С. Клочков, В. С. Мухортов, Н. М. Трухачев, Д. И. Шеффер

1

Стремление увеличить продолжительность кампании энергетических и исследовательских реакторов приводит к непрерывному росту запаса реактивности свежезагруженного аппарата. В наиболее распространенных водо-водяных системах этот запас составляет ~0,15 и имеет тенденцию возрастать по мере отработки новых активных зон. Одновременно разрабатываются и совершенствуются методы подавления избыточной реактивности: вводятся выгорающие поглотители, усложняются и умножаются механические системы — стержни, кассеты, компенсирующие решетки. Однако существующие методы обладают некоторыми недостатками. Так, применение самой совершенной системы выгорающих поглотителей не может обеспечить необходимого оперативного запаса реактивности (на температурный эффект, стационарное отравление, маневрирование мощностью, «борный разбаланс»), а механические устройства либо создают большие искажения поля тепловыделения (компенсирующие решетки), либо чрезмерно сложны и громоздки (системы из большого числа слабо поглощающих стержней с независимыми приводами). Кроме того, система стержней и их приводов обычно увеличивает необходимую высоту реактора.

Можно назвать три типа путей создания оперативного запаса реактивности:

1. Обычные поглощающие органы системы управления — стержни, кассеты, компенсирующие решетки и различные их модификации.

2. Изменение свойств замедлителя во время работы реактора, например, использование смесей обычной и тяжелой воды с переменной концентрацией компонент, растворение в замедлителе поглощающих веществ и их постепенное извлечение.

3. Изменение шага (или другая деформация) решетки активной зоны.

Использование обычных органов управления легко сочетать с изменением свойств замедлителя и весьма затруднительно с деформацией решетки. Любые методы создания оперативного запаса реактивности не исключают применения выгорающих поглотителей.

Возможности обычных систем компенсации хорошо изучены, и практически эти системы всегда оказываются довольно «жесткими», то есть содержат небольшое число сильно действующих исполнительных органов. Изменение свойств замедлителя в процессе эксплуатации реактора является примером «мягкого» регулирования, вносящего минимальные искажения в поле тепловыделения. Системы управления такого типа начинают внедряться на ряде реакторов.

Ниже обсуждаются особенности одной из возможных схем регулирования с помощью деформации решетки активной зоны.

Представим себе активную зону реактора, образованную правильной решеткой цилиндрических тепловыделяющих элементов, помещенных в жидкий замедлитель (например, в H_2O). Пусть верхние концы всех элементов закреплены в некоторой плоскости так, что каждый из них может независимо поворачиваться вокруг точки крепления. Пусть далее эти элементы свободно пропущены сквозь дистанционирующую плиту, отверстия в которой образуют сетку, повторяющую сетку точек крепления. Решетка и форма цилиндрического аппарата не зависят от расстояния между плоскостью шарниров и плоскостью дистанционирующей плиты. Начнем поворачивать эту плиту в горизонтальной плоскости вокруг центральной оси реактора. Тогда активная зона примет форму однополостного гиперболоида вращения. Решетка тепловыделяющих элементов будет деформирована так, что поверхностями постоянного шага окажется с большой точностью система эллипсоидов вращения, софокусных с гиперболоидом, образующим боковую границу. При заданных тепловыделяющих элементах и угле скручивания форма аппарата зависит также от расстояния между дистанционирующей плитой и плоскостью шарниров. Поэтому регулирование может осуществляться не только поворотом, но и изменением этого расстояния. Можно рассмотреть также случай, когда сетка отверстий в дистан-

ционирующей плите имеет шаг, отличный от шага сетки шарниров, и начальной формой активной зоны является не цилиндр, а усеченный конус. Однако по конструктивным соображениям и с точки зрения улучшения формы поля энерговыделения наиболее интересными представляются варианты, симметричные (или почти симметричные) относительно центральной плоскости активной зоны.

Разумеется, для реакторов, состоящих из отдельных тепловыделяющих элементов, охлаждаемых сплошным потоком воды, предложенные схемы неудобны вследствие изменения в процессе деформации активной зоны проходного сечения теплоносителя. Однако это обстоятельство не наблюдается в системах со сложными тепловыделяющими элементами — каналами, где межканальная вода служит только замедлителем.

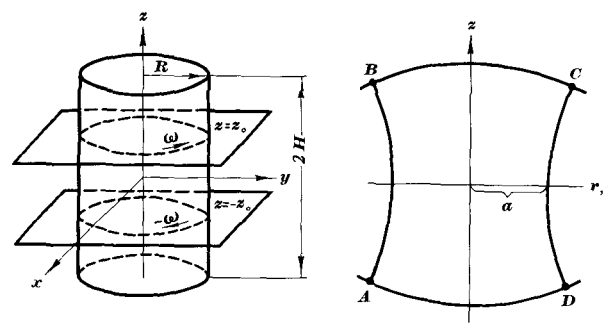
Зависимость реактивности от шага решетки цилиндрического реактора обычно немонотонна: при увеличении шага ϱ сначала растет, а затем уменьшается. Поэтому для регулирования реактора деформацией активной зоны можно использовать либо «левую» ветвь, соответствующую шагам решетки, меньшим оптимального, либо «правую», соответствующую большим шагам.

Заранее очевидно, что максимальная эффективность регулирования для правой ветви ограничена соображениями защиты от ядерных излучений. Действительно, в гетерогенном реакторе увеличение шага решетки приводит к росту положительной составляющей температурного эффекта, обусловленному выравниванием распределения тепловых нейтронов по ячейке. В достаточно разреженной системе полный температурный эффект и температурный коэффициент реактивности вблизи рабочей точки становятся положительными. Последнее обстоятельство и заставляет выбирать исходный шаг решетки не слишком большим. Минимальный шаг для левой ветви определяется диаметром канала, и возможная эффективность деформации зависит от разности реактивностей при оптимальном шаге и при касании каналов. Для каналов, в которых содержится небольшое количество внутреннего замедлителя, или в предельном случае для отдельных тепловыделяющих элементов распределение поля энерговыделения вдоль оси аппарата при скручивании может оказаться неустойчивым. Небольшая асимметрия решетки или внешней формы активной зоны относительно ее центральной плоскости при пережимании сечения замедлителя приводит к резкой асимметрии в распределении потока нейтронов.

При реализации аппаратов с деформируемой решеткой несколько затруднено размещение обычных быстродействующих органов аварийной защиты и автоматического регулирования. Одним из возможных вариантов конструктивного решения может служить выделение для этой цели освобожденной от каналов области вокруг оси аппарата или неподвижной группы центральных каналов, заранее скрученной или сближенной. При этом необходимо обратить внимание на увеличение эффективности быстродействующих органов регулирования и исключение значительных искажений радиальной составляющей нейтронного поля. Однако самой большой трудностью является необходимость иметь в недоступной в процессе работы области реактора значительное число кинематических пар или гибких элементов, обеспечивающих подвижность каналов. По существу жизненность обсуждаемой системы компенсации зависит именно от возможности гарантировать вполне надежную работу этих пар или элементов.

2

Для математического описания регулирования скручиванием решетки активной зоны рассмотрим цилиндрический реактор с эффективной высотой $2H$ и эффективным радиусом R.



Если плоскости $z = \pm z_0$ повернуть на углы $\pm\omega$ относительно вертикальной оси, то цилиндр перейдет в тело, ограниченное гиперболоидом вращения и поверхностью, которую с достаточной точностью можно принять за эллипсоид. В сечении этого тела плоскостью, проходящей через ось z, отрезки AD и BC представляют собой дуги эллипса

$$\frac{r^2}{a_э^2}+\frac{z^2}{b_э^2}=1,$$

а отрезки AB и DC — дуги софокусной с эллипсом гиперболы

$$\frac{r^2}{a_г^2}+\frac{z^2}{b_г^2}=1.$$

Фокусное расстояние для обеих кривых обозначим $2c$. Из простых геометрических соображений легко установить, что

$$a_г = a = R\cos\omega;$$
$$b_г = b = z_0 \operatorname{ctg}\omega;$$
$$a_э = [H^2 + (a^2+b^2)]^{1/2} = [H^2 + R^2\cos^2\omega + z_0^2 \operatorname{ctg}^2\omega]^{1/2};$$
$$b_э = H;$$
$$c^2 = R^2\cos^2\omega + z_0^2\operatorname{ctg}^2\omega.$$

Таким образом, параметры скрученного аппарата a, b, c полностью определены, если заданы эффективные высота и радиус цилиндра, угол поворота ω и расстояние между скручивающими плоскостями $2z_0$. Максимальный угол поворота определяется условием касания тепловыделяющих элементов диаметром d

$$\sin\omega \leqslant \left[\frac{1-(d/D)^2}{1+(d/D)^2(R/z_0)^2}\right]^{1/2},$$

где D — шаг ячейки в цилиндрическом аппарате ($\omega = 0$).

Краевая задача на отыскание критического параметра в одногрупповом приближении запишется следующим образом:

$$\Delta\Phi + \varkappa^2\Phi = 0; \qquad (1)$$

$$\Phi/\Sigma = 0, \qquad (2)$$

где Φ — поток тепловых нейтронов; Σ — эффективная поверхность аппарата; $\varkappa^2$ — материальный параметр, зависящий от координат, потока нейтронов и интеграла от потока по времени.

Нелинейное уравнение (1) можно рассматривать как квазистационарное.

Критическим параметром задачи о выгорании топлива можно считать либо угол ω, либо реактивность ρ. При сравнении с результатами критических опытов критическим параметром удобно считать величину эффективного радиуса R, а вместо вычисления $\varkappa^2$ по геометрическим и ядерным характеристикам решетки — вносить в расчет экспериментально определенную зависимость $\varkappa^2$ от площади ячейки S. Этим исключаются возможные ошибки расчета параметров размножения и возникает возможность легко оценить погрешности, вносимые грубостью описания реального аппарата одногрупповой моделью для реактора с эффективными размерами.

Решение краевой задачи удобно проводить в вырожденных эллипсоидальных координатах для сплюснутого эллипсоида вращения:

$$\begin{aligned} x &= c\,\mathrm{ch}\,\alpha\cdot\sin\beta\cdot\cos\varphi;\\ y &= c\,\mathrm{ch}\,\alpha\cdot\sin\beta\cdot\sin\varphi;\\ z &= c\,\mathrm{sh}\,\alpha\cdot\cos\beta. \end{aligned} \qquad (3)$$

Координатные поверхности суть сплюснутые эллипсоиды вращения $\alpha = \mathrm{const}$, однополостные гиперболоиды вращения $\beta = \mathrm{const}$ и плоскости $\varphi = \mathrm{const}$. Оператор Лапласа в этой системе координат имеет вид

$$\Delta\Phi = \frac{1}{c^2(\mathrm{ch}^2\alpha - \sin^2\beta)}\left[\frac{1}{\mathrm{ch}\,\alpha}\frac{\partial}{\partial\alpha}\left(\mathrm{ch}\,\alpha\frac{\partial\Phi}{\partial\alpha}\right) + \frac{1}{\sin\beta}\frac{\partial}{\partial\beta}\left(\sin\beta\frac{\partial\Phi}{\partial\beta}\right) + \left(\frac{1}{\sin^2\beta} - \frac{1}{\mathrm{ch}^2\alpha}\right)\frac{\partial^2\Phi}{\partial\varphi^2}\right].$$

Ограничимся случаем, когда решение не зависит от угла φ. При этом уравнение (1) примет форму

$$\frac{1}{\mathrm{ch}\,\alpha}\frac{\partial}{\partial\alpha}\left(\mathrm{ch}\,\alpha\frac{\partial\Phi}{\partial\alpha}\right) + \frac{1}{\sin\beta}\frac{\partial}{\partial\beta}\left(\sin\beta\frac{\partial\Phi}{\partial\beta}\right) + c^2(\mathrm{ch}^2\alpha - \sin^2\beta)\varkappa^2\Phi = 0. \qquad (1а)$$

Легко убедиться, что

$$S = \frac{\sqrt{3}}{2}\frac{D^2}{R^2}c^2\,\mathrm{ch}\,\alpha\left[\mathrm{ch}\,\alpha + \mathrm{sh}^2\alpha\times \ln\frac{1+\mathrm{ch}\,\alpha}{\cos\beta_1 + \sqrt{\mathrm{sh}^2\alpha + \cos^2\beta_1}} - \cos\beta_1\sqrt{\mathrm{sh}^2\alpha + \cos^2\beta_1}\right] = f \qquad (\alpha),$$

где $\sin\beta_1 = \frac{a}{c}$.

Для использования конечно-разностной схемы удобно ввести переменные

$$\xi = 1 - \cos\beta;$$
$$\eta = \mathrm{sh}\,\alpha$$

и привести уравнение (1) и условие (2) к виду

$$\frac{\partial}{\partial\eta}\left[(1+\eta^2)\frac{\partial\Phi}{\partial\eta}\right] + \frac{\partial}{\partial\xi}\left[\xi(2-\xi)\frac{\partial\Phi}{\partial\xi}\right] + c^2[\eta^2 + (1-\xi)^2]\varkappa^2(\xi, \eta, t, \Phi)\Phi = 0; \qquad (1б)$$

$$\Phi = 0 \text{ при } \xi = 1 - \cos\beta_1 \text{ или } \eta = \mathrm{sh}\,\alpha_1 = \frac{H}{c};$$

$$\frac{\partial\Phi}{\partial\eta} = 0 \text{ при } \xi = 0 \text{ или } \eta = 0. \qquad (2а)$$

(При численном решении можно ограничиться четвертью симметричной фигуры.)

Выражение для S в новых переменных есть

$$S = \frac{\sqrt{3}}{2}\frac{D^2}{R^2}c^2\sqrt{1+\eta^2}\left[\sqrt{1+\eta^2} + \eta^2\times \ln\frac{1+\sqrt{1+\eta^2}}{\cos\beta_1 + \sqrt{\eta^2+\cos^2\beta_1}} - \cos\beta_1\sqrt{\eta^2+\cos^2\beta_1}\right].$$

Нелинейное уравнение (1б) с граничными условиями уравнения (2а) решалось численными методами на электронно-вычислительной машине. Точность решения сверялась с аналитическими результатами для специальных случаев зависимости $\varkappa^2$ от координат.

3

Приемлемость математической модели уравнений (1), (2) анализировалась путем сравнения расчетных данных с экспериментальными, полученными для комплекта тепловыделяющих элементов, состоящего из стержней, содержащих UO_2 с 7%-ным обогащением в алюминиевых оболочках. Внешний диаметр стержней 11,4, длина 1200 *мм*. Вид двух сборок показан на рис. 1 и 2.

Сравнение проводилось по критическому числу тепловыделяющих элементов N при разных шагах решетки и углах скручивания:

$$N = \frac{2\pi}{\sqrt{3}}\frac{(R\cos\omega - \delta)^2}{D^2\cos^2\omega},$$

причем величина δ, описывающая влияние отражателя, считалась функцией только начального шага D. Зависимость $\varkappa^2$ (S) была полу-

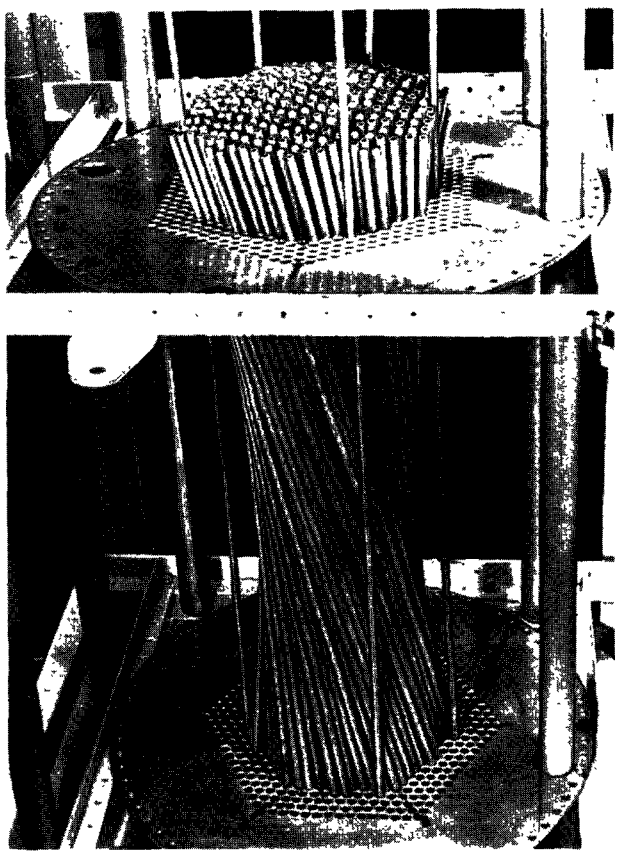


Рис. 1. Гиперболоидная сборка стержневых тепловыделяющих элементов

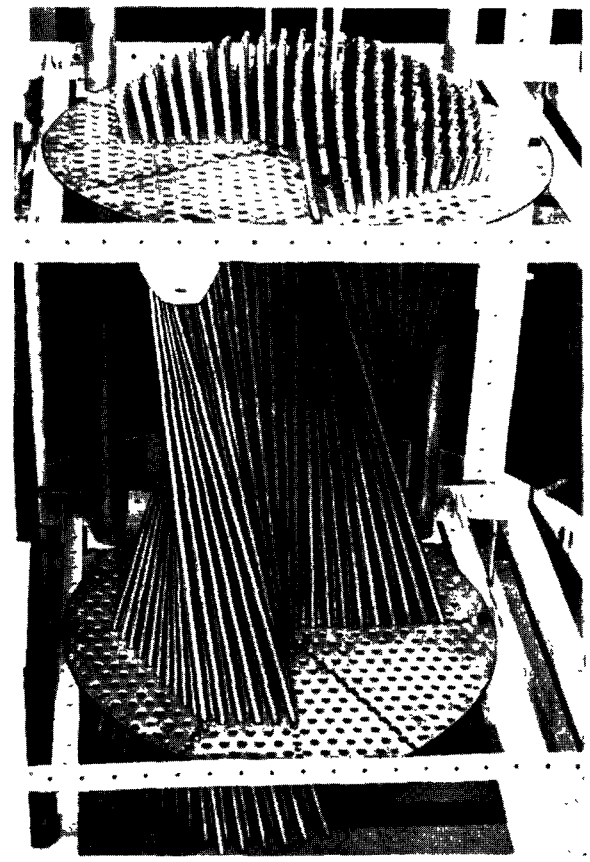


Рис. 2. Гиперболоидная сборка (часть тепловыделяющих элементов удалена)

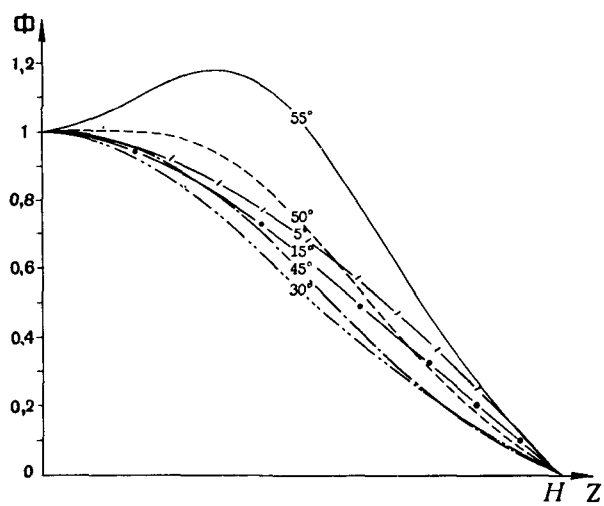


Рис. 3. Изменение распределения потока нейтронов вдоль оси сборки с начальным шагом 3 *см* при скручивании

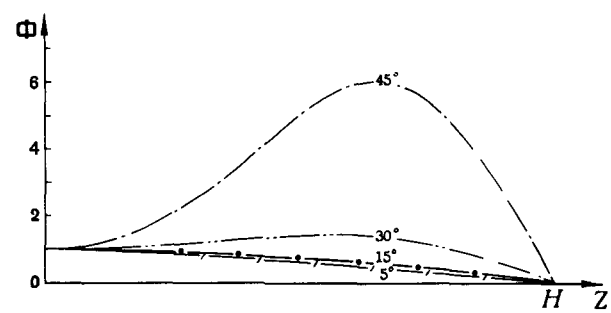


Рис. 4. Изменение распределения потока нейтронов вдоль оси сборки с начальным шагом 1,7 *см* при скручивании

чена из опытов с цилиндрическими системами. Совпадение расчетных и экспериментальных результатов оказалось вполне удовлетвори-

тельным. Достаточно точными являются и вычисленные распределения потока нейтронов по оси сборок (рис. 3, 4). Они были сравнены с распределениями, полученными с помощью полупроводникового кристаллического поверхностно-барьерного счетчика, регистрировав-

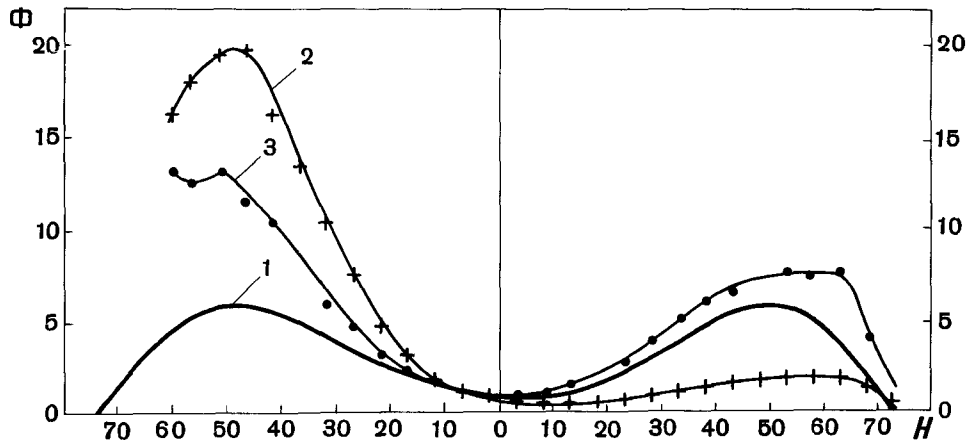


Рис. 5. Неустойчивость формы нейтронного поля:
1 — расчетная кривая для симметричной сборки;
2 — плоская нижняя граница активной зоны; *3* — частично симметризованная сборка

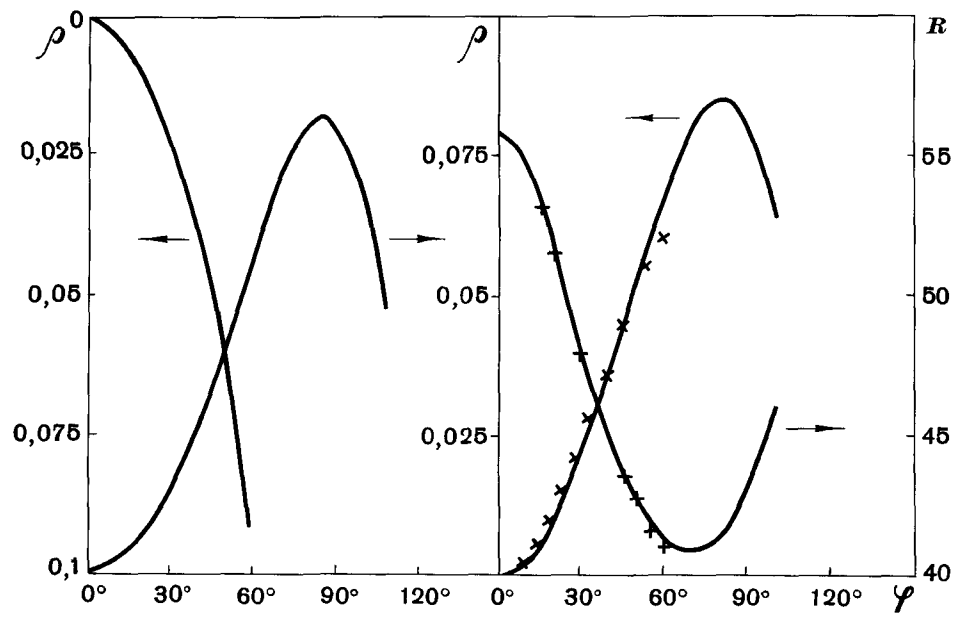


Рис. 6. Зависимость реактивности от угла скручивания для двух значений D ($\varphi=2\omega$)

Рис. 7. Зависимость ϱ и R от угла при скручивании канальной системы с $D=7$ *см*

шего осколки деления от мишени из U^{235}. Расхождение в полях отмечалось лишь для сборок с малым шагом, скрученных почти до касания тепловыделяющих элементов (рис. 5). Очевидной причиной этого расхождения была неидеальность геометрии опытов, в которых нижняя граница активной зоны была плоской, а верхняя — слишком выпуклой. Помещенная в качестве нижнего отражателя чаша из плексигласа значительно снизила асимметрию поля (кривая *3* на рис. 5), хотя ее кривизна была заметно меньше, чем необходимо для придания активной зоне правильной формы.

Для вычисления значения реактивности, компенсируемого скручиванием при фиксированном числе тепловыделяющих элементов $\varkappa^2$ в уравнении (1) заменялось на

$$\varkappa^{*2}=\varkappa^2(1-\varrho)-\varrho/M^2.$$

Зависимость критического параметра — реактивности ϱ от ω при двух значениях начального шага D дана на рис. 6.

Во всем интервале $0\leqslant\varrho\leqslant 0{,}09$ осевая неравномерность энерговыделения отличается от своего значения для начального состояния не больше чем на 20%, причем деформация

решетки с малым шагом улучшает, а разреженной ухудшает форму нейтронного поля. Соответствующие характеристики объемной неравномерности составляют ~30 и ~10%. Можно отметить, что процесс выгорания топлива благоприятствует выравниванию полей энерговыделения.

Вторая серия опытов была предпринята с каналами, представлявшими собой набор концентрических трубчатых тепловыделяющих элементов со стальными оболочками, вставленных один в другой. Фотография одной из сборок представлена на рис. 8. Вследствие наличия воды внутри канала зависимость $\varrho(D)$ не имела спадающей ветви при малых шагах и для регулирования можно было использовать только интервал D от 70 до ~50 *мм*. При этом зависимость $\varrho(\omega)$ изучалась экспериментально:

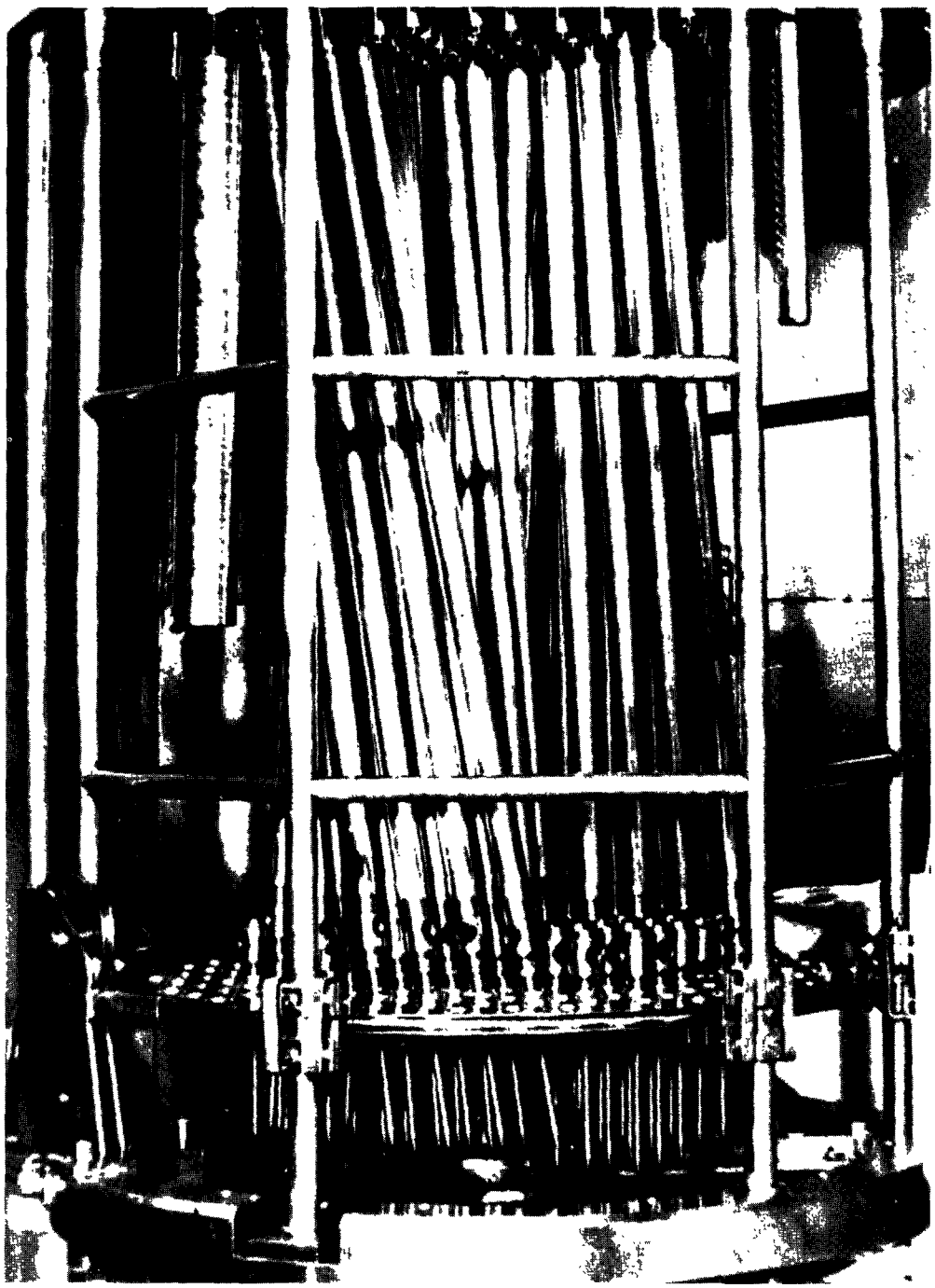


Рис. 8. Стенд для изучения гиперболоидных сборок

в критическую систему помещался дополнительный канал и измерялся период разгона. По обычным формулам период переводился в $\Delta\rho$ — изменение реактивности системы при догрузке. График зависимости $\Delta\rho$ от N интегрировался, и значения интегралов с верхним пределом 170, 160, . . ., 90, 85 каналов наносились в качестве экспериментальных точек на рис. 7. Для оценки действия возможных систем аварийной остановки реактора были проведены некоторые дополнительные опыты. В частности, исследовалось соответствие между углом скручивания и количеством добавленной в воду борной кислоты при условии $N = \text{const} = 152$. При величинах $\omega = 15$ и 20° концентрация H_3BO_3 составила 0,192 и 0,396 *г/л*. Эти значения еще очень далеки от предела растворимости и представляют возможность иметь в качестве аварийного средства небольшой объем высококонцентрированного раствора, вводимого в случае необходимости в активную зону.

Из этой же критической сборки удалялся центральный канал. Вместо него вставлялся стальной чехол диаметром 36 × 44 *мм*, и затем в этот чехол вводился пучок из семи борных стержней диаметром 8,5 *мм* каждый. Результаты опыта представлены в таблице.

	$\Delta\rho \cdot 10^{-3}$		
	$\varphi=20°$	$\varphi=30°$	$\varphi=45°$
Удаление центрального канала	8,6	10,7	11,7
Введение стального чехла	0	0	0
Введение пучка борных стержней	3,3	4,8	6,3

Очевидно, что такой пучок или один стержень соответствующего диаметра может служить автоматическим регулятором. Одновременно была подготовлена программа для расчета двухзонных по радиусу систем. Показано, что радиальное распределение потока в сборке с полостью, соответствующей отсутствию семи центральных каналов, вполне приемлемо. Всплеск потока нейтронов в полости способствует увеличению эффективности вводимых в нее поглощающих стержней, которые могут быть сделаны достаточно толстыми. Неподвижные каналы для поглотителей могут быть заранее скручены. Влияние водяного зазора между зоной поглотителей и рабочей зоной может привести к перенапряжению внутреннего кольца из 12 рабочих каналов, однако уменьшение концентрации ядерного топлива в этих каналах снимает опасность.

Рассматриваемая схема реактора приобретает законченный вид, если вместо шестиугольной сетки использовать кольцевое расположение каналов. В каждом кольце должно быть столько же каналов, сколько в соответствующем ряду шестиугольной сетки — 6, 12, 18 и т. д. Расстояние между кольцами выбирается так, что на каждый канал приходится одинаковый объем воды. Например, радиус внешнего кольца по осям каналов равен $\left[\frac{s}{\pi}\left(N - \frac{n}{2}\right)\right]^{1/2}$, где N — полное число ячеек, n — число ячеек во внешнем кольце. Экспериментально показано, что такой отход от правильной формы ячеек практически не влияет на реактивность.

ABSTRACT - RÉSUMÉ - АННОТАЦИЯ - RESUMEN

A/376 USSR

Compensation of large changes in the reactivity by deformation of the core lattice

By G. A. Bat *et al.*

Prolonging power reactor life entails an increase in the reactivity margin of the newly loaded reactor and, therefore, calls for the development of an effective compensating system for this margin. Along with the conventional systems such as shim rods and assemblies, burnable poisons and mixtures of heavy and light water, it seems useful to consider the possibility of controlling reactivity by means of a relatively slow deformation (variation of the effective spacing) of the core lattice in the moderator. This is easiest in the case of liquid-moderated reactors with channel type cores such as the type of the core employed in the reactors of the ice-breaker *Lenin*. Deformation of the lattice is, in a sense, similar to controlling the reactivity by changing the concentrations of a heavy and light water mixture, in that its effect does not cause considerable distortions of the energy release field accompanying the insertion of the permissible number of absorbing rods. However, the flexibility of the suggested method is high. The difficulties involved in the development of such control systems are due to the necessity of having a considerable number of kinematic pairs in inaccessible points of the reactor, to arrange "light" but quick acting control and safety components in the movable lattice and to adapt the system to operation at a varying temperature.

The work on the development of the new control system was carried out along three main lines: critical experiments, mathematical description (including calculation codes for high-speed computers) and design of the core.

Several series of critical experiments confirmed the effectiveness of this method of control and made it possible to find out its physical pecularities and work out simple but sufficiently accurate computer

codes. The experiments were carried out with individual fuel elements and with bundles in channels.

The paper describes several design schemes of cores with a deformable lattice.

A/376 URSS

Compensation des variations importantes de la réactivité par la déformation du réseau de la zone active

par G. A. Bat *et al.*

En cherchant à augmenter la durée de vie des réacteurs on en arrive à accroître la réserve de réactivité du réacteur fraîchement chargé, ce qui exige la mise au point de systèmes de compensation perfectionnés correspondant à une telle réserve. Parallèlement aux systèmes habituels (barres et ensembles de compensation, absorbants consommables, mélanges d'eau ordinaire et d'eau lourde) il a semblé utile d'étudier la possibilité de contrôler la réactivité au moyen d'une déformation relativement lente (modification du pas efficace) du réseau d'éléments combustibles dans le modérateur. Cette possibilité est réalisée le plus facilement dans les réacteurs à modérateur liquide ayant une structure à canaux de la zone active (analogue à celle des réacteurs du brise-glace *Lénine*). La déformation du réseau est, dans un sens, proche du contrôle par variation de la concentration du mélange $H_2O + D_2O$, puisque son efficacité n'est pas liée aux modifications importantes du champ d'émission d'énergie qui sont associées à l'introduction d'un nombre acceptable de barres absorbantes; cependant la souplesse de la méthode proposée est très grande. La difficulté de réalisation d'un tel système de compensation est liée à la nécessité d'avoir dans des points inaccessibles du réacteur un nombre important de couples cinématiques, de disposer dans un réseau mobile des organes de contrôle et de sécurité « légers » mais à action rapide et d'adapter le schéma de l'installation à un effet de température qui varie pendant le fonctionnement.

Les travaux relatifs à cette nouvelle méthode se sont développés dans trois directions principales: expériences critiques, représentation mathématique (y compris la programmation des calculs sur machines électroniques rapides), construction de la zone active.

Plusieurs séries d'expériences critiques ont permis de confirmer l'efficacité de cette méthode de contrôle, de mettre en évidence certaines de ses caractéristiques physiques et de construire des programmes de calcul simples, mais suffisamment précis. Les expériences ont été faites aussi bien avec des éléments combustibles séparés qu'avec des faisceaux (canaux).

Plusieurs schémas de zones actives à réseau déformable sont également donnés.

A/376 URSS

Compensación de grandes variaciones de la reactividad por deformación de la red del *núcleo del reactor*

por G. A. Bat *et al.*

La tendencia a aumentar el período de funcionamiento de los reactores de potencia tiene como consecuencia el aumento de la reserva de reactividad en el reactor recién cargado, lo que requiere la adaptación de sistemas desarrollados para la compensación de esa reserva. Junto con los sistemas ordinarios (barras y conjuntos de compensación, absorbentes consumibles, mezclas de agua ligera y agua pesada), cabe considerar la posibilidad de regular la reactividad mediante una deformación relativamente lenta (variación del paso eficaz) de la red de elementos combustibles en el moderador. Los reactores en los que existe esta posibilidad de la manera más sencilla son los que tienen moderador líquido y el núcleo es de estructura acanalada (del tipo del núcleo de los reactores del rompehielos « Lenin »). La deformación de la red se parece, en cierto sentido, al control por variación de la concentración de la mezcla $H_2O + D_2O$, ya que su eficacia no está ligada a las grandes alteraciones de la distribución de la potencia que supone la introducción de un número aceptable de barras de absorción; no obstante, la capacidad de maniobra del procedimiento propuesto es muy grande. Las dificultades de construcción de dicho sistema se refieren a la necesidad de tener, en sitios inaccesibles del reactor, un número considerable de pares cinemáticos, de disponer en la red móvil de órganos « fáciles », pero de acción rápida, para los sistemas de control y de seguridad, y de adaptar el esquema de la instalación a las variaciones de temperatura durante el funcionamiento.

Los trabajos relativos al nuevo sistema de control se dividen en tres clases fundamentales: experimentos críticos, representación matemática (incluidos los programas de cálculo para máquinas electrónicas rápidas) y proyecto del núcleo.

Algunas series de experimentos críticos han permitido confirmar la eficacia de este método de control, aclarar sus particularidades físicas y elaborar programas de cálculo sencillos, pero suficientemente precisos. Se han realizado experimentos con elementos combustibles aislados y con haces (canales).

También se presentan algunos esquemas de proyecto de núcleo con red deformable.

Solid state nuclear safety system

By L. Conti and M. Conti*

In the framework of the nuclear plant development, CNEN is carrying out a research and development programme on nuclear reactor control equipment known as SCIN (Control System for Nuclear Plants). Considerable attention has been devoted to safety problems and in this field, the Servomechanis Laboratory has developed a complete set of solid state instruments. The common features of these instruments are: fail-safe behaviour, solid state reliability and some degree of redundancy in design, and short actuating time. The nuclear reactor safety system can be divided into three different kinds of devices:

(*a*) Alarm situation detectors as safety amplifiers, radioactivity monitors, pressure and temperature trips;

(*b*) Logic networks which work out the alarm information and produce the intervention information (scram, setback, etc.);

(*c*) Magnet switch power supplies which supply the rod magnets (or magnetic clutches) and switch off when a dangerous situation is reached.

In our system, all the alarm information is shown by the voltage. Namely under normal conditions the voltage is +5 V, while under alarm conditions it is zero. In this way, an eventual breakdown in the alarm channel produces a safe action. All the +5 V signals are generated by electronic trip detectors. In the field of alarm situation detectors, we have designed a shut-down amplifier and an electrometer amplifier which are continuously tested by a high frequency signal. In this way, a high degree of reliability has been achieved. In order to process the alarm data safely a new set of pulsed logic blocks has been designed. In the field of switch power supplies, two devices have been developed which can supply dc loads up to 100 W and 5 kW respectively. Even these devices are fail-safe and wholly solid state.

ALARM DETECTORS

Shut-down amplifier

This instrument is a dc transistor amplifier which amplifies the current from the neutron sensitive ion chamber and produces alarm information when the trip level is reached. The trip level is continuously adjustable between 10^{-6} and 10^{-4} A [1].

The block diagram of this instrument is represented in Fig. 1. The high voltage to the ion chamber is supplied by a dc–dc converter. The high voltage smoothing network is designed so that some high frequency (15 kc/s) ripple is still present. This signal reaches the input of a dc amplifier, passing through the ion chamber capacitance, is amplified and is present at the output. The minimum voltage at the output is −10V, and when this level is reached the amplifier is in the overload condition and the 15 kc/s disappears at the output. The sensitivity of the amplifier can be varied by means of the potentiometer P_{101}. In this way also the input current which brings the amplifier in overload condition, i.e., the trip level, is varied. The test signal is picked up by the T transformer and is amplified by a band-pass amplifier. Finally, it is rectified and is present at the terminal U as +5 V dc voltage. Obviously there is no dc current when the trip level is reached and also in many other dangerous conditions as for instance failure in high voltage power supply, breakdown in high voltage cables, failure in the dc amplifier, in the potentiometer, in the transformer and in the band-pass amplifier.

The dc amplifier has been carefully designed to ensure the avoidance of regenerations at frequencies up to 15 kc/s, in case of failure. The band-pass amplifier tuned stages employ grounded base transistors with very high stability factors. In this device are also present a "high voltage abnormal" trip and a "high voltage cable disconnected" alarm circuit. The over-all accuracy of trip level is ±2% for an environmental temperature varying from 10 to 50 °C. There are two versions of this device: with a channel for chassis and with three channels for chassis (Fig. 2). As in all instruments of the SCIN programme there is a door in the front panel and in this way it is easy to perform operations inside the device as measurements, calibrations and substitutions of failed cards.

Power and safety amplifier

This device is substantially a linear current amplifier but is more sophisticated than conventional ones and accomplishes also the function of the period amplifier.

The sensitivity is adjustable between 10^{-10} A to 3.10^{-4} A (full scale) in fourteen ranges. The overall accuracy is ±2% and the rise time is better than

* Comitato Nazionale per l'Energia Nucleare, Casaccia, Rome.

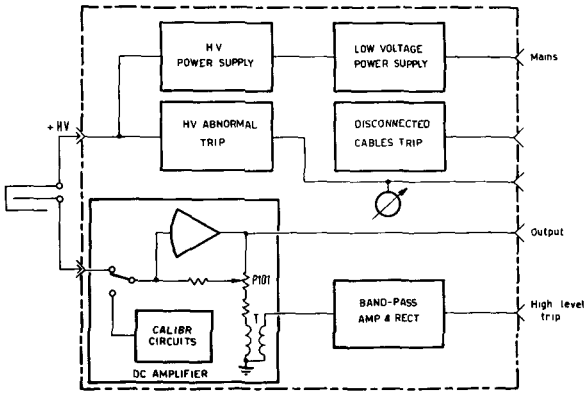


Figure 1. Shut-down amplifier. Block diagram

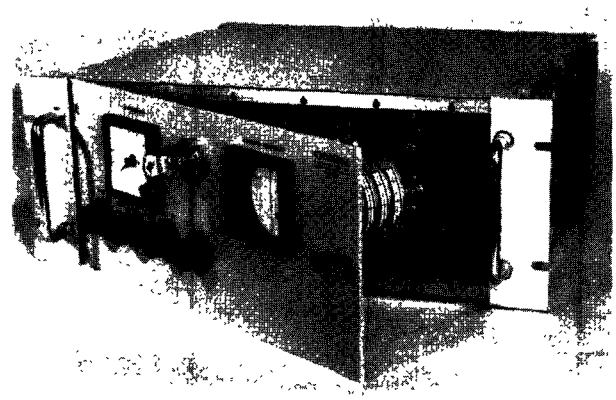


Figure 2. Shut-down amplifier

40 ms at the maximum sensitivity (5 000 pF at the input). As in the shut-down amplifier, correct operation is continuously tested with a 15 kc/s signal and so this device can be considered as a safety amplifier. There are two trip levels, the first at top level (adjustable between 80 and 95%) and the second at low level (5 to 15%) of each range. In this way it is necessary for the operator to measure in the range in which the device displays the best accuracy.

An automatic range switch circuit automatically increases or decreases the sensitivity whenever a low trip (10 to 20%) or a high trip (70 to 80%) is reached. This device is very useful when there are many amplifiers in operation. Besides, the automatic decrease in sensitivity is not immediate but occurs at a fixed time after the top trip has been reached. If the growth factor in neutron power is great, the high level trip is reached before the change in sensitivity has taken place and a period-like action results.

The change of sensitivity can also be performed manually. However it is not possible to perform more than about one change (decrease) in sensitivity per minute because of a delay circuit.

The block diagram of the whole instrument is represented in Fig. 3. The high voltage power supply is stabilized with a transistor dc amplifier. In this way very good stability in dc and in the low frequency range has been achieved. The first stage of the electrometer amplifier is an electrometer tube, the only vacuum tube of the whole instrumentation. As for the shut-down amplifier, the test signal produced for HV power supply passes through the compensated ion chamber, is amplified from the electrometer amplifier and the band-pass amplifier, is rectified and energizes the high level trip. This circuit is built with the logic blocks described below and is safe against all types of failure.

Also, in case of failure, care has been taken in designing the electrometer amplifier to avoid any regeneration at frequencies up 15 kc/s. Finally, the delay circuits employed in the automatic range switch are fail-safe in the sense that, in case of failure, no decrease is possible in delay time. As in the shut-down amplifier there are "abnormal HV" and "HV disconnected cable" trips.

ALARM SIGNALS PROCESSING NETWORK

The solid state logics are very attractive because of their characteristics of speed and compactness. Unfortunately the conventional dc logic suffers by lack of fail-safe features. In the logic blocks employed in our system the dc input signals are converted in pulse trains, are processed following the desired logic function and finally rectified at the output. The prescribed logic function can be synthesized from the standard basic blocks AND, OR and NOT.

The pulsed AND block is represented in Fig. 4(a) and is substantially a Hartley oscillator which can oscillate only when both the logic voltage and the internal clock pulse (3 μs with a repetition frequency of 10 kc/s) are present. The second transistor rectifies and amplifies this pulsed oscillation and at the output only a clock-like pulse is present. This signal can be employed as clock pulse for the next AND. This circuit has been tested systematically and its absolute fail-safe feature has been verified.

The OR circuit is represented in Fig. 4(b). It is fundamentally a direct coupled transistor OR gate. The limiting resistors in series with the base connections are used to de-couple external logic chains.

The NOT circuit is shown in Fig. 4(c) and works as follows. When the check pulse arrives, the transistor switches on and if the capacitor C is charged, a clock-like pulse is present at the output. So it is necessary for a +5 V bias voltage to be present. In case of failure no pulse can be present at the output because the transistor is a p-n-p-type.

Figure 4(d) shows a pulse dc converter fail-safe against any failure and speedy in action; its time delay is not greater than 150 μs. The input pulse is formed by means of the T_1C_1 tuned circuit, amplified and finally rectified into a standard +5 dc signal.

Figure 5 shows for instance a "two of three" logic built with these logic blocks. All the basic blocks are built in a standard package having dimensions of 5 $\times$ 3 $\times$ 1.5 cm. The overall delay time of the circuit is better than 0.7 ms. The operating conditions of the logic blocks and of the components used

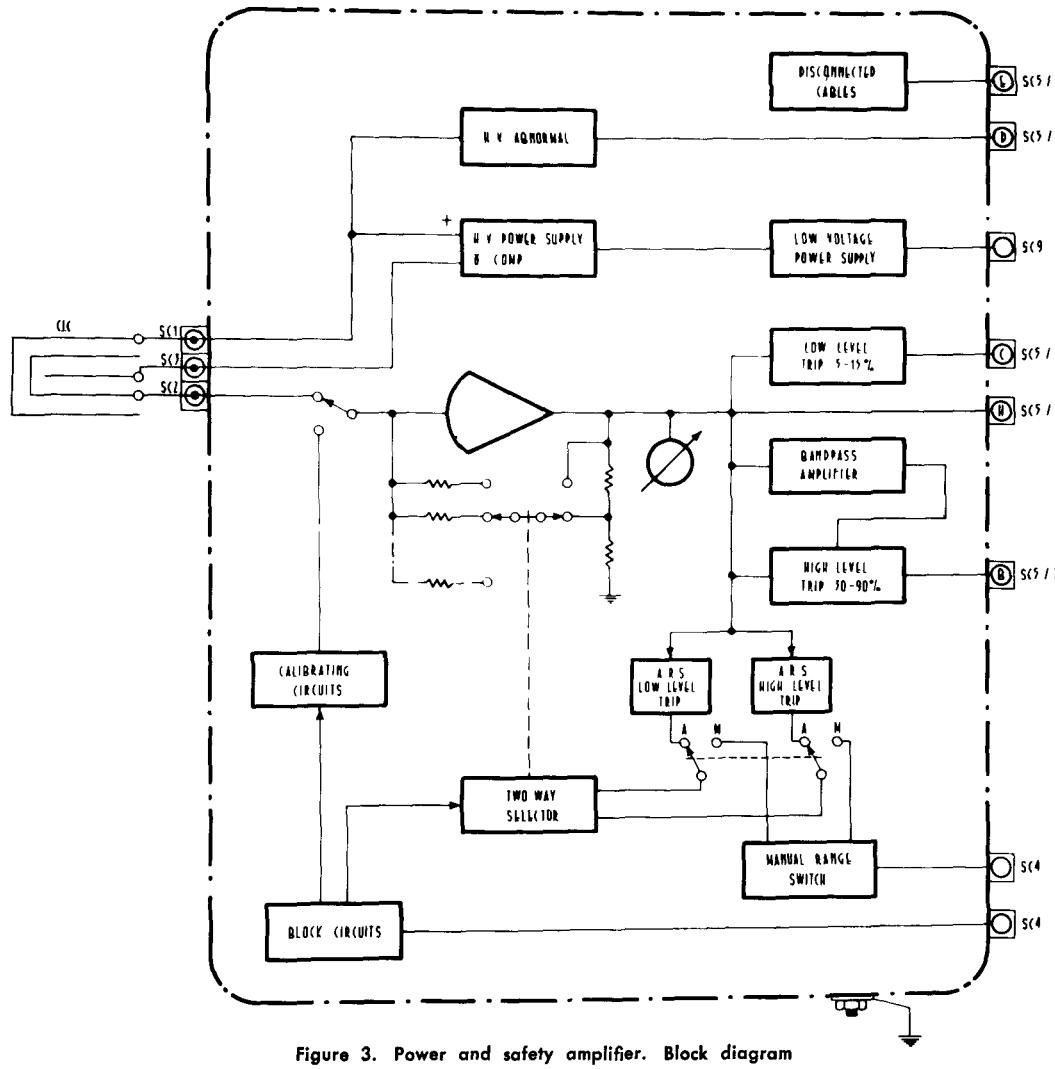


Figure 3. Power and safety amplifier. Block diagram

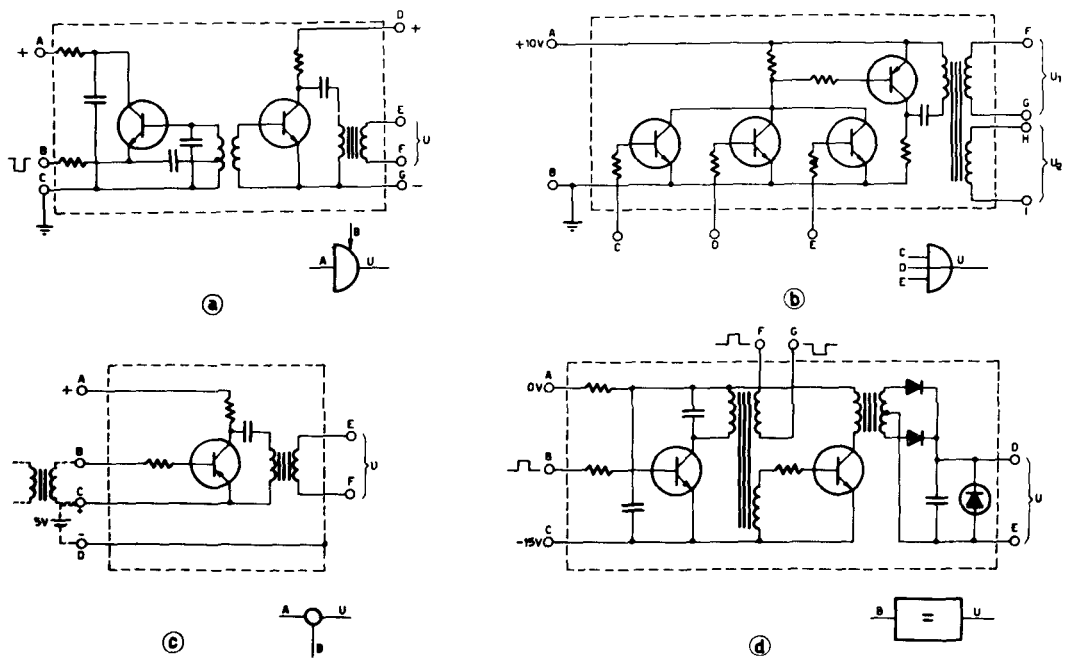


Figure 4. Pulsed logic blocks
(*a*) AND, (*b*) OR, (*c*) NOT, (*d*) pulse dc converter

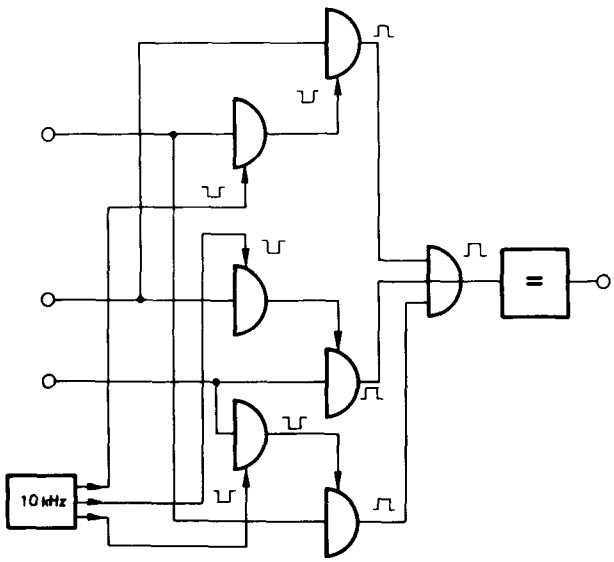


Figure 5. "Two of three" block diagram

in them are very conservative in order to increase the mean life of individual components. A further significant improvement in realiability can be achieved through some redundancy in design. For instance, it is possible to connect two "two of three" circuits in parallel. When the monitoring device shows that some blocks have failed, it is possible to replace them without any safety action.

SWITCH POWER SUPPLIES

The two power supplies described have been developed following the same principle of controlling a dc power supply by means of an ac transducer. In fact they are essentially power amplifiers whose input signal is taken from the logic system in the form of pulses, the absence of which constitutes the scram information.

This pulse train is converted into a square wave which drives the power stage. The output power is present at the secondary of the output transformer and can be employed as ac but more frequently it is rectified and so it is possible to supply standard dc loads as magnets and magnetic clutches. The coupling between the power supply and the load is electromagnetic and can be accomplished only if the inverter is conveniently excited. Flow of power directly from the power supply to the load is possible only if many failures occur at the same time. However it is not dangerous because the voltage rating of the load is much higher than that of the power supply. Therefore these devices are wholly fail-safe.

Figure 6 represents a block diagram of the 5 kW supply. The dc current provided by the pulse dc converter supplies the flip-flop which is triggered by a local 500 Hz clock generator and allows transmission of the square wave from the preamplifier to the power stage. In case of scram this transmission breaks down and the two SCR of the power stage are both switched off because of the third SCR which is switched on. The resistor in series with the dc supply of the inverter, and the related relay and delay networks, have the function of reducing the power supply voltage and allowing the inverter to start. The power inverter of the 5 kW unit is of the kind described by McMurray *et al.* [2] with some sophistications included in order to obtain very quick stopping and optimum power performance even in case of inductive load. The overall efficiency is about 90% and the maximum delay between the scram information and the disappearing of the output voltage is about 2 ms.

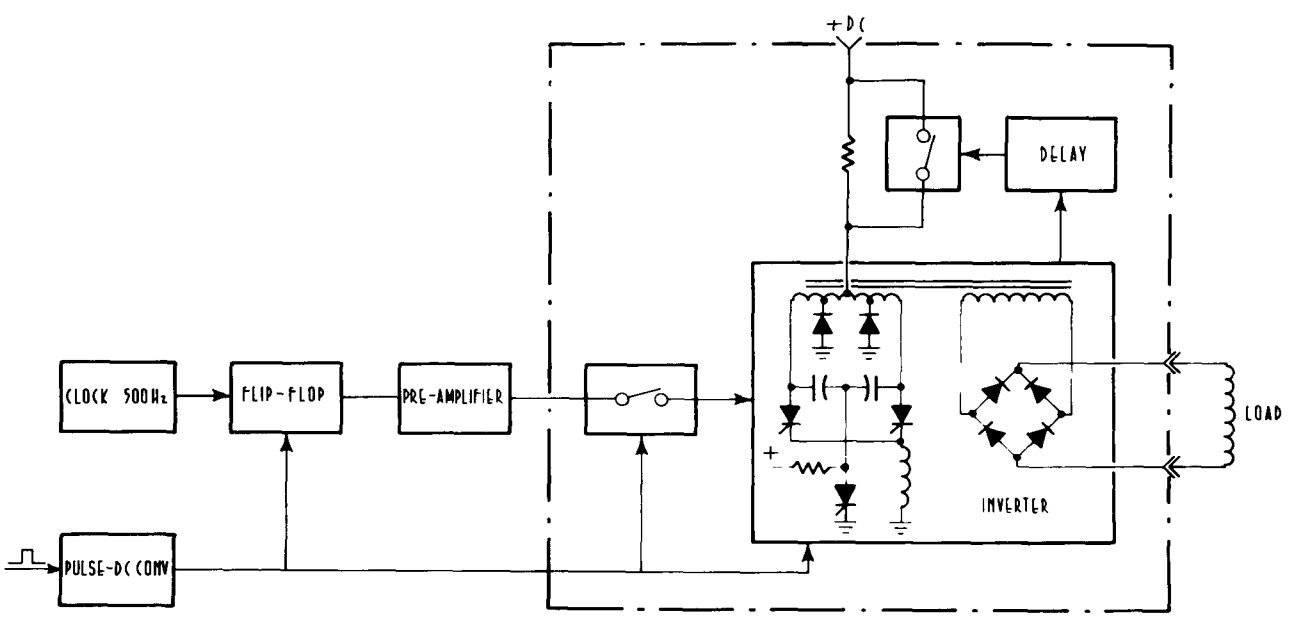


Figure 6. 5 kW switch power supply. Block diagram

For the 100 W unit, the block inside the dotted rectangle has to be replaced by a rather standard ac transistor power amplifier. No extinction circuits are required, the overall efficiency is about 85% and the maximum delay is about 1 ms.

ACKNOWLEDGEMENTS

The authors gratefully acknowledge the many helpful discussions held with Professor Sergio Barabaschi, Head of Technological Division of CNEN, and the invaluable contributions made by T. Businaro, P. Coda, A. Garroni, D. Malosti and D. Manzo in developing the various devices.

REFERENCES

1. Conti, M., and Garroni, A., Automazione e Strumentazione, *11*, 468-472 (1963).
2. McMurray, W., Communication and Electronics No. 57, 531-542 (1961).

ABSTRACT - RÉSUMÉ - АННОТАЦИЯ - RESUMEN

A/795 Italie

Instrumentation nucléaire de sécurité utilisant l'état solide

par L. Conti et M. Conti

Dans le cadre général du programme de développement nucléaire, le CNEN poursuit un programme de recherches et de développement portant sur l'équipement de contrôle des réacteurs et connu sous le nom de programme SCIN. Conformément à ce programme, le laboratoire Servomécanisme a réalisé une série relativement complète de dispositifs d'instrumentation nucléaire utilisant l'état solide.

En général, dans un système de sécurité on trouve:

a) Des détecteurs d'alarme (amplificateurs de sécurité, moniteurs de radioactivité, interrupteurs de sécurité de pression et de température, etc.);

b) Un circuit logique qui élabore les différents signaux d'alarme (par exemple: circuits « deux sur trois », circuits verrouillés, etc.);

c) L'amplificateur magnétique de puissance de commutation qui distribue le courant continu alimentant la commande d'arrêt instantané (aimants ou embrayages), ou le mécanisme de baisse de puissance.

Dans notre système, tous les signaux d'avertissement sont sous forme de tensions; plus précisément, en condition normale la tension est de +5 V, et en condition d'alerte la tension est nulle.

De cette façon, une éventuelle interruption dans les conducteurs d'avertissement provoque une réaction de sécurité. Tous les signaux de 5 V sont produits électroniquement par des détecteurs de déclenchement.

a) Dans le secteur des détecteurs d'alarme, nous avons mis au point un amplificateur électromètre (10^{-10} + 3.10^{-4} A, plusieurs échelles) et un amplificateur de sécurité (10^{-6} + 10^{-4} A, continuellement ajustable), qui font appel à une nouvelle méthode de contrôle continu. Dans les deux dispositifs, au puissant voltage des chambres d'ionisation compensées, est superposé un signal de contrôle de 15 000 Hz. Ce signal se propage à travers les câbles et la capacité des chambres jusqu'à l'amplificateur de courant continu stabilisé par réaction. A la sortie, un amplificateur à bande passante est relié aux amplificateurs situés au-delà du signal de contrôle. En dernier lieu, le signal est redressé et donne une tension de 5 V continus.

De cette façon, une panne quelconque dans le circuit (câble d'alimentation H. T., amplificateur courant continu) empêche la transmission du signal et la tension tombe de 5 V à zéro.

b) Le circuit logique réalisé par le CNEN reçoit les divers signaux d'alarme et provoque les signaux effectifs d'avertissement — toujours sous la forme 5 V — 0 V. Les caractéristiques les plus intéressantes de ce système sont la sécurité intrinsèque et la possibilité qu'il présente de synthétiser toute fonction logique partant des blocs fondamentaux ET, OU et NON. La sécurité intrinsèque est obtenue grâce à un système de modulation par impulsion.

Un quatrième bloc logique, le RAD, est un redresseur de courant à impulsions à sécurité intrinsèque entière, qui produit les signaux effectifs d'avertissement et, en général, les signaux à faible puissance de courant continu.

c) Afin d'alimenter l'électromécanisme, nous avons réalisé deux types d'amplificateurs de puissance de courant à impulsions à sécurité intrinsèque complète. Ces deux amplificateurs sont essentiellement des convertisseurs de courant à impulsion de commande.

Cette configuration convient pour éviter tout incident dangereux pouvant se produire avec les dispositifs interrupteurs de courant à état solide. Le premier amplificateur peut fournir jusqu'à 100 W et son dernier étage d'amplification est transistorisé. Le second peut fournir jusqu'à 5 kW avec un rendement d'environ 90%.

Dans les appareils logiques et d'alimentation, on peut utiliser quelques degrés de redondance de façon à améliorer l'efficacité de l'ensemble du système.

A/795 Англия и Франция

Система ядерной безопасности твердых тел

Л. Конти, М. Конти

В рамках своей программы по разработке ядерных реакторов Национальный комитет по атомной энергии (НКАЭ) осуществляет план исследований и разработок оборудования для контроля за ядерными реакторами, известный как программа SCIN. По этому проекту вспомогательная лаборатория разработала довольно полный набор ядерных устройств с использованием твердых тел.

В системе общей безопасности предусмотрены:

a) детекторы системы предупредительной сигнализации (усилители безопасности, радиоактивные дозиметры, переключатели давления и температуры и т. д.);

b) логическая схема, которая вырабатывает различные предупредительные сигналы (как, например, два из трех контуров, блокировочные контуры и т. д.);

c) магнитный усилитель переключения мощности, питающий постоянным током систему аварийной остановки (магниты или сцепления) или механизм остановки.

В системе все предупредительные сигналы разработаны по напряжениям; другими словами, при нормальных условиях напряжение равно + 5 *в*, а в условиях тревоги напряжение равно нулю.

Таким образом, любое возможное отключение в сигнальных каналах привело бы к безопасным мерам. Все сигналы в 5 *в* электронно генерируются детекторами выключающих устройств.

a) В секторе детекторов состояния тревоги мы разработали усилитель электрометра (от 10^{-1} до $3 \cdot 10^{-4}$ *а* для полной шкалы) и усилитель выключения с постоянной регулировкой от 10^{-6} до 10^{-4} *а*, где используется новый метод постоянного контроля.

В обоих устройствах контрольный сигнал в 15 000 *гц* налагается на высокое напряжение для компенсированных ионизационных камер. Этот сигнал проходит через провода и емкости к камере до стабилизированного усилителя обратного питания постоянного тока, на выходе которого он соединяется с усилителем полосы пропускания частот, который еще более усиливает контрольный сигнал. Наконец, этот сигнал выпрямляется в постоянный ток напряжением в 5 *в*. Таким образом, неисправность во всем канале (высоковольтный кабель питания, усилитель постоянного тока) мешает проходить сигналу далее и напряжение падает от 5 *в* до нуля.

b) Разработанная логическая схема получает предупредительные сигналы и вызывает возбуждающие и предупредительные сигналы, причем все находятся в диапазоне 5—0 *в*. Наиболее привлекательные особенности этого устройства состоят в его безотказности и возможности синтезировать любые логические функции, начиная от основных стандартных блоков AND, OR и NOT. Надежность достигается в результате системы модуляции импульсов. Четвертый логический блок представляет собой непрерывно действующий преобразователь импульсов постоянного тока, необходимый для производства возбуждающих или предупреждающих сигналов и обычно сигналов постоянного тока низкой энергии.

c) Для питания электромеханизма регулятора мы построили два типа надежных усилителей импульсов постоянного тока. Оба они являются в основном преобразователями импульса — пускового постоянного тока — постоянного тока. Эта конфигурация является необходимой для избежания любого небезопасного повреждения, которое может произойти, когда используются включающие устройства постоянного тока с использованием твердых тел. Первый усилитель может давать до 100 *вт*, и его последнюю ступень можно перевести на транзисторы. Второй усилитель может давать до 5 *квт* при к. п. д. около 90%.

В логических и силовых установках можно использовать некоторую степень избыточности для улучшения эффективности всей системы.

A/795 Italia

Instrumentación de seguridad nuclear de estado sólido

por L. Conti y M. Conti

En el marco general del programa de desarrollo de reactores nucleares, el CNEN está realizando un programa de investigación y desarrollo aplicado al equipo de control de un reactor nuclear, conocido como programa SCIN. Sobre este proyecto, el Laboratorio de Servomecanismos ha elaborado una serie relativamente completa de dispositivos de instrumentación nuclear de estado sólido.

En un sistema general de seguridad se encuentran los siguientes componentes:

a) Detectores de alarma (amplificadores de seguridad, monitores de radiactividad, disyuntores de presión y temperatura, etc.);

b) Un circuito lógico que gobierna las distintas señales de alarma (circuitos « dos de tres », circuitos de interconexión, etc.);

c) Un amplificador de potencia magnético, de conmutación, que suministra la corriente continua necesaria para accionar el dispositivo de parada brusca (electroimanes o embragues), o dispositivos de reducción de potencia.

En el sistema descrito, todas las señales de alarma se traducen en variaciones de tensión: en otras

palabras, en condiciones normales la tensión es +5 V, mientras que en condiciones de alarma baja a cero voltios.

De esta manera, cualquier interrupción en los canales de alarma hace funcionar un dispositivo de seguridad. Todas las señales de 5 V son generadas electrónicamente por detectores de disparo.

a) En el campo de los detectores de alarma localizados, se ha realizado un amplificador electrométrico (10^{-10} a 3.10^{-4} A (escala completa)) y un amplificador de seguridad continuamente ajustable entre 10^{-6} y 10^{-4} A, que utiliza un método nuevo de comprobación continua. En ambos dispositivos, se superpone una señal de 15 kilociclos a la alta tensión de las cámaras de ionización compensadas. Esta señal se propaga por los cables, y la capacidad de las cámaras, hasta el amplificador de corriente continua estabilizado por realimentación. A la salida se encuentra conectado un amplificador de paso de banda que amplifica la señal de comprobación. Finalmente, la señal se rectifica y se convierte en una señal continua de 5 V.

De esta manera, un fallo en cualquier punto del canal (cable de conexión de alimentación de alta tensión, amplificador de corriente continua) impide la propagación de la señal, con lo que la tensión cae de 5 V a cero.

b) El circuito lógico desarrollado por el CNEN recibe las distintas señales de alarma y da lugar a las señales de prevención o actuación, todas en forma de tensiones de 5 V–OV. Las cualidades más importantes de esta unidad son sus características de autoprotección, y la posibilidad de sintetizar cualquier función lógica, a partir de los bloques fundamentales AND, OR y NOT. La autoprotección se obtiene mediante un sistema de modulación de impulsos.

Un cuarto bloque lógico, el RAD, es un convertidor de impulsos en corriente continua, que sirve para generar las señales de prevención y actuación, y normalmente, señales de baja potencia de corriente continua.

c) Con la finalidad de alimentar el mecanismo electromagnético, se han construido dos tipos de amplificadores de impulsos de potencia a corriente continua completamente autoprotegidos. Ambos son esencialmente convertidores de impulsos de mando en corriente continua.

Esta configuración es adecuada para evitar cualquier fallo que puede ocurrir cuando se usan dispositivos interruptores de estado sólido. El primer amplificador puede suministrar hasta 100 W y su etapa de salida es transistorizada. El segundo amplificador puede entregar hasta 5 kW con un rendimiento aproximado de 90%.

Se puede utilizar cualquier grado de redundancia en las unidades lógicas y de alimentación, a fin de mejorar el rendimiento del sistema total.

Application of digital computer techniques to reactor operation

By M. A. Schultz* and F. C. Legler**

Large-scale installation of digital control equipment in conventional power stations has begun in the United States, and most of the newer electric utility installations use digital computer techniques in their operation. The reasons for the use of this type of equipment always reduce to economic factors, although reliability and safety considerations are steps toward this economic end. R. W. Ferguson [1] of Westinghouse has estimated that, for a conventional 300 MW(e) steam plant, the improvement in plant reliability and efficiency and the reduction of operating staff made possible by computer control might yield capitalized savings between $400 000 and $1 700 000. The added cost of digital equipment to effect these savings has been estimated at between $200 000 and $400 000. It is these economic factors that are the reasons most large nuclear power stations having the same owners as the conventional plants will ultimately be heavily computerized.

Granting the advantages of computer control, the reasons for using digital techniques as against analog ones for nuclear work are not obvious. For large installations, however, where hundreds of computational functions are required, analog computer hardware costs increase at a faster rate than digital computer costs for the same increase in the number of computations to be performed. Thus, an economic crossover point for selection of type of computation exists.

Estimates of the size computer required may be made on the basis of the number of inputs and recording points needed. This number varies from approximately 150 to 1 500 depending on the extensiveness of core fuel channel monitoring. For a large power reactor plant, Edwards [2] breaks down the estimated required inputs as given in Table 1.

It appears likely that the large number of calculations required by such data acquisition needs and safety functions will eventually tip the scales in favor of digital installations. Flexibility, ease of maintenance, smaller space requirements and reliability are secondary considerations in which the digital computer appears to have an advantage.

* Milletron, Incorporated, Irwin, Pennsylvania.
** U.S. Atomic Energy Commission, Washington, D.C.

In the nuclear reactor operation field in the United States, six extensive installations have been made of digital data acquisition and computational equipment. As yet, no plant has been installed with complete digital control, though studies have been made of the requirements. Some minor loops have been controlled, and special digital apparatus has been developed specifically for reactor control.

The intense preoccupation with reactor safety in the nuclear industry inevitably leads to the question "Can one rely on a complex digital computing machine rather than a man to control a reactor?" In perspective, the question has already been answered. Present-day reactor plants completely depend on complex analog circuits to protect the plant and public. The presence of the operator is of a supervisory nature. He is not expected, for example, to catch a one-second period excursion. Changing from analog to digital safety systems poses no additional hazard. Many of the safety logic systems already use conventional digital techniques, and simple arguments can be given for digital circuits and components on the grounds of greater reliability and ease of testing [3]. No automation proposal to date has recommended doing away with all people in the control room. The supervisory function always calls for a minimum of one operator. Thus, digital control of nuclear power plants will probably be incorporated into utility systems as fast as the economic factors justify them, and safety considerations will be similar to those of today's analog controlled plants.

DIGITAL SYSTEM FUNCTIONS

Five functions have been hypothesized for the digital computer in a nuclear reactor plant, as follows:

(*a*) Data acquisition and alarming;

(*b*) Computation of reactor and plant operating parameters;

(*c*) Programming of sequential events;

(*d*) Diagnostic calculations on system and computer malfunctions;

(*e*) Automatic control of minor and major loops.

A description of these functions follows, with examples of the state of the art in the United States.

Table 1. Input requirements for a nuclear power plant computer [2]

Type of input	Number of inputs	
	Minimum	Maximum
Transient	30	50
Steady state	300	600
On-off	30	100
Trend recording points	4	10
"Quick look points"	8	16
Incident recording points	30	50

Digital data acquisition and logging system

The first application of digital computing machines to reactors has been in data acquisition and logging, since there obviously was little risk in attaching these machines to a nuclear plant and a considerable amount of data could be handled expeditiously.

Shippingport installation

The most extensive use of a reactor data acquisition system in the USA has been at the Shippingport Plant located near Pittsburgh, Pennsylvania [4-6], where the Daystrom equipment was installed in 1961.

The Shippingport equipment is all solid state and consists of a signal input section, computer unit, instruction input section, and an output section. A block diagram of the system is shown in Fig. 1. The signal input section, containing multiplexer relays and an analog-to-digital converter, conditions all signals for processing by the computer unit. The computer unit consists of registers, logic, and memory units. A keyboard and tape reader make up the instruction input section, and typewriters and card punchers make up the output section.

Input data from 350 points of information are sampled at a rate of 5 points per second. The equipment can linearize, adjust scale factors, extract square roots, integrate, and perform all calculations required for presenting output information in readily usable engineering units. Logging is done continuously or at regular time intervals of 15, 30, 60, or 120 minutes. Read-out is in the form of printed sheets on typewriters or in the form of punched cards. There is also provision for logging certain points on demand by the operator between normal logging intervals.

Enrico Fermi fuel sub-assembly logger [7]-[8]

In the Fermi plant, two complete sets of Datex automatic logging equipment have been provided to insure proper accounting of the core and blanket sub-assemblies. This equipment consists of programmers to receive input signals which indicate the position of the fuel handling equipment and a Flexowriter to log the information. A block diagram of the duel system is given in Fig. 2.

One of the data loggers is located in the fuel and repair building to log all operations of the steam cleaning machine, the sodium-filled transfer tank, and the cask car while it is in the fuel and repair building. A separate data logger is located in the main control room to log all operations of the transfer rotor, rotating shield plug, offset handling mechanism, and the cask car while it is in the reactor building. The data logger systems compare the operation performed with the desired operation as shown on the program tape. Any error is annunciated in the main control room or in the fuel and repair building, and prevents operation of the offset handling mechanism gripper until a correction is made.

Hanford rod data logger [9]

This system is a portion of an integrated data and temperature monitoring setup supplied by Information Systems, Incorporated. The rod data logger's basic function consists of scanning continuously 87 rod position input points, and providing logging and visual display outputs under manual control of the operator. All circuits are composed of solid state passive elements. Fig. 3 shows the block diagram of the system.

The 87 inputs are scanned at a rate of ten per second. Each analog input is applied to a high impedance differential amplifier and digitized by a twelve-bit analog-to-digital converter, and the output is supplied to a logging typewriter and/or digital read-out display. Manual controls enable the operator to select the interval between log printouts and the input point displayed on the digital read-outs. Although the outputs are manually selected and may be periodic, input point scanning is automatically and continuously performed by a scanner driven by a control counter. The counter also directs the scanner to select a fixed voltage input point, thus enabling the rod data logger to perform a self-check during each scan cycle.

Computation of reactor and plant operating parameters

The digital computer can be expected to provide a number of physics and operating type constants and parameters for direct use in reactor operations. The only on-line operating digital computer in the USA at present performing this function is the Big Rock Point scheduling computer installed at the Consumers Power Company reactor at Charlevoix, Michigan [10, 11]. The primary purpose of this installation is to schedule control rod positions for maximum fuel burn-up, and to calculate reactor plant performance to operate at the highest possible reactor power density.

The computer is a GE-312 control processing system with a 40 000-word magnetic drum memory, and a one-matrix 384 contact single-channel scanner-distributor. The system currently accepts approximately 95 input signals from core flux, rod positions,

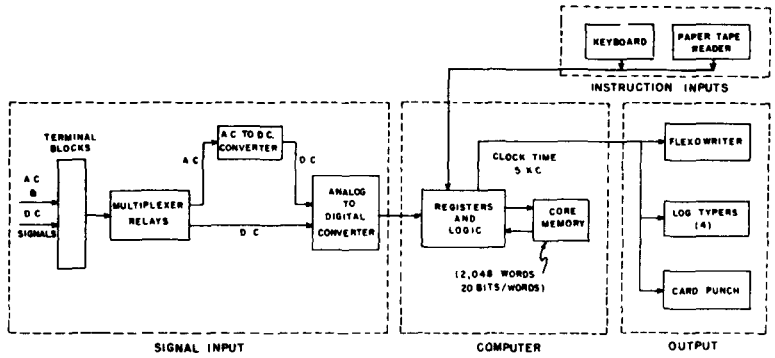


Figure 1. Shippingport data acquisition system

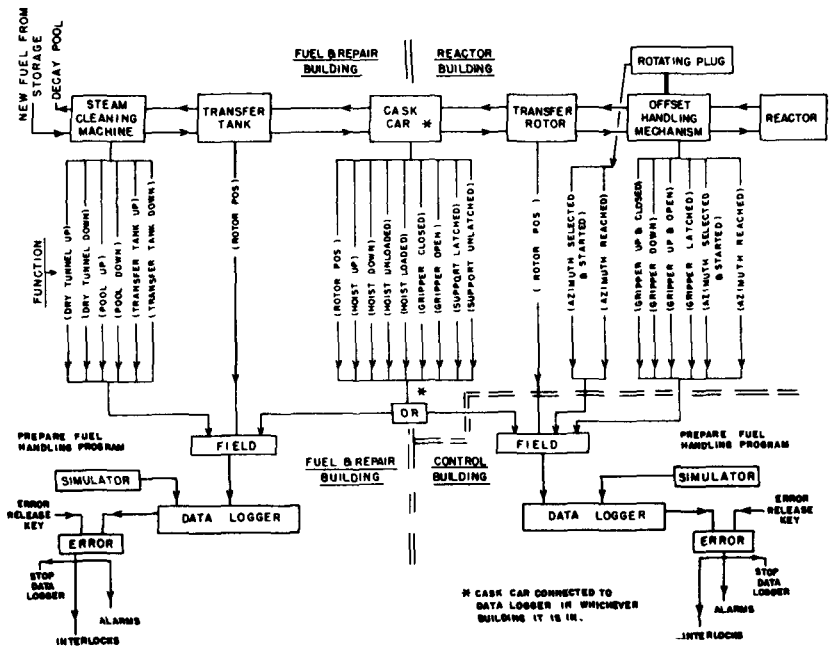


Figure 2. Fermi plant fuel sub-assembly logger

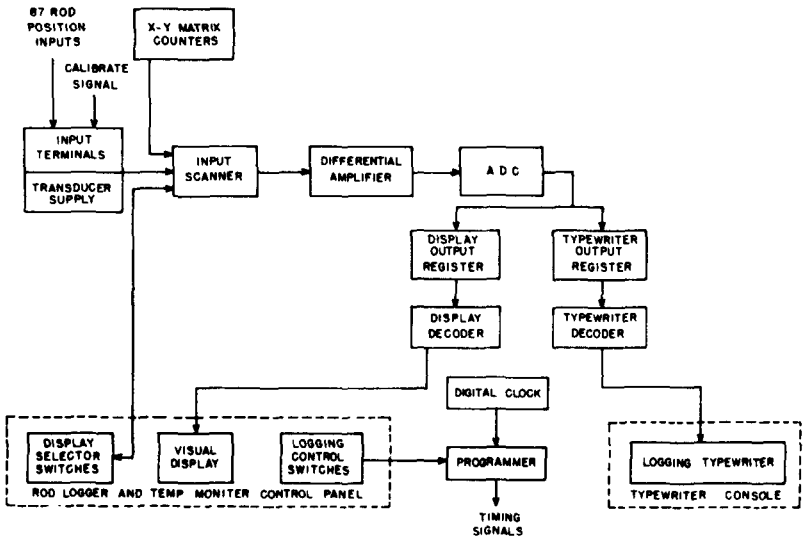


Figure 3. Hanford rod position data logger

and plant thermal variables. A scan of these variables is made once each hour for the purpose of calculations, and every five minutes to check for failed or out-of-limit sensors. In the event of a malfunctioning input, programming provision is made to insert typical data at that input point by the operator.

Table 2 shows the form of the output data during an early run made in May 1963. The computer contains the program routines and modules indicated in Table 3. The original programming was written and intercompared with a laboratory computer using FORTRAN.

The on-line computer at Big Rock Point has operated continuously since 12 February 1963, but some of its program and routines were not completed at that early date. On 14 August 1963, a six-month availability test was completed. The computer system was unavailable only for a total of 20 hours and 5 minutes during this interval, or the computer demonstrated an availability of 99.5%. The results obtained from this installation have been most satisfactory.

Programming and check-outs

Another obvious set of functions for a digital computer is to assist in cutting down the time it takes to put and keep a plant on line. Prior to the start-up of most nuclear plants, an enormous number of sub-systems and components must be checked. Daily operational checks of many reactor systems are also required. For example, the PATHFINDER reactor nuclear instrumentation operational check list contains approximately 400 items. Current operating rules call for these checks to be made once a shift. Pre-start check lists are often longer. Present practice is to have a reactor operator or technician proceed down the list and check off whether this valve is in the correct position or whether this meter reads properly, etc. Most of the quantities checked off are easily susceptible to a simple on-off digital type response. The time involved in manually going through pre-start-up check lists ranges from 1 to 15 hours, depending on the operation and the complexity of the plant involved. Operational check lists usually require about one hour per shift.

An elementary on-off "light board" installation for checking pre-start-up conditions on the Westinghouse Testing Reactor was designed in 1959. The use of these on-off indicators was intended to reduce a 14-hour check-out to 20 minutes. Unfortunately, this reactor was taken out of service before the system was completely installed.

Diagnostic calculations

Although no digital computer is currently engaged in reactor plant diagnostics on a regular basis, several such uses have been proposed in a study by IBM [12]. Some of these functions are:

(*a*) Using the computer as a digital test meter.—As long as many analog signals are available both at the sensors and at the outputs of indicators or recorders, the computer can be used to measure and compare readings to find a malfunction between inputs and outputs.

(*b*) Comparison of related quantities.—As an example, the computer might be used to compare a log n channel with a linear power channel and with the integral of a period channel to aid in diagnostics.

(*c*) Logical analysis of combinations of anomalies.—When several variables show anomalous behavior at the same time, conclusions may be drawn from either the set of variables involved or the time sequence of the malfunctions.

(*d*) Self-checking.—Routines have been developed for conventional applications which enable the computer to check itself on a programmed or demand basis.

Control functions

The ultimate function of complete computerized reactor-plant control is several years away. Studies have been performed by IBM [12], Daystrom [13], General Electric [14], and others which provide a strong economic incentive to proceed to full digital automation. Meanwhile, experience in digital minor loop control is being obtained in process industries and space applications [15].

DIGITAL COMPONENTS AND TECHNIQUES

Nuclear instrumentation channels

In anticipation of the need for digital components and sub-systems in nuclear plant control, a start has been made toward developing these devices.

Ford digital start-up control system

Work was first accomplished in 1958 in conjunction with the aircraft nuclear propulsion program towards development of digital nuclear start-up channels. Ford Instrument Company proposed a semidigital start-up control for aircraft reactors [16]. This system used a conventional series of nuclear detectors and an analog counting rate meter and period meter. However, as this was an automatic start-up system based on period information, all of the period system logic was digital. Fig. 4 shows a block diagram of one-half of this system. A dual set of apparatus is used and each system has three overlapping channels; one for low, one for intermediate, and one for high power ranges. Each channel becomes operative at specified low counting rates and is cut out at specified high counting rates. Schmidt triggers define the period strata from analog level signals and auctioneering circuits select the shortest period. Rods are connected in banks or frames, and the reactor period signals are used to trigger control logic, which in turn controls shim rod position. Five control operations are provided for automatic period start-up; these are withdrawal of successive rod

Table 2

Limiting values in each core region with location										Average values in each core region						Relative power in each core ring
Minimum burn-out ratio		Core average heat flux / Peak heat flux (10^6Btu/HFT^2)		Peak fuel center temperature (°F)		Hot channel flow rate (10^6 lb/h)		Core average exit steam quality (%)	Peak channel exit steam quality (%)	Core average steam void fraction		Relative power			
		0.110													
3.4	3.5	0.280	0.268	2574.	2490.	0.193	0.188	5.0	6.7						
(5805 4)	(5806 4)	(5805 4)	(5608 4)	(5804L4)	(5608L4)	(5805 4)	(5806 4)	57 6		0.187		0.981	0.954		0.000
2.8		0.331		2655.		0.194		5.0	4.8	0.196	0.187				0.882
(5507 3)		(5604 3)		(5704L4)		(5507 3)									1.053
3.5	3.4	0.268	0.280	2490.	2574.	0.188	0.193	5.8		0.176		1.076			1.085
(5305 4)	(5306 4)	(5503 4)	(5306 4)	(5503L4)	(5307L4)	(5305 4)	(5306 4)	4.7	5.0	0.184	0.196	0.954	0.981		1.051

Excess Δk / Xenon Δk	Control rod sequence: Raise power	Control rod sequence: Lower power	Relative power in each axial zone	In-core flux monitor readings								Core flow: Steam flow (10^6 lb/h) / No. 2 pico %	Core press. (psia) / ΔH SUB (Btu/lb) / Core ΔP / ΔP error (psid)	Core size: Core Exp (MWd/t) / Gross MW (e) / Power density (kW/l)	Date / Time / Net MW(e) / Core thermal power
				1 A	2 A	3 A	4 A	5 A	6 A	7 A	8 A				
				1 B	2 B	3 B	4 B	5 B	6 B	7 B	8 B				
				1 C	2 C	3 C	4 C	5 C	6 C	7 C	8 C				
	000	000													
	000	000	0.9010	41.7	57.6	38.9	61.4	55.3	39.3	44.0	60.9	10.9	1 045.0	56.0	5 19 63
0.0792	000	000													
	000	000	1.2622	65.1	78.7	65.1	81.0	60.0	62.8	62.8	60.9	0.595	15.6		19 22
	000	000													
0.0030	000	000	0.8363	55.3	72.6	68.9	71.2	68.9	57.1	66.5	67.9	95.0	8.6	50.1	45.5
	000	000													
	000	000											0.46	44.0	155.0

Table 3. Program routines

Big Rock Point scheduling computer

Executive routine	Decimal dump	Channel flow rate module	Plant performance module	Reactivity balance [a]
Timer	Decimal punch	Nodal and peak power module	Control rod sequence module	
Analog scan	Decimal load	Heat flux and burn-out ratio module	Burn-up optimization module [a]	Power distribution [a]
Control rod scan	Sensor failure		Set-up for on-demand logs	Plant performance [a]
Set-up for periodic log	Clock conversion	Quality and void fraction module	Demand logs :	Exposure [a]
Periodic log	Calculation alarm	Reactivity module	Stability test reference	Fuel shuffling auxiliary program
Set-up for daily log	Thermodynamic properties	Exposure module	Xenon transient	
Daily log	Core thermal power module	Variance module	Control rod position [a]	
Set-up for monthly log	Axial power module (using in-core monitors)	Xenon transient module	Operating limits [a]	
Monthly log			Core performance	

[a] These features are not presently implemented.

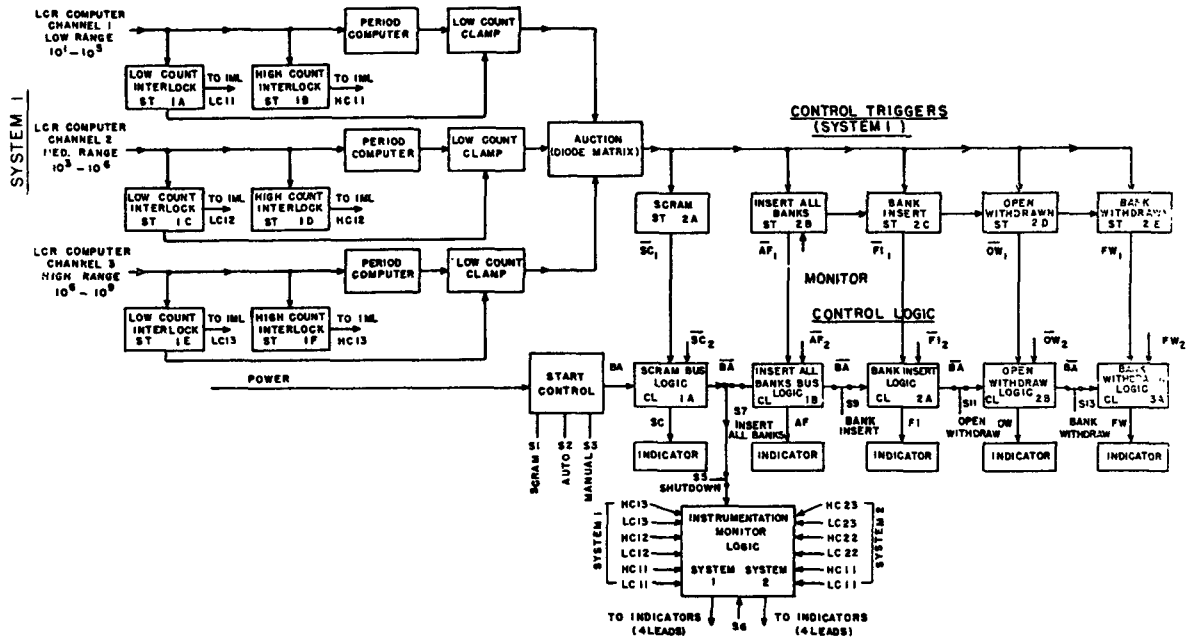


Figure 4. Ford digital start-up control system

banks, cessation of withdrawal, insertion of successive banks, insertion of all banks, and insertion of scram rods. An elaborate monitor logic circuit checks the proper operation of the system.

General Electric digital nuclear channel

A completely digital start-up channel has been constructed by Schmidt *et al.* at General Electric [17]. The unit operates on the premise that the original signals from a nuclear detector are essentially digitized pulses and consequently there is no need of any analog voltages to obtain level and period information. High reliability is claimed as all transistors are operated in a switching mode.

To cover a dynamic range of 9 decades in power, three fission counters are used as detectors. The three counters are positioned at different distances from the core so that each counter handles signals for three decades. A simplified block diagram of the channel is shown in Fig. 5. Three separate amplifier-shaping-discriminator circuits are used at the output of the detectors. Chamber commutation logic is set up to switch from one chamber to the other on the basis of high and low fixed counts per second. This arrangement eliminates the need for building identical level and doubling time circuits. The selected counter output is fed into forward and backward level counters. The level computation is performed by counting the pulses fed into the forward counter for a fixed interval of time of 1.28 seconds. The counts stored in the counter at the end of this interval are then read out and are proportional to the flux level in the reactor. These counts are converted into decimal level indication by a log matrix. Reactor level is displayed by two decimal indicators (tens digit and units digit) giving 30 discrete levels corresponding to 29 octaves in level.

The complete channel contains 198 transistors and thyristors and approximately 250 diodes. Of this number, approximately 80 transistors and thyristors and 150 diodes are required for the digital display and auxiliary functions. The unit occupies a volume of 0.85 cubic feet and consumes 20 watts of primary power.

Digital control rod drive system

The N.S.S. *Savannah* employs a digital control rod drive system [18], and this system is being considered for other reactors. Among the reasons for the selection of digital drive and control for these reactors are the extreme versatility of the system, excellent position accuracy and repeatability, and the no-drift feature of the on-off pulse motor. The

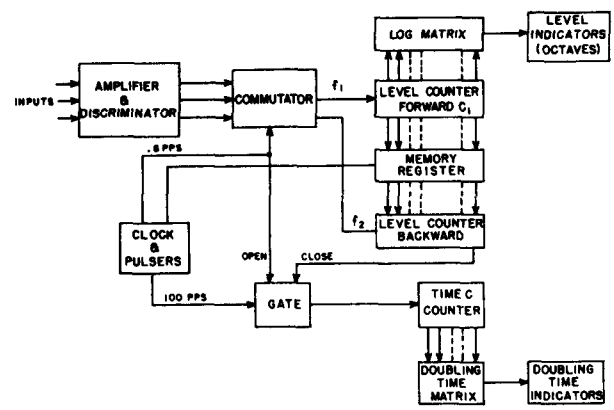


Figure 5. G.E. nuclear start-up channel

digital drive can be easily changed in speed and is compatible with present day solid state logic configurations. Commercial motors and drives are available from industrial sources.

N.S.S. *Savannah*-Marvel-Schebler control rod drive motor control system

The control rod drive motor is essentially a three-phase, multipole, synchronous-reluctance type motor. The power supply for the motor is dc and each phase winding is divided into two equal opposing wound legs. Power is supplied to three stator legs at a time in a predetermined sequence. A slotted rotor follows the rotating field.

A simple schematic of the motor windings and vector diagrams may be used to explain the rotating field of an elementary motor as follows: assume switches 1, 2, and 3 (see Fig. 6a) are closed to energize windings A_1, B_1, and C_1. The fluxes from windings A_1 and C_1 combine at an angle of 120° to produce the resultant vector ϕ_R which adds to the flux from winding B_1 to produce the total flux ϕ_T. The rotor aligns itself with the flux ϕ_T and remains aligned as long as ϕ_T is present. Opening switch 3 and closing switch 6 de-energizes winding A_1 and energizes winding A_2. The flux from the A phase now reverses since windings A_1 and A_2 are opposing wound. The total flux ϕ_T has now rotated through an angle of 60° (see step b). Repeating this energizing and de-energizing pattern for the remaining phases causes the field ϕ_T to rotate through 360° in 60° increments. The sequence must be reversed to reverse the direction of rotation. With a multipole machine, the incremental steps may be made as small as desired.

Since both windings of a phase-pair such as A_1-A_2, B_1-B_2, and C_1-C_2 are not simultaneously energized, silicon controlled rectifiers are paired off as bistable switches, where one side conducts while its counterpart is nonconductive (see Fig. 6b). As an example, when the A_1 side of the bistable becomes conductive and energizes winding A_1, the A_2 side becomes nonconductive, de-energizing the A_2 winding. Thus, by sequentially triggering the three bistables, the magnetic field of the motor will rotate and turn the rotor.

The sequential gating for the SCR's is performed by solid state AND and OR gates. The gating for one phase-pair (see Fig. 6c) is typical of the remaining two phase-pairs. Each AND gate has three inputs as follows: the first input from the SCR anode provides the present position of the magnetic field; the second input controls the direction of rotation; and the third input is the velocity control. There are 12 AND gates. Six AND gates establish the sequence for the counterclockwise rotation. Pairs of gates, i.e., AND gates 1 and 2, are controlled by the X velocity pulse while AND gates 3 and 4 are controlled by the Y velocity pulse. Therefore, the clockwise and counterclockwise commands select the six gates for sequence, and the X and Y velocity pulses trigger the SCR flip-flops in a manner directly proportional to the X-Y pulse rate which determines the motor speed.

The X and Y pulses are provided on separate control lines, and the pulses occur alternately in time with each pulse advancing the motor one increment. When the motor advances on an X pulse, for instance, additional X pulses will have no further effect upon the motor. Application of a Y pulse will then advance the motor another step. Thus, for continuous rotation, a pulse from one line must precede a pulse from the second line.

Generation of fixed or variable repetition rate pulses presents no problem, and the above system is completely compatible with present-day inputs or commands from digital computers.

Digital process sensing systems

The bulk of all process sensors are currently analog types, and digital information is obtained by some form of analog-to-digital conversion device. This apparatus usually has the disadvantage of complexity and it would be useful if digital process information could be obtained directly. A series of sensors and transducers has been developed by Ford

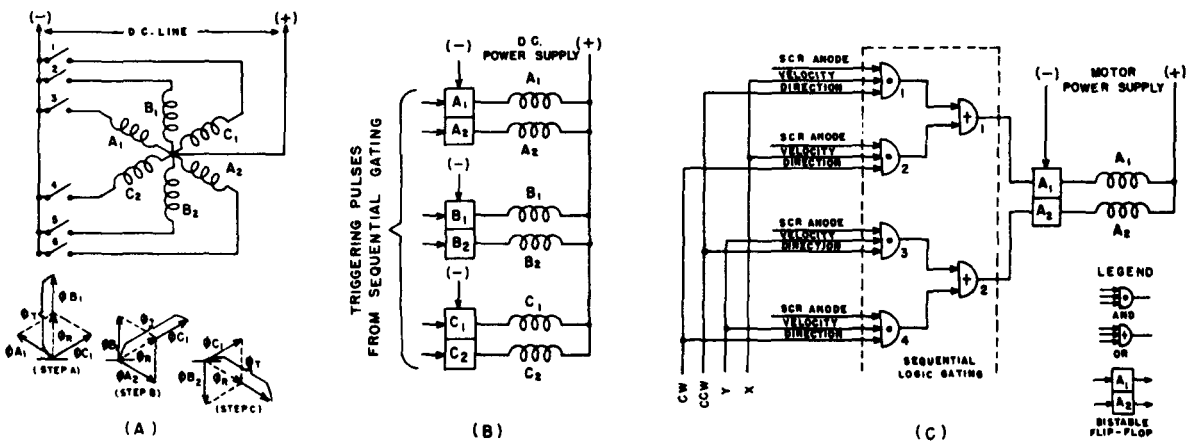


Figure 6. N.S.S. *Savannah* digital control rod drive

Instrument Company for the USAEC and US Maritime Administration [19-20]. These sensors may be used to measure temperature, pressure, liquid level, etc. The principle of operation uses reflected ultrasonic energy from a stepped target whose position is a function of the variable to be measured. Discrete pulse reflected echoes are obtained from the target and the number of these pulses is a direct measurement of the variable.

REFERENCES

1. Ferguson, R. W., *Computer Automation of Large Steam Power Plants, Symposium on the Role of Computers in Nuclear Power Plant Operation,* Nuclear News, Vol. 5, No. 5 (May 1962).
2. Edwards, R. A., *Digital Monitors for Nuclear Plants,* Nucleonics, *20,* No. 6 (June 1962).
3. Schultz, M. A., *Reactor Safety Instrumentation,* Nuclear Safety, *4,* No. 2 (December 1962).
4. Dressler, R. T., *The Shippingport Data Acquisition System, Part I, Symposium on the Role of Computers in Nuclear Power Plant Operation,* Nuclear News *5,* No. 5 (May 1962).
5. D'Amico, A. R., *The Shippingport Data Acquisition System, Part 2, Symposium on the Role of Computers in Nuclear Power Plant Operation,* Nuclear News *5,* No. 5 (May 1962).
6. Haas, W. E., *Automatic Data Logging and Computing System Performance Test,* Duquesne Light Company, DLCS-4000101 (1961).
7. Nickelson, T. S., *Enrico Fermi Atomic Power Plant Data Logger, Operating Procedure #1406,* Power Research Development Company (April 1962).
8. Herb, S. D., *Enrico Fermi Atomic Power Plant Preoperational Test Report – Data Loggers, X1-R,* Power Research Development Company (May 1963).
9. *On Line Computers for Power Reactors,* Nucleonics Special Report (June 1962).
10. Beckjord, E., Nucleonics, *20,* No. 6, 57 (June 1962).
11. Halladay, R. L., Quarterly Progress Report, GEAP-4391 (July-September 1963).
12. *Feasibility Study of Digital Computer Control of a Nuclear Power Plant,* International Business Machines Corporation, Oswego, New York (June 1960).
13. *Automation System for Nuclear Power Plants, Phase I Study,* Daystrom, Incorporated, Control Systems Division, Report CS-648, LaJolla, California (December 1960).
14. Rice, R. B., *et al., Automatic Control of T-7 Tanker Boiling Water Reactor Propulsion System,* GEAP-3528 (Rev. 1) (September 1960).
15. Kelley, E. A., and Nourse, T. M., *Experience with Direct Digital Control of Minor Loops,* Conference Paper CP 63-477, IEEE.
16. *Digital Startup Control for Aircraft Reactors,* Ford Instrument Company, NYO-8586 (March 1958).
17. Schmidt, J. D., Eriksen, B. K., and Peil, W., *A Digital Startup Control Unit for Nuclear Reactors,* IRE Transactions on Nuclear Science, Vol. N5-8, No. 3 (July 1961).
18. *Solid State Digital Control System,* Marvel-Schebler Products Division, Borg-Warner Corporation, Decatur, Illinois.
19. *All Digital Sensing and Control Systems for Marine Power Plant Applications,* Ford Instrument Company, Division of Sperry Rand Corporation, Long Island City, New York.
20. *Liquid Metal Sensing and Control Systems,* Ford Instrument Company, Division of Sperry Rand Corporation, Report SP 63-716, New York.

ABSTRACT - RÉSUMÉ - АННОТАЦИЯ - RESUMEN

A/273 Etats-Unis d'Amérique

Emploi de calculatrices numériques pour le contrôle des réacteurs

par M. A. Schultz et F. C. Legler

Plus de cinquante centrales classiques dont le contrôle est assuré au moyen de calculatrices numériques sont en service aux Etats-Unis. Les motifs d'ordre économique qui ont conduit à utiliser des calculatrices pour le contrôle des centrales brûlant des combustibles fossiles devraient également prévaloir en fin de compte pour les centrales nucléaires. On n'a pas encore installé aux Etats-Unis de système de contrôle nucléaire entièrement codé, mais plusieurs centrales utilisent des calculatrices comme dispositifs d'acquisition de données; il s'agit d'un premier pas vers leur utilisation pour la conduite du réacteur. Les auteurs comparent les installations existantes, prévoient les tendances futures et décrivent certains procédés et dispositifs spéciaux de contrôle qui sont actuellement en service ou à l'étude. Le mémoire contient aussi un exposé théorique du rôle que la calculatrice peut jouer dans les centrales nucléaires, et les auteurs analysent les problèmes de sécurité, de fiabilité et d'interaction des opérateurs que posent les systèmes de contrôle par calculatrices numériques qui sont proposés.

D'après des études menées par différentes entreprises, notamment IBM, Daystrom et Ford, on peut avantageusement et sans risque élargir le rôle de la calculatrice. Ces études prévoient cinq fonctions différentes qui peuvent être confiées à une calculatrice dans les centrales nucléaires. La première est l'enregistrement des données et le déclenchement d'un système d'alerte. Des dispositifs de ce type, utilisés pour les installations de Shippingport, Hanford et Enrico Fermi sont décrits. Une fois un appareil en place, la fonction de calcul de variables tels que l'empoisonnement par le xénon et le rendement de la centrale est une seconde extension simple de l'utilisation de la calculatrice. A Big Rock Point, l'utilisation d'une calculatrice numérique pour les calculs de gestion du combustible a donné toute satisfaction.

La troisième fonction de la calculatrice concerne

la programmation. Pour remplir ses autres fonctions, il faut que la calculatrice dispose de la plupart des informations et entrées détaillées provenant du réacteur et de la centrale. Une fois ces informations centralisées, il est logique de les utiliser pour programmer des séquences d'opérations, par exemple les opérations de vérifications avant démarrage, de démarrage automatique et d'arrêt automatique.

Une quatrième fonction de la calculatrice est de faire des calculs de diagnostic. Ces calculs sont de deux sortes: vérification de son bon fonctionnement par la calculatrice elle-même et types de calculs de comparaison entre installations en vue de contrôler les faux arrêts rapides ou le mauvais fonctionnement des appareils.

La cinquième et dernière fonction d'une calculatrice est d'assurer entièrement la commande de la centrale. Dans les industries de transformation, il est déjà courant d'utiliser des calculatrices pour commander des circuits secondaires, par exemple pour le règlage de la température. Il est également possible, en raison de la grande quantité d'entrées disponibles, de les utiliser pour assurer la souplesse de fonctionnement de la centrale nucléaire. C'est grâce à cette souplesse de fonctionnement que la centrale peut être constamment exploitée avec une efficacité maximale et c'est ce facteur qui détermine la rentabilité de l'installation d'une calculatrice.

Des dispositifs de pilotage de réacteur commandés par calculatrice numérique ont été mis au point par Ford et GE. Certains systèmes logiques numériques transistorisés sont couramment utilisés pour les circuits de sécurité. Le mémoire compare le système logique du mécanisme des barres du NSS *Savannah* aux programmes codés de commande de moteurs employés dans des industries de transformation. Les auteurs décrivent quelques dispositifs entièrement numériques pour la détermination de paramètres tels que la température et la pression, qui sont actuellement à l'étude.

A/273 США

Применение электронных цифровых вычислительных машин при эксплуатации реакторов

М. А. Шульц, Ф. С. Леглер

В США уже пущено в эксплуатацию свыше 50 тепловых электростанций, управляемых цифровыми вычислительными машинами. Те же экономические причины, которые привели к использованию вычислительных машин для управления электростанциями на органическом топливе, должны в конце концов обусловить использование таких машин для атомных электростанций. В США еще не разработано систем управления ядерными процессами, полностью построенных на цифровых вычислительных машинах, но на нескольких станциях цифровые машины используются для получения информации как первый шаг на пути к полным системам управления. Приводится сравнение существующих установок, дается прогноз будущих направлений развития и описываются некоторые элементы и методы из специализированных цифровых систем управления, которые используются или разрабатываются в настоящее время. Обсуждается вопрос о роли электронно-вычислительных машин в ядерной энергетике и рассматриваются вопросы безопасности, надежности и проблемы взаимодействия с персоналом предлагаемых электронных цифровых систем управления.

Исследования, проведенные фирмами «ИБМ», «Дэйстром», «Форд» и другими организациями, показывают, что области применения вычислительных машин могут быть расширены. В результате этих исследований было намечено пять возможных областей применения для атомных электростанций. Первое применение заключается в записи данных и сигнализации; описывается использование цифровых систем для этой цели на атомных электростанциях в Шиппингпорте, Ханфорде и на АЭС Энрико Ферми. Расчеты таких переменных величин, как отравление ксеноном и к. п. д. станции, представляют собой второе простое расширение применения вычислительной машины после ее установки. Результаты расчетов, связанных с использованием топлива, полученных с помощью цифровой машины на станции в Биг Рок-Пойнте оказались вполне удовлетворительными.

Третья область применения вычислительной машины связана с составлением программ. Для нормальной работы вычислительной машины необходимо подавать на ее вход большое количество подробных данных и входных сигналов от реактора и оборудования станции. После централизации этой информации можно использовать входные данные в последовательных стадиях программы, как, например, при предпусковой проверке, автоматическом пуске и остановке реактора.

Четвертая область применения вычислительной машины состоит в проведении двух видов диагностических расчетов: расчетов для проверки работы самой вычислительной машины и сравнительных расчетов для проверки ложных аварийных остановок или неисправности измерительных приборов.

Конечная цель применения вычислительной машины заключается в полном управлении станцией. Управление такими параметрами, как, например, температура, уже является обычным в химической промышленности. Переходное управление ядерной станцией также возможно вследствие наличия большого количества входных данных. Именно с переходным

управлением станция всегда может работать с наибольшей эффективностью, и именно эта особенность обусловливает рентабельность вычислительной машины.

Приборы цифрового управления реактором были разработаны фирмами «Форд» и «Дженерал электрик». Некоторые транзисторные цифровые логические системы используются сейчас в схемах безопасности. Логическая цифровая система привода стержней атомохода «Саванна» сравнивается с цифровыми приводами двигателей, которые используются в химическом производстве. Описываются несколько разрабатывающихся цифровых датчиков для измерения таких параметров, как температура и давление.

A/273 Estados Unidos de América

Aplicación de las técnicas de calculadoras digitales a la operación de reactores

por M. A. Schultz y F. C. Legler

Más de cincuenta centrales ordinarias de producción de energía controladas por calculadoras digitales han sido instaladas en los Estados Unidos. Las mismas razones económicas que han conducido a la elección de calculadoras electrónicas para el control de las centrales de producción de energía con combustibles fósiles deberán, en definitiva, conducir a su aplicación a las instalaciones nucleares de potencia. Aún no ha sido instalada en los Estados Unidos ninguna central nuclear con sistema de control realizado enteramente por calculadoras digitales, pero varias centrales utilizan estas calculadoras como instrumentos para la recopilación de datos en una etapa preliminar al control efectivo. Este documento compara las instalaciones existentes, indica las tendencias para el futuro y describe alguna de las componentes características del control digital, así como las técnicas que hasta ahora se utilizan y las que están en fase de desarrollo. Se incluye una especulación acerca del papel que las calculadoras pueden representar en el campo de la producción de energía nuclear; se estudian los problemas de seguridad, buen funcionamiento e interacción con el operador de los sistemas de control digital propuestos.

Se han realizado estudios por IBM, Daystrom, Ford y otros, que indican que el papel desempeñado por las calculadoras electrónicas puede ser ampliado con provechoso y buen funcionamiento. Cinco cometidos han sido proyectados en estos estudios para su aplicación a las centrales nucleares. El primer cometido es la recopilación de datos y la alarma y se describe el empleo de los sistemas digitales con este propósito en las centrales Shippingport, Handford y Fermi. El cálculo de variables tales como envenenamiento por xenón y rendimiento de la central representan una segunda y simple ampliación de la utilización de las calculadoras, una vez que la máquina está instalada. Los resultados de los cálculos acerca del manejo del combustible hechos por la calculadora digital de Big Rock Point han sido sumamente satisfactorios.

El tercer campo de trabajo de las calculadoras es la programación. Para que la calculadora pueda realizar los restantes cometidos debe disponer de la mayor parte de la información especificada, procedente del reactor y de la central. Una vez centralizada esta información, es lógico utilizarla en la programación de sucesiones de operaciones, tales como la comprobación previa en la puesta en marcha y los procedimientos de arranque y apagado automáticos.

Un cuarto cometido de la instalación de cálculo es efectuar cálculos de diagnosis. Estos son de dos clases: autodiagnosis para comprobar que la calculadora está trabajando correctamente y cálculos de comparaciones internas para comprobar la producción de caídas espúreas de barras o el defectuoso funcionamiento de los instrumentos.

La finalidad de una instalación de cálculo electrónico debe ser, en definitiva, el control completo de la central. El control de pequeños circuitos, tales como el control de la temperatura, es ya corriente en las industrias de producción en serie. El control de ajuste en las centrales nucleares es también factible debido a la gran cantidad de información disponible para su suministro a la calculadora. Es con el control de ajuste como puede operarse la central con la máxima eficacia y es esta característica lo que determina la economía de la instalación de cálculo.

Ford y General Electric han desarrollado instrumentos digitales de control de reactores. En la actualidad, son de uso corriente en circuitos de seguridad algunos sistemas lógicos digitales transistorizados. Se compara el sistema lógico digital de accionamiento de barras del NSS *Savannah* con el accionamiento digital de motores empleados en la producción en serie. Se describen unos pocos aparatos, todos digitales, que han sido desarrollados para la determinación de parámetros tales como temperatura y presión.

Un nouveau système de contrôle des réacteurs nucléaires

par I. Iftode, C. Tapu et C. Dobrescu*

Dans un mémoire antérieur [1], nous avons analysé l'utilité et les caractéristiques nécessaires d'un système de contrôle des réacteurs nucléaires. Le démarrage représente l'opération la plus difficile de l'exploitation du réacteur, et c'est pourquoi notre attention a été dirigée vers la simplification et l'amélioration des caractéristiques statiques et dynamiques de l'appareillage respectif. Le premier pas a été d'éliminer le « logarithmeur » sur une grande plage de variation de la puissance du réacteur et de le remplacer par un amplificateur opérationnel dont le gain varie automatiquement en échelons (les résistances de réaction) en fonction du signal à l'entrée (le courant de la chambre d'ionisation); ainsi, la tension à la sortie de l'amplificateur reste toujours entre les limites du fonctionnement optimum ($U_m - U_M$).

Pendant l'évolution de la puissance, le système de contrôle travaille en boucle fermée avec le réacteur à la condition dP/dt = constante (figure 1, variante A). Si on pouvait réaliser dans le circuit fermé une grande vitesse de variation de la réactivité, on pourrait alors obtenir une évolution linéaire de la puissance du réacteur dans un intervalle donné ($U_m - U_M$) et selon une courbe exponentielle approchée par des segments linéaires sur plusieurs intervalles. Dans ce cas, pour un intervalle de variation de la puissance de $U_M/U_m = k = 5$, la période de l'évolution varie de 2,5 fois, étant plus petite au commencement de l'intervalle.

La limitation de la vitesse de variation de la réactivité et l'introduction des constantes de temps au dérivateur nous ont permis de limiter la variation de la période et l'effet des fluctuations du système de réglage et du réacteur aux petits niveaux de puissance.

En intercalant un logarithmeur entre le circuit de mesure et celui de dérivation, on obtiendrait une amélioration du système de démarrage. La plage de variation de la puissance dans un intervalle étant plus petite qu'une décade ($K = 5$), il est possible d'obtenir par approximations la fonction logarithmique par 3-4 segments linéaires et d'utiliser la technique du calcul analogique pour sa réalisation physique (générateur de fonction à diodes). Dans ce cas, on peut diminuer la constante de temps du dérivateur, mais, à cause des fluctuations, elle reste pourtant assez grande.

En ajoutant le logarithmeur, en principe, le système de démarrage est équivalent au système classique; la différence réside seulement dans la réalisation physique du signal de commande. Le système de réglage pour le fonctionnement du réacteur à un niveau donné de puissance est classique.

De cette manière, si on retient la variation automatique du gain en échelons dans la chaîne de mesure, on peut éliminer le logarithmeur et le dérivateur en réalisant le signal de commande en régime dynamique par l'écart entre l'évolution de la puissance du réacteur $P(t)$ et une fonction donnée de temps (exponentielle, linéaire) de référence $P_o(t)$ (figure 1, variante B). Dans ce cas, on peut réaliser simplement les fonctions de référence $e^{\pm t/T}$ ou $\pm at$ au moyen des circuits linéaires.

Ces considérations sont à la base du système proposé.

Description fonctionnelle des éléments composants (figure 2)

1. Dans la chaîne de mesure, les courants des chambres d'ionisation passent par les résistances de réaction des amplificateurs opérationnels et sont transformés en tension. Si la position du commutateur manuel des intervalles CM ne correspond pas à celle du commutateur automatique CA, et si la tension à la sortie de l'amplificateur est $U < U_m$ ou $U > U_M$, alors CA passe automatiquement dans la position indiquée par CM et maintient $U_m < U < U_M$; U_m et U_M sont les tensions minimale et maximale qui définissent un intervalle de puissance et qui font travailler les relais R_m et R_M. On peut écrire:

$$U = R_r K_C P \quad \text{et} \quad U_M/U_m = k = \text{constante}$$

avec:

- R_r: résistance de réaction de l'amplificateur opérationnel
- K_C: constante de proportionnalité entre la puissance du réacteur et le courant de la chambre d'ionisation
- P: puissance du réacteur
- n: numéro d'ordre de l'intervalle

Si la puissance du réacteur évolue selon une exponentielle (avec une période constante) nous avons: $P = P_0\, e^{t/T}$ $\quad R_{r,n} = R_{r1}/K^{n-1}$ et donc $U_n = U_0\, (e^{t/T}/K^{n-1})$.

* Institut de physique atomique, Bucarest.

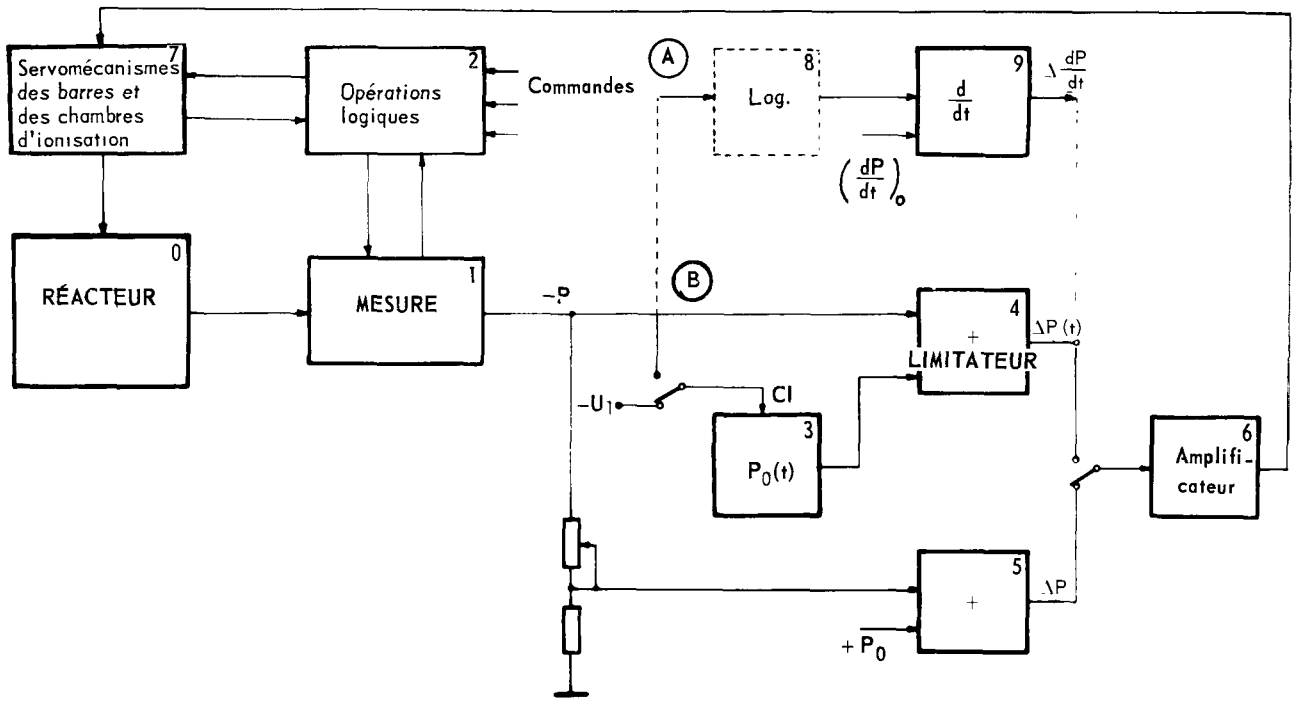


Figure 1. Schéma de principe du système de contrôle

Le temps correspondant à un intervalle d'évolution de la puissance est le même pour tous les intervalles: $\Delta t = T\ ln\ (U_M/U_m) = T\ ln\ K$.

Pour couvrir une grande plage de variation de la puissance (le démarrage du réacteur à partir de « zéro »), on utilise deux chambres d'ionisation: la première, compensée, pour les intervalles $n = 1$–9; et l'autre, non compensée, pour $n = 10$–12.

Lorsque la puissance passe dans l'intervalle $n = 10$, le système de contrôle passe sur la chambre d'ionisation non compensée fixe, et la chambre compensée se lève automatiquement.

Le relai R_{m0} ferme la boucle réacteur-système de contrôle pendant le démarrage. La tension U_{m0}, qui fait travailler le relais R_{m0}, représente ainsi le seuil de sensibilité du système et son niveau est imposé par l'influence des fluctuations et de la dérive sur le système de réglage aux petits niveaux de puissance.

2. L'unité des opérations logiques rend possible la réalisation logique et séquentielle de toutes les opérations nécessaires à un régime désiré de fonctionnement du réacteur.

3. Le générateur de fonctions de temps donne la fonction de temps de référence nécessaire aux régimes de fonctionnement dynamique du réacteur.

On accepte généralement une évolution exponentielle de la puissance pendant le démarrage et linéaire aux hauts niveaux de puissance, où apparaissent divers effets sur la réactivité (température, etc.). Au préalable, nous avons réalisé un démarrage exponentiel sur les neuf premiers intervalles, et une évolution linéaire de la puissance sur les autres (le générateur de fonctions devient intégrateur au moyen du relais R_r).

Pourtant, nous avons considéré qu'il était plus convenable d'avoir une évolution exponentielle de la puissance au début de chaque intervalle et linéaire ensuite (la diode Zener en parallèle sur le potentiomètre de période P_r). Dans ce cas, le temps d'arrivée au niveau nominal de puissance augmente de 20%, mais on obtient un fonctionnement plus facile du système de réglage à la stabilisation et au démarrage à partir de la zone supérieure de chaque intervalle.

Après chaque commutation de l'intervalle, la fonction de référence part d'une condition initiale déterminée par la tension à la sortie de la chaîne de mesure au début du nouvel intervalle.

Une autre attribution du générateur de référence est d'assurer les intervalles de temps après lesquels on donne les portions de réactivité positive, nécessaires pour s'approcher de la criticité ($U < U_{m0}$). Ces intervalles de temps sont déterminés par la tension de condition initiale U_1, par la « période » de la fonction $P_0(t)$, et par la tension maximum U_{M0}.

4. L'unité de signal d'erreur dynamique $\Delta P(t) = P(t) - P_0(t)$ a assuré l'évolution de la puissance selon les fonctions de temps de référence au démarrage du réacteur ou au passage d'un niveau de puissance à un autre. Ici, on réalise aussi la protection du réacteur pendant le régime du fonctionnement dynamique (le relais *Rd*).

Le filtre à l'entrée donne une constante de temps égale à celle du circuit de condition initiale de la fonction $P_0(t)$ pour éviter à la sortie les impulsions provoquées par la commutation des intervalles.

En outre, si la puissance du réacteur n'a pas atteint le seuil de sensibilité du système, l'unité a le rôle de comparateur et détermine la valeur de la

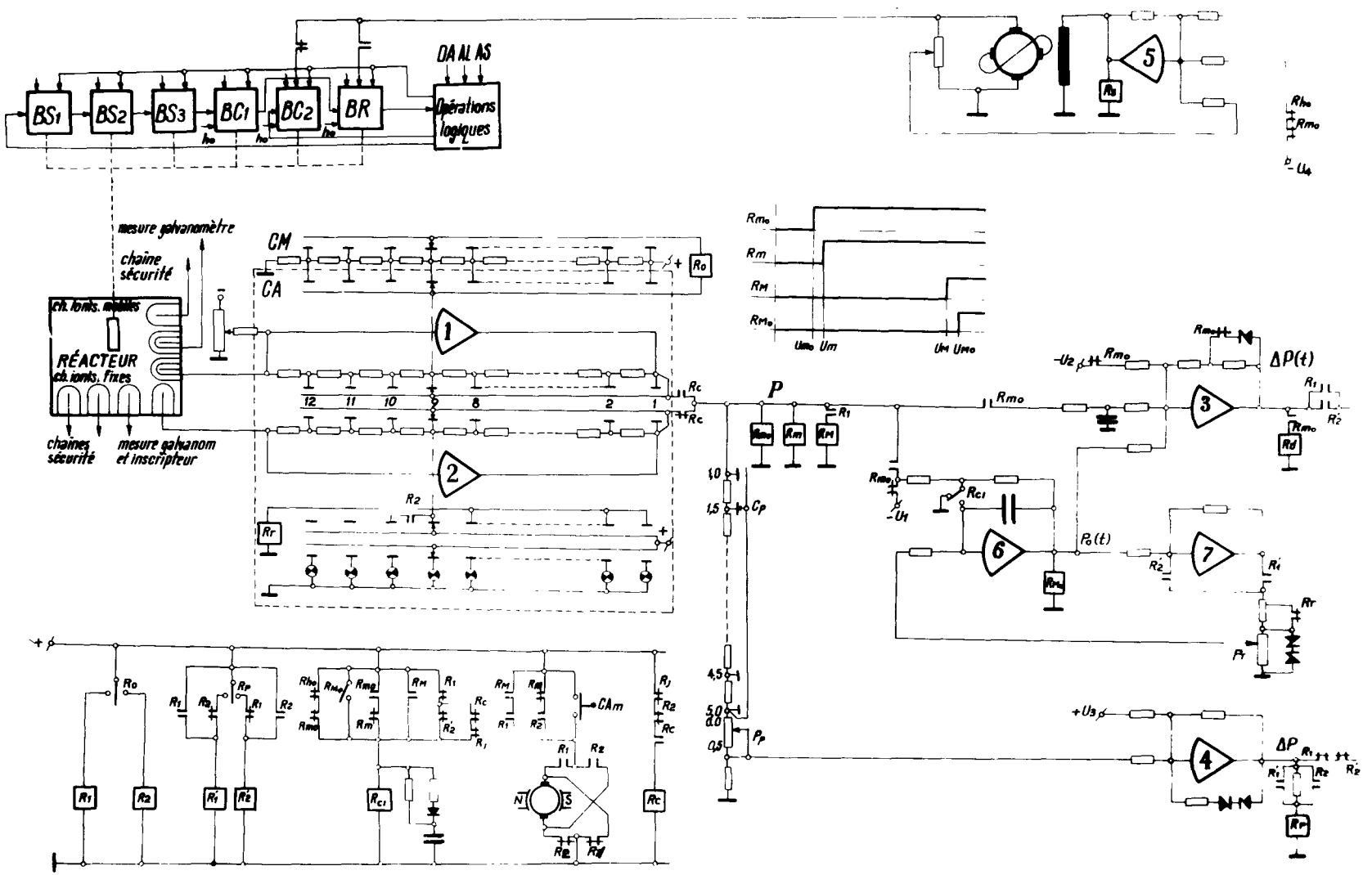


Figure 2. Schéma détaillé du système de contrôle

réactivité positive (la diode Zener dans le circuit de réaction de l'amplificateur) par la différence de tension $\Delta U = U_{M0} - U_2$.

5. L'unité signal d'erreur stationnaire $\Delta P = P - P_0$ est nécessaire pour le fonctionnement du réacteur à un niveau donné de puissance.

En régime dynamique, le relais *Rp* choisit le sens désiré de l'évolution de la puissance dans un intervalle en fonction du signe de ΔP. La sensibilité du relais *Rp* est maximum quand la puissance du réacteur évolue vers P_0 et se réduit ensuite à la valeur $\Delta P_0 = 8\%\ P_0$ quand le réacteur entre dans la phase de stabilisation et de fonctionnement à un niveau donné de puissance (ΔP_0 est plus petite que ΔP — variation donnée par un échelon du commutateur *Cp*).

Le commutateur *Cp* et le potentiomètre *Pp* sont connectés de telle manière qu'ils assurent dans le circuit fermé du réacteur-système de réglage un gain indépendant du niveau désiré de puissance.

6. L'amplificateur du signal d'erreur dynamique ou stationnaire possède un étage d'amplification en tension-amplificateur opérationnel et un étage de puissance-amplidyne, bouclés par un circuit commun de contre-réaction.

Si, à la sortie de l'amplificateur opérationnel, la tension dépasse une valeur donnée, alors le relais R_{dec} sépare tous les amplificateurs et arrête le réacteur.

La sortie de l'amplidyne commute sur la barre de compensation BC_2 ou sur la barre de réglage fin *BR*, selon qu'il est nécessaire ou non de réaliser une grande variation de puissance, en fonction du signal $|\Delta P| \gtrless \Delta P_0$, seuil de sensibilité du relais *Rp*. La barre de compensation BC_2, qui réalise le démarrage, monte à l'aide de l'amplificateur jusqu'à la position initiale h_0, à laquelle le réacteur n'atteint pas l'état critique. Si le réacteur arrive au seuil de sensibilité du système avant que la barre soit arrivée à la position h_0, alors le réacteur est arrêté rapidement.

7. L'unité de commande des barres et des chambres d'ionisation contient les relais et les moteurs appartenant au schéma de contrôle initial du réacteur.

8. La protection du réacteur, lorsque la puissance dépasse un niveau donné, est réalisée aussi au moyen des amplificateurs opérationnels connectés à une chambre d'ionisation mobile et à deux autres fixes. Le seuil de fonctionnement des relais de protection s'établit manuellement.

Pendant l'évolution de la puissance du réacteur, la protection est réalisée, comme on l'a vu, par l'écart entre la puissance et la fonction de référence (le relais *Rd*).

Dans la figure 2, on montre seulement les données nécessaires pour comprendre le principe de fonctionnement du schéma. Les détails relatifs aux interdictions, à la signalisation des pannes et aux éléments exécutifs ne sont pas inclus.

Description de divers régimes de fonctionnement de l'ensemble réacteur – système de contrôle

1. *Démarrage et stabilisation à un niveau donné de puissance.* Les vérifications nécessaires faites, on passe le système de contrôle sur « démarrage automatique » et on couple les amplificateurs opérationnels entre eux. On établit les limites h_0 qui déterminent les positions des barres BC_1, BC_2 et BC_3 auxquelles elles doivent arriver à vitesse normale. Ensuite on compense les tensions parasites à la sortie de la chaîne de mesure. On choisit le niveau désiré de puissance aux commutateurs *CM*, *Cp*, et au potentiomètre *Pp*.

En actionnant le bouton *DA*, le schéma de démarrage automatique est mis en fonction. A ce moment, les barres de sécurité BS_1, BS_2, BS_3 commencent à monter l'une après l'autre; puis la barre de compensation BS_1, la barre de réglage fin *BR*, et enfin la barre de compensation BC_2 par l'amplificateur jusqu'à la position préétablie h_0. Si le réacteur a démarré entre-temps et si la puissance atteint le seuil de sensibilité du schéma, alors toutes les barres tombent et arrêtent le réacteur, comme devant une situation imprévue; sinon, le générateur de référence fait sortir la barre BC_2, par portions préréglées, une portion toutes les 100 secondes, jusqu'au moment où la puissance arrive au seuil de sensibilité U_{M0}.

A ce moment, l'ensemble réacteur–système de contrôle fonctionne en circuit fermé au signal d'erreur $\Delta P(t)$, et l'évolution de la puissance se fait selon une exponentielle approximative.

Lorsque la puissance devient $P_M \equiv U_M$, le relais R_M fait commuter *CA* dans l'intervalle suivant et la tension se réduit *K* fois. En même temps, la fonction de référence $P_0(t)$ recommence à évoluer à partir de la nouvelle condition initiale $U_M = U_M/K$. Tout se répète jusqu'au moment où la puissance est arrivée au niveau désiré. Maintenant, l'erreur ΔP est petite, le relais *Rp* revient et fait passer tout le système sur le signal d'erreur stationnaire ΔP; la fonction de référence passe et reste ensuite sur la condition initiale $U \equiv P$: niveau désiré de puissance.

La barre BC_2 assure aussi la stabilisation, et c'est pourquoi elle est maintenue en circuit fermé, au moyen d'une constante de temps, encore 15 secondes, temps suffisant pour amener le réacteur à l'état critique. Ensuite, tout le système passe sur la barre de réglage fin *BR* et le gain dans le circuit augmente.

2. Le *passage d'un niveau de puissance à l'autre* se fait simplement par le choix de l'intervalle respectif au *CM* et du niveau désiré au commutateur *Cp* et au potentiomètre *Pp*; après quoi le système de contrôle fait le passage automatiquement. Si la variation de la puissance se fait lentement au moyen du *Pp*, de manière que le relais *Rp* ne soit pas actionné, alors le passage est réalisé par la barre *BR*. Il faut mentionner que, pour la diminution de la puissance, le générateur de fonctions donne la fonction $e^{-t/T}$ à la partie supérieure linéaire.

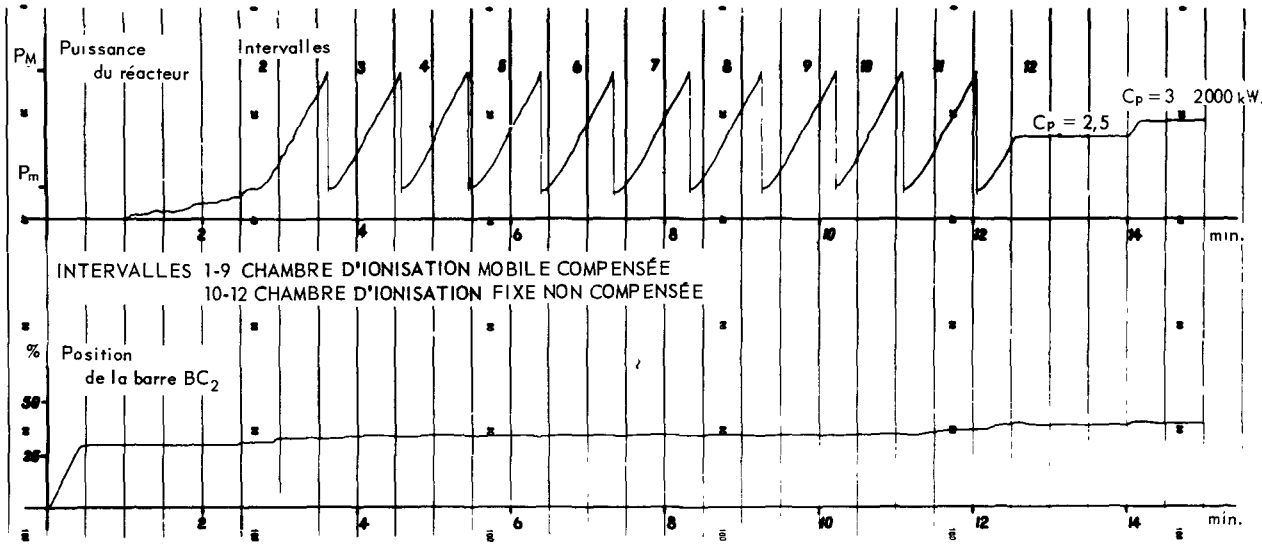


Figure 3. Démarrage du réacteur à partir du «zéro»; stabilisation au niveau de puissance 2 000 kW

3. Le *redémarrage immédiat* après l'arrêt du réacteur peut se faire si on met le commutateur *CM* dans l'intervalle où $U < U_{m0}$, au moyen du bouton CA_m, après quoi tout se répète comme plus haut. En ce cas, la réduction du gain dans le circuit se compense avec le fond existant de neutrons retardés.

4. L'*arrêt du réacteur* peut être fait soit à l'aide du bouton de sécurité *AS*, lorsque toutes les barres de sécurité tombent et que les barres de compensation entrent dans le cœur du réacteur à grande vitesse, soit à l'aide du bouton *AL*, lorsque les barres de compensation entrent à vitesse normale.

Caractéristiques des éléments importants

1. Les *amplificateurs* opérationnels sont du type à courant continu, semblables à ceux utilisés dans les calculatrices analogiques. Pour simplifier les opérations de maintenance et de réglage, tous les amplificateurs sont identiques. En considérant leurs conditions de travail dans le système de contrôle, la stabilisation automatique de la dérive n'est pas nécessaire.

Quelques caractéristiques

Tension maximum à la sortie pour une charge de 15 mA	± 100 V
Gain en circuit ouvert	$8 \cdot 10^4$
Courant de grille	$5 \cdot 10^{-11}$ A
Dérive à long terme, sommateur à gain 1	5 mV
Dérive intégrateur à constante d'intégration 1	25 mV/min

U_{m0}=13V; U_m=15V; U_M=75V; U_{M0}=85; $Rr_1 = 1{,}6 \cdot 10^{11}\Omega$.

2. L'*alimentation* de l'ensemble est réalisée à l'aide d'un stabilisateur ferro-résonant général, ce qui nous a permis de stabiliser électroniquement seulement les deux sources du premier et du second étage des amplificateurs opérationnels. Pour diminuer le bruit, les filaments de ces étages sont alimentés en courant continu.

3. Les *relais* R_0, R_{m0}, R_m, R_{M0}, R_M, R_{c1} sont des relais polarisés sensibles et rapides; les autres sont des relais électromagnétiques communs.

RESULTATS, CONCLUSIONS

Le système de contrôle réalisé a été vérifié et réglé au préalable dans le laboratoire au moyen de la calculatrice analogique FTR et a ensuite été monté dans la chambre de commande du réacteur VVR-S pour fonctionnement expérimental, après quoi le nouveau système va passer en exploitation normale.

Les courbes d'évolution de la puissance et la variation de la position de la barre BC_2 montrent la bonne qualité du démarrage, de la stabilisation à un niveau donné de puissance, et du passage d'un niveau de puissance à l'autre.

Dans la figure 3, on voit le démarrage du réacteur à partir du « zéro » et la stabilisation au niveau de puissance 2 000 kW. Bien que la dérive de l'amplificateur permette le fonctionnement du système dans le premier intervalle, les fluctuations extérieures imposent une grande constante de temps dans la chaîne de mesure. Ce fait nous a déterminés à commencer le démarrage à partir du second intervalle (constante de temps = 1 s).

La figure 4 représente le redémarrage du réacteur 20 minutes après l'arrêt et, plus loin, à divers régimes de fonctionnement, ainsi que la variation de la puissance au moyen des commutateurs *CM*, *Cp*, et du potentiomètre *Pp*.

Dans la figure 5, on peut voir le démarrage du réacteur à partir de « zéro », selon une courbe exponentielle jusqu'au dixième intervalle et linéairement ensuite.

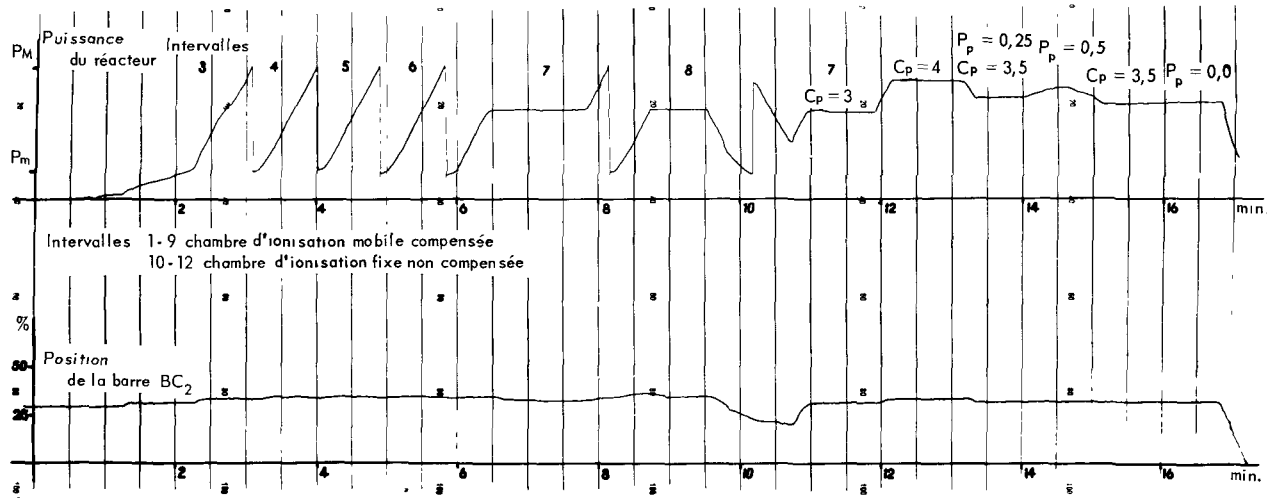


Figure 4. Redémarrage du réacteur 20 minutes après l'arrêt; divers régimes de fonctionnement. Variation de la puissance au moyen des commutateurs CM, Cp et du potentiomètre Pp

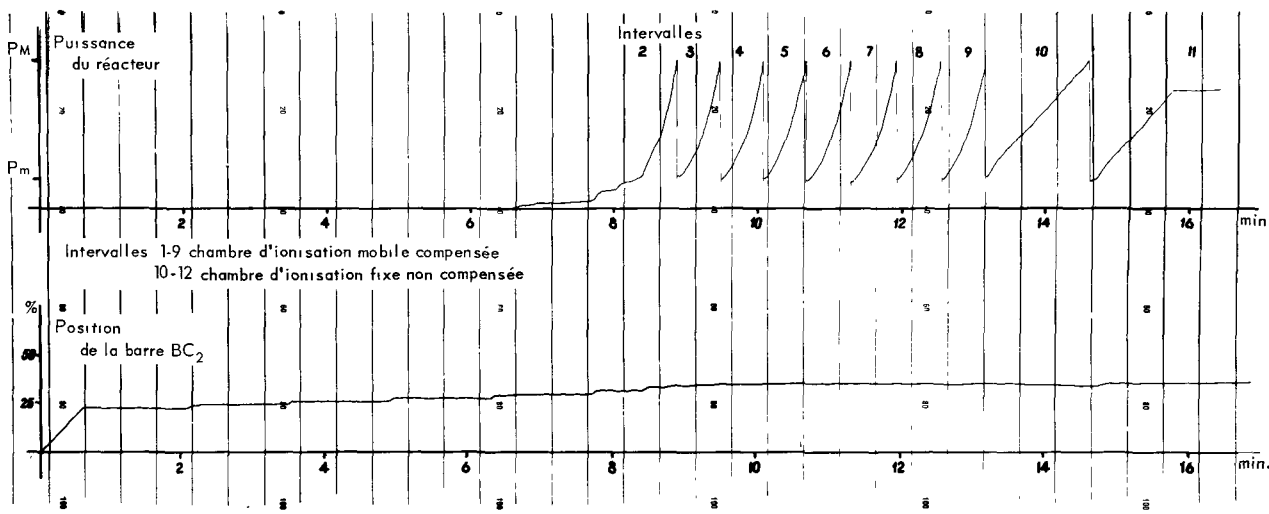


Figure 5. Démarrage exponentiel du réacteur à partir du «zéro»

Résumons les principaux avantages du système de contrôle proposé:

a) Le système permet de réaliser simplement et sûrement tous les divers régimes de fonctionnement d'un réacteur de recherche;

b) Le démarrage, opération difficile et dangereuse, est facilité par le fait qu'on élimine le logarithmeur et le dérivateur, éléments délicats, peu précis et sensibles aux fluctuations, éléments qui ont de grandes constantes de temps aux niveaux de basse puissance;

c) Il y a une chaîne unitaire de mesure de la puissance, ce qui permet au réacteur VVR-S un fonctionnement normal sur une grande plage de puissance 1W — 2 000 kW;

d) L'utilisation des amplificateurs opérationnels permet de réaliser les caractéristiques dynamiques et stationnaires nécessaires aux systèmes de contrôle au moyen d'éléments passifs avec une bonne stabilité dans le temps;

e) Du fait que les amplificateurs opérationnels sont tous identiques, sans stabilisation automatique de la dérive, et alimentés par des sources simplement stabilisées, les opérations de maintenance et de vérification sont facilitées et le nombre des pannes est diminué;

f) Pour des travaux expérimentaux, le système proposé peut être complété par une chaîne de mesure de la période (figure 1, variante A) et par d'autres éléments de calcul (par exemple, un calculateur de réactivité);

g) Le système peut être simplement adapté aux réacteurs énergétiques.

Actuellement, on étudie les possibilités d'amélioration de la sécurité de fonctionnement du nouveau

système: le remplacement des relais électromagnétiques par des relais statiques et l'utilisation d'amplificateurs magnétiques ou transistorisés.

REMERCIEMENTS

Nous tenons à remercier nos collègues A. Ionescu et C. Rîmbu, pour les travaux de construction, et le groupe d'opérateurs du réacteur VVR-S, pour l'assistance donnée pendant le fonctionnement expérimental.

REFERENCE

1. Iftode, I., Tapu, C., et Dobrescu, C., *An Automation System for Research Nuclear Reactors,* Revue roumaine de physique, *4* (1964).

ABSTRACT - RÉSUMÉ - АННОТАЦИЯ - RESUMEN

A/677 Romania

A new control system for nuclear reactors

By I. Iftode *et al.*

This paper describes an automatic control system covering the main operating conditions in research reactors, with special reference to VVR-S.

Since start-up is the most difficult operation in the running of a reactor, efforts have been made to simplify and improve essential equipment. Thus the logarithmic meter and the differentiator, both delicate components lacking in accuracy and sensitive to fluctuations, have been eliminated.

A unit system of power measurement over a wide power range has now been developed for start-up and for operating the reactor at various power levels. This has been achieved by using automatic switching which, by modifying in steps the gain in an operational amplifier (feed-back resistances as a function of ionisation chamber current) keeps the output voltages between the optimum operating limits: U_{min}–U_{max}.

During start-up or changing from one power level to another, the fault signal is $\Delta P(t) = P(t) - P_0(t)$, where $P(t)$ is the reactor power and $P_0(t)$ is a periodic time reference function (exponential, linear) with the same limits U_{min}–U_{max}; this function is derived simply using analogue techniques. The safety of the reactor is ensured by the signal $\Delta P(t) > \Delta P_0(t)$.

During operation at a given power level, the fault signal is $\Delta P = P - P_0$. The choice of appropriate signal is given automatically as a function of the value $|\Delta P| > \text{or} < \Delta P_0$.

A/677 Румыния

Новая система управления ядерных реакторов

И. Ифтоде *et al.*

Представлена система автоматического управления наиболее важных режимов работы исследовательских реакторов, в частности реактора ВВР-С.

Поскольку пуск является наиболее сложной операцией в эксплуатации реактора, основное внимание было направлено на упрощение и улучшение необходимой аппаратуры. Так, были исключены такие сложные, не обладающие большой точностью и чувствительные к флуктуациям элементы, как логарифматор и дифференциатор.

Помимо того, введена единая система измерения мощности на большой диапазон значений для пуска и работы на различных заданных уровнях мощности.

Это было достигнуто при помощи автоматического коммутатора, который путем ступенчатого изменения усиления операционного усилителя (сопротивление обратной связи в зависимости от тока ионизирующий камеры) поддерживает выходное напряжение в оптимальных рабочих пределах:

$$U_{min} - U_{max}.$$

Во время пуска или перехода с одного уровня мощности к другой, сигнал ошибки выражается через $\Delta P(t) = P(t) - P_0(t)$, где $P(t)$ — мощность реактора; $P_0(t)$ — эталонная периодическая функция времени (экспоненциальная, линейная) с теми же пределами: $U_{min} - U_{max}$ эта функция реализированна при помощи аналоговой модели. Защита реактора осуществляется сигналом $\Delta P(t) > \Delta P_0(t)$.

Во время работы на заданном уровне мощности сигналом ошибки является выражение $\Delta P = P - P_0$. Выбор соответствующего сигнала осуществляется автоматически в зависимости от значения $|\Delta P| \gtrless \Delta P_0$.

A/677 Rumania

Un nuevo sistema de control de los reactores nucleares

por I. Iftode *et al.*

Se presenta un sistema de control para los regímenes principales de los reactores de investigación, en particular del reactor VVR-S.

Puesto que se puede considerar la puesta en marcha como la operación más difícil, se ha buscado simplificar y mejorar la instrumentación correspondiente. Por eso se han eliminado el medidor loga-

rítmico y el diferenciador que son elementos delicados, poco precisos y sensibles a las fluctuaciones.

Asimismo se ha construido un sistema unitario de medida de potencia con un amplio intervalo de valores, que sirve para el arranque y para el funcionamiento a diversos niveles de potencia. Para ello se ha usado un conmutador automático que mantiene la tensión de salida entre los límites de funcionamiento óptimo U_{min}–U_{max} mediante el cambio por saltos, de la ganancia de un amplificador operacional (resistencias de reacción dependientes de la corriente de la cámara de ionización).

Mientras se arranca o cuando se cambia de nivel de potencia, la señal de error vale $\Delta P(t) = P(t) - P_0(t)$, donde $P(t)$ es la potencia y $P_0(t)$ es una función periódica del tiempo (exponencial, lineal), de referencia, cuyos límites son también U_m–U_M; dicha función se construye fácilmente mediante las técnicas de cálculo analógico. La protección del reactor se consigue mediante la señal $\Delta P(t) > P_0(t)$.

Mientras el reactor funciona a un nivel de potencia dado, la señal de error es $\Delta P = P - P_0$. La elección de la señal necesaria se realiza automáticamente en función del valor $|\Delta P| \gtrless \Delta P_0$.

Bradwell Nuclear Power Station: comparison of shielding performance with design calculations

By F. P. Youell,* A. K. McCracken** and P. Oliver*

During the commissioning and early operation of the Bradwell Nuclear Power Station, a series of radiation measurements was made through the core and shield layers of the reactors. This series formed part of an over-all programme of shielding experiments being carried out on the British Civil Nuclear Power Stations under the auspices of the Consortia, the UKAEA and the Generating Boards. The measurements were carried out by a joint team consisting of personnel from The Nuclear Power Group, responsible for the design, construction and commissioning of the station, from the UKAEA (Winfrith) Shielding Group stationed at Harwell and from the CEGB (Berkeley Nuclear Laboratories).

The purpose of the experiments was to provide data to test and improve design methods of calculation used in the UK [1] for power reactor shields. These methods have already been tested [2] for plane slab shields of simple configuration, both with and without penetrating ducts, by the UKAEA Shielding Group. However, such tests do not investigate the effects of the complex geometry found in the shields of large power reactors, in particular the effects of:

(*a*) The size and shape of the reactor core;

(*b*) Local perturbations due to structural members;

(*c*) Direct streaming along gas coolant channels from fuel elements.

To allow for these effects, various extensions to the methods of calculation are necessary and the purpose of this paper is to test these modified design methods by comparing the results of calculation with the experimental measurements obtained at Bradwell.

MEASUREMENTS: GENERAL

The general layout of the Bradwell core and shield is shown in Fig. 1. Measurements of fast and thermal neutron flux were made at points between the core/reflector boundary and the biological shield. In addition, gamma dose-rate distributions were measured in the biological shield. The measured fluxes span seven or eight decades, and consequently to obtain adequate counting statistics, measurements through the reflector, the pressure vessel and the thermal column were made at reactor powers of 20 and 200 kW(th), whilst measurements through the biological shield were made at approximately 500 MW(th).

To obtain these different conditions without using costly reactor time, it was necessary to phase the measurements into the reactor commissioning programme. As a result of this, during the 200 kW irradiation the bulk control rods were 40% inserted, causing severe axial distortion of core flux. This resulted in the flux in the upper regions of the core being depressed by a factor 6.5 compared with the condition in which the rods are withdrawn and the power is the same. This factor was obtained by measurement and confirmed by core calculations. Because of this, all measured fluxes above the core in the 200 kW run have been multiplied by 6.5. Fluxes at the side of the core at mid-height are relatively independent of rod insertion for fixed reactor power.

EXPERIMENTAL METHOD

Thermal and epithermal neutrons were detected by means of the $Mn^{55}(n,\gamma)Mn^{56}$ reaction and fast neutrons by means of the $S^{32}(n,p)P^{32}$ reaction. The active products of both reactions decay by β-emission with respective half-lives of 2.57 h and 14.3 d. The manganese foils, 1.3 cm in diameter, were punched from 0.013 cm sheet of manganese-nickel alloy which contained between 9 and 11% by weight of nickel. Sulphur was irradiated in the form of compressed pellets, 1.3 cm in diameter, of thickness 0.6 cm, and weight 1.49 gm. For a few measurements the higher sensitivity of the sulphur burning technique of Reinhardt and Davis [3] was required; for these, samples of sulphur were cast into Magnox cans. The activity of burnt samples was assessed by Geiger counting following the method of Parker [4] and pellet activity was measured either with plastic scintillators or Geiger counters.

The manganese foils were calibrated in the known flux of the thermal reactor GLEEP. In order to determine the reaction rate of Mn^{55}, the effective activation cross section of 13.8 barns [5] was used

* The Nuclear Power Group, Knutsford, Cheshire.
** United Kingdom Atomic Energy Authority, AEE Winfrith.

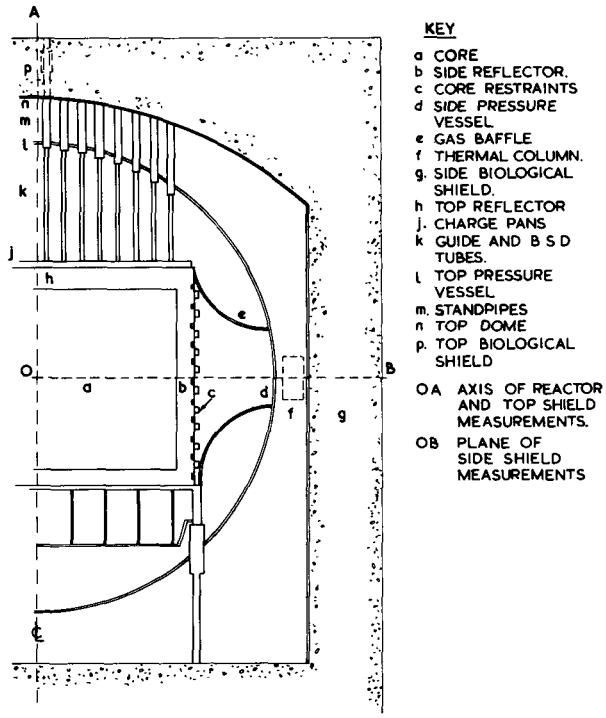


Figure 1. General arrangement of core and shield

and experimental values of thermal flux are reported in terms of reaction rate per atom of Mn^{55}.

Sulphur pellets were calibrated using the 14 MeV(d,t) reaction on the Harwell Cockcroft-Walton accelerator which was monitored by a standard U^{238} fission chamber. The cross sections used for the calibration were those of Hughes and Schwartz [6]. Pellets and burnt samples were inter-calibrated by comparing activities of numerous samples irradiated under identical conditions in experimental assemblies. All fast flux measurements are reported in units of reaction rate per atom S^{32}.

Gamma dose-rates were measured by means of small air-filled condenser ion chambers already described [7] elsewhere.

MEASUREMENTS AT THE SIDE OF THE CORE

Measurements were made on the reactor mid-plane as follows:

(*a*) Fast and thermal neutron flux distributions through the side reflector;

(*b*) Fast and thermal neutron fluxes on the inner and outer faces of the pressure vessel;

(*c*) Thermal neutron flux distribution in the thermal column;

(*d*) Fast and thermal neutron flux and gamma dose-rate distributions over a distance of 1 m into the biological shield.

Measurements (*a*), (*b*) and (*c*) were made with the reactor at low power (20 and 200 kW) and measurement (*d*) was made at approximately 500 MW. Further details are given below.

Flux distributions through the side reflector were measured by irradiating manganese foils and sulphur pellets in a 2.54 cm diameter hole provided for the purpose and which penetrated the reflector in the radial direction. The foils and pellets were contained in cavities in a 2.2 cm diameter graphite rod which reduced neutron streaming along the hole. Check experiments with foils and pellets placed at the inner ends of two other holes which only partially penetrated the reflector showed that neutron streaming was in fact negligible.

On the inner and outer faces of the pressure vessel, manganese foils were used for the measurement of thermal flux and in order to obtain greater sensitivity fast flux measurements were made using the sulphur burning technique.

The graphite thermal column (183 cm high, 284 cm wide and 92.7 cm thick) contains twelve ion chamber holes. These holes, 10 cm diameter, penetrate the column from the face remote from the reactor to within 20 cm of the inner face. In order to investigate the effect of flux depression due to an ion chamber, manganese foils were irradiated in two holes symmetrically disposed with respect to the horizontal axis of the column. One hole was left empty and the other contained an ion chamber.

For the measurements through the biological shield, small diameter (1.9 cm) holes had been provided during construction, penetrating the 259 cm thick concrete primary shield to various depths from the outer face. By irradiating manganese foils, sulphur pellets and condenser ion chambers at intervals along the axes of the holes, values of thermal and fast flux and gamma dose-rate were obtained. The detectors were separated and backed by concrete plugs to reduce radiation streaming along the holes.

The results of these measurements, made in a radial direction, are shown graphically in Figs. 2, 3a and 4.

MEASUREMENTS ABOVE THE CORE

Above the core, measurements were made on the reactor axis as follows:

(*a*) Fast and thermal neutron flux distributions through the top reflector and chargepans (the steel structure over the top reflector which is shown in Fig. 1);

(*b*) Fast and thermal neutron fluxes immediately above the chargepans over a fuel channel;

(*c*) Fast and thermal neutron fluxes at the inner face of the pressure vessel;

(*d*) Fast and thermal neutron flux distributions and gamma dose-rates through the biological shield. Measurements (*a*), (*b*) and (*c*) were made with the reactor at low power (20 and 200 kW) and measurement (*d*) was made at approximately 500 MW.

In the top reflector and chargepans, foils and pellets were taped to special Magnox supports which

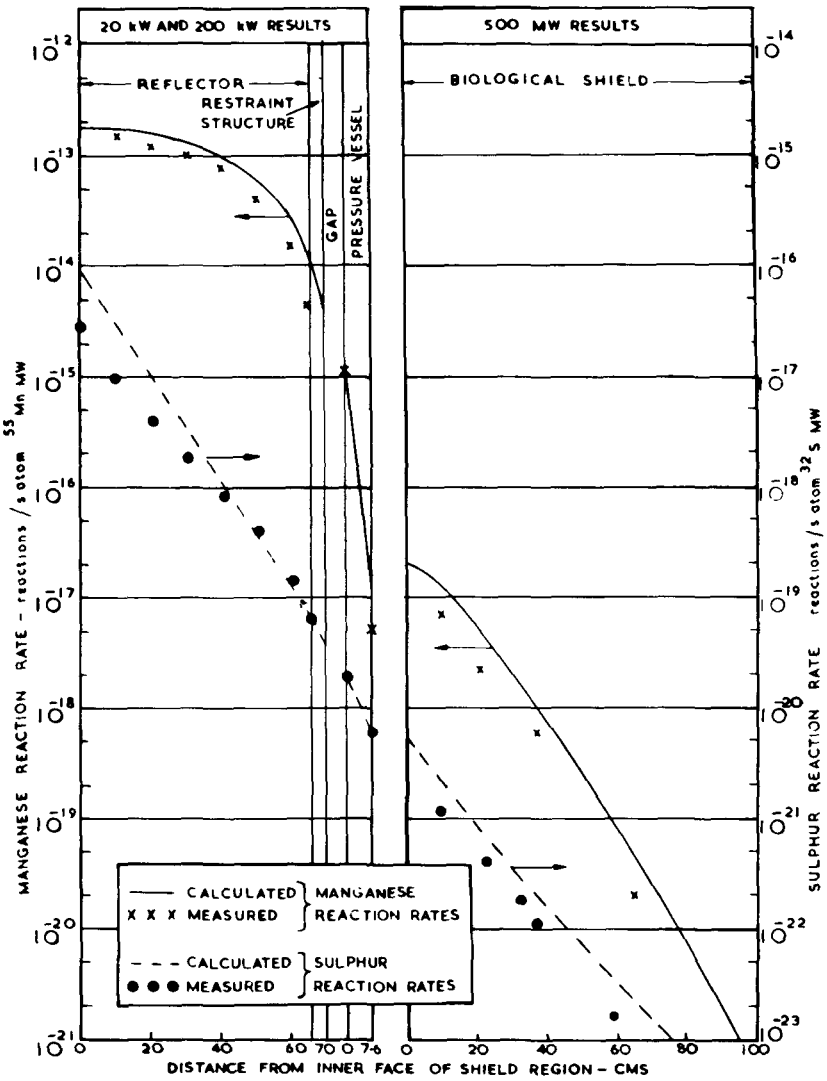


Figure 2. Manganese and sulphur reaction rates in side shield

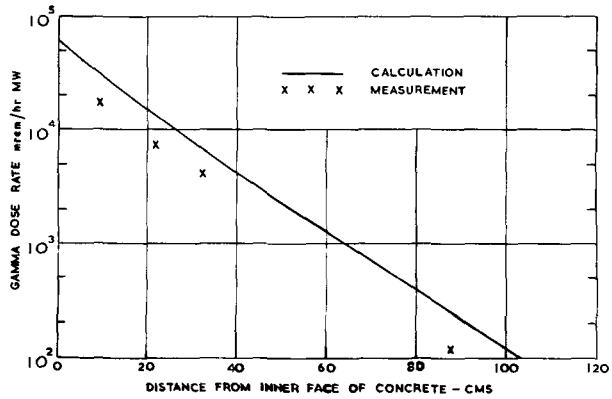


Figure 3a. Gamma dose-rate in side biological shield

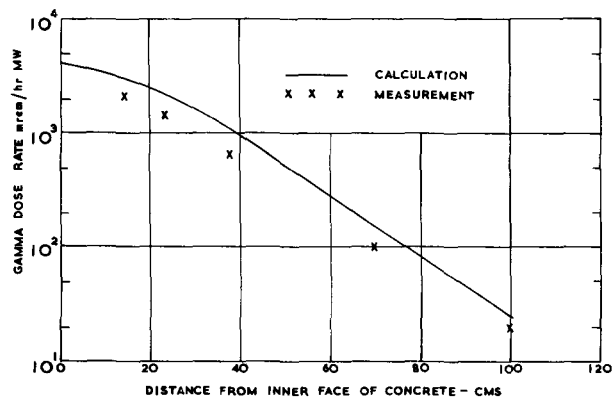


Figure 3b. Gamma dose-rate in top biological shield

were suspended from the chargepans. Above the chargepans, Magnox supports were again used to locate foils and pellets over the channels. In the vessel roof, manganese foils and sulphur samples were attached to local steelwork.

For the measurements through the top biological shield, holes similar to those through the side shield had been provided during construction and again manganese foils, sulphur pellets and condenser ion chambers were used.

The results of the above measurements are shown graphically in Figs. 3b and 5.

BASIS OF THE DESIGN CALCULATIONS

The design calculations for the Bradwell shields have been based upon the methods [1] developed by the UKAEA Shielding Group. In these methods neutron attenuation is calculated using a combination of removal and age-diffusion theory. Starting with the calculated power distribution in the core, removal theory is used to obtain the flux of penetrating neutrons which generates a distributed source (the removal source) in the shield for the multi-group diffusion equations.

Once the neutron distribution throughout the shield is known, the resulting capture gamma distribution may be calculated, thus obtaining the gamma dose-rate and nuclear heating at any desired position in the shield.

This type of calculation has been programmed in one dimensional geometry for the Ferranti Mercury digital computer in the programme series SHARN [8] - RASH E [9] - GASH [10]. SHARN calculates the removal neutron source distribution, RASH E solves the multi-group diffusion equations and GASH gives the capture gamma distribution. SHARN and GASH are restricted to plane geometry whilst RASH E can be used in plane, cylindrical or spherical geometry.

Comparisons of this removal/age-diffusion method with more rigorous transport codes such as NIOBE [11] have been carried out [12] in simple geometry and good agreement obtained, in spite of the semi-empirical nature of the removal concept.

In applying SHARN - RASH E - GASH to shields of large power reactors, modifications are necessary to allow for:

(*a*) The finite size of the core;

(*b*) Power variations in the core at right angles to the direction of neutron attenuation;

(*c*) The fact that many of the shield layers do not approximate to uniform slabs of material.

The amendment for (*c*) is important where shield layers, having high attenuating properties, are pierced in the direction of neutron attenuation by channels or large holes which are either empty or contain material of poor neutron attenuating properties. Simply smearing the material of the shield into a homogeneous slab can lead to a serious under-estimate of the neutron fluxes outside the shield layer. This is particularly so if the channels contain fuel, as fission neutrons are able to stream directly into the subsequent shield layers.

The treatments adopted for the calculation for the side and top shields are now described.

CALCULATIONS AT THE SIDE OF THE CORE

Here, the heterogeneous nature of the steel restraint structure surrounding the core (see Fig. 1) necessitates three calculations for the side shield as follows:

First, with the calculated power distribution in the core and the calculated fast and thermal fluxes at the core/reflector boundary, and omitting the steel of the restraint structure, SHARN - RASH E - GASH calculations are carried out through the side shield regions. Infinite cylindrical geometry is used for the RASH E calculation and due allowance is made for the different temperatures of the various regions.

A second calculation is carried out with the same conditions as for the first except that a complete steel layer equal in thickness to the actual restraint structure is included outside the reflector.

A third calculation is now carried out starting at the inside surface of the pressure vessel using input data obtained from the results of the previous two calculations, as follows:

(*a*) The removal source distributions in the pressure vessel and biological shield obtained in the first and second calculations are weighted according to the area of reflector respectively not covered and covered by the restraint structure. The weighted values are added and provide the removal source distribution for the third calculation;

(*b*) The epithermal and thermal out-currents leaving the reflector in the first calculation and leaving the steel restraint layer in the second calculation are similarly area-weighted and added to give, after application of a geometry factor, the true incident currents on the inside of the pressure vessel. This geometry factor is the calculated ratio of the current at the pressure vessel due to a finite cylindrical core with a cosine axial variation of flux, to that due to an infinite cylindrical core of constant axial flux, assuming cosine emission of current from the core;

(*c*) Using the removal sources of (*a*) and the incident neutron currents of (*b*) as input data, the third RASH E and GASH calculations are carried out through the pressure vessel and biological shield.

Thus the neutron distributions in the side reflector are given by the results of either the first or second calculation. Those in the restraint structure by the second calculation and those in the pressure vessel and biological shield by the third calculation.

The gamma dose rates in the biological shield are obtained as follows: the contribution from the

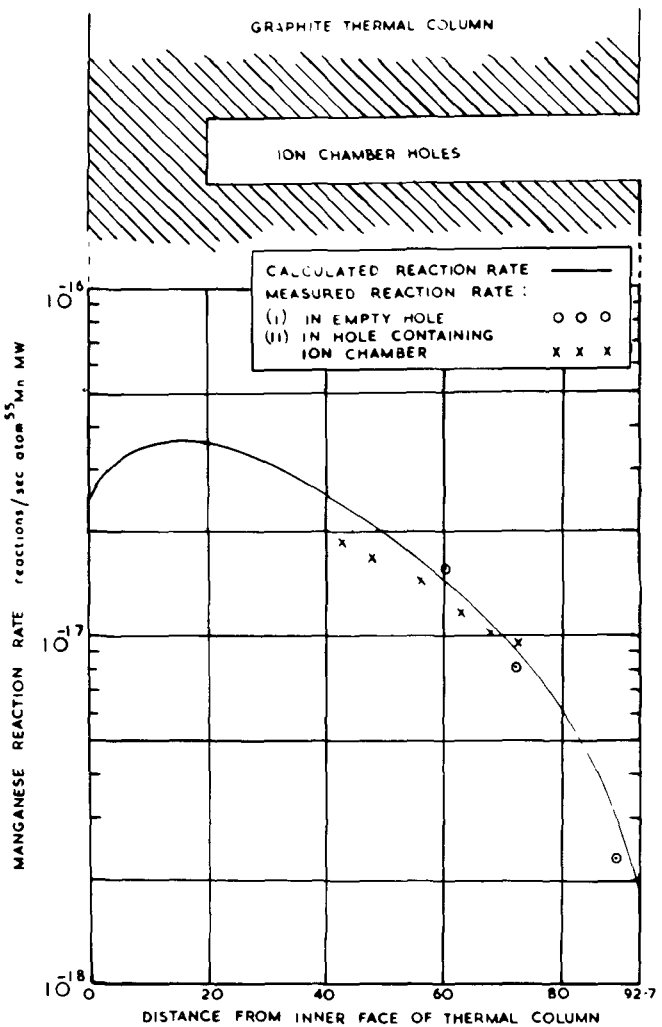


Figure 4. Manganese reaction rate in thermal column

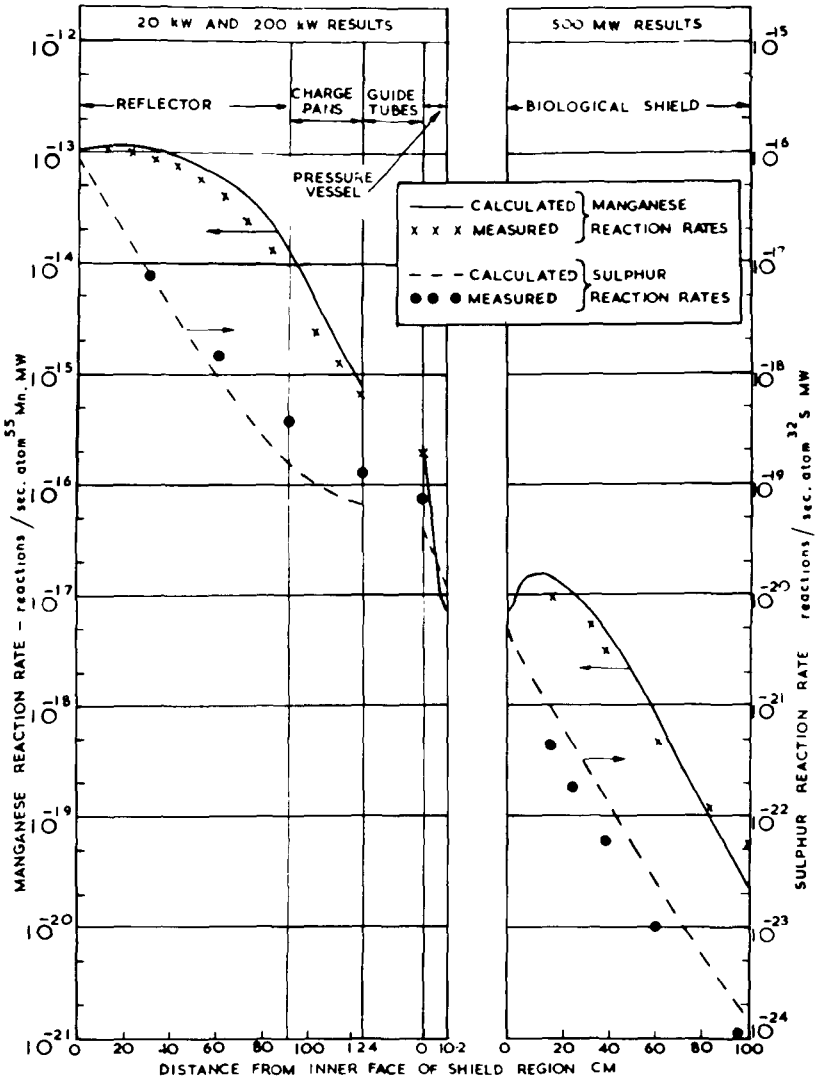


Figure 5. Manganese and sulphur reaction rates in top shield

reflector of the first calculation and that from the reflector and restraint structure of the second calculation are area-weighted and added. To this result are added the contributions from the pressure vessel and biological shield of the third calculation.

To obtain the thermal column neutron fluxes, the three calculations described above are repeated including a graphite layer equal in thickness to the thermal column in the region between the pressure vessel and biological shield. In that part of the column containing holes, allowance is made for neutron streaming by amending the epithermal slowing down lengths, the thermal diffusion length and the diffusion coefficients in the manner due to Behrens [13]. Further, to allow for leakage of thermal neutrons from the side of the column, a buckling term [1] is included in the multi-group equations.

The final calculated values of fast and thermal fluxes in the side shield regions are given in terms of sulphur and manganese reaction rates in the graphs of Fig. 2. The calculated gamma dose-rates in the biological shield are given in Fig 3a and the thermal column flux is shown in Fig. 4.

CALCULATIONS ABOVE THE CORE

Above the core, modifications to the SHARN - RASH E - GASH calculations must be made to allow for neutrons streaming along the channels in the top reflector, through the holes in the chargepans and between the guide tubes (see Fig. 1). The modifications adopted in this case differ from those used for the side shield owing to the high degree of collimation imposed by the geometry of the channels.

The general approach is to carry out calculations using homogenised shield regions and to superimpose on these calculations the contributions due to direct neutron streaming along the channels. The details of the calculations are as follows:

(*a*) For the homogenised calculations, SHARN - RASH E - GASH programmes are run with all shield regions smeared, the physical thickness of the region being retained and the density reduced to allow for voidage;

(*b*) For the streaming contribution in the channels of the reflector and chargepans, line-of-sight calculations are carried out taking as source the fuel elements and channel walls. In this calculation cosine emission of neutrons is assumed from the channel wall and the fuel element is considered as a self-absorbing cylindrical source. Allowance is made for the variation of axial flux down the channel;

(*c*) For the streaming contribution in the pressure vessel and shield regions beyond, a RASH E - GASH calculation is carried out using input data obtained as follows:

(i) A removal source distribution through the pressure vessel and subsequent regions, due to streaming of fission neutrons from the fuel through the reflector and chargepans, is calculated by a simple line-of-sight technique. Only fuel elements directly "visible" through the channels in the reflector and chargepans from the dose point are used in this calculation;

(ii) Thermal and epithermal neutron currents incident upon the underside of the pressure vessel are calculated by further line-of-sight calculations for which the effective sources are the neutron currents leaving the steel of the chargepans and walls of the channels. Cosine emission is assumed for the chargepan currents, which are obtained from the homogenised calculation of section (*a*) above. The currents leaving the channel walls are obtained from the calculated axial neutron flux distribution in the core and again cosine emission is assumed. By integrating over the complete area of chargepans and channel walls visible from the underside of the pressure vessel, allowance is made for the finite radius of the core, the radial distribution of power within the core and the effect of the steel guide tubes;

(*d*) The results of (*a*), (*b*) and (*c*) above are combined to give the total fluxes in the following manner:

(i) Neutron fluxes in the channels of the reflector and chargepans: add results of (*a*) and (*b*);

(ii) Neutron and gamma fluxes in the pressure vessel and beyond: add results of (*a*) and (*c*).

The results of (*d*) are shown in Figs. 3b and 5.

DISCUSSION OF RESULTS AND CONCLUSIONS

Examination of Figs. 2 to 5 shows that calculated values of neutron fluxes and gamma dose-rates, over an attenuation of seven or eight decades, are generally not more than a factor of 2 higher than measured values. This order of accuracy is usually acceptable in shielding design calculations as it implies an over-estimate of only 4% in predicting shield thicknesses. Two areas where results are at variance with this general picture are as follows.

In the outer regions of the top reflector and at the inner face of the top pressure vessel (see Fig. 5), the calculated values of fast neutron flux are lower than those measured. A possible reason for this is that streaming of fission neutrons from the fuel may not be adequately allowed for in the calculations, in that scattering from the walls of the channels is neglected in the line-of-sight approach described in this paper. Further work is being carried out by the UKAEA Shielding Group to investigate this effect.

In the inner regions of the side reflector (see Fig. 2), the calculated fast flux is a factor of 3 higher than measurement. This discrepancy is probably due to treating the core as a smeared volume source of fission neutrons, as recent calculations [14] carried out by the Shielding Group

show that by treating the core as a lattice of discrete line sources of fission neutrons, very good agreement with measurement is obtained. The simpler smeared treatment is adequate, however, in the outer regions of the reflector and beyond as the discrete nature of the fuel elements is no longer significant here.

Thus, it may be concluded that the general calculational technique described in this paper, namely that of an age-diffusion homogenised-slab approach followed by corrections for heterogeneity, provides a design tool having sufficient accuracy for power reactor shielding calculations.

ACKNOWLEDGEMENTS

The authors wish to acknowledge the help given by the many people involved in carrying out the measurements and calculations. Particular acknowledgement is due to A. Bardett, formerly of The Nuclear Power Group, J. Playle, CEGB Berkeley Nuclear Laboratories, E. J. Thomas, M. Stead and W. S. Sinclair, The Nuclear Power Group and G. Reddell, UKAEA. The authors also wish to thank J. Butler and A. Avery, UKAEA, and L. N. Snell, The Nuclear Power Group, for valuable discussions.

REFERENCES

1. Avery, A. F., Bendall, D. E., Butler, J., and Spinney, K. T., UKAEA report AERE-R3216 (1960).
2. Avery, A. F., Butler J., McCracken, A. K., and Packwood, A., Trans. Amer. Nucl. Soc., *5*, 2 (1962).
3. Reinhardt, P. W., and Davis, F. J., Health Physics, *1*, 2 (1958).
4. Parker, H., UKAEA report AERE-R3443 (1960).
5. Troubetzkoy, E. S., NDA-2133-4.
6. Hughes, D. J., and Schwartz, USAEC report BNL 325 (Second Edition) (1958).
7. Bardett, A., UKAEA report AEEW-R75 (1961).
8. Cesterton, B. K., and Sinclair, W. S., The Nuclear Power Group report TNPG 295.
9. Sinclair, W. S., and Pope, A. E., The Nuclear Power Group report TNPG 362.
10. Bendall, D. E., UKAEA report AERE-R2882 (1959).
11. Yetman, D., Eisenman B., and Rabinowitz, G., NDA-2143-18.
12. Butler, J., UKAEA, Winfrith, private communication.
13. Behrens, D. J., Proc. Phys. Soc. (London), *62*, Series A (1949).
14. Bendall, D. E., UKAEA, Winfrith, private communication.

ABSTRACT - RÉSUMÉ - АННОТАЦИЯ - RESUMEN

A/175 Royaume-Uni

Centrale nucléaire de Bradwell: performance du blindage par rapport aux calculs d'étude

par F. P. Youell *et al.*

Les résultats des mesures de radiation à travers les boucliers des réacteurs de Bradwell sont utilisés pour éprouver les méthodes de calcul employées dans l'étude des boucliers de réacteurs de puissance. Les méthodes utilisées au Royaume-Uni, qui se fondent sur une combinaison de la théorie de déplacement et la théorie de l'âge-diffusion, ont été mises au point par le Groupe Protection du UKAEA (Winfrith) et éprouvées à l'aide de boucliers en forme de plaque d'une configuration simple. Toutefois, afin de traiter les effets de la géométrie complexe des boucliers observés dans les gros réacteurs de puissance, il est nécessaire de prévoir différentes extensions à ces méthodes de calcul, et le présent document a pour but de mettre les méthodes modifiées à l'essai en comparant les résultats des calculs aux mesures expérimentales.

Les doses de neutrons thermiques ont été mesurées à l'aide de feuilles d'alliage manganèse-nickel. Les doses de neutrons rapides ont été mesurées à l'aide de pastilles et de blocs de soufre, et les débits de dose gamma à l'aide de chambres d'ionisation condensateurs. Le document rapporte les résultats concernant les mesures suivantes:

a) Les distributions de flux des neutrons rapides et thermiques à travers les réflecteurs latéraux et supérieur et à la surface du récipient de pression;

b) Les distributions de flux des neutrons rapides et thermiques et d'intensité de dose gamma à travers les boucliers biologiques latéraux et supérieurs;

c) Les distributions de flux des neutrons thermiques dans la colonne thermique.

Les auteurs exposent de manière détaillée les méthodes modifiées des calculs pour les boucliers latéraux et supérieurs de Bradwell, et se penchent particulièrement sur le traitement des couches de bouclier qui ne se rapprochent pas de plaques uniformes de matériau. A titre d'exemple, il convient de citer le bouclier supérieur où le réflecteur et les plaques de chargement sont percés par les canaux de combustible, ce qui permet aux neutrons de fission de s'écouler directement à partir des éléments de combustible jusqu'au caisson et au bouclier biologique supérieur.

Les flux de neutrons et de gammas mesurés et calculés s'accordent à un facteur de 2 près, sur des atténuations de 7 ou 8 décades. Il est donc démontré que les méthodes de calcul mises au point pour les systèmes à géométrie simple peuvent être étendues aux boucliers à configuration complexe des gros réacteurs de puissance.

A/175 Соединенное Королевство

Брадуэллская атомная электростанция—сравнение рабочих характеристик защиты реактора с проектными расчетами

Ф. П. Юэлл *et al.*

Для испытания методов расчета, применяемых при проектировании защиты энергетического реактора, использовались результаты радиационных измерений защиты реакторов в Брадуэлле. Методы расчета, используемые в Великобритании и основанные на комбинировании теории утечки и диффузионной возрастной теории, были разработаны Уинфритской группой защиты реактора Управления по атомной энергии и испытывались на защитных плитах простой конфигурации. Однако для определения эффектов сложной геометрии, имеющих место в защите крупных энергетических реакторов, требуется расширить возможности этих методов расчета защиты, и как раз задачей данного доклада является описание испытаний модифицированных методов путем сравнения полученных результатов расчета с экспериментальными измерениями.

Измерения скорости реакции тепловых нейтронов проводились на фольгах из сплава марганца и никеля. Скорость реакции быстрых нейтронов измерялась с использованием таблеток и блочков из серы, а мощность дозы гамма-излучения — при помощи интегрирующих камер.

Приводятся результаты измерений:

a) распределения быстрых и тепловых нейтронов через боковой и верхний отражатели и на поверхностях корпуса под давлением;

b) распределение быстрых и тепловых нейтронов, а также мощности доз гамма-излучения через боковую и верхнюю биологические защиты;

c) распределение тепловых нейтронов в тепловой колонне.

В докладе подробно описываются модифицированные методы расчетов для боковой и верхней защит реакторов в Брадуэлле, причем особое внимание уделяется расчетам, связанным с защитными слоями, которые не аппроксимируются к однородным пластинам материала. В качестве примера приводится верхняя защита, где отражатель и загрузочные устройства пронизываются топливными каналами, в результате чего нейтроны деления могут проникать прямо из тепловыделяющих элементов в корпус под давлением и в верхнюю биологическую защиту.

Результаты экспериментальных измерений и расчетов нейтронных потоков и мощностей доз гамма-излучения совпадают в пределах коэффициента, равного 2, при ослаблении излучения в 70—80 раз. Таким образом, в докладе показывается, что методы расчета, разработанные для систем с простой геометрией, могут быть модифицированы в целях их применения при расчете защит сложной конфигурации для крупных энергетических реакторов.

A/175 Reino Unido

Central nuclear de Bradwell. Comparación de la efectividad del blindaje con los cálculos del diseño

por F. P. Youell *et al.*

Los resultados de mediciones de la radiación que atraviesa los blindajes de los reactores de Bradwell se utilizan para comprobar métodos de cálculo usados en el diseño del blindaje para reactores de potencia. Los métodos usados en el Reino Unido, basados en una combinación de la teoría de la remoción y de la edad y difusión, han sido desarrollados por el UKAEA (Winfrith) Shielding Group y comprobados utilizando blindajes formados por configuraciones simples de planchas. Sin embargo, para analizar los efectos de geometría complicada que se da en los blindajes de grandes reactores de potencia, son necesarias varias extensiones de estos métodos de cálculo siendo el propósito de este informe comprobar los métodos modificados comparando los resultados del cálculo con las mediciones experimentales.

Se midieron las velocidades de reacción para neutrones térmicos utilizando laminillas de aleación de manganeso y níquel. Las velocidades de reacción para neutrones rápidos se midieron con pastillas y bloques de azufre y la dosis gamma con cámaras de ionización. Se presentan resultados de mediciones de:

a) Distribuciones de flujo de neutrones rápidos y térmicos a través de los reflectores lateral y superior y de la vasija de presión;

b) Distribuciones de flujo de neutrones rápidos y térmicos y dosis gamma a través de los blindajes biológicos lateral y superior;

c) Distribuciones de flujo de neutrones térmicos en la columna térmica.

Se describen con detalle los métodos modificados de cálculo para los blindajes lateral y superior de Bradwell, habiéndose prestado particular atención a las capas de blindaje que no son aproximadamente planchas uniformes de material. Un ejemplo de esto lo facilita el blindaje superior, donde el reflector y recipiente de carga están atravesados por los canales de combustible, permitiendo a los neutrones de fisión salir directamente desde los elementos de combustible a la vasija de presión y blindaje biológico superior.

Los valores calculados y medidos de los flujos neutrónicos y dosis gamma coinciden, dentro de un factor 2, para atenuaciones de 7 a 8 décadas. Así se demuestra que los métodos de cálculo desarrollados para sistemas de geometría simple pueden extenderse hasta llegar a ser aplicables a las complejas configuraciones de los blindajes de grandes reactores de potencia.

Recent advances in reactor shielding in the United States

By E. P. Blizard * and P. S. Mittelman **

The saying "The more things change, the more they are the same" could well be applied to shielding. When reactors first required shielding, the pundits observed that any shielding problem could be solved if one knew the sources and the cross sections and had sufficient computing capacity. We have now spent many years measuring sources and cross sections and we have made tremendously powerful computers, but we still cannot solve *all* shielding problems, although there are many that we can solve. Of the radiation sources, most are very well known. The fission sources, neutrons and gamma rays, have been well measured, and thermal-neutron-capture gamma rays for most nuclides are well known, but inelastic-scattering gamma rays remain largely unmeasured. Similarly with cross sections, it is inelastic scattering which remains least well known.

In the past few years, shielding research has been reoriented into two quite different directions: first, it has moved into the very demanding problems of shielding reactors for space applications. In early versions of shields for these reactors, the attenuations will not be large, but the geometry will be complicated and weight savings will be crucial. The difficulties of doing experiments on earth which will give shielding information pertinent to the vacuum condition of outer space have been investigated, and some experiments have been found to be feasible, although considerable analysis will be needed to make them reliably meaningful.

Second, it has turned to shielding studies of general applicability. Also evident are improvements in instruments and techniques of shield study, such as the development of new spectrometers. Neutron spectra in water or LiH shields have been measured. Calculational methods for attenuation have been devised, compared with experiment, and used. A new technique has been devised for designing a minimum-weight shield systematically, superseding the older optimization methods. And an information center has been started to collect, collate, and make available the totality of useful shielding literature. While reactor shielding experiments are waning, the general knowledge continues to grow and become better known. The purpose of the present paper is to review this progress as it has been pursued in the United States during the last few years.

* Oak Ridge National Laboratory, Oak Ridge, Tennessee.
** United Nuclear Corporation, White Plains, New York.

THEORETICAL METHODS OF SHIELD DESIGN

The development of high-speed computers and their associated programs has led to a virtual revolution in both the philosophy and the practice of shield analysis since the last Geneva Conference. One can now calculate the penetration of radiation through thick multilayered shields at reasonable cost and at an accuracy that is essentially limited only by the available cross-section information. This confidence arises from comparisons of theoretical and experimental evaluations of the same problem.

The emphasis in shield analysis has shifted strongly toward the solution of neutron transport problems. This is because most primary gamma-ray problems are simply solved by calculating the uncollided flux and multiplying it by a build-up factor (and even for multilayered shields build-up factors that yield answers of acceptable accuracy can be devised) whereas neutron transport problems require a complete solution of the spatial and energy variation of the flux in order to determine the dose and the sources of secondary gamma radiation. The various techniques currently used to solve neutron transport problems can be categorized as numerical integration, point kernel (sometimes combined with numerical integration), and Monte Carlo.

Numerical integration techniques

The major development in numerical integration techniques has been the development of the NIOBE (Numerical Integration of the Boltzmann Equation) computer program by Preiser *et al.* [1]. This program solves without significant physical approximation the neutron or gamma-ray transport problem in spherical multilayered geometries and yields the angular flux as a function of energy (256 values) and position both throughout the shield and on its surface. It has been successfully used in a variety of shielding problems (see below). It can, however, yield incorrect answers in certain situations: for example, if the angular flux cannot be well represented by a Legendre polynomial expansion of order 16 or if the angular distribution changes markedly at the interface between two media and the spatial mesh has not been properly established.

The Carlson S_n method, a numerical integration technique first developed for reactivity calculations, has been adapted to shielding calculations [2] by modifications which allow for the incorporation of a high degree of anisotropic scattering and of the proper angle-energy slowing-down relationship. Preliminary experience with this program indicates that it agrees with accurate Monte Carlo results.

Shure has attacked the problem of developing a shield analysis technique which is rapid and sufficiently accurate for metal-hydrogenous shield designs. Initially, a heuristic approach combined results from a P_1 multigroup program with those using a point kernel [3]. A more recent technique [4] is based upon results from the P3MG program [5], a multigroup program that solves the P_3 approximation to the one-dimensional Boltzmann transport equation for all non-thermal groups and solves the double P_1 approximation in the thermal energy range. Slowing down in hydrogen is treated exactly in the P_3 approximation, whereas slowing down in heavy elements is accounted for by age theory or, when proper constants are available, by the Greuling-Goertzel approximation. P_2 and P_3 components of the scattering cross sections for elements other than hydrogen may be included in the total and transport cross sections. Transverse buckling terms are included only in the P_1 equations. The results obtained with this technique are far superior to those obtained with the simple P_1 approximation and are in good agreement with experiments on water-steel shields out to a 150 cm penetration. The technique can be applied in slab, cylindrical, or spherical geometry.

Although not developed since the last Geneva meeting, the moments method for neutrons in infinite homogeneous media has been significantly improved. Recent versions of the technique as embodied in the Renupak [6] program permit solutions at 400 energy values in minutes of computer time (IBM 7090). The moments of the fluxes can be fitted by sums of either exponentials or Gaussians. Instances in which neither fit is valid have been encountered in non-hydrogenous media, and additional fitting functions are under investigation.

Point kernel and combination techniques

These techniques attempt to compensate for the deficiencies of diffusion theory at high energy (where anisotropic scattering is important) by using kernels to describe the transport of the high-energy radiation. Such techniques have been extensively developed for both neutron and gamma-ray problems and are most useful in situations where the geometry is extremely complex.

For cases in which the angular distribution of radiation leaving a shield is important, a significant development has been the recognition, by Moteff [7], of the two components involved in the neutron attenuation process. The neutron dose at a detector is taken to be composed of a component which has been only slightly scattered, if at all, and a more diffuse component from larger angle scatterings. The contribution of the first component to the total dose at the detector is determined by using an exponential attenuation kernel with the narrow-beam removal cross sections due to Schamberger *et al.* [8]. The contribution from the second component is evaluated by using the removal cross sections given by Chapman and Storrs [9] to calculate the shield penetration, applying angular distributions determined from experiments, and integrating over the shield surface. This technique has greatly improved the reliability of the dose estimate, expecially for shadow-shield geometries.

The computer programs GE 14-0, 14-1, and 14-2 [10] and GD/FW L-63 [11] have combined the relatively simple point kernel transport calculation with geometry routines capable of handling figures of revolution. The result is an analysis program of considerable utility, which in many instances, and particularly in the case of gamma-rays, yields answers with useful accuracy.

Several shield analysis programs have been prepared which treat one or more high-energy groups by removal theory and handle the slowing-down fluxes by multi-group diffusion techniques. The Hanford-MAC [12] and ANL-RE-122 [13] programs are widely used programs of this type.

Monte Carlo techniques

Perhaps the greatest advances in our ability to predict the performance of shield configurations have arisen with the rapid development of the Monte Carlo method and its application to a wide variety of problems. Some of the Monte Carlo programs which are of relatively general interest and are well documented and available are listed in Table 1.

Significant progress has been made in the development of variance reduction techniques which, coupled with the high speeds of modern computers, allow for the rapid solution of transport problems even when the radiation must penetrate to regions of phase space having low *a priori* probability.

The work of Kalos on the theory of importance sampling [14] has clarified the physical and mathematical role of the importance function. Of perhaps greater significance, Kalos has shown how practical importance functions can be developed to fit particular situations. Such importance functions have been applied to deep penetration problems (>100 mean free paths in hydrogen) that have been successfully solved within minutes of computing time.

Steinberg's study of generalized quota sampling [15] provides a technique which can significantly reduce the running time for a given statistical accuracy in a number of situations. He has developed a practical method of performing quota sampling from a number of variables simultaneously. Values

of variables are not chosen randomly over their allowed ranges. Instead, the range of each variable is divided into sub-intervals and each time that a new value is to be chosen it is picked, independently of the others, from a sub-interval not previously used. Steinberg has shown formally that this procedure reduces the variance of the average value of a set of histories. The technique has been applied in a variety of Monte Carlo programs such as TRIGR P (see Table 1).

Table 1. Monte Carlo codes in current use

Code name	Problem solved	Coding language	Machine	General remarks
		I. *One-dimensional programs*		
TRG — TRIGR P. [29]	Gamma penetration through multilayered slabs	SAP	IBM 704	Source monodirectional and monoenergetic: importance sampling used to produce very fast program
GD-FW-C-18 [30]	Neutron and gamma penetration through multilayered slab shields	FAP-SAP	IBM 7090 IBM 7094	Computes source of secondary gammas and then dose due to secondaries
UNC — SAGE [31]	Gamma penetration through multilayered spherical assemblies	Fortran-FAP Fortran	IBM 7090 CDC 1604A	Gamma source distributed through shells piecewise exponentially. External dose and interior fluxes calculated. Splitting and Russian roulette used
UNC — SANE [31] I II	Neutron penetration through spherical multilayered shields	Fortran-FAP Fortran	IBM 7090 CDC 1604A	Neutron source distributed through shells. Neutron fluxes and dose at interior and exterior points computed. SANE I uses particle splitting. SANE II uses analytic importance functions
		II. *Two-dimensional program*		
GE-18-0 [32]	Neutron and gamma penetration through cylindrically symmetric configurations	FAP	IBM 704 IBM 7090	Sources may be distributed through configuration. Calculates secondary gamma sources and heating as well as emergent radiation. Uses particle splitting
		III. *Three-dimensional programs*		
ORNL-05R [33]	Neutron transport in arrays of bodies bounded by quadratic surfaces	Fortran and/or FAP Fortran and/or CODAP	IBM 7090 IBM 7094 CDC 1604A	Arbitrary source. Generates neutron interaction tape. Various scoring routines may be used to get desired answers. Uses particle splitting and exponential transformation
UNC — ADONIS [34]	Neutron or gamma transport in arrays of boxes	Fortran	IBM 7090 CDC 1604A	Arbitrary source. Calculates neutron or gamma fluxes. Produces secondary gamma source tape. Uses particle splitting
GE — FMC-N,G [35]	Neutron and gamma penetration in bodies bounded by quadratic surfaces	FAP-SAP	IBM 704 IBM 7090	Has importance sampling. Arbitrary source distribution

A problem of considerable practical importance is that of evaluating the flux at a point detector located in a scattering medium. Kalos has shown that the conventional Monte Carlo solution to this problem, involving the use of last-flight estimators, has infinite variance. As a result, the Monte Carlo answer to such a problem converges very slowly to the correct answer. After a large number (n) of histories it converges as $(n)^{-\frac{1}{2}}$. To improve the convergence, Kalos developed a finite variance estimator [16] which in effect determines, after any given collision, the contribution of the particle to the flux after one more collision. The position at which this additional collision occurs may not be chosen at random but must be picked from a special distribution function.

SHIELD SYNTHESIS

The design of minimum weight shields, which is important for mobile reactors, has traditionally relied strongly on the experience and intuition of the shield designer. As the result of the work of G. Young, E. Troubetzkoy, M. Kalos, and M. Slater, a formal procedure for the synthesis of such shields has been developed [17]. Its application to real shield problems has resulted in impressive weight reductions for mobile reactor shields.

The technique of shield synthesis applies the calculus of variations to the problem of minimizing shield weight subject to certain constraints. These constraints are as follows:

(a) The dose should be less than or equal to a specified value;

(b) The properties of a mixture of materials should be a linear combination of the properties of the individual components. A material can be a single element or a chemical compound.

All materials are assigned a set of values for the following parameters: fast-neutron attenuation parameter (Y); medium-energy neutron attenuation parameter (y) (these neutrons are assumed to be responsible for secondary gamma-ray production); secondary gamma-ray production parameter (z); gamma-ray attenuation parameter (λ); and density (ρ). If each parameter is considered to be a coordinate axis in multi-dimensional space, then the parameter values for any material are the coordinates of a point in that space. If all materials are thus plotted in space, the resulting figure can be used to indicate which is the optimum sequence of materials in the shield configuration. The imposition of these constraints leads to a set of simultaneous nonlinear equations, which, for a given choice of shield materials, must be solved for the radii of the various shield regions.

From the shield synthesis work accomplished to date, a number of results have been obtained which clearly define the requirements for the most compact and light-weight shield. These are listed below:

(a) No region of the shield can consist of a mixture of more than two materials;

(b) The innermost layer of the shield and the outermost layer must be single materials;

(c) If a layer of the shield is a single material, it must be adjoined either by a layer consisting of one of its nearest neighbors on the multi-dimensional surface or by a mixture of itself and one of its nearest neighbors;

(d) If a layer of the shield is a mixture of two materials, it must be preceded by a layer of one component and followed by a layer of the other;

(e) The composition of the mixture must vary with radius (r) in such a way that $\lambda - y = 1/r$;

(f) Only those materials on a certain portion of the outer surface of the multi-dimensional figure can be present in the shield.

EXPERIMENTAL RESEARCH

Reactor shielding experiments in recent years have been addressed to the dual aims of giving insight into the ways in which shields attenuate and of checking in detail the calculations of high speed computers. Insight is needed to enable us better to devise shield calculational methods, the need being greater currently because shield applications are no longer simply the classical ones in which an operating reactor is wrapped in a thick shield and the persons to be protected are just outside. For example, for a power plant that can be transported overland and set up in the field, keeping the operators at a considerable distance from the shielded reactor would enable a savings in shield weight. But in an optimized case such as this, the top of the shield would be thin, and therefore the angular distribution of the radiation emitted from this shield would be important. Or in a reactor used for auxiliary power on a space vehicle, the shield may be a truncated cone curved at the base for minimum weight, making the angular dependence of penetrating radiation important. And in this case the payload may be instruments whose sensitivity to radiation remains to be determined, so that in the absence of a single detector to indicate damage, such as the dosimeter for effects on humans, the energy spectra would have to be measured. Another variation in the shielding problems being encountered today is the thinness of some shields, which often means that scattered and secondary radiation build-up is in transition and not in the pseudo-equilibrium observed in the usual thick shields. Still another is the separation of source and shield so that the radiation incident is collimated but not necessarily incident normally.

Our capability for solving these problems with computers varies, but the complications often stymie the standard moments method or NIOBE, and multigroup P3MG is proven only against the complication of lamination. Monte Carlo methods are capable of handling complications, but, if they are to give reliable results in reasonable running times,

the user must insert a set of biases which are founded in his understanding of the problem. Since it is dangerous (or impossible) to acquire this understanding from the computations themselves, experiments are carried out to reveal the workings of shields.

Because high performance neutron shields are almost always hydrogenous, materials of this type are studied most, water being the standard material and lithium hydride the most likely candidate for exacting applications. In one series of experiments, Western [18] made detailed measurements of the penetration of a narrow beam of reactor radiation through slabs of 3% borated polyethylene and lead. The slabs were relatively thin: up to 15 in. for the borated polyethylene and 6 in. for the lead. As a consequence, the uncollided flux of neutrons or gamma rays was very evident in the observed angular distributions of the penetrating radiation. Figure 1 shows the fast neutron dose-rate as measured at different angles from the slab normal for five slab thicknesses. It is seen that the radiation is easily described as a fairly sharp peak in line with the source beam (0°) and a scattered component of nearly constant shape. The former is attenuated faster than the latter and extrapolation indicates that the strong central peak would merge into the scattered component at about 125 cm. For the purpose of analyzing these thinner slabs, however, the two-component concept, which had previously been put forward by Moteff [7], was used by Beissner [19] in applying the method of invariant embedding to parallel calculations. Beissner's results are on the whole in good agreement, but simple modifications of his theory which would be easy to use are not reliable for high energy neutrons.

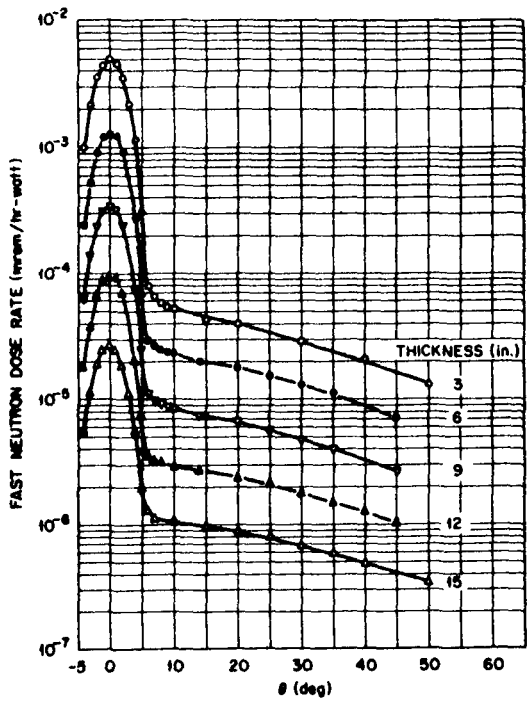


Figure 1. Angular distribution of fast neutron dose rate from particular thicknesses of 3% borated polyethylene slabs (R = 192 in)

In a more recent series of measurements, Verbinski [20] studied fast neutron attenuation in LiH, since this problem will be of direct importance in the design of high performance shields such as those for space power applications of reactors. Using an electron linear accelerator and a lead target, he was able to obtain a pulsed neutron source of energy much like that of uranium-235 fission (Fig. 2). Unfortunately it was necessary for him to use a lead filter to reduce the bremsstrahlung flash which would otherwise overload his scintillator detector. This was achieved by using a 20 cm cube of lead both as the source and as the filter; recesses on opposite sides of the cube permitted the entry of electrons to its center and "venting" of the excess beam. The dual disadvantage of the filter is that it enriches the low-energy end of the spectrum by neutrons inelastically scattered in lead and that it hardens the spectrum above about 4 MeV because of the drop-off of the lead cross section with increasing energy. The spectrum of the source which was used is shown in Fig. 3, along with the leakage spectra for LiH. These spectra were obtained by time-of-flight techniques with a 50 m flight path. Spectra computed with the NIOBE code [1], using the measured source spectrum and assuming the source to be a 10 cm radius sphere and the LiH to be a concentric spherical shell of inner radius 37 cm, are also shown in Fig. 3. The calculations do not reflect the spectral detail of the measurements around the $4\frac{1}{2}$ MeV peak in the Li cross section. This is understandable on the basis of the different geometries. The experiment is essentially a good geometry measurement, emphasizing uncollided flux, whereas in the calculation scattered neutrons are more likely to be counted.

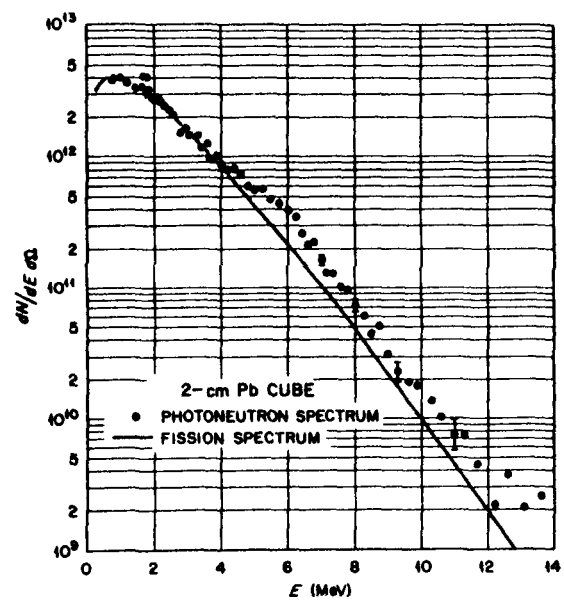


Figure 2. Spectrum of neutrons from 2 cm lead cube

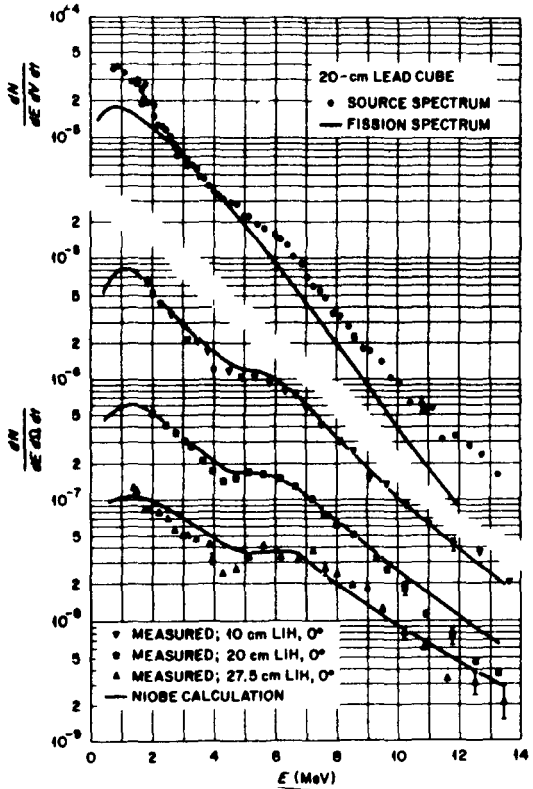


Figure 3. Neutron spectrum from 20 cm lead cube and normal leakage spectra through three thicknesses of LiH

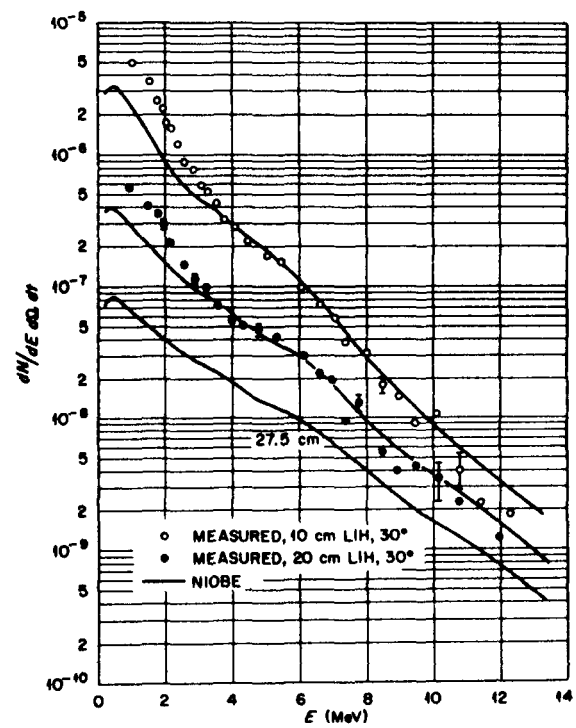


Figure 4. Comparison of measured spectra from 10 and 20 cm of LiH with NIOBE calculation. Data at 30° to normal

Since scattering implies energy reduction, the calculations mostly count neutrons that have travelled at more than one energy (one before and one after scattering) with a resultant smearing in sensitivity to the cross-section structure. Unfortunately, at this point, the agreement between calculation and experiment deteriorates. For measurements at 30° to the exit normal of the slab, the experiments show an upward trend below 3 MeV which the calculations do not follow (Fig. 4). This discrepancy is not yet resolved. A more serious discrepancy exists in the comparison of attenuation as measured by sulfur foil activation. The calculations give an attenuation which is smaller than the experimental value by a factor of about two for the 27.5 cm slab, and a relaxation length 25% greater than that observed. It is the intention of Verbinski to have other calculations made with a different method such as the ORNL 05R code.

More recently, Verbinski and co-workers [21] have applied their time-of-flight techniques to studies of the spectra of neutrons penetrating water slabs up to 40 cm thick. Although the instrument calibration had not been completed at this writing, the detail in the spectra (Fig. 5) is interesting for two reasons. First, it shows the expected spectrum hardening. Second, it shows the resonance structure in the oxygen cross section much exaggerated, the reason being that the observations are made on the beam axis, so that the uncollided flux is principally what is measured. Measurements at 30° to the exit normal show much less structure in the spectra, as is to be expected for scattered radiation. These data will afford a useful test for calculations, but no such test has yet been made.

Although measurements of spectra in shields by time-of-flight techniques are interesting and useful, they are not as directly pertinent to reactor shielding as measurements with a reactor source, for which this technique is of course not suited. The development of spectrometers for shielding research has been difficult and costly. A new one, using semiconductors to record the energies of the Li^6 $(n,\alpha)H^3$ reaction products, has been developed and used by Bokhari *et al.* [22]. Resolution is excellent and the detector can work in a high gamma-ray background, but sensitivity is still not as high as desirable. Spectra in water of outwardly directed neutrons from the Bulk Shielding Reactor I at Oak Ridge National Laboratory (ORNL) for distances up to 60 cm are shown in Fig. 6. Other spectra were taken of neutrons travelling other than normally outward.

A question which has beset shield designers for some time is the effect of angle of incidence of radiation on a shield. This was studied for gamma-rays some years ago by Kirn, Kennedy, and Wyckoff [23], and by Scofield and Haggmark [24]. Recently, similar work has been done by Cain *et al.* [25] using the elevatable reactor at the ORNL Tower Shielding Facility. Using slabs of concrete of different thicknesses mounted over a hole in the ground, and moving the reactor in air on a 100 ft radius arc in the overhead vertical plane, they studied the penetration of reactor neutrons (dose was measured) as

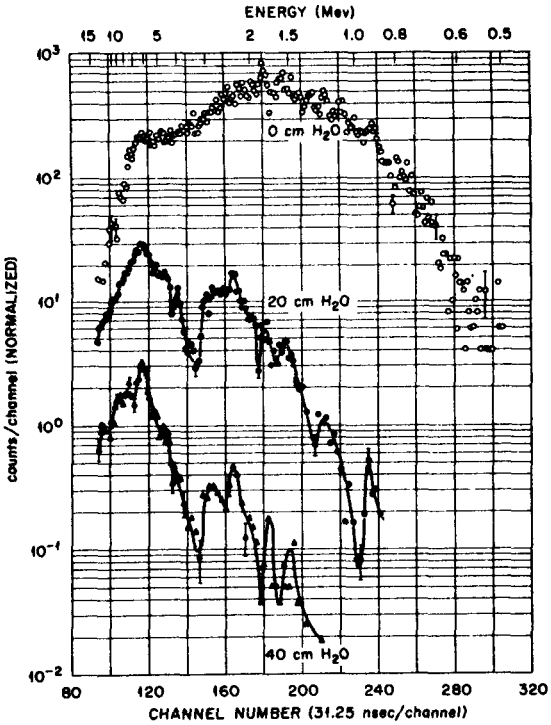


Figure 5. Comparison of leakage spectra through 20 and 40 cm of water with unattenuated source spectrum (0° from slab normal)

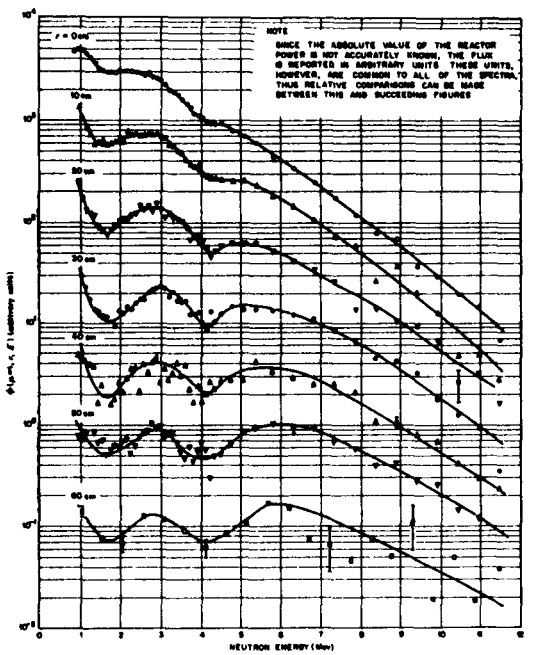


Figure 6. BSR-1 fast neutron spectra at $\theta = 0°$ and $r = 0$, 10, 20, 30, 40, 50, and 60 cm

a function of angle of incidence. The results, Fig. 7, show that the relaxation length is constant with penetration up to thicknesses of 36 in., and that, with the exception of very short transition regions at the beginning, the relaxation length is independent of the angle of incidence of the radiation. Measurements were made as a function of depth in the hole

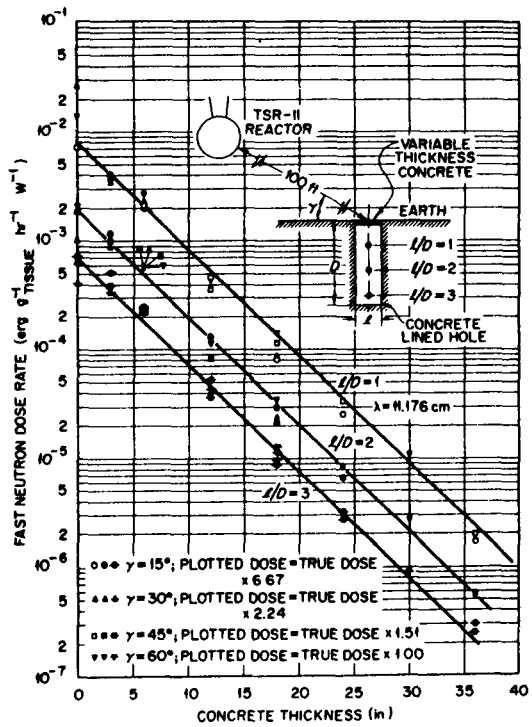


Figure 7. Normalized fast neutron dose rate vs concrete thickness

(in units of the diameter of the hole, l/D on the figure), which gives an indication of the angular distribution of the penetrating radiation. Since all the curves for different depths in the hole are parallel, the angular distribution is again essentially constant for all angles of incidence. A number of other conclusions can be drawn from the data which were obtained in this series of experiments.

An interesting new technique has been developed and used by Schamberger, Celnik and Ross [26], for the direct experimental determination of overall neutron-induced gamma-ray production in simple shield configurations. The neutron source they used was Po-Be and the detector was a NaI(Tl) scintillator. Simple geometry experiments provided a check not only on the Monte Carlo calculational technique (ADONIS, see Table 1) but also on the gamma-ray production cross sections which were used. Agreement was generally good, but the experiments indicated that improvements were needed in the data for inelastic scattering gamma-ray production.

SURVEYS OF RADIATION LEVELS AROUND OPERATING REACTORS

In a program to assess the performance of installed reactor shields, ORNL assembled a set of supersensitive radiation-detecting instruments on a van-type truck which could be driven to a reactor site. Included were an anthracene scintillation gamma-ray dosimeter and a large BF_3 counter. The BF_3 counter was used to measure both thermal and

fast neutrons. For the latter, it was covered with a specially designed Cd-covered polyethylene moderator [27]. Surveys of radiation levels were made at the following reactors: the University of Florida reactor, the University of Illinois TRIGA Mark II, the Westinghouse Testing Reactor, the Virginia Polytechnic Institute UTR 10, the University of Virginia Nuclear Research Reactor, and the ORNL Graphite Reactor. During the surveys, the reactors were operated at full power, and the operators were advised of locations with above normal levels. In general, the shield designs were found to be satisfactory and levels at least as low as required.

In a special project, the truck was put on board the N.S. *Savannah*, and a very complete survey was made of the exterior of the reactor's shield. Not only were one minute integration-type measurements taken on each square yard of the shield's exterior, but the whole exterior was scanned with the instruments. The scanning person listened with earphones for abnormal increases in the detector count rate. As was the case for the stationary reactors, the *Savannah* shield was found to be sound and to have no areas of excessive leakage.

RADIATION SHIELDING INFORMATION CENTER

Recognizing the importance of collecting, preserving, and disseminating radiation shielding information, the U.S. Atomic Energy Commission has instituted at ORNL a radiation shielding information center. The center collects documents with information pertinent to radiation shielding, evaluates these documents as to their pertinence to a variety of subject categories, and makes a record of the references and evaluation on a high-speed computer tape. The tape is then used to print a bibliography of radiation shielding, the most recent edition of which was distributed in September 1963 [28].

In addition, the center collects radiation shielding computer codes for the purpose of making them more generally available. Codes which are received are studied and made operable at ORNL, if it is possible to do so, with either the IBM-7090 or the CDC-1604 computer. The codes and pertinent documentation are then forwarded to the relevant computer manufacturers who have in these two cases agreed to make them available to requesters free of charge. The center's program for studying computer codes is aimed at determining those problems for which the several codes are best suited. The center also serves as a source of bibliographic type information on radiation shielding to all persons who request its assistance.

REFERENCES

1. Preiser, S., *et al., A Program for the Numerical Integration of the Boltzmann Transport Equation*, ARL Technical Report 60-314, U.S. Department of Commerce, Washington, D.C. (Dec. 1960).
2. Alexander, J. H., and Hinman, G. W., *A Modified DSN Program for the Solution of the One-Dimensional Anisotropic Transport Equation*, General Atomics report GA-4972-GAPLSN (March 1964).
3. Anderson, D. C., and Shure, K., Nuclear Sci. Eng., *8* (3), 260 (1960).
4. Shure, K., *P-3 Multigroup Calculations of Neutron Attenuation*, Westinghouse Electric Corporation report WAPD-T-1563 (May 1963).
5. Bohl, H. Jr., *et al., P3MG1 — A One-Dimensional Multigroup P-3 Program for the Philco-2000 Computer*, Westinghouse Electric Corporation report WAPD-TM-272 (Sept. 1963).
6. Certaine, J., de Dufour, E., and Rabinowitz, G., Nuclear Sci. Eng., *12* (3), 446 (1962).
7. Moteff, J., in Proceedings of Nucleonics in Flight Symposium, Dallas, Texas, March 1961, p. 87, American Nuclear Society.
8. Schamberger, R. D., in *Reactor Handbook* (E. P. Blizard and L. S. Abbott, eds.), p. 84, *III*, B, Interscience, New York (1962).
9. Chapman, G. T., and Storrs, C. L., *Effective Neutron Removal Cross sections for Shielding*, USAEC report AECD-3978 (1955).
10. Martin, J. T., and Yalch, J. P., *Shielding Computer Program 14-0, 14-1, Reactor Shield Analysis*, General Electric Co. report XDC 59-2-16 (1959).
11. Peterson, D. M., *Shield Penetration Program*, General Dynamics Co. report GD/FW L-63, FZK 9-170, NARF-61-39T (Dec. 1961).
12. Peterson, E. G., *MAC — A Bulk Shielding Code*, HW-73381 (April 1962).
13. *Reactor Physics Constants*, USAEC report ANL-5800, Second Edition, p. 773 (July 1963).
14. Kalos, M. H., Nuclear Sci. Eng., *16* (2), 227 (1963).
15. Steinberg, H. A., Nuclear Sci. Eng., *15* (2), 142 (1963).
16. Kalos, M. H., Nuclear Sci. Eng., *16* (1), 111 (1963).
17. Troubetskoy, E. S., *Minimum Weight Shield Synthesis*, UNC 5017 (Part A) (1962).
18. Western, G. T., *Energy and Angular Distribution Experiment*, Vol. 1, NARF-62-16T (FZK-9-183-1) (Dec. 1962); Vol. 2, NARF-62-16T (FZK-9-183-2), General Dynamics Co. (Sept. 1963).
19. Beissner, R. E., *An Analysis of Fast Neutron Energy-Angle Distributions*, NARF-63-5T (FZK-9-186), General Dynamics Co. (Aug. 1963).
20. Verbinski, V. V., Trans. Am. Nucl. Soc., *6*, 190 (June 1963).
21. Verbinski, V. V., *et al.*, in USAEC report ORNL-3499, *1*, 108 (1963).
22. Bokhari, M. S., Verbinski, V. V., and Kington, J. D., in USAEC report ORNL-3499, *1*, 98 (1963).
23. Kirn, F. S., Kennedy, R. J., and Wyckoff, H. O., Radiology, *63*, 94 (July 1954).
24. Scofield, N. E., and Haggmark, L. G., *Penetration of Plane Normal and Plane Slant Gamma Rays Through Slabs of Aluminum and Steel. II. Angular and Energy Spectra (Photon Number Flux)*, U.S. Naval Radiation Defence Laboratory report USNRDL-475 (Oct. 1960).
25. Cain, V. R., Holland, E. B., and Clifford, C. E., *Measurements of Radiation Intensities in Vertical Concrete-Lined Holes and an Adjoining Tunnel at the Tower Shielding Facility*, USAEC report ORNL-3513 (March 1964).
26. Schamberger, R., Celnik, J., and Ross, R., *Shield Small Source Experiments*, United Nuclear Corporation report UNC-5072 (MCR-1603) (Nov. 1963).

27. Blosser, T. V., and Freestone, R. M., Jr., Nucleonics, *21*, 56 (Feb. 1963).

28. *Cumulative Bibliography of Literature Examined by the Radiation Shielding Information Center*, USAEC report ORNL-RSIC-2 (Sept. 1963).

29. Steinberg, H., and Aronson, R., WADD TR-58-771.

30. Wells, M. B., *Monte Carlo Slab Geometry Shielding Code C-18, FZK-134*, Vol. 3 (December 1961).

31. Guber, W., Shapiro, M., *A Description of the SANE and SAGE Programs*, United Nuclear Corporation report UNUCOR-633 (1963).

32. MacDonald, J. E., Martin, J. T., and Jalch, J. P. P., *Specialized Reactor-Shield Monte Carlo Program 18-O*, XDC 61-1-91 (1961).

33. Kam, F. B. K., *et al.*, *The O5R Code*, ORNL-3622 (to be published).

34. Eisenman, B., Henessy, E., *ADONIS — An IBM-7090 Monte Carlo Shielding Code Which Solves the Transport of Neutrons and Gamma Rays in Three-Dimensional Rectangular Geometry*, United Nuclear Corporation report UNUCOR-635 (1963).

35. Loechler, J. J., MacDonald, J. E., *Flexible Monte Carlo Program*, General Electric Co. report APEX 706 (April, 1961).

ABSTRACT - RÉSUMÉ - АННОТАЦИЯ - RESUMEN

A/260 Etats-Unis d'Amérique

Progrès récents dans les protections des réacteurs aux Etats-Unis

par E. P. Blizard et P. S. Mittelman

La précision des méthodes employées pour les études des protections et l'amélioration des protections restent des facteurs importants de l'utilisation des réacteurs. Pour les grandes centrales nucléaires, cette importance tient à la nécessité de limiter le coût de la construction tout en assurant de bonnes performances; mais pour beaucoup d'autres utilisations, telles que la production d'énergie pour les engins spatiaux, la protection peut conditionner le succès même du projet, du fait des limitations de poids et de taille. C'est pourquoi on poursuit les recherches en vue d'améliorer les méthodes d'étude des protections, d'accroître la précision de l'évaluation des protections et d'améliorer les matériaux.

Aux Etats-Unis, les recherches et les réalisations dans ce domaine au cours des dernières années ont revêtu plusieurs aspects. Pour le calcul de l'atténuation due aux protections, on s'est efforcé de mettre à profit les progrès importants réalisés dans le domaine des ordinateurs. Pour ce qui est des méthodes d'étude des protections, la réalisation la plus récente est peut-être la mise au point d'une méthode de synthèse des protections consistant à choisir systématiquement les matériaux convenant le mieux aux diverses régions d'une protection. Cette méthode tient compte des anciennes méthodes d'optimisation. En ce qui concerne les instruments employés pour étudier les protections, la base même des progrès réalisés a été l'apparition du détecteur à semi-conducteur, qui a permis d'atteindre un pouvoir de résolution élevé dans la spectrométrie des neutrons. Grâce à cet appareil et à d'autres instruments, on a pu procéder à des mesures nouvelles et plus précises de divers matériaux de protection intéressants. La mise au point, dans le cadre de la recherche sur les protections, de méthodes de séparation permettant d'obtenir une meilleure évaluation d'un spectre a contribué à faire avancer la recherche expérimentale sur les protections; en outre, ces méthodes ont reçu de très larges applications dans d'autres domaines.

Les progrès les plus marquants récemment réalisés dans le calcul de l'atténuation due aux protections des réacteurs découlent en grande partie de l'application de la méthode de Monte-Carlo, pour laquelle on a encore perfectionné les méthodes d'échantillonnage selon l'importance et selon un choix raisonné et l'emploi des valeurs espérées. Une autre méthode — l'intégration numérique de l'équation de Bolzmann (code NIOBE) — s'est révélée très utile pour calculer les spectres de neutrons dans les protections, bien que, du fait des performances actuelles des calculatrices, cette méthode ne soit pas applicable pour mesurer les distributions de sources dans lesquelles la fraction diffusée vers l'avant peut prédominer. Lorsque la géométrie est complexe, il s'est révélé utile d'intégrer point par point des noyaux d'atténuation.

Les expériences relatives aux protections se sont surtout développées du point de vue de la précision des mesures. C'est ainsi que l'on a obtenu à l'aide d'un spectromètre à semi-conducteur les spectres de neutrons dans une protection constituée par de l'eau autour d'un réacteur. On a mesuré la propagation à travers le béton du rayonnement émis par une source collimatée, pour divers angles d'incidence. De même, on a fait des mesures précises de la production de rayons gamma secondaires dans divers matériaux de protection entourant une petite source de neutrons; on a utilisé les résultats de ces mesures comme données pour la méthode de synthèse des protections, dans laquelle l'étude des protections est fondée sur le choix de matériaux ou de mélange d'une efficacité optimale, en fonction de leur densité, de l'atténuation des neutrons et des rayons gamma, et de la production de rayons gamma secondaires.

La Commission de l'énergie atomique des Etats-Unis, reconnaissant l'importance des renseignements relatifs aux protections, a établi au Laboratoire national d'Oak Ridge un centre d'information sur les protections contre les rayonnements. Ce service

rassemble et évalue les renseignements relatifs aux protections, établit sur bandes magnétiques une liste annotée des sources et publie de temps à autre un bulletin (qui est une bibliographie annotée). Il rassemble également des programmes pour les calculs de protections, et étudie leurs avantages relatifs. Il aide aussi les spécialistes à trouver des renseignements sur la protection contre les rayonnements ou à obtenir des programmes.

A/260 США

Последние достижения в развитии защиты реактора в США

Э. П. Близард, П. С. Мителмен

Точность методов расчета защиты реактора и разработка усовершенствованных защит попрежнему имеют важное значение при расчетах ядерных реакторов. Для реакторов больших атомных электростанций необходимо обеспечить экономичную конструкцию, строго выдерживая при этом проектные характеристики, в то время как при использовании реакторов в энергетических источниках космических летательных аппаратов, защита играет основную роль в успехе проекта вследствие требований по ограничению веса и размера. Поэтому в настоящее время продолжается совершенствование методов расчета защиты, улучшения точности их анализа и повышения качества материалов для изготовления защиты.

Исследовательские работы в этих областях в США в последние годы велись в различных направлениях. Для основных расчетов ослабления радиации были использованы достижения техники вычислительных машин. Самым новым в развитии расчета защит является способ синтеза защиты. Этот метод заключается в систематическом выборе для разных слоев защиты материалов, обеспечивающих наилучшую эффективность; в нем использованы старые методы оптимизации. Главным достижением в приборах для изучения защиты является появление полупроводниковых детекторов, которые дали возможность получить высокое разрешение в нейтронной спектрометрии. Эти и другие новые приборы дали возможность провести новые и более точные измерения для некоторых защитных материалов. Разработанный в связи с исследованиями в области защиты метод «распутывания», который дает возможность получить наилучшую оценку спектра, например, по измеренному распределению амплитуд импульсов, оказался полезным не только при проведении экспериментальных исследований защиты, но также имеет широкое применение в других областях науки.

Наибольшее усовершенствование в основных расчетах защиты реакторов связано главным образом с методом Монте-Карло, для которого получили дальнейшее развитие методы значимости выборки, выборки по обобщенным группам и применение ожидаемых величин. Другой метод — численное интегрирование уравнения Больцмана (код NIOBE) — явился очень важным при расчете нейтронных спектров в защите, хотя современные возможности вычислительной техники не позволяют применить его к задачам, в которых исходные распределения имеют преобладающую составляющую рассеяния вперед. Для задач со сложной геометрией целесообразно проводить интегрирование точечных ядер ослабления.

Успехи в экспериментах по защите связаны главным образом с областью измерений. Так, полупроводниковый спектрометр был использован для получения нейтронных спектров в водяной защите вокруг реактора. Пропускание излучения через бетон было измерено для случая колиммированного источника под разными углами падения. Были проведены точные измерения возникающего вторичного гамма-излучения в различных материалах, окружающих маленький нейтронный источник. Результаты этих последних измерений были использованы в качестве входных данных для метода синтеза защиты. По этому методу защита строится систематическим выбором материалов или смесей материалов для получения оптимальной характеристики путем оценки плотности материалов, ослабления нейтронов и гамма-излучения, а также возникновения вторичного гамма-излучения.

Понимая важность систематизации информации по защите, Комиссия по атомной энергии США образовала Информационный центр по защите от излучения при Окриджской национальной лаборатории. Эта организация собирает и оценивает информацию по защите, записывает на ленте вычислительной машины аннотированный список источников и периодически публикует список этой информации. Этот центр также собирает коды для вычислительных машин по защите и оценивает их относительные возможности. Центр помогает находить информацию по защите от радиации или коды для вычислительных машин.

A/260 Estados Unidos de América

Recientes avances en blindaje de reactores en los Estados Unidos

por E. P. Blizard y P. S. Mittelman

La exactitud de los métodos de cálculo del blindaje y el desarrollo de blindajes perfeccionados siguen teniendo gran importancia en las aplicaciones de reactores nucleares. En reactores de grandes centrales nucleares, la importancia reside en la necesidad de una construcción barata en contraposición

a la garantía de eficacia del proyecto, mientras en otras muchas aplicaciones, como producción de energía para vehículos espaciales, el blindaje juega un papel primordial en el éxito del proyecto, debido a las limitaciones de tamaño y peso. Por esto continuamos esforzándonos en mejorar los métodos de proyecto de blindaje, para aumentar la exactitud de los cálculos y perfeccionar los materiales de blindaje.

La investigación y desarrollo en los Estados Unidos durante los últimos años, dedicados a estos puntos, han tomado diversos aspectos. En los cálculos de la atenuación a través del blindaje, se ha prodigado mucha inventiva en el aprovechamiento de los grandes progresos de las máquinas calculadoras. En los métodos de proyecto de blindaje, el avance más reciente puede que haya sido el desarrollo de una técnica de síntesis de blindaje, por la que se eligen sistemáticamente los materiales óptimos para las diversas zonas de un blindaje. Este método engloba también los antiguos métodos de optimización. En instrumentación para estudios de blindajes, la mejora clave ha sido la aparición del detector semiconductor, que ha proporcionado un gran poder de resolución en la espectrometría del neutrón. Con este y otros instrumentos se han hecho medidas nuevas y más claras en varios materiales útiles para blindaje. En relación con la investigación sobre blindajes, el desarrollo de técnicas de discriminación para obtener una estimación mejor de un espectro, por ejemplo a partir de una distribución medida de altura de impulsos, no sólo ha favorecido la investigación experimental sobre blindajes, sino también ha tenido un empleo científico amplio fuera del campo de los blindajes.

Los avances recientes que han tenido más éxito en el cálculo básico de atenuación de blindajes de reactores están relacionados principalmente con el método de Monte Carlo, para el cual se ha impulsado el desarrollo de las técnicas del muestreo con importancias, muestreo generalizado por cuotas y el uso de valores esperados. La integración numérica de la ecuación de Boltzmann (código NIOBE) ha sido otra técnica muy útil en el cálculo del espectro de neutrones en blindajes, aunque no es aplicable en las distribuciones de fuente en las que predomine la componente de dispersión tangencial, por las limitaciones de capacidad de las calculadoras actuales. En los casos en que la geometría es complicada, ha sido conveniente integrar punto a punto los núcleos de atenuación.

Los experimentos sobre blindajes han avanzado principalmente en lo referente al detalle de las medidas. De este modo se ha obtenido, con un espectrómetro con semiconductores, el espectro de neutrones en un blindaje de agua alrededor de un reactor. La transmisión de radiación en el hormigón se ha medido en el caso de una fuente colimada con diversos ángulos de incidencia. Se han hecho unas medidas claras de la producción de radiaciones gamma secundarias en diversos materiales de blindaje que rodeaban una pequeña fuente de neutrones. Estas últimas medidas se han realizado con objeto de proporcionar datos de partida para la técnica de síntesis de blindaje, con la que los blindajes se proyectan sistemáticamente eligiendo materiales o mezclas de materiales que den un rendimiento óptimo al tomar en consideración su densidad, atenuación de neutrones y radiación gamma y producción de radiación gamma secundaria.

La Comisión de Energía Atómica de Estados Unidos ha creado un Centro de información de blindaje a las radiaciones en el Oak Ridge National Laboratory, reconociendo así la importancia de tener al día la información sobre blindajes. Esta organización reúne y valora la información sobre blindajes, registra en cintas de calculadora listas de fuentes de información y publica periódicamente un boletín (que es una bibliografía comentada). También recopila códigos de cálculo de blindajes e investiga sus capacidades relativas. A petición de los proyectistas de blindajes les ayuda a encontrar información u obtener códigos.

Некоторые новые аспекты применения сопряженных функций и теории возмущений в расчетах реакторов и защиты

А. А. Абагян, Г. И. Дружинина, А. А. Дубинин, С. М. Зарицкий, В. В. Орлов, В. Я. Пупко, А. П. Суворов, Л. Н. Усачев, Р. П. Федоренко

Применение формул теории возмущений для определения критических параметров ядерного реактора оказалось весьма удобным в практике расчетов и экспериментальных исследований реакторов [1–5]. Работы [6, 7] расширили область применения теории возмущений для произвольных линейных функционалов в стационарных и нестационарных задачах переноса излучения с заданными источниками. В работе [8] получена формула теории возмущений для отношения чисел различных процессов в стационарном реакторе.

В разд. I обсуждается применение формул работы [8], расширяющих возможности исследований физических характеристик реакторов. Дается пример применения этой теории для вариантных расчетов коэффициента воспроизводства реактора-размножителя. Указывается на возможность использования этой теории для уточнения многогрупповой системы констант по результатам измерений на критических сборках.

В разд. II обсуждается применение формул теории возмущений для эффективного коэффициента размножения $k_{эфф}$ и отношения чисел различных процессов в реакторе для постановки вариационных задач об оптимальном распределении различных материалов в реакторе с произвольным спектром нейтронов [9]. Некоторые аналогичные задачи для $k_{эфф}$ применительно к реактору на тепловых нейтронах были рассмотрены в работе [4].

Разд. III посвящен использованию формул теории возмущений [7, 10] для оптимизации характеристик защиты.

Ввиду того что применение классических методов вариационного исчисления для задач защиты оказывается в ряде случаев затруднительным, процесс оптимизации проводится с использованием идей линейного программирования [11, 12].

I. ТЕОРИЯ ВОЗМУЩЕНИЙ ДЛЯ ОТНОШЕНИЯ ЧИСЕЛ ПРОЦЕССОВ В РЕАКТОРЕ*

1. Краткое изложение и некоторые уточнения вывода, сделанного в работе [8]

Хорошо известное в теории реакторов соотношение теории возмущений для определения критических параметров возмущенного реактора (см., например, [3])

$$-\int\left[\frac{1}{l'_{ai_{fs}}(\vec{r},E)}-\frac{1}{l_{ai_{fs}}(\vec{r},E)}\right]\times$$
$$\times F'(\vec{r},E,\vec{n})\,F^{+}_{\chi}(\vec{r},E,\vec{n})\,d\Omega dE dV+$$
$$+\int\left[w'(E,E',\vec{n},\vec{n}',\vec{r})-\right.$$
$$\left.-w(E,E',\vec{n},\vec{n}'\vec{r})\right]F'(\vec{r},E',\vec{n}')\times$$
$$\times F^{+}_{\chi}(\vec{r},E,\vec{n})\,d\theta+\int\left[\frac{\nu'(\vec{r},E',\vec{n}')}{l'_{f}(\vec{r},E')}\times\right.$$
$$\times\chi'(E,E',\vec{n},\vec{n}',\vec{r})-\frac{\nu(\vec{r},E',\vec{n}')}{l_{f}(\vec{r},E')}\times$$
$$\left.\times\chi(E,E',\vec{n},\vec{n}',\vec{r})\right]F'(\vec{r},E'\vec{n}')\times$$
$$\times F^{+}_{\chi}(\vec{r},E,\vec{n})\,d\theta=0, \qquad (1)$$

где

$$d\theta=d\Omega\,d\Omega'\,dE\,dE'\,dV,$$

получается из уравнения для потока нейтронов $F'(\vec{r},E,\vec{n})$ в возмущенном реакторе, параметры

* Раздел написан Л. Н. Усачевым и С. М. Зарицким.

которого обозначаются буквами со штрихами

$$\frac{\partial F'(\vec{r}, E, \vec{n})}{\partial S}+\frac{F'(\vec{r}, E, \vec{n})}{l'_{at_{fs}}}-$$
$$-\int w'(E, E', \vec{n}, \vec{n}', \vec{r})\times$$
$$\times F'(\vec{r}, E', \vec{n}')\,dE'\,d\Omega'=\int\frac{F'(\vec{r}, E', \vec{n}')}{l'_f(\vec{r}, E')}\times$$
$$\times\nu'(\vec{r}, E')\,\chi(E, E', \vec{n}, \vec{n}', \vec{r})\,dE'\,d\Omega', \quad (2)$$

и уравнения для ценности нейтронов в невозмущенном реакторе

$$\frac{-\partial F^+_\chi(\vec{r}, E, \vec{n})}{\partial S}+\frac{F^+_\chi(\vec{r}, E, \vec{n})}{l_{at_{fs}}}-$$
$$-\int w(E, E', \vec{n}, \vec{n}', \vec{r})\times$$
$$\times F^+_\chi(\vec{r}, E'\vec{n}')\,dE'\,d\Omega'=\int\frac{F^+_\chi(\vec{r}, E', \vec{n}')}{l'_f(\vec{r}, E)}\times$$
$$\times\nu(\vec{r}, E)\,\chi(E, E', \vec{n}, \vec{n}', \vec{r})\,dE'\,d\Omega'. \quad (3)$$

Чтобы получить соотношение (1), уравнения (2) и (3) перекрестно умножаются на F^+_χ и F, вычитаются одно из другого и интегрируются по всем энергиям, направлениям скоростей и объему реактора вплоть до внешней границы с пустотой.

Для получения соотношения теории возмущений по отношению к произвольному линейному функционалу от потока нейтронов в работе [7] были использованы аналогичные операции над взаимно сопряженными уравнениями, сформулированными в работе [6]. При этом рассмотрена наиболее общая нестационарная задача о распространении нейтронов от заданных источников.

Чтобы получить соотношение теории возмущений для отношения чисел процессов в стационарно работающем реакторе, описываемом однородными уравнениями, в работе [8] введено понятие ценности нейтрона любого предыдущего n-го цикла по отношению к процессу в выделенном (нулевом) цикле F^+_n. Система уравнений для этих ценностей при выводе искомого соотношения играет роль сопряженного уравнения. Если мы, например, интересуемся захватом в i-м изотопе, то эта система уравнений имеет вид

$$-\frac{\partial F^+_0}{\partial S}+\frac{F^+_0}{l_{at_{fs}}}-\int wF^+_0\,dE'\,d\Omega'=\frac{1}{l^i_a(\vec{r}, E)}, \quad (4а)$$
$$-\frac{\partial F^+_1}{\partial S}+\frac{F^+_1}{l_{at_{fs}}}-\int wF^+_1\,dE'\,d\Omega'=$$
$$=\frac{\nu}{l_f}\int\chi F^+_0\,d\Omega'\,dE', \quad (4б)$$
$$\cdots\cdots\cdots\cdots\cdots$$
$$-\frac{\partial F^+_n}{\partial S}+\frac{F^+_n}{l_{at_{fs}}}-\int wF^+_n\,dE'\,d\Omega'=$$
$$=\frac{\nu}{l_f}\int\chi F^+_{n-1}\,d\Omega'\,dE'. \quad (4в)$$

Последовательное решение уравнений (4а), (4б), (4в) совпадает с обычным ходом решения уравнения (3) методом последовательных приближений. Отсюда ясно, что при $n\to\infty$ $F^+_n\to\lambda_i F^+_\chi$. Используя сопряженность левых частей уравнений (3), (4а), (4б), (4в) и левой части уравнения для невозмущенного потока $F(\vec{r}, E, \vec{n})$ [уравнение (2) с параметрами без штрихов] и производя перекрестное умножение и вычитание, получаем цепочку равенств

$$a_i\equiv\int\frac{F}{l^i_a}\,d\Omega\,dE\,dV=\ldots=\int\frac{\nu\chi}{l_f}F^+_n\,Fd\theta=\ldots=$$
$$=\lambda_i\int\frac{\nu\chi}{l_f}F^+_\chi\,Fd\theta. \quad (4г)$$

Отсюда $\lambda_i=\frac{a_i}{\text{ЦНД}}$, где ЦНД $\equiv\int\frac{\nu\chi}{l_f}F^+_\chi Fd\theta$ — нормировочная ценность нейтронов деления.

Суммируя уравнения для F^+_0, F^+_1, ..., F^+_n, получаем уравнение для $\Phi^+_n=\sum_a^n F^+_a$

$$-\frac{\partial\Phi^+_n}{\partial S}+\frac{\Phi^+_n}{l_{at_{fs}}}-\int w\Phi^+_n\,dE'\,d\Omega'-$$
$$-\int\frac{\nu\chi}{l_f}\Phi^+_n\,dE'\,d\Omega'=-\int\frac{\nu\chi}{l_f}F^+_n\,dE'\,d\Omega'+\frac{1}{l^i_a}. \quad (5)$$

Производя ту же процедуру перекрестного умножения, интегрирования и вычитания с уравнениями (2) и (5), а также выделяя изменение числа интересующих нас процессов в реакторе, равное $\delta a_i\equiv a'_i-a_i\equiv\int\frac{F}{l^{i'}_a}dEd\Omega dV-$ $-\int\frac{F}{l^i_a}dEd\Omega dV$ и пользуясь соотношением (4г) $\int\frac{F}{l^i_a}dEd\Omega dV=\int\frac{\nu\chi}{l_f}F^+_nFd\theta$, получаем

$$\delta a_i=\int F'\left(\frac{1}{l^{i'}_a}-\frac{1}{l^i_a}\right)dE\,d\Omega\,dV+$$
$$+\int F'\Phi^+_{in}\left(\frac{1}{l'_{at_{fs}}}-\frac{1}{l_{at_{fs}}}\right)dE\,d\Omega\,dV-$$
$$-\int F'\Phi^+_{in}(w'-w)\,d\theta-\int\left(\frac{\nu'\chi'}{l'_f}-\frac{\nu\chi}{l_f}\right)F'\Phi^+_{in}\,d\theta+$$
$$+\int\frac{\nu\chi}{l_f}F^+_n(F'-F)\,d\theta. \quad (6)$$

Рассматривая только возмущения, оставляющие реактор критическим, то есть подчиняющиеся условию (1), замечаем, что во втором, третьем и четвертом членах правой части (6) можно заменить $\Phi^+_n=\sum_a^n F^+_a$, которая стремится к бесконечности при $n\to\infty$ на $\sum_a^n(F^+_a-\frac{a_i}{\text{ЦНД}}F^+_\chi)$, которая имеет конечный предел

$$\Phi^+=\sum_a^\infty\left(F^+_a-\frac{a_i}{\text{ЦНД}}F^+_\chi\right). \quad (7)$$

Последний член правой части при этом равняется

$$\frac{a_i}{\text{ЦНД}}\int\frac{\nu\chi}{l_f}F_\chi^+(F'-F)\,d\theta.$$

Физический смысл в критическом реакторе имеют отношения чисел процессов (например, отношение числа захватов к числу делений, то есть к мощности реактора) и изменения этих отношений при переходе от невозмущенного реактора к возмущенному.

Изменение отношения чисел захватов в i-м и j-м изотопах, равное

$$\delta\left(\frac{a_i}{a_j}\right)=\frac{a_i+\delta a_i}{a_j+\delta a_j}-\frac{a_i}{a_j}=\frac{a_i}{a_j}\left(\frac{\delta a_i}{a_i}-\frac{\delta a_j}{a_j}\right)\frac{a_j'}{a_j'},\quad(8)$$

можно записать, используя (6) при $n\to\infty$ и (7), в виде

$$\delta\left(\frac{a_i}{a_j}\right)=\frac{a_i}{a_j}\left\{\int\left[\frac{F''}{a_i'}\left(\frac{1}{l_a^{i'}}-\frac{1}{l_a^i}\right)-\frac{F''}{a_j'}\left(\frac{1}{l_a^{j'}}-\frac{1}{l_a^j}\right)\right]dE\,d\Omega\,dV+\right.$$
$$+\int F''\Psi^+\left(\frac{1}{l'_{ai_{fs}}}-\frac{1}{l_{ai_{fs}}}\right)dE\,d\Omega\,dV-$$
$$-\int F''\Psi^+(w'-w)\,d\theta-$$
$$\left.-\int\left(\frac{\nu'\chi'}{l_f'}-\frac{\nu\chi}{l_f}\right)F''\Psi^+\,d\theta\right\}.\quad(9)$$

Здесь $F''=F'\frac{a^j}{a_j'}$ — поток нейтронов в возмущенном реакторе, нормированный таким образом, чтобы число захватов в j-м изотопе совпало с этим числом в невозмущенном реакторе, а

$$\Psi^+=\frac{\Phi_i^+}{a_i'}-\frac{\Phi_j^+}{a_j'},\quad(10)$$

как это видно из соотношения (9) — функция имеющая смысл ценности нейтрона по отношению к рассматриваемому отношению чисел процессов.

Из соотношения (10) и линейности системы уравнений (4) ясно, что подставив в правую часть уравнения (4а) вместо $1/l_a^i$ линейную комбинацию $\left(\frac{1}{a_i l_a^i}-\frac{1}{a_j l_a^j}\right)$ и последовательно решая уравнения (4), получим сразу ψ^+ как сумму $\sum_\alpha^\infty F_\alpha^+$. При этом вместо двух решается одна система уравнений, и не требуется вычитать из каждого F_α^+ основную гармонику F_χ^+, как это делается в соотношении (7), так как каждым из слагаемых в правой части уравнения она возбуждается с одним и тем же коэффициентом 1/ЦНД, но разного знака. На эту комбинацию, которую целесообразно использовать при расчетах, было указано в работе [12]. В этой работе сделан вывод уравнения для ценности по отношению к дробно-линейному функционалу, исходя из введенного там понятия ценности по отношению к произвольному нелинейному функционалу и из баланса ценностей нейтронов, который был ранее использован в работах [3,7].

Для малых возмущений было показано, что в правой части уравнения для ценности должна стоять функциональная производная от указанного нелинейного функционала по потоку нейтронов. В интересующем нас случае дробно-линейного функционала эта производная равна $\frac{1}{a_i l_a^i}-\frac{1}{a_j l_a^j}$.

Описанный алгоритм теории возмущений был реализован нами практически с использованием 18-группового диффузионного приближения в программе на ЭВМ. Все примеры применения теории возмущений, описываемые ниже, были осуществлены или осуществляются в настоящее время с помощью этой программы.

2. Примеры применения формул теории возмущений

А. Вариантные расчеты реакторов. Изменения конструкции реактора с точки зрения нейтронной физики описываются обычно изменениями концентраций веществ в различных точках реактора. Поэтому для расчета вариантов конструкции реактора с помощью формул (1) и (9) изменения параметров реактора представляются в виде

$$\frac{1}{l'_{ai_{fs}}}-\frac{1}{l_{ai_{fs}}}=\sum_\alpha\delta\rho_\alpha\sigma_{ai_{fs}}^{(\alpha)};\quad w'-w=\sum_\alpha\delta\rho_\alpha w^{(\alpha)};$$
$$\frac{\nu'\chi'}{l_f'}-\frac{\nu\chi}{l_f}=\sum_\alpha\delta\rho_\alpha\left(\frac{\nu\chi}{l_f}\right)^{(\alpha)},$$

где $\sigma_{ai_{fs}}^{(\alpha)}$; $w^{(\alpha)}$; $\left(\frac{\nu\chi}{l_f}\right)^{(\alpha)}$ характеризуют взаимодействие нейтронов с ядрами сорта α.

Чтобы показать удобство применения формул теории возмущений для вариантных расчетов, запишем их для конкретного реактора. Рассмотрим реактор на быстрых нейтронах, который является упрощенной сферической моделью энергетического воспроизводящего реактора. В активной зоне реактора, радиус и объем которой равны 66 *см* и 1204 *л*, 35% объема занимает топливо — окись урана и плутония, 25% объема занимает сталь, 40% — натрий. Концентрации ядер кислорода, плутония, урана, стали и натрия в 1 $см^3$ активной зоны (умноженные на 10^{-24} равны соответственно $\rho_O^I=0{,}01288$, $\rho_9^I=0{,}001106$, $\rho_8^I=0{,}005334$, $\rho_{ст}^I=0{,}0214$, $\rho_{Na}^I=0{,}00888$. В зоне воспроизводства, толщина которой 60 *см*, $\rho_O^{II}=0{,}0272$, $\rho_9^{II}=0$, $\rho_8^{II}=0{,}01355$, $\rho_{ст}^{II}=0{,}0153$; $\rho_{Na}^{II}=0{,}00483$. В стальном отражателе толщиной 20 *см* $\rho_O^{III}=0$, $\rho_9^{III}=0$, $\rho_8^{III}=0$, $\rho_{ст}^{III}=0{,}072$, $\rho_{Na}^{III}=0{,}00345$. Полный коэффициент воспроизводства (КВ) и коэффициент

воспроизводства активной зоны (КВА) равны соответственно 1,458 и 0,595.

Соотношения, определяющие изменения критической концентрации плутония, КВ и КВА при равномерных по активной зоне и зоне воспроизводства изменениях концентраций различных веществ, удобно представить в виде

L	α								
	Pu^{239}	U^{233}	Na	Сталь	O	C	Осколки деления	Mo	Ni
L^{I}	—	0,0413	—0,000119	—0,00000844	—0,000181	—0,000175	0,0673	0,0205	—0,000117
L^{II}	—0,111	0,0000323	—0,0000880	—0,000123	—0,0000658	—0,0000363	—0,0000461	—0,0000839	—0,000193
$L^{I}_{КВ}$	—831	67,9	—10,1	—8,82	—9,23	—11,1	—9,87	—9,54	—12,0
$L^{II}_{КВ}$	315	3,7	—1,72	—3,46	—0,886	—0,502	—52,8	—17,9	—5,48
$L^{I}_{КВА}$	—935	184	6,00	2,55	5,83	7,80	—2,06	—0,947	1,90
$L^{II}_{КВА}$	5,43	—0,422	0,297	0,249	0,272	0,304	0,196	0,135	0,416

$$\delta\varrho_9^I = \sum_N \sum_{\alpha \neq 8,9} L^{\alpha N}\, \delta\varrho_\alpha^N + L_8^I\,(\delta\varrho_8^I + \delta\varrho_9^I);$$

$$\frac{\delta КВ}{КВ} = \sum_N \sum_\alpha L_{КВ}^{\alpha N}\, \delta\varrho_\alpha^N\,; \quad \frac{\delta КВА}{КВА} = \sum_N \sum_\alpha L_{КВА}^{\alpha N} \delta\varrho_\alpha^N\,. \tag{11}$$

Здесь N — номер зоны. Коэффициенты L, $L_{КВ}$, $L_{КВА}$ формул (11) приведены в таблице.

Эти коэффициенты рассчитаны для малых возмущений, то есть в предположении $F' = F$ и $F'' = F$. Для нахождения пределов применимости этих формул и для выяснения причин возможных расхождений упомянутая программа позволяет делать расчеты с F' и F''.

Б. **Влияние неточности констант.** При расчете коэффициентов для соотношений (11) получаются также коэффициенты, характеризующие влияние неточности в константе любого вещества в любой группе на критическую концентрацию и коэффициент воспроизводства как полный, так и в активной зоне. С помощью этих коэффициентов можно проделать анализ, аналогичный тому, который был выполнен в работе Моорхэда [14]. Напомним, что указанные коэффициенты в работе [14] определялись прямым расчетом.

В. **Анализ экспериментов на критических сборках для уточнения системы констант.** Соотношения теории возмущений уравнения (1) и (9) можно рассматривать как линейные, связывающие разности наблюдаемых и расчетных значений различных величин с неточностями в системе многогрупповых констант, которые, по предположению, вызывают несогласие расчета и эксперимента. Применение соотношений теории возмущений, понимаемых в указанном смысле, для анализа опытов на критических сборках и для планирования таких опытов может дать систематический метод уточнения системы многогрупповых констант для расчета реакторов. Для каждой критической сборки, на которой проводятся эксперименты, можно рассчитать коэффициенты линейных соотношений, связывающих изменение критической концентрации и изменения наблюдаемых на опыте отношений чисел различных процессов с изменениями групповых констант. Имея большое число указанных соотношений для нескольких критических сборок и для многих отношений чисел процессов, можно поставить задачу о подборе констант, наилучшим образом описывающих всю совокупность экспериментов. Такие задачи в наиболее общей постановке могут решаться методами линейного программирования [11], а в частных простых случаях их можно решать простым подбором.

В качестве отношения чисел процессов могут быть использованы отношения чисел делений и захватов в различных изотопах, измеренные в различных точках, а также интегрально по зонам реактора. Могут быть использованы и такие легко измеряемые величины, как реактивности от помещения различных образцов. Действительно, реактивность, обусловленная образцом, помещенным в критический реактор, может быть записана в виде отношения [см. уравнение (3)] $\frac{k-1}{k} = \frac{a_i}{a_j}$, где

$$a_i \equiv \int \frac{FF_\chi}{l_{ai f_s}^{обр}}\, dE\, d\Omega\, dV + \int w_{обр}\, FF_\chi^+\, d\theta + \int \left(\frac{\nu\chi}{l_f}\right)_{обр} FF_\chi^+\, d\theta \tag{12}$$

— дополнительная ценность нейтронов, возникающая за единицу времени при внесении образца,

$$a_j \equiv \text{ЦНД} \equiv \int \left[\frac{\nu\chi}{l_f} + \left(\frac{\nu\chi}{l_f}\right)_{обр}\right] FF_\chi^+\, d\theta \tag{13}$$

— ценность нейтронов деления, испускаемых во всем реакторе за единицу времени. Отсюда видно, что для вычисления вариаций реактивности $\delta\left(\frac{k-1}{k}\right)$ можно воспользоваться тем же алгоритмом, что и для других отношений чисел

процессов. Надо лишь заметить, что в правой части уравнения (4а) в этом случае вместо $1/l_a^i$ и $1/l_a^j$ должны стоять величины, которые, если их умножить на поток нейтронов F и проинтегрировать по энергиям, направлениям скоростей и объему реактора, дадут a_i и a_j, определенные соотношениями (12) и (13). Таким образом, следует заменить в уравнении (4а) и в последующих соотношениях

$$1/l_a^i \to -\frac{F_\chi^+}{l_{aifs}^{\text{обр}}} + \int w_{\text{обр}}\left(E,\ E',\ \vec{n},\ \vec{n}',\ \vec{r}\right) \times$$

$$\times F_\chi^+\left(\vec{r}, E', \vec{n}'\right) dE' d\Omega' + \int \left(\frac{\nu\chi}{l_f}\right)_{\text{обр}} F_\chi^+ \, dE' d\Omega', \quad (14)$$

$$1/l_a^j \to \int \left[\frac{\nu\chi}{l_f} + \left(\frac{\nu\chi}{l_f}\right)_{\text{обр}}\right] F_\chi^+ \, dE' \, d\Omega'. \quad (15)$$

Формула (9) с учетом формул (14) и (15) учитывает не только возможные неточности в константах образцов, но и неточности в константах, описывающих реактор, а также изменение спектра реактора в результате влияния внесенного образца.

Аналогичным образом может быть получена вариация среднего времени жизни мгновенных нейтронов, являющаяся отношением ценности всех нейтронов в реакторе, к ценности нейтронов деления, испускаемых за одну секунду [3]. В этом случае в формулах (4)—(9) надо заменить

$$a_i \to \int \frac{FF_\chi^+}{v} dE \, d\Omega \, dV; \quad 1/l_a^i \to \frac{F_\chi^+}{v};$$

$$a_j \to \int FF_\chi^+ \frac{\nu\chi}{l_f} d\theta; \quad 1/l_a^j \to \int F_\chi^+ \frac{\nu\chi}{l_f} dE \, d\Omega. \quad (16)$$

Такой анализ уже начал производиться при обработке экспериментальных данных, полученных на сборках БФС [15].

Изложенное развитие теории возмущений существенно расширяет область ее применения, которая не ограничивается, конечно, приведенными примерами (см., например,[8]). В частности, становится возможным решение задачи об оптимизации коэффициента воспроизводства или каких-либо других отношений чисел процессов, которое обсуждается в следующем разделе.

II. ИСПОЛЬЗОВАНИЕ ФУНКЦИОНАЛОВ ТЕОРИИ ВОЗМУЩЕНИЙ В ВАРИАЦИОННЫХ ЗАДАЧАХ ОБ ОПТИМАЛЬНОМ РАСПРЕДЕЛЕНИИ МАТЕРИАЛОВ В ЯДЕРНЫХ РЕАКТОРАХ*

Пользуясь теорией возмущений, можно в общем случае ставить задачи об оптимальном распределении различных материалов в реакторе с точки зрения достижения наивыгоднейших свойств, обусловленных действием этих материалов. Примерами таких задач является проблема минимизации критической загрузки реактора и проблема максимального коэффициента воспроизводства в реакторе-размножителе. Идея подхода к решению такой проблемы состоит в формулировании вариационной задачи на отыскание экстремума соответствующего функционала, вариация которого выражается с помощью формул теории возмущений. При этом одновременно может быть зафиксировано какое-то количество других функционалов или условий неинтегрального вида, так что на языке вариационного исчисления мы будем иметь дело с изопериметрической задачей или задачей на условный экстремум [16]. В первой из упоминавшихся задач функционалом является эффективный коэффициент размножения реактора $k_{\text{эфф}}$, вариация которого записывается с помощью формул теории возмущений [3]. Во второй задаче используется формула теории возмущений [8] для дробно-линейного функционала, представляющего собой отношение чисел двух различных процессов в реакторе. Формулы теории возмущений содержат функции эффективности различных материалов, описывающих влияние на величину варьируемого функционала изменения содержания этих материалов. Это позволяет сформулировать вариационную задачу на поиск оптимального распределения данного материала в реакторе.

Ниже рассматривается проблема сведения к минимуму критической загрузки и проблема максимального коэффициента воспроизводства. По аналогии с рассматриваемыми можно сформулировать другие вариационные задачи по оптимизации характеристик реактора (максимальная компенсирующая способность поглощающего материала и др.).

1. Постановка задачи о минимуме критической загрузки реактора

Имеется ядерный реактор с определенными размерами и заданным содержанием конструкционных материалов. При некоторой равномерной концентрации U^{235} в активной зоне реактор имеет определенные значения $k_{\text{эфф}}$ и критической загрузки G_5. Каким образом следует проварьировать по активной зоне распределение U^{235}, чтобы добиться снижения критической загрузки без изменения $k_{\text{эфф}}$, если это возможно?

Подобная проблема рассматривалась Гертцелем [17] для случая теплового реактора с одинаковым замедлителем в активной зоне и отражателе. Методика расчета таких реакторов рассматривается также в книгах [4,18].

В настоящем докладе условие минимизации критической загрузки рассматривается в общем случае для реактора с произвольным спектром нейтронов.

Для определенности предполагаем, что варьируя концентрации U^{235} $\rho_5(\vec{r})$ в точке $\vec{r}$, мы

* Раздел написан В. Я. Пупко и Г. И. Дружининой.

одновременно изменяем содержание только одного компонента k, концентрация которого есть $\rho_k(\vec{r})$. В общем случае существует принципиальная возможность уменьшения критической загрузки данного реактора с $\rho_5 = \text{const} < \rho_{5,0}$ путем соответствующего перераспределения U^{235} в активной зоне. Проблема рассматривается в два этапа: ставится вариационная задача на максимум $k_{эфф}$ при заданной загрузке G_5, а затем обсуждается переход к задаче о минимуме G_5 при фиксированном $k_{эфф}$.

2. Достижение максимума $k_{эфф}$ в реакторе с заданной нагрузкой

Варьируя $\rho_5(\vec{r})$, будем искать максимум $k_{эфф}$ при следующем изопериметрическом условии:

$$G_5 = C \int_{V_{аз}} \rho_5(\vec{r})\, dV. \qquad (17)$$

В соответствии с методом Эйлера [16] строим функционал

$$I(\rho_5) = k_{эфф} + \lambda_1 G_5 \qquad (18)$$

и ищем его безусловный экстремум. Выражение для вариации запишется

$$\delta I(\rho_5) = \delta k_{эфф}(\rho_5) + \lambda_1 \int_{V_{аз}} \delta\rho_5(\vec{r})\, dV. \qquad (19)$$

Первый член выразим с помощью формул теории возмущений [3]

$$\delta k_{эфф}(\rho_5) = \int_{V_{аз}} f(\vec{r}, \rho_5)\, \delta\rho_5(\vec{r})\, dV. \qquad (20)$$

Символом $f(\vec{r}, \rho_5)$ обозначена результирующая ценность нейтронов, генерируемых ежесекундно в точке $\vec{r}$ одним ядром делящегося вещества в результате всех процессов взаимодействия нейтронов с U^{235}. Функция $f(\vec{r}, \rho_5)$ в последующем изложении называется функцией эффективности U^{235}. Зависимость этой функции от $\vec{\rho_5}(r)$ является функциональной. Структура ее такова

$$f(\vec{r}, \rho_5) = f^{(5)}(\vec{r}, \rho_5) - \frac{\rho_{k0}}{\rho_{5,0}} f^{(k)}(\vec{r}, \rho_5), \qquad (21)$$

где $\rho_{5,0}$; ρ_{k0} — концентрации материалов, соответствующие их максимальной плотности. В общем случае

$$f^{15}(\vec{r}, \rho_5) = \frac{k_{эфф}}{ЦНД}\left\{\int_0^\infty \int_{\vec{\Omega}'} \int_0^\infty \int_{\vec{\Omega}} F(\vec{r}, E', \vec{\Omega}') \times \right.$$
$$\times \left[\sigma_f(E') \frac{\nu_f(E')}{k_{эфф}} \chi(E, E', \vec{\Omega}\,\vec{\Omega}') + \right.$$
$$\left. + W^{(5)}(E' \to E, \vec{\Omega}\,\vec{\Omega}')\right] F^+(\vec{r}, E', \vec{\Omega}) \times$$
$$\times dE'\, d\vec{\Omega}'\, dE\, d\vec{\Omega} - \int_0^\infty \int_{\vec{\Omega}} F(\vec{r}, E, \vec{\Omega}) \times$$
$$\left. \times F^+(\vec{r}, E, \vec{\Omega})\, \sigma^{(5)}_{ai_5}(E)\, dE\, d\vec{\Omega}\right\},$$
$$f^{(k)}(\vec{r}, \rho_5) = \frac{k_{эфф}}{ЦНД}\left\{\int_0^\infty \int_{\vec{\Omega}} \int_0^\infty \int_{\vec{\Omega}'} F(\vec{r}, E' \vec{\Omega}') \times \right.$$
$$\times W^{(k)}(E' \to E, \vec{\Omega}\ \vec{\Omega}') F^+(\vec{r}, E, \vec{\Omega}) \times$$
$$\times dE'\, d\vec{\Omega}'\, dE\, d\vec{\Omega} - \int_0^\infty \int_{\vec{\Omega}} F(\vec{r}, E, \vec{\Omega}) \times$$
$$\left. \times \sigma^{(k)}_{ai_5} F^+(\vec{r}, E, \vec{\Omega})\, dE\, d\vec{\Omega}\right\}, \qquad (22)$$

где ЦНД — нормировочная ценность нейтронов деления. Из условия экстремума $\delta I(\rho_5) = 0$ при использовании уравнений (19) и (20) получим уравнение Эйлера рассматриваемой вариационной задачи

$$f(\vec{r}, \rho_5) = \text{const}. \qquad (23)$$

Уравнение (23) есть необходимое условие оптимального рассредоточения заданного количества U^{235} по активной зоне, обеспечивающего максимум $k_{эфф}$ в реакторе с произвольным спектром нейтронов *. Физический смысл этого условия понятен: если функция эффективности U^{235} всюду в активной зоне постоянна, то каждый грамм делящегося вещества в любой точке работает равноценным образом. По смыслу вывода следует, что здесь рассматриваются такие реакторы, для которых при концентрациях U^{235} $0 < \rho_5(\vec{r}) < \rho_{5,0}$ существует экстремум функционала $k_{эфф}(\rho_5)$.

Уравнение (23) позволяет обосновать метод экспериментального определения хода концентрации U^{235} в реакторе, для которого реализуется максимум $k_{эфф}$ при заданной загрузке. Оно может служить также критерием правильности решения и должно использоваться при проведении численных расчетов таких реакторов. Последние выполняются методом итераций, в процессе которых добиваются сведения к постоянному значению функции эффективности U^{235} по объему активной зоны. Возможная итерационная схема расчета заключается в постепенном перераспределении U^{235} по активной зоне в соответствии с ходом рассчитываемой функции эффективности U^{235}.

3. Переход от задачи на максимум $k_{эфф}$ к задаче на минимум загрузки

Пусть для различных значений загрузок рассматриваемого реактора G_5^{I}, G_5^{II}, ... найдены функции $\rho_5^{I}(\vec{r})$, $\rho_5^{II}(\vec{r})$, ..., обеспечивающие максимально достижимые значения $k^{I}_{эфф}$, $k^{II}_{эфф}$, ... Из рис. 1 следует, что при $(\partial k_{эфф}/\partial G_5)_{V_{аз}} > 0$ для любого требующегося значения $k'_{эфф}$ за-

* В книге А. Вейнберга и Е. Вигнера[4] отмечается такое же требование для минимизации критической загрузки теплового реактора.

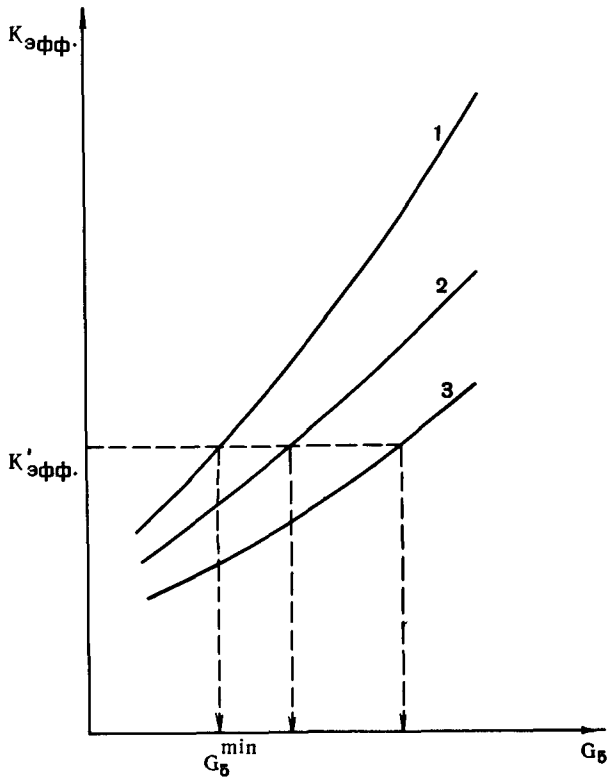


Рис. 1. Схематический график зависимости ($k_{эфф}$ — требуемое значение $k'_{эфф}$)

1 — $\rho_5(\vec{r})$ обеспечивает $k^{max}_{эфф}$; *2* — $\rho_5 = \text{const}$; *3* — $\rho_5 = \rho_5(\vec{r})$, но не оптимально

грузка реактора, соответствующая кривой *1*, будет наименьшей. В связи со сказанным необходимо специально проанализировать знак производной $(\partial k_{эфф}/\partial G_5)_{V_{аз}}$ в реакторах различного типа.

Используя формулы теории возмущений, можно показать, что

$$\left(\frac{\partial k_{эфф}}{\partial G_5}\right)_{V_{аз}} = \frac{\text{const}}{V_{аз}} \int\limits_{V_{аз}} f\,dV = \text{const}\,\bar{f}.$$

Минимизация критической загрузки реактора при $\bar{f}<0$ требует дополнительного рассмотрения. Аналогично доказательству в работе [19] для реакторов с $\rho_5 = \text{const}$ можно показать, что и при переменной концентрации U^{235} детали хода функции $G_5 = f(V_{аз})$ для реакторов различного типа определяются соотношением фактора утечки нейтронов из реактора и показателя эффективности делящегося вещества в реакторе $\eta \sim \bar{f}$. На рис. 2 приведены схематические графики зависимости $G_5 = f(V_{аз})$ для различных по спектру реакторов. Во всех случаях, кроме участка CD, показатель эффективности U^{235} $\eta>0$. На участке CD происходит обесценивание U^{235} ($\eta<0$) и изменяется наклон кривой $G_5 = f(V_{аз})$. Причинами такого

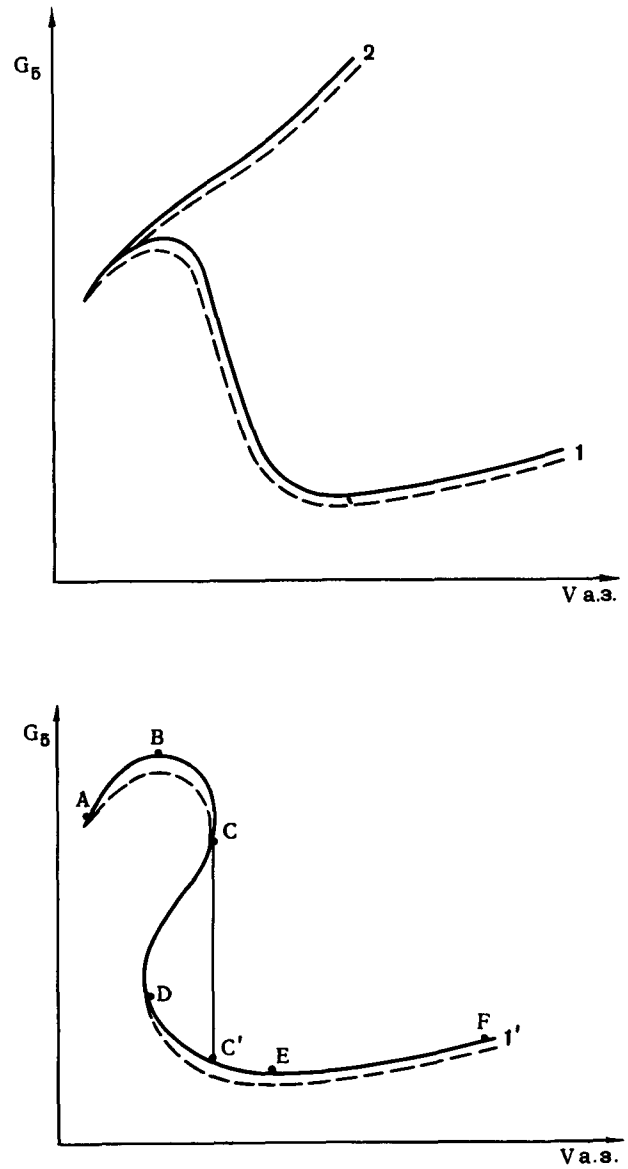


Рис. 2. Схематические графики зависимости $G_5 = f(V_{аз})$:
—— — критические загрузки при $\rho_5 = \text{const}$;
------ — минимизированные критические загрузки.
1 — разбавление U^{235} упруго рассеивающим замедлителем; *2* — разбавление U^{235} неупругим рассеивателем

явления могут быть, например, повышенный радиационный захват нейтронов в делящемся веществе, наличие в реакторе сильных резонансных поглотителей, применение водородсодержащего замедлителя и т. д. Изменение наклона кривой $G_5 = f(V_{аз})$ на участке CD приводит к тому, что из таких реакторов при неизменном объеме активной зоны можно без ущерба для реактивности извлекать в определенных пределах U^{235}, заменяя его замедлителем. Таким образом, минимизация критической загрузки реакторов с $\eta<0$ формально сводится к переходу с участка CD на участок $C'D$.

4. О неравномерности плотности делений в реакторах с минимизированной загрузкой

Перераспределение делящегося вещества в реакторе может неблагоприятно сказаться на коэффициенте неравномерности тепловыделения по активной зоне, поскольку для минимизации загрузки целесообразно перекладывать U^{235} из периферийных областей реактора ближе к центральным. При минимизации критической загрузки реакторов с малыми размерами возникает необходимость наряду с перераспределением делящегося вещества ближе к центру реактора создать одновременно и локальное повышение концентрации U^{235} на периферии активной зоны [17], что несколько улучшает неравномерность поля энерговыделения.

В случае, когда максимум плотности делений из-за смягчающего действия отражателя лежит на границе с последним, обеднение периферийных областей активной зоны U^{235} в пользу центральных способствует одновременно как улучшению неравномерности тепловыделения, так и выигрышу в загрузке реактора.

В гетерогенном реакторе на медленных нейтронах, в котором за счет постепенного увеличения объемной доли замедлителя от центра к периферии активной зоны достигается радиальное выравнивание среднего энерговыделения в отдельных твэлах, может одновременно происходить выравнивание функции эффективности U^{235} по твэлам. Ввиду практической важности вопроса о неравномерности энергсвыделения можно сформулировать вариационную проблему минимизации критической загрузки реактора с наложением ограничения по коэффициенту неравномерности плотности делений в активной зоне.

Метод получения уравнения Эйлера для этой задачи аналогичен вышеописанному. При выводе принимается во внимание изопериметрическое условие на объемный коэффициент неравномерности K_V, а выражение для $\delta K_V(\rho_5)$ составляется на основании формулы работы [8]. В результате получается условие постоянства по активной зоне функции эффективности U^{235}, имеющей для рассматриваемой задачи специальное выражение.

5. Вариационная задача на максимум коэффициента воспроизводства (КВ) в реакторе-размножителе

Имеется реактор-размножитель с заданными размерами и материалами активной зоны и отражателя. Предположим, что реактор сжигает U^{238} и Pu^{239} и накапливает Pu^{239}. Коэффициент воспроизводства ядерного горючего во всем реакторе по определению равен

$$\text{КВ}=\frac{a_8}{a_{f_9}}=$$

$$=\frac{\int\limits_{V_p}\int\limits_0^\infty\int\limits_{\Omega} F\left(\vec{r}, E, \vec{\Omega}\right)\rho_8\left(\vec{r}\right)\sigma_a^8(E)\,dE\,d\vec{\Omega}\,dV}{\int\limits_{V_p}\int\limits_0^\infty\int\limits_{\Omega} F\left(\vec{r}, E, \vec{\Omega}\right)\rho_9\left(\vec{r}\right)\sigma_{af}^9\,dE\,d\,\vec{\Omega}\,dV}. \quad (24)$$

Соотношение между концентрациями U^{238} $\rho_8(\vec{r})$ и Pu^{239} $\rho_9(\vec{r})$ в каждой точке реактора $\vec{r}$ можно варьировать с сохранением условия

$$\rho_8\left(\vec{r}\right)+\alpha\rho_9\left(\vec{r}\right)=\beta, \quad (25)$$

где α и β — некоторые заданные параметры твэла.

Каким способом следует распределить по объему реактора концентрации $\rho_8(\vec{r})$ и $\rho_9(\vec{r})$, чтобы без изменения $k_{\text{эфф}}$ достичь максимума КВ?

Выражения для вариации основного функционала δКВ и изопериметрическое условие $\delta k_{\text{эфф}}=0$ заимствуем из работы [8]. Варьируемой функцией будем считать $\rho_8(\vec{r})$, так как $\rho_9(\vec{r})$ связано с ней соотношением (25).

Учитывая сказанное, запишем:

$$\delta\text{КВ}=\int\limits_{V_p}\varphi\left(\vec{r}, \rho_8\right)\delta\rho_8\left(\vec{r}\right)dV, \quad (26)$$

$$\delta k_{\text{эфф}}=\frac{1}{\text{ЦНД}}\int\limits_{V_p}\xi\left(\vec{r}, \rho_8\right)\delta\rho_8\left(\vec{r}\right)dV=0, \quad (27)$$

где функция $\varphi(r, \rho_8)$ и $\xi(r, \rho_8)$ имеют вид

$$\frac{\varphi\left(\vec{r}, \rho_8\right)}{\text{КВ}}=\int\limits_0^\infty\int\limits_{\Omega}\left\{\left[\frac{\sigma_a^8(E)}{a_8}+\frac{\sigma_{af}^9(E)}{\alpha a_{f_9}}\right]-\right.$$

$$\left.-\left[\sigma_{ai_{f_8}}^8(E)-\frac{\sigma_{ai_{f_8}}^9(E)}{\alpha}\right]\Phi^+\left(\vec{r}, E, \vec{\Omega}\right)\right\}\times$$

$$\times F'\left(\vec{r}, E, \vec{\Omega}\right)dE\,d\vec{\Omega}+\int\limits_0^\infty\int\limits_{\Omega'}\int\limits_0^\infty\int\limits_{\Omega}\times$$

$$\times\left\{\left[W^8\left(E'\to E, \vec{\Omega}\,\vec{\Omega}'\right)-\frac{W^8\left(E'\to E, \vec{\Omega}\,\vec{\Omega}'\right)}{\alpha}\right]+\right.$$

$$+\left[\nu_f^8(E')\sigma_f^8(E')\chi_8\left(E, E', \vec{\Omega}\,\vec{\Omega}'\right)-\right.$$

$$\left.\left.-\frac{1}{\alpha}\nu_f^9(E')\sigma_f^9(E')\chi_9\left(E, E', \vec{\Omega}\,\vec{\Omega}'\right)\right]\right\}\times$$

$$\times F'\left(\vec{r}, E', \vec{\Omega}'\right)\Phi^+\left(\vec{r}, E, \vec{\Omega}\right)dE'\,d\vec{\Omega}'\,dE\,d\vec{\Omega}, \quad (28)$$

$$\xi\left(\vec{r}, \rho_8\right)=\int\limits_0^\infty\int\limits_{\Omega'}\int\limits_0^\infty\int\limits_{\Omega}\left\{\left[W^8\left(E'\to E, \vec{\Omega}\,\vec{\Omega}'\right)-\right.\right.$$

$$\left.-\frac{1}{\alpha}W^9\left(E'\to E, \vec{\Omega}\,\vec{\Omega}'\right)\right]+$$

$$+\left[\nu_f^8(E')\sigma_f^8(E')\chi_8\left(E, E', \vec{\Omega}\,\vec{\Omega}'\right)-\right.$$

$$\left.\left.-\frac{1}{\alpha}\nu_f^9(E')\sigma_f^9(E')\chi_9\left(E, E', \vec{\Omega}\,\vec{\Omega}'\right)\right]\right\}\times$$

$$\times F'\left(\vec{r}, E', \vec{\Omega}'\right) F^{+}\left(\vec{r}, E, \vec{\Omega}\right) dE' d\vec{\Omega}' dE d\vec{\Omega} -$$

$$-\int_0^{\infty}\int_{\Omega}\left[\sigma^{s}_{ai_fs}(E)-\frac{1}{\alpha}\sigma^{g}_{ai_fs}(E)\right]\times$$

$$\times F'\left(\vec{r}, E, \vec{\Omega}\right) F^{+}\left(\vec{r}, E, \vec{\Omega}\right) dE\, d\vec{\Omega}. \quad (29)$$

С помощью соотношений (26) и (27) находим уравнение Эйлера для рассматриваемой задачи

$$\theta\left(\vec{r}, \rho_s\right)=\frac{\varphi\left(\vec{r}, \rho_s\right)}{\xi\left(\vec{r}, \rho_s\right)}=\text{const}. \quad (30)$$

Полученное условие постоянства в реакторе функции эффективности U^{238} для рассматриваемой задачи может быть использовано в численных расчетах для поиска оптимального распределения U^{238} $\rho_s(\vec{r})$.

III. ОПТИМИЗАЦИЯ ФИЗИЧЕСКИХ ХАРАКТЕРИСТИК ЗАЩИТЫ ОТ ИЗЛУЧЕНИЙ*

1. Постановка задачи

Основной задачей конструирования и расчета защиты реактора является нахождение такого расположения защитных материалов (тяжелого и легкого компонентов, поглотителя нейтронов и т. п.), которое обеспечивает выполнение некоторой совокупности требований. Эти требования обычно заключаются в минимальности веса или габаритов защиты при выполнении определенных условий (заданных дозах за защитой, тепловыделениях и т. п.).

Данная задача, таким образом, может быть сформулирована как вариационная задача об оптимуме некоторой величины (F_0) при заданных значениях ряда других величин ($F_1, F_2, \ldots, F_k, \ldots, F_m$).

В некоторых простых случаях она может быть решена как классическая вариационная задача (работы Е. Близарда, Л. Р. Кимеля, Э. Е. Петрова, Д. В. Панкратова, Г. А. Лисочкина и др.[20-22]). Однако в более сложных случаях, когда происходит сильная деформация спектра излучений (например, при введении сильных поглотителей для подавления захватного γ-излучения), приходится описывать процессы в защите сложной многогрупповой системой уравнений и использование классических методов оказывается затруднительным. Кроме того, классические методы применимы в задачах, когда оптимум достигается во внутренней области допустимых изменений концентраций материалов [$0\leqslant\rho_q(\vec{r})\leqslant\rho_q^0$, где $\rho_q(\vec{r})$— концентрация q-го материала в точке $\vec{r}$, ρ_q^0— ее максимальное значение]. В практических задачах, однако, нередко имеет место ситуация, при которой в некоторых областях часть материалов ставить невыгодно, а в других выгодно поставить материал с максимальной плотностью.

Общий подход к решению задачи об оптимальном расположении защитных материалов может быть основан на использовании метода последовательных приближений, n-й шаг которого заключается в переходе от распределений

$$\rho_q^{(n)}\left(\vec{r}\right) \text{ к } \rho_q^{(n+1)}\left(\vec{r}\right)=\rho_q^{(n)}\left(\vec{r}\right)+\delta\rho_q^{(n)}\left(\vec{r}\right).$$

Функции $\delta\rho_q^{(n)}(\vec{r})$ должны быть выбраны так, чтобы:

а) минимизируемая величина F_0 уменьшилась бы как можно больше;

б) величины $F_1, F_2, \ldots, F_m$ оставались равными заданным значениям;

в) переход $\rho_q^{(n)}\left(\vec{r}\right)\to\rho_q^{(n+1)}\left(\vec{r}\right)$ оставался бы в области допустимых значений функций $\rho_q(\vec{r})$.

Для того чтобы выбрать $\delta\rho_q^{(n)}\left(\vec{r}\right)$ необходимо знать, к каким изменениям величины F_k приведет изменение плотностей материалов $\delta\rho_q^{(n)}\left(\vec{r}\right)$ в различных точках $\vec{r}$. Если $\delta\rho_q^{(n)}\left(\vec{r}\right)$ выбирать достаточно малыми, то можно воспользоваться для определения вариаций δF_k формулами теории малых возмущений [7,10], выражающих δF_k через функции потока и «опасности» нейтронов, которые являются решениями основного и сопряженного уравнений в предыдущей итерации. Эти формулы позволяют вычислить функции

$$h_q^k\left(\vec{r}\right)=-\frac{\delta F_k}{\delta\rho_q\left(\vec{r}\right)},$$

являющиеся «эффективностью» материала q в точке $\vec{r}$ по отношению к величине F_k. Знание функций эффективности позволяет нам целесообразным образом выбирать значение $\delta\rho_q^{(n)}\left(\vec{r}\right)$ в каждой итерации. Например, в задаче о безусловном экстремуме $\delta\rho_q^{(n)}\left(\vec{r}\right)$ можно выбрать в виде

$$\delta\rho_q^{(n)}\left(\vec{r}\right)=A\cdot h_q^{(n)}\left(\vec{r}\right),$$

так что там, где эффективность q-го материала по отношению к F_0 максимальна, добавляется большее количество этого материала, там, где $h_q(\vec{r})$ отрицательна, его количество убавляется. Разумеется, для того чтобы можно было пользоваться теорией малых возмущений, необходимо выбирать достаточно малые $\delta\rho_q(\vec{r})$, что может быть обеспечено соответствующим подбором величины A.

Для построения численного алгоритма поисков оптимального решения можно воспользоваться идеями линейного программирования [11,12].

* Раздел написан В. В. Орловым, А. А. Абагяном, Р. П. Федоренко, А. А. Дубининым, А. П. Суворовым.

2. Теория возмущений для характеристик защиты. Функция эффективности защитных материалов

Физические характеристики защиты F_0, F_1..., F_k, ..., F_m в общем случае зависят от потока нейтронов γ-квантов и распределения защитных материалов $\rho_q(\vec{r})$.

Распределение потока нейтронов в стационарном случае описывается уравнением

$$\vec{\Omega}\nabla\varphi + \Sigma(E)\,\varphi - \int d\vec{\Omega}' \int dE' \times \times \varphi\left(\vec{r}, \vec{\Omega}, E\right) \Sigma\left(\vec{\Omega}' \to \vec{\Omega}, E' \to E\right) = = q\left(\vec{r}, \vec{\Omega}, E\right), \quad (31)$$

где $\Sigma(E)$ — полное макроскопическое сечение взаимодействия;

$\Sigma(\vec{\Omega}' \to \vec{\Omega}, E' \to E)$ — дифференциальное сечение, характеризующее переход нейтронов из пучка $(\vec{\Omega}', E')$ в пучок $(\vec{\Omega}, E)$ (здесь учитываются упругие и неупругие переходы, а также деление);

$q(\vec{r}, \vec{\Omega}, E)$ — распределение источников нейтронов.

Среда, в которой мы ищем решение уравнения (31), занимает объем V, ограниченный поверхностью S.

Различные физические характеристики защиты можно записать в виде

$$F_k = \int_V \varphi\left(\vec{r}, \vec{\Omega}, E\right) \times \times P_k\left(\vec{r}, \vec{\Omega}, E\right) d\vec{\Omega}\, dE\, d\vec{r} + \Phi\left[\rho_q\left(\vec{r}\right)\right], \quad (32)$$

где первый член характеризует величины, обусловленные различными процессами взаимодействия нейтронов при прохождении их через защиту. Например, это может быть доза по захватному γ-излучению на поверхности защиты, тепловыделение от нейтронов и захватных γ-квантов, нейтронная доза и т. п. Член $\Phi[\rho_p(\vec{r})]$ характеризует величины, обусловленные внешними источниками γ-квантов (например, γ-кванты из активной зоны). Мы воспользовались здесь приближенным методом учета γ-квантов, хотя описание их с помощью кинетического уравнения не вызвало бы принципиальных затруднений.

Вес защиты есть функционал вида

$$F_0 = \int \sum_q \rho_q\left(\vec{r}\right) dV.$$

Введем в рассмотрение сопряженное к формуле (31) уравнение

$$-\vec{\Omega}\nabla\varphi_k^+ + \Sigma(E)\,\varphi_k^+ - -\int d\vec{\Omega}' \int dE' \varphi_k^+\left(\vec{r}, \vec{\Omega}, E'\right) \times \times \Sigma\left(\vec{\Omega} \to \vec{\Omega}', E \to E'\right) = \frac{\delta F_k}{\delta\varphi}, \quad (33)$$

где $\frac{\delta F_k}{\delta\varphi}$ — функциональная производная F_k по φ.

В случае линейной зависимости от φ функционалов типа (32)

$$\frac{\delta F_k}{\delta\varphi} = P_k\left(\vec{r}, \vec{\Omega}, E\right).$$

Как было показано в работах [6,7,10,13], сопряженная функция $\varphi_k^+(\vec{r}, \vec{\Omega}, E)$ описывает изменение величины F_k, если в «точку» $(\vec{r}, \vec{\Omega}, E)$ впущен один дополнительный нейтрон. В защите эта функция характеризует «опасность» нейтрона по отношению к нейтронной дозе за защитой, дозе по захватному γ-излучению, тепловыделению и т. п.

Знание потоков и функций «опасности» позволяет сформулировать теорию возмущений для различных функционалов.

Можно показать, что

$$\delta F_k = = -\int \varphi_k^+\left(\vec{r}, \vec{\Omega}, E\right) \delta L\varphi\left(\vec{r}, \vec{\Omega}, E\right) d\vec{r}\, d\vec{\Omega} dE + + \int \delta P\left(\vec{r}, \vec{\Omega}, E\right) \varphi\left(\vec{r}, \vec{\Omega}, E\right) d\vec{r}\, d\vec{\Omega}\, dE + + \int \delta q\left(\vec{r}, \vec{\Omega}, E\right) \varphi^+\left(\vec{r}, \vec{\Omega}, E\right) d\vec{r}\, d\vec{\Omega}\, dE + + \int \sum_q \frac{\delta\Phi}{\delta\rho_q} \delta\rho_q\left(\vec{r}\right) d\vec{r}, \quad (34)$$

где δL, δP и δq есть изменения, обусловленные вариацией плотности материалов $\delta\rho_q(\vec{r})$ в операторе кинетического уравнения (31), а также правых частей уравнений (31) и (33).

Как было указано выше, функция эффективности материала q по отношению к различным функционалам F_k имеет вид

$$h_q^k\left(\vec{r}\right) = -\frac{\delta F_k}{\delta\rho_q\left(\vec{r}\right)}. \quad (35)$$

Функция эффективности характеризует изменение функционалов F_k при внесении единичного количества материала q в точку $\vec{r}$. Величины $h_q^k(\vec{r})$ можно вычислить при использовании формулы теории возмущений (34).

Тогда изменение функционалов δF_k при изменении плотности материала q в единице объема около точки $\vec{r}$ на величину $\delta\rho_q(\vec{r})$ будет равно

$$\delta F_k = h_q^k\left(\vec{r}\right) \delta\rho_q\left(\vec{r}\right) + \frac{\delta\Phi}{\delta\rho_q} \delta\rho_q\left(\vec{r}\right).$$

Таким образом, знание функций эффективности дает информацию о том, к каким изменениям в различных функционалах будет приводить некоторое малое изменение плотностей материалов $\delta\rho_q(r)$.

3. Процесс минимизации

Проведение последовательных операций по минимизации некоторого функционала F_0 при условии, что на остальные функционалы F_1 ...

F_m наложены определенные условия

$$F_k \leqslant D_k, \quad k=1, 2, \ldots, m, \qquad (36)$$

заключается в том, что необходимо на каждом этапе определить такие значения $\delta\rho_q(r)$, которые уменьшали бы значение минимизируемого функционала F_0 при соблюдении условий (36).

Запишем $\rho_q(r)$ в виде $\rho_q(r)=\rho_q^0 U_q(r)$, где ρ_q^0— теоретическая плотность материала q

$$0 \leqslant u_q(r) \leqslant 1 \text{ и } \sum_q u_q(r) \leqslant 1. \qquad (37)$$

Выражение $u_q(r)$, называемое далее управлением, будем рассматривать как кусочно-постоянную функцию, равную u_{qj} на интервале Δr_j. Представим u_{qj} в виде вектора $\vec{u}_j$, компонентами которого являются u_{qj}. Запишем $\delta\rho_{qj}$ в виде $\delta\rho_{qj}=S_{qj}\delta u_{qj}$, где δu_{qj}—вариации вектора $\vec{u}_j$, использование которых с положительными весами не выводит $\vec{u}_j$ из области (37) (δu_{qj} и $-\delta u_{qj}$ считаются «разными», некоторые из них могут быть «запрещены»). S_{qj}— некоторые числа, удовлетворяющие ограничениям

$$0 \leqslant S_{qj} \leqslant S_{qj}^0. \qquad (38)$$

Вариациям δu_{qj} соответствуют векторы $\vec{h}_{qj}$, компонентами которых являются определенные выше эффективности h_{qj}^k материала q в точке j по отношению к функционалу F_k.

Вектор $\vec{h}_{qj}$ принадлежит пространству R_{m+1} размерности $(m+1)$. При построении векторов $\vec{h}_{qj}$ в пространстве R_{m+1} необходимо ввести метрику, так как разные компоненты векторов $\vec{h}_{qj}$ имеют разные размерности и различные порядки величин. Метрика может быть введена, например, путем изменения масштабов по разным компонентам (то есть действием некоторой диагональной матрицы) так, чтобы средние значения компонент векторов $\vec{h}_{qj}$ стали примерно одинаковыми.

Все дальнейшие построения основаны на линейной теории малых возмущений. Задача варьирования теперь ставится в следующей форме.

Необходимо найти такие числа S_{qj}, удовлетворяющие ограничениям (38), чтобы для управления $u_{qj}^*=u_{qj}+S_{qj}\cdot\delta u_{qj}$ выполнялись условия (37) и (36) и чтобы при этом было отрицательным приращением минимизируемого функционала

$$\delta F_0 = \sum_{qj} S_{qj} h_{qj}^0 \Delta r_j.$$

Множество точек

$$\vec{\xi} = \sum_{qj} S_{qj} \vec{h}_{qj} \Delta r_j$$

при всевозможных S_{qj}, подчиненных неравенствам (38), образуют выпуклый замкнутый многогранник R, который будем называть областью достижимости. R — ограниченная область пространства R_{m+1}.

Рассмотрим для определенности случай, когда условия (36) имеют вид равенств. Тогда задача сводится к поиску точки пересечения луча $\vec{l}_0$ с направлением $(-1, 0, 0, \ldots, 0)$ с границей области R (в общем случае к поиску одной из точек пересечения некоторого пространства, точки которого удовлетворяют условиям (36), с границей области). Рассмотрим один из простых, но практически достаточно эффективных способов определения S_{qj} (Подробнее этот вопрос освещен в работе [23]).

Процесс варьирования состоит из ряда элементарных актов, в каждом из которых управление меняется только на одном Δr_j для одного компонента q. Выбирается такая вариация, следствием которой является возможно большее понижение минимизируемого функционала при возможно меньшем нарушении условий (36). Такая вариация выбирается из условий минимальности угла между векторами $\vec{h}_{qj}$ и $\vec{l}_0$. Перейдем от u_{qj} к $u_{qj}^*=u_{qj}+S_{qj}\cdot\delta u_{qj}$. Следствием этого будет смещение точки $\vec{\xi}$ в точку $\vec{\xi}^*=\vec{\xi}+S_{qj}\vec{h}_{qj}\Delta r_j$, отстоящую от оси $\vec{l}_0$ на расстоянии $\rho(\xi^*)$.

Вторым элементарным актом варьирования является восстановление граничных условий (36). В этом случае вариация управления выбирается из условия минимальности угла между векторами $\vec{h}_{qj}$ и $(0, \xi^1, \xi^2, \ldots, \xi^k, \ldots, \xi^m)$.

Аналогично перебираются все имеющиеся в нашем распоряжении векторы $\vec{h}_{qj}$. На этом заканчивается итерация, пересчитываются векторы $\vec{h}_{qj}$ при полученных в предыдущей итерации управлениях u_{qj}^*, и затем начинается новая итерация.

Возможен и другой способ определения чисел S_{qj}, смысл которого заключается в выборе некоторого расстояния ρ_1 от оси $(-1, 0, 0, \ldots, 0)$ (некоторого нарушения граничных условий), которое в процессе итераций стремится к нулю. Тогда S_{qj} определяется из соотношения

$$\rho(\vec{\xi}) = \rho(S_{qj}, \vec{h}_{qj}, \Delta r_j) = S_{qj}\rho(\vec{h}_{qj})\Delta r_j = \rho_1.$$

Процесс останавливается, если нельзя подобрать такие S_{qj}, при помощи которых можно уменьшить функционал F_0, не нарушая условий (36).

Критерий оптимальности может быть сформулирован следующим образом. Оптимальной является такая композиция (такие значения управлений u_{qj}), векторы $\vec{h}_{qj}$ которой образуют выпуклый конус, не содержащий вектора с минимизируемым направлением $\vec{l}_0$. Указанный принцип минимизации применим, разумеется, в равной мере и к реакторным задачам.

ЛИТЕРАТУРА

1. A. Weinberg. Amer. Journ. of Phys. *20*, 401 (1952).
2. С. Глесстон, Э. Эдлунд. Основы теории ядерных реакторов, М., ИЛ, 1954.
3. Л. Н. Усачев. Уравнение для ценности нейтронов, кинетика реактора и теория возмущений. В кн. «Реакторостроение и теория реакторов». М., Изд-во АН СССР, 1955 (Докл. совет. делегации на Международ. конф. по мирному использ. атомной энергии. Женева, 1955).
4. А. Вейнберг, Е. Вигнер. Физическая теория ядерных реакторов. М., ИЛ, 1961.
5. Г. И. Марчук. Методы расчета ядерных реакторов. М., Госатомиздат, 1961.
6. Б. Б. Кадомцев. О функции влияния в теории переноса лучистой энергии. Докл. АН СССР, *113*, № 3 (1957).
7. Г. И. Марчук, В. В. Орлов. К теории сопряженных функций. В сб. «Нейтронная физика». М., Госатомиздат, 1961.
8. Л. Н. Усачев. Теория возмущений для коэффициента воспроизводства и других отношений чисел различных процессов в реакторе. Атомная энергия, декабрь (1963).
9. В. Я. Пупко. Использование функционалов теории возмущений в вариационных задачах об оптимальном распределении материалов в ядерных реакторах. (В печати.)
10. А. А. Абагян, В. В. Орлов, Г. И. Родионов. О функциях опасности нейтронов при расчете защиты от излучения. В сб. «Вопросы физики защиты реакторов». М., Госатомиздат, 1963.
11. Д. Б. Юдин, Е. Г. Гольдштейн. Линейное программирование. М., Физматгиз, 1963.
12. Л. С. Понтрягин, В. Г. Болтянский, Р. В. Гамкрелидзе. Математическая теория оптимальных процессов. М., Физматгиз, 1961.
13. В. В. Орлов. О функциях ценности и теории возмущений для расчетов характеристик реакторов. Атомная энергия. (В печати).
14. T. Moorhead. The Effects of Erros in Cross-section Data on Calculation for a Large Dilute East Reactor. International Atomic Energy Seminar on the Physics of Fast and Intermediate Reactors, Vienna, August, 1961.
15. А. И. Лейпунский и др. Экспериментальные исследования по физике быстрых реакторов, наст. издание, P/362.
16. М. А. Лаврентьев, Л. А. Люстенник. Курс вариационного исчисления. М., ГИТТЛ, 1950.
17. G. Goertzel. Minimum Critical Mass and Flat Flux. J. Nucl. Energy, *2*, No. 3 (1956).
18. А. Д. Галанин. Теория ядерных реакторов на тепловых нейтронах. М., Атомиздат, 1959.
19. В. Я. Пупко. Анализ зависимости между критической загрузкой и критическим объемом для реакторов различного типа. Приложение № 1 к журналу «Атомная энергия» (1958).
20. Е. Близард. Выбор оптимальной по весу защиты. Материалы комиссии по атомной энергии. Т. 1, М., ИЛ, 1956.
21. Л. Р. Кимель. Определение оптимальной формы защитного барьера. Атомная энергия, *7* вып. 3 (1959).
22. Г. А. Лисочкин. Условие оптимума для биологической защиты от нескольких источников излучения. Атомная энергия, *15*, вып. 1 (1963).
23. Р. П. Федоренко. Приближенное решение некоторых задач оптимального управления. «Ж. вычислит. и математ. физ.» (В печати.)

ABSTRACT - RÉSUMÉ - АННОТАЦИЯ - RESUMEN

A/364 USSR

Some new aspects of using adjoint functions and perturbation theory in reactor and shielding calculations

By A. A. Abagyan *et al.*

Aspects of applications of adjoint equations to investigate some reactor and radiation shielding problems are presented. In this paper, a new application of perturbation theory recently developed by one of the authors (*Atomnaya energia*, No. 12, 1963) is considered in which one can obtain not only reactivity changes but also variations of a number of other reactor characteristics represented as a ratio of any two values of neutron-induced processes in the reactor. Among such values one can mention, for example, a breeding ratio. Computation algorithm is described and some applications of this perturbation theory are given.

In this report adjoint equations and perturbation theory techniques are applied to find the minimum reactor critical mass in the general case. The conception of efficiency function of the fissionable material in the reactor is introduced. Constancy of this function within the reactor core is shown to be the condition for the reactor critical mass to be a minimum. The algorithm of numerical calculations of minimum critical mass based on iterations, with the efficiency function of fissionable material having a constant value, is discussed. The material efficiency conception in the reactor and the corresponding algorithm for the determination of this optimum distribution of material can be extended to other reactor materials (for example, moderator, absorber and U^{238} distribution in a breeder reactor).

In addition to the above-mentioned applications of adjoint equations to reactor problems, the applications of non-homogeneous adjoint equations to investigation and design of radiation shielding are also considered. Physical meaning of the adjoint function as a hazard function for neutrons with regard to processes in shielding is shown. The perturbation theory formulae for the most general cases of medium and source parameter changes are derived.

The efficiency function conception of shielding material for various processes in shielding is introduced. The condition of optimum shielding material distribution is formulated on the basis of the efficiency function conception already mentioned.

A/364 URSS

Nouveaux aspects de l'application des fonctions adjointes et de la théorie des perturbations aux calculs des réacteurs et des protections

par A. A. Abagyan *et al.*

Les auteurs examinent certains aspects de l'application des équations adjointes à la solution de plusieurs problèmes que posent les réacteurs et la protection contre le rayonnement. En premier lieu, ils étudient l'utilisation d'une théorie des perturbations, récemment établie par l'un d'entre eux (*Atomnaya energia,* n° 12, 1963), dans le calcul des variations de la réactivité et de plusieurs autres paramètres du réacteur qui s'expriment par un rapport entre deux nombres quelconques d'évènements ayant lieu dans ce réacteur. Parmi ces caractéristiques, on peut indiquer notamment le rapport de surgénération. Les auteurs décrivent l'algorithme de ces calculs et donnent plusieurs exemples montrant l'efficacité de cette méthode des perturbations.

En second lieu, ils étudient les possibilités d'appliquer ce procédé de calcul à la solution du cas général de la réduction au minimum de la charge critique d'un réacteur. Les auteurs introduisent la notion de fonction importance de la matière fissile dans le réacteur et montrent que pour minimiser la charge critique du réacteur il faut que cette fonction soit constante dans le cœur. Ils discutent l'algorithme du calcul numérique d'un réacteur à charge critique minimale, fondé sur des itérations par rapport à la fonction importance constante de la matière fissile. La notion d'importance de la matière fissile dans un réacteur et l'algorithme correspondant du calcul de la distribution optimale de cette dernière peuvent également être appliqués à d'autres matériaux pour réacteurs (par exemple, ralentisseur, absorbeur et uranium 238 dans un réacteur surgénérateur).

En troisième lieu, les auteurs envisagent l'utilisation d'équations adjointes non homogènes pour l'étude et le calcul des protections. Ils montrent la signification physique de la fonction adjointe en tant que fonction exprimant le « danger » des neutrons en ce qui concerne les divers processus induits dans les protections et établissent les formules de la théorie des perturbations pour le cas le plus général de variation des paramètres du milieu et de la source.

Les auteurs introduisent la notion de fonction d'efficacité du matériau de protection par rapport aux divers processus dont il est le siège. En partant de cette notion, ils formulent la condition de la distribution optimale des matériaux de protection.

A/364 URSS

Algunos aspectos nuevos de la aplicación de las funciones adjuntas y de la teoría de perturbaciones en los cálculos de reactores y de blindajes

por A. A. Abagyan *et al.*

En la memoria se examinan cuestiones relativas a la utilización de las ecuaciones adjuntas en el estudio de algunos problemas de reactores y de blindaje contra la radiación. Se considera la aplicación de una teoría de perturbaciones, desarrollada recientemente por uno de los autores (*Atomnaya Energia,* N° 12, 1963), al cálculo de las variaciones de la reactividad y de toda una serie de otros parámetros del reactor que se expresan mediante la razón de dos números cualesquiera de procesos que ocurren en el reactor. Entre estas magnitudes cabe mencionar, por ejemplo, el coeficiente de reproducción. Se describe el algoritmo de dichos cálculos y se presentan algunos ejemplos que ponen de relieve la eficacia de la citada teoría de perturbaciones.

A continuación, se considera la aplicación del método de las ecuaciones adjuntas y de la teoría de perturbaciones a la resolución del problema de minimizar la carga crítica del reactor en el caso general. Se introduce el concepto de importancia del material fisible en el reactor y se demuestra que para minimizar la carga crítica hace falta que la importancia sea constante en el núcleo. Se discute un algoritmo iterativo de cálculo numérico de reactores con carga crítica mínima, basado en una importancia del material fisible constante. El concepto de importancia del material fisible en el reactor y el correspondiente algoritmo para determinar la distribución óptima del mismo se pueden aplicar también a otros materiales del reactor (por ejemplo, el moderador, el absorbente y el uranio-238 en un reactor reproductor).

Junto a la utilización de las ecuaciones adjuntas en los problemas antes enumerados, en la memoria se consideran algunas cuestiones relativas al empleo de ecuaciones adjuntas no homogéneas para el estudio y cálculo de blindajes. Se pone de manifiesto el sentido físico de la función adjunta como función que expresa la peligrosidad de los neutrones para diferentes procesos en el blindaje. Se obtienen fórmulas de la teoría de perturbaciones para el caso más general de variación de los parámetros del medio y de la fuente.

Se introduce el concepto de función de eficacia del material de blindaje respecto de diferentes procesos en el mismo. Basándose en ese concepto, se formula la condición de distribución óptima de los materiales de blindaje.

Новые результаты физического исследования защиты

О. И. Лейпунский, С. Г. Цыпин, А. А. Абагян, В. Н. Аваев, С. П. Белов, Е. Б. Брешенкова, Г. А. Васильев, А. П. Веселкин, В. К. Даруга, С. Ф. Дегтярев, В. А. Дулин, Ю. А. Егоров, Ю. А. Казанский, Л. Р. Кимель, В. А. Климанов, В. И. Кухтевич, Е. С. Матусевич, В. П. Машкович, М. Е. Нетеча, А. В. Никитин, В. В. Орлов, Ю. В. Орлов, Ю. В. Панкратьев, А. М. Панченко, В. И. Попов, В. К. Сахаров, Б. И. Синицын, Л. А. Трыков, Б. П. Шеметенко

В настоящем докладе приведены результаты новых экспериментальных и теоретических исследований различных вопросов защиты.

Разд. 1 содержит данные о поле излучения от точечного мононаправленного источника, которые позволяют получить сведения о поле излучений от источников различной формы.

В разд. 2 приведена детальная информация об угловом энергетическом и пространственном распределении потока нейтронов и γ-лучей как внутри сред, так и на их границах. Приведены данные об образовании, выходе и способах подавления захватного γ-излучения; об оптимизации физических характеристик защиты; о спектральных, угловых характеристиках излучений, рассеянных в воздухе.

Разд. 3 посвящен экспериментальному и теоретическому определению дозового фактора накопления нейтронного излучения для различных защитных сред, представляющих практический интерес.

РАЗДЕЛ 1. ПОЛЕ ИЗЛУЧЕНИЙ ОТ МОНОНАПРАВЛЕННЫХ ИСТОЧНИКОВ

Большое разнообразие конфигураций радиоактивных источников, встречающееся во всех областях применения атомной энергии, затрудняет определение полей излучения в защитных средах, окружающих радиоактивные вещества. Это делает необходимым поиски таких простых источников, по известному полю излучения которых можно составить поле излучения любой сложной конфигурации источников. Наиболее богатые возможности представляет точечный мононаправленный моноэнергетический источник (тонкий луч), который является самым элементарным источником.

Изучение поля точечного мононаправленного источника может быть выполнено методом решения кинетического уравнения транспорта γ-квантов и нейтронов, методом Монте-Карло и экспериментальным методом. Этим исследованиям посвящено много работ [1–23]. Решение кинетического уравнения представляет большие трудности и до настоящего времени еще не произведено до конца [7, 16, 21, 22]. Методом Монте-Карло выполнены расчеты поля излучения от тонкого луча с начальной энергией γ-квантов 0,66 *Мэв* при распространении в железе на расстояниях до длин свободных пробегов излучения и для воздуха на расстояниях меньше длины свободного пробега от тонкого луча γ-квантов и нейтронов различных энергий [9]. Большое число переменных затрудняет применение метода Монте-Карло. Недостаточность теоретических данных по полю излучения тонкого луча принудила прибегнуть к экспериментальному исследованию.

§ 1. Измерение поля излучения тонкого луча γ-квантов

Тонкий луч создавался сильной коллимацией излучения точечных изотропных источников Cs^{137}, Co^{60}, Na^{24}. Измерения производились в условиях бесконечной геометрии. В качестве детекторов использовали сцинтилляционный счетчик с органическим кристаллом и малогабаритный галогенный счетчик со специальными фильтрами. При помощи этих фильтров сглаживалась зависимость показаний прибора от энергии γ-квантов [23], так что показания детекторов (*имп/мин*) пропорциональны потоку рассеянной энергии (*Мэв/см²·мин*). В табл. 1 указаны материалы, энергии γ-квантов

Таблица 1. Материалы, энергии γ-квантов и максимальные расстояния (в длинах свободного пробега), на которых изучались функции распределения тонкого луча

Изучаемые материалы	Энергия γ-квантов E_0, *Мэв*					
	0,66		1,25		2,76	
	$\mu_0 z$	$\mu_0 \rho$	$\mu_0 z$	$\mu_0 \rho$	$\mu_0 z$	$\mu_0 \rho$
Вода	4	3	4	2	—	—
Алюминий . .	7	3	5	3	3	2
Бетон	6	3	4	2	—	—
Железо	7	4	5	3	4	3
Свинец	6	4	5	3	3	3

и максимальные расстояния, на которых изучались функции распределения тонкого луча. На рис. 1 в виде примера показано пространственное распределение рассеянной энергии $\Phi_0(\vec{r}, \vec{r}_0, E_0, \vec{\Omega}_0)$ в точках $\vec{r}$ от тонкого луча с начальной энергией γ-квантов $E_0 = 2{,}76$ *Мэв*, испущенных из точки $\vec{r}_0$ в направлении $\vec{\Omega}_0$ в алюминии. Заметим, что $\Phi_0(\vec{r}, \vec{r}_0, E_0, \vec{\Omega}_0) \equiv \Phi_0(z, \rho)$, так как предполагается, что $\vec{r}_0 = 0$, луч направлен по оси z, а z, ρ — цилиндрические координаты; распределение по φ изотропно. Ход кривых для функций распределения $\Phi_0(z, \rho)$, показанных на рис. 1, типичен для других материалов и энергий. На рис. 2 приведены функции $\Phi_0(z, \rho)$ для ряда материалов от тонкого луча с начальной энергией 1,25 *Мэв* для $\mu_0 z = 2$. На рис. 3 приведено пространственно-энергетическое распределение γ-квантов в воде от тонкого луча с начальной энергией квантов 0,66 *Мэв* $G_0(z, \rho, E)$ в цилиндрической системе координат.

Распределение рассеянного излучения в воде от тонкого луча в плоскости, нормальной направлению луча $\Phi_0(z, \rho)$, для точек, отстоящих от источника более чем на одну длину свободного пробега, может быть описано выражением

$$\Phi_0(z, \rho) = E_0 e^{-\mu_0 z} \mu_0^2 \mu_0 z \Phi(\alpha \mu_0 \rho) \ \textit{Мэв/см}^2 \cdot \textit{сек}, \quad (1)$$

где E_0 — мощность источника, *Мэв/сек*, — линейный коэффициент ослабления; $\Phi(\alpha\mu_0\rho)$ — функция Кинга, $\alpha = \sqrt{\frac{2\pi\mu_0 z}{3(B-1)}}$; B — энергетический фактор накопления плоского мононаправленного источника. Для материалов с атомными номерами, большими, чем у воды, в выражении (1) вместо $\Phi(\alpha\mu_0\rho)$ следует записать $E_i(-\alpha\mu_0\rho)$.

§ 2. Измерения поля нейтронов от дискового мононаправленного источника

Для экспериментальных исследований пространственно-энергетических распределений нейтронов использовался дисковый мононаправленный источник. Этот источник в силу осевой симметрии является наиболее удобным среди плоских ограниченных мононаправленных источников. Измерения функций распределений производились на установке Б-2 [12, 19] реактора БР-5, представляющей собой дисковый мононаправленный источник диаметром $2a \simeq 30$ *см* (см. § 1 разд. 2). Измерения производились в воде, железе и углероде. В виде примера на рис. 4—6 представлены функции распределений указанного источника нейтронов деления в воде, измеренные индикаторами по реакции $P^{31}(n, p)Si^{31}$ в железе, измеренные индикаторами по реакции $Al^{27}(n,\alpha)Na^{24}$, и в углероде по реакции $S^{32}(n, p)P^{32}$. Для сравнения на рис. 5 приведены также расчетные данные [16]. На рис. 7 показаны функции $\Phi_{\text{диск}}(z, \rho, a)$ для одной толщины $z = 30$ *см* для ряда материалов и источника Б-2, измеренные индикаторами по реакции $S^{32}(n, p)P^{32}$.

Нетрудно показать, что для функции пространственного распределения можно совершить преобразование от дискового мононаправленного источника к плоскому мононаправленному источнику по формуле

$$\Phi^{\text{пл. мон}}(z) = c \int_0^{2\pi} d\varphi \int_0^{\infty} \Phi^{\text{диск}}(z, \rho, a)\, \rho d\rho. \quad (2)$$

Зная функцию пространственного распределения от дискового мононаправленного источника $\Phi_{\text{диск}}(z, \rho, a)$, при соответствующих упрощающих предположениях можно совершить обратное преобразование к тонкому лучу [13, 19].

РАЗДЕЛ 2. РАСПРЕДЕЛЕНИЕ И ГЕНЕРАЦИЯ ИЗЛУЧЕНИЯ В РАЗЛИЧНЫХ ЗАЩИТНЫХ СРЕДАХ

§ 1. Установки для исследования защиты

Установка Б-2 [12] была сооружена на реакторе быстрых нейтронов БР-5 [24] для исследования прохождения нейтронов через различные защитные материалы и сборки (рис. 8). Существенным отличием Б-2 от известных в литературе установок является использование дискового мононаправленного источника, позволяющего получить более детальную информацию об излучении в исследуемой защите (рис. 9).

Реактор РИЗ — урановодный реактор нулевой мощности для исследования образования, выхода и способов подавления захватного γ-излучения в защите (рис. 10). Специальная верхняя защита из карбида бора и висмута позволяла получить хорошее соотношение потоков выходящих нейтронов и γ-лучей.

§ 2. Прохождение нейтронов

Исследовалось прохождение быстрых нейтронов реактора БР-5 с энергией $E > 2 \div 3$ *Мэв*

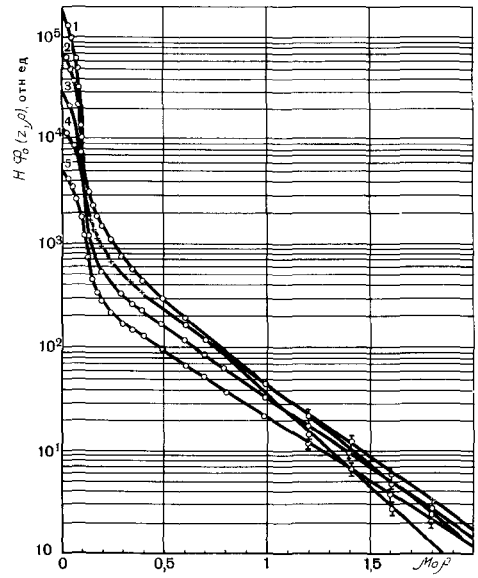


Рис. 1. Функция распределения тонкого луча в алюминии для начальной энергии γ-квантов 2,76 *Мэв* для расстояний $\mu_0 z$ (в длинах свободного пробега):
1—0,68; *2*—1,37; *3*—2,05; *4*—2,77; *5*—3,4

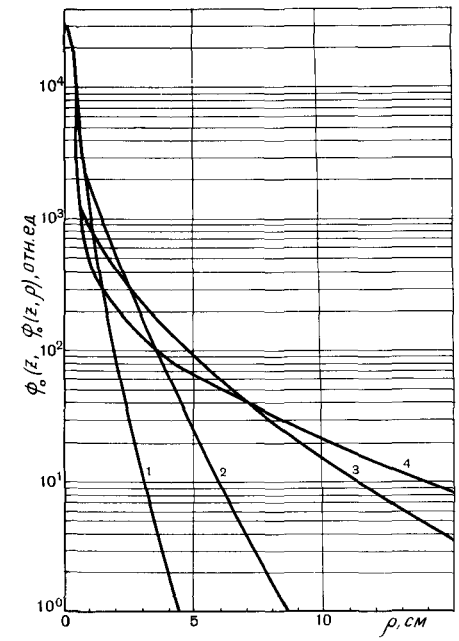


Рис. 2. Функция распределения тонкого луча для начальной энергии γ-квантов 1,25 *Мэв* в зависимости от ϱ для $\mu_0 z$-2 для материалов:
1—свинец; *2*—железо; *3*—алюминий; *4*—вода

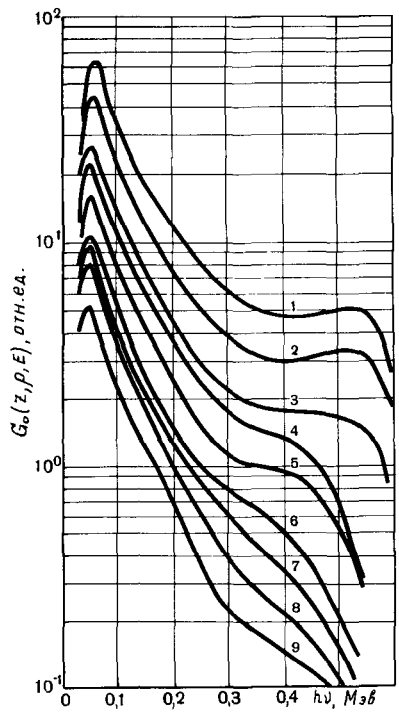


Рис. 3. Функция пространственно-энергетического распределения тонкого луча в воде для γ-квантов с начальной энергией 0,66 *Мэв* для точек с координатами (в *см*):

1—$z=19$, $\varrho=10{,}0$; *2*—$z=29{,}1$, $\varrho=10{,}0$;
3—$z=39$, $\varrho=10{,}0$; *4*—$z=19{,}1$, $\varrho=20{,}0$;
5—$z=29$, $\varrho=20{,}0$: *6*—$z=39{,}1$, $\varrho=20{,}0$;
7—$z=19$, $\varrho=30{,}0$; *8*—$z=29{,}1$, $\varrho=30{,}0$;
9—$z=39$, $\varrho=30{,}0$;

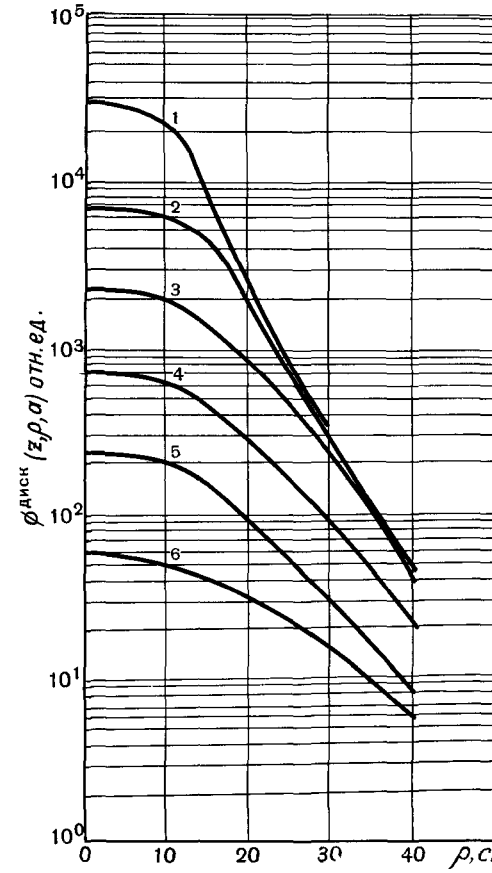


Рис. 4. Функция распределения дискового мононаправленного источника нейтронов деления в воде по измерению индикаторами по реакции $P^{31}(n, p)\,Si^{31}$ для z (в *см*):
1—16,5; *2*—30,0; *3*—40,0; *4*—50,0: *5*—60,0; *6*—72,5

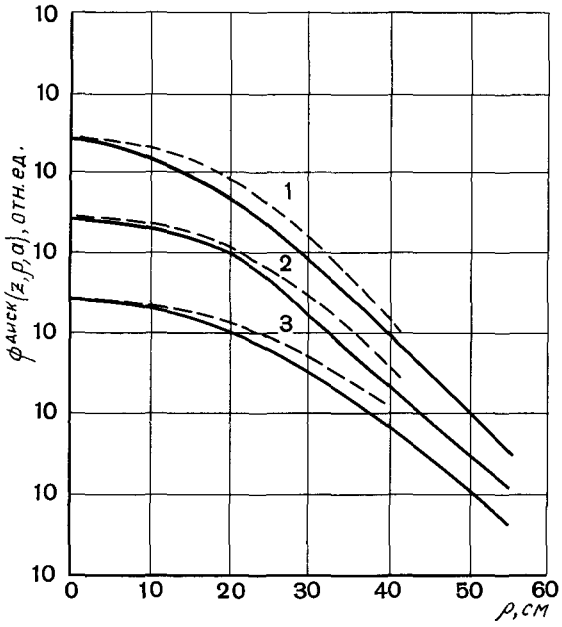


Рис. 5. Сравнение расчетных и экспериментальных данных (сплошные кривые — расчет по методу моментов: штриховые кривые — экспериментальные данные) по показаниям детектора по реакции $Al^{27}(n, d)Na^{24}$ в различных плоскостях z в зависимости от расстояния до центрального луча ϱ для дискового мононаправленного источника для z (в *см*):
1 — 27,1; *2* — 38,8; *3* — 50,5

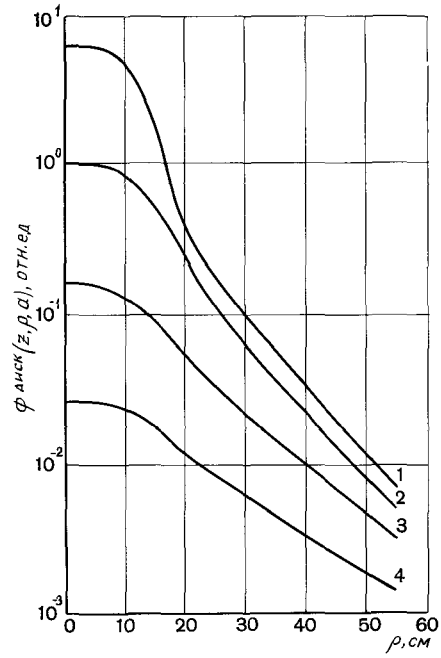


Рис. 6. Функция распределения дискового мононаправленного источника нейтронов деления в углероде по измерению индикаторами по реакции $S^{32}(n, p)P^{32}$ для z (в *см*):
1 — 10,0; *2* — 30,0; *3* — 50,0; *4* — 70,0

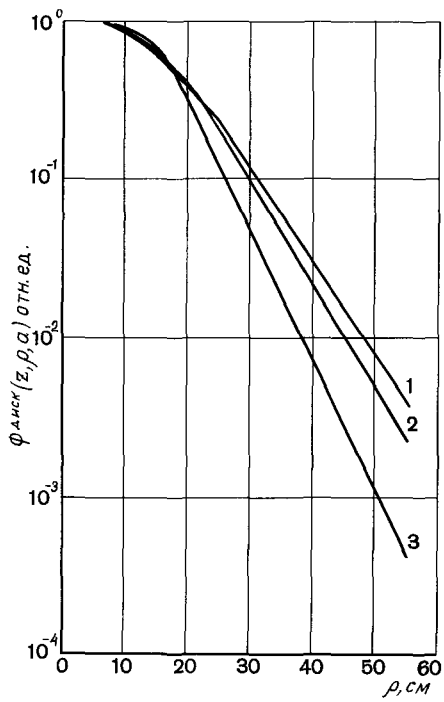


Рис. 7. Функция распределения дискового мононаправленного источника нейтронов деления по измерению индикаторами по реакции $S^{32}(n, p)P^{32}$ в зависимости от ϱ для $z = 30$ *см* для материалов:
1 — углерод; *2* — железо; *3* — вода

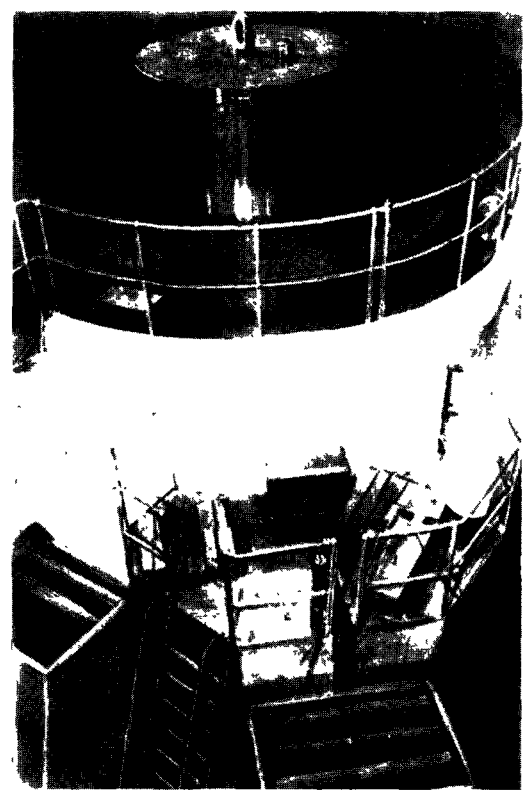


Рис. 8. Установка В-2 для исследования защиты

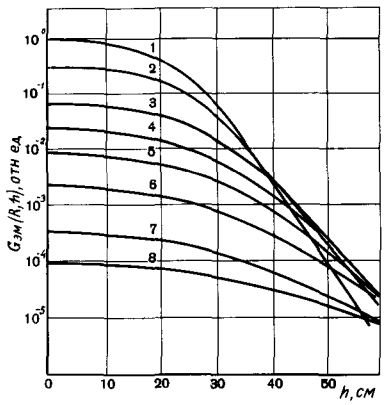


Рис. 9. Функции ослабления дискового мононаправленного источника спектра деления, измеренные пороговым детектором $P^{31}(n, p)Si^{31}$ (n — расстояние от оси диска) для различных толщин гидрида лития R (в *см*):
1 — $R=16{,}5$ *см*; *2* — $R=26{,}5$ *см*; *3* — $R=39\ 5$ *см*; *4* — $R=49{,}5$ *см*; *5* — $R=59{,}5$ *см*; *6* — $R=72$ *см*; *7* — $R=82{,}5$ *см*; *8* — $R=92{,}5$ *см*



Рис. 10. Общий вид реактора РИЗ

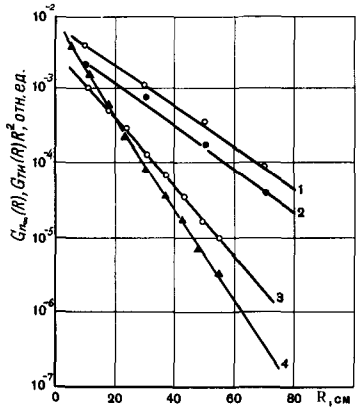


Рис. 11. Распределение потоков быстрых нейтронов в гидриде лития ($\varrho=0{,}82$ *г/см*^{3}) и в углероде ($\varrho=1{,}67$ *г/см*^{3}) от источника нейтронов деления:
1 — расчет методом моментов [25] для реакции $S^{32}(n, p)P^{32}$, геометрия исключена умножением R^1 (углерод); *2* — расчет методом моментов [25] для реакции $Al^{27}(n, \alpha)Na^{24}$, геометрия исключена умножением на R^2 (углерод); *3* — измерения детектором $Al^{27}(n, \alpha)Na^{24}$, источник плоский мононаправленный (гидрид лития); *4* — расчет дозы методом моментов [9] от точечного изотропного источника, геометрия исключена умножением на R^2 (гидрид лития); △ — Измерения детектором $P^{31}(n, p)Si^{31}$ и $S^{32}(n, p)P^{32}$, источник плоский мононаправленный (гидрид лития); ○ — измерения индикатором $S^{32}(n, p)P^{32}$, источник плоский мононаправленный (углерод); ⊙ — измерения индикатором $Al^{27}(n, \alpha)Na^{24}$, источник плоский мононаправленный (углерод)

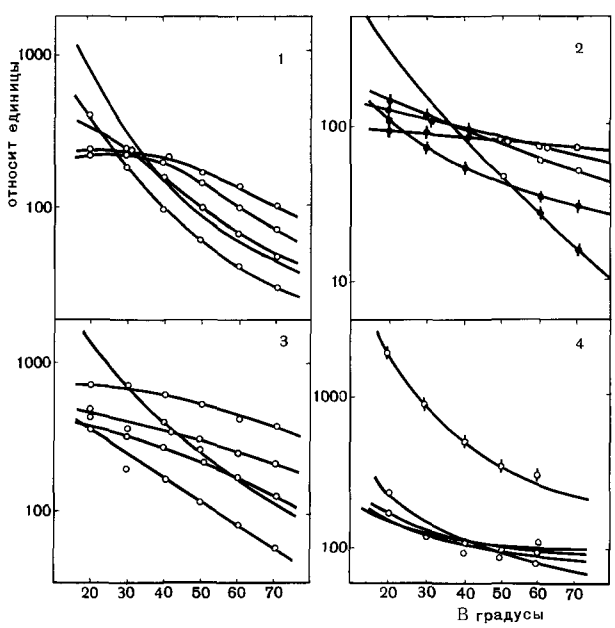


Рис. 12. Угловое распределение энергетических групп нейтронов для воды (*1*), углерода (*2*), железа (*3*) и свинца (*4*):
○ — группа 3,1—3,4 *Мэв*; ◑ — группа 2,1—3,1 *Мэв*; △ — группа 1,4—2,1 *Мэв*; ◒ — группа 0,8—1,4 *Мэв*; ○ — группа 0,5—0,8 *Мэв*;

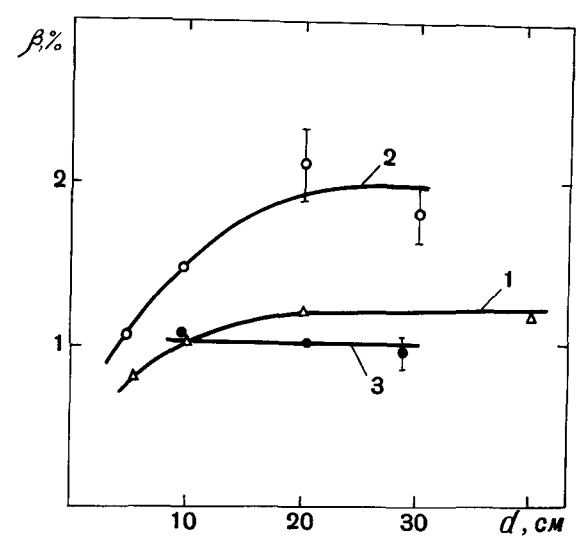


Рис. 13. Зависимость коэффициента вторичного излучения от толщины защиты из железа (*1*), никеля (*2*) и никеля с 2% вес. бора (*3*)

в гидриде лития и углероде в условиях бесконечной геометрии. Результаты измерений, приведенные на рис. 11, сравниваются с расчетами [9, 25]. Удовлетворительное согласие расчетов с экспериментами свидетельствует о корректности расчетной методики и правильности выбранных сечений.

В средах, не содержащих водород, распределение потока нейтронов с энергией $E > 2 \div 3$ *Мэв* для толщин защиты R от 2 до 15—20 длин свободных пробегов аппроксимируется следующим выражением: $\Phi(R) \sim \sim \exp(-qR)$. В качестве q здесь могут быть использованы следующие величины: сечение выведения $\Sigma_{\text{чет}}$, если рассматривать группу нейтронов с энергией выше 3 *Мэв* [26]; сечения, полученные из обратных длин релаксации $\Sigma_{1/\lambda}$ для группы нейтронов с энергией выше 3 *Мэв* [26]; асимптотические сечения Σ_{as}, полученные из решения односкоростного кинетического уравнения в транспортном приближении [26] с использованием систем групповых констант [27, 28] для групп 1,4 — ∞, 2,5 — ∞ *Мэв*.

В табл. 2 приведены параметры, почерпнутые из многочисленных литературных источников или полученные авторами настоящего доклада, которые экспериментально изучали прохождение нейтронов в бесконечно протяженных защитных средах из углерода, натрия, железа, а также в смесях железо — углерод и железо — кислород.

Угловое энергетическое распределение быстрых нейтронов исследовалось экспериментально с помощью методики, приведенной в [29, 30]. Источником нейтронов служила реакция $D(D, n)\,He^3$ (энергия 3,4 *Мэв*). На рис. 12 в качестве примера показаны угловые распределения энергетических групп нейтронов для H_2O, C, Fe и Pb. Угловая зависимость групп рассеянных нейтронов в телесном угле $d\Omega$ от 3,1 до 3,4 *Мэв* может быть представлена в виде $\exp(-\Theta/\Theta_0)$, где Θ_0 для H_2O, C и Al около 20°, а для сред с $A > 30$ около 35°. Угловое распределение дозы быстрых нейтронов с энергией выше 0,4 *Мэв* для сред с $A > 30$ можно представить такой же функцией с параметром $2/3\pi \leqslant \Theta_0 \geqslant \pi$. Для H_2O и углов $\Theta > 10°$ $\Theta \sim 45°$. Представление угловых распределений однопараметровой функцией имеет точность 10%.

Таблица 2. Сравнение сечений выведения, сечений, полученных из обратных длин релаксаций и асимптотических сечений

Элемент	$\sigma_{\text{чет}}$ [37], *барн*	$\sigma_{1/\lambda}$, *барн*	σ_{as}, *барн*	
			1,4—∞ *Мэв*	2,5—∞ *Мэв*
Литий	1,01	1,07	1,03 [28]	
Бериллий	1,07	1,15 [9]	1,20 [28]	
Бор*	0,97	1,12 [38]	1,12 [28]	
			1,00 [27]	
Углерод	0,81	0,75	0,95 [27]	
Кислород	0,74		0,74 [27]	
Натрий	1,26	1,50	1,36 [27]	
Магний	1,29		1,35 [27]	
Алюминий	1,30		1,42 [27]	
Кремний	1,37		1,23 [28]	
Калий	1,57		1,54 [28]	
			1,39 [27]	
Титан	1,82		1,62 [27]	
Хром	1,77		1,98 [27]	
Железо	1,98	1,81 [8]	1,87 [28]	
Никель	1,89	1,90 [26]	1,84 [27]	
Медь	2,04		2,04 [28]	
Цирконий	2,36		2,43 [27]	
Ниобий	2,37		2,30 [28]	
Молибден	2,38		2,85 [28]	
Барий	2,82		3,14 [28]	
Вольфрам	3,36		3,94 [27]	
Свинец	3,70		2,63 [27]	3,33 [27]
Висмут	3,50		2,62 [27]	3,53 [27]

* Величина $\sigma_{1/\lambda}$ для бора получена из измерений $\sigma_{1/\lambda}$ для B_4C [38] и $\sigma_{1/\lambda}$ равной 0,75 для углерода.

§ 3. Захватное γ-излучение и оптимизация защиты

Целесообразно вводить экспериментальные параметры, характеризующие выход захватного γ-излучения из различных защит. Одним из таких параметров является коэффициент вторичного γ-излучения β, равный отношению полного числа γ-квантов, выходящих из защиты, к полному числу вышедших нейтронов [31]. Показано, что β, начиная с определенной толщины защиты, остается постоянной, то есть

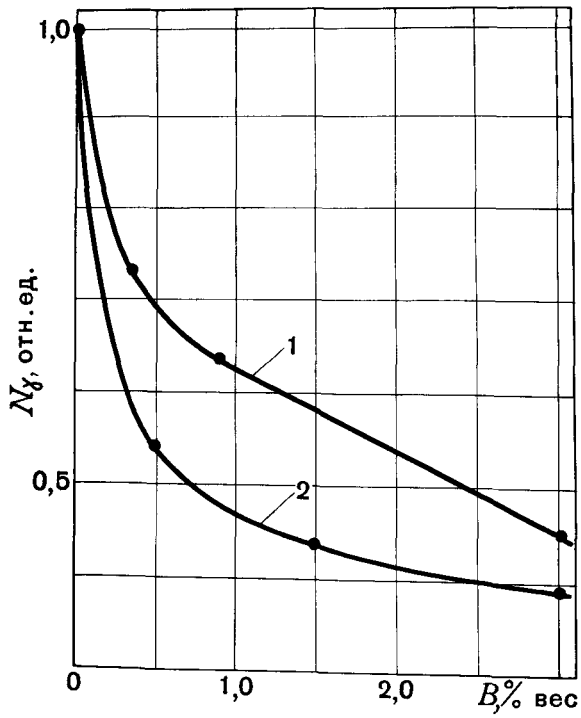


Рис. 14. Относительный выход захватного γ-излучения из железа (*1*) и никеля (*2*) в зависимости от весового содержания бора

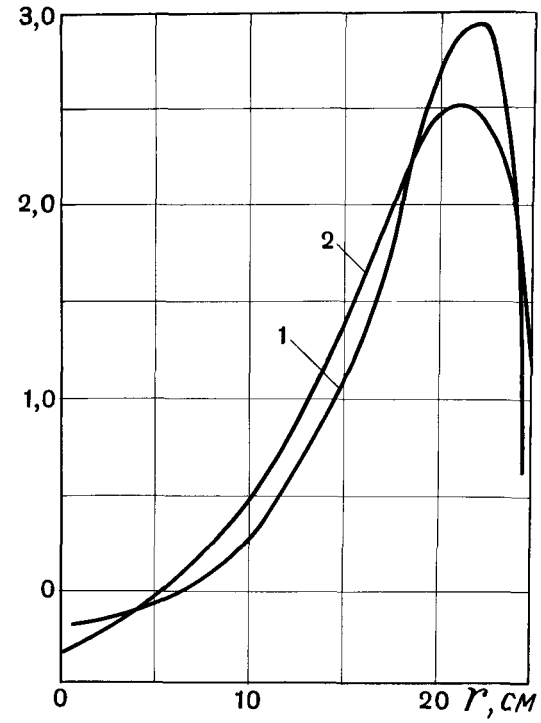


Рис. 15. Экспериментальная *1* и расчетная *2* функция эффективности водорода (0,11 *г/см*²) в никеле

определяется только свойствами среды. На рис. 13 в качестве примера даны коэффициенты β, измеренные на реакторе РИЗ для Fe, Ni, гомогенной смеси Ni с B.

Уменьшить выход захватного γ-излучения можно введением в защиту борсодержащих добавок. Было установлено, что введение бора эффективно уменьшает выход γ-лучей только при небольших его количествах (до 2—3 вес. %). На рис. 14 приведена типичная зависимость выхода γ-лучей из Fe и Ni от весовой концентрации B.

Различные характеристики защиты можно записать в виде

$$I_k = \int \Phi(\vec{r}, \vec{\Omega}, E) P_k(\vec{r}, \vec{\Omega}, E)\, d\vec{r}\, d\vec{\Omega}\, dE + \varphi[\varrho_i(r)].$$

Вес защиты есть функционал вида $P = \int \sum_i \varrho_i(\vec{r})\, dV$, где Φ — поток нейтронов; P_k характеризует процесс, обусловленный нейтронами (захватное γ-излучение, тепловыделение и т. п.); φ обусловлен внешними источниками γ-излучения; ϱ_i — плотность i материала.

Задача об оптимизации защиты в общем виде формулируется следующим образом. Необходимо найти минимальное значение величины I_0 при условии, что значения $I_1 \ldots I_k \ldots I_m$ не превышают определенного значения.

При использовании аппарата сопряженных функций и теории возмущений можно вычислить функции эффективности защитных материалов f_{ij}^k ($K = 0, 1 \ldots m$), характеризующих изменение функционалов I_k при внесении единичного количества материала i в точку j. Введем $(m+1)$-мерное пространство, компонентами которого являются ΔI_0, $\Delta I_1 \ldots \Delta I_m$, и выделим в нем направление минимизируемой величины $I_0 - \vec{S}_0$. Оптимальным является такое распределение защитных материалов $\varrho_i(\vec{r})$, при котором вектор f_{ij}, компонентами которого являются f_{ij}^k, образуют выпуклый конус, не содержащий вектора с минимизируемым направлением $\vec{S}_0$.

Заметим, что функции эффективности защитных материалов можно получить экспериментально и на основании этого производить оптимизацию экспериментальным путем. Функция эффективности водорода ($\varrho_H = 0{,}111$ *г/см*³) в никеле $f_{H\gamma}(r)$ по отношению к захватному γ-излучению была получена на реакторе РИЗ (рис. 15). Эта же функция была найдена расчетным путем по формулам теории возмущений [32]. Как видно из рис. 15, согласие удовлетворительное. Экспериментально показано также, что зависимость $f_{H\gamma}$ в максимуме от количества водорода линейна вплоть до 0,11 *г/см*³ водорода.

§ 4. Рассеяние нейтронов и γ-лучей в воздухе

В области расстояний R, малых по сравнению с длиной свободного пробега $1/\Sigma_t(E_0)$, происходит компенсация накопления многократно рассеянного излучения и поглощения. Вследствие этого пространственное распределение потока или мощности дозы оказывается пропорциональным $1/R$ (R — расстояние источник — детектор). Эта зависимость была подтверждена экспериментально авторами и расчетными работами [9, 33–36]. Зависимость $1/R$ существенно упрощает описание распространения рассеянного излучения различных источников в воздухе.

Введя относительный поток n_n, определяемый отношением рассеянного потока нейтронов в воздухе к потоку в вакууме в том же месте, пространственное распределение n_n от точечного изотропного источника записывается $n_n(R, E_0) = (2{,}15 \pm 0{,}2)\, R\, [\Sigma_t(E_0) - \Sigma_a(E_0)]\alpha(E_0)$, где $\Sigma_a(E_0)$ — сечение поглощения; $\alpha(E_0) = 1$ для $E_0 < 6$ *Мэв* и плавно меняется до 0,8 при $E_0 = 14$ *Мэв*. Аналогично для относительной мощности дозы D_n имеем $D_n(R, E_0) = B(E_0)\sqrt{\Sigma_t(E_0)}\, R$, где $B(E_0) = 0{,}195 \pm 0{,}02$ для $E_0 = 0{,}1 \div 6$ *Мэв* и $0{,}145 \pm 0{,}015$ для $E_0 = 7 \div 14$ *Мэв*. Величины n_n и D_n связаны зависимостью $n_n(R, E_0) = (1{,}1–1{,}2)\, D_n(R, E_0)$.

Из рассмотрения экспериментальных и расчетных данных следует, что с точностью ±20% геометрии мононаправленный источник — изотропный детектор и изотропный источник — мононаправленный детектор эквивалентны. Тогда соответствующие им распределения относительной мощности дозы P_n и Q_n можно записать как

$$P_n(R, E_0, h) = 2{,}2\sqrt{\Sigma_t}\cdot R\cdot \eta^{-\varkappa(E_0 h)} \text{ и}$$

$$Q_n(R, E_0, \psi) = 2{,}2\sqrt{\Sigma_t}\cdot R\psi^{-\varkappa(E_0\psi)},$$

где η и ψ углы ориентации мононаправленного источника и детектора соответственно; $\varkappa(E_0)$ для $E_0 = 0{,}1 \div 14$ *Мэв* меняется от 1,1 до 1,4 для η и ψ от 5 до 120°. Рис. 16 иллюстрирует зависимость P_n от η.

На рис. 17 приведено сравнение двух геометрий: точечный изотропный источник — мононаправленный детектор (эксперимент) и точечный мононаправленный источник — изотропный детектор (расчет). Из рис. 17 следует, что деградация спектра нейтронов от угла ориентации мала и энергетические распределения близки для двух геометрий.

Пространственное распределение относительной мощности дозы рассеянных γ-лучей для $0{,}5 < E_0 < 10$ *Мэв* от изотропного источника без учета аннигиляционного излучения имеет вид

$$D_\gamma(E_0, R) = 4{,}3\cdot 10^{-2} R \left[\left(7{,}7 - \frac{4{,}2}{1+\exp\left(\frac{E_0-2{,}5}{0{,}1}\right)}\right)E_0 + \frac{9}{1+\exp\left(\frac{E_0-2{,}5}{0{,}1}\right)}\right]^{-1} \pm$$

$\pm$ 20%, где $E_0 = 6$ *Мэв*, а R в *м*.

Пространственное распределение относительной мощности дозы рассеянных в воздухе γ-лучей от точечного мононаправленного источника выражается как

$$P_\gamma(E_0, R, h) = \begin{cases} \dfrac{0{,}48}{E_0} R\eta^{-1{,}78} & 20° < \eta < 90° \\ \dfrac{1{,}12\cdot 10^{-2}}{E_0} R\eta^{-0{,}95} & 90° < \eta < 180° \end{cases}$$

для энергии E_0 от 0,4 до 1,5 *Мэв* и без учета аннигиляционного излучения

$$P_\gamma(E_0, R, \eta) = \frac{Lc(\eta)(\pi - \eta) R}{T(E_0)\sin\eta}$$

для энергии $E_0 > 2$ *Мэв*. Здесь L — постоянная; $c(\eta)$ — комптоновское дифференциальное сечение; $T(E_0)$ — мощность дозы γ-лучей с энергией $E_0 \cdot P_\gamma(\eta)$ меняется с увеличением расстояния R (рис. 18).

Аналогично нейтронам для γ-лучей имеет место обратимость геометрии (рис. 19). На рис. 19 приведены экспериментальные значения энергетического распределения для $E_0 = 1{,}25$ *Мэв*, $\eta = \psi = 60°$ и $R = 16$ *м* от мононаправленного источника $P_\gamma(E)$ (изотропный детектор).

На рис. 20 показано, насколько расчет в однократном приближении занижает «мягкую» часть спектра. Расчетное распределение «испорчено» на энергетическое разрешение спектрометра.

РАЗДЕЛ 3. ДОЗОВЫЙ ФАКТОР НАКОПЛЕНИЯ НЕЙТРОНОВ

Предлагается метод расчета мощности дозы от нейтронов всего спектра. Метод основан на применении метода сечения выведения, многогруппового метода решения кинетического уравнения переноса нейтронов и введении понятия дозового фактора накопления нейтронного излучения, по форме аналогичного соответствующему понятию для γ-квантов.

За последнее время был развит и широко применяется в расчетах полуэмпирический метод сечения выведения, позволяющий относительно просто определить ослабление быстрых нейтронов с энергией выше 2—3 *Мэв*. Поэтому для нейтронного излучения дозовый фактор накопления удобно нормировать на мощность дозы быстрых нейтронов.

Для определения дозового фактора накопления относительно группы быстрых нейтронов был использован многогрупповой метод решения кинетического уравнения переноса ней-

тронов в диффузионно-возрастном приближении с точным учетом замедления на водороде.

На основании N-группового расчета нейтронных потоков и коэффициентов перевода нейтронного потока в мощность дозы [39] вычислялись пространственные распределения мощностей доз для каждой энергетической группы нейтронов $D_j(r)$. Дозовый фактор накопления рассчитывался по формуле

$$B(r) = \frac{\sum_{j=1} D_j(r)}{D_1(r)}. \qquad (3)$$

Рассматриваются следующие группы вопросов:

1. Энергетическое и пространственное распределение мощности дозы от нейтронов в однородных защитных материалах в бесконечной геометрии. В этом случае внешняя граница исследуемого слоя защиты предполагалась черной.

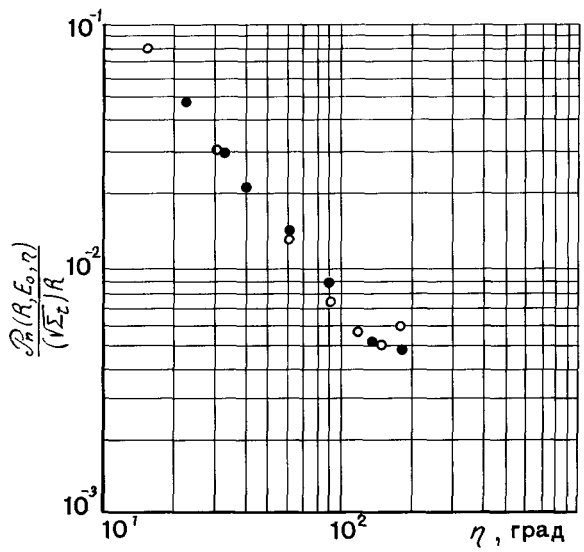


Рис. 16. Пространственное распределение относительной мощности дозы рассеянных в воздухе нейтронов для мононаправленного источника: ● — экспериментальные данные авторов $E_0=4{,}2$ *Мэв*; ○ — расчетные данные [9], усредненные по интервалу начальных энергий от 0,33 до 6 *Мэв*.

2. Энергетическое и пространственное распределение мощности дозы от нейтронов в различных композициях из защитных материалов, имитирующих возможные комбинации последних слоев биологической защиты. В этом случае геометрия является барьерной, но искаженной присутствием человека и рассеянием от окружающих стен и конструкций. Поэтому решено было за последним слоем композиции расположить 20 *см* полиэтилена, близкого по своим ядерно-физическим свойствам к биологической ткани, а нулевое значение многогрупповых потоков задать на экстраполированной границе за указанным материалом.

§ 1. Измерение спектра нейтронов и расчет доз

Расчет мощности дозы от нейтронов всего спектра производится в следующей последовательности. По методу сечения выведения сначала рассчитывается мощность дозы от быстрых нейтронов с использованием дозовых кривых ослабления в водородсодержащей защите. Затем в зависимости от конкретной композиции внешней части биологической защиты подбирается дозовый фактор накопления.

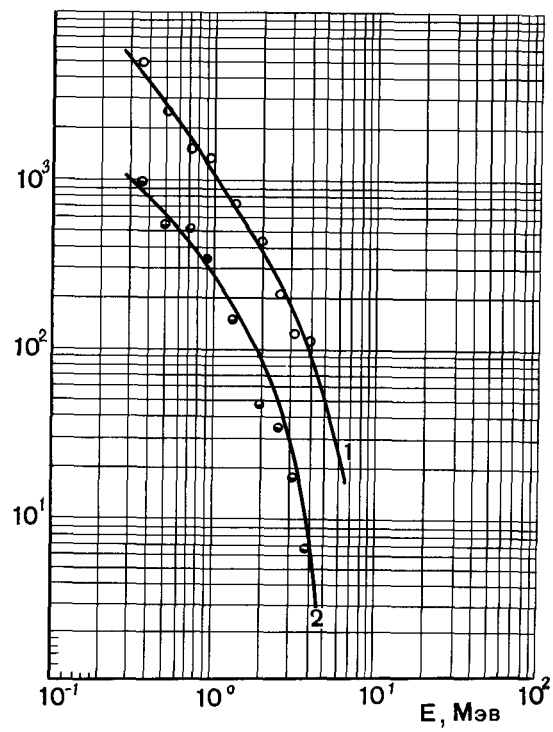


Рис. 17. Энергетическое распределение рассеянных в воздухе нейтронов от точечного изотропного и мононаправленного детектора $E=1{,}3$ *Мэв*, $R=14{,}3$ *м*; ○ — $\psi=30°$; ● — $\psi=180°$ (Экспериментальные авторов). Энергетическое распределение рассеянных в воздухе нейтронов от мононаправленного источника. По расчетным данным $E_0=1{,}3$ *Мэв*, $R=14{,}3$ *м*, кривая 1 — $\eta=30°$; кривая 2 — $180°$

Для усреднения ядерно-физических констант в области $10 \geqslant E_n \geqslant 0{,}7$ *Мэв* в дополнение к известным данным [25, 40] были выполнены измерения спектрального распределения нейтронов с энергией 0,9÷13 *Мэв* для некоторых гомогенных защитных материалов, в том числе для серпентинита, смеси полиэтилена с железом и со свинцом, смеси графита с железом. Константы для нейтронов 0,7 *Мэв* $\geqslant E_n \geqslant$ $\geqslant 0{,}4$ *эв* усреднялись по асимптотическим спектрам замедляющихся нейтронов. В ряде материалов оказалось необходимым специально измерить спектр нейтронов в надтепловой области энергий.

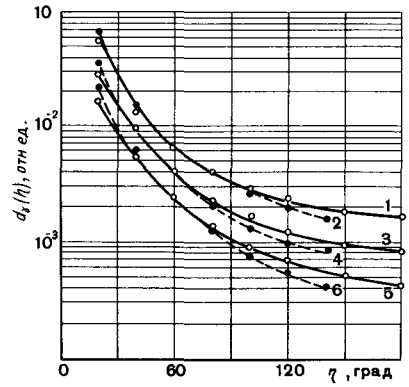


Рис. 18. Пространственное распределение мощности дозы рассеянного в воздухе γ-излучения от мононаправленного источника:
1 — $R=0{,}1\lambda$, $E_0=0{,}411$ *Мэв**;
2 — $R=1\eta E_0=0{,}411$ *Мэв*[10];
3 — $R=0{,}1\lambda$, $E_0=1{,}25$ *Мэв**;
4 — $R=1\lambda E_0=1{,}25$ *Мэв*[10];
5 — $R=0{,}2\lambda$, $E_0=1{,}9$ *Мэв**;
6 — $R=0{,}8\lambda E_0=1{,}9$ *Мэв*[10]

* Данные авторов

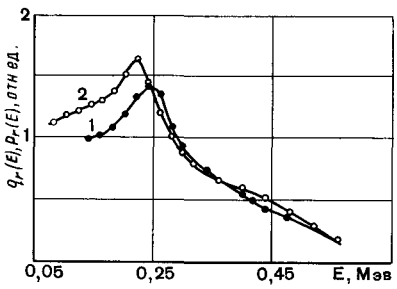


Рис. 19. Энергетическое распределение в воздухе γ-лучей от мононаправленного источника и изотропного детектора для $R=16$ *м*, $\eta=60°$, $E_0=1{,}25$ *Мэв*. (Кривая *1*) от изотропного источника и мононаправленного детектора для $R=16$ *м* и $\varphi=60°$, $E_0=1{,}25$ *Мэв* (кривая *2* данные авторов.)

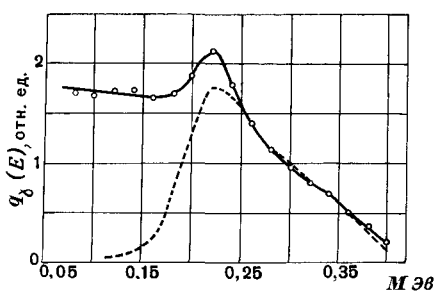


Рис. 20. Энергетическое распределение γ-лучей, рассеянных в воздухе от изотропного источника и мононаправленного детектора для $E_0=1{,}25$ *Мэв*, $\psi=90°$, $R=16$ *м*:
○ — экспериментальные данные: — — — — — расчет в однократном приближении; расчетное распределенре нормировано к экспоримен-тальному при $E=0{,}32$ *Мэв* (данные авторов)

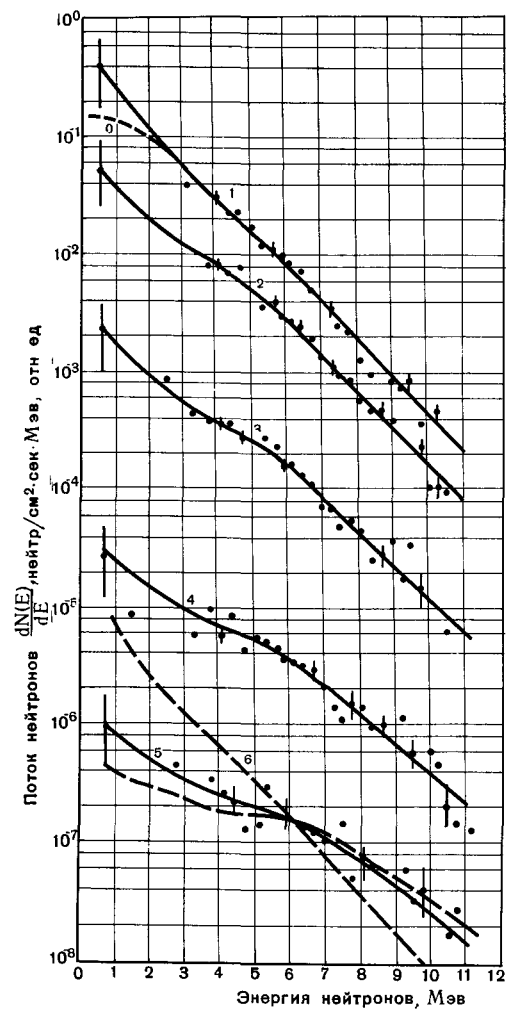


Рис. 21. Энергетическое распределечие быстрых нейтронов в смеси полиэтилен плюс железо:
○ — спектр нейтронов деления. Толщина: *1* — 0; *2* — 24,9; *3* — 81; *4* — 147; *5* — 215 *г/см²*; *6* — спектр за слоем 143 *г/см²*; *7* — спектр за слоем полиэтилена 72 *г/см²*

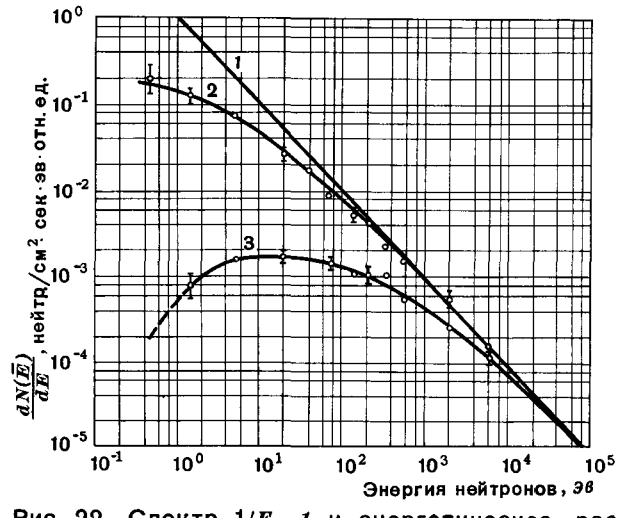


Рис. 22. Спектр $1/E$ *1* и энергетическое распределение надтепловых нейтронов в железе *2*, графите с бором *3*

Измерения энергетического распределения быстрых и промежуточных нейтронов были сделаны на исследовательском водо-водяном реакторе. Спектры быстрых нейтронов в диапазоне энергий 0,9—13 *Мэв* измерялись в условиях барьерной геометрии. Для измерений применялся однокристальный сцинтилляционный спектрометр с кристаллом стильбена и дискриминацией γ-фона.

Были измерены спектры быстрых нейтронов, прошедших через различные по толщине слои однородных материалов полиэтилена [41], графита, железа (Ст-3), свинца [40] и через различные по толщине слои смесей железа с полиэтиленом, свинца с полиэтиленом, железа с графитом. Рассматривалась также деформация спектра быстрых нейтронов при прохождении через серпентинит (SiO_2 — 39%, MgO — 37%, H_2O — 11,5%; Fe_2O_3 — 8,5%).

Энергетическое распределение надтепловых нейтронов исследовалось с помощью набора радиоактивных резонансных индикаторов методом «сравнения со спектром $1/E$». Измерения производились в условиях «полубесконечной» геометрии. Набор индикаторов позволял определять форму спектра в диапазоне энергий от 0,46 *эв* до 6 *кэв*. В качестве примера на рис. 21 представлены энергетические распределения быстрых нейтронов в смеси полиэтилена и железа и энергетический спектр надтепловых нейтронов в железе и графите с бором (рис. 22).

§ 2. Расчет дозовых факторов накопления

По формуле (3) были рассчитаны дозовые факторы накопления для следующих однородных материалов: вода, гомогенная железо-водная защита с 50%-ным объемным содержанием железа, полиэтилен, полиэтилен с 2,5%-ным весовым содержанием естественного бора, серпентинитовый бетон, смесь графита с бором (8% вес.), гидрид титана, гидрид титана с 2,5 вес. % бора, железо, железо с 0,8 вес. % бора, свинец и графит.

Кроме того, изучался вклад в полную дозу от нейтронов различных энергетических групп в защитных композициях, представляющих собой возможное расположение последних слоев реальной биологической защиты.

Во всех композициях в качестве первого слоя выбиралась водородсодержащая среда такой толщины, чтобы в ней устанавливался равновесный спектр, то есть как и в реальном случае, энергетический спектр нейтронов в последних слоях определялся нейтронами первой группы. В качестве первых слоев были рассмотрены следующие среды: вода, серпентинитовый бетон, железо-водная смесь, полиэтилен с бором и гидрид титана.

В качестве второго слоя во всех рассмотренных композициях был взят свинец разной толщины.

При проектировании биологической защиты ядерно-энергетических установок для получения заданной суммарной мощности дозы идут двумя путями: либо увеличивают толщину основного материала защиты (первого слоя), либо добавляют за свинцом слой блокирующего материала, который на малых толщинах сводил бы фактор накопления до минимально возможной величины.

В настоящей работе в качестве блокирующего слоя были изучены два водородсодержащих материала: полиэтилен с бором и гидрид титана с 2,5 вес. % B.

§ 3. Экспериментальное определение дозовых факторов накопления. Сравнение расчетных и экспериментальных данных

Для полиэтилена, серпентинита, гидрида титана с бором и композиции, состоящей из 50 *см* полиэтилена и 10 *см* свинца, были выполнены экспериментальные измерения дозовых факторов накопления. Фактор накопления определялся по отношению двух величин: полной мощности дозы от нейтронов всех энергий и мощности дозы, обусловленной нейтронами с $E_n \geqslant 2$ *Мэв*.

Таблица 3. Расчетные и экспериментальные значения дозовых факторов накопления для различных материалов и композиции

	Материал			
	полиэтилен	серпентинит	гидрид титана с бором	50 *см* полиэтилена + +10 *см* свинца
Экспериментальное значение фактора накопления	2,1	2,05	2,76	3,25
Рассчитанное значение фактора накопления	1,9	2,45	2,4	3,35

Полная мощность дозы определялась изодозным детектором [42]. Для измерения мощности дозы нейтронов с $E \geqslant 2$ *Мэв* использовался дозиметр быстрых нейтронов, в датчике которого применялась таблетка из плексигласа с ZnS (Ag).

В табл. 3 представлены экспериментальные и расчетные данные по факторам накопления для указанных однородных материалов и композиции. Как следует из сравнения расчетных и экспериментальных данных, отличие вычисленных дозовых факторов накопления от измеренных не превышает 20%.

ЛИТЕРАТУРА

1. L. V. Spenser and F. Stinson. Phys. Rev., *85*, 662 (1962).
2. W. P. Stinson. Nucleonics, *12*, 500 (1954).
3. Защита ядерных реакторов. Под ред. Т. Роквелла М., Изо-во иностр. лит., 1958.
4. M. I. Berger, L. V. Spenser. Rad. Res., *10*, 552 (1959).
5. В. А. Дулин, Ю. А. Казанский, В. П. Машкович, Е. А. Панов и С. Г. Цыпин. Атомная энергия, *9*, 315 (1960).
6. В. А. Дулин и др. Атомная энергия, *9*, 318 (1960).
7. Е. Б. Брешенкова и В. В. Орлов. Атомная энергия, *10*, 175 (1961).
8. В. П. Машкович, и С. Г. Цыпин. Атомная энергия, *11*, 251 (1961).
9. Reactor Handbook, vol. III. Part. B. Shielding. Blizard E. P., Editor, ORNL, N. Y., Lond., 1962.
10. В. И. Кухтевич и Б. П. Шеметенко. Атомная энергия, *12*, 204 (1962).
11. Л. Р. Кимель и О. И. Лейпунский Атомная энергия, *12*, 236 (1962).
12. С. Г. Цыпин. Атомная энергия, *12*, 300 (1962).
13. В. П. Машкович. В сб. «Вопросы дозиметрии и защиты от излучений». Под ред. В. И. Иванова Вып. 1, М., Госатомиздат, 1962, стр. 24.
14. О. И. Лейпунский, Л. Р. Кимель и А. М. Панченко. Атомная энергия, *14*, 577 (1963).
15. Л. Р. Кимель, А. М. Панченко и В. П. Терентьев. Атомная энергия, *15*, 328 (1963).
16. А. П. Суворов, Е. Б. Брешенкова и В. В. Орлов. В сб. «Вопросы физики защиты реакторов». Под ред. Д. Л. Бродера и др. М., Госатомиздат, 1963, стр. 30.
17. В. П. Машкович, В. К. Сахаров и С. Г. Цыпин. В сб. «Вопросы защиты реакторов». Под ред. Д. Л. Бродера и др. М., Госатомиздат, 1963, стр. 182.
18. Л. Р. Кимель и О. И. Лейпунский. В сб. «Вопросы физики защиты реакторов». Под ред. Д. Л. Бродера М., и др., Госатомиздат, 1963, стр. 220.
19. С. Г. Цыпин. В сб. «Вопросы физики защиты реакторов». Под ред. Д. Л. Бродера и др. М., Госатомиздат, 1963, стр. 243.
20. Л. Р. Кимель, А. М. Панченко и В. П. Терентьев. В сб. «Вопросы дозиметрии и защиты от излучений». Под ред. В. И. Иванова Вып. 2. М., Госатомиздат, 1963, стр. 6 и 26.
21. И. Г. Дядькин. «Ж. эксперим. и теорет. физ.», *34*, 1504 (1958).
22. В. В. Орлов и Г. И. Марчук. В сб. «Нейтронная физика». Под ред. П. А. Крупчицкого М., Атомиздат, 1961, стр. 30.
23. А. М. Панченко. Атомная энергия, 14, 408, (1963).
24. А. И. Лейпунский и др. Экспериментальные быстрые реакторы в СССР. Труды Второй международной конференции по мирному использованию атомной энергии. Женева, 1958 г. Доклады советских ученых, т. *2*. М., Атомиздат, 1959, стр. 215.
25. Гольдштейн. Основы защиты реакторов. М., Атомиздат, 1961.
26. Б. И. Синицын и С. Г. Цыпин, Атомная энергия, *12*, 306 (1962).
27. Л. П. Абагян, Н. О. Базазянц, И. И. Бондаренко и М. Н. Николаев. Групповые константы для расчета ядерных реакторов. М., Госатомиздат 1964.
28. И. В. Гордеев, Д. А. Кардашев, А. В. Малышев. Справочник по ядерно-физическим константам для расчетов реакторов. М., Атомиздат, 1960.
29. В. А. Дулин. и др. Приборы и техника эксперимента, № 2, 35 (1961).
30. В. А. Дулин, Ю. А. Казанский и И. В. Шугар. Атомная энергия, *14*, 488 (1963).
31. А. Т. Баков, Атомная энергия, *13*, 31 (1962).
32. А. А. Абагян, В. В. Орлов и Г. И. Родионов. О функциях опасности нейтронов при расчете защиты от излучений. В сб. «Вопросы физики защиты реакторов». Под ред. Д. Л. Бродера и др. М., Госатомиздат, 1963, стр. 7.
33. R. E. Lynch et al. A Monte Carlo Calculation of Air-Scattered Gamma Rays, ORNL, 1 (1958).
34. C. D. Zerby. A Monte Carlo Calculation of Air-Scattered Neutrons, ORNL-2277 (1957).
35. F. L. Keller, C. D. Zerby and J. Hilgenman. Monte Carlo Calculation of Flux and Dose Rates Resulting from Neutrons Multiply Scattered in Air, ORNL-2375 (1958).
36. C. R. Mehl. A Monte Carlo Calculation of the Neuron Flux from a Monoenergetic Point Source in Air, SC-4174 (TR), (1958).
37. Nucleonics, *20*, 158, (1962).
38. Д. Л. Бродер и др. Изучение пространственно-энергетических распределений нейтронов в различный средах. Труды Второй международной конференции по мирному использованию атомной энергии. Женева, 1958. Доклады советских ученых, т. *2*. М., ядорные реакторы и ядерная энергетика. Атомиздат, 1959, стр. 67.
39. М. И. Шальнов. Тканевая доза нейтронов. М., Атомиздат, 1960.
40. А. П. Веселкин, Ю. А. Егоров, Ю. В. Орлов и Ю. В. Панкратьев. Атомная энергия, *16*, 32 (1964).
41. В. Н. Аваев, Г. А. Васильев, А. П. Веселкин, Ю. А. Егоров, Ю. В. Орлов и Ю. В. Панкратьев. Атомная энергия, 15, 20 (1963).
42. Х. Д. Андросенко и Г. И. Смиренкин. Приборы и техника эксперимента, № 5, 64 (1962).

ABSTRACT - RÉSUMÉ - АННОТАЦИЯ - RESUMEN

A/377 USSR

New results of shielding research

By O. I. Leipunsky *et al.*

The rapid progress in the utilization of nuclear energy has given rise to a science of nuclear radiation shielding, one of the branches of which is the physics of shielding. The physics of shielding covers investigations of radiation fields, migration of radioisotopes and physical standardization of the biological effects of radiation.

The knowledge of radiation fields in matter is of special importance.

The development of the research techniques requires new experimental facilities and new theoretical approaches. The paper mentions new equipment for carrying out research in the field of shielding.

Many problems connected with gamma-ray and neutron fields have been solved in recent years. A prominent place is held in these investigations by a method whereby the field of an elementary radiation source is investigated first and then the field of a real source is treated as a superposition of the fields from the elementary sources. For a long time, an elementary source was taken to be a point isotropic source. However, a point mono-directional source ("narrow ray") is a more elementary source which can be used to form all sources treated before (isotropic point, isotropic plane and anisotropic sources). The paper presents the results of the experimental study of the fields from mono-directional point sources in various media and the empiric formulae which describe the results of the experiments. A useful contribution to the calculation of the field of a mono-directional point source can be made using adjoint functions for solving the kinetic equation of the transfer of γ quanta.

Calculation of shielding is connected with the evaluation of the biological effect of penetrating radiation. Hence the necessity exists for greater accuracy in determining the spectrum of neutrons coming through the shelding and for the evaluation of the radiation dose from intermediate energy neutrons. A "dose storage factor" was introduced to describe the doses. This "dose storage factor" was calculated for various compositions and various arrangements of the reactor shielding layers.

The extensive use of reactors poses an important problem of shield optimalization. The convenient methods for solving this problem are still being sought. One of such methods is the introduction of the function "effectiveness of the shielding material versus specific process". The mathematical methods of treating this function, particularly, the methods of the perturbation theory make it possible to find the conditions for the optimal composition of the shielding.

A/377 URSS

Résultats nouveaux d'études physiques sur la protection

par O. I. Leipunsky *et al.*

Les progrès rapides en matière d'utilisation de l'énergie nucléaire ont donné naissance à la science de la protection contre le rayonnement nucléaire, dont l'une des branches est la physique de la protection. Celle-ci comprend l'étude des champs de rayonnement, la migration des radioéléments, la normalisation physique des effets biologiques des rayonnements.

La connaissance des champs de rayonnement dans la matière est essentielle.

Le développement de ces études exige que soient créées de nouvelles possibilités expérimentales et de nouvelles méthodes théoriques. Le mémoire rappelle les installations récentes créées pour les études dans le domaine de la protection.

Bien des problèmes ont été résolus ces dernières années en ce qui concerne le champ de rayonnement gamma et de neutrons. Parmi les méthodes, une place importante revient à celle qui permet de résoudre le problème du champ de rayonnement d'une source élémentaire, le champ de la source réelle étant étudié ensuite comme superposition des champs de sources élémentaires. Pendant longtemps, la source élémentaire était considérée comme une source ponctuelle isotrope. Cependant plus élémentaire encore est la source ponctuelle unidirectionnelle (« faisceau mince ») dont on peut former toutes les sources étudiées précédemment (ponctuelle isotrope, plane isotrope ou anisotrope). On donne les résultats de l'étude expérimentale des champs et des sources ponctuelles unidirectionnelles dans différents milieux, ainsi que les formules empiriques qui décrivent ces résultats. Un apport utile au calcul du champ d'une source ponctuelle unidirectionnelle peut être fait par l'application des fonctions adjointes à la solution de l'équation de transfert des photons gamma.

La liaison avec l'évaluation de l'apparition sur le plan biologique des rayonnements pénétrants est caractéristique pour le calcul de la protection. De là la nécessité de connaître avec une plus grande précision le spectre des neutrons sortant de la protection et d'évaluer la dose due aux neutrons d'énergie intermédiaire. Pour caractériser les doses, on a introduit un « facteur d'accumulation de dose ». Ce facteur a été calculé pour différentes compositions et dispositions des enveloppes de protection du réacteur.

A mesure que les réacteurs deviennent plus nombreux, l'importance du problème de l'optimisation de la protection croit et on recherche encore dans ce domaine des moyens commodes de le résoudre. L'un de ces moyens est constitué par l'introduction de la fonction « efficacité du matériau de protection contre un processus donné ». L'étude de cette fonction par des méthodes mathématiques et, notamment par la méthode des perturbations, permet de trouver les conditions de la composition optimale de la protection.

A/377 URSS

Nuevos resultados de los estudios físicos sobre la protección

por O. I. Leipunsky *et al.*

El rápido progreso en la utilización de la energía nuclear ha originado la aparición de la ciencia de la protección contra las radiaciones nucleares, una de cuyas ramas está constituida por la física de la protección. La física de la protección comprende el estudio de los campos de radiación, la migración de los radioisótopos y el establecimiento de normas físicas relativas a los efectos biológicos de la radiación.

Es de particular importancia el conocimiento de los campos de radiación en la materia.

El desarrollo de la investigación exige crear nuevas posibilidades de experimentación y nuevos métodos teóricos. En la memoria se mencionan nuevas instalaciones para las investigaciones en el campo de la protección.

En los últimos años se han resuelto muchos problemas relativos a los campos de rayos gamma y de neutrones. Uno de los principales métodos consiste en determinar primero el campo creado por una fuente elemental y considerar luego el campo de una fuente real como superposición de campos producidos por fuentes elementales. Durante mucho tiempo se ha considerado como fuente elemental una fuente puntual isótropa. Sin embargo, una fuente más elemental está constituida por una fuente puntual colimada (monodireccional, "haz estrecho"), a partir de la cual pueden formarse todas las fuentes antes consideradas (puntual isótropa, plana isótropa o anisótropa). Se dan los resultados del estudio experimental de los campos y de las fuentes puntuales colimadas en diferentes medios, y fórmulas empíricas que describen estos resultados. Puede facilitarse el cálculo del campo producido por una fuente puntual colimada, empleando funciones adjuntas para la resolución de la ecuación de transporte de los fotones gamma.

El cálculo de la protección tiene una relación característica con la evaluación de la acción biológica de los rayos penetrantes. De aquí surge la necesidad de precisar el espectro de neutrones que salen del blindaje y evaluar la dosis de neutrones de energía intermedia. Para caracterizar las dosis se introdujo el "factor de acumulación de dosis". Este "factor de acumulación de dosis" ha sido calculado para diferentes composiciones y disposiciones de las capas del blindaje del reactor.

La amplia extensión de los reactores hace imprescindible la optimización de las protecciones. En este sentido, se buscan aún métodos cómodos para la solución del problema. Uno de ellos es la introducción de la función "importancia del material de blindaje con relación a un determinado proceso". Los métodos matemáticos de estudio de esta función, en particular los métodos de la teoría de perturbaciones, permiten encontrar las condiciones que determinan la composición óptima del blindaje.

Use of response matrix method for multi-layer shield design

By I. Kataoka*

The evaluation of photon transmission through stratified barriers has aroused interest because of its practical usefulness in radiation shield design. The only theoretical treatment applied satisfactorily to this problem has been the Monte-Carlo method.

Calculations by the Monte-Carlo method, however, are performed for a certain configuration of shielding, and usually a result so obtained cannot be applied to other cases. To overcome this inefficiency inherent to the Monte-Carlo calculation, a method—the response matrix method—is introduced and is described in this paper. In this method, an operator is prepared for an elementary part of the shielding by the Monte-Carlo method. It should include all the necessary information so that the result for the whole shielding can be synthetized from the operators for each elementary part. If the geometry is restricted to slab geometry, the energy of photons and the angle of the direction of photon motion to the normal to the slab surface would be enough to represent the condition of a photon. Though this concept is easily extended to other geometries, such as spherical geometry, it will cause great difficulty in practical treatment.

The operator concept was introduced by Peebles and Plesset [1] in which operators were evaluated by computing successive orders of scattering of photons in the elementary slab of material. In this slab, photons suffering more than three collisions were ignored. Yarmush, Zell and Aronson have developed this operator concept into the transmission matrix method [3, 4]. The matrices are deduced elementary matrices which depend on the material but not on its thickness. In evaluating elementary matrices, the formula for a single collision is used. Tsuruo has tried to utilize the operator taking account only of photons energy [5].

Though the response matrix method was originally introduced as an improvement on the Monte-Carlo method, it can suitably be defined as one case of the operator method in which the operators are prepared by the Monte-Carlo method.

DESCRIPTION OF THEORY

If the intensity of radiation reaching a barrier is I, and the transmitted and reflected radiations are I^T and I^R respectively (Fig. 1 (a)), the relation between I and I^T or I^R is recognized as a radiation response of an elementary slab and it is not necessary to consider the detailed behaviour of radiation in it. I can be the numerical flux, the energy flux, the energy current, the dose rate or any other radiation quantity.

In slab geometry, the state of a photon is represented by its energy, E and the angle of the direction of its motion to the normal of the slab surface, θ. By dividing these parameters into a finite number of groups, I is expressed as a form of matrix (Fig. 1 (b)). Then the response matrices for transmission T and reflection R are introduced, and

$$I^T = TI$$

$$I^R = RI$$

$$T \equiv (T_{ij}^{kl}) , R \equiv (R_{ij}^{kl}) .$$

If

$$I = I_{pq} = 1 \ ; \ p = k , q = 1$$

$$= 0 \ ; \ p \neq k \text{ and/or } q \neq 1 ,$$

then the elements of matrices are defined as the response of I by a barrier.

$$T_{ij}^{kl} = I_{ij}^T$$

$$R_{ij}^{kl} = I_{ij}^R$$

The precision of the calculation would improve as the number of groups is increased. The computation time to prepare the response matrices, however, will mount up in proportion to $(m \times n)$. The amount of data included in a response matrix is $(m \times n)^2$.

After trial calculations, the number and the ranges of groups shown in Fig. 1 (c) was chosen for general purpose shielding calculations for reactors and for most isotopes.

The rule for synthesizing a response matrix for two layers is easily deduced:

$$T_{1,2} = T_2(E - R_1R_2)^{-1}T_1$$

$$R_{1,2} = R_1 + T_1R_2(E - R_1R_2)^{-1}T_1$$

where suffixes 1,2 denote the first and the second barriers respectively, and $T_{1,2}$ and $R_{1,2}$ are the resultant response matrices of a stratified slab of two layers. E is the unit matrix. It takes about five seconds to synthesize the response of an additional layer using a medium speed computer.

* Ship Research Institute, Tokyo.

PREPARATION OF RESPONSE MATRICES

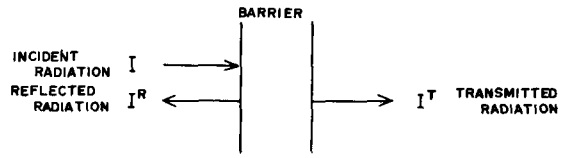
To reduce the counting variance in the Monte-Carlo calculation the technique applied by Berger [6] has been used to evaluate the response matrices of each material.

The response matrices for water, aluminium, iron and lead have been prepared. An example is illustrated in Table 1. History numbers are usually chosen in the range of 5 000-20 000. As can be seen from Table 1, the response matrix of the photon current, the energy current and the energy flux are computed at the same time by one case of calculation. In this table, each element of the matrix is arranged in the same order as shown in Fig. 1 (b) and the print-outs of elements which belong to higher energy groups than the group of the source energy are omitted since they are identically equal to zero. The pair production reaction of photons is counted, and using this data is made use of to take into account the effect of photons produced by the annihilation of positrons.

The output from one of the sample calculations is illustrated in Table 2. It shows the energy and angular distributions of incoming energy flux and also the energy flux transmitted through a stratified slab of 10 cm water, 1.8 cm iron and 2 cm lead.

Table 1. Example of response matrices evaluated by Monte-Carlo method

Alumi 2.000(00)cm	EO = 3.915(00)	WO = 1.000(00)−9.749(−01)	H = 1−20000			
0024693	9.466(−01)	8.716(−01)	9.372(−01)			
0002150	5.333(−02)	6.958(−03)	1.866(−02)			
0000000	0.000(00)	0.000(00)				
Number current, transmitted 9.466(−01)						
7.307(−06)	3.573(−05)	5.739(−05)	1.421(−05)	2.708(−05)	0.000(−00)	0.000(−00)
6.741(−04)	1.924(−03)	2.363(−03)	2.175(−03)	2.221(−03)	7.608(−04)	2.666(−04)
5.832(−03)	1.426(−02)	1.010(−02)	4.229(−03)	3.033(−03)	1.834(−03)	5.783(−04)
1.317(−04)	1.402(−03)	1.064(−02)	2.077(−02)	2.304(−02)	8.267(−03)	4.499(−04)
0.000(00)	0.000(00)	0.000(00)	4.397(−05)	6.186(−03)	2.134(−02)	8.039(−01)
Energy current, transmitted 8.716(−01)						
2.425(−07)	1.220(−06)	1.780(−06)	4.464(−07)	9.074(−07)	0.000(00)	0.000(00)
4.938(−05)	1.377(−04)	1.748(−04)	1.591(−04)	1.620(−04)	5.448(−05)	2.149(−05)
1.291(−03)	3.687(−03)	2.658(−03)	8.476(−04)	5.322(−04)	3.193(−04)	1.046(−04)
5.080(−05)	5.396(−04)	4.361(−03)	1.023(−02)	1.409(−02)	5.579(−03)	2.451(−04)
0.000(00)	0.000(00)	0.000(00)	3.370(−05)	4.952(−03)	1.853(−02)	8.028(−01)
Energy flux, transmitted 9.372(−01)						
1.400(−06)	3.403(−06)	3.246(−06)	6.482(−07)	1.036(−06)	0.000(00)	0.000(00)
4.195(−04)	4.188(−04)	3.271(−04)	2.226(−04)	1.896(−04)	5.814(−05)	2.138(−05)
4.282(−02)	1.110(−02)	5.074(−03)	1.211(−03)	6.233(−04)	3.348(−04)	1.046(−04)
2.826(−04)	1.466(−03)	7.896(−03)	1.421(−02)	1.655(−02)	5.919(−03)	2.456(−04)
0.000(00)	0.000(00)	0.000(00)	4.666(−05)	5.586(−03)	1.934(−02)	8.027(−01)
Number current, reflected 5.333(−02)						
2.423(−09)	5.826(−06)	3.198(−05)	0.000(00)	9.839(−06)	1.597(−05)	0.000(00)
6.122(−04)	2.222(−03)	2.253(−03)	2.416(−03)	1.802(−03)	1.091(−03)	4.782(−04)
4.408(−03)	9.136(−03)	9.949(−03)	7.746(−03)	5.937(−03)	3.864(−03)	1.352(−03)
4.542(−09)	0.000(00)	0.000(00)	0.000(00)	0.000(00)	0.000(00)	0.000(00)
0.000(00)	0.000(00)	0.000(00)	0.000(00)	0.000(00)	0.000(00)	0.000(00)
Energy current, reflected 6.958(−02)						
6.248(−11)	1.456(−07)	1.067(−06)	0.000(00)	3.310(−07)	4.717(−07)	0.000(00)
4.601(−05)	1.685(−04)	1.789(−04)	1.709(−04)	1.310(−04)	7.632(−05)	3.315(−05)
7.941(−04)	1.496(−03)	1.468(−03)	1.037(−03)	7.454(−04)	4.542(−04)	1.552(−04)
1.621(−09)	0.000(00)	0.000(00)	0.000(00)	0.000(00)	0.000(00)	0.000(00)
0.000(00)	0.000(00)	0.000(00)	0.000(00)	0.000(00)	0.000(00)	0.000(00)
Energy flux, reflected 1.886(−02)						
6.939(−10)	3.612(−07)	1.869(−06)	0.000(00)	3.637(−07)	4.967(−07)	0.000(00)
3.736(−04)	4.911(−04)	3.299(−04)	2.449(−04)	1.544(−04)	8.019(−05)	3.320(−05)
6.834(−03)	4.557(−03)	2.787(−03)	1.472(−03)	8.724(−04)	4.792(−04)	1.552(−04)
4.058(−08)	0.000(00)	0.000(00)	0.000(00)	0.000(00)	0.000(00)	0.000(00)
0.000(00)	0.000(00)	0.000(00)	0.000(00)	0.000(00)	0.000(00)	0.000(00)
Pair production reaction						
8.0908(00)	8.3889(00)	7.5722(00)	7.6121(00)	7.3826(00)		
7.1726(00)	7.2436(00)	7.0182(00)	7.1367(00)	6.8054(00)		



(a) RESPONSE OF RADIATION BY A BARRIER

$$I = \begin{pmatrix} I_{11}\ I_{12} \cdots I_{1j} \cdots I_{1n} \\ I_{21}\ I_{22} \cdots I_{2j} \cdots I_{2n} \\ \cdots\cdots\cdots\cdots \\ I_{i1}\ I_{i2} \cdots I_{ij} \cdots I_{in} \\ \cdots\cdots\cdots\cdots \\ I_{m1}\ I_{m2} \cdots I_{mj} \cdots I_{mn} \end{pmatrix}$$

i ; ENERGY GROUP

j ; GROUP OF ANGLE OF PHOTON MOTION

(b) ARRANGEMENT OF RADIATION INTENSITY MATRIX

i	1	2	3	4	5	6	7	8
ENERGY (MeV)	0.02	0.07	0.2	0.7	1.5	2.5	4.0	7.0
	-0.07	-0.2	-0.7	-1.5	-2.5	-4.0	-7.0	-10.0

j	1	2	3	4	5	6	7
COSINE OF ANGLE	0	0.2226	0.4338	0.6235	0.7818	0.9010	0.9749
	-0.2226	-0.4338	-0.6235	-0.7818	-0.9010	-0.9749	-1.0

(c) RANGE OF GROUPS FOR PRESENT CALCULATIONS

Figure 1

The arrangement of elements of the flux matrix is the same as in Fig. 1 (b). The right-hand column and the bottom row indicate the total.

The findings from trial calculations show that the synthesis procedure with about ten layers usually results in an over-estimation of 5 to 10 per cent. The exact amount of the accumulated error by slab synthesis calculation varies according to the material and thickness of the elementary slab. Bearing this fact in mind, the thickness of the elementary slab of each material should be so chosen that any slab thickness of that particular material, applied to common shielding design, can be expressed by a combination of several layers. It leads to the abandonment of the concept in which the operator for a slab of finite thickness is deduced from the operator of an extremely thin slab. This concept has been applied in the transmission matrix method.

Two thicknesses of elementary slab of each material were chosen in the response matrix method; 5 cm and 20 cm for water; 2 cm and 8 cm for aluminium; 1 cm and 4 cm for both iron and lead. The third, thinner layer will be introduced and the response matrices prepared for it. The purpose of

Table 2. Example of photon transmission calculation through stratified slab barriers by response matrix method

Energy flux (source):

1.000(−02)	1.000(−02)	1.000(−02)	1.000(−02)	2.000(−02)	2.000(−02)	2.000(−02)	1.000(−01)
0.000(00)	0.000(00)	2.000(−02)	3.000(−02)	5.000(−02)	5.000(−02)	5.000(−02)	2.000(−01)
0.000(00)	0.000(00)	0.000(00)	0.000(00)	0.000(00)	1.000(−01)	1.000(−01)	2.000(−01)
0.000(00)	0.000(00)	0.000(00)	0.000(00)	0.000(00)	0.000(00)	2.000(−01)	2.000(−01)
0.000(00)	0.000(00)	0.000(00)	0.000(00)	0.000(00)	0.000(00)	3.000(−01)	3.000(−01)
1.000(−02)	1.000(−02)	3.000(−02)	4.000(−02)	7.000(−02)	1.700(−01)	6.700(−01)	1.000(00)

Media :

Water 5.000(00)CM — Water 5.000(00)CM — Iron 1.000(00)CM — Iron 8.000(−01)CM — Lead 1.000 (00)CM — Lead 1.000(00)CM

Energy flux (transmitted):

5.711(−25)	1.408(−25)	5.461(−22)	1.370(−17)	2.609(−21)	5.541(−20)	7.322(−24)	1.376(−17)
1.716(−06)	1.150(−06)	8.139(−07)	9.698(−07)	5.016(−07)	1.582(−07)	7.570(−08)	5.385(−06)
6.108(−04)	9.893(−04)	1.209(−03)	1.270(−03)	1.039(−03)	1.071(−03)	6.910(−04)	6.881(−03)
8.888(−05)	4.208(−04)	1.657(−03)	4.118(−03)	7.151(−03)	5.421(−03)	1.035(−02)	2.921(−02)
1.226(−07)	1.400(−06)	2.259(−05)	1.808(−04)	2.118(−03)	7.349(−03)	3.948(−02)	4.915(−02)
7.016(−04)	1.412(−03)	2.889(−03)	5.571(−03)	1.030(−02)	1.384(−02)	5.053(−02)	8.525(−02)

Table 3. Example of calculation, the last 1 cm lead in Table 2 having been replaced by two layers of 0.5 cm lead

Energy flux (source):

1.000(00) . . . (*same as Table 2*)

Media :

Water 5.000(00)cm — Water 5.000(00)cm — Iron 1.000(00)cm — Iron 8.000(−01)cm — Lead 1.000(00)cm — Lead 5.000(−01)cm — Lead 5.000(−01)cm

Energy flux (transmitted):

1.239(−24)	3.868(−25)	5.902(−22)	1.512(−17)	2.948(−21)	5.552(−20)	2.255(−23)	1.518(−17)
1.845(−06)	1.229(−06)	8.802(−07)	1.015(−06)	5.289(−07)	1.665(−07)	8.028(−08)	5.745(−06)
6.225(−04)	1.021(−03)	1.288(−03)	1.359(−03)	1.099(−03)	1.120(−03)	7.088(−04)	7.221(−03)
8.909(−05)	4.225(−04)	1.660(−03)	4.105(−03)	7.104(−03)	5.371(−03)	1.037(−02)	2.912(−02)
1.193(−07)	1.355(−06)	2.215(−05)	1.766(−04)	2.097(−03)	7.265(−03)	3.949(−02)	4.905(−02)
7.136(−04)	1.446(−03)	2.971(−03)	5.642(−03)	1.030(−02)	1.375(−02)	5.057(−02)	8.540(−02)

supplementing the standard thickness is to avoid the error caused by thickness interpolations in some special cases which is discussed in a later section of this paper. There is no indication of the need for a fourth standard layer.

The interpolation of the energy flux or the energy current on the slab thickness is made on the following assumptions, (*a*) the photons which belong to one group of specific energy and angle will not fall into other groups during transmission through an elementary slab and (*b*) within an elementary slab the energy flux or the energy current of each group varies exponentially with transmission length.

One of the indications of the validity of these assumptions can be seen from the curves in the slab of the same material in Fig. 2.

TRANSMISSION CALCULATIONS AND DISCUSSION

Build-up factors for one-material slab

To examine the validity of the response matrix method in photon transmission calculation through a slab, the build-up factors for slabs of one material have been computed by applying this method and compared with the results of other theoretical calculations (Table 4). If account is taken of statistical errors inherent in the Monte-Carlo method, it is considered that the results are consistent.

Build-up factors for two-layer slabs

Comparison with Monte-Carlo calculation

Bowman and Trubey give the dose build-up factors for a stratified two-layer slab of lead and water, by applying the Monte-Carlo method [10, 11]. Corresponding calculations have been performed by the response matrix method. Some of the results are illustrated in Table 5 and in Fig. 3.

In Table 5, the failure of thickness interpolation is pointed out and this is discussed below. Apart from these cases, there is consistency.

Figure 3 indicates the different trend of dose build-up factors between the two methods for the

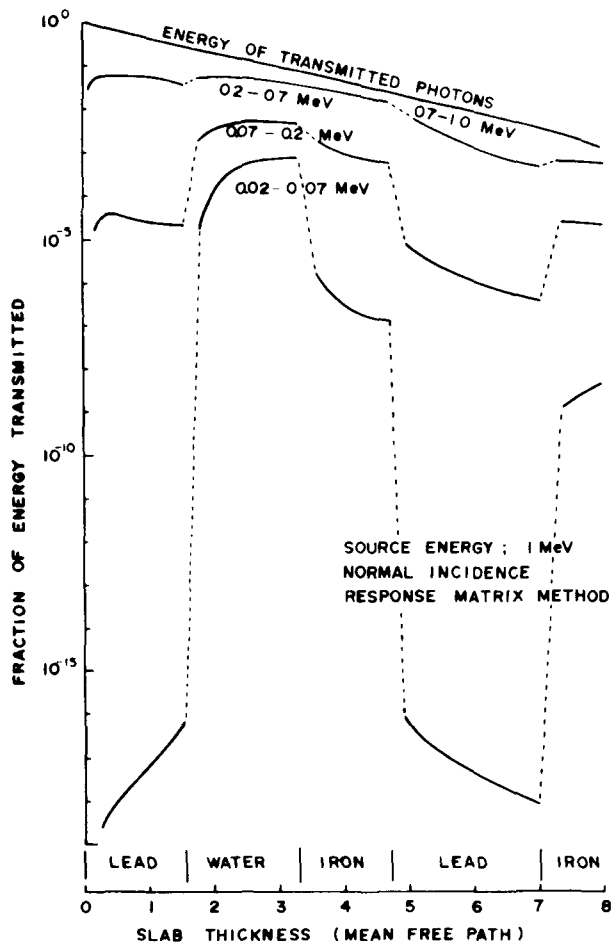


Figure 2. Energy transmission through stratified slabs

Table 4. Build-up factors for slab source energy 1MeV, normal incidence

Material	Thickness (mfp)	Energy build-up factor			Dose build-up factor			
		Moments method[a]	Monte-Carlo method [8]	Response matrix method	Moments method[a]	Monte-Carlo method[b]	Monte-Carlo method [10]	Response matrix method
Water	1	2.21	1.80	1.76	2.26	1.84	1.78	1.79
	2	3.28	2.72	2.61	3.39	2.81	2.62	2.65
	4	5.89	5.01	4.77	6.27	5.33	4.95	4.86
	6			7.77			8.00	7.92
Iron	1	1.89	1.72	1.70	1.92	1.74		1.73
	2	2.68	2.43	2.39	2.74	2.48		2.43
	4	4.45	4.07	4.08	4.57	4.18		4.16
	6			6.28				6.43
Lead	1	1.37	1.35	1.34	1.38	1.36	1.37	1.35
	2	1.65	1.63	1.62	1.68	1.66	1.61	1.63
	4	2.12	2.09	2.06	2.18	2.15	2.04	2.07
	6			2.55			2.48	2.57

[a] Build-up factors for infinite media. The rest are build-up factors behind finite slabs [7].

[b] From Table 10.14 of Ref. [9]; data are estimated by applying the ratio of the dose build-up factors to the energy build-up factors of the moments method, in column a, to the energy build-up factors which are shown in column b.

Table 5. Build-up factors for stratified slabs of lead and water (normal incident)

Slab thickness (mfp)		Energy build-up factor		Dose build-up factor		
		Response matrix method	Monte-Carlo method [8]	Response matrix method	Monte-Carlo method [11]	Monte-Carlo method[a]
Lead	Water	Lead followed by water				
1	0	1.34	1.35	1.35	1.37	1.36
0.75	0.25	(1.13)[b]		(1.13)[b]	1.53	
0.50	0.50	(1.38)[b]		(1.39)[b]	1.64	
0.25	0.75	1.58		1.60	1.73	
0	1	1.76	1.80	1.79	1.78	1.84
2	0	1.62	1.63	1.63	1.61	1.66
1.5	0.5	1.94		1.97	2.02	
1	1	2.20		2.23	2.33	
0.5	1.5	(2.20)[b]		(2.23)[b]	2.52	
0	2	2.61	2.72	2.65	2.62	2.81
4	0	2.06	2.09	2.07	2.04	2.15
3	1	2.89		2.93	3.10	
2	2	3.69		3.75	3.90	
1	3	4.26		4.33	4.48	
0	4	4.77	5.01	4.86	4.95	5.33
Water	Lead	Water followed by lead				
1	0	1.76	1.80	1.79	1.78	1.84
0.75	0.25	1.56		1.57	1.53	
0.50	0.50	1.43		1.44	1.43	
0.25	0.75	(1.13)[b]		(1.13)[b]	1.40	
0	1	1.34	1.35	1.35	1.37	1.36
2	0	2.61	2.72	2.65	2.62	2.81
1.5	0.5	2.00		2.03	1.97	
1	1	1.79		1.80	1.70	
0.5	1.5	1.69		1.70	1.62	
0	2	1.62	1.63	1.63	1.61	1.66
4	0	4.77	5.01	4.86	4.95	5.33
3	1	2.94		2.97	2.50	
2	2	2.56		2.58	2.16	
1	3	2.24		2.26	2.06	
0	4	2.06	2.09	2.07	2.04	2.15

[a] *From Table 10.14 of Ref. [9]. Data are estimated by applying the ratio of the dose build-up factors to the energy build-up factors of the moments method [7] to the energy build-up factors which are shown in column a.*

[b] Data in parentheses do not seem to be credible because of the failure of interpolation on the slab thickness. It is discussed in the text.

water-lead slab composition. Though the Monte-Carlo calculations should be considered more reliable than the response matrix method as a general rule, it does not necessarily follow that the response matrix method is not valid in these cases, since the experimental results seem to show the same drift as the response matrix calculations, rather than the Monte-Carlo calculations. The data from solutions by direct integration of the slab geometry transport equation are also indicated in Fig. 3.

Comparison with experimental measurements

Miyasaka *et al.* [13] have performed dose-rate measurements behind single and stratified slabs using a Co^{60} source and applying the technique of Kirn *et al.* [15]. Part of these data is illustrated in Fig. 4 together with the values obtained by the response matrix method. In view of the errors in both measurements and calculations, agreement is satisfactory.

Build-up factors for four-layer slabs

To evaluate the adaptability of the response matrix method to stratified slab calculations of more than two layers, the dose build-up factors of the experimental results by Mochizumi *et al.* [14] and of the response matrix calculations are shown in Fig. 5. Measured dose build-up factors for an iron slab indicate lower values than those by the response matrix method and by the Monte-Carlo calculation [8]. As described earlier both theoretical results are considered to be consistent. If account is taken of this difference of build-up factors for the iron slab, the response matrix method represents the behaviour of photons in the multiple layer slab barriers fairly well.

Discussion on validity of interpolation

The techniques of interpolation of the energy flux or current on slab thickness is valid if it is applied

to the slab which comes after one of the same material. One example is shown in Table 3. In this calculation two layers, of 0.5 cm lead slabs, are substituted for the last 1 cm lead slab in the configuration of Table 2. Comparison of the transmitted energy fluxes of Tables 2 and 3 illustrates the consistency not only of the total flux but also of the value of each element of the matrix and demonstrates the validity of the interpolation in this case.

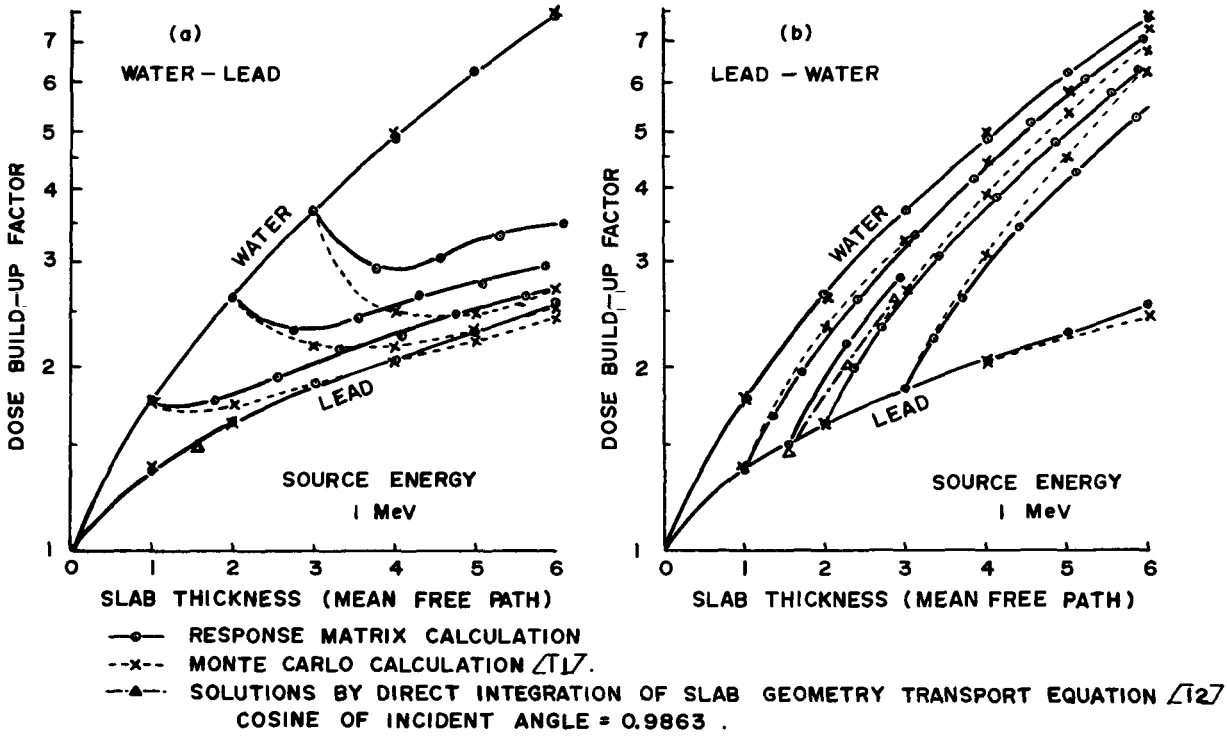


Figure 3. Dose build-up factors through stratified slabs (lead and water)

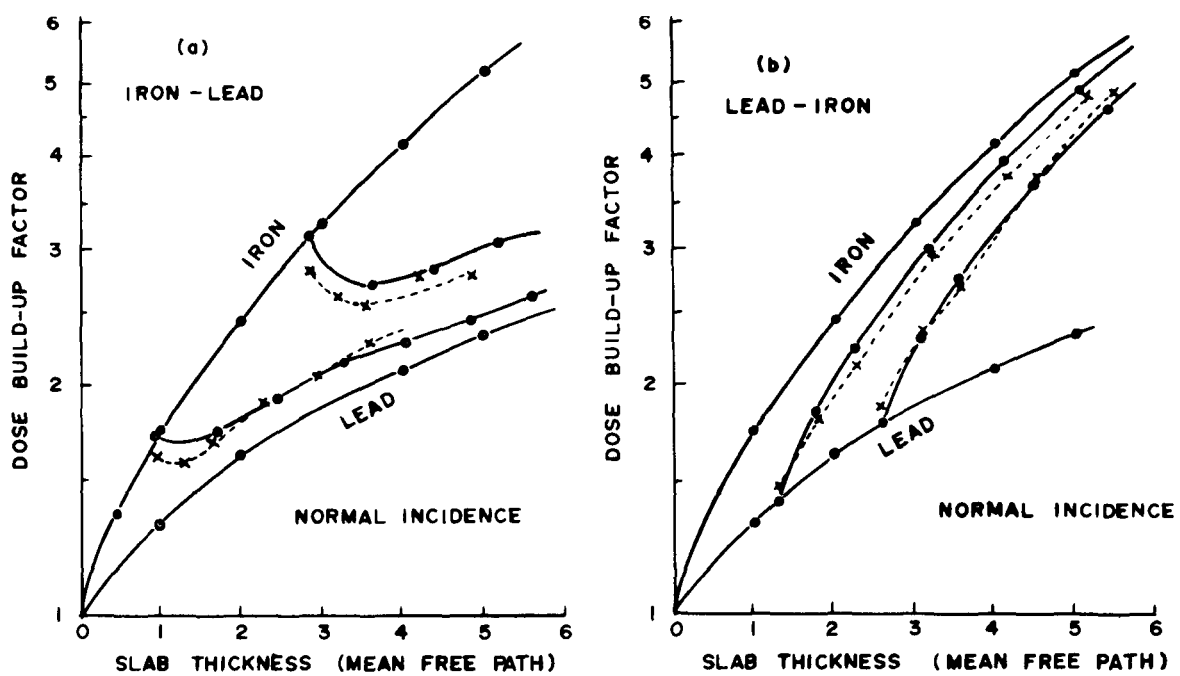


Figure 4. Dose build-up factors through stratified slabs (lead and iron)

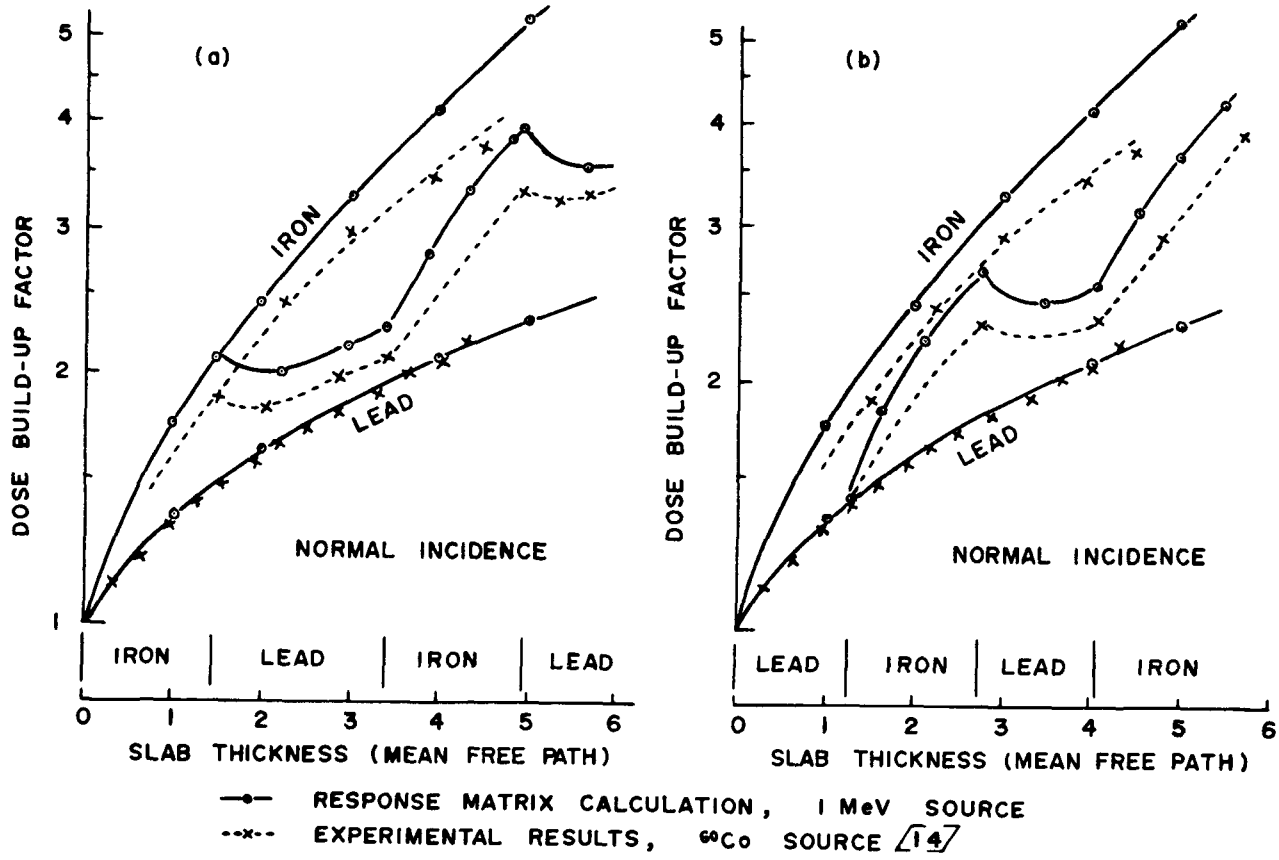


Figure 5. Dose build-up factors through stratified slabs (lead and iron)

When an interpolation is applied to a slab which is the first layer of a barrier or comes at the rear of a slab of different material, the interpolation is usually invalid. Rapid change in the photon intensity of each energy group makes interpolation difficult. The idea of the order of changes near the front face of barrier or behind the layer of different material can be seen in Fig. 2. To avoid this difficulty, the third standard thickness for which the response matrices will be prepared should be introduced in addition to the existing two standard layers already chosen for each material.

CONCLUSION

(*a*) The response matrix method mentioned above can be applied satisfactorily to the gamma-ray transmission problem in stratified slab barriers of different materials.

(*b*) The response matrices for water, aluminium, iron and lead have been prepared by the Monte-Carlo method.

(*c*) Since computation time for a synthesis calculation for a layer of slab is very short, the response matrix method can be used for practical design work for gamma-ray shielding.

(*d*) The response matrix calculation will give not only the total energy flux or current but also the energy and/or angular spectrum.

REFERENCES

1. Peebles, G. H., and Plesset, M. S., Phys. Rev., *81*, 430 (1951).
2. Peebles, G. H., USAEC report R-240 (1952).
3. Aronson, R., USAEC report WADC-TR-58-383 (1958).
4. Yarmush, D., Zell, J., and Aronson, R., USAEC report WADC-TR-59-772 (1960).
5. Tsuruo, A., J. Atomic Energy Soc. Japan, *6*, 91 (1964).
6. Berger, M. J., J. Res. Nat. Bur. Stands., *55*, 343 (1955).
7. Goldstein, H., and Wilkins, J. E., Jr., USAEC report NYO-3075 (1954).
8. Berger, M. J., and Doggett, J., J. Res. Nat. Bur. Stands., *56*, 89, (1956).
9. Blizard, E. P., and Abott, L. S. (ed.), *Reactor Handbook*, Vol. III, Part B, *Shielding*, p. 119, Interscience (1962).
10. Bowman, L. A., and Trubey, D. K., USAEC report CF-58-1-41 (1958).
11. Bowman, L. A., and Trubey, D. K., USAEC report ORNL-2609, p. 110 (1958).
12. Kataoka, I., and Takeuchi, K., to be published.
13. Miyasaka, S., Furuta, Y., Tsuruo, A., Tamura, K., and Kanemori, Y., 3rd National Nuclear Congress (1962).
14. Mochizuki, H., Tanaka, Y., Higashihara, Y., and Nagato, K., J. Atomic Energy Soc. Japan, *4*, 703 (1962).
15. Kirn, F. S., *et al.*, Radiology, *63*, 94 (1954).

ABSTRACT - RÉSUMÉ - АННОТАЦИЯ - RESUMEN

A/657 Japon

Application de la méthode des matrices de réponse aux projets de blindage à plusieurs couches

par I. Kataoka

Le mémoire présente une méthode pour calculer la transmission et la réflexion des rayons gamma dans le blindage en plaques à plusieurs couches. La méthode est basée sur le fait que la transmission et la réflexion des rayonnements dans une barrière peut être exprimée par un opérateur, dans ce cas par une matrice.

Peebles et Plesset ont indiqué que la méthode des matrices peut être appliquée au calcul des blindages. Les opérateurs ont été évalués pour des plaques élémentaires de fer et de plomb dans lesquelles les photons diffusés plus de trois fois étaient négligés. Yarmush, Zell et Aronson ont développé cette idée pour élaborer la méthode des matrices de transmission. Ces matrices sont déduites de matrices élémentaires qui ne dépendent que du matériau et non pas de l'épaisseur. En évaluant les matrices élémentaires, on utilise la formule pour une seule collision.

La méthode des matrices de réponse décrite dans le mémoire diffère de la méthode des matrices de transmission sur plusieurs points qui suivent. Les matrices de réponse élémentaires sont calculées par la méthode de Monte Carlo et par intégration directe des équations de transport et les distributions angulaires des rayons gamma sont divisées en groupes de direction. Les matrices de réponse de chaque matériau sont préparées pour deux épaisseurs différentes, c'est-à-dire forte et faible. Chaque matrice de réponse est calculée directement pour la barrière de cette épaisseur et n'est pas déduite des matrices d'une plaque élémentaire, c'est-à-dire d'une plaque extrêmement mince. Ceci empêche les erreurs de s'accumuler dans les calculs de la pénétration profonde.

Le flux numérique, flux d'énergie ou courant d'énergie des rayons gamma est divisé en groupes d'énergie et aussi en groupes angulaires. On a préparé les matrices de réponse pour l'eau, l'aluminium, le fer et le plomb. La distribution énergétique et angulaire des photons transmis et réfléchis dans le blindage à plusieurs couches peut être calculée en appliquant successivement les matrices de réponse de chaque plaque élémentaire aux rayonnements incidents.

Les exemples de calculs sont comparés avec les résultats de l'intégration directe de l'équation de transport et ceux d'autres calculs par la méthode de Monte Carlo.

A/657 Япония

Использование метода матричных характеристик для расчета конструкции многослойной защиты

И. Катаока

В докладе рассматривается метод расчета прохождения и отражения γ -лучей в многослойной пластинчатой защите. Метод основан на том факте, что прохождение и отражение радиации через барьер могут быть описаны оператором, в данном случае матрицей.

Пиблз и Плессе указали на применимость матричного метода для расчета защиты. Операторы были оценены для элементарных пластин железа и свинца, при этом фотоны, испытавшие более трех соударений, не учитывались. Ярмаш, Зелл и Аронсон развили эту концепцию применительно к матричному методу пропускания. Матрицы выводятся из элементарных матриц, которые зависят от материала, а не от толщины. При оценке элементарных матриц использовалась формула для однократных столкновений радиации.

Описанный в данном докладе метод матричных характеристик отличается от матричного метода пропускания в нескольких отношениях. Элементарные матричные характеристики рассчитываются по методу Монте-Карло и непосредственному интегрированию уравнений переноса и угловое распределение гамма-лучей делится на несколько групп. Матричные характеристики каждого материала берутся для двух различных толщин: тонкой и толстой. Каждая матричная характеристика определяется непосредственно для барьера данной толщины, а не выводится из матриц элементарной пластины, то есть предельно тонкой пластины. Это дает возможность исключить наложение ошибок при расчете глубины проникновения радиации.

Поток γ -лучей делится на группы по энергии и по направлению. Были подготовлены матричные характеристики для воды, алюминия, железа и свинца. Энергетическое и угловое распределение пропущенных и отраженных фотонов в многослойной защите может быть вычислено с использованием матричных характеристик каждой элементарной пластины по отношению к падающему излучению.

Расчеты сравниваются с результатами прямого интегрирования уравнения переноса и результатами расчетов по методу Монте-Карло.

A/657 Japón

Aplicación del método de matriz de respuesta al proyecto de blindaje de varias capas

por I. Kataoka

En esta memoria se presenta un método para calcular la transmisión y reflexión de rayos gamma en blindajes compuestos de varias capas planas. El método está basado en el hecho de que la transmisión y reflexión de radiaciones en una barrera puede expresarse por un operador, en este caso una matriz.

Peebles y Plesset han señalado la aplicabilidad del método matricial a los cálculos de blindaje. Se evaluaron los operadores para planchas elementales de hierro y plomo, sin tener en cuenta los fotones que experimentan más de tres colisiones. Yarmush, Zell y Aronson han desarrollado la idea hasta constituir el método de matrices de transmisión. Las matrices se deducen de matrices elementales, que dependen del material, pero no de su grosor. Para evaluar matrices elementales se utilizan las fórmulas para una sola colisión de las radiaciones.

El método de matriz de respuesta descrito en este documento difiere en varios puntos del método de matriz de transmisión. Por ejemplo, las matrices de respuesta elementales se calculan por el método de Monte Carlo y por integración directa de las ecuaciones del transporte y las distribuciones angulares de los rayos gamma se dividen en grupos de direcciones. Las matrices de respuesta de cada material están preparadas para dos diferentes espesores, delgado y grueso. Cada matriz de respuesta se calcula directamente para la barrera de este espesor, no deduciéndola de matrices de una lámina elemental, o sea, de una lámina extremadamente delgada. Esto evita la acumulación de errores en los cálculos de penetraciones profundas.

El flujo numérico, flujo de energía o corriente de energía de rayos gamma se ha dividido en grupos de energía y también en grupos direccionales.

Han sido preparadas las matrices de respuesta para agua, aluminio, hierro y plomo. La distribución en ángulo y energia de los fotones transmitidos y reflejados en el blindaje de varias planchas puede calcularse aplicando sucesivamente las matrices de respuesta de cada plancha elemental a las distribuciones incidentes.

Se comparan los cálculos de prueba con los resultados de la integración directa de la ecuación del transporte y de otros cálculos por el método de Monte Carlo.

A new shield design method and some attenuation studies in laminated biological shields

By E. Aalto*, L. Hjärne* and M. Leimdörfer**

When the Swedish effort in reactor shielding research and development was initiated some years ago, it was felt that a thorough knowledge of how to deal with problems concerning the penetration of radiation through laminated, massive shields in simple geometries should be the backbone of all subsequent shielding research. This report presents, in a condensed form, the most important results of our systematical work towards acquiring such knowledge. These are the NRN shield design method and the experimental study of the accuracy of this and other available design methods. The study is based on an extensive series of precision flux measurements in a great number of shield configurations.

THE NRN SHIELD DESIGN METHOD

Neutron transport

Most of the routine methods, at present used for predicting the penetration and slowing-down of neutrons in laminated reactor shields, are based upon the application of a fast neutron (removal) kernel which is inserted into a system of few-group or multi-group diffusion equations. Either an entirely empirical removal kernel [1, 2] or a more refined energy dependent kernel [3, 4] has been used, and the thermal neutron fluxes obtained generally seem to be in good agreement with experiments. These methods, however, are not capable of giving as detailed information on the neutron spectrum as is needed for predictions of biological dose-rates and radiation damage effects. In our method, presented at greater length in [5], the numerical advantages of the older methods are retained while a good description of the neutron spectrum is obtained.

We start by outlining the formalism at the fission process. The continuous energy spectrum of the neutrons released in fission is treated as a discrete array of δ-functions distributed systematically over the energy interval containing fission neutrons. The number of "spikes" is considered to be sufficiently large for an accurate representation of the fission spectrum to be obtained.

The flux of neutrons having suffered no collision or only strongly forward directed collisions, for historical reasons hereafter referred to as the removal flux, may be calculated by integration of an uncollided kernel over the core volume with a properly defined removal cross section, $\Sigma_{\text{rem}}(E_i)$, where E_i are the discrete points of the fission spectrum. In doing this, we again postulate that the neutrons which have suffered small-angle deviations encounter a Σ_{rem} at the energy at which they were released.

We define $\Sigma_{\text{rem}}(E_i)$ by the relation

$$\Sigma_{\text{rem}}(E_i) = \Sigma_{\text{tot}}(E_i) - 2\pi\int_{-1}^{1} w(\mu)\Sigma_{\text{el}}(E_i, \mu)\mathrm{d}\mu \quad (1)$$

where $w(\mu)$ is a weight function. We have chosen a Heaviside function $w(\mu) = H(\mu_0) = \begin{cases} 0; \mu < \mu_0 \\ 1; \mu \geqslant \mu_0 \end{cases}$

The parameter μ_0 is a boundary cosine, in the laboratory system of reference, defining a cone into which the virgin neutrons may be scattered without losing their character of being (virtually) unscattered. The rest of the notation is self-explanatory. This definition of the removal cross section departs from that used elsewhere, e.g. [5], namely,

$$\begin{aligned}\Sigma_{\text{rem}}(E_i) &= \Sigma_{\text{tot}}(E_i) - 2\pi\int_{-1}^{1}\mu\Sigma_{\text{el}}(E_i, \mu)d\mu \\ &= \Sigma_{\text{tot}}(E_i) - \bar{\mu}(E_i)\Sigma_{\text{el}}(E_i) \qquad (2)\end{aligned}$$

(equal to the transport cross section) in that it defines the degree of anisotropy allowed in the removal flux. (Eq. (1) is identical to Eq. (2) if $w(\mu) \equiv \mu$, but this is an unrealistic choice in the light of our model, as the weight function would then be negative for backward scattering and, in fact, permit the removal cross section to be greater than the total cross section). It may seem desirable that the energy degradation coupled to the deviation μ_0 is not stronger so that the neutrons are kept above the next lower energy point E_{i+1}. The strongest energy degradation is, of course, obtained with a hydrogen moderator having the scattering law $E = E' \cdot \mu^2$ (μ is the laboratory cosine), and therefore, we get the following condition

$$\mu_0 > (E_{i+1}/E_i)^{\frac{1}{2}} \qquad (3)$$

or for an arbitrary atomic mass A

$$\mu_0 > \tfrac{1}{2}(A+1)(E_{i+1}/E_i)^{\frac{1}{2}} - \tfrac{1}{2}(A-1)(E_i/E_{i+1})^{\frac{1}{2}} \qquad (4)$$

The optimum value of the parameter μ_0 was found to be about 0.6 to 0.65 by comparison between pre-

* AB Atomenergi, Stockholm.
** Research Institute of National Defence, Stockholm.

diction and experiment in a number of problems involving basically different shield configurations [15]. The value 0.60 was used in obtaining the results displayed below. It may be pointed out that the energy degradation corresponding to $\mu_o = 0.60$ may be large enough to remove a neutron from the removal group by scattering against very light nuclei if a dense removal group structure is used. We did not pay any special attention to this but kept all neutrons in the removal group if they were not deviated more than the prescribed angle. This partial overlap of the removal groups did not cause any difficulties. (This matter is discussed in more detail in [5].)

The removal fluxes are fitted as source terms into a multi-group diffusion scheme by the operation

$$\vec{S}_{rd} = C \cdot \vec{\phi}_{rem} \tag{5}$$

where $\vec{S}_{rd}$ is a vector of source terms in the diffusion equations, $\vec{\phi}_{rem}$ a vector of removal fluxes and C a conversion matrix. The matrix elements C_{ij} give the number of neutrons that are transferred from removal group i to diffusion group j by elastic and inelastic collisions per unit length

$$C_{ij} = \int_{E_{j+1}}^{E_j} \Sigma_{el}[E_i, \mu(E/E_i)]dE + \int_{E_{j+1}}^{E_j} \Sigma_{in}(E_i, E)dE . \tag{6}$$

The general expressions appearing in Eq. (6) contain elastic scattering angular distributions and inelastic scattering energy distributions with a discrete-level representation below a certain energy and a continuum above that energy. Inelastic scattering is considered isotropic. The operations in Eq. (6) are performed in the NRN method by a data preparation program, NECO, based on a library of cross sections with a representation similar to that of reference [6]. The integration of the removal fluxes

$$\phi_{rem,i} = \int_{\text{core volume}} \frac{e^{-\Sigma_{rem,i}\left|\vec{r}_c - \vec{r}_s\right|}}{4\pi\left|\vec{r}_c - \vec{r}_s\right|^2} \, dv \tag{7}$$

can be performed in box and slab geometries ($\vec{r}_c$ and $\vec{r}_s$ are points in the core and shield, respectively). The multi-group diffusion equations

$$D_j \Delta\phi_j - \Sigma_{abs,j}\phi_j + S_j = 0 \tag{8}$$

can be solved in one-dimensional plane, cylindrical, and spherical geometries. The D_j are defined

$$D_j = 1/3\Sigma_{tr,j} \tag{9}$$

with $\Sigma_{tr}(E) = \Sigma_{tot}(E) - \mu(E)\Sigma_{tot}(E) - \frac{4}{5}\Sigma_{abs,j}(E) + \frac{9}{5}\mu(E)\Sigma_{abs,j}(E)$

where $\Sigma_{abs,j}(E)$ is the probability per unit length that a neutron in diffusion group j be either physically absorbed or scattered below the lower energy boundary of group j. Group averaging of $\Sigma_{tr}(E)$, as well as of $\Sigma_{abs,j}(E)$, to obtain $\Sigma_{tr,j}$ and $\Sigma_{abs,j}$ is performed with a spectrum of the form E^{-c} in each group, where c is given values according to the expected shape of the results. The source term $\vec{S}_j$ is defined by

$$\vec{S}_j = S_{rd,j} + \sum_{j'<j} \phi_{j'} \Sigma_{j'\to j} \tag{10}$$

where $\Sigma_{j'\to j}$ equals the probability per unit length that a neutron in group j' be scattered, elastically or inelastically, into group j, again averaged over an assumed spectrum in group j'. In references [2-4], the slowing-down between groups is considered by age theory.

This latter treatment of slowing-down is not adequate in the MeV region as it does not allow for a general consideration of inelastic scattering. Moreover, moderation with light elements, especially hydrogen is outside the region of applicability of such a model. It is shown in [5] that the two methods of dealing with slowing-down converge, as they should, for heavy moderators. The NECO multi-group parameter program has an option for providing also such a diagonalized slowing-down matrix as is obtained from the age model, but that was not used when obtaining the results displayed here.

Gamma transport

The transport of photons produced in the reactor core and in the shield constitutes a self-contained problem. Most standard methods used at present for theoretical analyses of the migration of gamma-rays in shields rely on the build-up concept to account for the collided radiation component. These methods are rather questionable in heterogeneous configurations as build-up factors can not be obtained for each combination of materials and geometries. The method used in the NRN system is designed for arbitrarily laminated shields and employs the Monte Carlo technique with various departures from direct numerical simulation to accelerate the convergence of the calculation process. The essential "tricks" are the application of a modified exponential transformation which improves the forward penetrability of the sample photons and alters the spatial dependence of the source density to make it more favourable for Monte Carlo treatment. At present, only a one-dimensional plane geometry version of the associated programs exists (SALOME on the Ferranti Mercury and SALOMON on the IBM 7090), but spherical as well as cylindrical versions will be ready in the near future. A thorough description of the method is given in Refs. [7, 8, 9]. The output of the programs provides the penetration dose-rate, with a specification of the contributions from photons born in various predefined spatial regions, and the energy deposition rate in the same regions.

General remarks

At the moment the complete NRN design method is available for the Ferranti Mercury computer only, with the exception of the part for gamma transport which exists in a FORTRAN version (see above). The whole method will, however, soon be translated into FORTRAN. The necessary input data have been simplified as much as possible, and consist mainly of specifications regarding materials and geometry.

ATTENUATION MEASUREMENTS IN MASSIVE SHIELDS

Experimental facilities and instrumentation used

The experimental shielding facilities are situated around the pool of the R2-0 (100 kW) reactor at the Studsvik Research Center. These facilities [10] consist of a large (appr. 200 × 200 cm) window and a number of small (50 × 50 cm) windows. In the large window, detectors are placed in channels transverse to the axis towards the reactor. The only disadvantage observed in this facility is the unavoidable air gap (~ 30 cm) between the pool lining and the experimental set-up.

In the instrumentation we have tried to keep the movable part as simple as possible. The calibrated electronic equipment is permanently installed in laboratory rooms to minimize drifts because of various sources. This principle led to the use of the foil technique for the neutron measurements. Routines, automated as far as possible, have been worked out both for cadmium ratio measurements (Mn normally used) and double foil (Au-Cu) measurements, as well as for the threshold detectors, of which P(n, p) has been predominantly used.

Gamma measurements were performed using both primary (ion chambers and gamma dosimeters) and secondary instruments (films and G-M instruments). A rather thorough study of the sources of error (exposure rate, neutron interference and energy and material dependence) was performed.

For ion chambers, the neutron sensitivity is the most important source of error. Normally, no correction because of this factor seems to have been applied in this type of measurement. The fast neutron sensitivity of the ion chambers used was studied, [10] and, as a result, the observed ionization rates were corrected by multiplying them by a factor of 0.9.

The energy dependence of the chambers was studied experimentally by varying the thickness of a sleeve of air-equivalent material. No difference in the absorbed energy was observed between wall thicknesses from 250 to ~ 800 mg cm^{-2}. Even theoretically it can be shown that the disturbance that reaches the chamber because of electron non-equilibrium is small, < 15-5 per cent for the wall thicknesses mentioned. The exposure rates were so low that no error because of them was to be feared.

As for the gamma films, neutron interference has been shown to be negligible. The discrepancies between ion chamber and film measurements (up to 20-30 per cent) are explainable by the large energy dependence of the films.

Materials and configurations studied

Measurements were made in water (neutron fluxes only), in 6 configurations consisting mainly of magnetite concrete, and in 2 configurations of ordinary concrete. Besides, measurements were made in laminated Fe-D_2O [11].

Great importance must be attached to the accuracy of the physical data on the materials, for instance the errors originating from the uncertainties in concrete density are of the same order of magnitude as those from the uncertainty in design methods (see next section).

The reasons for studying the particular set of massive shield configurations reported here are twofold. First, we wanted to study the effect of introducing thin layers of heavy material (lead) into the shield. Secondly, as it is known that the translation between the experimental and calculational geometries is very difficult, we varied the thickness of the water layer nearest to the core, to get an idea of the sensitivity of the design methods to this type of small deviation.

Sources of error in the measurements described above

We divided item into the following main groups:

(*a*) Reactor power and the length of the runs;

(*b*) Differences between calculated and experimental geometries;

(*c*) Errors in the measurements for reasons other than those specified above;

(*d*) Variations within the materials studied.

The most important points are (*a*) and (*d*). In comparison to them, the others can generally be neglected. As to (*a*), it may be mentioned that the absolute reactor power has been determined with an accuracy estimated to be equal to ± 5 per cent. As to (*d*), the values with standard deviations obtained are:

magnetite concrete:

$$\rho = 3.74 \pm 0.05 \text{ g cm}^{-3},$$
$$w = 0.133 \pm 0.004 \text{ g cm}^{-3}$$

ordinary concrete:

$$\rho = 2.43 \pm 0.02 \text{ g cm}^{-3},$$
$$w = 0.165 \pm 0.004 \text{ g cm}^{-3}$$

(where ρ = density, w = water content). These errors in materials data give, after ~ 1.7 m penetration, a probable error of ~ 25-30 per cent in the dose attenuation in the magnetite concrete. The corresponding value for the ordinary concrete is ~ 10-15 per cent.

ATTENUATION MEASUREMENTS IN LAMINATED IRON AND HEAVY WATER

There exist well documented neutron flux measurements in configurations of iron and ordinary water, but no published data for iron and heavy water have been found. On the other hand, in heavy water reactor design work, heat generation and radiation damage rates in the region of reflector-thermal shield-pressure vessel ought to be known as precisely as possible. Thus, a series of measurements has been performed in order to check the accuracy of the available design methods in this case [11].

The effective cross section of the 2 × 2 m window was decreased to 1.5 × 1.5 m. The D_2O was kept in aluminium tanks to maintain the advantages of a dry facility. The configurations studied simulated the reflector-thermal shield-vessel wall and the top of a reactor core with thermal shields, respectively. An example of the results is presented in Fig. 10.

CALCULATIONS PERFORMED

Methods used

The methods used are:

1. The multi-group removal diffusion method developed at Harwell (RASH B3) [3].
2. Our NRN method presented [12].
3. NIOBE (Numerical Integration of Boltzmann-Equation) [13].

The reason for presenting results obtained by an older (RASH B_3) version of method 1 in these comparisons is that this method has been used to design the main shields of the R-3 (Ågesta) power reactor. We want to point out that there exists a later, improved version of this method even though it has not been used in this study. The multi-group parameters for the diffusion equations have been calculated using the MENDIP code [14].

On the application of the methods

We have been careful to avoid any adjusting of the input data directed towards obtaining good agreement between the measured and calculated values. A formal exception is the case of the NRN method, in which the scattering cosine μ_0 has first been experimentally determined [15], but this cosine has the same value (0.60) for all materials and should be considered as a "universal constant".

The calculations of neutron fluxes were performed, as far as possible, with equal input data in all the methods. The following points should be mentioned:

(*a*) The core was divided into an approximately equal number of volume elements in methods 1 and 2 for the "box"-geometry handling of removal sources. (8 × 8 × 16 vs. 6 × 6 × 12 elements);

(*b*) In method 3 a core, with radius 30 cm and with 10 radial source points was used;

(*c*) The geometry for the diffusion parts of methods 1 and 2 has a core radius of 30 cm;

(*d*) The same thermal neutron constants were used in methods 1 and 2.

COMPARISON OF THE MEASURED AND CALCULATED FLUXES

Quantities to be compared and their presentation

The composition and designation of configurations studied is shown in Fig. 1. We present comparisons between predicted and measured neutron fluxes in all the energy ranges covered by the foil detectors, mentioned above. The predicted epithermal fluxes (per unit lethargy) are given as average values over the range from 1 to 10 or 100 eV (assuming a $1/E$ spectrum). In the MeV range, the quantity given is the P(n, p)-reaction rate, marked A_P in the figures.

In the presentation of results, the ratios between values are given. A logarithmic scale is used as the deviations are expected to be of an exponential nature. All of the neutron fluxes are normalized to those obtained by the NRN method. Because method 1 does not enable the calculation of P-activity, the quantities compared are the total fluxes in the interval 0.3 to 2 MeV. The gamma exposure rates are normalized to those predicted by the finite

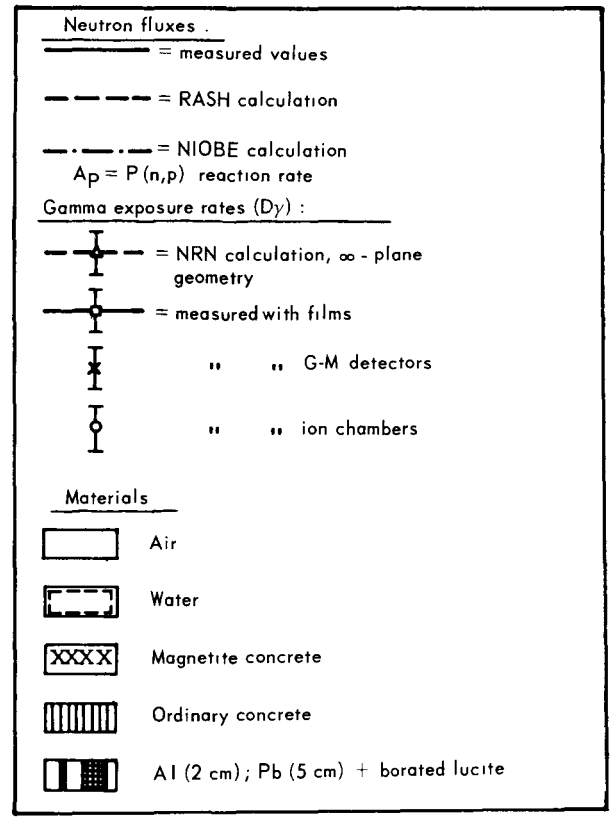


Figure 1. Explanation of signs

geometry gamma code (GASLIT) for method 1. This is because the gamma code available in the NRN method so far works in ∞-plane geometry only. The GASLIT calculation was based on experimentally determined lateral variations of the thermal flux throughout the shield.

Discussion of the results

In Figs. 2 to 8 the results are plotted at the measuring points only. Disregarding the geometrical disturbances close to the core, we see that the thermal flux by the NRN method is within a factor of 2 from the measured values. The agreement between epithermal fluxes is even better, except in water, where an under-estimation with a factor of 3 seems to prevail. The NIOBE results also agree well with the measured values. The RASH results, obtained by using the data recommended in [3] seem to have a discrepancy increasing with the penetration.

The agreement between the measured and NRN or NIOBE calculated P-reaction rates is good, too, except in water, where there is an over-estimation by a factor of 1.5 to 3.

As an example of the subtle material variations, we may look at configurations (2) and (3). Both are made, in principle, of the same concrete. Configuration (2), however, which is the massive pool wall, must have a slightly higher density and/or water contents of the concrete than configuration (3).

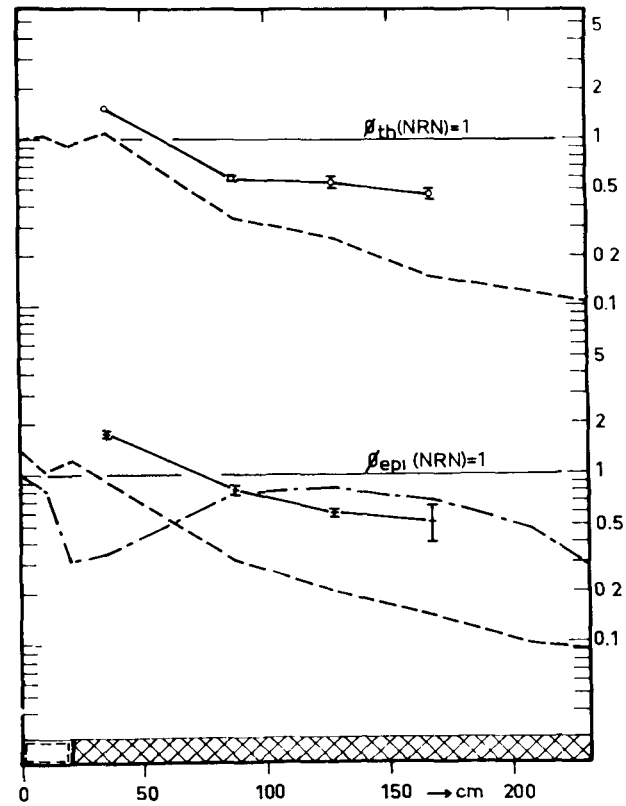


Figure 3. Thermal and epithermal fluxes in configuration 2

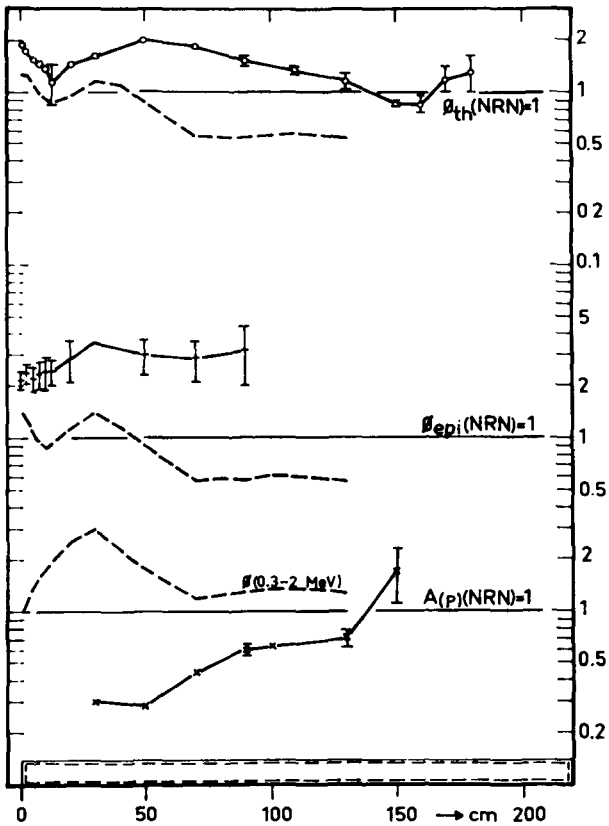


Figure 2. Neutron fluxes in configuration 1

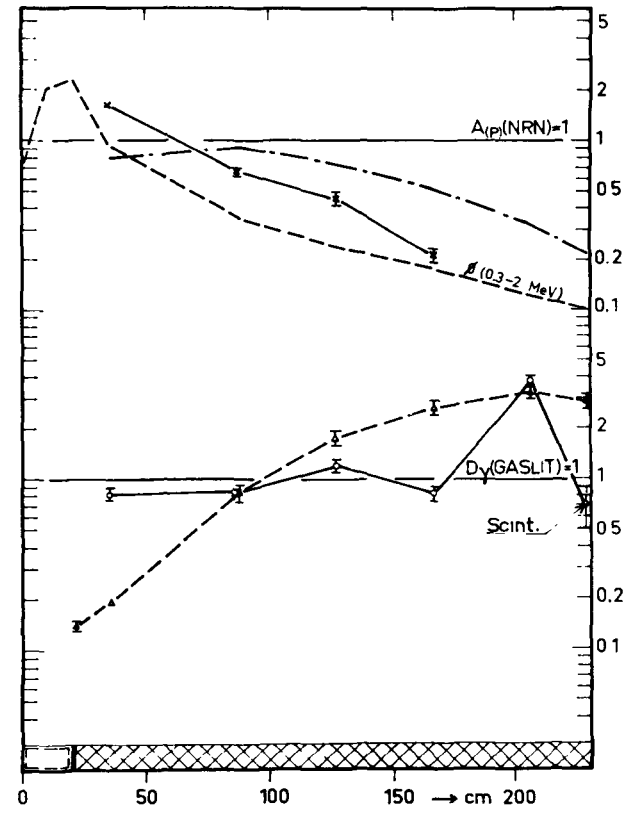


Figure 4. P(n, p) reaction and gamma exposure rates, configuration 2

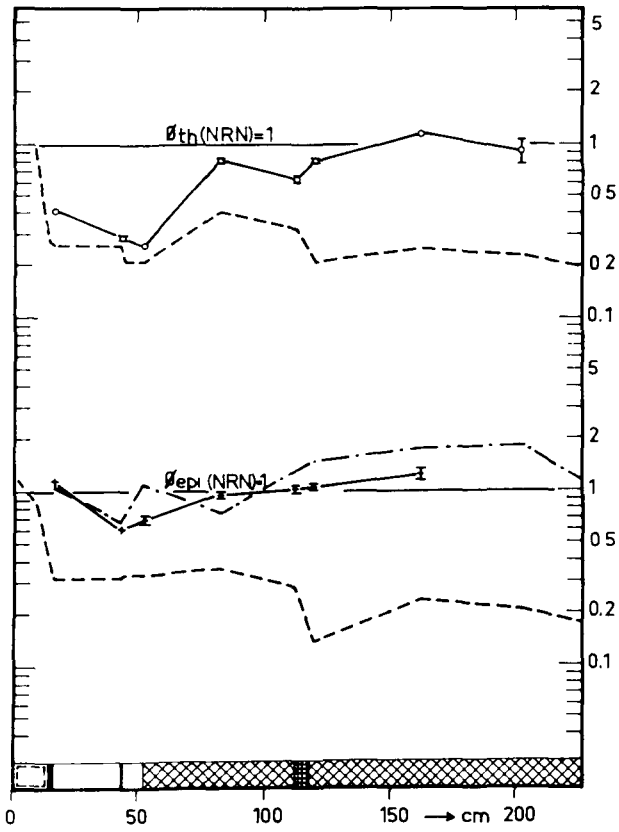


Figure 5. Thermal and epithermal fluxes in configuration 3

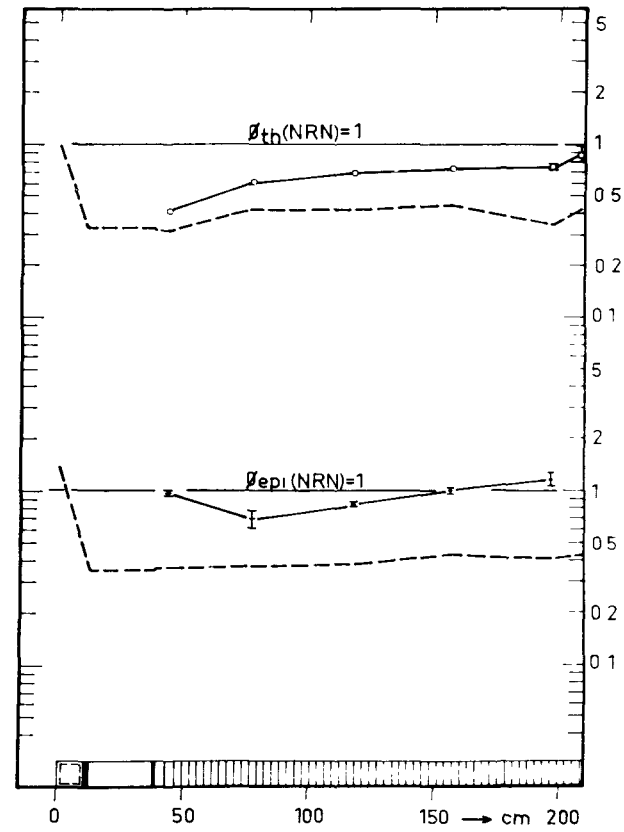


Figure 7. Thermal and epithermal fluxes in configuration 4

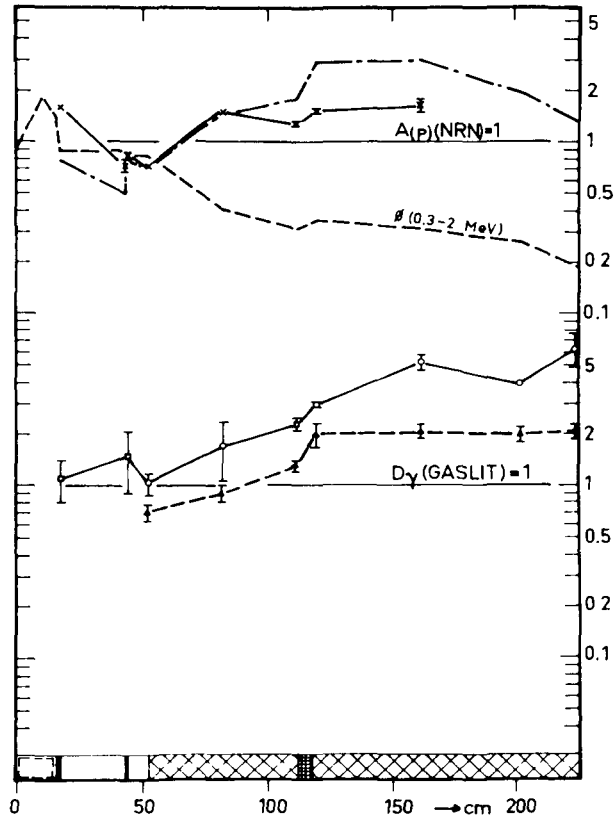


Figure 6. P(n, p) reaction and gamma exposure rates, configuration 3

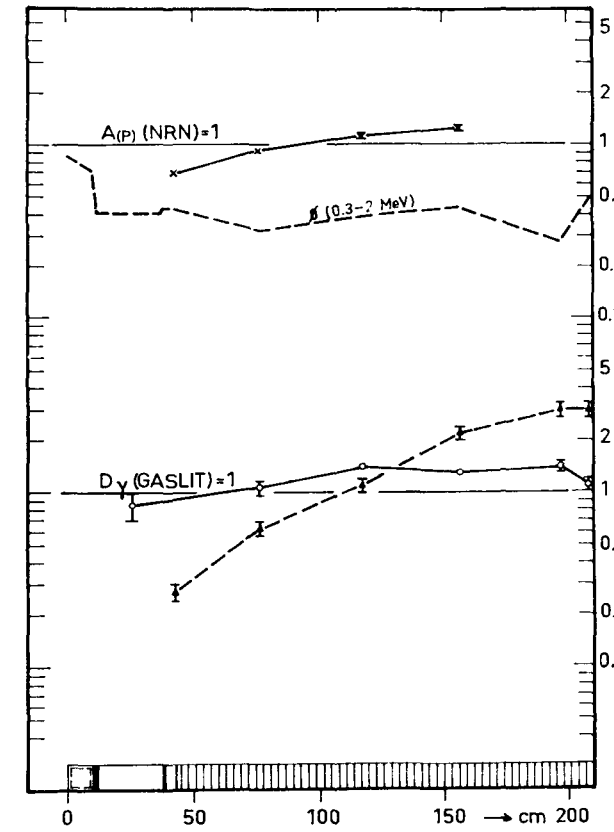


Figure 8. P(n, p) reaction and gamma exposure rates, configuration 4

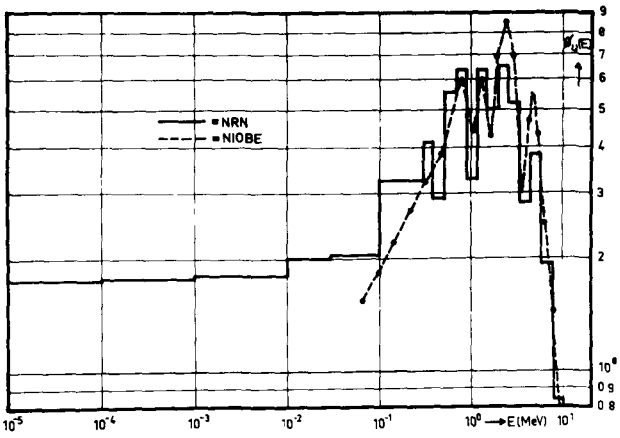


Figure 9. Neutron spectra by NRN and NIOBE methods after penetrating 20 cm water and 15 cm heavy concrete

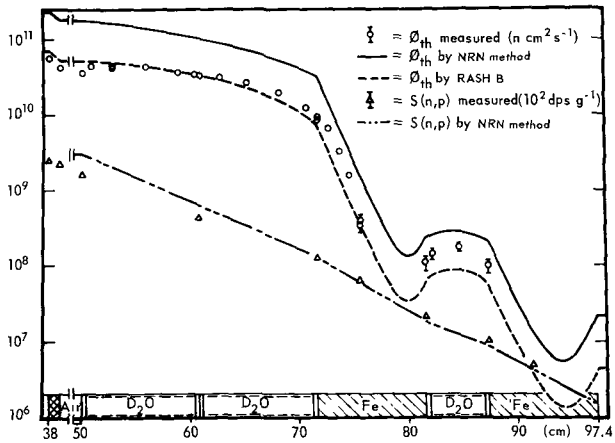


Figure 10. Measured and calculated thermal fluxes and S(n, p) reaction rates in laminated Fe-D_2O

As for the gamma exposure rates, configurations (2) and (4) are very homogeneous and thus ideal for the build-up factor type of calculation used in GASLIT. In these configurations, where the dose originates from the core and the innermost regions, the agreement is therefore very good (for method 1). The measured point at $z = 207$ cm in (2) is most probably too high because of a streaming effect. In configuration (3) with its Pb-layer and too low a photon source further out, the discrepancies between measurements and method 1 are greater. The results by the NRN method have a form that quite apparently could be "flattened out" by a suitable spherical geometry correction.

The neutron spectra obtained by NRN and NIOBE after an effective penetration approximately equal to that from a core to the vessel wall in a light-water reflected power reactor are compared in Fig. 9. No normalizing of the absolute values has been made. It should be pointed out that the computer times of the NRN and NIOBE have a ratio of $\sim$ 1:100, respectively. Figure 10 presents results in laminated Fe-D_2O. The absolute values are disturbed by the geometry close to the core but the detailed forms of the curves agree well for both methods shown.

CONCLUSIONS

The main difficulty in this type of study is the translation of the geometry of the experiment into a geometry accepted by the codes. The accuracy of the design methods studied is so good that the uncertainty from other factors (concrete density, geometry, source, normalisation) gives errors of the same order of magnitude as the calculation methods do. Thus, the accuracy to be expected (e.g., a factor of 2-3 after approximately 2 m penetration) cannot be improved by developing basically new design methods (except extending those existing to more suitable geometries). The accuracy in the determination of the basic materials and other data must, however, be improved.

REFERENCES

1. Albert, R. D. and Welton, T. A., USAEC report WAPD-15 (1950).
2. Cooper, C., Jones, J. D., Horton, C. C., *Some Design Criteria for Hydrogen-Metal Reactor Shields,* Proceedings of the Second International Conference on the Peaceful Uses of Atomic Energy, P/84, Vol. 13, p. 21, United Nations (1958).
3. Avery, A. F., *et al.,* UKAEA report AERE-R 3216 (1960).
4. Peterson, E. G., HW-73381 (1962).
5. Hjärne, L., and Leimdorfer, M., *A New Method for Predicting the Penetration and Slowing-down of Neutrons in Reactor Shields,* submitted for publication in Nuclear Sci. Eng.
6. Troubetzkoy, E., Kalos, M., Lustig, H., NDA 2111-3, Vol. C. (1959).
7. Leimdorfer, M., Nukleonik, *6,* 58 (1964).
8. Leimdorfer, M., Report FOA 4-A 4361-411 (1964). Trans. Chalmers Univ. of Technology, No. 286 (1964).
9. Leimdorfer, M., Report FOA 4-A 4366-411 (1964). Trans. Chalmers Univ. of Technology No. 287 (1964).
10. Aalto, E., and Nilsson, R., *Attenuation Measurements in Massive Biological Shields and a Study of the Accuracy of Some Design Methods,* AB Atomenergi report (to be issued in 1964).
11. Aalto, E., *Comparisons of Measured and Calculated Neutron Fluxes in Laminated Iron and Heavy Water,* AB Atomenergi report (1964); summary in Trans. Am. Nucl. Soc., *4,* 39 (1964).
12. Hjarne, L. (editor), *A User's Manual for the NRN Shield Design Method,* AB Atomenergi report AE-145 (1964).
13. Preiser, S., *et al.,* ARL Techn. Report 60-314 (1960).
14. Synge, M. J., SWP-P 67 (1960).
15. Aalto, E., and Fräki, R., *The Experimental Determination of the Scattering Angle (μ_0) in the NRN Shield Design Method* (to be published in 1964); the main results are reproduced in [5].

ABSTRACT - RÉSUMÉ - АННОТАЦИЯ - RESUMEN

A/684 Suède

Une nouvelle méthode de calcul d'écran et quelques études d'atténuation dans les écrans biologiques lamellaires

par E. Aalto *et al.*

Une méthode pour calculatrices électroniques a été élaborée pour le calcul de la pénétration de neutrons et de rayons gamma à travers les écrans massifs. L'atténuation et le ralentissement des neutrons sont traités par une combinaison des théories de déplacement du premier vol et de diffusion de groupes multiples. Le flux fonction de l'énergie de tels neutrons de fission n'ayant pas subi de collision, ou ayant seulement subi des collisions sous un faible angle, est calculé pour toute l'épaisseur de l'écran; ce flux donne des termes de source dans une série d'équations de diffusion multigroupes. Le ralentissement entre les groupes de diffusion est traité par un formalisme de collision discrète dans lequel il est tenu compte de la perte d'énergie moyenne correcte d'un neutron dans un groupe d'énergie donné. Les chocs inélastiques et la modération par les noyaux légers sont introduits naturellement étant donné que le ralentissement entre tous les groupes est permis.

Le transport des rayons gamma prenant naissance dans le cœur du réacteur et dans l'écran est calculé par la méthode de Monte-Carlo avec utilisation de différents procédés de réduction des variations, par exemple la transformation exponentielle au moyen de laquelle le mouvement de photons dirigé vers l'extérieur est accentué et la pente de la distribution de sources est modifiée, de manière à être plus favorable à l'application de la méthode de Monte-Carlo.

La méthode est entièrement codée pour la calculatrice Ferranti Mercury. Elle comprend une première partie donnant toutes les caractéristiques requises en matière de sections efficaces de neutrons. La section de transport gamma a été traduite en FORTRAN et existe également dans une version prévue pour la calculatrice IBM 7090.

L'avantage principal de cette méthode est qu'elle n'exige qu'une durée et une capacité d'emploi de calculatrice modestes par comparaison aux autres systèmes donnant les mêmes précision et qualité des résultats.

Une vaste série de mesures d'atténuation dans les écrans massifs a été effectuée au Centre d'étude et de recherche de Studsvik. Comme source de radiations on utilisa le réacteur R2–0 équipé de dispositifs spéciaux pour les études de boucliers. Des mesures ont été effectuées jusqu'à environ 2 m de pénétration dans un certain nombre de configurations d'eau-béton de magnétite-plomb, dans 2 configurations d'eau-béton ordinaire et jusqu'à des profondeurs de pénétration de 0,5 à 1 m dans des configurations lamellaires de fer et d'eau lourde. Les flux de neutrons aussi bien que de rayons gamma ont été mesurés sur toute l'épaisseur du bouclier.

Afin d'étudier la précision et la sûreté de la méthode décrite, il a été procédé à des calculs pour les mêmes configurations en utilisant les meilleures valeurs de départ disponibles. A titre de comparaison quelques calculs ont également été effectués avec *a*) une méthode antérieure de déplacement à 18 groupes combinée avec une application du facteur d'accumulation au transport gamma et *b*) une méthode de calcul des flux de neutrons par intégration numérique de l'équation de Boltzmann.

Les méthodes susmentionnées donnent des résultats qui concordent assez bien avec les valeurs mesurées, normalement avec un facteur de 2 à 3 après une pénétration de 2 m environ.

En ce qui concerne les facteurs de sécurité à utiliser lors du calcul de boucliers biologiques massifs, nous pouvons tirer la conclusion que la précision des meilleures méthodes existantes est si bonne que le manque de précision découlant d'autres facteurs (les sources de radiation ou la densité du béton, par exemple) donne des erreurs du même ordre de grandeur que celles résultant des méthodes de calcul.

A/684 Швеция

Новый метод конструирования защиты и некоторые исследования эффекта ослабления излучения в слоистых биологических защитных устройствах

Э. Аалто *et al.*

Разработан метод расчета с помощью счетно-вычислительной машины проникновения нейтронов и γ-лучей через сплошную защиту. Ослабление и замедление нейтронов рассчитывается на основе комбинирования теории спада нейтронов при первом пролете и многогрупповой диффузионной теории. Приводится расчет зависящего от энергии потока таких нейтронов деления через защиту, которые не сталкиваются или сталкиваются под очень небольшим углом. Этот поток является источником числовых значений для членов в серии многогрупповых диффузионных уравнений. Из числа диффузионных групп была рассчитана группа замедляющихся нейтронов с помощью теории формализма дискретных столкновений, в котором принимается во внимание средняя потеря энергии нейтроном в определенной энергетической группе. Естественно, учитывается также

неупругое рассеяние и замедление легких ядер, поскольку допустимо замедление между всеми группами.

Перенос γ-радиоактивности рождающейся в активной зоне реактора и в защите, рассчитывается по методу Монте-Карло с использованием различных вариаций, упрощающих методику расчета, например экспоненциального преобразования, посредством которого увеличивается извне направленное движение фотонов, и наклон источника распределения модифицирован таким образом, чтобы расчеты по методу Монте-Карло были более удобными.

В целом метод закодирован для счетно-вычислительной машины фирмы. «Ферранти». В первой части кода собраны данные по всем требующимся нейтронным сечениям. Раздел по переносу γ-радиоактивности закодирован в системе FORTRAN и существует в виде варианта для счетно-вычислительной машины IBM-7090.

Основным преимуществом описанного метода является то, что требуется умеренное количество машинного времени и памяти по сравнению с другими методами, дающими такие же результаты и с такой же точностью.

В Шведском научно-исследовательском центре в Студсвике были проведены серии измерений ослабления излучения в системах со сплошной защитой. Источником излучения служил реактор R2-0, снабженный специальным приспособлением для исследования защиты. Измерения проникающего излучения проводились на глубину приблизительно до 2 *м* в защитных системах различной конфигурации (вода — магнетитовый цемент — свинец, вода — обычный цемент) и на глубину до 0,5—1 *м* в слоистых защитных системах, состоящих из железа и тяжелой воды. Измерялись потоки как нейтронов, так и γ-излучения, проникавших через защиту.

Для определения точности и надежности описанного метода были проведены расчеты для этих же защитных систем с использованием наилучших исходных параметров. Для сравнения некоторые расчеты были проведены также *a*) по ранее описанному методу удаления 18 групп в сочетании с методом расчета предэкспоненциального множителя γ-переноса и *b*) по методу расчета потоков нейтронов численным интегрированием уравнения Больцмана.

Все описанные методы показали довольно хорошее совпадение результатов с измеренными значениями, обычно в пределах множителя 2—3 при глубине проникновения около 2 *м*.

Что касается коэффициентов безопасности, необходимых при конструировании массивных биологических защитных систем, авторы пришли к выводу, что точность наиболее употребительных методов настолько велика, что отклонения от других коэффициентов (например, для источников излучения, плотности бетона) приводят к ошибкам такого же порядка, что и при использовании расчетных методов.

A/684 Suecia

Un nuevo método de diseño de blindaje y algunos estudios de atenuación en blindajes biológicos laminados

por E. Aalto *et al.*

Se ha desarrollado un método para calcular la penetración de neutrones y rayos gamma a través de masas de blindaje utilizando una calculadora digital. La atenuación y la moderación de los neutrones se tratan mediante una combinación de la teoría de eliminación después del primer trayecto y de la teoría de difusión con varios grupos. Se calcula, a través de todo el blindaje, el flujo, en función de la energía, de los neutrones de fisión que, o no han sufrido ningún choque, o han experimentado únicamente colisiones con un pequeño ángulo; este flujo proporciona los términos del valor de la fuente en una serie de ecuaciones correspondientes a la difusión con varios grupos. La moderación entre los grupos de difusión se trata mediante un formalismo de colisiones discretas, en el que se tiene en cuenta el valor correcto del promedio de la pérdida de energía de un neutrón dentro de un grupo de energía determinado. Los choques inelásticos y la moderación por los núcleos ligeros se introducen de modo natural puesto que está permitida la moderación entre todos los grupos.

El transporte de la radiación gamma originada en el núcleo del reactor y en el blindaje se calcula con un esquema de Monte Carlo utilizando varias técnicas de reducción de la variancia como, por ejemplo, la transformación exponencial, por la que se favorece el movimiento de los fotones hacia el exterior y se modifica la pendiente de la distribución de la fuente en un sentido más favorable para el procedimiento de Monte Carlo.

El método completo está programado para una calculadora digital Ferranti Mercuri. Incluye una parte inicial que da todos los datos requeridos para las secciones eficaces neutrónicas. La sección de transporte gamma se ha traducido a FORTRAN y existe en una versión para la calculadora IBM 7090.

La ventaja fundamental del método presentado consiste en que requiere poco tiempo de una calculadora de pequeña capacidad, en comparación con otros sistemas que dan resultados de igual calidad y exactitud.

En el centro de investigación de Studsvik se ha realizado una amplia serie de medidas de atenuación en masas de blindaje. La fuente de radiación fue el reactor R2–0, provisto de dispositivos especiales para los estudios de blindaje. Las medidas se hicieron para penetraciones de 2 m aproximadamente

con diversas configuraciones de agua-hormigón de magnetita-plomo, con dos configuraciones de agua-hormigón ordinario y hasta valores de 0,5–1 m de penetración para configuraciones de planchas de hierro y agua pesada. Se midieron los flujos de neutrones y de radiación gamma a través de los blindajes.

Con objeto de estudiar la exactitud del método descrito se realizaron cálculos para esas mismas configuraciones utilizando los mejores datos de partida disponibles. Con fines comparativos, se realizaron también algunos cálculos con *a*) un método anterior de eliminación con 18 grupos, combinado con un tratamiento de factor de acumulación para el transporte gamma, y *b*) con un método que calcula flujos neutrónicos por integración numérica de la ecuación de Boltzmann.

Todos los métodos citados anteriormente dan una concordancia bastante satisfactoria con los valores medidos, estando los resultados comprendidos dentro de un factor 2–3 después de unos 2 m de penetración.

En cuanto a los factores de seguridad que deberán utilizarse al proyectar grandes blindajes biológicos, podemos llegar a la conclusión de que la exactitud de los mejores métodos existentes es tan buena que la incertidumbre procedente de otros factores (por ejemplo, las fuentes de radiación, la densidad del hormigón) da errores del mismo orden de magnitud que los métodos de cálculo.

Р/721 БССР

Описание ослабления нейтронного излучения ядерного реактора многослойной биологической защитой с помощью многогрупповой модели в диффузионном приближении

В. А. Наумов

ВВЕДЕНИЕ

За последние годы в ряде стран получили широкое развитие работы, связанные с использованием ядерных реакторов в качестве источника энергии в стационарных станциях большой мощности для производства электроэнергии и для транспортных установок. Реакторы подобных установок вследствие высокой тепловой напряженности активных зон являются мощными источниками радиации. При ослаблении излучений до уровней, безопасных для здоровья человека, толщина биологической защиты может достигать нескольких метров и весить сотни тонн. Поэтому главным требованием, предъявляемым к защите от излучений реактора, является требование к ее весу и размерам. Создание некоторых установок с атомными двигателями целиком зависит от решения этой проблемы. Опыт работы по проектированию стационарных атомных станций большой мощности показал важность решения вопросов защиты вследствие существенной зависимости экономичности станции от веса защиты. Создание защиты от излучений ядерного реактора в ограниченных весовых и габаритных пределах является трудной задачей. Она может быть эффективно решена в том случае, если в руках конструктора имеются достаточно надежные и простые методы расчета ослабления излучений реактора.

В настоящей работе сделана попытка перенести многогрупповые методы теории диффузии, используемые для расчета физических эффектов в активной зоне реактора, на расчеты ослабления потока нейтронов многослойной биологической защитой, а также обосновать их применимость для случаев металло-водных защит. На примере анализа расчетных и опытных данных по распределению потока нейтронов в биологических защитах действующих реакторов (исследовательского реактора типа ИРТ, СССР, и энергетического реактора типа APPR, США) показана пригодность предлагаемого метода для расчета тепловой и биологической защиты.

МЕТОД

Основные предположения и уравнения. К наиболее простой форме уравнений для потока нейтронов приводит использование широко распространенного в практике проектирования ядерных реакторов диффузионного приближения кинетического уравнения. Диффузионное приближение применялось рядом авторов и для создания методов расчета защиты от нейтронов [1]. Однако рассмотрение на основе предположений теории диффузии ограничивалось только замедляющимися и тепловыми нейтронами. При этом ослабление быстрых нейтронов задавалось при помощи какого-либо из полуэмпирических методов.

В данной работе в рамках теории диффузии рассматривается поведение потока тепловых, замедляющихся и быстрых нейтронов. Такое решение основывается на ряде особенностей механизма замедления нейтронов в металловодной защите:

а) Быстрые нейтроны в значительной степени замедляются вследствие неупругих столкновений с тяжелыми ядрами (железо, свинец). Неупругое рассеяние можно в первом приближении считать изотропным.

б) Быстрые нейтроны высоких энергий 4—6 *Мэв* возбуждают с большой вероятностью первые уровни ядер среднего веса (железо, никель, хром и др.) с небольшой относительной потерей энергии. Этот механизм взаимодействия нейтронов подобен упругому рассеянию.

в) Упругое рассеяние, в высшей степени анизотропное при высоких энергиях нейтронов практически на всех ядрах, не играет в механизме замедления существенной роли, а реакции поглощения быстрых нейтронов маловероятны.

г) В области энергий ниже порога неупругого рассеяния ядер железа и свинца основным процессом замедления нейтронов становится упругое рассеяние — изотропное или слабо анизотропное на всех ядрах (кроме водорода).

Перечисленные факторы создают предпосылки для применения к расчетам ослабления потока

быстрых (и тем более замедляющихся) нейтронов невысоких приближений метода сферических гармоник, когда угловое распределение нейтронов характеризуется небольшим числом членов ряда по сферическим функциям (в частности, в диффузионном приближении двумя членами). Вместе с тем, вследствие грубого представления углового распределения нейтронов, проникающих на большие расстояния в водородсодержащей защите, следует ожидать в этом методе ухудшения точности результатов с расстоянием от источника.

Биологическую защиту можно считать в первом приближении состоящей из ряда следующих одна за другой однородных сред. Рассмотрим одну из таких сред. Предполагается, что:

1) среда поглощает и рассеивает нейтроны;
2) неупругое рассеяние изотропно;
3) спектр нейтронов, неупруго рассеянных на тяжелых ядрах (свинец, U^{235}, U^{238}), согласно статистической теории Вайскопфа имеет вид максвелловского распределения. Закон неупругого рассеяния для ядер среднего веса (алюминий, железо, никель, хром) устанавливается по функциям возбуждения уровней ядер, рассчитанных на основе предположений оптической модели ядра [2];
4) упругое рассеяние не изотропно в системе координат, в которой центр масс нейтрона и рассеивающего ядра покоится. Анизотропия рассеяния учитывается с помощью линейного по углу закона рассеяния.

Тогда в соответствии с методом скалярный поток нейтронов $\Phi(r, E)$ как функция положения и энергии должна удовлетворять для стационарного случая следующему уравнению:

$$-D(E)\Delta\Phi(r, E)+\Sigma(E)\Phi(r, E)= \\ =\int_{E}^{E/\alpha}\Phi(r, E')\Sigma_s(E')W_{s_0}(E', E)\,dE'+ \\ +\int_{E}^{\infty}\Phi(r, E')\Sigma_{in}(E')W_{in_0}(E', E)\,dE' \quad (1)$$

с соответствующими реальной геометрии граничными условиями. В уравнении (1) W_{s_0}, W_{in_0} — коэффициенты разложения индикатрисс упругого W_s и неупругого W_{in} рассеяния, равные

$$W_{s_0}(E', E)=\frac{(A+1)^2}{4AE'}\left\{1+\frac{3}{2}\frac{A^2}{A^2-0{,}6}\left(\bar{\mu}_L-\frac{2}{3A}\right)\times\right. \\ \left.\times\left[(A+1)^2\frac{E}{E'}-(A^2+1)\right]\right\},$$

$$W_{in_0}(E', E)=4\pi W_{in}=E\exp\left[-\frac{E}{T(E')}\right]\times \\ \times\left\{T^2(E')\left[1-\left(1+\frac{E}{T(E')}\right)\exp\left(-\frac{E}{T(E')}\right)\right]\right\}^{-1},$$

а индикатриса упругого рассеяния:

$$W_s(\mu_0, E', E)=\frac{(A+1)^2}{16\pi\cdot AE'}\left\{1+\frac{3}{2}\frac{A^2}{A^2-0{,}6}\times\right. \\ \times\left(\bar{\mu}_L-\frac{2}{3A}\right)\left[(A+1)^2\frac{E}{E'}-(A^2+1)\right]\Big\}\times \\ \left.\times\delta\left[\mu_0-\left(\frac{A+1}{2}\sqrt{\frac{E}{E'}}-\frac{A-1}{2}\sqrt{\frac{E'}{E}}\right)\right]\right.$$

для $\alpha E'<E<E'$; μ_0 — косинус угла между направлениями нейтрона до и после рассеяния; $\bar{\mu}_L$ — средний косинус угла рассеяния в лабораторной системе координат. Остальные обозначения общепринятые.

Решение уравнения (1) для реальной геометрии защиты сопряжено с серьезными трудностями вследствие сложных зависимостей нейтронных поперечных сечений и индикатрисс упругого и неупругого рассеяния от энергии. Поэтому, интегро-дифференциальное уравнение, содержащее две переменные, пространственные координаты и энергию, интегрированием по выбранным энергетическим интервалам сводится к системе связанных дифференциальных, многогрупповых диффузионных уравнений. Каждое из уравнений системы описывает поведение в слое защиты потока (интегрального) нейтронов Φ_j определенного энергетического интервала ΔE_j и имеет вид:

$$D_j\Delta\Phi_j(r)-\Sigma_j\Phi_j(r)+\sum_{k=1}^{j-1}\Phi_k(r)\Sigma_{kj}^{in}+ \\ +\sum_{k=1}^{j-1}\Phi_k(r)\Sigma_{kj}^{s}=0, \quad (2)$$

где $\Sigma_j=\Sigma_{aj}+\sum_{k=j+1}^{N}\left(\Sigma_{jk}^{in}+\Sigma_{jk}^{s}\right)$;

$$\Sigma_{jk}^{in\,s}=\int_{\Delta E_k}dE\int_{\Delta E_j}\Phi(r, E')\Sigma_{in,\,s}(E')\times \\ \times W_{in_0s_0}(E', E)\,dE'/\Phi_j;$$

$$\Sigma_{aj}=\frac{\int_{\Delta E_j}\Sigma_a(E)\Phi(r, E)\,dE}{\Phi_j};$$

$$D_j=\frac{\int_{\Delta E_j}D(E)\nabla\Phi(r, E)\,dE}{\int_{\Delta E_j}\nabla\Phi(r, E)\,dE}.$$

Групповые константы не являются постоянными, а зависят от неизвестного пространственно энергетического распределения потоков нейтронов и не могут быть вычислены, если неизвестно искомое решение. Для преодоления этой трудности в расчетах констант были использованы спектры, формирующиеся в бесконечных средах с равномерно распределенными источниками нейтронов деления.

Выбор групп. Разбиение энергетического интервала было подчинено главной цели —

по возможности подробно описать основные процессы, влияющие на прохождение через металло-водную биологическую защиту ядерного реактора. Во внимание принимались зависимости нейтронных поперечных сечений от энергии для основных защитных материалов (вода, железо, свинец), функции перевода потока нейтронов в тканевую биологическую дозу, а также формы спектров потока нейтронов в однородных бесконечных средах воды, железа, свинца и графита. В соответствии с зависимостью указанных величин от энергии нейтрона весь диапазон энергий можно разбить на несколько больших областей.

1. Область спектра от 1,5 до 15 *Мэв*, где ход потока следует спектру деления в большинстве рассмотренных сред, характеризуется сильной анизотропией упруго рассеиваемых нейтронов и замедлением главным образом за счет неупругого рассеяния в средах, содержащих тяжелые ядра. Здесь образовано три группы: $j=1$ $4 Мэв < E < 15$ *Мэв*; $j=2$ $2{,}5$ *Мэв* $< E <$ $4{,}0$ *Мэв*; $j=3$ $1{,}5$ *Мэв* $< E <$ $2{,}5$ *Мэв*. Во всех этих группах полные сечения упругих рассеивателей кислорода и углерода, сечения неупругого рассеяния алюминия, железа, никеля, свинца и урана, а также коэффициент перевода потока нейтронов в тканевую дозу слабо зависят от энергии. Исключение составляет водород, сечение которого в первой группе меняется примерно в два раза и во второй группе — в пределах 40%.

2. В переходной области от спектра деления к спектру Ферми (от 0,3 *Мэв*) выделены две группы: $j=4$ $0{,}7 Мэв < E < 1{,}5 Мэв$; $j=5$ $0{,}3 Мэв < E < 0{,}7 Мэв$. Некоторую роль в замедлении нейтронов этих групп играет неупругое рассеяние в железе, свинце и уране, но в более легких средах упругое рассеяние (неизотропное в системе центра масс) является основным процессом.

3. Область спектра Ферми от 1 до 300 *кэв*, характерными особенностями взаимодействия нейтронов в которой являются изотропия упругого рассеяния, интерференция между потенциальным и резонансным рассеянием и слабое поглощение нейтронов. Резонансная структура полного сечения, появляющаяся вследствие интерференции, должна учитываться при осреднении сечений. Наличие провалов в полном сечении приводит к тому, что нейтрон при замедлении может приобретать энергию, близкую к энергии провала, и проходить большие расстояния в защите. Для учета этого эффекта выделено две группы: $j=6$ 40 *кэв* $< E <$ 300 *кэв*; $j=7$ 1 *кэв* $< E <$ 40 *кэв*.

4. Область от 0 до 1 *кэв*, где существенно поглощение нейтронов для многих защитных материалов, образована тремя группами: $j=8$ $6{,}7 < E < 1000$ *эв*; $j=9$ $E_{гр} < E < 6{,}7$ *эв*; $j=10$ $0 < E < E_{гр}$. Таким образом выбрано 10 энергетических групп. Последняя, десятая, группа объединяет нейтроны тепловых энергий. Ослабление потока тепловых нейтронов характеризуется эффективными сечениями, осредняемыми по спектру Максвелла [3]. Условное разделение тепловых и замедляющихся нейтронов величиной $E_{гр}$ перенесено из методов, используемых для расчета критических масс реакторов [3].

ТЕОРЕТИЧЕСКИЕ И ЭКСПЕРИМЕНТАЛЬНЫЕ ДАННЫЕ ПО ОСЛАБЛЕНИЮ ПОТОКА НЕЙТРОНОВ В ОДНОРОДНЫХ СРЕДАХ. КРИТЕРИЙ МЕТОДА

Многочисленные предположения, положенные в основу получения диффузионных многогрупповых уравнений, ограничивают пределы применимости метода и вызывают необходимость его теоретической и особенно экспериментальной проверки. Теоретическая проверка применимости метода к расчетам ослабления потока нейтронов в биологической защите не представляется возможной практически, так как она связана с определением пространственно углового энергетического распределения нейтронов в многослойной среде от области распределенных источников деления. Более простому анализу поддаются энергетические спектры потока нейтронов, формирующиеся в бесконечных однородных средах от сосредоточенных источников. Рассмотрение ослабления нейтронов различными однородными средами позволяет разделить ошибки, связанные с предположениями теории диффузии, от погрешностей, возникающих в результате неточного описания влияния на формирование потока нейтронов одной среды на другую, имеющих место в гетерогенной защите.

Поэтому в качестве критерия правильности результата, получаемого с помощью диффузионного 10-группового метода, были использованы точные энергетические спектры потока в однородных бесконечных средах, рассчитанные методом моментов [4], а также данные измерений ослабления нейтронов различными индикаторами (Cu^{63}, In^{115}, S^{32}, Th^{232} и др.). По типу взаимодействия нейтронов деления с ядрами атомов материалы, наиболее употребительные при конструировании металло-водных биологических защит, могут быть разделены условно на три класса сред:

1) среды, замедляющие нейтроны посредством упругого рассеяния с относительно небольшим вкладом неупругого рассеяния;

2) среды с преимущественным замедлением быстрых нейтронов вследствие неупругого рассеяния;

3) водородсодержащие среды.

В соответствии с этим делением были рассмотрены наиболее типичные защитные среды: графит, свинец, железо и вода.

Графит. Взаимодействие нейтронов спектра деления с графитом происходит через процесс

упругого рассеяния, так как первый уровень ядра углерода имеет энергию примерно 4,4 *Мэв*. Графит — слабо поглощающая нейтроны среда, поэтому ошибки в потоке должны быть связаны с неточным представлением углового распределения потока нейтронов и индикатриссы упругого рассеяния. Последняя неточность, проявляющаяся в случае анизотропного характера рассеяния в системе центра масс, ведет к недооценке вклада в поток нейтронов, рассеянных на малые углы. Опыт показывает [3], что предположение о линейности индикатриссы рассеяния является грубым для нейтронов спектра деления, энергии которых превышают 2,5 *Мэв* и особенно в области выше энергии первого уровня ядра углерода. Таким образом, надо ожидать существенных ошибок как в спектре потока нейтронов для $E>4{,}0$ *Мэв*, так и в низкоэнергетической области спектра на расстояниях от источника, где поток целиком определяется нейтронами, замедлившимися из области $E>4{,}0$ *Мэв*. Порядок величины расстояния, начиная с которого следует ожидать ошибок в потоке, может быть оценен для случая плоского изотропного источника деления, для которого групповые потоки — решения уравнения (2) — определяются через следующие рекуррентные соотношения:

$$\Phi_j=\sum_{k=1}^{j}A_k\alpha_{kj}\exp(-\varkappa_k x);$$

$$\alpha_{kj}=\frac{\sum_{m=k}^{j-1}\varkappa_{mj}^2\alpha_{km}}{\varkappa_j^2-\varkappa_k^2},\quad \alpha_{jj}=1; \qquad (3)$$

$$A_k=\frac{\left[\frac{\chi_k}{2D_k}-\sum_{m=1}^{k-1}\varkappa_m\alpha_{mk}A_m\right]}{\varkappa_k},$$

где x — расстояние от источника; $\varkappa_j^2=\Sigma_j/D_j$ и $\varkappa_{kj}^2=\Sigma_{kj}/D_j$.

Для графита плотностью 1670 *кг/м*^{3} $\varkappa_1=8{,}00$, $\varkappa_2=12{,}2$, $\varkappa_3=12{,}6$ *м*$^{-1}$; $D_1=0{,}0543$, $D_2=0{,}0306$, $D_3=0{,}0265$ *м* (χ — спектр деления).

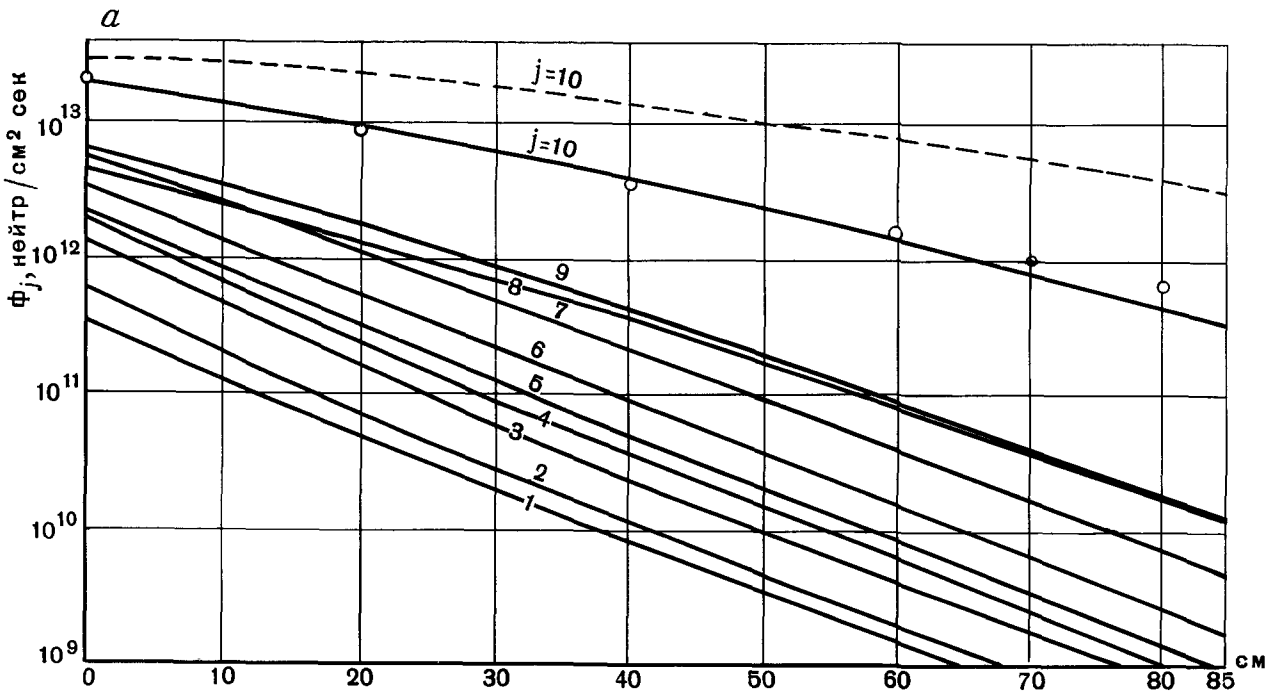
Нетрудно видеть, что поток нейтронов первой группы существенно (например, на порядок) превышает поток нейтронов, испускаемых источником в интервале $1{,}5\,Мэв<E<4\,Мэв$, начиная с расстояния

$$x\cong\frac{\left\{\ln\left[10\frac{\varkappa_1}{\varkappa_2}\cdot\frac{D_1}{\chi_1}\left(\frac{\chi_2}{D_2}+\frac{\chi_3}{D_3}\right)\right]\right\}}{(\varkappa_2-\varkappa_1)};\qquad x\cong 0{,}85\ м.$$

Энергетическое распределение потока нейтронов, рассчитанное по уравнениям (3), для расстояний $\gamma x=10$, 60, 90, 120 *г/см*^{2} сравнивалось с соответствующими данными методами моментов [4] (рис. 1). Наблюдается удовлетворительное согласие абсолютных энергетических спектров на расстояниях вплоть до 120 *г/см*^{2}. Максимальная ошибка около 40% проявляется на расстоянии $x=0{,}72$ *м* от источника в узкой области спектра $0{,}7\ Мэв<E<2{,}5\ Мэв$. Эти данные подтверждают высказанные выше соображения и указывают пределы применимости 10-группового метода для расчета ослабления потока нейтронов в графите с приемлемой для защиты точностью.

Железо, свинец. В железе и свинце ослабление быстрых нейтронов определяется главным образом неупругим рассеянием. Наиболее важно правильно определять ослабление железом и свинцом быстрых нейтронов с энергиями выше 4 *Мэв* и резонансных нейтронов с энергиями ниже порога неупругого рассеяния $E<0{,}85$ *Мэв*. Если быстрые нейтроны с $E>4$ *Мэв* относительно слабо замедляются водой и поэтому вносят существенный вклад в мощность дозы в металло-водной защите, то резонансные нейтроны являются наиболее проникающими в свинце и железе. Они обусловливают поток тепловых нейтронов в водяных слоях, следующих за свинцом или железом в свинцово-водной или железо-водной защите.

Для проверки групповых констант железа 10-групповым методом было рассчитано пространственно-энергетическое распределение потока нейтронов в бесконечном массиве железа плотностью 7,85 *г/см*^{3} для случая точечного изотропного источника деления мощностью 1 *нейтр/сек*. Наиболее близкими для сравнения с расчетными данными являются результаты измерений ослабления в железе нейтронов, испущенных мононаправленным пучком из реактора БР-5 [5]. Распределение быстрых нейтронов от мононаправленного пучка из реактора на быстрых нейтронах БР-5 измерялось пороговыми индикаторами Al^{27} (n,α) Na^{24}, S^{32} (n,p) P^{32} и ториевой камерой деления. Результаты опытов с мононаправленным источником реакторных нейтронов допускают сравнение с расчетными данными настоящей работы (рис. 2*а*), так как функция ослабления бесконечного плоского мононаправленного источника и функция ослабления точечного изотропного источника, умноженная на $4\pi r^2$, практически не отличаются от аналогичных функций в работе [7], а спектр быстрого реактора в области выше наинизшего порога реакций, идущих в использованных детекторах [реакции Th (n,f)], близок к спектру деления. Рассчитанные активности серных индикаторов, число делений ториевой камеры и соответствующие измеренные величины удовлетворительно согласуются на расстояниях до 60 *см* от источника. Максимальная разница в 30% наблюдается в числе делений ториевой камеры при $r=0{,}6$ *м*. Аналогичное сравнение по счету ториевой камеры от точечного изотропного источника нейтронов на 4 *Мэв* в свинце на расстояниях от источника до 0,52 *м* (рис. 2*б*) показало максимальную разницу между рассчитанными и измеренными данными, равную 20%. Проведенные сравнения указывают на то, что 10-групповой метод может быть использован для расчета быстрых



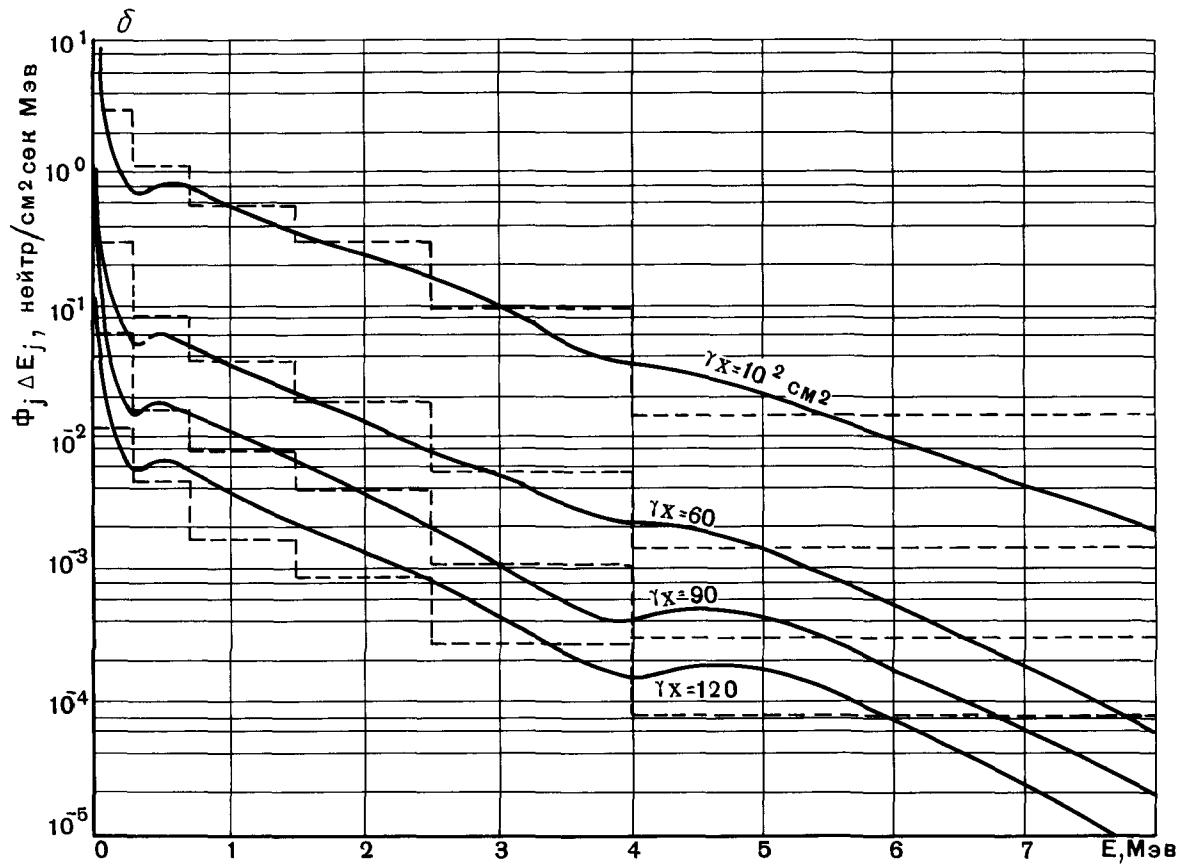


Рис. 1. Ослабление нейтронов в графите

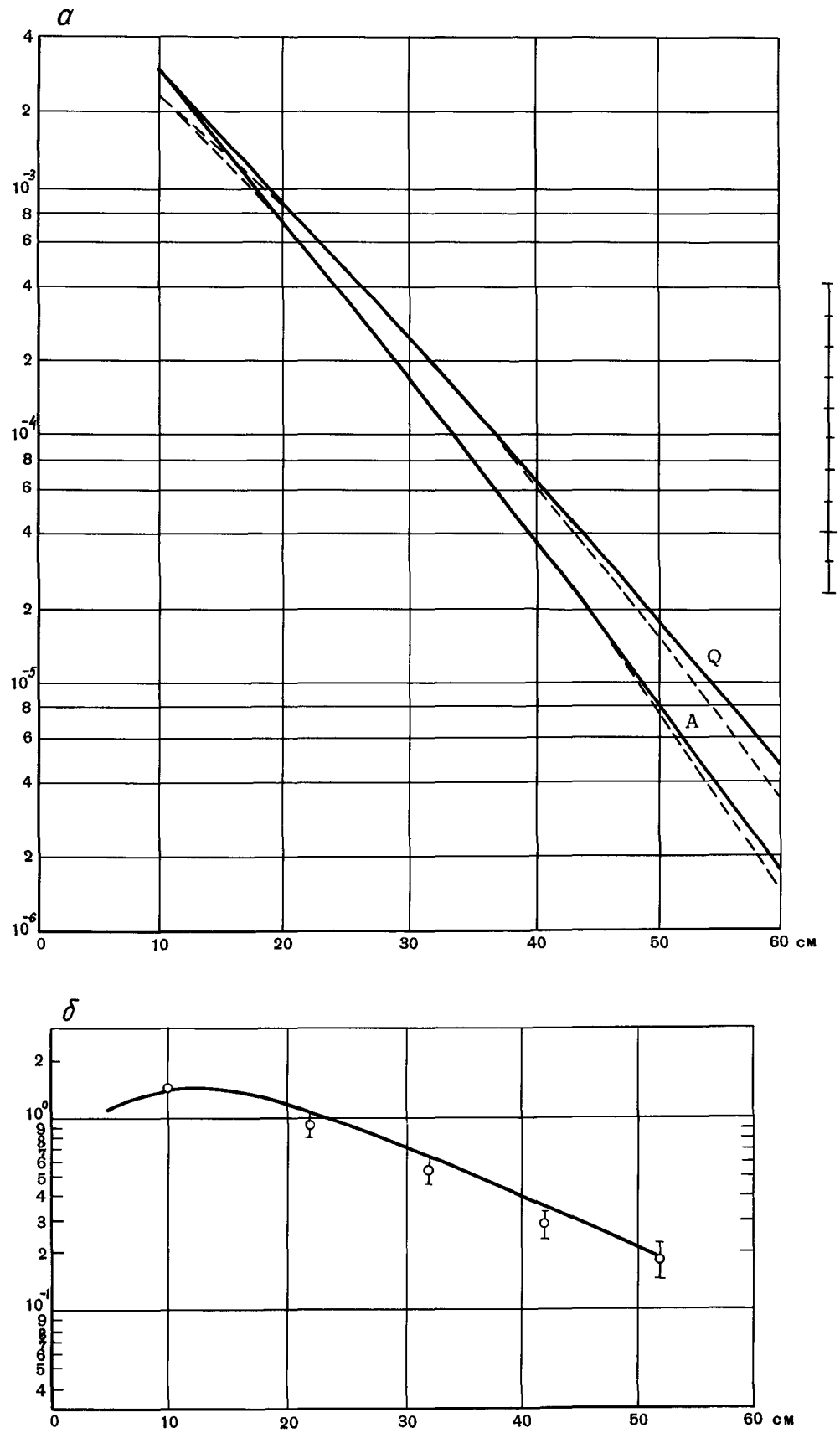


Рис. 2. Сравнение расчетных и экспериментальных данных по ослаблению нейтронов в железе и свинце

и резонансных нейтронов в железе и свинце на расстояниях до 0,6 *м* от источника.

Водородсодержащие среды. В силу того что рассеяние на ядрах водорода сферически симметрично в системе центра масс, замедление нейтронов водородом в диффузионном уравнении баланса (1) определяется точно, а недостатки теории диффузии должны быть связаны с линейным представлением угловой зависимости плотности нейтронов и с использованием закона диффузии. Последнее предположение означает, что нейтрон, рассеянный ядром водорода, изменяет направление своего движения на постоянный угол $\arccos\frac{2}{3}$. В действительности нейтрон изменяет направление в зависимости от того, в какую энергетическую группу он замедляется, причем для нейтронов деления средневзвешенный по энергиям нейтрона в пределах групп $W_{s_1}(E',E)=\frac{1}{E'}\sqrt{\frac{E}{E'}}$ меньше 2/3. Поэтому можно предполагать, что в случае диффузионного описания нейтроны проходят большие пути в водородсодержащей среде, чем в действительности. Действие этого эффекта рассеяния на водороде должно приводить к переоценке потока быстрых нейтронов на расстояниях от источника, на которых не сформировалось анизотропное угловое распределение. Если это так, то увеличение порядка приближения по-прежнему без точного учета корреляции между изменениями угла и энергии при рассеянии должно приводить к худшим результатам, чем в диффузионном приближении. Например, при описании ослабления нейтронов в P_2-приближении уравнение баланса в этом случае имеет вид, совпадающий по форме с уравнением диффузии, и отличается только константами [8]. В случае чистого водорода длина диффузии в P_2-приближении для первой энергетической группы наиболее проникающих нейтронов выражается через константы в диффузионном приближении и средний квадрат длины пробега по отношению к рассеянию следующим образом: $L_{P_2}^2=\frac{D_1}{\Sigma_1}+\frac{16}{15}\left(\frac{1}{\Sigma_s^2}\right)_1$.

Рассчитанные длины диффузии в различных приближениях приведены в табл. 1. Из таблицы видно, что использование последовательного P_1-приближения и P_2-приближения в обсуждаемой форме приведет к неоправданно сильному в P_1-и более слабому, чем в действительности, ослаблению в P_2-приближении.

Наличие тяжелых упругих рассеивателей в водородсодержащей среде, которые не замедляют нейтроны в сравнении с водородом, но конкурируют с ним в процессе рассеяния, должно улучшать результаты диффузионного метода из-за недооценки рассеяния на малые углы, а следовательно, и недооценки транспортной длины пробега нейтронов. Завышение и занижение транспортной длины пробега при описании замедления на водороде и кислороде

Таблица 1. Расчетные длины диффузии (в *м*) для водорода плотностью 111 *кг/м*³

Интервал, *Мэв*	Приближение			
	Диффузионное	P_1	P_2	Метод моментов[4]
$8<E<\infty$	0,157		0,22	
$4<E<\infty$	0,1105	0,0628	0,142	
$7{,}9<E<8{,}1$	0,130	0,0772	0,190	0,132

в воде приводит к компенсации ошибок диффузионного приближения. Этим в значительной степени следует объяснить хорошее согласие абсолютных спектров в воде на расстоянии до 0,9 *м* от точечного источника деления, рассчитанных 10-групповым методом и методом моментов (рис. 3*а*). Причем на расстоянии 0,9 *м* от источника разница в потоках по двум методам в интервале 0,3 *Мэв*$<E<$8 *Мэв* в среднем не превышает 30%. В таком же количественном соотношении находятся результаты расчета активации индия и аналогичные данные эксперимента в воде [9,11] (рис. 3*б*).

ПРИМЕНЕНИЕ МЕТОДА К РАСЧЕТАМ ТЕПЛОВОЙ ЗАЩИТЫ КОРПУСА И БИОЛОГИЧЕСКОЙ ЗАЩИТЫ

Точность расчета в реальной гетерогенной защите таких величин, как поток тепловых и промежуточных нейтронов, мощность дозы от нейтронов, источники γ-излучения, зависит в большинстве случаев от правильности описания ослабления быстрых нейтронов. Исключениями являются применяющиеся в качестве защитных экранов или деталей конструкции реактора толстые свинцовые или стальные плиты. В таких средах полный поток нейтронов, мощность дозы от нейтронов и источники захватного γ-излучения должны определяться резонансными нейтронами. Учет накопления резонансных нейтронов в металлах важен и в расчетах источников γ-излучения в металло-водной защите. Для получения правильных сведений по ослаблению резонансных нейтронов металлическими экранами необходим соответствующий выбор способа осреднения групповых констант.

Если для расчета потока резонансных нейтронов в толстых экранах из никеля, железа или свинца с размерами в несколько длин пробега сечения взаимодействия следует осреднять по спектру Ферми, то в тонких экранах металло-водной защиты — по спектру $\Phi(U)=\text{const}$, так как в последнем случае спектр формируется водородом, у которого в резонансной области $\Sigma=\text{const}$. Наиболее показательным в этом отношении является железо, у одного из изотопов которого в поперечном сечении наблюдается глубокий провал при 24 *кэв*. Длины диффузии для нейтронов седьмой группы, содержащей провал в сечении

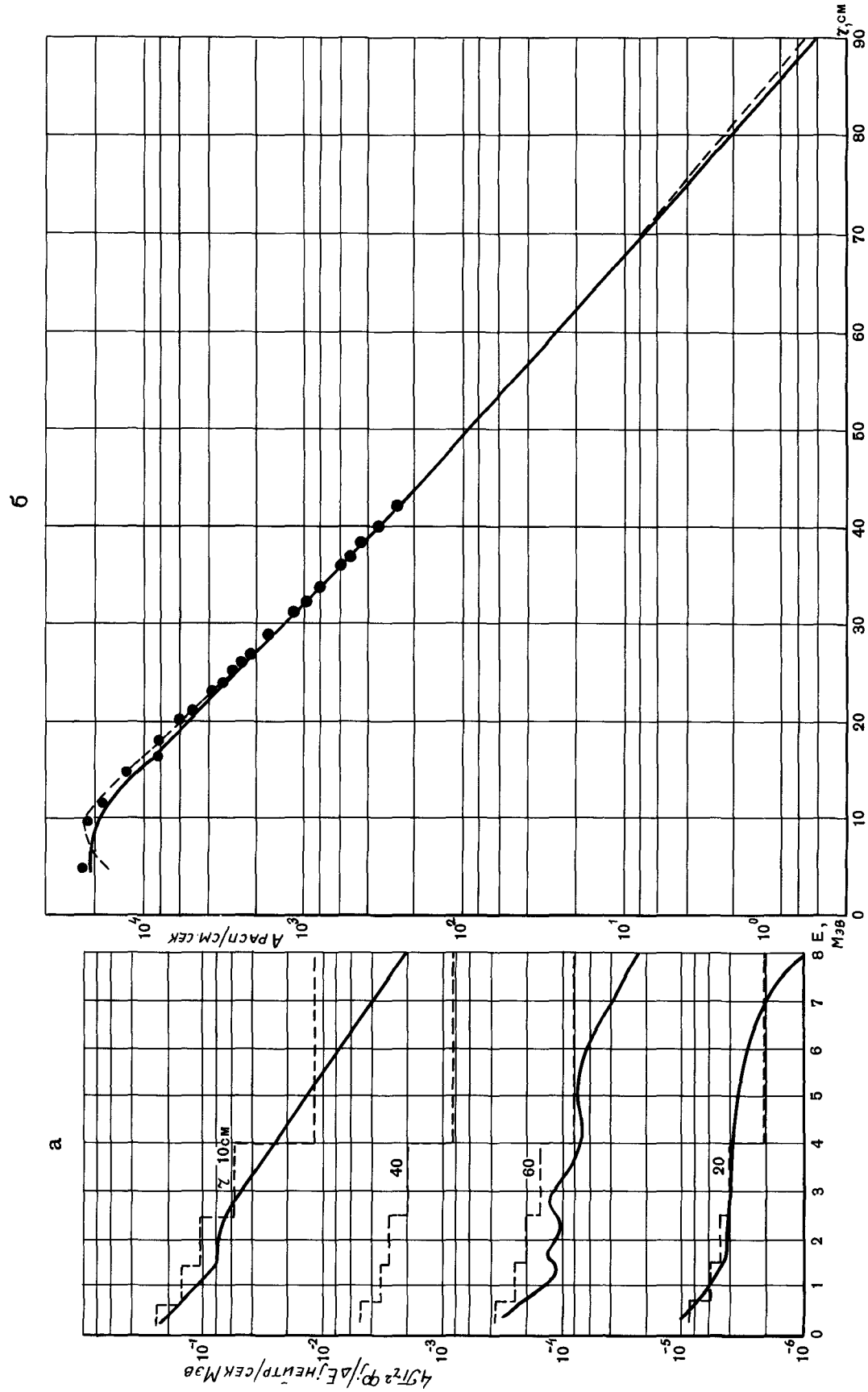


Рис. 3. Ослабление водой нейтронов от точечного источника спектра деления

рассеяния, вычисленные через групповые константы по двум способам осреднения, оказались равными соответственно: для спектра $\Phi(U)\sim 1/\Sigma(U)$ $L=\sqrt{D/\Sigma}=0{,}361$ *м* и для $\Phi(U)=\text{const}$ $L=0{,}16$ *м*. Первая величина хорошо согласуется с длиной релаксации промежуточных нейтронов, измеренной Бродером [6] в железе и равной 0,36 *м*. Вторая величина близка к длине замедления промежуточных нейтронов в железе железо-водной защиты $L=0{,}177$ *м*, полученной Купером и др. подгонкой расчетных данных по потоку к экспериментальным [1]. Групповые сечения для металлов, осредненные по двум типам спектра, приведены в табл. 2.

Таблица 2. Групповые длины диффузии для некоторых материалов, L_a — константы в группах 5 — 9 осреднены по спектру $\Phi(U)=1/\Sigma(U)$, $L_в$ — то же по спектру $\Phi(U)=\text{const}$

j	$E\min_j$, эв	Железо (7850 кг/м³)		Свинец (1130 кг/м³)		Вода (1000 кг/м³)	Графит (1670 кг/м³)
		L_a	$L_в$	L_a	$L_в$		$L_в$
1	$4\cdot10^6$	0,0521	0,0521	0,0633	0,0633	0,0752	0,125
2	$2{,}5\cdot10^6$	0,0461	0,0461	0,0789	0,0789	0,0545	0,082
3	$1{,}5\cdot10^6$	0,0532	0,0532	0,108	0,108	0,0447	0.0793
4	$0{,}7\cdot10^6$	0,0803	0,0803	0,172	0,172	0,0282	0,0653
5	$0{,}3\cdot10^6$	0,129	0,121	0,255	0,238	0,0210	0,0506
6	$40\cdot10^3$	0,209	0,179	0,256	0,246	0,0164	0,0606
7	$1\cdot10^3$	0,361	0,164	0,294	0,292	0,0134	0,0729
8	6,7	0,0662	0,0576	0,33	0,320	0,0145	0,0838
9	0,189	0,0372	0,0314	0,276	0,218	0,0114	0,0717

Удовлетворительные данные, полученные в расчетах ослабления быстрых нейтронов в однородных средах, создают предпосылки для применения 10-группового метода к расчетам пространственно энергетического распределения потока нейтронов в многослойной биологической защите в некоторой области расстояний от активной зоны.

К вопросам, связанным с применимостью метода для расчета ослабления нейтронов гетерогенной защитой, относятся: возможность использования 10-группового метода для расчета потока тепловых и замедляющихся нейтронов в тонких водяных прослойках, в сильно поглощающих средах и вблизи таких сред.

Проверке этих эффектов посвящена работа по анализу результатов расчета и измерений потоков нейтронов в защитных сборках, имитирующих тепловую защиту корпуса, корпус и часть биологической защиты ядерного реактора [10]. Сравнение результатов расчета потока нейтронов по активности медных индикаторов с результатами экспериментов позволило сделать следующие выводы.

1. 10-групповая система констант удовлетворительно описывает поведение потока нейтронов в стальных, стальных борированных и свинцовых экранах тепловой защиты корпуса. Совпадение рассчитанных и измеренных активностей в пределах 20—30% может служить основанием для вывода о пригодности метода для расчетов источников γ-излучения в железо- и свинцово-водных защитах толщиной до 0,4 *м*.

2. Максимальная разница между рассчитанными и измеренными величинами наблюдается в водородсодержащих средах, между борированными экранами (сильными поглотителями нейтронов) и достигает 30—40%. Эти отклонения могут быть связаны с асимметрией углового распределения нейтронов в сильно поглощающих нейтроны слоях, а также с отличием реального спектра потока нейтронов в этих слоях от принятого при осреднении групповых постоянных.

Большие возможности 10-группового метода демонстрируются обсчетами опытов по измерению распределения потока нейтронов золотыми индикаторами и мощности дозы от γ-лучей в железо-водной биологической защите американского реактора APPR [12] и потока тепловых нейтронов в тепловой графитовой колонне исследовательского погружного реактора ИРТ-2000 [13]. Сравнение измеренных и вычисленных активностей золотых индикаторов в биологической защите APPR показало, что 10-групповой метод удовлетворительно описывает ослабление потока нейтронов в биологической защите на глубине 1 *м*, то есть в области, которая обусловливает мощность дозы вне биологической защиты. На основе пространственно энергетического распределения потока нейтронов, полученного 10-групповым методом, было рассчитано распределение источников захватного γ-излучения, а затем с помощью построенных функций дозы — распределение мощности дозы в биологической защите APPR (рис. 4). Рассчитанная абсолютная полная мощность дозы в пределах 30% совпадает с измеренной на расстояниях до 1,40 *м* от центра активной зоны (лишь в одной точке защиты рассчитанная мощность дозы отличается от измеренной в 1,5 раза).

Расчеты ослабления потоков нейтронов в тепловой колонне реактора ИРТ-2000 были выполнены на электронно-вычислительной машине «Урал-1» Института математики и вычислительной техники АН БССР. Сравнение полученных данных с экспериментальными (см. рис. 1) показывает удовлетворительную точность расчета потока тепловых и замедляющих нейтронов в графите. Эта работа проявила одно из основных достоинств 10-группового метода — простоту и программируемость даже на таких машинах низкого класса (по памяти), как «Урал-1».

В заключение необходимо отметить, что, несмотря на удовлетворительное для защиты согласие расчетных и экспериментальных данных, требуется определенная осторожность в применении диффузионного многогруппового метода (особенно в случаях, которые не относятся к апробированным) из-за грубого представления углового распределения нейтронов, а также индикатриссы рассеяния.

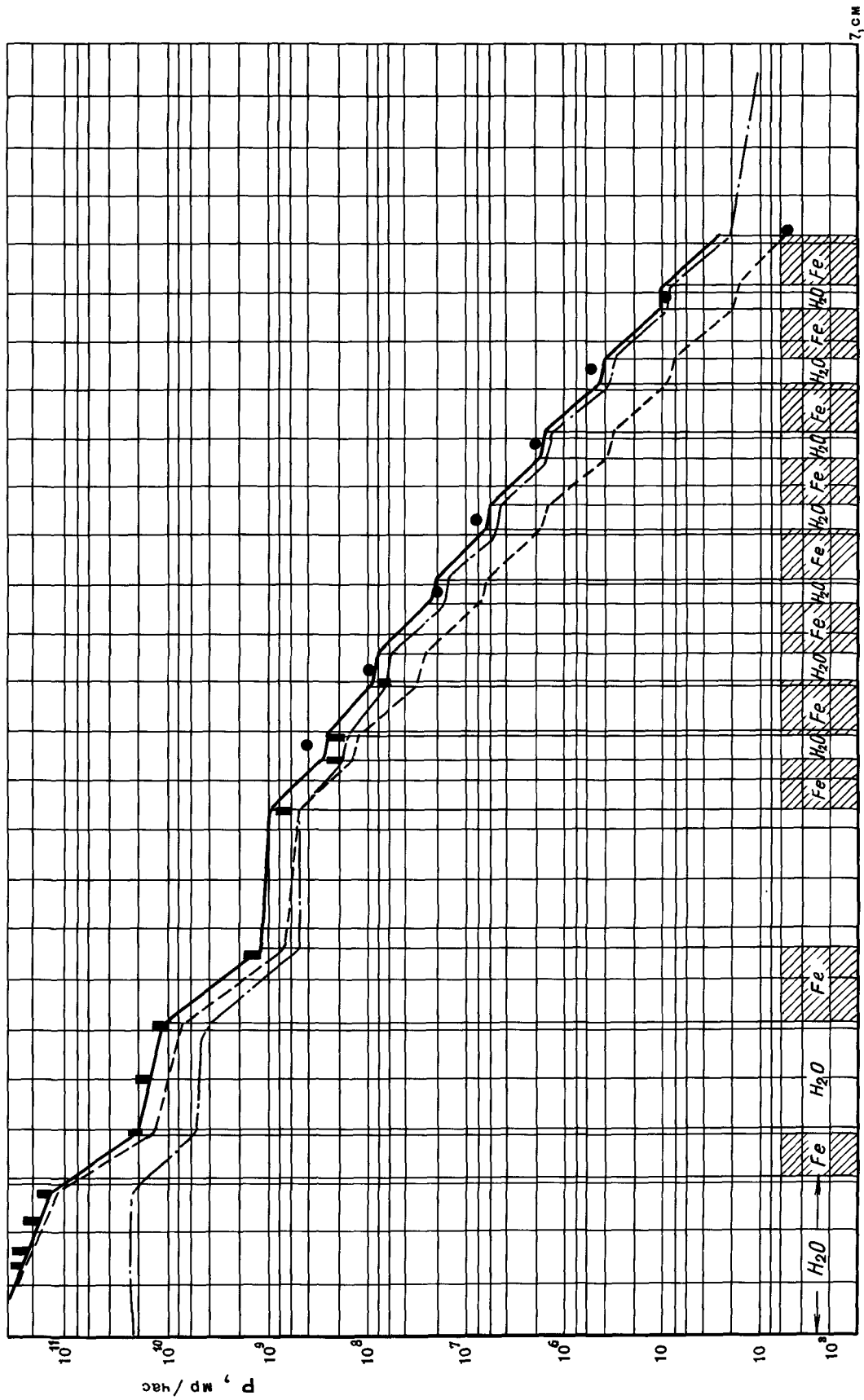


Рис. 4. Мощность дозы в тепловой защите корпуса и биологической защите реактора APPR

ЛИТЕРАТУРА

1. К. Купер, Дж. Джонс и К. Хортон. Труды Второй международной конференции по мирному использованию атомной энергии. Женева, 1958. Избранные доклады иностранных ученых, P/84. Т. 3. М., Атомиздат, 1959.
2. Д. Л. Бродер и др. Подбор системы функций возбуждения уровней при неупругом рассеянии нейтронов на ядрах железа, никеля и ниобия. В сб. «Вопросы физики защиты реакторов». М., Госатомиздат, 1963, стр. 132.
3. И. В. Гордеев, Д. А. Кардашев и А. В. Малышев. Справочник по ядерно-физическим константам для расчетов реакторов. М., Атомиздат, 1960.
4. Г. Гольдштейн. Основы защиты реакторов. М., Госатомиздат, 1961.
5. В. П. Машкович, С. Г. Цыпин. Атомная энергия, *2*, 3, 252 (1961).
6. Д. Л. Бродер, А. А. Кутузов, В. В. Левин, В. В. Орлов и А. Т. Турусова. Атомная энергия, *7*, 4, 313 (1959).
7. С. Г. Цыпин. Атомная энергия, *12*, 3, 500 (1962).
8. Г. Я. Румянцев. Атомная энергия, *10*, 1, 26 (1961).
9. Уилкинс, Хелленс, Цвайфел. Современное состояние эксперимента и теории замедления нейтронов в водородсодержащих средах. Материалы международной конференции по мирному использованию атомной энергии, Женева, 1955, P/597. Т. 5. М., Изд-во АН СССР, 1958.
10. Д. Л. Бродер, А. П. Кондрашев, А. А. Кутузов, В. А. Наумов, Ю. А. Сергеев и А. Т. Турусова. Атомная энергия, *12*, 2, 129 (1962).
11. Л. А. Герасева и В. В. Вавилов. Атомная энергия, *8*, 6, 556 (1960).
12. Галлахер. Краткая сводка проектных данных на основе трехлетнего опыта работы малого PWR. Доклад SMPR/52 на конференции по реакторам малой и средней мощности, Вена, сентябрь 1960.
13. В. В. Гончаров и др. Некоторые новые и реконструированные исследовательские тепловые реакторы. Труды Второй международной конференции по мирному использованию атомной энергии, Женева, 1958. Доклады советских ученых, P/2185. Т. 2. М., Атомиздат, 1959.

ABSTRACT - RÉSUMÉ - АННОТАЦИЯ - RESUMEN

A/721 Byelorussian SSR

Description of neutron radiation attenuation in-pile by multi-layer biological shielding on a multi-group model in diffusion approximation

By V. A. Naumov

On the basis of diffusion theory, a convenient calculation method for the neutron flux in the biological metal-water shielding of the pile is suggested in this paper. To describe neutron slowing down, the ten-group model is suggested in the range where the basic processes (elastic and inelastic scattering and absorption) determining the behaviour of the neutron flux in shielding are taken into account.

The method was approbised on calculations of neutron attenuation in the homogeneous shielding media water, graphite, iron, lead (with sources of a simple form) and in assemblies imitating thermal shielding and part biological shielding using zero power piles as a neutron source.

The study of attenuation of a fast neutron flux in homogeneous media such as water, graphite, iron and lead showed that the diffusion approximation may be used over a wider range than the theoretical limits. The region in which the diffusion theory correctly describes both the full neutron flux and power flux and the power flux distribution is extended by making a number of assumptions. First, the law of elastic scattering is assumed to be linear in the mass centre system. Secondly, the quantitative description of neutron slowing-down due to inelastic collisions is made with nuclei excitation function, which are obtained for example, from the optical model of a nuclei. This distinguishes the proposed method from the approach based on assumptions of isotropy of elastic scattering and Maxwell's form of the spectre of inelastic neutron scattering.

Comparison of copper indicator activities, calculated and measured in the shielding assemblies, has shown that a system comprising the ten-group constants satisfactorily describes neutron flux behaviour in water, steel, boron steel and lead thermal shielding of a reactor vessel. Maximum deviations of predicted values from experimentally measured ones are observed in the hydrogeneous media which are between the borated shields—strong neutron absorbers—and attain 30-40 per cent.

To verify the usefulness of this method for predictions of neutron attenuation in multi-layer biological shielding with the help of a ten-group constant system, the neutron flux spectra in a thermal column of the IRT-2000 research reactor and in the biological shielding of the power reactor APPR were calculated. The information obtained on the distribution of neutron fluxes was utilized for restoration of the dependences of some values experimentally measured on shielding thicknesses.

In the case of the IRT-2000 reactor these values were the thermal neutron flux and in the case of the APPR reactor the activities of gold foils and the dose rates from capture γ-radiation and fission γ-rays. Comparison of the predicted and experimental data showed their satisfactory agreement when attenuation of the neutron flux was more than 10^6.

The proposed method is notable for simplicity and can be readily programmed for electronic computers.

A/721 RSS de Biélorussie

Description de l'atténuation du rayonnement neutronique d'un réacteur par un bouclier biologique à plusieurs écrans, au moyen d'un modèle à plusieurs groupes dans une approximation de diffusion

par V. A. Naumov

L'auteur, se fondant sur la théorie de la diffusion, propose une méthode de calcul pratique du flux de neutrons dans le bouclier biologique métal-eau d'un réacteur nucléaire. Pour représenter le ralentissement des neutrons, il propose un modèle à dix groupes qui tient compte de tous les principaux processus (diffusion élastique et inélastique, absorption) qui déterminent le comportement du flux de neutrons dans le bouclier.

On a appliqué à titre d'essai cette méthode au calcul de l'atténuation des neutrons dans des milieux protecteurs homogènes: eau, graphite, fer, plomb (avec des sources de forme simple) et dans des assemblages simulant le bouclier thermique et une partie du bouclier biologique, avec des réacteurs de puissance nulle comme source de neutrons.

L'étude de l'atténuation d'un flux de neutrons rapides dans des milieux homogènes — eau, graphite, fer et plomb — a montré que l'approximation de diffusion est applicable dans un intervalle beaucoup plus vaste que celui des limites théoriques. La zone des distances pour lesquelles la théorie de diffusion définit correctement à la fois le flux de neutrons complet et la distribution du flux selon l'énergie s'étend considérablement si l'on admet certaines hypothèses. Premièrement, on suppose que la loi de diffusion élastique est linéaire dans le système du centre de masse. Deuxièmement, on décrit quantitativement le ralentissement des neutrons dû aux chocs inélastiques au moyen des fonctions d'excitation des noyaux (que l'on obtient, par exemple, à partir du modèle optique du noyau). A cet égard, la méthode proposée diffère de la méthode fondée sur les hypothèses relatives à l'isotropie de la diffusion élastique et à la forme maxwellienne du spectre de diffusion inélastique des neutrons.

La comparaison des activités des indicateurs en cuivre, calculées et mesurées dans les assemblages protecteurs, montre que le modèle à dix groupes choisi définit de façon satisfaisante le comportement du flux de neutrons dans les différents matériaux dont se compose le bouclier thermique d'une cuve de réacteur: eau, acier, acier au bore, plomb. Les écarts maximaux entre les chiffres calculés et les valeurs mesurées expérimentalement correspondent à des milieux hydrogénés situés entre des écrans au bore (caractérisés par une forte absorption des neutrons) et s'élèvent à 30 ou 40%.

Pour vérifier si la méthode permet de prévoir l'atténuation des neutrons par un bouclier biologique à plusieurs écrans au moyen d'un modèle à dix groupes, on a calculé les spectres du flux de neutrons dans la colonne thermique du réacteur de recherche IRT-2000 et dans le bouclier biologique du réacteur de puissance ARR. Les données obtenues sur la distribution du flux de neutrons selon l'énergie ont été utilisées pour tenir compte des variations des valeurs mesurées expérimentalement selon l'épaisseur de l'écran.

Ces valeurs étaient, pour le réacteur IRT-2000, le flux de neutrons thermiques et, pour le réacteur ARR, les activités de feuilles d'or et le débit de dose dû aux rayons γ de capture et de fission. La comparaison entre les données calculées et les données expérimentales a montré une concordance satisfaisante pour une atténuation du flux de neutrons supérieure à 10^6.

La méthode proposée se distingue par sa simplicité et peut être facilement incorporée dans les programmes des ordinateurs électroniques.

A/721 RSS de Bielorrusia

Cálculo de la atenuación de la radiación neutrónica de un reactor por un blindaje biológico de varias capas mediante un modelo de difusión con varios grupos

por V. A. Naumov

En la memoria se propone un método práctico, basado en la teoría de la difusión, para el cálculo del flujo neutrónico en un blindaje biológico de agua y metal de un reactor nuclear. Para representar la moderación de los neutrones se propone un modelo con diez grupos energéticos, mediante el cual se tienen en cuenta todos los procesos fundamentales que determinan el paso del flujo neutrónico por el blindaje (dispersión elástica e inelástica, absorción).

El método ha sido probado calculando la atenuación de los neutrones en medios homogéneos, utilizados como blindaje: agua, grafito, hierro, plomo (con fuentes de forma simple) y en un modelo de blindaje térmico y de una parte del biológico, utilizando reactores de potencia nula como fuente de neutrones.

El estudio de la atenuación del flujo de neutrones rápidos en medios homogéneos (agua, grafito, hierro y plomo) ha puesto de manifiesto que la teoría de la difusión es aplicable entre límites mucho más amplios que los límites teóricos. El intervalo de distancias en el que la teoría de la difusión describe correctamente tanto el flujo neutrónico total como su distribución energética aumenta considerablemente gracias a una serie de hipótesis. En primer lugar, se supone que la ley de dispersión elástica es lineal en el sistema del centro de masas. En segundo lugar, el comportamiento cuantitativo de la moderación neutrónica debida a choques inelásticos se representa mediante funciones de excitación de los

núcleos (obtenidas, por ejemplo, a partir del modelo óptico del núcleo). Estas dos hipótesis distinguen el método propuesto del que se basa en suponer isótropa la dispersión elástica y en admitir una forma maxwelliana para el espectro de los neutrones que han sufrido dispersión inelástica.

La comparación de las actividades de los indicadores de cobre, calculadas y medidas en modelos de blindaje, prueba que el sistema de constantes elegido para diez grupos representa satisfactoriamente el comportamiento del flujo neutrónico en las capas de agua, de acero, de acero al boro y de plomo que constituyen el blindaje térmico de la vasija del reactor. Las desviaciones máximas de los valores calculados de las medidas experimentales se observan en medios hidrogenados que se encuentran entre capas con boro, que absorben fuertemente los neutrones, y varían entre el 30 y el 40%.

Para comprobar si el método permite predecir, mediante un modelo de 10 grupos, la atenuación de los neutrones por un blindaje biológico de varias capas, se calcularon los espectros del flujo neutrónico en la columna térmica del reactor de investigaciones IRT-2000 y en el blindaje biológico del reactor de potencia ARR. La información obtenida acerca de la distribución energética del flujo neutrónico se empleó para establecer la ley de variación de las magnitudes medidas experimentalmente, en función del espesor de la capa.

En el caso del reactor IRT-2000, la magnitud en cuestión fue el flujo de los neutrones térmicos; en el del reactor ARR, las actividades de hojas de oro y la dosis debida a los rayos γ de captura y de fisión. La comparación entre los valores calculados y los experimentales mostró que concuerdan satisfactoriamente para una atenuación del flujo neutrónico superior a 10^6.

El método propuesto se distingue por su simplicidad y es fácil de programar para las calculadoras electrónicas.

Record of Session 3.5

Reactor control and shielding

Chairman: E. P. Blizard (United States of America)

Paper P/631 (presented by P. Kovanic)

DISCUSSION

M. A. SCHULTZ (United States of America): I should like to say a few words about similar moving detector instrumentation in the United States. As you may know, Dr. S. Hanauer describes, in paper P/229,* the all-transistorized moving detector system under test in the ORR reactor for ultimate use in the HIFIR reactor. This system is similar to yours and the one described in paper P/80 by Mr. Furet* except in the matter of period reading capability. I see that your mechanical system is capable of following periods as short as 2 s. My own feeling is that it should be possible to build a servo system that would follow 0.1 s periods. Dr. Hanauer and his colleagues at Oak Ridge, however, believe that in experimental reactors period protection should be provided down to a response time of a few milliseconds. Consequently, they have added a very fast electronic rate-of-change circuit, following the detector, to supplement the normal period circuit. They use this circuit for fast period information and the detector position for level information.

What is your opinion of this solution? Do you think fast period protection might be necessary? Secondly, I should like to know whether you use detector position trips as over-power scrams, or whether you rely on your fixed instrumentation for this purpose.

P. KOVANIC (Czechoslovakia): We agree that it should be possible to build a moving detector system which would *measure* reactor periods shorter than the 2 s indicated in our paper. The maximum velocity of the detector is chosen to correspond to the required period reading range. It should be stressed that this maximum velocity does *not* determine the response time of the period scram signal, which is related not to the detector's rate of movement but directly to its output signal. In normal conditions the magnitude of this signal stays within narrow limits for any given power of the reactor. It can go outside these limits only in an emergency period or when the tracking system is defective. The scram-signal circuits consist of electronic equipment which acts just as quickly as in systems employing stationary detectors. We can therefore get a response time of 1 ms in the period scram signal even though the moving detector mechanism may operate slowly.

We feel that the introduction of supplementary equipment as proposed by Dr. Hanauer in paper P/229 would be useful, but we do not believe that it is essential for fast period protection; such protection can be ensured perfectly well in systems using moving detectors. In our VVR-S reactor the moving detector systems produced the scram signals so fast that we had to provide for a response time of 0.1 s in order to give the operator time for manual adjustment of the control rods.

The answer to your second question is that we do use detector position trips for this purpose. Furthermore, we have so far kept part of the earlier emergency system, employing stationary detectors, as a form of reserve.

J. FURET (France): What is the maximum velocity of the moving detector? Is a limiting period maintained during start-up and does this entail stoppage or dropping of the control rods?

P. KOVANIC (Czechoslovakia): The maximum velocity of the moving detector is approximately 4 cm/s. When the reactor is started up by the automatic system, the velocity of the detector in the control system remains constant; the start-up period varied slightly in relation to the calibration curve (see Fig. 2 in the paper).

When the actual period of the reactor differs from the prescribed period, the automatic equipment transfers control of the reactor to another of the three moving detector systems, which up to that point has functioned as a measuring system. The detector in this new system then stops and the system automatically brings reactivity down to zero while keeping the power constant at the level that had been reached. Further power changes can be made only after the operator has given his permission.

We do not resort to cut-off (control rod "stoppage") because this can result in the reactor being stopped in a supercritical state.

J. WEILL (France): Have you observed variations in absolute power readings as a function of water

* Vol. 8, these Proceedings.

temperature, or as a result of the presence of experimental devices?

P. KOVANIC (Czechoslovakia): As far as we can see, the calibration of the moving detectors is not dependent on water temperature, and in any case the water temperature in the VVR-S reactor varies only within narrow limits. At the outset we did experience some difficulty owing to the presence of experimental devices in the immediate neighbourhood of the detector channels, and this applies particularly to the tubes that are not filled with water. Since then we have observed a few additional operating rules, in effect very simple rules, and there have been no more difficulties.

Y. EL-MESHAD (United Arab Republic): I understand that the neutron flux distribution sometimes deviates from an exponential distribution. Have you found any practical means of dealing with this problem?

P. KOVANIC (Czechoslovakia): While the installation was being designed we took a number of steps to correct these deviations, but subsequently it turned out that, from a practical point of view, they presented no problems.

B. G. DUBOVSKY (USSR): I feel that in high temperature reactors of high specific power, a category which encompasses practically all power reactors, the use of moving detectors in control and safety systems is not advisable. The fact is that moving detectors create an additional source of uncertainty in the functioning of those crucially important systems; moreover, the advantages to be derived from their use are not really so great. In the Soviet Union, in 1950, I used a method of bringing a reactor from the sub-critical state to a controlled power level which ensures perfect safety.* The method consists essentially in prescribing a specific rate of reactivity increase. It depends, of course, on having a small quantity of beryllium or beryllium oxide (about 10 kg) in the reactor to raise the neutron background, and on the use of control equipment of standard sensitivity. I have found the optimum rate to be 0.2% over a period of three minutes (in the form of a step increase followed by a three-minute pause).

All this, of course, is without prejudice to the usefulness of movable fission chambers as a means of controlling a reactor in the subcritical state.

Paper P/80 (presented by J. Furet)

DISCUSSION

K. WAGNER (Czechoslovakia): In your paper the systems employing moving detectors are divided into two groups, the first group consisting of measuring servo systems and the second of control systems. I should like to know whether the three moving detector systems in the OSIRIS reactor are designed as control systems only, or whether you intend to use them as measuring systems too.

In this same connection, I understand that the moving detectors in the TRITON and MÉLUSINE reactors are used only as control systems. Our experience suggests that their use as measuring systems is entirely practicable, and I should be interested to learn why they have not been used in this way.

J. FURET (France): When OSIRIS first goes into operation the three electronic assemblies associated with the three moving detectors will not be used to provide automatic start-up. The reactor will be started by manual operation of the control rods and the detectors will move individually in accordance with the programme described in the paper. Automatic start-up will be considered after experiments have been carried out on the installation.

In reply to your second question, the moving detector system has been in use in the TRITON reactor since 1962, although start-up is still affected by manual withdrawal of the control rods. This equipment thus belongs in the first of the two groups I mentioned.

B. G. DUBOVSKY (USSR): I should like to draw your attention to the possibility of using uranium thermopiles as neutron flux detectors in control and safety systems. Batteries of uranium-coated thermocouples work well at temperatures above 500 °C, and owing to their low electrical resistance the problem of electric leaks from the insulation of supply cables does not arise. Provided the thermopiles are well made, thermal lag can be kept sufficiently small. The experiments which I carried out in 1954 on the reactor of the first atomic power station gave satisfactory results.**

Paper P/647

There was no discussion of this paper.

Paper P/273 (read by title only)

DISCUSSION

A. G. FILIPPOV (USSR): I should like to ask Mr. Schultz whether reactivity is measured during start-up, and if so, how is it done?

M. A. SCHULTZ (United States of America): No, in none of the digital systems that have been used to date do we measure reactivity. The work done so far simply replaces direct analogue counting by digital counting.

Paper P/375 (presented by V. A. Kuznetsov)

DISCUSSION

J. A. THIE (United States of America): Mr. Kuznetsov has mentioned two excellent techniques for

* Atomnaya Energia (1957).

** Dubovsky, B. G., and Kitaev, V. Y., *O primenenii maloinertsionnoy termobatarei dlya izmerenia bolshikh neitronnyh potokov v yadernykh reaktorakh*, Atomnaya Energia, Supplement 1, p. 128 (1958).

measuring subcritical or negative reactivities, namely the reciprocal count rate method and the fuel addition method. There are other familiar methods, for example interchange of non-interfering control rods, rapid control rod insertion, exchange with chemical shim absorbers, and neutron random fluctuation analysis. If there are any other, less familiar methods of measuring subcritical reactivities, it would be interesting to hear about them from Mr. Kuznetsov.

V. A. KUZNETSOV (USSR): Apart from the well-known methods of measuring negative reactivities by means of a pulsed neutron source, I can add nothing new to the list of experimental techniques enumerated by Dr. Thie.

Paper P/179 (presented by J. Brown)

DISCUSSION

A. G. FILIPPOV (USSR): How consistent are the readings obtained from the thermocouples? Do you use any other signal devices for the same purpose?

J. BROWN (United Kingdom): The measurements of fuel element temperature are consistent to within $\pm$ 3 °C and we have found them to be extremely reliable. Very few failures have been observed since Bradwell and Berkeley started power operation. We place complete reliance on these temperature measurements for protection against the type of fault discussed (sector rod faults). In the paper, we explain that it is in fact not possible to use any other parameter. We have no in-pile flux detectors from which we can derive protection signals.

A. G. FILIPPOV (USSR): Are the sectors interrelated? In other words, do the control rods in each sector move independently and emit independent signals or are certain sectors with maximum buckling selected?

J. BROWN (United Kingdom): Each sector operates independently from its neighbours, but a common temperature demand signal is normally set. The stability rod will therefore take up a position giving the demanded gas outlet temperature from the sector. If, in the long term, a stability rod is found to drift from 50% insertion in the reactor, there are "trimming" rods which can then be used (on manual control) to return the stability rod to about 50% insertion, the position at which it is most effective. The relative positions of the stability rods, if one of them comes out of the core under fault conditions, are shown in Fig. 12 of the paper; as the temperature in adjacent sectors rises, so that adjacent stability rods penetrate deeper into the core, attempting to keep the gas temperature at its demanded value. The stability rods are thus, in a certain sense, "coupled" through the reactor.

P. BACHER (France): Have you observed any spatial instabilities in the stations now operating? Has the control system actually gone into service? Lastly, have you been able to compare the operation of this system with the theoretical predictions?

J. BROWN (United Kingdom): Something akin to spatial instability has been observed at Berkeley. The flux has been perturbed, and the resulting oscillations have not diverged but have died away only very slowly; the Berkeley reactor has a moderator temperature coefficient of almost 10 mN/°C. Thus we believe that we are on the threshold of instabilities.

The sector system is expected to be put into operation, on automatic control, at any moment. All modifications to the safety system mentioned in my oral presentation have been carried out and commissioning tests have been completed. The Berkeley reactor was shut down when I left for Geneva, but was due to start again at the beginning of September with the system in full operation.

Figures 18 and 19 show comparisons between the results of a commissioning experiment and the theoretical predictions used for this work, at Berkeley. The measured temperature increases show remarkably good agreement with theory.

P. B. BRANSON (United Kingdom): In this connection I should like to make two brief comments on topics which are dealt with more fully in paper P/180. The first concerns the methods used in transient analysis, particularly for gas-cooled reactors. We have heard of the recent development of large and complex three-dimensional models of reactor transient behaviour; however, even with the very fast computers now available, these three-dimensional models still require an excessive amount of computation time as well as great effort in the preparation and interpretation of the runs. These methods have an important place in detailed operational and safety studies once a design has been completed, but they are generally too expensive and clumsy for design purposes, for which one- and two-dimensional, and even point models, are still extensively used. It has been our experience to date, based on comparisons with both actual reactor behaviour and the elaborate three-dimensional calculations, that the simpler methods do in fact provide a sound basis for most design purposes.

My second comment concerns the need to consider in-pile control rods, such as spatial control or override rods, as an integral part of the over-all power flattening arrangement. This is most easily achieved by using movable absorbers on a common lattice with the controllers. Such a system has been used on the Hunterston reactor, for example, and it has been found possible in practice to achieve very good form factors, together with satisfactory control, while at the same time maintaining maximum operational flexibility by providing for differential insertion of the absorbers.

Paper P/260 (presented by E. P. Blizard)

DISCUSSION

V. V. ORLOV (USSR): Much of the Soviet work on the physics of shielding has been described in

papers presented at this Conference. However, having heard Dr. Blizard's interesting survey I should like to comment on two special points.

First, by using a set of conjugate kinetic equations and perturbation theory, we have devised a method of calculating what we call efficiency functions for different materials, a method which enables us, by means of successive approximations, to determine the optimum distribution of materials in the shielding. On this basis, a computer programme designed to produce optimized shielding data has been drawn up. We can thus find the shielding composition which will have minimum weight, dimensions and so on, while still satisfying certain prescribed conditions with regard to doses outside the shielding, heat release and other parameters.

Secondly, I should like to call your attention to the possibility of calculating the distribution in infinite media of radiations from a directional point source by the solution of a conjugate kinetic equation postulating an isotropic source. This method is considerably easier than a direct solution of the kinetic equation because it involves fewer independent variables.

H. WIJKER (Netherlands): The procedure described by Mr. Orlov seems to involve the changing of one parameter after another by small stages. Is this not rather time-consuming?

V. V. ORLOV (USSR): Much depends, of course, on the complexity of the individual problem. The computer programme is broad enough to handle a wide variety of problems and is usually more detailed than the situation demands. The time required is several hours.

P. S. MITTELMAN (United States of America): The technique described by Dr. Blizard and myself is designed both to synthesize and to optimize a shield. With the synthesis technique, the point is not to start with a set of materials and alter the thickness of various layers until a minimum weight is obtained, but rather to select a set of shield materials and then to establish analytically the shield design which will give minimum weight.

I should think it would be very difficult to derive a set of efficiency functions for materials at various points in a shield because the effectiveness of a given material at a given position is closely dependent on the materials which precede and follow it. If both the type of material and its position in the shield are treated as variables, the calculation becomes, I should think, nearly impossible.

V. V. ORLOV (USSR): I am not entirely in agreement with you. The programme I referred to consists in successive iterations, each of which involves only small changes in the concentration of the materials. It is assumed that the change is small enough in each case so that the conditions in which small perturbation theory will remain applicable are preserved. The interdependence which you mention, that is the influence of preceding and following layers, and so on, is fully taken into account. I can if necessary describe to you in greater detail after the meeting the way in which this is done.

Paper P/684 (presented by M. Leimdörfer)

DISCUSSION

F. P. YOUELL (United Kingdom): As you mention the United Kingdom RASH B code, I should like to make a few comments. First, your paper is interesting in that it provides further evidence of the value of the removal-diffusion treatment for neutron penetration of shields. The RASH B code has been used in this paper, but the scope of the model has now been extended to enable the neutron spectrum from 18 MeV down to thermal energies to be calculated in various types of laminated shield. This latest version of the code is known as RASH E; its versatility and accuracy are described in the UKAEA report AEEW-R361 by Dr. J. Butler.

In the United Kingdom, we feel that the accuracy now obtained for simple shield configurations is at present adequate, particularly when compared with the inaccuracies introduced by simplification of the complex geometry encountered in large power-reactor shields. Our main efforts are now directed towards extending the RASH method to treat these complex geometries. Paper P/175 describes various extensions of the standard method, designed to deal with certain heterogeneous shield regions encountered at Bradwell. Simply smearing the material of the shield into a homogeneous slab can lead to serious under-estimates of neutron fluxes, particularly when one is dealing with regions such as reflectors pierced by fuel channel arrays in gas-cooled reactors. From the results given in paper P/175 we conclude that the removal age – diffusion model, incorporating line-of-sight or similar corrections for heterogeneity, provides a valuable design tool for practical reactor shields.

G. H. MINTON (United States of America): Could you comment on the merit of the discrete ordinate method, or the higher-order spherical harmonic methods, in multigroup calculations for problems of the type discussed in your paper?

M. LEIMDÖRFER (Sweden): I believe it is mainly a matter of computer time. For instance, the NIOBE programme, which belongs to the group you mentioned, is about 100 times slower than our method.

Paper P/657

DISCUSSION

G. H. MINTON (United States of America): You state that "the photons which belong to one group of specific energy and angle will not fall into other groups during transmission through an elementary slab". Is this a characteristic of the Monte Carlo programme used in preparing the response matrix?

I. KATAOKA (Japan): No, it is not a characteristic

of the Monte Carlo programme. It relates only to the thickness interpolation procedure used in synthesizing the response matrices for the elementary slabs. To clarify this answer I should add that the calculations as a whole are considered as consisting of two separate parts. First comes the preparation of the response matrices for the elementary slabs of various materials; the user of the method needs only a table of the response matrices. Secondly, there is the actual calculation of photons transmitted (or reflected) through any desired stratified barriers. The synthesis of the response matrices and the calculation of thickness interpolation are performed at this stage of the calculation, which can be coded for any digital computer convenient to the user of this method. The author has prepared a code for an NEAC-2206 computer.

H. WIJKER (Netherlands): As the matrices contain only two parameters, the energy and the cosine of the angle, one can conclude that the procedure you describe only holds good for infinite plane homogeneous sources. In Figures 4 and 5 the results are compared with measurements made with a Co^{60} source. I wonder whether the source used in these experiments was a homogeneous plane source of reasonable dimensions.

I. KATAOKA (Japan): There is no direct connection between the Monte Carlo calculation and the actual arrangement of the source and detectors in the experiment. The final results were converted to values for slab geometry obtained from experimental measurements, and these are the results referred to in the paper.

Compte rendu de la séance 3.5

Contrôle des réacteurs; écrans de protection

Président: E. P. Blizard (Etats-Unis d'Amérique)

Mémoire P/631 (présenté par P. Kovanic)

DISCUSSION

M. A. SCHULTZ (Etats-Unis d'Amérique): Je voudrais dire quelques mots au sujet des détecteurs mobiles étudiés aux Etats-Unis et semblables à ceux décrits dans le mémoire. Comme vous le savez sans doute, M. S. Hanauer décrit, dans le mémoire P/229*, le système de détecteurs mobiles entièrement transistorisé qui est en cours d'essai dans le réacteur ORR et qui est destiné au réacteur HIFIR. Ce système est voisin du vôtre et de celui qui est décrit dans le mémoire P/80 par M. Furet*, sauf en ce qui concerne la possibilité de lire la période. Je vois que votre système mécanique est capable de suivre des périodes courtes, jusqu'à une limite inférieure de 2 s. Je crois personnellement qu'il serait possible de construire des servo-mécanismes qui suivraient des périodes de 0,1 s. M. Hanauer et ses collègues d'Oak Ridge pensent cependant que, pour les réacteurs expérimentaux, il faut assurer la protection en période jusqu'à un temps de réponse de quelques millisecondes. En conséquence, ils ont ajouté un circuit électronique très rapide de mesure de la vitesse de variation, qui suit le détecteur et complète le circuit de période normal. Ils utilisent ce circuit pour obtenir des informations sur les périodes très courtes, et la position du détecteur pour les mesures de niveau.

Que pensez-vous de cette solution? Pensez-vous que la protection pour les cas de périodes rapides est nécessaire? J'aimerais aussi savoir si vous utilisez les déclenchements liés à la position du détecteur pour les arrêts d'urgence en cas de barres de surpuissance, ou si vous vous fiez dans ce but à l'instrumentation fixe.

P. KOVANIC (Tchécoslovaquie): Je pense aussi qu'il serait possible de construire un détecteur mobile capable de *mesurer* des périodes de réacteur inférieures aux 2 s indiquées dans notre mémoire. La vitesse maximale du détecteur est choisie de façon à correspondre au domaine voulu de lecture de périodes. Il faut insister sur le fait que cette vitesse maximale *ne détermine pas* le temps de réponse du signal de période pour les chutes de barres, qui est lié non pas à la vitesse de déplacement du détecteur mais directement au signal émis par celui-ci. Dans les conditions normales, l'intensité de ce signal varie entre des limites très étroites pour une puissance donnée du réacteur. Il ne sort de ces limites qu'en période de danger, ou quand

* Voir les présents Actes, vol. 8.

le système de repérage est défectueux. Les circuits d'alerte sont des circuits électroniques qui agissent aussi rapidement que ceux des systèmes à détecteurs fixes. Nous pouvons donc obtenir un temps de réponse de 1 ms pour le signal d'alerte de période, même si le mécanisme du détecteur mobile fonctionne lentement.

Nous pensons que l'introduction d'équipement supplémentaire, comme le propose M. Hanauer dans le mémoire P/229, peut être utile, mais nous ne pensons pas qu'elle soit essentielle pour la protection contre les périodes très courtes; on peut parfaitement assurer cette protection dans les systèmes à détecteurs mobiles. Dans notre réacteur VVR-S, les systèmes de détecteurs mobiles produisaient les signaux d'alerte si rapidement que nous avons dû prévoir un temps de réponse de 0,1 s pour donner à l'opérateur le temps d'ajuster manuellement les barres de contrôle.

La réponse à votre seconde question est affirmative: nous utilisons les signaux de position des détecteurs dans ce but. De plus, nous avons conservé pour le moment une partie de l'ancien système d'urgence, qui utilise des détecteurs fixes, et sert de système de secours.

J. FURET (France): Quelle est la vitesse maximale du détecteur mobile? Maintenez-vous une période limite pendant le démarrage, et ceci entraîne-t-il l'arrêt ou la chute des barres de contrôle?

P. KOVANIC (Tchécoslovaquie): La vitesse maximale du détecteur mobile est voisine de 4 cm/s. Quand on fait démarrer le réacteur avec le système automatique, la vitesse du détecteur dans le système de contrôle reste constante; la période de démarrage varie légèrement en fonction de la courbe d'étalonnage (voir la figure 2 du mémoire).

Quand la période réelle du réacteur diffère de la période affichée, l'équipement automatique transfère le contrôle du réacteur à un autre des trois systèmes de détecteurs mobiles, qui avait jusque-là joué le rôle de système de mesure. Le détecteur de ce nouveau système s'arrête alors et le système fait automatiquement tomber la réactivité à zéro, tout en maintenant la puissance constante à la valeur qui avait été atteinte. De nouvelles variations de puissance ne peuvent se faire sans l'autorisation de l'opérateur.

Nous ne pratiquons pas l'arrêt des barres de contrôle parce que cette méthode peut conduire à bloquer le réacteur dans un état surcritique.

J. WEILL (France): Avez-vous observé des variations de la puissance absolue mesurée en fonction de la température de l'eau, ou en raison de la présence de dispositifs expérimentaux?

P. KOVANIC (Tchécoslovaquie): Il ne semble pas que l'étalonnage des détecteurs mobiles dépende de la température de l'eau, et, en tout cas, la température de l'eau du réacteur VVR-S ne varie qu'entre d'étroites limites. Au début, nous avons éprouvé quelques difficultés dues à la présence de dispositifs expérimentaux au voisinage immédiat des canaux des détecteurs, et ceci s'applique particulièrement aux tubes qui ne sont pas remplis d'eau. Depuis, nous avons appliqué quelques règles de procédure supplémentaires, des règles très simples, et nous n'avons plus eu de difficultés.

Y. EL-MESHAD (République arabe unie): Il semble que la distribution du flux de neutrons s'écarte parfois d'une distribution exponentielle. Avez-vous trouvé des moyens pratiques de faire face à ce problème?

P. KOVANIC (Tchécoslovaquie): Au cours de la mise au point du projet, nous avons pris un certain nombre de mesures pour corriger ces déviations, mais nous avons constaté par la suite que, du point de vue pratique, elles ne posaient pas de problème.

B. G. DUBOVSKY (URSS): Je pense que, dans les réacteurs à haute température et à puissance spécifique élevée, catégorie qui comprend pratiquement tous les réacteurs de puissance, il n'est pas judicieux d'utiliser des détecteurs mobiles dans les systèmes de contrôle et de sécurité. Les détecteurs mobiles créent, en effet, une source supplémentaire d'incertitude dans le fonctionnement de ces systèmes d'importance essentielle; de plus, les avantages que présente leur utilisation ne sont pas réellement grands. En Union soviétique, j'ai utilisé en 1950 une méthode qui permet d'amener en toute sécurité un réacteur de l'état sous-critique à un niveau de puissance contrôlé*. La méthode consiste essentiellement à prescrire une vitesse donnée d'augmentation de la réactivité. Il faut, bien entendu, avoir dans le réacteur une petite quantité de béryllium ou de glucine (environ 10 kg) pour augmenter le bruit de fond de neutrons, et disposer d'équipement de contrôle de sensibilité normale. J'ai trouvé que la vitesse optimale est de 0,2% sur une période de trois minutes (sous forme d'augmentation en une étape, suivie d'une pause de trois minutes).

Tout cela, naturellement, n'a rien à voir avec l'utilité des chambres de fission mobiles pour le contrôle d'un réacteur à l'état sous-critique.

Mémoire P/80 (présenté par J. Furet)

DISCUSSION

K. WAGNER (Tchécoslovaquie): D'après votre mémoire, les systèmes employant des détecteurs mobiles se divisent en deux groupes, le premier groupe comprenant les servo-mécanismes de mesure et le second les systèmes de contrôle. Je voudrais savoir si les trois systèmes de détecteurs mobiles du réacteur OSIRIS seront seulement des systèmes de contrôle, ou si vous envisagez de les utiliser aussi comme systèmes de mesure.

J. FURET (France): Au début du fonctionnement d'OSIRIS, les trois ensembles électroniques associés aux trois détecteurs mobiles ne seront pas utilisés

* Atomnaya Energia, 1957.

pour réaliser un démarrage automatique. Le réacteur démarrera par déplacement manuel des barres de contrôle, et les détecteurs se déplaceront individuellement selon le programme décrit dans le mémoire. On envisagera le démarrage automatique quand une certaine expérience aura été obtenue avec l'installation.

K. WAGNER (Tchécoslovaquie): Il semble que les détecteurs mobiles des réacteurs TRITON et MÉLUSINE ne sont utilisés que comme systèmes de contrôle. Notre expérience nous fait penser qu'il serait tout à fait possible de les utiliser comme systèmes de mesure, et je voudrais savoir pourquoi ils n'ont pas été ainsi utilisés.

J. FURET (France): Le système de détecteurs mobiles est utilisé dans le réacteur TRITON depuis 1962, mais le démarrage se fait toujours par déplacement manuel des barres de commande. Cet équipement fait donc partie du premier des deux groupes que j'ai mentionnés.

B. G. DUBOVSKY (URSS): Je voudrais attirer l'attention sur la possibilité d'utiliser des thermopiles à uranium comme détecteurs de flux de neutrons dans les systèmes de contrôle et de sécurité. Des batteries de thermocouples revêtus d'uranium fonctionnent bien aux températures supérieures à 500 °C, et, grâce à leur faible résistance électrique, le problème des fuites électriques par l'isolement des câbles d'alimentation ne se pose pas. A condition que les thermopiles soient bien construites, l'inertie thermique peut être suffisamment faible. Les expériences que j'ai faites en 1954 sur le réacteur de la première centrale atomique ont donné des résultats satisfaisants.*

Mémoire P/647

Ce mémoire n'a pas donné lieu à une discussion.

Mémoire P/273 (présenté seulement par son titre)

DISCUSSION

A. G. FILIPPOV (URSS): Je voudrais demander à M. Schultz si la réactivité est mesurée pendant le démarrage et, dans ce cas, comment cette mesure est faite.

M. A. SCHULTZ (Etats-Unis d'Amérique): Non, aucun des systèmes numériques utilisés jusqu'à présent ne sert à mesurer la réactivité. Les études faites jusqu'à maintenant ont simplement remplacé le comptage analogique direct par le comptage numérique.

Mémoire P/375 (présenté par V. A. Kuznetsov)

DISCUSSION

J. A. THIE (Etats-Unis d'Amérique): M. Kuznetsov a mentionné deux excellentes techniques de mesure des réactivités sous-critiques ou négatives, la méthode de l'inverse du taux de comptage et la méthode d'addition de combustible. Il y a d'autres méthodes usuelles, par exemple l'échange de barres de contrôle qui n'interfèrent pas, l'insertion rapide d'une barre de contrôle, l'échange avec des absorbeurs de compensation chimiques, et l'analyse des fluctuations aléatoires des neutrons. S'il y a d'autres méthodes, moins connues, pour mesurer les réactivités sous-critiques, il serait intéressant que M. Kuznetsov nous en parle.

V. A. KUZNETSOV (URSS): En dehors des méthodes bien connues de mesure des réactivités négatives à l'aide d'une source de neutrons pulsée, je ne peux rien ajouter de nouveau à la liste de techniques expérimentales énumérées par M. Thie.

Mémoire P/179 (présenté par J. Brown)

DISCUSSION

A. G. FILIPPOV (URSS): Quelle est la reproductibilité des mesures données par les thermocouples? Utilisez-vous d'autres mesures de signaux dans le même but?

J. BROWN (Royaume-Uni): Les mesures de température d'éléments combustibles sont correctes à $\pm$ 3 °C, et nous les avons trouvées très sûres. Il y a eu très peu d'incidents depuis la montée en puissance des réacteurs de Bradwell et de Berkeley. Nous avons toute confiance dans ces mesures de température pour assurer la protection contre le type de défaut discuté (barre de secteur défectueuse). Nous expliquons dans notre mémoire qu'il n'est pratiquement pas possible d'utiliser un autre paramètre. Nous n'avons pas de détecteurs de flux dans la pile qui pourraient nous donner des indications pour la sécurité.

A. G. FILIPPOV (URSS): Les secteurs sont-ils interconnectés? En d'autres termes, les barres de contrôle de chaque secteur se déplacent-elles indépendamment et émettent-elles des signaux indépendants, ou avez-vous choisi certains secteurs à laplacien minimal?

J. BROWN (Royaume-Uni): Chaque secteur fonctionne indépendamment de ses voisins, mais un signal commun de demande de température est normalement fixé. La barre de stabilité prendra donc une position qui donne la température voulue du gaz caloporteur à la sortie du secteur. Si, à long terme, une barre de stabilité s'écarte de la position d'insertion à 50% dans le réacteur, on peut utiliser des barres de « réglage fin » (par commande manuelle) pour ramener la barre de stabilité à une insertion voisine de 50%, position dans laquelle la barre en question a une efficacité maximale. Les positions relatives des barres de stabilité, si l'une d'entre elles sort du cœur dans certaines conditions, sont représentées sur la figure 12 de notre mémoire; si la température s'élève dans les secteurs voisins, les barres de stabilité adjacentes pénètrent davan-

* Dubovsky, B. G., and Kitaev, V. Y., *O primenenii maloinertsionnoy termobatarei dlya izmerenia bolshikh neitronnyh potokov v yadernykh reaktorakh,* Atomnaya Energia, Supplement 1, p. 128 (1958).

tage dans le cœur, pour maintenir la température du gaz à la valeur voulue. Les barres de stabilité sont donc, en un certain sens, « couplées » dans tout le réacteur.

P. BACHER (France): Avez-vous observé des instabilités spatiales dans les centrales actuellement en fonctionnement? Le système de contrôle a-t-il été mis en service? Enfin, avez-vous pu comparer le fonctionnement du système avec les prévisions théoriques?

J. BROWN (Royaume-Uni): Nous avons observé à Berkeley quelque chose qui ressemblait à une instabilité spatiale. Le flux a été perturbé, et les oscillations résultantes n'ont pas divergé mais elles ne se sont amorties que très lentement; le réacteur de Berkeley a un coefficient de température du modérateur de près de 10 mN/°C. Nous pensons donc que nous sommes à la limite des instabilités.

Nous comptons mettre en service sous peu le système des secteurs, en contrôle automatique. Toutes les modifications au système de sécurité que j'ai mentionnées dans ma présentation orale ont été faites, et les essais de mise en service sont terminés. Le réacteur de Berkeley était arrêté quand je suis parti pour Genève, mais il devait démarrer à nouveau au début de septembre, avec l'ensemble en plein fonctionnement.

Les figures 18 et 19 donnent les comparaisons entre les résultats des essais de mise en service et les prévisions théoriques utilisées dans cette étude, pour Barkeley. Les augmentations de température mesurées sont en très bon accord avec la théorie.

P. B. BRANSON (Royaume-Uni): A ce sujet, je voudrais faire deux brèves remarques sur des sujets qui sont plus complètement traités dans le mémoire P/180. La première remarque concerne les méthodes utilisées pour l'analyse des transitoires, en particulier pour les réacteurs refroidis au gaz. Nous avons entendu parler du développement des grands modèles complexes à trois dimensions pour l'étude du comportement transitoire des réacteurs; cependant, même avec les calculateurs très rapides maintenant disponibles, ces modèles à trois dimensions exigent encore un nombre excessif d'heures de calcul ainsi qu'un grand effort pour la préparation et l'interprétation de ces calculs. Ces méthodes jouent un rôle important dans les études détaillées de fonctionnement et de sécurité, une fois un projet achevé, mais elles sont généralement trop coûteuses et trop lourdes pour les études de projet, pour lesquelles on utilise encore beaucoup les modèles uni- et bi-dimensionnels et même les modèles par points. Notre expérience à ce jour, basée sur des comparaisons avec le comportement réel des réacteurs et les calculs complexes à trois dimensions, montre que les méthodes plus simples fournissent en fait des bases solides pour la plupart des études de projets.

Ma seconde remarque se rapporte à la nécessité de considérer les barres de commande en pile, telles que les barres de contrôle spatial, comme des parties intégrantes de l'ensemble général d'aplatissement du flux. Il est facile d'obtenir ce résultat en utilisant des absorbeurs mobiles sur un réseau commun avec les barres de contrôle. Un tel système a été utilisé pour le réacteur de Hunterston, par exemple, et il a permis d'obtenir en pratique d'excellents facteurs de forme, ainsi qu'un contrôle satisfaisant, tout en permettant de conserver la souplesse de fonctionnement maximale en permettant l'insertion différentielle des absorbeurs.

Mémoire P/260 (présenté par E. P. Blizard)

DISCUSSION

V. V. ORLOV (URSS): L'essentiel des travaux soviétiques sur la physique de la protection a été décrit dans les mémoires présentés à la Conférence. Cependant, après avoir entendu l'intéressant exposé de M. Blizard, je voudrais faire quelques commentaires sur deux points particuliers.

Le premier point, c'est qu'en utilisant un ensemble d'équations cinétiques conjuguées et la théorie des perturbations, nous avons imaginé une méthode pour le calcul de ce que nous appelons les fonctions d'efficacité pour différents matériaux, méthode qui nous permet, à l'aide d'approximations successives, de déterminer la distribution optimale des matériaux dans la protection. Un programme de calcul en vue de fournir des données de protection optimisées a été mis au point sur cette base. Nous pouvons ainsi trouver la composition de la protection qui aura le poids minimal, les dimensions minimales, et ainsi de suite, tout en satisfaisant à certaines conditions prescrites en ce qui concerne les doses à l'extérieur de la protection, le dégagement de chaleur et d'autres paramètres.

Le second point, c'est que je voudrais attirer l'attention sur la possibilité de calculer la distribution dans des milieux infinis des radiations venant d'une source ponctuelle directionnelle en résolvant une équation cinétique conjuguée qui suppose une source isotrope. Cette méthode est beaucoup plus facile que la solution directe de l'équation cinétique parce qu'elle comprend moins de variables indépendantes.

H. WIJKER (Pays-Bas): La procédure décrite par M. Orlov semble impliquer que l'on fait varier un paramètre après l'autre par petites étapes. Cette méthode n'est-elle pas très lente?

V. V. ORLOV (URSS): Tout dépend, assurément, de la complexité du problème particulier. Le programme de calcul est assez général pour permettre d'aborder des problèmes très variés, et donne généralement plus de détails qu'il n'en faut. Le temps nécessaire est de plusieurs heures.

P. S. MITTELMAN (Etats-Unis d'Amérique): La technique décrite par M. Blizard et moi-même est conçue à la fois pour synthétiser et pour optimiser une protection. Avec la technique de synthèse, il ne

s'agit pas de partir d'un ensemble de matériaux et de faire varier l'épaisseur de diverses couches pour obtenir un poids minimal, mais plutôt de choisir un ensemble de matériaux de protection et d'établir analytiquement le type de protection qui donnera le poids minimal.

Je pense qu'il serait très difficile de déterminer un ensemble de fonctions d'efficacité pour des matériaux en divers points d'une protection parce que l'efficacité d'un matériau donné dans une position donnée dépend étroitement des matériaux qui le précèdent et de ceux qui le suivent. Si le type de matériau et sa position dans la protection sont tous les deux considérés comme des variables, le calcul devient, à mon avis, presque impossible.

V. V. ORLOV (URSS): Je ne suis pas entièrement d'accord avec vous. Le programme dont j'ai parlé consiste en itérations successives, dont chacune ne comporte que de faibles changements dans la concentration des matériaux. On suppose que le changement est assez petit dans chaque cas pour conserver les conditions permettant d'appliquer la théorie des petites perturbations. On tient compte de façon complète de l'interdépendance dont vous avez parlé, c'est-à-dire l'influence des couches précédentes et suivantes, et ainsi de suite. Je pourrai, si vous le désirez, vous donner plus de détails après la séance.

Mémoire P/684 (présenté par M. Leimdörfer)

DISCUSSION

F. P. YOUELL (Royaume-Uni): Comme vous avez parlé du code anglais RASH B, je voudrais faire quelques commentaires. Le premier, c'est que votre mémoire est intéressant en ce qu'il donne des preuves supplémentaires de l'intérêt du traitement par diffusion-extraction pour la pénétration des neutrons dans les protections. Le code RASH B a été utilisé dans ce mémoire, mais le champ d'application du modèle a maintenant été étendu pour permettre de calculer le spectre de neutrons depuis 18 MeV jusqu'aux énergies thermiques dans divers types de protections à plusieurs couches. Cette dernière version du code est appelée RASH E; sa souplesse et sa précision sont décrites par M. J. Bútler dans le rapport AEEN-R/361 de l'UKAEA.

Nous pensons au Royaume-Uni que la précision obtenue maintenant pour des configurations simples des protections est suffisante, en particulier quand on la compare aux inexactitudes qu'introduit la simplification des géométries complexes que l'on rencontre dans les protections des grands réacteurs de puissance. Notre principal effort tend maintenant à étendre la méthode RASH au traitement de ces géométries complexes. Le mémoire P/175 décrit diverses extensions de la méthode type, destinées à certaines régions hétérogènes de la protection rencontrées à Bradwell. Le fait de considérer que le matériau de la protection est simplement étalé en une plaque homogène peut conduire à sous-estimer fortement les flux de neutrons, en particulier quand il s'agit de régions telles que les réflecteurs percés par les ensembles de canaux de combustibles dans les réacteurs à gaz. Les résultats donnés dans le mémoire P/175 nous permettent de conclure que le modèle de diffusion par âge, y compris des corrections de ligne visuelle ou des corrections analogues pour tenir compte des hétérogénéités, donne un instrument précieux dans la pratique pour les protections de réacteurs.

G. H. MINTON (Etats-Unis d'Amérique): Pourriez-vous faire quelques commentaires sur les avantages de la méthode des ordonnées discrètes, ou sur les méthodes d'harmoniques sphériques d'ordre supérieur, dans les calculs à plusieurs groupes pour des problèmes voisins de ceux qui sont discutés dans votre mémoire?

M. LEIMDÖRFER (Suède): Je crois que c'est surtout une question de temps de calcul à la machine. Par exemple, le programme NIOBE, qui fait partie du groupe que vous avez mentionné, est environ cent fois plus lent que notre méthode.

Mémoire P/657

DISCUSSION

G. H. MINTON (Etats-Unis d'Amérique): Vous dites que « les photons qui appartiennent à un groupe d'énergie et d'angle ne tomberont pas dans d'autres groupes au cours de la transmission à travers une couche élémentaire ». Ceci est-il une caractéristique du programme de Monte-Carlo utilisé pour préparer la matrice de réponse?

I. KATAOKA (Japon): Non, ce n'est pas une caractéristique du programme de Monte-Carlo. Il s'agit uniquement d'une conséquence de la procédure d'interpolation des épaisseurs que l'on utilise pour synthétiser les matrices de réponse pour les couches élémentaires. Pour rendre cette réponse plus claire, je devrais ajouter que les calculs consistent pratiquement en deux parties séparées. Il y a d'abord la préparation des matrices de réponse pour les couches élémentaires de divers matériaux; l'utilisateur de la méthode n'a besoin que d'une table de matrices de réponse. Il y a ensuite le calcul pratique des photons transmis (ou réfléchis) à travers n'importe quelle barrière stratifiée voulue. La synthèse des matrices de réponse et le calcul de l'interpolation d'épaisseur sont faits à ce stade du calcul, que l'on peut coder pour tout calculateur numérique convenant à l'utilisateur de cette méthode. L'auteur a préparé un code pour un calculateur NEAC-2206.

H. WIJKER (Pays-Bas): Comme les matrices ne contiennent que deux paramètres, l'énergie et le cosinus de l'angle, on peut en conclure que la procédure que vous décrivez ne s'applique qu'à des sources homogènes dans un plan infini. Dans les figures 4 et 5 les résultats sont comparés à des mesures réalisées avec une source de cobalt 60. Je

me demande si la source utilisée dans ces expériences était une source plane homogène de dimensions raisonnables.

I. Катаока (Japon): Il n'y a pas de lien direct entre le calcul de Monte-Carlo et la disposition pratique de la source et des détecteurs dans l'expérience. Les résultats définitifs ont été convertis en valeurs pour une géométrie de couche obtenues à partir des mesures expérimentales, et ce sont ces résultats que donne le mémoire.

Протокол заседания 3.5

Управление реакторами и защита

Председатель: Э. П. Близард (США)

Доклад P/631 (представил П. Кованиц)

ДИСКУССИЯ

М. А. ШУЛЬЦ (США): Я хочу сказать несколько слов об оборудовании с подвижными детекторами, используемом в США. Как Вы, вероятно, знаете, г-н Ганауэр в докладе P/229 * описал полностью транзистированную систему с подвижными детекторами, испытания которой в настоящее время производятся на исследовательском реакторе Окриджской национальной лаборатории. После завершения этих испытаний система будет применяться на реакторе HIFIR. Указанная система аналогична Вашей системе и системе, описанной в докладе P/80* г-ном Фюре. Однако она отличается от данных систем своими возможностями в измерении периода реактора. Видно, что Ваша механическая система обеспечивает измерение периодов, не превышающих 2 *сек*. Я полагаю, что можно создать следящую систему, позволяющую измерять периоды, равные 0,1 *сек*. Однако Ганауэр и его коллеги из Окриджа считают, что время срабатывания систем защиты по периоду экспериментальных реакторов должно составлять несколько миллисекунд. В связи с этим они в дополнение к обычной схеме измерения периода используют для определения скорости детекторов электронную схему с очень большим быстродействием. Эта схема позволяет быстро получать информацию о периоде, в то время как положение детектора дает информацию об уровне мощности.

Каково Ваше мнение о данном решении задачи? Считаете ли Вы, что быстрая защита по периоду является необходимой? Кроме того, я хотел бы узнать, используете ли Вы выключение по положению детектора для быстрого выключения реактора вследствие превышения уровня мощности или Вы использовали для этой цели Ваше оборудование со стационарными датчиками.

П. КОВАНИЦ (ЧССР): Мы согласны, что можно построить систему с подвижными детекторами, которая будет измерять периоды реактора, более короткие, чем 2 *сек*, указанные в докладе. Максимальная скорость детектора выбирается из имеющегося диапазона изменения периода. Хочу подчеркнуть, что эта максимальная скорость не определяет времени возникновения сигнала быстрого выключения реактора по периоду, поскольку последний связан не со скоростью движения детекторов, а непосредственно с их выходным сигналом. В нормальных условиях величина этого сигнала изменяется в узких пределах при любой заданной мощности реактора. Сигнал может отличаться от предельных значений, соответствующих нормальной работе, только в случае аварийного периода или при неисправности следящей системы. В контур сигнала быстрой остановки реактора входит электронное оборудование, быстродействие которого равно быстродействию оборудования систем, использующих стационарные детекторы. Следовательно, мы можем иметь время срабатывания сигнала быстрого выключения реактора по периоду, равное 1 *мсек*, при медленном механизме перемещения детекторов.

Мы считаем, что введение дополнительного оборудования, аналогичного предложенному г-ном Ганауэром в докладе P/229, будет полезным. Однако сомнительно, что оно может иметь существенное значение в обеспечении быстродействующей защиты по периоду. Данная защита может быть обеспечена в имеющихся системах, использующих подвижные детекторы. В нашем реакторе ВВР-С система с подвижными детекторами выдает сигналы аварии настолько быстро, что приходится увеличивать

* Настоящее издание, т. 8.

время срабатывания до 0,1 *сек*, чтобы дать возможность оператору осуществить ручное регулирование регулирующих стержней.

Отвечу теперь на Ваш второй вопрос.

Да, мы используем выключения по положению детектора для указанной цели. Кроме того, часть старой системы аварийной защиты со стационарными детекторами применяется в качестве резервной.

Ж. ФЮРЕ (Франция): Какова максимальная скорость движения детекторов? Поддерживается ли период в процессе пуска в определенных пределах и влечет ли это за собой остановку или опускание регулирующих стержней?

П. КОВАНИЦ (ЧССР): Максимальная скорость движения детектора приблизительно равна 4 *см/сек*. Если пуск реактора осуществляется автоматической системой, то скорость детекторов системы регулирования остается постоянной. Мощность реактора в период пуска мало отличается от указанной на калибровочной кривой (рис. 2 доклада).

Если измеренный период реактора отличается от установленного значения периода, автоматическое оборудование передает функции регулирования реактора трем системам с подвижными детекторами, которые до момента достижения установленного значения работают как измерительные системы. После этого детекторы останавливаются, а система автоматически снижает реактивность до нуля и поддерживает мощность на постоянном уровне, равном достигнутому значению. Дальнейшее изменение мощности может производиться только по желанию оператора.

Мы не прибегали к выключению (остановка при помощи регулирующих стержней), поскольку при этом реактор может быть остановлен в подкритическом состоянии.

Ж. ВЕЙЛ (Франция): Наблюдали ли Вы изменение абсолютной величины мощности в зависимости от температуры воды или как следствие присутствия экспериментальных устройств?

П. КОВАНИЦ (ЧССР): Насколько мы могли заметить, калибровка подвижных детекторов не зависит от температуры воды (во всех случаях температура воды в реакторе ВВР-С изменяется в узком диапазоне температур). Вначале мы испытывали некоторые затруднения, связанные с присутствием экспериментальных устройств в непосредственном соседстве с каналами детекторов, в частности, это относится к каналам, не заполненным водой. Впоследствии мы ввели несколько дополнительных очень простых правил эксплуатации, которые позволили нам устранить эти затруднения.

Ю. ЭЛЬ-МЕШАД (ОАР): Насколько я понял, распределение нейтронного потока отличается от экспоненциального распределения. Нашли ли Вы практический способ решения этой задачи?

П. КОВАНИЦ (ЧССР): Во время проектирования установки мы предусмотрели ряд мероприятий для уточнения этих отклонений, но впоследствии на основании практического опыта убедились, что они не создают каких-либо затруднений.

Б. Г. ДУБОВСКИЙ (СССР): Я не сторонник использования подвижных детекторов в системах регулирования и аварийной защиты энергонапряженных высокотемпературных реакторов, к которым относятся практически все энергетические ядерные реакторы. Надежность их, по-моему, недостаточна. Передвижение детекторов создает дополнительный источник неопределенности в работе этих исключительно важных систем, а преимущества, вытекающие из их использования, не так уж велики. В СССР в 1950 году я использовал метод пуска реактора из подкритического состояния и доведения его мощности до заданной величины, обеспечивающий высокую безопасность*. Метод основан на равномерном увеличении реактивности. Конечно, при этом существенно наличие в реакторе небольшого количества (порядка 10 *кг*) бериллия или окиси бериллия, используемых для увеличения нейтронного фона, и применение регулирующего оборудования стандартной чувствительности. Я считаю, что оптимальной является скорость увеличения реактивности, равная 0,2% за 3 *мин*, то есть скачкообразное увеличение реактивности на 0,2% и 3-минутная выдержка.

Все это, конечно, не исключает использования подвижных камер деления для регулирования реактора в подкритическом состоянии.

Доклад P/80 (представил Ж. Фюре)

ДИСКУССИЯ

К. ВАГНЕР (ЧССР): Описанная в Вашем докладе система с подвижными детекторами делится на две группы, первая из которых является измеряющей следящей системой, а вторая — регулирующей. Я хотел бы знать, спроектирована ли система реактора OSIRIS тремя подвижными детекторами исключительно для целей регулирования или Вы предполагаете использовать ее также как измерительную систему?

В связи с последним вопросом хотелось бы обратить внимание на то, что, насколько я понял, подвижные детекторы на реакторах TRITON и MELUSINE используются только в системах регулирования. Накопленный нами опыт показал, что использование подвижных детекторов в системах измерения практически полностью оправдано. Поэтому хотелось бы услышать, почему в Ваших измерительных системах не применяются подвижные детекторы?

* Атомная энергия (1957).

Ж. ФЮРЕ (Франция): Когда реактор OSIRIS впервые будет пущен в эксплуатацию, три комплекта электронного оборудования, связанного с тремя подвижными детекторами, не смогут обеспечить проведение автоматического пуска. Пуск реактора будет осуществлен путем ручного регулирования регулирующими стержнями, а детекторы будут перемещаться независимо друг от друга в соответствии с программой, описанной в докладе. Возможность автоматического пуска будет рассматриваться после проведения на установке необходимых экспериментов.

Теперь отвечу на Ваш второй вопрос. Система с подвижными детекторами использовалась на реакторе TRITON с 1962 года, хотя пуск реактора еще осуществляется вручную, путем извлечения регулирующих стержней.

Б. Г. ДУБОВСКИЙ (СССР): Я хочу обратить Ваше внимание на возможность использования урановых термобатарей в качестве детекторов нейтронного потока систем регулирования и аварийной защиты. Батареи, изготовленные из термоэлементов с покрытием из урана, хорошо работают при температурах, превышающих 500° С. Благодаря свойственному им малому омическому сопротивлению отпадают затруднения, связанные с электрическими утечками по изоляции кабелей питания. В хорошо изготовленных термобатареях тепловая инерция очень мала. Эксперименты, которые я провел в 1954 году на реакторе Первой атомной электростанции, дали хорошие результаты *.

Доклад P/647

По этому докладу дискуссии не было.

Доклад P/273 (зачитывается только название)

ДИСКУССИЯ

А. Г. ФИЛИППОВ (СССР): Я хочу спросить у г-на Шульца, измерялась ли реактивность в процессе пуска и, если да, то каким образом.

М. А. ШУЛЬЦ (США): Нет, для измерения реактивности цифровые системы не используются. В дальнейшем они могут быть использованы для этой цели после проведения простой замены аналоговых схем на цифровые.

Доклад P/375 (представил В. А. Кузнецов)

ДИСКУССИЯ

Дж. ТАЙ (США): Г-н Кузнецов упомянул два интересных метода измерения подкритической или отрицательной реактивности, а именно: метод обратного счета и метод наращивания высоты топлива в активной зоне. Существуют также другие методы, которые могут быть использованы для той же цели: например, метод, основанный на замене независимых друг от друга регулирующих стержней, метод, основанный на быстром внесении регулирующего стержня, метод обмена с корректировочными химическими поглотителями и метод, основанный на анализе случайных флуктуаций потока нейтронов. Знает ли г-н Кузнецов еще какие-либо менее известные в настоящее время методы измерения подкритической реактивности?

В. А. КУЗНЕЦОВ (СССР): За исключением хорошо известного метода измерения отрицательных реактивностей с помощью импульсного источника нейтронов, я не могу добавить ничего нового к экспериментальным методам, перечисленным г-ном ТАЙ.

Доклад P/179 (представил Дж. Браун)

ДИСКУССИЯ

А. Г. ФИЛИППОВ (СССР): Какова стабильность показаний термопар? Использовали ли Вы какие-либо другие датчики для тех же целей?

Дж. БРАУН (Соединенное Королевство): Результаты отдельных измерений температуры тепловыделяющих элементов отличались друг от друга не более чем на ±3° С, поэтому мы считали их достаточно надежными. С момента начала работы на полной мощности электростанций в Брадуэлле и Беркли имело место незначительное число нарушений работы термопар. В связи с этим мы полностью положились на надежность наших измерений температуры и использовали их для обеспечения защиты от повреждений рассматриваемого типа (повреждения секторного стержня). В докладе мы объясняем, почему нельзя использовать никакой другой параметр. Главным образом это связано с тем, что пока еще у нас нет детекторов нейтронного потока, обеспечивающих получение сигналов, предупреждающих об аварии.

А. Г. ФИЛИППОВ (СССР): Являются ли сектора взаимосвязанными? Другими словами, перемещаются ли регулирующие стержни в каждом секторе независимо, по своим сигналам, или выбираются сектора с максимальным лапласианом?

Дж. БРАУН (Соединенное Королевство): Каждый сектор работал независимо, но, как правило, устанавливалось общее требование к температуре. Поэтому стабилизирующий стержень принимал положение, которое обеспечивало требуемую температуру газа на выходе из сектора. Если в процессе эксплуатации будет обнаружено, что стабилизирующий стержень

* Б. Г. Дубовский, В. Я. Китаев. О применении малоинерционной термобатареи для измерения больших нейтронных потоков в ядерных реакторах, Атомная энергия, Приложение 1, 128 (1958).

отклонился от положения, соответствующего погружению в реактор, на 50%, то имеющиеся «уравновешивающие» стержни (с ручным управлением) позволят возвратить его в старое положение, в котором он наиболее эффективен. Относительное положение стабилизирующих стержней для случая, когда один из них выходит из активной зоны вследствие повреждения, показано на рис. 12 доклада; поскольку температура в смежных секторах при этом повышается, стабилизирующие стержни этих секторов проникают глубже в активную зону, пытаясь сохранить температуру газа на заданном уровне. Стабилизирующие стержни реактора, таким образом, в определенном смысле «связаны» между собой.

П. БАШЕР (Франция): Наблюдали ли Вы существование пространственной неустойчивости у действующих в настоящее время атомных электростанций? Действительно ли система регулирования вступила в строй? И наконец, не могли бы Вы сравнить работу этой системы с ее расчетными параметрами?

Дж. БРАУН (Соединенное Королевство): В Беркли наблюдалось нечто похожее на пространственную неустойчивость. Поток возмущался, а полученные в результате этого колебания не расходились, а очень медленно затухали; температурный коэффициент замедлителя реактора в Беркли при этом был равен приблизительно 10 *мнайл*/° С. Мы полагаем, что в описываемый момент находились на пороге появления неустойчивости.

В любой момент секторная система автоматически может быть запущена в эксплуатацию. Модернизация системы аварийной защиты, о которой я упоминал в докладе, в настоящее время завершена, кроме того, закончены испытания, связанные с введением системы в эксплуатацию. Реактор в Беркли был выключен после моего отъезда в Женеву. Он должен был начать работать вновь в начале сентября при 100%-ном использовании описанной системы.

На рис. 18 и 19 сравниваются результаты эксперимента в Беркли с соответствующими расчетными данными. Увеличение температуры, полученное экспериментально, находится в очень хорошем соответствии с теорией.

П. Б. БРЭНСОН (Соединенное Королевство): В этой связи мне хотелось бы сделать два коротких замечания по вопросам, которые более подробно изложены в докладе P/180. Первое касается методов, применявшихся при анализе переходных условий в реакторах с газовым теплоносителем. Мы слышали о проведенных в последнее время разработках больших, сложных трехмерных моделей поведения реакторов в переходном режиме; однако даже при использовании самых быстродействующих вычислительных машин, имеющихся в настоящее время, эти трехмерные модели потребуют большого времени на проведение вычислений, а также затраты больших усилий при подготовке программы и интерпретации режима работы. Эти методы сыграют большую роль в детальном изучении условий эксплуатации и безопасности реактора, однако для целей проектирования еще широко будет использоваться расчет, основанный на применении одно- и двухмерных и даже точечных моделей. Наш опыт сравнения реальных характеристик реактора и характеристик, полученных в результате вычислений по трехмерной модели, показал, что самые простые методы обеспечивают хорошую базу для проведения большинства практических работ.

Второе замечание касается необходимости рассмотрения регулирующих стержней, находящихся внутри реактора, например пространственных регулирующих и компенсирующих стержней, в качестве неотъемлемой части устройства для полного выравнивания мощности. Наиболее легко это достигается путем использования подвижных поглотителей в обычной решетке с управляющими устройствами. Такая система уже применялась, например, на хантерстонском реакторе. Там было обнаружено, что с помощью дифференцированного ввода поглотителей можно получить очень хорошие формфакторы, наряду с удовлетворительным регулированием, и в то же время достичь максимальной гибкости в работе.

Доклад P/260 (представил Э. П. Близард)

ДИСКУССИЯ

В. В. ОРЛОВ (СССР): Бóльшая часть работ, проведенных в Советском Союзе по физике защиты ядерных реакторов, была описана в докладах, представленных на настоящей конференции. Однако, прослушав интересный обзор, сделанный д-ром Близардом, мне хотелось бы остановиться на двух вопросах.

Во-первых, применяя аппарат сопряженных кинетических уравнений и теорию возмущений, мы создали метод расчета так называемых функций эффективности материалов — метод, позволяющий нам путем последовательных приближений определить оптимальное распределение материалов в защите. На его основе была составлена программа для вычислительной машины, рассчитанная на получение в конечном итоге оптимальных данных по защите. Таким образом, мы можем найти состав защиты, которая будет иметь минимальный вес, размеры и т. д. и в то же время удовлетворять определенным условиям в отношении доз излучения за ее пределами, в отношении выделения тепла и других параметров.

Во-вторых, мне хотелось бы обратить Ваше внимание на возможность вычисления распределения в бесконечной среде излучений от на-

правленного точечного источника путем решения сопряженного кинетического уравнения, постулирующего изотропный источник. Этот метод значительно проще, чем прямое решение кинетического уравнения, поскольку он включает меньшее число независимых переменных.

Г. ВИЙКЕР (Нидерланды): Процедура, описанная г-ном Орловым, по-видимому, включает последовательное изменение одного параметра за другим небольшими ступенями. Не требует ли все это слишком много времени?

В. В. ОРЛОВ (СССР): Многое зависит от сложности поставленных задач. Программа вычислительной машины достаточно универсальна и позволяет решать множество задач, как правило, более подробно, чем это необходимо. На проведение расчетов обычно требуется несколько часов.

П. С. МИТТЕЛМАН (США): Метод, описанный д-ром Близардом и мною, позволяет синтезировать и оптимизировать защиту. При использовании метода синтеза расчет начинается не с выбора группы материалов и изменения толщины различных слоев до тех пор, пока не будет получен минимальный вес, а с выбора ряда материалов защиты и аналитического определения конструкции защиты, которая будет иметь минимальный вес.

Я думаю, что очень трудно получить аппарат функций эффективности для материалов различных точек защиты, так как эффективность данного материала в данном положении сильно зависит от материалов, которые предшествуют ему и идут за ним. Если тип материала и его положение рассматриваются как переменные, то расчет становится, по моему мнению, почти невозможным.

В. В. ОРЛОВ (СССР): Я с Вами не совсем согласен. Программа, о которой я говорил, состоит из последовательных итераций, каждая из которых несет небольшие изменения в концентрации материалов. Допускается, что изменение достаточно мало́ для каждого случая, так что сохраняются условия, при которых может быть применена теория малых возмущений. Взаимная зависимость, о которой Вы говорили, — влияние предшествующих и последующих слоев и т. д. — полностью учитывается. Более подробное доказательство я смогу привести после совещания.

Доклад P/684 (представил М. Леймдорфер)

ДИСКУССИЯ

Ф. П. ЙОУЭЛЛ (Соединенное Королевство): Поскольку Вы упомянули программу RASH B, принятую в Соединенном Королевстве, я должен сказать несколько слов. Во-первых, Ваш доклад интересен тем, что он со всей очевидностью показал ценность приближения диффузионного решения для расчета ослабления нейтронов в защите. В данном докладе использована программа RASH B, но созданная в настоящее время для расчета многослойных защит различного типа разновидность этой программы позволяет проводить оценки для нейтронного спектра от 18 *Мэв* до тепловых энергий. Эта программа получила название RASH E. Ее универсальность и точность показаны в отчете AEEW-R/361 Управления по атомной энергии Соединенного Королевства г-ном Батлером.

В Соединенном Королевстве мы считаем, что полученная в настоящее время точность для случая простой конфигурации защиты является удовлетворительной, особенно если сравнивать ее с погрешностями, обусловленными упрощением сложных геометрий защит больших энергетических реакторов. Нашей задачей в настоящее время является расширение применения RASH-метода на эти сложные геометрии. В докладе P/175 описаны различные способы применения стандартного метода при проектировании некоторых частей гетерогенной защиты реакторов в Брадуэлле. Упрощающее предположение о том, что материал защиты является гомогенным, ведет к серьезной переоценке нейтронного потока, особенно в такой области, как отражатели, через которые проходит ряд топливных каналов реакторов с газовым охлаждением. Результаты, приведенные в докладе P/175, позволяют сделать заключение, что модель возрастной диффузии с поправками на гетерогенность дает возможность получить хороший метод расчета защит реактора.

Г. Г. МИНТОН (США): Что Вы можете сказать о пригодности метода дискретных ординат или метода сферических гармоник высокого порядка, используемых в многогрупповых вычислениях, для решения задач, аналогичных указанным в Вашем докладе?

М. ЛЕЙМДОРФЕР (Швеция): Эти методы хуже главным образом тем, что требуют больше времени на проведение расчетов с использованием вычислительной машины. Так, программа NIOBS, которая применяется с указанными Вами методами, приблизительно в 100 раз медленнее, чем наш метод.

Доклад P/657 (представил И. Катаока)

ДИСКУССИЯ

Г. Г. МИНТОН (США): Вы утверждаете, что «фотоны, относящиеся к определенной группе энергии и углу, не будут попадать в другие группы во время прохождения через элементарную пластину». Является ли это особенностью метода Монте-Карло, используемого при разработке матрицы чувствительности?

И. КАТАОКА (Япония): Нет, это не является особенностью метода Монте-Карло.

Сказанное относится только к процедуре интерполяции толщины, применяемой при синтезировании матриц чувствительности для элементарных пластин. Для того чтобы ответ был более ясным, я должен добавить, что вычисления в целом рассматриваются как состоящие из двух отдельных частей. Во-первых, идет подготовка матриц чувствительности для элементарных пластин из различных материалов. Использующему этот метод требуется только таблица матриц чувствительности. Во-вторых, имеется расчет фотонов, переданных (или отраженных) через любые многослойные барьеры. Синтез матриц чувствительности и вычисление интерполяции толщины выполняются на стадии вычисления, которая может быть закодирована для любой цифровой вычислительной машины, удобной для использующего этот метод. Автор приготовил программу для вычислительной машины NEAS-2206.

Г. ВИЙКЕР (Нидерланды): Так как матрицы содержат только два параметра — энергию и косинус угла, можно сделать вывод, что процедура, которую Вы описали, хорошо подходит только к бесконечно плоским однородным источникам. На рис. 4 и 5 результаты сравниваются с измерениями, сделанными с источником Co^{60}. Мне бы хотелось знать, действительно ли источник, использованный в этих экспериментах, представлял собой однородный плоский источник разумных размеров.

И. КАТАОКА (Япония): Нет, прямой связи между вычислениями Монте-Карло и действительным устройством источника и детекторов в эксперименте не имеется. Окончательные результаты были преобразованы к значениям геометрии пластины, полученной из экспериментальных измерений. Именно на эти результаты делались ссылки в докладе.

Acta de la Sesión 3.5

Control y blindaje de reactores

Presidente: E. P. Blizard (Estados Unidos de América)

Documento P/631 (presentado por P. Kovanic)

DISCUSIÓN

M. A. SCHULTZ (Estados Unidos de América): Me gustaría decir unas palabras acerca de unos sistemas de detectores móviles similares, construidos en los Estados Unidos. Ya sabrá Vd. que el Dr. S. Hanauer describe, en la memoria P/229 *, el sistema de detector móvil totalmente transistorizado que está en pruebas en el reactor ORR para su utilización futura en el reactor HIFIR. Este sistema es similar al suyo y al descrito por el Sr. Furet en la memoria P/80, excepto en el aspecto de su capacidad de medida de período. Ya veo que su sistema mecánico es capaz de seguir períodos de hasta 2 s. Creo que debería ser posible construir un servosistema que siguiese períodos de 0,1 s. Sin embargo el Dr. Hanauer y sus colegas de Oak Ridge creen que en los reactores experimentales la protección por medida del período debería extenderse hasta un tiempo de respuesta de unos pocos milisegundos. Por lo tanto han añadido un circuito electrónico de « velocidad de cambio » muy rápido a continuación del detector, para suplementar el circuito normal de período. Para medir períodos rápidos emplean este circuito, y la posición del detector para medir el nivel.

¿Cuál es su opinión acerca de esta solución? ¿Cree Vd. que podría ser necesaria una protección contra períodos rápidos? En segundo lugar, me gustaría saber si Vds. emplean señales procedentes de la posición del detector como indicación de potencia superior a la normal para originar la parada de emergencia o si confían esta misión a su instrumentación fija.

P. KOVANIC (Checoslovaquia): Estamos de acuerdo en que debería ser posible construir un sistema con detector móvil que *midiese* períodos más cortos que los 2 s indicados en nuestra memoria. La velocidad máxima del detector se escogió de manera que correspondiera al intervalo de medida necesario. Se debe recalcar que esta velocidad máxima *no* determina el tiempo de respuesta de la señal de parada de emergencia por período, la cual no está relacionada con la velocidad de movimiento del detector sino directamente con la señal que proporciona. En condiciones normales la magnitud de esta señal permanece dentro de estrechos límites para cualquier potencia del reactor. Puede salir fuera de estos límites solamente en un período de emergencia o cuando el sistema de movimiento sea defectuoso. Los circuitos que proporcionan la señal de parada de emergencia están formados por componentes

* Véase estas Actas, Vol. 8.

electrónicos que actúan con la misma rapidez que cualquier sistema que emplee detectores estacionarios. Podemos por lo tanto obtener un tiempo de respuesta de 1 ms en la señal de apagado de emergencia por período aún cuando los mecanismos de movimiento del detector actúen lentamente.

Creemos que la introducción de equipo suplementario tal como propone el Dr. Hanauer en la memoria P/229 sería útil, pero no creemos sea esencial para la protección de período rápido; esta protección puede asegurarse perfectamente en sistemas que empleen detectores móviles. En nuestro reactor VVR-S los sistemas de detector móvil proporcionaban las señales de disparo de emergencia con tal rapidez que fue necesario adaptarlas a un tiempo de respuesta de O,1 s para dar tiempo al operador para el ajuste manual de las barras de control.

La respuesta a su segunda pregunta es afirmativa; empleamos señales de disparo originados por la posición del detector con ese propósito. Además, hemos mantenido hasta el momento parte del antiguo sistema de emergencia, que emplea detectores estacionarios como una especie de reserva.

J. FURET (Francia): ¿Cuál es la velocidad máxima del detector móvil? ¿Se mantiene un período límite durante la puesta en marcha e implica esto la parada o la caída de las barras de control?

P. KOVANIC (Checoslovaquia): La velocidad máxima del detector móvil es aproximadamente 4 cm/s. Cuando se pone en marcha el reactor mediante el sistema automático la velocidad del detector permanece constante. El período durante la puesta en en marcha varió ligeramente con respecto a la curva de calibración (ver figura 2 en la memoria).

Cuando el período real del reactor difiere del período prescrito, el equipo automático transfiere el control del reactor a otro de los tres sistemas de detector móvil que hasta este momento había funcionado como un sistema de medida. El detector de este nuevo sistema se para y el sistema lleva la reactividad automáticamente a cero al mismo tiempo que mantiene la potencia constante al nivel que había alcanzado. No se realizan cambios ulteriores de potencia hasta que el operador da su consentimiento.

No recurrimos a parar las barras de control porque esto puede dar como resultado que se pare el reactor en estado supercrítico.

J. WEILL (Francia): ¿Han observado Vds. que existan variaciones en la indicación absoluta de potencia en función de la temperatura del agua, o como resultado de la presencia de dispositivos experimentales?

P. KOVANIC (Checoslovaquia): No hemos observado que la calibración de los detectores móviles dependa de la temperatura del agua, y en cualquier caso, la temperatura del agua en el reactor VVR-S varía sólo dentro de un margen muy pequeño. Al principio experimentamos algunas dificultades a causa de la presencia de aparatos experimentales en la vecindad de los canales de los detectores, especialmente en el caso de tubos que no están llenos de agua. Desde entonces hemos seguido unas cuantas normas de operación adicionales, muy sencillas, y no hemos tenido más dificultades.

Y. EL-MESHAD (República Arabe Unida): La distribución de flujo de neutrones se desvía a veces de una distribución exponencial. ¿Han encontrado alguna manera práctica de resolver esta dificultad?

P. KOVANIC (Checoslovaquia): Mientras se diseñaba la instalación se tomaron varias medidas para corregir esas desviaciones, pero, posteriormente, se encontró que, desde un punto de vista práctico, no presentaban problemas.

B. G. DUBOVSKY (URSS): Me parece que en los reactores de alta temperatura y gran potencia específica (una categoría que comprende prácticamente todos los reactores de potencia) no es aconsejable el empleo de detectores móviles en los sistemas de control y seguridad. De hecho los detectores móviles crean una fuente adicional de incertidumbre en el funcionamiento de esos sistemas de importancia crucial; además, las ventajas que se derivan de su empleo no son en realidad tan grandes. En la Unión Soviética, en 1950, empleé un método para llevar un reactor desde el estado subcrítico a un nivel de potencia controlado que garantiza una seguridad perfecta*. El método consiste esencialmente en fijar una velocidad específica de incremento de reactividad. Depende, por supuesto, de tener en el reactor una pequeña cantidad de berilio u óxido de berilio (aproximadamente 10 kg) para aumentar el fondo de neutrones, y del empleo de un equipo de control de sensibilidad normal. He encontrado que la velocidad óptima es 0,2% durante un período de tres minutos (en forma de un incremento en escalón seguido por una pausa de tres minutos).

Todo esto, por supuesto, sin detrimento de la utilidad de las cámaras de fisión móviles como un medio de controlar un reactor en el estado subcrítico.

Documento P/80 (presentado por J. Furet)

DISCUSIÓN

K. WAGNER (Checoslovaquia): En su memoria los sistemas que emplean detectores móviles se dividen en dos grupos, el primero consta de servosistemas de medida y el segundo de sistemas de control. Me gustaría saber si los tres sistemas de detector móvil del reactor OSIRIS están diseñados solamente como sistemas de control o si se trata de usarlos también como sistemas de medida.

En relación con esto, creo que los detectores móviles en los reactores TRITON y MÉLUSINE se emplean únicamente como sistemas de control. Nuestra experiencia indica que su utilización como

* Atomnaya Energia (1957).

sistemas de medida es totalmente practicable y me gustaría saber por qué no se han usado para este fin.

J. FURET (Francia): Cuando se ponga en funcionamiento por primera vez el OSIRIS, los tres conjuntos electrónicos asociados a los tres detectores móviles no serán empleados para proporcionar arranque automático. El reactor se pondrá en marcha por operación manual de las barras de control y los detectores se moverán individualmente de acuerdo con el programa descrito en la memoria. Se pensará en la puesta en marcha automática después de que se hayan hecho experimentos con la instalación.

En contestación a su segunda pregunta, el sistema de detector móvil se ha empleado en el reactor TRITON desde 1962, aunque el arranque se realiza todavía por retirada manual de las barras de control. Este equipo se clasifica por lo tanto en el primero de los dos grupos que he mencionado.

B. G. DUBOVSKY (URSS): Me gustaría llamar su atención sobre la posibilidad de emplear termopilas de uranio como detectores de flujo de neutrones en los sistemas de control y seguridad. Las baterías de termopares recubiertos de uranio funcionan bien a temperaturas por encima de 500 °C y, a causa de su baja resistencia eléctrica, no se presentan problemas de fugas eléctricas a través del aislante de los cables de alimentación. Si las termopilas están bien contruidas el retardo térmico puede hacerse suficientemente corto. Los experimentos que llevé a cabo en 1954 en el reactor de la primera central atómica dieron resultados satisfactorios *.

Documento P/647

No hubo discusión de esta memoria.

Documento P/273 (solamente se leyó el título)

DISCUSIÓN

A. G. FILIPPOV (URSS): Me gustaría preguntar al Sr. Schultz si se mide la reactividad durante la puesta en marcha y, si es así, cómo se hace.

M. A. SCHULTZ (Estados Unidos de América): No, no medimos la reactividad en ninguno de los sistemas digitales usados hasta la fecha. En el trabajo realizado hasta ahora se sustituye simplemente la cuenta analógica directa por una cuenta digital.

Documento P/375 (presentado por V. A. Kuznetsov)

DISCUSIÓN

J. A. THIE (Estados Unidos de América): El Sr. Kuznetsov ha mencionado dos técnicas excelentes para medir reactividades subcríticas o negativas, a saber, el método de la recíproca de la velocidad de cuenta y el de la adición de combustible. Hay otros métodos bien conocidos, tales como el intercambio de barras de control que no se interfieran, la inserción rápida de una barra de control, el intercambio con absorbentes disueltos para compensación y el análisis de las fluctuaciones al azar de los neutrones. Si hay otros métodos menos familiares de medida de reactividades subcríticas sería interesante que el Sr. Kuznetsov nos dijese algo acerca de ellos.

V. A. KUZNETSOV (URSS): Aparte de los métodos, ampliamente conocidos, de medida de reactividades negativas por medio de una fuente pulsante de neutrones, no puedo añadir nada nuevo a la lista de técnicas experimentales enumeradas por el Dr. Thie.

Documento P/179 (presentado por J. Brown)

DISCUSIÓN

A. G. FILIPPOV (URSS): ¿Qué crédito merecen las lecturas obtenidas de los termopares? ¿Emplean Vds. algún otro sistema de señales con el mismo propósito?

J. BROWN (Reino Unido): Las medidas de temperatura del elemento combustible son reproducibles hasta $\pm$ 3 °C y nos parece que merecen toda confianza. Se han observado muy pocas averías desde que Bradwell y Berkeley empezaron a funcionar en carga. Nosotros concedemos plena confianza a estas medidas de temperatura como protección contra el tipo de avería que se discute (avería de una barra de un sector). En la memoria explicamos que, de hecho, no resulta posible utilizar ningún otro parámetro. No disponemos de detectores de flujo internos al reactor de los que podamos derivar señales de protección.

A. G. FILIPPOV (URSS): ¿Están los sectores relacionados entre sí? En otras palabras, ¿se mueven independientemente las barras de control de cada sector y emiten señales independientes o han sido seleccionados ciertos sectores con laplaciana máxima?

J. BROWN (Reino Unido): Cada sector opera independientemente de los que están contiguos, pero se utiliza una señal común como demanda de temperatura. La barra estabilizadora tomará así una posición que dé como resultado la temperatura requerida de salida del gas del sector. Si, a largo plazo, resultara que una barra estabilizadora derivase hasta más de un 50% de inserción en el reactor, existen barras de ajuste fino que pueden ser utilizadas (con control manual) para volver la barra estabilizadora a un 50% de inserción aproximadamente, que es la posición en la cual resulta más eficaz. Las posiciones relativas de las barras estabilizadoras, si una de ellas se sale fuera del núcleo en caso de avería en el reactor, aparecen representadas en la figura 12 de la memoria; cuanto más crece la temperatura en los sectores adyacentes, tanto más

* Dubovsky, B. G., and Kitaev, V. Y., *O primenenii maloinertsionnoy termobatarei dlya izmerenia bolshikh neitronnyh potokov v yadernykh reaktorakh*, Atomnaya Energia, Supplement 1, p. 128 (1958).

penetran las barras estabilizadoras adyacentes en el núcleo, tratando de mantener la temperatura del gas en el valor prefijado. Las barras estabilizadoras resultan así, en cierto modo, « acopladas » a través del reactor.

P. BACHER (Francia): ¿Han observado Vds. algún tipo de inestabilidad espacial en las centrales que actualmente están funcionando? ¿Ha entrado ya en servicio este sistema de control? Por último, ¿han podido Vds. comparar la forma de funcionar este sistema con las predicciones teóricas?

J. BROWN (Reino Unido): En Berkeley se ha observado algo parecido a una inestabilidad espacial. Al ser perturbado el flujo, las oscilaciones resultantes, aunque no divergentes, se amortiguaron muy lentamente; el reactor de Berkeley tiene un coeficiente de temperatura del moderador de casi 10 mN/°C. Por eso creemos que nos encontramos en el umbral de las inestabilidades.

Se espera que el sistema de sectores sea puesto en funcionamiento, con control automático, de un momento a otro. Todas las modificaciones en el sistema de seguridad mencionadas en mi presentación oral han sido ya llevadas a cabo y han finalizado las pruebas de puesta en servicio. El reactor de Berkeley estaba parado cuando salí para Ginebra y se había fijado la nueva puesta en marcha, con todo el sistema en funcionamiento, para principios de septiembre.

Las figuras 18 y 19 muestran comparaciones entre los resultados de un experimento de puesta en servicio y las predicciones teóricas utilizadas para este trabajo en Berkeley. Los incrementos de temperatura medidos concuerdan muy bien con la teoría.

P. B. BRANSON (Reino Unido): En relación con esto me gustaría hacer dos comentarios breves sobre temas tratados con más profundidad en el trabajo P/180. El primero está relacionado con los métodos empleados en el análisis de transitorios, especialmente para reactores refrigerados por gas. Tenemos noticias del desarrollo reciente de modelos tridimensionales para el comportamiento transitorio del reactor; sin embargo, estos modelos tridimensionales todavía necesitan un tiempo de cálculo excesivo aún con las máquinas de cálculo muy rápidas disponibles en la actualidad, así como un gran esfuerzo en la preparación e interpretación de los resultados. Estos métodos desempeñan un papel importante en los estudios detallados de funcionamiento y seguridad, una vez que se ha terminado el proyecto, pero, en general, son demasiado costosos y lentos a efectos de diseño, para lo cual todavía se emplean ampliamente modelos uni y bidimensionales e incluso puntuales. Nuestra experiencia hasta el momento, basada en comparaciones entre el comportamiento real del reactor y los cálculos tridimensionales refinados, muestra que los métodos más sencillos proporcionan de hecho una base sólida para la mayor parte de los problemas de diseño.

Mi segundo comentario se relaciona con la necesidad de considerar las barras de control internas, tales como barras de control espacial o sobrecompensación, como una parte integral del sistema completo de aplanamiento del flujo. Esto se consigue muy fácilmente mediante el empleo de absorbentes móviles que formen parte de la misma red de los de control.

Este sistema se ha empleado, por ejemplo, en el reactor de Hunterston, haciendo posible alcanzar muy buenos factores de forma y al mismo tiempo un control satisfactorio y manteniendo la máxima flexibilidad de funcionamiento mediante la posibilidad de inserción diferencial de los absorbentes.

Documento P/260 (presentado por E. P. Blizard)

DISCUSIÓN

V. V. ORLOV (URSS): Una gran parte del trabajo soviético sobre la física del blindaje ha sido descrito en memorias presentadas en esta Conferencia. Sin embargo, después de oir el interesante examen del Dr. Blizard, me gustaría comentar dos puntos especiales.

Primeramente, hemos ideado un método para calcular lo que llamamos « funciones de eficacia » para diferentes materiales por medio de un conjunto de ecuaciones cinéticas conjugadas y de la teoría de perturbaciones (método que nos permite, por medio de aproximaciones sucesivas, determinar la distribución óptima de materiales en el blindaje). Sobre esta base se ha realizado un programa para calculadora con el propósito de obtener datos optimizados de blindaje. De este modo podemos hallar la composición del blindaje que posea peso mínimo, dimensiones mínimas, etc., sin dejar de satisfacer ciertas condiciones preestablecidas referentes a dosis en el exterior del blindaje, liberación de calor y otros parámetros.

En segundo lugar, desearía llamar su atención sobre la posibilidad de calcular la distribución en medios infinitos de radiaciones procedentes de una fuente puntual direccional mediante la solución de una ecuación cinética conjugada para una fuente que se supone isotrópica. Este método es considerablemente más fácil que la resolución directa de la ecuación cinética porque implica un número menor de variables independientes.

H. WIJKER (Países Bajos): El procedimiento descrito por el Sr. Orlov parece implicar el cambio de un parámetro tras otro en pequeñas etapas. ¿No requiere esto bastante tiempo?

V. V. ORLOV (URSS): Depende en gran parte, desde luego, de la complejidad del problema particular de que se trata. El programa de la calculadora tiene suficiente capacidad para tratar una amplia variedad de problemas y generalmente es más detallado de lo que la situación exige. El tiempo requerido es de varias horas.

P. S. MITTELMAN (Estados Unidos de América): La técnica descrita por el Dr. Blizard y por mí ha sido ideada tanto para sintetizar como para optimizar un blindaje. Con la técnica de síntesis el propósito no es comenzar con un conjunto de materiales y variar el grosor de varias capas hasta obtener un peso mínimo, sino más bien seleccionar un conjunto de materiales de blindaje y entonces establecer analíticamente el proyecto de blindaje que dé un peso mínimo.

Supongo que sería muy arduo deducir un conjunto de funciones de eficacia para los materiales presentes en diversos puntos de un blindaje, porque la eficacia de un material dado en una posición dada, depende estrechamente de los materiales que le preceden y le siguen. Si se tratan a la vez como variables el tipo de material y su posición en el blindaje, supongo que el cálculo se hace casi imposible.

V. V. ORLOV (URSS): No estoy enteramente de acuerdo con Vd. El programa al que me he referido consiste en iteraciones sucesivas, cada una de las cuales lleva consigo sólo pequeños cambios en las concentraciones de los materiales. Se supone que en cada caso el cambio es lo suficientemente pequeño para que se conserven las condiciones en las que es aplicable la teoría de perturbaciones pequeñas. La interdependencia que Vd. menciona (la influencia de las capas precedentes y siguientes, etc.) se tiene en cuenta. Si es necesario puedo describir a Vd. con mayor detalle, después de la reunión, la manera de hacer esto.

Documento P/684 (presentado por M. Leimdörfer)

DISCUSIÓN

F. P. YOUELL (Reino Unido): Como Vd. menciona el programa de cálculo RASH B del Reino Unido, me gustaría hacer unos breves comentarios. Primero, su memoria es interesante porque proporciona una prueba adicional de la valía del método de remoción-difusión para la penetración de neutrones en blindajes. En esta memoria se ha utilizado el programa de cálculo RASH B, pero el campo de acción del modelo ha sido ya ampliado a fin de permitir el cálculo, en varios tipos de blindaje estratificado, del espectro neutrónico desde 18 MeV hasta energías térmicas. Esta última versión del programa se conoce como RASH E; su versatilidad y precisión han sido expuestas por el Dr. J. Butler en la memoria ABEW-R361 de la UKAEA.

En el Reino Unido tenemos la sensación de que la precisión ya conseguida para configuraciones sencillas de blindaje es en la actualidad satisfactoria, particularmente si se la compara con las inexactitudes introducidas al simplificar la compleja geometría que se encuentra en los blindajes de los grandes reactores de potencia. Nuestros principales esfuerzos se dirigen ahora hacia la extensión del método RASH para tratar estas geometrías complejas. La memoria P/175 describe varias ampliaciones del método normal que se ha propuesto para tratar ciertas regiones heterogéneas de blindaje halladas en Bradwell. Suponer todo el material del blindaje homogeneizado en una simple losa, puede conducir a serias subestimaciones de los flujos neutrónicos, sobre todo cuando se trata de regiones tales como reflectores atravesados por muchos canales de combustible en reactores refrigerados por gas. De los resultados dados en la memoria P/175 llegamos a la conclusión de que el modelo edad de remoción y difusión, junto con correcciones de camino directo o similares para la heterogeneidad, proporciona un valioso instrumento para los proyectos de blindajes de reactores.

C. H. MINTON (Estados Unidos de América): ¿Podría Vd. hacer algún comentario sobre la bondad del método de ordenadas discretas, o los métodos de armónicos esféricos de órdenes elevados, en cálculos de varios grupos para problemas del tipo discutido en su memoria?

M. LEIMDORFER (Suecia): Yo creo que se trata principalmente de una cuestión de tiempo de calculadora. Por ejemplo, el programa NIOBE, que pertenece al grupo que Vd. ha mencionado, es aproximadamente 100 veces más lento que nuestro método.

Documento P/657

DISCUSIÓN

C. H. MINTON (Estados Unidos de América): Usted afirma que «los fotones que pertenecen a un grupo de energía y ángulo no pasarán a los otros grupos durante la transmisión a través de una losa elemental». ¿Es esto una característica del programa de Monte Carlo utilizado en la preparación de la matriz de respuesta?

I. KATAOKA (Japón): No, no es una característica del programa de Monte Carlo. Se refiere únicamente al procedimiento de interpolación de espesor utilizado para sintetizar las matrices de respuesta para las losas elementales. Para aclarar esta respuesta debo añadir que los cálculos se consideran en conjunto como compuestos de dos partes separadas. Primero viene la preparación de las matrices de respuesta para las losas elementales de varios materiales; el que emplea el método necesita únicamente una tabla de las matrices de respuesta. En segundo lugar está el cálculo de los fotones transmitidos (o reflejados) a través de la barrera estratificada que se desee. La síntesis de las matrices de respuesta y el cálculo de interpolación de espesor se realizan en esta etapa del cálculo, que puede ser programado para cualquier calculadora digital que convenga al usuario del método. El autor ha preparado un programa para una calculadora NEAC-2206.

H. WIJKER (Países Bajos): Como las matrices contienen solamente dos parámetros, la energía y el coseno del ángulo, se puede llegar a la conclusión

de que el procedimiento que Vd. describe es satisfactorio únicamente para fuentes homogéneas planas e infinitas. En las figuras 4 y 5 se comparan los resultados con medidas realizadas con una fuente de Co^{60}. Me pregunto si la fuente utilizada en estos experimentos era una fuente plana homogénea de dimensiones razonables.

I. KATAOKA (Japón): No existe relación directa entre el cálculo de Monte Carlo y la verdadera disposición de la fuente y detectores en el experimento. Los resultados finales fueron convertidos en valores para geometría plana a partir de las medidas experimentales, y estos son los resultados a que se hace referencia en la memoria.

PEACEFUL USES OF ATOMIC ENERGY

Proceedings of the Third International Conference held at Geneva, 31 August-9 September 1964

The full list of the sixteen volumes comprising the multilingual edition of the Proceedings is given below. The sessional titles are included to show the main subjects dealt with in each individual volume.

Volume 1

Progress in Atomic Energy

Programme of the Conference

A Opening of the Conference

B New Economic Data. Energy Needs in Coming Years and the Role of Nuclear Power in Meeting these Needs

1.6 Technical and Economic Aspects of the Use of Nuclear Power

C International Collaboration in Nuclear Reactor Projects, including Developments of Major Co-operative Installations

H Closing of the Conference

Evening Lecture

Scientific Exhibition

Volume 2

Reactor Physics

3.1 New Developments in Reactor Physics

Volume 3

Reactor Studies and Performance

3.2 Lattice Studies and Critical Experiments

3.3 Reactor Performance

Volume 4

Reactor Control

3.4 Reactor Kinetics

3.5 Reactor Control and Shielding

Volume 5

Nuclear Reactors — I. Gas-cooled and Water-cooled Reactors

1.1 Gas-cooled and Graphite-moderated Reactors

1.2 Light-water Reactors

1.3 Heavy-water and Organic Reactors

Volume 6

Nuclear Reactors — II. Fast Reactors and Advanced Concepts

1.4 Fast Reactor Physics and Breeders

1.5 Superheating and Advanced Concepts

1.7 Reactors of Special Applications. Future Developments

Volume 7

Research and Testing Reactors

D Research Reactors

1.9 High Flux Reactors for Material Testing

1.8 Very High Flux Reactors, Construction and Uses

Volume 8

Reactor Engineering and Equipment

1.10 Heat Transfer

1.11 Hydraulic Problems of Reactor Engineering

3.7 Reactor Plant Equipment

Volume 9

Reactor Materials

2.8 Structural Materials

2.9 Structural and Control Materials and Moderators

2.4 Corrosion Studies. Non-destructive Testing

Volume 10

Nuclear Fuels — 1. Fabrication and Reprocessing

2.3 Fuel Element Fabrication and Experience

2.6 Fuel Reprocessing, Part I

2.7 Fuel Reprocessing, Part II

Volume 11

Nuclear Fuels — II. Types and Economics

2.5 Economics of the Fuel Cycle

2.1 Metallic and Various Fuels

2.2 Ceramic Fuels

Volume 12

Nuclear Fuels — III. Raw Materials

2.11 Resources and Requirements

2.12 Prospecting Techniques and Recovery from Ores

2.10 Isotope Separation

Volume 13

Nuclear Safety

3.9 Nuclear Safety Research

3.8 Chemical Processing Plant Safety; Fuel Transport

3.6 Reactor Safety; Location and Containment; Reactor Tests

Volume 14

Environmental Aspects of Atomic Energy and Waste Management

3.10 Safety Aspects of Large-scale Use of Atomic Energy. Measurement and Limitation of Exposure in Radiation Emergencies

3.11 Radioactive Waste Management

Volume 15

Special Aspects of Nuclear Energy and Isotope Applications

E Controlled Nuclear Fusion

4.1 Direct Conversion of Heat to Electricity

F Applications of Isotopes and Radiation Sources in the Physical Sciences

G Applications of Isotopes and Radiation Sources in the Life Sciences

4.2 Miscellaneous Applications of Atomic Energy

Volume 16

List of Papers and Indexes

List of Papers

Author Index

Country Index

Sessional Index